

**Applications of Palladium-Catalyzed Enantioselective Decarboxylative Alkylation in
Natural Products Total Synthesis**

Thesis by

Ryan Michael McFadden

In Partial Fulfillment of the Requirements

for the Degree of

Doctor of Philosophy

California Institute of Technology

Pasadena, California

2008

(Defended December 11, 2007)

© 2008

Ryan Michael McFadden

All Rights Reserved

To Marcia
for her love and support

Acknowledgments

There are so many people I want thank for guiding me during my graduate student years. First and foremost, I am grateful to my advisor and mentor, Brian Stoltz. He has encouraged and challenged me from the very first day I arrived in the lab. His passion for chemistry is contagious, and he is a creative teacher who makes our science come to life. I truly admire the tenacity, openness, and flexibility he models to us, his students, as he manages our laboratory. He has given me incredible academic opportunities, allowing me to tackle both methodology and total synthesis while granting me freedom to explore my own ideas. The advice and support he has lent me over the years will never be forgotten.

I am also grateful to my committee members. My chairperson, Professor Bob Grubbs, encouraged me when my science was challenging, helping me to find my niche as a chemist. I have enjoyed my interactions with Professor Goddard and his group over the years. Our collaborations on both hypervalent iodine and palladium chemistry have been rewarding. Professor Hsieh-Wilson has also played a key role during my time at Caltech, helping give me a deeper understanding about biochemistry, inspiring me as I begin a career in medicinal chemistry. Although not an official committee member, I also want to thank Professor Dervan. It was a joy helping teach his class, and our discussions about science were rewarding.

I want to express my gratitude to Dr. Hicham Fenniri for mentoring me while I was an undergraduate in his lab at Purdue University. His encouragement for me to pursue graduate work in organic chemistry was valuable, and he taught me the importance of effective scientific communication. His patience and fascination with chemistry were great models to me. Professor Timothy Zwier is also acknowledged, as

are the many students in his lab at Purdue who took the time to mentor me during my first undergraduate research experience.

A special thanks also goes to Eli Lilly for their funding of my research and education over the years, especially in graduate school. Neil Rapp, Mike Kelly, Jim Schwengel, Kelly Kuchenbrod, and Jim Kimsey also deserve a warm thanks. These teachers helped foster my love of learning and went out of their way to give me opportunities to grow as a scientist. It all started with that vinegar and baking soda science fair project!

It has been a privilege to collaborate with so many talented scientists over the years. Dan Caspi and Dave Ebner were my first partners in crime. In our early days we investigated many flavors of oxidative kinetic resolutions. We used to draw straws to see who would get the GC next? One of us always got stuck doing runs at 4 a.m.— it built character, though! It was also a joy to work with Julius Su from the Goddard group on hypervalent iodine chemistry. He is an enthusiastic, friendly, and brilliant person, and I wish him continued success. Thanks goes to Scott Virgil for helpful discussions—he is always excited to talk chemistry, and we are glad to have him at Caltech.

Next, I want to give a shout out to my baymates past and present. John “JZ” Zepernick was a hard-working guy with an ability to make anybody laugh about anything. It was always lively when we chatted about politics, and it wasn’t surprising when he went to campaign for Howard Dean because he was doing what he loved. Jenny Roizen was a very personable baymate, and continues to be a great friend. Our conversations about everything from Dave Matthews to Dar Williams were memorable. Gene Lee showed that you could do chemistry and still be a family man. Nat Sherden and

I had so much fun talking about chemistry that it's a wonder we actually got any done! He introduced me to Zwan, the Smashing Pumpkins, and other great music. We had this barbecue once—I've never seen someone eat so much steak! Last, but not least, is Narae Park. Her bubbly enthusiasm is awesome, and I have learned a lot about chemistry from her. She has really encouraged me and helped me laugh at my mistakes! And what would graduate school have been like without Jenn Stockdill, my unofficial baymate? Whenever chemistry was going rough she'd be around to cheer me up and get me thinking about solutions instead of problems. Not only is she a talented chemist, but also a true friend. She was always game for ice cream, coffee, or Amigo's—whichever was in order!

I want to thank all of the postdocs who have come through the Stoltz Lab too. Richmond Sarpong was a mentor and taught me the ropes when I was a newbie in the lab. Zoltán Novák was my lunchtime friend, and we'd compare/swap dishes our wives had made. He showed me what REAL Hungarian goulash was supposed to taste like. Charles Liu is a talented chemist and made short work of some tough natural products. I look forward to seeing him again when I get to Gilead; they are privileged to have him on their team. A huge thanks goes out to Dave White for his advice, wisdom, and suggestions about the job interviewing process. It was a great experience working with him and Mike Krout on the enantioselective decarboxylative alkylation chemistry.

I owe Neil Garg a big thanks for taking the time to help me get started in the lab. When I came to Caltech as a prospective student, I remember meeting him and seeing how much he loved working for Brian. Whether he was taking prospectives for a hike to Switzer's or presenting a poster, Neil went out of his way to make us feel welcome. His enthusiasm really got me excited to join the Stoltz lab, and I am so glad that I did.

A special thanks goes out to Team Tsuji, including Doug Behenna, JT Mohr, Andy Harned, Kousuke Tani, Sandy Ma, Nat Sherden, Jeff Servesko, Akihiko Iwashita, Smaranda Miranescu, John Keith, Julius Su, Jenny Roizen, John Enquist, Mike Krout, Dave White, Toyoki Nishimata, Masaki Seto, Thomas Jensen, and anyone else I may have forgotten. The length of this list is a huge tribute to Doug Behenna, who performed some of the first investigations into the enantioselective Tsuji allylation. His insight and discoveries have paved the way for numerous projects in the group, including my own.

I also want to thank Dr. Gomez and Dr. Selke from Cal State LA, as well as the PREM program. It was an honor to speak at the 2006 inaugural PREM conference in San Diego, and it was a fantastic experience working with Jacqueline Malette. Although she may have learned things from me while I was her mentor for two summers, I think I learned even more. A huge thanks also goes out to the Caltech MURF program, which made the experience possible.

There are many behind-the-scenes folks who are the oil for the research engine. Scott Ross and Chris Brandow have kept our NMR facility running and have gone out of their way on several occasions to help me out. Mona Shahgholi and Naseem Torian have been a huge help with mass spectrometry needs. If it is broken, Tom Dunn can fix it. I can't even keep track of all of my broken stirplates he's repaired. Rick Gerhart has repaired an equally large number of my broken flash columns. Mike Day and Larry Henling have helped provide the X-ray crystallographic data presented in this thesis. Dian Buchness and Laura Howe have helped immensely with the administrative details of my time here—more than I'm probably aware of!

My parents have shown me so much love and support, and worked so hard to provide me with opportunities that helped bring me here. The Liems are my new family and have provided me great comfort, love, and hospitality. Erin, Kevin, Pete, and Kimi, thanks for cheering me on, saying, “You can do it!” God has helped me through. Finally, I want to thank my loving wife, Marcia. Her care, support, prayers, and encouragement have kept me going. And I know the lab will miss her awesome cooking!

ABSTRACT

The catalytic enantioselective preparation of all-carbon quaternary stereocenters within rings via alkylation is a major challenge in synthetic organic chemistry. Many important natural products and biologically active pharmaceuticals contain this motif. We have developed palladium-catalyzed decarboxylative alkylations capable of generating all-carbon quaternary stereocenters in good yield with high enantioselectivity.

Alkylated products are readily elaborated to synthetically useful cyclic scaffolds. The enantioselective decarboxylative alkylation is thus utilized to prepare intermediates previously reported in the total syntheses of classic natural products. Herein, we disclose modern formal syntheses of (–)-Thujopsene, (–)-Dysidiolide, and (–)-Aspidospermine.

The longer-term goal was to apply this new enantioselective catalysis to the total syntheses of natural products with novel carbocyclic architectures. Our methodology is demonstrated during the first protecting group-free enantioselective total synthesis of (+)-dichroanone, a 4a-methyltetrahydrofluorene. The [6-5-6] tricyclic natural products family has members with important biological activity, and our route to (+)-dichroanone may provide general access to related compounds. During our synthetic endeavors, a novel Kumada-benzannulation approach to the aromatic portion of (+)-dichroanone was developed, along with a unique synthesis of a hydroxy-*p*-benzoquinone from a phenol. The absolute stereochemistry of the natural product was verified for the first time during our total synthesis.

Significant progress has been made toward the total synthesis of the marine meroterpenoid liphagal, a potent and selective phosphatidylinositol 3-kinase α inhibitor. The enantioselective decarboxylative alkylation has been employed, and an acetylene [2 + 2] photoaddition / ring-opening sequence is used to construct the 7-membered ring. New understanding about the reactivity of [6-7] bicyclic scaffolds has been gathered, and the information applied during preparation of liphagal's benzofuran motif. Our efforts have led to a functionally diverse array of liphagal analogues, which may be used for structure-activity-relationship studies with phosphatidylinositol 3-kinases.

Table of Contents

Dedication	iii
Acknowledgments	iv
Abstract	ix
Table of Contents	x
List of Figures	xviii
List of Schemes	xxvi
List of Tables	xxx
List of Abbreviations	xxxii
 Chapter One: Enantioselective Alkylations Generating All-Carbon Quaternary Stereocenters Within Rings	 1
1.1 Background	1
1.2 Auxilliary-Based Methods for Alkylation	1
<i>Koga's t-Butyl Glycine Esters</i>	1
<i>Meyers' Valinol Auxilliary</i>	2
<i>Enders' RAMP and SAMP Hydrazone Auxilliary</i>	3
1.3 Catalytic Alkylations for Generating Quaternary Stereocenters without Pd	4
<i>Chiral Phase Transfer Catalysis</i>	4
<i>Shibasaki's Lanthanide Sodium Binol Catalyzed Enantioselective Michael Reaction</i>	6
<i>Jacobsen's Chromium Salen Catalyzed Alkylation</i>	6
1.4 Palladium Catalysis for Enantioselective Alkylation of Prochiral Enolates	7
<i>Hayashi's Allyl Palladium Catalysis</i>	7
<i>Early Work by Trost Surrounding Pd-Catalyzed Alkylation</i>	8
<i>Ito's BINAP-Pd Catalyst</i>	11
<i>Enantioselective Pd-Catalyzed Decarboxylative Alkylation</i>	11

<i>Other Enantioselective Decarboxylative Alkylation Methodologies</i>	14
1.5 Concluding Remarks	15
1.6 Notes and Citations	16
<hr/>	
Chapter Two: Enantioselective Formal Total Syntheses of Natural Products	
Using Palladium-Catalyzed Decarboxylative Alkylation	21
2.1 Introduction	21
2.2 Formal Total Synthesis of (–)-Thujopsene	21
<i>Background</i>	21
<i>Structural Analysis of Thujopsene</i>	22
<i>Formal Total Synthesis of (–)-Thujopsene</i>	24
2.3 Formal Total Synthesis of (–)-Dysidiolide	27
<i>Background</i>	27
<i>Retrosynthetic Analysis</i>	28
<i>Formal Total Synthesis of (–)-Dysidiolide</i>	29
2.4 Formal Total Synthesis of (–)-Aspidospermine	30
<i>Background</i>	30
<i>Retrosynthetic Analysis</i>	32
<i>Two Routes to the Alkylated Vinylogous Ester: Formal Synthesis of Aspidospermine</i>	32
2.5 Other Targets for Formal Total Synthesis	34
<i>Goniomitine</i>	34
<i>Jiadifenin</i>	35

<i>Fillion's Approach to Taiwaniaquinol B</i>	105
<i>Node's Synthesis of Dichroanal B</i>	107
<i>Trauner's Synthesis of Taiwaniaquinoids</i>	109
<i>Challenges to Address</i>	112
3.3 First Retrosynthetic Analysis of Dichroanone	113
<i>Complexities of the Dichroanone Architecture</i>	113
<i>Retrosynthetic Analysis of Dichroanone</i>	113
3.4 Synthesis of the Tricyclic Core	114
<i>Preparation of a Racemic Bicyclic Enone</i>	114
<i>6π-Electrocyclization Approach to the Third Ring</i>	117
<i>Robinson Annulation of the Enone</i>	119
3.5 Synthesis of a Dichroanone Isomer	120
<i>α-Hydroxylation</i>	120
<i>Synthesis of an Isomer of Dichroanone</i>	121
3.6 Second Retrosynthetic Analysis of Dichroanone	123
<i>Lessons Learned</i>	123
<i>Retrosynthetic Revisions</i>	123
<i>Substrate and Catalyst Control in Pd-Catalyzed Enantioselective Alkylations</i>	124
<i>Enantioenrichment Strategy</i>	126
3.7 Preparation and Manipulation of a Tricyclic Phenol	127
<i>Attempted Aryl Triflate Synthesis</i>	127
<i>Kumada Coupling and Benzannulation</i>	128
<i>Preparation of an Unstable Phenol</i>	130
<i>Protecting Group Strategies</i>	131

3.8	Total Synthesis of Dichroanone	132
	<i>Preparation of an o-Quinone</i>	132
	<i>Thiol Additions into the o-Quinone</i>	133
	<i>Completion of Dichroanone</i>	135
3.9	Attempts to Prepare Other Natural Products	137
	<i>Toward Taiwaniaquinone H</i>	137
	<i>Toward Taiwaniaquinol D</i>	138
3.10	Concluding Remarks	139
3.11	Experimental Procedures	140
	<i>Materials and Methods</i>	140
	<i>Syntheses of Compounds Related to Dichroanone</i>	142
	<i>Methods for the Determination of Enantiomeric Excess</i>	189
3.12	Notes and Citations	190
<hr/>		
	Appendix Three: Synthetic Summary of the Enantioselective Total Syntheses of (+)-Dichroanone	198
	Appendix Four: Spectra of Compounds Relevant to Chapter 3	200
	Appendix Five: X-Ray Crystallographic Data Relevant to Chapter 3	269
<hr/>		
	Chapter Four: Progress Toward the Catalytic Enantioselective Total Synthesis of Liphagal	282
4.1	Background	282
	<i>Isolation of the First Liphagane Natural Product, Liphagal</i>	282
	<i>Biological Activity of Liphagal</i>	282

<i>Phosphatidylinositol 3-Kinases and their Biology</i>	283
<i>Biosynthetic Proposals</i>	284
4.2 Andersen's Racemic Total Synthesis of Liphagal	286
<i>Retrosynthetic Analysis</i>	286
<i>Preparation of the Fragments</i>	287
<i>Completion of Racemic Liphagal</i>	288
4.3 First Retrosynthetic Analysis of Liphagal	290
<i>Challenges for Synthesizing Liphagal</i>	290
<i>Retrosynthetic Analysis</i>	291
4.4 A Photochemical Approach to the [6-7] Ring System	292
<i>Synthesis of the Bicyclic Enone Antipode</i>	292
<i>Photochemical Investigations</i>	293
<i>A Photochemical Rearrangement Pathway</i>	294
<i>Formal 4π Electrocyclic Ring Expansion</i>	296
<i>Elaboration of the [6-7] Core</i>	297
4.5 Attempts to Install the Benzofuran Moiety of Liphagal	298
<i>An Aryloxime Model System</i>	298
<i>An Aryloxime Approach to Liphagal</i>	299
<i>A Mukaiyama Michael-Based Benzofuran Synthesis</i>	300
<i>Mukaiyama Michael Approach to Liphagal</i>	302
<i>α-Arylation Strategy</i>	304
<i>α-Arylation Attempts on the [6-7] Bicyclic System</i>	306
4.6 Positional Blocking Strategies Applied to the Key Benzofuran Synthesis	307
<i>Retrosynthetic Revisions</i>	307
<i>Attempted Arylation of the Dienone</i>	308

<i>Exocyclic Olefin Substrates</i>	308
<i>Quaternization of C(8)</i>	309
4.7 Approaches Based on Arylation of [6-5] Systems	311
<i>Retrosynthetic Revisions</i>	311
<i>Attempted Photoaddition to an Aryl Enone</i>	312
<i>Successful Arylation of the Keto-Cyclobutene</i>	313
<i>Changes In the Ring Expansion</i>	314
<i>Effects of the Aryl Group on Subsequent Chemistry</i>	316
<i>Optimized Electrocyclic Ring Expansion</i>	318
<i>Functionalization of the Dienone</i>	319
4.8 Completion of the Benzofuran Ring	321
<i>Preparation of a Dihydrobenzofuran</i>	321
<i>Controlled Oxidation of the Dihydrobenzofuran</i>	323
<i>Installation of the Aldehyde Functionality</i>	324
<i>Proposed Endgame for the Total Synthesis of Liphagal</i>	325
4.9 Analogues for PI3K Biological Screening	326
4.10 Concluding Remarks	328
4.11 Experimental Procedures	328
<i>Materials and Methods</i>	328
<i>Syntheses of Compounds Related to Liphagal</i>	330
<i>Methods for the Determination of Enantiomeric Excess</i>	393
4.12 Notes and Citations	394

Appendix Six: Synthetic Summary of Efforts Toward the Enantioselective Total Syntheses of Liphagal	402
Appendix Seven: Spectra of Compounds Relevant to Chapter 4	405
Appendix Eight: X-Ray Crystallographic Data Relevant to Chapter 4	503
Appendix Nine: Compounds Submitted for PI3K Biological Screening	529
Appendix Ten: Cross References to Characterization Binders and Notebooks	537
<hr/>	
Comprehensive Bibliography	559
About the Author	574
<hr/>	

List of Figures

Chapter Two: Enantioselective Formal Total Syntheses of Natural Products Using Palladium-Catalyzed Decarboxylative Alkylation	21
Figure 2.1 Natural Products from <i>Thujopsis dolabrata</i>	22
Figure 2.2 Representative Aspidosperma Alkaloids	31

Appendix Two: Spectra of Compounds Relevant to Chapter 2	67
Figure A2.1 ¹ H NMR (300 MHz, CDCl ₃) of compound 100 .	68
Figure A2.2 Infrared spectrum (NaCl/CDCl ₃) of compound 100 .	69
Figure A2.3 ¹³ C NMR (75 MHz, CDCl ₃) of compound 100 .	69
Figure A2.4 ¹ H NMR (300 MHz, CDCl ₃) of compound 75 .	70
Figure A2.5 Infrared spectrum (NaCl/CDCl ₃) of compound 75 .	71
Figure A2.6 ¹³ C NMR (75 MHz, CDCl ₃) of compound 75 .	71
Figure A2.7 ¹ H NMR (300 MHz, CDCl ₃) of compound 143 .	72
Figure A2.8 Infrared spectrum (NaCl/CDCl ₃) of compound 143 .	73
Figure A2.9 ¹³ C NMR (75 MHz, CDCl ₃) of compound 143 .	73
Figure A2.10 ¹ H NMR (300 MHz, CDCl ₃) of compounds 99A and 99B .	74
Figure A2.11 Infrared spectrum (NaCl/CDCl ₃) of compounds 99A and 99B .	75
Figure A2.12 ¹³ C NMR (75 MHz, CDCl ₃) of compounds 99A and 99B .	75
Figure A2.13 ¹ H NMR (300 MHz, CDCl ₃) of compounds 103A and 103B .	76
Figure A2.14 Infrared spectrum (NaCl/CDCl ₃) of compounds 103A and 103B .	77
Figure A2.15 ¹³ C NMR (75 MHz, CDCl ₃) of compounds 103A and 103B .	77
Figure A2.16 ¹ H NMR (300 MHz, CDCl ₃) of compound 104 .	78
Figure A2.17 Infrared spectrum (NaCl/CDCl ₃) of compound 104 .	79
Figure A2.18 ¹³ C NMR (75 MHz, CDCl ₃) of compound 104 .	79
Figure A2.19 ¹ H NMR (300 MHz, CDCl ₃) of compound 94 .	80
Figure A2.20 Infrared spectrum (NaCl/CDCl ₃) of compound 94 .	81
Figure A2.21 ¹³ C NMR (75 MHz, CDCl ₃) of compound 94 .	81
Figure A2.22 ¹ H NMR (300 MHz, CDCl ₃) of compound 113 .	82
Figure A2.23 Infrared spectrum (NaCl/CDCl ₃) of compound 113 .	83
Figure A2.24 ¹³ C NMR (75 MHz, CDCl ₃) of compound 113 .	83
Figure A2.25 ¹ H NMR (300 MHz, CDCl ₃) of compound 112 .	84
Figure A2.26 Infrared spectrum (NaCl/CDCl ₃) of compound 112 .	85
Figure A2.27 ¹³ C NMR (75 MHz, CDCl ₃) of compound 112 .	85
Figure A2.28 ¹ H NMR (300 MHz, CDCl ₃) of compound 109 .	86
Figure A2.29 Infrared spectrum (NaCl/CDCl ₃) of compound 109 .	87
Figure A2.30 ¹³ C NMR (75 MHz, CDCl ₃) of compound 109 .	87
Figure A2.31 ¹ H NMR (300 MHz, CDCl ₃) of compound 121 .	87
Figure A2.32 Infrared spectrum (NaCl/CDCl ₃) of compound 121 .	89
Figure A2.33 ¹³ C NMR (75 MHz, CDCl ₃) of compound 121 .	89
Figure A2.34 ¹ H NMR (300 MHz, CDCl ₃) of compound 79 .	90

Figure A2.35	Infrared spectrum (NaCl/CDCl ₃) of compound 79 .	91
Figure A2.36	¹³ C NMR (300 MHz, CDCl ₃) of compound 79 .	91
Figure A2.37	¹ H NMR (300 MHz, CDCl ₃) of compound 125 .	92
Figure A2.38	Infrared spectrum (NaCl/CDCl ₃) of compound 125 .	93
Figure A2.39	¹³ C NMR (75 MHz, CDCl ₃) of compound 125 .	93
Figure A2.40	¹ H NMR (300 MHz, CDCl ₃) of compound 124 .	94
Figure A2.41	Infrared spectrum (NaCl/CDCl ₃) of compound 124 .	95
Figure A2.42	¹³ C NMR (75 MHz, CDCl ₃) of compound 124 .	95
Figure A2.43	¹ H NMR (300 MHz, CDCl ₃) of compound 120 .	96
Figure A2.44	Infrared spectrum (NaCl/CDCl ₃) of compound 120 .	97
Figure A2.45	¹³ C NMR (75 MHz, CDCl ₃) of compound 120 .	97

Chapter Three:	The Catalytic-Enantioselective, Protecting Group-Free Total Synthesis of (+)-Dichroanone	98
Figure 3.1	[6-5-6] Natural Products	99

Appendix Four:	Spectra of Compounds Relevant to Chapter 3	200
Figure A4.1	¹ H NMR (300 MHz, CDCl ₃) of compound 222 .	201
Figure A4.2	Infrared spectrum (KBr) of compound 222 .	202
Figure A4.3	¹³ C NMR (75 MHz, CDCl ₃) of compound 222 .	202
Figure A4.4	¹ H NMR (300 MHz, CDCl ₃) of compound 101 .	203
Figure A4.5	Infrared spectrum (NaCl/CDCl ₃) of compound 101 .	204
Figure A4.6	¹³ C NMR (75 MHz, CDCl ₃) of compound 101 .	204
Figure A4.7	¹ H NMR (300 MHz, CDCl ₃) of compound 100 .	205
Figure A4.8	Infrared spectrum (NaCl/CDCl ₃) of compound 100 .	206
Figure A4.9	¹³ C NMR (75 MHz, CDCl ₃) of compound 100 .	206
Figure A4.10	¹ H NMR (300 MHz, CDCl ₃) of compound 75 .	207
Figure A4.11	Infrared spectrum (NaCl/CDCl ₃) of compound 75 .	208
Figure A4.12	¹³ C NMR (75 MHz, CDCl ₃) of compound 75 .	208
Figure A4.13	¹ H NMR (300 MHz, CDCl ₃) of compound 244 .	209
Figure A4.14	Infrared spectrum (NaCl/CDCl ₃) of compound 244 .	210
Figure A4.15	¹³ C NMR (75 MHz, CDCl ₃) of compound 244 .	210
Figure A4.16	¹ H NMR (300 MHz, CDCl ₃) of compound 245A and 245B .	211
Figure A4.17	Infrared spectrum (NaCl/CDCl ₃) of compound 245A and 245B .	212
Figure A4.18	¹³ C NMR (75 MHz, CDCl ₃) of compound 245A and 245B .	212
Figure A4.19	¹ H NMR (300 MHz, CDCl ₃) of compound 219 .	213
Figure A4.20	Infrared spectrum (NaCl/CDCl ₃) of compound 219 .	214
Figure A4.21	¹³ C NMR (75 MHz, CDCl ₃) of compound 219 .	214
Figure A4.22	¹ H NMR (300 MHz, CDCl ₃) of compound 143 .	215
Figure A4.23	Infrared spectrum (NaCl/CDCl ₃) of compound 143 .	216

Figure A4.24	^{13}C NMR (75 MHz, CDCl_3) of compound 143 .	216
Figure A4.25	^1H NMR (300 MHz, CDCl_3) of compound 246 .	217
Figure A4.26	Infrared spectrum (KBr) of compound 246 .	218
Figure A4.27	^{13}C NMR (125 MHz, CDCl_3) of compound 246 .	218
Figure A4.28	^1H NMR (300 MHz, C_6D_6) of compound 229 .	219
Figure A4.29	^{13}C NMR (75 MHz, C_6D_6) of compound 229 .	220
Figure A4.30	^{19}F NMR (282 MHz, C_6D_6) of compound 229 .	221
Figure A4.31	^1H NMR (300 MHz, CDCl_3) of compound 231 .	222
Figure A4.32	Infrared spectrum ($\text{NaCl}/\text{CDCl}_3$) of compound 231 .	223
Figure A4.33	^{13}C NMR (75 MHz, CDCl_3) of compound 231 .	223
Figure A4.34	^1H NMR (300 MHz, CDCl_3) of compound 233 .	224
Figure A4.35	Infrared spectrum (KBr) of compound 233 .	225
Figure A4.36	^{13}C NMR (75 MHz, CDCl_3) of compound 233 .	225
Figure A4.37	^1H NMR (300 MHz, CDCl_3) of compound 234 .	226
Figure A4.38	Infrared spectrum ($\text{NaCl}/\text{CDCl}_3$) of compound 234 .	227
Figure A4.39	^{13}C NMR (75 MHz, CDCl_3) of compound 234 .	227
Figure A4.40	^1H NMR (300 MHz, C_6D_6) of compound 235 .	228
Figure A4.41	Infrared spectrum (NaCl/neat) of compound 235 .	229
Figure A4.42	^{13}C NMR (75 MHz, C_6D_6) of compound 235 .	229
Figure A4.43	^1H NMR (300 MHz, CDCl_3) of compound 236A .	230
Figure A4.44	Infrared spectrum ($\text{NaCl}/\text{CDCl}_3$) of compound 236A .	231
Figure A4.45	^{13}C NMR (75 MHz, CDCl_3) of compound 236A .	231
Figure A4.46	^1H NMR (300 MHz, CDCl_3) of compound 236B .	232
Figure A4.47	Infrared spectrum ($\text{NaCl}/\text{CDCl}_3$) of compound 236B .	233
Figure A4.48	^{13}C NMR (75 MHz, CDCl_3) of compound 236B .	233
Figure A4.49	^1H NMR (300 MHz, CDCl_3) of compound 237 .	234
Figure A4.50	Infrared spectrum ($\text{NaCl}/\text{CDCl}_3$) of compound 237 .	235
Figure A4.51	^{13}C NMR (75 MHz, CDCl_3) of compound 237 .	235
Figure A4.52	^1H NMR (300 MHz, CDCl_3) of compound 240 .	236
Figure A4.53	Infrared spectrum ($\text{NaCl}/\text{CDCl}_3$) of compound 240 .	237
Figure A4.54	^{13}C NMR (125 MHz, CDCl_3) of compound 240 .	237
Figure A4.55	^1H NMR (300 MHz, C_6D_6) of compound 250 .	238
Figure A4.56	Infrared spectrum ($\text{NaCl}/\text{hexane}$) of compound 250 .	239
Figure A4.57	^{13}C NMR (75 MHz, C_6D_6) of compound 250 .	239
Figure A4.58	^{19}F NMR (282 MHz, C_6D_6) of compound 250 .	240
Figure A4.59	^1H NMR (300 MHz, CDCl_3) of compound 252 .	241
Figure A4.60	Infrared spectrum ($\text{NaCl}/\text{CDCl}_3$) of compound 252 .	242
Figure A4.61	^{13}C NMR (75 MHz, CDCl_3) of compound 252 .	242
Figure A4.62	^1H NMR (300 MHz, CDCl_3) of compound 253 .	243
Figure A4.63	Infrared spectrum ($\text{NaCl}/\text{CDCl}_3$) of compound 253 .	244
Figure A4.64	^{13}C NMR (75 MHz, CDCl_3) of compound 253 .	244
Figure A4.65	^1H NMR (300 MHz, CDCl_3) of compound 254 .	245
Figure A4.66	Infrared spectrum ($\text{NaCl}/\text{CDCl}_3$) of compound 254 .	246
Figure A4.67	^{13}C NMR (75 MHz, CDCl_3) of compound 254 .	246
Figure A4.68	^1H NMR (300 MHz, CDCl_3) of compound 242 .	247
Figure A4.69	Infrared spectrum (KBr) of compound 242 .	248

Figure A4.70	^{13}C NMR (75 MHz, CDCl_3) of compound 242 .	248
Figure A4.71	^1H NMR (300 MHz, CDCl_3) of compound 255 .	249
Figure A4.72	^1H NMR (300 MHz, CDCl_3) of compound 256 .	250
Figure A4.73	Infrared spectrum ($\text{NaCl}/\text{CDCl}_3$) of compound 256 .	251
Figure A4.74	^{13}C NMR (125 MHz, CDCl_3) of compound 256 .	251
Figure A4.75	^1H NMR (300 MHz, CDCl_3) of compound 257 .	252
Figure A4.76	Infrared spectrum ($\text{NaCl}/\text{CDCl}_3$) of compound 257 .	253
Figure A4.77	^{13}C NMR (75 MHz, CDCl_3) of compound 257 .	253
Figure A4.78	^1H NMR (300 MHz, CDCl_3) of compound 258 .	254
Figure A4.79	Infrared spectrum ($\text{NaCl}/\text{CDCl}_3$) of compound 258 .	255
Figure A4.80	^{13}C NMR (75 MHz, CDCl_3) of compound 258 .	255
Figure A4.81	^1H NMR (300 MHz, CDCl_3) of compound 259 .	256
Figure A4.82	Infrared spectrum ($\text{NaCl}/\text{CDCl}_3/\text{D}_2\text{O}$) of compound 259 .	257
Figure A4.83	^{13}C NMR (125 MHz, CDCl_3) of compound 259 .	257
Figure A4.84	^1H NMR (300 MHz, C_6D_6) of compound 260 .	258
Figure A4.85	Infrared spectrum (NaCl/neat) of compound 260 .	259
Figure A4.86	^1H NMR (300 MHz, CDCl_3) of compound 150 .	260
Figure A4.87	Infrared spectrum (KBr) of compound 150 .	261
Figure A4.88	^{13}C NMR (75 MHz, CDCl_3) of compound 150 .	261
Figure A4.89	Infrared spectrum ($\text{NaCl}/\text{CHCl}_3$) of compound 150 .	262
Figure A4.90	^1H NMR (300 MHz, CDCl_3) of compound 267 .	263
Figure A4.91	Infrared spectrum ($\text{NaCl}/\text{CHCl}_3$) of compound 267 .	264
Figure A4.92	^{13}C NMR (75 MHz, CDCl_3) of compound 267 .	264
Figure A4.93	^1H NMR (300 MHz, CDCl_3) of compound 268 .	265
Figure A4.94	Infrared spectrum ($\text{NaCl}/\text{CHCl}_3$) of compound 268 .	266
Figure A4.95	^{13}C NMR (125 MHz, CDCl_3) of compound 268 .	266
Figure A4.96	^1H NMR (300 MHz, CDCl_3) of compound 269 .	267
Figure A4.97	Infrared spectrum ($\text{NaCl}/\text{CHCl}_3$) of compound 269 .	268
Figure A4.98	^{13}C NMR (125 MHz, CDCl_3) of compound 269 .	268

Chapter Four: Progress Toward the Catalytic Enantioselective Total Synthesis of Liphagal	282
Figure 4.1 The Structure of Liphagal	282
Figure 4.2 Selected Inhibitors of PI3K α	284
Figure 4.3 Selected Molecules For PI3K Biological Activity Studies	326

Appendix Seven: Spectra of Compounds Relevant to Chapter 4	405
Figure A7.1 ^1H NMR (300 MHz, CDCl_3) of compounds 307A and 307B .	406
Figure A7.2 Infrared spectrum (KBr) of compounds 307A and 307B .	407

Figure A7.3	^{13}C NMR (75 MHz, CDCl_3) of compounds 307A and 307B .	407
Figure A7.4	^1H NMR (300 MHz, C_6D_6) of compound 312 .	408
Figure A7.5	Infrared spectrum ($\text{NaCl}/\text{CHCl}_3$) of compound 312 .	409
Figure A7.6	^{13}C NMR (125 MHz, C_6D_6) of compound 312 .	409
Figure A7.7	^1H NMR (300 MHz, C_6D_6) of compound 313 .	410
Figure A7.8	Infrared spectrum (NaCl/neat) of compound 313 .	411
Figure A7.9	^{13}C NMR (75 MHz, C_6D_6) of compound 313 .	411
Figure A7.10	^1H NMR (300 MHz, CDCl_3) of compound 318 .	412
Figure A7.11	Infrared spectrum ($\text{NaCl}/\text{CDCl}_3$) of compound 318 .	413
Figure A7.12	^{13}C NMR (75 MHz, CDCl_3) of compound 318 .	413
Figure A7.13	^1H NMR (300 MHz, CDCl_3) of compound 305 .	414
Figure A7.14	Infrared spectrum ($\text{NaCl}/\text{CDCl}_3$) of compound 305 .	415
Figure A7.15	^{13}C NMR (75 MHz, CDCl_3) of compound 305 .	415
Figure A7.16	^1H NMR (300 MHz, CDCl_3) of compound 304 .	416
Figure A7.17	Infrared spectrum ($\text{NaCl}/\text{CDCl}_3$) of compound 304 .	417
Figure A7.18	^{13}C NMR (75 MHz, CDCl_3) of compound 304 .	417
Figure A7.19	^1H NMR (300 MHz, CDCl_3) of compounds 319A .	418
Figure A7.20	Infrared spectrum ($\text{NaCl}/\text{CDCl}_3$) of compounds 319A .	419
Figure A7.21	^{13}C NMR (75 MHz, CDCl_3) of compound 319A .	419
Figure A7.22	^1H NMR (300 MHz, CDCl_3) of compound 321 .	420
Figure A7.23	Infrared spectrum ($\text{NaCl}/\text{CDCl}_3$) of compound 321 .	421
Figure A7.24	^{13}C NMR (75 MHz, CDCl_3) of compound 321 .	421
Figure A7.25	^1H NMR (300 MHz, CDCl_3) of compound 322 .	422
Figure A7.26	Infrared spectrum ($\text{NaCl}/\text{CDCl}_3$) of compound 322 .	423
Figure A7.27	^{13}C NMR (75 MHz, CDCl_3) of compound 322 .	423
Figure A7.28	^1H NMR (300 MHz, CDCl_3) of compound 323A and 323B .	424
Figure A7.29	Infrared spectrum ($\text{NaCl}/\text{CDCl}_3$) of compound 323A and 323B .	425
Figure A7.30	^{13}C NMR (75 MHz, CDCl_3) of compound 323A and 323B .	425
Figure A7.31	^1H NMR (300 MHz, CDCl_3) of compound 331 .	426
Figure A7.32	Infrared spectrum ($\text{NaCl}/\text{CDCl}_3$) of compound 331 .	427
Figure A7.33	^{13}C NMR (75 MHz, CDCl_3) of compound 331 .	427
Figure A7.34	^1H NMR (300 MHz, CDCl_3) of compound 334 .	428
Figure A7.35	Infrared spectrum (KBr) of compound 334 .	429
Figure A7.36	^{13}C NMR (75 MHz, CDCl_3) of compound 334 .	429
Figure A7.37	^1H NMR (500 MHz, CDCl_3) of compound 338 .	430
Figure A7.38	Infrared spectrum ($\text{NaCl}/\text{CDCl}_3$) of compound 338 .	431
Figure A7.39	^{13}C NMR (125 MHz, CDCl_3) of compound 338 .	431
Figure A7.40	^1H NMR (500 MHz, CDCl_3) of compound 339 .	432
Figure A7.41	Infrared spectrum (KBr) of compound 339 .	433
Figure A7.42	^{13}C NMR (125 MHz, CDCl_3) of compound 339 .	433
Figure A7.43	^1H NMR (500 MHz, CDCl_3) of compound 340 .	434
Figure A7.44	Infrared spectrum ($\text{NaCl}/\text{CHCl}_3/\text{CDCl}_3$) of compound 340 .	435
Figure A7.45	^{13}C NMR (125 MHz, CDCl_3) of compound 340 .	435
Figure A7.46	^1H NMR (300 MHz, C_6D_6) of compound 342 .	436
Figure A7.47	Infrared spectrum (NaCl/neat) of compound 342 .	437
Figure A7.48	^{13}C NMR (75 MHz, C_6D_6) of compound 342 .	437

Figure A7.49	^1H NMR (500 MHz, CDCl_3) of compound 348 .	438
Figure A7.50	Infrared spectrum (KBr) of compound 348 .	439
Figure A7.51	^{13}C NMR (125 MHz, CDCl_3) of compound 348 .	439
Figure A7.52	^1H NMR (500 MHz, CDCl_3) of compound 349 .	440
Figure A7.53	Infrared spectrum ($\text{NaCl}/\text{CDCl}_3$) of compound 349 .	441
Figure A7.54	^{13}C NMR (125 MHz, CDCl_3) of compound 349 .	441
Figure A7.55	^1H NMR (300 MHz, C_6D_6) of compound 350 .	442
Figure A7.56	Infrared spectrum (KBr) of compound 350 .	443
Figure A7.57	^{13}C NMR (75 MHz, C_6D_6) of compound 350 .	443
Figure A7.58	^1H NMR (500 MHz, CDCl_3) of compound 351 .	444
Figure A7.59	Infrared spectrum ($\text{NaCl}/\text{CDCl}_3$) of compound 351 .	445
Figure A7.60	^{13}C NMR (125 MHz, CDCl_3) of compound 351 .	445
Figure A7.61	^1H NMR (500 MHz, CDCl_3) of compound 352 .	446
Figure A7.62	Infrared spectrum ($\text{NaCl}/\text{CHCl}_3$) of compound 352 .	447
Figure A7.63	^{13}C NMR (125 MHz, CDCl_3) of compound 352 .	447
Figure A7.64	^1H NMR (300 MHz, C_6D_6) of compound 357 .	448
Figure A7.65	Infrared spectrum ($\text{NaCl}/\text{CH}_2\text{Cl}_2$) of compound 357 .	449
Figure A7.66	^{13}C NMR (75 MHz, C_6D_6) of compound 357 .	449
Figure A7.67	^1H NMR (300 MHz, C_6D_6) of compound 358 .	450
Figure A7.68	Infrared spectrum ($\text{NaCl}/\text{CH}_2\text{Cl}_2$) of compound 358 .	451
Figure A7.69	^{13}C NMR (75 MHz, C_6D_6) of compound 358 .	451
Figure A7.70	^1H NMR (300 MHz, C_6D_6) of compound 359 .	452
Figure A7.71	Infrared spectrum ($\text{NaCl}/\text{CH}_2\text{Cl}_2$) of compound 359 .	453
Figure A7.72	^{13}C NMR (75 MHz, C_6D_6) of compound 359 .	453
Figure A7.73	^1H NMR (300 MHz, CDCl_3) of compounds 361A , 361B , and 361C .	454
Figure A7.74	Infrared spectrum ($\text{NaCl}/\text{CDCl}_3$) of compounds 361A , 361B , and 361C .	455
Figure A7.75	^{13}C NMR (75 MHz, CDCl_3) of compound 361A , 361B , and 361C .	455
Figure A7.76	^1H NMR (300 MHz, CDCl_3) of compound 362 .	456
Figure A7.77	Infrared spectrum ($\text{NaCl}/\text{CDCl}_3$) of compound 362 .	457
Figure A7.78	^{13}C NMR (75 MHz, CDCl_3) of compound 362 .	457
Figure A7.79	^1H NMR (300 MHz, C_6D_6) of compound 363 .	458
Figure A7.80	Infrared spectrum ($\text{NaCl}/\text{CH}_2\text{Cl}_2$) of compound 363 .	459
Figure A7.81	^{13}C NMR (75 MHz, C_6D_6) of compound 363 .	459
Figure A7.82	^1H NMR (500 MHz, C_6D_6) of compound 369 .	460
Figure A7.83	Infrared spectrum ($\text{NaCl}/\text{CHCl}_3$) of compound 369 .	461
Figure A7.84	^{13}C NMR (125 MHz, C_6D_6) of compound 369 .	461
Figure A7.85	^1H NMR (500 MHz, C_6D_6) of compound 356 .	462
Figure A7.86	Infrared spectrum ($\text{NaCl}/\text{CHCl}_3$) of compound 356 .	463
Figure A7.87	^{13}C NMR (125 MHz, C_6D_6) of compound 356 .	463
Figure A7.88	^1H NMR (500 MHz, C_6D_6) of compound 370 .	464
Figure A7.89	Infrared spectrum ($\text{NaCl}/\text{CHCl}_3$) of compound 370 .	465
Figure A7.90	^{13}C NMR (125 MHz, C_6D_6) of compound 370 .	465
Figure A7.91	^1H NMR (300 MHz, CDCl_3) of compound 373 .	466

Figure A7.92	Infrared spectrum (NaCl/CDCl ₃) of compound 373 .	467
Figure A7.93	¹³ C NMR (75 MHz, CDCl ₃) of compound 373 .	467
Figure A7.94	¹ H NMR (300 MHz, C ₆ D ₆) of compound 374 .	468
Figure A7.95	Infrared spectrum (NaCl/CHCl ₃) of compound 374 .	469
Figure A7.96	¹³ C NMR (75 MHz, C ₆ D ₆) of compound 374 .	469
Figure A7.97	¹ H NMR (300 MHz, CDCl ₃) of compound 375 .	470
Figure A7.98	Infrared spectrum (NaCl/CHCl ₃) of compound 375 .	471
Figure A7.99	¹³ C NMR (75 MHz, CDCl ₃) of compound 375 .	471
Figure A7.100	¹ H NMR (300 MHz, CDCl ₃) of compound 376 .	472
Figure A7.101	Infrared spectrum (NaCl/CHCl ₃) of compound 376 .	473
Figure A7.102	¹³ C NMR (75 MHz, CDCl ₃) of compound 376 .	473
Figure A7.103	¹ H NMR (300 MHz, CDCl ₃) of compound 377 .	474
Figure A7.104	Infrared spectrum (NaCl/CDCl ₃) of compound 377 .	475
Figure A7.105	¹³ C NMR (75 MHz, CDCl ₃) of compound 377 .	475
Figure A7.106	¹ H NMR (300 MHz, CDCl ₃) of compound 379 .	476
Figure A7.107	Infrared spectrum (NaCl/CDCl ₃) of compound 379 .	477
Figure A7.108	¹³ C NMR (75 MHz, CDCl ₃) of compound 379 .	477
Figure A7.109	¹ H NMR (300 MHz, CDCl ₃) of compound 380 .	478
Figure A7.110	Infrared spectrum (NaCl/CDCl ₃) of compound 380 .	479
Figure A7.111	¹³ C NMR (75 MHz, CDCl ₃) of compound 380 .	479
Figure A7.112	¹ H NMR (300 MHz, CDCl ₃) of compound 381 .	480
Figure A7.113	Infrared spectrum (NaCl/CDCl ₃) of compound 381 .	481
Figure A7.114	¹³ C NMR (75 MHz, CDCl ₃) of compound 381 .	481
Figure A7.115	¹ H NMR (300 MHz, CDCl ₃) of compound 382 .	482
Figure A7.116	Infrared spectrum (NaCl/CDCl ₃) of compound 382 .	483
Figure A7.117	¹³ C NMR (75 MHz, CDCl ₃) of compound 382 .	483
Figure A7.118	¹ H NMR (300 MHz, CDCl ₃) of compound 383 .	484
Figure A7.119	Infrared spectrum (NaCl/CDCl ₃) of compound 383 .	485
Figure A7.120	¹³ C NMR (125 MHz, CDCl ₃) of compound 383 .	485
Figure A7.121	¹ H NMR (300 MHz, CDCl ₃) of compound 385 .	486
Figure A7.122	Infrared spectrum (NaCl/CDCl ₃) of compound 385 .	487
Figure A7.123	¹³ C NMR (125 MHz, CDCl ₃) of compound 385 .	487
Figure A7.124	¹ H NMR (300 MHz, CDCl ₃) of compound 388 .	488
Figure A7.125	Infrared spectrum (NaCl/CDCl ₃) of compound 388 .	489
Figure A7.126	¹³ C NMR (125 MHz, CDCl ₃) of compound 388 .	489
Figure A7.127	¹ H NMR (300 MHz, CDCl ₃) of compound 389 .	490
Figure A7.128	Infrared spectrum (NaCl/CDCl ₃) of compound 389 .	491
Figure A7.129	¹³ C NMR (75 MHz, CDCl ₃) of compound 389 .	491
Figure A7.130	¹ H NMR (300 MHz, CDCl ₃) of compound 390 .	492
Figure A7.131	Infrared spectrum (NaCl/CDCl ₃) of compound 390 .	493
Figure A7.132	¹³ C NMR (75 MHz, CDCl ₃) of compound 390 .	493
Figure A7.133	¹ H NMR (300 MHz, CDCl ₃) of compound 391 .	494
Figure A7.134	Infrared spectrum (NaCl/CDCl ₃) of compound 391 .	495
Figure A7.135	¹³ C NMR (75 MHz, CDCl ₃) of compound 391 .	495
Figure A7.136	¹ H NMR (300 MHz, CDCl ₃) of compound 386 .	496
Figure A7.137	Infrared spectrum (NaCl/CDCl ₃) of compound 386 .	497

Figure A7.138	^{13}C NMR (75 MHz, CDCl_3) of compound 386 .	497
Figure A7.139	^1H NMR (500 MHz, CDCl_3) of compound 394 .	498
Figure A7.140	Infrared spectrum ($\text{NaCl}/\text{CDCl}_3$) of compound 394 .	499
Figure A7.141	^{13}C NMR (125 MHz, CDCl_3) of compound 394 .	499
Figure A7.142	^1H NMR (300 MHz, CDCl_3) of compound 395 .	500
Figure A7.143	^1H NMR (500 MHz, CDCl_3) of compound 396 .	501
Figure A7.144	Infrared spectrum ($\text{NaCl}/\text{CDCl}_3$) of compound 396 .	502
Figure A7.145	^{13}C NMR (125 MHz, CDCl_3) of compound 396 .	502

List of Schemes

Chapter One: Enantioselective Alkylations Generating All-Carbon Quaternary Stereocenters Within Rings	1
Scheme 1.1 Koga's Alkylation of Cycloalkene Carbaldehydes	2
Scheme 1.2 Meyers' Valinol Auxilliary Method and Synthesis of Cuparenone	3
Scheme 1.3 RAMP and SAMP Technology	4
Scheme 1.4 Phase Transfer Catalysis for Stereoselective Alkylation	5
Scheme 1.5 Shibasaki's Direct Michael Reaction	6
Scheme 1.6 Hayashi's Enantioselective Alkylation of β -dicarbonyls	8
Scheme 1.7 Trost Ligands for Asymmetric Pd-Catalyzed Alkylation	9
Scheme 1.8 Other Substrate Classes Investigated by Trost	10
Scheme 1.9 Three Example of Enantioselective Decarboxylative Alkylation	12
Scheme 1.10 Trost's Enantioselective Decarboxylative Alkylations	14
Scheme 1.11 Blechert's Ring Expansion/Enolate Alkylation Cascade	15
<hr/>	
Chapter Two: Enantioselective Formal Total Syntheses of Natural Products Using Palladium-Catalyzed Decarboxylative Alkylation	21
Scheme 2.1 Srikrishna and Anebouselvy's Approach to (-)-Thujopsene	23
Scheme 2.2 Retrosynthetic Analysis of (-)-Thujopsene	24
Scheme 2.3 Preparation of Diastereomeric Alcohols	25
Scheme 2.4 Completion of the Carboxylic Acid	26
Scheme 2.5 Danishefsky's Approach to (\pm)-Dysidiolide	28
Scheme 2.6 Retrosynthetic Analysis of the Keto-Olefin	28
Scheme 2.7 Formal Synthesis of (-)-Dysidiolide	29
Scheme 2.8 Meyers' Approach to Unnatural (+)-Aspidospermine	31
Scheme 2.9 Retrosynthetic Analysis of the γ -Allyl Enone	32
Scheme 2.10 Two Decarboxylative Alkylation Methods Tested	33
Scheme 2.11 A Possible Formal Synthesis of Goniomitine	34
Scheme 2.12 Danishefsky's Intermediates in the Jiadifenin Synthesis	35
Scheme 2.13 Other Natural Products Targeted for Formal Synthesis	36
<hr/>	
Appendix One: Synthetic Summaries of the Formal Total Syntheses of (-)-Thujopsene, (-)-Dysidiolide, and (-)-Aspidospermine	63
Scheme A1.1 Formal Total Synthesis of Thujopsene	64
Scheme A1.2 Formal Total Synthesis of Dysidiolide	65
Scheme A1.3 Formal Total Synthesis of Aspidospermine	66

Chapter Three: The Catalytic-Enantioselective, Protecting Group-Free Total Synthesis of (+)-Dichroanone	98
Scheme 3.1 Banerjee's Retrosynthetic Analysis	101
Scheme 3.2 Preparation of the Aromatic Coupling Partner	102
Scheme 3.3 Union of the Coupling Partners	103
Scheme 3.4 Installation of the Isopropyl Moiety	103
Scheme 3.5 Completion of (±)-Dichroanal B	104
Scheme 3.6 Total Synthesis of (±)-Dichroanone (150)	105
Scheme 3.7 Retrosynthesis of Taiwaniquinol B	105
Scheme 3.8 Beginning of the Synthesis	106
Scheme 3.9 Fillion's Total Synthesis of (±)-Taiwaniquinol B	107
Scheme 3.10 Node's Retrosynthetic Analysis	107
Scheme 3.11 Total Synthesis of Racemic Dichroanal B	108
Scheme 3.12 Trauner's Retrosynthetic Analysis	109
Scheme 3.13 Completion of Racemic Taiwaniquinol B	110
Scheme 3.14 Application of the Nazarov Triflation	111
Scheme 3.15 Total Synthesis of Racemic Taiwaniquinol D	112
Scheme 3.16 First Retrosynthetic Analysis of Dichroanone	114
Scheme 3.17 Synthesis of 2,2,6-trimethylcyclohexanone	115
Scheme 3.18 Completion of the Bicyclic Enone	116
Scheme 3.19 Fallis' Benzannulation	118
Scheme 3.20 Attempted Electrocyclization	119
Scheme 3.21 Robinson Annulation Approach	120
Scheme 3.22 Installing an Extra Oxygen Atom	121
Scheme 3.23 Synthesis of a Dichroanone Isomer	122
Scheme 3.24 Second Retrosynthetic Analysis of Dichroanone	124
Scheme 3.25 Substrate and Catalyst Control in a Diastereoselective Alkylation	125
Scheme 3.26 Preparation of the Bicyclic Enone	126
Scheme 3.27 Enantioenrichment of the Bicyclic Enone	127
Scheme 3.28 Proposed Routes to the Aryl Triflate	128
Scheme 3.29 Kumada Coupling Strategy	129
Scheme 3.30 Synthesis of the Two Aldehydes	130
Scheme 3.31 Instability of a Key Phenol	131
Scheme 3.32 Studies with the Methyl Ether	132
Scheme 3.33 Preparation of the <i>o</i> -Quinone	133
Scheme 3.34 Nucleophilic Additions of Thiophenol	134
Scheme 3.35 The Switch to Pentafluorothiophenol	135
Scheme 3.36 Total Synthesis of (+)-Dichroanone	136
Scheme 3.37 One-Step Synthesis of Dichroanone from the Phenol	137
Scheme 3.38 Preparation of a Taiwaniquinone H Isomer.	138
Scheme 3.39 A Potential Route to Taiwaniquinol B or E	139

Appendix Three: Synthetic Summary of the Enantioselective Total Synthesis of (+)-Dichroanone	198
Scheme A3.1 Enantioselective Total Synthesis of (+)-Dichroanone	199
<hr/>	
Chapter Four: Progress Toward the Catalytic Enantioselective Total Synthesis of Liphagal	282
Scheme 4.1 Possible Biosynthesis of Liphagal from Siphonodictyal	285
Scheme 4.2 Alternative Cationic Cyclization Proposal	286
Scheme 4.3 Andersen's Retrosynthesis of Liphagal	287
Scheme 4.4 Synthesis of the Aromatic Piece	287
Scheme 4.5 Preparation of the Carboxylic Acid Coupling Partner	288
Scheme 4.6 Completion of the Natural Product	289
Scheme 4.7 First Retrosynthetic Analysis of Liphagal	291
Scheme 4.8 Preparation of the Bicyclic Enone	292
Scheme 4.9 Angularly-Fused Cyclobutanes	293
Scheme 4.10 Photoadducts from the Acetylene [2 + 2]	294
Scheme 4.11 Mechanism of the Oxa-Di- π -Methane Rearrangement	295
Scheme 4.12 Reversion of the Bicyclobutane to the Cyclobutene	296
Scheme 4.13 Ring Opening of the Cyclobutene	296
Scheme 4.14 Functionalization of the [6-7] Ring System	297
Scheme 4.15 Aryloxime Cyclization Reaction	298
Scheme 4.16 Failed Attempts to Prepare a Benzofuran Using an <i>O</i> -Aryloxime	299
Scheme 4.17 Benzoquinone Mukaiyama Michael Model System	300
Scheme 4.18 Synthesis of a More Substituted Quinone	301
Scheme 4.19 A Complex Quinone Model System	302
Scheme 4.20 Attempted Mukaiyama Michael Reaction	303
Scheme 4.21 Arylation/CuI Cyclization Strategy	304
Scheme 4.22 Synthesis of a Complex Aryl Halide	305
Scheme 4.23 Attempted Arylation of the [6-7] System	306
Scheme 4.24 Second Retrosynthesis of Liphagal	307
Scheme 4.25 Attempted Dienone Arylation	308
Scheme 4.26 Vinylogous Substrates	309
Scheme 4.27 Quaternized Substrates	310
Scheme 4.28 A New Retrosynthesis	311
Scheme 4.29 Photochemistry of the Aryl Enone	312
Scheme 4.30 Arylation of the Cyclobutene	313
Scheme 4.31 Side Product Formation During the Electrocyclic Opening	314
Scheme 4.32 Mechanism of the Cargill Rearrangement	315
Scheme 4.33 Observation of Friedel-Crafts Chemistry	316
Scheme 4.34 The Chemistry of the Aryl Dienone	317
Scheme 4.35 Bromination Solution for Ring Expansion	318
Scheme 4.36 Early Reduction Methods	319
Scheme 4.37 Methylation and Epimerization Studies	320

Scheme 4.38 Failed Attempts to Prepare the Benzofuran	322
Scheme 4.39 Making the Necessary C–O Bond	323
Scheme 4.40 Careful Oxidation to the Benzofuran	323
Scheme 4.41 Further Functionalizations	325
Scheme 4.42 Proposed Total Synthesis of Liphagal	326

Appendix Six: Synthetic Summary of Efforts Toward the Total Synthesis of Liphagal	402
---	-----

Scheme A6.1 Toward the Enantioselective Total Synthesis of Liphagal: Part 1	403
Scheme A6.2 Toward the Enantioselective Total Synthesis of Liphagal: Part 2	404

List of Tables

Chapter One: Enantioselective Alkylations Generating All-Carbon Quaternary Stereocenters Within Rings	1
Table 1.1 Enantioselective Alkylation of Tributyl Tin Enolates	7
Table 1.2 Enantioselective Cinnamylation of β -Diketones	11
Table 1.3 Substrate Scope of the Enantioselective Decarboxylative Alkylation	13
<hr/>	
Appendix Nine: Compounds Submitted for PI3K Biological Screening	529
Table A9.1 Compounds Submitted for PI3K Biological Screening: Part 1	530
Table A9.1 Compounds Submitted for PI3K Biological Screening: Part 2	531
Table A9.1 Compounds Submitted for PI3K Biological Screening: Part 3	532
Table A9.1 Compounds Submitted for PI3K Biological Screening: Part 4	533
Table A9.1 Compounds Submitted for PI3K Biological Screening: Part 5	534
Table A9.1 Compounds Submitted for PI3K Biological Screening: Part 6	535
Table A9.1 Compounds Submitted for PI3K Biological Screening: Part 7	536
<hr/>	
Appendix Ten: Cross References to Characterization Binders and Notebooks	537
Table A10.1 Cross References for Compounds from Chapter 2: Thujopsene	538
Table A10.2 Cross References for Compounds from Chapter 2: Dysidiolide	539
Table A10.3 Cross References for Compounds from Chapter 2: Aspidospermine	540
Table A10.4 Cross References for Compounds from Chapter 3: Dichroanone: Part 1	541
Table A10.5 Cross References for Compounds from Chapter 3: Dichroanone: Part 2	542
Table A10.6 Cross References for Compounds from Chapter 3: Dichroanone: Part 3	543
Table A10.7 Cross References for Compounds from Chapter 3: Dichroanone: Part 4	544
Table A10.8 Cross References for Compounds from Chapter 3: Dichroanone: Part 5	545
Table A10.9 Cross References for Compounds from Chapter 3: Dichroanone: Part 6	546
Table A10.10 Cross References for Compounds from Chapter 3: Dichroanone: Part 7	547

Table A10.11 Cross References for Compounds from Chapter 4: Liphagal: Part 1	548
Table A10.12 Cross References for Compounds from Chapter 4: Liphagal: Part 2	549
Table A10.13 Cross References for Compounds from Chapter 4: Liphagal: Part 3	550
Table A10.14 Cross References for Compounds from Chapter 4: Liphagal: Part 4	551
Table A10.15 Cross References for Compounds from Chapter 4: Liphagal: Part 5	552
Table A10.16 Cross References for Compounds from Chapter 4: Liphagal: Part 6	553
Table A10.17 Cross References for Compounds from Chapter 4: Liphagal: Part 7	554
Table A10.18 Cross References for Compounds from Chapter 4: Liphagal: Part 8	555
Table A10.19 Cross References for Compounds from Chapter 4: Liphagal: Part 9	556
Table A10.20 Cross References for Compounds from Chapter 4: Liphagal: Part 10	557
Table A10.21 Cross References for Compounds from Chapter 4: Liphagal: Part 11	558

List of Abbreviations

2,6-DTBP	2,6-di- <i>tert</i> -butyl pyridine
2D-TLC	2-dimentional thin-layer chromatography
$[\alpha]^{xx}_D$	specific rotation at xx °C at the sodium D line wavelength
Å	angstrohm
Ac	acetyl
Am	amyl
app.	apparent
aq	aqueous
Ar	aryl substiuent
atm	atmosphere(s)
BINOL	1,1'-bi-(2-naphthol)
BINAP	2,2'-bis(diphenylphosphino)-1,1'-binaphthyl
Bn	benzyl
bp	boiling point
Bu	butyl
<i>i</i> -Bu	<i>iso</i> -butyl
<i>n</i> -Bu	<i>normal</i> -butyl
<i>s</i> -Bu	<i>secondary</i> -butyl
<i>t</i> -Bu	<i>tertiary</i> -butyl
<i>tert</i> -Bu	<i>tertiary</i> -butyl
^{13}C	carbon 13 isotope
c	centi

<i>c</i>	<i>cyclo</i> or concentration (value in g/dL, for optical rotation)
calc'd	calculated
CAN	ceric ammonium nitrate
CCDC	Cambridge Crystallographic Data Centre
conc.	concentrated
<i>m</i> -CPBA	<i>meta</i> -chloroperbenzoic acid
δ	chemical shift of (value in parts per million)
d	doublet or day(s)
D	deuterium
DABCO	1,4-diazabicyclo[2.2.2]octane
dba	dibenzylideneacetone
DCC	dicyclohexyl carbodiimide
DDQ	2,3-dichloro-5,6-dicyano-1,4-benzoquinone
DIBAL	di- <i>iso</i> -butyl alane
dmdba	di-(3',5'-dimethoxybenzylidene)-acetone
DMA	<i>N,N'</i> -dimethyl acetamide
DMAP	4-(<i>N,N'</i> -dimethylamino)-pyridine
DME	1,2-dimethoxyethane
DMF	<i>N,N'</i> -dimethyl formamide
DMP	Dess-Martin periodinane
DMS	dimethylsulfide
DMSO	dimethylsulfoxide
Dod	dodecyl

dppp	1,3-diphenylphosphinopropane
dr	diastereomeric ratio
ϵ	extinction coefficient
equiv	equivalents
<i>E</i>	engegen olefin geometry
ee	enantiomeric excess
EI	electron impact (method)
ESI	electrospray ionization (method)
Et	ethyl
^{19}F	fluorine 19 isotope
FAB	fast atom bombardment (method)
g	gram
GC	gas chromatography
gCOSY	gradient correlation spectroscopy
Grubbs II	the Grubbs second-generation metathesis catalyst
η^n	hapto, n = number of atoms coordinated to the metal
h	hour(s)
[H]	conceptual reduction
^1H	hydrogen 1 isotope
<i>c</i> -hexane	cyclohexane
<i>n</i> -Hex	<i>normal</i> -hexyl
HPLC	high performance liquid chromatography
HRMS	high-resolution mass spectrometry

Hz	hertz (s^{-1})
<i>i</i>	<i>iso</i>
IBX	1-hydroxy-1-oxo-1(λ^5),2-benz[d]-iodoxol-3-one
IC ₅₀	concentration required for 50% growth inhibition
IR	infrared (spectroscopy)
<i>J</i>	coupling constant (in Hz)
<i>J</i> _x	coupling constant with x-type of splitting
KHMDS	potassium bis(trimethylsilyl)-amide
λ_{max}	wavelength at a local maximum of absorption
LA	Lewis acid
LAH	lithium tetrahydridoaluminate
LCMS	tandem liquid chromatography / mass spectrometry
LDA	lithium diisopropyl amide
LiHMDS	lithium bis(trimethylsilyl)-amide
LRMS	low-resolution mass spectrometry
LSB	lanthanum sodium binol catalyst
μ	micro
m	multiplet, milli, or meter
<i>m</i>	<i>meta</i>
M	mega, metal, or molar (mol / L)
Me	methyl
min	minute(s)
mol	mole(s)

mp	melting point
Ms	methanesulfonyl
MS	molecular sieves
MVK	methyl vinyl ketone
n	nano
<i>n</i>	<i>normal</i>
NBS	<i>N</i> -bromosuccinimide
NaHMDS	sodium bis(trimethylsilyl)-amide
NMR	nuclear magnetic resonance (spectroscopy)
nOe	nuclear Overhauser effect
nOesy-1D	1-dimensional nuclear Overhauser effect difference spectroscopy
[O]	conceptual oxidation
<i>o</i>	<i>ortho</i>
<i>p</i>	<i>para</i>
PCC	pyridinium chlorochromate
Pd / C	Pd ⁰ supported on activated carbon
PMHS	poly(methyl hydrosiloxane), trimethylsilyl terminated
PFPSH	pentafluorothiophenol
Ph	phenyl
PHOX	2-(triphenylphosphino-2'-yl)-oxazoline-derived ligand
PI3K	phosphatidylinositol-3-kinase
PI3K α	α isoform of phosphatidylinositol-3-kinase
ppm	parts per million

PPTS	pyridinium <i>para</i> -toluene sulfonate
Pr	propyl
<i>i</i> -Pr	<i>iso</i> -propyl
Pyr	pyridine
q	quartet
R	substituent group
R _f	retention factor
<i>R</i>	rectus chiral configuration
RAMP	(<i>R</i>)-1-amino-2-(methoxymethyl)pyrrolidine
REDAL	sodium bis(2-methoxyethoxo)-dihydridoaluminate
ref.	Reference
rel.	relative
s	singlet
<i>S</i>	sinister chiral configuration
<i>s</i>	<i>secondary</i>
SAMP	(<i>S</i>)-1-amino-2-(methoxymethyl)pyrrolidine
salen	<i>N,N'</i> -bis(salicylidene)-1,2-diaminoethane-derived ligand
sat.	saturated
sp	sublimation point
TBAT	tetra- <i>n</i> -butylammoniumdifluorotriphenylsilicate
TBDPS	<i>tert</i> -butyl diphenyl silyl
Tf	trifluoromethanesulfonyl
THF	tetrahydrofuran

TLC	thin-layer chromatography
TMEDA	<i>N,N,N',N'</i> -tetramethyl 1,2-diaminoethane
TMS	trimethylsilyl
TES	triethylsilyl
TBS	<i>tert</i> -butyl dimethylsilyl
TMG	tetramethyl guanidine
Ts	<i>para</i> -toluenesulfonyl
t	triplet
<i>t</i>	<i>tertiary</i>
<i>tert</i>	<i>tertiary</i>
UV	ultraviolet
Vis	visible
w/w	weight per weight
yr	year(s)
<i>Z</i>	zusammen olefin geometry

CHAPTER ONE

Enantioselective Alkylations Generating All-Carbon Quaternary Stereocenters Within Rings

1.1 Background

The catalytic enantioselective preparation of all-carbon quaternary stereocenters has proven challenging for the synthetic chemist.¹ Many elegant methods have been demonstrated, including Diels-Alder reactions,² cyclopropanations,³ desymmetrizations,⁴ Heck reactions,⁵ acylations,⁶ electrocyclizations,⁷ arylations,⁸ and transformations catalyzed by organic molecules.⁹ Another significant approach is the alkylation of prochiral enolates to generate all-carbon quaternary stereocenters.^{10,11} Of particular interest are those alkylative methods where the newly formed stereocenter is within a ring because this motif is found in numerous natural products and biologically important pharmaceuticals.

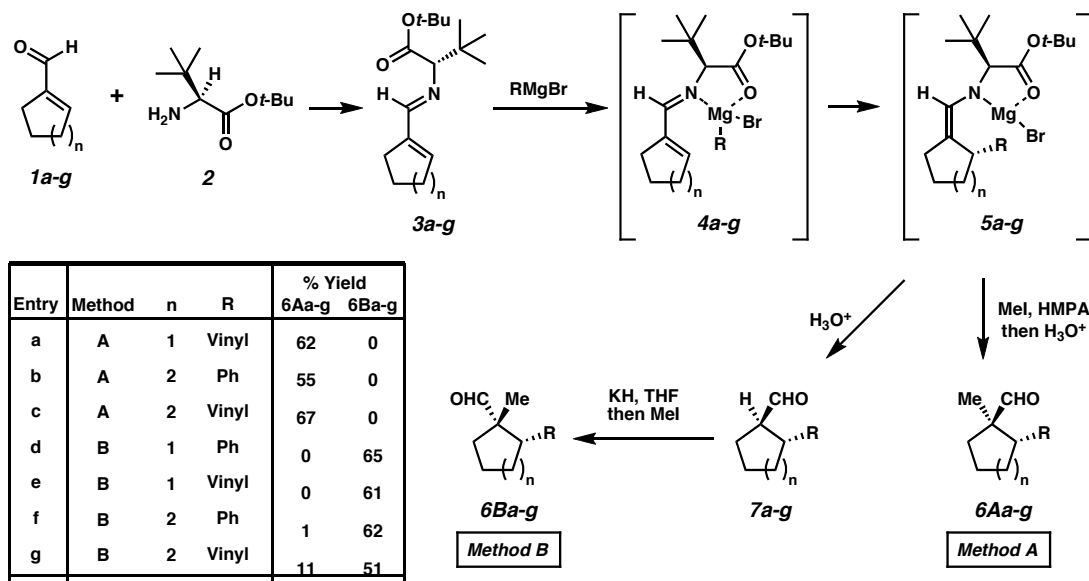
1.2 Auxilliary-Based Methods for Alkylation

1.2.1 Koga's *t*-Butyl Glycine Esters

Koga demonstrated one of the first auxiliary-based methods for setting all-carbon quaternary stereocenters within rings via alkylation.¹² Cycloalkene carbaldehydes (e.g., **1a-g**) were condensed with a *t*-butyl glycine ester (**2**) (Scheme 1.1). Diastereoselective conjugate addition of a Grignard reagent to **3a-g** generated metalloenamines **5a-g**, which were alkylated with iodomethane and hydrolyzed furnishing **6Aa-g**. Alternatively, the auxiliary could be removed after the 1,4-Grignard addition and the resulting aldehydes **7a-g** alkylated with iodomethane, giving diastereomers **6Ba-g**. Both alkylation processes

were highly diastereoselective, and the α -quaternary aldehydes could be accessed in high ee. The auxiliary could also be recycled after completion of the sequences.

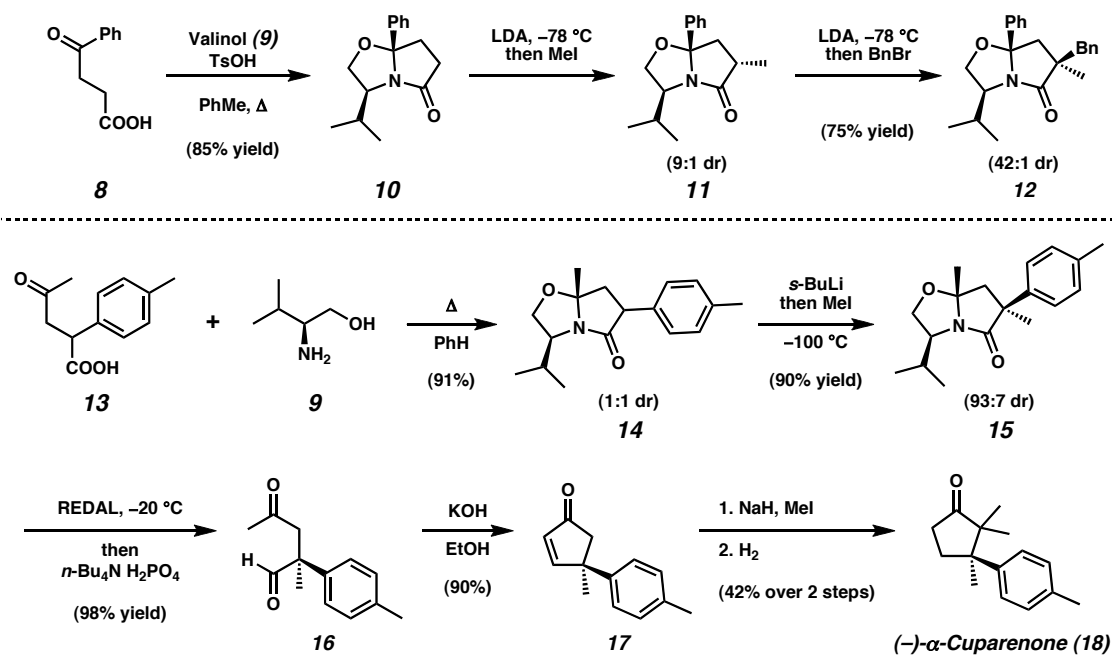
Scheme 1.1 Koga's Alkylation of Cycloalkene Carbaldehydes



1.2.2 Meyers' Valinol Auxilliary

Meyers condensed various γ -keto acids (e.g., **8**) with valinol (**9**) to prepare chiral bicyclic lactams (e.g., **10**, Scheme 1.2).¹³ A series of two alkylations were performed, leading to α -quaternary lactams (e.g., **12**) with high diastereoselectivity. Although the first alkylation usually occurred with 9:1 dr or greater, enantioenriched monoalkylated product was usually not obtained presumably due to epimerization during lactam hydrolysis. However, quaternary dialkylated compounds such as **12** were not epimerizable. Hence, the auxiliary could be cleaved under a variety of conditions and the linear product elaborated to a variety of enantioenriched all-carbon quaternary compounds.

Scheme 1.2 Meyers' Valinol Auxilliary Method and Synthesis of Cuparenone



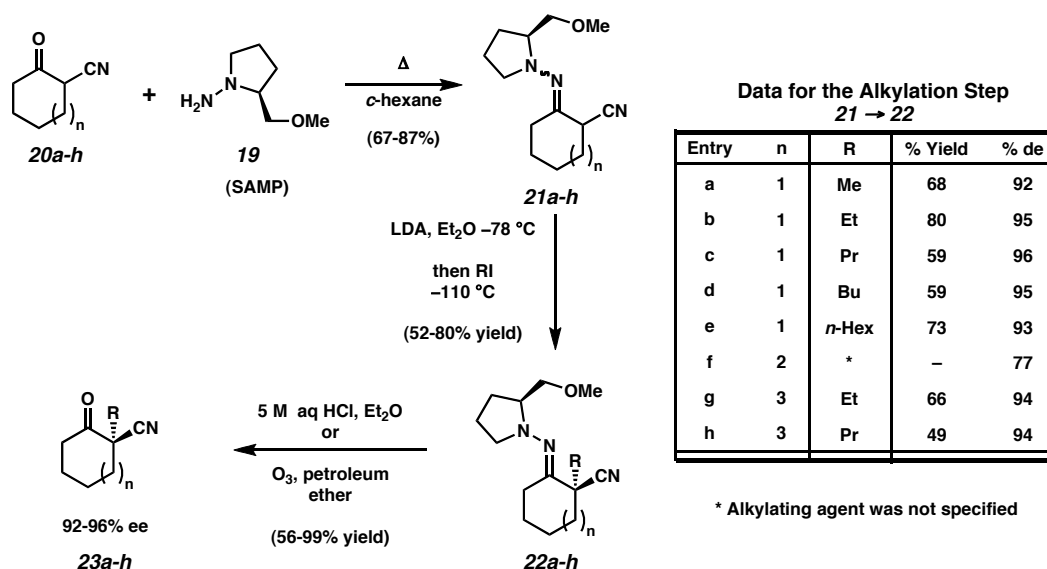
Treatment of pure, crystalline dialkylated lactam **15** with REDAL led to γ -keto aldehyde **16** in 91% yield (Scheme 1.2). Cyclization of **16** under aldol condensation conditions furnished cyclopentenone **17**, which was then alkylated twice with iodomethane. The product was reduced, providing **(-)-α-cuparenone (18)** in 98% ee.¹⁴ This amino alcohol methodology was also used toward the syntheses of other natural products including **(+)-mesembrine**,¹⁵ **(-)-grandisol**,¹⁶ and **(+)-aspidospermine**.¹⁷

1.2.3 Enders' RAMP and SAMP Hydrazone Auxilliary

Enders demonstrated that cyclic ketones themselves could be used as the prochiral enolate precursor. By condensing chiral hydrazine auxiliaries such as *(R)*-1-amino-2-(methoxymethyl)pyrrolidine (RAMP) or *(S)*-1-amino-2-(methoxymethyl)pyrrolidine (SAMP) (**19**) onto β -cyanoketones (e.g., **20a-h**), hydrazones **21a-h** were generated

(Scheme 1.3).¹⁸ Metalloenamine formation was achieved by treating the hydrazones with LDA. Diastereoselective alkylation at low temperature furnished alpha quaternary hydrazones **22a-h** that were readily cleaved (either via acidic hydrolysis or ozonolysis) to afford enantioenriched ketones **23a-h**. This diastereoselective alkylation chemistry is amenable to the preparation of enantioenriched cyclohexanones and cyclooctanones, but 7-membered ring substrates suffer from lower levels of enantioselectivity. Brunner, Kraus, and Lautenschlager described a conceptually similar diastereoselective Michael reaction mediated by an α -methylbenzylamine auxiliary.¹¹

Scheme 1.3 RAMP and SAMP Technology



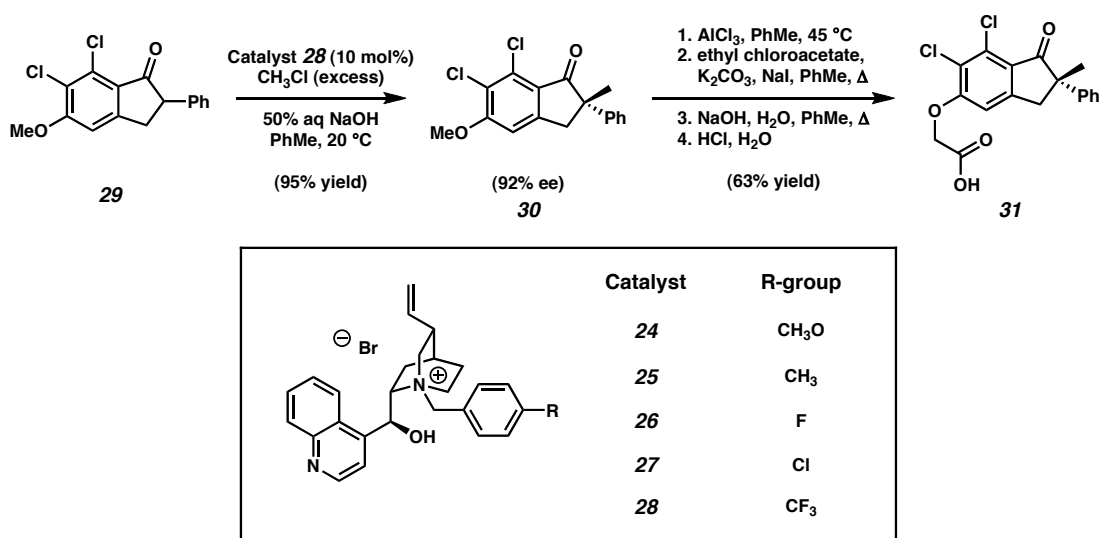
1.3 Catalytic Alkylations for Generating Quaternary Stereocenters without Pd

1.3.1 Chiral Phase Transfer Catalysis

Catalytic methods for generating all-carbon quaternary stereocenters via alkylation were an attractive alternative to the use of auxiliaries. One of the first

examples employed a chiral phase transfer catalyst, **28**, derived from a cinchona alkaloid (Scheme 1.4).¹⁹ When a biphasic solution of indanone **29** was treated with chloromethane and catalytic **28**, aryl methyl ketone **30** was obtained in 95% yield and 92% ee. This molecule was later advanced to the uricosuric (+)-indacrinone (MK-0197) **31** via a sequence of demethylation and phenolic oxygen alkylation.

Scheme 1.4 Phase Transfer Catalysis for Stereoselective Alkylation

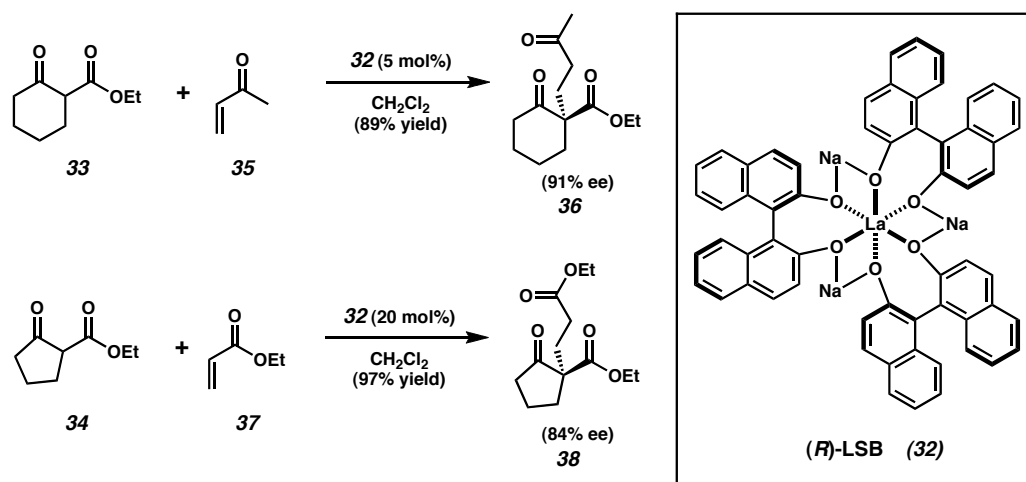


Ion pairing was invoked as the key enantiodetermining interaction. When more polar solvents such as CH₂Cl₂ were substituted for toluene, a drop in enantioselectivity was observed. When substituents R on the catalyst became more electron-withdrawing, a corresponding elevation in ee was observed. A Hammett plot of log (ee/ee₀) versus the σ values for these R-groups gave $\rho = 0.21 \pm 0.02$. A counterion effect of the alkylator was also found. If iodomethane was used instead of chloromethane, there was a decrease in product ee.

1.3.2 Shibasaki's Lanthanide Sodium Binol Catalyzed Enantioselective Michael Reaction

Shibasaki demonstrated a catalytic enantioselective direct Michael reaction of β -ketoesters with α,β -unsaturated carbonyls. Using a chiral complex **32** derived from lanthanum and BINOL, highly enantioselective formation of α -quaternary compounds was possible (Scheme 1.5).²⁰ A few of the reported examples of the direct Michael addition employed cyclic β -ketoesters such as **33** and **34**. Notably, both 5 and 6-membered ring sizes were tolerated. A variety of Michael acceptors including methyl vinyl ketone (**35**) and ethyl acrylate were amenable to the chemistry.

Scheme 1.5 Shibasaki's Direct Michael Reaction



1.3.3 Jacobsen's Chromium Salen Catalyzed Alkylation

Jacobsen recently reported a catalytic preparation of enantioenriched, α -quaternary cycloalkanones.²¹ Readily distilled tri-*n*-butyltin enolates (e.g., **39a-f**) underwent alkylation in the presence of a chromium salen catalyst (*R*- or *S*-**40**) when treated with activated alkyl iodides and bromides (Table 1.1). A large range of

electrophiles displayed compatibility with the catalyst system, giving rise to a variety of products. 5, 6, and 7-membered ring substrates perform very well in this system, providing a range of cyclic ketones in excellent yield and high ee. The mode of catalyst action is uncertain, but investigations are ongoing.

Table 1.1 Enantioselective Alkylation of Tributyl Tin Enolates

(*R,R*)-Salen CrCl (*R*-40, A)

(*S,S*)-Salen CrCl (*S*-40, B)

Entry	R ² X	Catalyst	Product	%Yield	%ee
a		A		84	94
b		B		81	96
c		A		67	95
d		B		80	85
e		B		43	90
f		A		58	92

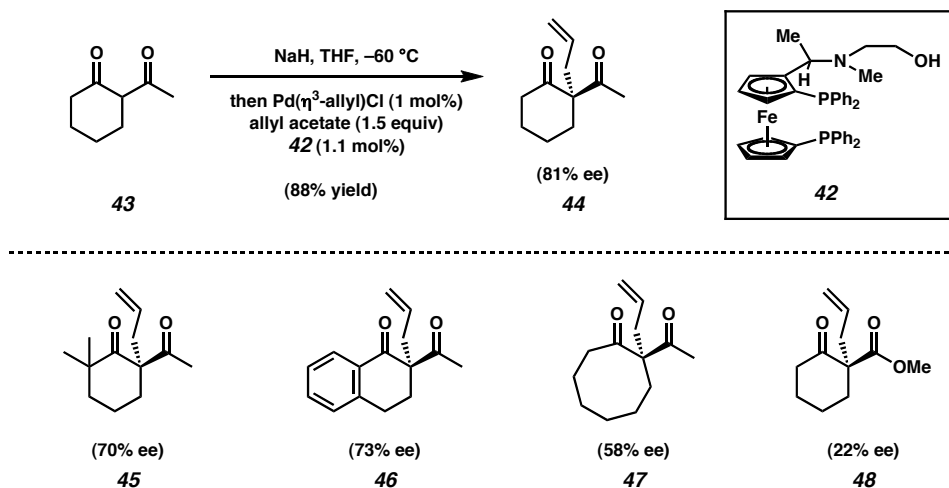
1.4 Palladium Catalysis for Enantioselective Alkylation of Prochiral Enolates

1.4.1 Hayashi's Allyl Palladium Catalysis

The attack of prochiral enolates upon η^3 -allyl palladium (II) complexes was also recognized as a powerful method for generating all-carbon quaternary stereocenters.

Hayashi pioneered this type of reaction during an exploration of Pd-catalyzed alkylation of β -dicarbonyls (Scheme 1.6).²² Investigations revealed ferrocenyl catalyst **42** as a superior ligand for the transformation of **43** to **44**. Diverse substrates were screened, and most displayed only limited stereoselectivity. Ultimately, allyl diketone **44** was prepared in a maximum 81% ee. Other activated carbonyl compounds including but not limited to **45**, **46**, **47**, and **48** were also accessible, with modest degrees of enantioselectivity. Optical activity was observed for 7-membered ring substrates, but 5-membered ring examples displayed very low stereoselectivity. Inspired by Hayashi's work, Ito also investigated these enantioselective alkylations using a crown-ether-modified phosphinoferrocenes with modest success.²³

Scheme 1.6 Hayashi's Enantioselective Alkylation of β -dicarbonyls

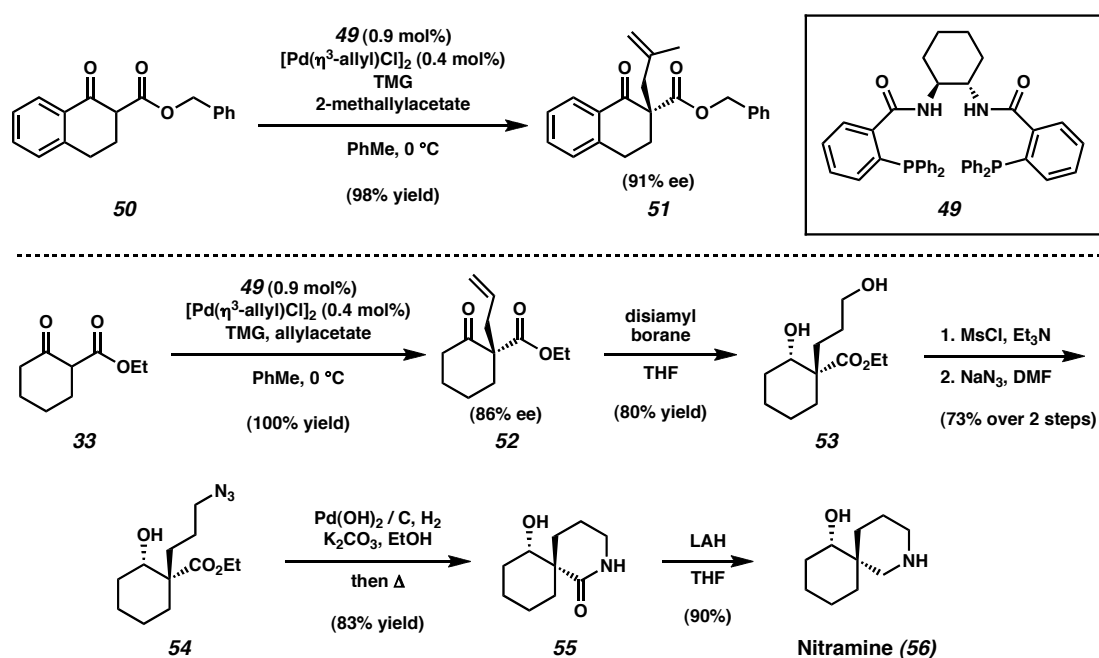


1.4.2 Early Work by Trost Surrounding Pd-Catalyzed Alkylation

In an effort to improve the yield, scope, and enantioselectivity of ketone alkylations catalyzed by palladium, Trost developed new ligands (e.g., **49**) designed to

project stereochemical information closer to the site of C–C bond formation (Scheme 1.7).²⁴ Substrates with a single acidic site could be alkylated in high yield with excellent enantioselectivity. Tetramethyl guanidine (TMG) was more effective than other bases for direct deprotonation. Trost applied this method during a short total synthesis of the alkaloid nitramine (**56**).^{24a}

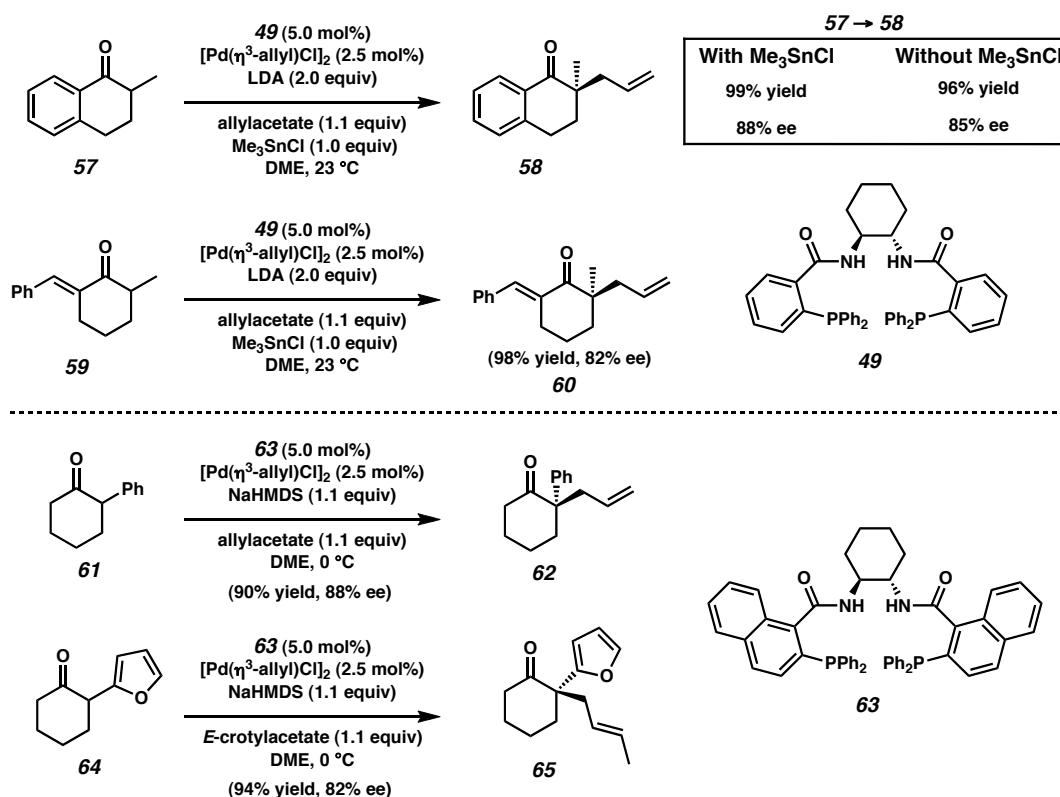
Scheme 1.7 Trost Ligands for Asymmetric Pd-Catalyzed Alkylation



Trost later developed other asymmetric catalyses, allowing the enantioselective alkylation of less acidic substrates. His next system used LDA as a base (Scheme 1.8).^{24b} Occasionally, addition of Me₃SnCl to the reaction mixture gave an elevation in ee, although good enantioselectivity could be achieved with LDA alone. Tetralones were ideal substrates for this chemistry because of their single-site acidity. However, alkylidene blocking groups could be installed to prevent enolization at unwanted sites in

non-tetralone examples (e.g. **59**), giving access to α -quaternary cycloalkanones in high ee. Hou and Dai later reported another Pd-catalyzed asymmetric alkylation using ferrocenylphosphines similar to the ones reported by Trost.²⁵

Scheme 1.8 Other Substrate Classes Investigated by Trost



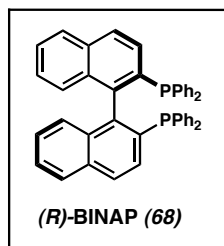
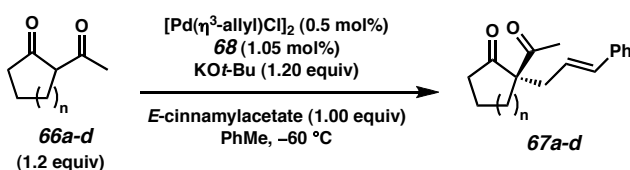
Trost developed another Pd-catalyzed alkylation employing NaHMDS as the base, and α -arylcyclohexanone substrates were investigated (Scheme 1.8). Once again, single-site acidity inherent in the substrate aided regioselective C–C bond formation. 2-Furyl cyclohexanone **64** could be crotylated to give a single olefin isomer of **65** with high yield and stereoselectivity.^{24c} Trost's Pd-catalyst manifold was one of the first systems

able to install branched and cyclic allyl fragments at the carbonyl α position with high enantioselectivity.

1.4.3 Ito's BINAP-Pd Catalyst

Another catalyst system recently described by Ito was capable of building quaternary stereocenters with branched allyl substituents.²⁶ (*R*)-BINAP (**68**) was used in conjunction with a Pd source. Using *E*-cinnamylacetate, Ito prepared a variety of α -quaternary- β -dicarbonyls (Table 1.2). A great variety of ring sizes were compatible with the chemistry, and enantioselectivities were uniformly in the 70-85% range.

Table 1.2 Enantioselective Cinnamylation of β -Diketones



Entry	n	%yield	%ee
a	1	92	81
b	2	99	85
c	3	95	77
d	4	90	84

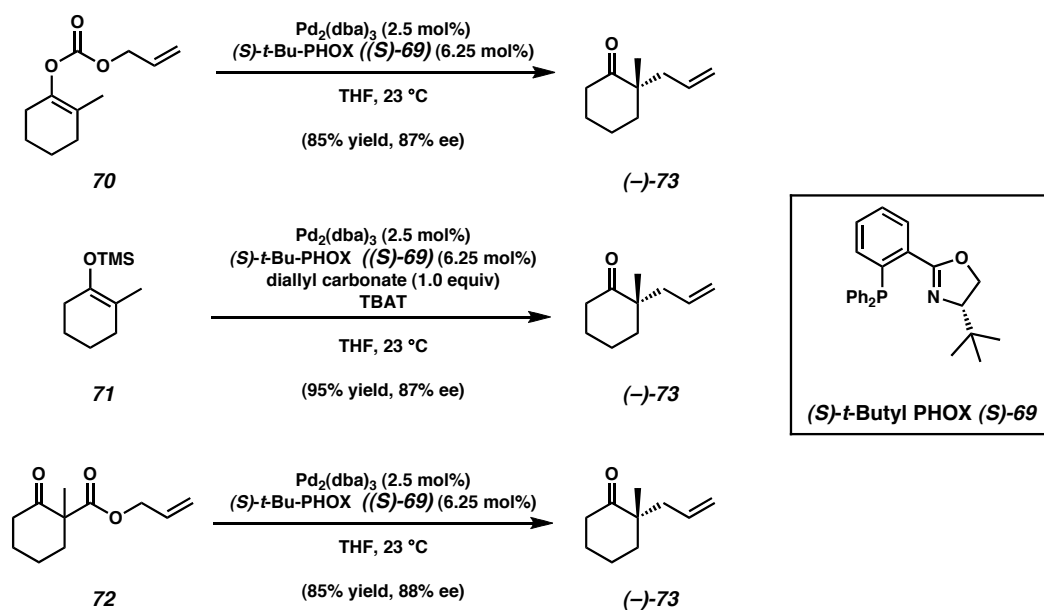
yield base on *E*-cinnamylacetate

1.4.4 Enantioselective Pd-Catalyzed Decarboxylative Alkylation

We became interested in the challenge of designing a catalyst system capable of generating all-carbon quaternary stereocenters from cyclic ketones with multiple acidic sites. Three palladium-catalyzed enantioselective decarboxylative alkylations²⁷ were

developed based on analogous racemic systems reported by Tsuji and Saegusa in the 1980's (Scheme 1.9).²⁸ Chiral *t*-butyl-phosphinooxazolines (e.g., (*S*)-*t*-Bu-PHOX ((*S*)-**69**)) are used in each of the catalyst manifolds, and the electronic and steric features of the ligand are readily modified to enhance reactivity and enantioselectivity.²⁹

Scheme 1.9 Three Example of Enantioselective Decarboxylative Alkylation

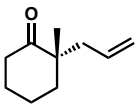
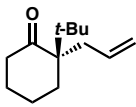
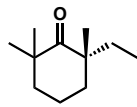
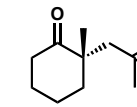
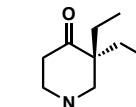
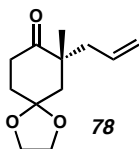
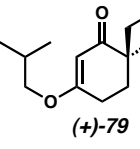
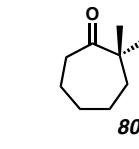
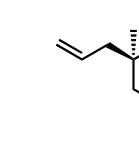


The first method employs allyl enol carbonates such as **70**, wherein the prochiral enolate and allyl fragment are part of the same starting material (Scheme 1.9).³⁰ A second variation of this catalysis utilizes silyl enol ethers (e.g., **71**) and diallyl carbonate, an external allyl source. The fluoride promoter tetra-*n*-butyl ammonium difluorotriphenylsilicate (TBAT) facilitates desilylation and generation of the prochiral enolate for alkylation.³⁰ The third asymmetric alkylation involves a stereoablative enantioselective transformation³¹ of racemic β -ketoesters. Deallylation of substrate **72**

followed by decarboxylation leads to a prochiral enolate, which is enantioselectively alkylated to generate allyl ketone **(-)-73**.³²

Many substrate classes were investigated (Table 1.3).^{30,32} The substrate can harbor considerable steric congestion near the site of C–C bond formation as evidenced by *t*-butyl ketone product **74**. Steric bulk at other positions is also tolerated (e.g., **(-)-75**). It is also possible to bring in substituents at the 2-position of the allyl fragment (**76**), and heteroatoms can also be part of the substrate (e.g., **77** and **78**). Vinylogous ester substrates (e.g., **79**) and 7-membered rings (e.g., **80**) are also well tolerated by the catalyst system. For the first time, two enantioselective decarboxylative alkylations can be performed sequentially, giving **81** in high ee.

Table 1.3 Substrate Scope of the Enantioselective Decarboxylative Alkylation

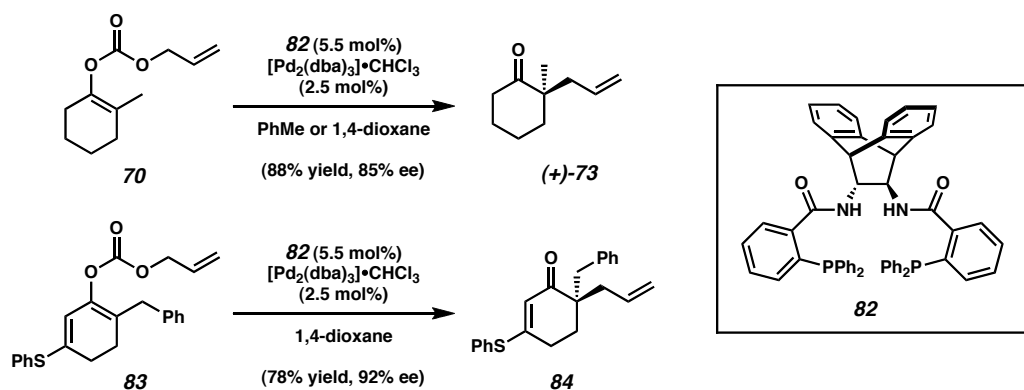
 (-)-73 89% yield 88% ee	 74 55% yield* 82% ee	 (-)-75 94% yield 92% ee	 76 89% yield 91% ee	 77 91% yield 92% ee
 78 94% yield 86% ee	 (+)-79 82% yield 86% ee	 80 83% yield 87% ee	 81 76% yield 92% ee, 4:1 dr	

*Yield after Wacker oxidation to the corresponding diketone

1.4.5 Other Enantioselective Decarboxylative Alkylation Methodologies

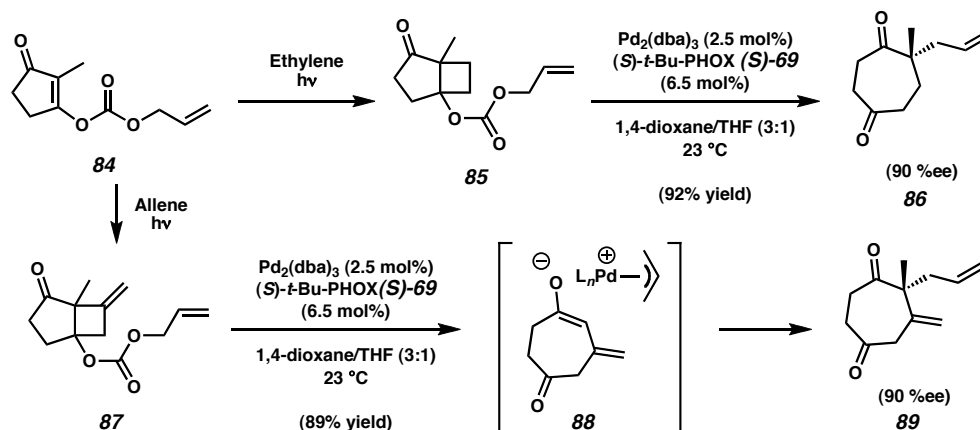
Subsequent to our investigations into Pd-catalyzed decarboxylative alkylation, the Trost lab published a similar technology using ligand **82** (Scheme 1.10).³³ A variety of enantioenriched cyclic all-carbon quaternary ketones and vinylogous thioesters are available using this chemistry. Yields and enantioselectivities are high, and both allyl enol carbonates and allyl β -ketoesters can be used.

Scheme 1.10 Trost's Enantioselective Decarboxylative Alkylations



A clever means to generate the prochiral enolate for enantioselective alkylation was recently reported by Blechert.³⁴ Enol carbonates such as **84** can undergo [2 + 2] photoaddition with ethylene or allene (Scheme 1.11). Treatment of the bicyclo[3.2.0]heptanes with Pd^0 and (*S*)-*t*-Bu-PHOX ((*S*)-**69**) induces a retro-aldol ring expansion. The resulting enolates are enantioselectively alkylated, generating α -quaternary cycloheptanediones. In the case of **87**, the intermediate enolate **88** does not undergo γ -alkylation. Consequently, the exo-methylene group is retained. These transformations represent enantioselective de Mayo reactions.³⁵

Scheme 1.11 Blechert's Ring Expansion/Enolate Alkylation Cascade



1.5 Concluding Remarks

Numerous methods have been developed addressing the generation of all-carbon quaternary stereocenters within rings via alkylation. Certain technologies have even been applied to the syntheses of pharmaceuticals and natural products. Early alkylation approaches utilized chiral auxiliaries, but in more recent years catalytic methods have been developed. Among these technologies are the versatile alkylations catalyzed by palladium. Three very powerful methods for generating all-carbon quaternary stereocenters via enantioselective decarboxylative allylation have recently been developed in our labs. Enol carbonates, silyl enol ethers, and β -ketoester substrates can be readily elaborated to α -quaternary ketones. Our goal has been to use these enantioselective Pd-catalyzed alkylations to synthesize biologically relevant natural products with novel skeletal structures.

1.6 Notes and Citations

- (1) For excellent reviews on enantioselective preparation of all-carbon-quaternary stereocenters, see: (a) Corey, E. J.; Guzman-Perez, A. *Angew. Chem., Int. Ed.* **1998**, *37*, 388-401. (b) Christoffers, J.; Mann, A. *Angew. Chem., Int. Ed.* **2001**, *40*, 4591-4597. (c) Douglas, C. J.; Overman, L. E. *Proc. Natl. Acad. Sci. U.S.A.* **2004**, *101*, 5363-5367.
- (2) (a) Evans, D. A.; Johnson, J. S. In *Comprehensive Asymmetric Catalysis*; Jacobsen, E. N., Pfaltz, A., Yamamoto, H., Eds.; Springer: New York, **1999**; Vol. 3, pp 1177-1235. (b) Maruoka, K. In *Catalytic Asymmetric Synthesis*, 2nd ed.; Ojima, I., Ed.; Wiley-VCH: New York, **2000**; pp 467-491. (c) Corey, E. J. *Angew. Chem., Int. Ed.* **2002**, *41*, 1650-1667. (d) Hayashi, U. In *Cycloaddition Reactions in Organic Synthesis*; Kobayashi, S.; Jorgensen, K. A., Eds.; Wiley-VCH: New York, **2002**; pp 5-56. (e) Ryu, D. U.; Corey, E. J. *J. Am. Chem. Soc.* **2003**, *125*, 6388-6390. (f) Evans, D. A.; Wu, J. *J. Am. Chem. Soc.* **2003**, *125*, 10162-10163.
- (3) (a) Denmark, S. E.; O'Connor, S. P. *J. Org. Chem.* **1997**, *62*, 584-594. (b) Pfaltz, A. In *Comprehensive Asymmetric Catalysis*; Jacobsen, E. N., Pfaltz, A., Yamamoto, H., Eds.; Springer: New York, **1999**; Vol. 2, pp 513-538. (c) Lydon, K. M.; McKerver, M. A. In *Comprehensive Asymmetric Catalysis*; Jacobsen, E. N.; Pfaltz, A.; Yamamoto, H., Eds.; Springer: New York, **1999**; Vol. 2, pp 539-580. (d) Charette, A. B.; Lebel, H. In *Comprehensive Asymmetric Catalysis*; Jacobsen, E. N.; Pfaltz, A.; Yamamoto, H., Eds.; Springer: New York, **1999**; Vol. 2, pp 581-603. (e) Doyle, M. P. In *Catalytic Asymmetric Synthesis*, 2nd ed.; Ojima, I., Ed.; Wiley-VCH: New York, **2000**; pp 191-228.

-
- (4) (a) Hajos, Z. G.; Parrish, D. R. *J. Org. Chem.* **1974**, *39*, 1615-1621. (b) Watanabe, N.; Ogawa, T.; Ohtake, Y.; Ikegami, S.; Hashimoto, S. *Synlett* **1996**, 85-86. (c) Wu, M. H.; Hansen, K. B.; Jacobsen, E. N. *Angew. Chem., Int. Ed.* **1999**, *38*, 2012-2014. (d) Davies, H. M. L.; Beckwith, R. E. *J. Chem. Rev.* **2003**, *103*, 2861-2903.
- (5) (a) Sato, Y.; Sodeoka, M.; Shibasaki, M. *J. Org. Chem.* **1989**, *54*, 4738-4739. (b) Carpenter, N. E.; Kucera, D. J.; Overman, L. E. *J. Org. Chem.* **1989**, *54*, 5845-5848. (c) Donde, A.; Overman, L. E. In *Catalytic Asymmetric Synthesis*, 2nd ed.; Ojima, I., Ed.; Wiley-VCH: New York, **2000**; pp 675-697. (d) Dounay, A. B.; Overman, L. E. *Chem. Rev.* **2003**, *103*, 2945-2963.
- (6) (a) Buono, G.; Chiodi, O.; Wills, M. *Synlett* **1999**, 377-388. (b) France, S.; Guerin, D. J.; Miller, S. J.; Lectka, T. *Chem. Rev.* **2003**, *103*, 2985-3012. (c) Mermerian, A. H.; Fu, G. C. *J. Am. Chem. Soc.* **2003**, *125*, 4050-4051. (d) Shaw, S. A.; Aleman, P.; Vedejs, E. *J. Am. Chem. Soc.* **2003**, *125*, 13368-13369. (e) Hills, I. D.; Fu, G. C. *Angew. Chem., Int. Ed.* **2003**, *42*, 3921-3924.
- (7) (a) Enders, D.; Bartsch, M.; Backhaus, D.; Runsink, J.; Raabe, G. *Liebigs Ann.* **1996**, 1095-1116. (b) Yoon, T. P.; Dong, V. M.; MacMillan, D. W. C. *J. Am. Chem. Soc.* **1999**, *121*, 9726-9727. (c) Yoon, T. P.; MacMillan, D. W. C. *J. Am. Chem. Soc.* **2001**, *123*, 2911-2912.
- (8) (a) Spielvogel, D. J.; Buchwald, S. L. *J. Am. Chem. Soc.* **2002**, *124*, 3500-3501. (b) Bella, M.; Kobbelaar, S.; Jørgensen, K. A. *J. Am. Chem. Soc.* **2005**, *127*, 62-63.
- (9) (a) Liu, T.-Y.; Long, J.; Li, B.-J.; Jiang, L.; Li, R.; Wu, Y.; Ding, L.-S.; Chen, Y.-C. *Org. Biomol. Chem.* **2006**, *4*, 2097-2099. (b) Bell, M.; Poulsen, T. B.; Jørgensen, K. A. *J. Org. Chem.* **2007**, *72*, 3053-3056.

-
- (10) For selected examples of prochiral enolate catalytic asymmetric alkylation not discussed in this chapter, see: (a) Kim, Y.-S.; Matsunaga, S.; Das, J.; Sekine, A.; Ohshima, T.; Shibasaki, M. *J. Am. Chem. Soc.* **2000**, *122*, 6506-6507. (b) Hamashima, Y.; Hotta, D.; Sodeoka, M. *J. Am. Chem. Soc.* **2002**, *124*, 11240-11241. (c) Taylor, M. S.; Jacobsen, E. N. *J. Am. Chem. Soc.* **2003**, *125*, 11204-11205. (d) Mase, N.; Tanaka, F.; Barbas, C. F., III *Angew. Chem., Int. Ed.* **2004**, *43*, 2420-2423. (e) Hamashima, Y.; Sakamoto, N.; Hotta, D.; Somei, H.; Umebayashi, N.; Sodeoka, M. *Angew. Chem., Int. Ed.* **2005**, *44*, 1525-1529. (f) Nemoto, T.; Fukuda, T.; Matsumoto, T.; Hitomi, T.; Hamada, Y. *Adv. Synth. Catal.* **2005**, *347*, 1504-1506.
- (11) For an example of a diastereoselective Michael reaction mediated by a chiral amine auxiliary, see: Brunner, H.; Kraus, J.; Lautenschlager, H. J. *Monatsch. Chem.* **1988**, *119*, 1161-1167.
- (12) Kogen, H.; Tomioka, K.; Hashimoto, S.-i.; Koga, K. *Tetrahedron Lett.* **1980**, *21*, 4005-4008.
- (13) Meyers, A. I.; Harre, M.; Garland, R. *J. Am. Chem. Soc.* **1984**, *106*, 1146-1148.
- (14) Meyers, A. I.; Lefker, B. A. *J. Org. Chem.* **1986**, *51*, 1541-1544.
- (15) Meyers, A. I.; Hanreich, R.; Wanner, K. T. *J. Am. Chem. Soc.* **1985**, *107*, 7776-7778.
- (16) Meyers, A. I.; Fleming, S. A. *J. Am. Chem. Soc.* **1986**, *108*, 306-307.
- (17) Meyers, A. I.; Berney, D. *J. Org. Chem.* **1989**, *54*, 4673-4676.
- (18) (a) Enders, D.; Zamponi, A.; Raabe, G.; Runsink, J. *Synthesis* **1993**, 725-728. (b) Enders, D.; Zamponi, A.; Schäfer, T.; Nübling, C.; Eichenauer, H.; Demir, A. S.; Raabe, G. *Chem. Ber.* **1994**, *127*, 1707-1721.

-
- (19) (a) Dolling, U.-H.; Davis, P.; Grabowski, E. J. J. *J. Am. Chem. Soc.* **1984**, *106*, 446-447. (b) Bhattacharya, A.; Dolling, U.-H.; Grabowski, E. J. J.; Karady, S.; Ryan, K. M.; Weinstock, L. *Angew. Chem., Int. Ed.* **1986**, *25*, 476-477.
- (20) (a) Sasai, H.; Emori, E.; Arai, T.; Shibasaki, M. *Tetrahedron Lett.* **1996**, *37*, 5561-5564. (b) Shibasaki, M.; Yoshikawa, N. *Chem. Rev.* **2002**, *102*, 2187-2209.
- (21) Doyle, A. G.; Jacobsen, E. N. *J. Am. Chem. Soc.* **2005**, *127*, 62-63.
- (22) Hayashi, T.; Kanehira, K.; Hagihara, T.; Kumada, M. *J. Org. Chem.* **1988**, *53*, 113-120.
- (23) Sawamura, M.; Nagata, H.; Sakamoto, H.; Ito, Y. *J. Am. Chem. Soc.* **1992**, *114*, 2586-2592.
- (24) (a) Trost, B. M.; Radinov, R.; Grenzer, E. M. *J. Am. Chem. Soc.* **1997**, *119*, 7879-7880. (b) Trost, B. M.; Schroeder, G. M. *J. Am. Chem. Soc.* **1999**, *121*, 6759-6760. (c) Trost, B. M.; Schroeder, G. M.; Kristensen, J. *Angew. Chem., Int. Ed.* **2002**, *41*, 3492-3495.
- (25) You, S.-L.; Hou, X.-L.; Dai, L.-X.; Zhu, X.-Z. *Org. Lett.* **2001**, *3*, 149-151.
- (26) Kuwano, R.; Uchida, K.-i.; Ito, Y. *Org. Lett.* **2003**, *5*, 2177-2179.
- (27) For reviews on enantioselective decarboxylative alkylations, see: (a) You, S.-L.; Dai, L.-X. *Angew. Chem., Int. Ed.* **2006**, *45*, 5246-5248. (b) Mohr, J. T.; Stoltz, B. M. *Chem. Asian J.* **2007**, (In Press: DOI: 10.1002/asia.200700183).
- (28) (a) Shimizu, I.; Yamada, T.; Tsuji, J. *Tetrahedron Lett.* **1980**, *21*, 3199-3202. (b) Tsuda, T.; Chujo, Y.; Nishi, S.; Tawara, K.; Saegusa, T. *J. Am. Chem. Soc.* **1980**, *102*, 6381-6384. (c) Tsuji, J.; Minami, I.; Shimizu, I. *Tetrahedron Lett.* **1983**, *24*, 1793-1796. (d) Tsuji, J.; Minami, I.; Shimizu, I. *Chem. Lett.* **1983**, 1325-1326.

-
- (29) For additional details on ligand modification, see: Tani, K.; Behenna, D. C.; McFadden, R. M.; Stoltz, B. M. *Org. Lett.* **2007**, *9*, 2529-2931.
- (30) Behenna, D. C.; Stoltz, B. M. *J. Am. Chem. Soc.* **2004**, *126*, 15044-15045.
- (31) For an excellent review on stereoablative enantioselective transformations, see: Mohr, J. T.; Ebner, D. C.; Stoltz, B. M. *Org. Biomol. Chem.* **2007**, *5*, 3571-3576.
- (32) Mohr, J. T.; Behenna, D. C.; Harned, A. M.; Stoltz, B. M. *Angew. Chem., Int. Ed.* **2005**, *44*, 6924-6927.
- (33) (a) Trost, B. M.; Xu, J. *J. Am. Chem. Soc.* **2005**, *127*, 2846-2847. (b) Trost, B. M.; Xu, J. *J. Am. Chem. Soc.* **2005**, *127*, 12180-17181. (c) Trost, B. M.; Xu, J.; Reichle, M. *J. Am. Chem. Soc.* **2007**, *129*, 282-283.
- (34) Schulz, S. R.; Blechert, S. *Angew. Chem., Int. Ed.* **2007**, *46*, 3966-3970.
- (35) Crimmins, M. T. *Chem. Rev.* **1988**, *88*, 1453-1473.

CHAPTER TWO

Enantioselective Formal Total Syntheses of Natural Products Using Palladium-Catalyzed Decarboxylative Alkylation

2.1 Introduction

The enantioselective generation of all-carbon quaternary stereocenters is a challenge for the modern organic chemist.¹ A recent tool added to the arsenal of methods in this field has been palladium-catalyzed decarboxylative alkylation.² This method has allowed for the preparation of diverse cyclic α -quaternary allyl ketones and vinylogous esters, with high functional group tolerance. Recently, we developed three methods for generating enantioenriched α -quaternary ketones in the presence of a Pd(0) source and a chiral phosphinooxazoline ligand. The first two methods utilize silyl enol ether and enol carbonate substrates, respectively,³ while the third method employs racemic allyl β -ketoesters.⁴ Since the enantioenriched products prepared are well suited for further synthetic elaboration, we sought to advance them to intermediates reported in total syntheses of classic molecules. Herein we disclose catalytic enantioselective formal syntheses of an array of challenging natural products bearing at least one all-carbon quaternary stereocenter.

2.2 Formal Total Synthesis of (–)-Thujopsene[†]

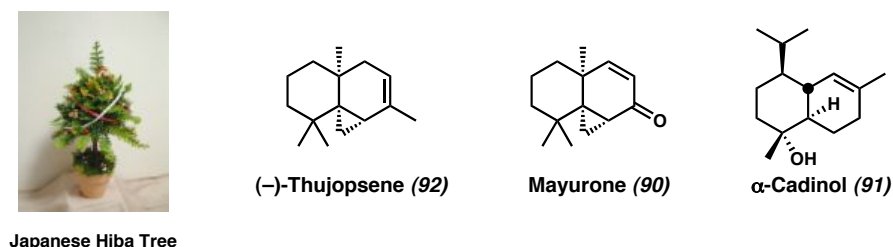
2.2.1 Background

The Japanese Hiba tree, *Thujopsis dolabrata*, has been used for centuries as decoration and within traditional architecture.⁵ The plant is a member of the order

[†] This work on (–)-thujopsene was done in collaboration with Jacqueline Malette.

Cupressaceae, and its fragrant wood oil contains many sesquiterpene natural products, including mayurone (**90**),⁶ α -cadinol (**91**),⁷ and (–)-thujopsene (**92**)⁸ (Figure 2.1). The wood oil has been shown to have potent deterrent effects against dust mites; thus, in addition to its ornamental value, the hiba tree also provides an environmentally benign means of pest control.⁹

Figure 2.1 Natural Products from *Thujopsis dolabrata*



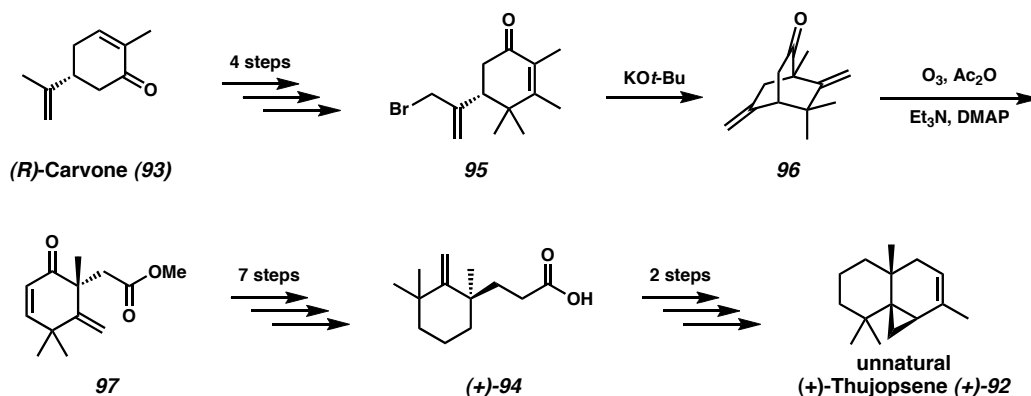
2.2.2 Structural Analysis of Thujopsene

(–)-Thujopsene (**92**) bears many features that have made it an attractive target to synthetic chemists. In addition to its tricyclo[5.4.0.0^{1,3}]undecane skeleton, the compound contains three contiguous all-carbon quaternary centers, two of which are stereogenic, and one that is also part of a cyclopropane (Scheme 2.1).¹⁰ Additionally, the natural product is a hydrocarbon with few functional group handles for retrosynthetic analysis.

Inspired by the interesting structure of (–)-thujopsene (**92**), several groups have reported racemic approaches to the natural product.¹¹ In addition, at least two enantioselective routes have been completed.¹² Srikrishna and Anebouselvy reported an enantiospecific route to the (+)-thujopsene (+)-**92** from (*R*)-carvone (**93**).¹³ During their total synthesis, the authors prepare carboxylic acid (+)-**94** over 13 steps (Scheme 2.1).

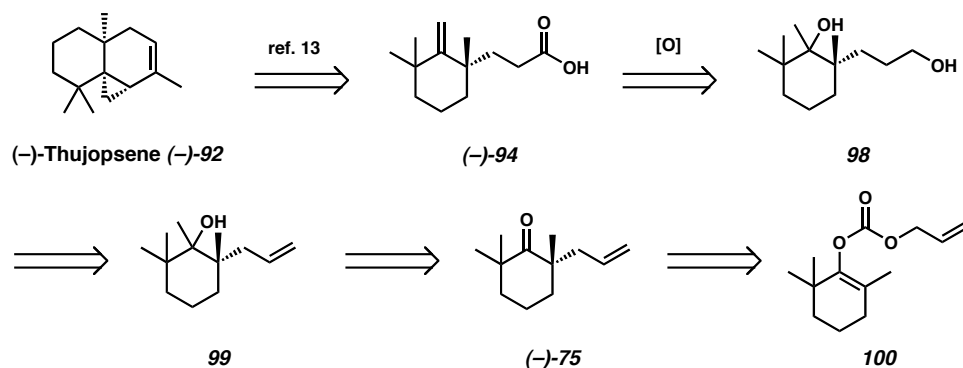
We anticipated that we could intercept this intermediate in an efficient manner using our enantioselective decarboxylative allylation chemistry.

Scheme 2.1 Srikrishna and Anebouselvy's Approach to (–)-Thujopsene



We designed a retrosynthesis of the carboxylic acid (–)-**94** (Scheme 2.2). It was anticipated that the acid functionality might arise via selective oxidation of diol **98**. We believed the olefinic moiety present in (–)-**94** might be installed by acid-mediated elimination concomitant with primary alcohol oxidation. The terminal alcohol could be installed by hydroboration-oxidation of the olefin **99**. This bis-homoallylic alcohol could potentially come from allyl ketone (–)-**75**, available in 91% ee from enol carbonate **100**. This allyl enol carbonate is readily prepared from 2,2,6-trimethylcyclohexanone (**101**).

Scheme 2.2 Retrosynthetic Analysis of (–)-Thujopsene

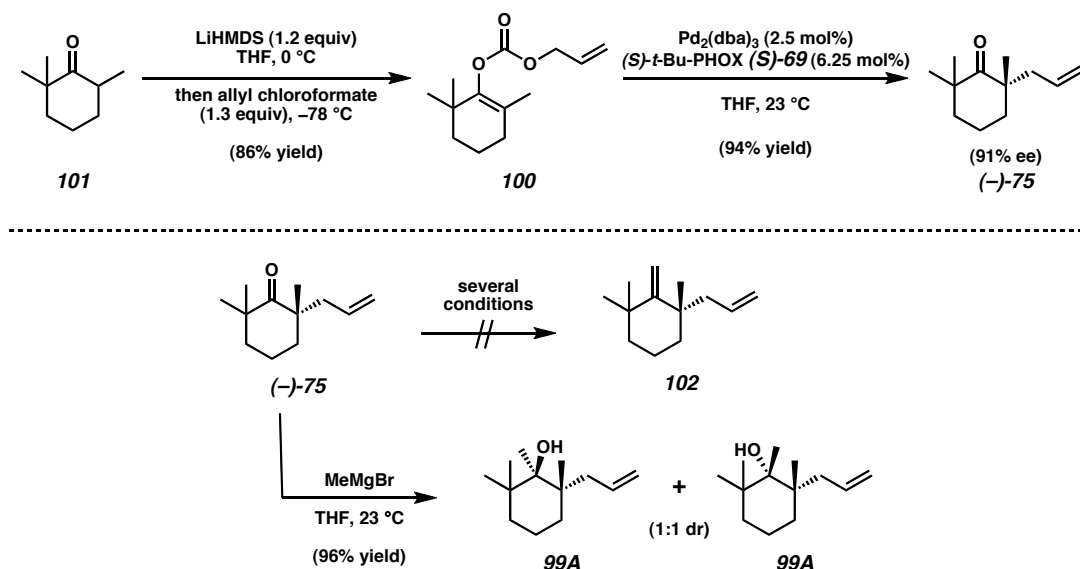


2.2.3 Formal Total Synthesis of (–)-Thujopsene

We commenced our formal total synthesis of (–)-thujopsene ((–)-92) by treatment of **101** with LiHMDS in THF followed by allyl chloroformate, furnishing known enol carbonate **100** in excellent yield (Scheme 2.3). This substrate smoothly underwent Pd-catalyzed enantioselective decarboxylative allylation in the presence of (*S*)-*t*-Bu PHOX ((*S*)-69), giving allyl ketone (–)-75 in 94% yield and 91% ee.¹⁴ Rigorous exclusion of air and moisture was crucial for obtaining high yield and enantioselectivity.¹⁵

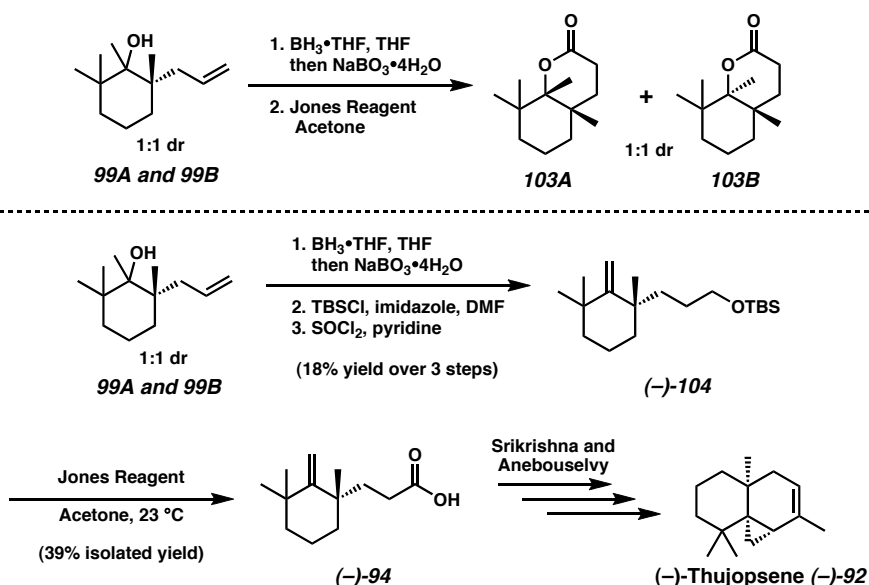
The next task was the installation of the exocyclic methylene of (–)-94. Attempted Wittig olefination failed to produce bis-olefin **102**, presumably due to the steric congestion proximal to the ketone. Although direct methylenation of ketone (–)-75 was not workable, addition of methyl magnesium bromide at 23 °C gave a 1:1 mixture of homoallylic alcohols **99A** and **99B** in excellent yield.

Scheme 2.3 Preparation of Diastereomeric Alcohols



The **99A/99B** mixture was carried through a two-step sequence of hydroboration/oxidation and Jones oxidation (Scheme 2.4). It was anticipated that under highly acidic oxidizing conditions, the tertiary alcohols present would be eliminated, removing a stereocenter and installing the requisite exocyclic olefin present in **(-)-94**. Oxidation of the primary alcohol (installed during the hydroboration) to a carboxylic acid was also anticipated. In the event, two diastereomeric lactones **103A** and **103B** were obtained as the sole isolated products in 1:1 dr. Apparently, primary alcohol oxidation is more rapid than any tertiary alcohol elimination.

Scheme 2.4 Completion of the Carboxylic Acid



The formation of the lactones **103A** and **103B** necessitated revision of our synthetic plan. We subjected the mixture of diastereomeric alcohols **99A** and **99B** to hydroboration, followed by oxidative workup with $\text{NaBO}_3 \cdot 4\text{H}_2\text{O}$ (Scheme 2.4). The product mixture was purified, then treated with TBSCl and imidazole in dry DMF. This resulted in selective protection of the primary alcohol installed during the hydroboration/oxidation sequence. The combined, purified monoprotected diols were treated with thionyl chloride in pyridine, affecting a net dehydration reaction, providing silyl ether **(-)-104** in 18% yield over three steps from the mixture of **99A** and **99B**. The purified TBS ether was exposed briefly to the Jones reagent, accomplishing silyl ether cleavage *and* primary alcohol oxidization to a carboxylic acid. This oxidative transformation furnished **(-)-94**, thus completing the formal total synthesis of **(-)-thujopsene ((-)-92)**.

2.3 Formal Total Synthesis of (–)-Dysidiolide

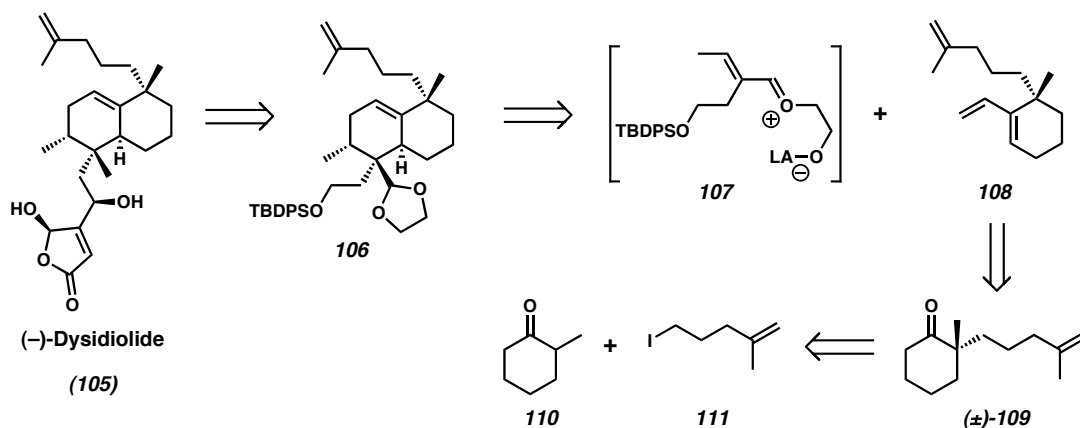
2.3.1 Background

Dysidiolide (**105**) was isolated from the marine sponge *Dysidea etheria* and found to have inhibitory activity toward the protein phosphatase cdc25, with an IC₅₀ value of 9.4 μ M (Scheme 2.5).¹⁶ This enzyme belongs to a protein family involved in dephosphorylation of cyclin-dependent kinases.¹⁷ Thus, inhibitors of cdc25 might allow for targeted cell-cycle disruption in cancer cell lines.¹⁶

Initial investigations into the structure of the natural product were made using NMR techniques; however, many of the signals in the ¹³C NMR spectrum were broad.¹⁶ Fortuitously, the relative stereochemistry of the sesterterpene **105** was determined via single-crystal X-ray diffraction. Dysidiolide (**105**) was found to have a butenolide ring and six stereocenters, two that were of the all-carbon quaternary variety. Several groups have reported total syntheses of this natural product,¹⁸ three of which are enantioselective.^{18a,18b,18h,18l,19}

In Danishefsky's racemic approach, the cyclohexene ring of **106** was installed via diastereoselective Diels-Alder reaction of a transient dioxolenium dienophile (**107**) with a chiral vinylcyclohexene (**108**) (Scheme 2.5).^{18j} Diene **108** was prepared from α -quaternary ketone (\pm)-**109** in racemic form. This keto-olefin was synthesized via alkylation of the thermodynamic lithium enolate of 2-methylcyclohexanone (**110**) with 5-iodo-2-methyl-1-pentene (**111**). We believed that our catalytic decarboxylative alkylation chemistry might allow for an enantioselective synthesis of (–)-**109**, constituting a formal total synthesis of (–)-dysidiolide (**105**).

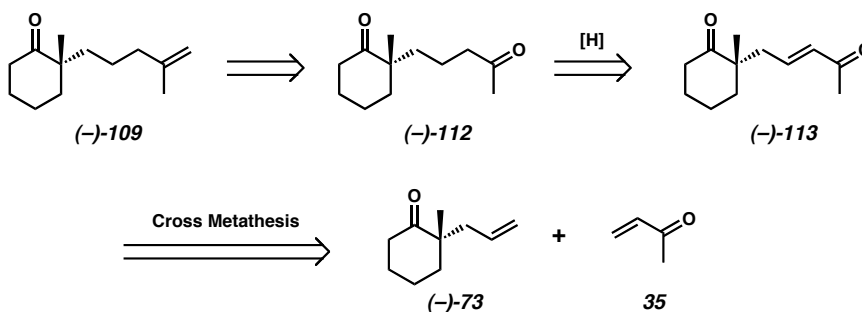
Scheme 2.5 Danishefsky's Approach to (±)-Dysidiolide



2.3.2 Retrosynthetic Analysis

Looking at the target keto-olefin (–)-109, we reasoned that the geminally di-substituted olefin could be prepared from a diketone (–)-112 (Scheme 2.6). Based on steric arguments, we believed selective olefination of the less-hindered distal ketone moiety would be possible. Diketone (–)-112 could easily arise from keto-enone (–)-113 via olefination. Retrosynthetically, (–)-113 could come from methyl vinyl ketone (35) and the α -quaternary cyclohexanone (–)-73, readily available in enantioenriched form through our enantioselective decarboxylative allylation chemistry.

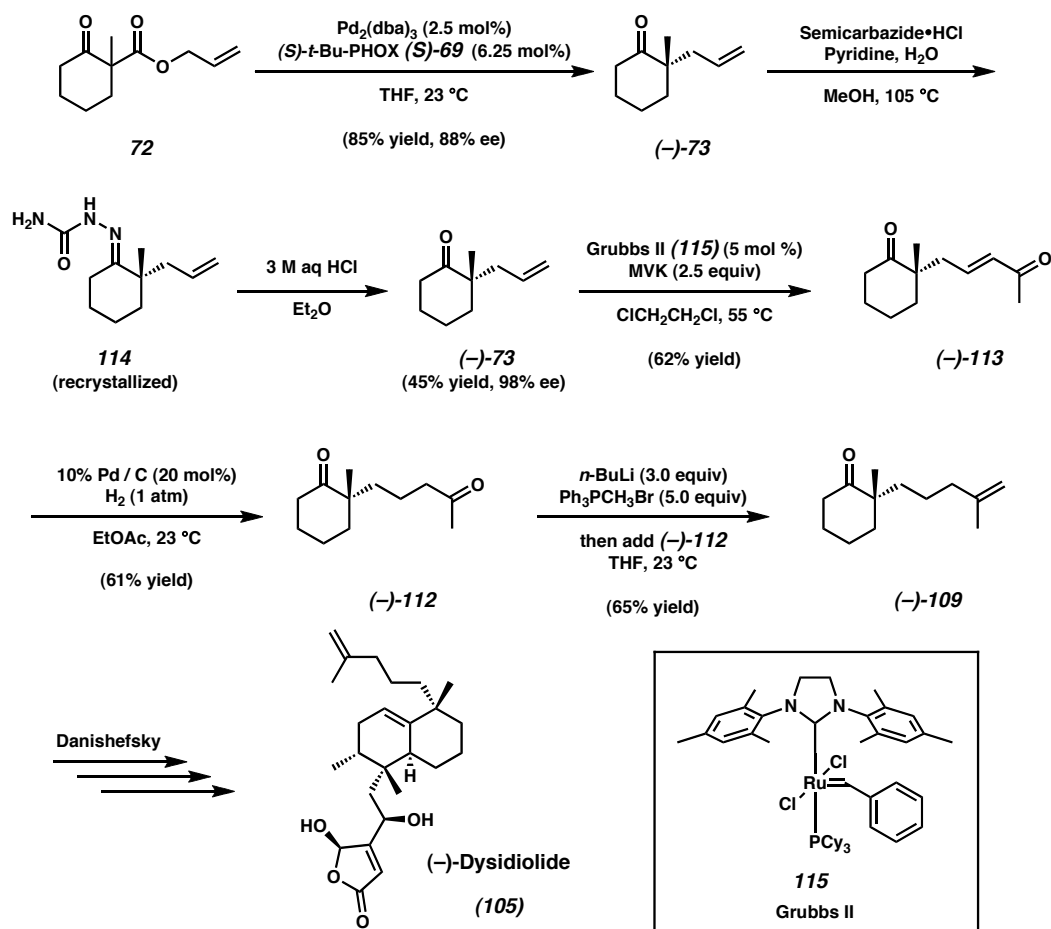
Scheme 2.6 Retrosynthetic Analysis of the Keto-Olefin



2.3.3 Formal Total Synthesis of (–)-Dysidiolide

Our synthesis commenced by treating known allyl β-ketoester **72** with catalytic $\text{Pd}_2(\text{dba})_3$ and (*S*)-*t*-Bu-PHOX ((*S*)-**69**), furnishing 2-allyl-2-methylcyclohexanone ((–)-**79**) in 85% yield and 88% ee (Scheme 2.7).⁴ The allyl ketone was enriched to 98% ee via the semicarbazone **114**.³ Using the Grubbs 2nd generation metathesis catalyst (**115**), allyl ketone (–)-**73** was crossed with methyl vinyl ketone (**35**) in reasonable yield. The ketone (–)-**113** was then reduced to diketone (–)-**112** using Pd/C and H_2 .

Scheme 2.7 Formal Synthesis of (–)-Dysidiolide



A Wittig reaction seemed ideal for installation of the geminally disubstituted olefin. However, it was critical that the methyl triphenyl phosphonium salt be completely deprotonated because any unreacted base led to side reactions of the starting material.²⁰ Due to their limited solubility, NaH and KO*t*-Bu failed to react completely with the phosphonium salt. However, *n*-BuLi reacted completely for preparation of the phosphorus ylide. Treatment of the ylide with (–)-**112** resulted in chemoselective methylenation of the distal ketone. This completed (–)-**109** and thus our formal synthesis of (–)-dysidiolide ((–)-**105**).

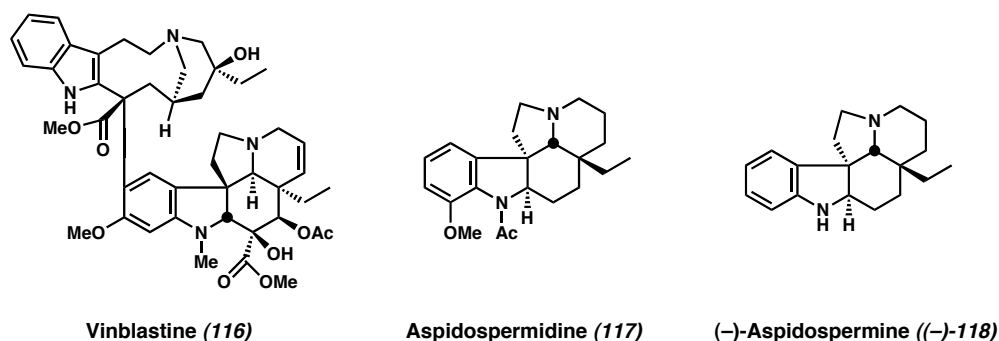
2.4 Formal Total Synthesis of (–)-Aspidospermine[†]

2.4.1 Background

The aspidosperma alkaloids have garnered much attention over the years as targets for synthetic chemists. Most of the 250 compounds in this large class share a common pentacyclic core, from the complex vinca alkaloids such as vinblastine (**116**) (used as a chemotherapeutic) to the simpler aspidospermidine (**117**) (Figure 2.2).²¹ To address the challenging synthetic features of the aspidosperma alkaloids, many clever synthetic approaches have been reported, highlighted by the seminal work of Stork and Dolfini²² along with Ban and co-workers.²³

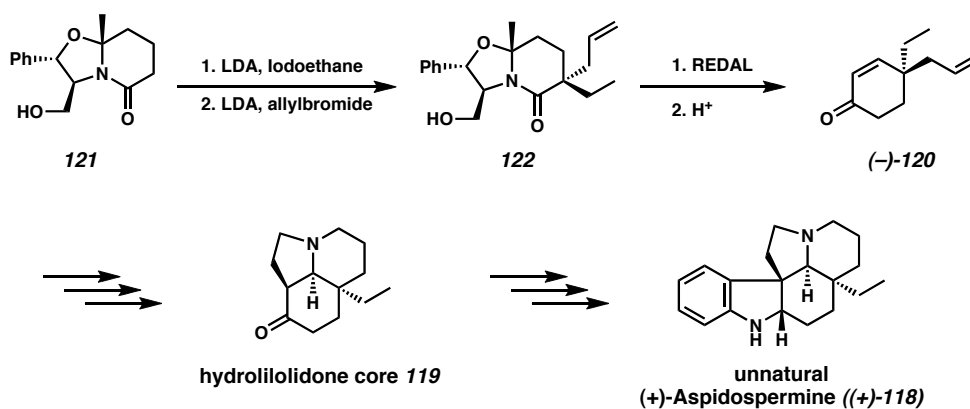
[†] This work on (–)-aspidospermine was done in collaboration with David E. White and Michael R. Krout.

Figure 2.2 Representative Aspidosperma Alkaloids



One popular target within this natural product family is aspidospermine ((-)-**118**). Although not as medicinally potent as certain other members of the aspidosperma class, it has served as a testing ground for chemists venturing into this alkaloid realm. In 1989, Meyers reported an enantioselective synthesis of the (4a*S*,8a*R*,8*S*)-hydrolilolidone core **119**^{22,23,24} present in aspidospermine ((+)-**118**), and thus a formal synthesis of the alkaloid itself (Scheme 2.8).²⁵ One of the precursors to the core structure, prepared in enantioenriched form, was enone (-)-**120**. Contrasting Meyers' approach, which employed a chiral auxiliary, we thought a catalytic enantioselective alkylative strategy would be ideal for a formal total synthesis of aspidospermine ((-)-**118**).

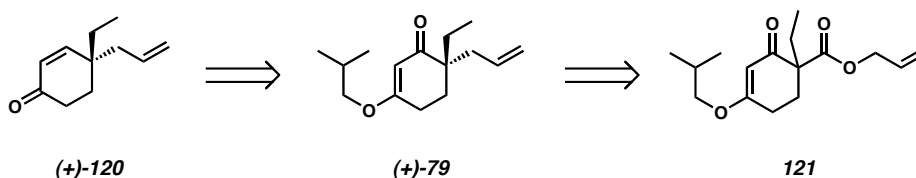
Scheme 2.8 Meyers' Approach to Unnatural (+)-Aspidospermine



2.4.2 Retrosynthetic Analysis

One challenge associated with **(+)-120** was its γ -stereogenicity. To address this issue retrosynthetically, we installed oxygenation at the β -carbon (Scheme 2.9). A reasonable retron was vinylogous ester **(+)-79**. This retrosynthetic plan simplified the problem of γ -chirality to one of α -stereogenicity. The allyl vinylogous ester could potentially arise from α -allyloxycarbonyl vinylogous ester **121** via enantioselective allylation. One goal during this formal synthesis was to finish the target compound (**(+)-120**) with an ee of at least 90%. Overall, our proposed forward synthetic sequence is an enantioselective form of Stork-Danheiser chemistry.²⁶

Scheme 2.9 Retrosynthetic Analysis of the γ -Allyl Enone

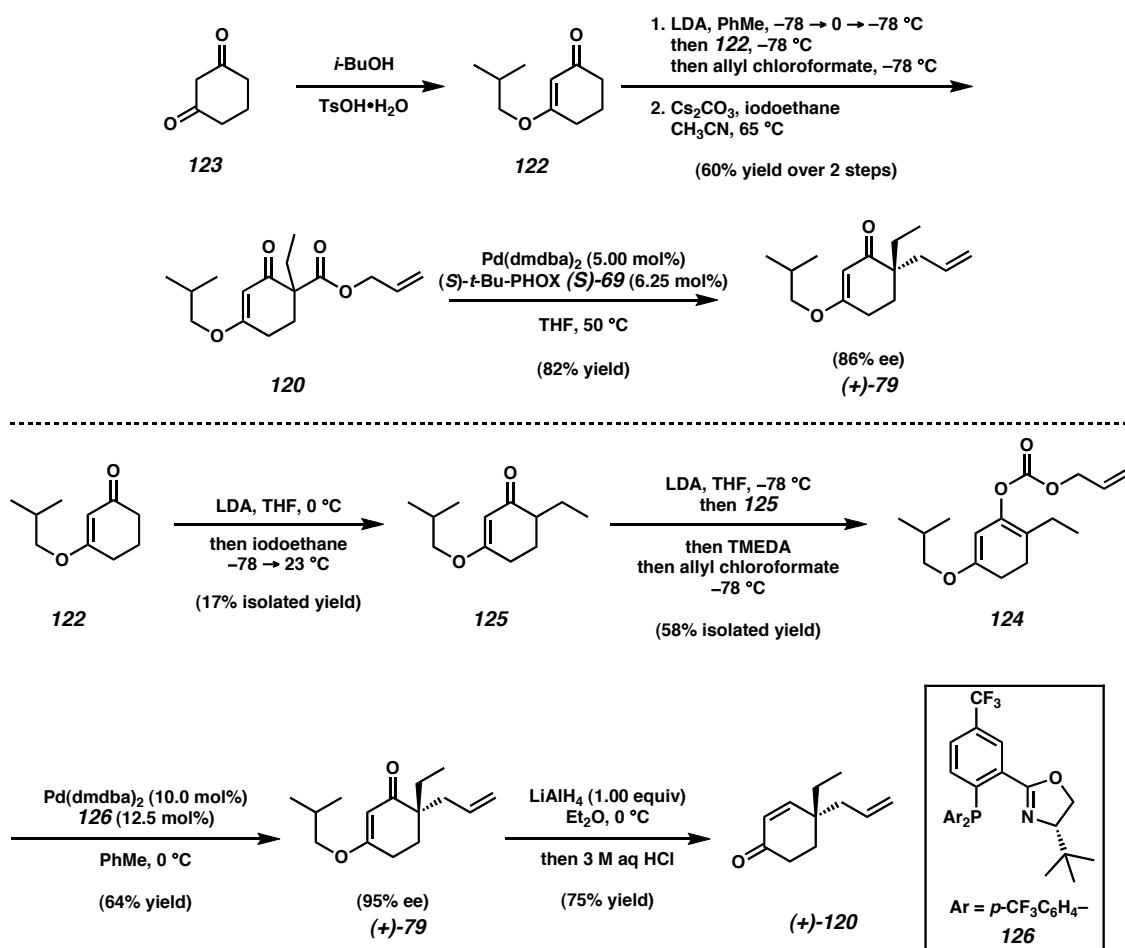


2.4.3 Two Routes to the Alkylated Vinylogous Ester: Formal Synthesis of Aspidospermine

We started our formal synthesis with the known isobutyl vinylogous ester **122**, readily available from 1,3-cyclohexanedione (**123**) (Scheme 2.10). Compound **122** was selectively acylated on carbon with allylchloroformate, furnishing a vinylogous β -diester as a tautomeric mixture. This composite was immediately subjected to alkylation with iodoethane in acetonitrile under basic conditions, providing **120** in good yield. When we performed the decarboxylative allylation, we obtained allyl vinylogous ester **(+)-79** in

82% yield and 86% ee. The higher temperature used was necessary to achieve complete conversion, but it came with the cost of lowered enantioselectivity.

Scheme 2.10 Two Decarboxylative Alkylation Methods Tested



An alternative route to (+)-79 was developed, demonstrating the versatility of our decarboxylative alkylation chemistry. We discovered it was possible to prepare 124 in reasonable yield from 125 (Scheme 2.10).²⁷ Using the tris-trifluoromethyl PHOX ligand 126 at reduced temperatures in toluene allowed for the synthesis of (+)-79 in 64% isolated yield and 95% ee. The product allyl vinylogous ester (+)-79 was then treated

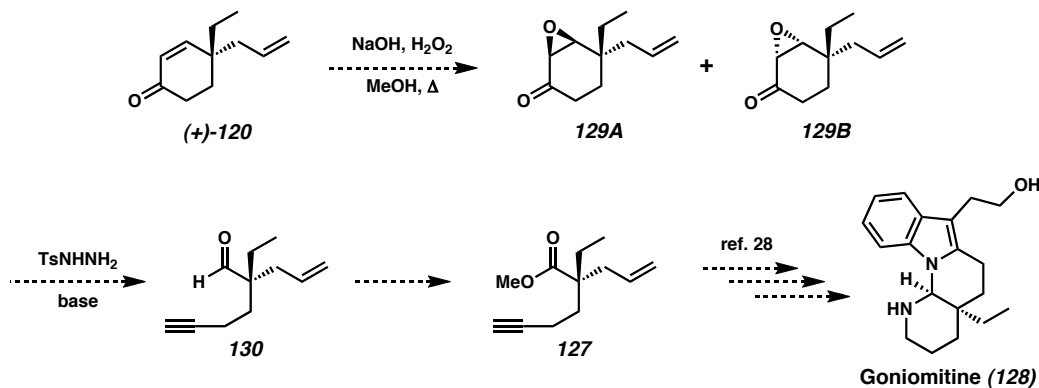
with LiAlH_4 in Et_2O , giving selective 1,2-reduction. Hydrolysis of the crude product with 3 M aqueous HCl gave rise to enone **(+)-120**, resulting in a formal synthesis of **(-)-aspidospermine**.

2.5 Other Targets for Formal Total Synthesis

2.5.1 Goniomitine

Some of the intermediates we prepared during our formal synthesis endeavors might find use in other contexts. For instance, ester **127** has been reported as an intermediate in the total synthesis of goniomitine (**128**) (Scheme 2.11).²⁸ We envision that enone **(+)-120** might be elaborated to ester **127**, constituting a formal total synthesis of goniomitine (**128**). The enone **(+)-120** could undergo nucleophilic epoxidation to give **129A** and **129B**. These diastereomeric epoxides, when condensed with *p*-toluenesulfonylhydrazide and treated with base, are anticipated to undergo an Eschenmoser-Tanabe fragmentation. This transformation would lead to alkyne **130**, which could be oxidized and esterified to give the desired ester **127**.

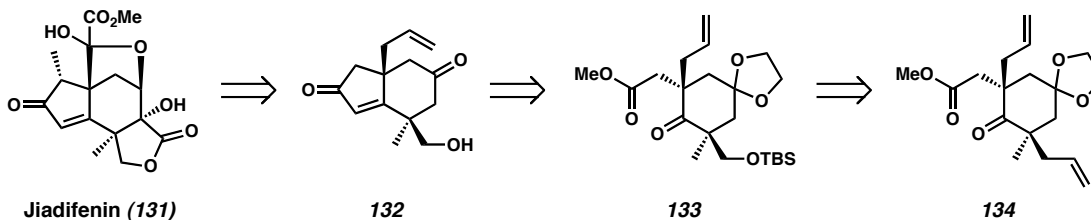
Scheme 2.11 A Possible Formal Synthesis of Goniomitine



2.5.2 Jiadifenin

The neurotrophic natural product jiadifenin (**131**) is another structurally interesting target, which has been synthesized in racemic form by Danishefsky.²⁹ This synthesis proceeds through a chiral, racemic tetrasubstituted cyclohexanone **133**. Considering the possibility of performing two stereoselective alkylations on a single molecule, it might be possible to intercept Danishefsky's intermediate **133** in enantioenriched form (Scheme 2.12).

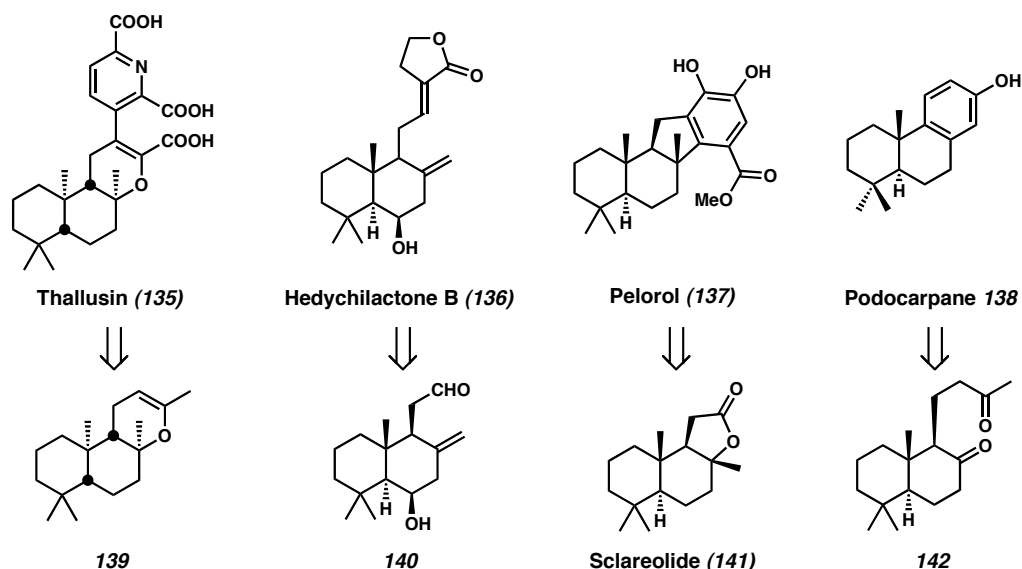
Scheme 2.12 Danishefsky's Intermediates in the Jiadifenin Synthesis



2.5.3 Other Natural Products

There are many other potential uses for chiral non-racemic quaternary compounds available through our chemistry. Formal syntheses of natural products including, but not limited to, (–)-thallusin (**135**),³⁰ hedychilactone (**136**),³¹ (–)-pelorol (**137**),³² and podocarpene **138**³³ could all be envisioned (Scheme 2.13). Yang's synthesis of Pelorol itself even began with another natural product, sclareolide (**141**).³² Our enantioselective decarboxylative alkylation chemistry is anticipated to find widespread use in the synthesis of functionally diverse quaternary-carbon entities.

Scheme 2.13 Other Natural Products Targeted for Formal Synthesis



2.6 Concluding Remarks

The development of a Pd-catalyzed method for generating all-carbon quaternary stereocenters has set the stage for formal total syntheses of an array of natural products including terpenes and alkaloids. An efficient route to the sesquiterpene (–)-thujopsene ((–)-**92**)¹³ has been delineated, featuring the installation of a sterically congested exocyclic olefin. We have also intercepted a key intermediate in Danishefsky’s synthesis of dysidiolide ((–)-**105**),^{18j} demonstrating chemoselective modification of the allyl group installed during the palladium catalysis. Finally, we have shown that the various starting materials utilized in our alkylation method can provide great flexibility in overall synthetic design, allowing us to overcome obstacles associated with enantioselectivity. The use of an allyl enol carbonate (**124**) derived from a vinylogous ester (**125**), as opposed to an allyl vinylogous β-diester (**120**), allowed for the highly enantioselective synthesis of a quaternary allyl vinylogous ester ((+)-**79**). Using traditional Stork-

Danheiser chemistry, a formal total synthesis of (–)-Aspidospermine ((–)-**118**) was achieved.²⁵ We anticipate that formal total syntheses of other natural products are soon to follow, lending us additional insight into synthetic elaborations of compounds with all-carbon quaternary stereocenters.

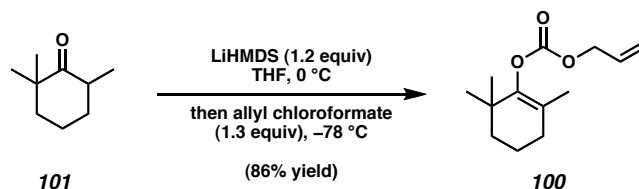
2.7 Experimental Procedures

2.7.1 Materials and Methods

Unless stated otherwise, reactions were conducted in flame-dried glassware under an atmosphere of nitrogen using anhydrous solvents (either freshly distilled or passed through activated alumina columns). Chloroform, stabilized with ethanol, was stored in the dark over oven-dried 4Å molecular sieves. Absolute ethanol, methanol, and *N,N*-dimethyl acetamide were used as purchased. 2,2,6-Trimethylcyclohexanone (**101**) was used as received. TMEDA and *i*-Pr₂NH were distilled from CaH₂. All other commercially obtained reagents were used as received unless specified otherwise. (*S*)-*t*-Bu-PHOX ligand (**S**)-**69** was prepared according to known methods.^{3,34} (*S*)-2-(tris-*p*-trifluoromethylphenylphosphin-2'-yl)-4-*t*-butyloxazoline (**126**) was also prepared according to the published procedure.^{3,34b} Reaction temperatures were controlled using an IKAmag temperature modulator. Thin-layer chromatography (TLC) was conducted with E. Merck silica gel 60 F254 pre-coated plates (0.25 mm) and visualized using UV at 254 nm, *p*-anisaldehyde, potassium permanganate, and iodine vapor over sand. TLC data include R_f, eluent, and method of visualization. ICN silica gel (particle size 0.032-0.063 mm), SilliaFlash P60 Academic silica gel (0.040-0.063 mm), or Florisil (Aldrich) was

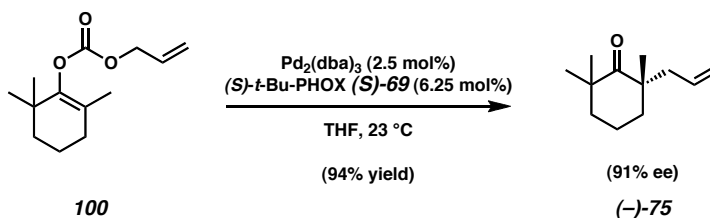
used for flash column chromatography. Analytical chiral HPLC analyses were performed with an Agilent 1100 Series HPLC using a chiralcel OD or AD normal-phase column (250 x 4.6 mm) employing 2.0-3.0% ethanol in hexane isocratic elution and a flow rate of 0.1 mL/min with visualization at 254nm. Analytical chiral GC analysis was performed with an Agilent 6850 GC using a GT-A column (0.25m x 30.00m) employing an 80 °C isotherm and a flow rate of 1.0 mL/min. ^1H NMR spectra were recorded on a Varian Mercury 300 (at 300 MHz) or a Varian Inova 500 (at 500 MHz) and are reported relative to the residual solvent peak (δ 7.26 for CDCl_3 and δ 7.16 for C_6D_6). Data for ^1H NMR spectra are reported as follows: chemical shift (δ ppm), multiplicity, coupling constant (Hz),³⁵ and integration. ^{13}C NMR spectra were recorded on a Varian Mercury 300 (at 75 MHz) or a Varian Inova 500 (at 125 MHz) and are reported relative the residual solvent peak (δ 77.2 for CDCl_3 and δ 128.4 for C_6D_6). Data for ^{13}C NMR spectra are reported in terms of chemical shift, and integration (where appropriate). IR spectra were recorded on a Perkin Elmer Spectrum BXII spectrometer and are reported in frequency of absorption (cm^{-1}). IR samples were thin films deposited on sodium chloride plates by evaporation from a solvent (usually CDCl_3), which is recorded. Optical rotations were measured with a Jasco P-1010 polarimeter, using a 100 mm path-length cell. High-resolution mass spectra were obtained from the California Institute of Technology Mass Spectral Facility. Melting points were determined on a Thomas-Hoover melting point apparatus and are uncorrected.

2.7.2 Syntheses of Compounds Related to Thujopsene



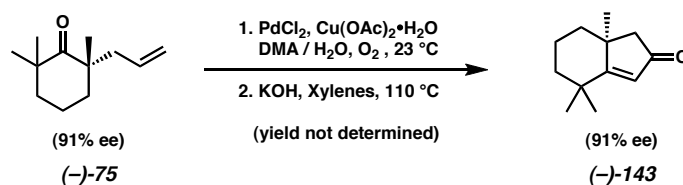
Enol Carbonate 100. A solution of LiHMDS (1.0 M in THF, 57.5 mL, 57.5 mmol) was added to THF (300 mL), then cooled to 0 °C. A solution of 2,2,6-trimethylcyclohexanone (**101**) (6.67 g, 47.6 mmol) in THF (10 mL) was added. The reaction was stirred at 0 °C for 1 h, then cooled to $-78\text{ }^{\circ}\text{C}$ and fitted with an addition funnel, which was charged with a solution of allyl chloroformate (6.56 mL, 61.8 mmol) in THF (200 mL). The solution was added dropwise over 30 min. Then the reaction was warmed to 23 °C. After 13 h, the reaction was poured into a mixture of sat. aq NH_4Cl (100 mL), water (100 mL), and hexane (100 mL). After 10 min, the organic phase was collected and the aqueous phase extracted with Et_2O (3 x 75 mL). All organic layers were combined, washed with brine (100 mL), dried (Na_2SO_4), filtered, and concentrated. The residue was purified by flash chromatography on silica gel (2:98 Et_2O /hexane eluent), affording enol carbonate **100** (9.19 g, 86% yield) as a clear oil. R_f 0.43 (1:9 EtOAc /hexane), (*p*-Anisaldehyde, blue spot); ^1H NMR (300 MHz, CDCl_3): δ 5.96 (app. ddt, $J_{d1} = 17.1\text{ Hz}$, $J_{d2} = 10.7\text{ Hz}$, $J_t = 5.8\text{ Hz}$, 1H), 5.38 (app. ddq, $J_{d1} = 17.3\text{ Hz}$, $J_{d2} = 8.3\text{ Hz}$, $J_q = 1.4\text{ Hz}$, 1H), 5.28 (app. ddq, $J_{d1} = 10.5\text{ Hz}$, $J_{d2} = 4.4\text{ Hz}$, $J_q = 1.1\text{ Hz}$, 1H), 4.65 (app. ddt, $J_{d1} = 10.2\text{ Hz}$, $J_{d2} = 5.7\text{ Hz}$, $J_t = 1.4\text{ Hz}$, 2H), 2.05 (t, $J = 5.5\text{ Hz}$, 2H), 1.77-1.52 (m, 4H), 1.50 (s, 3H), 1.04 (s, 6H); ^{13}C NMR (75 MHz, CDCl_3): δ 153.5, 148.1, 131.8, 120.9, 119.1, 68.7, 39.4, 35.1, 31.4, 26.9, 19.3, 16.7; IR (NaCl/ CDCl_3): 2965, 2934, 2868, 2838, 1759, 1459, 1363, 1271, 1238,

1138, 1025, 993, 937 cm^{-1} ; HRMS-EI⁺ (m/z): $[M]^+$ calc'd for $\text{C}_{13}\text{H}_{20}\text{O}$, 224.1413; found, 224.1408.



Allyl Ketone (-)-75. A round bottom flask was flame-dried under argon and cycled into the glovebox. It was charged with $\text{Pd}_2(\text{dba})_3$ (242 mg, 0.264 mmol, 6.25 mol%) and $(S)\text{-}t\text{-Bu-PHOX } ((S)\text{-69})$ (256 mg, 0.661 mmol, 2.5 mol%). Then, THF (317 mL) was introduced. The red mixture was stirred for 20 min at 25 °C. Then, enol carbonate **100** (2.37 g, 10.57 mmol, 1.00 equiv) in THF (10 mL) was added. After the reaction was gauged complete using TLC analysis, it was removed from the glovebox, then concentrated. PhH (~20 mL) was added. After concentrating a second time, more PhH (~20 mL) was added. The solution was purified by flash chromatography on silica gel (2:98 Et_2O /hexane eluent), affording allyl ketone **(-)-75** (1.72 g, 94% yield) as a clear oil in 91% ee as determined by chiral HPLC analysis. R_f 0.48 (1:9 EtOAc /hexane), (I_2 /sand, brown spot); ^1H NMR (300 MHz, CDCl_3): δ 5.64 (dddd, $J = 17.1$ Hz, 10.5 Hz, 7.7 Hz, 6.9 Hz, 1H), 5.05 (app. ddt, $J_{d1} = 6.3$ Hz, $J_{d2} = 2.2$ Hz, $J_t = 1.1$ Hz, 1H), 4.98 (app. ddt, $J_{d1} = 13.8$ Hz, $J_{d2} = 2.5$ Hz, $J_t = 1.4$ Hz, 1H), 2.32 (app. ddt, $J_{d1} = 13.8$ Hz, $J_{d2} = 6.9$ Hz, $J_t = 1.4$ Hz, 1H), 2.16 (app. ddt, $J_{d1} = 13.8$ Hz, $J_{d2} = 6.9$ Hz, $J_t = 1.4$ Hz, 1H) 1.87-1.47 (m, 6H), 1.15 (s, 3H), 1.09 (s, 3H), 1.08 (s, 3H); ^{13}C NMR (75 MHz, CDCl_3): δ 219.8, 134.7, 118.0, 47.7, 44.6, 44.0, 39.9, 37.0, 28.0, 27.3, 25.7, 17.9; IR (NaCl/ CDCl_3): 3077, 2979,

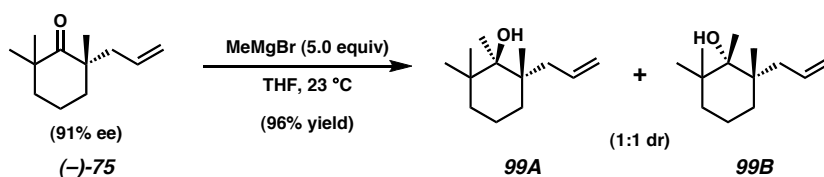
2964, 2933, 2869, 1697, 1463, 1382, 999, 914 cm^{-1} ; HRMS-EI⁺ (m/z): $[\text{M}]^+$ calc'd for $\text{C}_{12}\text{H}_{20}\text{O}$, 180.1514; found, 180.1506; $[\alpha]_{\text{D}}^{24} -36.3^\circ$ (c 0.140, CHCl_3), 91% ee.



Bicyclic Enone (-)-143. A round-bottom flask was charged with PdCl_2 (10 mg, 56 μmol), $\text{Cu(OAc)}_2\cdot\text{H}_2\text{O}$ (30 mg, 0.16 mmol), *N,N*-dimethylacetamide (3.0 mL), and water (0.5 mL). Then, allyl ketone (-)-75 (20 mg, 0.11 mmol) was introduced. The system was cooled to -78°C and evacuated with vacuum and back-filled with O_2 from a balloon (3 x). The mixture was warmed to 23°C and stirred vigorously for 40 h under a balloon of O_2 . The reaction was then diluted with H_2O (50 mL) and extracted with hexanes (3 x 25 mL). All organic phases were combined, dried (Na_2SO_4), filtered, and concentrated. The residue was purified by flash chromatography on silica gel (15:85 EtOAc:hexane eluent), affording a diketone as a clear oil, which was immediately used in the next reaction.

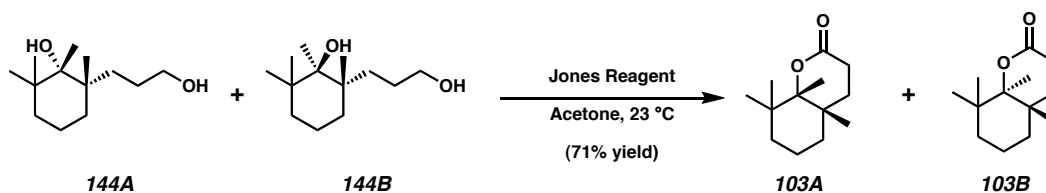
To a solution of this diketone (10 mg, 51 μmol) in xylenes (1.0 mL) was added freshly powdered KOH (3.0 mg, 54 μmol). The reaction was heated to 110°C for 16 h. The reaction was cooled to 23°C and directly loaded onto a preparative TLC plate (20:80 EtOAc/hexane eluent), affording bicyclic enone (-)-143 (yield not determined) as a clear, fragrant oil in 91% ee as determined by chiral HPLC assay. R_f 0.37 (1:4 EtOAc/hexane), (UV, 254 nm); mp $9\text{--}11^\circ\text{C}$ (Et_2O); ^1H NMR (300 MHz, CDCl_3): δ 5.82 (s, 1H), 2.29 (app. s, 2.29, 2H), 1.93 (app. dq, $J_d = 10.5$ Hz, $J_q = 2.8$ Hz, 1H), 1.83 (app. tt, $J = 13.5$ Hz, 3.3 Hz, 1H), 1.71–1.54 (m, 2H), 1.40 (app. ddd, $J = 12.4$ Hz, 8.0 Hz, 3.9 Hz, 1H),

1.36 (app. ddd, $J = 8.0$ Hz, 3.3 Hz, 2.0 Hz, 1H), 1.35 (s, 3H), 1.25 (s, 3H), 1.20 (s, 3H); ^{13}C NMR (75 MHz, CDCl_3): δ 208.1, 194.4, 126.4, 54.7, 44.3, 41.5, 40.6, 36.5, 31.3, 27.4, 26.2, 19.1; IR (NaCl/ CDCl_3): 2997, 2987, 2960, 2929, 2868, 2847, 1712, 1696, 1600, 1459, 1261, 1166 cm^{-1} ; HRMS- EI^+ (m/z): $[\text{M}]^+$ calc'd for $\text{C}_{12}\text{H}_{18}\text{O}$, 178.1358; found, 178.1356; $[\alpha]_{\text{D}}^{25} -87.2^\circ$ (c 0.280, CHCl_3), 91% ee.



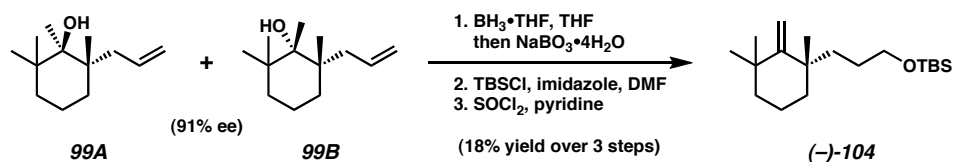
Alcohols 99A and 99B. A round-bottom flask was charged with a solution of allyl ketone **(-)-75** (1.02 g, 5.65 mmol, 1.00 equiv, 91% ee) and THF (55.5 mL). Then, methyl magnesium bromide (3.0 M in Et_2O , 9.25 mL, 27.8 mmol, 5.00 equiv) was gradually introduced at 23 °C. After 24 h, the reaction was carefully quenched at 0 °C with sat. aq NH_4Cl (30 mL). Then H_2O (50 mL) was added, along with hexanes (50 mL). The biphasic mixture was extracted with Et_2O (2 x 30 mL). All organic layers were combined, dried (Na_2SO_4), filtered, and concentrated. The wet residue was taken up in CHCl_3 and dried again with Na_2SO_4 , then filtered. The filtrate was concentrated, giving a 1:1 mixture of diastereomeric alcohols **99A** and **99B** (1.04 g, 94% yield) as a colorless oil. R_f 0.59 (10:90 EtOAc /hexane), (*p*-Anisaldehyde, violet spot); ^1H NMR (300 MHz, CDCl_3) (both diastereomers): δ 5.84 (app. dddd, $J = 19.4$ Hz, 14.6 Hz, 7.4 Hz, 7.2 Hz, 2H), 5.01 (app. d, $J = 11.1$ Hz, 2H), 5.00 (app. d, $J = 14.6$ Hz, 2H), 2.44 (app. ddd, $J = 12.6$ Hz, 11.1 Hz, 7.5 Hz, 2H), 2.07 (app. ddd, $J = 19.4$ Hz, 13.6 Hz, 7.7 Hz, 2H), 1.62-1.46 (m, 4H), 1.44-1.36 (m, 4H), 1.28-1.10 (m, 2H), 1.14 (app. s, 6H), 1.07 (s, 3H), 1.06 (s, 3H), 1.10 (s,

3H), 0.99 (s, 3H), 0.98-0.86 (m, 2H), 0.97 (s, 3H), 0.95 (s, 3H); ^{13}C NMR (75 MHz, CDCl_3) (both diastereomers): δ 136.8, 136.4, 117.0, 116.8, 78.2, 77.9, 43.8, 42.0, 41.6, 41.2, 39.2, 39.0, 37.2, 36.9, 33.6, 33.0, 28.3, 28.2, 26.6, 25.8, 22.9, 22.2, 18.6, 18.5, 18.3, 18.1; IR (NaCl/ CDCl_3): 3504 (broad), 3074, 2930, 2867, 1638, 1454, 1378, 1305, 1071, 998, 910 cm^{-1} ; HRMS-EI $^+$ (m/z): $[\text{M}]^+$ calc'd for $\text{C}_{13}\text{H}_{24}\text{O}$, 196.1827; found, 196.1803.



Lactones 103A and 103B. A round-bottom flask containing a mixture of diastereomeric diols **144A** and **144B** (50.0 mg, 0.234 mmol) was charged with acetone (ACS grade, 5 mL). Jones reagent (1.0 M aq CrO_3 and 4.0 M aq H_2SO_4) was added dropwise at 23 °C until a red coloration persisted. The reaction was carefully quenched with sat. aq Na_2SO_3 (excess), followed by 6 M aq HCl (10 mL). The reaction was then extracted with Et_2O (8 x 15 mL). All organic layers were combined, washed with brine (2 x 15 mL), dried (Na_2SO_4), filtered, and concentrated in vacuo, giving lactones **103A** and **103B** (34.7 mg, 71% combined yield) as a mixture of diastereomers that were not separated. The mixture is a yellow, fragrant oil. R_f 0.20 (20:80 EtOAc/hexane), (*p*-Anisaldehyde, blue spot); ^1H NMR (300 MHz, CDCl_3)(major diastereomer only): δ 2.71-2.42 (m, 2H), 2.07-1.84 (m, 1H), 1.72-1.63 (m, 1H), 1.58-1.26 (m, 3H), 1.33 (s, 3H), 1.26-0.95 (m, 3H), 1.12 (s, 3H), 1.05 (app. s, 6H); ^{13}C NMR (75 MHz, CDCl_3)(major diastereomer only): δ 172.4, 91.2, 39.0, 36.3, 35.3, 33.2, 32.6, 27.3, 26.1, 25.6, 24.9, 18.2, 17.8; IR (NaCl/ CDCl_3): 2934,

2874, 1770, 1732, 1463, 1398, 1382, 1349, 1274, 1254, 1175, 1112, 1073, 1047, 965 cm^{-1} ; HRMS-EI⁺ (m/z): $[\text{M}]^+$ calc'd for $\text{C}_{13}\text{H}_{22}\text{O}_2$, 210.1619; found, 210.1620.

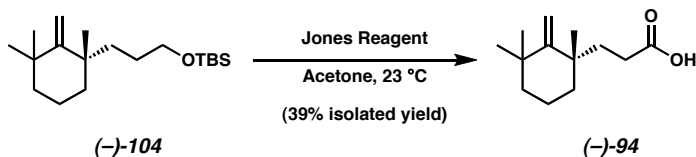


Methylene Cyclohexane (-)-104. A round-bottom flask containing a mixture of diastereomeric alcohols **99A** and **99B** (900 mg, 4.59 mmol, 1.00 equiv, 91% ee) and THF (25 mL) was cooled to 0 °C and treated with $\text{BH}_3\cdot\text{THF}$ (1.0 M in THF, 11.5 mL, 11.5 mmol, 2.5 equiv). The reaction was warmed to 23 °C and stirred for 6 h. Then the reaction was cooled to 0 °C, and H_2O (25 mL) was carefully added, followed by $\text{NaBO}_3\cdot 4\text{H}_2\text{O}$ (3.05 g, 19.82 mmol, 4.32 equiv). The biphasic reaction was stirred vigorously at 23 °C for 28 h and 6 M aq HCl (10 mL) was added. The reaction was diluted with hexanes, and the organic phase was collected. The aqueous layer was extracted with EtOAc (3 x 20 mL). All organic layers were combined, dried (Na_2SO_4), filtered, and concentrated. The residue was purified by flash chromatography on silica gel (10:90 EtOAc:hexane \rightarrow 30:70 EtOAc:hexane \rightarrow 50:50 EtOAc:hexane eluent), giving an oil containing two diastereomeric products, which was immediately used in the next reaction.

This mixture was transferred to a round-bottom flask, and imidazole (recrystallized, 344 mg, 5.05 mmol) was introduced, followed by a solution of TBSCl (726 mg, 4.82 mmol) in anhydrous, argon-degassed DMF (5.0 mL) at 23 °C. After 2.5 h, the reaction was diluted with H_2O (50 mL). The mixture was extracted with Et_2O (3 x 50

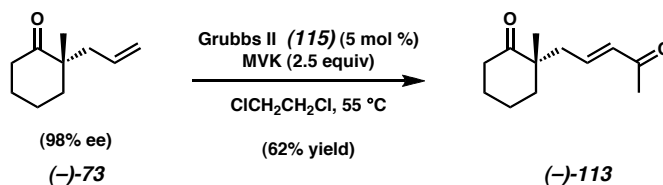
mL). All organic layers were combined, dried (Na_2SO_4), filtered, and concentrated. The residue was purified by flash chromatography on silica gel (10:90 EtOAc:hexane eluent), affording a diastereomeric mixture of silyl ethers. This composite was carried on to the next reaction without further characterization.

The mixture of silyl ethers was transferred to a round-bottom flask, which was charged with pyridine (freshly distilled from CaH_2 , 5.0 mL). After cooling to 0 °C, SOCl_2 (192 μL , 2.64 mmol) was slowly introduced. After 1 h, H_2O (50 mL) was carefully added, followed by Et_2O (50 mL). The organic phase was collected, and the aqueous layer was extracted with Et_2O (2 x 20 mL). All organic layers were combined, washed with 1.0 M aq CuSO_4 (6 x 10 mL), dried (Na_2SO_4), filtered, and concentrated. The residue was purified by flash chromatography on silica gel (1:99 Et_2O :hexane \rightarrow 5:95 Et_2O :hexane eluent), giving pure methylene cyclohexane (–)-**104** (306.3 mg, 18% yield from **99A** and **99B**) as a colorless oil. R_f 0.71 (10:90 EtOAc/hexane), (*p*-Anisaldehyde, blue spot); ^1H NMR (300 MHz, CDCl_3): δ 5.00 (app. s, 1H), 4.79 (app. s, 1H), 3.57 (app. t, J = 6.6 Hz, 2H), 1.80-1.64 (m, 2H), 1.62-1.16 (m, 8H), 1.11 (s, 3H), 1.10 (s, 3H), 1.04 (s, 3H), 0.89 (s, 9H), 0.04 (s, 6H); ^{13}C NMR (75 MHz, CDCl_3): δ 160.5, 108.7, 64.1, 41.8, 40.8, 39.4, 36.6, 36.5, 32.8, 29.9, 29.8, 28.4, 26.2 (3C), 18.7, 18.6, 5.0 (2C); IR (NaCl/ CDCl_3): 3100, 2955, 2929, 2858, 1623, 1472, 1382, 1361, 1255, 1100, 940, 900, 836, 774 cm^{-1} ; HRMS-EI $^+$ (m/z): $[\text{M}]^+$ calc'd for $\text{C}_{19}\text{H}_{38}\text{SiO}$, 310.2692; found, 310.2689. $[\alpha]_D^{24}$ –18.8° (c 1.90, CHCl_3), 91% ee.

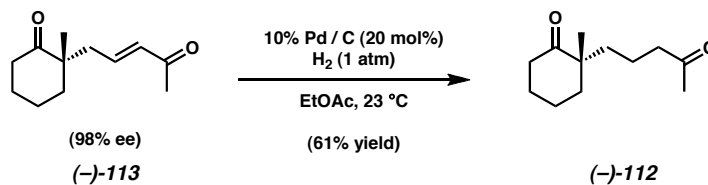


Carboxylic Acid (-)-94. A vessel containing methylene cyclohexane (-)-104 (90.2 mg, 0.291 mmol) was charged with acetone (ACS grade, 5.0 mL), then treated with Jones reagent (1.0 M CrO₃, 4.0 H₂SO₄ in H₂O)(1.0 mL, dropwise from a glass pipet) at 23 °C. After 10 min, the reaction was carefully quenched with sat. aq Na₂SO₃ (2 mL). CHCl₃ (10 mL) was added, followed by 6 M aq HCl (5.0 mL). After 10 min, the reaction was diluted with H₂O (15 mL) and extracted with CHCl₃ (3 x 25 mL). All organic layers were combined, dried (Na₂SO₄), filtered, and concentrated. The residue was purified by flash chromatography on silica gel (20:80 EtOAc:hexane eluent), giving carboxylic acid (-)-94 (24.1 mg, 39% yield) as a colorless oil. *R_f* 0.17 (10:90 EtOAc/hexane), (*p*-Anisaldehyde, blue spot); ¹H NMR (300 MHz, CDCl₃): δ 5.06 (app. s, 1H), 4.80 (app. s, 1H), 2.36-2.04 (m, 3H), 1.82-1.66 (m, 2H), 1.60-1.30 (m, 5H), 1.11 (s, 3H), 1.10 (s, 3H), 1.05 (s, 3H); ¹³C NMR (75 MHz, CDCl₃): δ 159.3, 109.6, 41.5, 40.6, 39.2, 36.5, 34.7, 32.7, 29.61, 29.56, 18.6; IR (NaCl/CDCl₃): 3000 (broad), 2927, 1708, 1462, 1414, 1380, 1296, 1095, 902 cm⁻¹; HRMS-EI⁺ (*m/z*): [M]⁺ calc'd for C₁₃H₂₂O, 210.1620; found, 210.1618. [α]_D²⁴ -27.8° (*c* 1.205, CHCl₃), 91% ee.

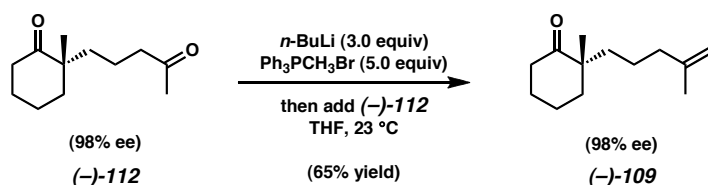
2.7.3 Syntheses of Compounds Related to Dysidiolide



Keto-Enone (–)-113. A vial was charged with allyl ketone (–)-73 (45.2 mg, 0.297 mmol, 1.0 equiv, 98% ee), followed by a solution of methyl vinyl ketone (61.8 μL , 0.743 mmol, 2.5 equiv) in 1,2-dichloroethane (1.5 mL). Then, Grubbs 2nd generation catalyst (12.6 mg, 14.9 μmol , 5 mol%) was added. The vessel was sealed and warmed to 55 $^\circ\text{C}$ for 24 h. The reaction transitioned from maroon to deep green. The reaction was cooled to 23 $^\circ\text{C}$ and concentrated. The residue was purified by flash chromatography on silica gel (hexane \rightarrow 20:80 EtOAc:hexane eluent), giving keto-enone (–)-113 (35.7 mg, 62% yield) as a pale brown oil. R_f 0.23 (20:80 EtOAc/hexane), (UV, 254 nm); ^1H NMR (300 MHz, CDCl_3): δ 6.70 (app. dt, $J_d = 15.9$ Hz, $J_t = 7.4$ Hz, 1H), 6.03 (app. d, $J = 15.9$ Hz, 1H), 2.50–2.26 (m, 2H), 2.40 (app. d, $J = 6.9$ Hz, 1H), 2.39 (app. d, $J = 6.9$ Hz, 1H), 2.22 (s, 3H), 1.91–1.81 (m, 2H), 1.80–1.60 (m, 4H), 1.12 (s, 3H); ^{13}C NMR (75 MHz, CDCl_3): δ 214.6, 198.4, 144.1, 134.2, 48.7, 41.0, 38.9, 38.7, 27.4, 26.9, 23.1, 21.1; IR (NaCl/ CDCl_3): 2935, 2866, 1704, 1672, 1626, 1426, 1361, 1254, 1124, 986 cm^{-1} ; HRMS- EI^+ (m/z): $[\text{M}]^+$ calc'd for $\text{C}_{12}\text{H}_{18}\text{O}_2$, 194.1307; found, 194.1336. $[\alpha]_D^{22} -1.14^\circ$ (c 1.415, CHCl_3), 98% ee.



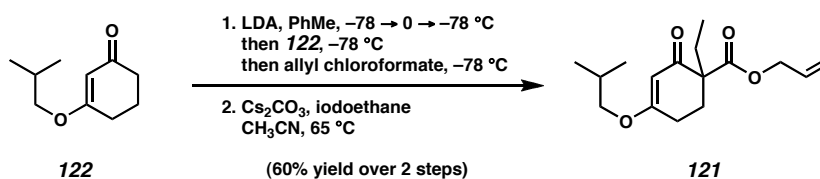
Diketone (-)-112. A round-bottom flask containing keto-enone (-)-113 (28.0 mg, 0.144 mmol, 1.0 equiv) in EtOAc (3.0 mL) was sparged with argon for 2 min. Pd/C (10% w/w) (30.6 mg, 28.8 μmol , 20 mol) was introduced, and the reaction was cooled to -78 $^\circ\text{C}$. It was purged/backfilled with vacuum/ H_2 (1 atm) (3 x) and warmed to 23 $^\circ\text{C}$ and stirred under H_2 (1 atm) for 12 h. More EtOAc (5 mL) was added, and the reaction was sparged with argon to remove residual H_2 . The material was filtered through a plug of silica gel with the aide of EtOAc. The filtrate was concentrated, affording diketone (-)-112 (17.3 mg, 61% yield) as a pale yellow oil. R_f 0.26 (20:80 EtOAc/hexane), (*p*-Anisaldehyde, peach spot); ^1H NMR (300 MHz, CDCl_3): δ 2.40 (app. t, $J = 6.6$ Hz, 2H), 2.36 (app. t, $J = 5.5$ Hz, 2H), 2.11 (s, 3H), 1.90-1.44 (m, 9H), 1.36 (app. d, $J = 7.7$ Hz, 1H), 1.15 (s, 3H); ^{13}C NMR (75 MHz, CDCl_3): δ 216.0, 208.8, 48.6, 44.0, 39.2, 38.9, 37.0, 30.1, 27.6, 22.7, 21.2, 18.2; IR (NaCl/ CDCl_3): 2936, 2865, 1705, 1452, 1360, 1167, 1123, 1099 cm^{-1} ; HRMS- EI^+ (m/z): $[\text{M}]^+$ calc'd for $\text{C}_{12}\text{H}_{20}\text{O}_2$, 196.1463; found, 196.1469. $[\alpha]_D^{22} -42.3^\circ$ (c 0.865, CHCl_3), 98% ee.



Keto-Olefin (-)-109. A round-bottom flask was charged with methyl triphenyl phosphonium bromide (weighed in glovebox, 260 mg, 0.688 mmol, 5.0 equiv). THF (5.5

mL) was introduced, followed by *n*-BuLi (2.5 M in hexane, 165 μ L, 0.413 mmol, 3.0 equiv) at 23 °C. After stirring for 1 h, a solution of diketone (–)-**112** (27.0 mg, 0.138 mmol, 1.0 equiv) in THF (2.0 mL) was added. 30 min later, the reaction was quenched with sat. aq NH₄Cl (4.0 mL). Then, the reaction was diluted with H₂O (20 mL) and hexane (15 mL). The biphasic mixture was extracted with EtOAc (4 x 20 mL). All organic layers were combined, dried (Na₂SO₄), filtered, and concentrated. The residue was purified by flash chromatography on silica gel (hexane \rightarrow 2:98 EtOAc:hexane eluent), giving keto-olefin (–)-**109** (17.3 mg, 65% yield) as a colorless oil. *R*_f 0.75 (20:80 EtOAc/hexane), (*p*-Anisaldehyde, blue spot); ¹H NMR (300 MHz, CDCl₃): δ 4.70 (app. s, 1H), 4.65 (app. s, 1H), 2.46-2.26 (m, 2H), 1.98 (app. t, *J* = 7.1 Hz, 2H), 1.94-1.84 (m, 1H), 1.82-1.50 (m, 5H), 1.68 (s, 3H), 1.47-1.39 (m, 1H), 1.38 (app. ddd, *J* = 26.4 Hz, 12.6 Hz, 4.1 Hz, 1H), 1.22-1.10 (m, 2H), 1.14 (s, 3H); ¹³C NMR (75 MHz, CDCl₃): δ 216.3, 145.7, 110.3, 48.7, 39.6, 39.0, 38.4, 37.2, 27.7, 22.8, 22.5, 21.7, 21.2; IR (NaCl/CDCl₃): 3074, 2936, 2865, 1707, 1650, 1452, 1376, 1260, 1096, 1020, 886, 804 cm⁻¹; HRMS-EI⁺ (*m/z*): [M]⁺ calc'd for C₁₃H₂₂O, 194.1671; found, 194.1680. [α]_D²¹ –49.8° (*c* 0.865, CHCl₃), 98% ee.

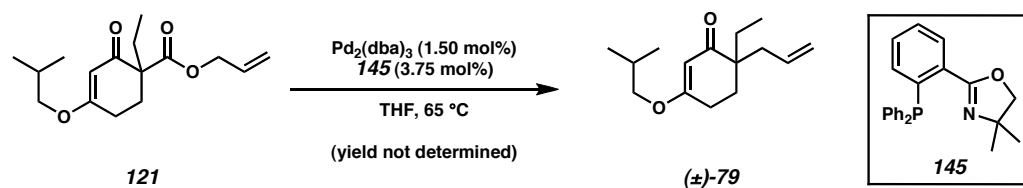
2.7.4 Syntheses of Compounds Related to Aspidospermine



α -Ethyl- α -Allyloxycarbonyl Vinylogous Ester 121. A round-bottom flask was flamedried under argon and charged with dry PhMe (320 mL). Then, *i*-Pr₂NH (12.81 mL, 91.3 mmol, 2.05 equiv) was introduced. The reaction was cooled to $-78 \text{ }^{\circ}\text{C}$, and *n*-BuLi (2.5 M in hexane, 35.68 mL, 89.2 mmol, 2.00 equiv) was added slowly. The reaction was warmed to $0 \text{ }^{\circ}\text{C}$ for 15 min, then promptly cooled back to $-78 \text{ }^{\circ}\text{C}$. Then, a solution of vinylogous acid **122** (7.50 g, 44.6 mmol, 1.00 equiv) in PhMe (20 mL) was added at $-78 \text{ }^{\circ}\text{C}$ over a 5 min period. After 40 min had passed, the reaction was treated with allyl chloroformate (4.97 mL, 46.8 mmol, 1.05 equiv) over a 5 min timeframe at $-78 \text{ }^{\circ}\text{C}$. After 15 min, the reaction was warmed to $23 \text{ }^{\circ}\text{C}$ and stirred for 1 h, during which the reaction went from yellow to orange. Then, 1.0 M aq KHSO₄ (127 mL) was added with vigorous stirring, causing the reaction to turn yellow. The organic phase was collected. The aqueous layer was extracted with Et₂O (2 x 50 mL). All organic layers were combined, dried (Na₂SO₄), filtered, and concentrated, giving a crude α -allyloxycarbonyl vinylogous ester as an orange oil, which was immediately used in the next reaction.

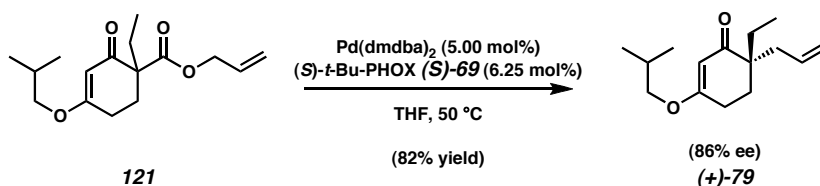
A round-bottom flask containing the crude vinylogous ester was charged with CH₃CN (45 mL), followed by iodoethane (14.26 mL, 178.4 mmol, 4.0 equiv relative to **122**). Anhydrous Cs₂CO₃ (29.06 g, 89.2 mmol, 2.0 equiv relative to **122**) was introduced, and the reaction was stirred vigorously at $65 \text{ }^{\circ}\text{C}$ for 12 h. The reaction was cooled to $23 \text{ }^{\circ}\text{C}$ and filtered over glass frits. The filtrate was concentrated in vacuo, and the residue

was purified by flash column chromatography on silica gel (hexane \rightarrow 15:85 EtOAc:hexane eluent), giving semipure **121**. The product-containing fractions were combined and concentrated, and the resulting residue was purified on a second silica gel flash column (5:95 EtOAc:CH₂Cl₂ eluent), giving pure α -ethyl- α -allyloxycarbonyl vinylogous ester **121** (7.47 g, 60% yield over 2 steps) as a yellow oil. R_f 0.44 (20:80 EtOAc/hexane), (*p*-Anisaldehyde, brownish-blue spot); ¹H NMR (300 MHz, CDCl₃): δ 5.83 (ddt, J_{d1} = 16.2 Hz, J_{d2} = 10.7 Hz, J_t = 5.7 Hz, 1H), 5.31 (s, 1H), 5.24 (app. ddd, J = 16.2 Hz, 2.9 Hz, 1.5 Hz, 1H), 5.15 (app. ddd, J = 10.7 Hz, 2.9 Hz, 1.5 Hz, 1H), 4.56 (app. dt, J_d = 5.4 Hz, J_t = 1.5 Hz, 2H), 3.54 (d, J = 6.7 Hz, 2H), 2.68-2.28 (m, 2H), 2.42-2.26 (m, 1H), 1.99 (dq, J_d = 22.2 Hz J_q = 7.4 Hz, 1H), 1.97-1.85 (m, 2H), 1.78 (dq, J_d = 22.2 Hz, J_q = 7.4 Hz, 1H), 0.92 (d, J = 6.9 Hz, 6H), 0.86 (t, J = 7.4 Hz, 3H); ¹³C NMR (75 MHz, CDCl₃): δ 195.8, 176.8, 171.6, 131.9, 118.2, 102.2, 74.9, 65.5, 56.3, 27.77, 27.76, 27.0, 26.4, 19.1, 9.1; IR (NaCl/CDCl₃): 3083, 2963, 2939, 2879, 1731, 1664, ,1610, 1470, 1384, 1236, 1195, 1178, 1119, 998, 919 cm⁻¹; HRMS-EI⁺ (m/z): [M]⁺ calc'd for C₁₆H₂₄O₄, 280.1687; found, 280.1687.



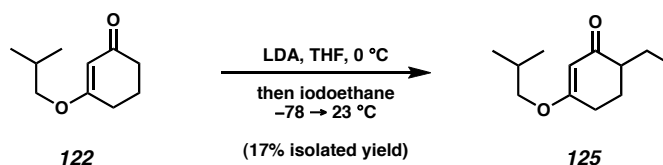
Racemic Allyl Vinylogous Ester (±)-79. In the glovebox, a vial was charged with Pd₂(dba)₃ (2.5 mg, 2.68 μmol, 1.50 mol%), then removed from the glovebox. Phosphinooxazoline **145** (2.4 mg, 6.71 μmol, 3.75 mol%) was then added, followed by THF (800 μL). The reaction was stirred for 30 min at 23 °C. Then, a solution of

α -ethyl- β -allyloxycarbonyl vinylogous ester **120** (50.0 mg, 0.179 mmol, 1.00 equiv) in THF (1.0 mL) was introduced. The vial was sealed and heated to 65 °C for 24 h. The reaction was cooled to 23 °C and split into two portions. Both portions were concentrated and purified on separate preparative silica gel TLC plates (20:80 EtOAc:hexane eluent), giving racemic allyl vinylogous ester (\pm)-**79** (yield not determined) as a colorless oil. The material was used for chiral HPLC assay development. Characterization is reported on pages 52 and 53 below.



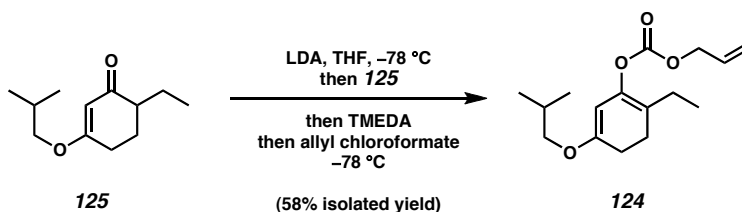
Allyl Vinylogous Ester (+)-79 (86% ee). In the glovebox, a flamedried round-bottom flask was charged with Pd(dmdba)₂ (40.8 mg, 50.0 μ mol, 5.00 mol%) and (*S*)-*t*-butyl phosphinooxazoline (24.2 mg, 62.5 μ mol, 6.25 mol%) and removed from the glovebox. THF (30 mL) was added, and the reaction stirred at 23 °C for 30 min. Then, a solution of α -ethyl- β -allyloxycarbonyl vinylogous ester **121** (280 mg, 1.00 mmol, 1.00 equiv) in THF (3.0 mL) was added. The reactor was quickly fitted with a reflux condenser, and the reaction was heated to 50 °C under N₂ for 24 h. During this time the reaction went from orange to green. The reaction was cooled to 23 °C and concentrated. The residue was purified by flash chromatography on silica gel (hexane \rightarrow 5:95 EtOAc:hexane eluent), giving allyl vinylogous ester (+)-**79** (193.4 mg, 82% yield) in 86% ee (as determined by chiral HPLC assay) as a yellow oil. *R*_f 0.58 (20:80 EtOAc/hexane), (UV, 254 nm); ¹H NMR (300 MHz, CDCl₃): δ 5.73 (app. dddd, *J* = 17.0 Hz, 10.5 Hz, 7.7 Hz, 6.9 Hz, 1H), 5.24 (s, 1H), 5.08-5.04 (m, 1H), 5.04-5.00 (m, 1H), 3.57 (d, *J* = 6.6 Hz, 2H), 2.42 (app.

td, $J_t = 6.6$ Hz, $J_d = 2.5$ Hz, 2H), 2.38 (app. dd, $J = 14.0$ Hz, 7.1 Hz, 1H), 2.19 (app. dd, $J = 14.0$ Hz, 7.1 Hz, 1H), 1.85 (app. t, $J = 6.6$ Hz, 2H), 2.01 (app. septuplet, $J = 6.6$ Hz, 1H), 1.61 (dq, $J_d = 22.2$ Hz, $J_q = 7.4$ Hz, 1H), 1.55 (dq, $J_d = 22.2$ Hz, $J_q = 7.4$ Hz, 1H), 0.97 (d, $J = 6.6$ Hz, 6H), 0.84 (t, $J = 7.4$ Hz, 3H); ^{13}C NMR (75 MHz, CDCl_3): δ 203.0, 176.0, 134.8, 117.8, 102.0, 74.8, 46.6, 39.4, 29.0, 27.9, 27.6, 25.8, 19.2, 8.5; IR (NaCl/ CDCl_3): 3074, 2963, 2936, 2878, 1652, 1612, 1384, 1193, 1178, 1003 cm^{-1} ; HRMS-EI $^+$ (m/z): $[\text{M}]^+$ calc'd for $\text{C}_{15}\text{H}_{24}\text{O}_2$, 236.1776; found, 236.1788. $[\alpha]_D^{24} +10.4^\circ$ (c 0.675, CHCl_3), 86% ee.



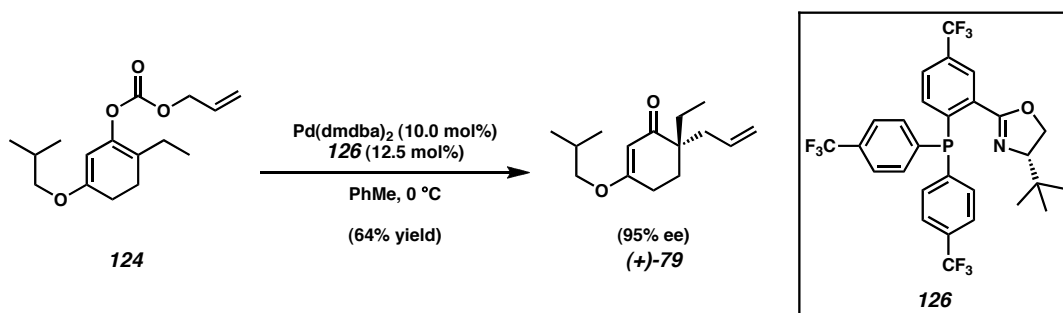
Ethyl Vinylogous Ester 125. A round-bottom flask was charged with THF (90 mL), and $i\text{-Pr}_2\text{NH}$ (4.55 mL, 32.7 mmol, 1.10 equiv) was introduced. The reaction was cooled to 0 $^\circ\text{C}$, and $n\text{-BuLi}$ (2.5 M in hexane, 12.48 mL, 31.2 mmol, 1.05 equiv) was added slowly. 30 min later, a solution of vinylogous ester **122** (5.00 g, 29.7 mmol, 1.00 equiv) in THF (10 mL) was introduced. After 1 h, the reaction was cooled to -78°C , and iodoethane (4.75 mL, 59.4 mmol, 2.00 equiv) was rapidly added. The reaction was allowed to warm to 23 $^\circ\text{C}$ over 4 h, during which it turned deep orange. The reaction was then quenched with sat. aq NH_4Cl (20 mL). Then, the reaction was diluted with H_2O (50 mL) and hexane (30 mL). The organic phase was collected, and the aqueous layer extracted with EtOAc (2 x 30 mL). All organic layers were combined, dried (Na_2SO_4), filtered, and concentrated. The residue was purified by flash chromatography on silica gel (5:95 EtOAc:hexane \rightarrow 20:80 EtOAc:hexane eluent), giving two sets of fractions. The first

contained impure **125** (which was not factored into the yield calculation), but the second set was combined and concentrated, affording pure ethyl vinylogous ester **125** (1.00 g, 17% isolated yield) as a pale yellow oil. R_f 0.43 (20:80 EtOAc/hexane), (UV, 254 nm); ^1H NMR (300 MHz, CDCl_3): δ 5.23 (s, 1H), 3.42 (d, $J = 6.6$ Hz, 2H), 2.37 (app. t, $J = 6.2$ Hz, 2H), 2.10-1.96 (m, 2H), 1.98 (septuplet, $J = 6.6$ Hz, 1H), 1.88-1.72 (m, 1H), 1.76-1.60 (m, 1H), 1.38 (app. dq, $J_d = 22.2$ Hz $J_q = 7.4$ Hz, 1H), 0.91 (d, $J = 6.6$ Hz, 6H), 0.88 (t, $J = 7.4$ Hz, 3H); ^{13}C NMR (75 MHz, CDCl_3): δ 210.6, 177.0, 102.3, 74.7, 46.6, 27.9, 27.8, 25.7, 22.5, 19.1, 11.5; IR (NaCl/ CDCl_3): 2961, 2875, 1659, 1610, 1470, 1384, 1368, 1239, 1222, 1194, 990 cm^{-1} ; HRMS- EI^+ (m/z): $[\text{M}]^+$ calc'd for $\text{C}_{12}\text{H}_{20}\text{O}_2$, 196.1463; found, 196.1461.



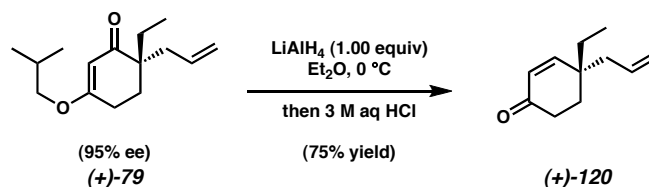
Enol Carbonate 124. A flamedried round-bottom flask under argon was charged with THF (28 mL), and $i\text{-Pr}_2\text{NH}$ (858 μL , 6.12 mmol, 1.20 equiv) was introduced. The reaction was cooled to 0 $^\circ\text{C}$, and $n\text{-BuLi}$ (2.5 M in hexane, 2.20 mL, 5.51 mmol, 1.08 equiv) was added slowly. After 30 min, the reaction was cooled to -78°C , and a solution of ethyl vinylogous ester **125** (1.00 g, 5.10 mmol, 1.00 equiv) in THF (3.0 mL) was added dropwise. After 30 min, TMEDA (918 μL , 6.12 mmol, 1.20 equiv) was added slowly below the solvent interface. Once 1 h had passed, a solution of allyl chloroformate (595 μL , 5.61 mmol, 1.10 equiv) in THF (3.0 mL) was added slowly below the solvent level. White precipitate began to form and the reaction was yellow. After 35 min,

conversion had reached 65% (as determined by ^1H NMR), and sat. aq NaHCO_3 (20 mL) was added at -78°C . The reaction was warmed to 23°C and diluted with hexanes (30 mL) and H_2O (30 mL). The organic phase was collected. The aqueous layer was extracted with EtOAc (3 x 30 mL). All organic layers were combined, dried (Na_2SO_4), filtered, and concentrated. The residue was concentrated from PhH, and then purified by rapid flash chromatography on florisil (5:95 EtOAc:hexane eluent), giving enol carbonate **124** (823 mg, 59% yield, 89% yield based on starting material consumption) as a yellow oil. R_f 0.65 (20:80 EtOAc/hexane), (UV, 254 nm); ^1H NMR (300 MHz, CDCl_3): δ 5.95 (app. ddt, $J_{d1} = 17.1$ Hz, $J_{d2} = 10.4$ Hz, $J_t = 5.8$ Hz, 1H), 5.37 (app. d, $J = 17.1$ Hz, 1H), 5.27 (app. d, $J = 10.4$ Hz, 1H), 4.72 (s, 1H), 4.65 (app. d, $J = 5.8$ Hz, 2H), 3.44 (d, $J = 6.6$ Hz, 2H), 2.30 (app. t, $J = 4.4$ Hz, 1H), 2.04 (app. q, $J = 7.4$ Hz, 2H), 1.94 (septuplet, $J = 6.6$ Hz, 1H), 0.95 (t, $J = 7.4$ Hz, 3H), 0.92 (d, $J = 6.6$ Hz, 6H); ^{13}C NMR (75 MHz, CDCl_3): δ 158.3, 153.6, 140.1, 131.6, 119.1, 117.1, 91.8, 74.0, 68.8, 28.0, 27.3, 25.7, 22.4, 19.4, 12.4; IR (NaCl/ CDCl_3): 3086, 2963, 2936, 2876, 2832, 1759, 1677, 1635, 1471, 1383, 1368, 1244, 1200, 1156, 1120, 1090, 1042, 993, 948 cm^{-1} ; HRMS-EI $^+$ (m/z): $[\text{M}]^+$ calc'd for $\text{C}_{16}\text{H}_{24}\text{O}_4$, 280.1675; found, 280.1676.



Allyl Vinylogous Ester (+)-79 (95% ee). A flamedried round-bottom flask in the glovebox was charged with Pd(dmdba)_2 (40.8 mg, 50.0 μmol , 10.0 mol%) and

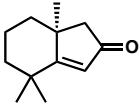
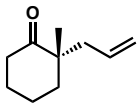
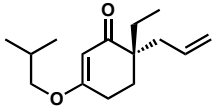
phosphinooxazoline **126** (37.0 mg, 62.5 μ mol, 12.5 mol%) and removed from the glovebox. PhMe (14.7 mL) was introduced, and the reaction was stirred at 23 °C for 30 min and cooled to 0 °C. A solution of enol carbonate **124** (140 mg, 0.5 mmol, 1.00 equiv) in PhMe (2.0 mL) was introduced. After 9 h, the reaction was concentrated in vacuo to a total volume of ~3 mL, and the solution was directly loaded onto a silica gel flash column, then purified chromatographically (5:95 EtOAc:hexane eluent), giving allyl vinylogous ester **(+)-79** (75.1 mg, 64% yield) as a yellow oil in 95% ee as determined by chiral HPLC assay. $[\alpha]_D^{24} +10.7^\circ$ (*c* 1.502, CHCl₃), 95% ee. Other characterization data can be found on pages 52 and 53 above.



γ -Ethyl- γ -Allyl Enone **(+)-120.** A round-bottom flask was charged with allyl vinylogous ester **(+)-79** (50.0 mg, 0.212 mmol, 95% ee, 1.00 equiv), and the reactor was purged with vacuum/argon (1 x). Et₂O (10.0 mL) was introduced, and the reaction was cooled to 0 °C. LiAlH₄ (8.0 mg, 0.212 mmol, 1.00 equiv) was then added, and the reaction was stirred for 1 h. The 3 M aq HCl (10.0 mL) was very cautiously added at 0 °C. Once the addition was complete, the reaction was warmed to 23 °C and stirred vigorously for 5 h. The reaction was transferred to a separatory funnel and extracted with Et₂O (3 x 10 mL). All organic layers were combined, dried (Na₂SO₄), filtered, and concentrated. The residue, which contained some H₂O, was dissolved in CHCl₃ and dried with Na₂SO₄. The mixture was filtered, and the filtrate was concentrated, affording γ -ethyl- γ -allyl enone **(+)-120**

(26.2 mg, 75% yield) as a colorless, volatile oil. R_f 0.57 (20:80 EtOAc/hexane), (UV, 254 nm) ^1H NMR (300 MHz, CDCl_3): δ 6.69 (d, $J = 10.4$ Hz, 1H), 5.91 (d, $J = 10.4$ Hz, 1H), 5.74 (app. ddt, $J_{d1} = 16.7$ Hz, $J_{d2} = 9.9$ Hz, $J_t = 7.4$ Hz, 1H), 5.10 (app. d, $J = 9.9$ Hz, 1H), 5.08 (app. d, $J = 16.7$ Hz, 1H), 2.42 (app. t, $J = 6.9$ Hz, 2H), 2.21 (app. d, $J = 7.4$ Hz, 2H), 1.86 (app. t, $J = 6.9$ Hz, 2H), 1.53 (dq, $J_d = 22.2$ Hz, $J_q = 7.4$ Hz, 1H), 1.47 (dq, $J_d = 22.2$ Hz, $J_q = 7.4$ Hz, 1H), 0.90 (t, $J = 7.4$ Hz, 3H); ^{13}C NMR (75 MHz, CDCl_3): δ 199.9, 158.3, 133.7, 128.4, 118.7, 41.9, 38.7, 34.0, 30.6, 30.4, 8.5; IR (NaCl/ CDCl_3): 3077, 2966, 2929, 2880, 1682, 1452, 1387, 916, 800 cm^{-1} ; HRMS- EI^+ (m/z): $[\text{M}]^+$ calc'd for $\text{C}_{11}\text{H}_{16}\text{O}$, 164.1201; found, 164.1207. $[\alpha]^{25}_{\text{D}} +27.5^\circ$ (c 0.524, CHCl_3), 95% ee.

2.7.5 Methods for the Determination of Enantiomeric Excess

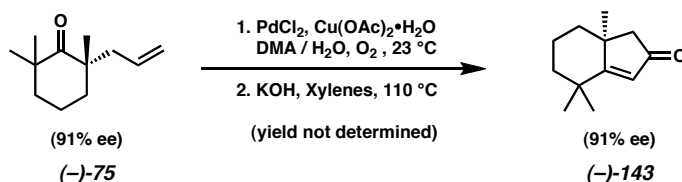
Entry	Substrate	Assay	Column	Method	Retention Time (min)	
1.	 (S)-(-)-143	Enantiomeric Excess	Chiral HPLC	3%EtOH/Hex monitor@254nm	Minor (R)	9.1
			Chiralcel AD Column	20 min	Major (S)	10.2
2.	 (S)-(-)-73	Enantiomeric Excess	Chiral GC	100 °C isotherm	Major (S)	11.1
			Agilent GT-A Column	40 min	Minor (R)	12.7
3.	 (S)-(+)-79	Enantiomeric Excess	Chiral HPLC	2%EtOH/Hex monitor@254nm	Major (S)	7.4
			Chiralcel OD Column	20 min	Minor (R)	8.2

2.8 Notes and Citation

- (1) For reviews on catalytic enantioselective methods for quaternary stereocenter generation, see: (a) Corey, E. J.; Guzman-Perez, A. *Angew. Chem., Int. Ed.* **1998**, *37*, 388-401. (b) Christoffers, J.; Mann A. *Angew. Chem., Int. Ed.* **2001**, *40*, 4591-4597. (c) Douglas, C. J.; Overman, L. E. *Proc. Natl. Acad. Sci. U.S.A.* **2004**, *101*, 5363-5367.
- (2) For a review of enantioselective decarboxylative alkylations, see: Mohr, J. T.; Stoltz, B. M. *Chem. Asian J.* **2007**, (In Press: DOI: 10.1002/asia.200700183).
- (3) Behenna, D. C.; Stoltz, B. M. *J. Am. Chem. Soc.* **2004**, *126*, 15044-15045.
- (4) Mohr, J. T.; Behenna, D. C.; Harned, A. M.; Stoltz, B. M. *Angew. Chem., Int. Ed.* **2005**, *44*, 6924-6927.
- (5) The famous Japanese building Konjiki-do, a structure within the Chuson-ji Temple of Iwate Prefecture, was constructed of wood from *Thujopsis dolabrata*. It is speculated that the terpenes in the wood oil, which have antifungal and insecticidal properties, have preserved the wood. For this reason, the temple lasted around 840 years without significant restoration. For an account, see: Yoshihiko, I.; Yasuhiro, M.; Yoshikazu, S.; Toshihoro, O.; Nakao, I. *Biocontrol science* **2006**, *11*, 49-54.
- (6) Mayurone was originally isolated from *Mayur pankhi*, see: (a) Chetty, G. L.; Dev, S. *Tetrahedron Lett.* **1965**, *6*, 3773-3776. It was later found in *Thujopsis dolabrata*, see: (b) Ito, S.; Endo, K.; Honma, H.; Ota, K. *Tetrahedron Lett.* **1965**, *6*, 3777-3781.
- (7) α -Cadinol has been implicated as an active contributor to the disease-resistance of *Thujopsis dolabrata*, see: Yatagai, M. *Aroma Res.* **2007**, *8*, 88-93.

-
- (8) (a) Yano, M. *J. Soc. Chem. Ind. Jpn.* **1913**, *16*, 443. (b) Uchida, S. *J. Soc. Chem. Ind. Jpn.* **1928**, *31*, 501.
- (9) (a) Miyazaki, Y. *Mokuzai Gakkaishi* **1996**, *42*, 624-626. (b) Yatagai, M. *Curr. Top. Phytochem.* **1997**, *1*, 85-97. (c) Hiramatsu, Y.; Miyazaki, Y. *J. Wood. Sci.* **2001**, *47*, 13-17.
- (10) For the establishment of the relative stereochemistry of thujopsene, see: (a) Nozoe, T.; Takeshita, H.; Ito, S.; Ozeki, T.; Seto, S. *Chem. Pharm. Bull.* **1960**, *8*, 936-938. (b) Norin, T. *Acta Chem. Scand.* **1961**, *15*, 1676-1694. (c) Sisido, K.; Nozaki, H.; Imagawa, T. *J. Org. Chem.* **1961**, *26*, 1964-1967. (d) Norin, T. *Acta Chem. Scand.* **1963**, *17*, 738-748.
- (11) (a) Dauben, W. G.; Ashcraft, A. C. *J. Am. Chem. Soc.* **1963**, *85*, 3673-3676. (b) Beuchi, G.; White, J. D. *J. Am. Chem. Soc.* **1964**, *86*, 2884-2887. (c) Anderson, P. L. Use of Cyclopropyl Intermediates in Angular Methylation and a Total Synthesis of dl-Thujopsene. Ph. D. Dissertation, University of Michigan, Ann Arbor, MI, USA, **1967**. (d) Mori, K.; Ohki, M.; Kobayashi, A.; Matsui, M. *Tetrahedron*, **1970**, *26*, 2815-2819. (e) McMurry, J. E.; Blaszcak, L. C. *J. Org. Chem.* **1974**, *39*, 2217-2222. (f) Branca, S. J.; Lock, R. L.; Smith, A. B., III *J. Org. Chem.* **1977**, *42*, 3165-3168.
- (12) (a) Johnson, C. R.; Barbachyn, M. R. *J. Am. Chem. Soc.* **1982**, *104*, 4290-4291. (b) Lee, E.; Shin, I.-J.; Kim, T.-S. *J. Am. Chem. Soc.* **1990**, *112*, 260-264.
- (13) Srikrishna, A.; Anebuselvy, K. *J. Org. Chem.* **2001**, *66*, 7102-7106.

(14) The determination of the enantiomeric excess of the allylketone was achieved by a 2-step derivatization to the bicyclic enone **(-)-143**:



(15) It was advantageous to run the reaction in a glovebox. See supporting information for details.

(16) Gunasekera, S. P.; McCarthy, P. J.; Kelly-Borges, M. *J. Am. Chem. Soc.* **1996**, *118*, 8759-8760.

(17) (a) Millar, J. B. A.; Russel, P. *Cell* **1992**, *68*, 407-410. (b) Barrate, B.; Meijer, L.; Galaktionov, K.; Beach, D. *Anticancer Res.* **1992**, *12*, 873-880.

(18) (a) Corey, E. J.; Roberts, B. E. *J. Am. Chem. Soc.* **1997**, *119*, 12425-12431. (b) Roberts, B. E. The Enantioselective Total Synthesis of the Marine Terpenes Fuscol and Dysidiolide. Ph. D. Dissertation, Harvard University, Cambridge, MA, USA, **1997**. (c) Boukouvalas, J.; Cheng, Y.-X.; Robichaud, J. *J. Org. Chem.* **1998**, *63*, 228-229. (d) Magnuson, S. R.; Sepp-Lorenzino, L.; Rosen, N.; Danishefsky, S. J. *J. Am. Chem. Soc.* **1998**, *120*, 1615-1616. (e) Miyaoka, H.; Kajiwara, Y.; Yamada, Y. *Tetrahedron Lett.* **2000**, *41*, 911-914. (f) Takahashi, M.; Dodo, K.; Hashimoto, Y.; Shirai, R. *Tetrahedron Lett.* **2000**, *41*, 2111-2114. (g) Demeke, D.; Forsyth, C. *Org. Lett.* **2000**, *2*, 3967-3969. (h) Miyaoka, H.; Kajiwara, Y.; Hara, Y.; Yamada, Y. *J. Org. Chem.* **2001**, *66*, 1429-1435. (i) Nishimura, N. I. Total Synthesis of Dysidiolide. II. [2+2] to [4+2] Rearrangements. Ph. D. Dissertation, University of California, Los

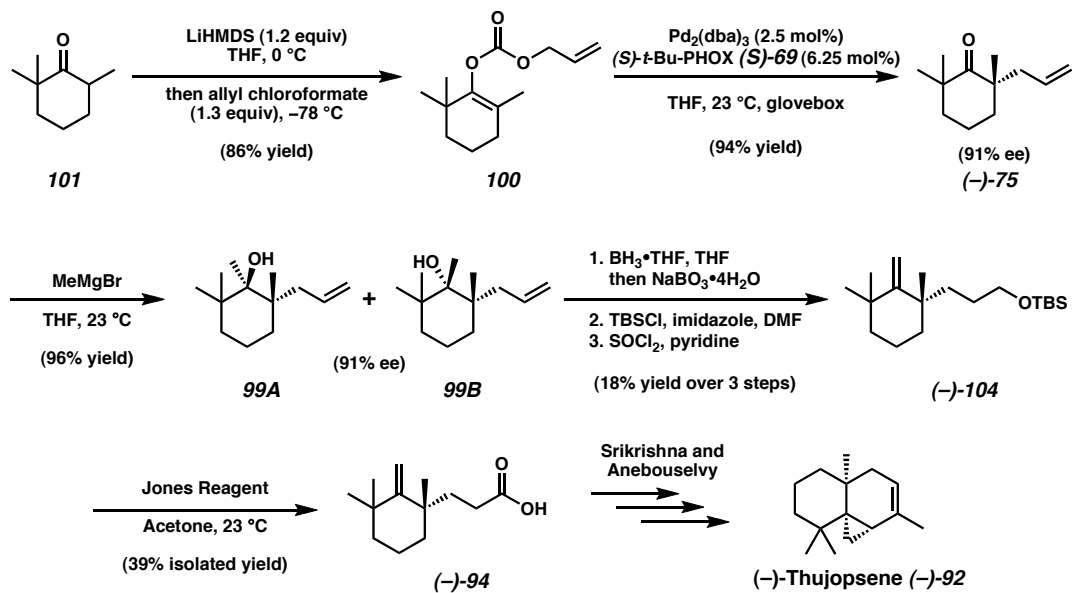
-
- Angeles, CA, USA, **2001**. (j) Miyaoka, H.; Yamada, Y. *Bull. Chem. Soc. Jpn.* **2002**, *75*, 203-222. (k) Demeke, D.; Forsyth, C. J. *Tetrahedron* **2002**, *58*, 6531-6544. (l) Caille, S. Enantioselective Syntheses of the Sesterterpenoid (–)-Dysidiolide and Structurally Related Analogues. Ph. D. Dissertation, University of British Columbia, Vancouver, BC, Canada, **2002**. (m) Demeke, D. Total Synthesis of Dysidiolide and Cacospongionolide F: A General Approach to the Synthesis of Labadane, Isolabadane, and Clerodane Polyterpenes. Ph. D. Dissertation, Univ. of Minnesota, Minneapolis, MN, USA, **2003**.
- (19) An enantioselective formal total synthesis of (–)-dysidiolide ((–)-**150**) has also been reported, see: Jung, M. E.; Nishimura, N. *Org. Lett.* **2001**, *3*, 2113-2115.
- (20) The side products appeared to arise via intramolecular aldol condensation:
- CC(=O)CCC1CCCCC1=O $\xrightarrow{\text{Base}}$ CC(=O)C1=CC2CCCCC2C1
 (-)-112 i
- (21) Saxton, J. E. In *The Alkaloids*; Cordell, G. A., Ed.; Academic Press: New York, **1998**; Vol. 51, Chapter 1.
- (22) Stork, G.; Dolfini, J. E. *J. Am. Chem. Soc.* **1963**, *85*, 2872-2873.
- (23) Ban, Y.; Sato, Y.; Inoue, I.; Nagai, M.; Oishi, T.; Terashima, M.; Yonematsu, O.; Kanaoka, Y. *Tetrahedron Lett.* **1965**, *6*, 2261-2268.
- (24) Lawton, G.; Saxton, J. E.; Smith, A. J. *Tetrahedron* **1977**, *33*, 1641-1653.
- (25) Meyers, A. I.; Berney, D. *J. Org. Chem.* **1989**, *54*, 4673-4676.
- (26) Stork, G.; Danheiser, R. L. *J. Org. Chem.* **1973**, *38*, 1775-1776.
- (27) Unreacted starting material (**125**) could be recovered at the end of the reaction.

-
- (28) Takano, S.; Sato, T.; Inomata, K.; Ogasawara, K. *J. Chem. Soc., Chem. Commun.* **1991**, 7, 462-464.
- (29) Cho, Y. S.; Carcache, D. A.; Tian, Y.; Li, Y.-M.; Danishefsky, S. J. *J. Am. Chem. Soc.* **2004**, 126, 14358-14359.
- (30) Gao, X.; Matsuo, Y.; Snider, B. B. *Org. Lett.* **2006**, 8, 2123-2126.
- (31) Jung, M. E.; Murakami, M. *Org. Lett.* **2007**, 9, 461-463.
- (32) Yang, L.; Williams, D. E.; Mui, A.; Ong, C.; Krystal, G.; van Soest, R.; Andersen, R. *J. Org. Lett.* **2005**, 7, 1073-1076.
- (33) Roldán, E. A.-M.; Santiago, J. L. R.; Chahboun, R. *J. Nat. Prod.* **2006**, 69, 563-566.
- (34) (a) Peer, M.; de Jong, J. C.; Kiefer, M.; Langer, T.; Riech, H.; Schell, H.; Sennhenn, P.; Sprinz, J.; Steinhagen, H.; Wiese, B.; Helmchen, G. *Tetrahedron* **1996**, 52, 7547-7583. (b) Tani, K.; Behenna, D. C.; McFadden, R. M.; Stoltz, B. M. *Org. Lett.* **2007**, 9, 2529-2931.
- (35) When a subscript is shown with the coupling constant, it indicates what type of splitting the constant is associated with. For example (td, $J_t = 5.0$ Hz, $J_d = 3.3$ Hz, 1H) indicates that the triplet splitting has a 5.0 Hz coupling constant and the doublet has a 3.3 Hz coupling constant.

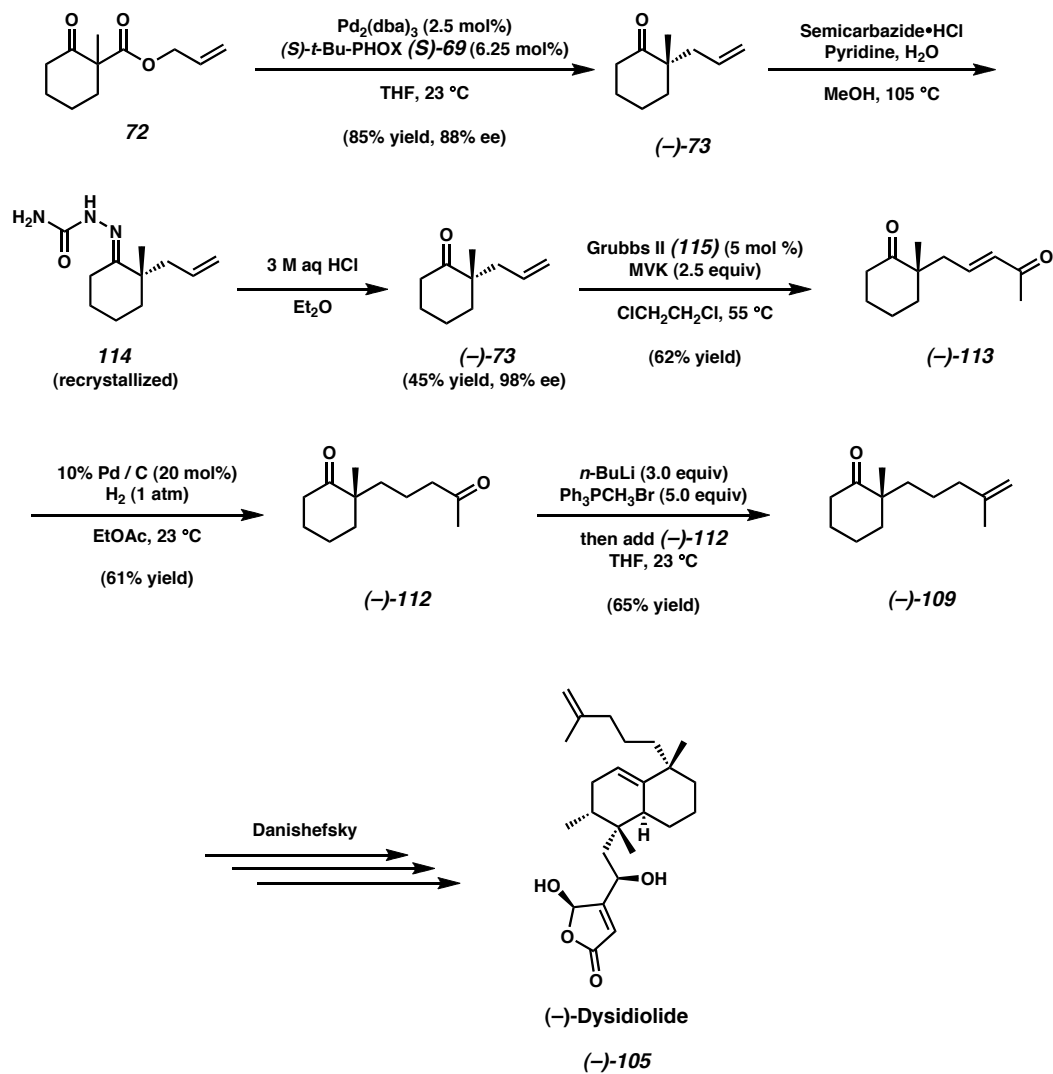
Appendix ONE

Synthetic Summaries of the Formal Total Syntheses of (-)-Thujopsene, (-)-Dysidiolide, and (-)-Aspidospermine

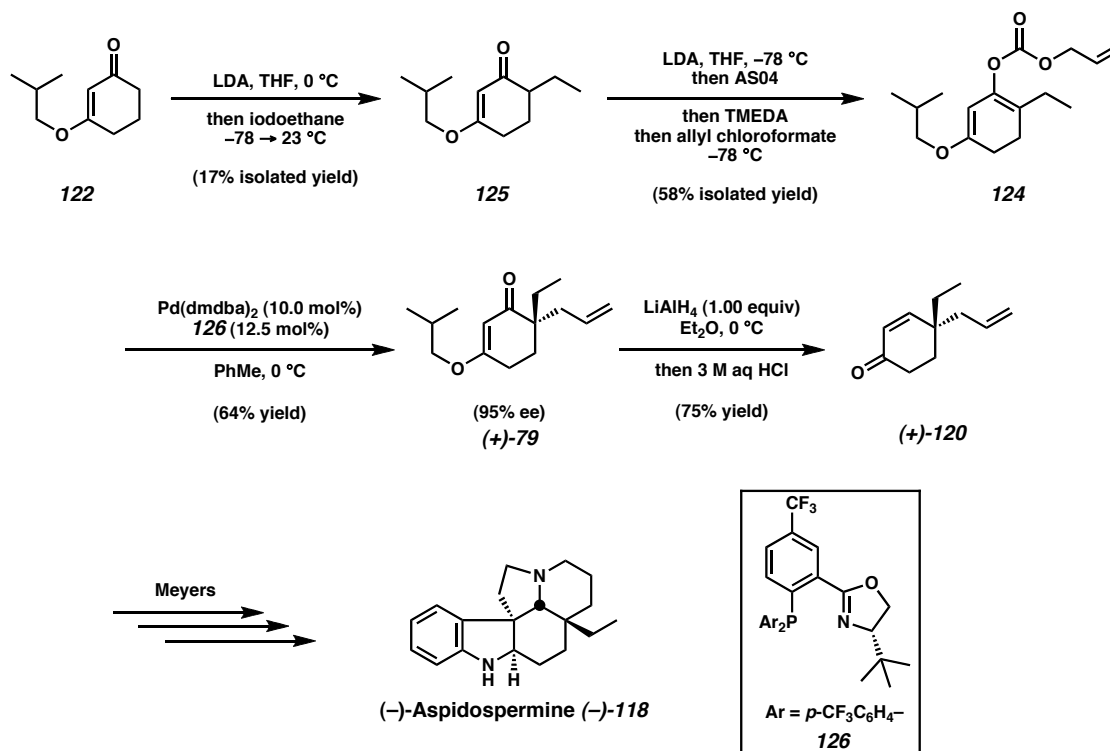
Scheme A1.1 Formal Total Synthesis of Thujopsene



Scheme A1.2 Formal Total Synthesis of Dysidiolide



Scheme A1.3 Formal Total Synthesis of Aspidospermine



Appendix TWO

Spectra of Compounds Relevant to Chapter 2

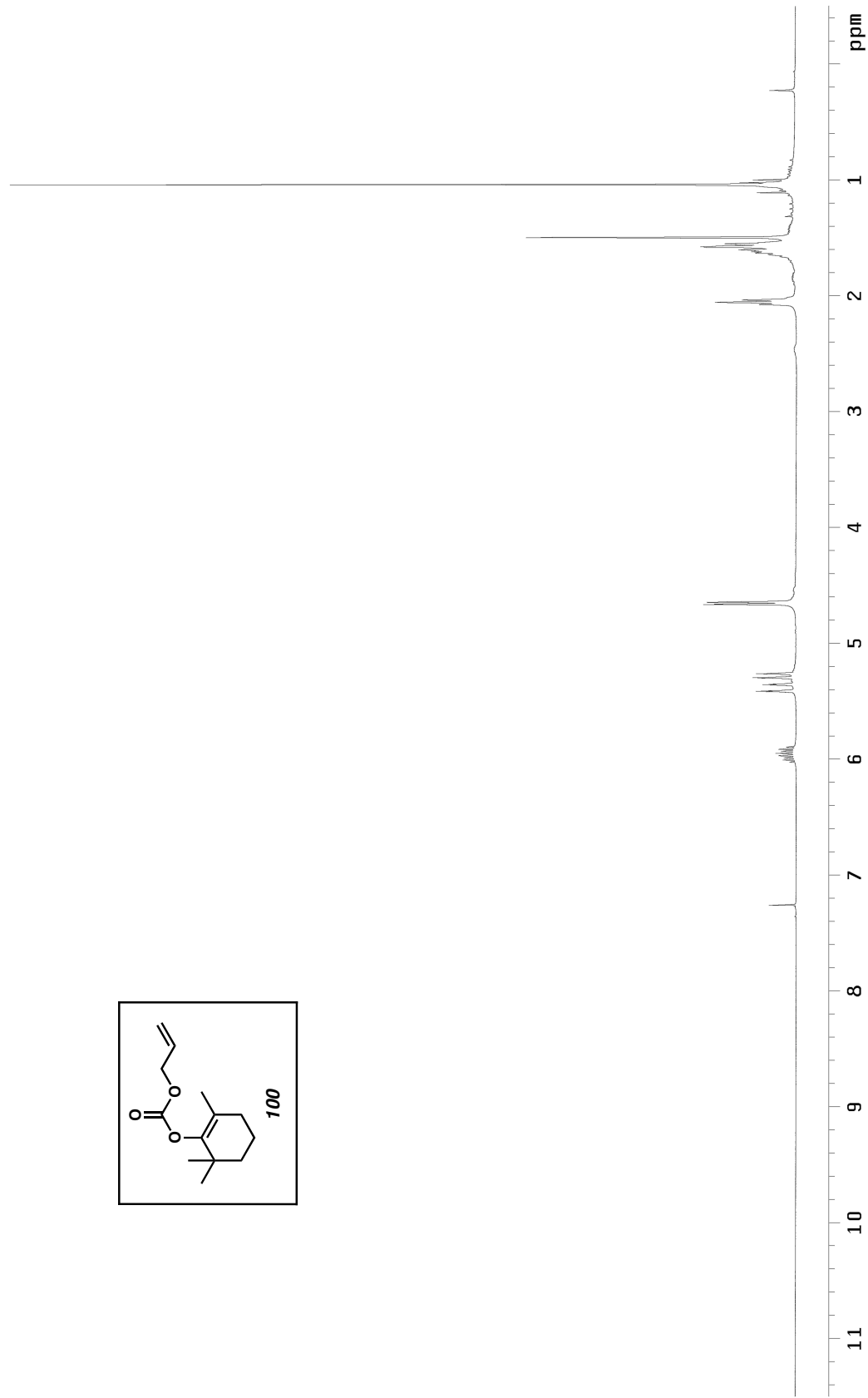
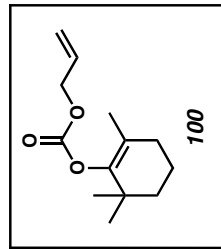


Figure A2.1 ^1H NMR (300 MHz, CDCl_3) of compound **100**.

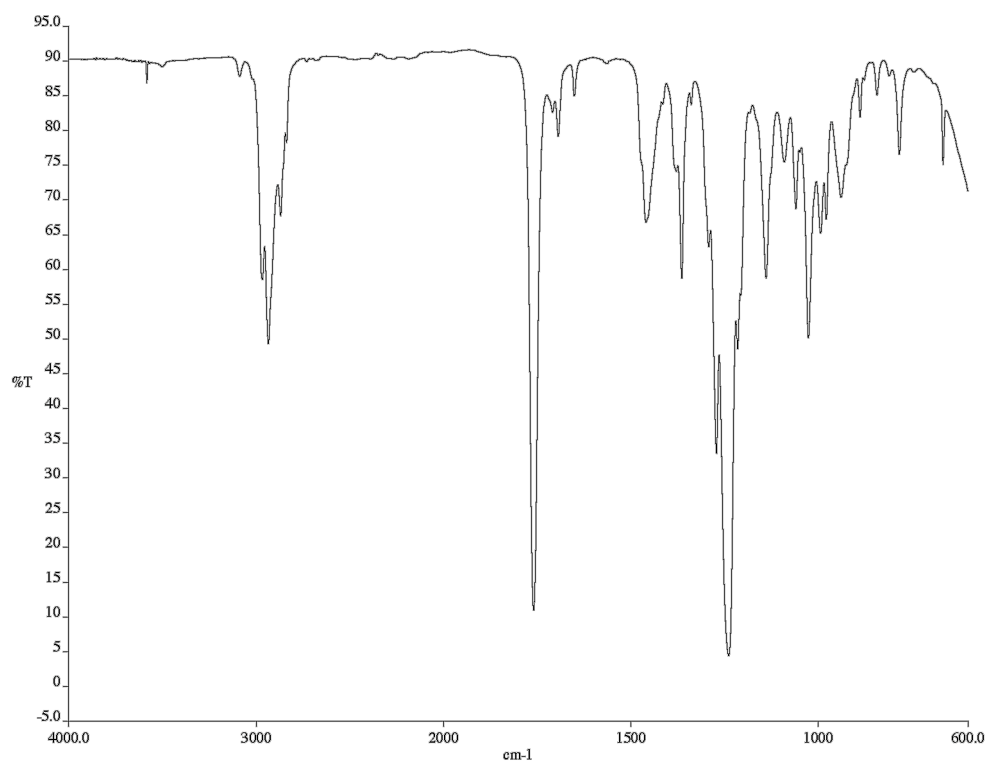


Figure A2.2 Infrared spectrum (NaCl/CDCl₃) of compound **100**.

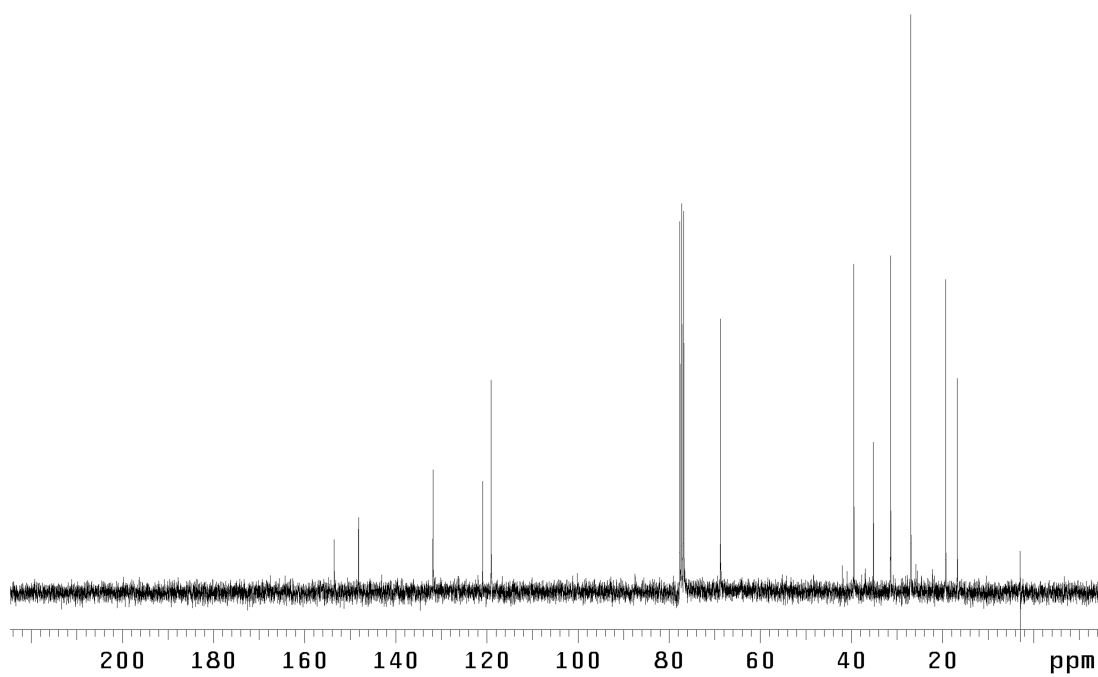


Figure A2.3 ¹³C NMR (75 MHz, CDCl₃) of compound **100**.

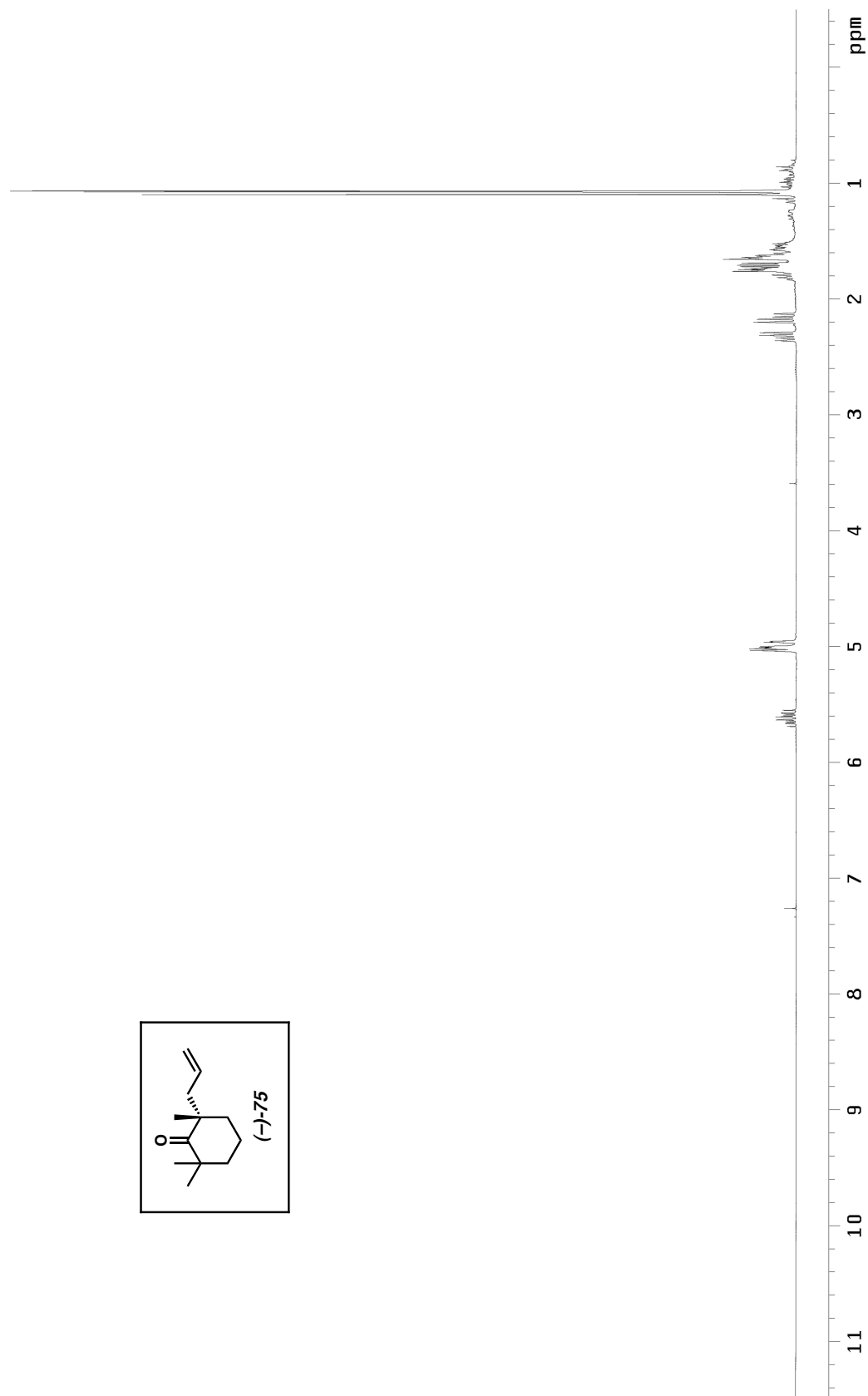


Figure A2.4 ^1H NMR (300 MHz, CDCl_3) of compound **75**.

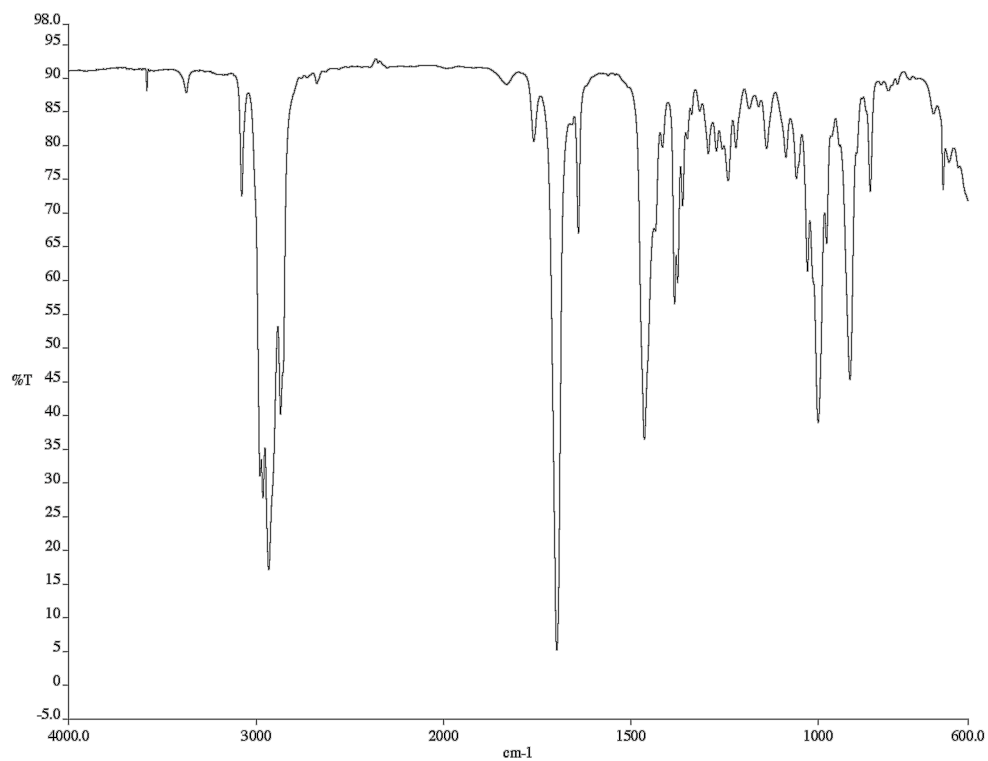


Figure A2.5 Infrared spectrum (NaCl/CDCl₃) of compound **75**.

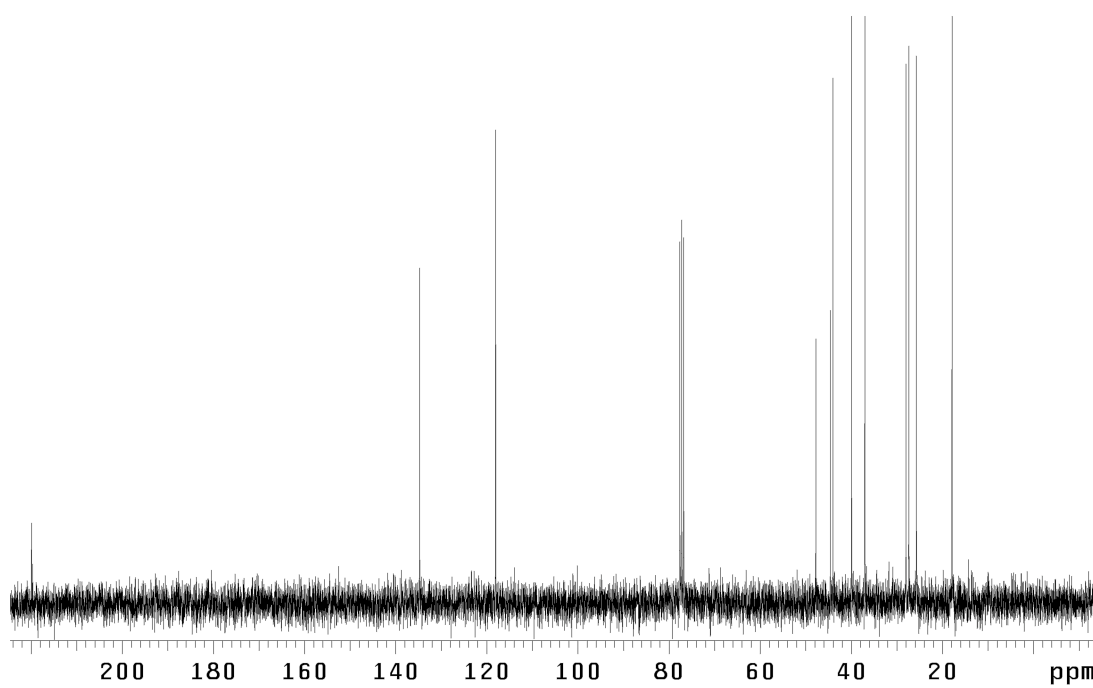


Figure A2.6 ¹³C NMR (75 MHz, CDCl₃) of compound **75**.

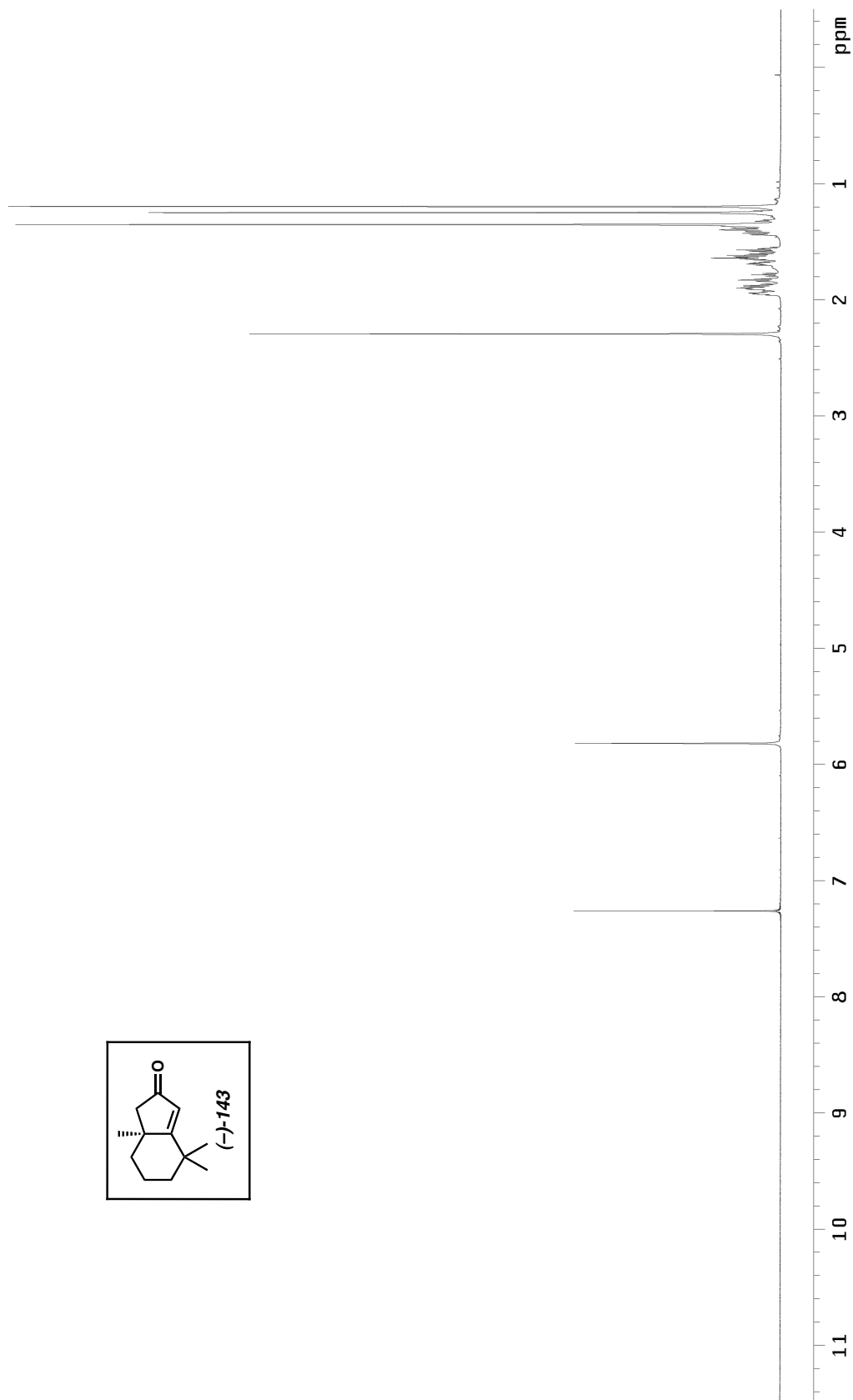
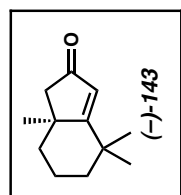


Figure A2.7 ^1H NMR (300 MHz, CDCl_3) of compound **143**.

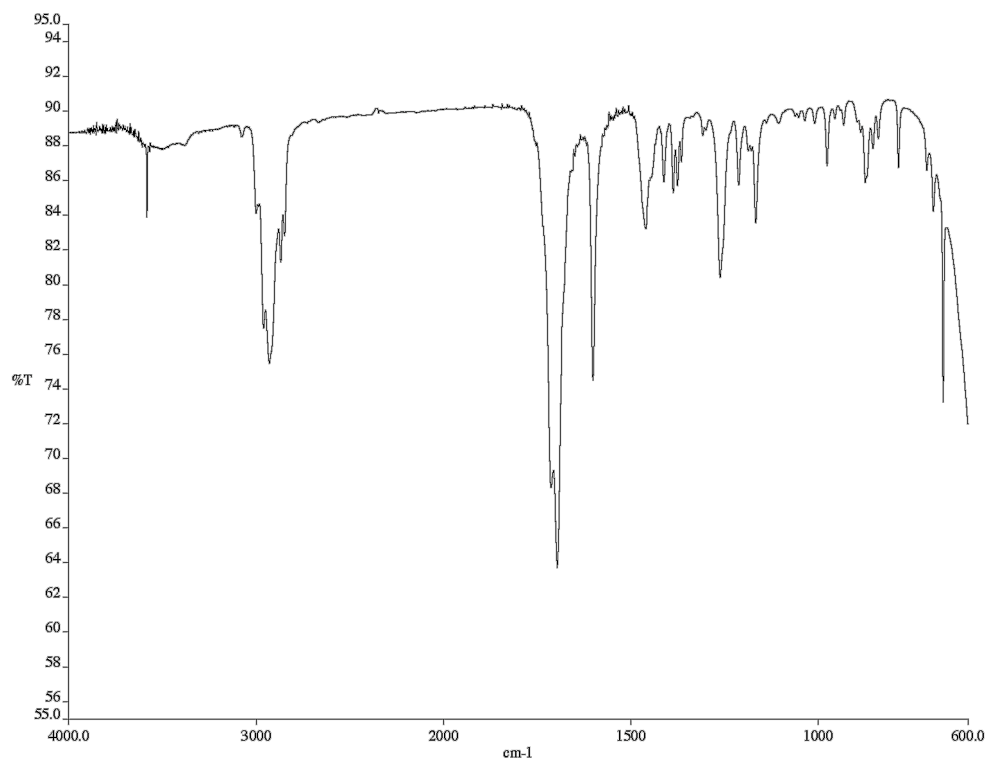


Figure A2.8 Infrared spectrum (NaCl/CDCl₃) of compound **143**.

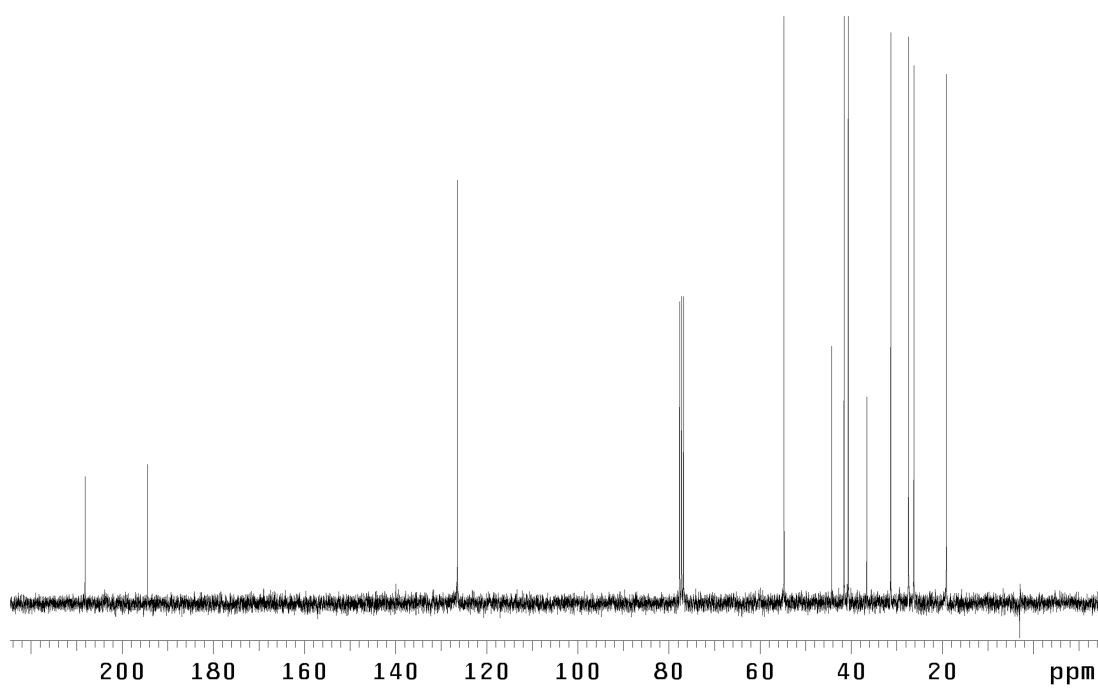


Figure A2.9 ¹³C NMR (75 MHz, CDCl₃) of compound **143**.

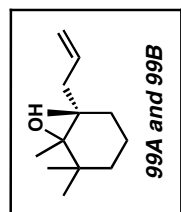
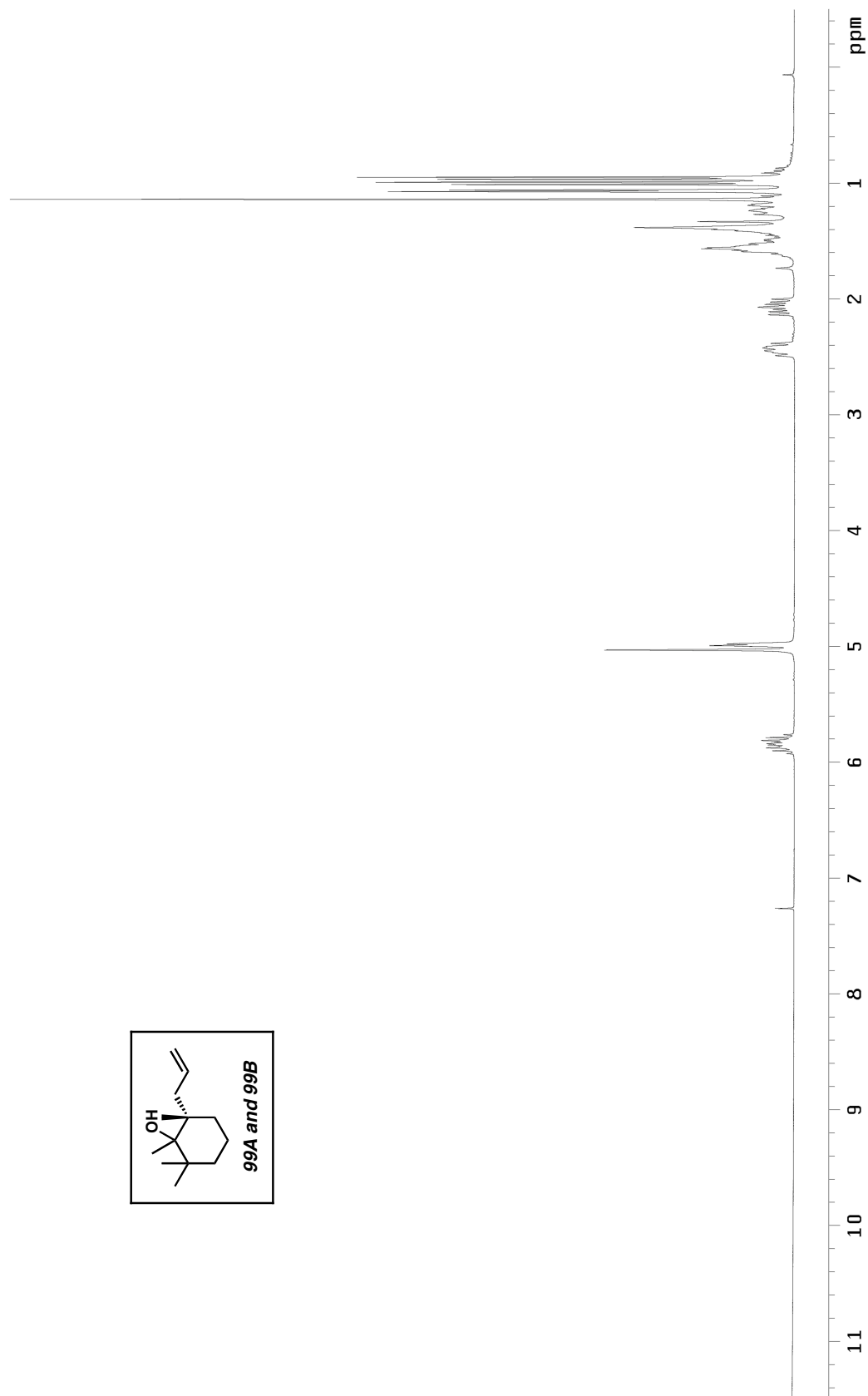


Figure A2.10 ^1H NMR (300 MHz, CDCl_3) of compounds **99A** and **99B**.

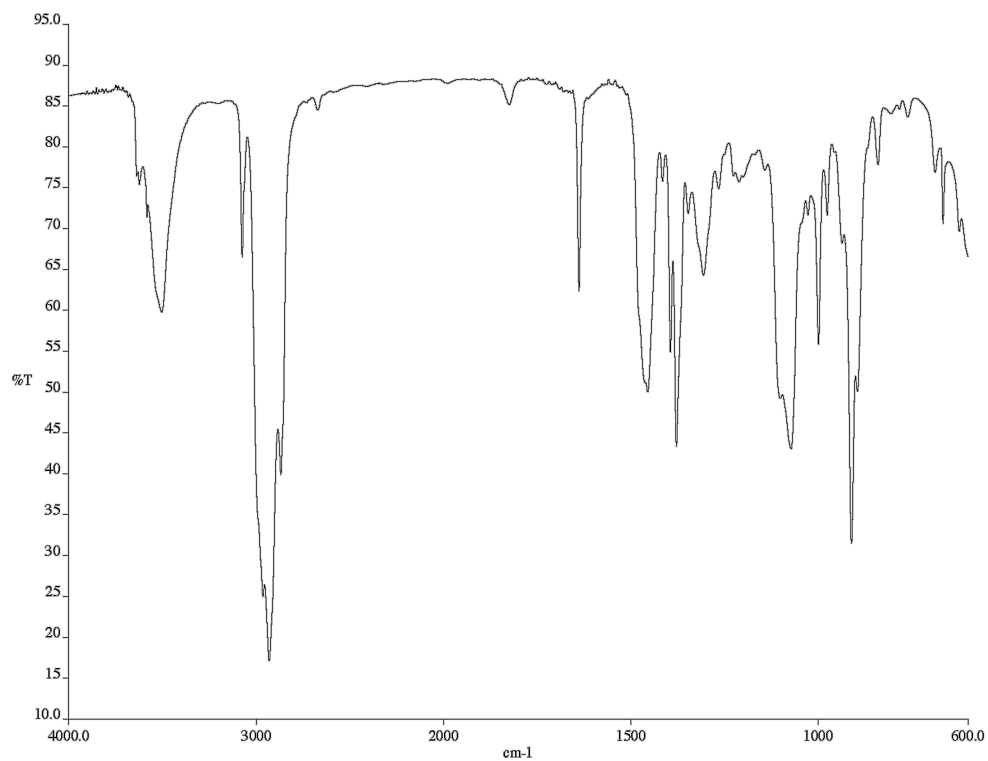


Figure A2.11 Infrared spectrum (NaCl/CDCl₃) of compounds **99A** and **99B**.

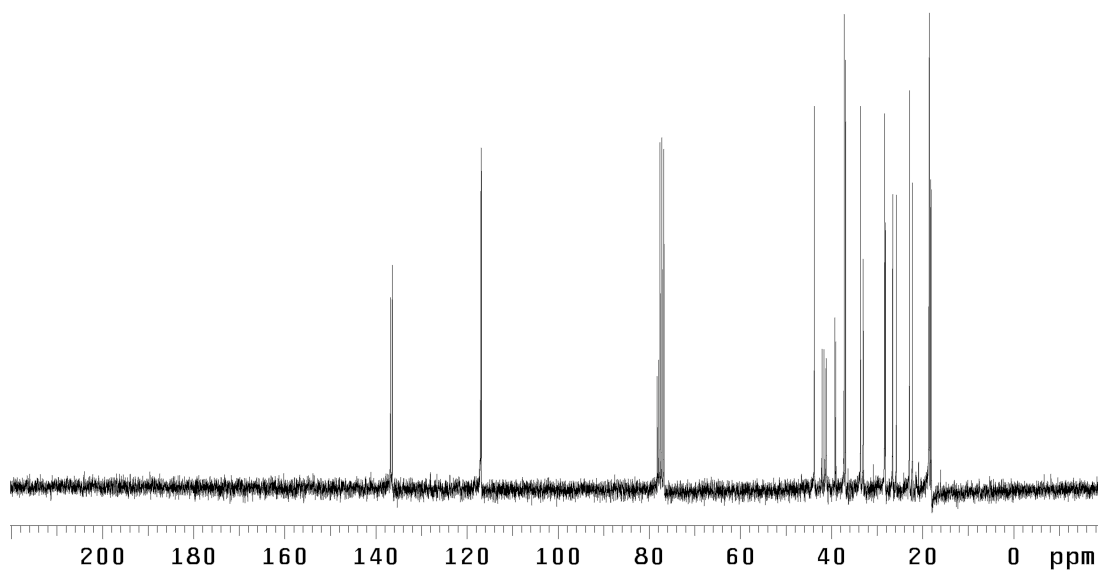


Figure A2.12 ¹³C NMR (75 MHz, CDCl₃) of compounds **99A** and **99B**.

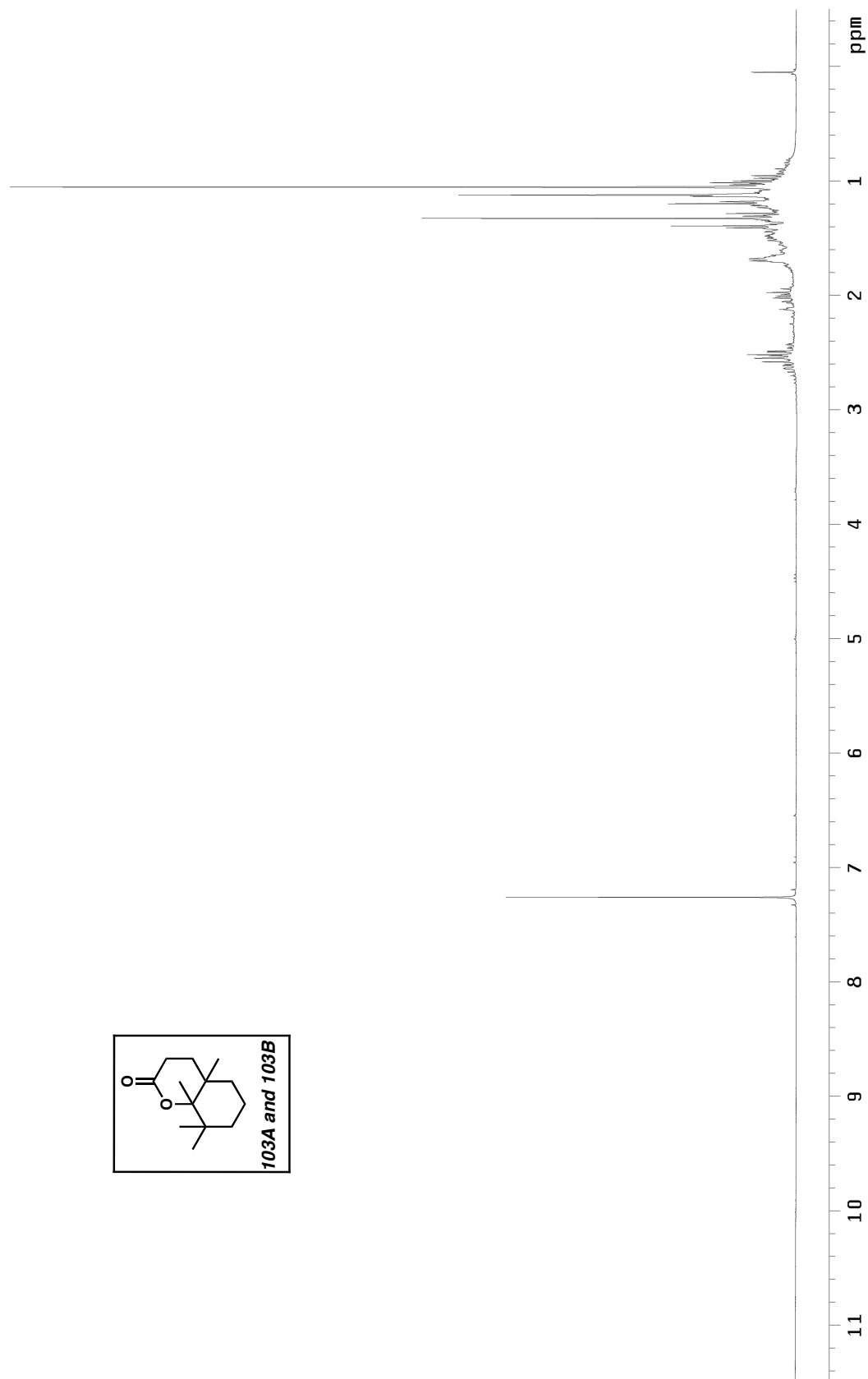


Figure A2.13 ^1H NMR (300 MHz, CDCl_3) of compounds **103A** and **103B**.

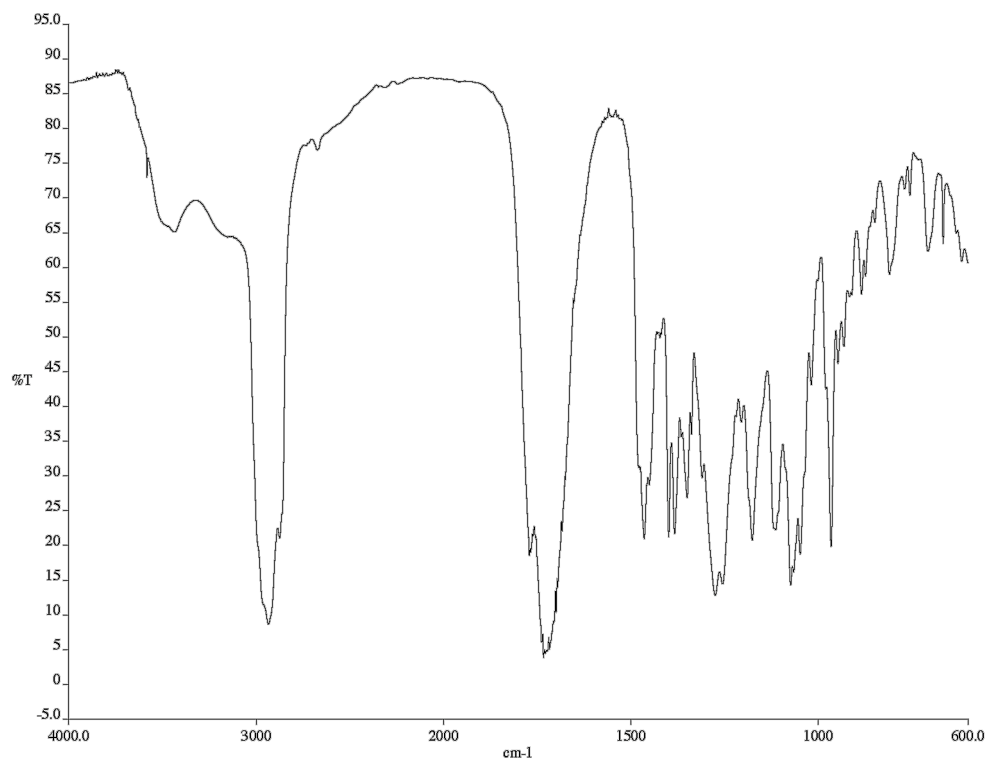


Figure A2.14 Infrared spectrum (NaCl/CDCl₃) of compounds **103A** and **103B**.

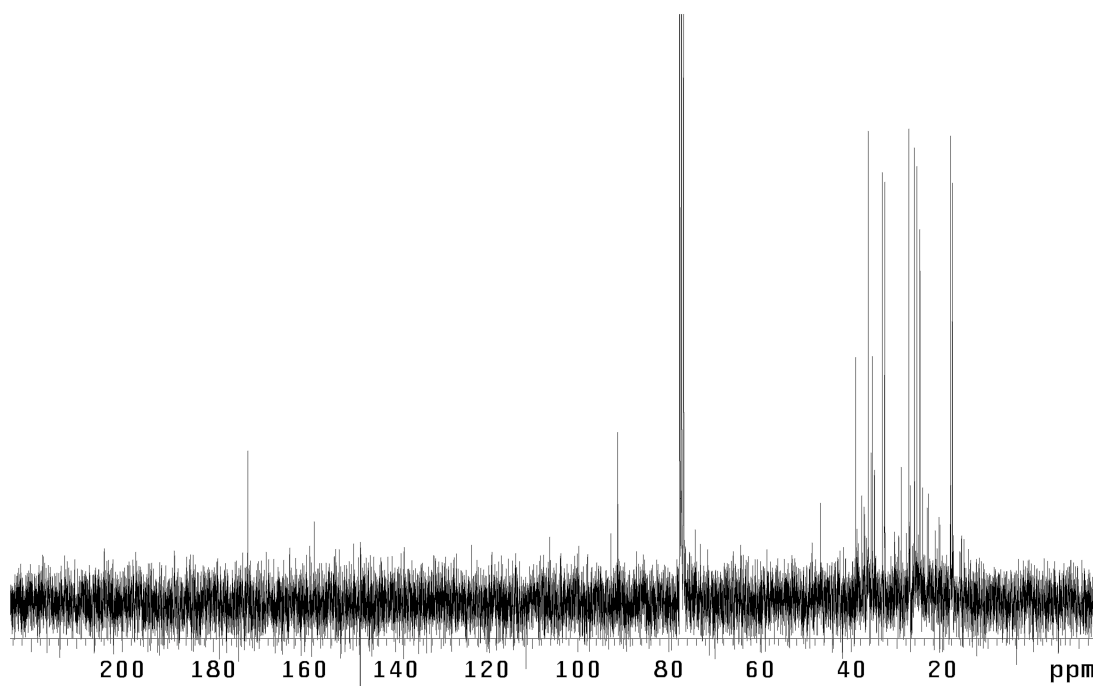


Figure A2.15 ¹³C NMR (75 MHz, CDCl₃) of compounds **103A** and **103B**.

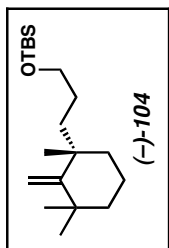
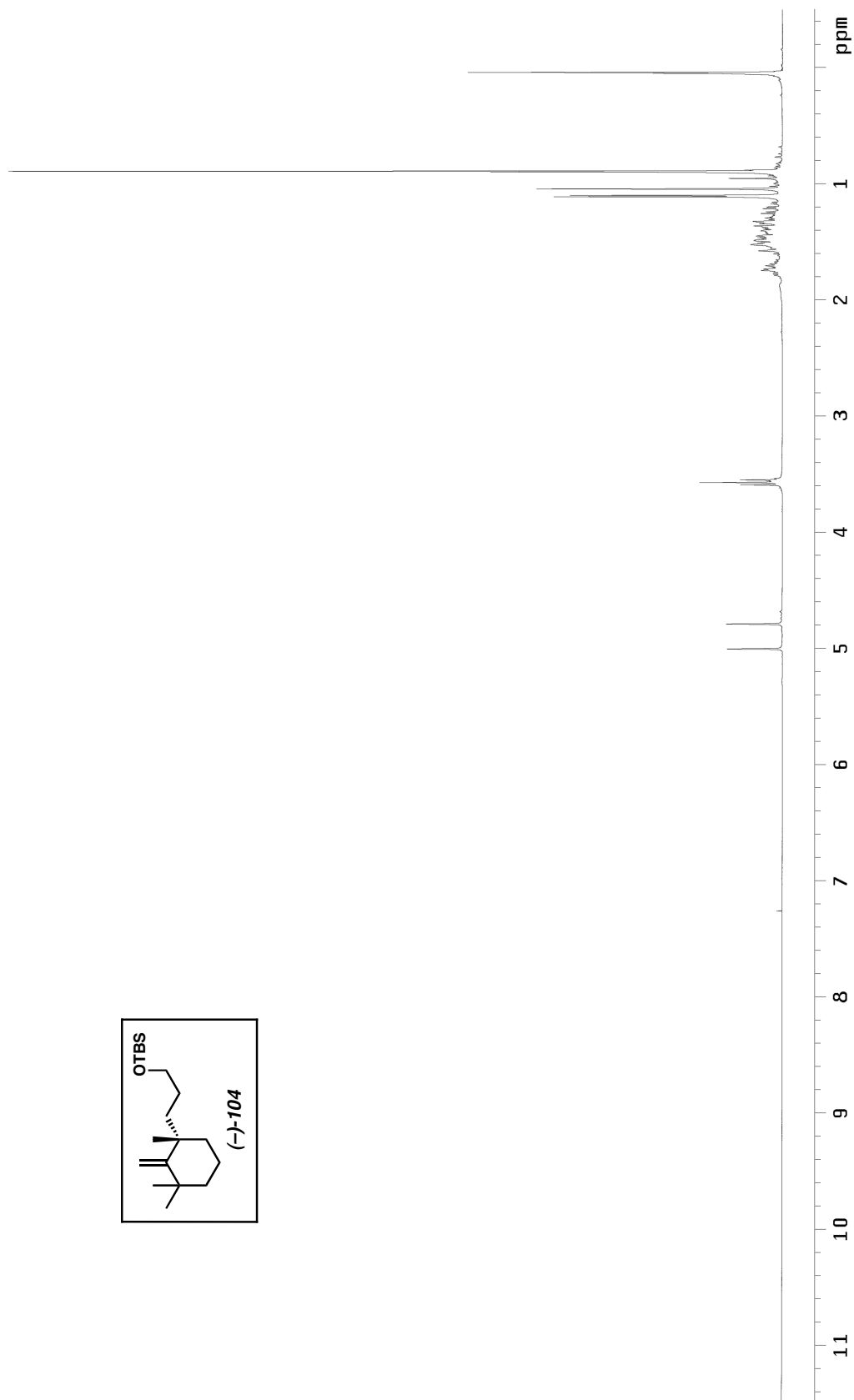


Figure A2.16 ^1H NMR (300 MHz, CDCl_3) of compound **104**.

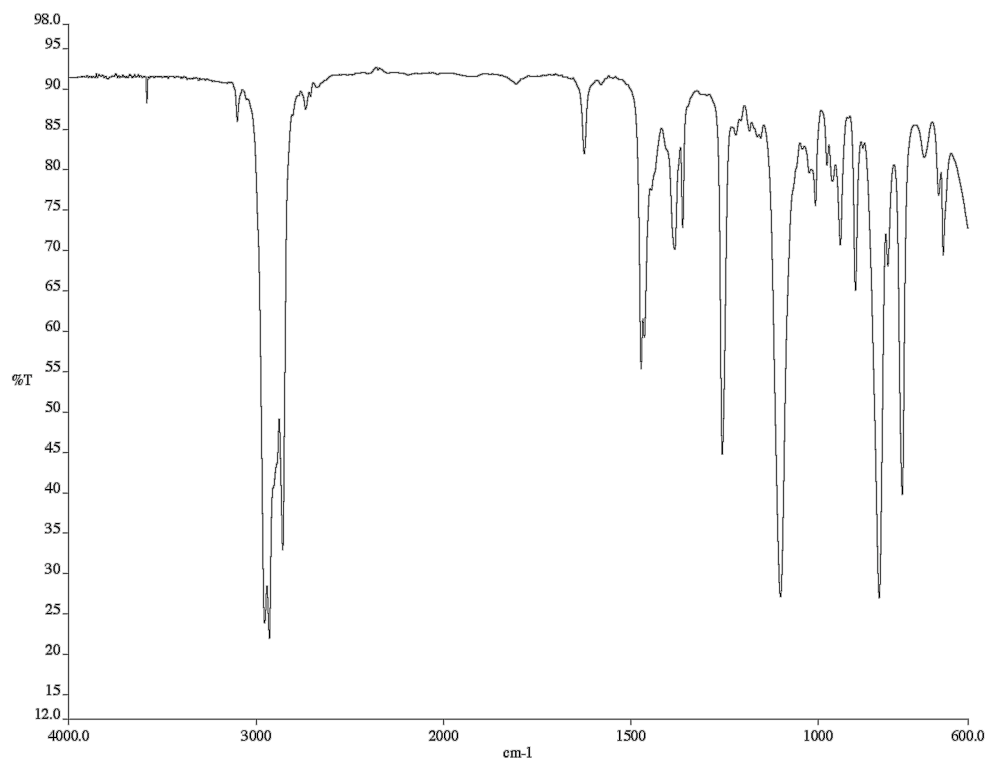


Figure A2.17 Infrared spectrum (NaCl/CDCl₃) of compound **104**.

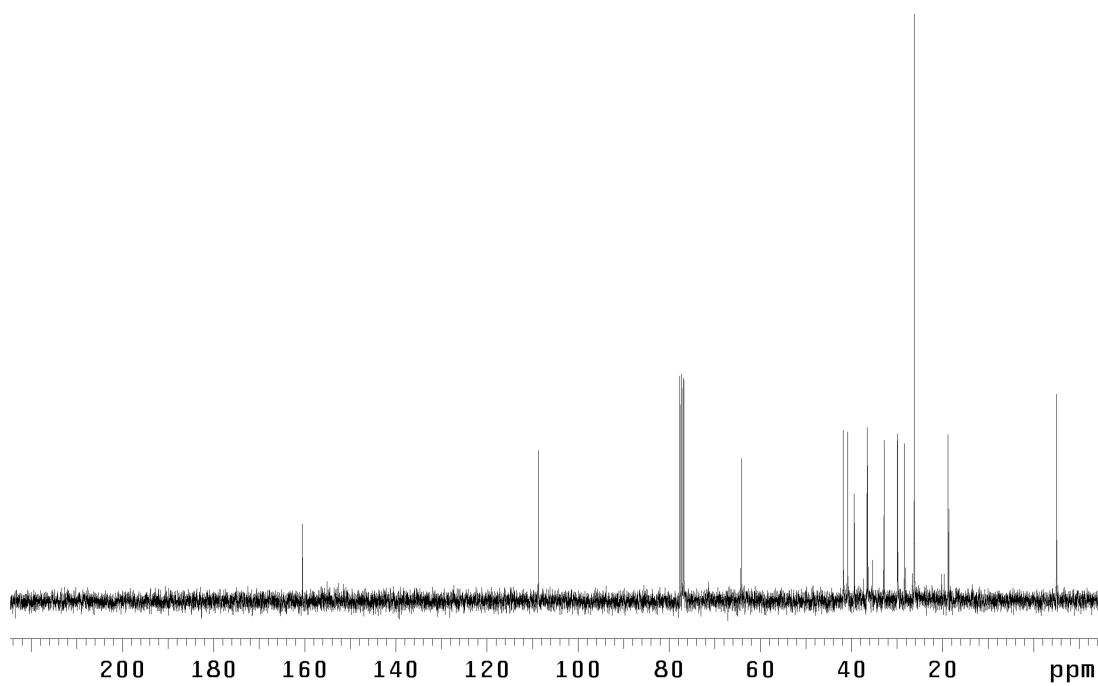


Figure A2.18 ¹³C NMR (75 MHz, CDCl₃) of compound **104**.

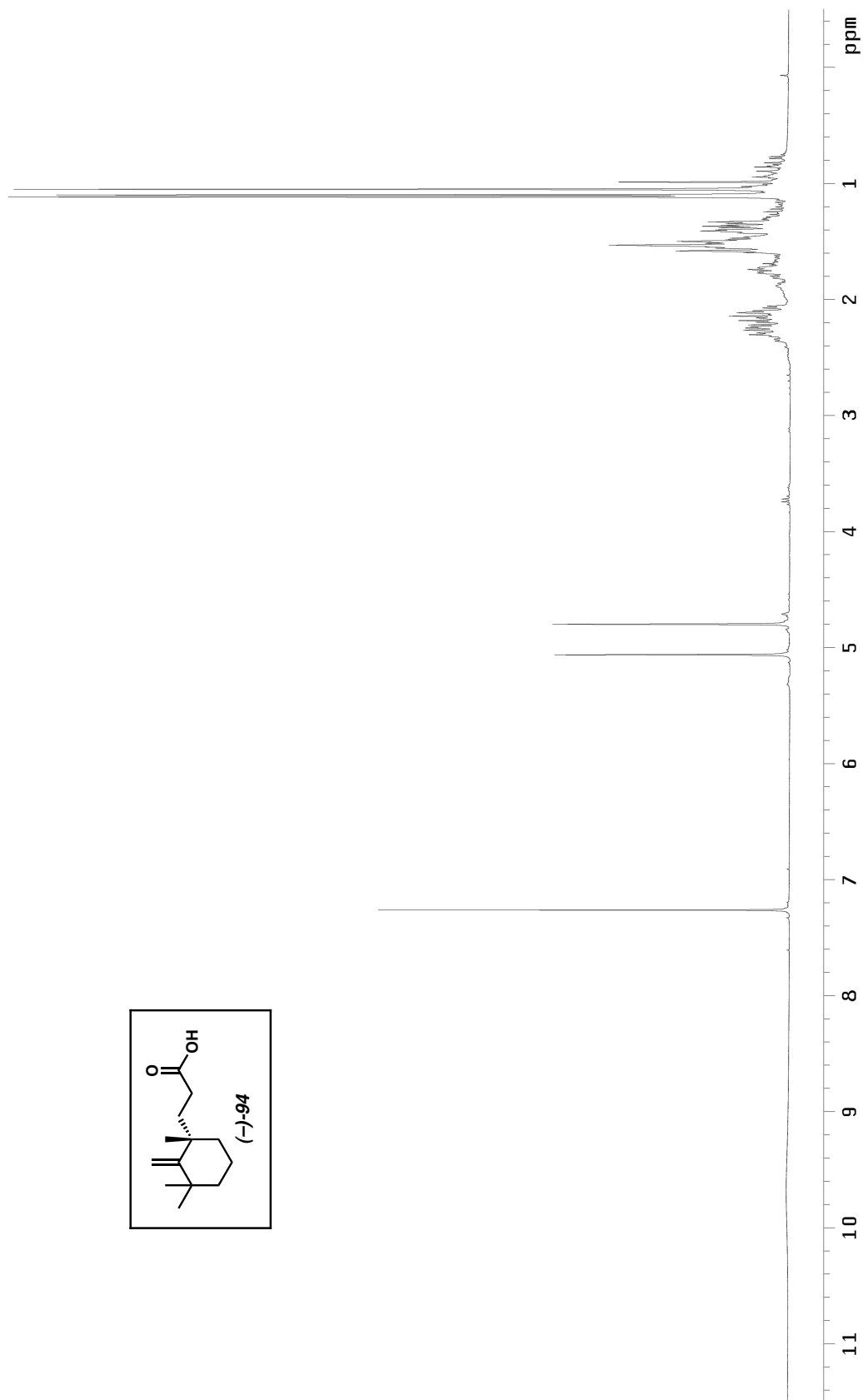
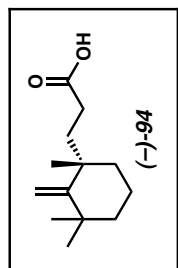


Figure A2.19 ¹H NMR (300 MHz, CDCl₃) of compound **94**.

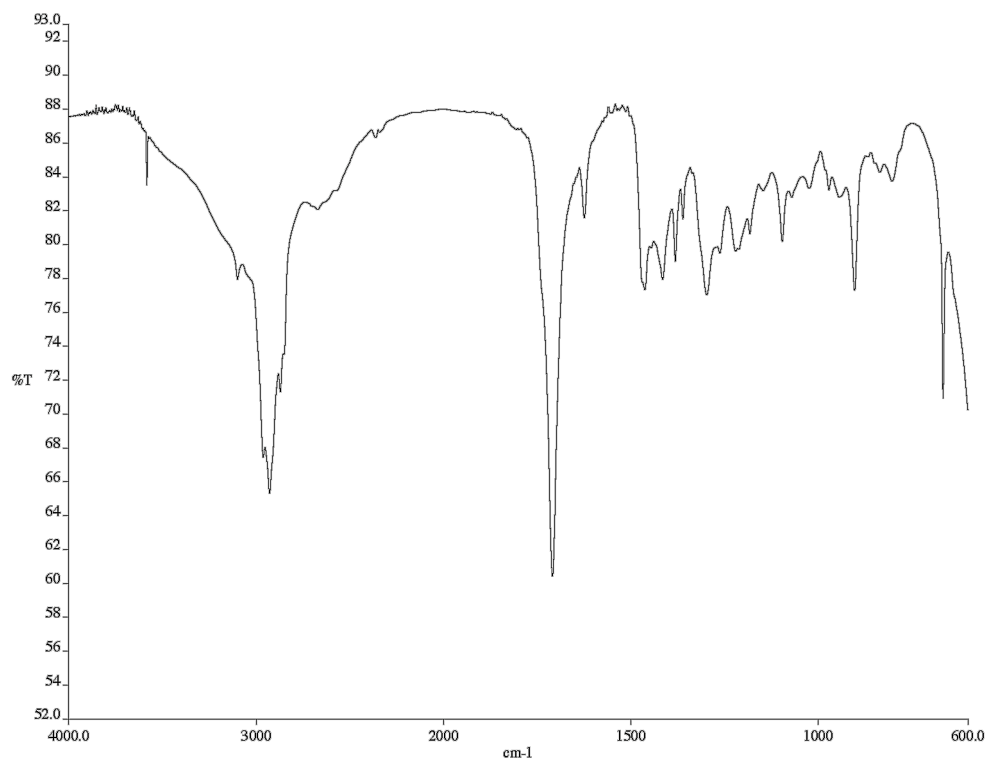


Figure A2.20 Infrared spectrum (NaCl/CDCl₃) of compound **94**.

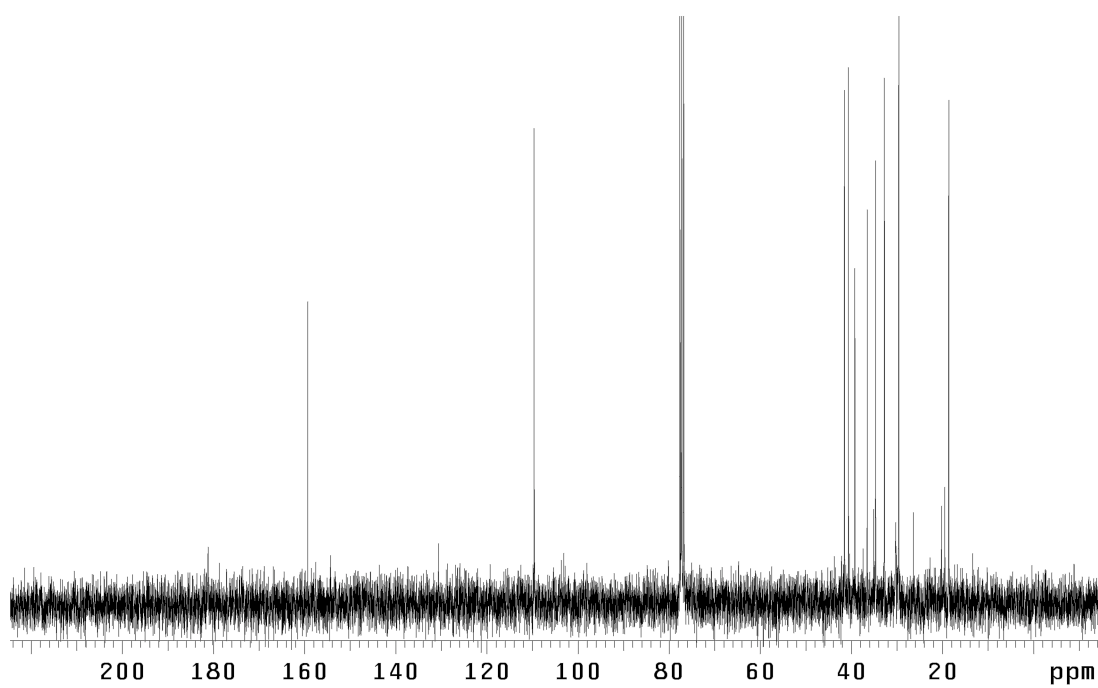


Figure A2.21 ¹³C NMR (75 MHz, CDCl₃) of compound **94**.

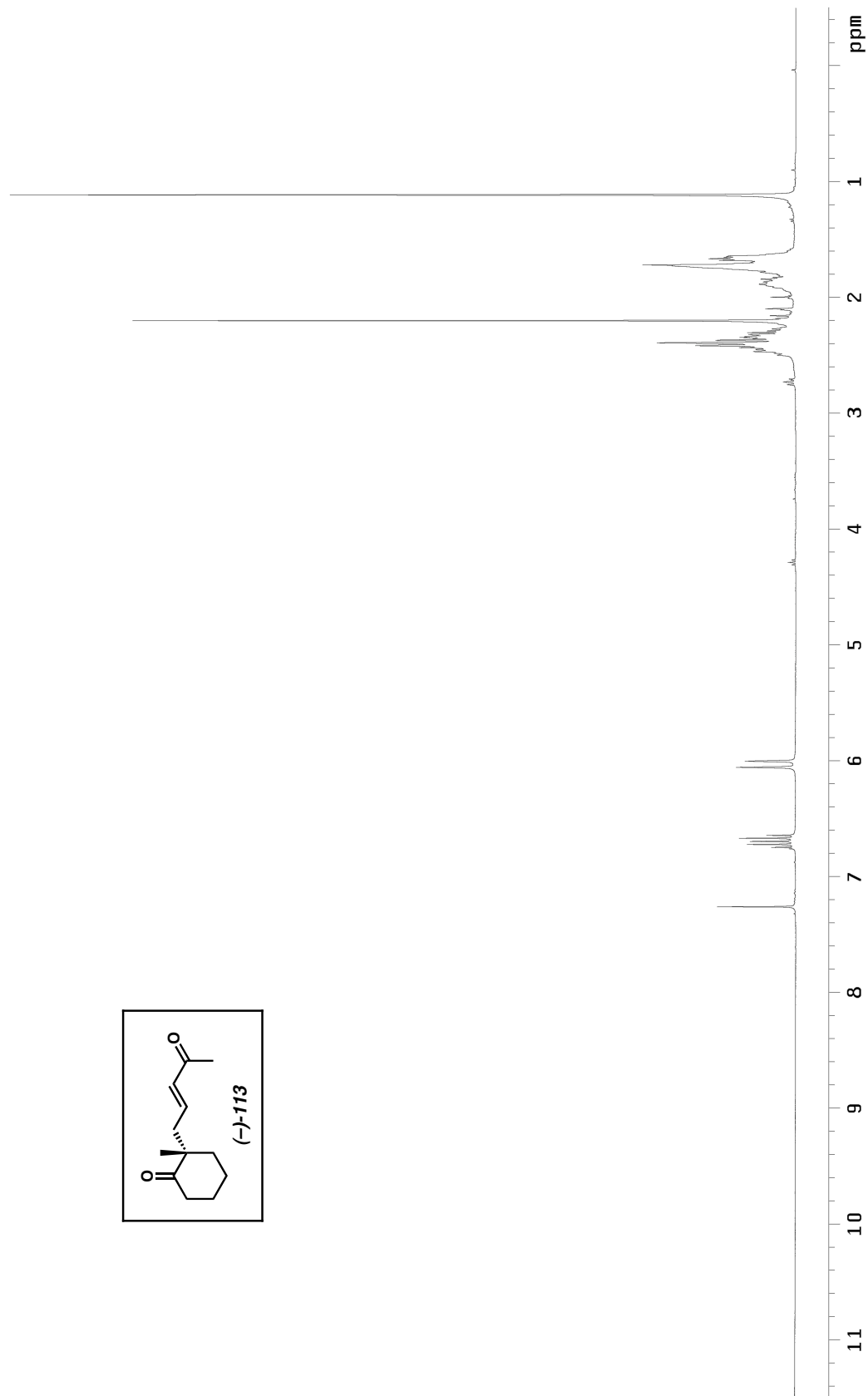
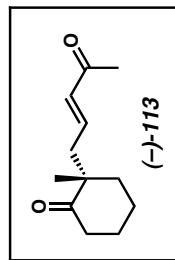


Figure A2.22 ^1H NMR (300 MHz, CDCl_3) of compound **113**.

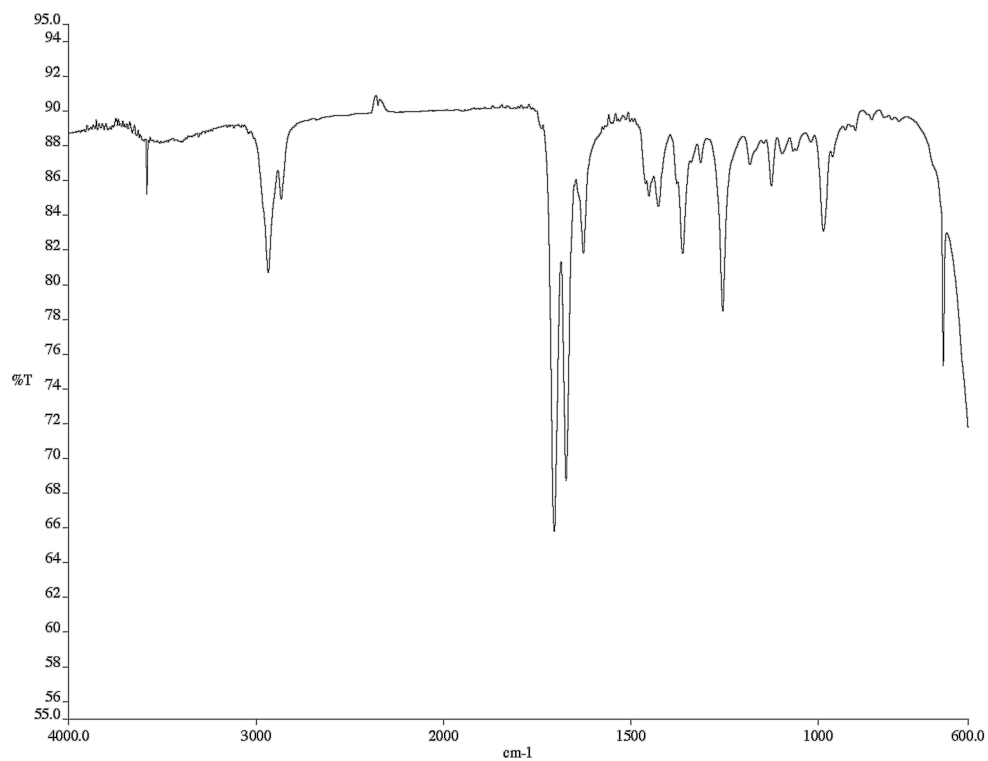


Figure A2.23 Infrared spectrum (NaCl/CDCl₃) of compound **113**.

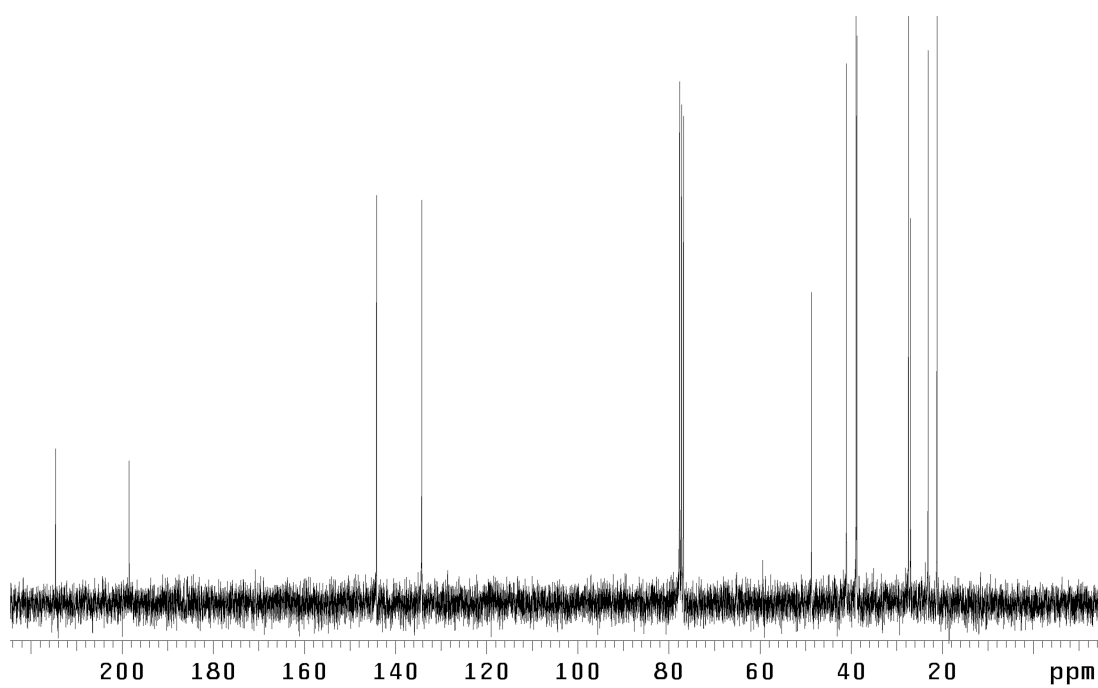


Figure A2.24 ¹³C NMR (75 MHz, CDCl₃) of compound **113**.

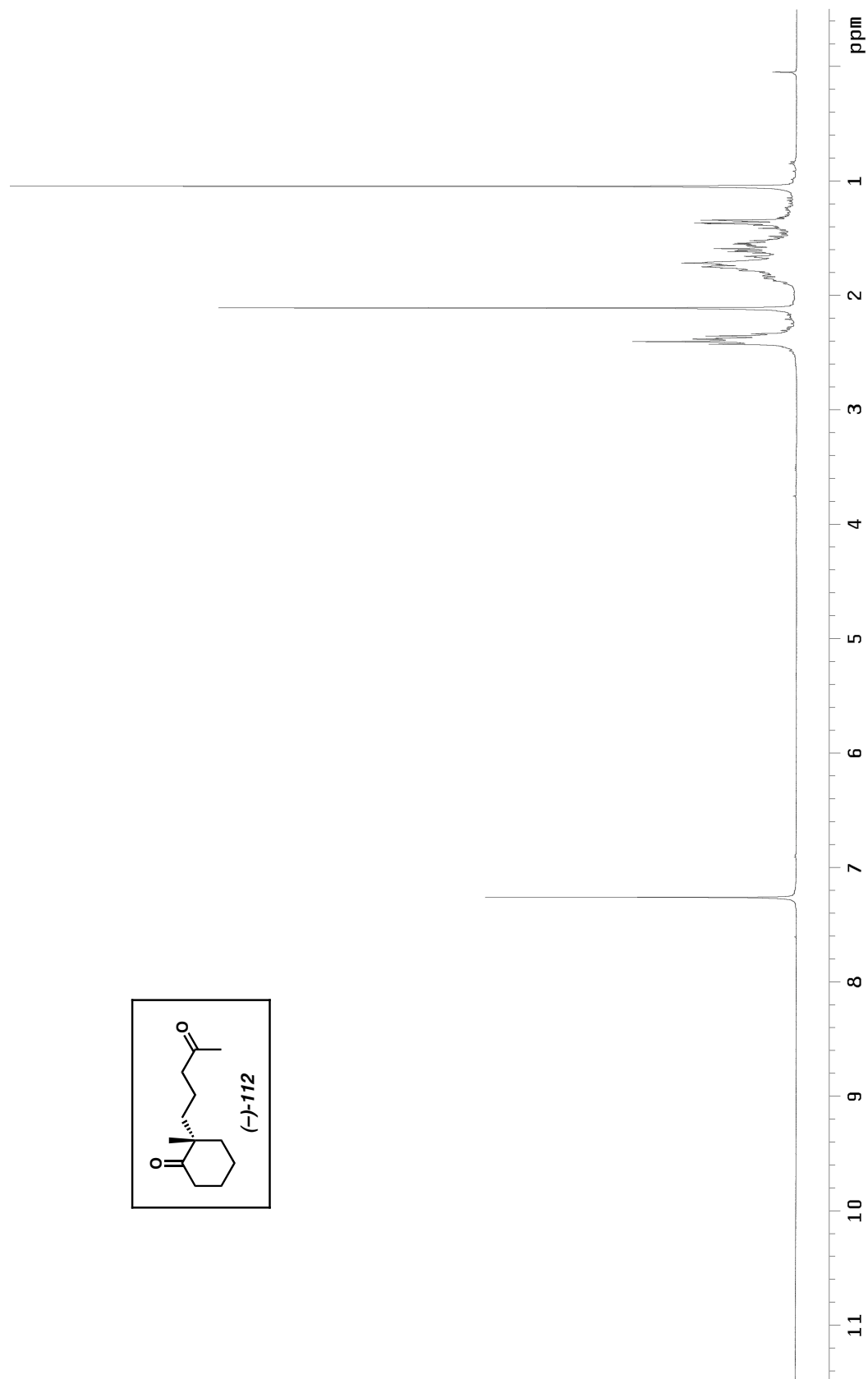
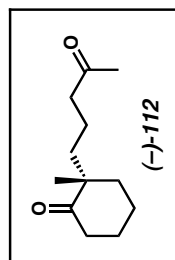


Figure A2.25 ^1H NMR (300 MHz, CDCl_3) of compound **112**.

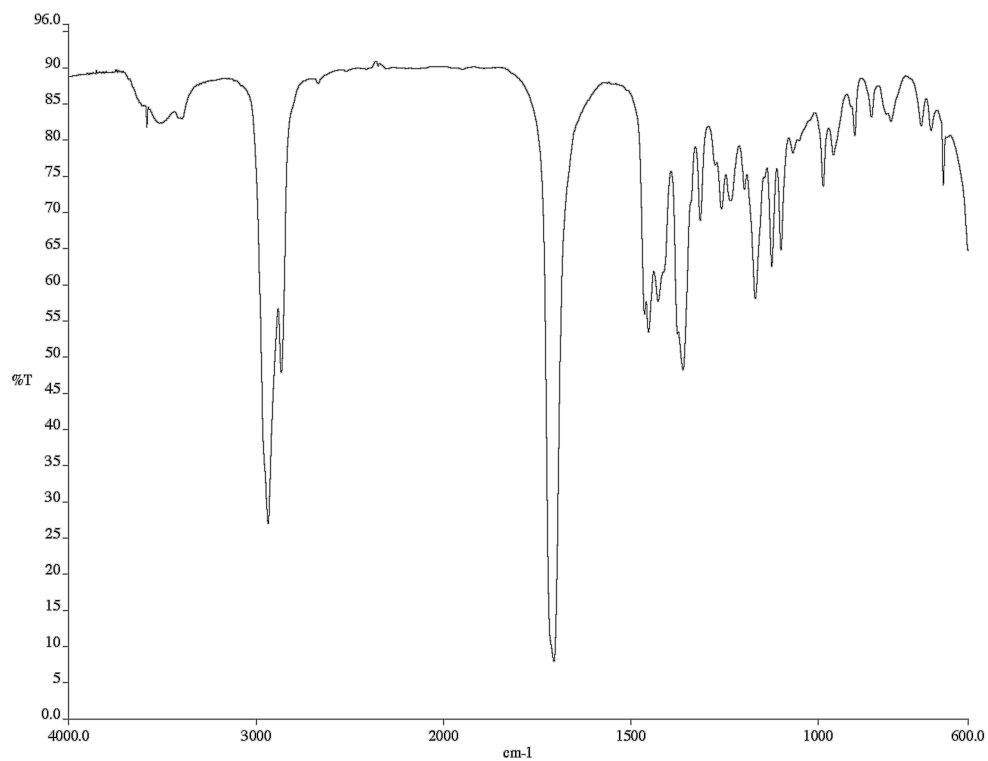


Figure A2.26 Infrared spectrum (NaCl/CDCl₃) of compound **112**.

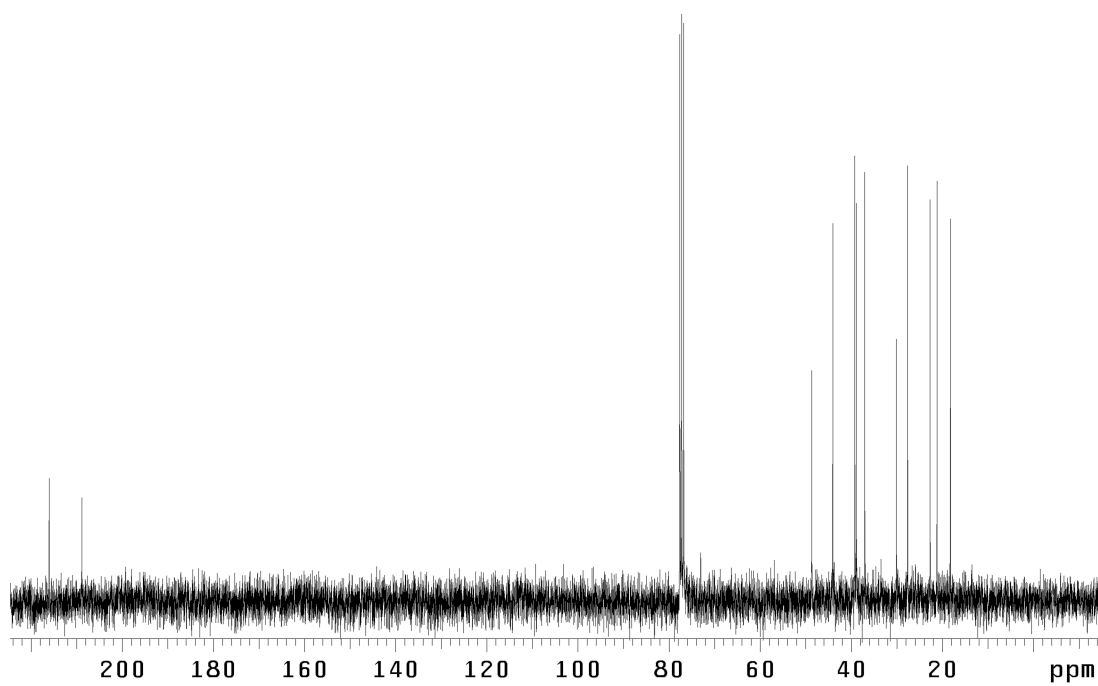


Figure A2.27 ¹³C NMR (75 MHz, CDCl₃) of compound **112**.

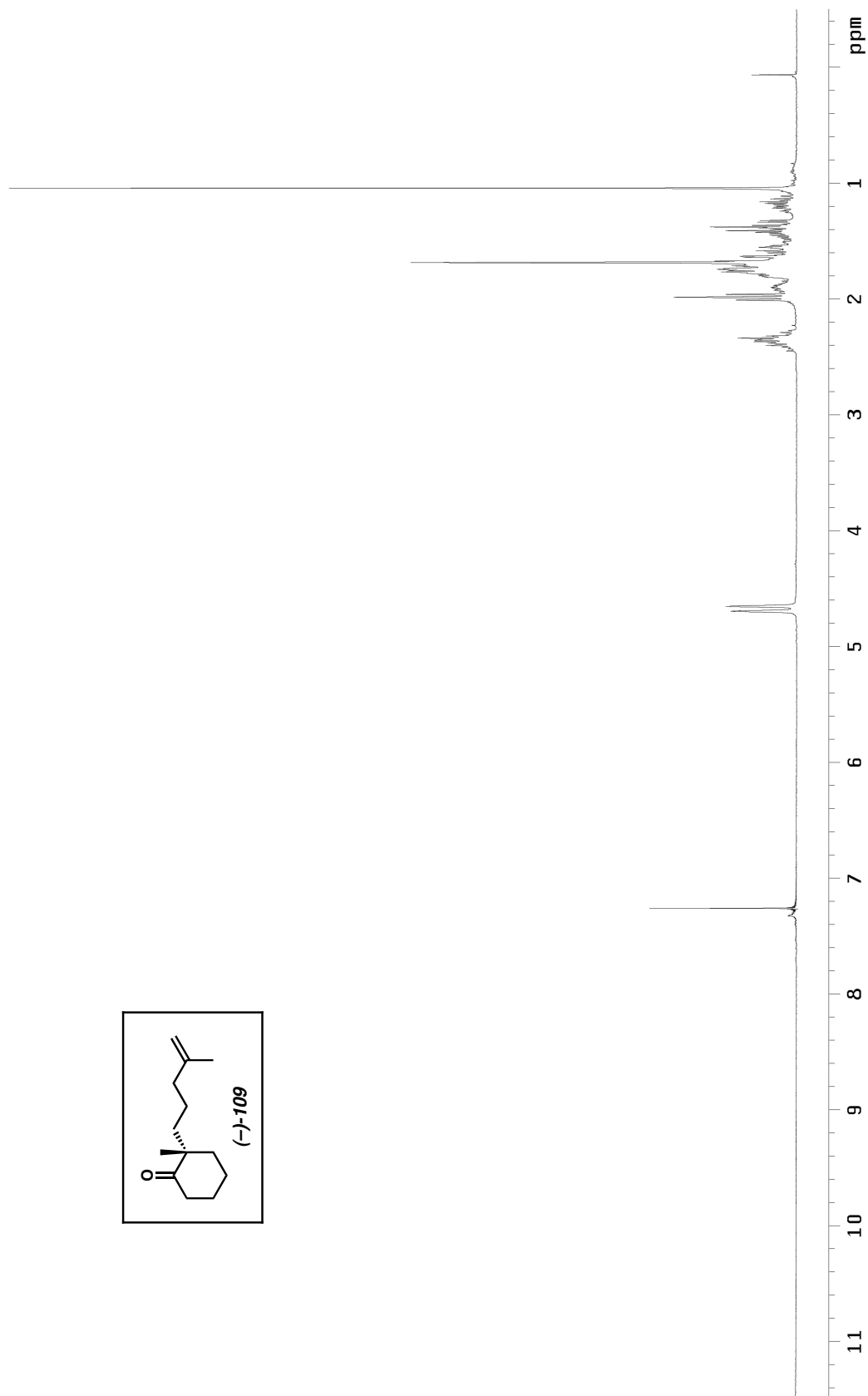
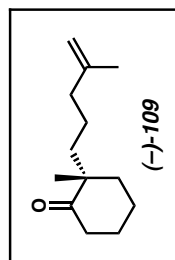


Figure A2.28 ^1H NMR (300 MHz, CDCl_3) of compound **109**.

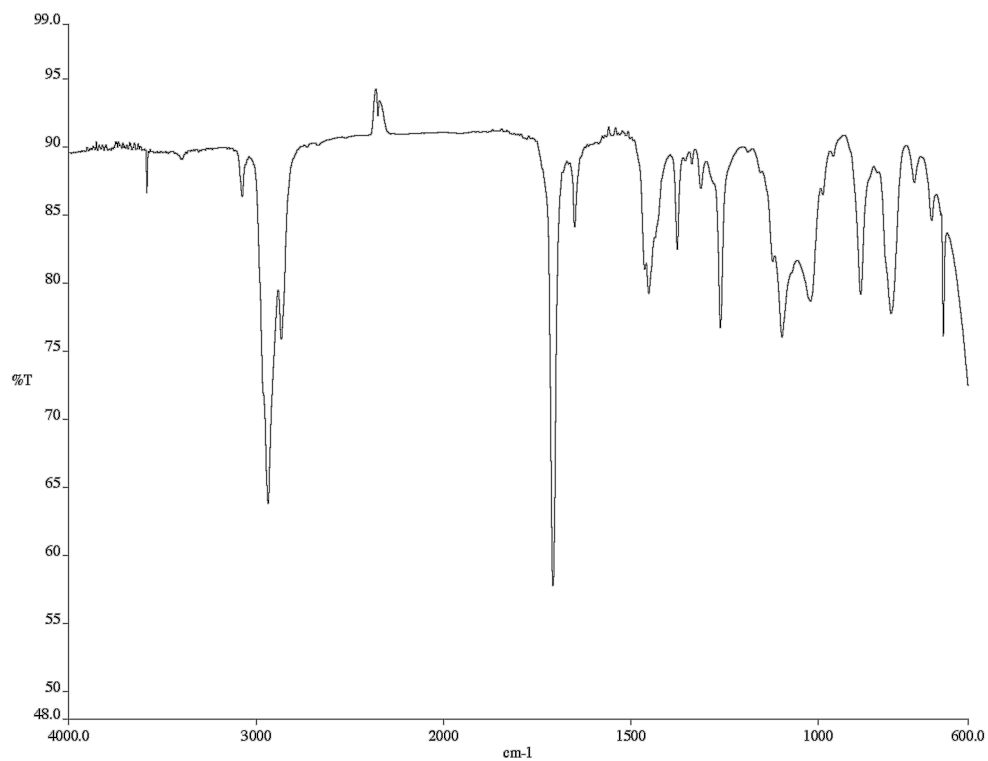


Figure A2.29 Infrared spectrum (NaCl/CDCl₃) of compound **109**.

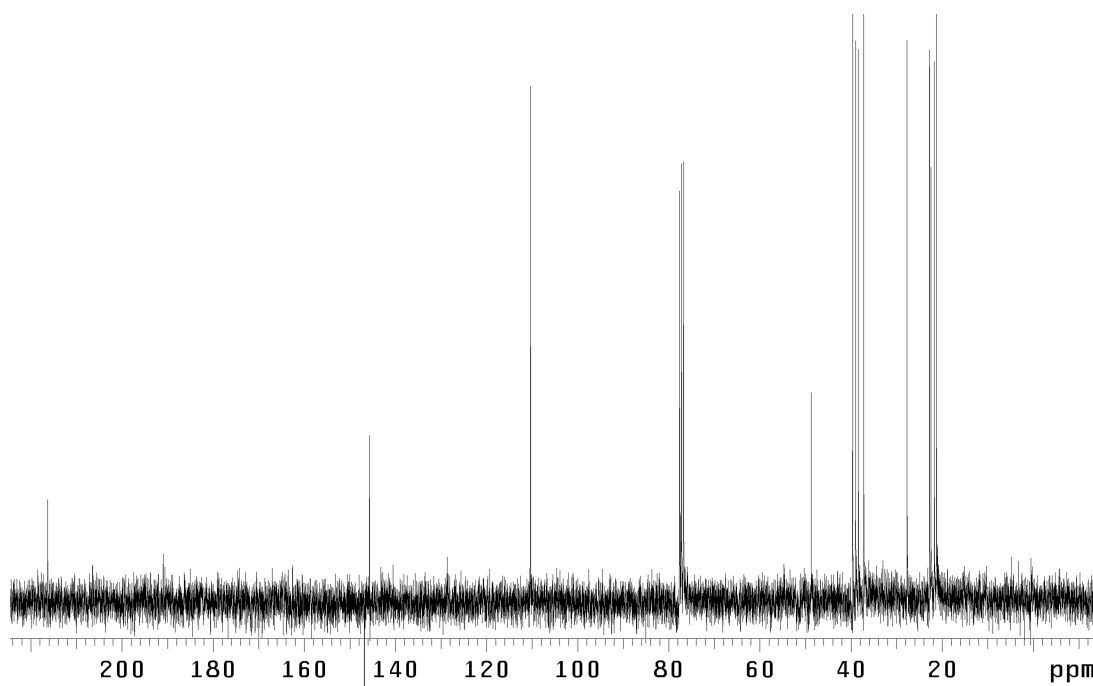


Figure A2.30 ¹³C NMR (75 MHz, CDCl₃) of compound **109**.

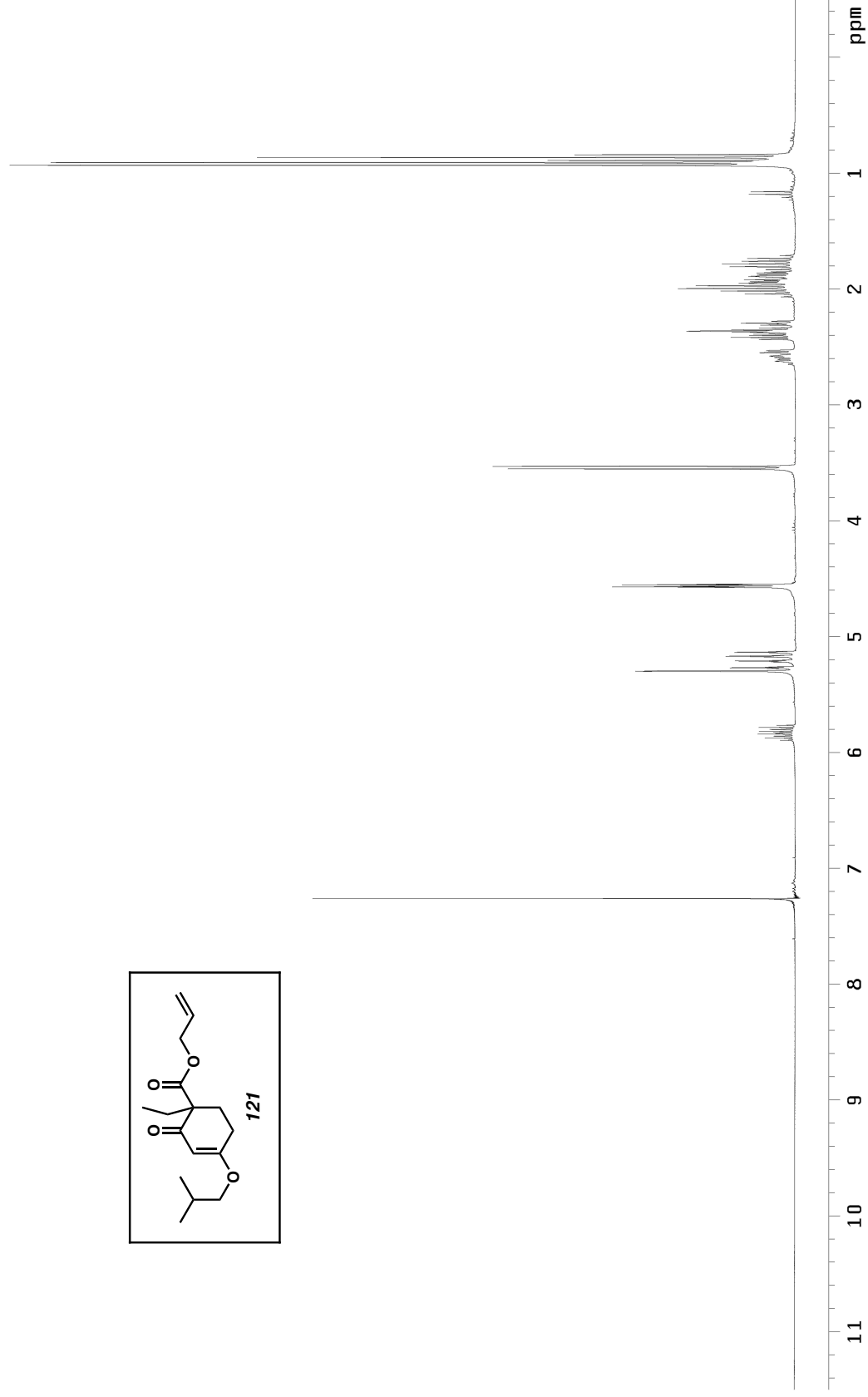
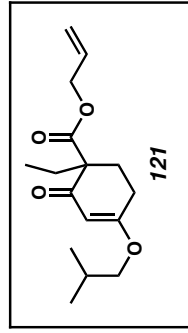


Figure A2.31 ^1H NMR (300 MHz, CDCl_3) of compound **121**.

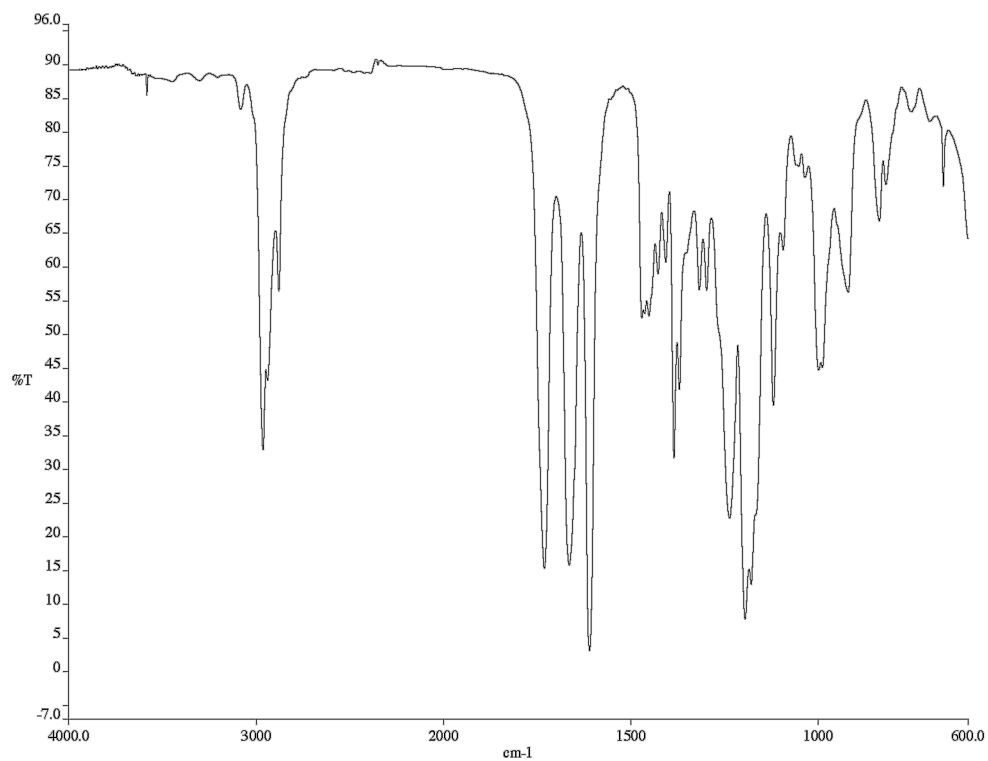


Figure A2.32 Infrared spectrum (NaCl/CDCl₃) of compound **121**.

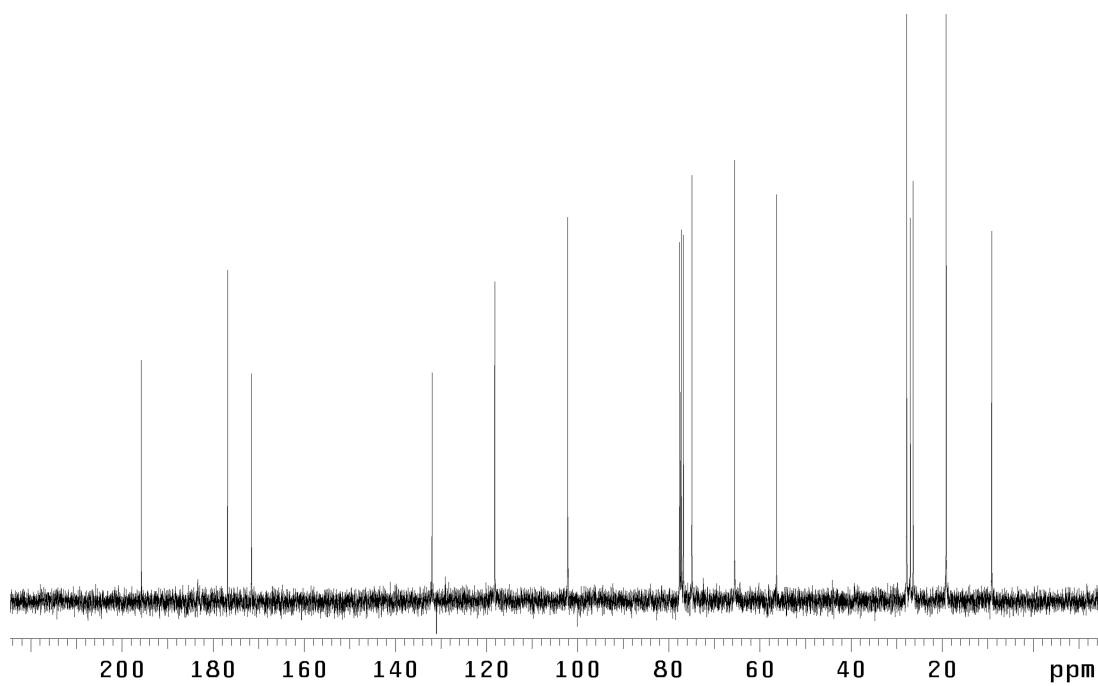
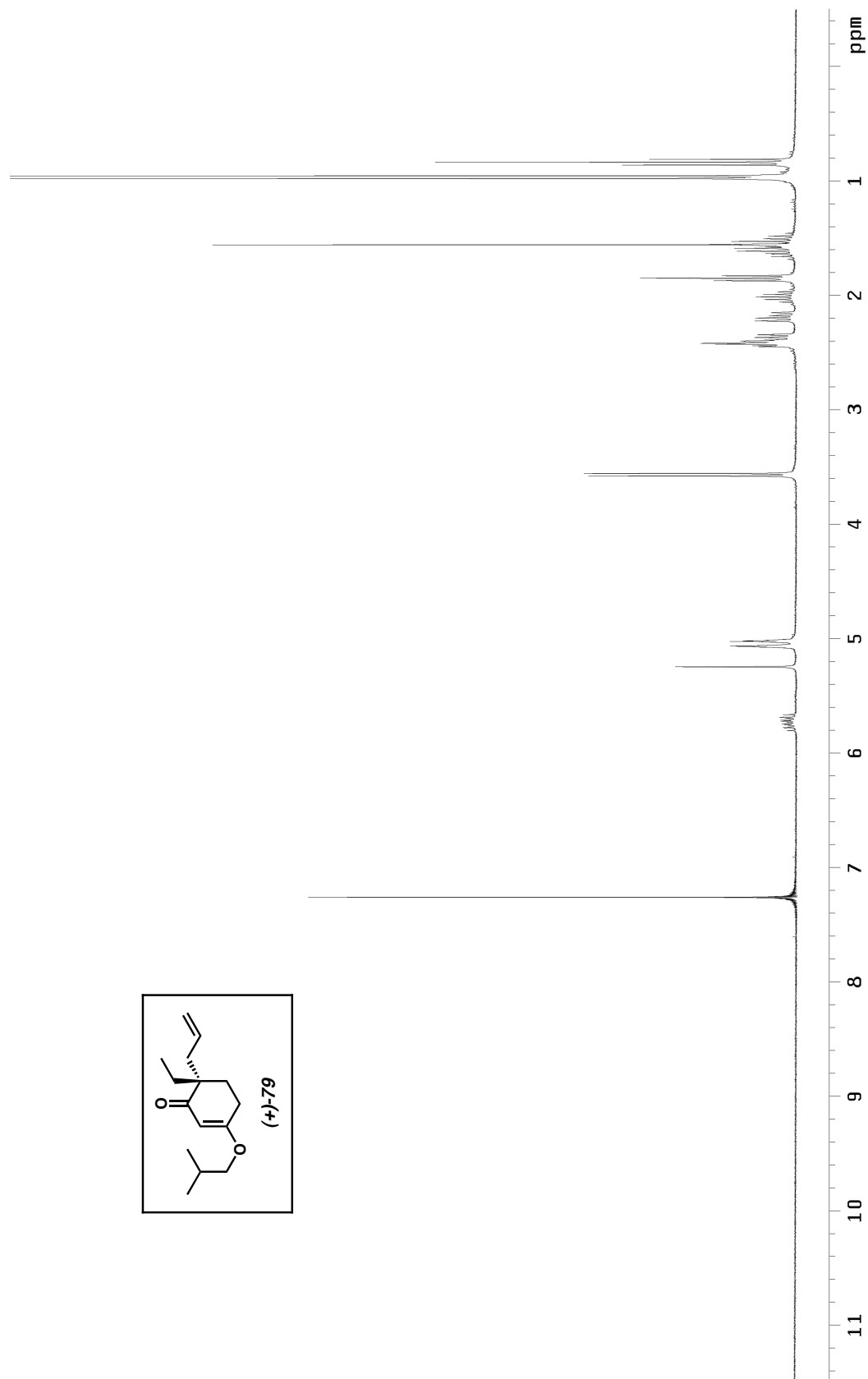


Figure A2.33 ¹³C NMR (75 MHz, CDCl₃) of compound **121**.

Figure A2.34 ^1H NMR (300 MHz, CDCl_3) of compound **79**.

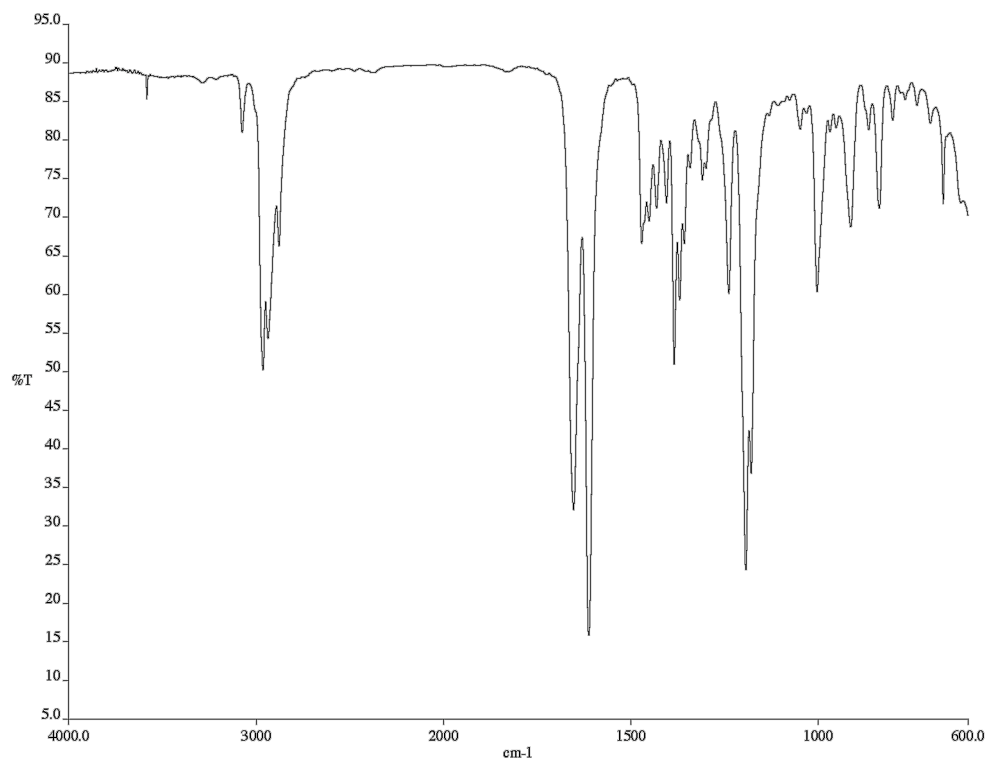


Figure A2.35 Infrared spectrum (NaCl/CDCl₃) of compound **79**.

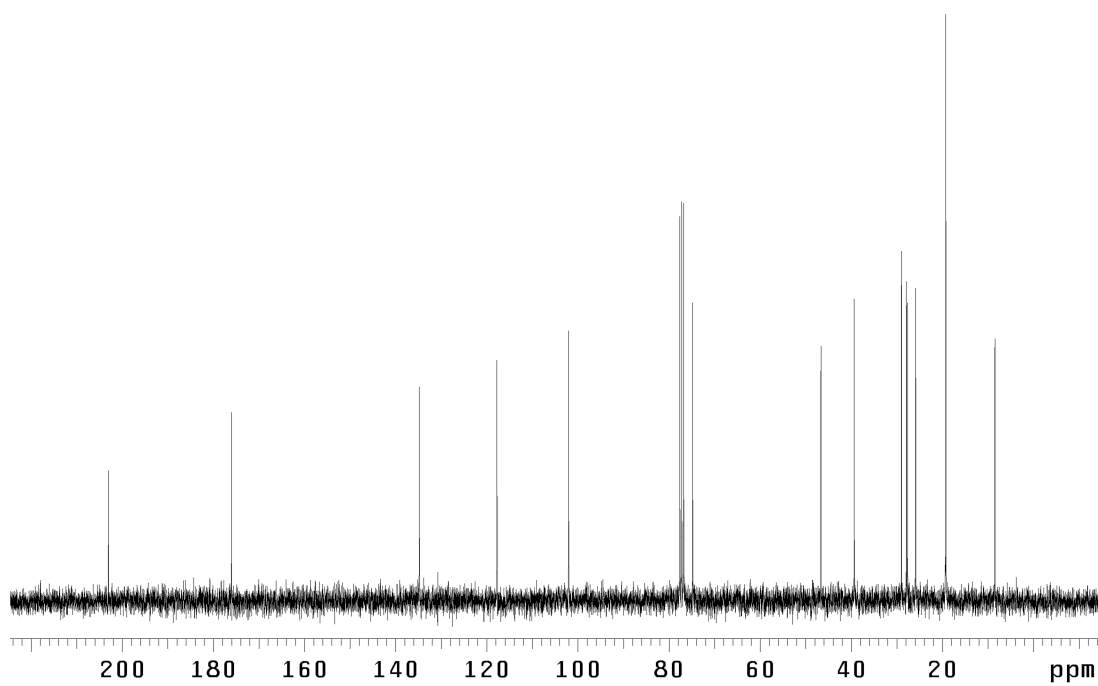


Figure A2.36 ¹³C NMR (300 MHz, CDCl₃) of compound **79**.

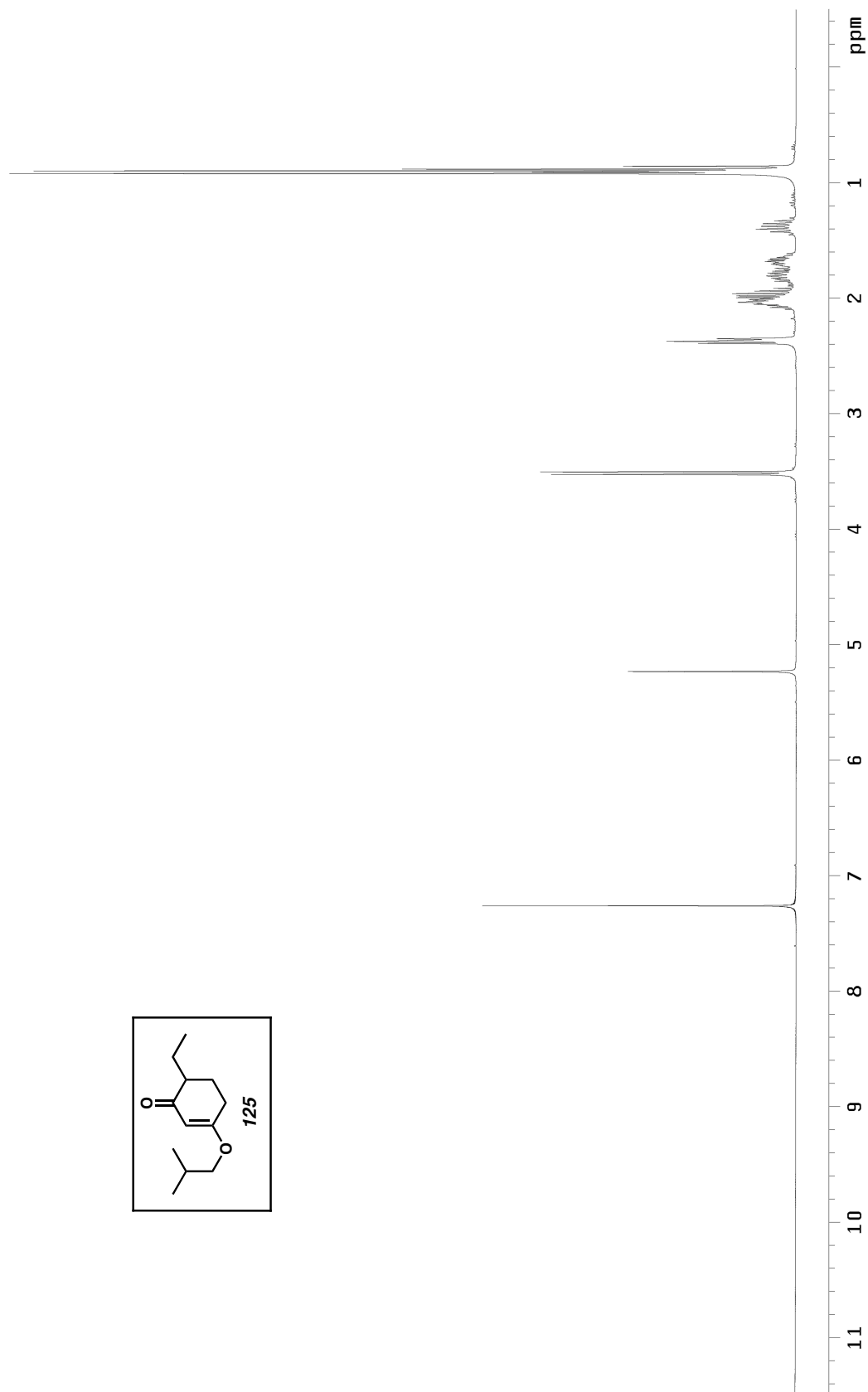
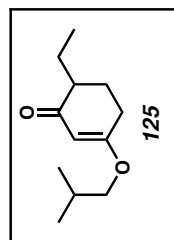


Figure A2.37 ^1H NMR (300 MHz, CDCl_3) of compound **125**.

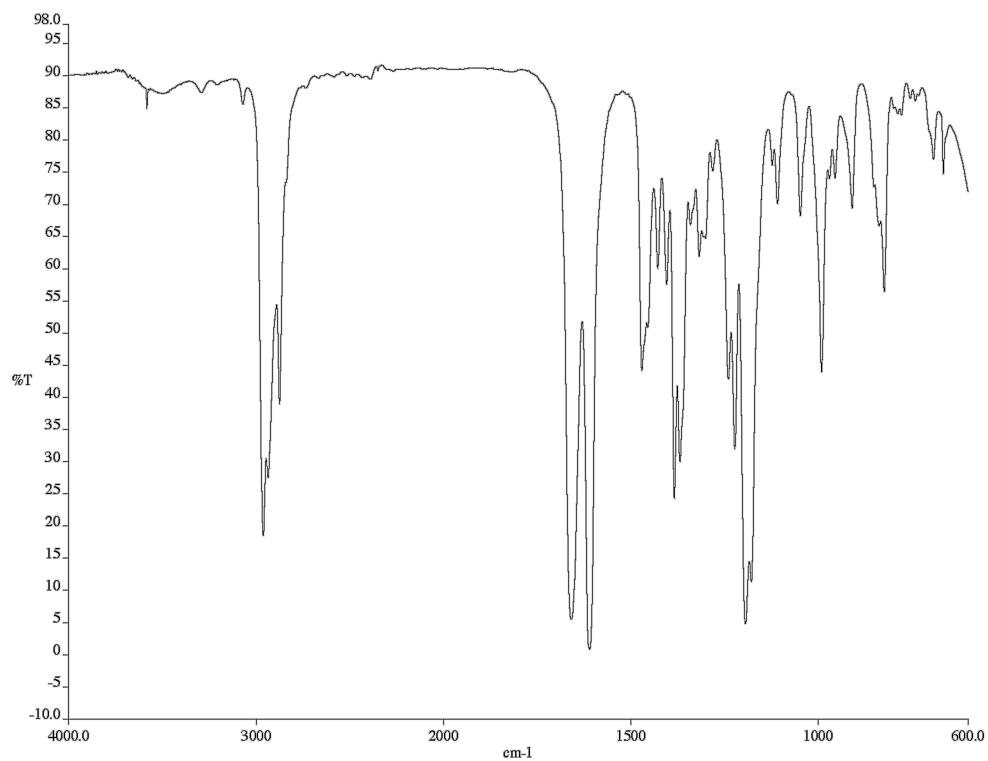


Figure A2.38 Infrared spectrum (NaCl/CDCl₃) of compound **125**.

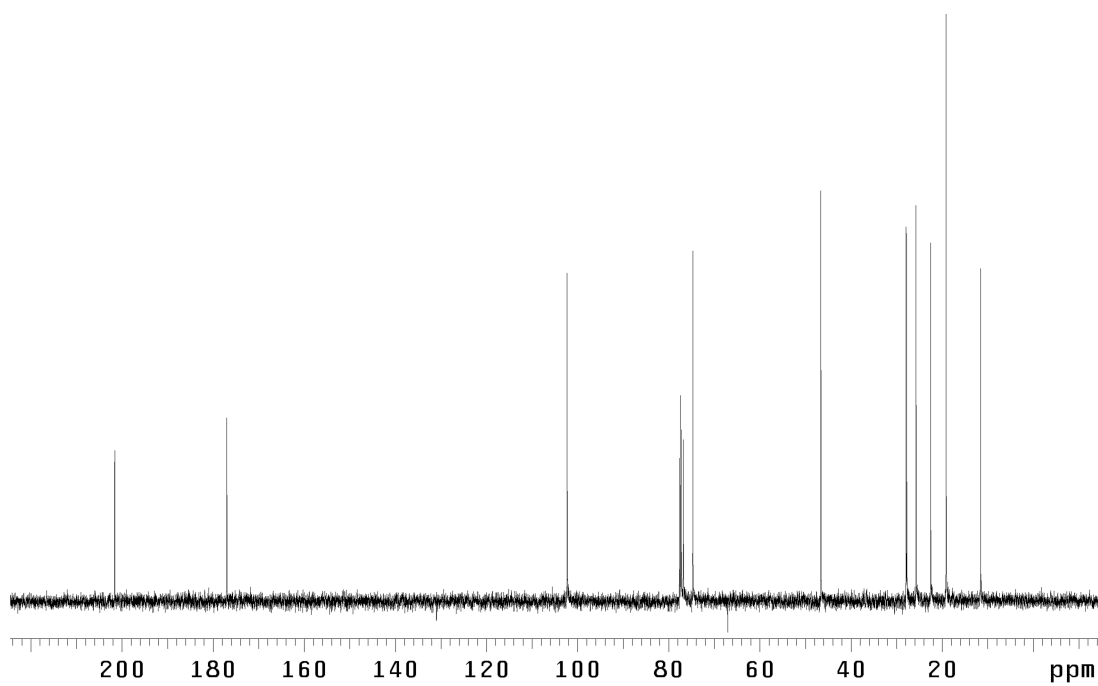


Figure A2.39 ¹³C NMR (75 MHz, CDCl₃) of compound **125**.

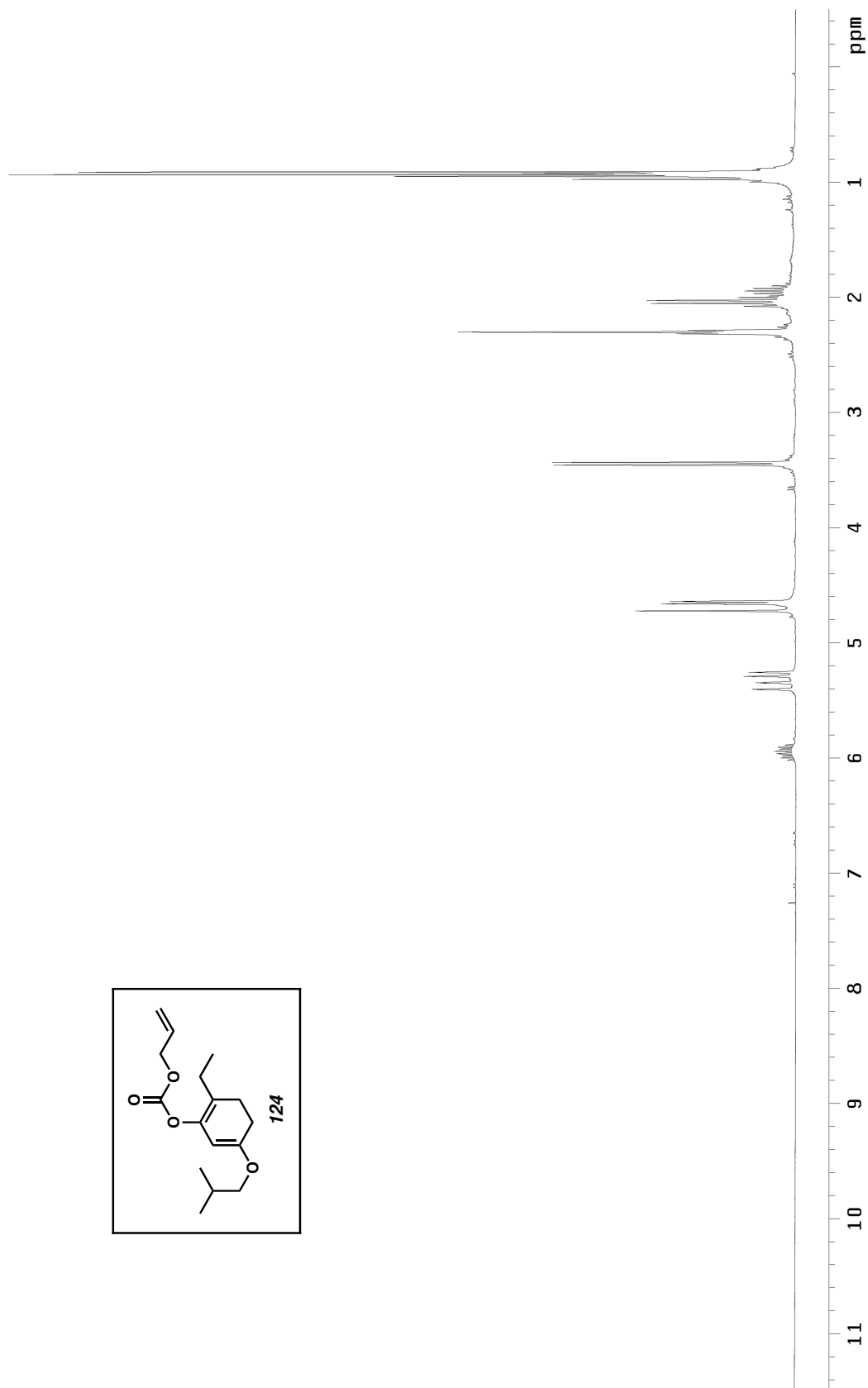


Figure A2.40 ^1H NMR (300 MHz, CDCl_3) of compound **124**.

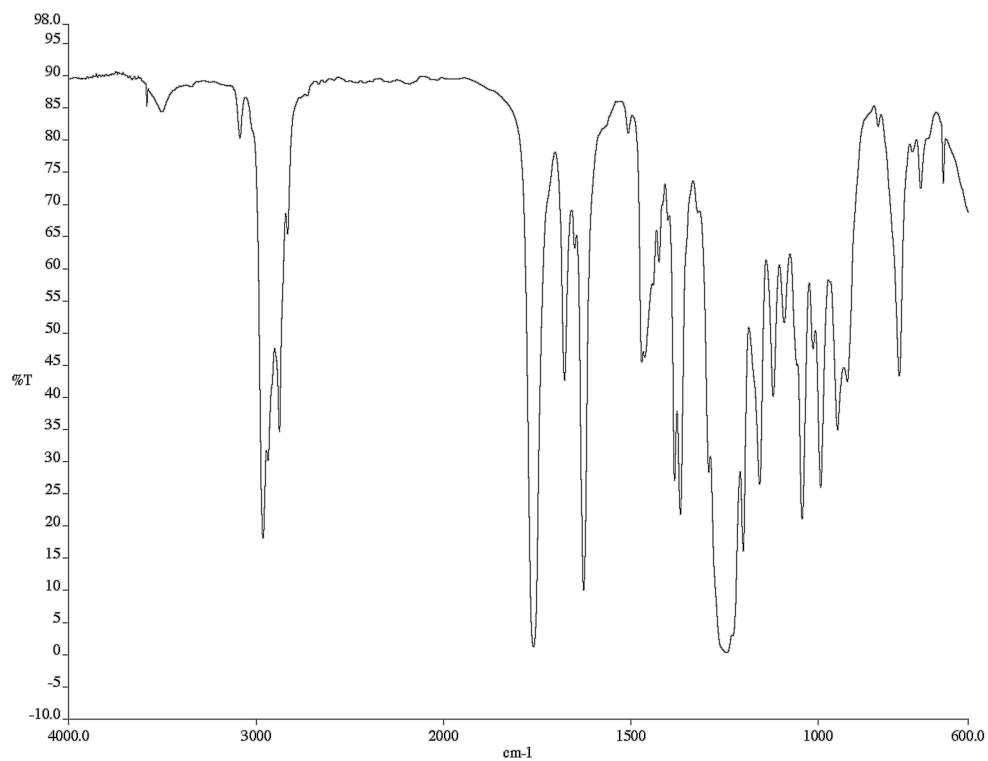


Figure A2.41 Infrared spectrum (NaCl/CDCl₃) of compound **124**.

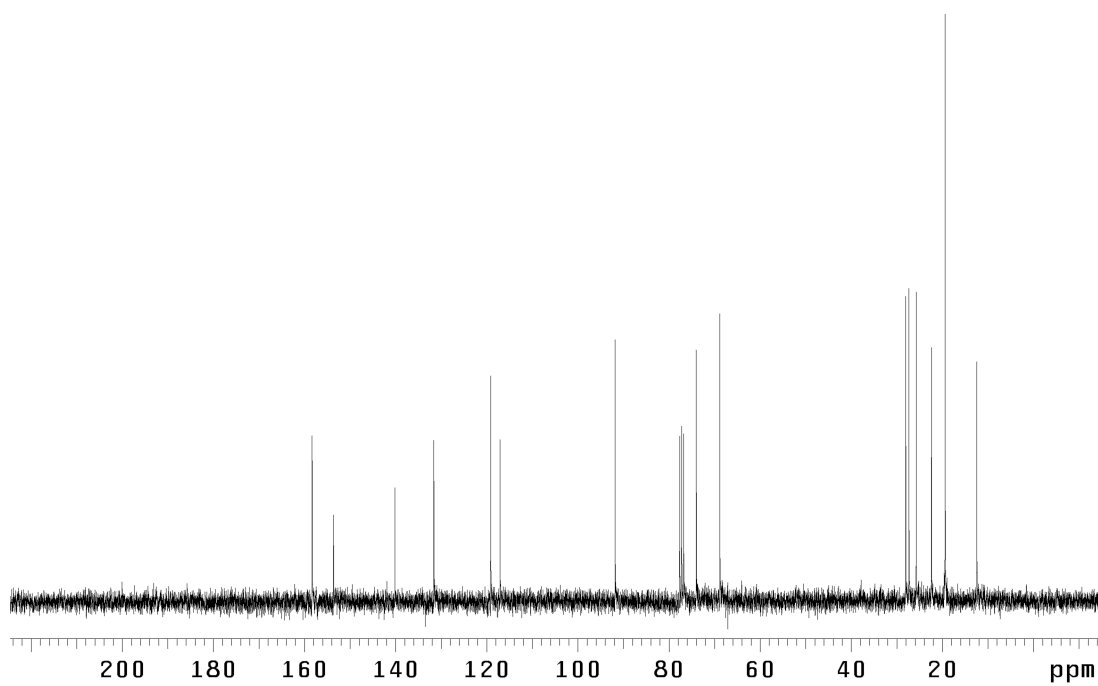


Figure A2.42 ¹³C NMR (75 MHz, CDCl₃) of compound **124**.

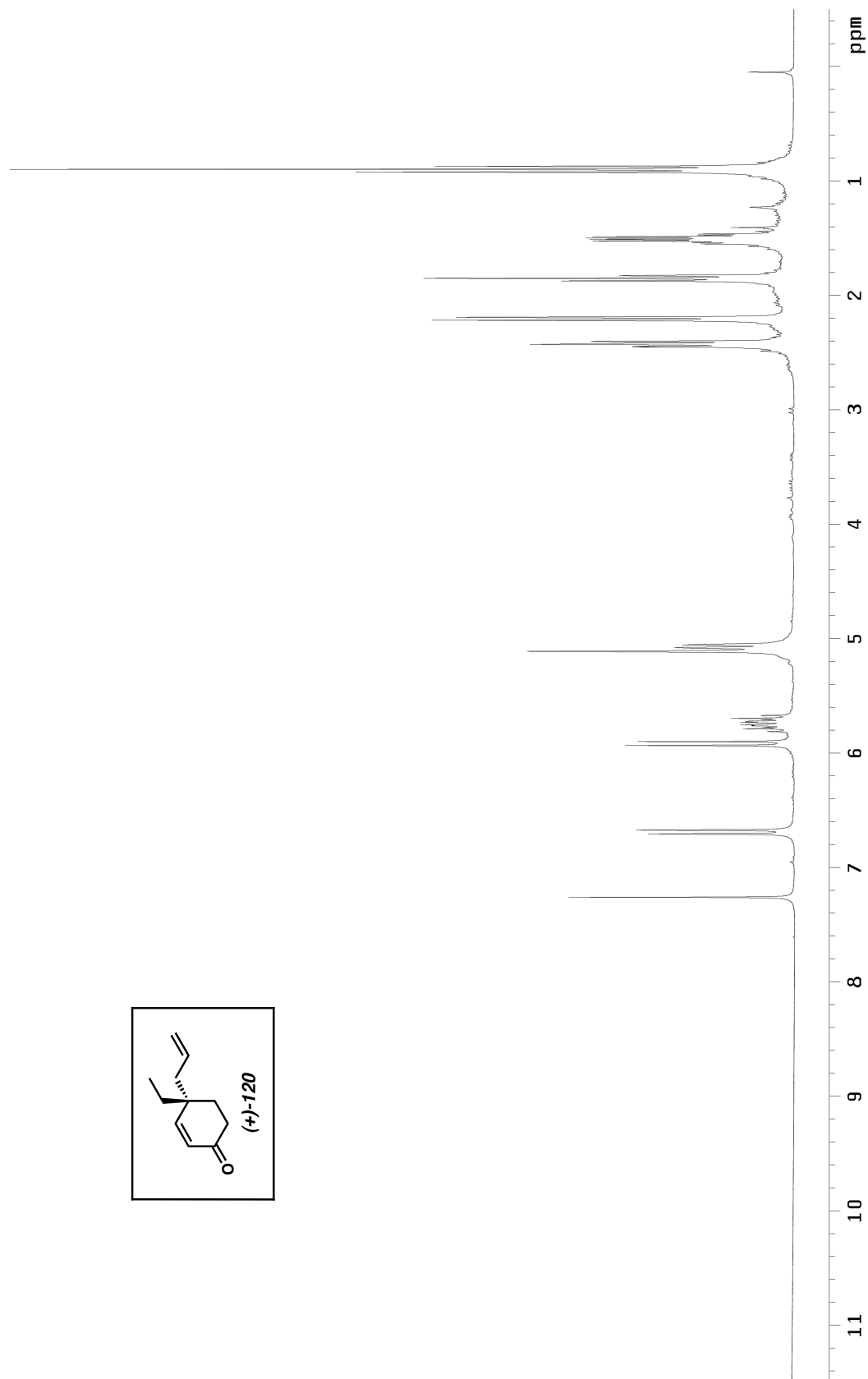


Figure A2.43 ^1H NMR (300 MHz, CDCl_3) of compound **120**.

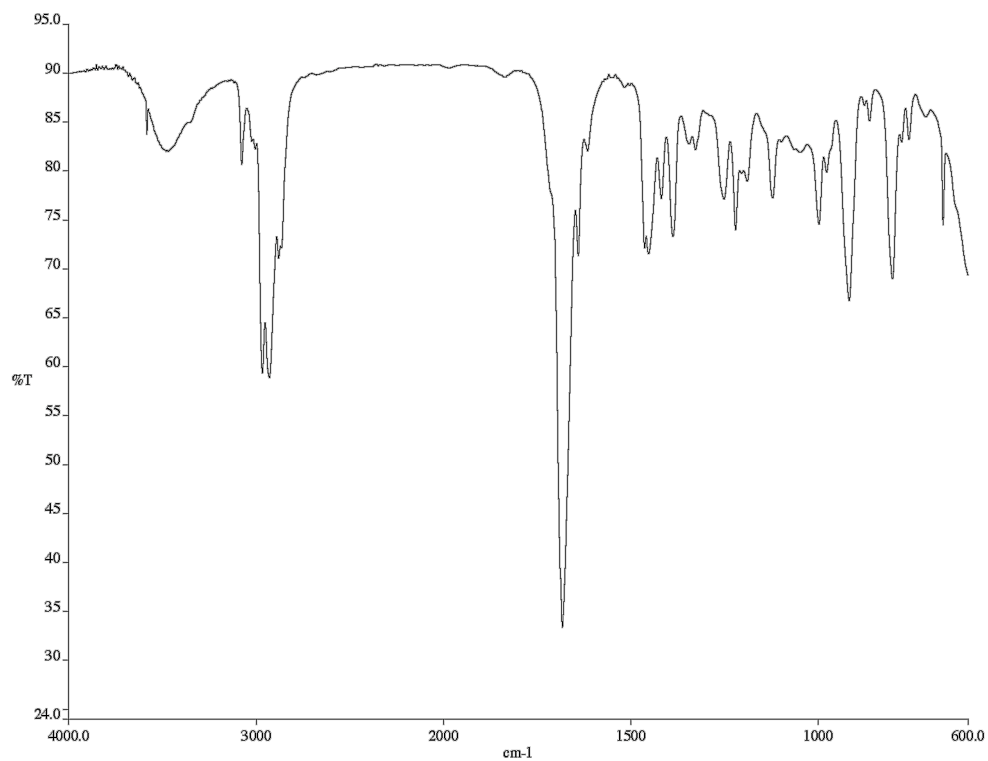


Figure A2.44 Infrared spectrum (NaCl/CDCl₃) of compound **120**.

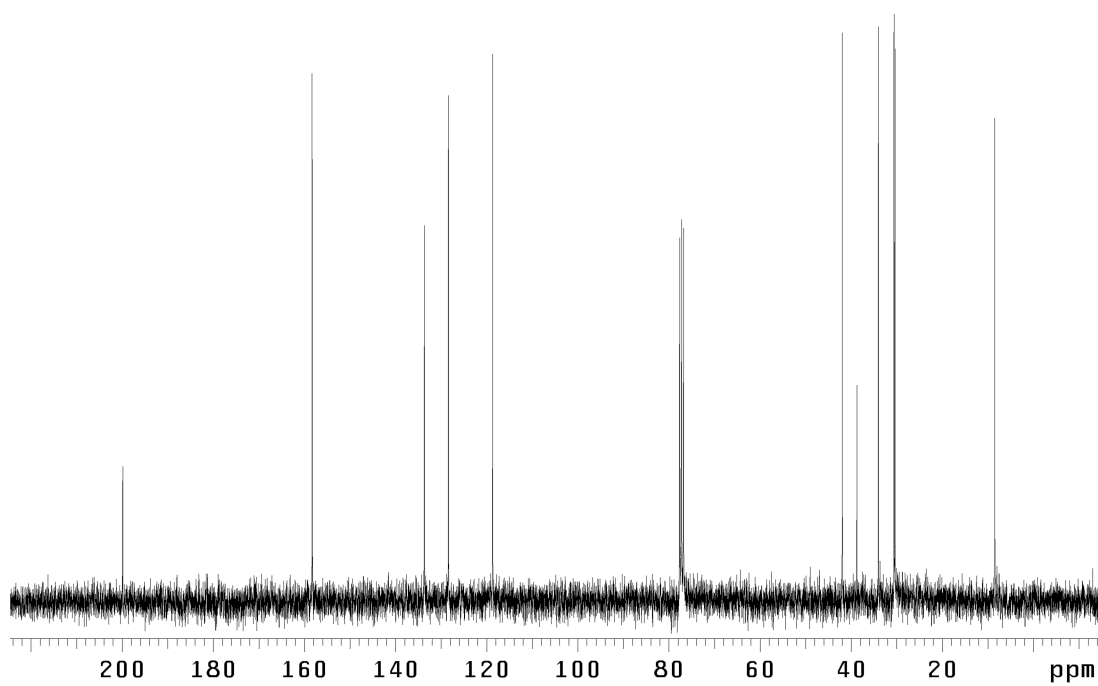


Figure A2.45 ¹³C NMR (75 MHz, CDCl₃) of compound **120**.

CHAPTER THREE†

The Catalytic-Enantioselective, Protecting Group-Free Total Synthesis of (+)-Dichroanone

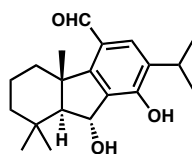
3.1 Natural Products with a [6-5-6] Carbocyclic Skeleton

3.1.1 Tricyclic Terpenoids Isolated from *Thuja standishii*, *Taiwania cryptomerioides*, and *Salvia dichroantha*

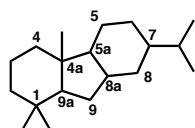
There is a growing class of natural products found that share a [6-5-6] tricyclic core. Whereas the homologous abietane diterpene skeletal structure **146**, which has a [6-6-6] carbocyclic scaffold, has been known for many years, this new 4a-methyltetrahydrofluorene class has only recently been uncovered (Figure 3.1). Three plant species are known to produce molecules with this tricyclic architecture. The first, *Thuja standishii*, yields standishinal (**147**), a substituted benzaldehyde.¹ The second, *Taiwania cryptomerioides*, has yielded the largest contingent of [6-5-6] natural products to date, where each member features a highly oxidized aromatic ring.² Finally, and most recently, natural products in this 4a-methyltetrahydrofluorene family have also been discovered in *Salvia dichroantha*, a flowering plant native to Turkey.³ Three 4a-methyltetrahydrofluorenes have been isolated from the root extract of this plant: dichroanal A (**148**), dichroanal B (**149**), and (–)-dichroanone ((–)-**150**). The biosyntheses of these compounds, though not fully understood, may begin from preformed abietanes (**146**). If this is true, the abietane cores may undergo oxidation and central ring restructuring, leading to rearranged 4a-methyltetrahydrofluorene diterpenoids (e.g., taiwaniaquinone D (**151**)).^{2a} Occasionally, a one-carbon excision may occur, leading to norditerpenoid variants (e.g., dichroanone ((–)-**150**).

†(Pages 140-189 reproduced in part from *J. Am. Chem. Soc.* **2006**, *128*, 7738; supporting information.)

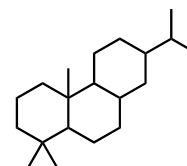
Figure 3.1 [6-5-6] Natural Products

Thuja standishii

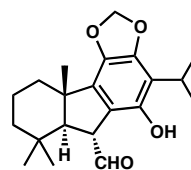
Standishinal (147)



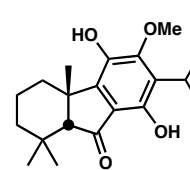
4a-methyltetrahydrofluorene skeleton (152)



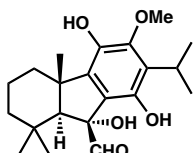
Abietane Skeleton (146)

Taiwania cryptomerioides

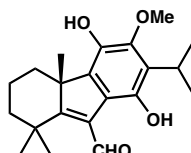
Taiwaniaquinol A (153)



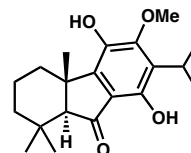
Taiwaniaquinol B (154)



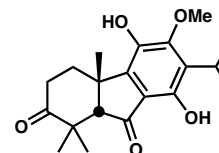
Taiwaniaquinol C (155)



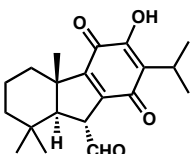
Taiwaniaquinol D (156)



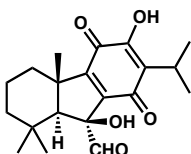
Taiwaniaquinol E (157)



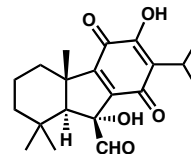
Taiwaniaquinol F (158)



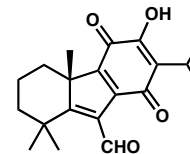
Taiwaniaquinone A (159)



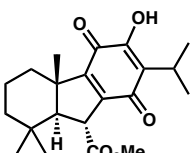
Taiwaniaquinone B (160)



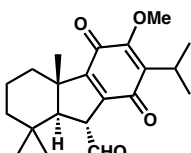
Taiwaniaquinone C (161)



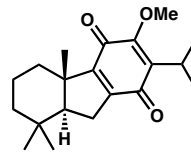
Taiwaniaquinone D (161)



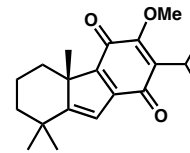
Taiwaniaquinone E (162)



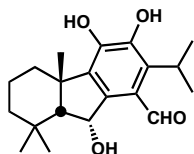
Taiwaniaquinone F (163)



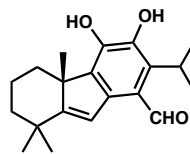
Taiwaniaquinone G (164)



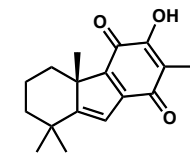
Taiwaniaquinone H (165)

Salvia Dichroantha

Dichroanal A (148)



Dichroanal B (149)



(-)-Dichroanone (-)-150

3.1.2 *Biological Activity of the 4a-Methyltetrahydrofluorene Family*

Little is known of the biological activity of this family of natural products. However, standishinal (**147**) has been found to inhibit aromatase, an enzyme involved in the biosynthesis of estrogen.⁴ Thus, it is believed that molecules in the family could be used to develop agents targeting estrogen-dependent carcinomas.^{2d} It is possible that other members of the [6-5-6] carbocyclic class might have similar biological activity to standishinal (**147**), and we anticipate that a general synthetic route to members of this family would allow for detailed structure-activity-relationship studies.

3.1.3 *Structural Characteristics of the 4a-Methyltetrahydrofluorene Family*

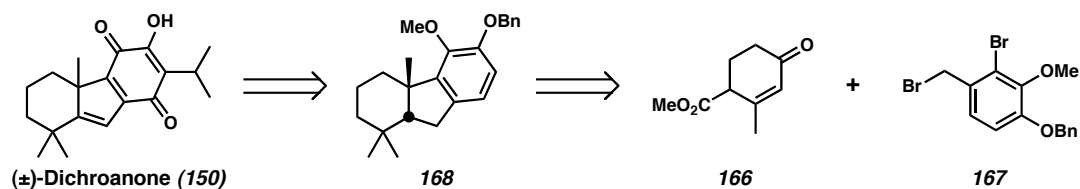
In addition to the unique tricyclic ring structure found in the 4a-methyltetrahydrofluorene natural products, some other features are noteworthy. The compounds each possess all-carbon quaternary stereocenters adjacent to an aromatic or quinoid ring. These highly oxidized ring systems pose another synthetic challenge. In most cases, the aromatic or quinoid ring is fully substituted, and in every case there is an isopropyl substituent at C(7) (Figure 3.1). Some members of the family display *p*-quinones, a potentially sensitive functional group for the synthetic chemist. The attractive features and unique [6-5-6] ring topologies of these molecules have inspired a number of total syntheses. When we initially became interested in these compounds as synthetic targets, the absolute stereochemistries of the molecules were unknown.

3.2 Synthetic Studies on [6-5-6] Carbocyclic Natural Products

3.2.1 Banerjee's Approach to the 4a-Methyltetrahydrofluorenes

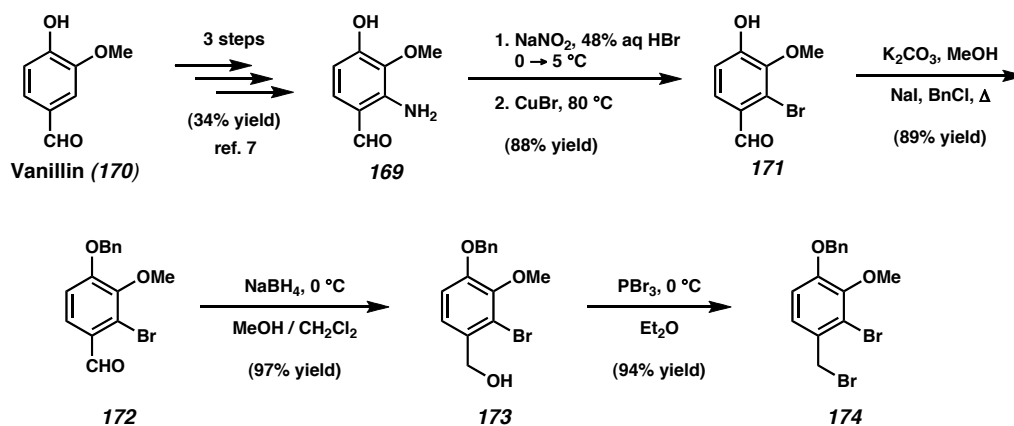
Banerjee published the first total syntheses of members of the 4a-methyltetrahydrofluorene family in 2003.⁵ The molecules completed in the group's first report included (±)-dichroanal B (**149**) and (±)-dichroanone (**150**), but later Banerjee also published total syntheses of (±)-taiwaniaquinol B (**154**) and (±)-taiwaniaquinones H and D (**151** and **154**, respectively).⁶ Their route to these racemates was designed to handle the challenges associated with the quaternary stereocenter, while taking a convergent approach to the construction of the tricyclic core (Scheme 3.1). Two 6-membered carbocyclic fragments (**166** and **167**) were separately assembled and subsequently coupled to prepare the central 5-membered ring of the natural products.

Scheme 3.1 Banerjee's Retrosynthetic Analysis



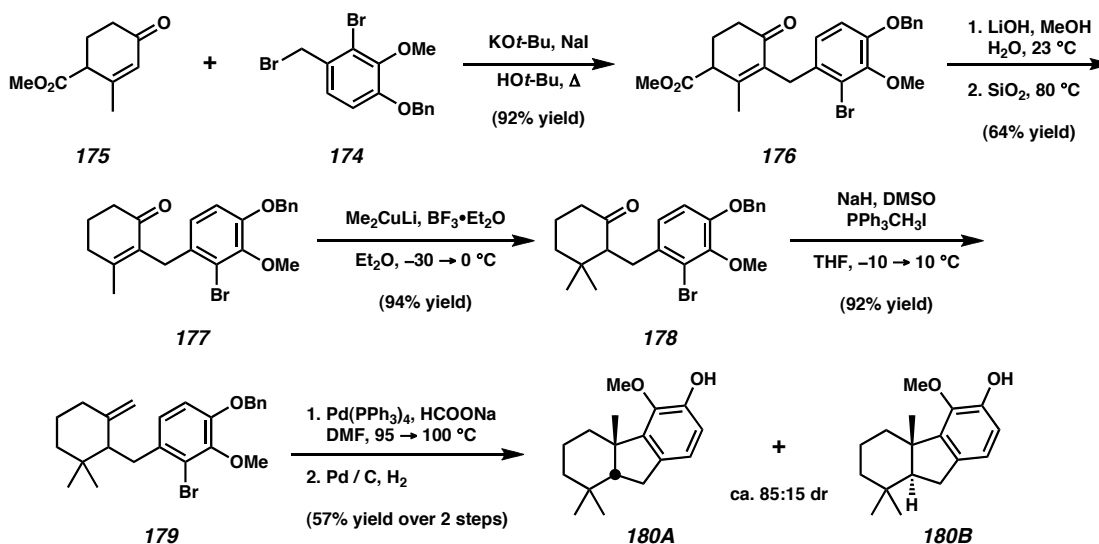
Banerjee's synthesis of the aromatic portion of the natural products began with the preparation of tetrasubstituted arene **169**, according to a published method (Scheme 3.2).⁷ With aniline **169** in hand, Sandmeyer chemistry allowed the installation of a bromine atom. Benzylolation of phenol **171** under Finkelstein conditions followed by reduction of the aldehyde functionality furnished benzylic alcohol **173**. Treatment with PBr_3 provided the first coupling partner, **174**, in excellent yield.

Scheme 3.2 Preparation of the Aromatic Coupling Partner



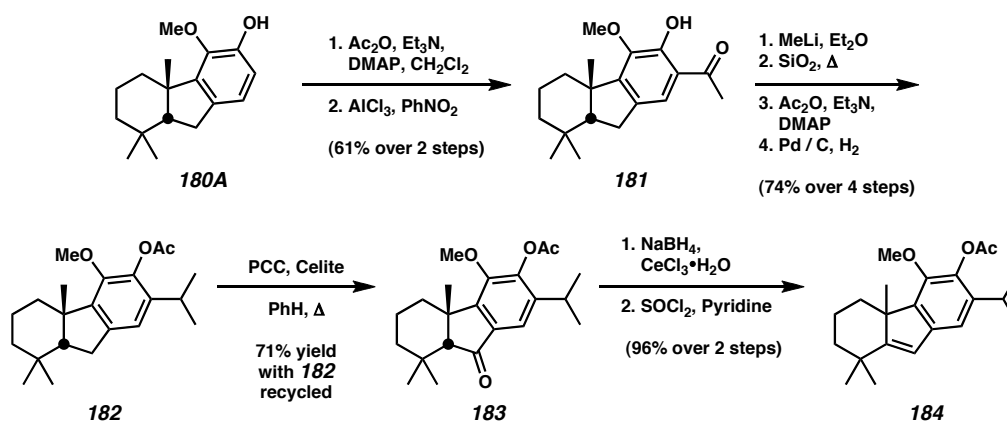
The other coupling fragment **175** was then appended to the benzylic bromide **174** in an alkylation reaction (Scheme 3.3). The use of **175** as opposed to its ethyl ester variant (Hagemann's ester) was crucial, as the attempted decarboxylation of the ethyl ester variant of **175** led to multiple products. Treatment of **177** with Gilman's reagent installed the geminal dimethyl functionality on the cyclohexane ring of **178**. Methylenation was followed by an intramolecular reductive Heck cyclization, closing the central 5-membered ring, while producing two separable diastereomers. The tricycle **180A**, bearing *cis*-ring fusion at the C(4a) and C(9a) positions, was carried onward through the synthesis.

Scheme 3.3 Union of the Coupling Partners



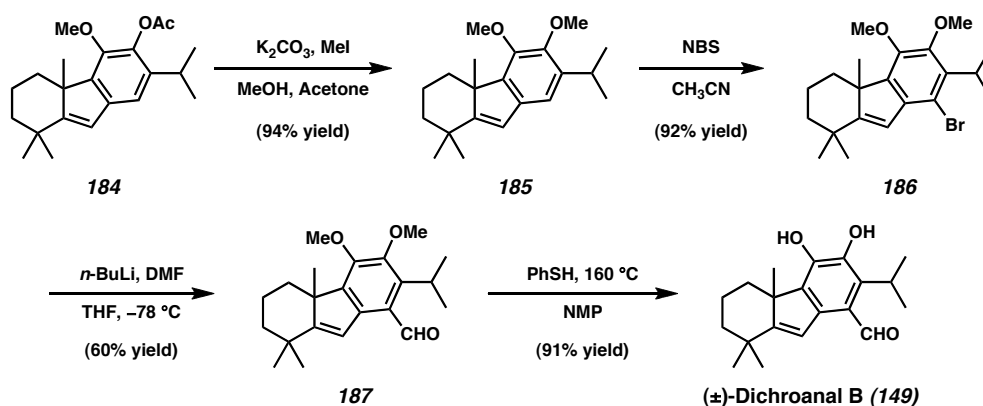
The next focus of the synthesis was the installation of the isopropyl moiety. Acylation of **180A** and Fries rearrangement,⁸ followed by a 4-step sequence of events, led to the acetate-protected catechol **182** (Scheme 3.4). Oxidation of the 5-membered ring with PCC gave ketone **183**, which was reduced and dehydrated with SOCl_2 , furnishing the styrene **184**. At this point the synthesis diverged into two paths.

Scheme 3.4 Installation of the Isopropyl Moiety

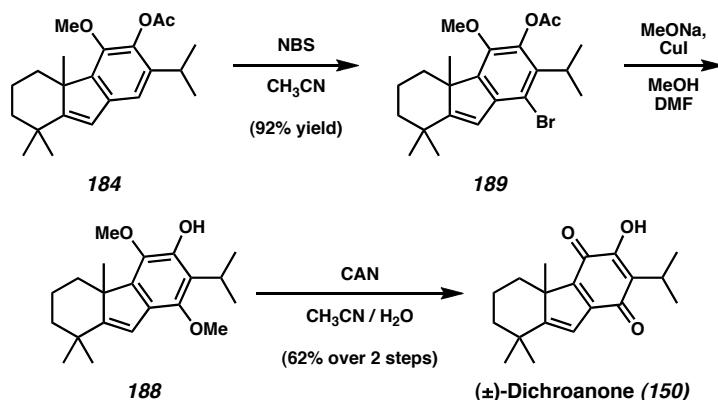


(±)-Dichroanal B (**149**) was prepared as follows (Scheme 3.5). A portion of protected catechol **184** was converted via saponification and methylation to the veratrole **185**. Chemoselective bromination of the aromatic portion of the molecule furnished **186** in excellent yield. Metal-halogen exchange was followed by DMF quench and nucleophilic demethylation with thiophenol, completing the first total synthesis of (±)-dichroanal B (**149**).⁹

Scheme 3.5 Completion of (±)-Dichroanal B



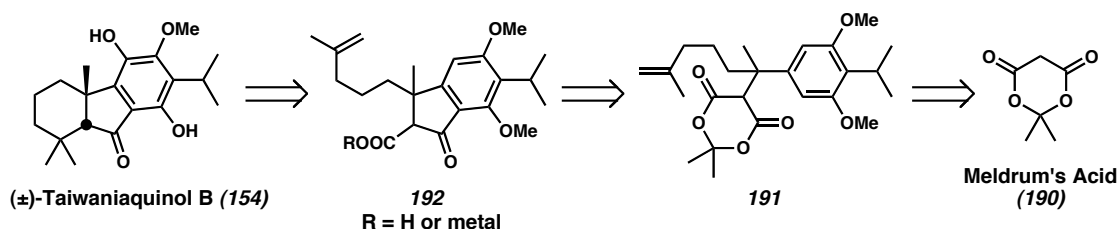
Alternatively, styrene **184** could also be carried on to (±)-dichroanone (**150**) (Scheme 3.6). Selective bromination of **184**, followed by a copper(I)-promoted methoxylation reaction, furnished the bis-(methyl)hydroquinone **188**. When this molecule was treated with ceric ammonium nitrate in water and acetonitrile, (±)-dichroanone (**150**) was produced in 62% yield from **189**.¹⁰

Scheme 3.6 Total Synthesis of (±)-Dichroanone (**150**)

3.2.2 Fillion's Approach to Taiwaniaquinol B

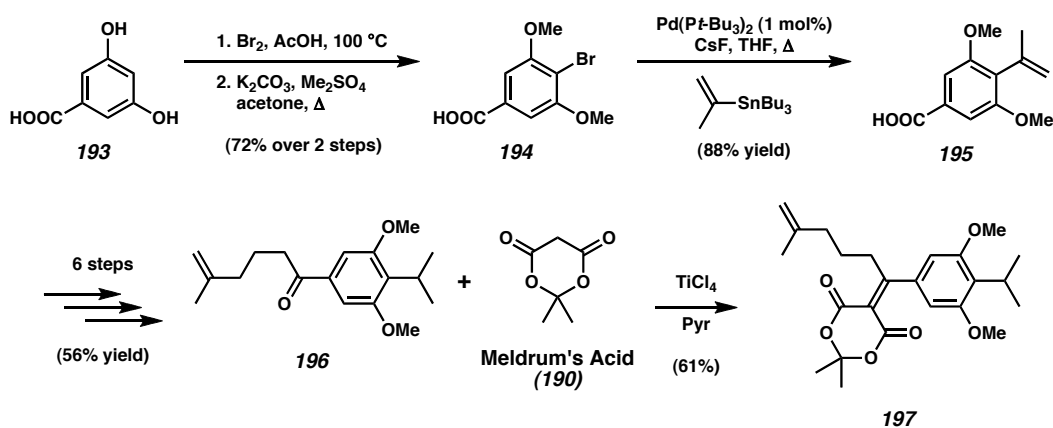
Fillion's group has also published a total synthesis of a 4a-methyltetrahydrofluorene diterpenoid, (±)-taiwaniaquinol B (**154**).¹¹ Their synthetic design was inspired by the powerful versatility of Meldrum's acid (**190**) (Scheme 3.7). It was envisioned that the tricyclic scaffold of (±)-taiwaniaquinol B (**154**) might be assembled in one step from the branched compound **191** via **192**. It was known that Meldrum's acid analogues, such as **191**, are prone to retro [4+2] cycloadditions, leading to thermal loss of acetone. Fillion postulated that the reactive ketene generated would acylate the nearby arene, forming indanone **192**. After a decarboxylation event and *tert*-alkylation, the final ring of the natural product could be assembled.

Scheme 3.7 Retrosynthesis of Taiwaniaquinol B



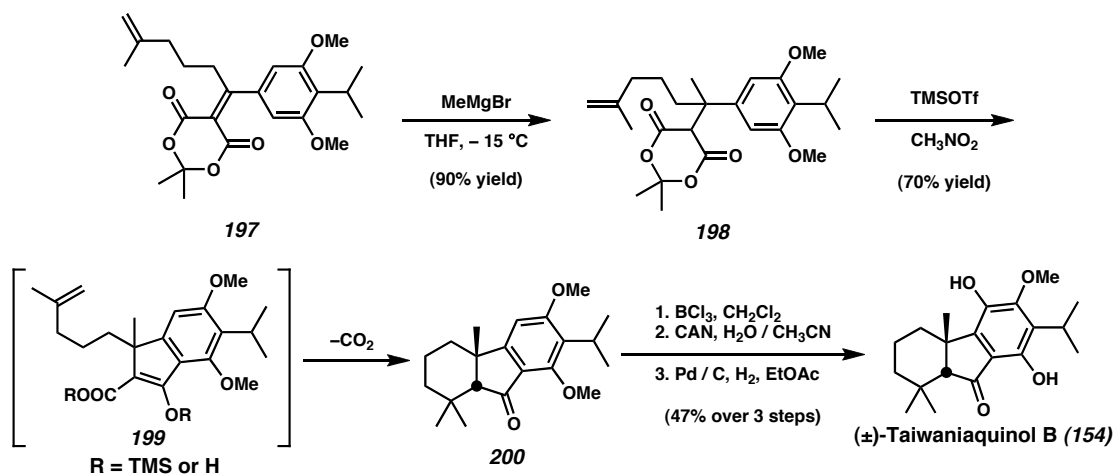
The synthesis commenced with 3,5-dihydroxybenzoic acid (**193**) (Scheme 3.8). Regioselective bromination, followed by bis-methylation and Stille coupling of 2-propenyl stannane, furnished the styrene **195**. A 5-step elaboration of **195** to the geminally substituted alkene **196** was followed by Knoevenagel condensation with Meldrum's acid (**190**), affording **197**.

Scheme 3.8 Beginning of the Synthesis



Chemoselective conjugate addition of MeMgBr to **197** gave the branched compound **198**, poised for the key cyclization reaction (Scheme 3.9). In a unique reaction cascade, treatment of **198** with stoichiometric TMSOTf induced a Friedel-Crafts acylation, followed by decarboxylation and acid-mediated *tert*-alkylation of a putative enolate **199**. This quickly assembled the *cis*-fused [6-5-6] tricyclic framework with complete diastereoselectivity. The arene **200** was readily elaborated to (±)-taiwaniaquinol B (**154**) after selective demethylation and oxidation to the hydroquinone oxidation state.¹²

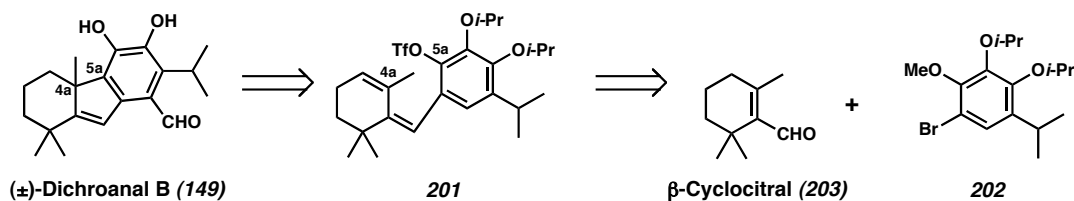
Scheme 3.9 Fillion's Total Synthesis of (±)-Taiwaniaquinol B



3.2.3 Node's Synthesis of Dichroanal B

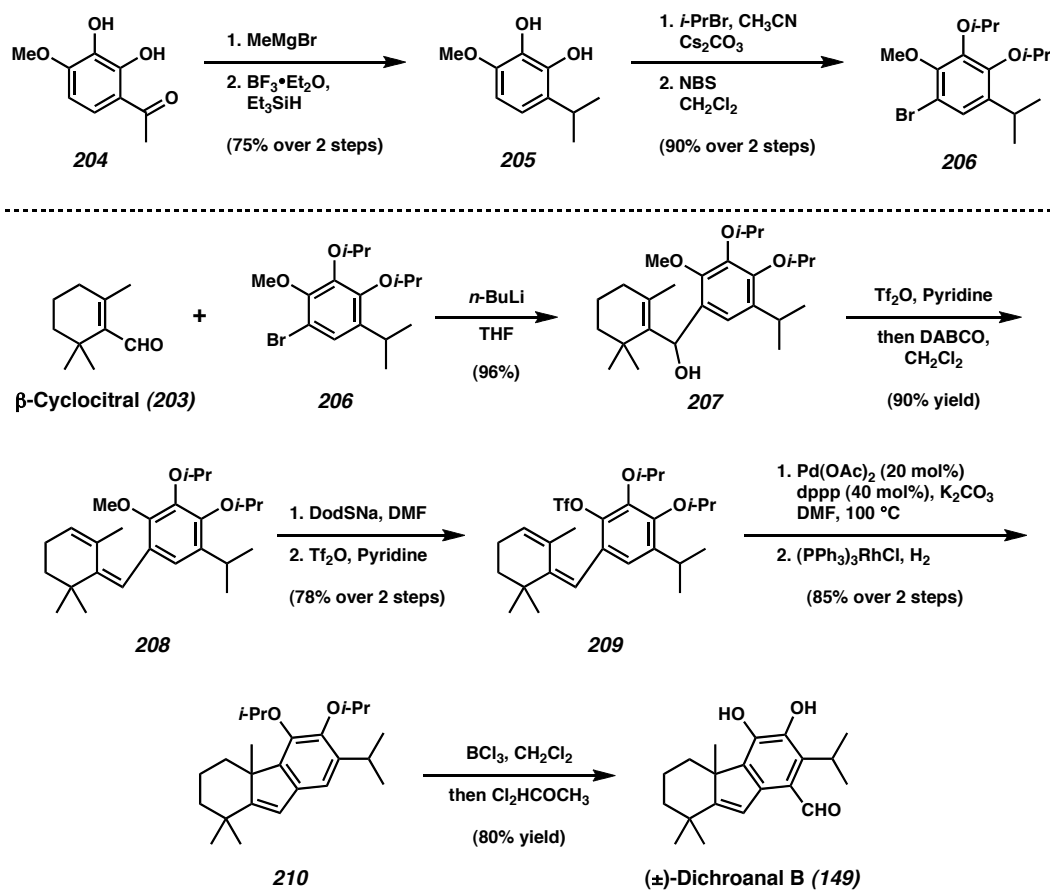
The Node group designed an efficient synthesis of (±)-dichroanal B (**149**) that employed a convergent approach.¹³ As Banerjee had done,^{5,6} Node made a key retrosynthetic disconnection across C(4a) and C(5a). A 5-*exo*-intramolecular Heck cyclization was the reaction of choice for the desired C-C bond formation (Scheme 3.10). Node decided to use an endocyclic olefin at the point of cyclization (C(4a)), leading to an overall oxidatively neutral Heck cyclization. The substrate for this transformation, **201**, could come from two fragments: the arene **202** and β-cyclocitral (**203**).¹⁴

Scheme 3.10 Node's Retrosynthetic Analysis



To begin the synthesis of (±)-dichroanal B (**149**), tetrasubstituted arene **204** was treated with MeMgBr, followed by a Lewis-acid-promoted reduction with Et₃SiH (Scheme 3.11). The two free hydroxyls of **205** were protected as isopropyl ethers, and the resulting compound was chemoselectively brominated with *N*-bromosuccinimide in excellent yield, furnishing **206**.

Scheme 3.11 Total Synthesis of Racemic Dichroanal B



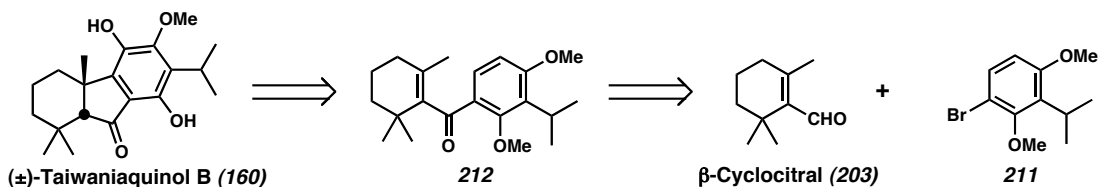
With aryl bromide **206** in hand, a lithium-halogen exchange was performed, and the resulting lithio-arene was treated with β -cyclocitral (**203**),¹⁴ resulting in 1,2-addition (Scheme 3.11). Chemoselective dehydration of **207** with triflic anhydride and DABCO

furnished the *s-trans*-diene **208** in high yield. Selective demethylation of the aryl methyl ether in the presence of two *i*-Pr ethers was achieved with sodium dodecanethiolate, and the unmasked hydroxyl group was triflated, affording **209**. The key intramolecular Heck cyclization proceeded as intended, and the resulting disubstituted olefin moiety was selectively hydrogenated with Wilkinson's catalyst and H₂. The tricyclic styrene product **210** was treated with BCl₃ followed by α,α -dichloromethyl methyl ether, completing the total synthesis of (\pm)-dichroanal B (**149**).¹⁵

3.2.4 Trauner's Synthesis of *Taiwaniaquinoids*

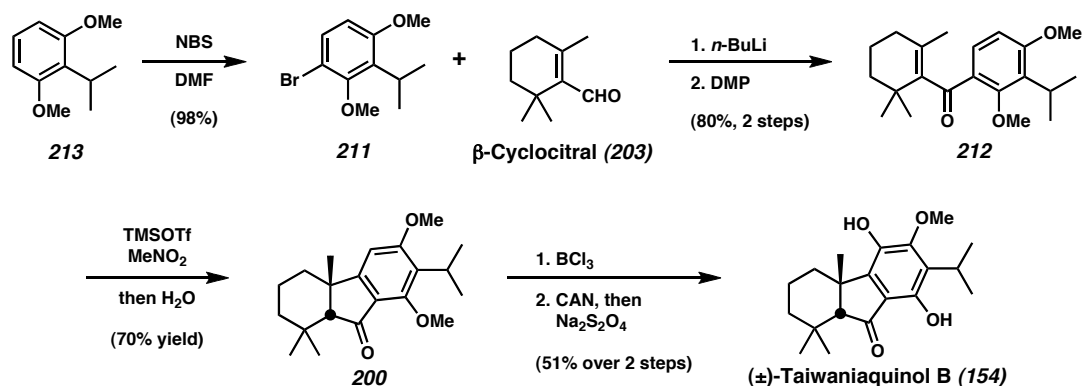
The Trauner group has also sought to address the challenges presented by the 4a-methyltetrahydrofluorene natural products.¹⁶ Their efforts culminated in the total syntheses of (\pm)-taiwaniaquinols B and D (**160** and **151**), along with (\pm)-taiwaniaquinone H (**165**) and (\pm)-dichroanone (**150**). Their investigations demonstrated the generality of their route toward preparation of several members of this natural product family. Key to the Trauner's retrosynthetic analysis was the possibility of building the central 5-membered ring using a Nazarov cyclization (Scheme 3.12). Like the Node's synthesis,¹³ this one would also begin with the unification of an arene fragment (**211**) and β -cyclocitral (**203**).¹⁴

Scheme 3.12 Trauner's Retrosynthetic Analysis



To begin the syntheses, 2,6-dimethoxycumene (**213**)¹⁷ was monobrominated with *N*-bromosuccinimide in DMF (Scheme 3.13). Subsequent lithium halogen exchange, followed by 1,2-addition to β -cyclocitral (**203**),¹⁴ furnished an aryl vinyl carbinol. Oxidation with Dess-Martin periodinane gave aryl ketone **212**, which was poised for the key Nazarov cyclization. Upon treatment of **212** with TMSOTf in nitromethane, followed by aqueous workup, the *cis*-fused product **200** was obtained in good yield as a single diastereomer. Key to the success of this reaction was the use of MeNO₂ as the solvent because less polar alternatives resulted in poor conversion. Although **200** had already been prepared in Fillion's synthesis of (\pm)-taiwaniaquinol B (**154**) (Scheme 3.9),¹¹ the Trauner group published a different endgame involving monodeprotection and CAN-mediated oxidation (Scheme 3.13).¹⁸

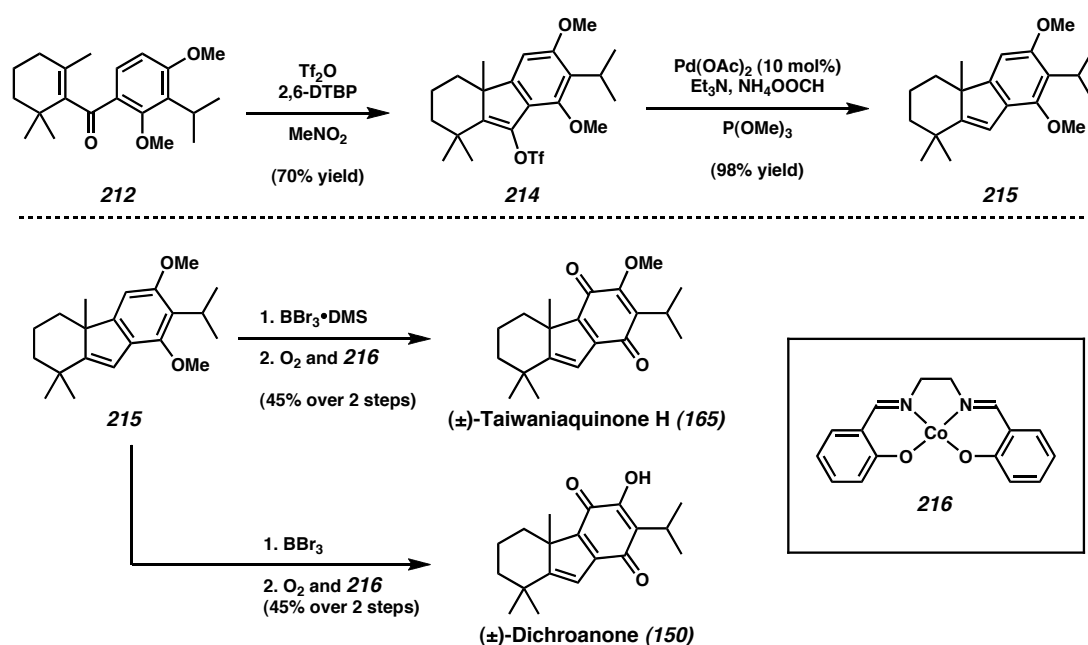
Scheme 3.13 Completion of Racemic Taiwaniaquinol B



Using alternative Lewis acids in the Nazarov cyclization was possible, ultimately leading to the completion of other natural products (Scheme 3.14). If triflic anhydride was employed in lieu of TMSOTf, along with a base, a stable enol triflate (**214**) could be isolated. After completion of the Nazarov triflation, Pd-catalyzed reductive detriflation

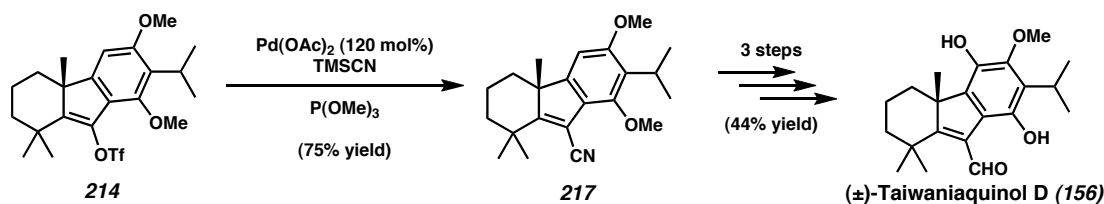
furnished the useful styrene **215**, which was carried onward to (±)-dichroanone (**150**) and (±)-taiwaniaquinone H (**165**). Of note, the compound **215** could be either mono- or di-demethylated with judicious choice of Lewis acid. To install the final oxygen atom in both natural products,¹⁹ a cobalt(II) *N,N'*-bis-salicylidene-ethylenediamine catalyst (**216**) was used with molecular oxygen as the terminal oxidant.

Scheme 3.14 Application of the Nazarov Triflation



The enol triflate **214** was also converted to a vinyl nitrile **217** in the presence of superstoichiometric $\text{Pd}(\text{OAc})_2$, $\text{P}(\text{OMe})_3$, and TMSCN (Scheme 3.15). After a short series of oxidation state adjustments, the total synthesis of (±)-taiwaniaquinol D (**156**) was achieved.²⁰ Trauner's syntheses of these natural products showed the broad utility of the Nazarov cyclization.

Scheme 3.15 Total Synthesis of Racemic Taiwanaiquinol D



3.2.5 Challenges to Address

Each group mentioned in the previous sections made great contributions toward understanding the chemistry of 4a-methyltetrahydrofluorene natural products.²¹ However, there was room for improvement in the syntheses of members of this class. Most of the synthetic strategies had focused attention on forming the central 5-membered ring. Although this allowed for a convergent approach to the tricyclic core, it required bringing in an aryl fragment with protecting groups. Even after the central rings were formed, there were usually numerous functional group interconversions before the total syntheses were complete. Perhaps most significant was that none of the reported methods were enantioselective. The absolute stereochemistries of these natural products was still uncertain, despite biosynthetic hypotheses.^{2b,c,22} We believed that using our catalytic enantioselective decarboxylative alkylation chemistry, we could address all of these matters in a concise total synthesis. Our primary target molecule would be dichroanone (**150**), but we envisioned that our route provide a general access to many members of the 4a-methyltetrahydrofluorene class (**152**, Figure 3.1).

3.3 First Retrosynthetic Analysis of Dichroanone

3.3.1 Complexities of the Dichroanone Architecture

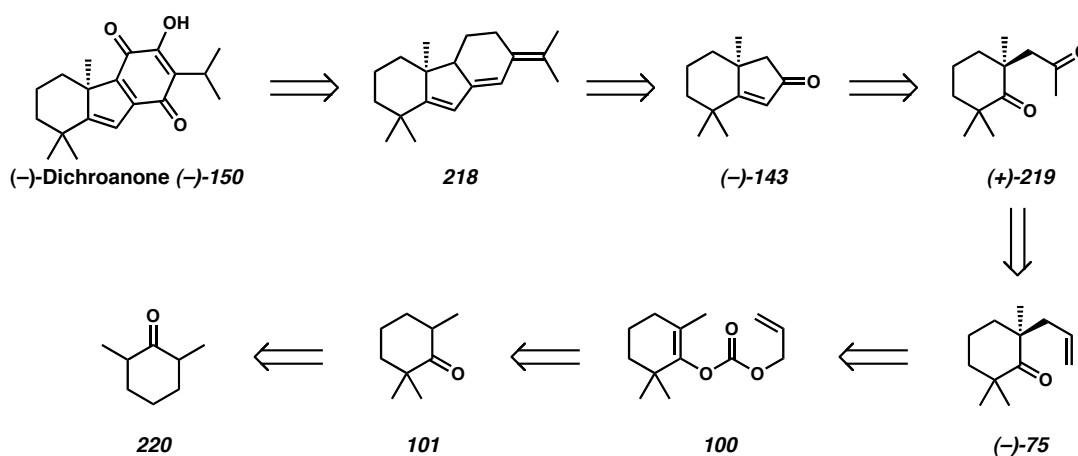
One goal of our total synthesis was to determine the absolute stereochemistry of the natural product by using our enantioselective decarboxylative alkylation to set the all-carbon-quaternary stereocenter. The second endeavor was to design a synthesis amenable to completion of related natural products. The pioneering work of Banerjee,^{5,6} Fillion,¹¹ Node,¹³ and Trauner¹⁶ provided a wealth of knowledge about the behavior of 4a-methyltetrahydrofluorenes. Previous syntheses had, without exception, dealt with protection of the aromatic oxygen atoms. To address this matter, we reasoned that the three oxygen atoms of dichroanone (**150**) could be installed at a late synthetic stage, possibly avoiding the need for protecting groups entirely. Our retrosynthesis would also need to address the challenge of selectively functionalizing the fully substituted *p*-quinone ring.

3.3.2 Retrosynthetic Analysis of Dichroanone

Our first retrosynthetic analysis of dichroanone (**150**) began with the removal of the oxygen atoms and the isopropyl group. It was reasoned that the natural product could be assembled from tricyclic hydrocarbon **218** (Scheme 3.16). This compound might arise from a simpler enone ((-)-**143**) via annulation. We anticipated that enone (-)-**143** could be easily prepared from diketone (+)-**219** using intramolecular aldol condensation. This 1,4-dicarbonyl compound could arise from allyl ketone (-)-**75**. Using our group's Pd-catalyzed enantioselective alkylation chemistry, (-)-**75** would originate from enol

carbonate **100**. The enol carbonate would ultimately come from commercially available 2,6-dimethylcyclohexanone (**220**).

Scheme 3.16 First Retrosynthetic Analysis of Dichroanone



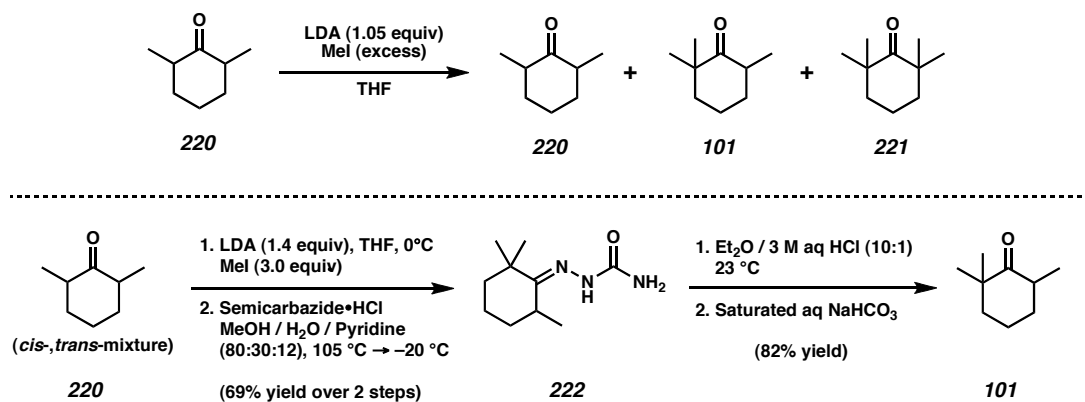
3.4 Synthesis of the Tricyclic Core

3.4.1 Preparation of a Racemic Bicyclic Enone

The first decision made during the total synthesis of (+)-dichroanone ((+)-150) was which commercially available starting material to use. 2,2,6-trimethylcyclohexanone (**101**) was an ideal choice, but its cost was prohibitive for use in batches larger than one gram.²³ To facilitate the large-scale production of material, we decided to use the less-costly 2,6-dimethylcyclohexanone (**220**), available as a *cis*, *trans* mixture.²⁴ Upon attempted methylation of **220** with iodomethane and LDA, a mixture of desired product **101**, unreacted starting material **220**, and bis-methylation adduct 2,2,6,6-tetramethylcyclohexanone (**221**) was obtained (Scheme 3.17). Initially we were encouraged because **101** was the major product of the reaction. Unfortunately, **220**, **101**, and **221** had very similar chromatographic properties and boiling points. Even careful fractional distillation was ineffective as a separation technique.

To address this issue and obtain large quantities of pure **101**, we decided to push the methylation reaction toward overalkylation, ensuring that no unreacted starting material would remain (Scheme 3.17). Once the reaction was complete, we took advantage of the steric differences between **101** and **221**. Upon treatment of the crude mixture with semicarbazide hydrochloride under basic conditions, we observed crystallization of the semicarbazone **222**. Presumably, the analogous semicarbazone of **221** is unable to form due to the extreme steric hindrance by the four methyl groups, leaving unreacted **221** in the mother liquors. Acidic hydrolysis of the desired semicarbazone **222** afforded pure 2,2,6-trimethylcyclohexanone (**101**) after distillation. This method allowed for the production of large batches of this compound without any chromatography.

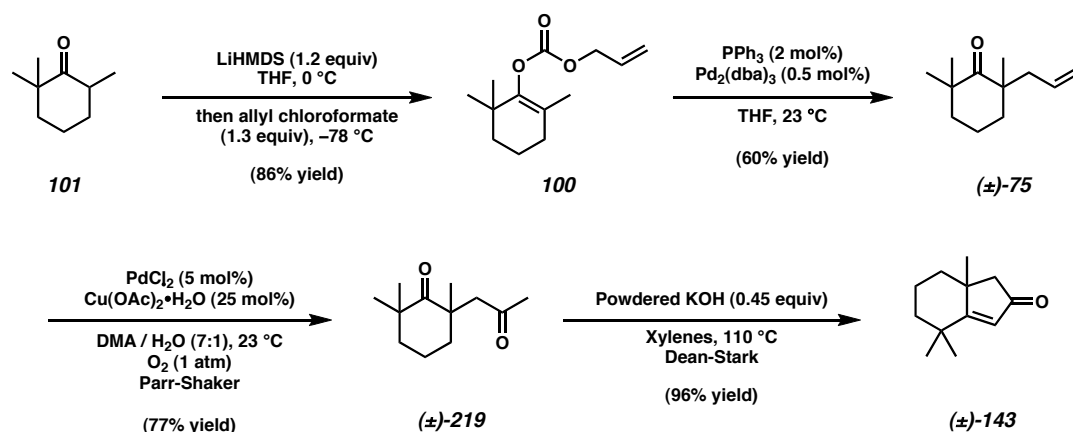
Scheme 3.17 Synthesis of 2,2,6-trimethylcyclohexanone



The 2,2,6-trimethylcyclohexanone (**101**) was smoothly converted to the allyl enol carbonate **100** via enolization with LiHMDS and allyl chloroformate trapping (Scheme 3.18).²⁵ Conveniently, we found that if PPh₃ was employed as an achiral ligand, a

racemic Tsuji allylation²⁶ could be conducted with as little as 0.5 mol% $\text{Pd}_2(\text{dba})_3$ and 2 mol% PPh_3 ligand. Use of enantioselective conditions required low substrate concentration (0.033 M) to achieve the highest degree of enantioselectivity. Hence, large solvent volumes were needed for high material throughput. However, using the PPh_3 -based non-enantioselective system, reactions could be performed at high concentrations (0.2 M). Although large-scale reactions could now be performed, care had to be taken during purification, as the allyl ketone (\pm)-**75** was found to be volatile.²⁷ Initial investigations into the total synthesis would be conducted with racemic material. Once chemistry was well established, the enantioselective synthesis would be undertaken.

Scheme 3.18 Completion of the Bicyclic Enone



We believed that a Wacker oxidation would be ideal for installation of a second ketone moiety of (\pm)-**219** (Scheme 3.18).²⁸ On small scale, this proved to be the case. However, when larger reactions were performed, catalyst lifetime was poor. Initially, we tried increasing the catalyst loadings of Pd and Cu or heating the reaction to higher temperature. These approaches met with limited success, though. We hypothesized that

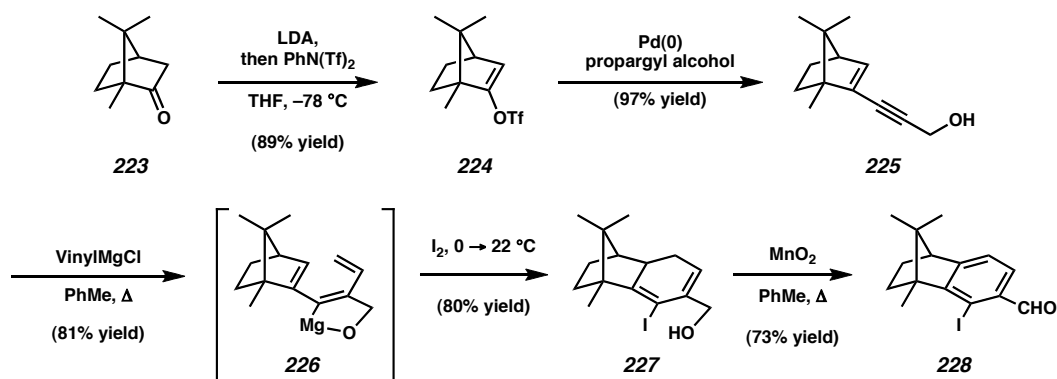
inefficient catalyst turnover was due to poor reoxidation of the palladium after substrate oxidation. Without enough O₂ in solution, Pd⁰ could not be regenerated. To increase the amount of O₂ uptake in these Wacker oxidations, we placed the reactions on a Parr shaker under a balloon of oxygen. With the increased oxygenation and headspace-solvent interaction, our oxidation reaction became very efficient on increased scale.

Finally, an intramolecular aldol condensation of diketone (**±**)-**219** was attempted. Conditions involving KOH and ethanol,²⁹ though capable of the transformation, were not high yielding in this case. Fortunately, if the reaction was performed in xylenes with azeotropic removal of water under Dean-Stark conditions,³⁰ bicyclic enone (**±**)-**143** could be prepared in excellent yield.³¹ Employing the methods we had developed, more than 17 grams of enone (**±**)-**143** was prepared in racemic form.

3.4.2 *6 π -Electrocyclization Approach to the Third Ring*

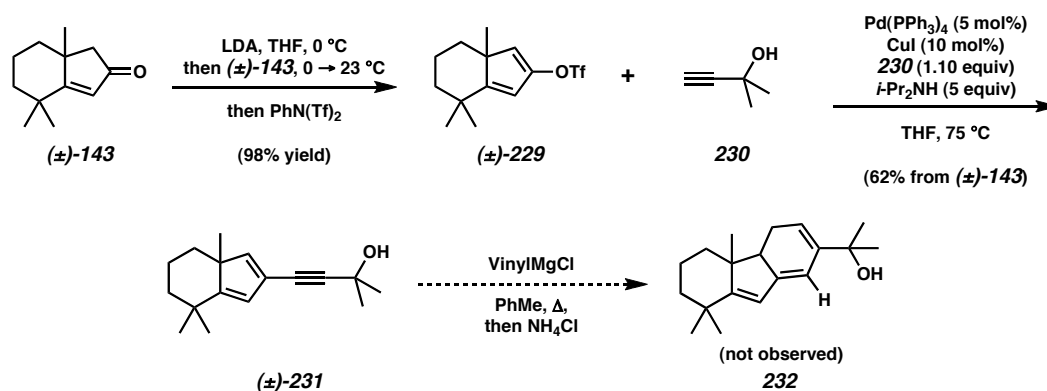
With the second carbocyclic ring of the natural product in place, we began to think of methods for installing the third ring. Fallis had recently reported a 6 π -electrocyclization approach toward the benzannulation of certain ketones (Scheme 3.19).³² In his method, a ketone (e.g., **223**) was converted to an enol triflate **224** and coupled to a propargyl alcohol under Sonogashira conditions. When alcohol **225** was treated with vinyl magnesium halide, a directed carbomagnesiation took place. The new triene **226** could then undergo 6 π -electrocyclization. The resulting diene product (**227**) could be treated with a proton or electrophiles such as iodine then oxidized to an aromatic system (e.g., **228**).

Scheme 3.19 Fallis' Benzannulation



We hoped that this benzannulation approach might be applicable to our system (Scheme 3.20). If the method succeeded, we could install both the aromatic ring of dichroanone (**150**) and the isopropyl group. Enone (**(±)**-**143**) could be readily converted to enol triflate (**(±)**-**229**) via treatment with LDA and *N*-phenyl triflimide. Gratifyingly, Sonogashira coupling of 2-methyl but-3-yn-2-ol (**230**) in the presence of $\text{Pd(PPh}_3)_4$ and CuI went smoothly, giving (**(±)**-**231**). However, all attempts at directed carbometallation with vinyl magnesium halides were unsuccessful in our hands. Perhaps the switch from the primary propargylic alcohols typically used by Fallis (*e.g.*, propargyl alcohol) to our tertiary one (**230**) was responsible in part for the difficulty with our reaction.

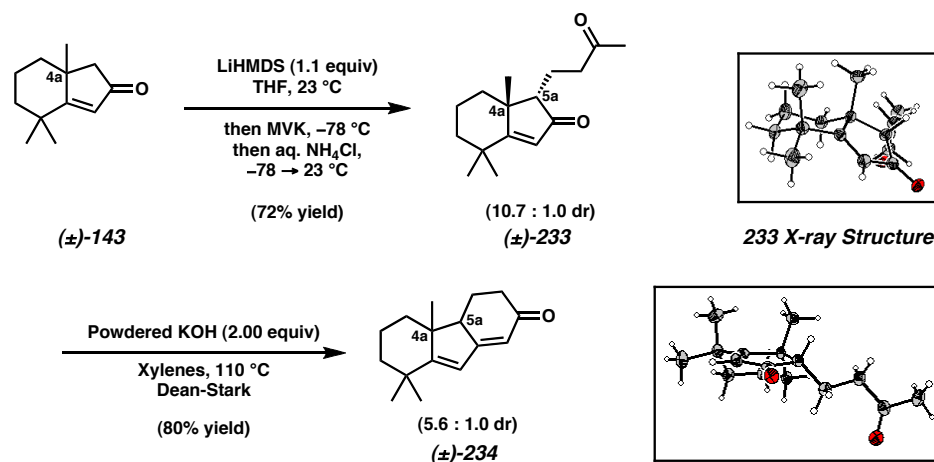
Scheme 3.20 Attempted Electrocyclization



3.4.3 Robinson Annulation of the Enone

Enolization of bicyclic enone (±)-143 and trapping with *N*-phenyltriflimide had been a facile process, but when other electrophiles such as iodomethane, allyl chloroformate, or allyl bromide were used to trap the enolate, complex mixtures of products were obtained. Usually, it appeared that *O*-functionalization was competitive with *C*-functionalization. Thus, we turned toward the possibility of a two-step Robinson annulation. Fortunately, Michael addition of the lithium enolate of (±)-143 into methyl vinyl ketone (**35**) gave primarily one product (Scheme 3.21). Initially, the yield was low, but careful optimization of the temperature, rate of MVK (**35**) addition, base, and equivalents of **35** increased the yield from the low 30% range to 72% with a 10.7:1 dr. X-ray crystallographic analysis of (±)-233 revealed that the methyl group at C(4a) and the ketone chain at C(5a) in the major diastereomer possessed an *anti* configuration.

Scheme 3.21 Robinson Annulation Approach



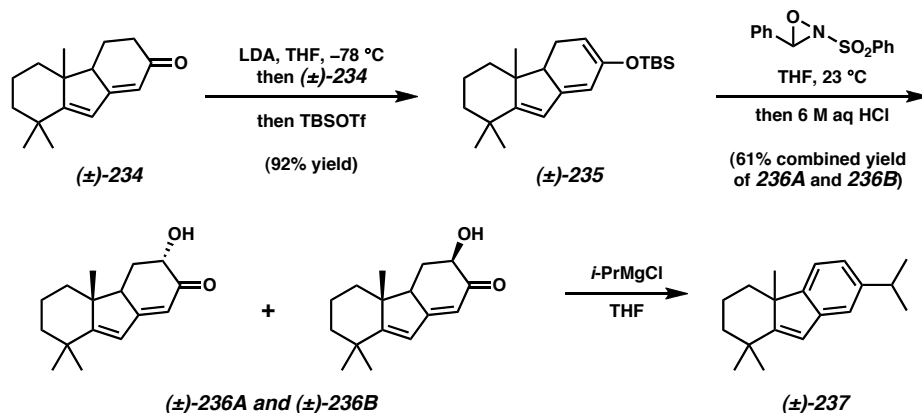
To complete the two-step Robinson annulation, an intramolecular aldol condensation was necessary. We turned to the conditions previously used to prepare bicyclic enone (\pm) -143 (Scheme 3.21). When 0.45 equivalents of KOH were used, conversion of (\pm) -233 to (\pm) -234 was limited. However, if 2.00 equivalents of KOH were employed, the final ring closure proceeded smoothly. Thus, tricyclic enone (\pm) -234 was isolated in 80% yield and 5.6:1 dr. Although there had been some epimerization at C(5a), we were not concerned because this stereocenter would later be removed.

3.5 Synthesis of a Dichroanone Isomer

3.5.1 α -Hydroxylation

Our next challenges included bringing the newly formed cyclohexenone ring to aromaticity and installing the isopropyl group. Direct addition of isopropylmetal species into the carbonyl of (\pm) -234 were met with limited success and led to complex mixtures (Scheme 3.22). To provide an extra synthetic handle, we decided to install another oxygen on the cyclohexenone ring of (\pm) -234.

Scheme 3.22 Installing an Extra Oxygen Atom



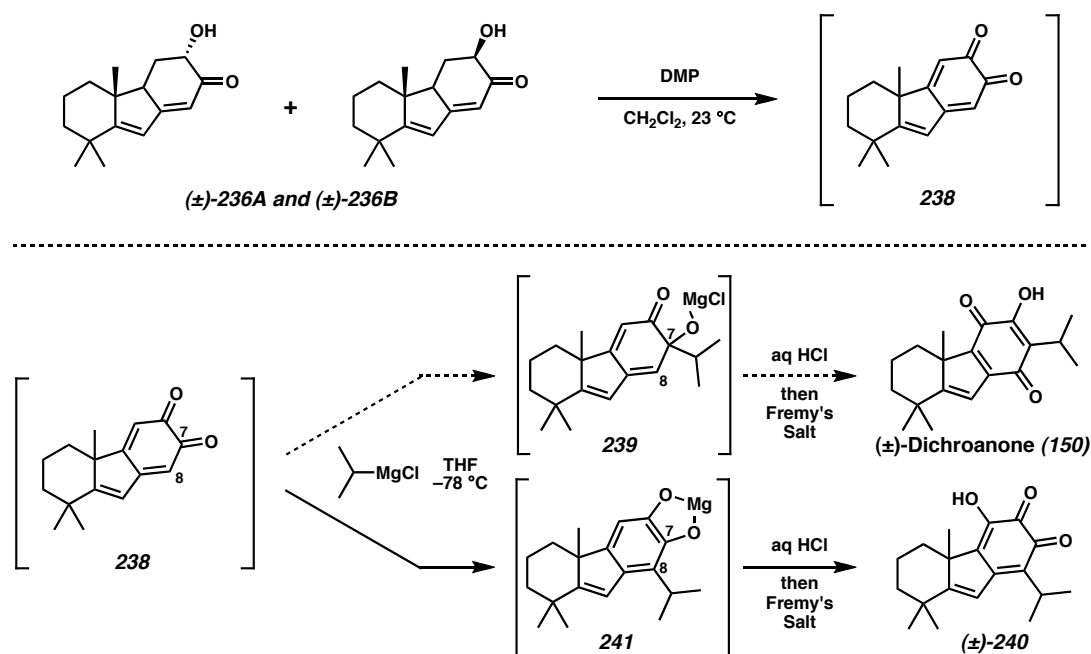
To this end, we treated tricyclic enone **(±)-234** with LDA, followed by TBSOTf, furnishing silyl enol ether **(±)-235**. A battery of oxidation conditions were tested for synthesizing an α -hydroxyketone, including MoOPH,^{33,34} Rubottom oxidation,³⁵ dimethyl dioxirane,³⁶ and methyl phenyl dioxirane.³⁷ The Davis oxaziridine³⁸ proved most effective for this transformation, giving two partially separable diastereomeric acyloins **(±)-236A** and **(±)-236B** in 61% combined yield. Attempts to protect the hydroxyl groups met with limited success. Direct addition of isopropyl magnesium halide to the acyloins resulted in a complex mixture, containing traces of the hydrocarbon **(±)-237**. This was encouraging to us, and we thought that a further increase in the oxidation state of the starting material for the Grignard addition could potentially lead to arenes with oxygen functionality.

3.5.2 Synthesis of an Isomer of Dichroanone

To test the hypothesis regarding the increased oxygenation and its effect on Grignard addition, we treated the mixture of acyloins **(±)-236A** and **(±)-236B** with Dess-

Martin periodinane. The reaction became bright red, indicating the possible presence of an *o*-quinone such as **238** (Scheme 3.23). Unfortunately, we were unable to isolate the product in pure form, perhaps due to its high instability. Instead, we subjected the crude product to isopropyl magnesium chloride in THF at $-78\text{ }^{\circ}\text{C}$. Gratifyingly, a reaction occurred, and the putative *o*-quinone **238** was consumed. Unfortunately, the product proved too unstable to isolate. We hypothesized, erroneously, that an isopropyl group had been successfully introduced at C(7) via 1,2-addition to the carbonyl, leading to a non-aromatic species **239**. If this had been true, acid-mediated rearrangement and oxidation might have potentially led to (\pm)-dichroanone (**150**).

Scheme 3.23 Synthesis of a Dichroanone Isomer



We tested our theory by first stirring the crude Grignard product mixture with aqueous HCl, then rapidly chromatographing the resulting reaction product. The isolated species was immediately heated in the presence of Fremy's salt (potassium nitroso

disulfonate radical), producing a product that was purified on preparative HPLC. nOe analysis revealed that an isopropyl group had indeed been added to the desired ring. However, it had undergone an overall 1,6-addition to the *o*-quinone **238** at C(8), ultimately leading to an isomer of dichroanone ((\pm)-**240**).

3.6 Second Retrosynthetic Analysis of Dichroanone

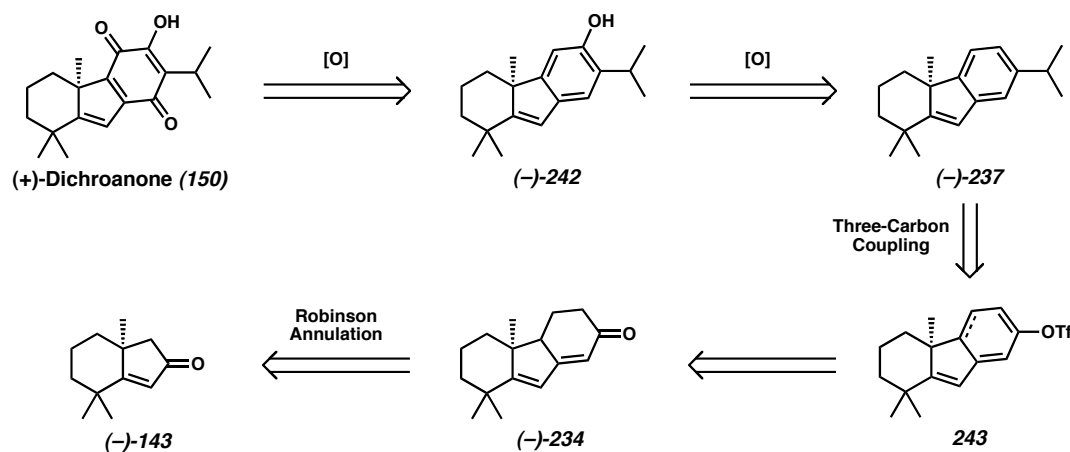
3.6.1 *Lessons Learned*

It was abundantly clear that an effective total synthesis of dichroanone (**150**) was going to require careful installation of the isopropyl group. This functionalization would need to take precedence over oxygenation of the aromatic ring of the 4a-methyltetrahydrofluorene skeleton (**152**). Fortunately, we had already shown it was possible to construct all of the rings in the natural product, and we were hopeful that the tricyclic enone **234** could still be an intermediate in our synthetic route.

3.6.2 *Retrosynthetic Revisions*

Our second-generation retrosynthetic analysis of dichroanone ((+)-**150**) began with the removal of the two quinoid oxygen atoms (Scheme 3.24). This simplified the system to a target phenol molecule (–)-**242**, which could be prepared from an arene such as (–)-**237**. This hydrocarbon could arise via coupling of an isopropyl metal and either an aryl or dienyl triflate (**243**) derived from tricyclic enone (\pm)-**234** and a three-carbon coupling partner. The tricyclic enone (\pm)-**234** would still be prepared from (–)-**143**, and from this point back, the retrosynthesis would remain largely unchanged.

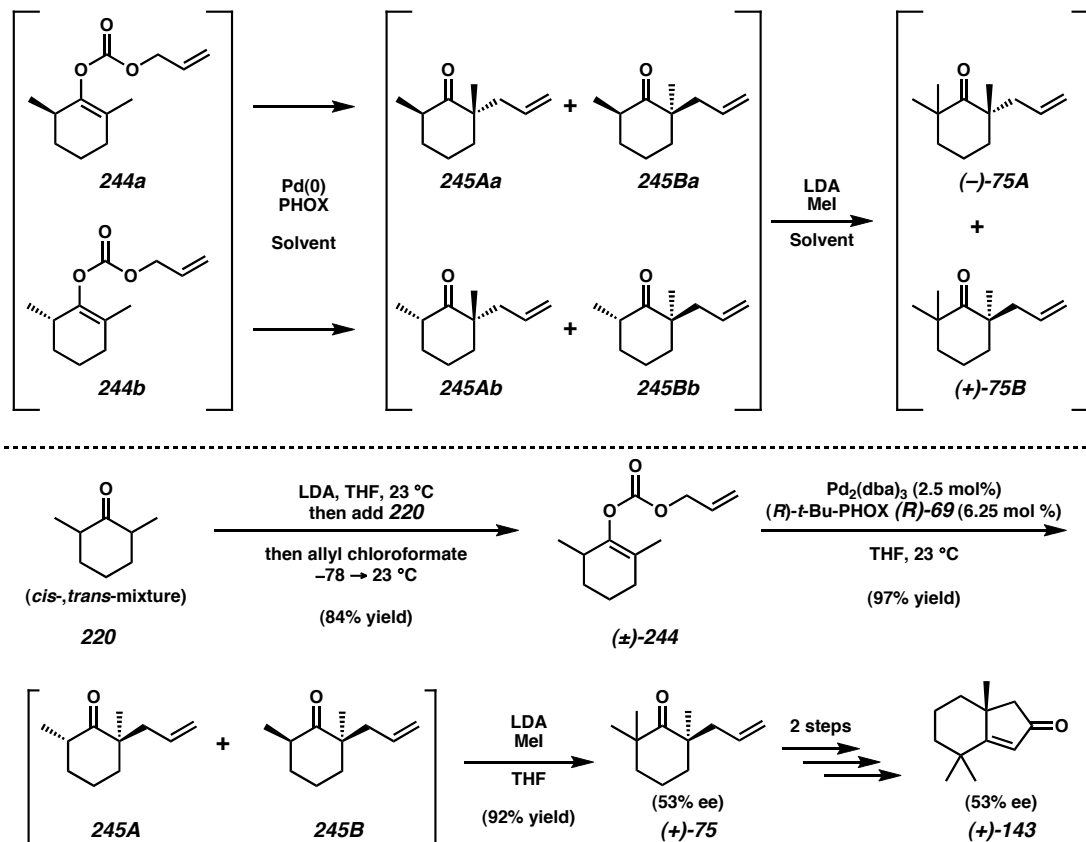
Scheme 3.24 Second Retrosynthetic Analysis of Dichroanone



3.6.3 Substrate and Catalyst Control in Pd-Catalyzed Enantioselective Alkylations

It was somewhat challenging to prepare pure 2,2,6-trimethylcyclohexanone (**101**), so we wondered if a Pd-catalyzed enantioselective decarboxylative alkylation could be performed with the chiral, yet racemic enol carbonate (\pm)-**244**, derived from 2,6-dimethylcyclohexanone (**220**) (Scheme 3.25). Assuming a 100% stereoselective, fully (*R*)-catalyst-controlled reaction, a 1:1 mixture of two allyl ketones **245Ba** and **245Bb**, each with 99% ee, would be formed. Alternatively, if the reaction were substrate controlled and/or less enantioselective, the catalyst might occasionally form the undesired diastereomers. This might lead to a mixture of four products **245Aa**, **245Ab**, **245Ba**, and **245Bb**. Upon inspection, one can see that **245Aa** and **245Bb** are enantiomeric, as are **245Ab** and **245Ba**. If the mixture of all four compounds were alkylated with LDA and iodomethane, two enantiomeric products (*-*)-**75A** and (*+*)-**75B** would be produced. However, if the (*R*)-PHOX ligand catalyst system were completely dominant over the substrate stereochemistry and fully enantioselective, only enantiomer (*+*)-**75B** would be seen after alkylation. This was the desired scenario.

Scheme 3.25 Substrate and Catalyst Control in a Diastereoselective Alkylation

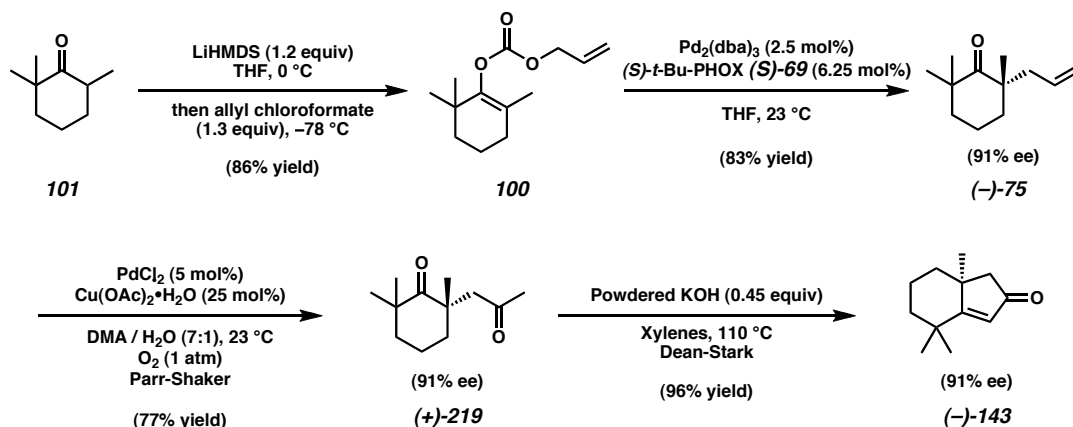


To test the viability of this approach, racemic **244** was prepared in high yield and treated with (*R*)-*t*-Bu-PHOX (**R**)-**69** and Pd₂(dba)₃ in THF (Scheme 3.25). A rapid reaction led to a mixture of two diastereomeric products **245A** and **245B**. This mixture was then treated with LDA and iodomethane, giving two enantiomers of allyl ketone **(-)-75**. Wacker oxidation of **(+)-75** was followed by intramolecular aldol condensation. The enone **(+)-143** was studied by chiral HPLC, revealing only a 53% ee. This indicated a fair degree of substrate control for this enantioselective decarboxylative alkylation. Although this method involving the enol carbonate **(±)-DM32** was not enantioselective enough for application in the synthesis, insight was gained into the catalyst/substrate control bias.

3.6.4 Enantioenrichment Strategy

Using the methods described earlier in this chapter, we prepared the enol carbonate of 2,2,6-trimethylcyclohexanone, **100** (Scheme 3.26). Pd-catalyzed enantioselective decarboxylative allylation furnished tetrasubstituted allyl ketone (–)-**75** in 83% yield and 91% ee, but we wanted to prepare dichroanone ((+)-**150**) in greater than 96% ee. A crystalline intermediate (such as a semicarbazone or oxime) within our synthetic route could perhaps be recrystallized to achieve high enantioenrichment. Because 2,2,6,6-tetramethylcyclohexanone (**221**) had been unable to form a semicarbazone, we were concerned that tetrasubstituted allyl ketone (–)-**75** would also be unable to do so. This meant that we would need to find some other crystalline species later in our synthesis that could be enantioenriched via recrystallization.

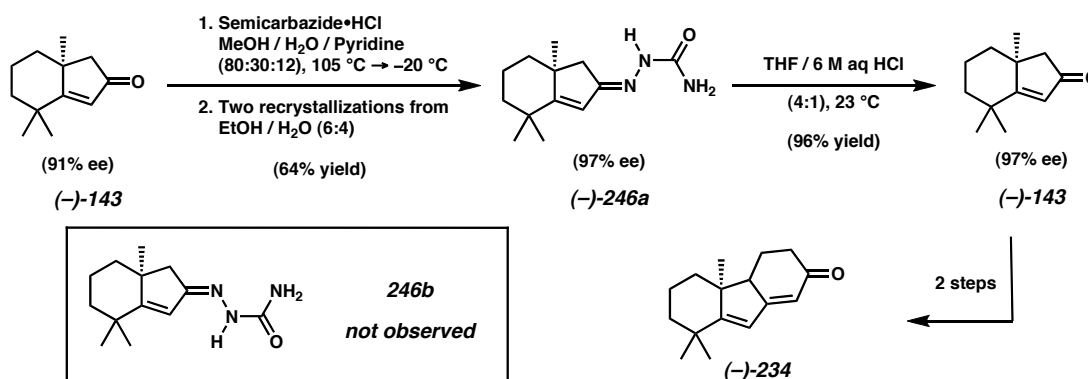
Scheme 3.26 Preparation of the Bicyclic Enone



Thus, we advanced material to the bicyclic enone (–)-**143**. We thought this might be a suitable candidate for conversion to a crystalline imine analog, but we were aware that two imines (–)-**246a** and **246b** were possible. If they both formed, this could make an

enantioenrichment recrystallization problematic. To our delight, when **(-)-143** was treated with semicarbazide hydrochloride and base, a single geometric isomer of semicarbazone, **(-)-246a** was formed, as indicated by nOesy-1D experiments. After two recrystallizations from ethanol/water³⁹ followed by acidic hydrolysis, **(-)-143** was obtained in 97% ee. Using our two-step Robinson annulation, we accessed tricyclic enone **(±)-234** and became ready for further investigations.

Scheme 3.27 Enantioenrichment of the Bicyclic Enone

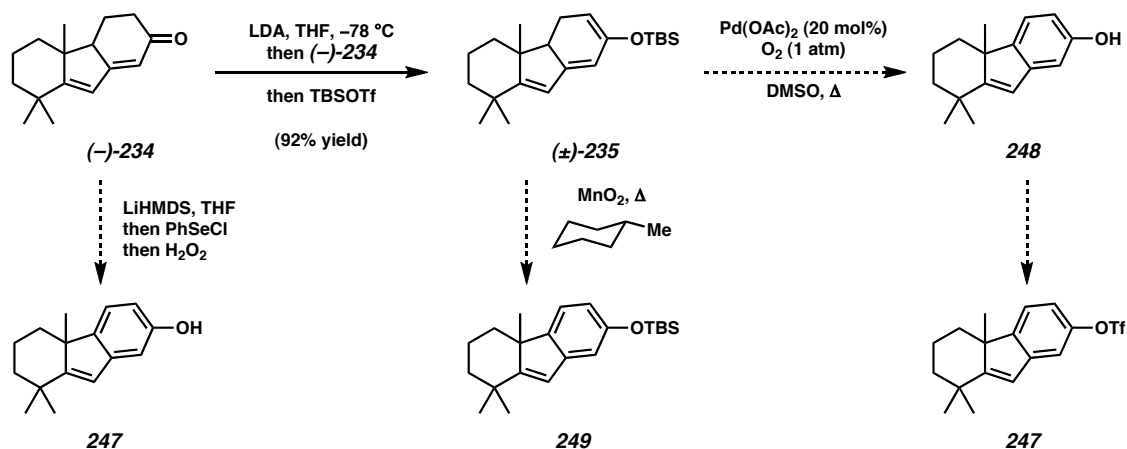


3.7 Preparation and Manipulation of a Tricyclic Phenol

3.7.1 Attempted Aryl Triflate Synthesis

With tricyclic enone **(±)-234** in hand, we thought aryl triflate **248** would be a good target. Our first goal was to increase the oxidation state of the enone ring to an aromatic level (Scheme 3.28). Treatment of racemic **(±)-234** with LiHMDS, followed by PhSeCl and a hydrogen peroxide workup, appeared to yield some of the desired phenol **247**. Unfortunately, the method proved difficult to optimize and was not pursued further.

Scheme 3.28 Proposed Routes to the Aryl Triflate



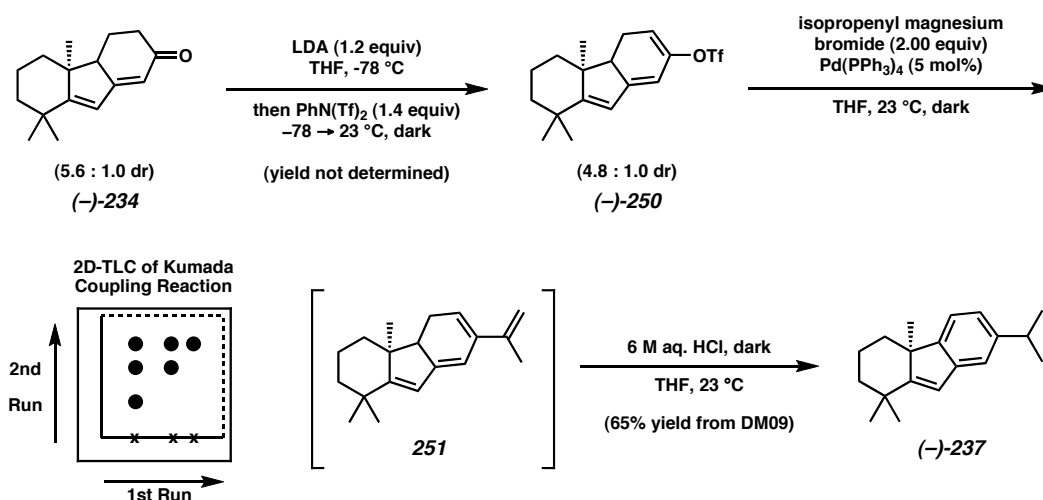
Preparation of TBS enol ether (±)-**235** had been facile, so we tested aromatization chemistry developed by Corey and Lazerwith.⁴⁰ Treatment of (±)-**235** with MnO₂ in methylcyclohexane did not affect oxidation in our hands. The Saegusa-Ito oxidation of silyl enol ethers to enones also appeared viable in this scenario.⁴¹ When we applied this method, it looked as though phenol **247** was present, but achieving catalyst turnover was difficult. Thus, synthesis of the aryl triflate **248** was not pursued further.

3.7.2 Kumada Coupling and Benzannulation

Considering the facile preparation of silyl enol ether (±)-**235**, it was not surprising that enol triflate (–)-**250** was also readily accessible. We believed that coupling of an isopropenyl metal species to this compound might allow access to a tetraene **251**. If this could be prepared, we anticipated that the oxidation state of the isopropenyl olefin could be transposed into the adjacent six-membered ring, affecting aromatization (Scheme 3.29). Toward this end, we attempted a Kumada coupling of enol triflate (–)-**250** and

isopropenyl magnesium bromide in THF. Triflate (–)-**250** was fully consumed during the reaction, but several products were observed.

Scheme 3.29 Kumada Coupling Strategy



After LCMS analysis of the crude reaction mixture was performed, three UV-active peaks were found, each bearing the mass of the desired product. Furthermore, two-dimensional TLC analysis revealed that two of the three products were unstable on silica gel. The one with the lowest retention factor (R_f) converted irreversibly to a mixture of the other two. The middle R_f compound converted irreversibly to the highest R_f product only.

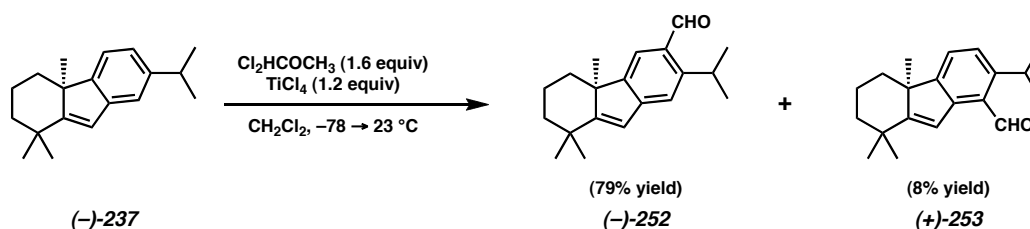
Based on these observations, we reasoned that acid-promoted rearrangements were occurring, and that the two low- R_f spot were olefin isomers of **251**.⁴² We believed the high- R_f product was the thermodynamic product of the rearrangement and, possibly, arene (–)-**237**. To test this hypothesis, a completed Kumada coupling reaction was quenched with 6 M aqueous HCl, and allowed to stir at $23\text{ }^{\circ}\text{C}$ for several hours in the dark. To our delight, arene (–)-**237** was formed as the only isolable product in 65%

overall yield from bicyclic enone (\pm)-**234**. This novel Kumada benzannulation achieved the installation of the aromatic ring system while placing the isopropyl group in the correct position for completion of dichroanone ((+)-**150**).

3.7.3 Preparation of an Unstable Phenol

Aromatic hydrocarbon (–)-**237** presented us with the daunting challenge of selective functionalization of the arene. Fortunately, we discovered that treatment of (–)-**237** with TiCl_4 and α,α -dichloromethyl methyl ether in CH_2Cl_2 at low temperature produced a mixture of two separable aldehydes in a 10:1 ratio (Scheme 3.30). The major aldehyde isomer was studied using nOesy-1D experiments and found to have the structure (–)-**252**, whereas the minor one ((+)-**253**) was substituted *ortho* to the styrenyl vinyl group.

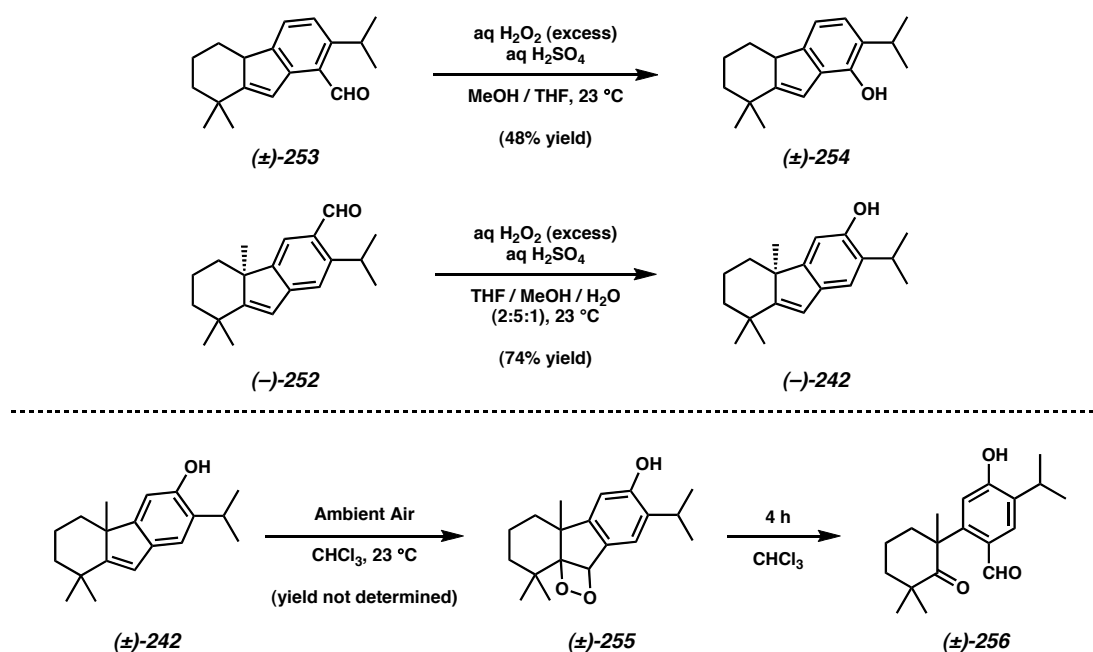
Scheme 3.30 Synthesis of the Two Aldehydes



Both aldehydes could be converted to their corresponding phenols (–)-**242** and (\pm)-**254** via Baeyer-Villiger oxidation under acidic conditions. For simplicity, we decided to carry on the major phenol (–)-**242** (Scheme 3.31). We discovered, however, that this phenol was very unstable. It had to be prepared and used within a single day for any

practical chemistry. Careful observation of the compound by ^1H NMR in CDCl_3 revealed the formation of a new and highly unstable peroxide species (\pm)-**255**, which decomposed over a four-hour period (in solution) to a new compound. Careful isolation and characterization of this entity showed it to be keto-aldehyde (\pm)-**256**, which presumably forms by retro $[2 + 2]$ cycloaddition of the peroxide (\pm)-**255**. If (–)-**242** was allowed to stand in the solid state under ambient air, it slowly oxidized to (\pm)-**255**. This decomposition mode has been surmised for other electron-rich styrenes found in nature.⁴³

Scheme 3.31 Instability of a Key Phenol

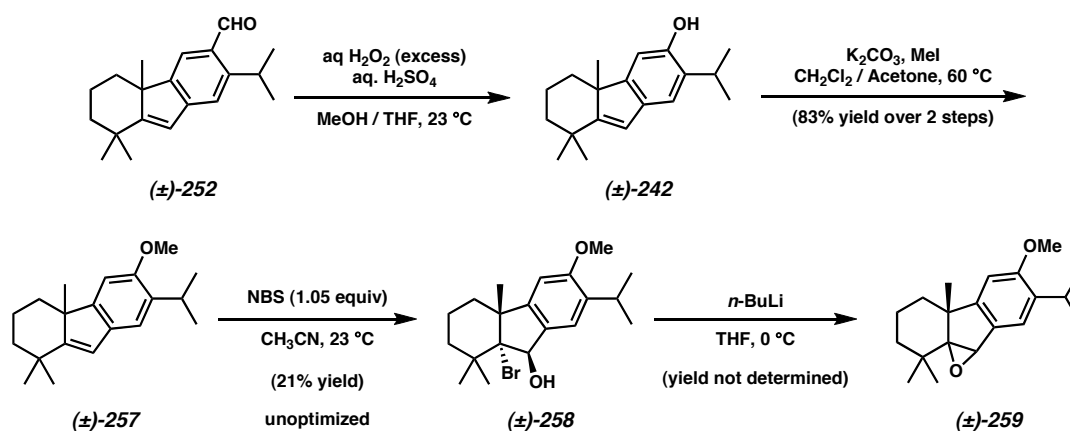


3.7.4 Protecting Group Strategies

It initially seemed wise to protect unstable phenol (–)-**242**. When treated with base and iodomethane, phenol (\pm)-**242** was transformed into methyl ether (\pm)-**257** (Scheme 3.32). Directed *o*-lithiation of (\pm)-**257** was unsuccessful, perhaps due to the

nearby quaternary carbon at C(4a). Formylation of the aryl ring under a variety of conditions also failed. When methyl ether (\pm)-**257** was treated with *N*-bromosuccinimide in wet CH₃CN, bromohydrin (\pm)-**258** was produced. Its relative stereochemical configuration was determined by nOesy-1D experiments. It was also possible to convert this bromohydrin into epoxide (\pm)-**259**. Although investigations with the methyl ether (\pm)-**257** were not fruitful in the progression toward dichroanone ((+)-**150**), we believed that compounds (\pm)-**258** and (\pm)-**259** might eventually find use in the total synthesis of taiwaniaquinol B (**154**) or other bioactive molecules.⁴⁴

Scheme 3.32 Studies with the Methyl Ether



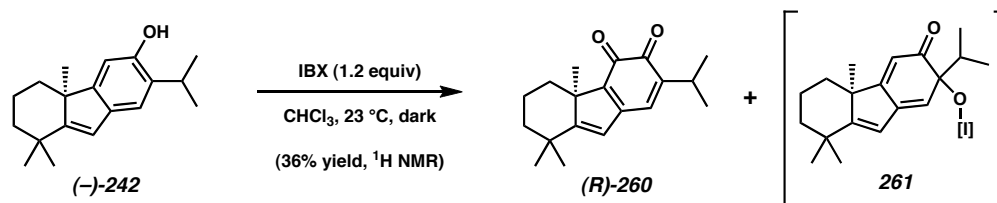
3.8 Total Synthesis of Dichroanone

3.8.1 Preparation of an *o*-Quinone

The preparation of phenol (–)-**242** had become a bottleneck in the synthesis, but installation of the second oxygen atom of the aromatic system was still explorable. We made *o*-quinone (*R*)-**260** our target compound (Scheme 3.33). Screening many conditions revealed a few methods capable of producing the *o*-quinone. The most successful reagent

for this transformation was IBX, used under a set of conditions developed by Pettus.⁴⁵ We could isolate the *o*-quinone (***R***)-**260** chromatographically, but the yield was poor because most of the compound decomposed on the flash column. Additionally, we believed that most of the starting material was forming a different oxidation byproduct **261**,^{45,46} although it could not be isolated in pure form. In order to determine the actual yield of *o*-quinone (***R***)-**260**, we turned to NMR methods.⁴⁷ The maximum yield of *o*-quinone (***R***)-**260** was found to be 36%. Any further synthetic manipulations on (***R***)-**260** would need to be done in solution without direct isolation due to the extreme instability of this *o*-quinone. Although the yield was modest at best, we hoped that (***R***)-**260** could be used as a precursor for dichroanone ((+)-**150**).

Scheme 3.33 Preparation of the *o*-Quinone

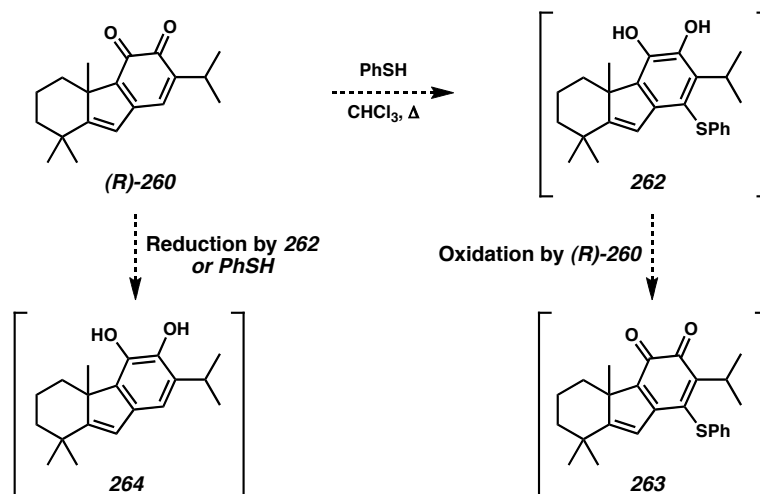


3.8.2 Thiol Additions into the *o*-Quinone

We began to treat the filtered chloroform solution of *o*-quinone (***R***)-**260** (from the IBX reaction) with a variety of nucleophiles. The goal was to install a functional handle at the unsubstituted position of the *o*-quinone. Amongst the list of reagents tested were anhydrous HCl, MgBr₂, and ethanethiol. In most cases, incomplete reaction, poor chemoselectivity, or both were encountered. When we turned to aryl thiol nucleophiles,

smoother reactions were observed. The sulfur atom appeared to undergo a conjugate 1,4-addition into the remaining unsubstituted *o*-quinone ring position (Scheme 3.34).

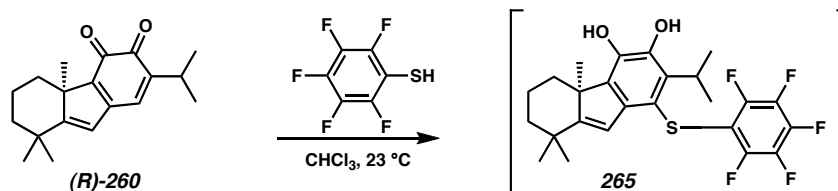
Scheme 3.34 Nucleophilic Additions of Thiophenol



When thiophenol was used, an unstable catechol could be detected in the ^1H NMR of a rapidly chromatographed, yet crude, product sample. Although this compound could not be isolated by itself in pure form, two broad singlets between 4 and 6 ppm in CDCl_3 were observed in the crude ^1H NMR spectrum, which were possibly catechol hydroxyl protons. As we allowed a given reaction of **(R)-260** with thiophenol to progress, more products began to form. It was possible that the unreacted *o*-quinone **(R)-260** could have been oxidizing the catechol **262** as it formed (Scheme 3.34), leading to **263** and **264**. Alternatively, hydride transfer from thiophenol to **(R)-260** could also explain the presence of the isolated catechol. It was not possible to ascertain with full certainty the structure of the catechol observed in the crude ^1H NMR.

Although we were not fully certain about what was happening during the thiophenol transformation, we decided to believe the theory of product **262** oxidation by starting material (*R*)-**260**. A potential solution to this hypothetical problem would have been to produce a catechol (via conjugate addition) too electron-deficient to be oxidized by unreacted (*R*)-**260**. A good thiol candidate for accomplishing this was pentafluorothiophenol (PFPSH). To our delight, when a solution of *o*-quinone (*R*)-**260** was treated with this reagent, a much smoother reaction was observed as compared to the PhSH transformation (Scheme 3.35). Although we suspected the presence of catechol **265** after PFPSH addition to (*R*)-**260**, no stable product could be isolated from the reaction. Our options were now very limited.

Scheme 3.35 The Switch to Pentafluorothiophenol

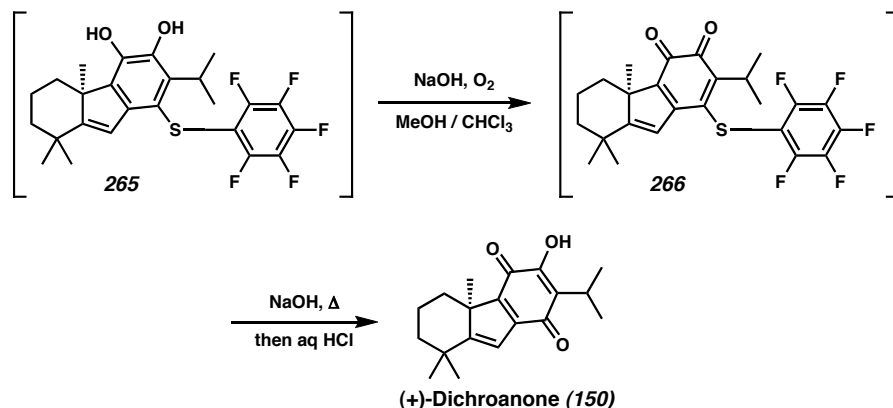


3.8.3 Completion of Dichroanone

The best method for dealing with the putative catechol **265** was to simply let it oxidize. We took the completed nucleophilic addition reaction and added methanol, NaOH, and a balloon of O_2 . As the bright yellow reaction was stirred, it gradually became a deep reddish-brown color. We took this as evidence that the catechol was being converted to another *o*-quinone **266**, which was also too unstable to isolate (Scheme 3.36). The hypothesis that **266** was an *o*-quinone led us to make a strategic decision. **266**

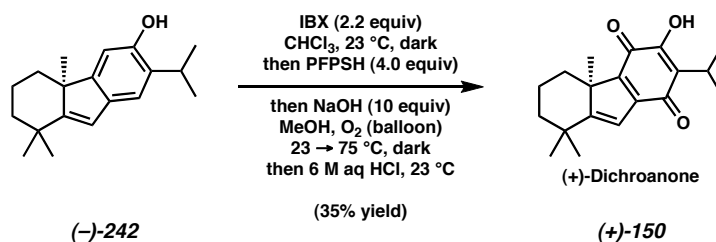
was not only an *o*-quinone, but also an activated, electron-deficient vinylogous thioester. Since NaOH was already in the reaction, we attempted a vinylogous saponification by warming the reaction.⁴⁸

Scheme 3.36 Total Synthesis of (+)-Dichroanone



The isolation chemists had indicated that dichroanone (**150**) was a bright red solid. Our reaction was a chalky brown color. However, when we quenched the reaction with aqueous HCl, a beautiful reaction color change to a translucent bright orange-red was observed. To our delight, aqueous workup and column chromatography on silica gel provided (+)-dichroanone ((+)-**150**) as a stable, bright red solid in 35% overall yield from phenol (–)-**242** (Scheme 3.37). The material was identical in all respects to the natural product reported by the isolation chemists,³ with the exception of its sign of rotation. Not only was our synthesis completed in 11 steps and 4% overall yield from commercial material, but it required no protecting groups.⁴⁹

Scheme 3.37 One-Step Synthesis of Dichroanone from the Phenol

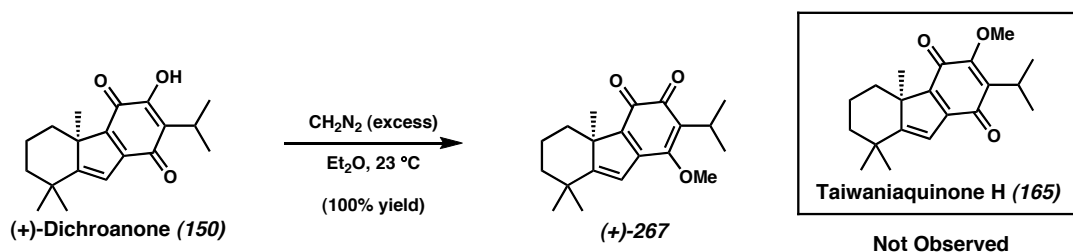


3.9 Attempts to Prepare Other Natural Products

3.9.1 Toward *Taiwaniaquinone H*

Taiwaniaquinone H (**165**) appeared to be the vinylogous methyl ester or dichroanone (**150**). Considering the similarity between these two natural products, we decided to try methylating **150** in an attempted synthesis of **165** (Scheme 3.38). Treatment of ethereal solutions of **150** with diazomethane gave quantitative conversion to a single compound, which we initially thought was *taiwaniaquinone H* (**165**). Closer examination of the spectral data for this species revealed some differences from the authentic natural product.^{2d} Many of the ^{13}C NMR resonances differ, and two in our sample were $> \delta$ 180 ppm, more consistent with an *o*-quinone moiety. The resonances in the ^1H NMR differed as well, especially the vinylogous methyl ester CH_3 protons (δ 3.86 ppm in our sample, but δ 3.96 ppm for the natural product.) The carbonyls in the IR spectrum were also different. For these reasons, we believe that we have prepared (+)-**267** and not *taiwaniaquinone H* (**165**).^{6,50}

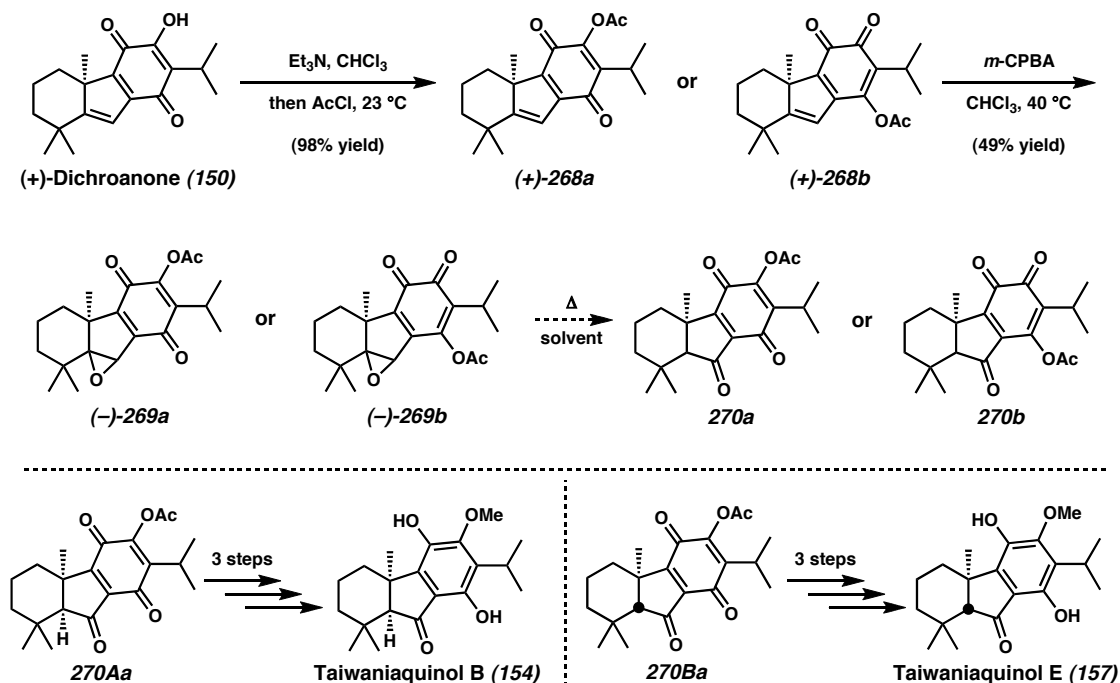
Scheme 3.38 Preparation of a Taiwaniaquinone H Isomer.



3.9.2 Toward Taiwaniaquinol D

Treatment of dichroanone (**150**) first with base followed by acetyl chloride gave a single vinylogous anhydride (+)-**268a** (or ((+)-**268b**) (Scheme 3.39). It was possible to selectively oxidize the trisubstituted olefin spanning C(9) and C(9a) with *m*-CPBA, affording a single epoxide diastereomer (either (–)-**269a** or (–)-**269b**). Preliminary experiments have revealed that epoxide (–)-**269a** (or (–)-**269b**) may rearrange to a ketone **270a** (or **270b**) under thermal conditions. This product could potentially be transformed into taiwaniaquinol B (**154**) or E (**157**) after deacetylation, methylation, and reduction. The epoxide (–)-**269a** (or (–)-**269b**) might also be bioactive, as certain other oxiranyl quinones have been.⁴⁴

Scheme 3.39 A Potential Route to Taiwaniaquinol B or E



3.10 Concluding Remarks

We have reported the first catalytic-enantioselective, protecting group-free total synthesis of (+)-Dichroanone ((+)-**150**), establishing the absolute stereochemistry of the natural product.⁴⁹ Our synthesis has showcased the power of our enantioselective decarboxylative alkylation in the context of a total synthesis. We have developed a novel Kumada coupling-aromatization strategy, as well as a new method for generating a hydroxy *p*-benzoquinone from a phenol. Investigations were also made into synthesizing other natural products in the family.

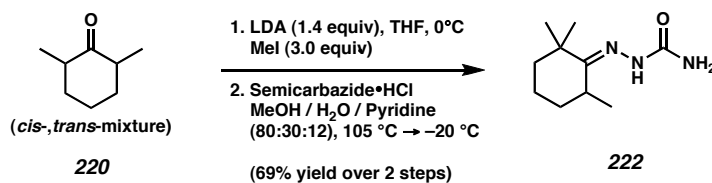
3.11 Experimental Procedures

3.11.1 Materials and Methods

Unless stated otherwise, reactions were conducted in flame-dried glassware under an atmosphere of nitrogen using anhydrous solvents (either freshly distilled or passed through activated alumina columns). Chloroform, stabilized with ethanol, was stored in the dark over oven-dried 4Å molecular sieves. Methanol, absolute ethanol, and *N,N*-dimethyl acetamide were used as purchased. 2,6-dimethylcyclohexanone (**220**), purchased from Aldrich,²⁴ was fractionally distilled from CaSO₄ at ambient pressure prior to use. TMEDA, pyridine, *i*-Pr₂NH, and Et₃N were distilled from CaH₂. All other commercially obtained reagents were used as received, unless specified otherwise. The Davis oxaziridine was prepared according to the method of Davis.³⁸ IBX was prepared by the method of Santagostino.⁵¹ (*R*)- and (*S*)-*t*-Bu-PHOX ligands (**(R)-69** and (**R**)-69 were prepared according to known methods.⁵² Reaction temperatures were controlled using an IKAmag temperature modulator. Thin-layer chromatography (TLC) was conducted with E. Merck silica gel 60 F254 pre-coated plates (0.25 mm) and visualized using UV at 254 nm or 356 nm, *p*-anisaldehyde, ceric ammonium molybdate, potassium permanganate, and iodine vapor over sand. TLC data include *R_f*, eluent, and method of visualization. ICN silica gel (particle size 0.032-0.063 mm) was used for flash column chromatography. Analytical chiral HPLC analyses were performed with an Agilent 1100 Series HPLC using a chiralcel AD normal-phase column (250 x 4.6 mm) employing 2.0-3.0% ethanol in hexane isocratic elution and a flow rate of 0.1 mL/min with visualization at 254nm. Analytical chiral GC analysis was performed with an Agilent 6850 GC using a GT-A column (0.25m x 30.00m) employing an 80 °C isotherm and a flow rate of 1.0

mL/min. ^1H NMR spectra were recorded on a Varian Mercury 300 (at 300 MHz) or a Varian Inova 500 (at 500 MHz) and are reported relative to the residual solvent peak (δ 7.26 for CDCl_3 and δ 7.16 for C_6D_6). Data for ^1H NMR spectra are reported as follows: chemical shift (δ ppm), multiplicity, coupling constant (Hz),⁵³ and integration. ^1H - ^1H homodecoupling and nOesy 1D experiments were conducted at 300 MHz. In nOe drawings, the tail of the arrow denotes the proton being saturated, and the head the proton receiving spin transfer energy. ^{13}C NMR spectra were recorded on a Varian Mercury 300 (at 75 MHz) or a Varian Inova 500 (at 125 MHz) and are reported relative to the residual solvent peak (δ 77.2 for CDCl_3 and δ 128.4 for C_6D_6). Data for ^{13}C NMR spectra are reported in terms of chemical shift. ^{19}F NMR spectra were recorded on a Varian Mercury 300 (at 282 MHz) and are reported in terms of chemical shift without the use of a reference peak. IR spectra were recorded on a Perkin Elmer Spectrum BXII spectrometer and are reported in frequency of absorption (cm^{-1}). IR samples were thin films deposited on sodium chloride plates by evaporation from a solvent (usually CDCl_3), which is recorded. Optical rotations were measured with a Jasco P-1010 polarimeter, using a 100 mm path-length cell. High-resolution mass spectra were obtained from the California Institute of Technology Mass Spectral Facility. Melting points were determined on a Thomas-Hoover melting point apparatus and are uncorrected. Boiling points are measured directly during distillation and are uncorrected. UV-Vis spectra were collected on an Agilent 8453 UV-Vis spectroscopy system and are reported as follows: λ_{max} (nm) then $\log(\epsilon)$ ($\text{M}^{-1}\cdot\text{cm}^{-1}$). Crystallographic data for (\pm)-**233** have been deposited at the CCDC, 12 Union Road, Cambridge CB2 1EZ, UK. Copies can be obtained on request, free of charge, by quoting the publication citation and the deposition number 293604.

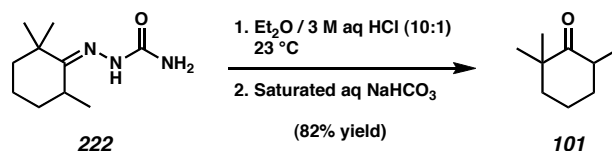
3.11.2 Syntheses of Compounds Related to Dichroanone



Semicarbazone 222. To a solution of *i*-Pr₂NH (16.6 mL, 119 mmol) in THF (400 mL) was added *n*-BuLi (44.4 mL, 2.55 M in hexanes, 113.2 mmol) in a dropwise fashion at 0 °C. After 30 min, a solution of 2,6-dimethylcyclohexanone (**220**) (10.0 g, 79.3 mmol, mixture of *cis* and *trans* isomers) in THF (10 mL) was added. After 1 h, Iodomethane (14.8 mL, 237.9 mmol) was added quickly, and the reaction was warmed to 23 °C. After 1 h, the reaction was poured into a round-bottom flask containing sat. aq NH₄Cl (100 mL) and H₂O (100 mL). After stirring 10 min, the reaction was diluted with H₂O (75 mL) and pentanes (75 mL). The aqueous layer was extracted with pentanes (3 x 100 mL). All organic layers were combined, washed with brine (100 mL), dried (Na₂SO₄), filtered, concentrated, and distilled under N₂ at ambient pressure, affording ketone mixture of 2,2,6-trimethylcyclohexanone (**101**) and 2,2,6,6-tetramethyl cyclohexanone (9.57 g) as a clear, fragrant oil, which was used without further characterization.

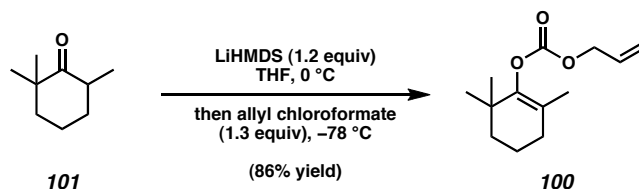
To a solution of this ketone mixture (9.56 g), in MeOH (160 mL), water (60 mL), and pyridine (24 mL) was added semicarbazide hydrochloride (14.0g, 126.1 mmol). The reaction was refluxed at 105 °C for 30 min. Then, the heating was turned off, and the reaction was allowed to cool to 23 °C in the oil bath. Then, the reaction was cooled to -20 °C for 36 h. The white crystals that formed were filtered and washed with water, then dried in vacuo over P₂O₅, giving **222** (10.8 g, 69% over 2 steps from **220**) as a white,

crystalline solid. R_f 0.45 (10:90 MeOH/CH₂Cl₂), (I₂/Sand, brown spot); mp 203-205 °C (water); ¹H NMR (300 MHz, CDCl₃): δ 8.39 (s, broad, 1H), 6.05 (s, broad, 1H), 5.67 (s, broad, 1H), 2.92-2.79 (m, 1H), 1.84-1.66 (m, 1H), 1.64-1.31 (m, 5H), 1.13 (s, 3H), 1.13 (d, J = 7.7 Hz, 3H), 1.12 (s, 3H), 1.11-1.08 (m, 1H); ¹³C NMR (75 MHz, CDCl₃): δ 160.7, 158.8, 40.3, 38.0, 31.7, 29.6, 29.2, 28.3, 18.0, 17.1; IR (KBr): 3463, 3186, 2970, 2931, 2868, 2856, 1689, 1577, 1465, 1384, 1110, 1086 cm⁻¹; HRMS-FAB⁺ (m/z): [M+H]⁺ calc'd for C₁₀H₂₀N₃O, 198.1606; found, 198.1602.



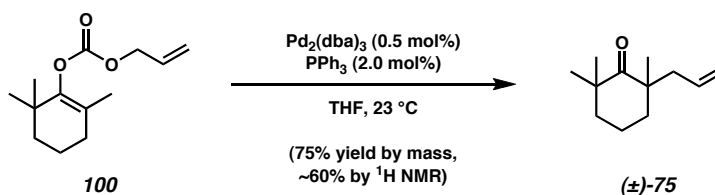
2,2,6-Trimethyl Cyclohexanone (101). To a suspension of semicarbazone **222** (10.9 g, 55.0 mmol) in Et₂O (400 mL) and water (20 mL) was added 6 M aq HCl (20 mL) in a dropwise fashion. The biphasic mixture was stirred vigorously at 23 °C for 3 h. Then, sat. aq NaHCO₃ (300 mL) was added cautiously at 0 °C. After 30 min, the organic phase was collected. The aqueous phase was extracted with Et₂O (2 x 100 mL). All organic layers were combined, dried (Na₂SO₄), filtered, and concentrated. The residue was distilled at ambient pressure under N₂, affording 2,2,6-trimethylcyclohexanone (**101**) (6.51 g, 82% yield) as a clear, fragrant oil. R_f 0.48 (1:9 EtOAc/hexane), (*p*-Anisaldehyde, yellow spot); bp 178-180 °C (760 mmHg); ¹H NMR (300 MHz, CDCl₃): δ 2.54 (app. septuplet, J = 6.6 Hz, 1H), 1.99-1.88 (m, 1H), 1.77 (tdd, J_t = 26.7 Hz, J_{d1} = 13.2 Hz, J_{d2} = 3.8 Hz, 1H), 1.65 (app. dq, J_d = 13.2 Hz, J_q = 2.8 Hz, 1H), 1.52 (app. dddd, J = 13.7 Hz, 6.6 Hz, 4.1 Hz, 2.9 Hz, 1H), 1.42 (app. td, J_t = 13.2 Hz, J_d = 4.1 Hz, 1H), 1.19 (app. ddd, J = 26.1 Hz, 13.2

Hz, 3.9 Hz, 1H), 1.06 (s, 3H), 0.91 (s, 3H), 0.86 (d, $J = 6.3$ Hz, 3H); ^{13}C NMR (75 MHz, CDCl_3): δ 217.1, 45.1, 41.8, 40.7, 36.7, 25.6, 25.2, 21.5, 14.9; IR (NaCl/ CDCl_3): 2967, 2930, 2869, 2853, 1707, 1471, 1455, 1384, 1376, 1127, 1019, 993, 957, 857 cm^{-1} ; HRMS- EI^+ (m/z): $[\text{M}]^+$ calc'd for $\text{C}_9\text{H}_{16}\text{O}$, 140.1201; found, 140.1203.

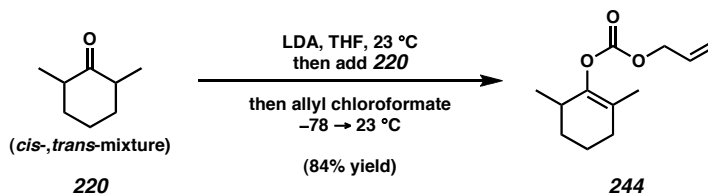


Enol Carbonate 100. A solution of LiHMDS (1.0 M in THF, 57.5 mL, 57.5 mmol) was added to THF (300 mL), then cooled to 0 °C. A solution of pure 2,2,6-trimethylcyclohexanone (**101**) (6.67 g, 47.6 mmol) in THF (10 mL) was added. The reaction was stirred at 0 °C for 1 h, then cooled to −78 °C and fitted with an addition funnel, which was charged with a solution of allyl chloroformate (6.56 mL, 61.8 mmol) in THF (200 mL). The solution was added dropwise over 30 min. Then, the reaction was warmed to 23 °C. After 13 h, the reaction was poured into a mixture of sat. aq NH_4Cl (100 mL), water (100 mL), and hexane (100 mL). After 10 min, the organic phase was collected and the aqueous phase extracted with Et_2O (3 x 75 mL). All organic layers were combined, washed with brine (100 mL), dried (Na_2SO_4), filtered, and concentrated. The residue was purified by flash chromatography on silica gel (2:98 Et_2O /hexane eluent), affording enol carbonate **100** (9.19 g, 86% yield) as a clear oil. R_f 0.43 (1:9 EtOAc /hexane), (*p*-Anisaldehyde, blue spot); ^1H NMR (300 MHz, CDCl_3): δ 5.96 (app. ddt, $J_{d1} = 17.1$ Hz, $J_{d2} = 10.7$ Hz, $J_t = 5.8$ Hz, 1H), 5.38 (app. ddq, $J_{d1} = 17.3$ Hz, $J_{d2} = 8.3$ Hz, $J_q = 1.4$ Hz, 1H), 5.28 (app. ddq, $J_{d1} = 10.5$ Hz, $J_{d2} = 4.4$ Hz, $J_q = 1.1$ Hz, 1H),

4.65 (app. ddt, $J_{d1} = 10.2$ Hz, $J_{d2} = 5.7$ Hz, $J_t = 1.4$ Hz, 2H), 2.05 (t, $J = 5.5$ Hz, 2H), 1.77-1.52 (m, 4H), 1.50 (s, 3H), 1.04 (s, 6H); ^{13}C NMR (75 MHz, CDCl_3): δ 153.5, 148.1, 131.8, 120.9, 119.1, 68.7, 39.4, 35.1, 31.4, 26.9, 19.3, 16.7; IR (NaCl/ CDCl_3): 2965, 2934, 2868, 2838, 1759, 1459, 1363, 1271, 1238, 1138, 1025, 993, 937 cm^{-1} ; HRMS-EI $^+$ (m/z): $[\text{M}]^+$ calc'd for $\text{C}_{13}\text{H}_{20}\text{O}$, 224.1413; found, 224.1408.

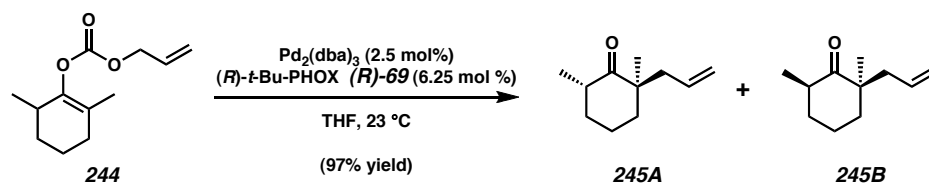


Allyl Ketone (±)-75. A round-bottom flask was flame-dried under argon and charged with $\text{Pd}_2(\text{dba})_3$ (81.6 mg, 89.0 μmol , 0.5 mol%) and PPh_3 (93.6 mg, 0.357 mmol, 2.0 mol%). The system was evacuated with vacuum and back-filled with argon (3 x). Then THF (90 mL) was introduced. The red mixture was stirred vigorously for 2 min at 25 °C. Then, enol carbonate **100** (4.00 g, 17.8 mmol, 1.00 equiv) was added, and the reaction immediately turned green. After 2 h, the reaction was filtered through a plug of silica gel with the aid of THF, and the filtrate was concentrated to ~20 mL total volume. The material was transferred to a round-bottom flask and fitted with a short-path distillation head under N_2 . The THF was distilled away at ambient pressure, then the racemic allyl ketone **(±)-75** was distilled in semipure form as a yellow oil (2.40 g, 75% yield by mass, ~60% yield by ^1H NMR). bp: 62-75 °C (8 mmHg). Other characterization data can be found on pages 40 and 41 (chapter 2).



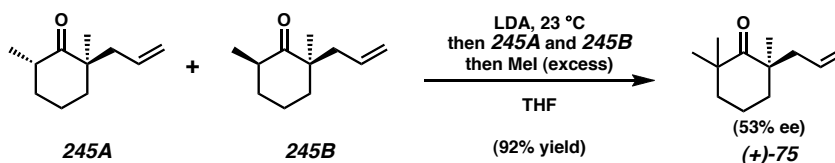
Enol Carbonate 244. A round-bottom flask was charged with THF (200 mL) and *i*-Pr₂NH (13.33 mL, 95.2 mmol, 1.2 equiv) and cooled to 0 °C. *n*-BuLi (2.5 M in hexanes, 34.9 mL, 87.2 mmol, 1.1 equiv) was added dropwise. After 30 min, 2,6-dimethylcyclohexanone (**220**) (*cis,trans* mixture) (10.0 g, 79.3 mmol, 1.0 equiv) was added along with THF (10 mL). After 1.5 h at 23 °C, the reactor was fitted with an addition funnel, which was charged with a solution of allyl chloroformate (10.1 mL, 95.2 mmol, 1.20 equiv) in THF (100 mL). The reaction was cooled to −78 °C, and the chloroformate solution was added dropwise over a 30 min period. Then, the reaction was allowed to warm to 23 °C. After 15 h, the reaction was quenched with sat. aq NH₄Cl (100 mL) and diluted with H₂O (100 mL) and hexanes (100 mL). The organic phase was collected and the aqueous layer extracted with Et₂O (2 x 100 mL). All organic layers were combined, dried (Na₂SO₄), filtered, and concentrated to an orange oil. This oil was fractionally distilled through a vacuum-jacketed Vigreux column fitted with a vacuum jacketed short path head at 8 mmHg. A forerun (~1 mL, bp 50-96 °C) was collected, followed by a main fraction (bp 96-106 °C) that contained enol carbonate **244** (13.93 g, 84% yield) as a colorless, fragrant oil. *R_f* 0.43 (10:90 EtOAc/hexane), (*p*-Anisaldehyde, turquoise spot); ¹H NMR (300 MHz, CDCl₃): δ 5.95 (app. ddt, *J*_{d1} = 17.3 Hz, *J*_{d2} = 10.4 Hz, *J*_t = 5.7 Hz, 1H), 5.37 (app. dd, *J* = 17.3 Hz, 1.4 Hz, 1H), 5.27 (app. dd, *J* = 10.4 Hz, 1.4 Hz, 1H), 4.64 (app. d, *J* = 5.7 Hz, 2H), 2.46 (app. d, broad, *J* = 4.7 Hz, 1H), 2.13 (app. dd, *J* = 6.1 Hz, 4.9 Hz, 2H), 1.84 (app. dddd, *J* = 12.6 Hz, 8.5 Hz, 5.8 Hz, 3.0 Hz, 1H), 1.72-1.48 (m,

2H), 1.55 (s 3H), 1.40 (app. dddd, $J = 12.4$ Hz, 8.5 Hz, 6.3 Hz, 3.3 Hz, 1H), 1.00 (d, $J = 7.1$ Hz, 3H); ^{13}C NMR (75 MHz, CDCl_3): δ 153.2, 146.0, 131.7, 121.1, 118.7, 68.5, 31.8, 31.3, 30.7, 20.1, 18.2, 16.1; IR (NaCl/ CDCl_3): 2934, 2875, 1755, 1454, 1366, 1245, 1229, 1132, 1035 cm^{-1} ; HRMS-EI $^+$ (m/z): $[\text{M}]^+$ calc'd for $\text{C}_{12}\text{H}_{18}\text{O}_3$, 210.1256; found, 210.1248.



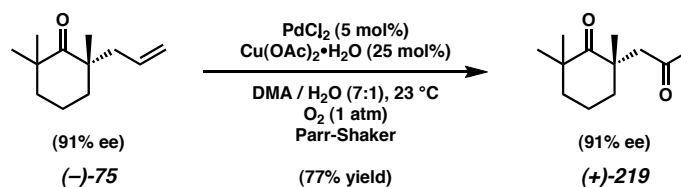
Diastereomeric Allyl Ketones 245A and 245B. A round-bottom flask was flamedried under argon, then cycled into a glovebox. The flask was charged with $\text{Pd}_2(\text{dba})_3$ (54.5 mg, 0.119 mmol, 2.5 mol%, 5 mol% Pd), $(R)\text{-}t\text{-Bu-PHOX}$ (57.6 mg, 0.149 mmol, 6.25 mol%), followed by THF (70 mL). After stirring for 15 min, a solution of enol carbonate **244** (500 mg, 2.38 mmol) and THF (9.0 mL) was added. The reaction went from orange to green. After 6 h at 23 °C, the reaction was cycled out of the glovebox and concentrated in vacuo (10 °C bath temperature). The resulting oil was purified by flash chromatography on silica gel (3:97 Et_2O :hexane eluent), affording **245A** and **245B** as a mixture of diastereomers in 7:3 dr (major diastereomer not identified) and 53% ee (as determined by derivatization to enone (+)-**143** and ee assay) (384 mg total, 97% yield) as a colorless, fragrant, volatile oil. R_f 0.45 (1:9 EtOAc :hexane), (I_2/Sand , brown spot); ^1H NMR (300 MHz, CDCl_3): δ 5.80 (app. ddt, $J_{d1} = 16.5$ Hz, $J_{d2} = 10.7$ Hz, $J_t = 7.2$ Hz, 0.6H), 5.60 (app. ddt, $J_{d1} = 21.2$ Hz, $J_{d2} = 9.6$ Hz, $J_t = 7.4$ Hz, 1.4H), 5.08-4.86 (m, 4H), 2.62 (app. qq, $J = 12.6$ Hz, 6.3 Hz, 1.4H), 2.53 (app. dd, $J = 14.3$ Hz, 7.4 Hz, 0.6H), 2.26-

1.70 (m, 8H), 1.86-1.36 (m, 8H), 1.15 (s, 1.8H), 1.01 (s, 4.2H), 0.994 (d, $J = 7.4$ Hz, 1.8H), 0.986 (d, $J = 6.3$ Hz, 4.2H); ^{13}C NMR (75 MHz, CDCl_3): δ 216.6, 216.3, 135.3, 133.2, 118.0, 117.5, 48.9, 47.9, 43.1, 41.9, 41.5, 41.2, 40.1, 38.8, 36.7, 36.5, 23.2, 22.6, 21.4, 21.2, 15.1, 15.0; IR (NaCl/ CDCl_3): 3077, 2970, 2931, 2870, 2854, 1706, 1640, 1455, 1377, 1126, 999, 914 cm^{-1} ; HRMS- EI^+ (m/z): $[\text{M}]^+$ calc'd for $\text{C}_{11}\text{H}_{18}\text{O}$, 166.1358; found, 166.1357.

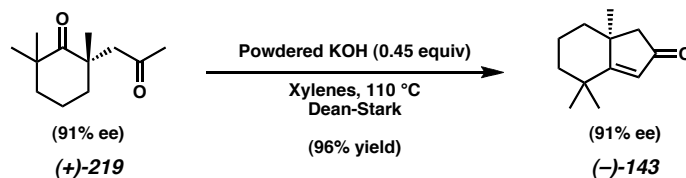


Allyl Ketone (+)-75. A round-bottom flask was charged with THF (20 mL) and $i\text{-PrNH}_2$ (556 μL , 3.97 mmol, 2.20 equiv), then cooled to 0 °C. $n\text{-BuLi}$ (2.5 M in hexanes, 1.44 mL, 3.61 mmol, 2.05 equiv) was added dropwise, and the reaction stirred for 30 min. Then, a solution of diastereomeric allyl cyclohexanones **245A** and **245B** (291 mg, 1.76 mmol, 1.00 equiv) in THF (4.0 mL) was added, and the reaction was warmed to 23 °C. After 2 h, Iodomethane (561 μL , 9.00 mmol, 5.00 equiv) was introduced. After the reaction was complete, sat. aq NH_4Cl (5 mL) was added. 10 min later, the reaction was diluted with hexanes (10 mL) and H_2O (10 mL). The organic phase was collected and the aqueous layer extracted with Et_2O (3 x 20 mL). All organic layers were combined, dried (Na_2SO_4), filtered, and concentrated at 10 °C in vacuo. The residue was purified by flash chromatography on silica gel (hexane \rightarrow Et_2O /hexane 4:96 eluent) affording allyl ketone **(+)-75** (291 mg, 92% yield) in 53% ee as determined by derivatization to enone **(+)-143**.

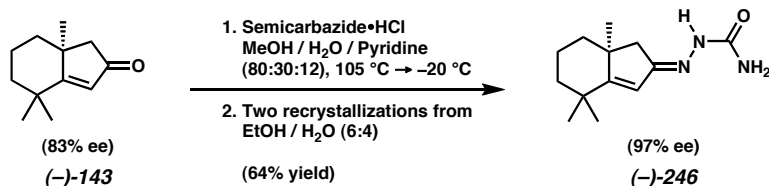
and chiral HPLC assay. Characterization data can be found on pages 40 and 41 (chapter 2).



Diketone (+)-219. A Parr flask was charged with PdCl_2 (74.5 mg, 0.420 mmol, 5 mol%), $\text{Cu(OAc)}_2 \cdot \text{H}_2\text{O}$ (381 mg, 2.10 mmol, 25 mol%), *N,N*-dimethyl acetamide (17.5 mL), and water (2.5 mL). Then allyl ketone (-)-75 (1.51 g, 8.39 mmol, 1.0 equiv) was introduced. The system was cooled to -78 °C and evacuated with vacuum and back-filled from a balloon of O_2 (3 x). The mixture was warmed to 23 °C and placed on a Parr shaker for 24 h under a balloon of O_2 . The reaction was then directly loaded onto a silica gel column and purified by flash chromatography (15:85 Et_2O :pentane \rightarrow 25:75 Et_2O :pentane eluent), affording diketone (+)-219 (1.27 g, 77% yield) as a clear oil. R_f 0.44 (1:4 EtOAc :hexane), (KMnO_4 , yellow spot); ^1H NMR (300 MHz, CDCl_3): δ 3.26 (AB spin system, d, $J_{\text{AB}} = 18.4$ Hz, 1H), 2.32 (AB spin system, d, $J_{\text{AB}} = 18.4$ Hz, 1H), 2.05 (s, 3H), 2.00-1.72 (m, 3H), 1.71-1.53 (m, 2H), 1.47 (app. ddd, $J = 12.0$ Hz, 5.4 Hz, 2.8 Hz, 1H), 1.16 (s, 3H), 1.11 (s, 3H), 1.10 (s, 3H); ^{13}C NMR (75 MHz, CDCl_3): δ 220.7, 206.9, 55.7, 45.0, 44.4, 38.9, 36.9, 30.2, 27.9, 27.8, 27.0, 18.2; IR (NaCl/ CDCl_3): 2965, 2943, 2924, 2868, 1715, 1694, 1463, 1394, 1379, 1360, 1147, 1034 cm^{-1} ; HRMS- EI^+ (m/z): $[\text{M}]^+$ calc'd for $\text{C}_{12}\text{H}_{20}\text{O}_2$, 196.1463; found, 196.1456; $[\alpha]_D^{27} +71.96^\circ$ (c 0.200, CHCl_3), 91% ee.

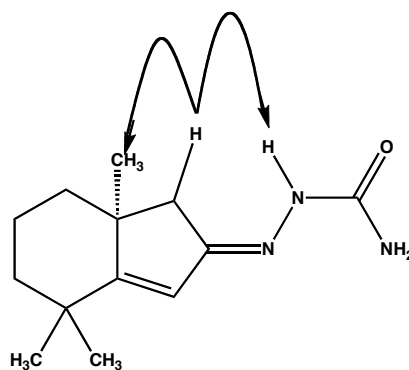


Bicyclic Enone (–)-143. To a solution of diketone (+)-219 (1.21 g, 6.15 mmol, 1.0 equiv) in xylenes (25 mL) was added freshly powdered KOH (155 mg, 2.76 mmol, 0.45 equiv). The reactor was fitted with a Dean-Stark trap and heated to 110 °C for 11 h. The reaction was cooled to 23 °C and directly loaded onto a column of silica gel and purified by flash chromatography (pentane → 5:95 Et₂O/pentane → 50:50 Et₂O/pentane eluent), affording bicyclic enone (–)-143 (1.06 g, 96% yield) as a clear, fragrant oil, which was fully characterized after enantioenrichment (page 152 below); $[\alpha]_D^{25} -87.21^\circ$ (*c* 0.280, CHCl₃), 91% ee.

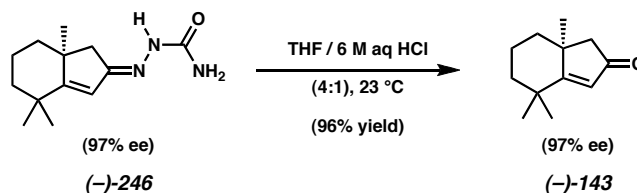


Bicyclic Semicarbazone (–)-246. To a suspension of bicyclic enone (–)-143 (1.70 g, 9.51 mmol, 83% ee) in MeOH (27.1 mL), water (10.2 mL), and pyridine (4.07 mL) was added semicarbazide hydrochloride (1.91 g, 17.1 mmol). The reaction was refluxed at 105 °C for 2 h. Then, the reaction was cooled to –20 °C for 36 h. The crystals that formed were filtered and washed with water, then suspended in absolute EtOH (115 mL). The suspension was heated to 95 °C, at which point it became a solution. Water was added dropwise until cloudiness persisted for 30 seconds even with stirring (76.6 mL). EtOH (200 μL) was added to remove the clouding. Then the heat was turned off, and the

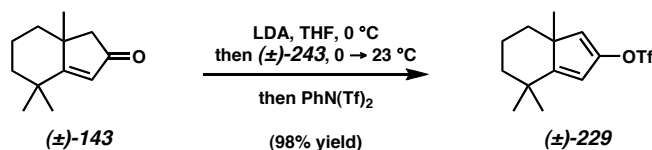
reaction was allowed to cool in the oil bath to 23 °C. After 10 h, the crystals were filtered and suspended in EtOH (100 mL). The suspension was heated to 100 °C, and water (72 mL) was added dropwise as before, followed by EtOH (200 μ L). The white, flaky crystals were grown in the same way and collected by filtration, washed with water, and dried over P₂O₅ in vacuo, giving enantioenriched bicyclic semicarbazone (–)-**246** (1.43 g, 64%) as a single imine geometric isomer in 97% ee as determined by chiral HPLC analysis. *R_f* 0.46 (10:90 MeOH/CH₂Cl₂), (UV, 254 nm); mp 227–229 °C (water); ¹H NMR (300 MHz, CDCl₃): δ 7.55 (s, broad, 1H), 5.86 (s, 1H), 5.80 (s, broad, 1H), 5.12 (s, broad, 1H), 2.42 (AB spin system, d, *J*_{AB} = 16.8 Hz, 1H), 2.29 (AB spin system, d, *J*_{AB} = 16.8 Hz, 1H), 1.89 (app. d, *J* = 12.9 Hz, 1H), 1.78 (app. tt, *J* = 13.8 Hz, 3.0 Hz, 1H), 1.61–1.48 (m, 2H), 1.37–1.30 (m, 1H), 1.28 (s, 1H), 1.29–1.23 (m, 1H), 1.17 (s, 1H); ¹³C NMR (125 MHz, CDCl₃): δ 46.6 (broad), 44.8 (broad), 41.7, 41.0, 36.0 (broad), 31.4, 29.9, 27.7, 26.7, 19.5; IR (KBr): 3469, 3235 (broad), 3191 (broad), 3137 (broad), 2998, 2984, 2958, 2938, 2911, 2863, 1692, 1661, 1572, 1477, 1460, 1420, 1093 cm^{–1}; HRMS-FAB⁺ (*m/z*): [M+H]⁺ calc'd for C₁₃H₂₂N₃O, 236.1761; found, 236.1763; [α]_D²⁵ –103.70° (*c* 0.100, CHCl₃), 97% ee. ¹H–¹H nOesy-1D spectra were obtained for (–)-**246** (300 MHz, CDCl₃); the results are shown below:



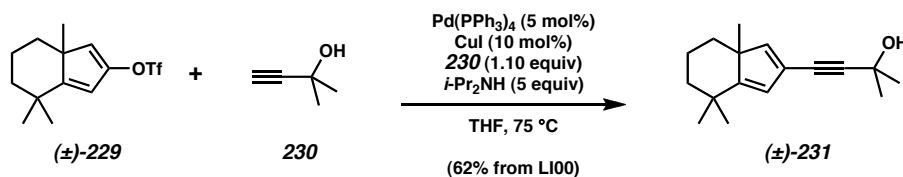
nOe's detected for (–)-**246**



Enantioenriched Bicyclic Enone (-)-143. To a suspension of enantioenriched bicyclic semicarbazone (-)-246 (1.30 g, 5.53 mmol, 97% ee) in THF (120 mL) was added aqueous 6 M aq HCl (30 mL) in a dropwise fashion. After stirring vigorously for 12 h at 23 °C, the biphasic mixture was cooled to 0 °C, and sat. aq NaHCO₃ (72 mL) was added cautiously. After stirring for 10 min, the reaction was diluted with water (75 mL) and hexane (75 mL), and the organic phase was collected. The aqueous phase was extracted with Et₂O (3 x 75 mL). All organic layers were combined, washed with brine (75 mL), dried (Na₂SO₄), filtered, and concentrated, giving enantioenriched bicyclic enone (-)-143 (944 mg, 96% yield, 97% ee) as a clear, fragrant oil. *R_f* 0.37 (1:4 EtOAc/hexane), (UV, 254 nm); mp 9-11 °C (Et₂O); ¹H NMR (300 MHz, CDCl₃): δ 5.82 (s, 1H), 2.29 (app. s, 2.29, 2H), 1.93 (app. dq, *J_d* = 10.5 Hz, *J_q* = 2.8 Hz, 1H), 1.83 (app. tt, *J* = 13.5 Hz, 3.3 Hz, 1H), 1.71-1.54 (m, 2H), 1.40 (app. ddd, *J* = 12.4 Hz, 8.0 Hz, 3.9 Hz, 1H), 1.36 (app. ddd, *J* = 8.0 Hz, 3.3 Hz, 2.0 Hz, 1H), 1.35 (s, 3H), 1.25 (s, 3H), 1.20 (s, 3H); ¹³C NMR (75 MHz, CDCl₃): δ 208.1, 194.4, 126.4, 54.7, 44.3, 41.5, 40.6, 36.5, 31.3, 27.4, 26.2, 19.1; IR (NaCl/CDCl₃): 2997, 2987, 2960, 2929, 2868, 2847, 1712, 1696, 1600, 1459, 1261, 1166 cm⁻¹; HRMS-EI⁺ (*m/z*): [*M*]⁺ calc'd for C₁₂H₁₈O, 178.1358; found, 178.1356; [*α*]_D²⁴ -102.40° (*c* 0.200, CHCl₃), 97% ee.

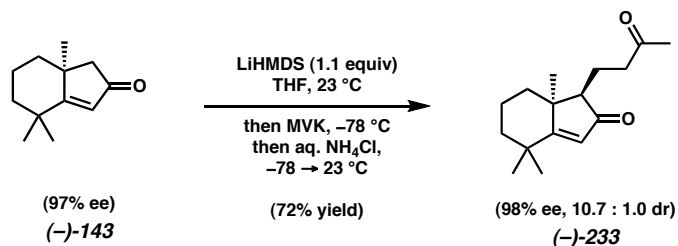


Dienyl Triflate (±)-229. A round-bottom flask was charged with THF (16 mL) and freshly distilled *i*-Pr₂NH (256 μL, 1.82 mmol, 1.30 equiv) and cooled to 0 °C. *n*-BuLi (2.5 M in hexanes, 673 μL, 1.68 mmol, 1.20 equiv) was added dropwise. After 30 min, a solution of bicyclic enone (±)-143 (250 mg, 1.40 mmol, 1.00 equiv) in THF (2 mL) was added dropwise. Then, the reaction was warmed to 23 °C and stirred for 1.5 h. Finally, a solution of *N*-phenyl triflimide (651 mg, 1.82 mmol, 1.3 equiv) in THF (2 mL) was added. At 16 h, the reaction was diluted with Et₃N (5 mL), and the reaction was concentrated to ~5 mL total volume. Hexane (10 mL) was added, and the reaction was directly loaded onto a column of silica gel and purified by rapid flash column chromatography (5:5:90 Et₃N:Et₂O:hexane eluent), affording dienyl triflate (±)-229 (427 mg, yield not determined) as an oil. The compound was immediately used in the next reaction. *R_f* (not determined); ¹H NMR (300 MHz, C₆D₆): δ 5.68 (app. d, *J* = 1.7 Hz, 1H), 5.65 (app. d, *J* = 1.7 Hz, 1H), 1.61 (app. ddd, *J* = 12.7 Hz, 4.7 Hz, 3.0 Hz, 1H), 1.48 (app. qt, *J_q* = 13.6 Hz, *J_t* = 3.3 Hz, 1H), 1.36-1.28 (m, 1H), 1.31-1.19 (m, 1H), 0.96 (s, 3H), 0.93 (s, 3H), 0.90 (s, 3H), 0.78 (app. dt, *J_d* = 12.9 Hz, *J_t* = 4.4 Hz, 1H), 0.72 (app. dt, *J_d* = 12.9, *J_t* = 4.0 Hz, 1H); ¹³C NMR (75 MHz, C₆D₆): δ 165.8, 147.7, 130.3, 116.9, 51.9, 42.9, 37.3, 36.0, 30.9, 24.6, 20.0, 19.6; ¹⁹F NMR (282 MHz, C₆D₆): δ -74.11, -71.69; IR: (not obtained); HRMS: (not performed).



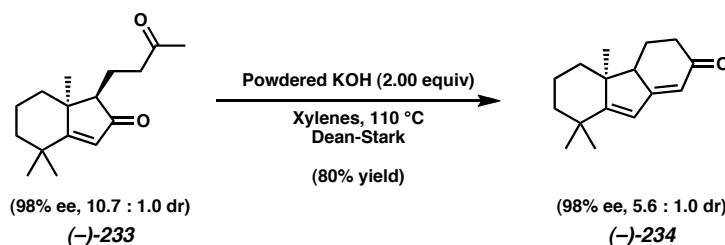
Propargylic Alcohol (±)-231. A round-bottom flask was charged with CuI (27 mg, 0.14 mmol, 10 mol%), followed by a solution of $\text{Pd(PPh}_3)_4$ (80 mg, weighed in glovebox, 70 μmol , 5 mol%) in THF (10 mL) (reaction was yellow). Then, freshly distilled $i\text{-Pr}_2\text{NH}$ (981 μL , 7.00 mmol, 5.0 equiv) was added (reaction became black), followed immediately by a solution of dienyl triflate (±)-229 (434 mg, 1.40 mmol, 1.0 equiv) in THF (10 mL) (reaction turned maroon). Finally, a solution 2-methyl-3-butyn-2-ol (**230**) (149 μL , 1.54 mmol, 1.1 equiv) in THF (5.0 mL) was introduced slowly (reaction became orange). The reaction was heated to 75 $^\circ\text{C}$ for 20 h. Then, the reaction was cooled to 23 $^\circ\text{C}$ and filtered through celite with the aide of hexane and Et_2O . The filtrate was concentrated, then purified by flash column chromatography on silica gel (10:90 Et_2O :hexane eluent). The product-containing fractions, which contained semipure (±)-**231**, were combined and concentrated. The residue was purified on a second silica gel flash column (10:90 Et_2O :hexane \rightarrow 20:80 Et_2O :hexane \rightarrow 50:50 Et_2O :hexane eluent), giving bicyclic enone (±)-**143** (22.7 mg, 9% yield) and propargylic alcohol (±)-**231** (211 mg, 62% yield over 2 steps from (±)-**243**) R_f (not determined); ^1H NMR (300 MHz, CDCl_3): δ 6.36 (app. s, 1H), 5.79 (app. s, 1H), 2.42-2.22 (m, 1H), 1.88 (app. d, $J=13.9$ Hz, 1H), 1.76 (app. t, $J = 13.2$ Hz, 1H), 1.60-1.48 (m, 1H), 1.54 (s, 6H), 1.18 (s, 3H), 1.15 (s, 3H), 1.11 (s, 3H), 0.96 (app. t, $J = 11.8$ Hz, 1H), 0.93 (app. t, $J = 12.9$ Hz, 1H); ^{13}C NMR (75 MHz, CDCl_3): δ 163.2, 150.8, 122.2, 121.6, 94.8, 78.9, 65.7, 54.2, 42.8, 36.8, 35.5, 31.6, 30.9, 24.7, 20.0, 19.6; IR (NaCl/ CDCl_3): 3369 (broad), 3071, 2919,

2245, 1694, 1602, 1455, 1369, 1300, 1234, 1164 cm^{-1} ; HRMS-FAB⁺ (m/z): $[M]^+$ calc'd for $\text{C}_{17}\text{H}_{24}\text{O}$, 244.1827; found, 244.1827.



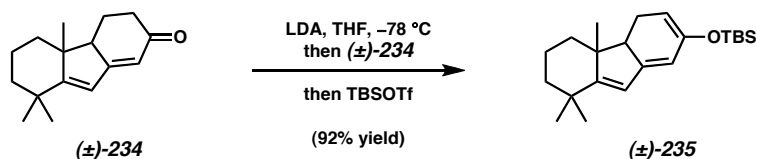
Keto-Enone (–)-233. To a solution of LiHMDS (0.943M in THF, 3.27 mL, 3.09 mmol) in THF (29 mL) at 23 °C was added a solution of enantioenriched bicyclic enone (–)-143 (981 mg, 5.51 mmol) in THF (12 mL) in a dropwise fashion over 3 min. After 1 h, the reaction was cooled to –78 °C, and methyl vinyl ketone (**35**) (257 μL , 3.09 mmol) was added quickly. After 5 min, the reaction was quenched with a 1:1 mixture of sat. aq NH_4Cl (5 mL) and water (5 mL) at –78 °C. Then, the reaction was warmed to room temperature and diluted with hexanes (20 mL) and H_2O (20 mL). After collecting the organic phase, the aqueous phase was extracted with Et_2O (3 x 15 mL). All organic layers were combined, washed with brine (20 mL), dried (Na_2SO_4), filtered, and concentrated. The residue was purified by flash chromatography on silica gel (1:9 Et_2O /pentane \rightarrow 2:8 Et_2O /pentane \rightarrow 4:6 Et_2O /pentane eluent), affording starting material (–)-143 (49.3 mg, 10% yield) as a colorless oil and keto-enone (–)-233 (500 mg, 72% yield) as a colorless oil, which formed pale yellow crystals from the melt under reduced pressure. The solid was of 98% ee as determined by chiral HPLC analysis. Two separate crystals of racemic (\pm)-233 were analyzed by X-ray diffraction; each proved to be the same diastereomer (relative stereochemistry is depicted in the product above). R_f 0.20 (1:4 EtOAc /hexane), (UV, 254 nm); mp 67–69 °C (Et_2O /pentane) (98% ee), mp 62–64 °C (Et_2O /pentane) (83%

ee) mp 42-44 °C (Et₂O/pentane) (0% ee); ¹H NMR (300 MHz, CDCl₃), (major diastereomer): δ 5.76 (s, 1H), 2.89 (qd, *J*_q = 9.1 Hz, *J*_d = 5.2 Hz, 1H), 2.70 (ddd, *J* = 18.2 Hz, 8.8 Hz, 6.6 Hz, 1H), 1.99 (dd, *J* = 10.7 Hz, 5.0 Hz, 1H), 2.16 (s, 3H), 1.94-1.78 (m, 2H), 1.72-1.49 (m, 4H), 1.45 (dd, *J* = 13.2 Hz, 3.9 Hz, 1H), 1.35 (s, 3H), 1.33 (app. dd, *J* = 14.1 Hz, 4.4 Hz, 1H), 1.25 (s, 3H), 1.19 (s, 3H); ¹³C NMR (75 MHz, CDCl₃), (major diastereomer): δ 211.0, 208.9, 193.1, 124.8, 58.1, 47.2, 41.7, 41.4, 36.7, 35.2, 31.2, 30.2, 28.3, 26.4, 21.3, 18.8; IR (KBr): 3009, 2958, 2943, 2897, 2871, 1710, 1691, 1598, 1460, 1420, 1381, 1372, 1357, 1269, 1161 cm⁻¹; HRMS-EI⁺ (*m/z*): [M]⁺ calc'd for C₁₆H₂₄O₂, 248.1776; found, 248.1774; [α]_D²⁷ -15.79° (*c* 0.220, CHCl₃), 98% ee.



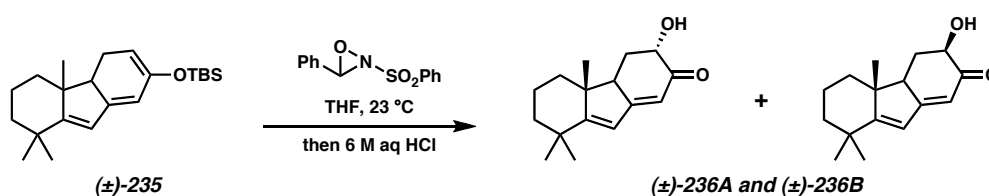
Tricyclic Dienone (-)-234. To a solution of keto-enone (-)-233 (457 mg, 1.60 mmol, 1.00 equiv) in xylenes (18 mL) was added freshly powdered KOH (207 mg, 3.69 mmol, 2.00 equiv). The reactor was fitted with a Dean-Stark trap and heated to 110 °C for 14 h in the dark. The reaction was cooled to 23 °C and directly loaded onto a column of silica gel and purified by flash chromatography (pentane → 2:8 Et₂O:pentane → 6:4 Et₂O:pentane eluent), affording tricyclic dienone (-)-234 (336 mg, 80% yield) as a yellow oil. The product was a mixture of two diastereomers as determined by ¹H NMR. *R*_f 0.28 (1:4 EtOAc/hexane), (UV, 254 nm), (first diastereomer) *R*_f 0.19 (1:4 EtOAc/hexane), (UV 254 nm), (second diastereomer); ¹H NMR (300 MHz, CDCl₃), (major diastereomer): δ 6.05 (s, 1H), 5.76 (d, *J* = 2.5 Hz, 1H), 2.52 (app. ddd, *J* = 14.3

Hz, 5.5 Hz, 2.5 Hz, 1H), 2.50 (app. ddd, $J = 14.9$ Hz, 3.6 Hz, 2.8 Hz, 1H), 2.29 (ddd, $J = 17.0$ Hz, 13.5 Hz, 5.2 Hz, 1H), 1.98-1.72 (m, 4H), 1.56 (app. d, $J = 12.4$ Hz, 2H), 1.39-1.24 (m, 2H), 1.16 (s, 6H), (1.05 (s, 3H); ^{13}C NMR (75 MHz, CDCl_3), (major diastereomer): δ 200.1, 179.3, 171.7, 122.9, 117.2, 55.3, 49.1, 41.2, 40.1, 37.9, 35.7, 31.3, 27.7, 23.9, 22.4, 19.1; IR (NaCl/ CDCl_3): 2930, 2868, 2847, 1659, 1652, 1619, 1616, 1585, 1457, 1418, 1385, 1372, 1320, 1273, 1244, 1194, 1181, 970, 887 cm^{-1} ; HRMS-EI $^+$ (m/z): $[\text{M}]^+$ calc'd for $\text{C}_{16}\text{H}_{22}\text{O}$, 230.1671; found, 230.1668; $[\alpha]_D^{25} -224.40^\circ$ (c 0.550, CHCl_3), 98% ee.



Silyl Enol Ether (\pm)-235. A round-bottom flask was charged with THF (12.5 mL) and $i\text{-Pr}_2\text{NH}$ (395 μL , 2.82 mmol, 1.3 equiv), then cooled to 0 $^\circ\text{C}$. $n\text{-BuLi}$ (2.5 M in hexanes, 1.05 mL, 2.61 mmol, 1.2 equiv) was added dropwise. After 30 min, the reaction was cooled to -78°C , and a solution of tricyclic dienone (\pm)-234 (500 mg, 2.17 mmol, 1.0 equiv) in THF (2.86 mL) was added slowly. After 30 min, TBSOTf (698 μL , 3.04 mmol, 1.4 equiv) was introduced. The reaction was kept at -78°C for 30 min, then warmed to 23 $^\circ\text{C}$. Once the reaction was gauged complete, it was concentrated in vacuo to ~ 4 mL total volume, then diluted with hexanes (15 mL) and Et_3N (1.0 mL). The solution was directly loaded onto a column of silica gel and rapidly purified by flash column chromatography (5:5:9 $\text{Et}_3\text{N}:\text{Et}_2\text{O}:\text{hexane}$ eluent), affording silyl enol ether (\pm)-235 (690 mg, 92% yield) as a bright yellow oil. R_f not determined (compound is unstable on silica gel); ^1H NMR (300 MHz, C_6D_6)(major diastereomer only): δ 5.90 (s, 1H), 5.76 (s, 1H),

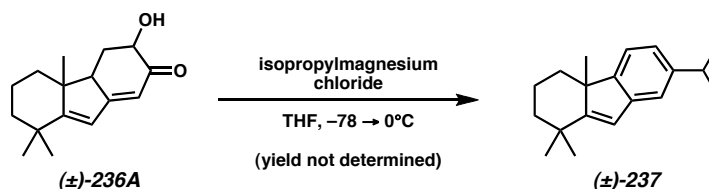
5.01-4.97 (m, 1H), 2.39 (app. dd, $J = 14.0$ Hz, 6.8 Hz, 1H), 2.26 (app. s, 1H), 2.01-1.93 (m, 1H), 1.74-1.08 (m, 6H), 1.08 (s, 3H), 1.07 (s, 3H), 1.02 (s, 9H), 0.98 (s, 3H), 0.20 (s, 6H); ^{13}C NMR (75 MHz, C_6D_6): δ 169.1, 151.7, 150.4, 123.0, 113.9, 100.0, 51.7, 48.6, 41.4, 40.9, 35.5, 32.1, 28.2, 26.4, 23.7, 21.4, 20.0, 18.8, 3.8; IR (NaCl/neat film): 3049, 2928, 2858, 1651, 1587, 1472, 1362, 1252, 1224, 1151, 1006, 926, 839, 780 cm^{-1} ; HRMS- EI^+ (m/z): $[\text{M}]^+$ calc'd for $\text{C}_{22}\text{H}_{36}\text{OSi}$, 344.2536; found, 344.2532.



Acyloins (±)-236A and (±)-236B. A round-bottom flask containing silyl enol ether (±)-**235** (600 mg, 1.74 mmol, 1.00 equiv) was charged with THF (25 mL). Then, the Davis oxaziridine (1.15 g, 2.18 mmol, 1.25 equiv) was introduced at 23 °C. Once the starting material was consumed, the reaction was concentrated in vacuo. The resulting residue was triturated with Et_2O and filtered to remove solids. The filtrate was concentrated and dissolved in THF (25 mL) and 6 M aq HCl (16 mL) was added, causing a color change from colorless to bright yellow. After 5 min, the reaction was diluted with H_2O and hexanes, and the organic phase was collected. The aqueous layer was extracted with Et_2O (3 x). All organic layers were combined, dried (Na_2SO_4), filtered, and concentrated. The residue was purified by flash column chromatography on silica gel (10:90 EtOAc:hexane \rightarrow 20:80 EtOAc:hexane \rightarrow 50:50 EtOAc:hexane \rightarrow EtOAc eluent), giving two acyloin products, (±)-**236A** and (±)-**236B**, whose relative configurations were not assigned. The high R_f product, (±)-**236A** (70 mg, 17% yield), was obtained in semipure form and had

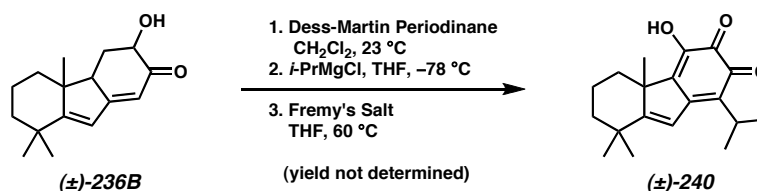
the following characteristics: R_f (not measured) (UV, 254 nm); ^1H NMR (300 MHz, CDCl_3): δ 6.07 (s, 1H), 5.82 (app. dd, $J = 20.4$ Hz, 2.5 Hz, 1H), 4.12 (app. dddd, $J = 12.7$ Hz, 5.0 Hz, 2.5 Hz, 1.9 Hz, 1H), 3.95 (s, broad, 1H), 2.70 (app. dddd, $J = 12.7$ Hz, 6.9 Hz, 4.4 Hz, 2.8 Hz, 1H), 2.60-2.48 (m, 2H), 2.41-2.29 (m, 1H), 2.32 (app. td, $J_t = 16.8$ Hz, $J_d = 5.2$ Hz, 1H), 1.93-1.51 (m, 4H), 1.17 (app. s, 6H), 1.07 (s, 3H); ^{13}C NMR (75 MHz, CDCl_3) (not obtained due to modest purity of compound); IR (NaCl/ CDCl_3): 3460 (broad), 2931, 2868, 2847, 1655, 1613, 1582, 1459, 1320, 1212, 1182, 1107, 887 cm^{-1} ; HRMS-EI $^+$ (m/z): $[\text{M}]^+$ calc'd for $\text{C}_{16}\text{H}_{22}\text{O}$, 246.1620; found, 246.1616.

The low R_f product, (\pm)-**236B** (176 mg, 44% yield) was also obtained in semipure form and had the following characteristics: R_f (not measured) (UV, 254 nm); ^1H NMR (300 MHz, CDCl_3): δ 6.08 (s, 1H), 5.75 (app. d, $J = 2.5$ Hz, 1H), 4.06 (app. t, $J = 3.0$ Hz, 1H), 3.80 (s, broad, 1H), 2.97 (app. ddd, $J = 11.3$ Hz, 4.4 Hz, 2.5 Hz, 1H), 2.10 (app. ddd, $J = 13.5$ Hz, 4.7 Hz, 3.0 Hz, 1H), 1.90 (app. ddd, $J = 25.0$ Hz, 13.5 Hz, 10.2 Hz, 1H), 1.90-1.70 (m, 2H), 1.60-1.50 (m, 2H), 1.40-1.17 (m, 2H), 1.16 (s, 3H), 1.15 (s, 3H), 1.05 (s, 3H); ^{13}C NMR (75 MHz, CDCl_3): δ 198.6, 181.2, 173.5, 123.1, 114.6, 70.5, 49.5, 49.1, 41.2, 39.7, 35.9, 31.2, 30.5, 27.8, 22.9, 19.0; IR (NaCl/ CDCl_3): 3386 (broad), 2960, 2927, 2868, 2848, 1643, 1612, 1582, 1459, 1327, 1164, 1058, 888 cm^{-1} ; HRMS-EI $^+$ (m/z): $[\text{M}]^+$ calc'd for $\text{C}_{16}\text{H}_{22}\text{O}$, 246.1620; found, 246.1630.



Arene (\pm)-237. A vial was charged with a solution of acyloin (\pm)-**236A** (25 mg, 0.102 mmol, 1.00 equiv) and THF (2.0 mL). After cooling to -78°C , $i\text{-PrMgCl}$ (1.84 M in

THF, 166 μ L, 3.00 equiv) was added slowly. After 10 min, the reaction was allowed to warm to 0 $^{\circ}$ C. 10 min later, the reaction was quenched with sat. aq NH_4Cl (400 μ L). Then H_2O (2 mL) was added, and the material extracted with Et_2O (3 x 4 mL). All organic layers were combined, dried (Na_2SO_4), filtered, and concentrated. The residue was purified by preparative TLC on silica gel (EtOAc /hexane 30:70 eluent), affording trace arene (\pm)-**237** (yield not determined) as a colorless oil. Characterization data for this compound can be found on page 164 below.



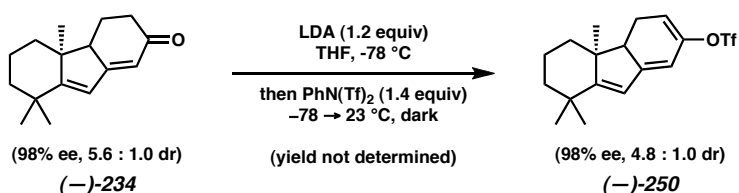
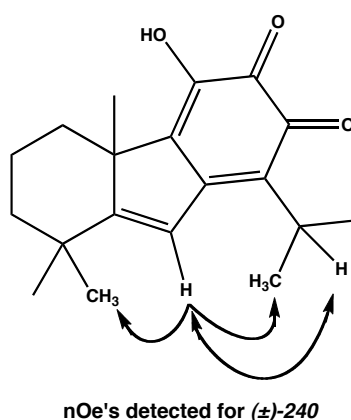
Isodichroanone (\pm)-**240**. A solution of acyloin (\pm)-**236B** (475 mg, 1.93 mmol, 1.0 equiv) in CH_2Cl_2 (100 mL) was treated with Dess-Martin Periodinane (1.634 g, 3.86 mmol, 2.0 equiv) at 23 $^{\circ}$ C for 2 h. The reaction was then filtered through silica gel presaturated with $\text{Et}_3\text{N}/\text{CH}_2\text{Cl}_2$. The filtrate was adsorbed to \sim 3 mL of silica gel and immediately purified by flash chromatography on silica gel (20:80 EtOAc :hexane eluent), giving an orange oily product (231 mg) which was immediately used in the next reaction.

60 mg of this orange oil was concentrated several times from THF, dissolved in THF (20 mL), and cooled to $-78\text{ }^{\circ}\text{C}$. $i\text{-PrMgCl}$ (1.84 M in THF, 135 μ L, 0.248 mmol) was then added, causing the reaction to turn from bright red to bright green. After 40 min had passed, the reaction was treated with 6 M aq HCl (3.0 mL) $-78\text{ }^{\circ}\text{C}$, and the reaction quickly turned orange-red. The reaction was warmed to 23 $^{\circ}$ C and stirred for 3 h. Then H_2O (15 mL) was added, and organic phase was collected. The aqueous layer was

extracted with Et₂O (3 x 10 mL). All organic layers were combined, dried (Na₂SO₄), filtered, and adsorbed to 750 μ L of silica gel. The material was purified by flash column chromatography on silica gel (10:90 EtOAc:hexane \rightarrow 20:80 EtOAc:hexane eluent), and the orange product (mass not determined) was immediately used in the next reaction.

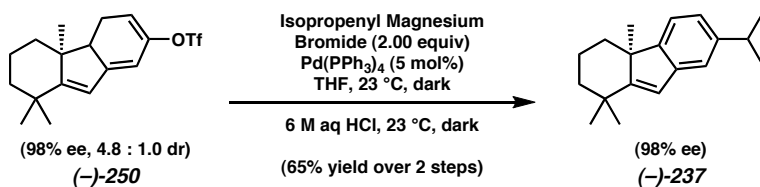
The orange product of the grignard reaction was dissolved in THF (20 mL). Fremy's Salt (potassium nitroso disulfonate, radical)(424 mg, 1.61 mmol) was introduced, and the reaction was heated to 60 °C for 5.5 h. The reaction was cooled to 23 °C and filtered through a short plug of silica gel. The filtrate was concentrated and quickly partitioned between EtOAc (20 mL) and H₂O (20 mL). The organic layer was collected, dried (Na₂SO₄), filtered, and concentrated. The residue was purified by flash column chromatography on silica gel (5:95 EtOAc:hexane \rightarrow 20:80 EtOAc:hexane eluent), giving a bright red series of fractions. These fractions were combined and concentrated. The residue was subjected to preparative HPLC (normal phase silica gel column, 10-20 mesh)(10:90 EtOAc:hexane \rightarrow 30:70 EtOAc:hexane gradient elution), giving isodichroanone (\pm)-**240** (~3 mg) as a red semisolid. *R_f* (not determined); ¹H NMR (300 MHz, CDCl₃): δ 7.07 (s, 1H), 6.55 (s, 1H), 3.34 (septuplet, *J* = 6.9 Hz, 1H), 2.11 (app. d, *J* = 13.2 Hz, 1H), 1.96 (app. qt, *J_q* = 13.6 Hz, *J_t* = 3.6 Hz, 1H), 1.75-1.48 (m, 4H), 1.46 (s, 3H), 1.35 (d, *J* = 6.9 Hz, 6H), 1.31 (s, 3H), 1.29 (s, 3H); ¹³C NMR (125 MHz, CDCl₃): δ 178.9, 171.4, 155.3, 151.1, 150.3, 131.2, 124.9, 121.1, 120.4, 50.1, 42.3, 38.7, 36.9, 31.1, 30.5, 29.9, 29.5, 27.4, 25.7, 25.4, 21.21, 21.17, 19.5 (4 extra carbons are noted; compound is only semipure); IR (NaCl/CDCl₃): 3267 (broad), 2961, 2930, 2871, 1738, 1641, 1574, 1403, 1100 cm⁻¹; LRMS-EI⁺ (*m/z*): [*M*]⁺ calc'd for C₁₉H₂₄O₃, 300; found, 300. ¹H-¹H homodecoupling experiments (600 MHz, CDCl₃) were performed on

(\pm)-**240**: The signal at δ 3.34 (septuplet, J = 6.9 Hz, 1H) was suppressed with a decoupling current, resulting in a splitting change at δ 1.35 (d, J = 6.9 Hz, 6H \rightarrow app. s, 6H). This information allowed for key nOe's to be correctly assigned. ^1H - ^1H nOesy-1D spectra were obtained for (\pm)-**240** (600 MHz, CDCl_3); the results are shown below:



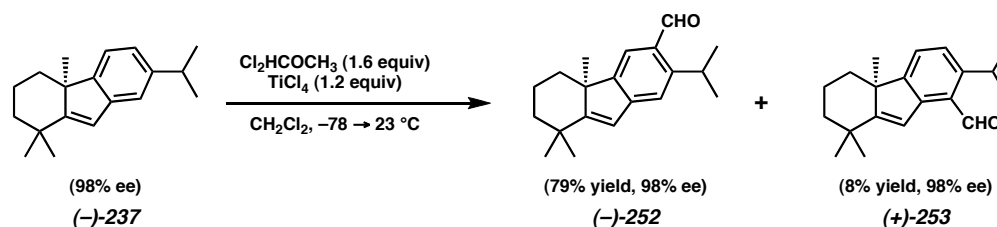
Tricyclic Enol Triflate ($-$)-250. A solution of $i\text{-Pr}_2\text{NH}$ (186 μL , 1.33 mmol) in THF (17 mL) was cooled to $0\text{ }^{\circ}\text{C}$, and $n\text{-BuLi}$ (2.55 M in hexanes, 482 μL , 1.23 mmol) was added dropwise. After 30 min, the reaction was cooled to $-78\text{ }^{\circ}\text{C}$, and a solution of tricyclic dienone ($-$)-**234** (236 mg, 1.03 mmol) in THF (3 mL) was added dropwise over 5 min. After 30 min, a solution of N -phenyl triflimide (513 mg, 1.44 mmol) in THF (6 mL) was added. 30 min later, the reaction was wrapped in foil and warmed to $23\text{ }^{\circ}\text{C}$. After 5 h, the reaction was diluted with Et_3N (5 mL) and concentrated to $\sim 5\text{ mL}$ total volume. Then hexane (10 mL) and more Et_3N (2 mL) were added, and the reaction was concentrated to $\sim 5\text{ mL}$ a second time. The reaction was filtered through a 5-inch plug of silica that had

been pre-eluted with Et₃N/Et₂O/hexane (5:20:75) and eluted with the same solvent mixture. The eluate was concentrated, giving crude, unstable tricyclic enol triflate **(-)-250** (yield not determined) as an orange gel, which was immediately used in the next reaction. ¹H NMR revealed the product to be an inseparable mixture of diastereomers. *R_f* 0.80 (2:8:1 EtOAc/hexane/Et₃N, TLC plate is pre-eluted), (Ceric Ammonium Molybdate, blue spot) (both diastereomers); ¹H NMR (300 MHz, C₆D₆): δ 5.66 (s, 1H), 5.58 (app. dd, *J* = 2.5 Hz, 2.2 Hz, 1H), 5.31 (app. dtd, *J*_{d1} = 6.6 Hz, *J*_t = 2.2 Hz, *J*_{d2} = 1.1 Hz, 1H), 1.95 (ddd, *J* = 29.2 Hz, 20.0 Hz, 2.5 Hz, 1H), 1.93 (ddd, *J* = 50.6 Hz, 19.8 Hz, 2.8 Hz, 1H), 1.64 (app. dt, *J*_d = 14.8 Hz, *J*_t = 6.9 Hz, 1H), 1.61-1.43 (m, 2H), 1.33-1.17 (m, 2H), 1.11 (app. dd, *J* = 12.7 Hz, 3.0 Hz, 1H), 0.97 (s, 6H), 0.96-0.80 (m, 1H), 0.77 (s, 3H); ¹³C NMR (75 MHz, C₆D₆): δ 172.7, 153.0, 149.1, 132.3, 131.4, 130.3, 122.5, 111.2, 107.7, 50.1, 48.7, 41.0, 40.2, 35.6, 31.8, 27.7, 23.1, 20.9, 19.6; ¹⁹F NMR (282 MHz, C₆D₆): δ -71.6, -74.4 (major diastereomer), -74.5 (minor diastereomer); IR (NaCl/hexane): 2961, 2931, 2868, 2848, 1649, 1579, 1445, 1420, 1246, 1209, 1144, 1096, 1059, 907, 880, 862 cm⁻¹; HRMS-EI⁺ (*m/z*): [M]⁺ calc'd for C₁₇H₂₁F₃O₃S, 362.1164; found, 362.1166; [α]_D²⁵ -11.24° (*c* 0.700, hexane), 98% ee.



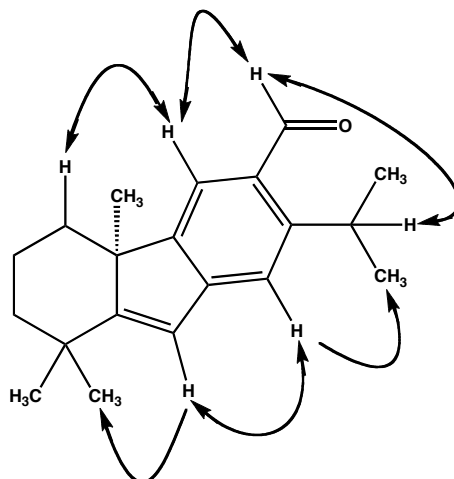
Arene (-)-237. To a solution of crude tricyclic enol triflate **(-)-250** (~371 mg, 1.03 mmol) in THF (50 mL) was added isopropenyl magnesium bromide (0.5 M in THF, 4.12 mL, 2.06 mmol), and the round-bottom flask was immediately covered in foil. Then a

solution of $\text{Pd}(\text{PPh}_3)_4$ (29.5 mg, 0.0515 mmol, weighed in glovebox) in THF (5 mL) was promptly added at 23 °C. After 1 h, 6 M aq HCl (5.5 mL) was added in a dropwise manner. After 16 h at 23 °C, the reaction was diluted with water (40 mL) and hexane (40 mL), and the organic phase was collected. The aqueous phase was extracted with Et_2O (3 x 30 mL). All organic layers were combined, washed with brine (30 mL), dried (Na_2SO_4), filtered, and adsorbed onto silica gel. The adsorbed product was purified by flash chromatography on silica gel (hexane eluent), affording arene **(-)-237** (170 mg, 65% yield from tricyclic dienone **(-)-234**) as a colorless oil. R_f 0.43 (hexane), (UV 254 nm); ^1H NMR (300 MHz, CDCl_3): δ 7.21 (d, $J = 1.4$ Hz, 1H), 7.19 (d, $J = 7.7$ Hz, 1H), 7.04 (dd, $J = 7.7$ Hz, 1.4 Hz, 1H), 6.40 (s, 1H), 2.96 (septuplet, $J = 6.9$ Hz, 1H), 2.18 (ddd, $J = 12.7$ Hz, 4.7 Hz, 3.0 Hz, 1H), 2.00 (app. qt, $J_q = 13.8$ Hz, $J_t = 4.3$ Hz, 1H), 1.74-1.60 (m, 2H), 1.41 (s, 3H), 1.35 (s, 3H), 1.32 (d, $J = 6.9$ Hz, 6H), 1.29 (s, 3H), 1.15 (td, $J_t = 12.9$ Hz, $J_d = 3.7$ Hz, 1H), 1.05 (td, $J_t = 13.2$ Hz, $J_d = 3.7$ Hz, 1H); ^{13}C NMR (75 MHz, CDCl_3): δ 164.4, 152.9, 147.2, 142.4, 122.4, 121.0, 120.8, 118.6, 50.8, 42.8, 38.3, 35.7, 34.3, 31.5, 25.5, 24.54, 24.51, 23.7, 20.0; IR (NaCl/ CDCl_3): 3061, 2995, 2959, 2928, 2866, 2845, 1616, 1479, 1458, 1382, 1369, 1362, 886, 820 cm^{-1} ; HRMS- EI^+ (m/z): $[\text{M}]^+$ calc'd for $\text{C}_{19}\text{H}_{26}$, 254.2035; found, 254.2046; $[\alpha]_D^{24} -80.74^\circ$ (c 0.320, CHCl_3), 98% ee.



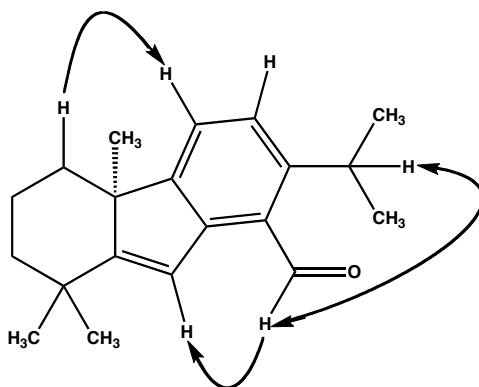
Aldehydes (-)-252 and (+)-253. A solution of arene **(-)-237** (156 mg, 0.614 mmol) in CH_2Cl_2 (15 mL) was cooled to -78°C and α,α -dichloromethyl, methyl ether (89.0 μL ,

0.982 mmol) was introduced, followed by TiCl_4 (81.0 μL , 0.736 mmol). After 1 h, the deep red mixture was warmed to 23 $^\circ\text{C}$, and 1 h later the reaction was poured onto a slurry of crushed ice (40 mL) and CH_2Cl_2 (10 mL). After stirring vigorously for 1 h, the organic phase was collected. The aqueous phase was extracted with CH_2Cl_2 (3 x 20 mL). All organic layers were combined, washed with water (20 mL), sat. aq NaHCO_3 (30 mL), and brine (30 mL), then dried (Na_2SO_4), filtered, and adsorbed onto silica gel. The adsorbed products were separated by flash chromatography on silica gel (1:99 Et_2O /hexane \rightarrow 2:98 Et_2O /hexane \rightarrow 5:95 Et_2O /hexane eluent), affording desired aldehyde (–)-**252** (137 mg, 79% yield) as a colorless oil. R_f 0.40 (1:9 EtOAc /hexane), (UV, 254 nm); ^1H NMR (300 MHz, CDCl_3): δ 10.39 (s, 1H), 7.73 (s, 1H), 7.33 (s, 1H), 6.42 (s, 1H), 3.96 (app. septuplet, $J = 6.9$ Hz, 1H), 2.20 (app. d, $J = 12.9$ Hz, 1H), 1.96 (app. qt, $J_q = 13.2$ Hz, $J_t = 3.3$ Hz, 1H), 1.56–1.72 (m, 2H), 1.39 (s, 3H), 1.33 (d, $J = 6.9$ Hz, 3H), 1.32 (d, $J = 6.9$ Hz, 3H), 1.31 (s, 3H), 1.25 (s, 3H), 1.10 (td, $J_t = 13.2$ Hz, $J_d = 3.9$ Hz, 1H), 0.99 (td, $J_t = 13.5$ Hz, $J_d = 3.9$ Hz, 1H); ^{13}C NMR (75 MHz, CDCl_3): δ 191.9, 170.2, 152.6, 151.4, 148.5, 129.2, 122.6, 121.1, 117.9, 51.3, 42.6, 37.9, 36.1, 31.3, 27.7, 25.1, 24.4, 24.3, 23.2, 19.7; IR (NaCl/ CDCl_3): 3066, 2995, 2962, 2930, 2867, 2847, 2801, 2753, 2717, 2252, 1690, 1674, 1613, 1552, 1472, 1459, 1420, 1383, 1370, 1267, 1180, 1163, 906, 891 cm^{-1} ; HRMS-EI $^+$ (m/z): $[\text{M}]^+$ calc'd for $\text{C}_{20}\text{H}_{26}\text{O}$, 282.1984; found, 282.1991; $[\alpha]_D^{24}$ -109.22° (c 1.205, CHCl_3), 98% ee. ^1H - ^1H nOesy-1D spectra were obtained for (–)-**252** (300 MHz, CDCl_3); the results are shown below:

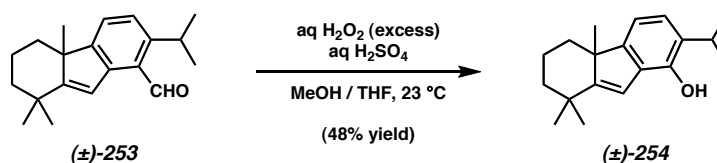


nOe's detected for (-)-252

Undesired aldehyde (+)-**253** (13.3 mg, 8% yield) was also isolated as a colorless oil. R_f 0.48 (1:9 EtOAc/hexane), (UV, 356 nm); ^1H NMR (300 MHz, CDCl_3): δ 10.71 (s, 1H), 7.37 (d, $J = 7.7$ Hz, 1H), 7.19 (s, 1H), 7.17 (d, $J = 7.7$ Hz, 1H), 3.89 (septuplet, $J = 6.9$ Hz, 1H), 2.17 (app. dd, $J = 12.9$ Hz, 1.7 Hz, 1H), 1.97 (app. qt, $J_q = 14.0$ Hz, $J_t = 3.9$ Hz, 1H), 1.74-1.58 (m, 2H), 1.37 (s, 3H), 1.35 (s, 3H), 1.33 (d, $J = 6.9$ Hz, 3H), 1.32 (d, $J = 6.9$ Hz, 3H), 1.26 (s, 3H), 1.11 (td, $J_t = 12.9$ Hz, $J_d = 3.9$ Hz, 1H), 0.96 (td, $J_t = 13.2$ Hz, $J_d = 3.6$ Hz, 1H); ^{13}C NMR (75 MHz, CDCl_3): δ 192.8, 169.3, 154.3, 149.7, 144.3, 125.9, 125.7, 121.6, 120.1, 50.0, 42.7, 37.9, 36.1, 31.4, 28.2, 25.2, 24.60, 24.55, 23.1, 19.8; IR (NaCl/ CDCl_3): 2994, 2962, 2930, 2867, 2846, 2777, 2754, 1682, 1591, 1571, 1456, 1417, 1254, 1183, 1176, 1109, 882, 828 cm^{-1} ; HRMS-EI⁺ (m/z): $[\text{M}]^+$ calc'd for $\text{C}_{20}\text{H}_{26}\text{O}$, 282.1984; found, 282.1990; $[\alpha]_D^{26} +1.15^\circ$ (c 0.665, CHCl_3), 98% ee. ^1H - ^1H nOesy-1D spectra were obtained for (+)-**253** (300 MHz, CDCl_3); the results are shown below:

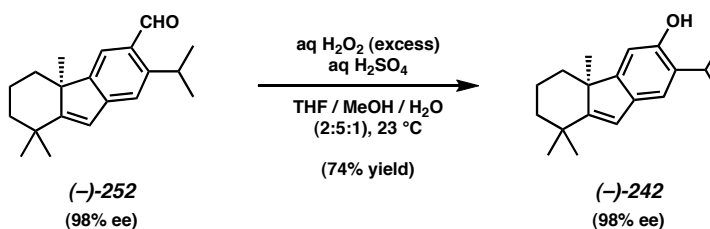


nOe's detected for (+)-253



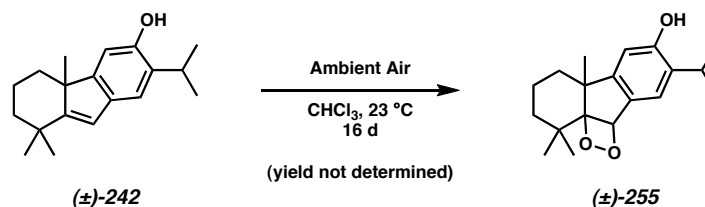
Tricyclic Phenol (±)-254. A round-bottom flask was charged with a solution of aldehyde (±)-253 (35 mg, 0.124 mmol) in THF (500 μL). MeOH (3 mL) was added, followed by 30% aq H_2O_2 (500 μL) at 23 $^\circ\text{C}$. Then, conc. aq H_2SO_4 (3 drops from a glass pipet) was added. After 1 h, more 30% aq H_2O_2 (500 μL) was added. After 48 h, the reaction was added to a biphasic mixture of NaHSO_3 (1.2 g), H_2O (20 mL), CH_2Cl_2 (20 mL), and hexanes (10 mL). The organic phase was collected, and the aqueous layer was extracted with CH_2Cl_2 (3 x 15 mL). All organic layers were combined, washed with brine, dried (Na_2SO_4), filtered, and adsorbed onto 1.0 mL of silica gel. The material was purified by flash chromatography on silica gel (1:99 Et_2O :hexane \rightarrow 8:92 Et_2O :hexane eluent), giving tricyclic phenol (±)-254 (16.2 mg, 48% yield). R_f (not determined); ^1H NMR (300 MHz, CDCl_3): δ 7.00 (d, $J = 7.7$ Hz, 1H), 6.84 (d, $J = 7.7$ Hz, 1H), 6.45 (s, 1H), 4.68 (s,

1H), 3.21 (app. septuplet, $J = 6.9$ Hz, 1H), 2.12 (ddd, $J = 12.7$ Hz, 4.7 Hz, 3.0 Hz, 1H), 1.96 (app. qt, $J_q = 13.6$ Hz, $J_t = 3.9$ Hz, 1H), 1.71-1.56 (m, 2H), 1.37 (s, 3H), 1.32 (s, 3H), 1.29 (d, $J = 6.9$ Hz, 3H), 1.28 (d, $J = 6.9$ Hz, 3H), 1.25 (s, 3H), 1.12 (app. td, $J_t = 12.9$ Hz, $J_d = 3.9$ Hz, 1H), 1.01 (app. td, $J_t = 13.2$ Hz, $J_d = 3.6$ Hz, 1H); ^{13}C NMR (75 MHz, CDCl_3): δ 163.4, 154.8, 145.7, 132.2, 128.6, 122.4, 115.4, 114.1, 51.5, 43.0, 38.4, 35.8, 31.5, 27.1, 25.6, 23.8, 23.2, 23.1, 20.0; IR (NaCl/ CDCl_3): 3400 (broad), 2961, 2928, 2866, 2845, 1478, 1436, 1295, 1202 cm^{-1} ; HRMS-EI $^+$ (m/z): $[\text{M}]^+$ calc'd for $\text{C}_{19}\text{H}_{26}\text{O}$, 270.1984; found, 270.1989.



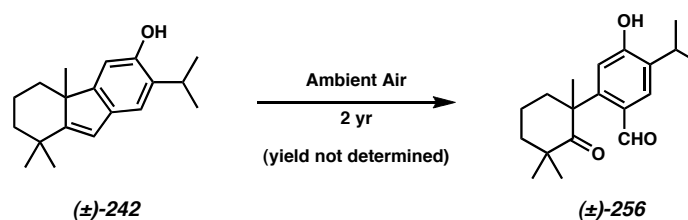
Phenol (–)-242. To a solution of aldehyde (–)-252 (135 mg, 0.478 mmol) in THF (5.4 mL) and MeOH (13.5 mL) at 23 °C was added 30% aq H_2O_2 (2.70 mL, 23.8 mmol) immediately followed by conc. aq H_2SO_4 (245 μL). After 1 h, the reaction was cautiously added to an ice-cold mixture of NaHSO_3 (1.62 g, 15.6 mmol), water (54 mL), and Et_2O (20 mL). After 5 min, the reaction was diluted with water (10 mL) and hexane (20 mL), and the organic phase was collected. The aqueous phase was extracted with Et_2O (3 x 40 mL). All organic layers were combined, washed with brine (20 mL), dried (Na_2SO_4), filtered, and adsorbed on silica gel. The adsorbed product was purified by flash chromatography on silica gel (2:98 Et_2O /hexane \rightarrow 10:90 Et_2O /hexane eluent), affording phenol (–)-242 (95.0 mg, 74% yield) as a white, unstable powder. R_f 0.56 (1:4

EtOAc/hexane), (UV, 254 nm); mp 105-106 °C (dec.) (Et₂O/hexane); ¹H NMR (300 MHz, CDCl₃, degassed with argon): δ 7.11 (s, 1H), 6.68 (s, 1H), 6.29 (s, 1H), 4.57 (s, 1H, vanishes with D₂O addition), 3.19 (app. quintet, *J* = 6.9 Hz, 1H), 2.07 (app. d, *J* = 12.4, 1H), 1.94 (app. qt, *J*_q = 13.5 Hz, *J*_t = 3.3 Hz, 1H), 1.62 (app. s, 1H), 1.58 (app. s, 1H), 1.34 (s, 3H), 1.28 (s, 3H), 1.27 (d, *J* = 6.9 Hz, 3H), 1.26 (d, *J* = 6.9 Hz, 3H), 1.22 (s, 3H), 1.10 (td, *J*_t = 13.2 Hz, *J*_d = 3.6 Hz, 1H), 1.01 (td, *J*_t = 13.2 Hz, *J*_d = 3.6 Hz, 1H); ¹³C NMR (75 MHz, CDCl₃): δ 162.0, 154.3, 150.0, 135.5, 132.4, 120.5, 117.9, 109.4, 50.9, 42.8, 38.2, 35.5, 31.4, 27.2, 25.6, 23.8, 23.1, 20.0; IR (KBr): 3393 (broad), 3057, 2988, 2965, 2934, 2909, 2868, 2837, 1459, 1431, 1382, 1362, 1286, 1166, 1076, 1004, 894, 856 cm⁻¹; HRMS-EI⁺ (*m/z*): [*M*]⁺ calc'd for C₁₉H₂₆O, 270.1984; found, 270.1993; [*α*]_D²⁴ -73.23° (*c* 0.080, CHCl₃), 98% ee.



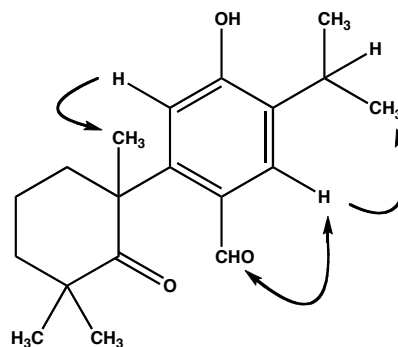
Peroxide (±)-255. A sample of purified phenol (±)-242 (~50 mg) was dissolved in PhH (~5 mL) under an ambient air headspace (solution was colorless), then stored at < 0 °C, such that the solution froze. At 16 days, the frozen sample was found to be peach-colored. The solution was adsorbed to 750 μL of silica gel and rapidly chromatographed (8:92 Et₂O:hexane → 20:80 Et₂O:hexane eluent), giving one set of fractions containing peroxide (±)-255 (yield not determined) as a white powder. An NMR tube was charged with a solution of (±)-255 (~5 mg) and CDCl₃ (700 μL) and immediately analyzed by ¹H NMR. *R_f* (not measured, but lower than phenol (±)-242 in EtOAc:hexane 20:80); ¹H

NMR (300 MHz, CDCl_3): δ 6.62 (s, 1H), 5.90 (s, 1H), 5.06 (s, 1H), 3.19 (app. septuplet, $J = 6.9$ Hz, 1H), 1.76 (app. dd, $J = 14.0$ Hz, 3.4 Hz, 1H), 1.69 (s, 3H), 1.64-1.49 (m, 2H), 1.34 (s, 3H), 1.37-1.19 (m, 3H), 1.262 (app. d, $J = 6.9$ Hz, 3H), 1.261 (app. d, $J = 6.9$ Hz, 3H), 1.16 (s, 3H); ^{13}C NMR (not measured; compound decomposed before acquisition completion); IR (not performed); HRMS (not performed). If the solution of (\pm)-**255** was allowed to stand for an additional 4 h, noticeable conversion to keto-aldehyde (\pm)-**256** was observable in the ^1H NMR. For characterization of (\pm)-**256**, see page 170 and 171 below.

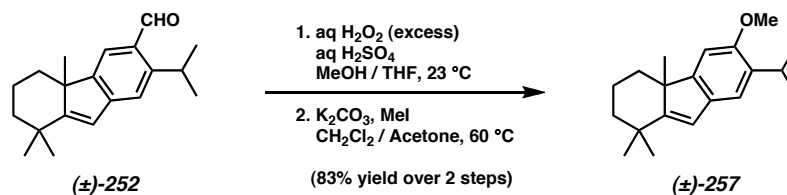


Keto Aldehyde (\pm)-256. A vial containing pure phenol (\pm)-**242** (~5 mg, evaporated from PhH) was left open to the air for a brief period of time and stored in the dark at 23 °C for 2 yr. The vial was then opened and found to contain pure (\pm)-**256** (~5 mg, yield not determined) as yellow-brown needles. R_f 0.22 (20:80 EtOAc/hexane), (UV, 254 nm); mp 181-185 °C (dec.); ^1H NMR (300 MHz, CDCl_3): δ 9.70 (s, 1H), 7.60 (s, 1H), 6.94 (s, 1H), 5.61 (app. d, $J = 7.1$ Hz, 1H), 3.16 (app. septuplet, $J = 6.9$ Hz, 1H), 2.44 (app. td, $J_t = 12.9$ Hz, $J_d = 3.9$ Hz, 1H), 2.17 (app. td, $J_t = 12.9$ Hz, $J_d = 3.6$ Hz, 1H), 1.98 (app. qt, $J_q = 13.7$ Hz, $J_t = 3.0$ Hz, 1H), 1.76-1.64 (m, 2H), 1.62 (s, 3H), 1.60-1.52 (m, 1H), 1.29 (s, 3H), 1.27 (app. d, $J = 6.9$ Hz, 3H), 1.26 (app. d, $J = 6.9$ Hz, 3H), 1.26 (s, 3H). The signal at δ 5.61 (app. d, $J = 7.1$ Hz, 1H) vanishes when D_2O is shaken into the ^1H NMR sample; ^{13}C NMR (125 MHz, CDCl_3): δ 218.2, 191.5, 158.8, 147.1, 138.0, 132.5, 125.5, 116.2,

52.9, 44.7, 40.0, 37.9, 30.3, 27.1, 26.6, 25.5, 22.5, 22.1, 18.7; IR (NaCl/CDCl₃): 3272 (broad), 2962, 2927, 2869, 1684, 1612, 1579, 1460, 1425, 1345, 1274, 999, 909, 734 cm⁻¹; HRMS-FAB⁺ (*m/z*): [M+H]⁺ calc'd for C₁₉H₂₇O₃, 303.1960; found, 303.1953. ¹H-¹H nOesy-1D spectra were obtained for (±)-**256** (300 MHz, CDCl₃); the results are shown below:

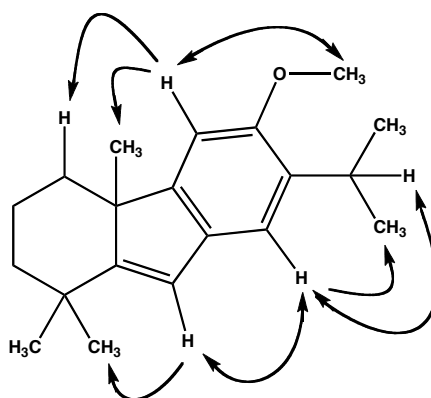


nOe's detected for (±)-**256**

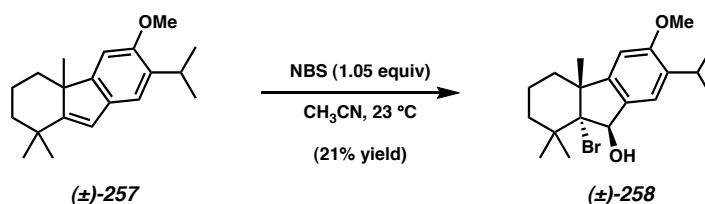


Aryl Methyl Ether (±)-257**.** A round-bottom flask was charged with a solution of aldehyde (±)-**252** (35 mg, 0.124 mmol), THF (1.0 mL), and MeOH (2.5 mL). 30% aq H₂O₂ (500 μL) was added, followed by conc. aq H₂SO₄ (3 drops from a glass pipet). After 1.2 h at 23 °C, the reaction was added slowly to a biphasic mixture of NaHSO₃ (600 mg), H₂O (20 mL), CH₂Cl₂ (20 mL), and hexanes (10 mL). The organic phase was collected, and the aqueous layer extracted with CH₂Cl₂ (3 x 15 mL). All organic layers were then combined, washed with brine (20 mL), dried (Na₂SO₄), filtered, and concentrated.

The crude product was taken up in CH₂Cl₂ (200 μ L) and transferred to a Schlenk tube. Acetone (ACS grade, 800 μ L) was added, followed by K₂CO₃ (155 mg, 1.12 mmol) and iodomethane (70 μ L, 1.12 mmol). The tube was sealed and heated to 60 °C behind a blast shield for 20 h. Then the reaction was cooled to 23 °C and filtered over glass frits with the aid of acetone. The filtrate was adsorbed onto 750 μ L of silica gel and purified by flash chromatography on silica gel (3:97 Et₂O:hexane eluent), giving aryl methyl ether (\pm)-**257** (26.4 mg, 83% yield from (\pm)-**252**) as a white powder. *R_f* (not determined); ¹H NMR (300 MHz, CDCl₃): δ 7.16 (s, 1H), 6.82 (s, 1H), 6.33 (s, 1H), 3.87 (s, 3H), 3.35 (app. septuplet, *J* = 6.9 Hz, 1H), 2.13 (app. ddd, *J* = 12.7 Hz, 4.7 Hz, 3.0 Hz, 1H), 1.98 (app. qt, *J_q* = 14.0 Hz, *J_t* = 3.9 Hz, 1H), 1.73-1.59 (m, 2H), 1.39 (s, 3H), 1.31 (s, 3H), 1.26 (s, 3H), 1.25 (app. d, *J* = 6.9 Hz, 3H), 1.24 (app. d, *J* = 6.9 Hz, 3H), 1.13 (app. td, *J_t* = 12.7 Hz, *J_d* = 3.9 Hz, 1H), 1.04 (app. td, *J_t* = 12.9 Hz, *J_d* = 3.6 Hz, 1H); ¹³C NMR (75 MHz, CDCl₃): δ 162.0, 154.7, 153.9, 135.1, 134.8, 120.6, 117.9, 104.9, 56.1, 51.2, 43.0, 38.4, 35.6, 31.5, 26.9, 25.7, 24.0, 23.3, 23.2, 20.1; IR (NaCl/CDCl₃): 3059, 2960, 2929, 2866, 2844, 1620, 1593, 1571, 1484, 1463, 1417, 1309, 1289, 1221, 1082, 1065, 1032, 888 cm⁻¹; HRMS-EI⁺ (*m/z*): [M]⁺ calc'd for C₂₀H₂₈O, 284.2140; found, 284.2131. ¹H-¹H nOesy-1D spectra were obtained for (\pm)-**257** (300 MHz, CDCl₃); the results are shown below:

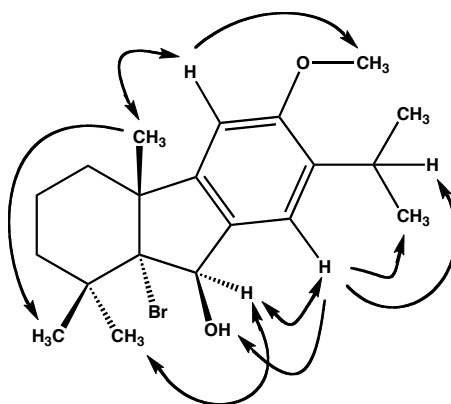


nOe's detected for (±)-257

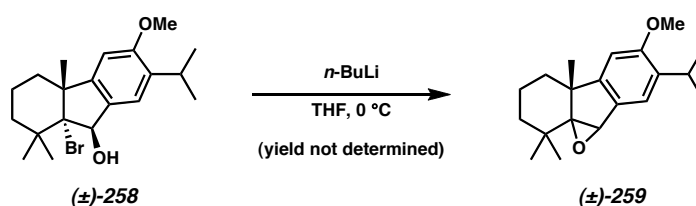


Bromohydrin (±)-258. A round-bottom flask was charged with a solution of aryl methyl ether (±)-**257** (28 mg, 99 μmol , 1.0 equiv) and CH_3CN (1.0 mL). To this was added a solution of *N*-bromo succinimide (18.4 mg, 0.103 mmol, 1.05 equiv) in CH_3CN (1.0 mL) at 23 °C. As time passed, the reaction went from colorless to yellow. At 16 h, the reaction was diluted with CH_2Cl_2 (20 mL) and adsorbed to 750 μL of silica gel and purified by flash chromatography on silica gel (2:98 Et_2O :hexane eluent), affording bromohydrin (±)-**258** (8.0 mg, 21% yield). R_f (not determined); ^1H NMR (300 MHz, CDCl_3): δ 7.22 (s, 1H), 6.57 (s, 1H), 4.98 (app. d, $J = 12.5$ Hz, 1H), 3.83 (s, 3H), 3.28 (app. septuplet, $J = 6.9$ Hz, 1H), 2.56 (app. d, $J = 12.5$ Hz, 1H), 1.81-1.61 (m, 4H), 1.76 (s, 3H), 1.51-1.40 (m, 1H), 1.37 (s, 3H), 1.36-1.26 (m, 1H), 1.26 (s, 3H), 1.20 (app. d, $J = 6.9$ Hz, 3H), 1.19 (app. d, $J = 6.9$ Hz, 3H). The signal at δ 2.56 (app. d, $J = 12.5$ Hz, 1H) vanishes when D_2O is shaken into the ^1H NMR sample; concomitantly, the signal at δ

4.98 converges: (app. d, $J = 12.5$ Hz, 1H \rightarrow app. s, 1H) ; ^{13}C NMR (75 MHz, CDCl_3): δ 157.2, 148.5, 136.0, 133.1, 121.9, 110.2, 103.1, 77.2 (?), 55.7, 51.7, 41.6, 40.8, 39.4, 30.8, 28.7, 27.0, 24.7, 23.1, 22.9, 18.5; IR (NaCl/ CDCl_3): 3538 (broad), 2938, 2867, 1615, 1592, 1492, 1464, 1392, 1305, 1289, 1223, 1093, 1070, 906 cm^{-1} ; LRMS-EI $^+$ (m/z): $[\text{M}]^+$ calc'd for $\text{C}_{20}\text{H}_{29}\text{O}_2^{79,81}\text{Br}$, 380 and 382; found, 380 and 382. ^1H - ^1H nOesy-1D spectra were obtained for (\pm)-**258** (300 MHz, CDCl_3); the results are shown below:

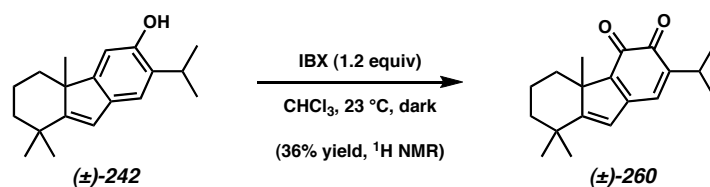


nOe's detected for (\pm)-**258**



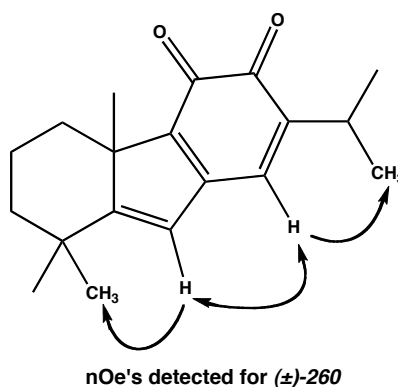
Aryl Epoxide (\pm)-259. A round-bottom flask was charged with a solution of bromohydrin (\pm)-**258** (6.2 mg, 16.3 μmol) and THF (5.0 mL) and cooled to 0 $^\circ\text{C}$. (n -BuLi, 2.5 M in hexanes, 7 μL , 17.5 μmol) was added. 10 min later, the reaction was treated with D_2O (1.0 mL), then warmed to 23 $^\circ\text{C}$. After 15 min, the reaction was diluted with hexanes (5 mL). The organic layer was collected, dried (Na_2SO_4), filtered, and concentrated, giving aryl epoxide (\pm)-**259** (yield not determined) R_f (not determined); ^1H

NMR (300 MHz, CDCl₃): δ 7.24 (s, 1H), 6.60 (s, 1H), 5.53 (app. d, J = 5.8 Hz, 1H), 3.85 (s, 3H), 3.28 (app. septuplet, J = 6.9 Hz, 1H), 2.26 (app. t, J = 13.4 Hz, 1H), 1.95-1.71 (m, 3H), 1.73 (s, 3H), 1.62-1.52 (m, 2H), 1.45 (s, 3H), 1.37 (s, 3H), 1.21 (app. d, J = 6.9 Hz, 3H), 1.20 (app. d, J = 6.9 Hz, 3H); ¹³C NMR (75 MHz, CDCl₃): δ 158.0, 136.2, 133.7, 122.4, 104.5, 84.7, 55.7, 40.1, 39.4, 31.7, 27.5, 27.1, 23.0, 22.8, 19.6; IR (NaCl/CDCl₃): 3434, 2959, 2933, 2873, 1615, 1492, 1464, 1376, 1308, 1226, 1058, 1018 cm⁻¹; HRMS-EI⁺ (m/z): [M+H]⁺ calc'd for C₂₀H₂₉O₂, 301.2168; found, 301.2168. ¹H-¹H homodecoupling experiments (300 MHz, CDCl₃) were performed on (±)-**259**: The signal at δ 6.60 (s, 1H) was suppressed with a decoupling current, resulting in no detectable splitting changes. The signal at δ 5.53 (app. d, J = 5.8 Hz, 1H) was suppressed with a decoupling current, resulting in no detectable splitting changes. It is hypothesized that this signal is not really a doublet, but rather 2 singlets that arise from 2 diastereomers of (±)-**259**.



***o*-Quinone (±)-260.** To a rapidly stirred solution of phenol (±)-**242** (25 mg, 0.0925 mmol) in CHCl₃ (5 mL) wrapped in foil was added IBX (30.5 mg, 0.102 mmol) in nine portions over a 9 h period at 23 °C. After 11 h, the reaction was filtered through glass frits with the aide of CHCl₃. 80% (by volume) of the solution was carried onward; the remaining 20% was saved. The 80% of maroon filtrate to be processed was diluted with hexane (15 mL) and concentrated to ~4 mL total volume. More hexane was added (20

mL), and the solution was concentrated again to ~4 mL. This process was repeated two more times; then the solution was purified by flash chromatography on silica gel (1:9 Et₂O/hexane eluent), affording unstable *o*-quinone (\pm)-**260** (4.3 mg, 20% yield based on 80% of starting material) as a purple powder. The compound was suitable for partial characterization: *R_f* 0.55 (1:4 EtOAc/hexane), (visible, purple spot); ¹H NMR (300 MHz, CDCl₃): δ 6.86 (s, 1H), 6.15 (s, 1H), 2.98 (app. quintet, *J* = 6.9 Hz, 1H), 2.41 (app. dd, *J* = 12.4 Hz, 1.7 Hz, 1H), 1.95-2.20 (m, 1H), 1.89 (app. qt, *J_q* = 13.2 Hz, *J_t* = 2.5 Hz, 1H), 1.72 (app. d, *J* = 12.7 Hz, 1H), 1.60 (s, 3H), 1.43 (s, 3H), 1.24 (s, 3H), 1.11-1.21 (m, 1H), 1.12 (d, *J* = 6.9 Hz, 3H), 1.11 (d, *J* = 6.9 Hz, 3H), 1.00-1.08 (m, 1H); IR (NaCl/CH₂Cl₂): 3418 (broad), 3035, 2961, 2932, 2869, 1959, 1682, 1631, 1580, 1517, 1464, 1433, 1403, 1369, 1287, 1230, 1172, 1009 cm⁻¹; HRMS-FAB⁺ (*m/z*): [M+H]⁺ calc'd for C₁₉H₂₅O, 285.1855; found, 285.1851. ¹H-¹H nOesy-1D spectra were obtained for (\pm)-**260** (300 MHz, CDCl₃); the results are shown below:



The following experiment was employed for determining actual yield of (\pm)-**260**: To a rapidly stirred solution phenol (–)-**242** (25.4 mg, 0.0940 mmol) in CHCl₃ (5 mL) in the dark was added IBX (30.2 mg, 0.1018 mmol) in one portion. After 15 h, the reaction was filtered through glass frits with the aid of CHCl₃. The filtrate was partially concentrated and CDCl₃ was added; this was repeated iteratively until there was less than

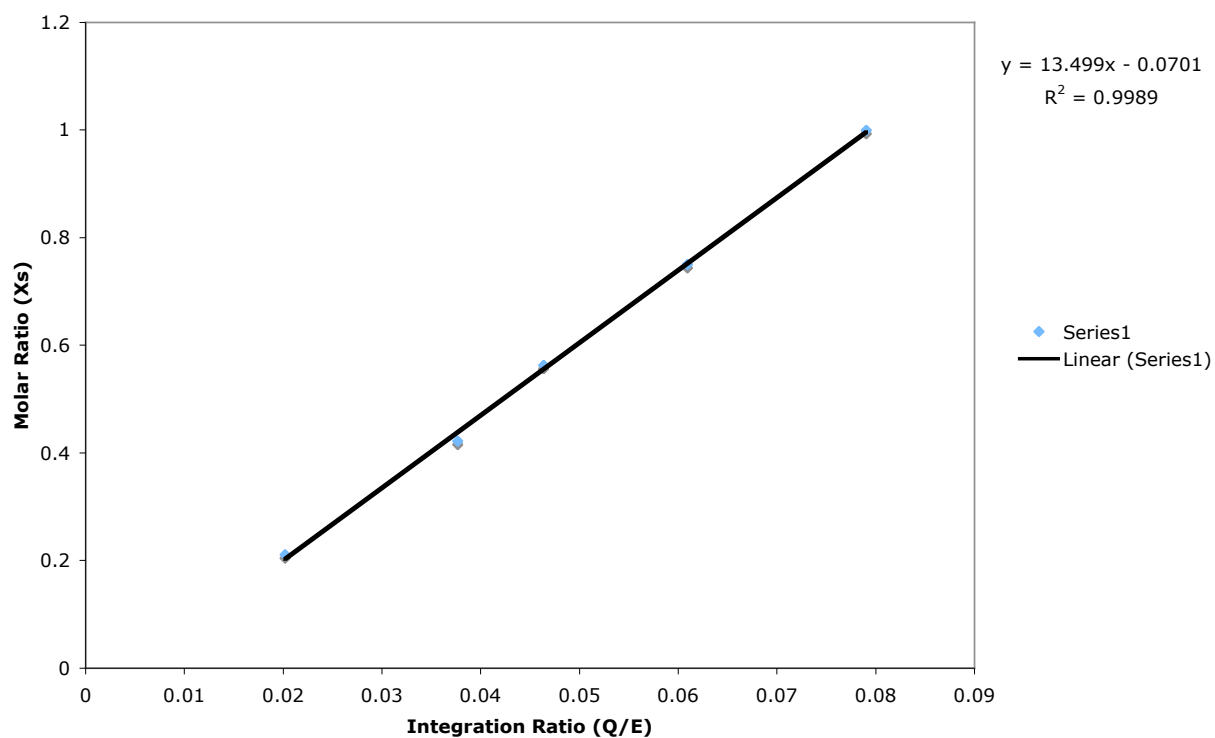
2% CHCl_3 by volume and ~ 3 mL total volume of solution. The solution was transferred to a 5.00 mL volumetric flask, and EtOAc (51.0 μL , 0.522 mmol, internal standard) was added. The flask was diluted to 5 mL using CDCl_3 , giving a solution of unknown that was 0.0188 M in (\pm) -**260** (assuming a 100% yield) and 0.104 M in EtOAc, with a theoretical molar ratio, X_T , of 1:5.55 (maximum theoretical analyte: internal standard). In a separate 2.00 mL volumetric flask, analytically pure racemic *o*-quinone (\pm) -**260** (4.3 mg, 0.0151 mmol) from earlier in this procedure was dissolved in 2.0 mL of a stock solution of EtOAc (20.5 μL , 0.209 mmol, internal standard) and CDCl_3 (5.00 mL), giving a solution with a molar ratio X_S of 1:5.55 (analyte/internal standard). This analyte solution was serially diluted with the stock internal standard solution, giving four more solutions with molar ratios of $0.750X_S$, $0.563X_S$, $0.422X_S$, and $0.211X_S$. These four solutions, along with the original $1.000X_S$ solution, were analyzed by ^1H NMR, and the peak integration ratios δ 6.86 (analyte): δ 4.08 (internal standard) were determined. A calibration curve of molar ratio vs. integration ratio was prepared. The unknown was also analyzed by ^1H NMR to obtain its integration ratio. The value of X_T (molar ratio) for the unknown was extrapolated from the equation of the least-squares best-fit line for the calibration curve, and was found to be $0.363X_S$. This corresponds to a 36% yield of racemic *o*-quinone (\pm) -**260**.

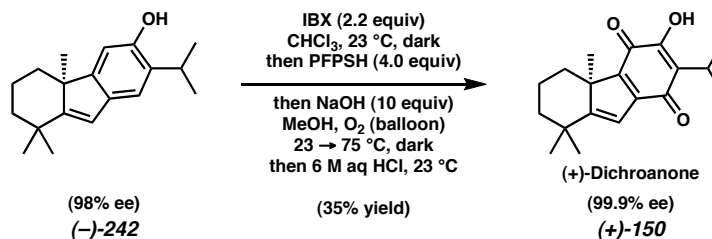
Calibration Curve and Extrapolation Data for *o*-Quinone (\pm)-260 Yield Assay

	(\pm)-260	Int. Std.	Q/E Ratio	
Calibration	Integration $\delta 6.86$	Integration $\delta 4.08$	(\pm)-260/Int.Std.	Yield (X_S)
	5.37	67.95	0.0790	1.00
	4.46	73.20	0.0609	0.750
	3.62	78.07	0.0464	0.563
	2.99	79.35	0.0377	0.422
	1.72	85.11	0.0202	0.211
Extrapolation	Unknown	Internal Std.	Unknown/Int.Std.	Yield (X_T)
	2.50	78.00	0.0321	0.363

Calibration Curve for *o*-Quinone (\pm)-260 Yield Assay

Calibration Curve: Molar Ratio vs. Integration Ratio





(R)-(+)-Dichroanone ((+)-150). Phenol **(-)-242** (79.8 mg, 0.295 mmol) was dissolved in CHCl₃ (16 mL) that had been degassed with argon for 10 min and shaken over oven-dry MS4Å. IBX (99.0 mg, 0.354 mmol) was added under argon with vigorous stirring in the dark at 23 °C. At 19 h, the reaction was filtered through glass frits with the aid of CHCl₃. The filtrate, which contained enantioenriched *o*-quinone **(R)-260** (36% yield by ¹H NMR), was immediately used without further purification. To this solution was added pentafluorothiophenol (157 μL, 1.18 mmol) at 23 °C in the dark. After 2 h, the maroon reaction had become yellow-orange, and TLC revealed complete consumption of the *o*-quinone **(R)-260**. At this time, a solution of powdered NaOH (118 mg, 2.95 mmol) in MeOH (16 mL) was introduced. An O₂ balloon was attached, and the reaction became deep red over the next 2 h. Then, the mixture was refluxed under a balloon of O₂ at 75 °C in the dark for another 3 h. After cooling to 23 °C, the O₂ balloon was removed and substituted for an N₂ atmosphere. 6 M aq HCl (1.60 mL) was added dropwise and stirring was continued at 23 °C as the reaction became bright orange-red, and a white precipitate formed. After 30 min, the reaction was diluted with water (20 mL) and hexane (20 mL), and the organic phase was collected. The aqueous phase was extracted with Et₂O (3 x 20 mL). All organic layers were combined, washed with brine (20 mL), dried (Na₂SO₄), filtered, and concentrated to ~2 mL total volume. This suspension was purified by flash chromatography on silica gel (2:98 Et₂O/hexane eluent), affording semipure (+)-

dichroanone ((+)-**150**) as an oily, unpleasant-smelling, red solid. The residue was dissolved in hexane and adsorbed onto silica gel. The material was purified by flash chromatography on a second column of silica gel (2:98 Et₂O/hexane eluent), affording (*R*)-(+)-dichroanone ((+)-**150**) (31.0 mg, 35% yield from phenol (–)-**242**, 99% yield from *o*-quinone (*R*)-**260**) as an odorless, amorphous red solid. The product had a 99.9% ee as determined by chiral HPLC. The compound had the same spectroscopic and physical properties as the natural sample and bore the opposite sense of optical rotation, establishing the absolute stereochemistry of natural dichroanone to be (*S*). *R_f* 0.61 (1:4 EtOAc/hexane), (visible, orange-red spot); mp 119–120 °C (PhH); ¹H NMR (300 MHz, CDCl₃): δ 7.31 (s, 1H), 6.44 (s, 1H), 3.21 (septuplet, *J* = 7.2 Hz, 1H), 2.37 (app. ddd, *J* = 13.2 Hz, 5.0 Hz, 2.8 Hz, 1H), 1.92 (app. qt, *J_q* = 13.8 Hz, *J_t* = 3.3 Hz, 1H), 1.70 (app. dq, *J_d* = 13.2 Hz, *J_q* = 2.5 Hz, 1H), 1.62 (app. dddd, *J* = 14.2 Hz, 6.6 Hz, 3.9 Hz, 2.7 Hz, 1H), 1.45 (s, 3H), 1.28 (s, 3H), 1.24 (d, *J* = 7.2 Hz, 3H), 1.23 (d, *J* = 7.2 Hz, 3H), 1.23 (s, 3H), 1.11 (app. dt, *J_d* = 13.2 Hz, *J_t* = 4.4 Hz, 1H), 1.07 (app. dt, *J_d* = 13.2 Hz, *J_t* = 4.4 Hz, 1H); ¹³C NMR (75 MHz, CDCl₃): δ 185.9, 178.4, 177.2, 152.6, 149.0, 147.9, 122.9, 118.1, 55.5, 43.5, 37.5, 37.1, 31.1, 24.9, 24.1, 20.3, 20.2, 19.2; IR (KBr): 3326, 2959, 2925, 2868, 1628, 1519, 1459, 1367, 1357, 1287, 1170, 1127, 1107, 992, 966 cm^{–1} (NaCl/CHCl₃): 3350, 2960, 2932, 2873, 1637, 1527, 1470, 1368, 1358, 1317, 1242, 1104, 990, 966 cm^{–1}; HRMS-EI⁺ (*m/z*): [*M*]⁺ calc'd for C₁₉H₂₄O₃, 300.17255; found, 300.17265; UV-Vis λ_{max} nm (log ε): 253(4.0), 332 (3.9); [α]_D²⁷ +99.60° (*c* 0.0055, dioxane), 99.9% ee.

Comparison of Natural (*S*)-(-)-Dichroanone and Synthetic (*R*)-(+)-Dichroanone ((+)-**150**)

¹ H NMR of Dichroanone, CDCl ₃ ¹			
Synthetic (+), 300 MHz		Natural (-), 300 MHz ²	
Shift (ppm)	Multiplicity/Coupling (Hz)	Shift (ppm)	Multiplicity/Coupling (Hz)
7.31	s	7.31	s
6.44	s	6.45	s
3.21	septet, 7.2	3.22	septet, 7.0
2.37	ddd, 13.2, 5.0, 2.8	2.38	br. dd, ca. 13, ca. 2
1.92	qt, q = 13.8, t = 3.3	1.93	m
1.7	dq, d = 13.2, q = 2.5	1.71	ddd, 7.5, 2.5, 2.5
1.62	dddd, 14.2, 6.6, 3.9, 2.7	ca. 1.6	m
1.45	s	1.46	s
1.28	s	1.29	s
1.24	d, 7.2	1.25	d, 7.0
1.23	d, 7.2	1.24	d, 7.0
1.23	s	1.24	s
1.11	dt, d = 13.2, t = 4.4	ca. 1.1	m
1.07	dt, d = 13.2, t = 4.4	ca. 1.1	m

¹ Note that the chemical shifts of the synthetic (+)-Dichroanone ((+)-**150**) are uniformly 0.01 ppm upfield relative to the shifts for natural (-)-Dichroanone ((+)-**150**). This could be due to the reference value used by the isolation chemists. The chemical shift reference for the synthetic material was δ 7.26 ppm in accord with Cambridge Isotopes Laboratory, Inc.

² ¹H NMR, ¹³C NMR, IR, UV-Vis, and optical rotation data have been reproduced from the isolation paper. See: Kawazoe, K.; Yamamoto, M.; Takaishi, Y.; Honda, G.; Fujita, T.; Sezik, E.; Yesilada, E. *Phytochemistry* **1999**, 50, 493-497.

Comparison of Natural (*S*)-(-)-Dichroanone and Synthetic (*R*)-(+)-Dichroanone ((+)-**150**)

¹³ C NMR of Dichroanone, CDCl ₃		IR of Dichroanone, KBr	
Synthetic (+), 75 MHz	Natural (-), 75 MHz	Synthetic (+)	Natural (-)
Shift (ppm)	Shift (ppm)	Wavenumber (cm ⁻¹)	Wavenumber (cm ⁻¹)
185.9	185.8	3326	3324
178.4	178.3	2959	2958
177.2	177.3	2925	-
152.6	152.6	2868	-
149.0	149.0	1628	1627
147.9	148.0	1519	1520
122.9	123.0	1459	1457
118.1	118.1	1367	-
55.5	55.5	1357	-
43.5	43.6	1287	1288
37.5	37.5	1170	-
37.1	37.1	1127	-
31.1	31.0	1107	-
24.9	24.9	992	-
24.1	24.1	966	-
20.3	20.3		
20.2	20.2		
-	20.2		
19.2	19.2		

UV-Vis Spectrum of Dichroanone		Specific Optical Rotation of Dichroanone	
Synthetic (+)	Natural (-)	Synthetic (+)	Natural (-)
λ_{\max} (nm), (log ϵ)	λ_{\max} (nm), (log ϵ)	$[\alpha]^{27}_{\text{D}}$, (c 0.0055) (in dioxane, 99.9%ee)	$[\alpha]^{25}_{\text{D}}$, (c 0.67) ³ (in dioxane, 100%ee)
253 (4.0)	253 (4.0)	+99.60°	-99.3°
332 (3.9)	332 (4.0)		

³ An attempt was made to measure the specific optical rotation of synthetic (-) dichroanone ((+)-**150**) at c = 0.67 as reported by the isolation chemists; however, due to the cell path length used (100 mm) on the polarimeter, no sodium-D (589 nm) light was transmitted through the orange-red solution, making an accurate measurement difficult. To circumvent this issue, a lower concentration was employed.

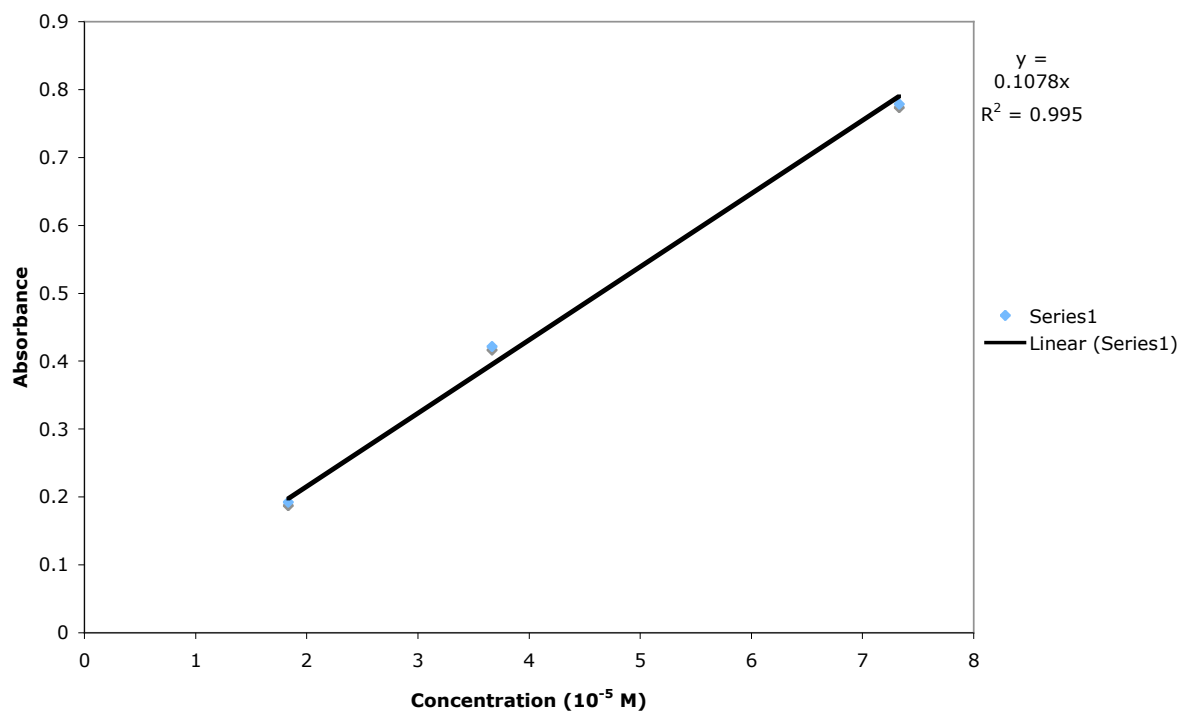
Determination of Absorption Maxima and Extinction Coefficients for (*R*)-(+)-Dichroanone ((+)-150). A sample of (+)-Dichroanone ((+)-150) (11.0 mg, 0.0366 mmol) was dissolved in dioxane (2.00 mL) in a volumetric flask, giving a 0.183 M solution. This solution was serially diluted to the following concentrations (10^{-5} M): 7.329, 4.217, and 1.925. UV-Vis spectra of the three diluted samples were obtained using a 1-cm path length quartz cuvette, and absorbances at 253 nm and 332 nm were measured. A least-squares line of absorbance vs. concentration (constrained to fit the origin) was calculated for both 253 nm and 332 nm absorbance sets. The slope of the least-squares-fit line gave the molar extinction coefficients: λ_{max} nm (log ϵ): 253(4.0), 332 (3.9).

Data Points for UV-Vis Spectra of (*R*)-(+)-Dichroanone ((+)-150)

Concentration (10^{-5} M)	Abs at 253 nm	Abs at 332 nm
7.329	0.7783	0.5974
3.665	0.4217	0.3369
1.832	0.1925	0.1542

UV-Vis Data for (*R*)-(+)-Dichroanone ((+)-150)

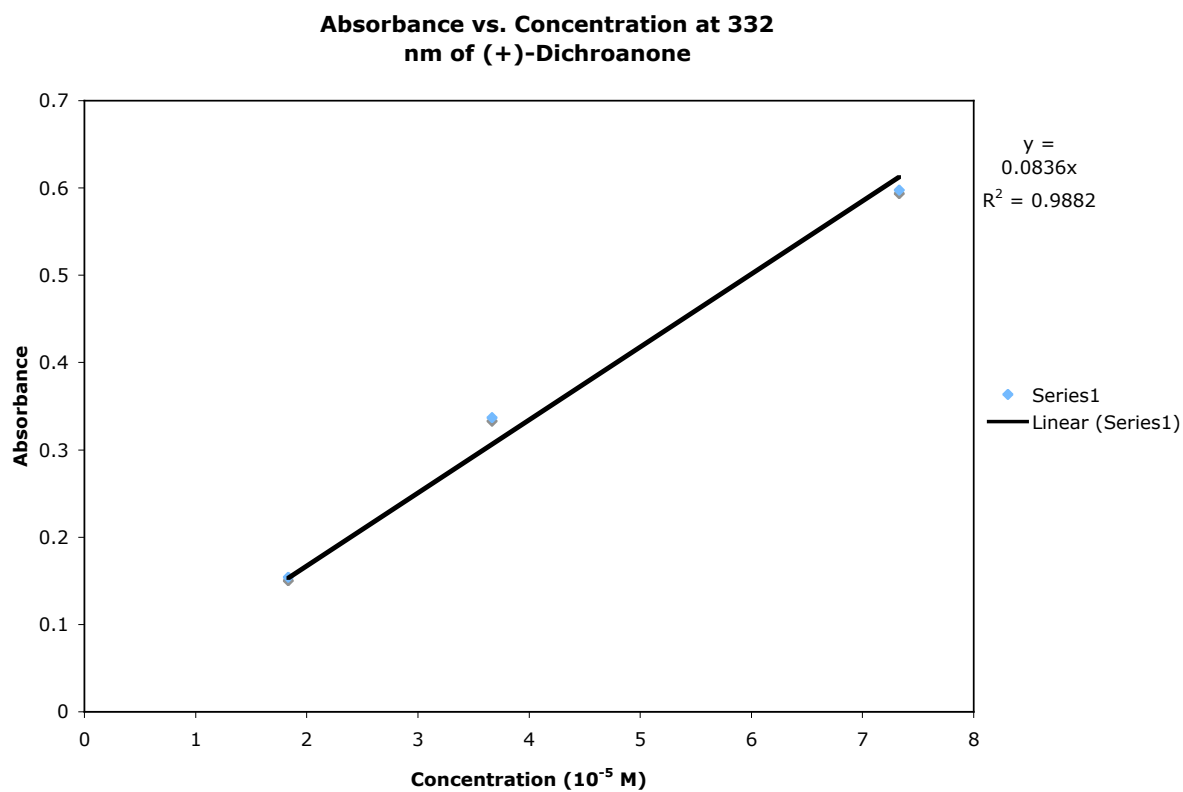
Absorbance vs. Concentration at 253 nm of (+)-Dichroanone



$$\epsilon_{253} = 10780 \text{ L / (mol} \cdot \text{cm)}; \log(\epsilon_{253}) = 4.0^4$$

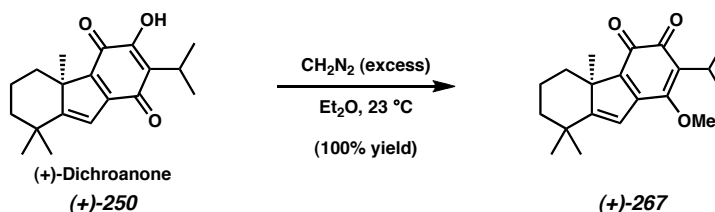
⁴ For this graph, the equation of best fit is equivalent to Beer's Law, $A = \epsilon lc$, where l is a constant (1 cm, the path length of the sample in the quartz cuvette) and ϵ is the slope of the least squares line, constrained to run through the origin. Thus, ϵ is in units of $[\text{cm}^{-1} \cdot (10^{-5} \text{ M})^{-1}]$ or more simply, $\epsilon = 100000 \cdot (\text{slope}) \cdot \text{L / (mol} \cdot \text{cm)}$. Hence, $\epsilon_{253} = 10780 \text{ L / (mol} \cdot \text{cm)}$, and $\log(\epsilon_{253}) = 4.0$.

UV-Vis Data for (*R*)-(+)-Dichroanone (+)-150

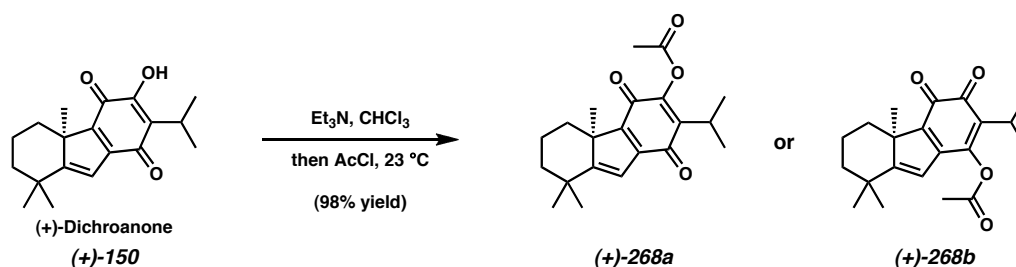


$$\epsilon_{332} = 8360 \text{ L} / (\text{mol} \cdot \text{cm}); \log(\epsilon_{332}) = 3.9^5$$

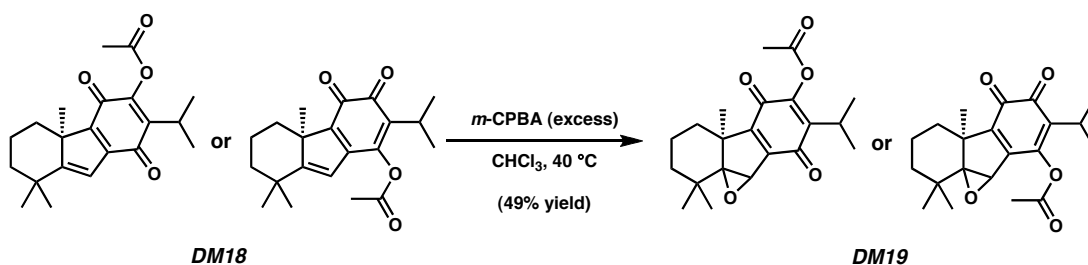
⁵ For this graph, the equation of best fit is equivalent to Beer's Law, $A = \epsilon lc$, where l is a constant (1 cm, the path length of the sample in the quartz cuvette) and ϵ is the slope of the least squares line, constrained to run through the origin. Thus, ϵ is in units of $[\text{cm}^{-1} \cdot (10^{-5} \text{ M})^{-1}]$ or more simply, $\epsilon = 100000 \cdot (\text{slope}) \cdot \text{L} / (\text{mol} \cdot \text{cm})$. Hence, $\epsilon_{332} = 8360 \text{ L} / (\text{mol} \cdot \text{cm})$, and $\log(\epsilon_{332}) = 3.9$.



***O*-Methyl Dichroanone (+)-267.** A vial was charged with dichroanone ((+)-150) (3.0 mg, 10 μ mol), and a solution of diazomethane (2.0 M in Et₂O, 2.0 mL, 4 mmol) was added. After 1 h at 23 $^{\circ}$ C, 63 μ L of silica gel was carefully added, and the reaction was adsorbed onto the silica. The reaction was then purified on a pipet flash column loaded with silica gel (10:90 Et₂O:hexane eluent), affording *O*-methyl dichroanone (+)-267 (3.1 mg, quantitative yield) as an orange powder. *R*_f 0.65 (20:80 EtOAc/hexane), (visible, orange spot); mp 85-88 $^{\circ}$ C (Et₂O/hexane); ¹H NMR (300 MHz, CDCl₃): δ 6.37 (s, 1H), 3.86 (app. d, *J* = 1.1 Hz, 3H), 3.25 (septuplet, *J* = 7.1 Hz, 1H), 2.40 (app. d, *J* = 13.2 Hz, 1H), 1.92 (app. qt, *J*_q = 13.8 Hz, *J*_t = 3.3 Hz, 1H), 1.70-1.60 (m, 2H), 1.44 (s, 3H), 1.27 (s, 3H), 1.23 (d, *J* = 7.1 Hz, 3H), 1.22 (s, 3H), 1.22 (d, *J* = 7.1 Hz, 3H), 1.11 (dt, *J*_d = 13.5 Hz, *J*_t = 3.9 Hz, 1H), 1.06 (dt, *J*_d = 13.2 Hz, *J*_t = 3.6 Hz, 1H); ¹³C NMR (75 MHz, CDCl₃): δ 186.5, 180.0, 175.8, 157.5, 150.7, 146.0, 136.2, 116.9, 61.6, 55.8, 43.5, 37.4, 36.9, 31.1, 25.0, 24.6, 20.9, 20.3, 19.3, 15.6; IR (NaCl/CHCl₃): 2961, 2931, 2874, 1645, 1615, 1583, 1534, 1472, 1458, 1359, 1292, 1264, 1156, 1092, 1026 cm⁻¹; HRMS-EI⁺ (*m/z*): [M]⁺ calc'd for C₂₀H₂₆O₃, 314.1882; found, 314.1868. [α]_D²⁵ +68.34 $^{\circ}$ (*c* 0.068, CHCl₃), 99.9% ee.



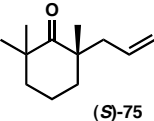
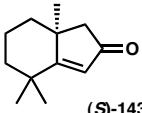
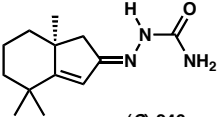
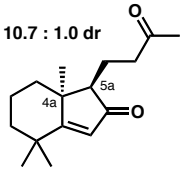
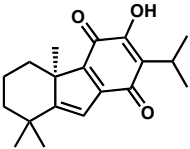
***O*-Acetyl Dichroanone (+)-268.** To a solution of dichroanone ((+)-150) (5.0 mg, 16.7 μmol) in CHCl_3 (4.0 mL) was added Et_3N (100 μL), causing the solution to turn from yellow-orange to indigo. After 5 min at 23 $^\circ\text{C}$, acetyl chloride (50 μL) was introduced, and the reaction became bright yellow. After 5 min, sat. aq NaHCO_3 (2.0 mL) was carefully added, followed by H_2O (2.0 mL). The organic phase was collected, and the aqueous layer was extracted with CHCl_3 (2 x 4 mL). All organic layers were combined, dried (Na_2SO_4), filtered, and adsorbed onto 125 μL of silica gel. The material was purified on a pipet silica gel flash column (5:95 Et_2O :hexane eluent), giving *O*-acetyl dichroanone (+)-268 (5.6 mg, 98% yield) as a yellow semisolid. R_f 0.62 (20:80 EtOAc /hexane), (visible, yellow-orange spot); mp 59-61 $^\circ\text{C}$ (CHCl_3); ^1H NMR (300 MHz, CDCl_3): δ 6.39 (s, 1H), 3.15 (septuplet, $J = 7.1$ Hz, 1H), 2.42 (app. d, $J = 13.2$ Hz, 1H), 2.36 (s, 3H), 1.91 (app. qt, $J_q = 13.5$ Hz, $J_t = 3.3$ Hz, 1H), 1.73-1.58 (m, 2H), 1.44 (s, 3H), 1.28 (s, 3H), 1.22 (app. d, $J = 6.9$ Hz, 6H), 1.22 (s, 3H), 1.12 (dt, $J_d = 13.2$ Hz, 1H), 1.07 (dt, $J_d = 12.6$ Hz, $J_t = 2.7$ Hz, 1H); ^{13}C NMR (125 MHz, CDCl_3): δ 185.2, 176.6, 175.2, 168.5, 150.9, 150.4, 146.5, 138.8, 116.8, 56.0, 43.5, 36.9, 37.4, 31.1, 25.3, 25.0, 20.65, 20.61, 20.3, 19.2; IR ($\text{NaCl}/\text{CHCl}_3$): 2963, 2932, 2874, 1777, 1652, 1594, 1534, 1462, 1368, 1352, 1292, 1184, 1158, 1010, 921, 864 cm^{-1} ; HRMS-FAB $^+$ (m/z): $[\text{M}+\text{H}]^+$ calc'd for $\text{C}_{21}\text{H}_{27}\text{O}_4$, 343.1909; found, 343.1918. $[\alpha]_D^{26} +82.61^\circ$ (c 0.0280, CHCl_3), 99.5% ee.



***O*-Acetyl Dichroanone Epoxide (–)-269.** A Schlenk tube was charged with *m*-CPBA (99% pure, 27.7 mg, 0.161 mmol, 10.0 equiv). A solution of *O*-acetyl dichroanone (+)-**268** (5.5 mg, 16.1 μmol , 1.0 equiv) in CHCl_3 (5.0 mL) was introduced. The vessel was sealed and warmed to 40 $^\circ\text{C}$ for 17 h. Then, a second portion of *m*-CPBA (99% pure, 27.7 mg, 0.161 mmol, 10.0 equiv) was added. The reaction was stirred for an additional 7 h at 40 $^\circ\text{C}$ and concentrated. The residue was purified by flash pipet column chromatography on silica gel (5:95 Et_2O :hexane eluent), giving semipure (–)-**269**. This material was purified on a second flash pipet column with silica gel (5:95 Et_2O :hexane eluent), affording pure *O*-acetyl dichroanone epoxide (–)-**269** (3.3 mg, 49% yield) as a single diastereomer in the form of a pale yellow oil. R_f 0.55 (20:80 EtOAc /hexane), (*p*-Anisaldehyde, green-yellow spot); ^1H NMR (500 MHz, CDCl_3): δ 4.17 (s, 1H), 3.12 (app. quintet, $J = 6.9$ Hz, 1H), 2.32 (s, 3H), 2.26 (app. ddd, $J = 13.2$ Hz, 5.4 Hz, 2.9 Hz, 1H), 1.78 (app. qt, $J_q = 14.2$ Hz, $J_t = 2.9$ Hz, 1H), 1.68 (app. ddd, $J = 13.7$ Hz, 5.4 Hz, 2.9 Hz, 1H), 1.58–1.44 (m, 1H), 1.55 (s, 3H), 1.48 (s, 3H), 1.36 (app. td, $J_t = 13.7$ Hz, $J_d = 3.4$ Hz, 1H), 1.30 (app. td, $J_t = 13.7$ Hz, $J_d = 3.9$ Hz, 1H), 1.21 (app. d, $J = 6.9$ Hz, 3H), 1.20 (app. d, $J = 6.9$ Hz, 3H), 1.17 (s, 3H); ^{13}C NMR (125 MHz, CDCl_3): δ 184.6, 178.2, 168.2, 155.9, 149.6, 145.8, 139.9, 75.2, 59.9, 49.5, 40.1, 36.8, 32.1, 28.0, 25.4, 23.8, 20.53, 20.47, 19.2, 17.5; IR (NaCl/ CHCl_3): 2966, 2936, 2874, 1778, 1658, 1608, 1457,

1370, 1318, 1182, 1164, 1132, 1008, 920, 890 cm^{-1} ; HRMS-FAB⁺ (m/z): $[\text{M}]^+$ calc'd for $\text{C}_{21}\text{H}_{26}\text{O}_5$, 358.1780; found, 358.1790. $[\alpha]_D^{26} -27.28^\circ$ (c 0.140, CHCl_3), 99.5% ee.

3.11.3 Methods for the Determination of Enantiomeric Excess

Entry	Substrate	Assay	Column	Method	Retention Time (min)	
1.	 (<i>S</i>)-75	Enantiomeric Excess	Chiral GC	80 °C isotherm	Major (<i>S</i>)	29.1
			Agilent GT-A Column	40 min	Minor (<i>R</i>)	30.5
2.	 (<i>S</i>)-143	Enantiomeric Excess	Chiral HPLC	3%EtOH/Hex monitor@254nm	Minor (<i>R</i>)	9.1
			Chiralcel AD Column	20 min	Major (<i>S</i>)	10.2
3.	 (<i>S</i>)-246	Enantiomeric Excess	Chiral HPLC	10%EtOH/Hex monitor@254nm	Minor (<i>R</i>)	9.3
			Chiralcel AD Column	20 min	Major (<i>S</i>)	12.1
4.	 Major Diastereomer: (4a <i>S</i> , 5a <i>R</i>)-233	Enantiomeric Excess	Chiral HPLC	4%EtOH/Hex monitor@254nm	Minor (4a <i>S</i> , 5a <i>R</i>)	17.6
			Chiralcel AD Column	40 min	Major (4a <i>R</i> , 5a <i>S</i>)	28.5
5.	 (<i>R</i>)-(+)-Dichroanone-(150)	Enantiomeric Excess	Chiral HPLC	0.3%EtOH/Hex monitor@254nm	Minor (<i>S</i>)	18.3
			Chiralcel AD Column	30 min	Major (<i>R</i>)	21.1

3.12 Notes and Citations

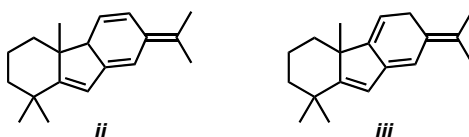
- (1) For the isolation of standishinal, see: Ohtsu, H.; Iwamoto, M.; Ohishi, H.; Matsunaga, S.; Tanaka, R.; *Tetrahedron Lett.* **1999**, *40*, 6419-6422.
- (2) Several isolations of 4a-methyltetrahydrofluorene natural products from *Taiwania cryptomerioides* have been reported: (a) Lin, W.-H.; Fang, J.-M.; Cheng, Y.-S. *Phytochemistry* **1995**, *40*, 871-873. (b) Lin, W.-H.; Fang, J.-M.; Cheng, Y.-S. *Phytochemistry* **1996**, *42*, 1657-1663. (c) Chang, C.-I.; Chien, S.-C.; Lee, S.-M.; Kuo, Y.-H. *Chem. Pharm. Bull.* **2003**, *51*, 1420-1422. (d) Chang, C.-I.; Chang, J.-Y.; Kuo, C.-C.; Pan, Y.-H.; Kuo, W.-Y. *Planta Med.* **2005**, *71*, 72-76.
- (3) For isolations of 4a-methyltetrahydrofluorene natural products from *Salvia dichroantha*, see: Kawazoe, K.; Yamamoto, M.; Takaishi, Y.; Honda, G.; Fujita, T.; Sezik, E.; Yesilada, E. *Phytochemistry* **1999**, *50*, 493-497.
- (4) (a) Iwamoto, M.; Ohtsu, H.; Tokuda, H.; Nishino, H.; Matsunaga, S.; Tanaka, R. *Bioorg. Med. Chem.* **2001**, *9*, 1911-1921. (b) Minami, T.; Iwamoto, M.; Ohtsu, H.; Ohishi, H.; Tanaka, R.; Yoshitake, A. *Planta Med.* **2002**, *68*, 742-745.
- (5) Banerjee, M.; Mukhopadhyay, R.; Achari, B.; Banerjee, A. Kr. *Org. Lett.* **2003**, *5*, 3931-3933.
- (6) Banerjee, M.; Mukhopadhyay, R.; Achari, B.; Banerjee, A. Kr. *J. Org. Chem.* **2006**, *71*, 2787-2796.
- (7) Burger, A. P. N.; Brandt, E. V.; Roux, D. G. *Phytochemistry* **1983**, *22*, 2813-2817.
- (8) (a) Blatt, A. H. *Org. React.* **1942**, *1*, 342-369. (b) Gammill, R. B. *Tetrahedron Lett.* **1985**, *26*, 1385-1388.

-
- (9) Banerjee's longest linear sequence to Dichroanal B (**149**) is 28 steps from vanillin (**170**) with a 0.88% overall yield. Vanillin (**170**) costs \$26 for 100 g (\$0.26/g) from Aldrich.
- (10) Banerjee's longest linear sequence to dichroanone (**150**) is 27 steps from vanillin (**170**) with a 1.1% overall yield. See also reference 9.
- (11) Fillion, E.; Fishlock, D. *J. Am. Chem. Soc.* **2005**, *127*, 13144-13145.
- (12) Fillion's longest linear sequence to taiwaniaquinol B (**154**) is 15 steps from 3,5-dimethoxybenzoic acid (**193**) with a 6.4% overall yield. 3,5-dihydroxybenzoic acid (**193**) costs \$30 for 100 g (\$0.30/g) from Aldrich.
- (13) Planas, L.; Mogi, M.; Takita, H.; Kajimoto, T.; Node, M. *J. Org. Chem.* **2006**, *71*, 2896-2898.
- (14) β -cyclocitral (**203**) can be purchased from Alfa Aesar at \$118 for 50 g (\$2.36/g).
- (15) Node's longest linear sequence to dichroanal B (**149**) is 11 steps from 2',3'-dihydroxy-4'-methoxyacetophenone (**204**) with a 31% overall yield. From TCI America Organic Chemicals, 2',3'-dihydroxy-4'-methoxyacetophenone (**204**) costs \$246 for 25 g (\$9.84/g).
- (16) Liang, G.; Xu, Y.; Seiple, I. B.; Trauner, D. *J. Am. Chem. Soc.* **2006**, *128*, 11022-11023.
- (17) Trauner does not specify how 2,6-dimethoxycumene (**213**) is prepared.
- (18) Trauner's longest linear sequence to taiwaniaquinol B (**154**) is 6 steps from 2,6-dimethoxycumene (**213**) with a 28% overall yield. See reference 17.

-
- (19) Taiwaniaquinone H (**165**) is prepared in 7 steps and 24% overall yield from 2,6-dimethoxycumene (**213**). Dichroanone is prepared in 7 steps and 24% overall yield from the same starting material (**213**). See reference 17.
- (20) Taiwaniaquinol D (**156**) is prepared in 8 steps and 18% overall yield from 2,6-dimethoxycumene (**213**). See reference 17.
- (21) Subsequent to our work, additional synthetic studies of 4a-methyltetrahydrofluorenes were presented, see: Himkus, J. M.; Majetich, G. Total synthesis of (±)-dichroanone and studies toward related diterpenoids. Abstracts, 58th Southeast Regional Meeting of the American Chemical Society, Augusta, GA, United States, November 1-4 (**2006**), SRM06-633.
- (22) The absolute stereochemistry of taiwaniaquinone A (**159**) was speculated by analogy to the abietanes in the taxodiaceae family. For information, see reference 2b. There has also been debate about how these [6-5-6] tricyclic natural products are named. As an alternative to the description “4a-methyltetrahydrofluorene” or “taiwaniaquinoid”, some favor the “5(6→7)abeoabietane type” nomenclature for the diterpene members and “6-nor-5(6→7)abeoabietane type” nomenclature for the norditerpenoids. For more information, see reference 2c.
- (23) 2,2,6-trimethylcyclohexanone (**101**) costs \$48/g from Aldrich.
- (24) 2,6-dimethylcyclohexanone (**220**), sold as a *cis,trans* mixture from Aldrich, costs \$48 for 25 g (\$1.92/g).
- (25) Aboulhoda, S. J.; Hénin, F.; Muzart, J.; Thorey, C. *Tetrahedron Lett.* **1995**, *36*, 4795-4796.
- (26) Tsuji, J.; Minami, I.; Shimizu, I. *Tetrahedron Lett.* **1983**, *24*, 1793-1796.

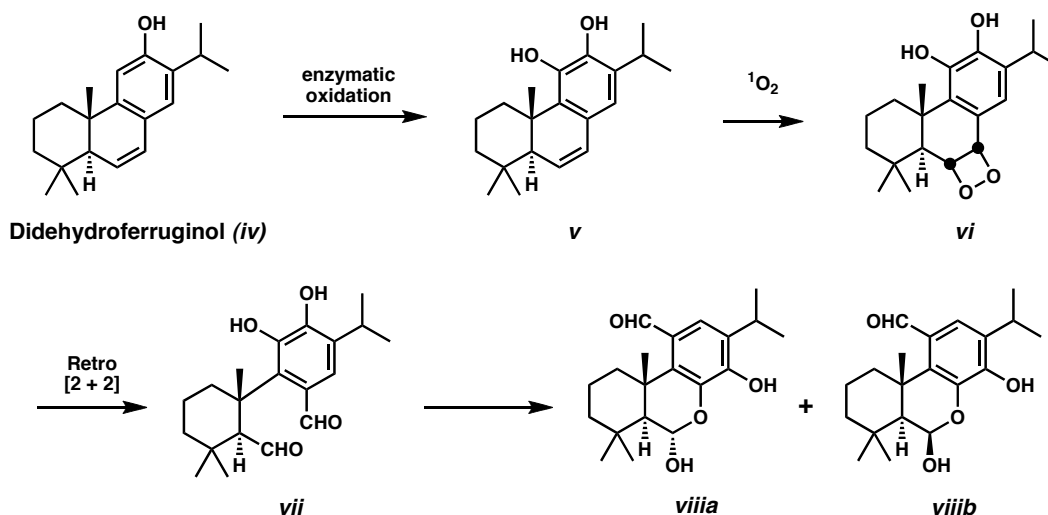
-
- (27) Typically, when solvated samples of 2-allyl-2,6,6-trimethylcyclohexanone (**75**) were concentrated in vacuo, the external bath temperature was kept at less than 10 °C to reduce unwanted evaporation of the compound, while still allowing distillation of the solvent.
- (28) Smith, A. B., III; Cho, Y. S.; Friestad, G. K. *Tetrahedron Lett.* **1998**, *39*, 8765-8768.
- (29) These conditions worked well for a similar substrate. See: Behenna, D. C.; Stoltz, B. *M. J. Am. Chem. Soc.* **2004**, *126*, 15044-15045.
- (30) Although xylenes do not reflux at this temperature, the xylene-water azeotrope does and can be removed. Refluxing at greater than 110 °C was avoided as it led to decomposition.
- (31) Thomas, A. F.; Ozainne, M.; Guntz-Dubini, R. *Can. J. Chem.* **1980**, *58*, 1810-1820.
- (32) Tessier, P. E.; Nguyen, N.; Clay, M. D.; Fallis, A. G. *Org. Lett.* **2005**, *7*, 767-770.
- (33) For the use of MoOPH in the synthesis of α -hydroxyketones, see: Vedejs, E.; Engler, D. A.; Teclschow, J. E. *J. Org. Chem.* **1978**, *43*, 188-196.
- (34) (a) For the preparation of the DMPU analogue of MoOPH, see: Daniewski, A. R.; Wojciechowska, W. *Synth. Commun.* **1986**, *16*, 535-536. (b) For application of the aforementioned analogue toward α -hydroxyketone synthesis, see: Anderson, J. C.; Smith, S. C. *Synlett* **1990**, 107-108.
- (35) (a) Rubottom, G. M.; Juve, H. D., Jr. *J. Org. Chem.* **1983**, *48*, 422-425. (b) Katsumura, S.; Isoe, S. *Chem. Lett.* **1982**, 1689-1692.
- (36) Adam, W.; Chan, Y.-Y.; Cremer, D.; Gauss, J.; Scheutzwow, D.; Schindler, M. *J. Org. Chem.* **1987**, *52*, 2800-2803.

- (37) Nakamura, N.; Nojima, M.; Kusabayashi, S. *J. Am. Chem. Soc.* **1987**, *109*, 4969-4973.
- (38) (a) Davis, F. A.; Lamendola, J., Jr.; Nadir, U.; Kluger, E. W.; Sedergran, T. C.; Panunto, T. W.; Billmers, R.; Jenkins, R., Jr.; Turchi, I. J.; Watson, W. H.; Chen, J. S.; Kimura, M. *J. Am. Chem. Soc.* **1980**, *102*, 2000-2005. (b) For use of the Davis oxaziridine in preparation of α -hydroxylketones, see: Davis, F. A.; Sheppard, A. C. *J. Org. Chem.* **1987**, *52*, 955-957. (c) A practical synthesis of the Davis oxaziridine using Oxone® has been reported: Davis, F. A.; Chattopadhyay, S.; Towson, J. C.; Lal, S.; Reddy, T. *J. Org. Chem.* **1988**, *53*, 2087-2089.
- (39) The sample of bicyclic enone (–)-**143** used in this recrystallization sequence was a combination of several lots of enone product and had a net ee of 83%.
- (40) Corey, E. J.; Lazerwith, S. E. *J. Am. Chem. Soc.* **1998**, *120*, 12777-12782.
- (41) Ito, Y.; Saegusa, T. *J. Org. Chem.* **1978**, *43*, 1011-1013.
- (42) Two hypothetical olefin isomers corresponding to the two low- R_f species are shown below:

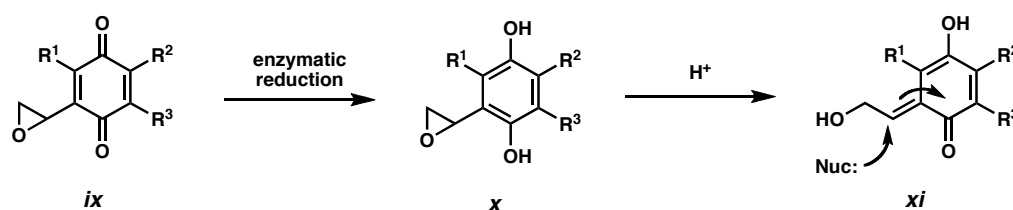


- (43) Luis, J. G.; Grillo, T. A. *Tetrahedron*, **1993**, *49*, 6277-6284. The authors believe that a dioxetane (**vi**) might explain the formation of **viii**a and **viii**b from the natural product 6,7-didehydroferruginol (**iv**). The compound (**iv**) might be enzymatically

oxidized to catechol **v**. In the presence of singlet dioxygen, dioxetane **vi** could arise. A formal 4π -electrocyclic ring opening would lead to aldehyde **vii**, and cyclization of an aromatic hydroxyl onto the cyclohexanecarbaldehyde moiety could produce either or both of the anomers **viii**a and **viii**b. See below:



- (44) Syper, L.; Mlochowski, J.; Kloc, K. *Tetrahedron* **1983**, *39*, 781-792. A number of oxiranyl quinones of type **ix** have been synthesized and evaluated for bioalkylation activity. Their mode of action is believed to begin with bioreduction to **x** followed by epoxide opening, generating the alkylator **xi**. See below:



- (45) Magdziak, D.; Rodriguez, A. A.; Van De Water, R. W.; Pettus, T. R. R. *Org. Lett.* **2002**, *4*, 285-288.
- (46) (a) The oxidation products of phenols by iodine (III) reagents has been studied computationally, see: Kurti, L.; Hurczegh, P.; Visy, J.; Simonyi, M.; Antus, S.; Pelter,

-
- A. J. Chem. Soc., Perkin Trans. 1: Organic and Bio-Organic Chemistry* **1999**, 4, 379-380. (b) phenolic oxidative dearomatization has been used in the total synthesis of aquaticol: Gagnepain, J.; Castet, F.; Quideau, S. *Angew. Chem., Int. Ed.* **2007**, 46, 1533-1535.
- (47) A calibration curve of ^1H NMR signal integration (ratio to EtOAc internal standard) versus mass for known amounts of pure, chromatographed *o*-quinone was prepared. Filtered product mixture from an actual IBX oxidation was doped with EtOAc, and a sample was analyzed for the integration ratio versus internal standard. The value was used to extrapolate the amount of *o*-quinone present using the calibration curve. For more details, see the experimental section.
- (48) For a discussion about quinoid vinylogous esters and vinylogous anhydride hydrolysis during synthetic investigations on analogues of the natural product asteriquinone, see: Kaji, A.; Saito, R.; Hata, Y.; Kiriya, N. *Chem. Pharm. Bull.* **1999**, 47, 77-82.
- (49) We have reported our synthesis: McFadden, R. M.; Stoltz, B. M. *J. Am. Chem. Soc.* **2006**, 128, 7738-7739.
- (50) Banerjee reported the conversion of (\pm)-dichroanone (**150**) to (\pm)-taiwaniaquinol-H (**165**) in the presence of K_2CO_3 and iodomethane in a 2:1 acetone/methanol solvent mixture. See reference 6 for details.
- (51) Frigerio, M.; Santagostino, M.; Sputore, S. *J. Org. Chem.* **1999**, 64, 4537-4538.
- (52) (a) Peer, M.; de Jong, J. C.; Kiefer, M.; Langer, T.; Riech, H.; Schell, H.; Sennhenn, P.; Sprinz, J.; Steinhagen, H.; Wiese, B.; Helmchen, G. *Tetrahedron* **1996**, 52, 7547-7583. (b) Behenna, D. C.; Stoltz, B. M. *J. Am. Chem. Soc.* **2004**, 126, 15044-15045.

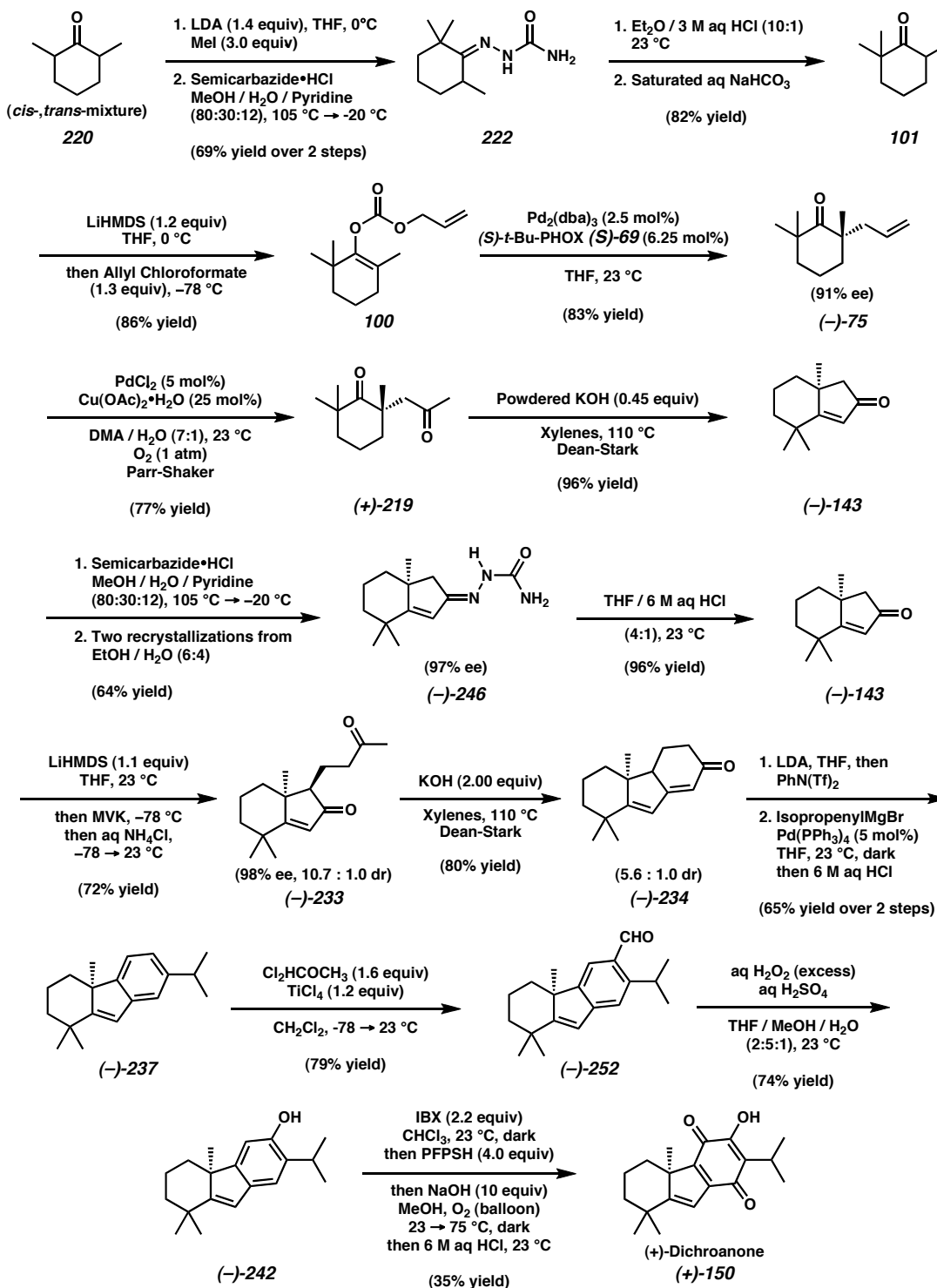
(c) Tani, K.; Behenna, D. C.; McFadden, R. M.; Stoltz, B. M. *Org. Lett.* **2007**, *9*, 2529-2931.

(53) When a subscript is shown with the coupling constant, it indicates what type of splitting the constant is associated with. For example, (td, $J_t = 5.0$ Hz, $J_d = 3.3$ Hz, 1H) indicates that the triplet splitting has a 5.0 Hz coupling constant and the doublet has a 3.3 Hz coupling constant.

Appendix THREE

Synthetic Summary of the Enantioselective Total Synthesis of (+)-Dichroanone

Scheme A3.1 Enantioselective Total Synthesis of (+)-Dichroanone



Appendix FOUR

Spectra of Compounds Relevant to Chapter 3

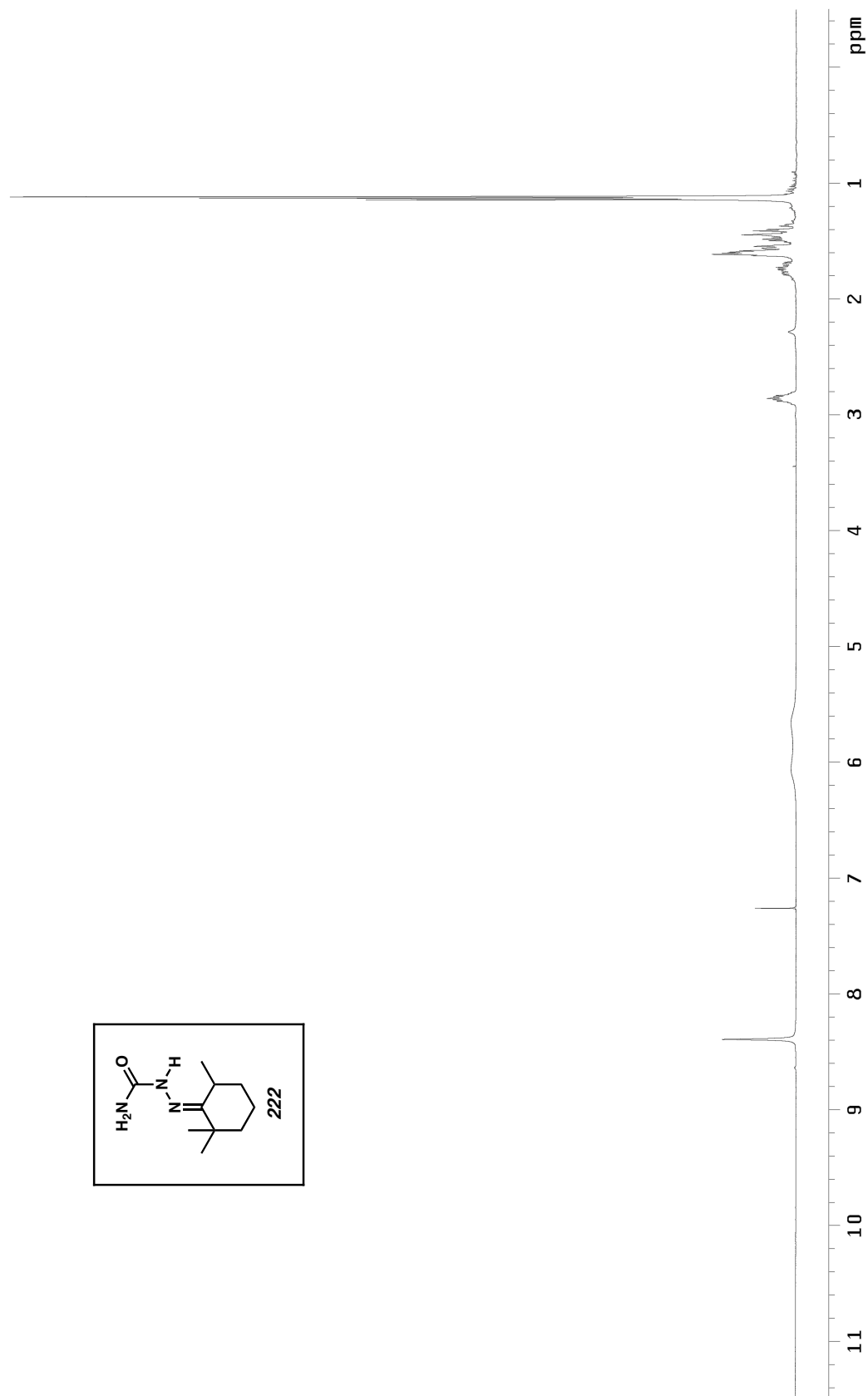


Figure A4.1 ^1H NMR (300 MHz, CDCl_3) of compound **222**.

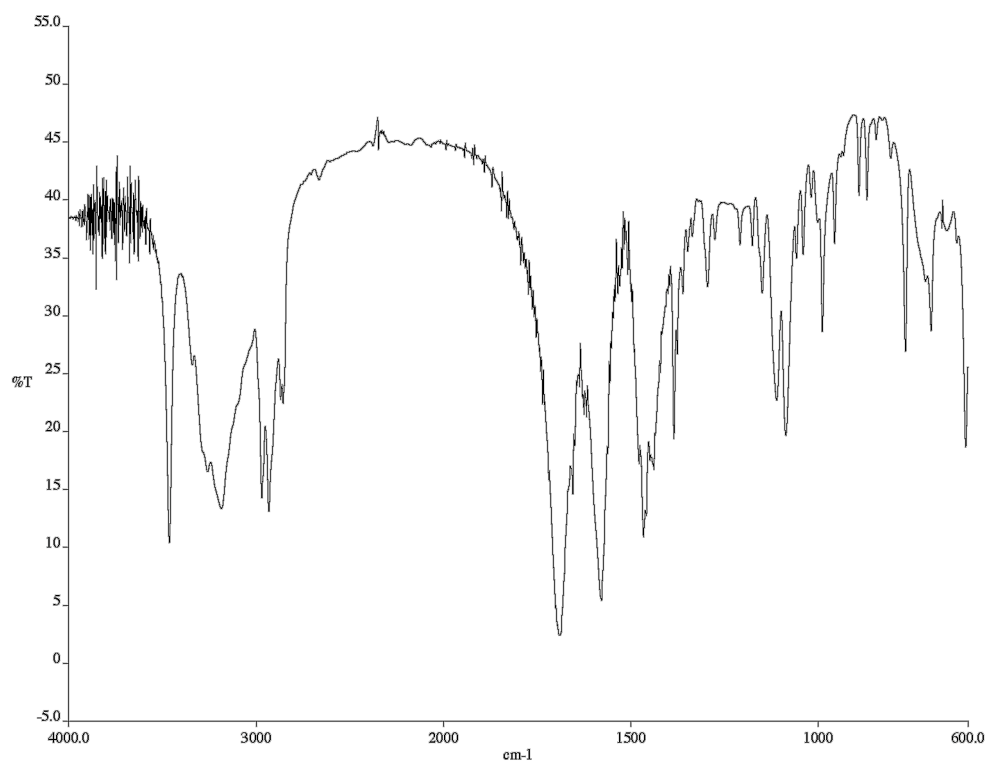


Figure A4.2 Infrared spectrum (KBr) of compound **222**.

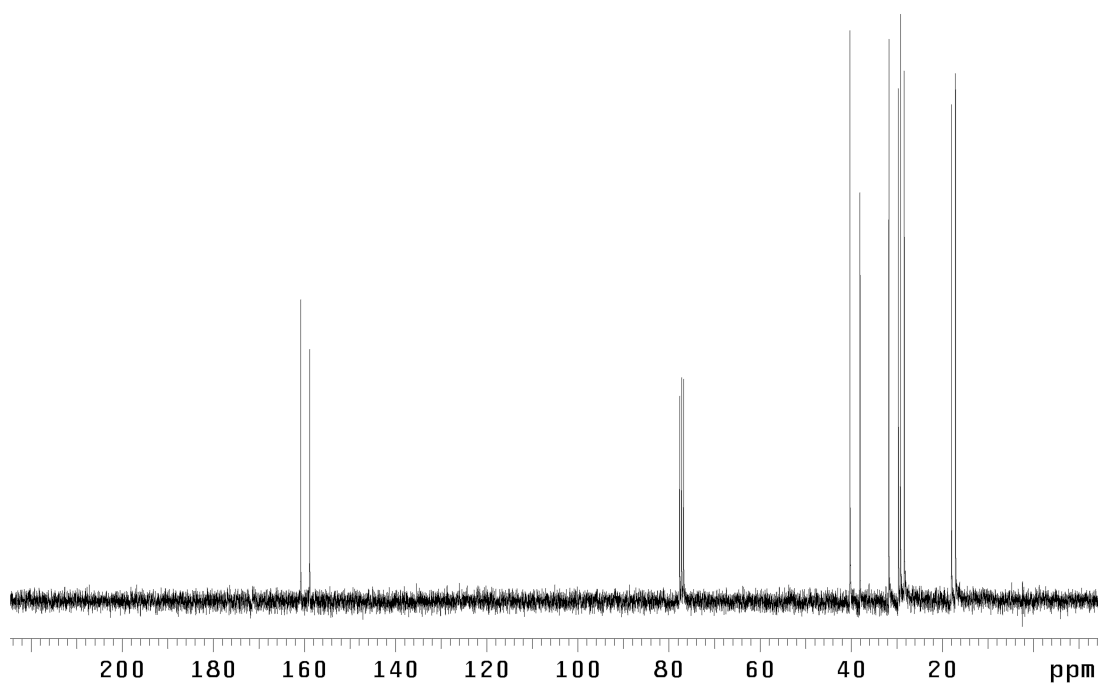


Figure A4.3 ¹³C NMR (75 MHz, CDCl₃) of compound **222**.

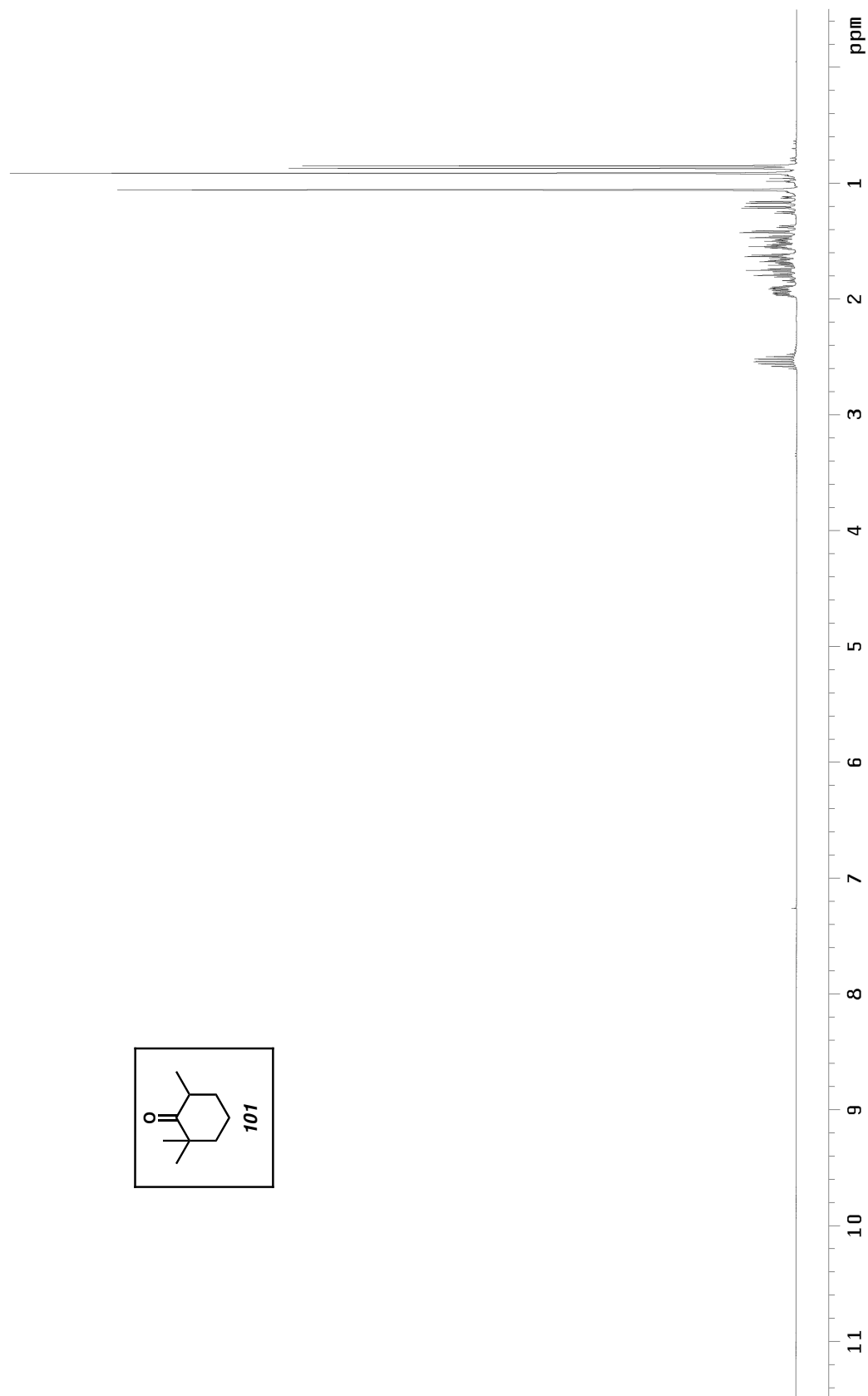


Figure A4.4 ^1H NMR (300 MHz, CDCl_3) of compound **101**.

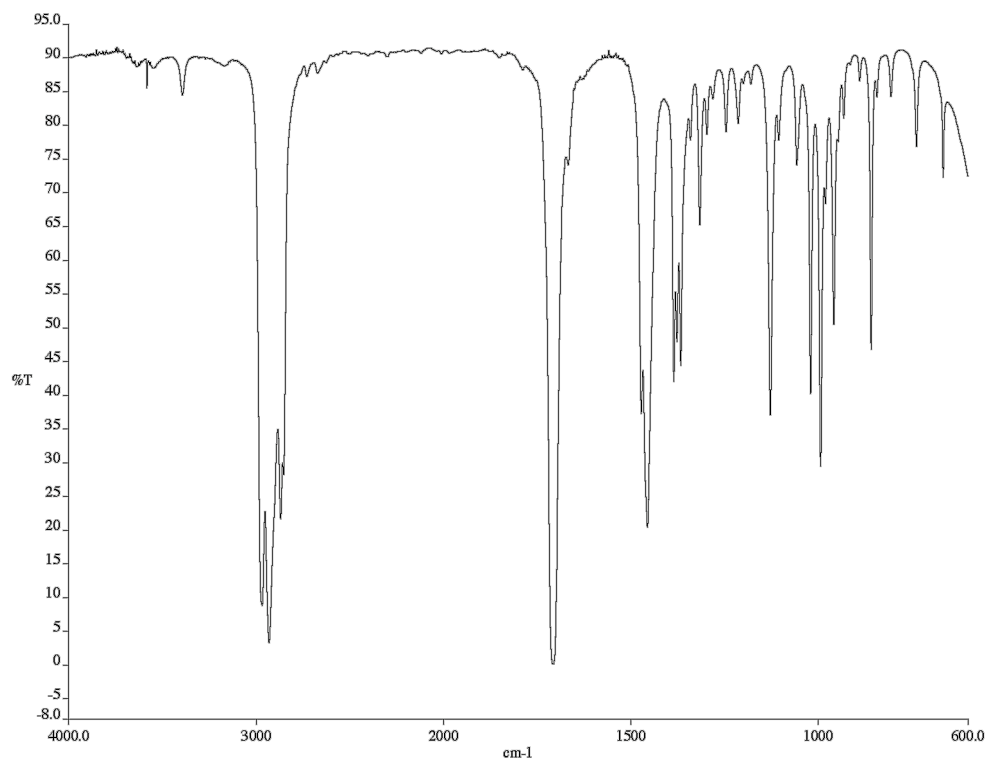


Figure A4.5 Infrared spectrum (NaCl/CDCl₃) of compound **101**.

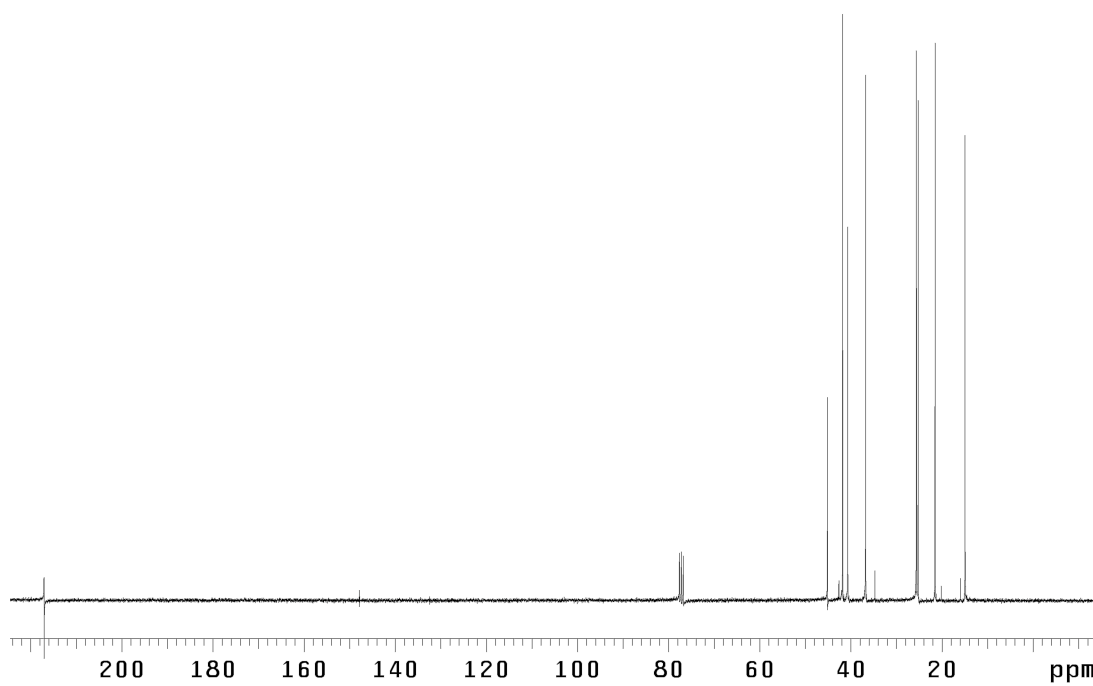


Figure A4.6 ¹³C NMR (75 MHz, CDCl₃) of compound **101**.

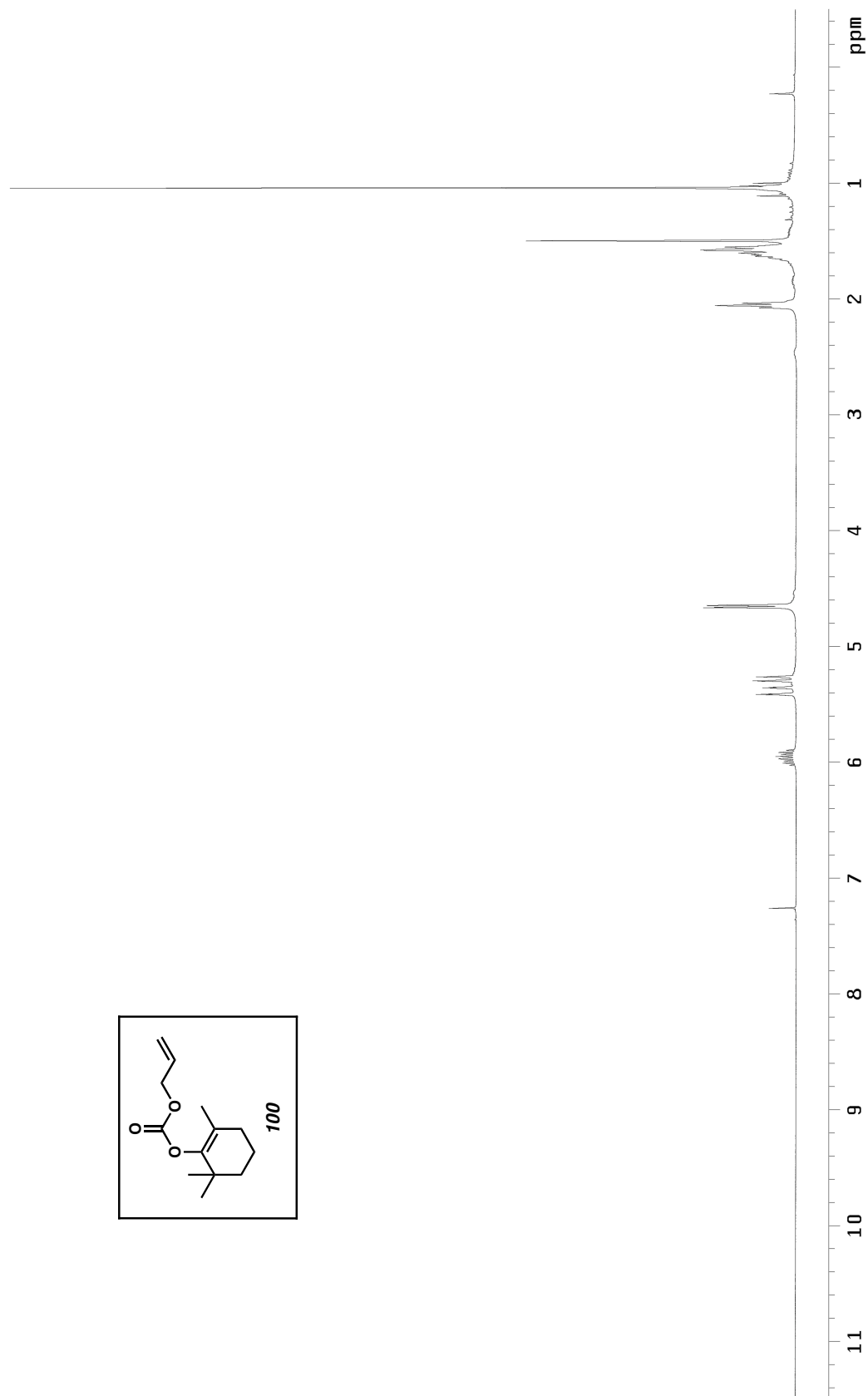


Figure A4.7 ^1H NMR (300 MHz, CDCl_3) of compound **100**.

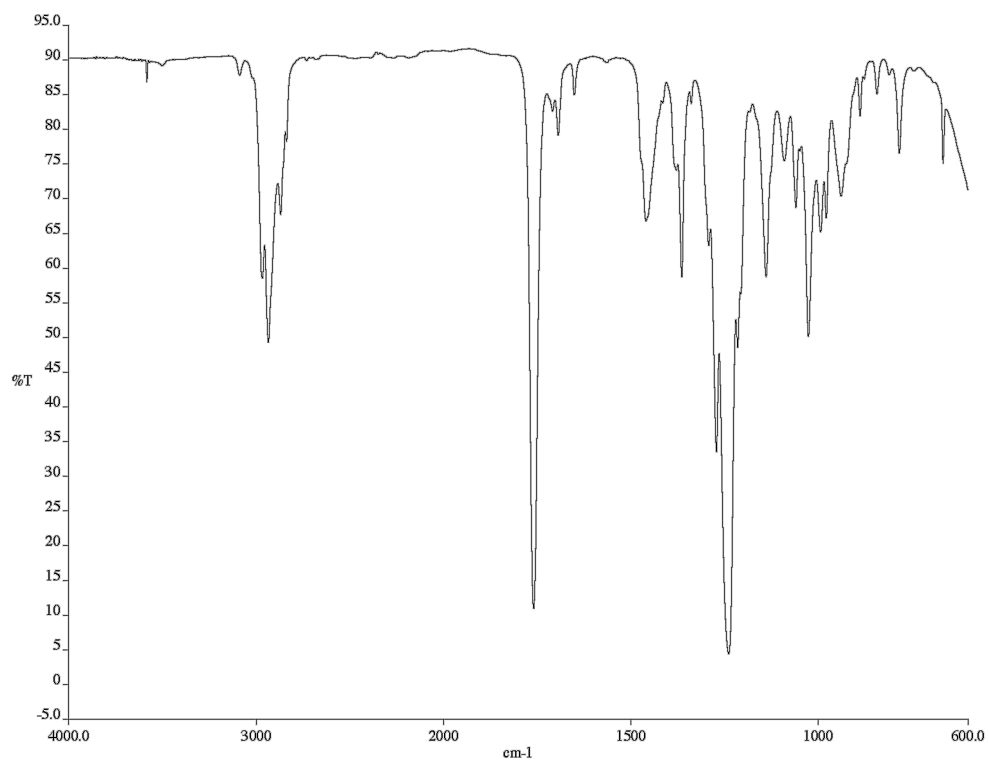


Figure A4.8 Infrared spectrum (NaCl/CDCl₃) of compound **100**.

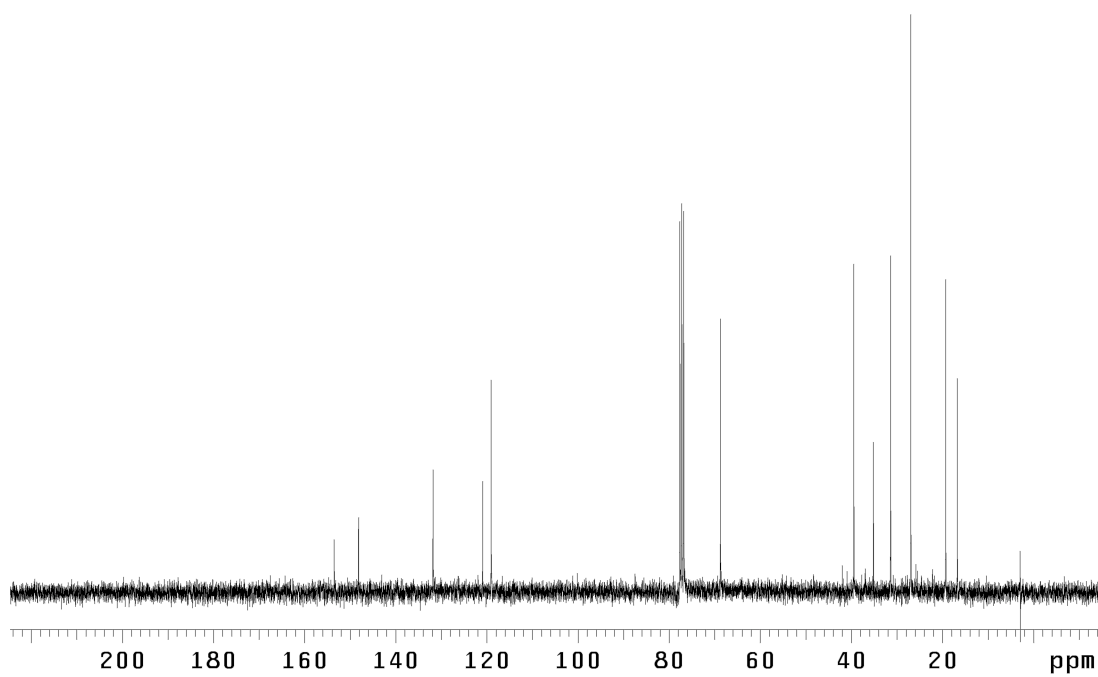


Figure A4.9 ¹³C NMR (75 MHz, CDCl₃) of compound **100**.

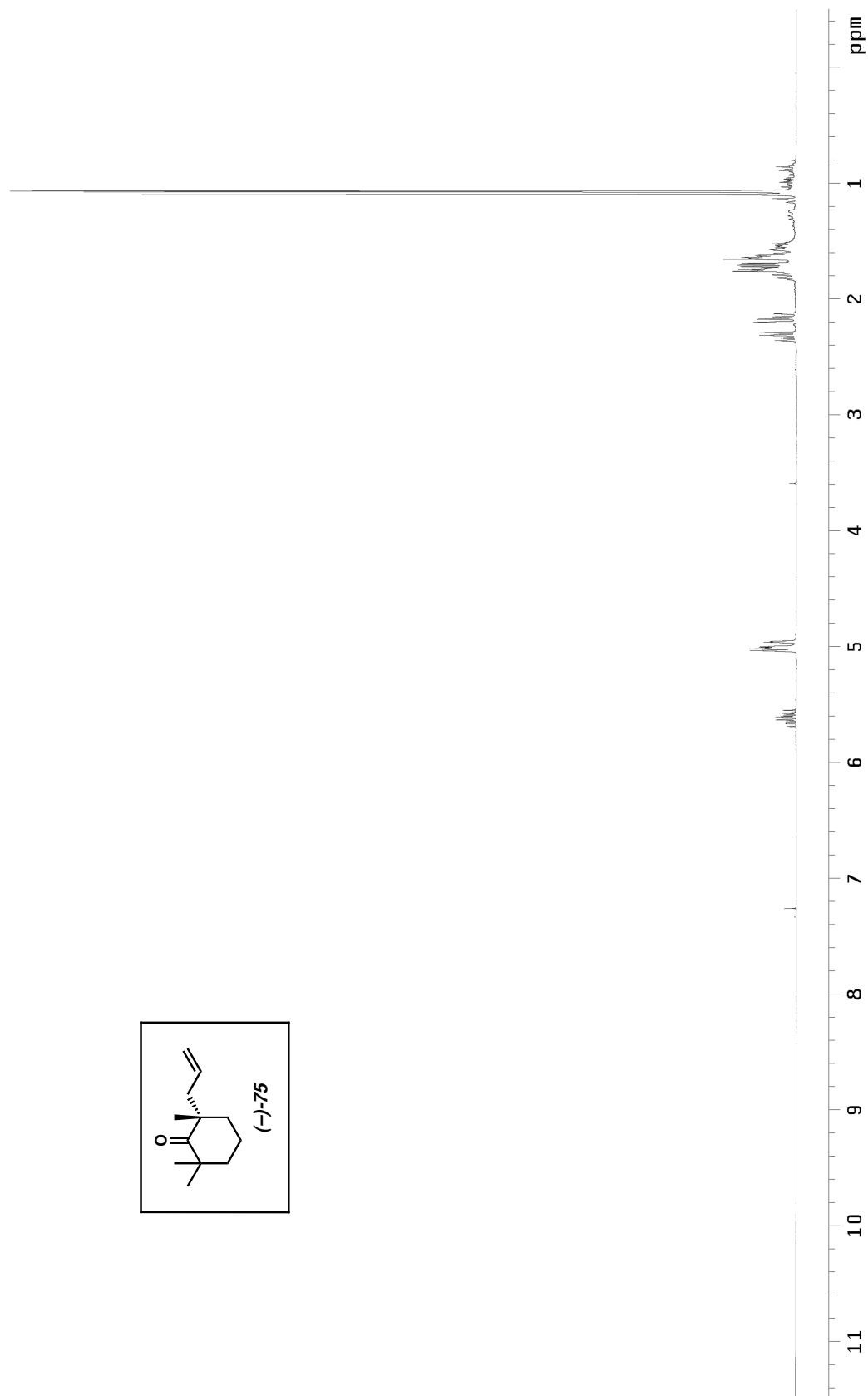


Figure A4.10 ¹H NMR (300 MHz, CDCl₃) of compound **75**.

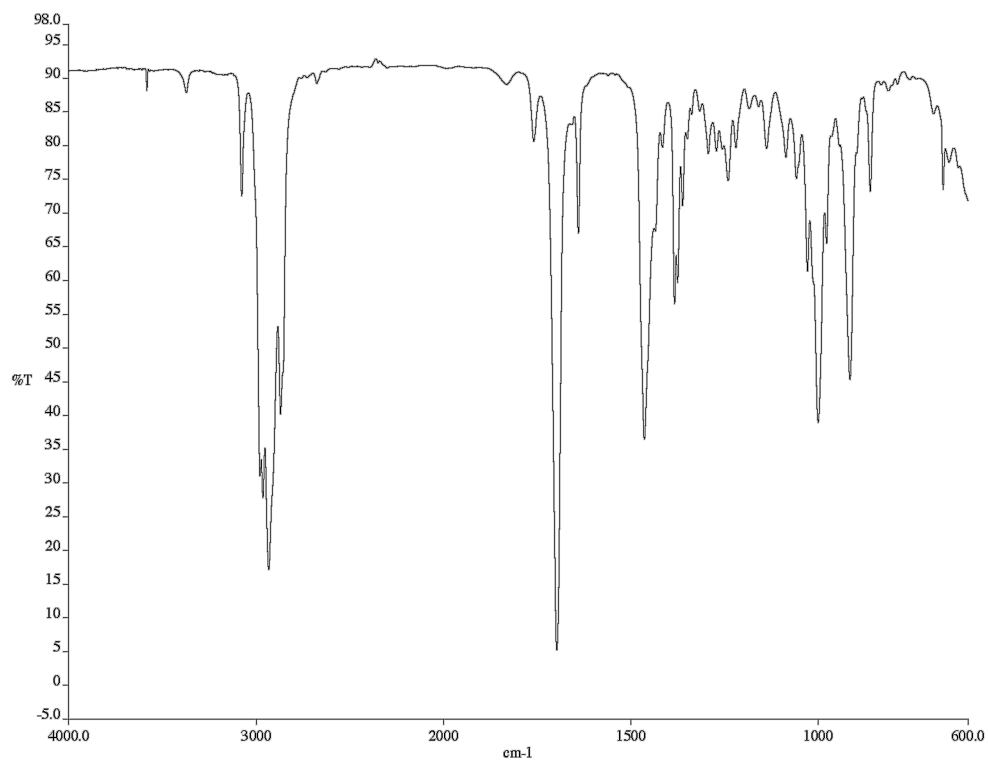


Figure A4.11 Infrared spectrum (NaCl/CDCl₃) of compound **75**.

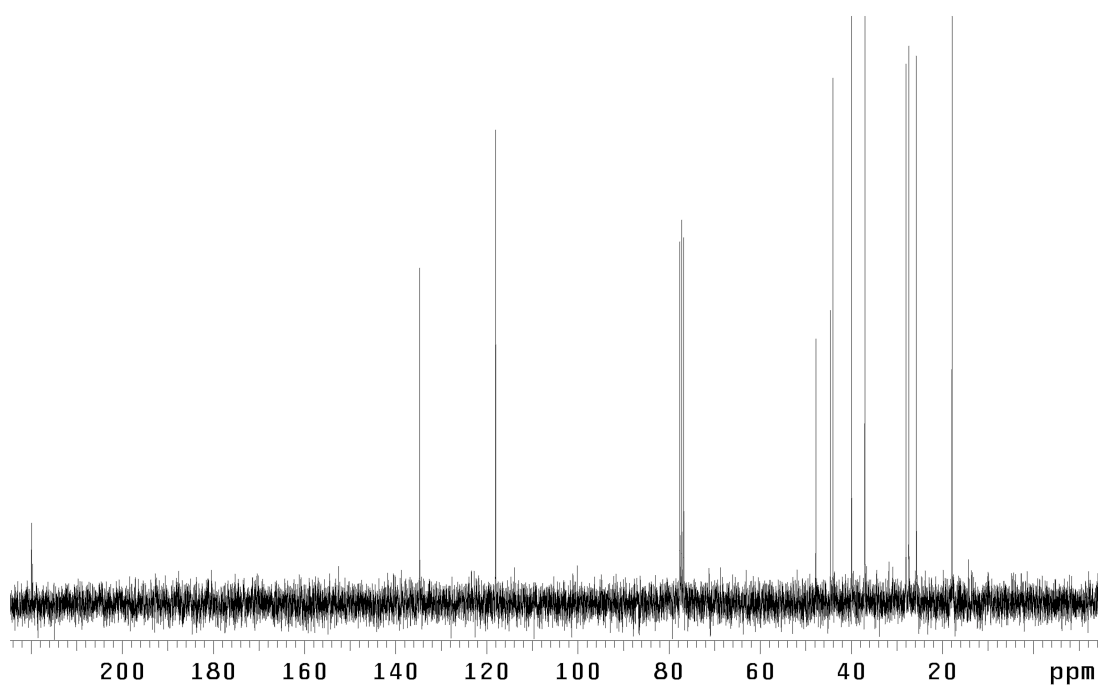


Figure A4.12 ¹³C NMR (75 MHz, CDCl₃) of compound **75**.

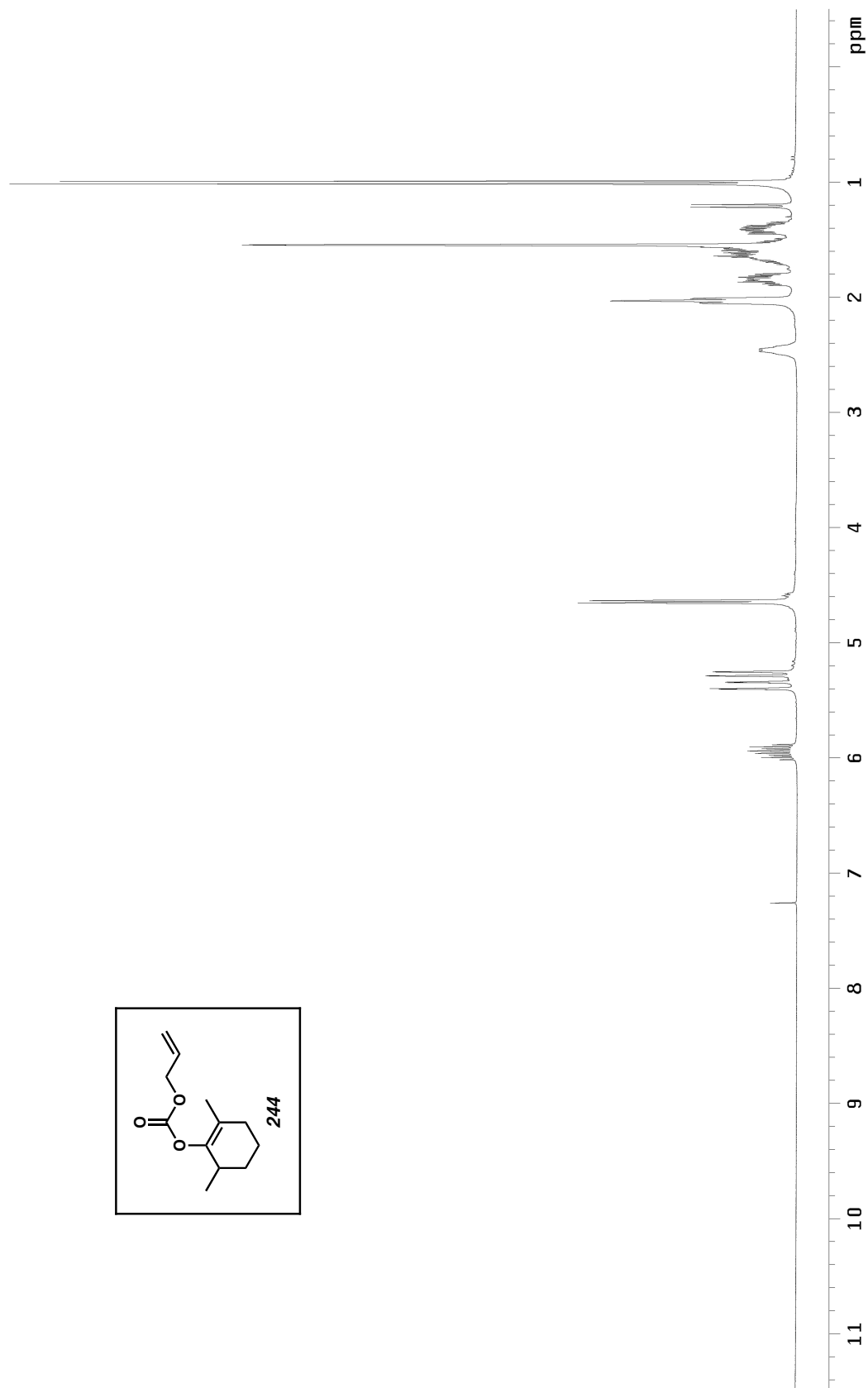


Figure A4.13 ^1H NMR (300 MHz, CDCl_3) of compound 244.

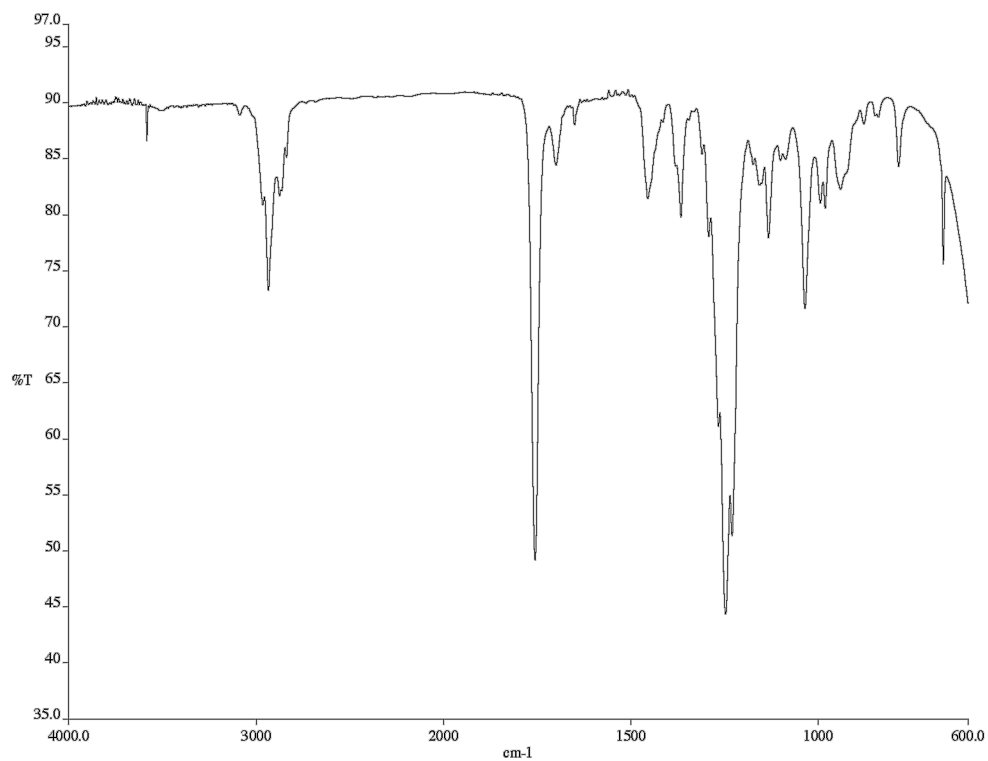


Figure A4.14 Infrared spectrum ($\text{NaCl}/\text{CDCl}_3$) of compound **244**.

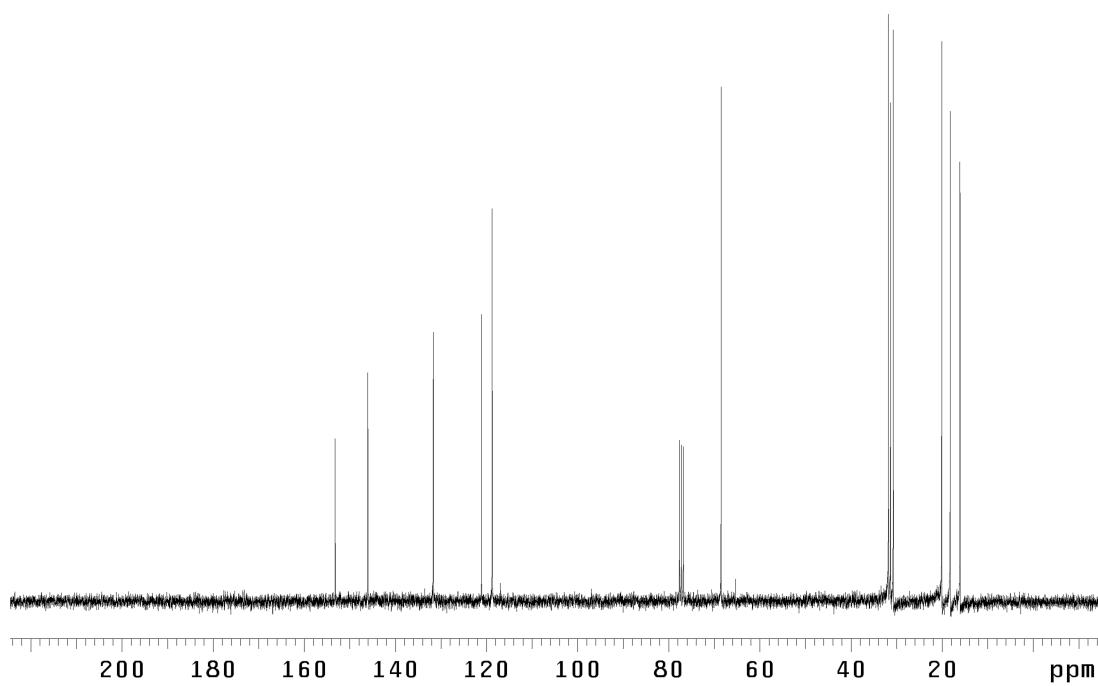


Figure A4.15 ^{13}C NMR (75 MHz, CDCl_3) of compound **244**.

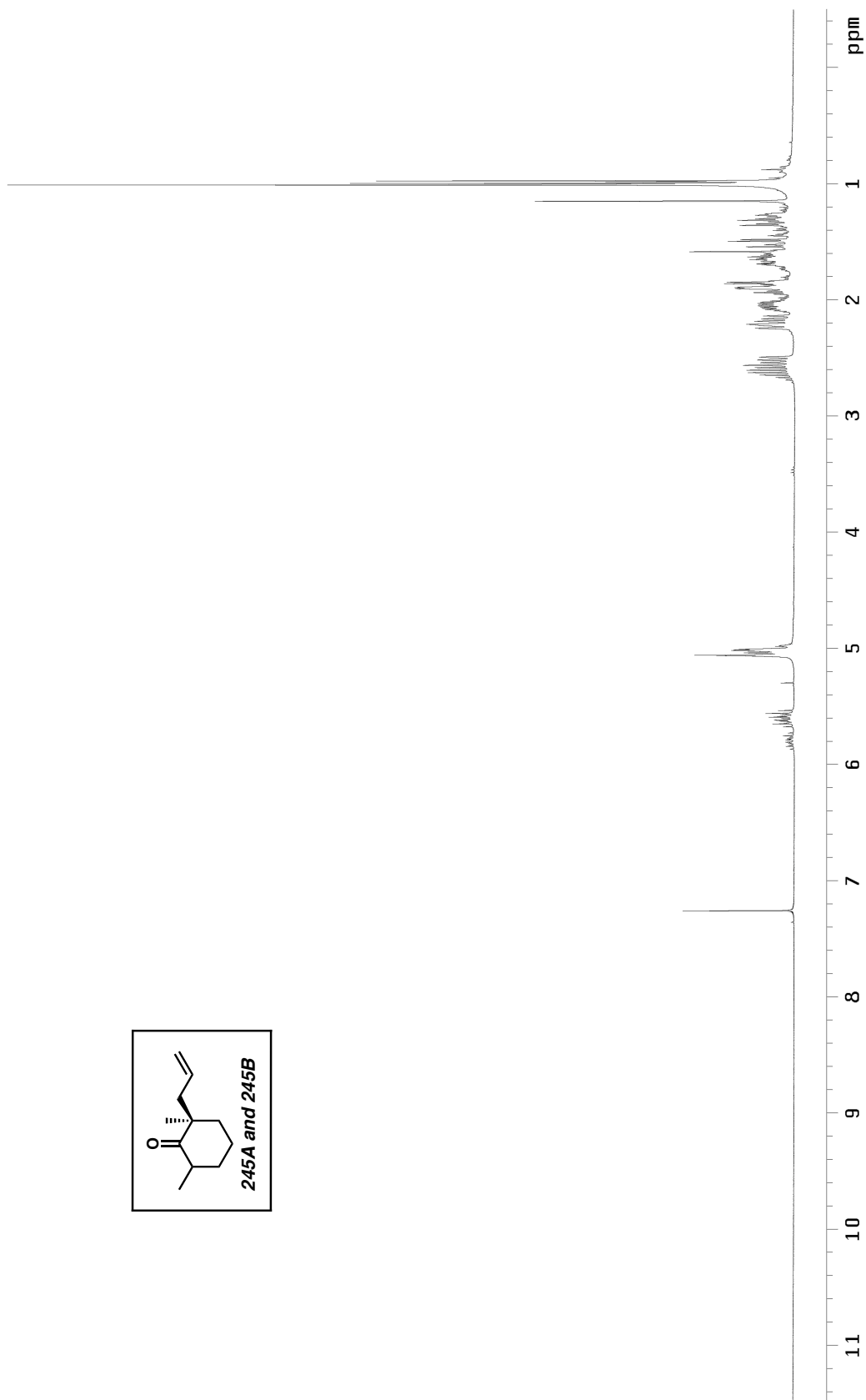
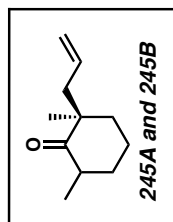


Figure A4.16 ^1H NMR (300 MHz, CDCl_3) of compound **245A** and **245B**.

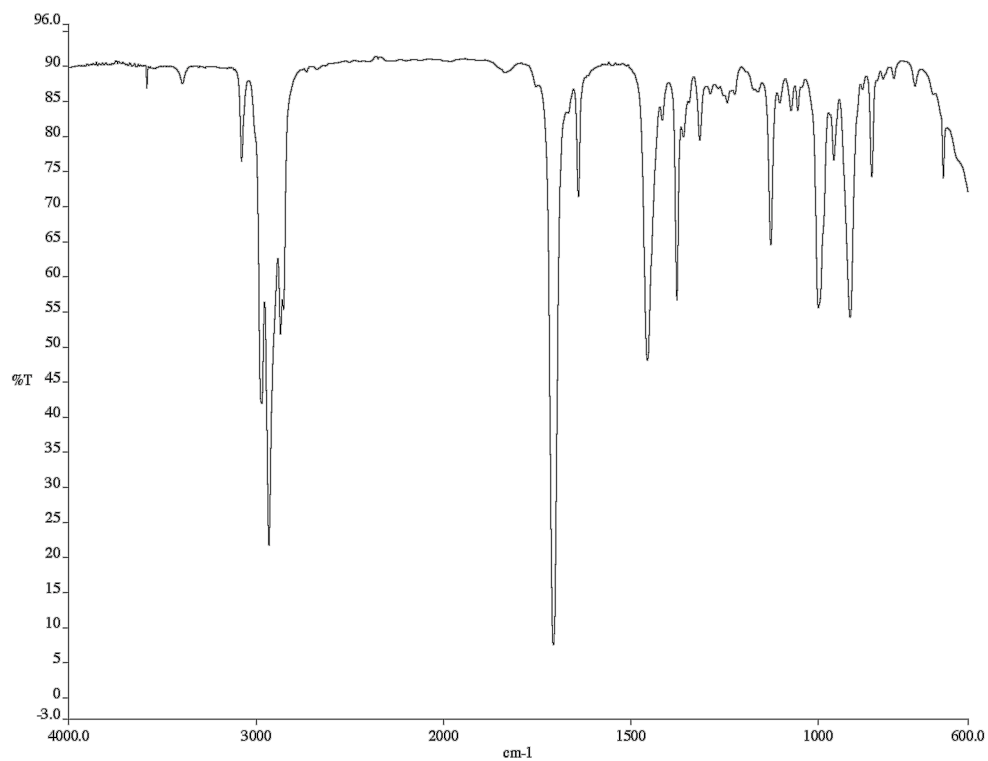


Figure A4.17 Infrared spectrum (NaCl/CDCl₃) of compound **245A** and **245B**.

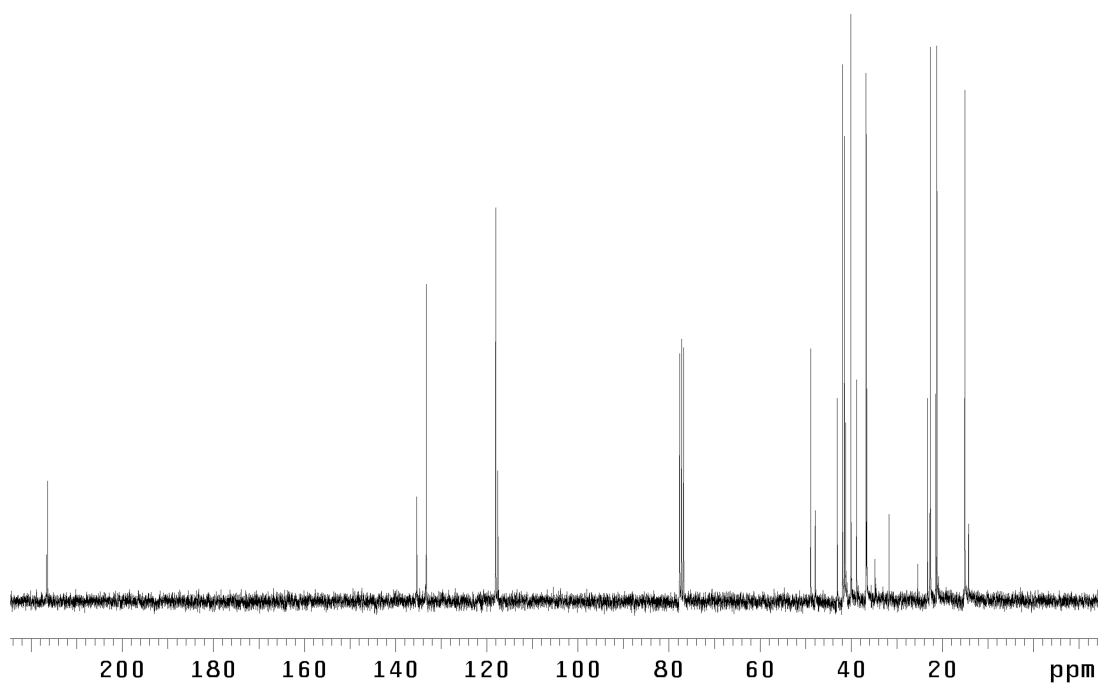


Figure A4.18 ¹³C NMR (75 MHz, CDCl₃) of compound **245A** and **245B**.



Figure A4.19 ^1H NMR (300 MHz, CDCl_3) of compound **219**.

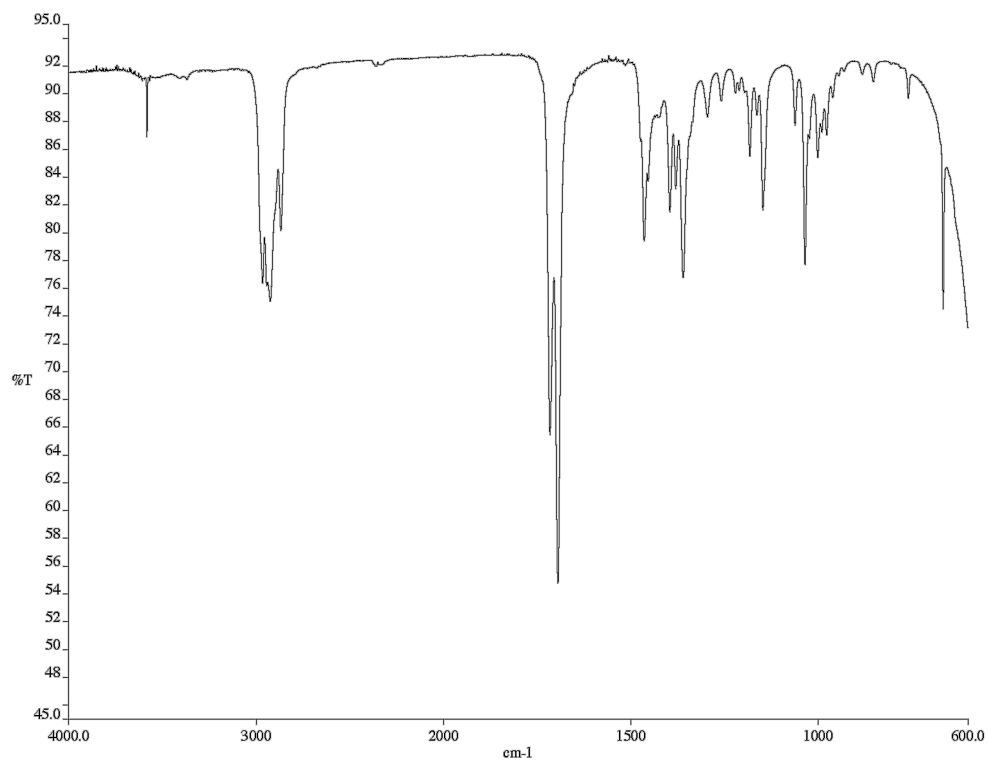


Figure A4.20 Infrared spectrum ($\text{NaCl}/\text{CDCl}_3$) of compound **219**.

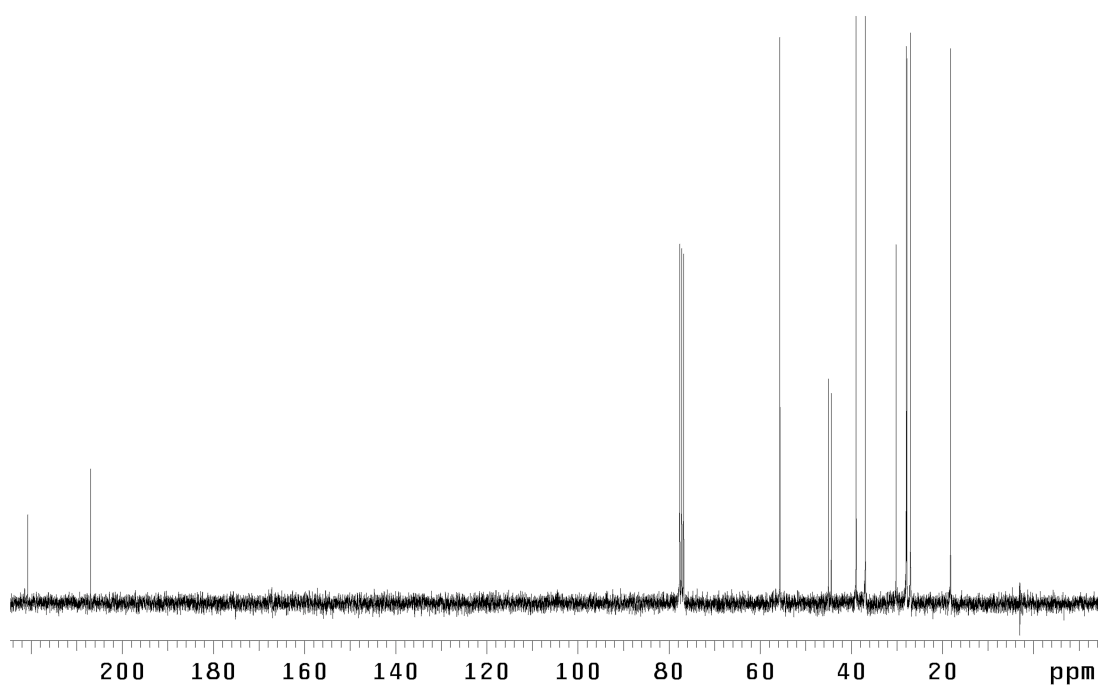


Figure A4.21 ^{13}C NMR (75 MHz, CDCl_3) of compound **219**.

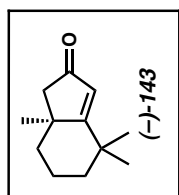
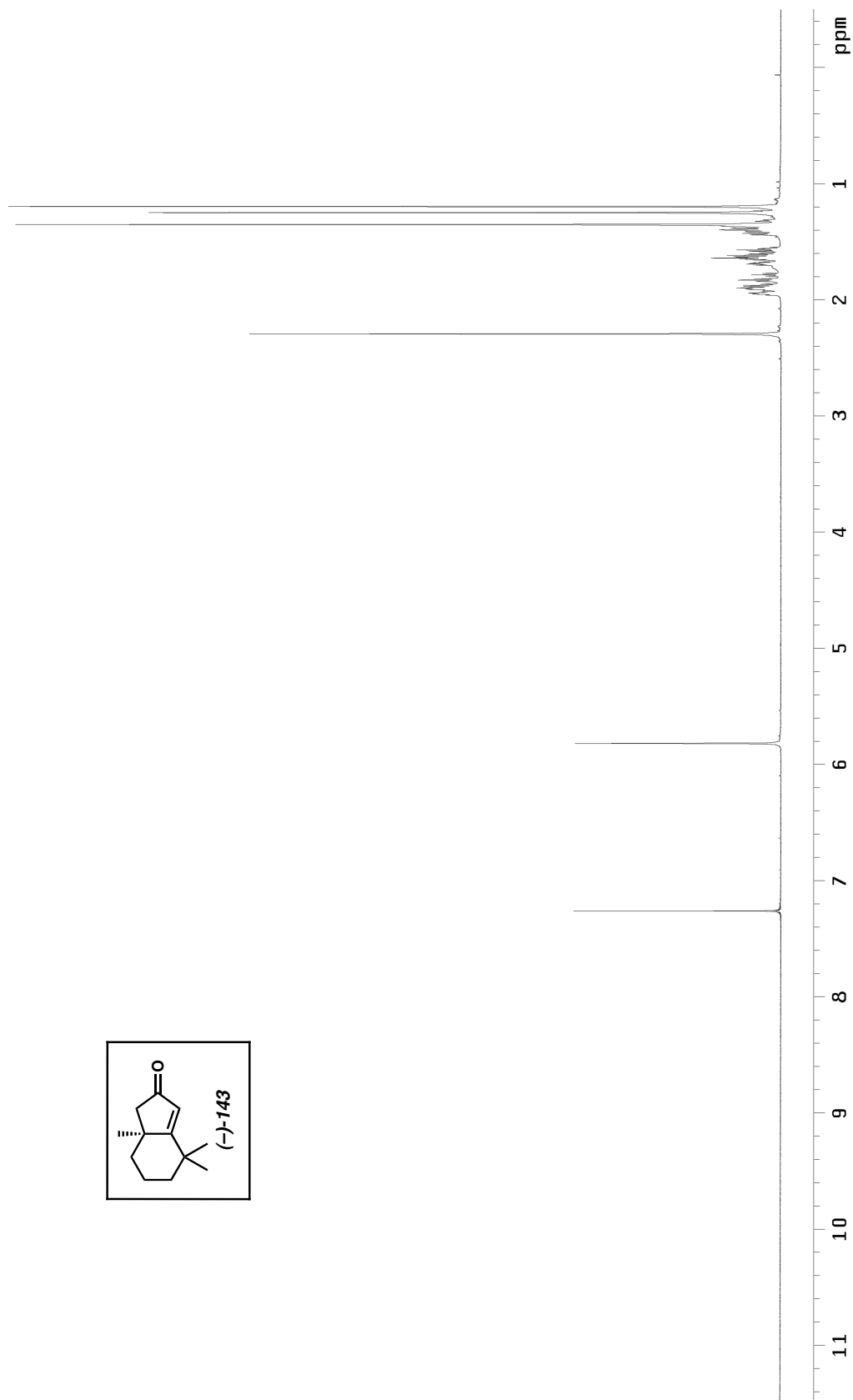


Figure A4.22 ^1H NMR (300 MHz, CDCl_3) of compound **143**.

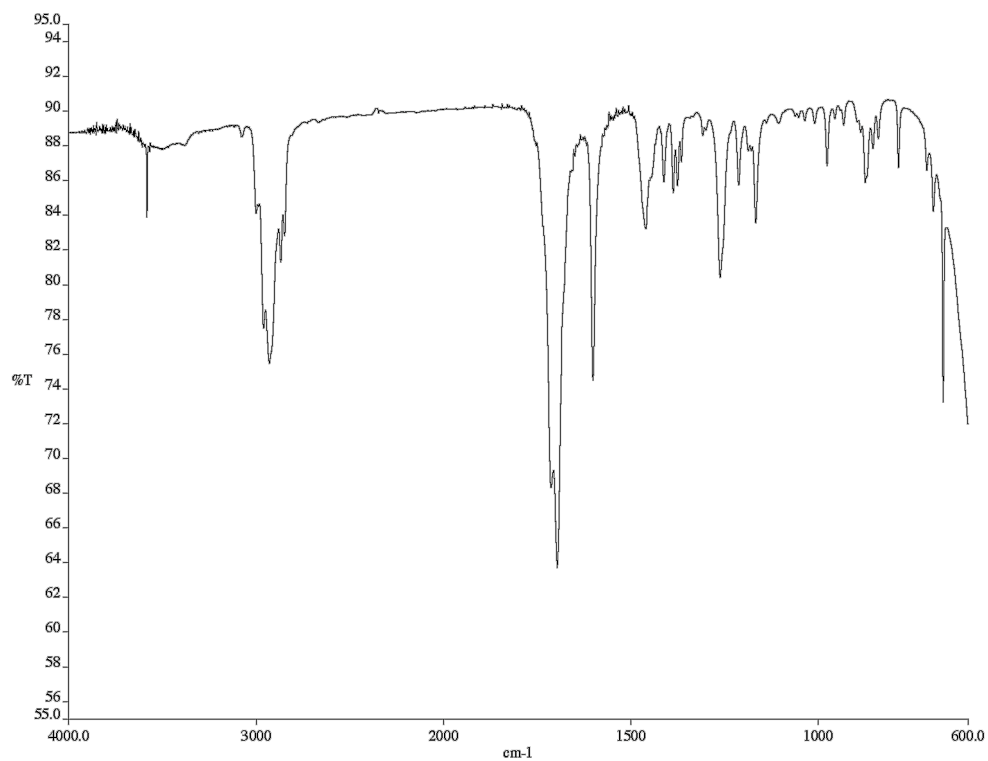


Figure A4.23 Infrared spectrum (NaCl/CDCl₃) of compound **143**.

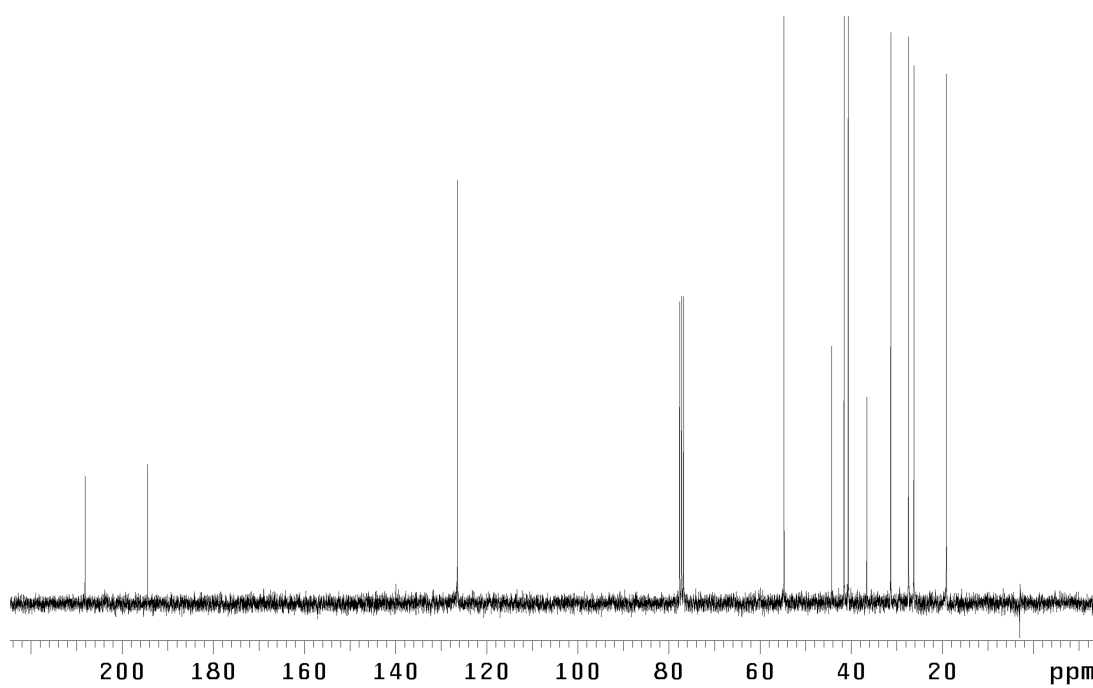


Figure A4.24 ¹³C NMR (75 MHz, CDCl₃) of compound **143**.

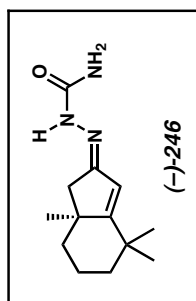
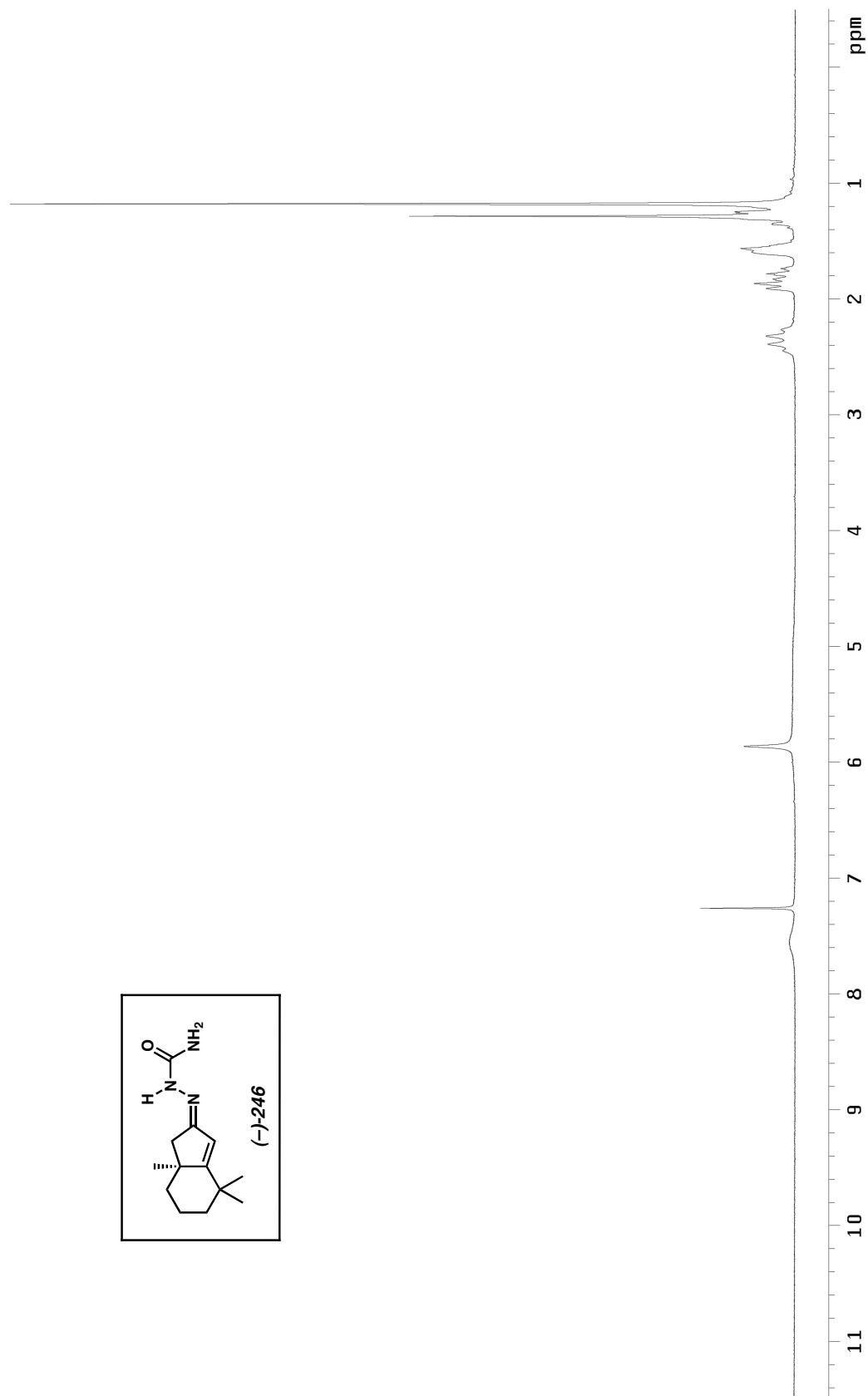


Figure A4.25 ^1H NMR (300 MHz, CDCl_3) of compound **246**.

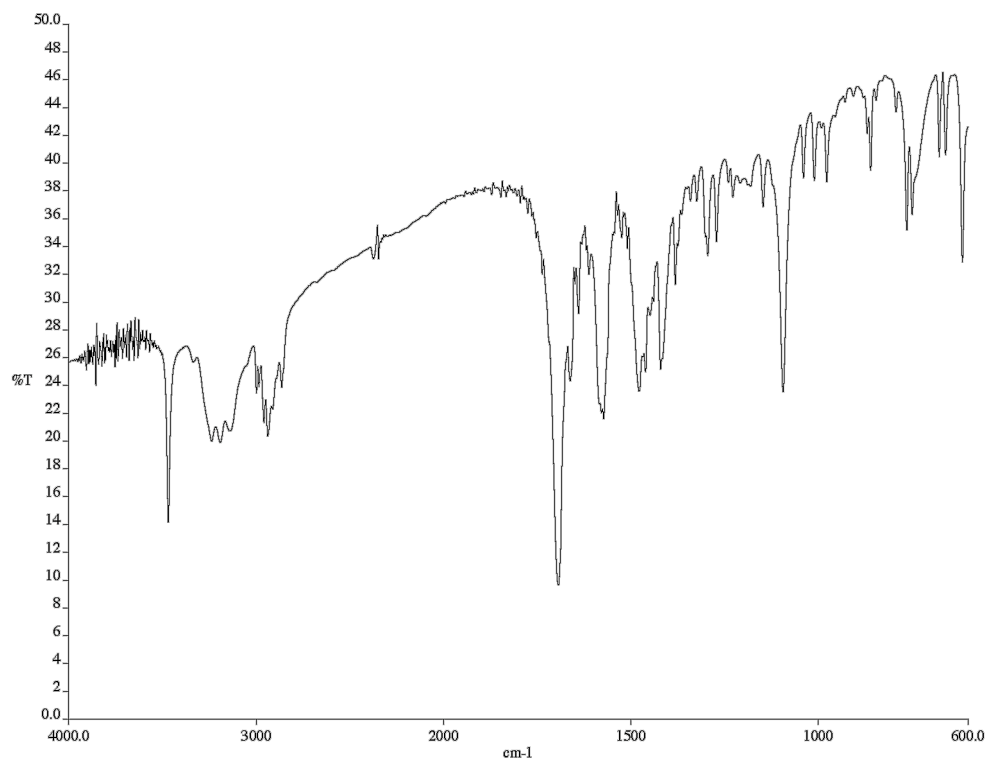


Figure A4.26 Infrared spectrum (KBr) of compound **246**.

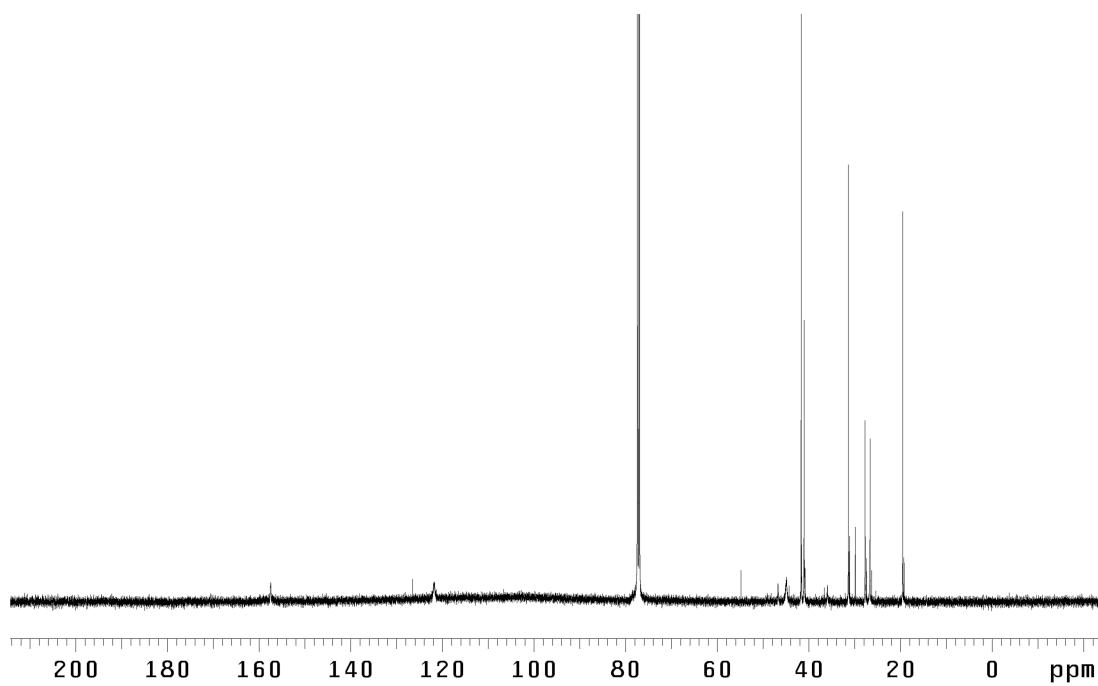


Figure A4.27 ¹³C NMR (125 MHz, CDCl₃) of compound **246**.

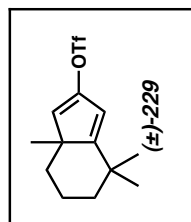
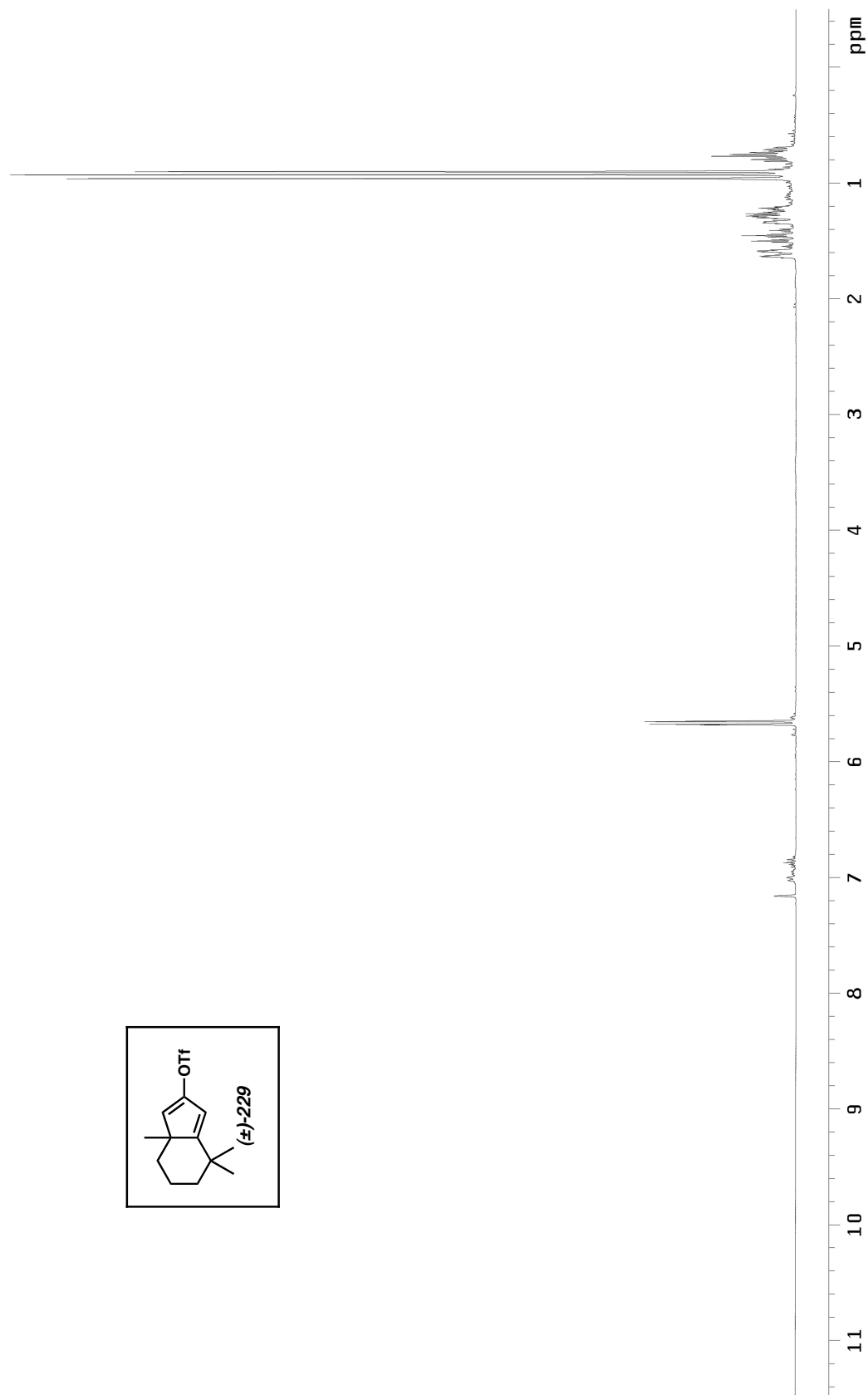


Figure A4.28 ^1H NMR (300 MHz, C_6D_6) of compound **229**.

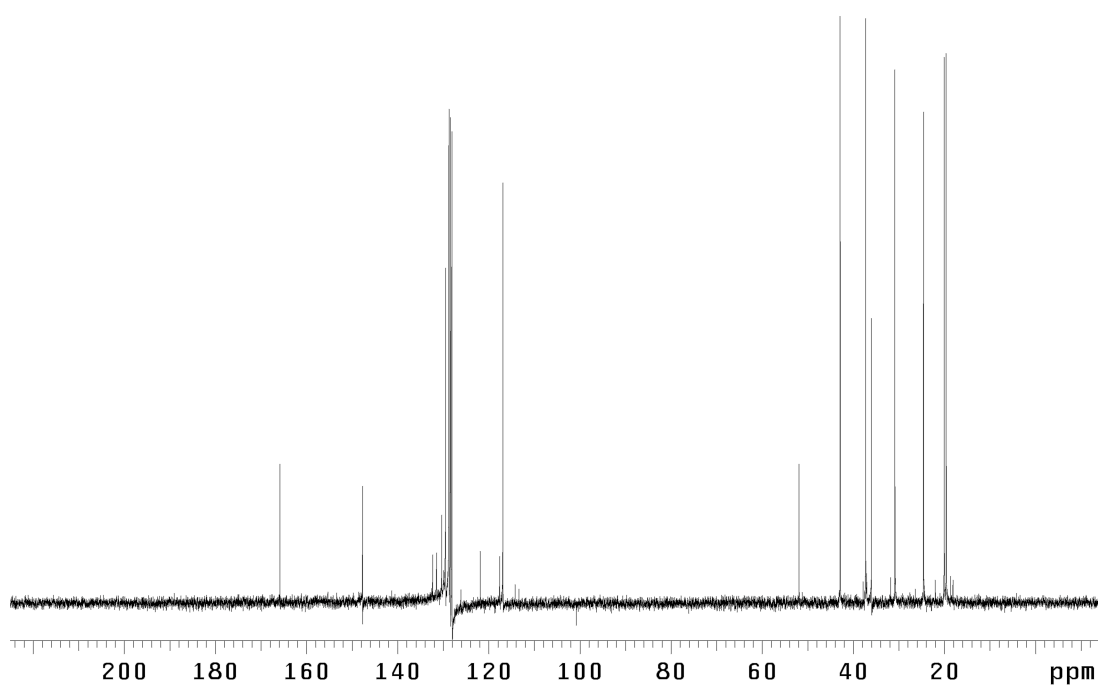


Figure A4.29 ^{13}C NMR (75 MHz, C_6D_6) of compound **229**.

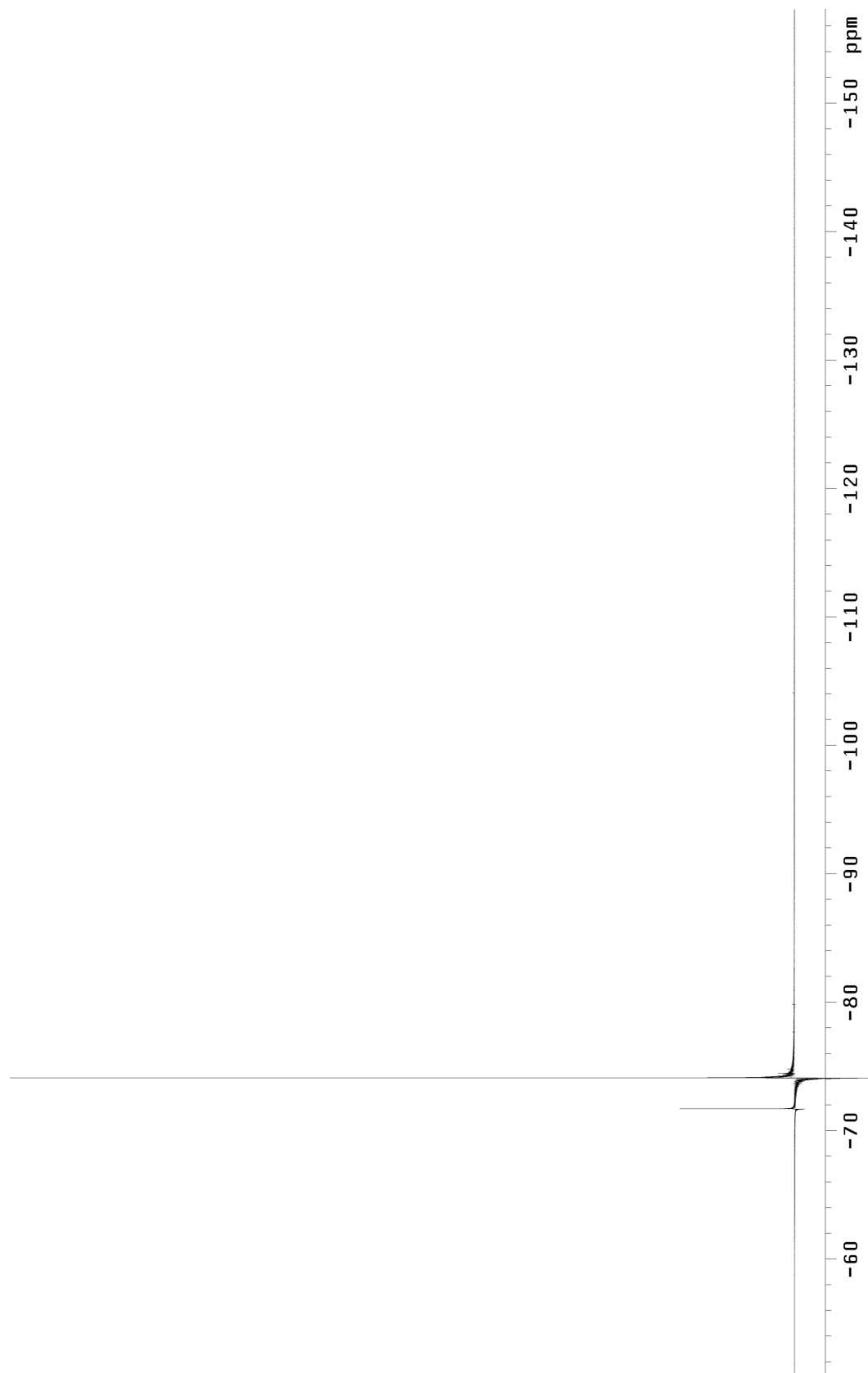


Figure A4.30 ^{19}F NMR (282 MHz, C_6D_6) of compound **229**.

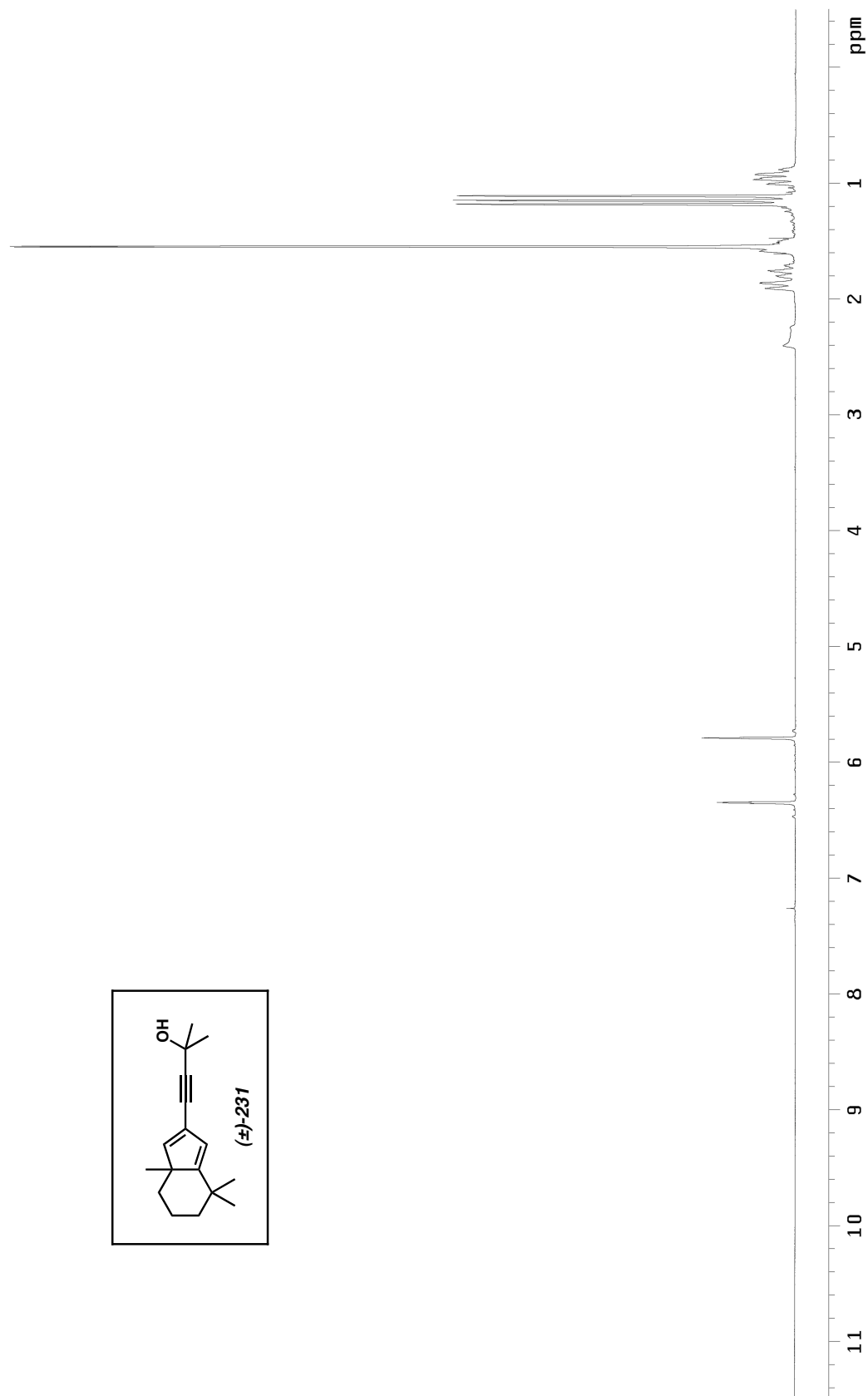


Figure A4.31 ^1H NMR (300 MHz, CDCl_3) of compound **231**.

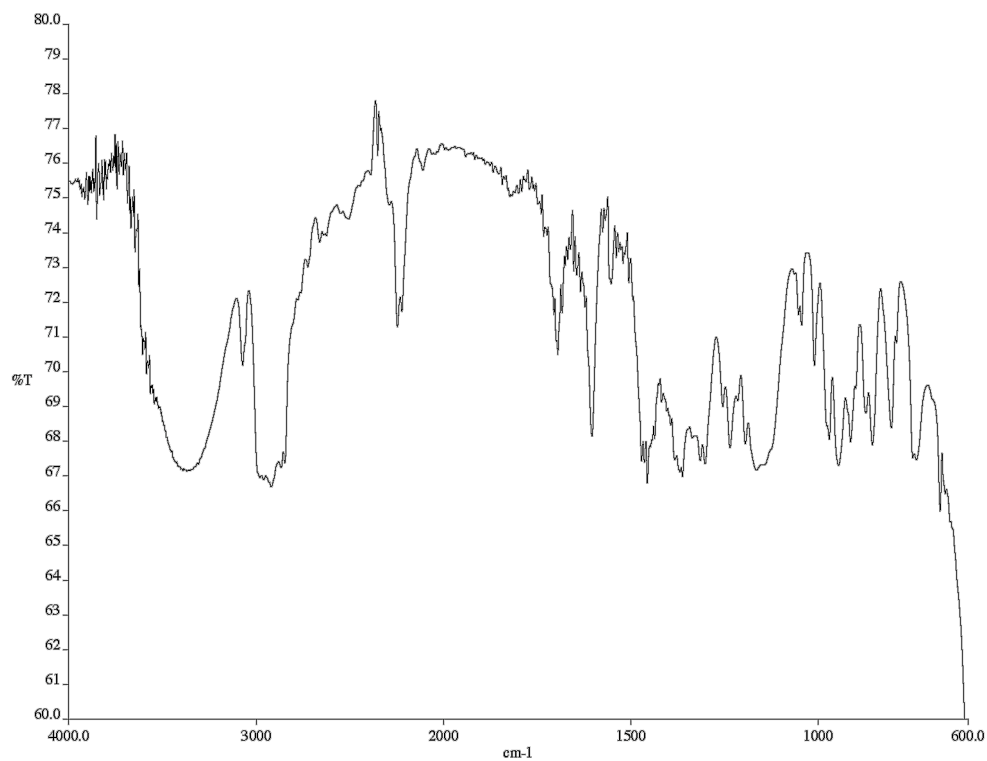


Figure A4.32 Infrared spectrum (NaCl/CDCl₃) of compound **231**.

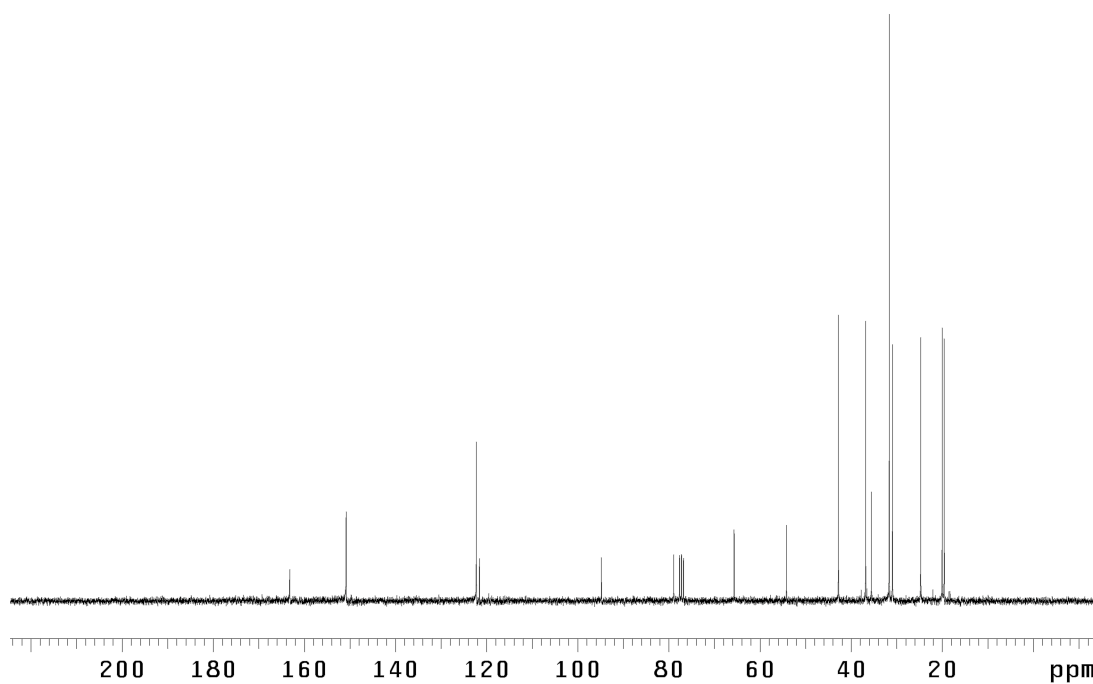


Figure A4.33 ¹³C NMR (75 MHz, CDCl₃) of compound **231**.

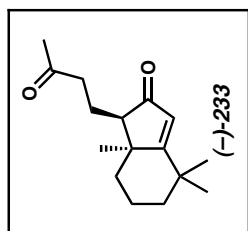
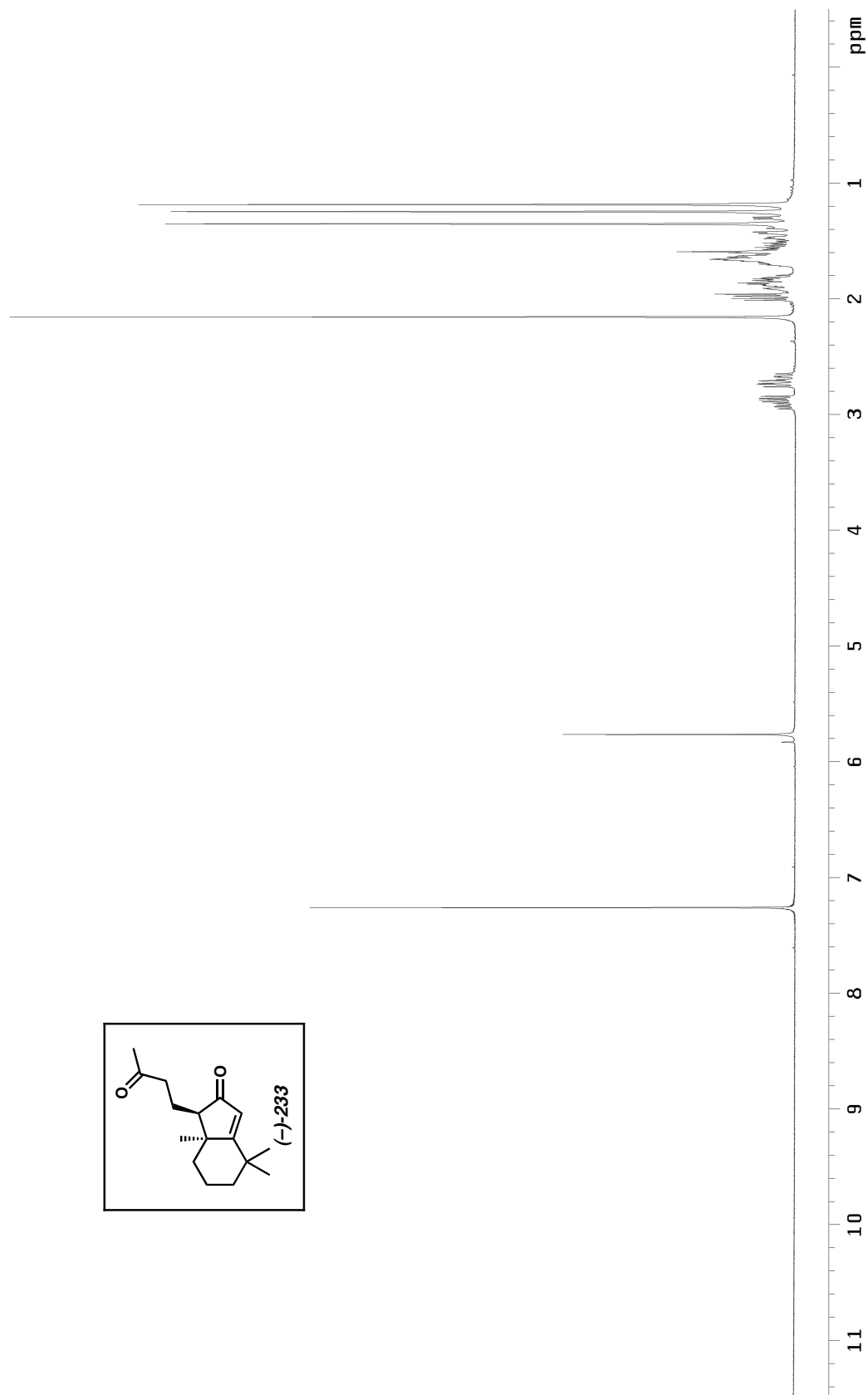


Figure A4.34 ^1H NMR (300 MHz, CDCl_3) of compound **233**.

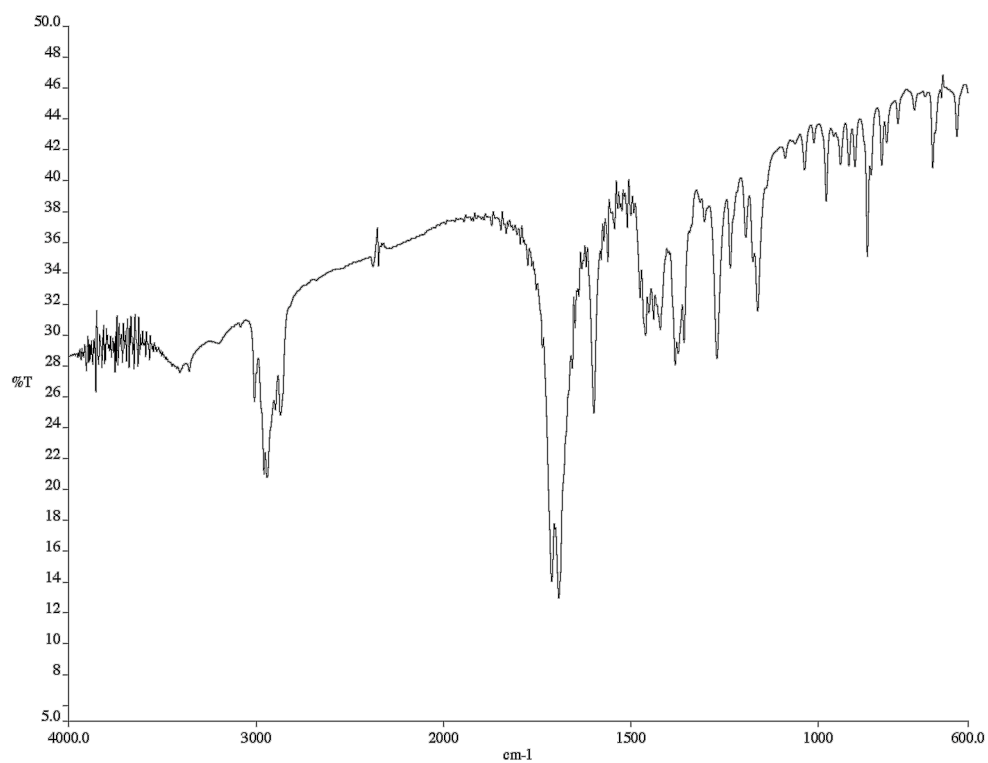


Figure A4.35 Infrared spectrum (KBr) of compound **233**.

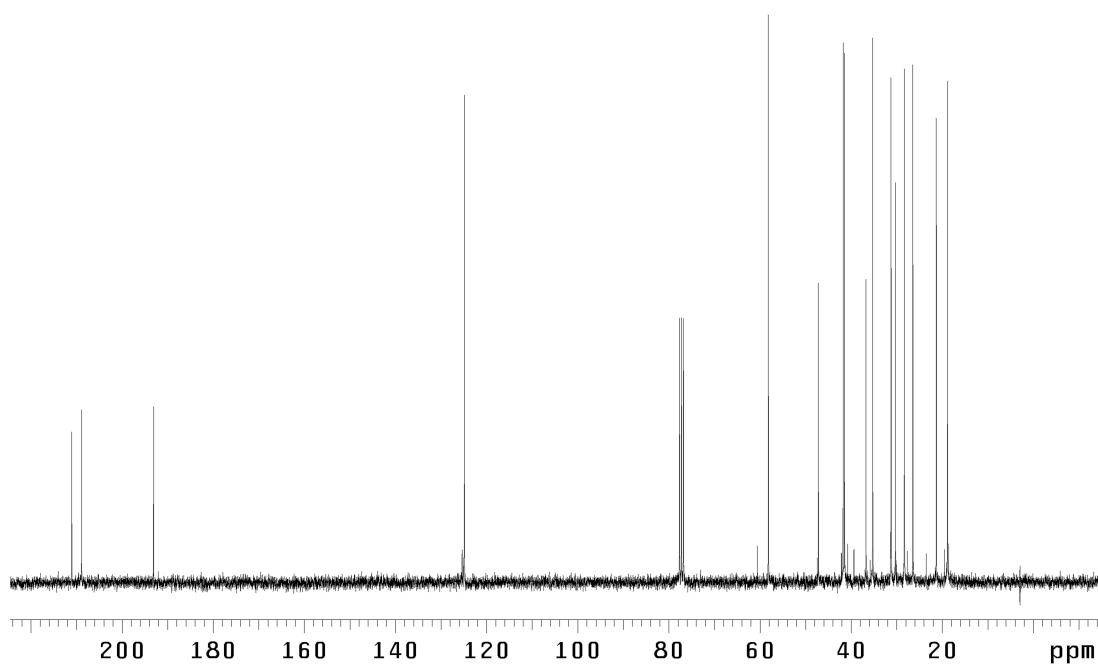


Figure A4.36 ¹³C NMR (75 MHz, CDCl₃) of compound **233**.

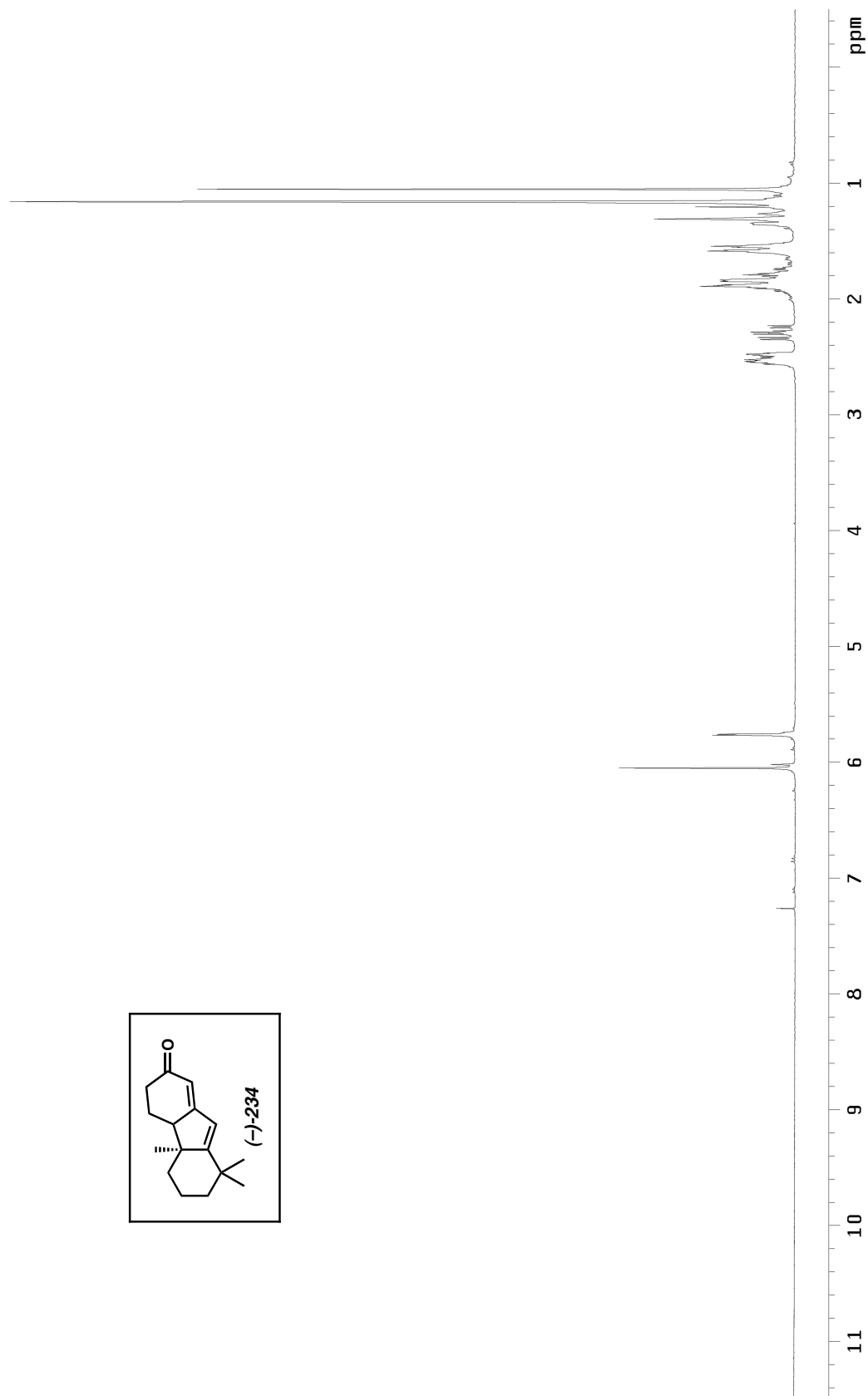


Figure A4.37 ^1H NMR (300 MHz, CDCl_3) of compound **234**.

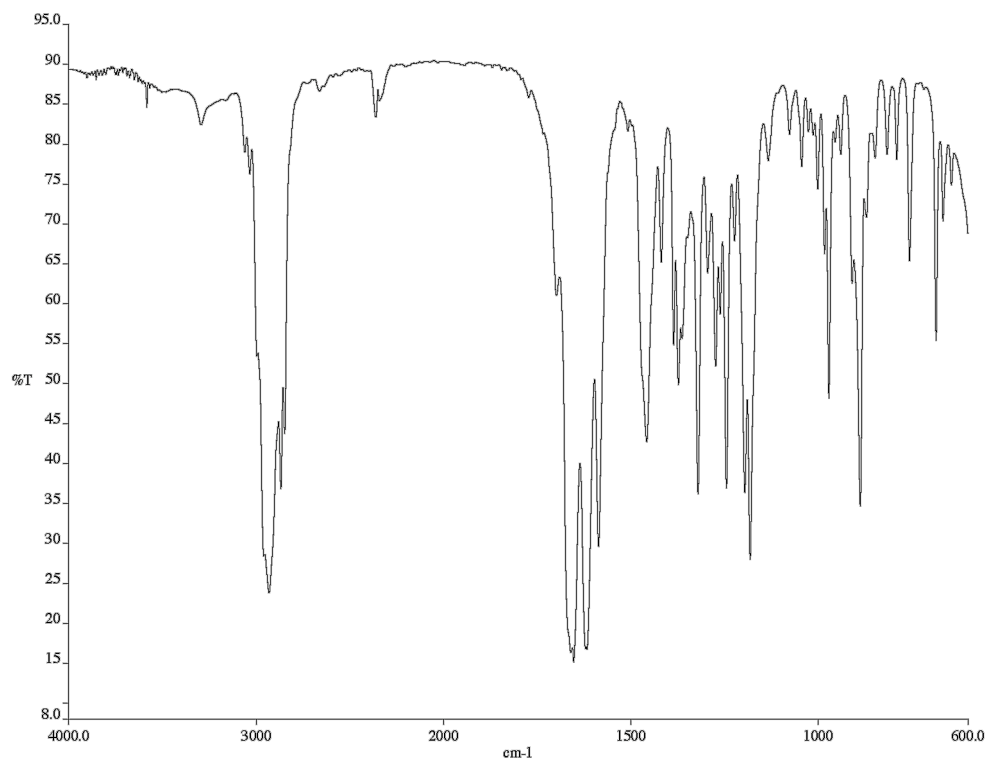


Figure A4.38 Infrared spectrum (NaCl/CDCl₃) of compound **234**.

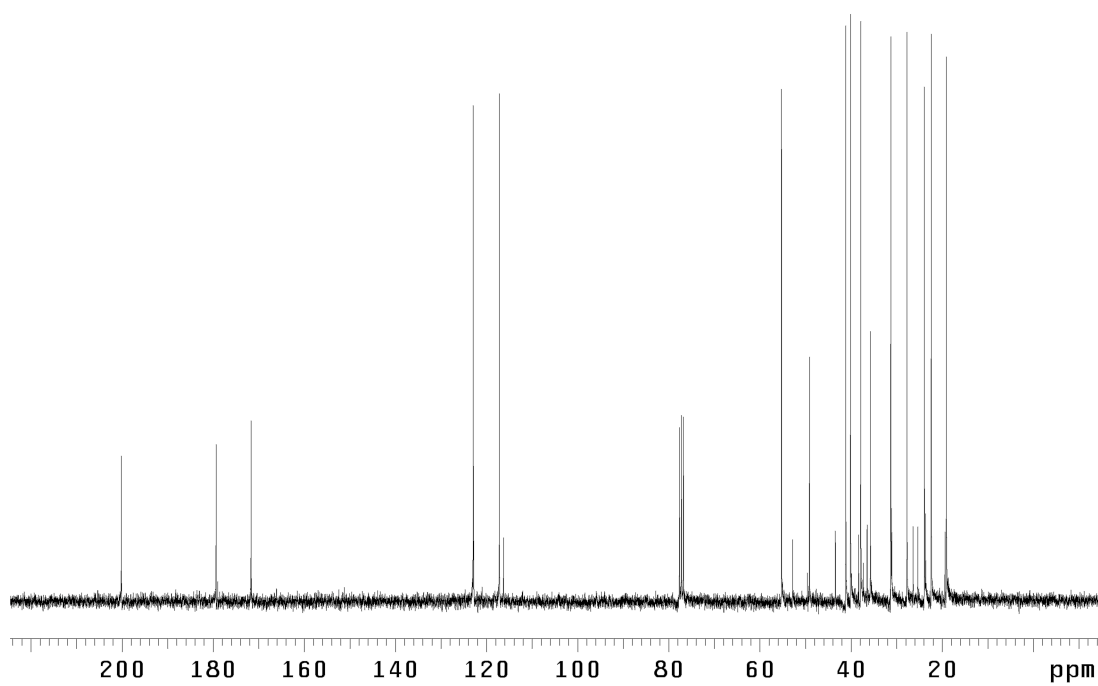


Figure A4.39 ¹³C NMR (75 MHz, CDCl₃) of compound **234**.

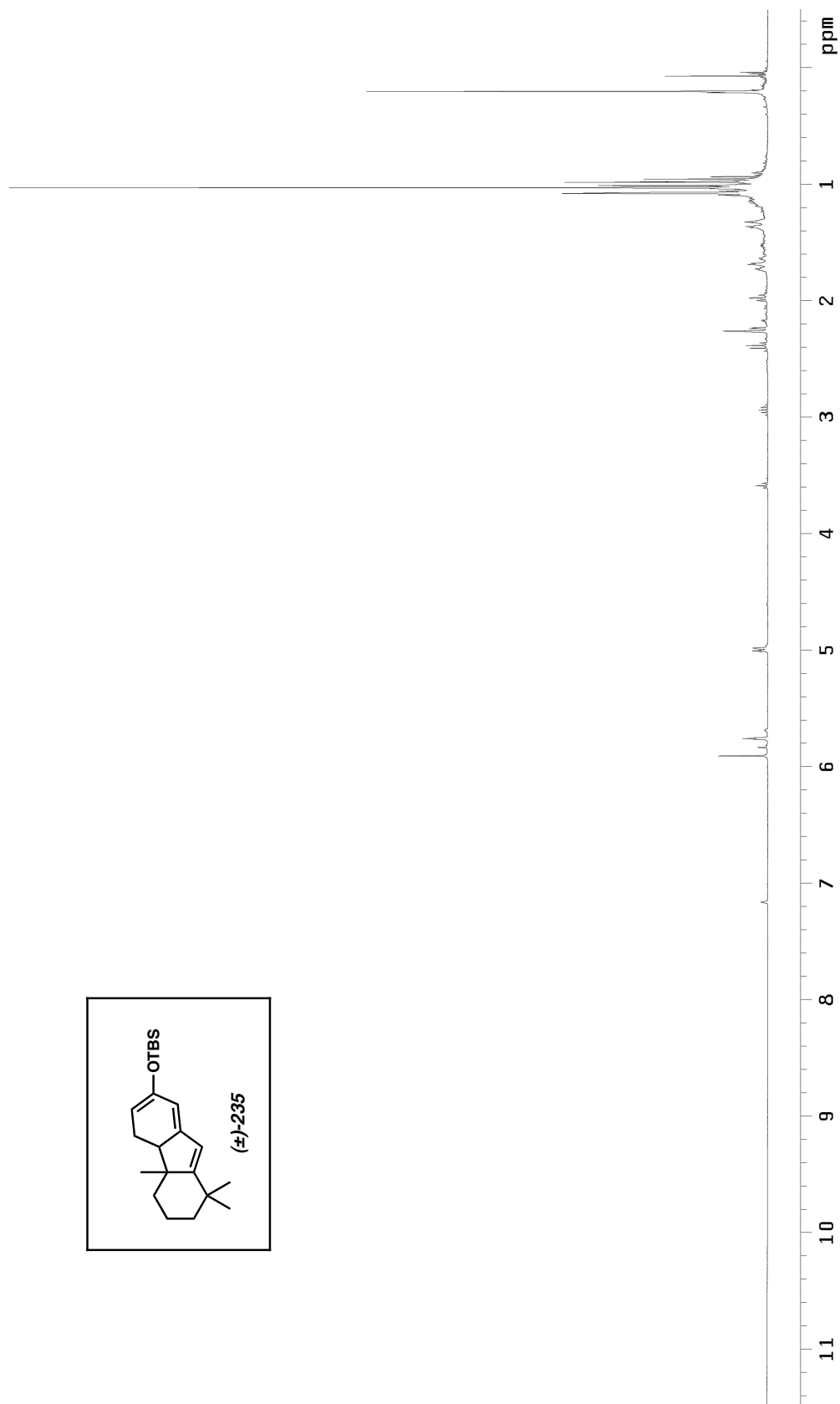


Figure A4.40 ^1H NMR (300 MHz, C_6D_6) of compound **235**.

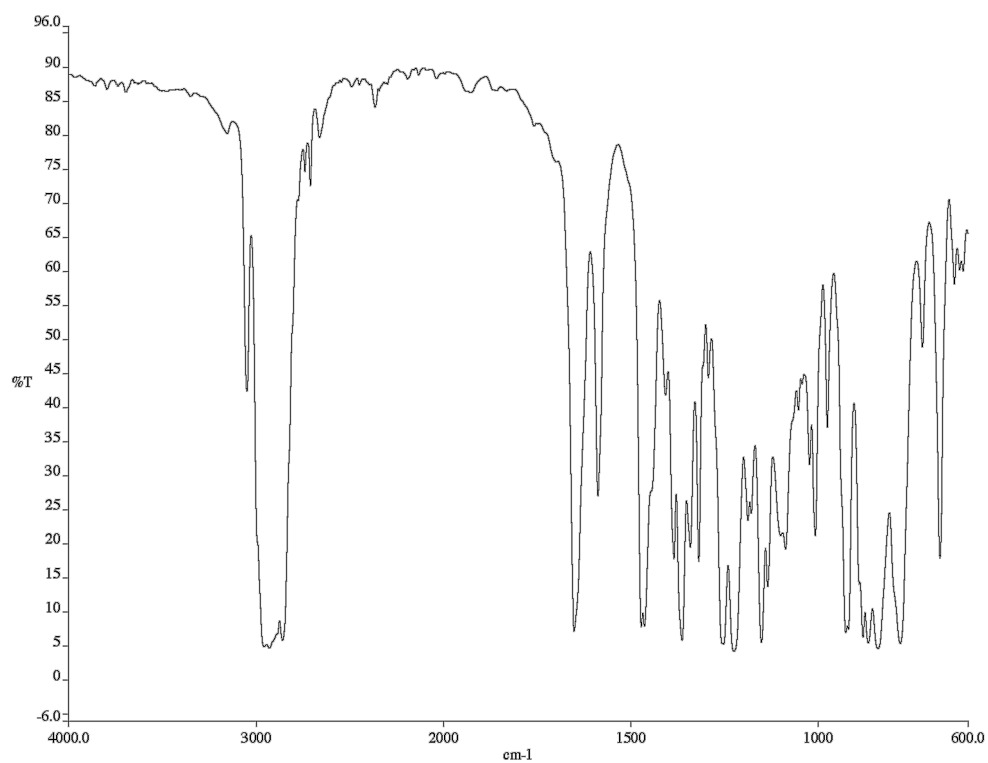


Figure A4.41 Infrared spectrum (NaCl/neat) of compound **235**.

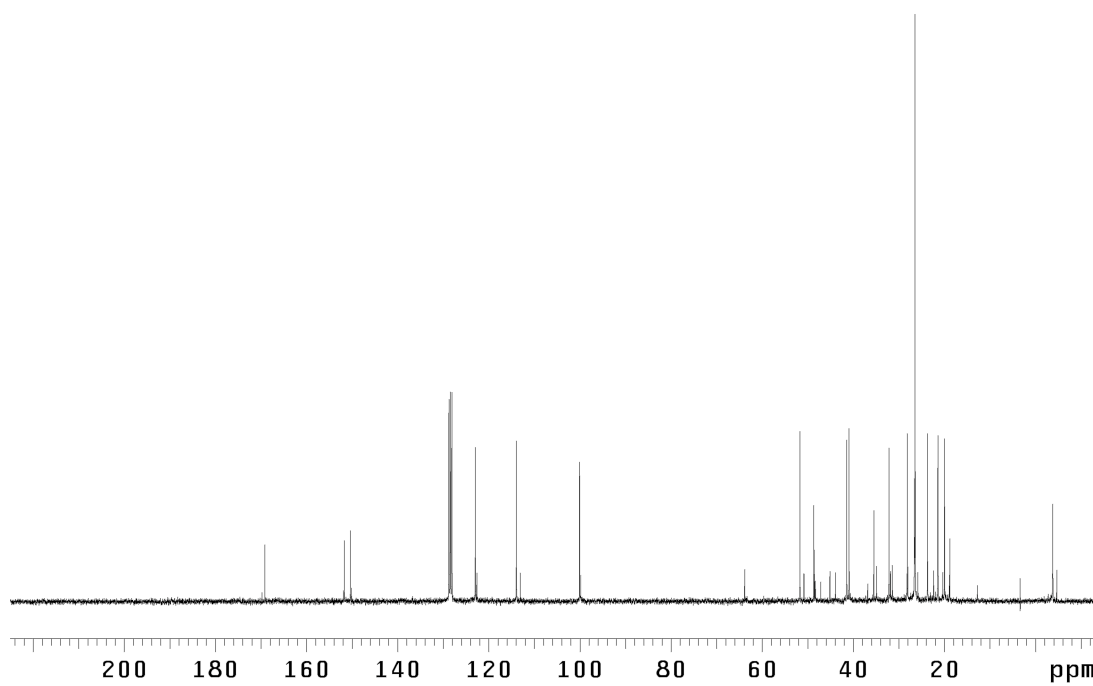


Figure A4.42 ¹³C NMR (75 MHz, C₆D₆) of compound **235**.

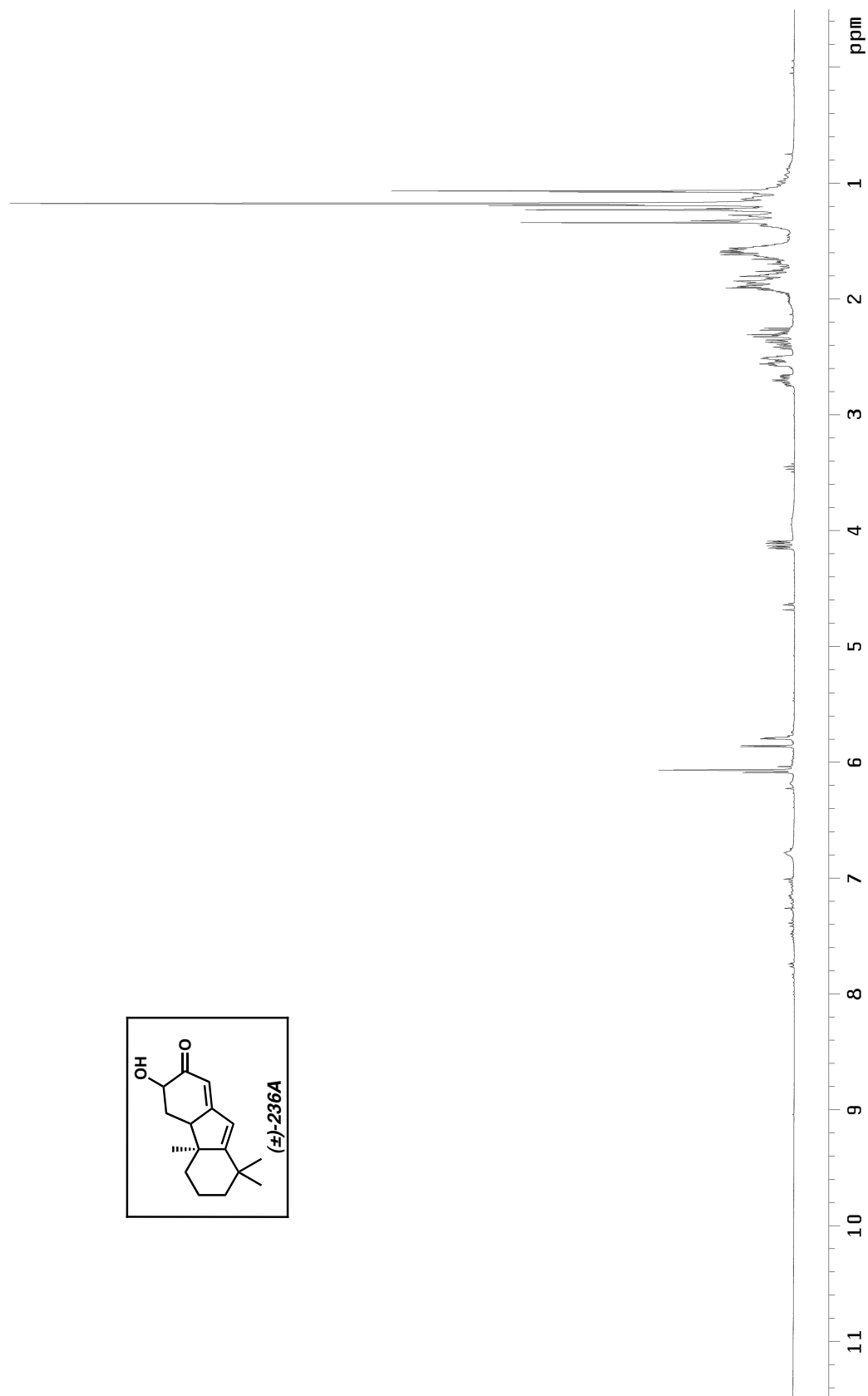


Figure A4.43 ¹H NMR (300 MHz, CDCl₃) of compound **236A**.

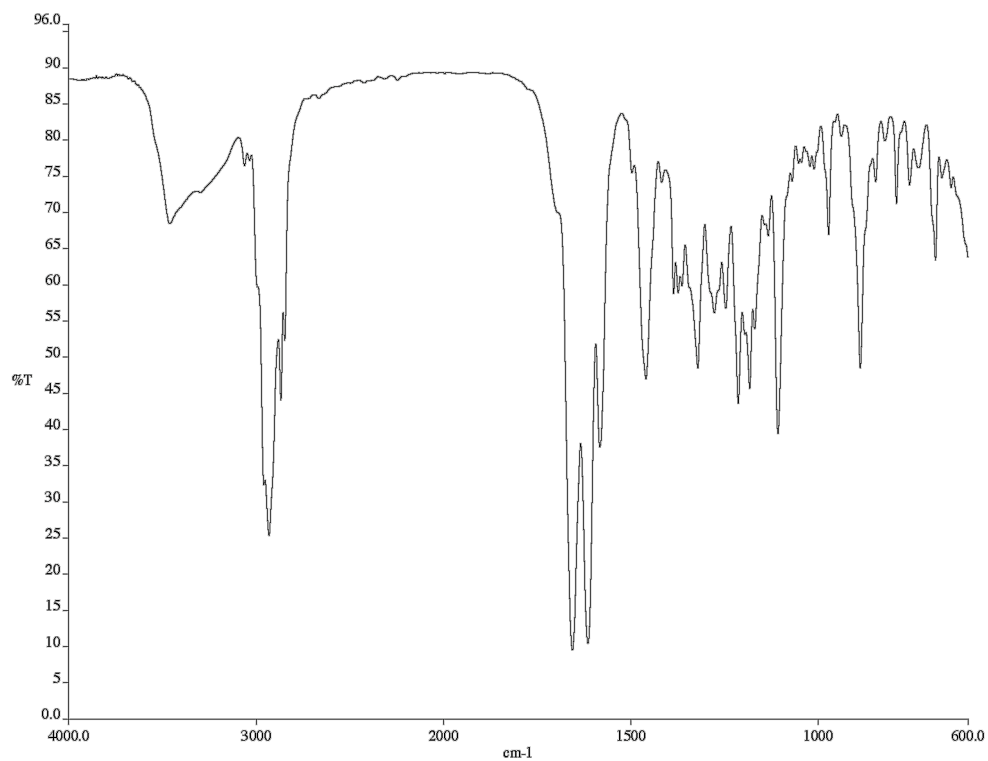


Figure A4.44 Infrared spectrum (NaCl/CDCl₃) of compound **236A**.

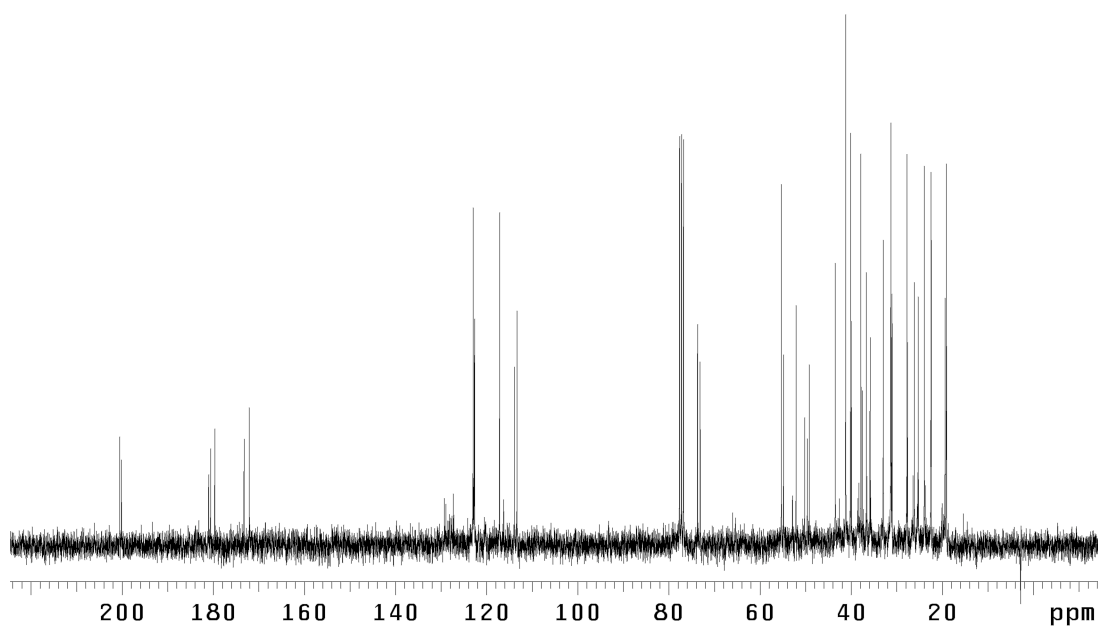


Figure A4.45 ¹³C NMR (75 MHz, CDCl₃) of compound **236A**.

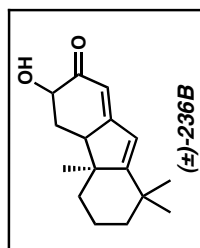


Figure A4.46 ^1H NMR (300 MHz, CDCl_3) of compound **236B**.

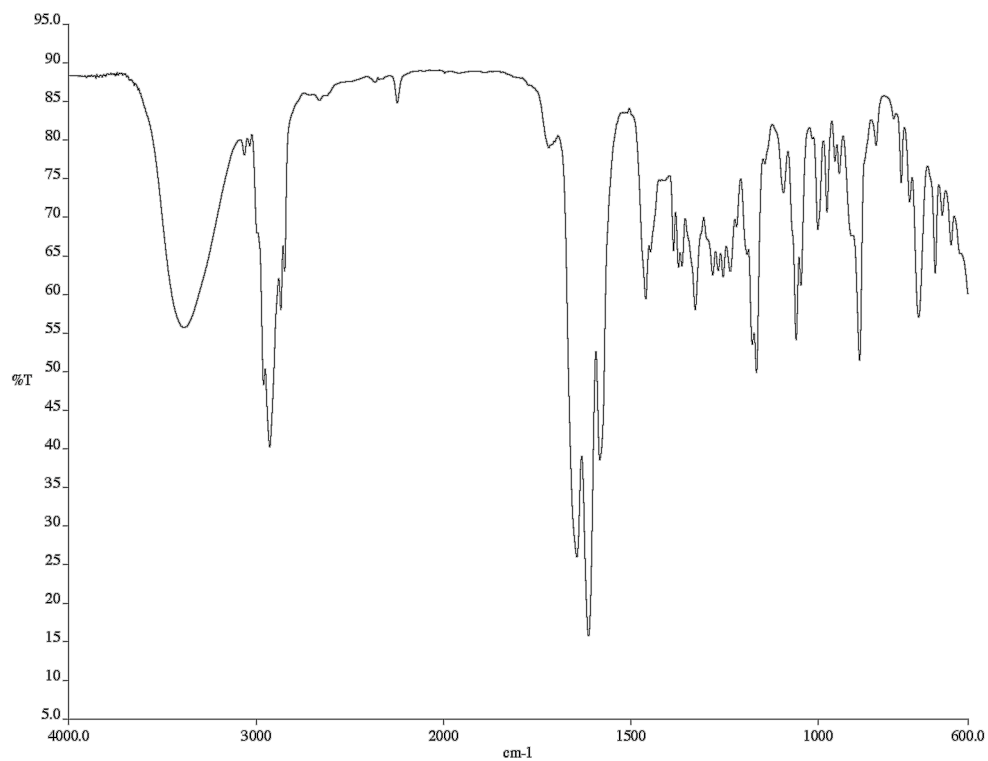


Figure A4.47 Infrared spectrum (NaCl/CDCl₃) of compound **236B**.

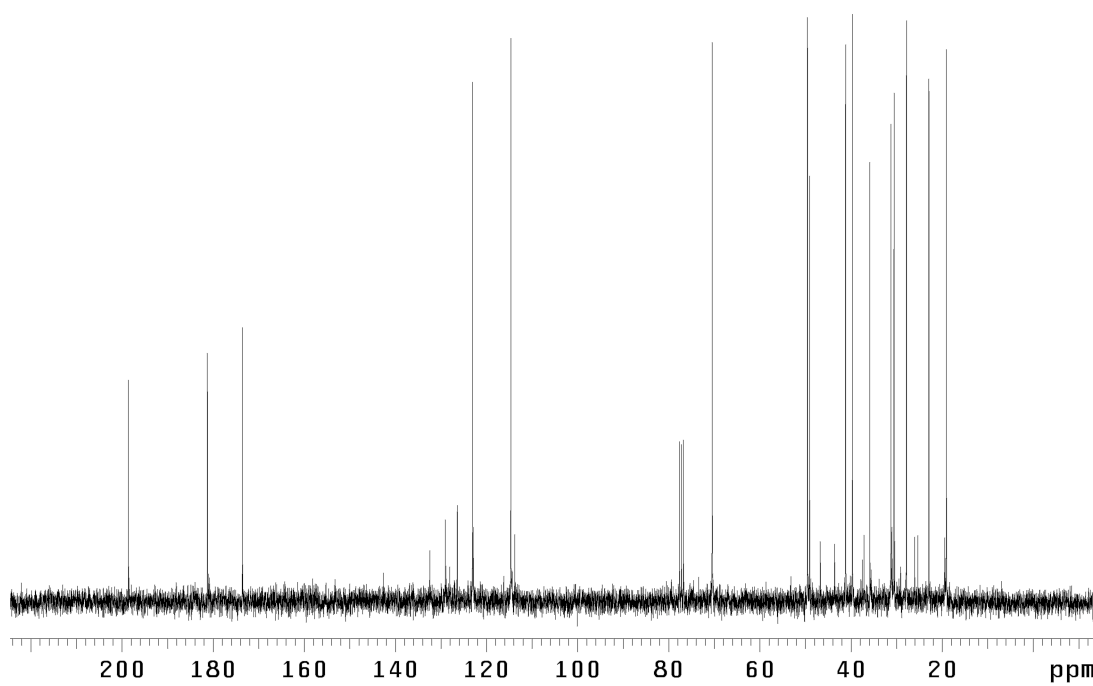


Figure A4.48 ¹³C NMR (75 MHz, CDCl₃) of compound **236B**.

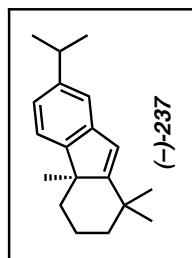
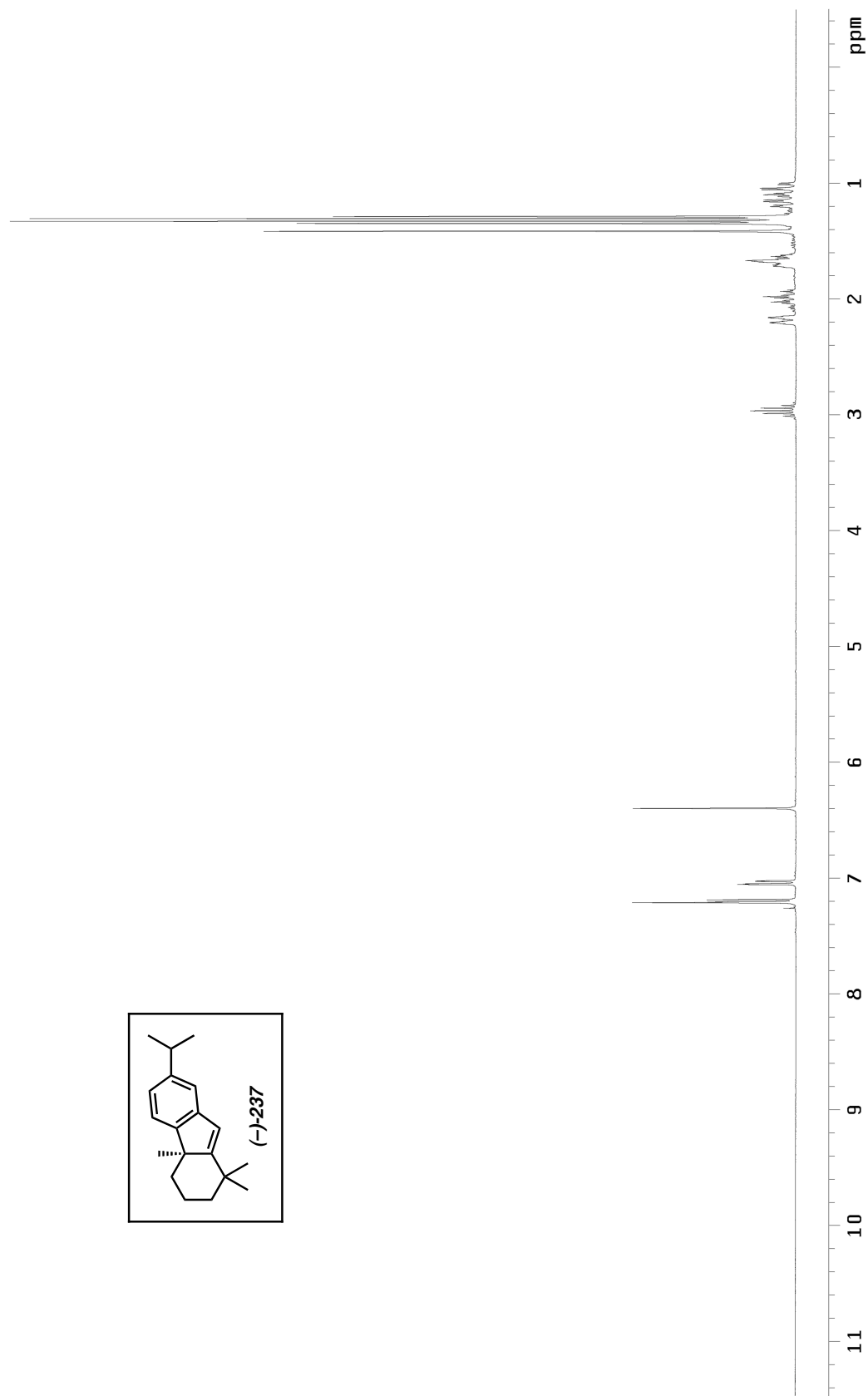


Figure A4.49 ^1H NMR (300 MHz, CDCl_3) of compound **237**.

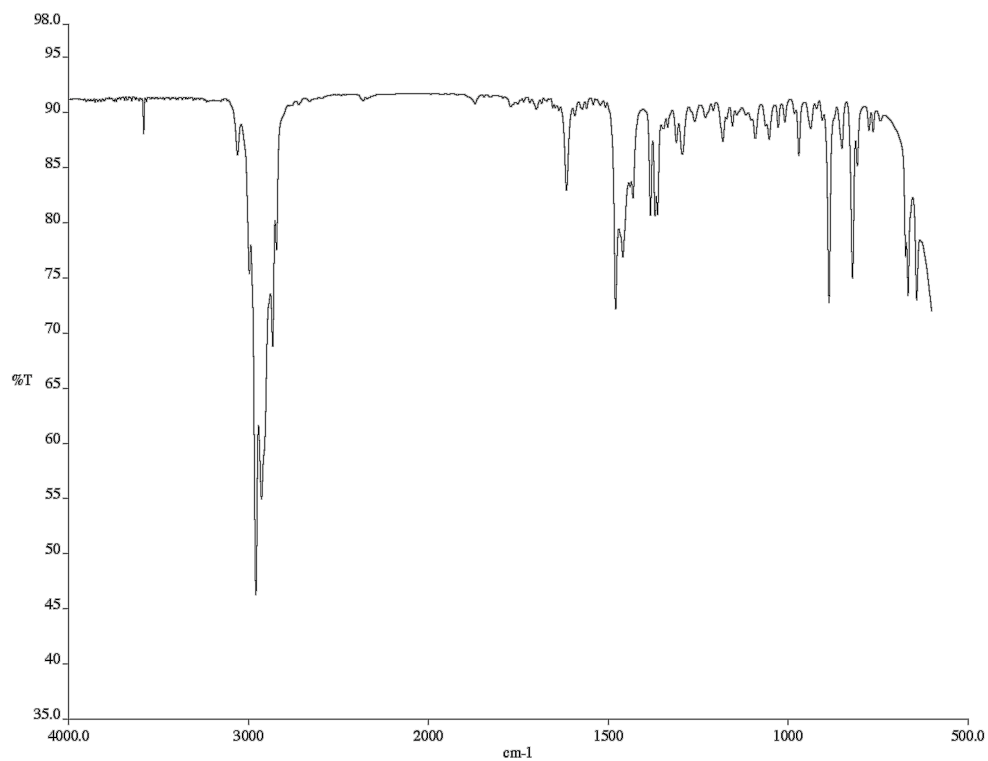


Figure A4.50 Infrared spectrum (NaCl/CDCl₃) of compound **237**.

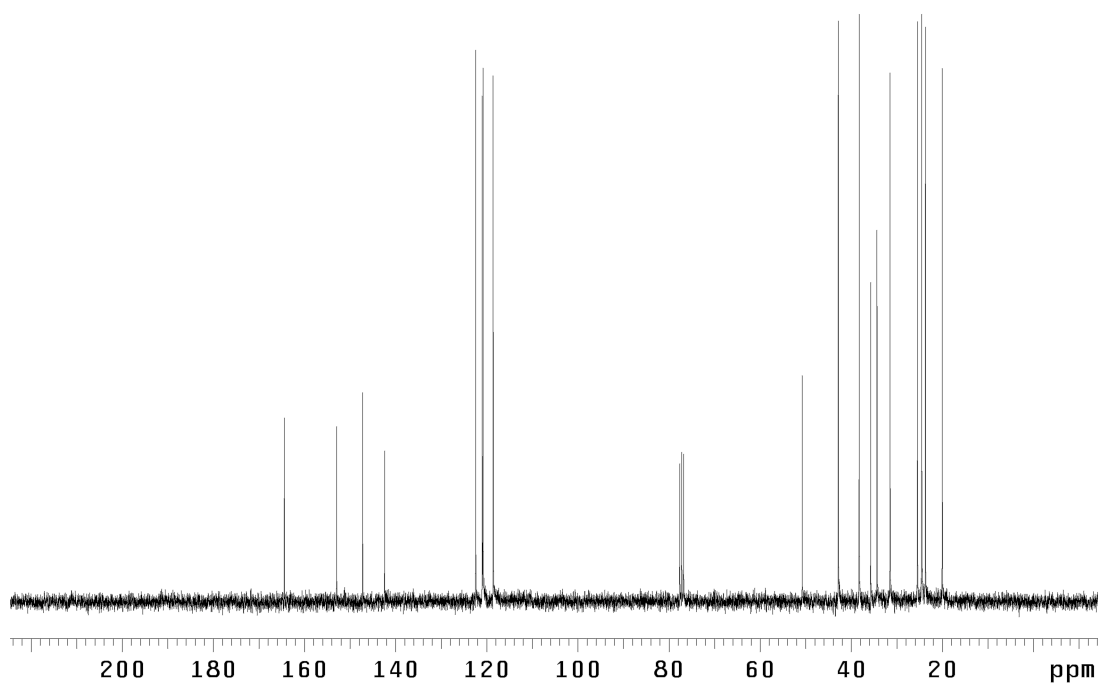


Figure A4.51 ¹³C NMR (75 MHz, CDCl₃) of compound **237**.

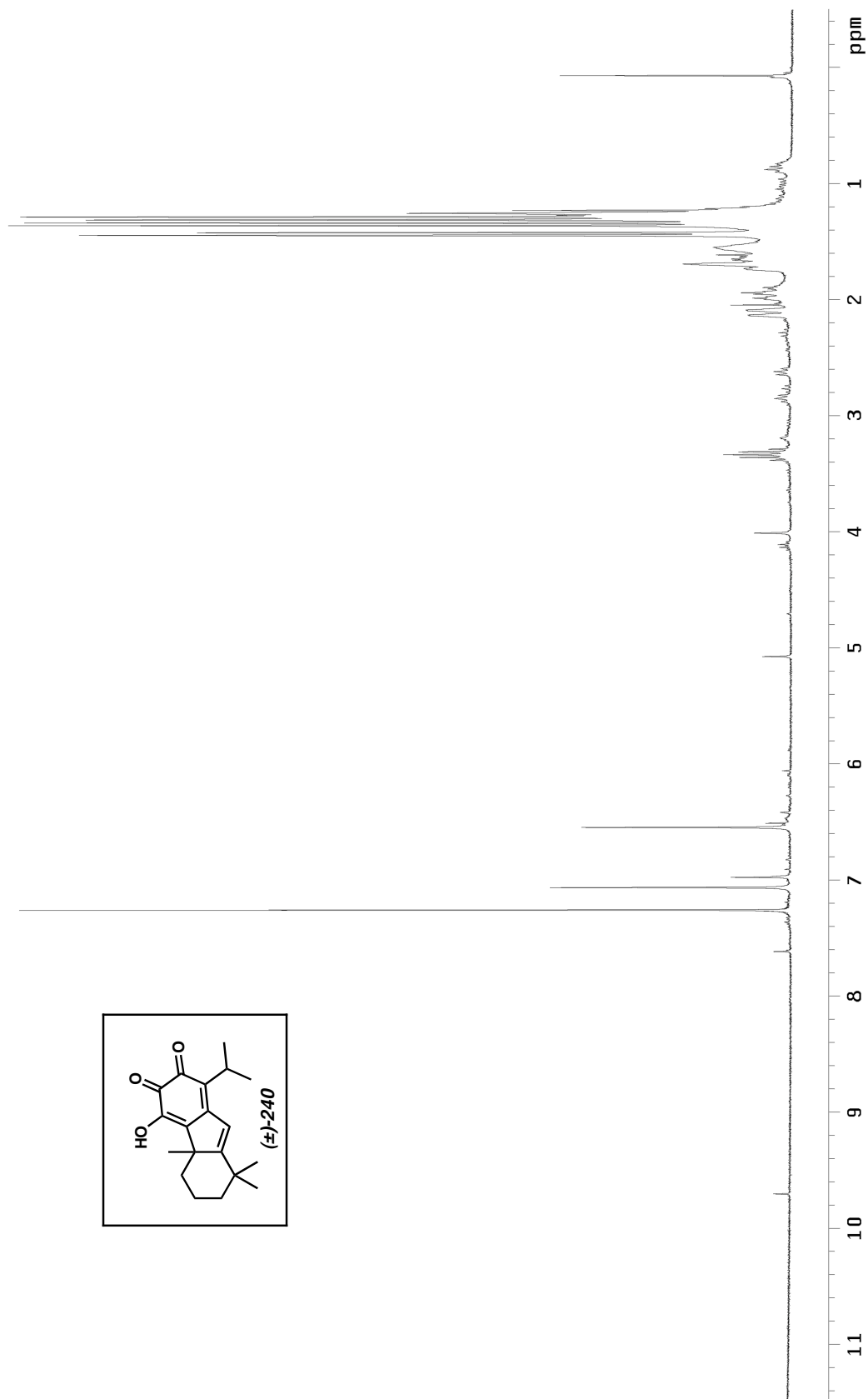


Figure A4.52 ^1H NMR (300 MHz, CDCl_3) of compound **240**.

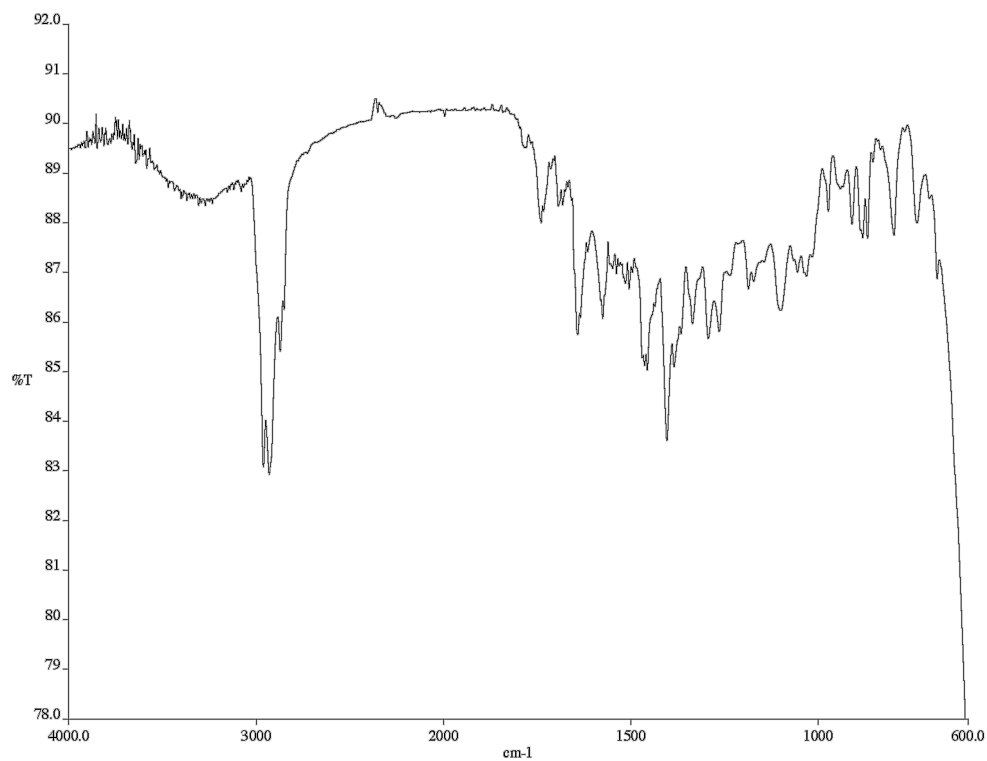


Figure A4.53 Infrared spectrum (NaCl/CDCl₃) of compound **240**.

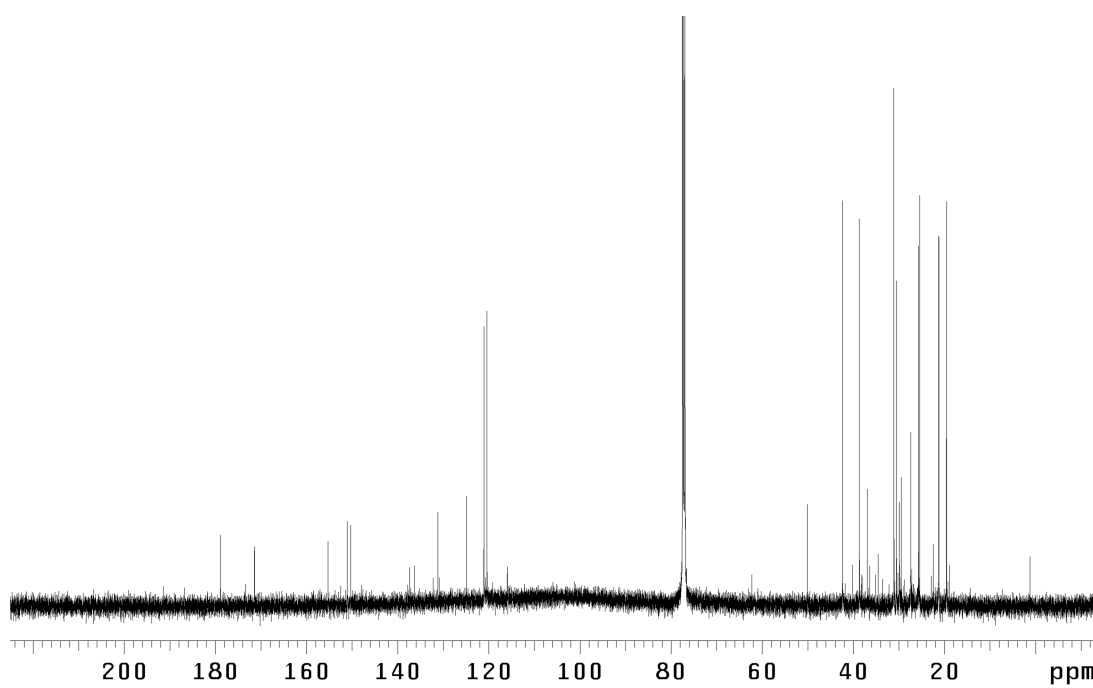


Figure A4.54 ¹³C NMR (125 MHz, CDCl₃) of compound **240**.

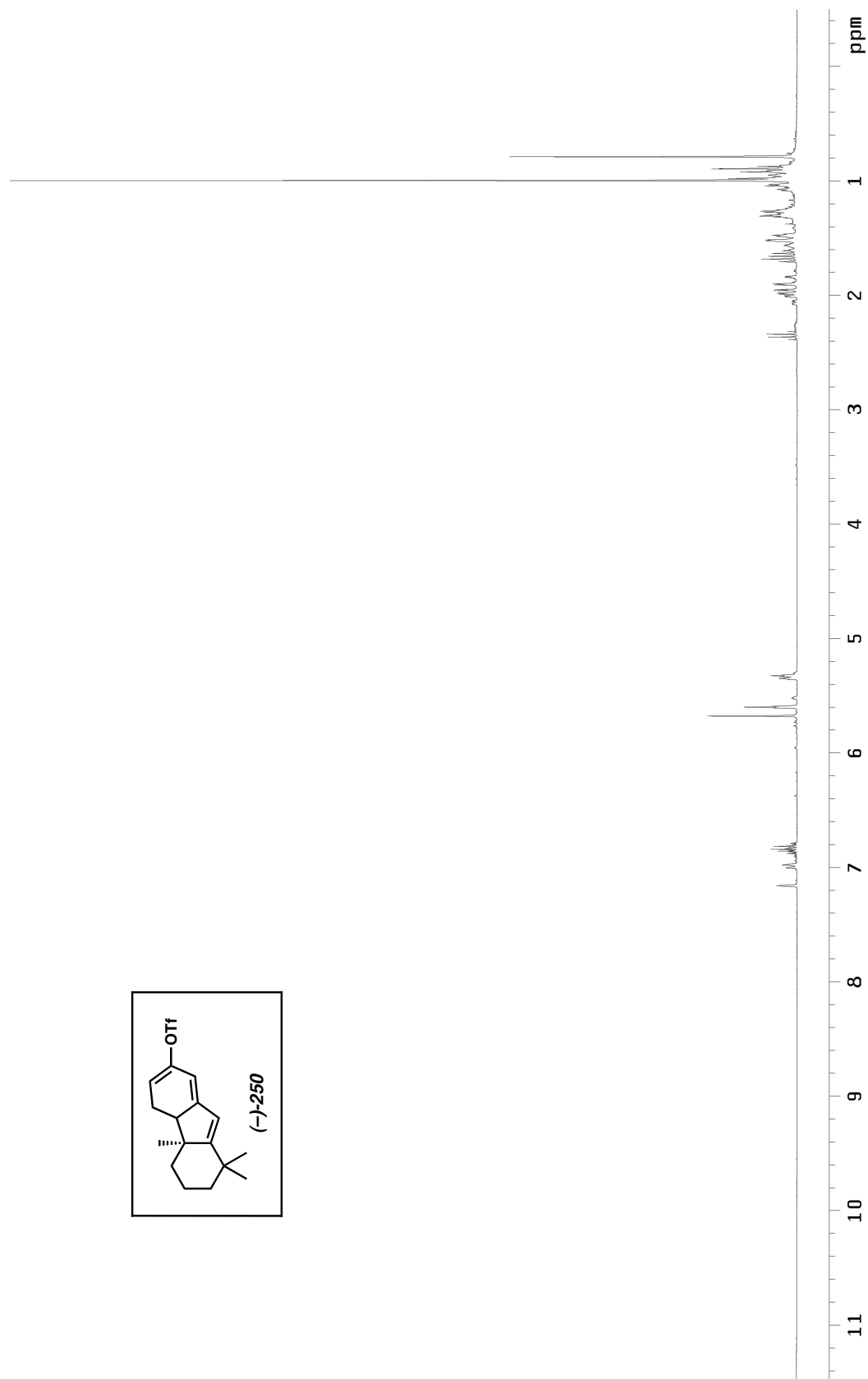


Figure A4.55 ^1H NMR (300 MHz, C_6D_6) of compound **250**.

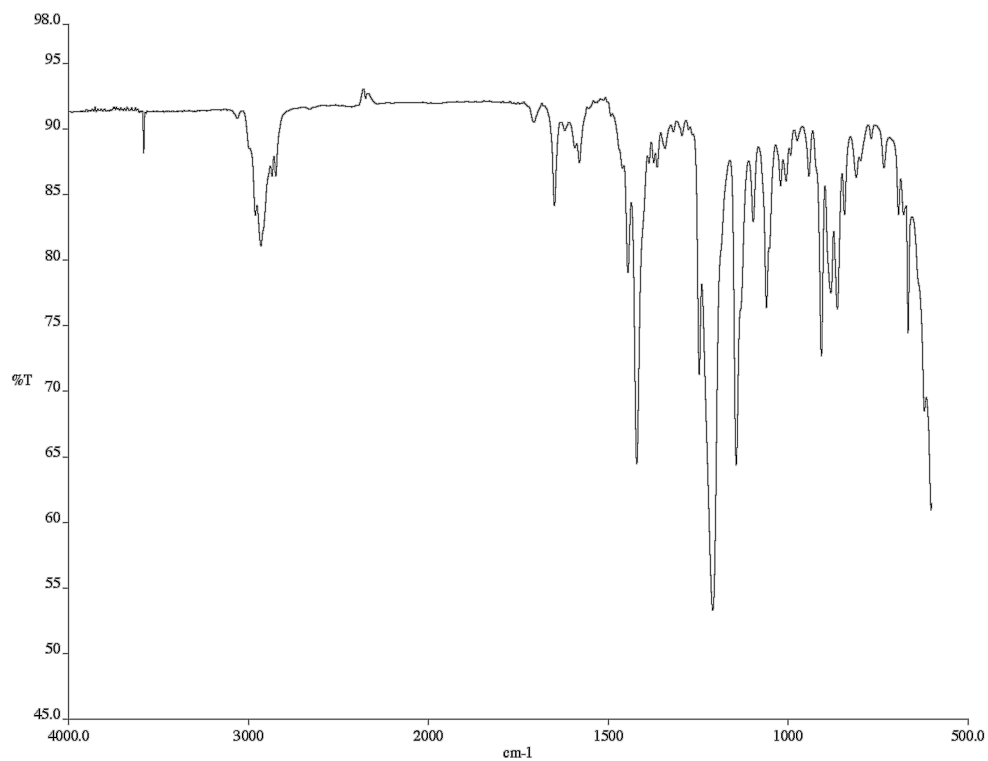


Figure A4.56 Infrared spectrum (NaCl/hexane) of compound **250**.

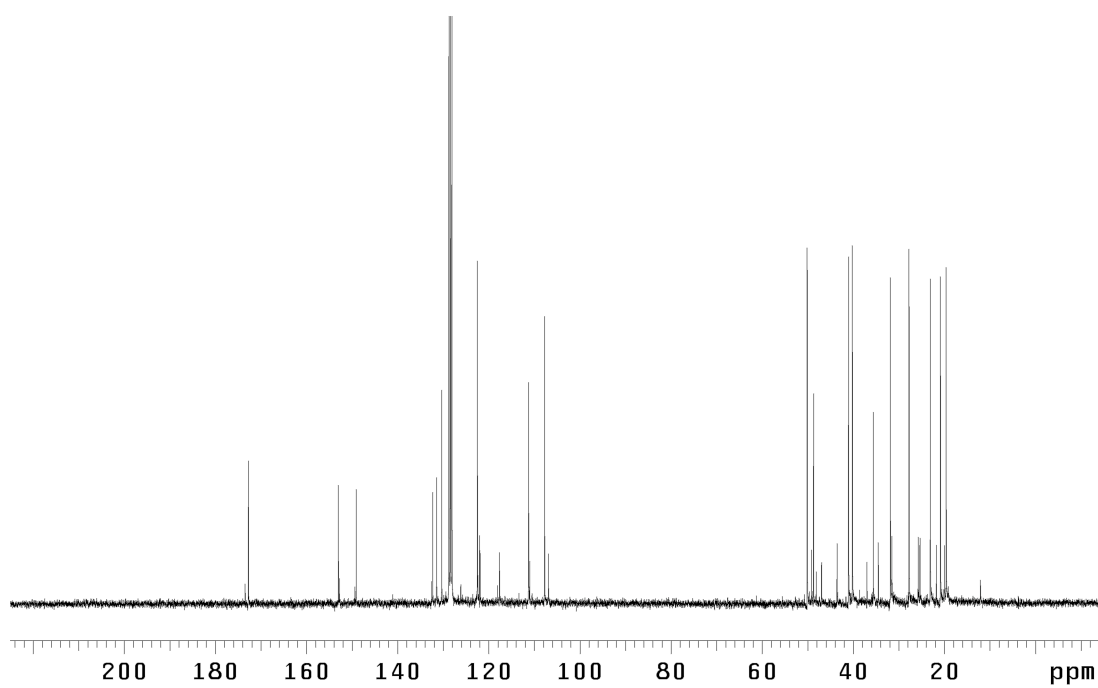


Figure A4.57 ¹³C NMR (75 MHz, C₆D₆) of compound **250**.

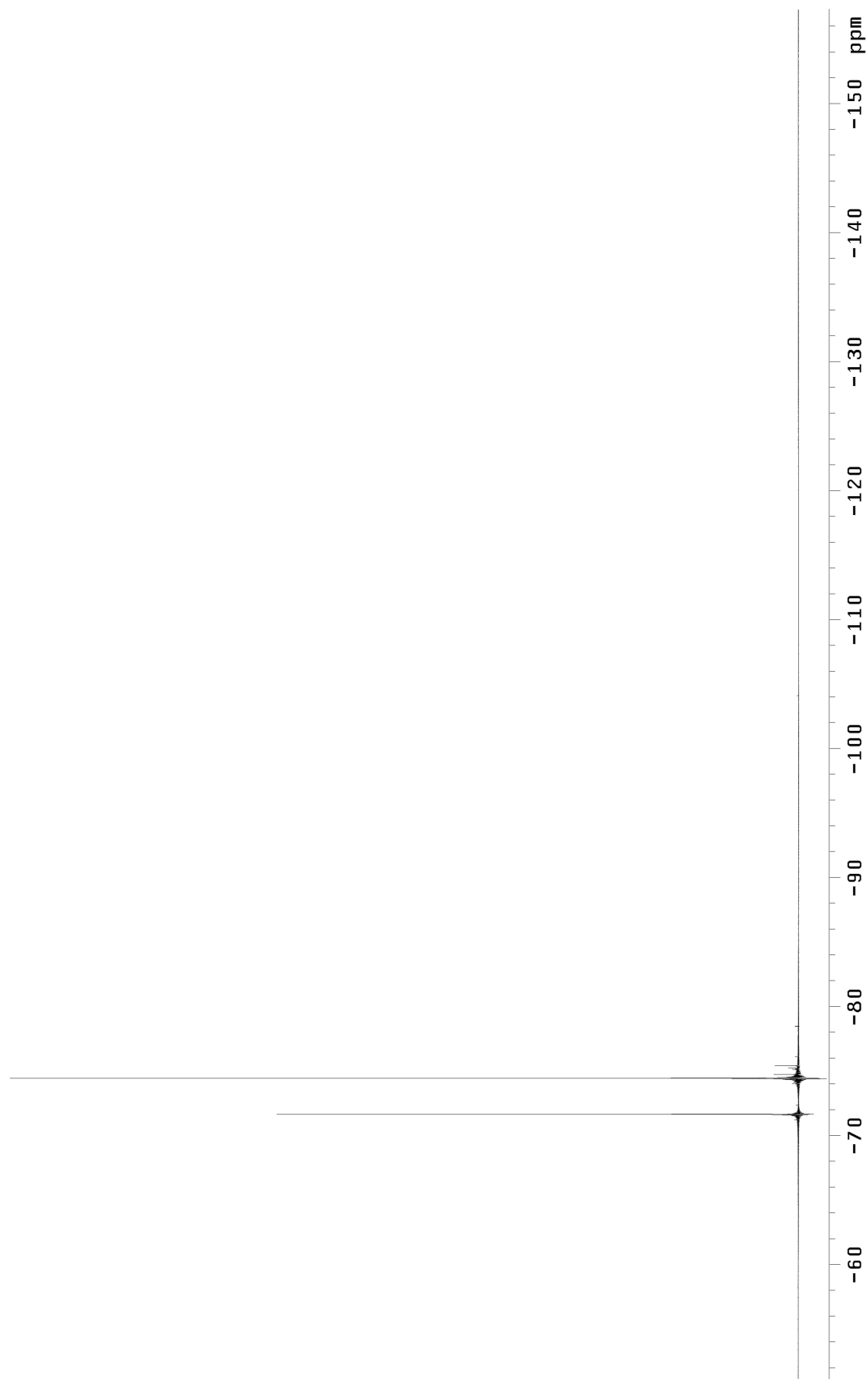


Figure A4.58 ^{19}F NMR (282 MHz, C_6D_6) of compound **250**.

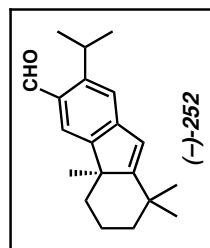
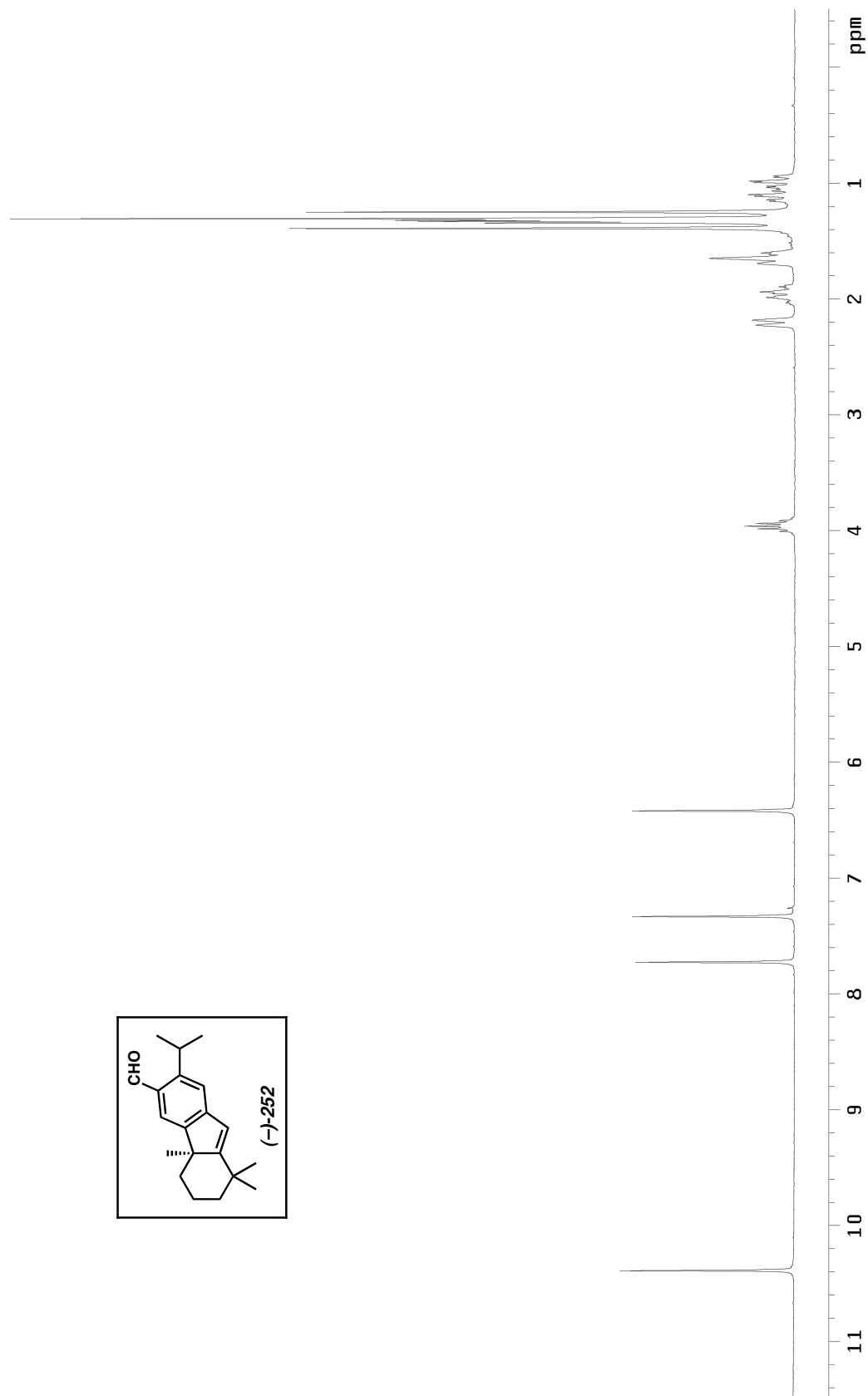


Figure A4.59 ^1H NMR (300 MHz, CDCl_3) of compound **252**.

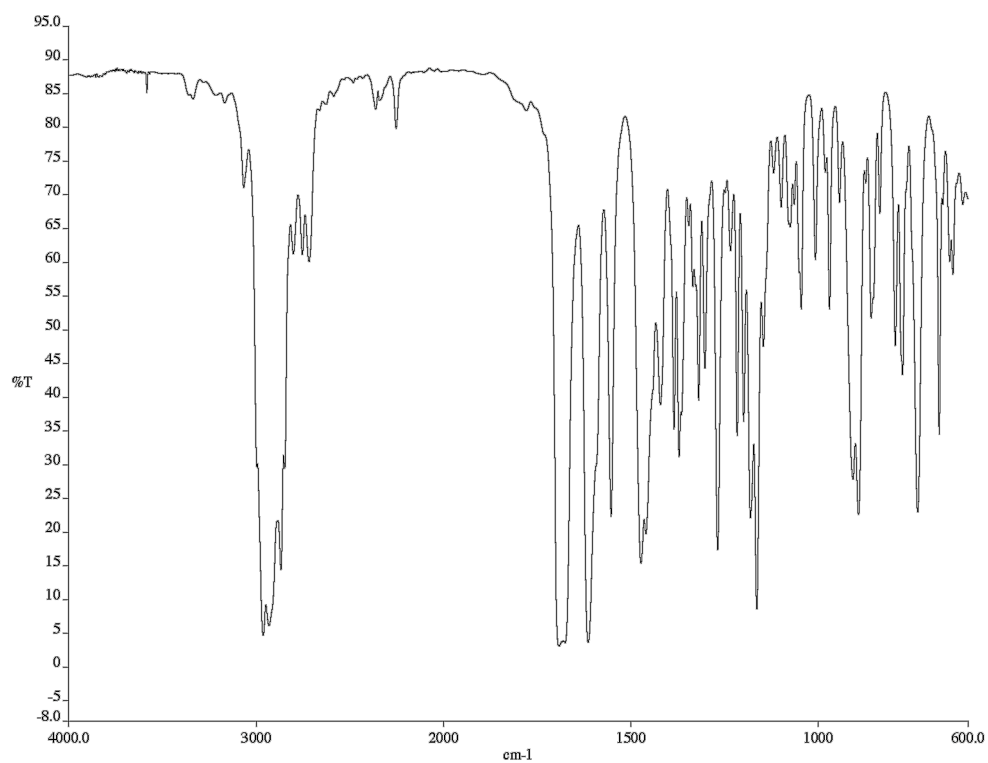


Figure A4.60 Infrared spectrum (NaCl/CDCl₃) of compound **252**.

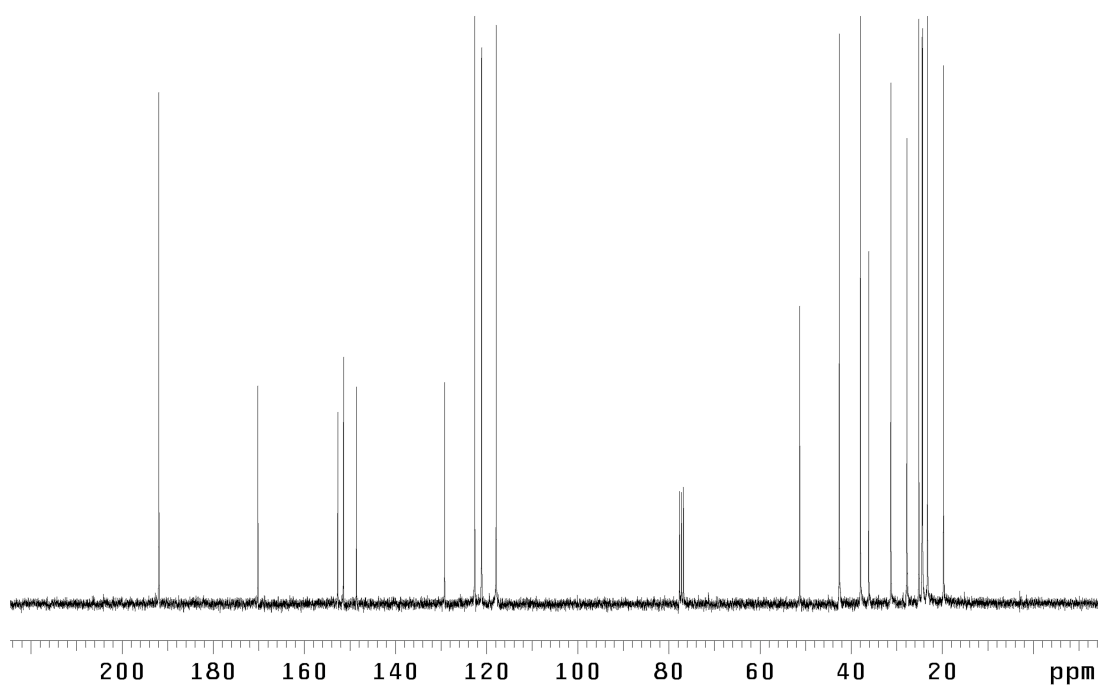


Figure A4.61 ¹³C NMR (75 MHz, CDCl₃) of compound **252**.

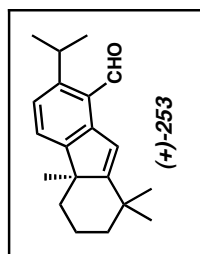
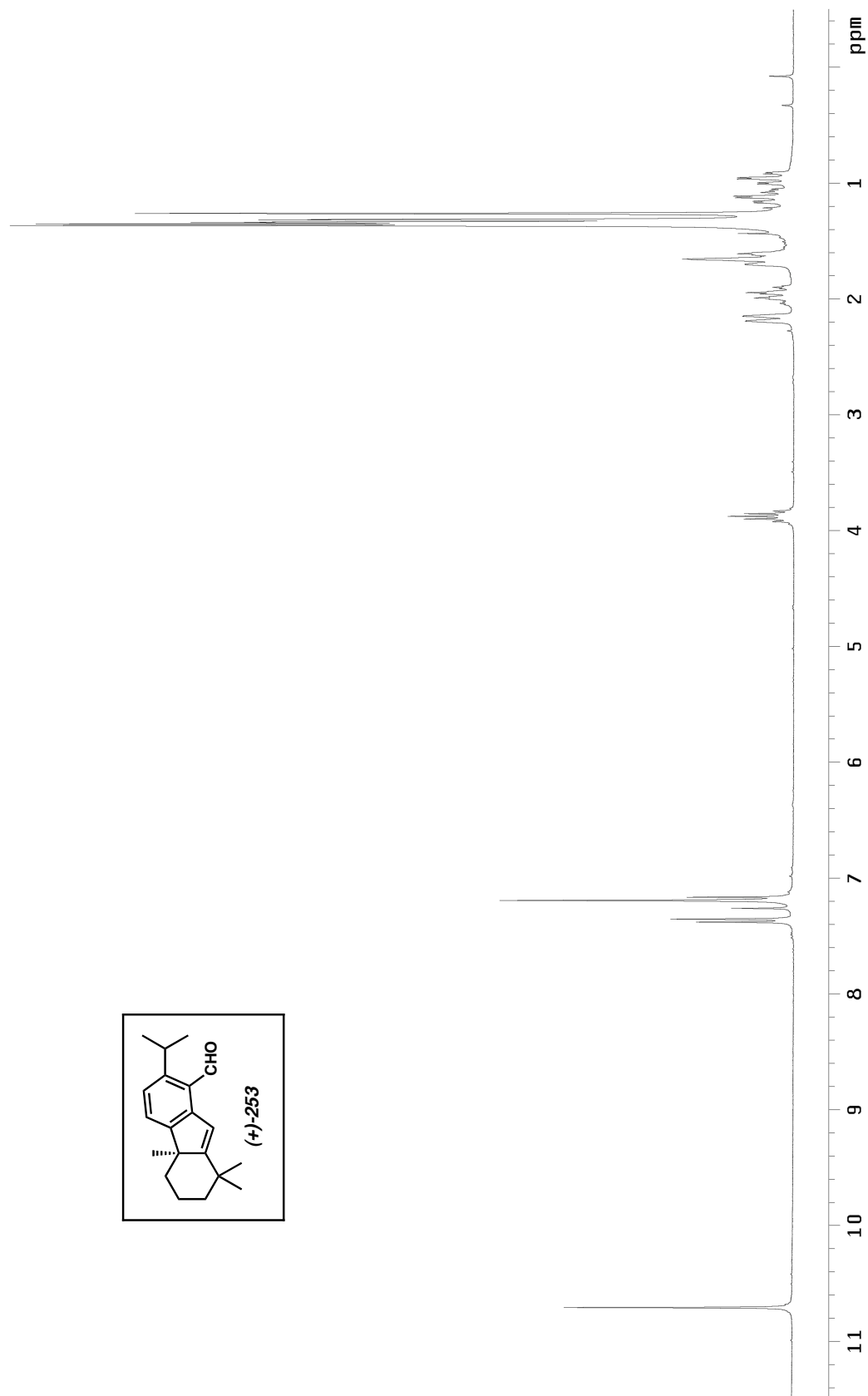


Figure A4.62 ¹H NMR (300 MHz, CDCl₃) of compound **253**.

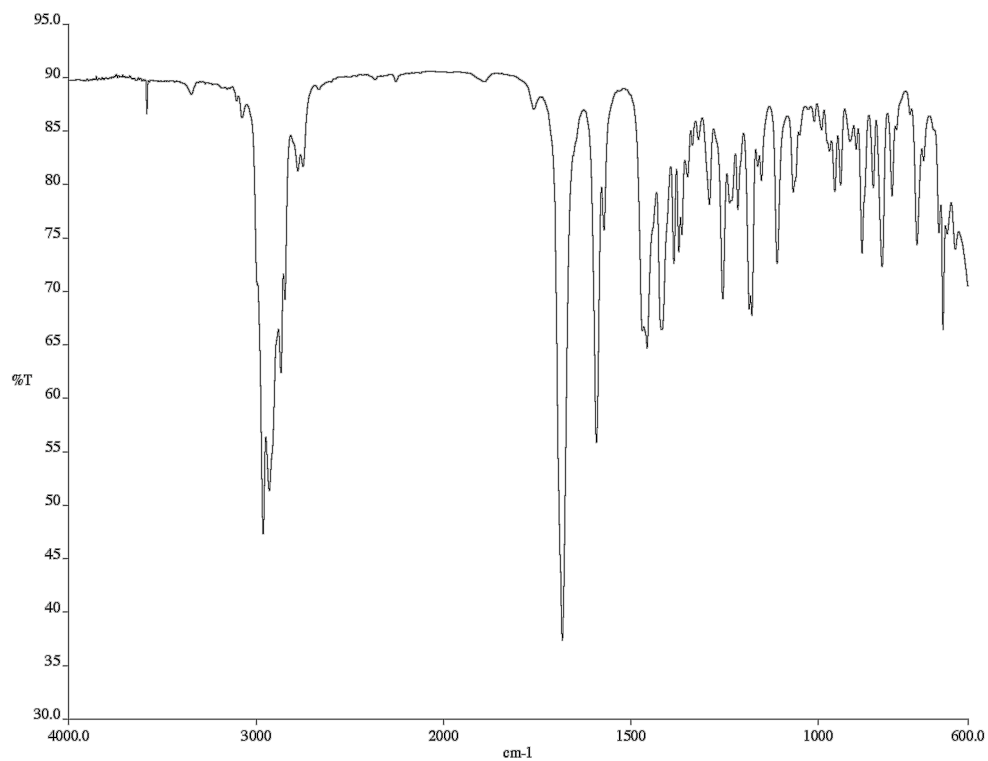


Figure A4.63 Infrared spectrum (NaCl/CDCl₃) of compound **253**.

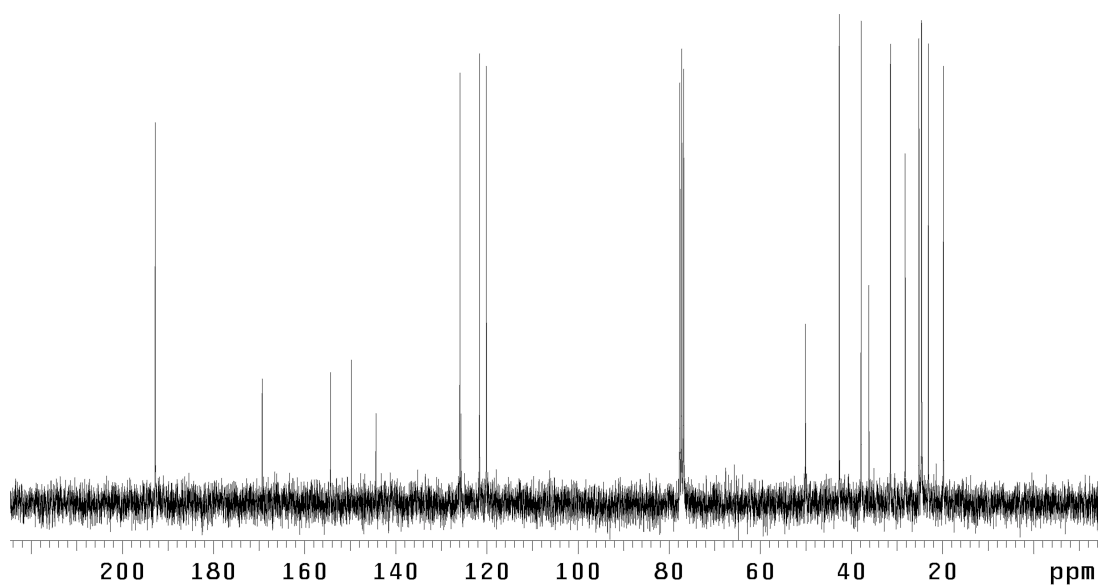


Figure A4.64 ¹³C NMR (75 MHz, CDCl₃) of compound **253**.

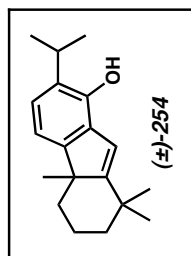
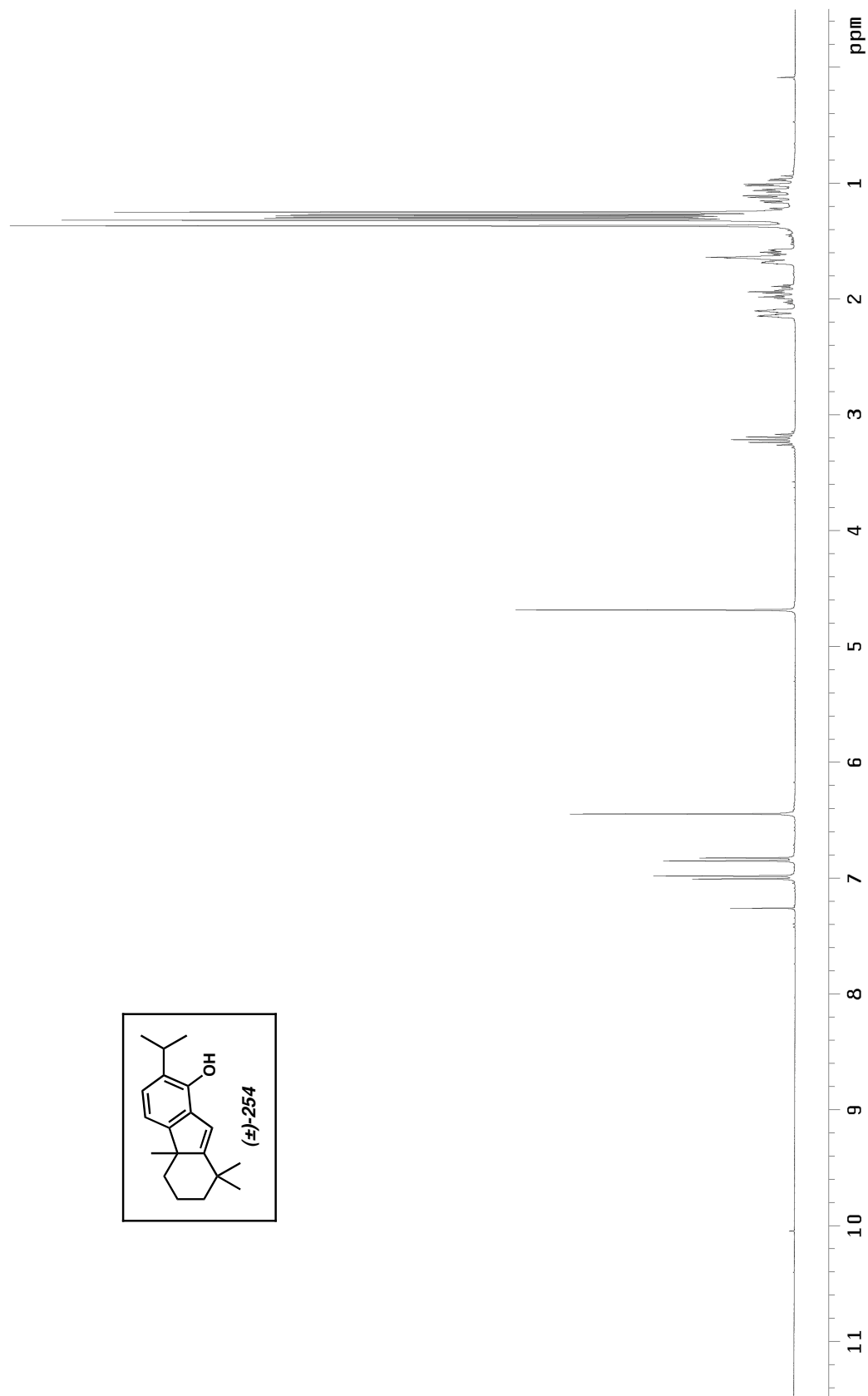


Figure A4.65 ^1H NMR (300 MHz, CDCl_3) of compound **254**.

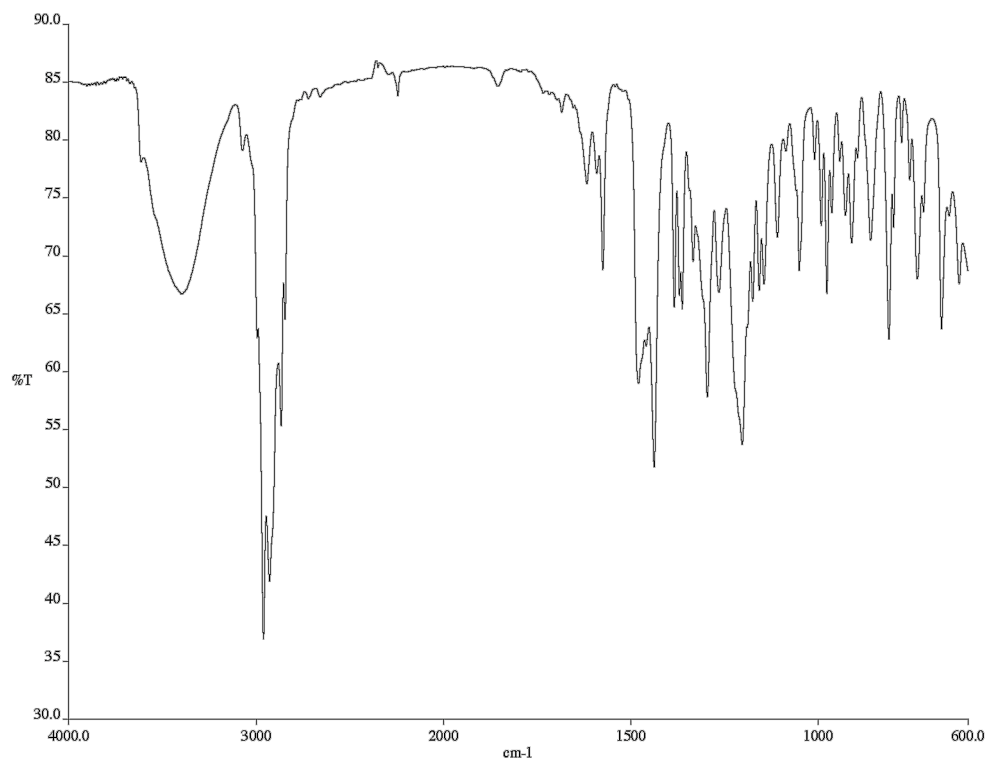


Figure A4.66 Infrared spectrum (NaCl/CDCl₃) of compound **254**.

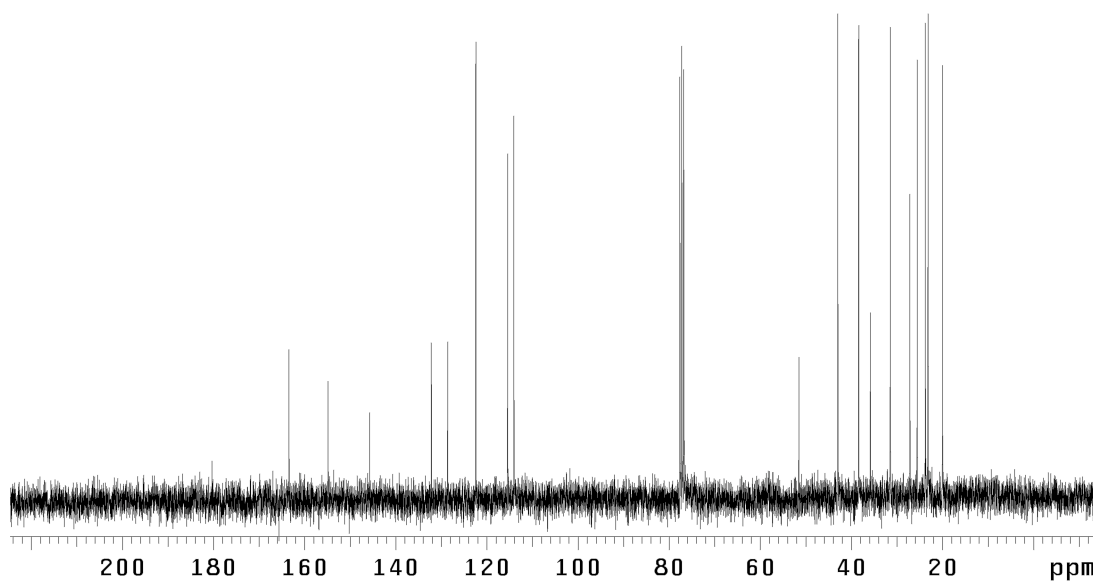


Figure A4.67 ¹³C NMR (75 MHz, CDCl₃) of compound **254**.

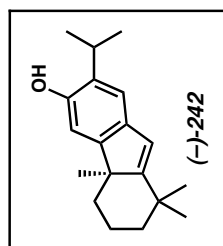


Figure A4.68 ¹H NMR (300 MHz, CDCl₃) of compound **242**.

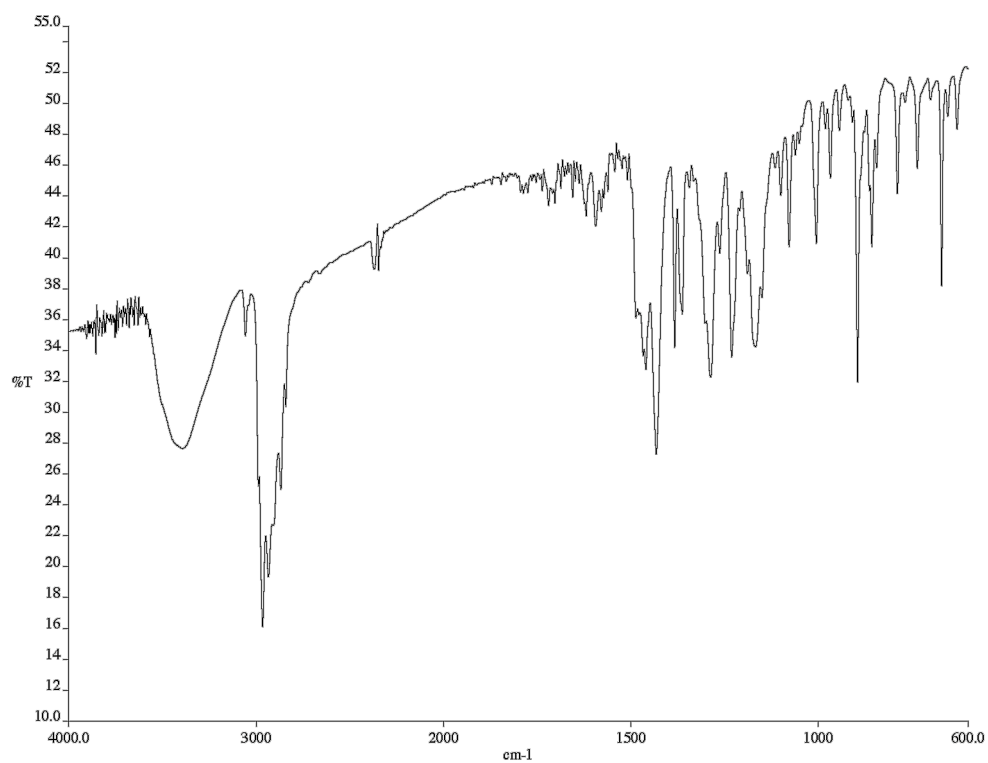


Figure A4.69 Infrared spectrum (KBr) of compound **242**.

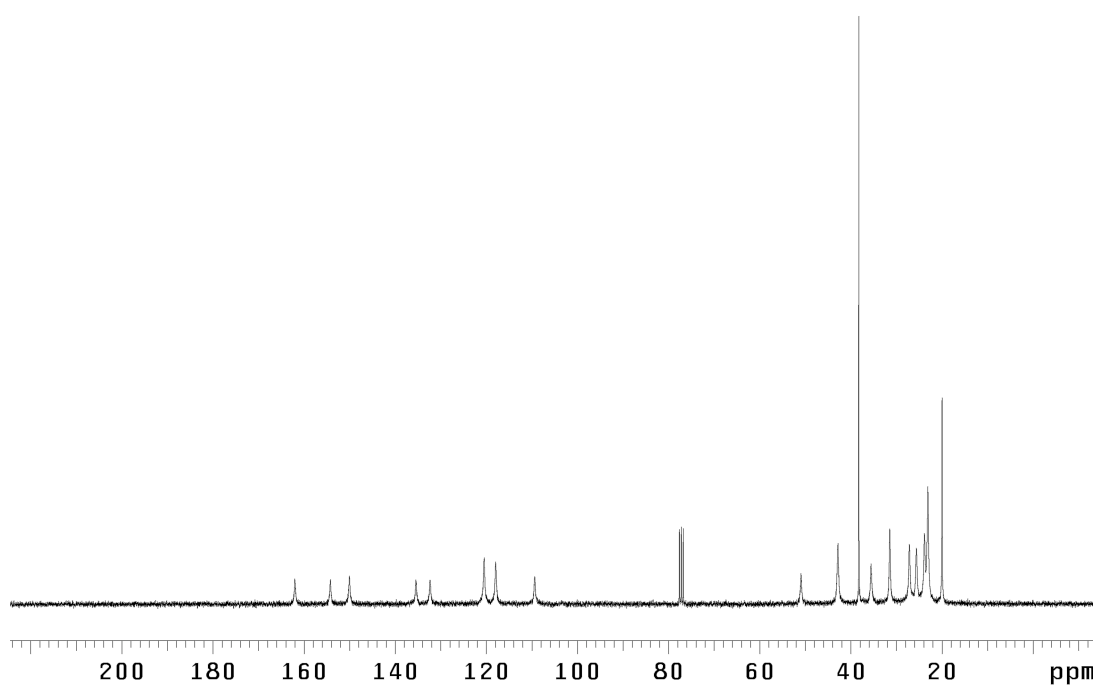


Figure A4.70 ¹³C NMR (75 MHz, CDCl₃) of compound **242**.

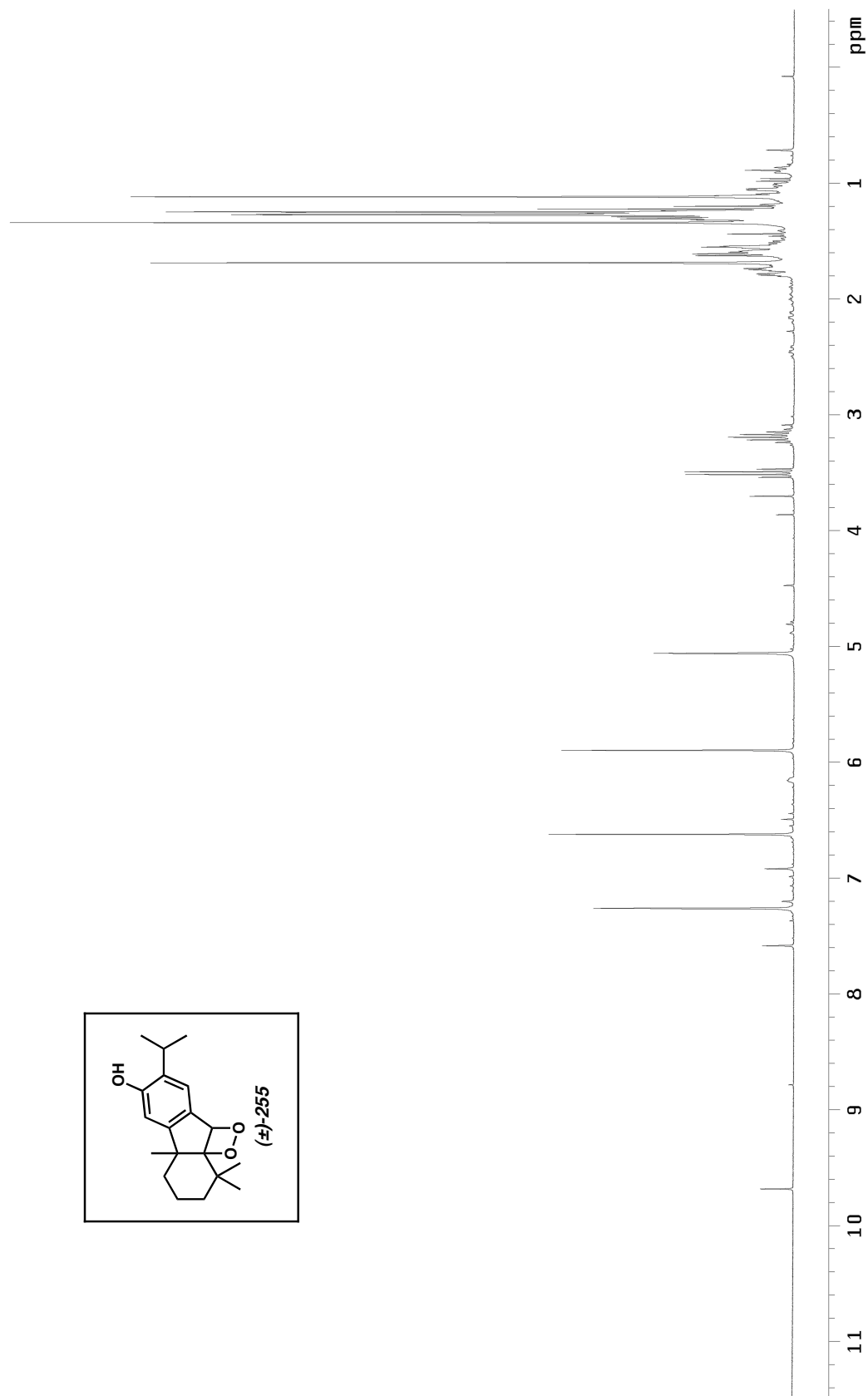


Figure A4.71 ^1H NMR (300 MHz, CDCl_3) of compound **255**.

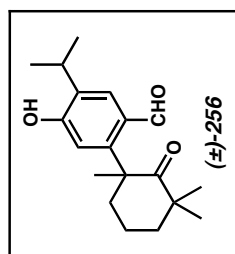
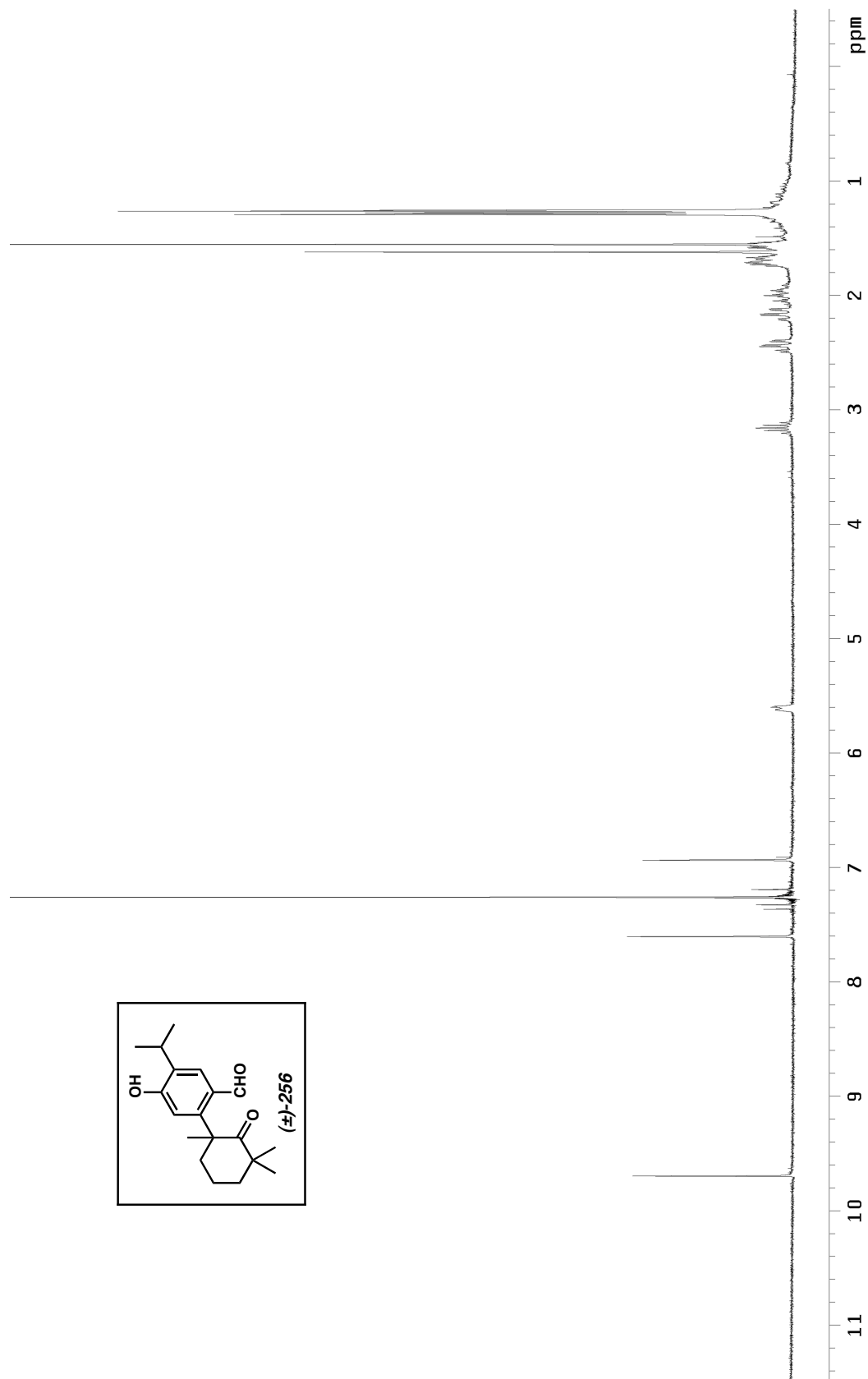


Figure A4.72 ^1H NMR (300 MHz, CDCl_3) of compound **256**.

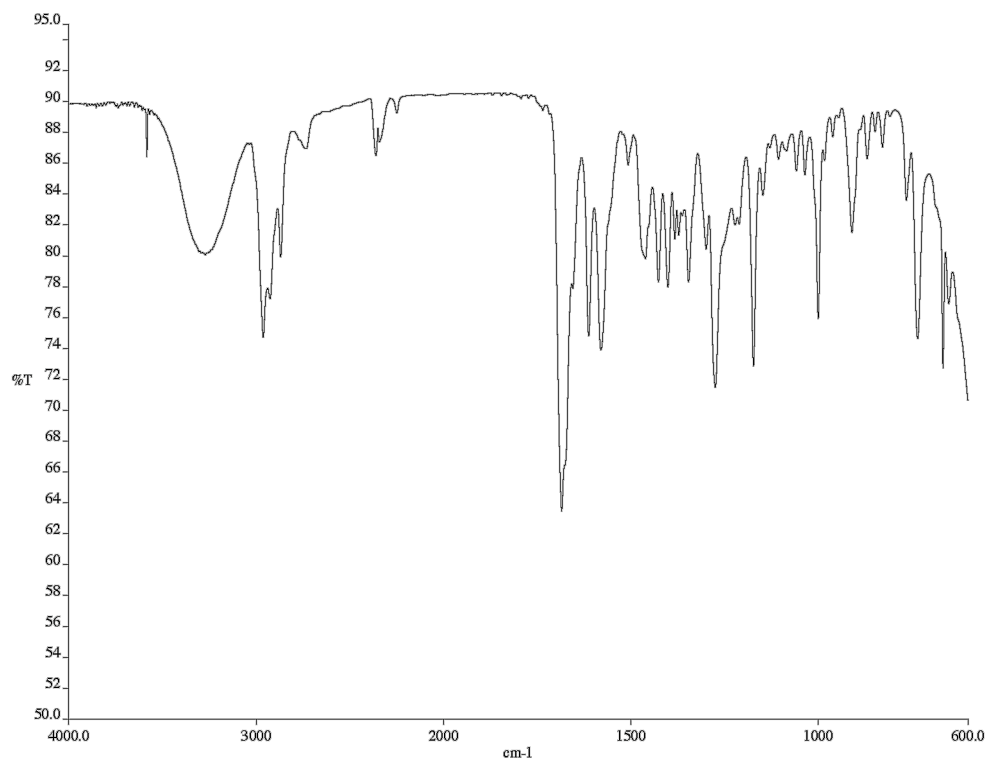


Figure A4.73 Infrared spectrum (NaCl/CDCl₃) of compound **256**.

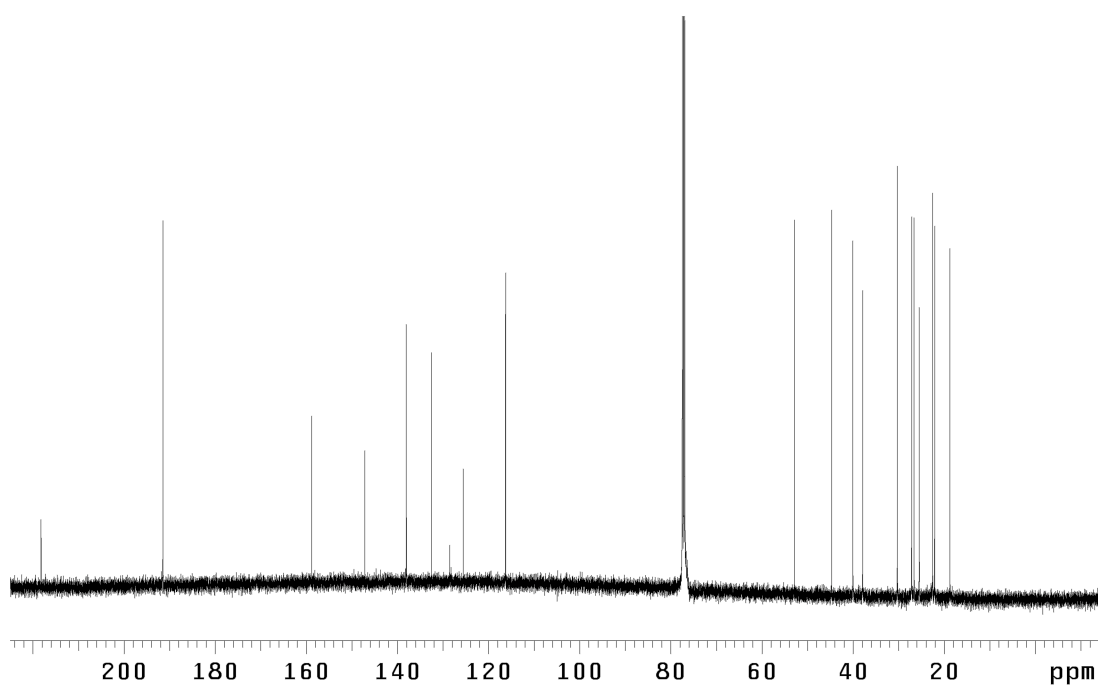


Figure A4.74 ¹³C NMR (125 MHz, CDCl₃) of compound **256**.



Figure A4.75 ^1H NMR (300 MHz, CDCl_3) of compound **257**.

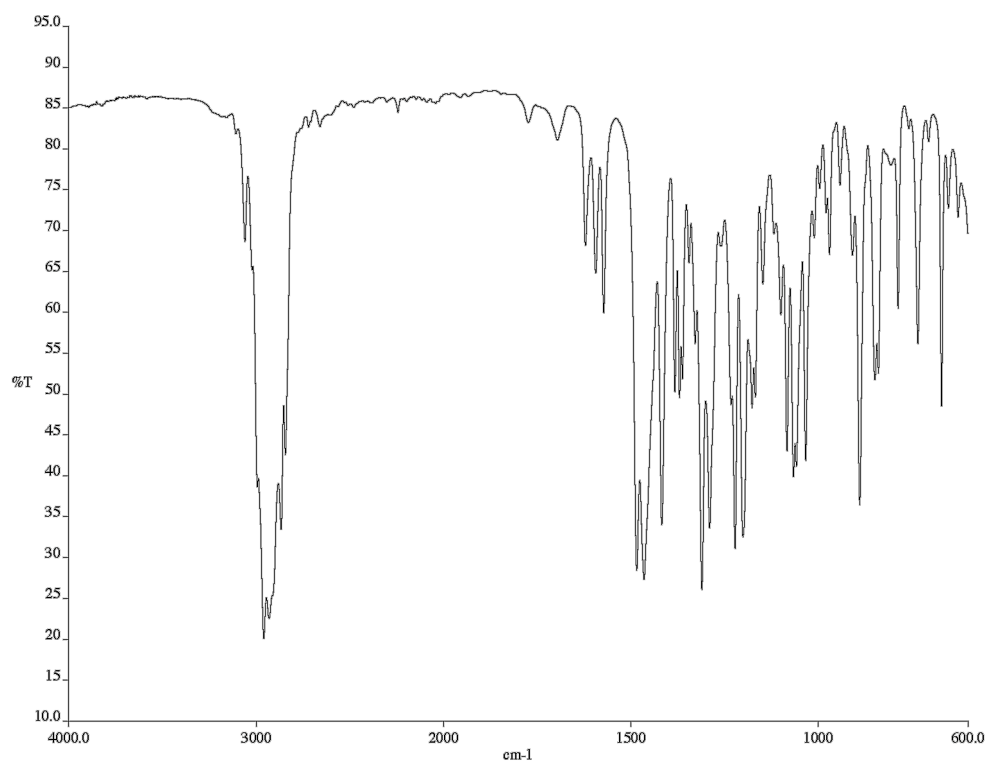


Figure A4.76 Infrared spectrum (NaCl/CDCl₃) of compound **257**.

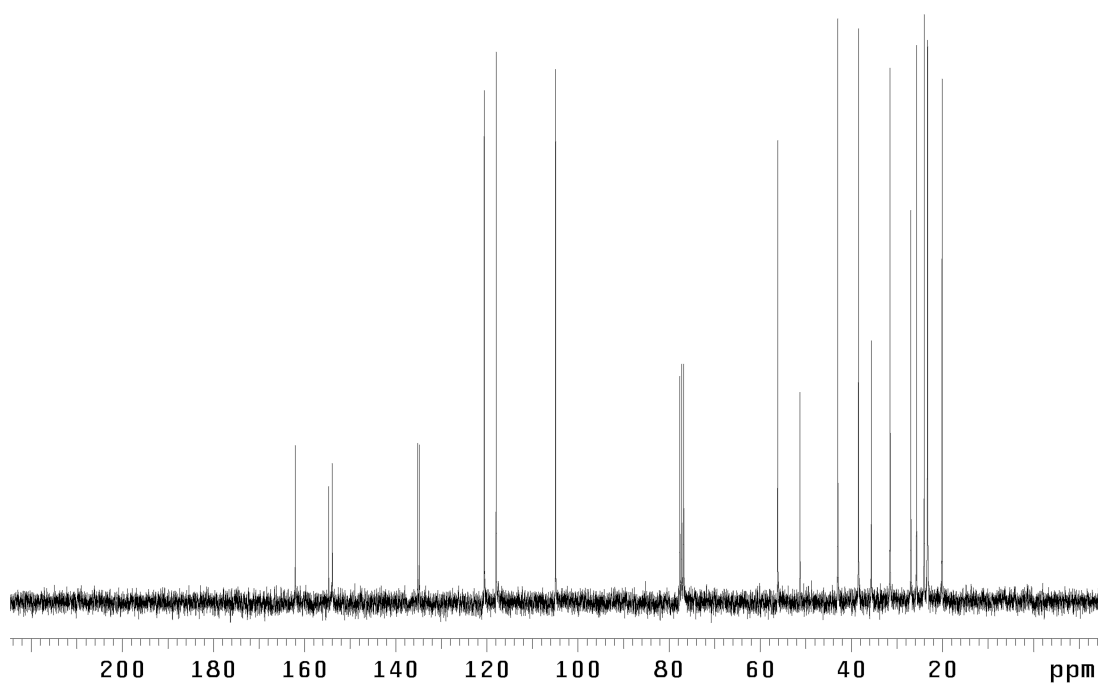


Figure A4.77 ¹³C NMR (75 MHz, CDCl₃) of compound **257**.

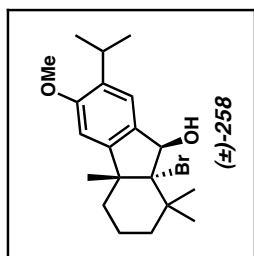


Figure A4.78 ^1H NMR (300 MHz, CDCl_3) of compound **258**.

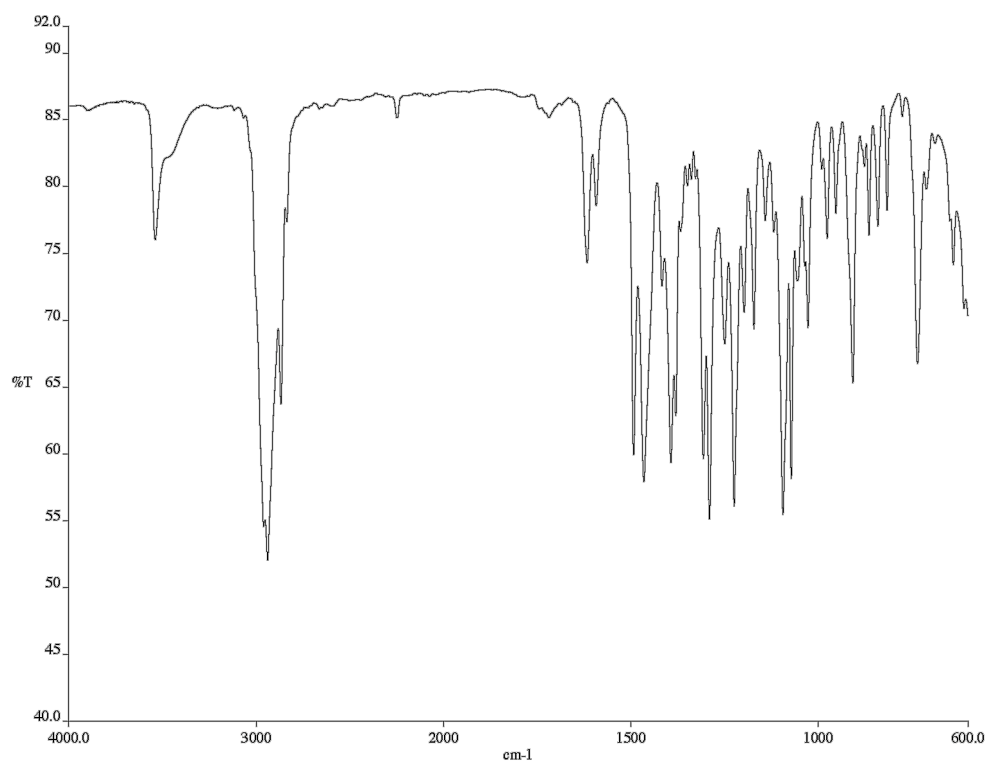


Figure A4.79 Infrared spectrum (NaCl/CDCl₃) of compound **258**.

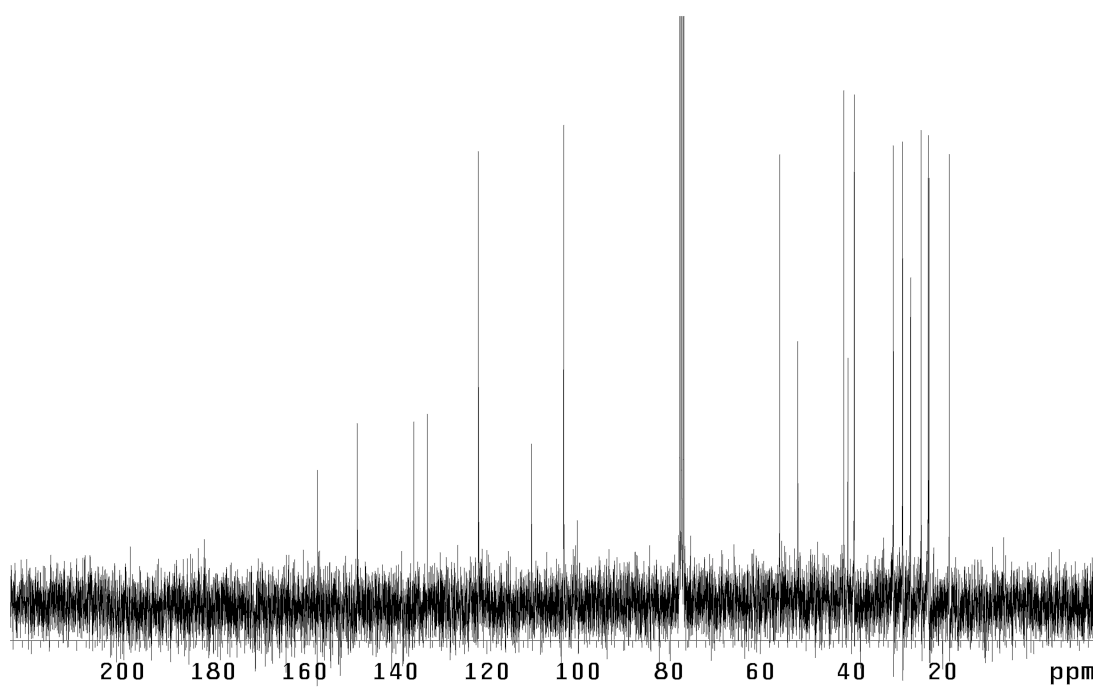


Figure A4.80 ¹³C NMR (75 MHz, CDCl₃) of compound **258**.

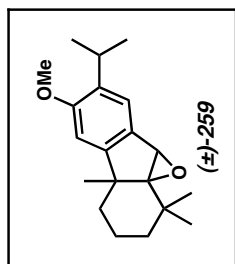


Figure A4.81 ¹H NMR (300 MHz, CDCl₃) of compound **259**.

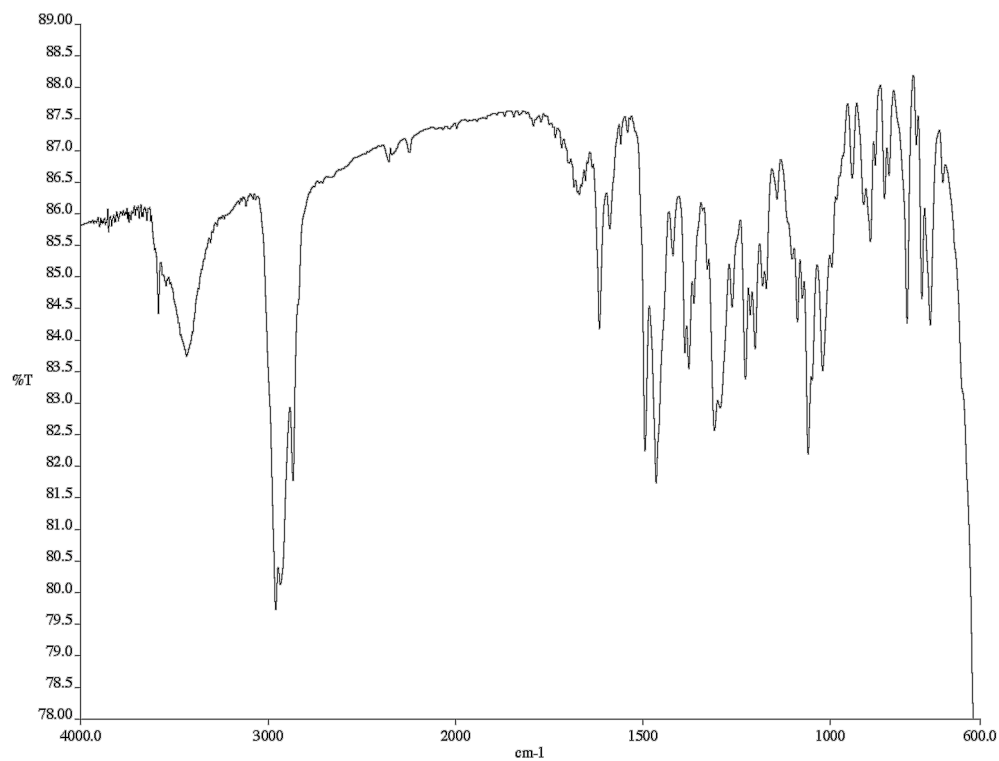


Figure A4.82 Infrared spectrum (NaCl/CDCl₃/D₂O) of compound **259**.

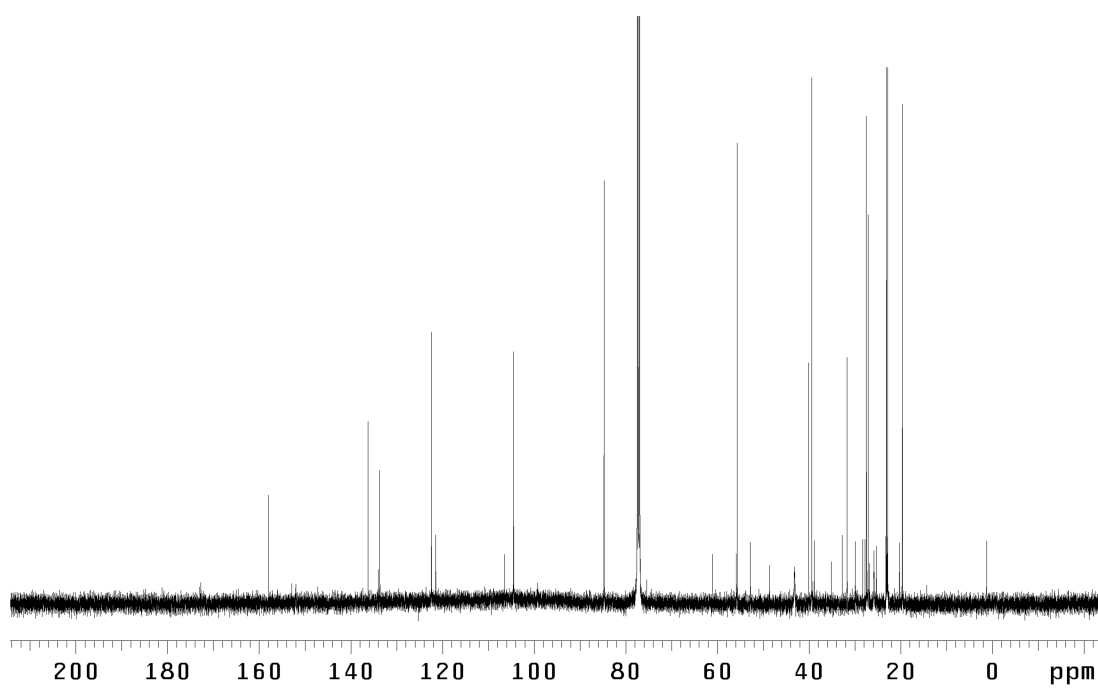


Figure A4.83 ¹³C NMR (125 MHz, CDCl₃) of compound **259**.

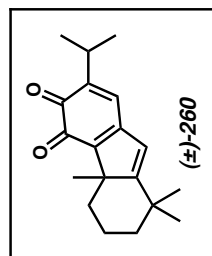
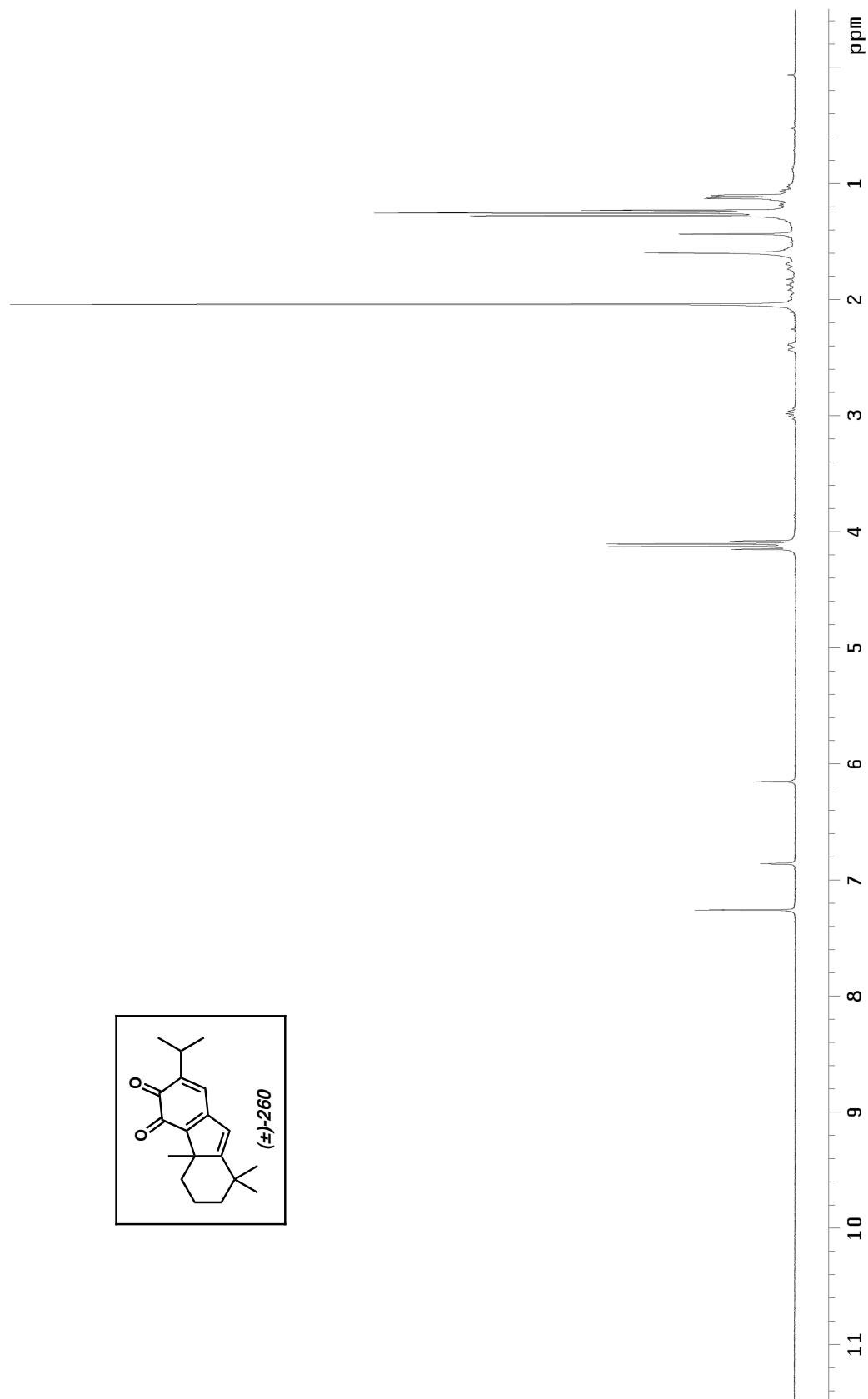


Figure A4.84 ^1H NMR (300 MHz, C_6D_6) of compound **260**.

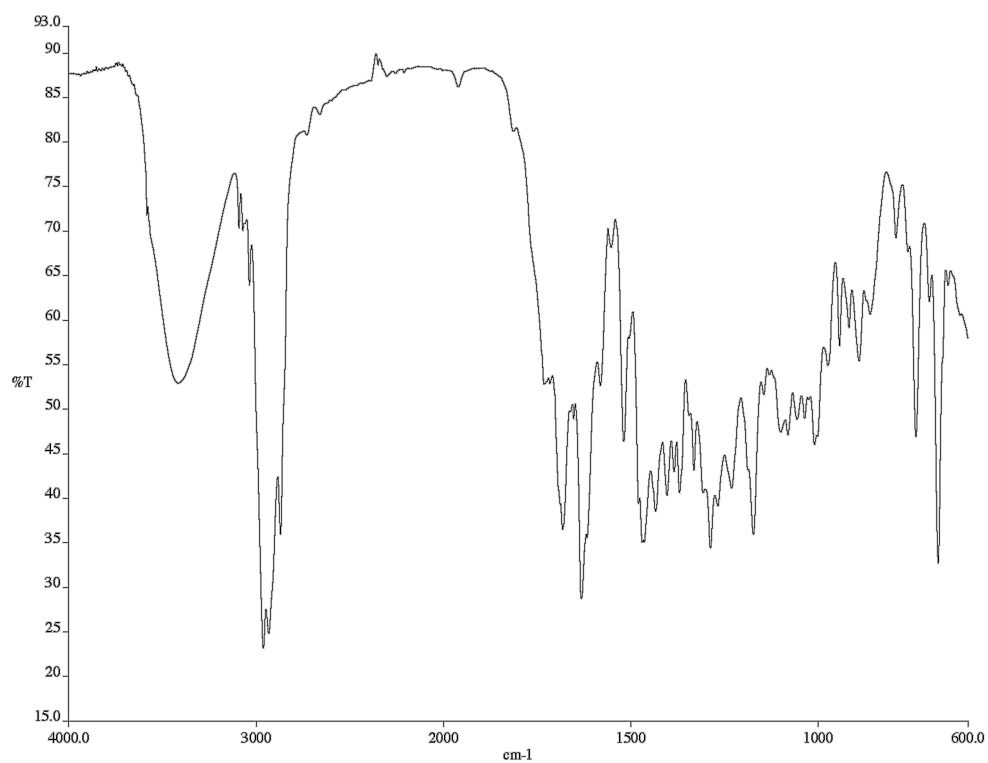


Figure A4.85 Infrared spectrum (NaCl/neat) of compound **260**.

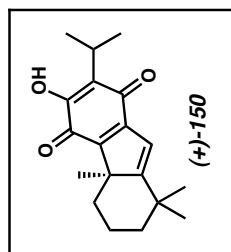
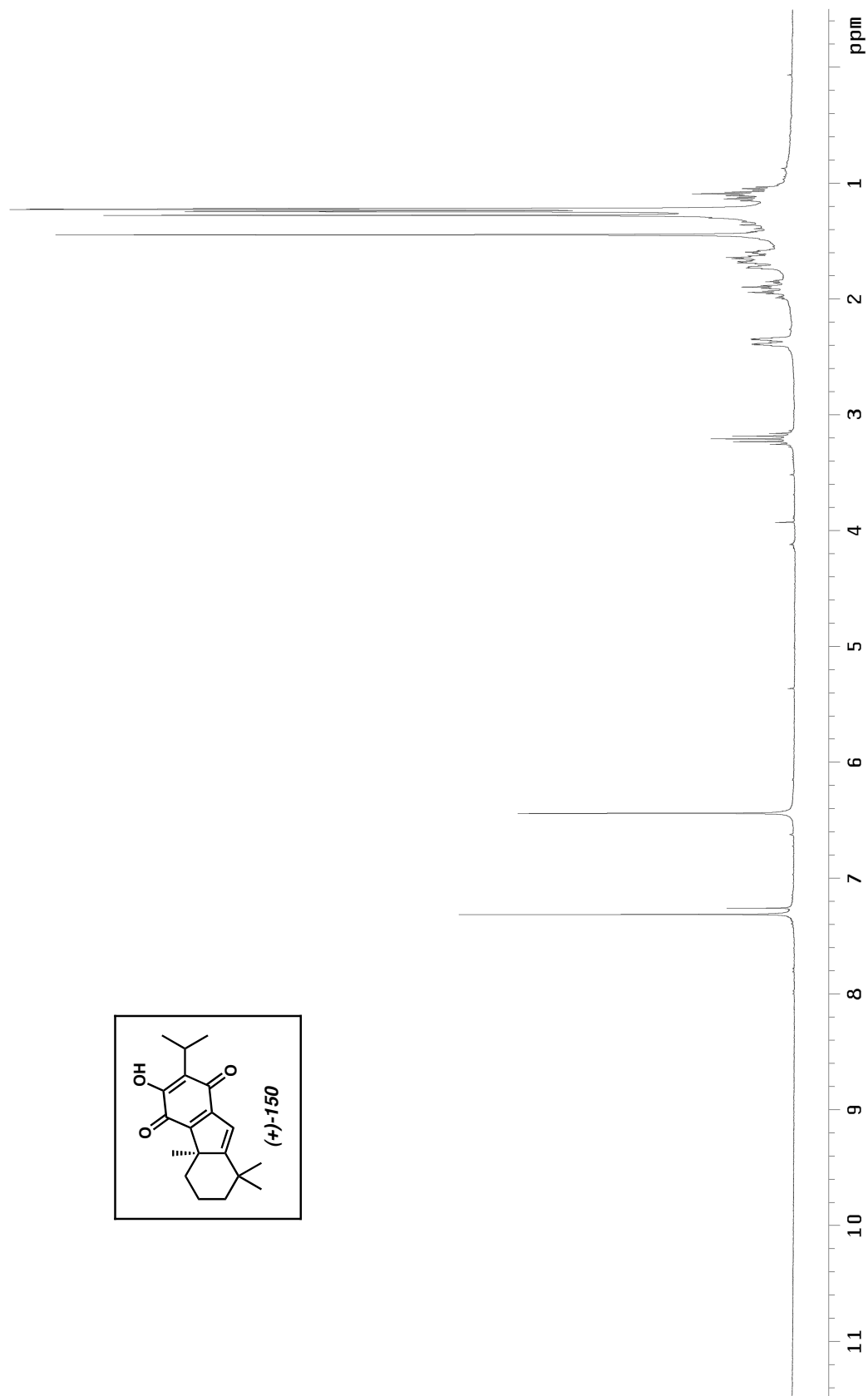


Figure A4.86 ^1H NMR (300 MHz, CDCl_3) of compound **150**.

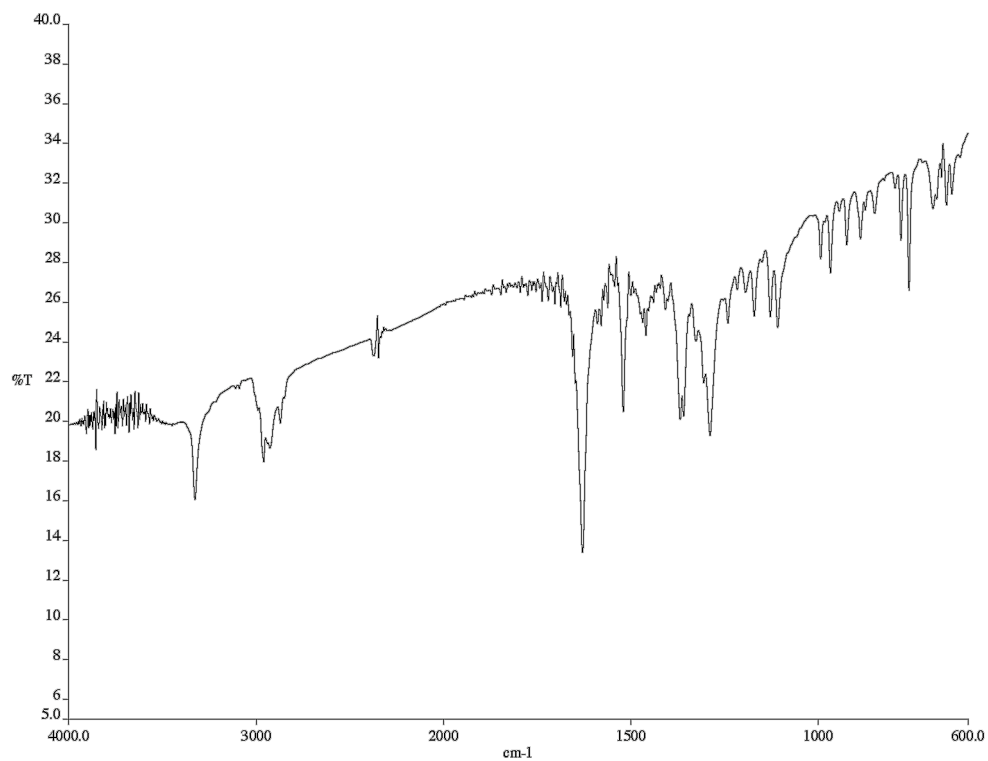


Figure A4.87 Infrared spectrum (KBr) of compound **150**.

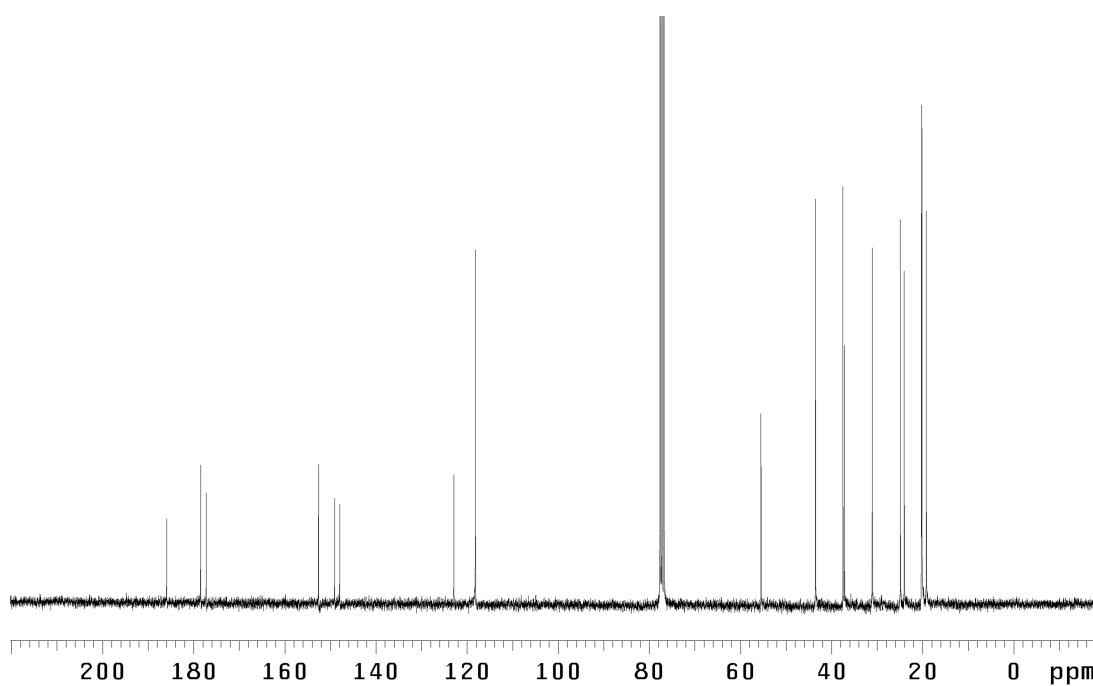


Figure A4.88 ¹³C NMR (75 MHz, CDCl₃) of compound **150**.

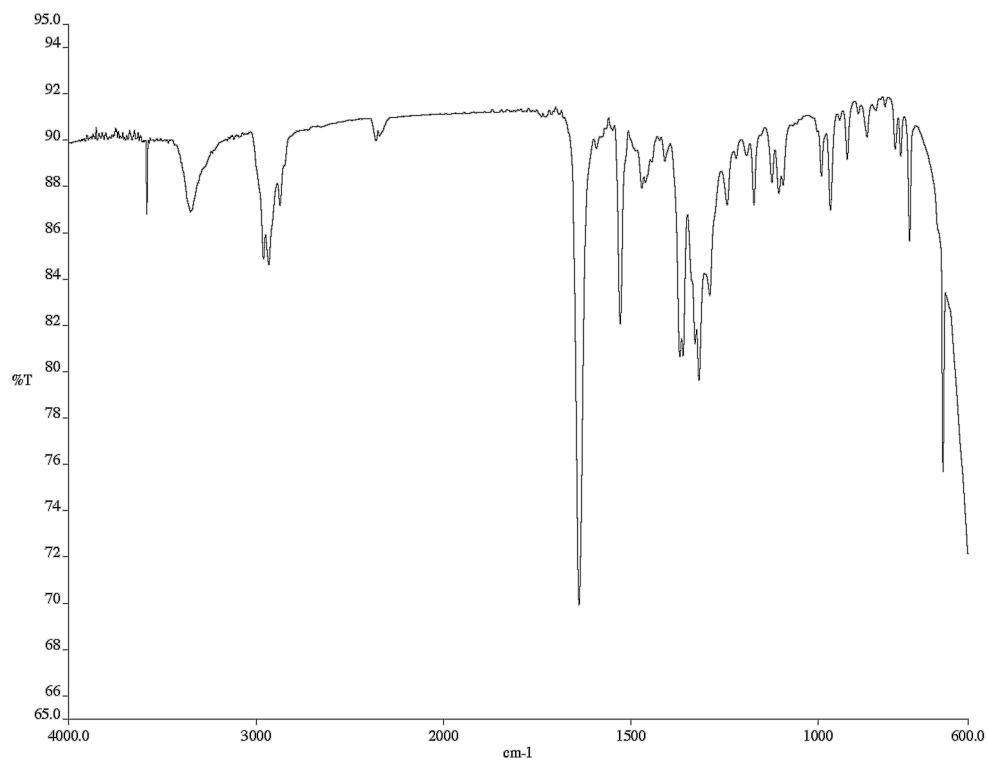


Figure A4.89 Infrared spectrum (NaCl/CHCl₃) of compound **150**.

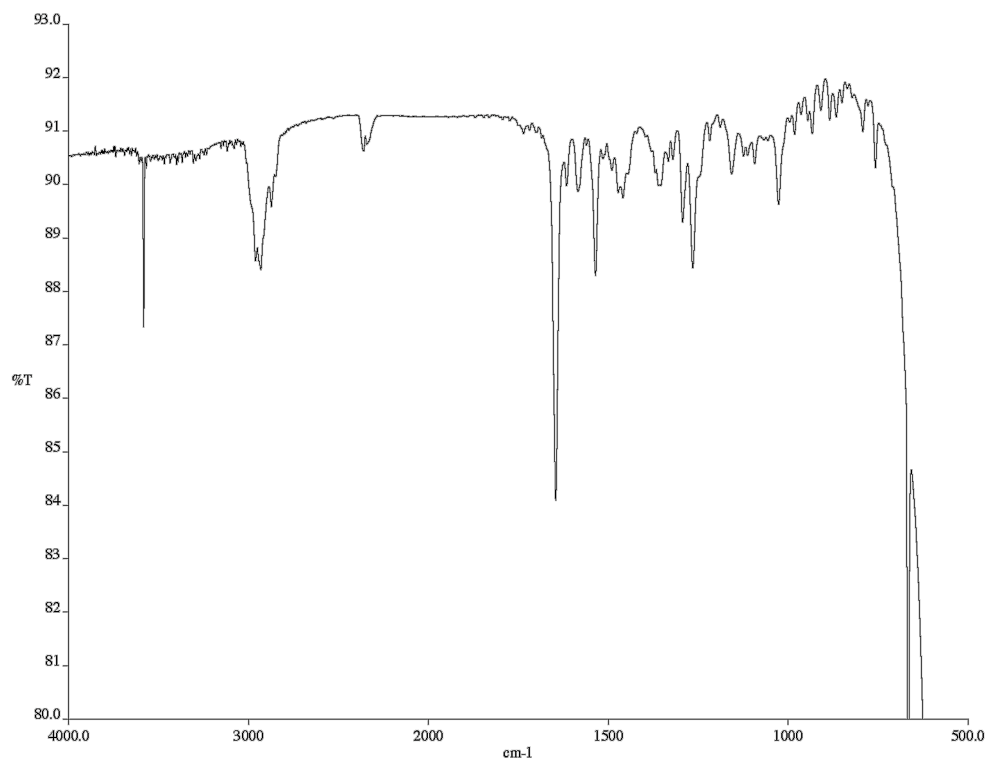


Figure A4.91 Infrared spectrum (NaCl/CHCl₃) of compound **267**.

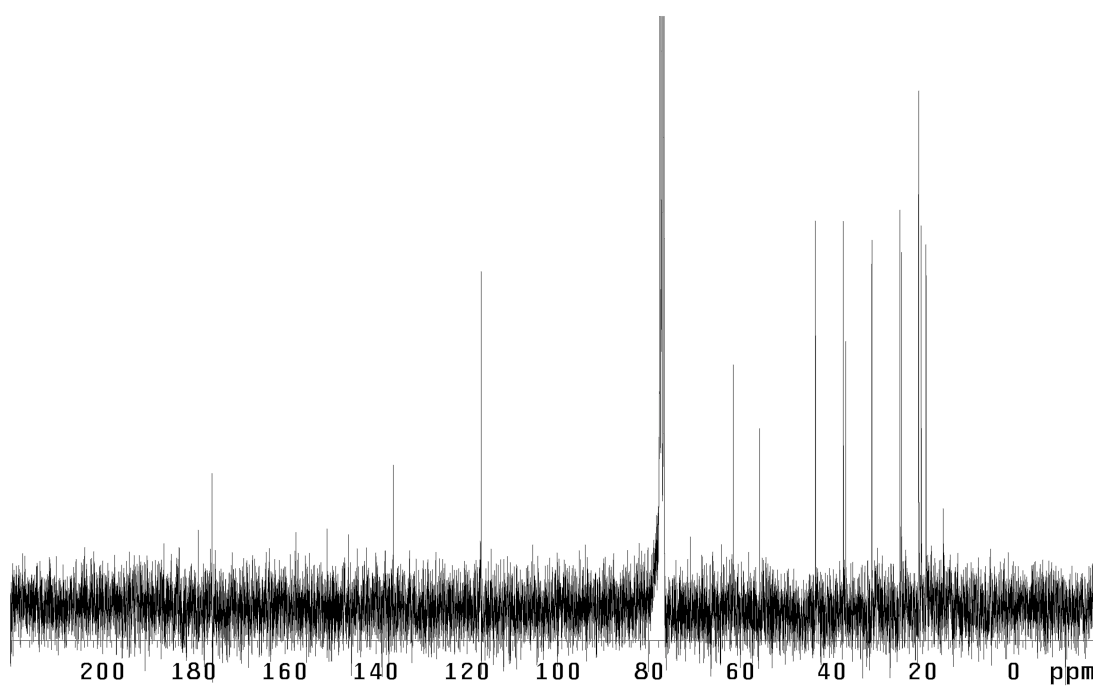
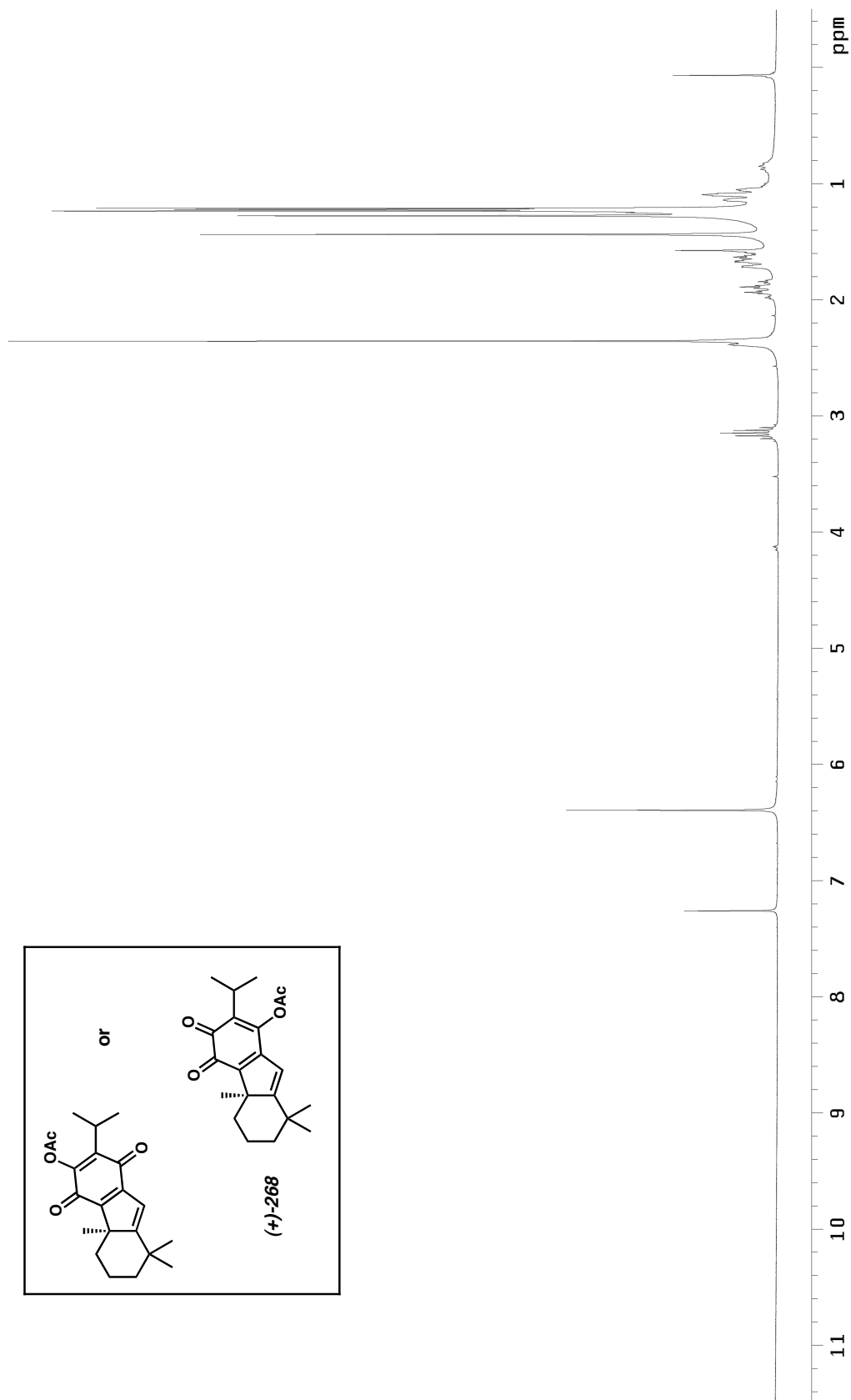


Figure A4.92 ¹³C NMR (75 MHz, CDCl₃) of compound **267**.

Figure A4.93 ^1H NMR (300 MHz, CDCl_3) of compound **268**.

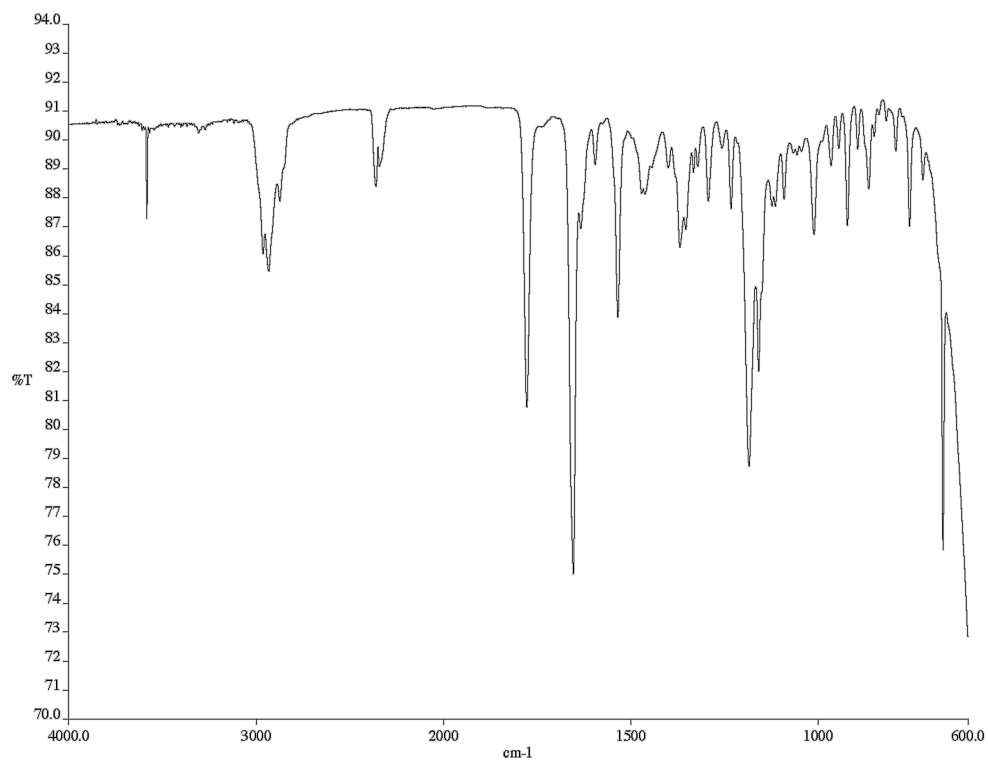


Figure A4.94 Infrared spectrum (NaCl/CHCl₃) of compound **268**.

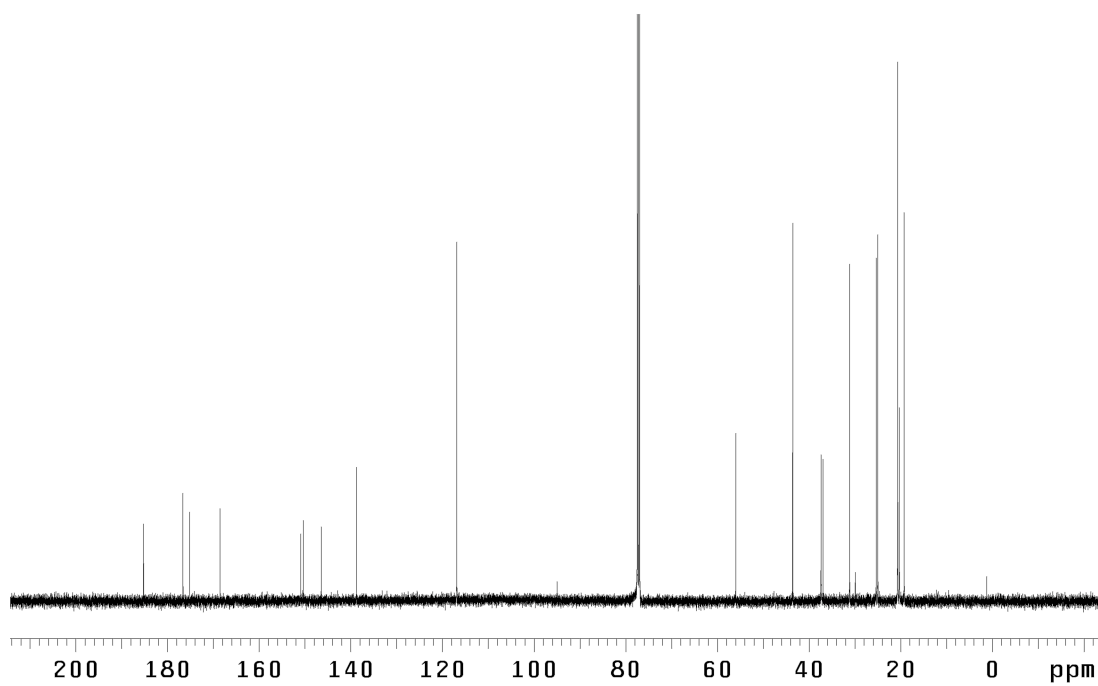
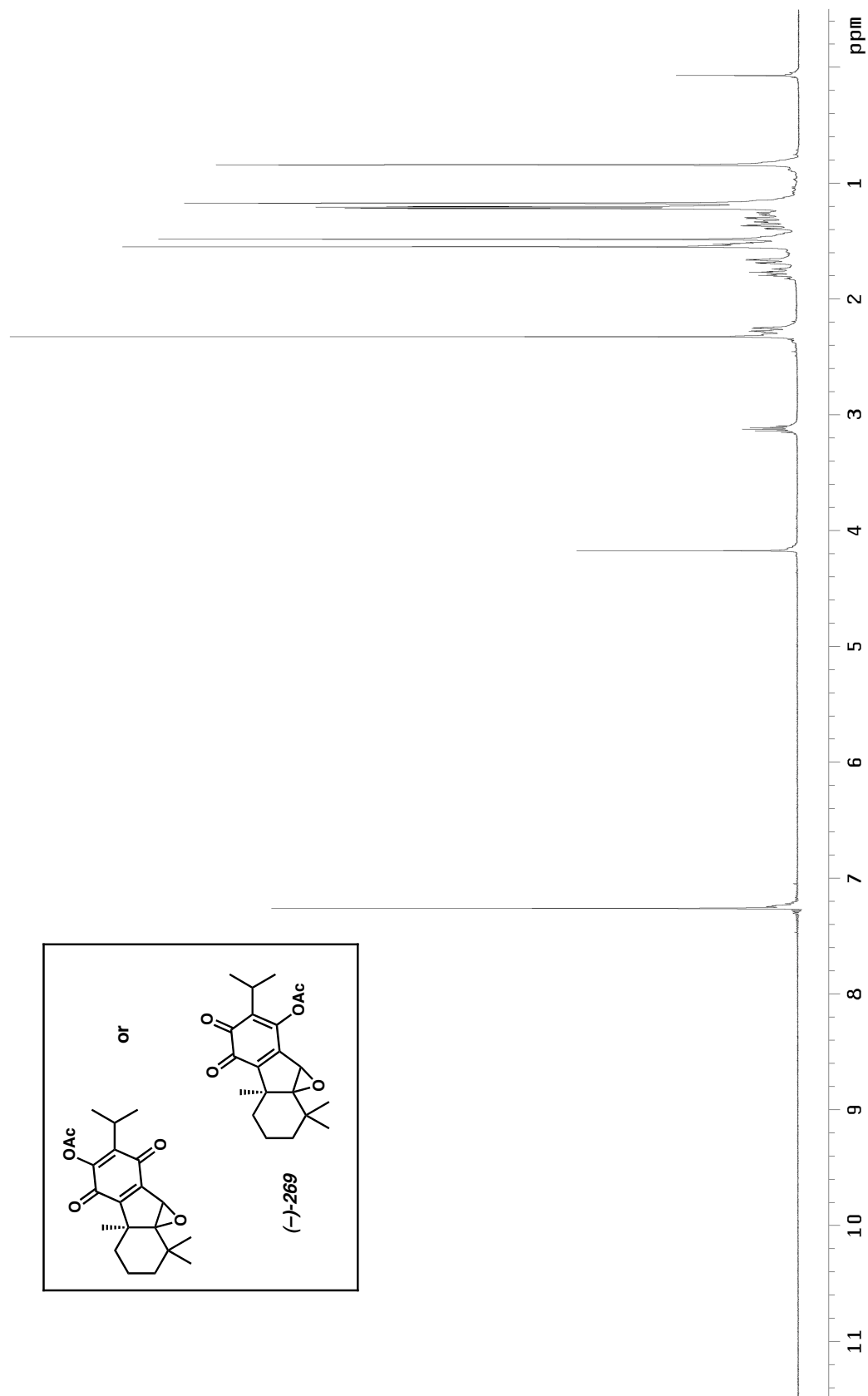


Figure A4.95 ¹³C NMR (125 MHz, CDCl₃) of compound **268**.

Figure A4.96 ^1H NMR (300 MHz, CDCl_3) of compound **269**.

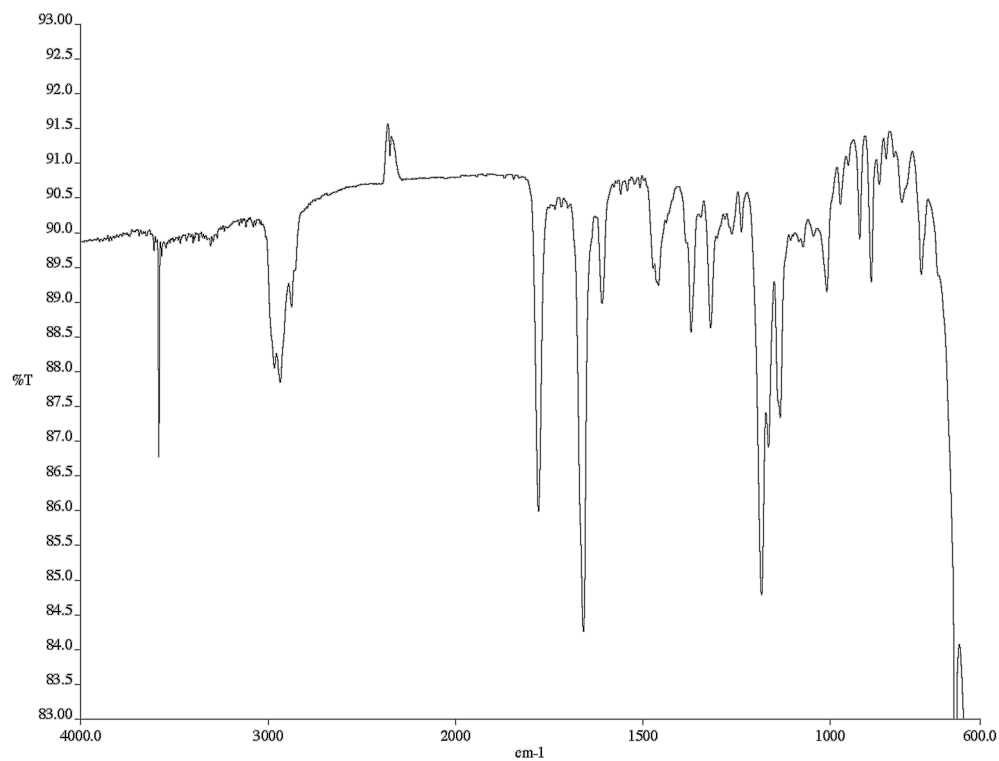


Figure A4.97 Infrared spectrum (NaCl/CHCl₃) of compound **269**.

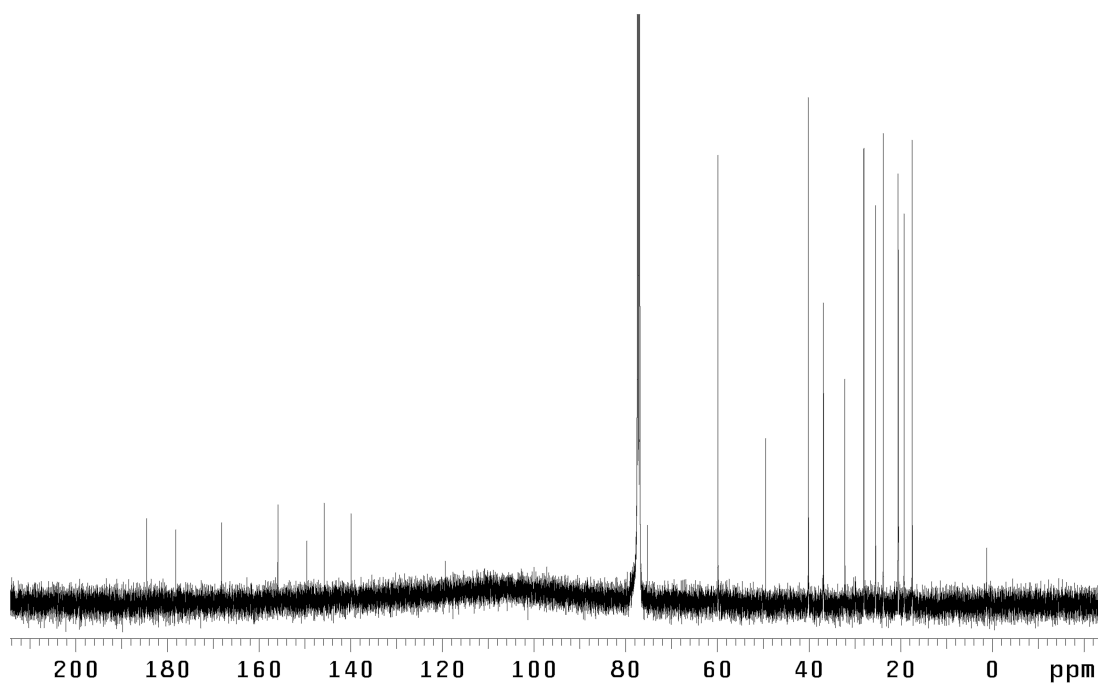


Figure A4.98 ¹³C NMR (125 MHz, CDCl₃) of compound **269**.

Appendix FIVE

X-Ray Crystallographic Data Relevant to Chapter 3

CALIFORNIA INSTITUTE OF TECHNOLOGY
BECKMAN INSTITUTE
X-RAY CRYSTALLOGRAPHY LABORATORY

Date 22 December 2005

Crystal Structure Analysis of:

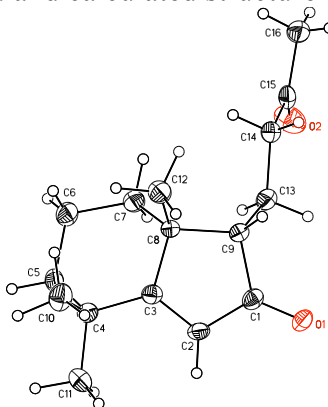
233

(shown below)

For	Investigator: Ryan McFadden	ext. 6131
	Advisor: B. M. Stoltz	ext. 6064
	Account Number: BMS1.SQUIBB-2.22-GRANT.SQUIBB1	
By	Michael W. Day	116 Beckman ext. 2734 e-mail: mikeday@caltech.edu

Contents

Table 1. Crystal data
Figures Figures
Table 2. Atomic Coordinates
Table 3. Full bond distances and angles
Table 4. Anisotropic displacement parameters
Table 5. Hydrogen atomic coordinates
Table 6. Observed and calculated structure factors (available upon request)



233

Note: The crystallographic data have been deposited in the Cambridge Database (CCDC) and have been placed on hold pending further instructions from me. The deposition number is 293604. Ideally, the CCDC would like the publication to contain a footnote of the type: "Crystallographic data have been deposited at the CCDC, 12 Union Road, Cambridge CB2 1EZ, UK and copies can be obtained on request, free of charge, by quoting the publication citation and the deposition number 293604."

Table 1. Crystal data and structure refinement for 233 (CCDC 293604).

Empirical formula	$C_{16}H_{24}O_2$	
Formula weight	248.35	
Crystallization Solvent	From melt	
Crystal Habit	Plate	
Crystal size	0.36 x 0.27 x 0.03 mm ³	
Crystal color	Colorless	
Data Collection		
Type of diffractometer	Bruker SMART 1000	
Wavelength	0.71073 Å MoK α	
Data Collection Temperature	100(2) K	
θ range for 3103 reflections used in lattice determination	2.82 to 27.84°	
Unit cell dimensions	a = 7.2276(13) Å b = 9.3724(17) Å c = 10.3744(18) Å	$\beta = 92.231(3)^\circ$
Volume	702.2(2) Å ³	
Z	2	
Crystal system	Monoclinic	
Space group	P2 ₁	
Density (calculated)	1.175 Mg/m ³	
F(000)	272	
Data collection program	Bruker SMART v5.630	
θ range for data collection	1.96 to 27.87°	
Completeness to $\theta = 27.87^\circ$	93.6 %	
Index ranges	$-9 \leq h \leq 9, -11 \leq k \leq 12, -13 \leq l \leq 13$	
Data collection scan type	ω scans at 3 ϕ settings	
Data reduction program	Bruker SAINT v6.45A	
Reflections collected	6194	
Independent reflections	2968 [$R_{\text{int}} = 0.0422$]	
Absorption coefficient	0.075 mm ⁻¹	
Absorption correction	None	
Max. and min. transmission	0.9977 and 0.9734	

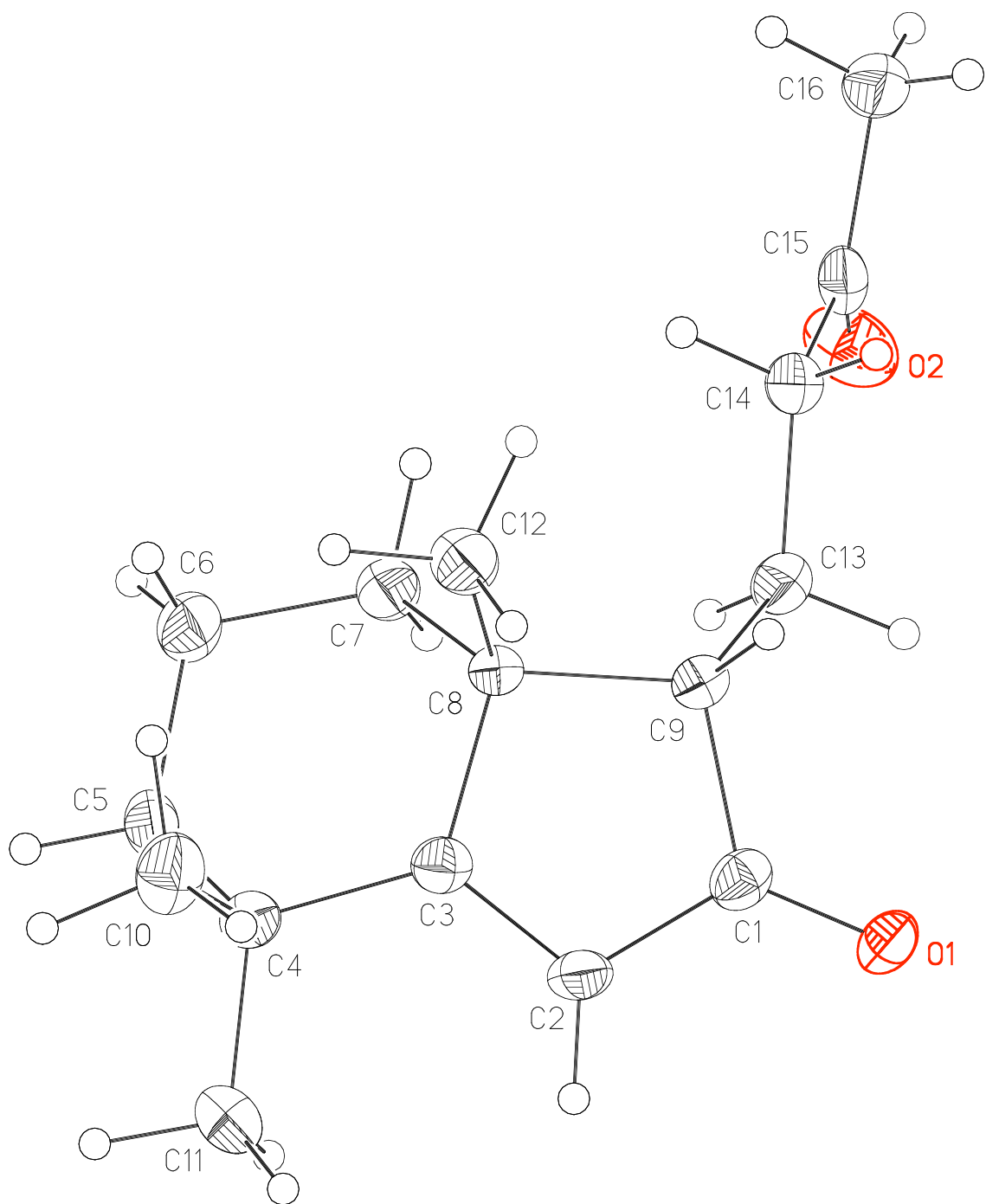
Table 1 (cont.)**Structure solution and Refinement**

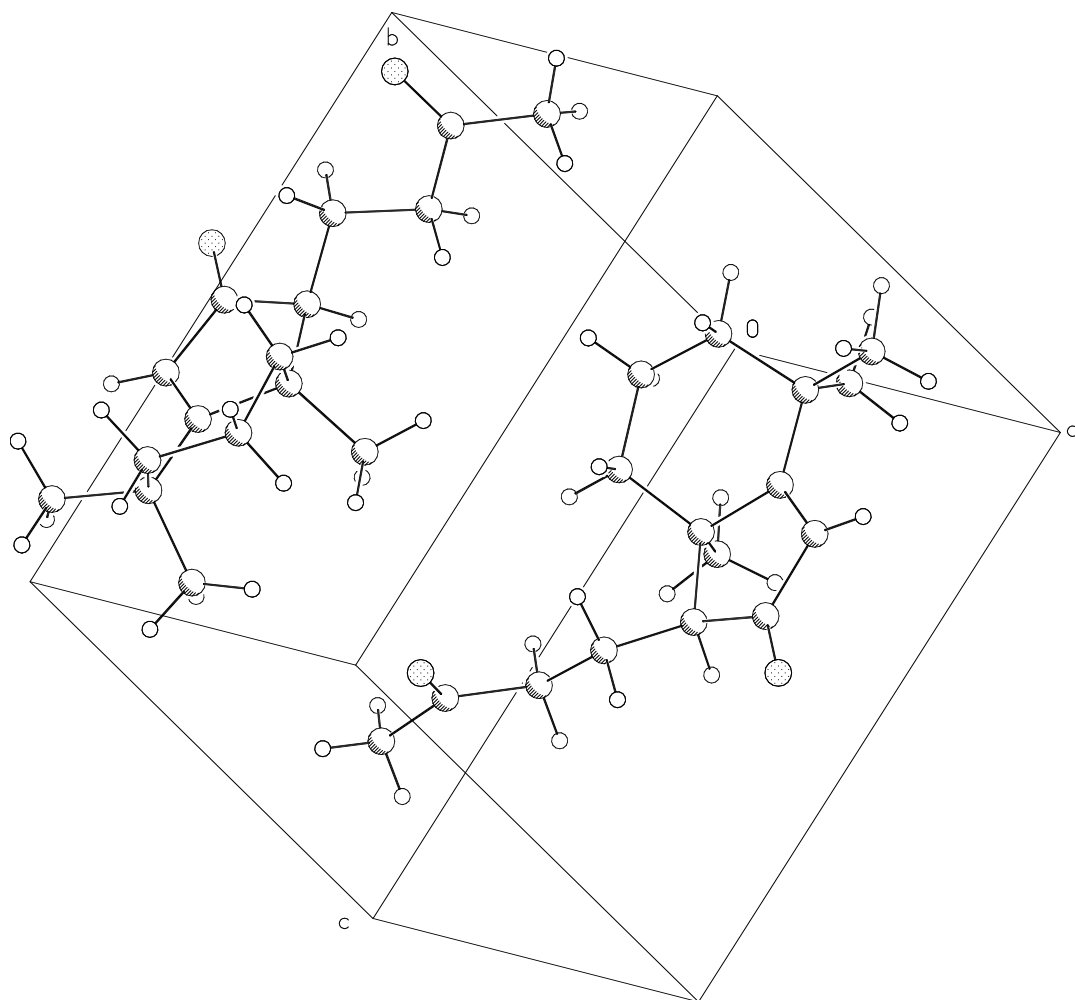
Structure solution program	Bruker XS v6.12
Primary solution method	Direct methods
Secondary solution method	Difference Fourier map
Hydrogen placement	Difference Fourier map
Structure refinement program	Bruker XL v6.12
Refinement method	Full matrix least-squares on F^2
Data / restraints / parameters	2968 / 1 / 259
Treatment of hydrogen atoms	Unrestrained
Goodness-of-fit on F^2	1.379
Final R indices [$I > 2\sigma(I)$, 2464 reflections]	$R_1 = 0.0417$, $wR_2 = 0.0708$
R indices (all data)	$R_1 = 0.0528$, $wR_2 = 0.0729$
Type of weighting scheme used	Sigma
Weighting scheme used	$w = 1/\sigma^2(F_o^2)$
Max shift/error	0.000
Average shift/error	0.000
Absolute structure determination	Not able to determine
Absolute structure parameter	-0.5(12)
Largest diff. peak and hole	0.279 and -0.197 e. \AA^{-3}

Special Refinement Details

Refinement of F^2 against ALL reflections. The weighted R-factor (wR) and goodness of fit (S) are based on F^2 . Conventional R-factors (R) are based on F , with F set to zero for negative F^2 . The threshold expression of $F^2 > 2\sigma(F^2)$ is used only for calculating R-factors(gt), etc., and is not relevant to the choice of reflections for refinement. R-factors based on F^2 are statistically about twice as large as those based on F , and R-factors based on ALL data will be even larger.

All esds (except the esd in the dihedral angle between two l.s. planes) are estimated using the full covariance matrix. The cell esds are taken into account individually in the estimation of esds in distances, angles and torsion angles; correlations between esds in cell parameters are only used when they are defined by crystal symmetry. An approximate (isotropic) treatment of cell esds is used for estimating esds involving l.s. planes.





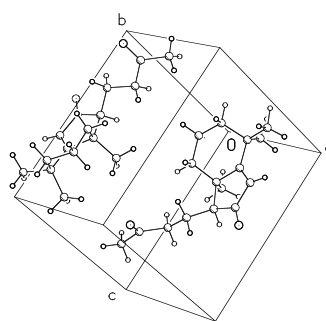
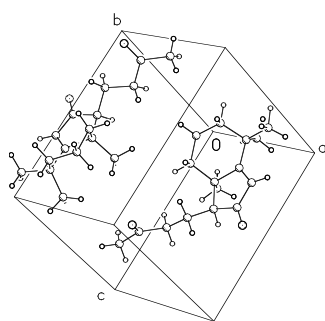


Table 2. Atomic coordinates ($\times 10^4$) and equivalent isotropic displacement parameters ($\text{\AA}^2 \times 10^3$) for 233 (CCDC 293604). $U(\text{eq})$ is defined as the trace of the orthogonalized U^{ij} tensor.

	x	y	z	U_{eq}
O(1)	-2410(2)	8958(1)	3790(1)	26(1)
O(2)	3287(2)	11505(2)	1446(1)	43(1)
C(1)	-1126(2)	8961(2)	4599(2)	22(1)
C(2)	-1246(2)	9098(2)	5978(2)	24(1)
C(3)	438(2)	9136(2)	6569(2)	21(1)
C(4)	845(2)	9489(2)	7970(2)	24(1)
C(5)	2195(3)	10768(2)	7999(2)	25(1)
C(6)	3847(3)	10570(2)	7160(2)	30(1)
C(7)	3246(3)	10291(2)	5743(2)	25(1)
C(8)	1987(2)	8962(2)	5616(2)	19(1)
C(9)	904(2)	8804(2)	4288(2)	22(1)
C(10)	1666(3)	8214(2)	8718(2)	33(1)
C(11)	-912(3)	9929(3)	8641(2)	37(1)
C(12)	3162(3)	7620(2)	5848(2)	28(1)
C(13)	1425(3)	9737(2)	3163(2)	25(1)
C(14)	3226(3)	9280(2)	2556(2)	26(1)
C(15)	3946(3)	10329(2)	1605(2)	27(1)
C(16)	5601(3)	9861(3)	880(2)	32(1)

Table 3. Bond lengths [Å] and angles [°] for 233 (CCDC 293604).

O(1)-C(1)	1.2264(18)	C(2)-C(3)-C(8)	112.01(14)
O(2)-C(15)	1.209(2)	C(4)-C(3)-C(8)	121.71(14)
C(1)-C(2)	1.442(2)	C(3)-C(4)-C(11)	111.34(16)
C(1)-C(9)	1.522(2)	C(3)-C(4)-C(10)	111.95(16)
C(2)-C(3)	1.342(2)	C(11)-C(4)-C(10)	106.99(18)
C(2)-H(2)	0.934(16)	C(3)-C(4)-C(5)	106.74(15)
C(3)-C(4)	1.508(2)	C(11)-C(4)-C(5)	108.48(17)
C(3)-C(8)	1.531(2)	C(10)-C(4)-C(5)	111.33(16)
C(4)-C(11)	1.528(3)	C(6)-C(5)-C(4)	113.88(17)
C(4)-C(10)	1.532(3)	C(6)-C(5)-H(5B)	111.9(11)
C(4)-C(5)	1.546(3)	C(4)-C(5)-H(5B)	108.7(11)
C(5)-C(6)	1.516(3)	C(6)-C(5)-H(5A)	112.0(10)
C(5)-H(5B)	1.02(2)	C(4)-C(5)-H(5A)	109.7(10)
C(5)-H(5A)	0.975(18)	H(5B)-C(5)-H(5A)	99.7(14)
C(6)-C(7)	1.539(3)	C(5)-C(6)-C(7)	111.68(17)
C(6)-H(6B)	1.01(2)	C(5)-C(6)-H(6B)	114.1(11)
C(6)-H(6A)	0.98(2)	C(7)-C(6)-H(6B)	107.2(11)
C(7)-C(8)	1.545(3)	C(5)-C(6)-H(6A)	107.9(11)
C(7)-H(7A)	0.974(19)	C(7)-C(6)-H(6A)	106.5(12)
C(7)-H(7B)	0.939(19)	H(6B)-C(6)-H(6A)	109.3(16)
C(8)-C(12)	1.532(3)	C(6)-C(7)-C(8)	111.21(16)
C(8)-C(9)	1.565(2)	C(6)-C(7)-H(7A)	113.1(11)
C(9)-C(13)	1.518(3)	C(8)-C(7)-H(7A)	108.5(11)
C(9)-H(9)	1.02(2)	C(6)-C(7)-H(7B)	109.4(11)
C(10)-H(10A)	1.03(2)	C(8)-C(7)-H(7B)	110.4(11)
C(10)-H(10B)	0.96(2)	H(7A)-C(7)-H(7B)	104.0(15)
C(10)-H(10C)	1.05(2)	C(3)-C(8)-C(12)	113.62(16)
C(11)-H(11A)	0.96(2)	C(3)-C(8)-C(7)	107.62(16)
C(11)-H(11C)	1.03(2)	C(12)-C(8)-C(7)	109.11(14)
C(11)-H(11B)	1.02(2)	C(3)-C(8)-C(9)	103.04(12)
C(12)-H(12C)	1.00(2)	C(12)-C(8)-C(9)	108.39(16)
C(12)-H(12B)	0.97(2)	C(7)-C(8)-C(9)	115.09(15)
C(12)-H(12A)	1.009(19)	C(13)-C(9)-C(1)	112.16(15)
C(13)-C(14)	1.529(3)	C(13)-C(9)-C(8)	119.48(16)
C(13)-H(13A)	1.04(2)	C(1)-C(9)-C(8)	104.92(14)
C(13)-H(13B)	1.006(19)	C(13)-C(9)-H(9)	103.6(11)
C(14)-C(15)	1.500(3)	C(1)-C(9)-H(9)	105.4(10)
C(14)-H(14B)	0.975(18)	C(8)-C(9)-H(9)	110.6(11)
C(14)-H(14A)	0.967(17)	C(4)-C(10)-H(10A)	114.3(12)
C(15)-C(16)	1.503(3)	C(4)-C(10)-H(10B)	108.7(14)
C(16)-H(16B)	0.90(3)	H(10A)-C(10)-H(10B)	112.0(18)
C(16)-H(16C)	0.96(2)	C(4)-C(10)-H(10C)	107.4(12)
C(16)-H(16A)	0.97(2)	H(10A)-C(10)-H(10C)	104.8(18)
		H(10B)-C(10)-H(10C)	109.3(19)
O(1)-C(1)-C(2)	127.29(15)	C(4)-C(11)-H(11A)	113.8(14)
O(1)-C(1)-C(9)	124.39(15)	C(4)-C(11)-H(11C)	106.3(11)
C(2)-C(1)-C(9)	108.32(14)	H(11A)-C(11)-H(11C)	108.7(18)
C(3)-C(2)-C(1)	111.57(15)	C(4)-C(11)-H(11B)	110.4(12)
C(3)-C(2)-H(2)	124.9(10)	H(11A)-C(11)-H(11B)	112.6(19)
C(1)-C(2)-H(2)	123.5(10)	H(11C)-C(11)-H(11B)	104.5(17)
C(2)-C(3)-C(4)	125.86(16)	C(8)-C(12)-H(12C)	110.1(10)

H(12C)-C(12)-H(12B)	106.1(17)
C(8)-C(12)-H(12A)	108.9(11)
H(12C)-C(12)-H(12A)	110.9(15)
H(12B)-C(12)-H(12A)	112.3(18)
C(9)-C(13)-C(14)	113.31(16)
C(9)-C(13)-H(13A)	108.5(10)
C(14)-C(13)-H(13A)	112.1(10)
C(9)-C(13)-H(13B)	105.7(11)
C(14)-C(13)-H(13B)	109.2(11)
H(13A)-C(13)-H(13B)	107.7(14)
C(15)-C(14)-C(13)	114.19(17)
C(15)-C(14)-H(14B)	104.2(11)
C(13)-C(14)-H(14B)	112.2(10)
C(15)-C(14)-H(14A)	108.8(11)
C(13)-C(14)-H(14A)	111.8(11)
H(14B)-C(14)-H(14A)	104.9(16)
O(2)-C(15)-C(14)	122.82(18)
O(2)-C(15)-C(16)	120.97(19)
C(14)-C(15)-C(16)	116.17(19)
C(15)-C(16)-H(16B)	107.5(13)
C(15)-C(16)-H(16C)	109.2(12)
H(16B)-C(16)-H(16C)	111(2)
C(15)-C(16)-H(16A)	111.7(14)
H(16B)-C(16)-H(16A)	107.1(19)
H(16C)-C(16)-H(16A)	110.2(18)

Table 4. Anisotropic displacement parameters ($\text{\AA}^2 \times 10^4$) for 233 (CCDC 293604). The anisotropic displacement factor exponent takes the form: $-2\pi^2 [h^2 a^{*2} U^{11} + \dots + 2 h k a^* b^* U^{12}]$

U^{11}	U^{22}	U^{33}	U^{23}	U^{13}	U^{12}
O(1)180(6)	311(7)	286(7)	-27(7)	-40(5)	-6(6)
O(2)528(10)	395(9)	366(9)	77(7)	117(7)	126(8)
C(1)197(9)	186(9)	286(10)	-22(10)	-10(7)	-15(9)
C(2)158(9)	286(11)	280(10)	-46(9)	48(8)	-18(9)
C(3)198(8)	187(10)	235(9)	-13(8)	25(7)	-10(8)
C(4)194(9)	276(11)	245(11)	-31(8)	19(8)	-18(8)
C(5)275(11)	285(12)	188(11)	-24(9)	-14(9)	-29(9)
C(6)274(12)	334(13)	283(12)	-24(10)	12(9)	-113(10)
C(7)229(11)	262(11)	253(11)	-14(9)	23(10)	-34(9)
C(8)155(8)	232(9)	182(9)	-7(9)	19(6)	-2(9)
C(9)165(9)	281(11)	216(10)	-13(9)	3(7)	10(9)
C(10)356(14)	334(13)	304(13)	45(10)	-32(11)	-83(11)
C(11)333(13)	531(16)	245(12)	-85(11)	59(10)	-24(12)
C(12)284(13)	285(12)	257(12)	15(10)	6(11)	65(10)
C(13)204(10)	305(12)	242(11)	9(9)	-16(8)	13(9)
C(14)220(10)	350(13)	197(10)	-4(9)	-5(8)	19(9)
C(15)263(11)	354(13)	181(10)	-50(9)	-51(8)	21(9)
C(16)247(12)	456(14)	253(12)	20(12)	25(10)	-38(11)

Table 5. Hydrogen coordinates ($\times 10^4$) and isotropic displacement parameters ($\text{\AA}^2 \times 10^3$) for 233 (CCDC 293604).

	x	y	z	U_{iso}
H(12C)	3900(30)	7703(19)	6684(19)	18(5)
H(14B)	4240(20)	9170(20)	3197(17)	24(5)
H(2)	-2360(20)	9190(20)	6393(15)	17(4)
H(16B)	5270(30)	9080(30)	420(20)	55(7)
H(5B)	1470(30)	11670(20)	7763(19)	31(6)
H(14A)	3110(20)	8356(19)	2145(16)	11(4)
H(5A)	2570(20)	10993(18)	8889(18)	17(5)
H(6B)	4700(30)	9760(20)	7443(19)	31(5)
H(9)	1030(20)	7790(20)	3938(18)	26(5)
H(13A)	1470(20)	10800(20)	3472(16)	20(5)
H(7A)	4290(30)	10165(18)	5186(17)	21(5)
H(16C)	6600(30)	9650(20)	1480(20)	35(6)
H(6A)	4550(30)	11460(20)	7172(18)	25(5)
H(7B)	2630(20)	11100(20)	5405(17)	20(5)
H(10A)	2990(30)	7960(20)	8490(20)	44(6)
H(11A)	-1810(30)	9180(30)	8690(20)	55(7)
H(12B)	2340(30)	6820(30)	5940(20)	45(7)
H(12A)	4000(30)	7490(20)	5104(19)	28(6)
H(11C)	-500(30)	10220(20)	9560(20)	33(5)
H(11B)	-1450(30)	10830(30)	8240(20)	44(6)
H(16A)	5970(30)	10580(20)	270(20)	42(6)
H(10B)	840(30)	7420(30)	8610(20)	46(7)
H(13B)	370(30)	9650(20)	2503(19)	26(5)
H(10C)	1770(30)	8500(20)	9690(20)	54(7)

CHAPTER FOUR

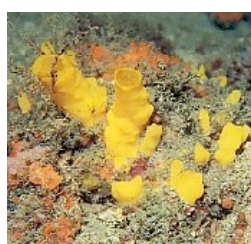
Progress Toward the Catalytic Enantioselective Total Synthesis of Liphagal

4.1 Background

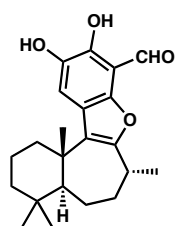
4.1.1 Isolation of the First Liphagane Natural Product, Liphagal

Liphagal (**271**), a tetracyclic meroterpenoid natural product, was recently isolated from the sponge *Aka coralliphaga*, native to Dominica (Figure 4.1).¹ Anderson, who isolated the natural product, assigned its structure and relative stereochemistry using multidimensional NMR techniques, later confirming the structural assignment via racemic total synthesis.¹ When Andersen isolated the molecule, he named its unprecedented framework, hallmarked by its unusual [6-7-5-6] tetracyclic core, the “liphagane” skeleton (**272**). To the best of our knowledge, no other liphaganes have been reported to date.

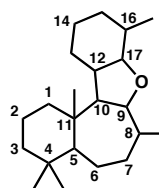
Figure 4.1 The Structure of Liphagal



Aka coralliphaga



Liphagal (**271**)



Liphagane
Skeleton **272**

4.1.2 Biological Activity of Liphagal

Liphagal (**271**) was isolated via bioactivity-guided extraction and reverse-phase chromatography. In particular, the isolation chemists were searching for potent inhibitors of phosphatidylinositol 3-kinase α (PI3K α) using a fluorescence polarization assay developed in SF9 insect cells.¹ Liphagal (**271**) was found to have an IC_{50} value of 100

nM against PI3K α in this primary assay. Secondary assays of the compound revealed substantial cytotoxicity toward various cancer cell lines. Against LoVo (human colon) cells, liphagal (**271**) displayed an IC₅₀ of 0.58 μ M, and against another cell line, CaCo (human colon), the IC₅₀ value was 0.67 μ M. Additionally, some cytotoxicity toward a breast cancer cell line, MDA-468 was observed (IC₅₀ = 1.58 μ M). Without a doubt, this natural product has significant biological activity and could be useful as a lead structure for chemotherapeutics development.

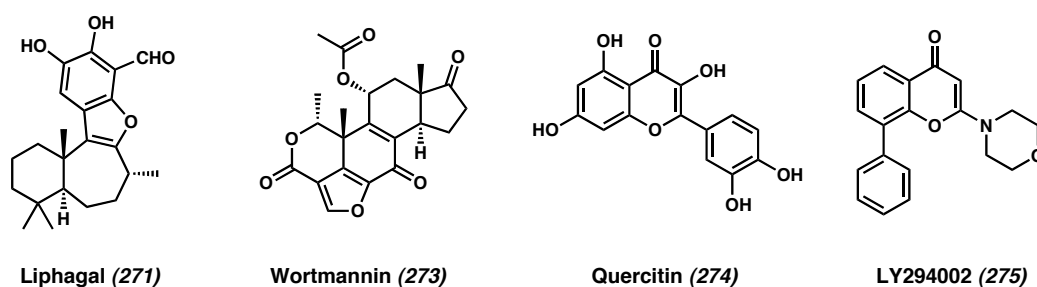
4.1.3 *Phosphatidylinositol 3-Kinases and their Biology*

Potentially the most significant finding about liphagal (**271**) is its selective inhibition of PI3K α relative to other PI3K's¹ because there are numerous kinases in the human genome.² The PI3K family of enzymes is intimately involved in numerous cellular pathways spanning proliferation, survival, adhesion, movement, differentiation, membrane trafficking, glucose transport, neurite outgrowth, and superoxide production in cells.³ Selective inhibitors of individual isoforms of these enzymes would allow for the targeting of specific diseases spanning cancer, cardiovascular disease, and autoimmune disorders.^{3,4} Liphagal (**271**) has an IC₅₀ of 100 nM against PI3K α and is at least 10-fold more potent against this isoform of the enzyme compared to any other PI3K.

Many natural product and synthetic inhibitors of PI3K's are known, but selective inhibition of an individual isoform is rare. Although the natural product wortmannin (**273**) shows an IC₅₀ of 12 nM toward PI3K α , it has nearly equal potency against several other related enzymes (Figure 4.2).^{1,5} Quercitin (**274**) and other molecules have already

been used in chemical genetics studies to understand the roles of certain PI3K's in cell signaling. Second generation synthetic molecules designed to mimic natural products (e.g., LY294002 (**275**)) have been developed and studied by the pharmaceutical industry.^{1,5,6} Though somewhat selective, molecules such as LY294002 (**275**) lack the potency of liphagal (**271**).¹ With its unique biological activity and potentially novel mode of action, liphagal (**271**) promises to be useful in the development of new therapeutics and as a chemical tool for studying cellular signaling and disease states.

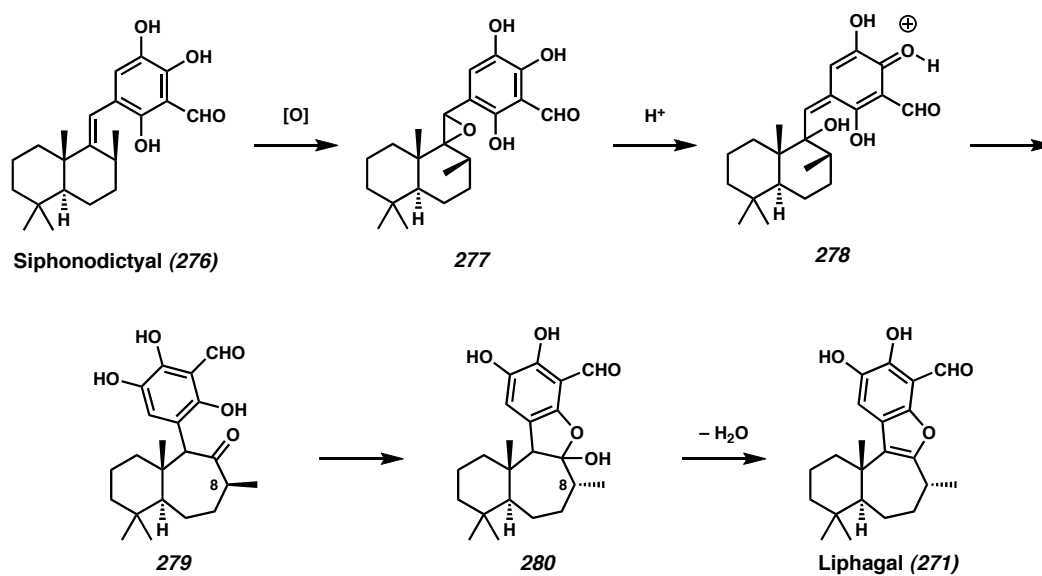
Figure 4.2 Selected Inhibitors of PI3K α



4.1.4 Biosynthetic Proposals

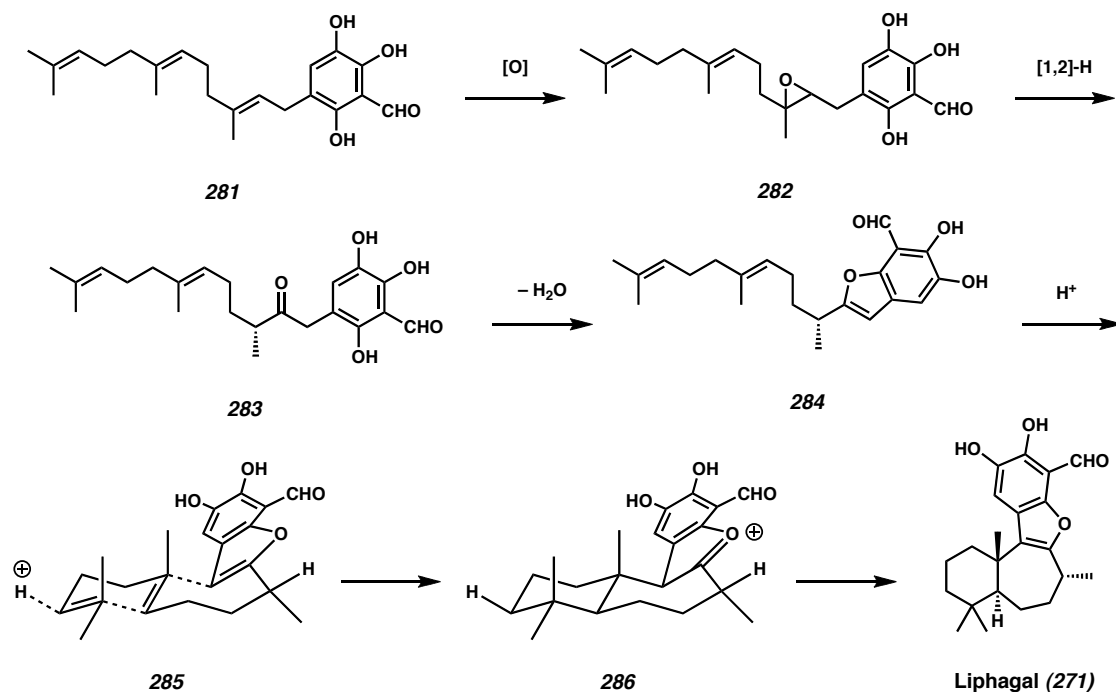
Andersen proposed that liphagal (**271**) could have one of several biosynthetic origins.¹ One of the first hypotheses discussed was the natural product's potential origination from siphonodictyal B (**276**) (Scheme 4.1). Oxidation of the trisubstituted olefin of **276** could be followed by an epoxide fragmentation-triggered ring expansion, generating the 7-membered ring of **279**. Epimerization of the C(8) stereocenter and phenolic condensation might ultimately lead to liphagal (**271**).

Scheme 4.1 Possible Biosynthesis of Liphagal from Siphonodictyal



Alternatively, the biosynthesis of **271** could begin with the polyisoprenylated arene **281** (Scheme 4.2). Oxidation of the olefin proximal to the electron-rich aromatic core, followed by a formal [1,2] H-shift, would lead to ketone **283**. A dehydrative cyclization might lead to the substituted benzofuran **284**, poised for an acid-induced polyene cyclization cascade. If a diastereoselective series of ring closures occurs, liphagal (**271**) could arise. It was this latter theory that inspired Andersen to complete the first and only total synthesis of liphagal (**271**) reported to date.¹

Scheme 4.2 Alternative Cationic Cyclization Proposal

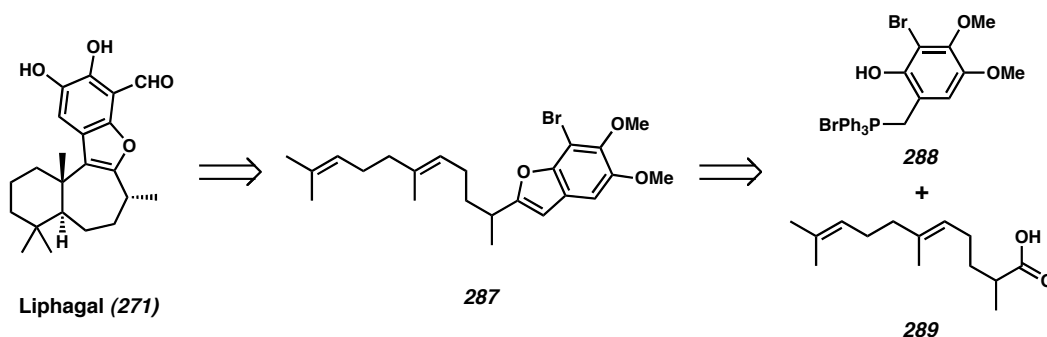


4.2 Andersen's Racemic Total Synthesis of Liphagal

4.2.1 Retrosynthetic Analysis

Andersen designed his retrosynthesis for the natural product based on the polyene cyclization cascade biosynthetic hypothesis.¹ Accordingly, liphagal (**271**) could arise from a diolefinic precursor **287** containing an electron-rich benzofuran moiety (Scheme 4.3). This aromatic system would serve as the terminating nucleophile in a biomimetic, acid-mediated polyene cyclization cascade. Retrosynthetically, **287** could be prepared from two fragments, a substituted phenol **288** and a carboxylic acid **289**, that could be unified via Wittig cyclization.

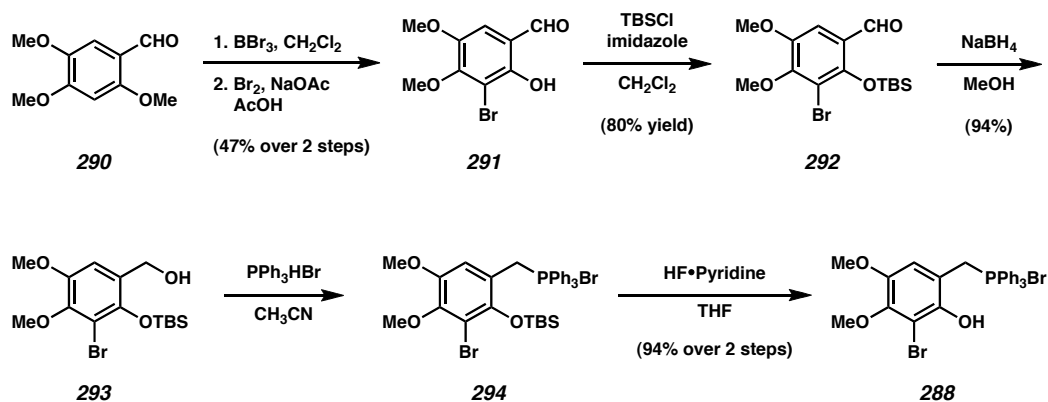
Scheme 4.3 Andersen's Retrosynthesis of Liphagal



4.2.2 Preparation of the Fragments

To begin the synthesis, the known aldehyde **290** was selectively demethylated and treated with bromine in buffered acetic acid to furnish 4,5-dimethoxy-3-bromosalicylaldehyde (**291**) in modest yield (Scheme 4.4). Protection of the free phenol with TBSCl and reduction of the benzaldehyde moiety led to the benzylic alcohol **293**. Treatment of **293** with triphenylphosphonium bromide in acetonitrile installed a quaternary phosphonium salt, giving **288** after treatment with HF•pyridine.

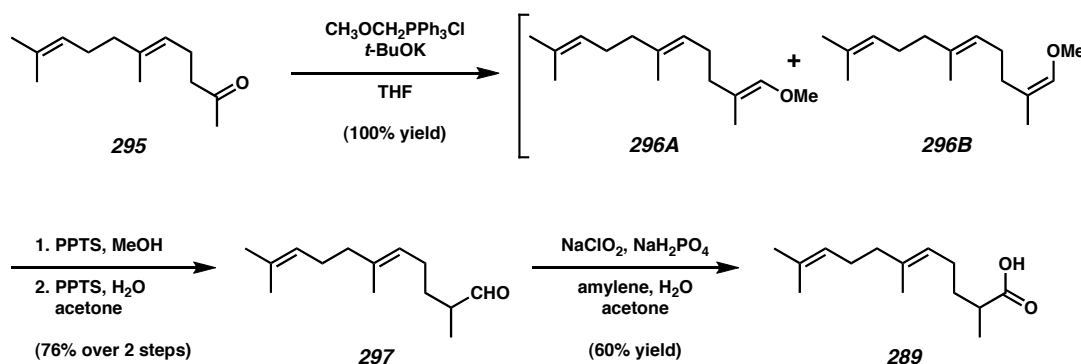
Scheme 4.4 Synthesis of the Aromatic Piece



The synthesis of the second fragment began with geranylacetone (**295**). When treated with methoxymethylene triphenylphosphonium chloride and base, **295** was

transformed to a mixture of methyl vinyl ethers **296A** and **296B** (Scheme 4.5). Conversion to the dimethyl acetal and hydrolysis afforded aldehyde **297** in good yield. Upon oxidation of **297** with buffered sodium chlorite, the requisite carboxylic acid **289** was complete.

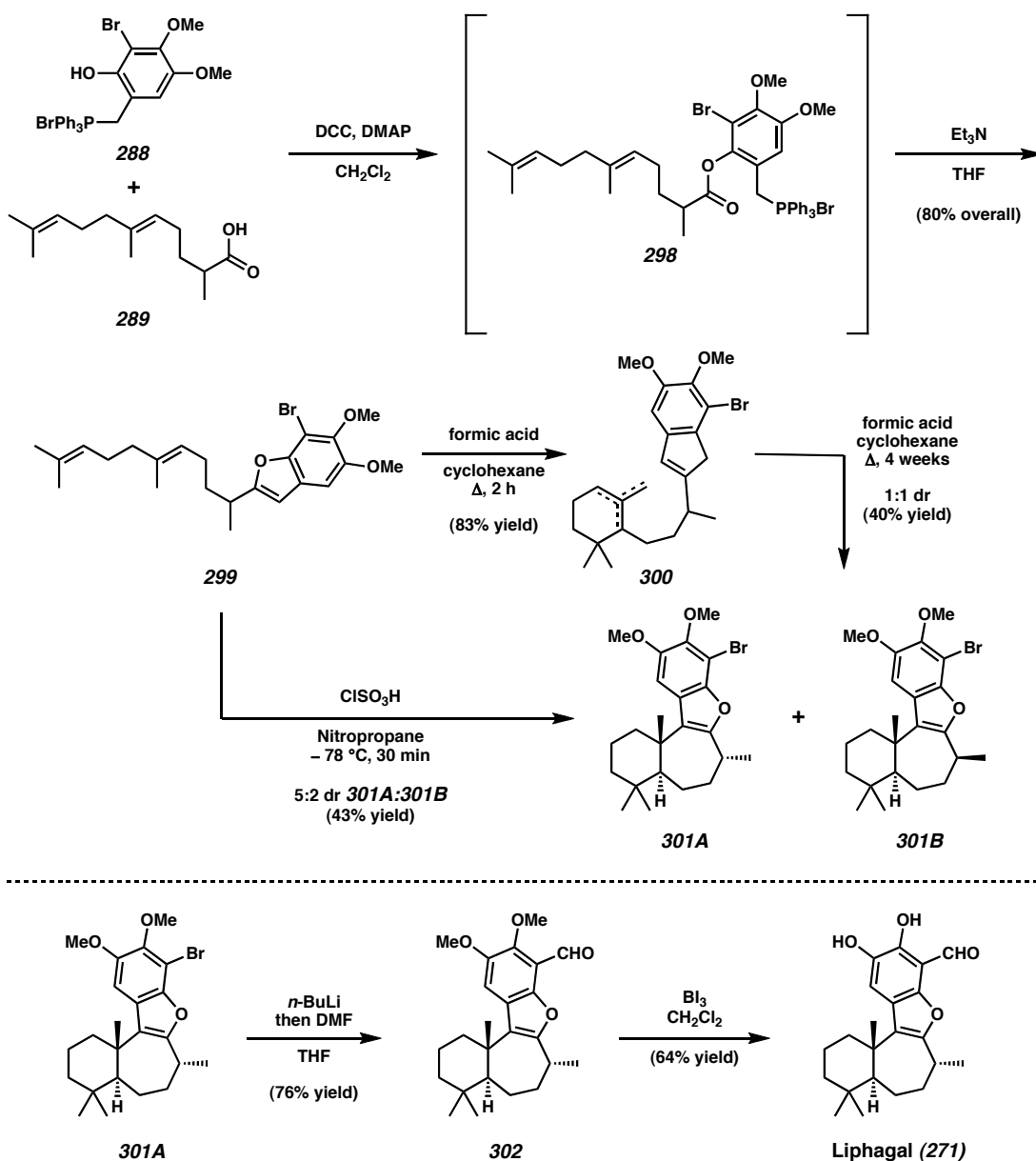
Scheme 4.5 Preparation of the Carboxylic Acid Coupling Partner



4.2.3 Completion of Racemic Liphagal

Once coupling partners **288** and **289** were complete, they were linked together using DCC and DMAP (Scheme 4.6). The intermediate **298** was not isolated, but rather subjected to mildly basic conditions, affecting an intramolecular Wittig cyclization of the resulting benzyl phosphonium ylide onto the carbonyl of the ester. The outcome was the completion of benzofuran **299**. Initially, the polyene cyclization approach was tested with formic acid as the promoter. Although the 6-membered ring cyclization to **300** readily occurred within two hours, more forcing conditions were necessary to close the 7-membered ring of the natural product. Unfortunately, the final ring closure had occurred with poor diastereoselectivity and modest conversion even over a four-week period.

Scheme 4.6 Completion of the Natural Product



Ultimately, these challenges were surmounted when the precursor **299** was treated with chlorosulfonic acid in nitropropane (as opposed to formic acid) at low temperature. In this case both requisite ring closures occurred during a thirty-minute timeframe, favoring the correct diastereomer **301A** in 5:2 dr for completion of the synthesis. Metal halogen exchange followed by DMF quench was used to install the aldehyde of **302**.

Didemethylation with BI_3 at $-78\text{ }^\circ\text{C}$ then completed Andersen's total synthesis of (\pm)-liphagal (**271**).⁷

4.3 First Retrosynthetic Analysis of Liphagal

4.3.1 *Challenges for Synthesizing Liphagal*

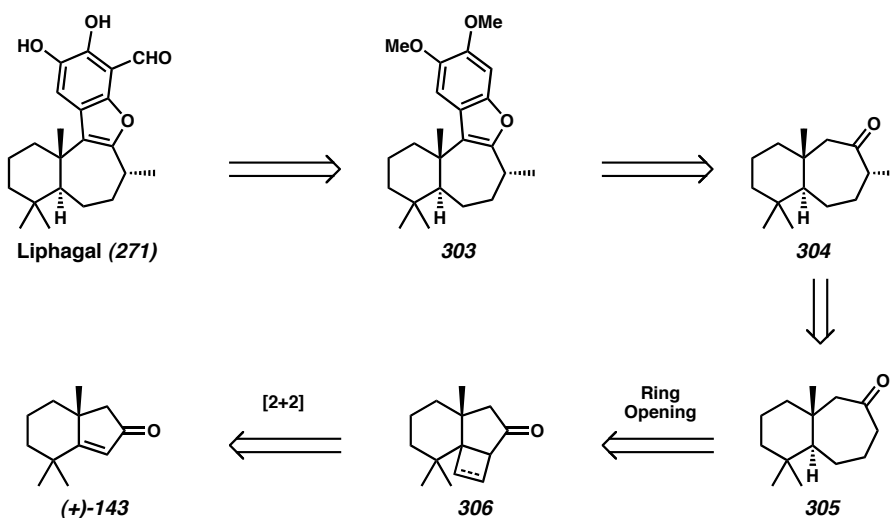
We became interested in liphagal (**271**) as a synthetic target for several reasons. First, the molecule has a unique carbocyclic architecture including a highly oxidized benzofuran ring system, saturated *trans*-fused [6-7] bicyclic domain, and three stereocenters. One of these is an all-carbon quaternary stereocenter. When we began the endeavor of synthesizing liphagal (**271**), the absolute stereochemistry of the natural product was unknown, but we anticipated that our enantioselective decarboxylative alkylation could be used to set the quaternary stereocenter, eventually determining the absolute stereochemistry of the natural product. Finally, our total synthesis would also serve to develop and apply new synthetic methods, while gaining insight about the chemistry of [6-7] bicyclic systems.

Andersen's synthesis employed a biosynthetic approach to the molecule in an elegant manner.¹ However, in light of the natural product's significant biological activity, we wanted an approach more amenable to the synthesis of analogues. Having derivatives in hand, we could probe the structure-activity-relationship of the natural product with respect to PI3K's, determining which moieties are necessary pharmacophores for activity.

4.3.2 Retrosynthetic Analysis

Examination of liphagal (**271**) revealed potentially sensitive catechol and aldehyde moieties; thus we opted to install them toward the end of the synthesis. Therefore, we thought liphagal (**271**) could arise from a protected benzofuran (**303**) (Scheme 4.7). We anticipated that the benzofuran might originate from the bicyclic ketone (\pm)-**304** via an annulation sequence. Bicyclic methyl ketone (\pm)-**304** might be accessible from the simpler cycloheptanone (\pm)-**305**, which could be synthesized from an angularly-fused [6-5-4] cyclobutane or cyclobutene **306** via ring opening. The 4-membered ring of **306** could arise from photoaddition of ethylene or acetylene to a bicyclic enone (+)-**143**. We decided to prepare the enantiomer of the enone (–)-**143** present in the dichroanone synthesis since we thought that liphagal (**271**) belonged to the same enantiomeric series as natural (–)-dichroanone ((–)-**150**).⁸

Scheme 4.7 First Retrosynthetic Analysis of Liphagal

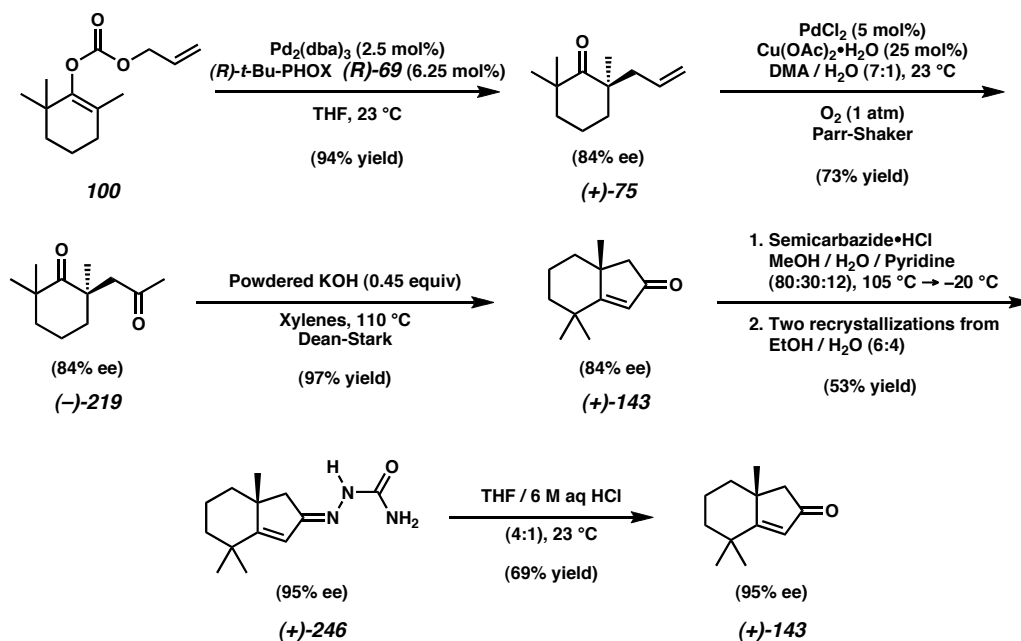


4.4 A Photochemical Approach to the [6-7] Ring System

4.4.1 Synthesis of the Bicyclic Enone Antipode

Our total synthesis effort commenced with enol carbonate **100**, prepared during our dichroanone synthesis.⁸ Treatment of **100** with catalytic (*R*)-*t*-Bu-PHOX (*R*)-**69** and Pd₂(dba)₃ resulted in the preparation of allyl ketone (+)-**75** in 84% ee (Scheme 4.8). Wacker oxidation of (+)-**75** led to the 1,4-diketone (–)-**219** in good yield.⁹ This compound was cyclized under aldol condensation conditions, furnishing the bicyclic enone (+)-**143** in high yield.¹⁰ After transformation to the semicarbazone (+)-**246** followed by recrystallization, the ee was elevated to 95%. Hydrolysis under acidic conditions gave the enantioenriched bicyclic enone (+)-**143**, which would be used to investigate the preparation of the 7-membered ring of liphagal (**271**).¹¹

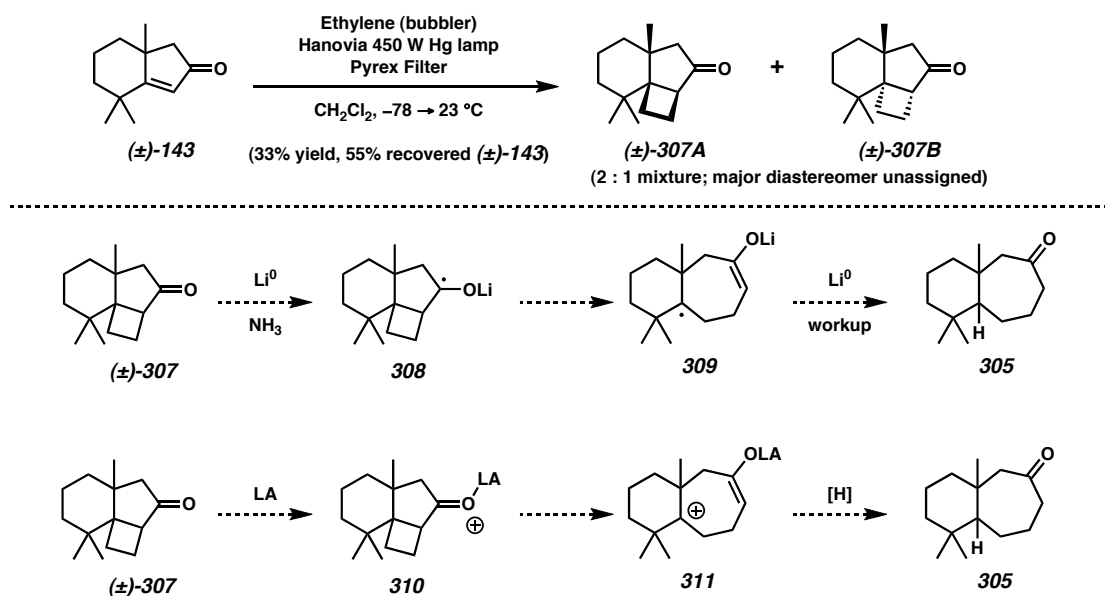
Scheme 4.8 Preparation of the Bicyclic Enone



4.4.2 Photochemical Investigations

To build a 7-membered ring compound from our [6-5] bicyclic enone, a 2-carbon spacer would need to be inserted. We hoped that photoaddition of ethylene in a [2 + 2] sense to our bicyclic enone **(+)-143** would accomplish this goal.^{12,13} To this end, a solution of **(±)-143** in CH₂Cl₂ was saturated with ethylene gas at low temperature and irradiated with light from a medium-pressure mercury lamp. To our delight, a slow but productive cycloaddition occurred, and two diastereomeric, angularly fused cyclobutanes **(±)-307A** and **(±)-307B** were obtained in a modest yield (Scheme 4.9).

Scheme 4.9 Angularly-Fused Cyclobutanes

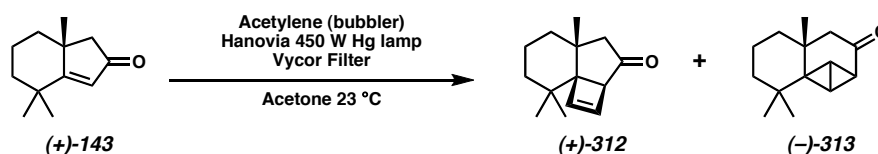


We believed that a reductive ring opening of the 4-membered rings of **(±)-307A** and **(±)-307B** could be achieved. One might envision reduction of the ketone to a cyclobutyl carbinyl radical **308**, possibly prone to cyclobutane ring fragmentation. A second 1-electron reduction of **309** and protonations might lead to the desired **(±)-305**. However, when we treated the cyclobutanes **(±)-307A** and **(±)-307B** with Li⁰ in liquid

ammonia, none of the desired ring-opening product (\pm)-**305** could be isolated. An alternative approach was Lewis acid-mediated ring expansion of the 4-membered ring.¹⁴ Coordination of the carbonyl by a Lewis acid would develop a partial positive charge on carbon. The developing cyclobutyl carbinyl cation **310** might rearrange with C–C bond fragmentation. However, we found no conditions effective for this transformation.

We hypothesized that switching from a cyclobutane to a more strained cyclobutene would facilitate ring opening.¹⁵ To this end, we bubbled acetylene gas through a solution of the bicyclic enone (+)-**143** in acetone while irradiating the reaction through a vycor filter (Scheme 4.10).¹⁶ Gratifyingly, the starting material was almost completely consumed in less than 12 hours. TLC analysis revealed the presence of at least two products. One was a single diastereomer of the desired angularly-fused cyclobutene (+)-**312**, a chromatographically stable, yet volatile solid.¹⁷ At the time, we did not know which cyclobutene diastereomer had formed, but later investigations would reveal its identity. The second major product of the photoreaction was bicyclobutane (–)-**313**, a compound isolable in pure form, yet unstable to silica gel.^{18,19}

Scheme 4.10 Photoadducts from the Acetylene [2 + 2]

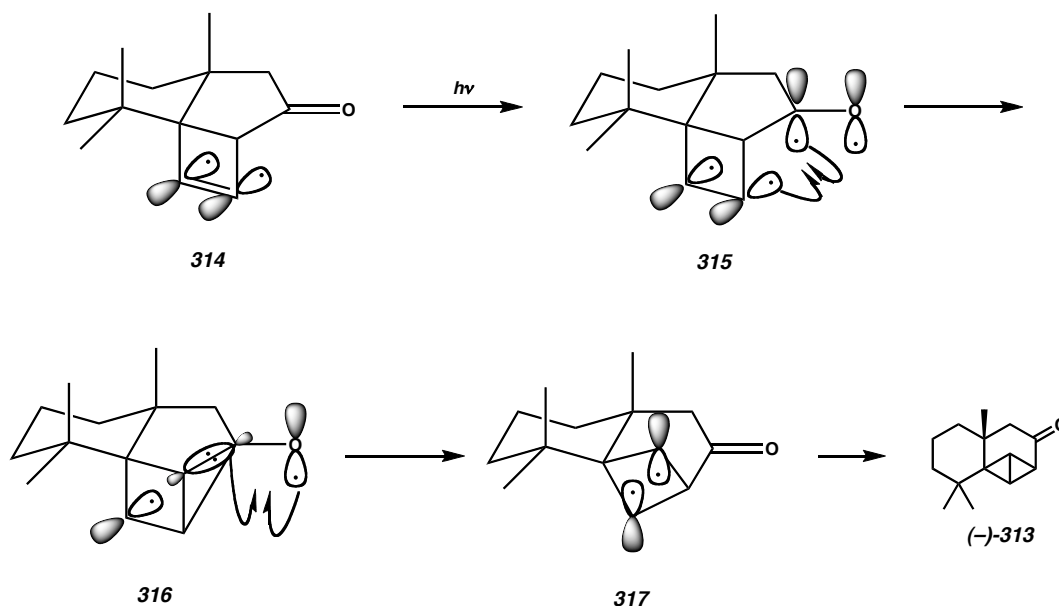


4.4.3 A Photochemical Rearrangement Pathway

Cyclobutanes bearing an olefin β,γ relative to a ketone can undergo an oxa-di- π -methane rearrangement under photochemical conditions.^{20,21} The mechanism is believed

to begin with excitation of the carbonyl chromophore **314** (Scheme 4.11). Diradical **315** will then combine with the π -system of the olefin, leading to another diradical **316**. One of the bonds in the newly formed cyclopropane ring can then rupture, with concomitant regeneration of the carbonyl C–O π -bond. Once **317** has formed, the 1,3-diradical collapses, forming bicyclo[1.1.0]butane (–)-**313**.

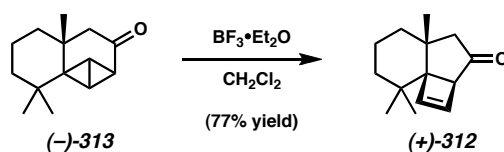
Scheme 4.11 Mechanism of the Oxa-Di- π -Methane Rearrangement



A significant portion of the mass balance in our acetylene photoaddition was bicyclobutane (–)-**313**, making our reaction somewhat unattractive as an early synthetic step in a total synthesis. Gratifyingly, when pure (–)-**313** was treated with $\text{BF}_3 \cdot \text{Et}_2\text{O}$ in CH_2Cl_2 , clean conversion to a single diastereomer of (+)-**312** was observed (Scheme 4.12).^{22,23} This cyclobutene had the same relative configuration as the one directly isolated from the acetylene photoaddition, meaning our [2 + 2] method could effectively install vicinal all-carbon quaternary stereocenters in greater than 99:1 dr. Operationally,

we could perform the photoaddition, chromatograph the crude products, then treat the mixture of (+)-**312** and (–)-**313** with $\text{BF}_3 \cdot \text{Et}_2\text{O}$, obtaining diastereopure (+)-**312**.

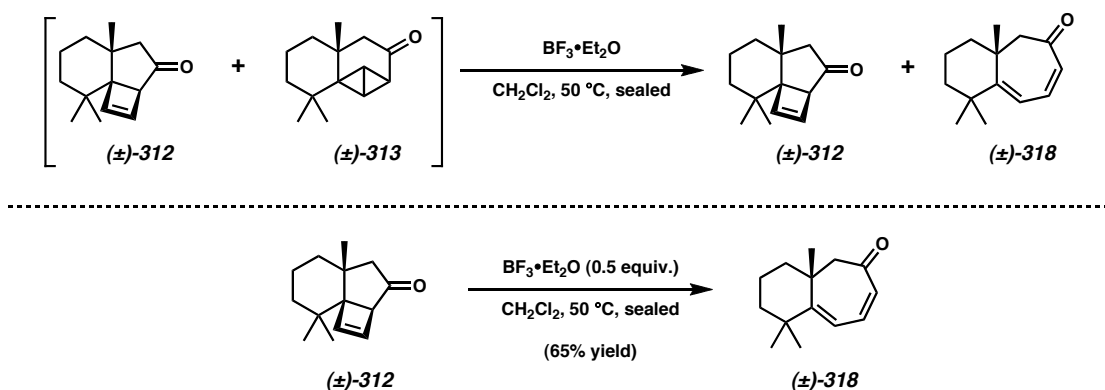
Scheme 4.12 Reversion of the Bicyclobutane to the Cyclobutene



4.4.4 Formal 4π Electrocyclic Ring Expansion

Heating a sample of unseparated (\pm)-**312** and (\pm)-**313** that had been treated with $\text{BF}_3 \cdot \text{Et}_2\text{O}$ led to the formation of a new product (Scheme 4.13). Careful isolation showed that it was a doubly unsaturated, bicyclic ketone (\pm)-**318**. This serendipitous discovery allowed for the streamlined synthesis of the [6-7] carbocyclic framework we needed. Later we learned that (\pm)-**318** could be prepared directly from the cyclobutene (+)-**312**, in what constituted a formal 4π -electrocyclic ring-opening.²⁴

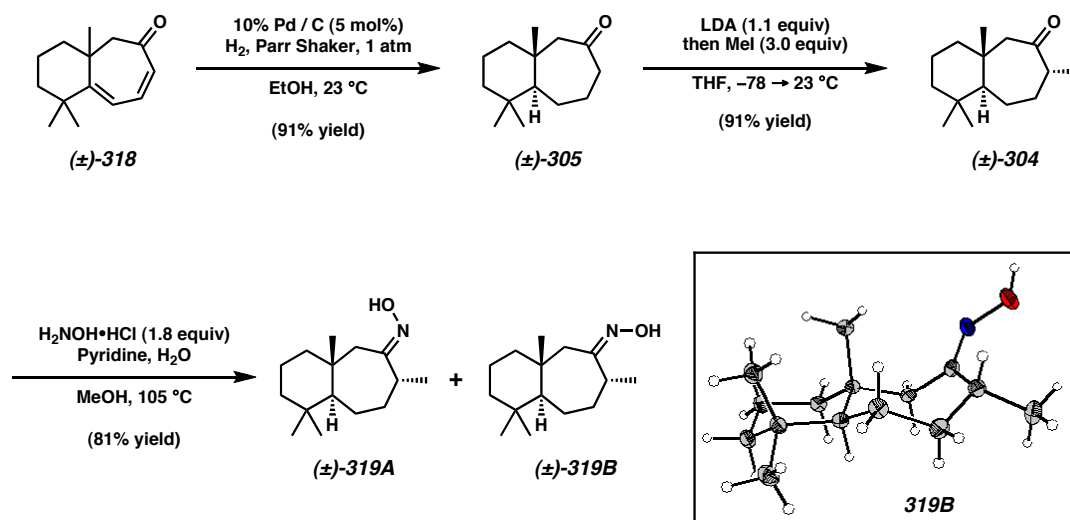
Scheme 4.13 Ring Opening of the Cyclobutene



4.4.5 Elaboration of the [6-7] Core

The bicyclic dienone (\pm)-**318** could be readily hydrogenated to the fully saturated cycloheptanone (\pm)-**305** in good yield (Scheme 4.14). Fortunately, a single diastereomer was produced during this transformation. At the time, we were unable to assign the relative stereochemistry of the compound because it was recalcitrant to nOe analysis. We attempted methylation of the carbonyl using LDA and iodomethane trapping, which produced methyl ketone (\pm)-**304** as a single diastereomer in high yield. This compound was then converted to a mixture of two oxime isomers (\pm)-**319A** and (\pm)-**319B**, one of which was obtained in crystalline form suitable for X-ray crystallographic analysis. The structural data revealed that all stereochemistry present was analogous to that of the natural product. Our next major task was installation of the benzofuran present in liphagal (**271**).

Scheme 4.14 Functionalization of the [6-7] Ring System



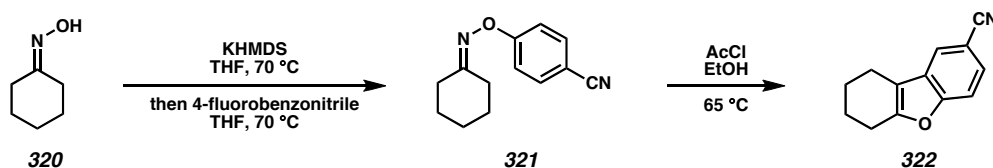
4.5 Attempts to Install the Benzofuran Moiety of Liphagal

4.5.1 An Aryloxime Model System

We had a number of systems designed to model benzofuran installation. The first concept we explored was based on the Fischer indole synthesis.²⁵ In a Fischer indole synthesis, an aryl hydrazone undergoes a [3,3] sigmatropic rearrangement, ultimately leading to an indole. There were a few examples of the analogous transformation with a *O*-aryloximes.^{26,27}

As a model study, we deprotonated the oxygen atom of cyclohexanoxime (**320**) with KHMDS and added 4-fluorobenzonitrile, furnishing the desired *O*-aryloxime **321** (Scheme 4.15). The choice and number of equivalents of base in this transformation were both crucial. Weaker bases led to complex product mixtures, as did excess base.

Scheme 4.15 Aryloxime Cyclization Reaction

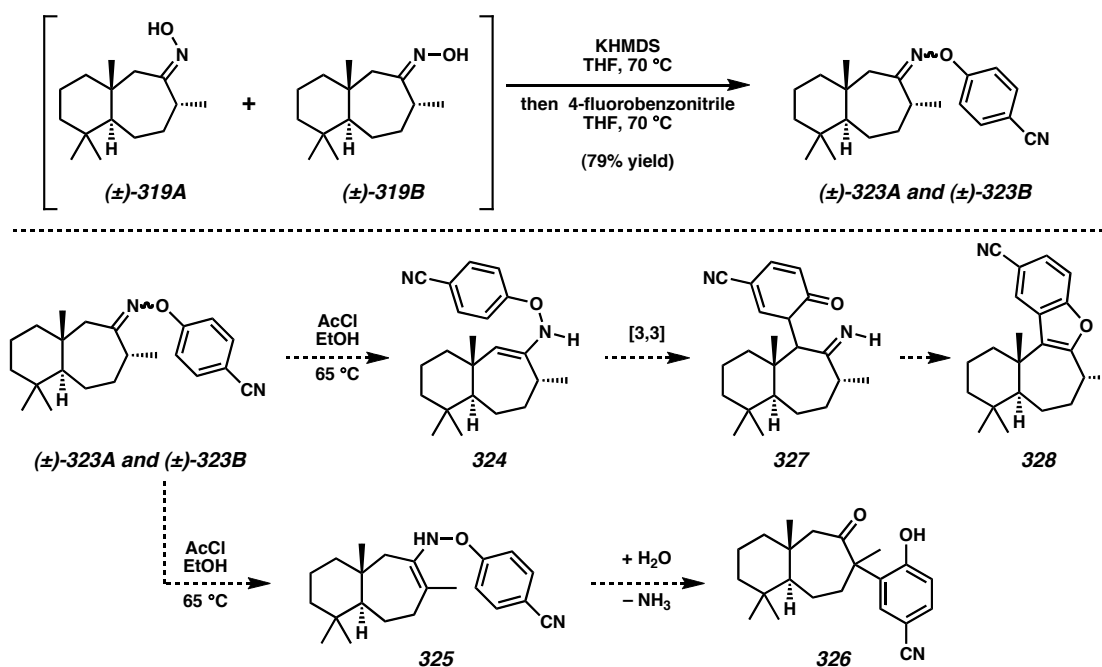


With model *O*-aryloxime **321** in hand, we screened several conditions for the benzofuran synthesis. Ultimately, we found very mild conditions that could achieve the desired transformation. When **321** was added to a pre-stirred solution of acetyl chloride in ethanol and warmed to 65 °C, an acid-promoted sequence of events led to the desired benzofuran **322**. With a working reaction in hand, we began investigation in the context of the liphagane framework.

4.5.2 An Aryloxime Approach to Liphagal

We took the readily prepared mixture of oximes (\pm)-**319A** and (\pm)-**319B** and synthesized aryloximes (\pm)-**323A** and (\pm)-**323B**, without separation. We believed the favored enehydroxylamine tautomer **324** would be formed when (\pm)-**323A** and (\pm)-**323B** were treated with acid (Scheme 4.16). Although we realized the difficulty of making a C–C bond near an all-carbon quaternary stereocenter, we anticipated that an intramolecular [3,3] sigmatropic cyclization mode would overcome this challenge. Unfortunately, there was no desired C–C bond formation at the desired position under acidic conditions. We speculated that an alternative enehydroxylamine tautomer **325** formed during the reaction, and [3,3] sigmatropic rearrangement led to a product **326** incapable of forming a benzofuran. Despite our efforts, we were unable to prepare the desired benzofuran **328** using the aryloxime methodology.

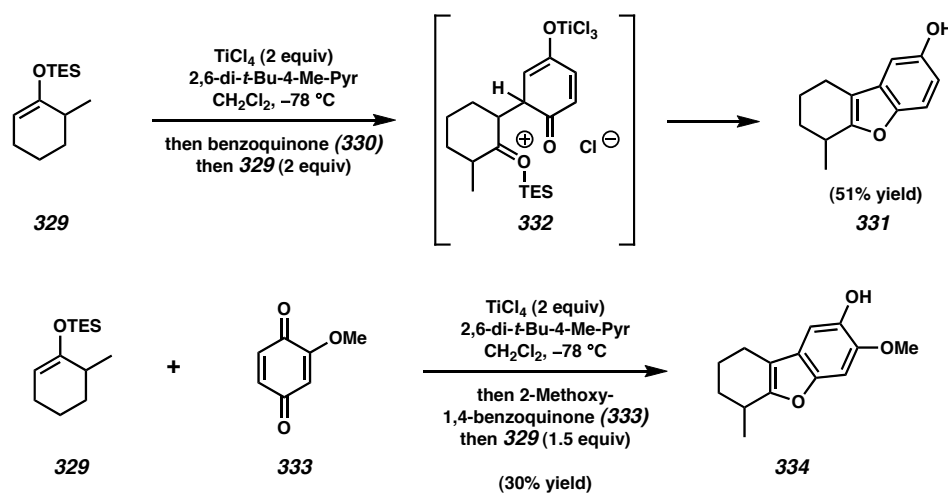
Scheme 4.16 Failed Attempts to Prepare a Benzofuran Using an *O*-Aryloxime



4.5.3 A Mukaiyama Michael-Based Benzofuran Synthesis

The problem of regioselective C–C bond formation necessary for the benzofuran installation merited attention. We thought that regioselectivity in the bond-forming event might be possible using a preformed enolate. A model system to test this hypothesis was designed. We anticipated that silyl enol ether **329** might undergo conjugate addition into 1,4-benzoquinone (**330**) in the presence of Lewis acid (Scheme 4.17). After the initial C–C bond formation, a condensation would lead to a substituted benzofuran **331**. To the best of our knowledge, this type of reaction was unexplored in the literature.

Scheme 4.17 Benzoquinone Mukaiyama Michael Model System

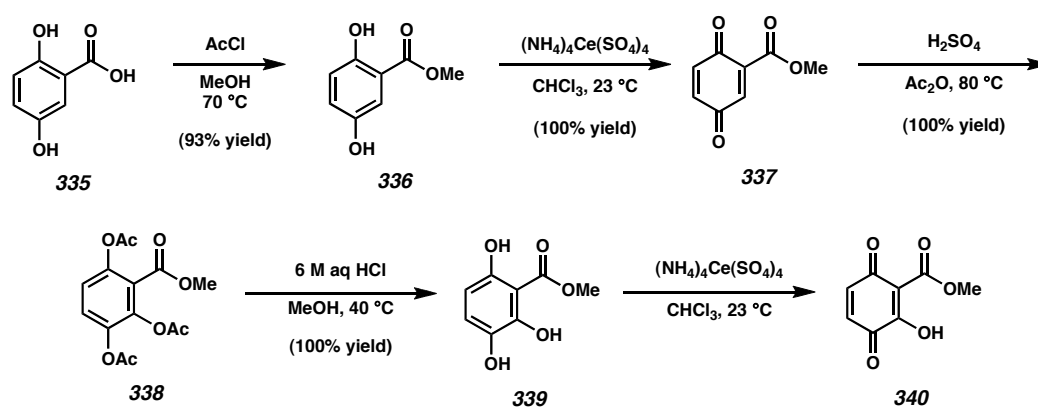


We prepared the known silyl enol ether **329** and screened its reactivity with 1,4-benzoquinone (**330**) in the presence of various acid promoters. We discovered that little or no productive reaction occurred in the absence of base, but when 2,6-di-*t*-Bu-4-methyl pyridine was employed for this transformation, it appeared to have no interaction with the Lewis acid used. One could envision the propensity of intermediate **332** toward

rearomatization. If this happened, an equivalent of HX would be generated. In the absence of base, the acid could desilylate the starting material; often we saw 2-methylcyclohexanone during these reactions. TiCl_4 emerged as a superior promoter for the overall transformation, and optimization revealed 2.0 equivalents of the Lewis acid relative to the benzoquinone (**330**) to be ideal. Under fully optimized conditions, hydroxybenzofuran **331** was accessible in 51% isolated yield from benzoquinone.

Other more complex quinone acceptors could be envisioned. 2-Methoxy-1,4-benzoquinone (**333**) also underwent a productive reaction with **329** in 30% yield based on benzoquinone. Of interest, **334** was the only benzofuran isolated, an indication that the 5-position of **333** was the most electrophilic. Based on this observation, we began to prepare more complex benzoquinones for this chemistry during our initial optimization stage (Scheme 4.18). With the right substrate design, the Mukaiyama Michael product could contain functionality similar to liphagal (**271**) (Scheme 4.19).

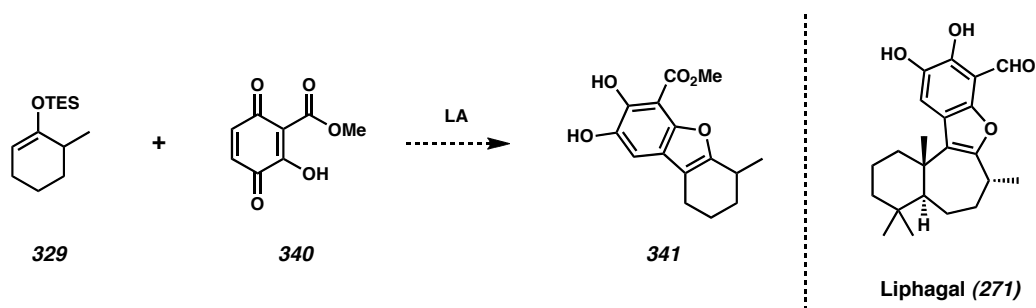
Scheme 4.18 Synthesis of a More Substituted Quinone



To this end, commercially available gentisic acid (**335**) was esterified in acidic methanol, furnishing **336** in high yield.²⁸ A chloroform solution of the methyl ester **336**

was stirred with solid ceric ammonium sulfate,²⁹ producing the unstable *p*-quinone **337** in near-quantitative yield after a filtration workup. Thiele-Winter acetoxylation of the solid quinone in acetic anhydride with sulfuric acid gave a remarkably clean conversion to triacetate **338**.³⁰ Acidic hydrolysis of the three acetates led to trihydroxyarene **339** in excellent yield. When **339** was stirred with ceric ammonium sulfate in chloroform, **340** became available. One could envision that addition of silyl enol ether **229** into the most electrophilic carbon of **340** (the 6-position) might ultimately lead to a substituted benzofuran **341** remarkably similar to liphagal (**271**) (Scheme 4.19). However, we were unable to prepare **341** using **340** presumably due to the instability of **340** in the presence of both Lewis acids and Brønsted bases. It was also surprisingly difficult to functionalize the vinylogous acid oxygen of **340**. Thus, we discontinued the use of this complex *p*-benzoquinone for obtaining a benzofuran.

Scheme 4.19 A Complex Quinone Model System

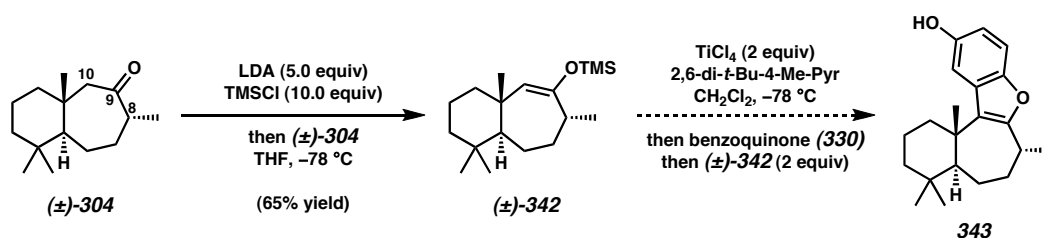


4.5.4 Mukaiyama Michael Approach to Liphagal

Although the complex benzoquinone **340** was not amendable to our model system, the success we had with **330** and **333** was encouraging. Thus, we began to synthesize a silyl enol ether appropriate for the synthesis of liphagal (**271**). When methyl

ketone (\pm)-**304** was added to a preformed mixture of TMSCl and LDA at $-78\text{ }^{\circ}\text{C}$, silyl enol ether (\pm)-**342** was isolated as the major product (Scheme 4.20).³¹ When other methods, such as hard enolization with silyl triflate quench or soft enolization, were used, (\pm)-**342** was never observed in the product mixture.³² As we had observed with the aryl oximes (\pm)-**323A** and (\pm)-**323B**, there seemed to be a strong tendency toward generation of an olefin between C(8) and C(9) in these systems.

Scheme 4.20 Attempted Mukaiyama Michael Reaction

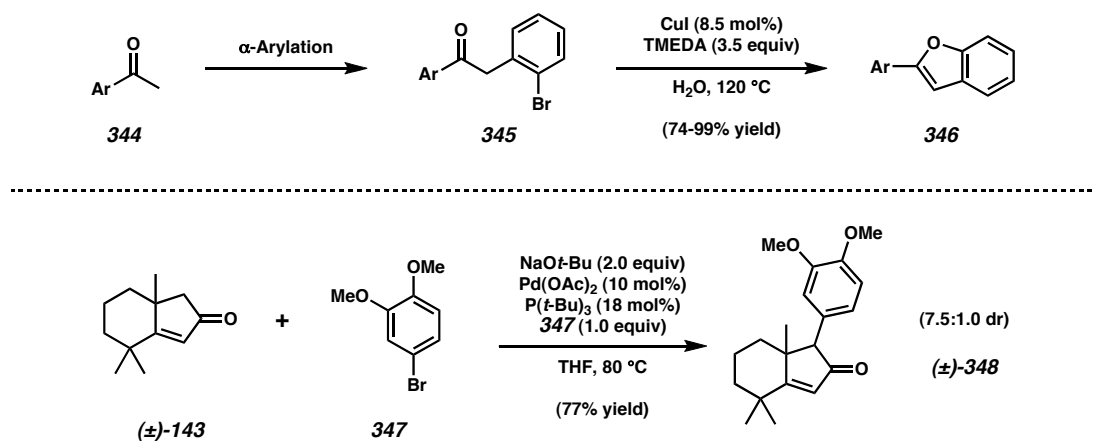


With silyl enol ether (\pm)-**342** in hand, we tested our benzoquinone Mukaiyama Michael strategy with *p*-benzoquinone (**330**). Unfortunately, we never observed C–C bond formation at the correct position. Usually, desilylated ketone (\pm)-**304** was the major product isolated. Qualitatively, we observed that (\pm)-**342** was much more acid-labile than the corresponding silyl enol ether **329** (Scheme 4.19). We tested different Lewis acids, silyl groups, and ingredient addition orders, but we never obtained the desired benzofuran **343**. Perhaps the transition state for C–C bond formation was too sterically hindered, or maybe transannular strain within the 7-membered ring was responsible for the lack of desired reactivity.

4.5.5 α -Arylation Strategy

In addition to our aryloxime and Mukaiyama Michael concepts for benzofuran synthesis, we had another model. Recently, SanMartin and Domínguez demonstrated that α -aryl ketones bearing *ortho* halogenation (e.g., **345**) could undergo a smooth transformation to benzofurans such as **346** (Scheme 4.21).³³ The reactions were typically run “on water”³⁴ using catalytic CuI and superstoichiometric TMEDA. We found that this chemistry was readily duplicated on simple compounds, but we needed a method for installing an analogous aromatic ring in the real system. Hence, we investigated α -arylations of a model ketone (+)-**143** using standard Buchwald-Hartwig conditions.³⁵ Gratifyingly, upon heating (+)-**143** and 4-bromoveratrole (**347**) in the presence of NaOt-Bu, Pd(OAc)₂, and P(*t*-Bu)₃, aryl ketone (\pm)-**348** was produced in good yield.

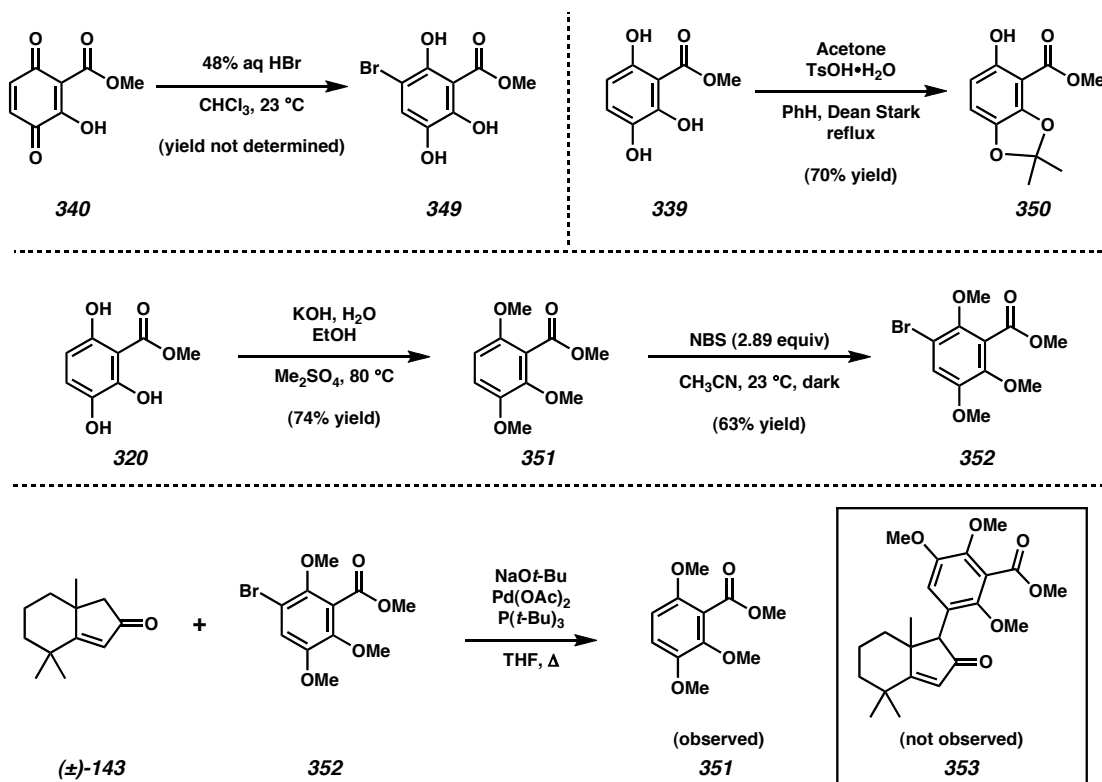
Scheme 4.21 Arylation/CuI Cyclization Strategy



With this initial result using (\pm)-**143**, we wanted to test more substituted aryl halide partners related to **349** in the Buchwald-Hartwig coupling. To this end, we treated the quinone **340** prepared earlier from gentisic acid (**335**) with HBr, achieving

chemoselective bromination of the arene. (Scheme 4.22). Although the transformation worked, the compound **349** was chromatographically unstable and unsuitable for further synthetic manipulation. Protection of the hydroxy groups would be necessary to improve compound stability. Triol **339** could be converted to its acetonide **350** in 70% yield, but the chemistry was hard to reproduce on larger scale. The best method for installation of bromide functionality began with global methylation of **339**. This transformation was challenging because use of strong bases led to decomposition during the protection. Nevertheless, carefully controlled use of KOH in dimethyl sulfate and ethanol furnished **351** in 74% yield from **339**. This compound was regioselectively brominated with excess *N*-bromosuccinimide in acetonitrile, giving the desired **352**.

Scheme 4.22 Synthesis of a Complex Aryl Halide

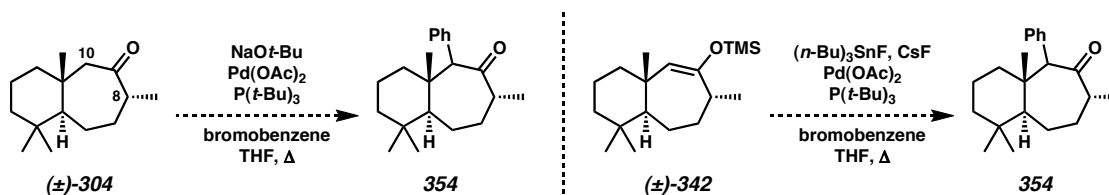


With aryl bromide **352** in hand, we tried to α -arylate (+)-**143** under conditions previously utilized to prepare (\pm)-**348**. Unfortunately, only dehalogenated arene **351** was observed under the conditions tested. Although this indicated that oxidative addition was possible, the steric demand for later steps in the catalytic cycle had become too great. Although minor optimizations were tested for preparation of **353**, we could not achieve arylation of (+)-**143** with **352**.

4.5.6 α -Arylation Attempts on the [6-7] Bicyclic System

The next step in our investigation was the attempted arylation of methyl ketone (\pm)-**304**, a substrate further along the synthetic route to liphagal (**271**). Test reactions did not lead to any of the desired C–C bonded product **354** (Scheme 4.23). We speculated that α -arylation of C(8) was perhaps competing with the desired pathway. Attempts were made using modified conditions for α -arylation of silyl enol ethers.³⁶ However, when (\pm)-**342** was tested using these methods, only (\pm)-**304** was observed. Considering the difficulty encountered with the requisite benzofuran C–C bond formation on our [6-7] systems, our retrosynthesis needed revision.

Scheme 4.23 Attempted Arylation of the [6-7] System

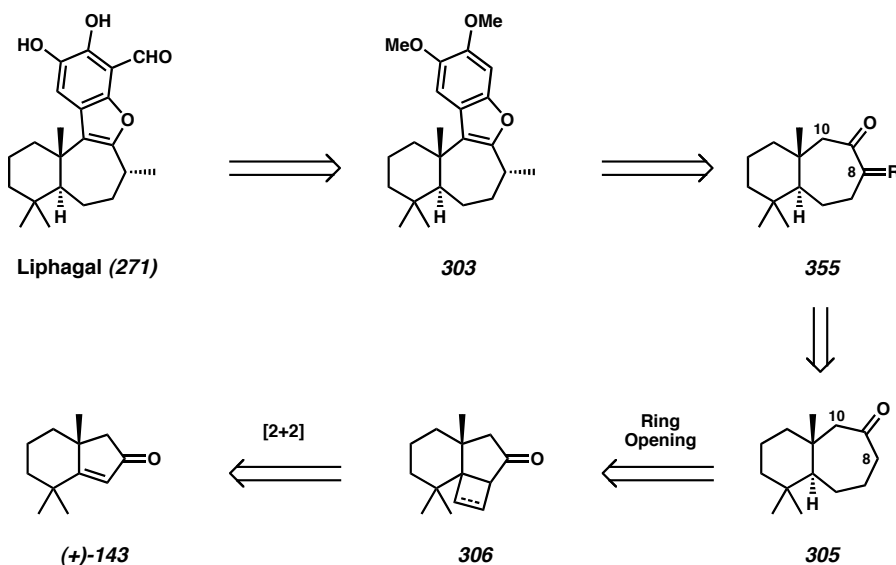


4.6 Positional Blocking Strategies Applied to the Key Benzofuran Synthesis

4.6.1 Retrosynthetic Revisions

Our previous experiments on the [6-7] ring system had demonstrated the difficulty of forming an exocyclic C–C bond at C(10) (Scheme 4.24). One reason for this observation could be competitive reactivity at C(8). We hypothesized that mitigation of unwanted C(8) chemistry would be achieved by completely blocking the position, forcing chemistry at C(10). Modifying the previous retrosynthesis, the benzofuran **303** could arise from a C(8)-blocked species **355**. This carbonyl-containing entity could be prepared from (\pm)-**305**. Once the key carbon bond at C(10) was established, the functionality at C(8) could be altered for installation of the requisite methyl group. Otherwise, our retrosynthetic analysis would remain unchanged.

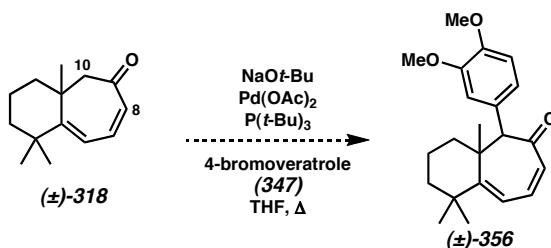
Scheme 4.24 Second Retrosynthesis of Liphagal



4.6.2 Attempted Arylation of the Dienone

Compound (\pm)-**318** displayed the necessary characteristics we were searching for during the retrosynthetic revisions. Given the sp^2 hybridization at C(8), enolization should occur selectively at C(10). Thus, we attempted Buchwald-Hartwig α -arylation of (\pm)-**318** using 4-bromoveratrole (Scheme 4.25). A productive reaction occurred; however, the purified product was not arylated at C(10). Control reactions in the absence of Pd and phosphine ligand revealed that (\pm)-**318** was unstable in the presence of NaOt-Bu. The product of the attempted arylation did contain a veratrole group, but its location on the [6-7] framework could not be unambiguously assigned. Hence, we discontinued arylation studies with (\pm)-**318**.

Scheme 4.25 Attempted Dienone Arylation

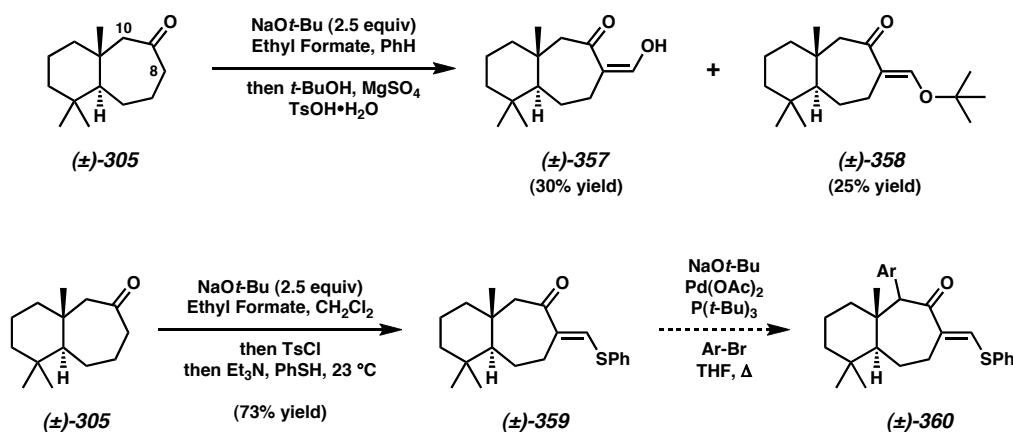


4.6.3 Exocyclic Olefin Substrates

Although substrate (\pm)-**318** was not amenable to arylation, we anticipated that an exocyclic olefin could efficiently block C(8). Ketone (\pm)-**305** was subjected to excess ethyl formate and NaOt-Bu, followed by an attempted vinylogous esterification using *t*-BuOH (Scheme 4.26). We were pleased to observe both the vinylogous acid (\pm)-**357** and the vinylogous ester (\pm)-**358**, each in modest yield. Conceptually, one could envision conversion of the exocyclic methylene of (\pm)-**357** or (\pm)-**358** to a methyl group (Scheme

4.26) via reduction. Since the vinylogous acid (\pm)-**357** was not ideal for α -arylation, and conversion to (\pm)-**358** was difficult, we targeted a vinylogous thioester (\pm)-**359**.

Scheme 4.26 Vinylogous Substrates



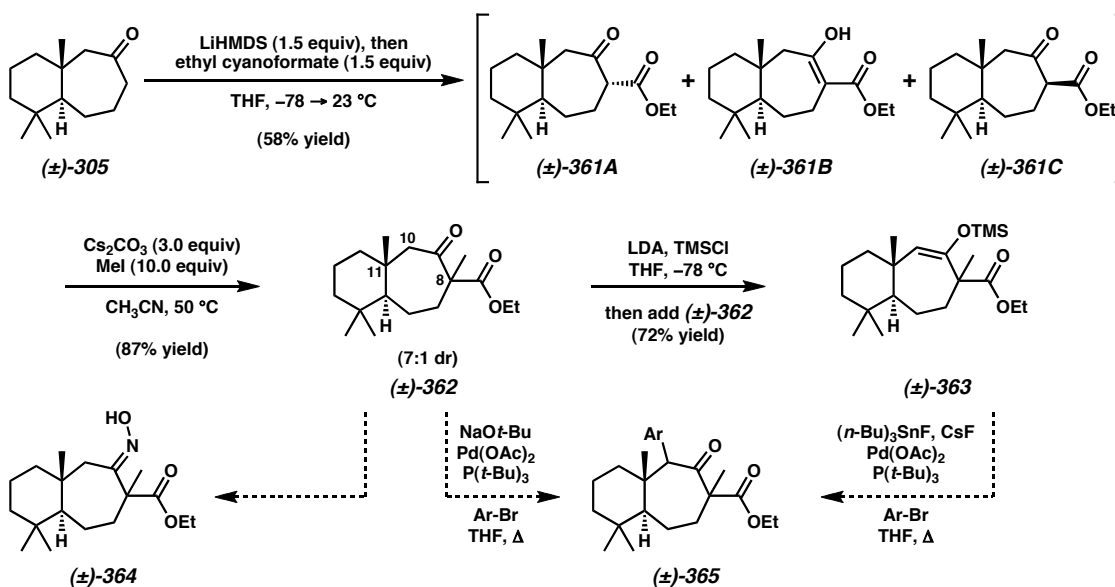
The vinylogous acid (\pm)-**357** was treated with TsCl, and the intermediate vinylogous mixed anhydride underwent conjugate addition/elimination with thiophenol. Thus, in a one-pot sequence, (\pm)-**305** could be rapidly transformed into (\pm)-**359**. When α -arylation of vinylogous thioester (\pm)-**359** was attempted, we observed no C–C bond formation at C(10), but rather vinylogous saponification to give (\pm)-**358**. To remedy this situation, we tried to prepare an *N*-methyl, *N*-phenyl vinylogous amide, but efforts to do so were fruitless. Considering these results, we decided to develop an alternative blocking strategy.

4.6.4 Quaternization of C(8)

Observing that sp^2 hybridization of C(8) was not a viable method for achieving arylation of C(10), we decided to transform C(8) into a non-enolizable, quaternary sp^3 carbon. Treatment of bicyclic ketone (\pm)-**305** with LiHMDS followed by ethyl

cyanohydrin at low temperature gave a tautomeric mixture of the β -ketoesters (\pm)-**361A**, (\pm)-**361B**, and (\pm)-**361C** (Scheme 4.27). This crude isolate was immediately methylated in acetonitrile, furnishing quaternized (\pm)-**362** in high dr.³⁷ We attempted α -arylation of (\pm)-**362**, but did not observe any bond formation at C(10).

Scheme 4.27 Quaternized Substrates



At this point, we questioned whether enolization was even possible. Looking at (\pm)-**362** we could see that transannular strain might develop between substituents at C(8) and C(11) during an enolization. Despite this, silyl enol ether (\pm)-**363** was readily obtained when (\pm)-**362** was treated with a preformed mixture of LDA and TMSCl.³¹ We also tested the Hartwig-modified conditions for α -arylation of (\pm)-**363**,³⁶ but these efforts were fruitless. The silyl enol ether was also screened with our benzoquinone Mukaiyama Michael conditions, yet no C–C bonded product could be isolated. Perhaps most surprising of all, when we attempted several conditions for oxime formation on β -

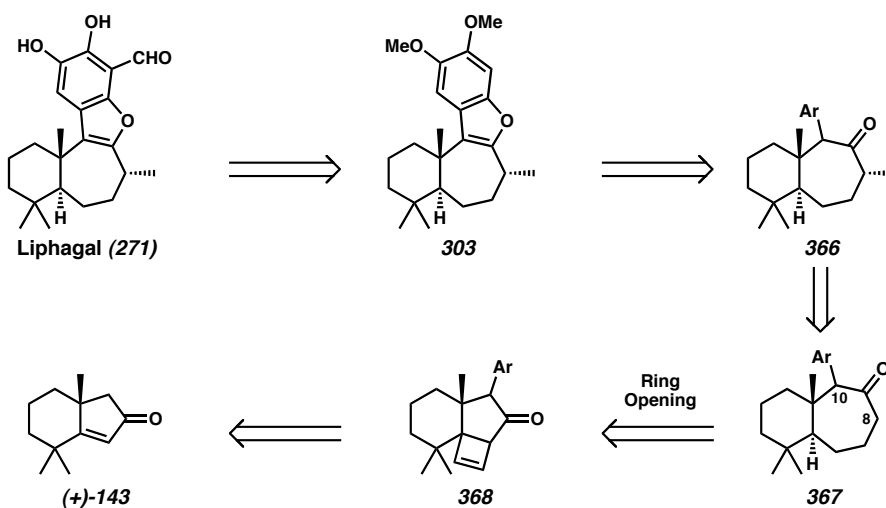
ketoester (\pm)-**362** at C(9), no condensation was realized. This meant that we could not access an *O*-aryloxime for a [3,3] sigmatropic rearrangement. Based on all of these observations, we concluded that the environment around C(10) was not conducive to C–C bonding, so more retrosynthetic revisions were in order.

4.7 Approaches Based on Arylation of [6-5] Systems

4.7.1 Retrosynthetic Revisions

A somewhat significant retrosynthetic revision was required to address the necessary C(10) exocyclic C–C bond construction. The most efficacious strategic adjustment might be to arylate a [6-5] carbocyclic species and subsequently perform the ring expansion (Scheme 4.28). This meant that the arene would be carried through many synthetic steps prior to benzofuran closure. We were unsure of what effects this would have on later stereoselective transformations but believed that previously developed chemistry would be applicable to this new strategy.

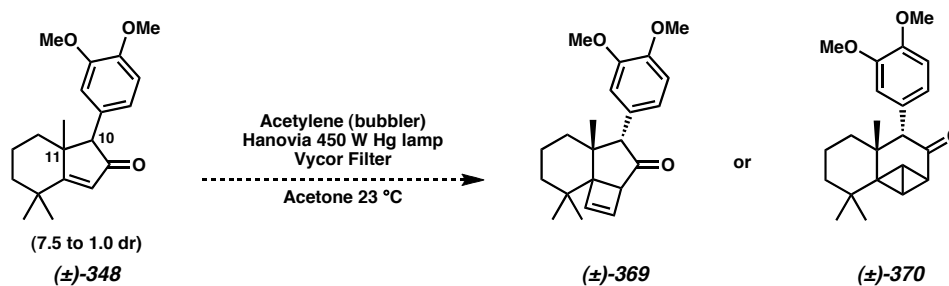
Scheme 4.28 A New Retrosynthesis



4.7.2 Attempted Photoaddition to an Aryl Enone

The aryl enone (\pm)-**348** previously prepared in the context of a model system appeared to be a good starting point for further investigations (Scheme 4.29). Although we did not know which diastereomer of (\pm)-**348** was the major one, it likely had an *anti* relationship between the aryl group at C(10) and the axial methyl at C(11). This assumption was made based on the crystallographic data observed for Michael adduct **233** from the dichroanone synthesis, which existed in a 10.7:1.0 dr.⁸ Results obtained later in the synthesis would further support our hypothesis. We ran an acetylene [2 + 2] photocyclization with (\pm)-**348** under conditions similar to those used for (+)-**312**, but never observed a productive reaction.

Scheme 4.29 Photochemistry of the Aryl Enone



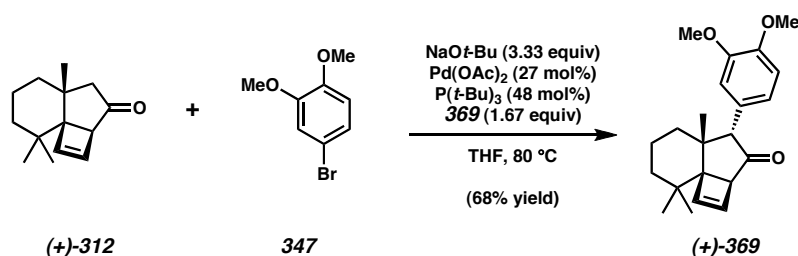
Two theories might explain the lack of reactivity, the first of which is a steric argument. Given the relative stereochemistry described, the aryl group of (\pm)-**348** would sit directly beneath the olefin moiety. This might block the α -face, preventing the first photoaddition step. The axial quaternary methyl groups would potentially hinder the β -face of the olefin as well. Another argument for the lack of reactivity could be a photophysical one. Presumably, the first step of the net [2 + 2] cycloaddition is an

excitation of the enone chromophore. The nearby aryl group of (\pm)-**348** has a significant absorption cross section in the UV and lies physically close to the enone. Thus, a fluorescent resonant energy transfer from the excited enone to the aryl group could induce a new state incapable of exciplex formation with acetylene.

4.7.3 Successful Arylation of the Keto-Cyclobutene

Our only other option for C–C bond formation at C(10) was to α -arylate the angularly-fused cyclobutene (**+**)-**312**. We were delighted to find that (**+**)-**312** reacted cleanly with 4-bromoveratrole under the Buchwald-Hartwig conditions, furnishing a single diastereomer of (**+**)-**369** (Scheme 4.30). At the time, we did not know the relative stereochemistry of the aryl ketone (**+**)-**369**, but a serendipitous discovery would later elucidate this matter. The arylation, though clean, required a slight excess of 4-bromoveratrole, elevated catalyst loadings, and longer reaction times in part due to steric demands. Nonetheless, we were pleased to finally have the C–C bond necessary for the benzofuran moiety of liphagal (**271**).

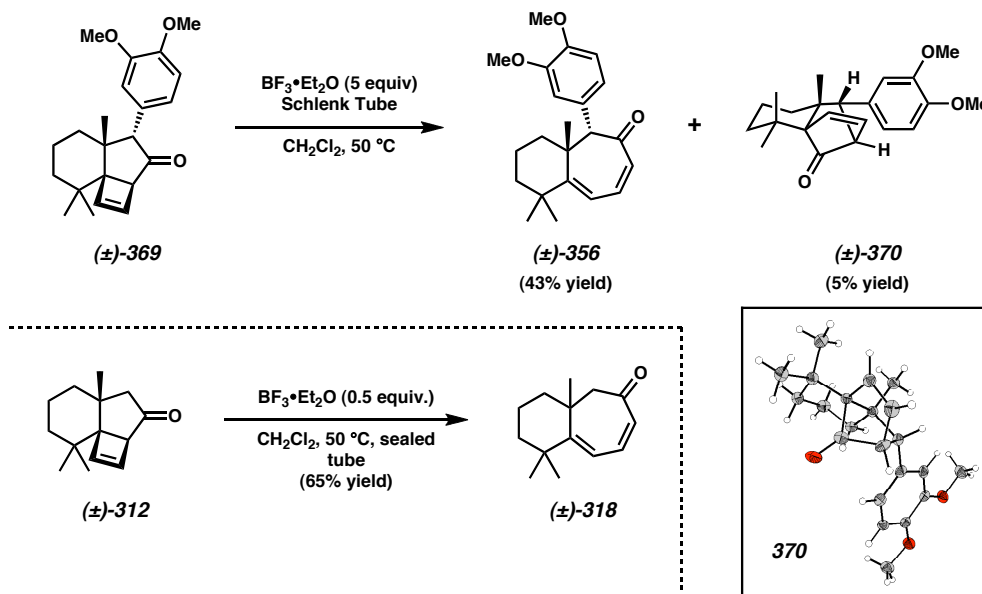
Scheme 4.30 Arylation of the Cyclobutene



4.7.4 Changes In the Ring Expansion

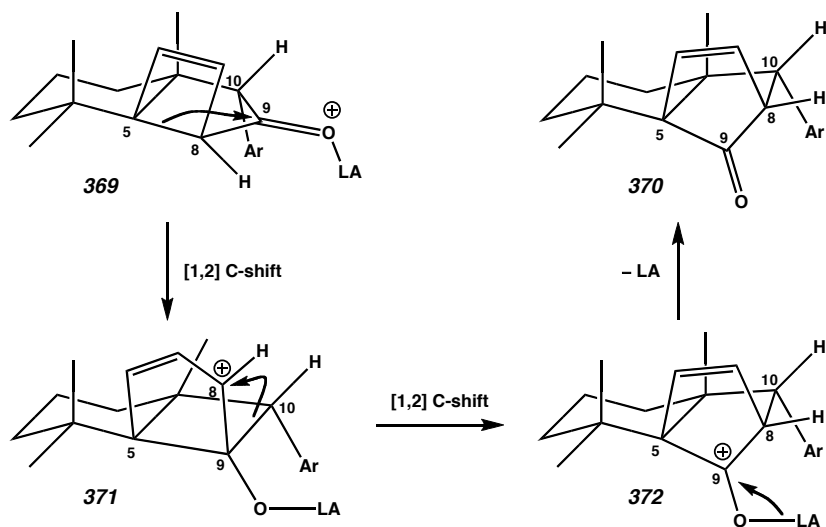
Once we had formed the requisite C–C bond at C(10), we tested our formal retro 4π electrocyclization chemistry using (+)-**369**. Gratifyingly, we could advance material through to (\pm)-**356** without loss of stereochemical information at C(10) (Scheme 4.31). Despite this, we noticed a substantial drop in yield for this reaction compared to the analogous transformation (lacking the aryl group) from (+)-**312** to (\pm)-**318**. Noticeable quantities of an unusual side product, (\pm)-**370**, were now also present. Fortuitously, X-ray quality crystals of the polycyclic ketone (\pm)-**370** could be obtained, and its relative stereochemistry was established. We had encountered a rearrangement mode of cyclobutene-containing ketones described by Cargill.³⁸ Clearly, small changes to our cyclobutene (*c.f.* (+)-**312** and (+)-**369**) could have dramatic effects upon its reactivity.³⁹

Scheme 4.31 Side Product Formation During the Electrocyclic Opening



Mechanistically, the transformation from (+)-**369** to (±)-**370** happens by a series of concerted C–C bond migrations.³⁸ Activation of the carbonyl with Lewis acid induces development of a partial positive charge at C(9) (Scheme 4.32). The bond between C(5) and C(8) of **369** undergoes a [1,2] C-shift, generating an allylic carbocation **371**. The bond between C(9) and C(10) of the resulting cyclobutane then migrates via [1,2] C-shift into the carbocation at C(8), generating homoallylic carbocation **372** centered at C(9). Lewis acid dissociation quenches the carbocation, giving (±)-**370**. Based on the relative stereochemistry of (±)-**370**, we could backtrack through this mechanism, determining the relative configuration of (+)-**369**, (±)-**318**, and by analogy, (±)-**348** (Scheme 4.29).

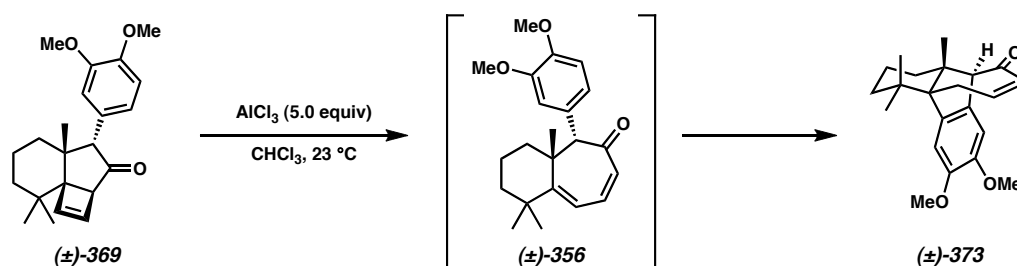
Scheme 4.32 Mechanism of the Cargill Rearrangement



It was worthwhile to screen other Lewis acids for the electrocyclic ring opening. Many others we tested led to the Cargill product (±)-**370**. Curiously, when we treated (±)-**369** with AlCl_3 in CHCl_3 , no Cargill product (±)-**370** was observed. However, a new species (±)-**373** was noticed instead of the desired (±)-**356** (Scheme 4.33). After

confirmation of its relative stereochemistry and structure, we could see that (\pm)-**373** was the result of an intramolecular Friedel-Crafts cyclization of (\pm)-**356**. This gave us some insight into the conformational preferences of aryl ketone (\pm)-**356**. Apparently, the electron-rich veratrole moiety sits directly underneath the olefinic π -system. When the carbonyl is activated, a 1,6-addition of the arene into the doubly unsaturated system may occur.

Scheme 4.33 Observation of Friedel-Crafts Chemistry



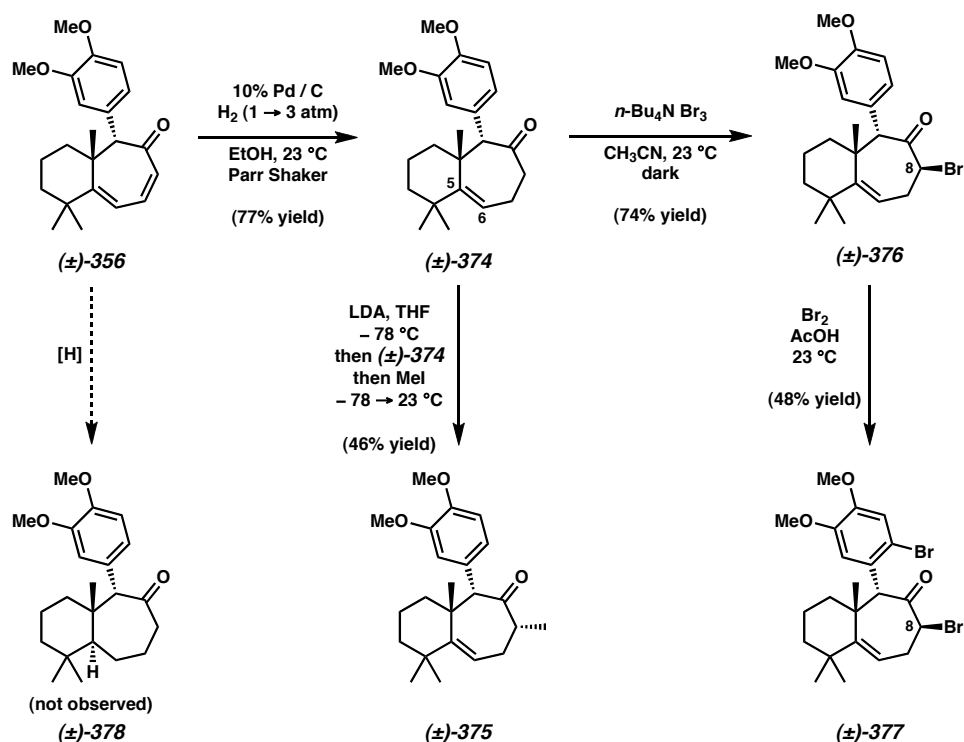
4.7.5 Effects of the Aryl Group on Subsequent Chemistry

The observation of the Friedel-Crafts chemistry presaged some of the discoveries we would later make. With arylated dienone (\pm)-**356** in hand, we tested our hydrogenation reaction developed for the transformation of (\pm)-**318** to (\pm)-**305**. A reaction occurred, but the product, (\pm)-**374**, still contained the trisubstituted olefin spanning C(5) and C(6) (Scheme 4.34). More forcing conditions were attempted to reduce this alkene, but all were unsuccessful. The close proximity of the sterically large arene and C(5)–C(6) olefin α face is believed to prevent hydrogenation.

We hoped that this olefin could be reduced stereoselectively on the α face once the benzofuran moiety of the liphagane skeleton was installed. To this end, we tested

some of our other previously developed chemistry. (\pm)-**374** was treated with LDA and iodomethane, furnishing (\pm)-**375** in 46% yield and 3:1 dr with a 38% recovery of unreacted (\pm)-**374**. nOesy-1D analysis of (\pm)-**375** revealed that the major diastereomer possessed correct relative stereochemistry at C(8).

Scheme 4.34 The Chemistry of the Aryl Dienone



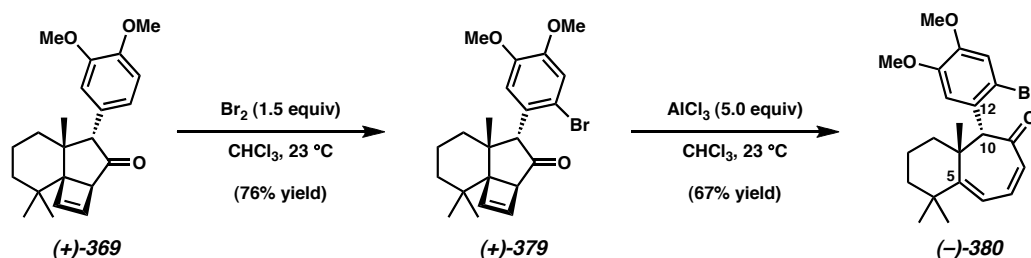
We anticipated that an aryl bromide handle would be useful for closure to a benzofuran later in the synthesis. Treatment of (\pm)-**374** with $(n\text{-Bu})_4\text{N Br}_3$ in CH_3CN led to bromination of only C(8), whereas stronger conditions applied to (\pm)-**376** could also chemoselectively brominate the aromatic ring, furnishing dibromide (\pm)-**377**. Although we had halogenated the arene, we now had an unwanted alkyl bromide at C(8).

Bromination of the arene prior to ring expansion of the cyclobutene could potentially avoid this problem.

4.7.6 Optimized Electrocyclic Ring Expansion

We believed that the electron-rich nature of the veratrole moiety in (\pm)-**369** was responsible for conversion of (\pm)-**356** to (\pm)-**373** during the Lewis acid-promoted ring expansion. We also wanted a bromine atom on our aromatic ring for the eventual benzofuran synthesis. Bromination of the arene (\pm)-**356** could attenuate the unwanted Friedel-Crafts pathway by making the aromatic ring less electron-rich. The bromide might also change the dihedral angle about C(10)–C(12), precluding a conformation requisite for nucleophilic attack on C(5) (Scheme 4.35).

Scheme 4.35 Bromination Solution for Ring Expansion

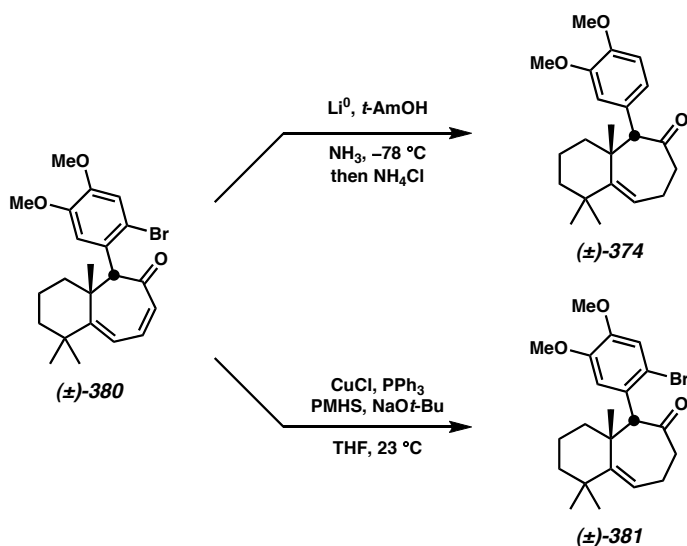


To test our hypotheses, (+)-**369** was treated with Br₂ in CHCl₃, leading to (+)-**379** in good yield and excellent chemoselectivity (Scheme 4.35). To our delight, when bromoveratrole-substituted cyclobutene (+)-**379** was treated with AlCl₃ in CHCl₃, a very clean rearrangement to (-)-**380** occurred devoid of both Friedel-Crafts and Cargill rearrangement side products.

4.7.7 Functionalization of the Dienone

We needed to reduce the two alkenes within the 7-membered ring of (\pm)-**380**, and hoped that a dissolving metal reduction might efficiently reduce both olefins. However, when (\pm)-**380** was treated with Li^0 and *t*-AmOH in liquid ammonia, only 1,4 reduction and dehalogenation were observed (Scheme 4.36). We realized that conjugation of the γ,δ olefin to the other π -systems was somewhat limited. Even if we could suppress dehalogenation, it would be difficult to achieve 1,6-reduction using dissolving metal reductions.

Scheme 4.36 Early Reduction Methods

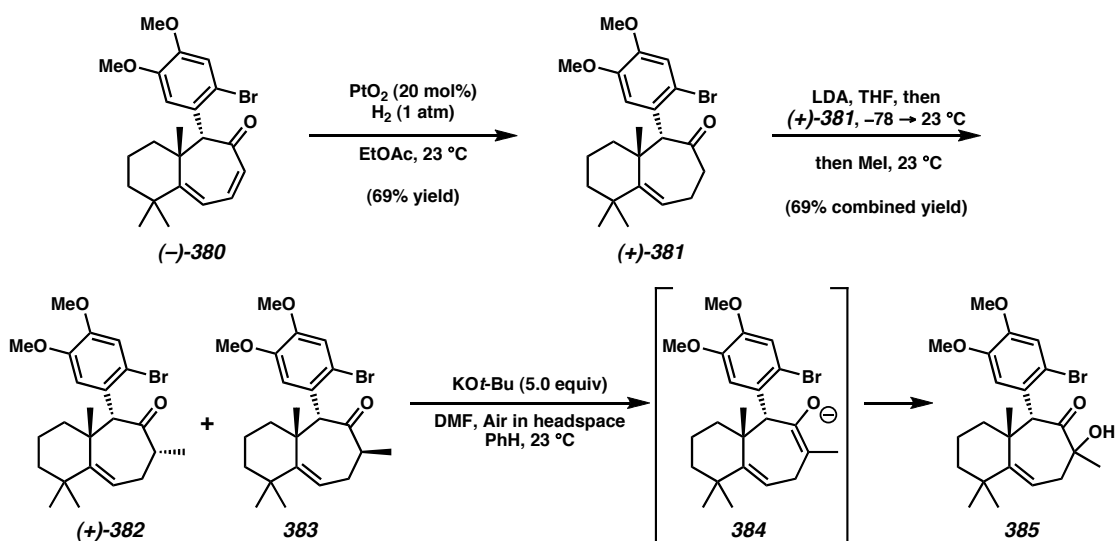


One method that was useful initially was a copper hydride conjugate reduction of (\pm)-**380** to (\pm)-**381**.⁴⁰ The advantage of this approach was its high chemoselectivity; no debromination was ever observed. One of the disadvantages of this method was its poor

reproducibility. Although many reaction variables were screened, yields ranged from 0-56%. It was too risky to use this procedure during scale-up.

Ultimately, the best means for reduction of (–)-**380** proved to be hydrogenation with Adams' catalyst in EtOAc (Scheme 4.37). The choice of solvent was critical, as substantial debromination was observed in EtOH when PtO₂ was used. In no instance was reduction of the γ,δ olefin observed, consistent with previous data obtained.

Scheme 4.37 Methylation and Epimerization Studies



Now that the dienone had been reduced, methylation of (+)-**381** was tested. Gratifyingly, treatment of (+)-**381** with LDA, followed by iodomethane, installed the methyl group of (+)-**382** in 5:2 dr, favoring the desired diastereomer (Scheme 4.37). Although conversion in this reaction was generally incomplete, the two diastereomers (+)-**382** and **383** were fully separable, and most of the unreacted starting material could be recovered. We made a significant discovery when we tried to epimerize **383** to the

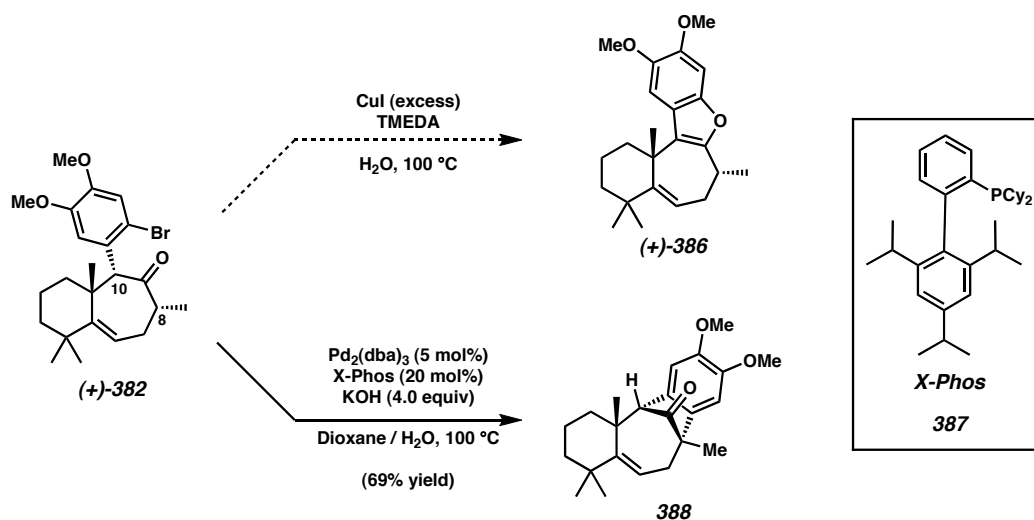
desired (+)-**382**. The enolate **384** was presumably very unstable because we could never reisolate any (+)-**382** or **383**. Instead, the only discernable product from any epimerization attempt was the acyloin **385**. The relative configuration of this species was not determined.

4.8 Completion of the Benzofuran Ring

4.8.1 Preparation of a Dihydrobenzofuran

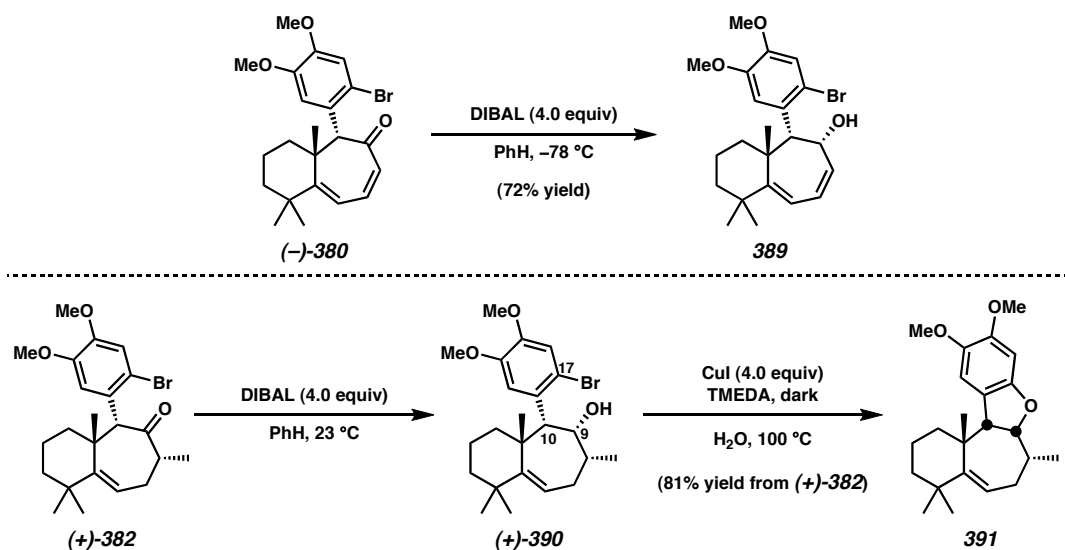
With the bromoveratrole (+)-**382** in hand, we were finally ready to close the benzofuran. (+)-**382** was treated with excess CuI in TMEDA and H₂O rigorously degassed with argon (Scheme 4.38).³³ Unfortunately, but not surprisingly, in light of the enolate instability of **384**, we never observed any C–O bond formation or (+)-**386**. We turned instead to an alternative method described by Buchwald. When certain aryl halides are heated in the presence X-Phos ligand **387** and Pd₂(dba)₃ in dioxane/H₂O with KOH, conversion of the aryl halide to a phenol is observed.⁴¹ We hoped to access a phenol, which upon dehydrative cyclization might lead to benzofuran (+)-**386**. We were excited when we observed full conversion of (+)-**382** to a single, stable product. To our surprise, the product **388** was the result of a clean intramolecular α -arylation. This reactivity again highlights the strong preference of our [6,7] carbocyclic ketone systems toward enolization at C(8) compared to C(10).

Scheme 4.38 Failed Attempts to Prepare the Benzofuran



We needed a creative way to make the C(17)-O bond while avoiding unwanted reactions at C(8). During another study, dienone (–)-**380** could be diastereoselectively reduced to allylic alcohol **389** in good yield, so we believed it would be possible to perform the analogous transformation on (+)-**382** (Scheme 4.39). To our delight, treatment of (+)-**382** with DIBAL in benzene at $23\text{ }^\circ\text{C}$ gave complete conversion to (+)-**390** as a single diastereomer. The relationship between the protons at C(9) and C(10) was *syn*, so we anticipated that cyclization of the C(9) oxygen of (+)-**390** onto C(17) would be possible. When we treated (+)-**390** with excess CuI in $\text{TMEDA}/\text{H}_2\text{O}$ ³³ we obtained dihydrobenzofuran **391** as the exclusive product. Finally, the fourth ring the liphagane skeleton (**272**, Figure 4.1) was in place.

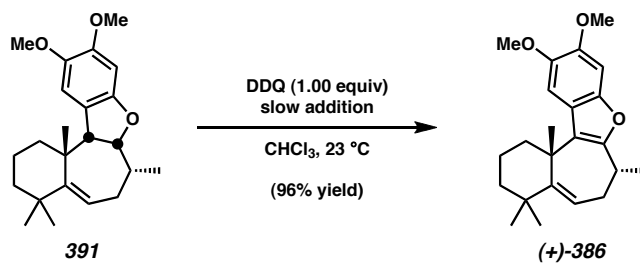
Scheme 4.39 Making the Necessary C–O Bond



4.8.2 Controlled Oxidation of the Dihydrobenzofuran

At last we were poised for the installation of the benzofuran. Treatment of dihydrobenzofuran **391** in high dilution with one equivalent of DDQ over a three-hour timeframe at 23 °C gave a 96% yield of benzofuran **(+)-386** (Scheme 4.40). The methods developed for this reaction were critical. If more than one equivalent of DDQ was used or the addition was too rapid, overoxidation byproducts were observed.

Scheme 4.40 Careful Oxidation to the Benzofuran

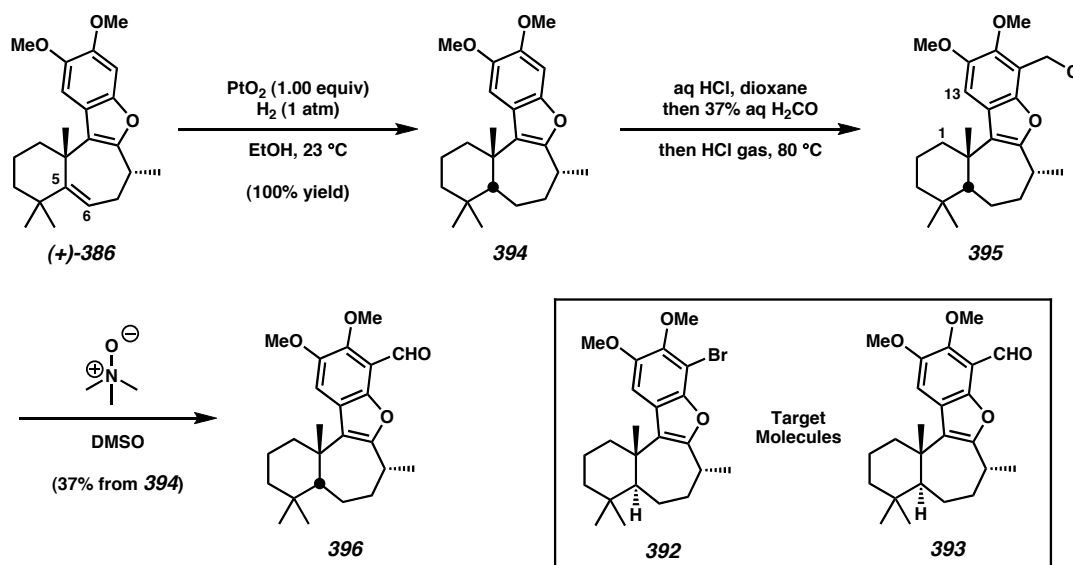


4.8.3 Installation of the Aldehyde Functionality

Although all of the rings in the natural product were present, we still needed to install the aldehyde functionality. We hoped to intercept a compound reported in Andersen's racemic total synthesis, either aryl bromide **392** or aldehyde **393**.¹ We tried a few conditions for hydrogenation of the C(5)–C(6) double bond, and quickly discovered that PtO₂ / H₂ reduction at 1 atm in EtOH produced a single diastereomeric product **394** (Scheme 4.41). At the time, we could not tell which diastereomer we had produced. We were hopeful that *trans* ring fusion across C(5) and C(11) was achieved based on similar reactions with [6-6] carbocycles.⁴² Literature examples of more relevant [6-7] systems were nearly scarce,⁴³ but we anticipated stereoselection in our hydrogenation might follow the same trends seen for [6-6] systems.

With our hydrogenated 7-membered ring benzofuran **394**, we targeted **392**. Under all conditions tested, we failed to observe any bromination of our arene. Instead, oxidation of the 7-membered ring was more common. Undaunted, we decided to pursue **393**. We tested many methods of direct formylation or cyanation, but had limited success. Instead, we came to rely upon a two-step sequence. Condensation of **394** with aqueous formaldehyde in HCl-saturated dioxane produced a single isomer of benzyl chloride **395**, which was partially characterized (Scheme 4.41). Most importantly, a key nOe was observed between the aryl proton at C(13) and a proton on C(1).⁴⁴ This confirmed the position of the benzylic chloride moiety. To our delight, when **395** was treated with trimethylamine *N*-oxide in DMSO,⁴⁵ benzaldehyde **396** was the major product in 37% yield from **394**. However, we had prepared the C(5) epimer of Andersen's aldehyde **393**.⁴⁶

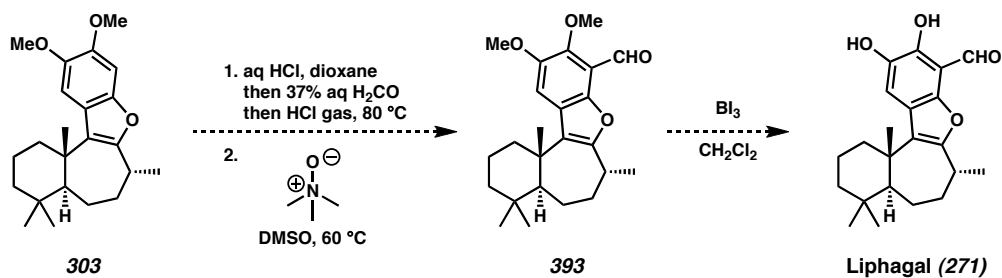
Scheme 4.41 Further Functionalizations



4.8.4 Proposed Endgame for the Total Synthesis of Liphagal

If the preparation of **303** were possible, chloromethylation of the benzofuran followed by oxidation using the Taylor-Ganem modification of the Kornblum oxidation⁴⁵ would lead to Andersen's aldehyde **393** (Scheme 4.42). This would constitute a formal total synthesis of **271**. Didemethylation of **393** with BI_3 at low temperature¹ would then complete the catalytic enantioselective total synthesis of liphagal (**271**).

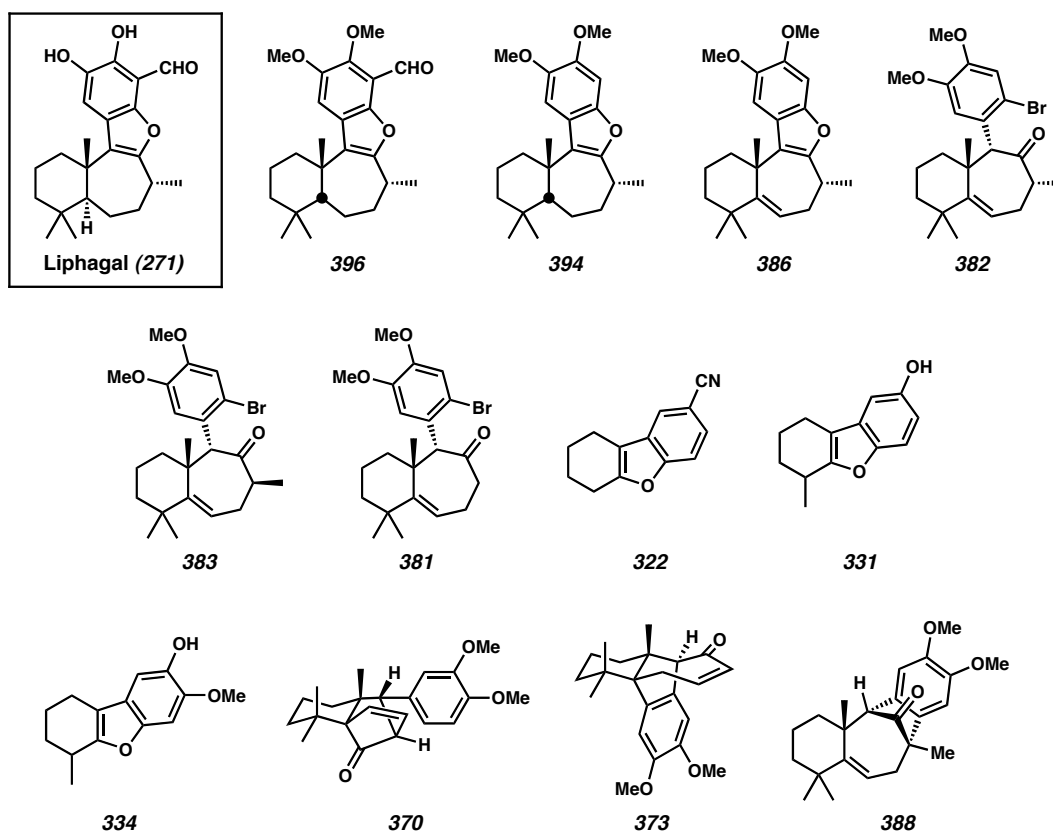
Scheme 4.42 Proposed Total Synthesis of Liphagal



4.9 Analogues for PI3K Biological Screening

A large number of potential candidates for PI3K biological screening have been prepared during our synthetic investigations toward liphagal (**271**). Many of these molecules could be used for structure-activity-relationship studies (Figure 4.3). Specifically, we can probe the functional groups of our compounds that are mandatory for biological activity.

Figure 4.3 Selected Molecules For PI3K Biological Activity Studies



Screening of aldehyde **396** may determine if the catechol pharmacophore is necessary for liphagal's potency and selectivity in PI3K α inhibition assays (Figure 4.3). Liphaganes including **396**, **394**, and **386** could ascertain the effect of aldehyde

functionality (or lack thereof) on biological activity. The importance of the benzofuran could be studied using compounds **382**, **383**, **381**, and others. Furthermore, the biological significance of the [6-7] carbocyclic system of the liphaganes (**272**, Figure 4.1) might be understood using model compounds **322**, **331**, and **334**. Additional structure activity relationship data may be garnered from the polycyclic compounds **370**, **373**, and **388**. A large collection of molecules prepared during this synthesis will be sent for biological screening against PI3K enzymes.⁴⁷

4.10 Concluding Remarks

Herein we have reported significant progress toward the catalytic enantioselective total synthesis of the meroterpenoid liphagal (**271**). Our route displays the utility of the enantioselective decarboxylative alkylation chemistry developed in our laboratory and sets the absolute stereochemistry of the natural product. We have also developed a powerful method for expanding [5-4] cyclobutene ring systems into 7-membered rings. The photoaddition of acetylene to a bicyclic enone sets vicinal quaternary stereocenters in a very congested molecule with high diastereoselectivity. These synthetic endeavors toward liphagal (**271**) have done much to elucidate the stereochemical proclivities of [6-7] carbocyclic frameworks. Furthermore, our synthesis of the benzofuran portion of the natural product demonstrated a creative solution to the problems posed by the inherent 7-membered ring chemistry. Importantly, many interesting compounds have been prepared during this synthetic investigation that could help elucidate the structure-activity-relationship between liphaganes (**272**) and PI3K enzymes.

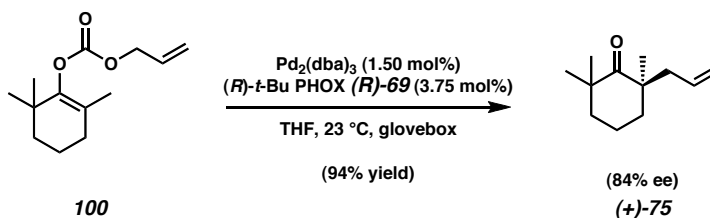
4.11 Experimental Procedures

4.11.1 Materials and Methods

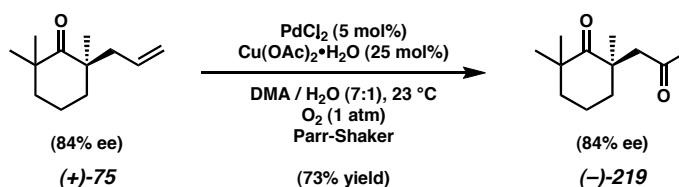
Unless stated otherwise, reactions were conducted in flame-dried glassware under an atmosphere of nitrogen using anhydrous solvents (either freshly distilled or passed through activated alumina columns). Chloroform was stabilized with ethanol and stored in the dark unless indicated otherwise. Methanol and *N,N*-dimethyl acetamide were used as purchased. TMEDA and *i*-Pr₂NH were distilled from CaH₂. 2,6-dimethylcyclohexanone (**220**) was fractionally distilled from CaSO₄ at ambient pressure prior to use. Dimethyl sulfate was fractionally distilled through a Vigreux column prior to use. All other commercially-obtained reagents were used as received, unless specified otherwise. (*R*)-*t*-Bu-PHOX ligand (**R**)-**69** was prepared according to known methods.⁴⁸ Reaction temperatures were controlled using an IKAmag temperature modulator. Thin-layer chromatography (TLC) was conducted with E. Merck silica gel 60 F254 pre-coated plates (0.25 mm) and visualized using UV at 254nm or 356 nm, *p*-anisaldehyde, ceric ammonium molybdate, potassium permanganate, and iodine vapor over sand. TLC data include R_f, eluent, and method of visualization. ICN silica gel (particle size 0.032-0.063 mm) or SilliaFlash P60 Academic silica gel (0.040-0.063 mm) was used for flash column chromatography. Analytical chiral HPLC analyses were performed with an Agilent 1100 Series HPLC using a chiralcel AD normal-phase column (250 x 4.6 mm) employing 2.0-3.0% ethanol in hexane isocratic elution and a flow rate of 0.1 mL/min with visualization at 254nm. Analytical chiral GC analysis was performed with an Agilent 6850 GC using a GT-A column (0.25m x 30.00m) employing an 80 °C isotherm and a flow rate of 1.0 mL/min. ¹H NMR spectra were recorded on a Varian Mercury 300 (at 300 MHz) or a

Varian Inova 500 (at 500 MHz) and are reported relative to the residual solvent peak (δ 7.26 for CDCl_3 and δ 7.16 for C_6D_6). Data for ^1H NMR spectra are reported as follows: chemical shift (δ ppm), multiplicity, coupling constant (Hz),⁴⁹ and integration. ^1H - ^1H nOesy 1D experiments were conducted at 300 MHz. In nOe drawings, the tail of the arrow denotes the proton being saturated, and the head the proton receiving spin transfer energy. ^1H - ^1H gCOSY experiments were performed at 300 MHz or 500 MHz. ^1H - ^1H homodecoupling experiments were performed at 300 MHz. ^{13}C NMR spectra were recorded on a Varian Mercury 300 (at 75 MHz) or a Varian Inova 500 (at 125 MHz) and are reported relative the residual solvent peak (δ 77.2 for CDCl_3 and δ 128.4 for C_6D_6). Data for ^{13}C NMR spectra are reported in terms of chemical shift. IR spectra were recorded on a Perkin Elmer Spectrum BXII spectrometer and are reported in frequency of absorption (cm^{-1}). IR samples were usually thin films deposited on sodium chloride plates by evaporation from a solvent (usually CDCl_3), which is recorded. Optical rotations were measured with a Jasco P-1010 polarimeter, using a 100 mm path-length cell. High-resolution mass spectra were obtained from the California Institute of Technology Mass Spectral Facility. Melting points were determined on a Thomas-Hoover melting point apparatus and are uncorrected. Boiling points are measured directly during distillation and are uncorrected. Sublimation points are measured directly. Crystallographic data have been deposited at the CCDC, 12 Union Road, Cambridge CB2 1EZ, UK. Copies can be obtained on request, free of charge, by quoting the publication citation and either deposition number 606034 for (\pm)-**319** or 634511 for (\pm)-**370**.

4.11.2 Syntheses of Compounds Related to Liphagal

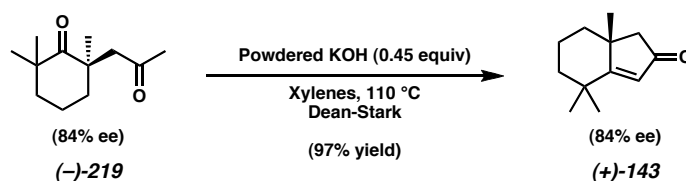


Allyl Ketone (+)-75. In the glovebox, a flamedried round-bottom flask was charged with $\text{Pd}_2(\text{dba})_3$ (181 mg, 0.198 mmol) and $(R)\text{-}t\text{-Bu-PHOX } (R)\text{-}69$ (192 mg, 0.495 mmol). Dry THF (390 mL) was added at 23 °C. After 30 min, a solution of enol carbonate **100** in THF (10 mL) was added. After 24 h, the reaction was removed from the glovebox and concentrated in vacuo at < 10 °C (product is volatile). The residue was purified by flash chromatography on silica gel (pentane \rightarrow 4:96 Et_2O :pentane \rightarrow 8:92 Et_2O :pentane eluent), giving allyl ketone **(+)-75** (2.23 g, 94% yield) as a colorless oil in 84% ee as determined by chiral HPLC. $[\alpha]_D^{25} +36.0^\circ$ (c 0.855, CHCl_3), 84% ee. Other characterization data for this compound can be found on pages 40 and 41 (chapter 2).

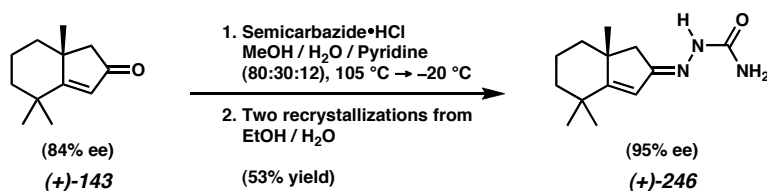


Diketone (-)-219. A Parr flask was charged with PdCl_2 (432 mg, 2.44 mmol) and $\text{Cu}(\text{OAc})_2 \cdot \text{H}_2\text{O}$ (2.27 g, 12.2 mmol), followed by H_2O (6.0 mL). A solution of allyl ketone **(+)-75** (4.39 g, 24.4 mmol) in DMA (42.0 mL) was introduced. The reaction was cooled to -78°C , then evacuated/backfilled (vacuum/ O_2) (3 x). The reaction was warmed to 23 °C and placed on a Parr Shaker under 1 atm of O_2 for 28 h. The reaction was

directly loaded onto a column of silica gel and purified by flash chromatography (20:80 Et₂O:hexane eluent), giving diketone (–)-**219** (3.51 g, 73% yield) in 84% ee as determined by chiral HPLC. $[\alpha]_D^{26} -70.3^\circ$ (*c* 0.970, CHCl₃), 84% ee. Other characterization data for this compound can be found on page 149 (chapter 3).

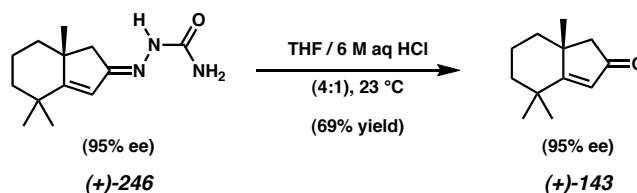


Bicyclic Enone (+)-143. A round-bottom flask was charged with a solution of diketone (–)-**219** (3.48 g, 17.7 mmol) in xylenes (75 mL). Powdered KOH (448 mg, 7.98 mmol) was added. The reaction was fitted with a Dean-Stark trap and reflux condenser, then heated to 110 °C for 22 h. Then, the reaction was cooled to 23 °C. It was directly loaded onto a column of silica gel and purified by flash chromatography (hexane → 40:60 Et₂O:hexane eluent), giving bicyclic enone (+)-**143** (3.06 g, 97% yield) in 84% ee as determined by chiral HPLC. $[\alpha]_D^{26} +90.7^\circ$ (*c* 0.865, CHCl₃), 84% ee. Other characterization data for this compound can be found on page 152 (chapter 3).



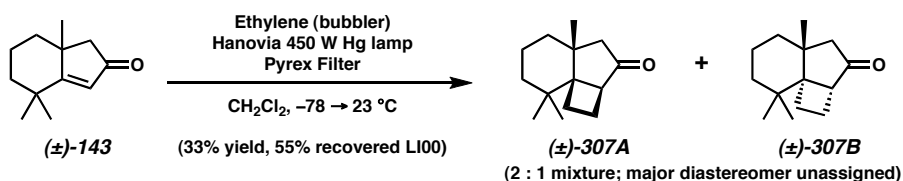
Bicyclic Semicarbazone (+)-246. A round-bottom flask containing the scalemic bicyclic enone (+)-**143** (3.04 g, 17.06 mmol, 1.00 equiv, 84% ee) was charged with MeOH (48.6 mL), H₂O (18.2 mL), and pyridine (7.30 mL). Semicarbazide hydrochloride (3.42 g, 30.7

mmol, 1.80 equiv) was added. The reaction was heated to 105 °C for 4 h and cooled to –20 °C overnight. The white crystals that formed were filtered, washed with H₂O, dried in the air, and transferred to a new round-bottom flask. Absolute EtOH (200 mL) was added gradually at 100 °C. H₂O (160 mL) was gradually added. A persistent cloudiness developed, but had cleared by 2 min. The heat was turned off, and the flask allowed to cool to gradually to 23 °C overnight.⁵⁰ The crystals were filtered and redissolved in EtOH (180 mL) at 100 °C. H₂O (130 mL) was added as before. The heating bath was turned off, and the system allowed to cool to 23 °C. The crystals were collected after 2 days via filtration. They were dried in vacuo over P₂O₅, giving **(+)-246** (2.45 g, 53% yield) in 95% ee as determined by chiral HPLC. Other characterization data for this compound can be found on page 151 (chapter 3).



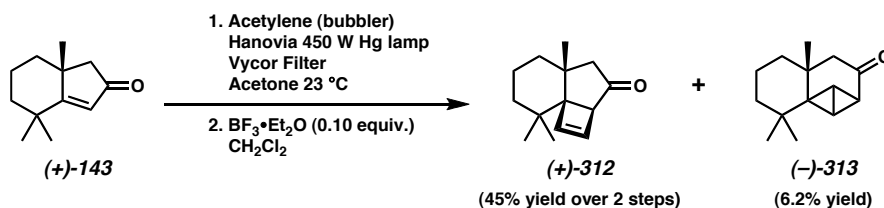
Bicyclic Enone (+)-143. A round-bottom flask containing the bicyclic semicarbazone **(+)-246** (2.37 g, 10.1 mmol, 95% ee) was charged with THF (50 mL) and 6 M aq HCl (20 mL). The reaction was stirred vigorously at 23 °C for 18 h. It was diluted with hexanes (20 mL), and the organic phase was collected. The aqueous layer was extracted with CH₂Cl₂ (3 x 30 mL) followed by with EtOAc (3 x 30 mL). All organic layers were combined, dried (Na₂SO₄), filtered, and concentrated. The residue was purified by flash chromatography on silica gel (20:80 EtOAc:hexane eluent), giving enantioenriched bicyclic enone **(+)-143** (3.06 g, 69% yield) in 95% ee as determined by chiral HPLC.

$[\alpha]_D^{25} +107.5^\circ$ (c 1.415, CHCl_3), 95% ee. Other characterization data for this compound can be found on page 152 (chapter 3).



Cyclobutenes (\pm)-307A and (\pm)-307B. A 500 mL glass photoreactor was charged with a solution of racemic bicyclic enone (\pm)-143 (950 mg, 5.33 mmol) in CH_2Cl_2 (240 mL). The solution was degassed with argon for 10 min. A quartz cooling jacket was inserted into the reactor. A hanovia medium pressure 450 W mercury lamp, jacketed with a pyrex filter, was inserted into the quartz cooling jacket. The reactor was cooled externally to -78°C and internally with water circulation in the quartz cooling jacket. The reaction was kept under a positive pressure of N_2 . Ethylene gas was bubbled through steadily using a needle for 10 min. Then, the bubbling was stopped and the solution irradiated. More ethylene was bubbled in every hour for 10 min time intervals until 2 hours had passed. Seeing that not much starting material had converted to product, the external temperature was carefully elevated to 23°C , and ethylene was bubbled through steadily for another 2 hours. The reaction was concentrated. Benzene was added, and the reaction was concentrated a second time. The residue was then taken up in benzene and wet-loaded onto a silica gel column then purified by flash chromatography (20:80 Et_2O :pentane \rightarrow 50:50 Et_2O :pentane eluent), affording an inseparable mixture of cyclobutenes (\pm)-307A and (\pm)-307B (368 mg, 33% yield, 2:1 dr, major diastereomer not identified) as a waxy white semisolid. R_f 0.55 (1:4 EtOAc /hexane), (p -Anisaldehyde, red

spot); mp 203-205 °C; ^1H NMR (300 MHz, CDCl_3): δ 2.91 (AB spin system, d, J_{AB} = 16.5 Hz, 1.33H), 2.78 (AB spin system, d, J_{AB} = 16.8 Hz, 0.67H), 2.53 (app. d, J = 12.2 Hz, 0.67H), 2.49 (app. d, J = 8.0 Hz, 1.33H), 2.32-1.90 (m, 6H), 1.79 (AB spin system, d, J_{AB} = 16.8 Hz, 0.67H), 1.76 (AB spin system, d, J_{AB} = 16.5 Hz, 1.33H), 1.70-1.16 (m, 14H), 1.08 (s, 4H), 1.01 (s, 2H), 1.00 (s, 2H), 0.97 (s, 4H), 0.95 (s, 4H), 0.85 (s, 2H); ^{13}C NMR (75 MHz, CDCl_3): δ 220.8, 220.4, 57.8, 55.2, 54.2, 54.0, 48.3, 45.3, 43.5, 41.1, 36.3, 35.7, 34.7, 34.3, 33.4, 30.1, 29.6, 28.3, 27.2, 24.6, 24.2, 22.3, 22.0, 20.1, 19.9; IR (KBr): 2931, 1736, 1466, 1390, 1269, 1156 cm^{-1} ; HRMS-EI $^+$ (m/z): $[\text{M}]^+$ calc'd for $\text{C}_{14}\text{H}_{22}\text{O}$, 206.1671; found, 206.1669. In addition, unreacted (\pm)-**143** (527 mg, 55% yield) was also recovered.



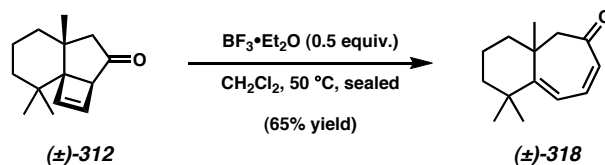
Cyclobutene (+)-312 and Bicyclobutane (-)-313. A 1.5 L glass photoreactor was charged with a solution of bicyclic enone (**(+)-143**) (1.207 g, 6.77 mmol) in acetone (ACS grade)(1.0L). The solution was degassed with argon for 10 min. A quartz cooling jacket was inserted into the reactor. A hanovia medium pressure 450 W mercury lamp, jacketed with a vycor filter, was inserted into the quartz cooling jacket. The reactor was cooled externally to 0 °C and internally with water circulation in the quartz cooling jacket. The reactor was also fitted with a reflux condenser with circulated ethylene glycol/water at a temperature of 5 °C, and the reaction was kept under a positive pressure of N_2 . Acetylene gas was bubbled through steadily using a needle as the solution was

irradiated for 10 h. The reaction was concentrated. The residue was then taken up in benzene and wet-loaded onto a silica gel column then purified by flash chromatography (5:95 EtOAc:hexane \rightarrow 20:80 EtOAc:hexane eluent), affording a crude mixture of cyclobutene (+)-**312** and bicyclobutane (–)-**313**, which was carried on to the next reaction. Additionally, an analytically pure sample of bicyclobutane (–)-**313** (85.2 mg, 6.2% yield) was obtained as a pale yellow oil, which was unstable on silica gel. R_f 0.45 (1:4 EtOAc/hexane), (*p*-Anisaldehyde, red spot); ^1H NMR (300 MHz, C_6D_6): δ 2.48 (app. dd, $J = 3.9$ Hz, 2.5 Hz, 1H), 1.80 (app. d $J = 16.3$ Hz, 1H), 1.75 (app. d, $J = 16.3$, 1H), 1.68 (app. dd, $J = 9.9$ Hz, 2.5 Hz, 1H), 1.59 (app. dd, $J = 9.9$ Hz, 3.9 Hz, 1H), 1.31–1.15 (m, 6H), 0.94 (s, 3H), 0.85 (s, 3H), 0.52 (s, 3H); ^{13}C NMR (75 MHz, C_6D_6): δ 208.5, 60.4, 55.8, 48.3, 41.7, 40.7, 36.9, 33.4, 29.1, 28.3, 27.0, 18.6, 16.7, 14.9; IR (NaCl/neat film): 3092, 2927, 1713, 1456, 1390, 1377, 1276, 1226, 1041, 979, 812, 797 cm^{-1} ; HRMS-EI $^+$ (m/z): $[\text{M}]^+$ calc'd for $\text{C}_{14}\text{H}_{20}\text{O}$, 204.1514; found, 204.1519. $[\alpha]_D^{25} -22.04^\circ$ (c 1.65, C_6H_6), 95% ee. Unreacted starting material (±)-**143** (146.8mg, 12% yield) was also recovered.

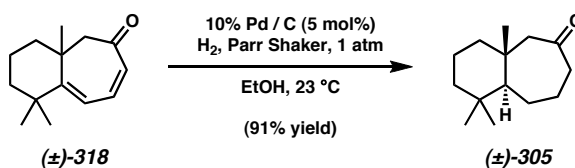
An analytically pure sample of cyclobutene (+)-**312** was obtained in the following manner. A round-bottom flask containing analytically pure bicyclobutane (–)-**313** (80.0 mg, 0.392 mmol) in CH_2Cl_2 (5 ml) was treated with $\text{BF}_3 \cdot \text{Et}_2\text{O}$ (5 μL) at 23 $^\circ\text{C}$. After 10 min, the reaction was added dropwise to a rapidly stirred suspension of brine (10 mL), sat. aq NaHCO_3 (10 mL), and CH_2Cl_2 (20 mL). The organic layer was collected, and the aqueous phase was extracted with CH_2Cl_2 (2 x). The organic layers were combined, dried (Na_2SO_4), filtered, and concentrated. The residue was taken up in benzene and purified by flash chromatography on silica gel (5:95 EtOAc:hexane eluent), affording cyclobutene

(+)-**312** (61.6 mg, 77% yield) as a waxy white, volatile semisolid. R_f 0.58 (1:4 EtOAc/hexane), (*p*-Anisaldehyde, red spot); mp 54-139 °C (amorphous), sublimation point, sp: < 23 °C (3 mmHg); ^1H NMR (300 MHz, C_6D_6): δ 6.00 (app. dd, $J = 2.8$ Hz, 0.6 Hz, 1H), 5.93 (app. dd, $J = 2.8$ Hz, 1.4 Hz, 1H), 3.00 (app. s, 1H), 2.87 (AB spin system, d, $J_{AB} = 16.0$ Hz, 1H), 1.58 (AB spin system, app. dd, $J_{AB} = 16.0$ Hz, $J = 1.7$ Hz, 1H), 1.36 (app. ddt, $J_{d1} = 27.2$ Hz, $J_{d2} = 12.7$ Hz, $J_t = 3.0$ Hz, 1H), 1.23-0.95 (m, 5H), 0.85 (s, 3H), 0.83 (s, 3H), 0.81 (s, 3H); ^{13}C NMR (75 MHz, C_6D_6): δ 123.0, 142.8, 138.4, 65.4, 58.9, 52.2, 39.0, 37.3, 36.1, 33.6, 28.5, 25.4, 22.2, 18.9; IR (NaCl/ CHCl_3): 3130, 3040, 2925, 2870, 2845, 1733, 1456, 141, 1388, 1378, 1212, 1160, 754, 726 cm^{-1} ; HRMS-EI $^+$ (m/z): $[\text{M}]^+$ calc'd for $\text{C}_{14}\text{H}_{20}\text{O}$, 204.1514; found, 204.1523; $[\alpha]_D^{26} +694.99^\circ$ (*c* 1.232, C_6H_6), 95% ee.

The crude mixture of cyclobutene (+)-**312** and (–)-**313** prepared above (excluding the pure isolated (–)-**313**) was dissolved in CH_2Cl_2 (50 mL) and treated with $\text{BF}_3 \cdot \text{Et}_2\text{O}$ (86 μL) at 23 °C for 10 min. The reaction was added dropwise to a rapidly stirred suspension of brine (50 mL), sat. aq NaHCO_3 (50 mL), and CH_2Cl_2 (50 mL). The organic layer was collected, and the aqueous phase was extracted with CH_2Cl_2 (2 x). The organic layers were combined, dried (Na_2SO_4), filtered, and concentrated. The residue was taken up in benzene and purified by flash chromatography on silica gel (5:95 EtOAc:hexane eluent), affording semipure cyclobutene (+)-**312** (578 mg, 45% yield over 2 steps as determined by ^1H NMR). A contaminant (with a structure similar to the product) with a mass of 265 mg was also present, as determined by ^1H NMR. The semipure cyclobutene (+)-**312** was used in subsequent reactions without further purification.

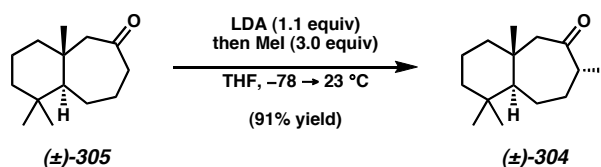


Cycloheptadienone (±)-318. A flamedried Schlenk tube under N₂ was charged with a solution of cyclobutene (+)-312 (125 mg, 0.600 mmol) and CH₂Cl₂ (20 mL). Then, BF₃•Et₂O (38 μL, 0.300 mmol) was added. The tube was sealed, and the yellow solution was heated to 50 °C for 9 h. The reaction was cooled to 23 °C and concentrated to ~5 mL. The solution was directly loaded onto a silica gel column and purified by flash chromatography (8:92 EtOAc:hexane eluent), affording cycloheptadienone (±)-318 (81.8 mg, 65% yield) as a pale yellow oil. *R*_f 0.52 (20:80 EtOAc/hexane), (*p*-Anisaldehyde, rose spot, UV, 254 nm); ¹H NMR (300 MHz, CDCl₃): δ 6.60 (dd, *J* = 11.8 Hz, 8.8 Hz, 1H), 6.10 (d, *J* = 8.8 Hz, 1H), 6.00 (app. dd, *J* = 11.8 Hz, 1.9 Hz, 1H), 2.79 (AB spin system, d, *J*_{AB} = 14.0 Hz, 1H), 2.16 (AB spin system, app. dd, *J*_{AB} = 14 Hz, *J* = 1.9 Hz, 1H), 1.80-1.30 (m, 6H), 1.20 (s, 3H), 1.12 (s, 3H), 1.01 (s, 3H); ¹³C NMR (75 MHz, CDCl₃): δ 200.7, 169.7, 139.4, 129.1, 119.4, 56.7, 41.9, 39.5, 38.2, 35.5, 32.9, 31.8, 20.4, 18.0; IR (NaCl/CDCl₃): 3030, 2961, 2932, 2867, 1660, 1571, 1461, 1420, 1372, 1312, 1233, 986 cm⁻¹; HRMS-FAB⁺ (*m/z*): [M+H]⁺ calc'd for C₁₄H₂₁O, 205.1592; found, 205.1583.



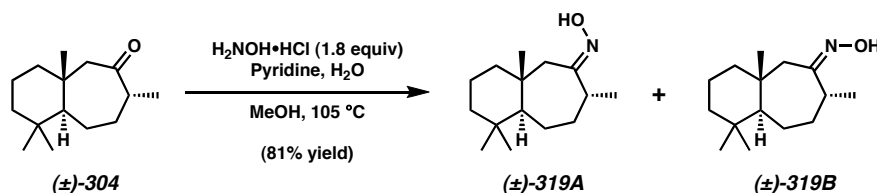
Cycloheptanone (±)-305. A Parr flask was charged with 10% w/w Pd/C (150 mg, 0.142 mmol), followed by a solution of cycloheptadienone (±)-318 (580 mg, 2.84 mmol) and

absolute ethanol (120 mL). The reaction was placed on a Parr shaker under H₂ (1 atm) at 23 °C for 4 h. The reaction was sparged with argon, then filtered through celite with the aide of Et₂O. The filtrate was concentrated and purified by flash chromatography on silica gel (Et₂O:hexane 10:90 eluent), affording cycloheptanone (\pm)-**305** (536 mg, 91% yield) as a colorless oil. *R_f* 0.58 (20:80 EtOAc/hexane), (*p*-Anisaldehyde, yellow spot); ¹H NMR (300 MHz, CDCl₃): δ 2.58 (AB spin system, d, *J*_{AB} = 12.4 Hz, 1H), 2.45 (app. dt, *J*_d = 18.4 Hz, *J*_t = 3.6 Hz, 1H), 2.24 (app. ddd, *J* = 19.2 Hz, 13.2 Hz, 4.1 Hz, 1H), 2.06 (AB spin system, *J*_{AB} = 12.4 Hz, 1H), 2.02-1.86 (m, 2H), 1.68-1.46 (m, 2H), 1.44-1.30 (m, 3H), 1.30-1.10 (m, 4H), 0.91 (s, 3H), 0.87 (s, 3H), 0.79 (s, 3H); ¹³C NMR (75 MHz, CDCl₃): δ 214.9, 61.6, 59.2, 43.4, 43.3, 42.4, 36.5, 34.7, 33.8, 26.1, 24.8, 21.7, 19.3, 19.1; IR (NaCl/CDCl₃): 2929, 1696, 1457, 1258 cm⁻¹; HRMS-EI⁺ (*m/z*): [M]⁺ calc'd for C₁₄H₂₄O, 208.1827; found, 208.1824.



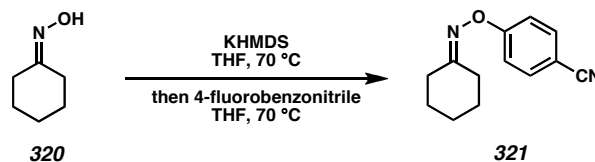
Methylcycloheptanone (\pm)-304. A flamedried round-bottom flask was charged with THF (7.7 mL) and *i*-Pr₂NH (130 μ L, 0.922 mmol) and cooled to 0 °C. *n*-BuLi (2.5 M in hexanes, 338 μ L, 0.845 mmol) was added dropwise. After 30 min, the reaction was cooled to -78 °C. THF (5.7 mL) was added, followed by a solution of cycloheptanone (\pm)-**305** (160 mg, 0.768 mmol) in THF (2.0 mL). After 1 h, MeI (144 μ L, 2.31 mmol) was added. After another hour had passed, the reaction was warmed to 23 °C and stirred for 1 h. The reaction was quenched with sat. aq NH₄Cl (5 mL) followed by H₂O (10 mL). Hexanes (10 mL) and Et₂O (15 mL) were added. The organic layer was collected, and the

aqueous layer was extracted with Et₂O (3 x 15 mL). All organic layers were combined, washed with brine (15 mL), dried (Na₂SO₄), filtered, and concentrated. The residue was purified by flash chromatography on silica gel (EtOAc:hexane 8:92 eluent), affording methylcycloheptanone (**(±)-304**) (147 mg, 86% yield) as a yellow oil. *R_f* 0.61 (20:80 EtOAc/hexane), (*p*-Anisaldehyde, purple spot); ¹H NMR (300 MHz, CDCl₃): δ 2.54 (AB spin system, d, *J*_{AB} = 11.6 Hz, 1H), 2.28-2.14 (m, 1H), 1.96 (AB spin system, d, *J*_{AB} = 11.6 Hz, 1H), 1.93 (app. d, *J* = 8.6 Hz, 1H), 1.87 (app. d, *J* = 8.6 Hz, 1H), 1.58 (app. ddt, *J*_{d1} = 14.3 Hz, *J*_{d2} = 13.5 Hz, *J*_t = 3.6 Hz, 1H), 1.43-1.30 (m, 3H), 1.30-1.12 (m, 3H), 1.16-0.88 (m, 2H), 1.01 (d, *J* = 7.4 Hz, 3H), 0.88 (s, 3H), 0.84 (s, 3H), 0.75 (s, 3H); ¹³C NMR (75 MHz, CDCl₃): δ 216.9, 59.3, 59.2, 47.9, 43.0, 42.3, 36.6, 34.6, 34.2, 33.7, 24.9, 21.6, 19.6, 19.5, 19.2; IR (NaCl/CDCl₃): 2927, 2868, 2846, 1697, 1458, 1385, 1367, 1274, 971 cm⁻¹; HRMS-EI⁺ (*m/z*): [*M*]⁺ calc'd for C₁₅H₂₆O, 222.1984; found, 222.1979.



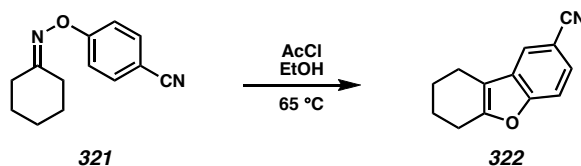
Methylcycloheptanoximes (±)-319A and (±)-319B. A vial containing methylcyclohexanone (**(±)-304**) (70 mg, 0.315 mmol) in MeOH (882 μL) was treated with H₂O (329 μL) and pyridine (133 μL). Then hydroxylamine hydrochloride (39.4 mg, 0.567 mmol) was introduced. The vial was sealed and heated to 105 °C. After 11 h, the residue was diluted with Et₂O, CHCl₃, and H₂O. The suspension was extracted with Et₂O (3 x). Organic layers were combined, dried (Na₂SO₄), filtered, and concentrated, giving methylcycloheptanoxime (2 imine geometric isomers) (**(±)-319A** and (**(±)-319B**) (61 mg,

81% yield) as a white powder. R_f 0.25 (3:97 MeOH/DCM), (KMnO₄, yellow spot); mp 153-155 °C (CHCl₃); ¹H NMR (300 MHz, CDCl₃) (major imine geometric isomer (±)-**319A**): δ 8.62 (s, broad, 1H), 3.04 (app. sept, $J_{\text{sept}} = 6.9$ Hz, 1H), 2.16 (AB spin system, d, $J_{\text{AB}} = 12.9$ Hz, 1H), 1.98-1.82 (m, 1H), 1.85 (AB spin system, d, $J_{\text{AB}} = 12.9$ Hz, 1H), 1.75 (app. dd, $J = 12.9$ Hz, 9.1 Hz, 1H), 1.61 (app. tt, $J = 13.5$ Hz, 3.6 Hz, 1H), 1.46-1.40 (m, 1H), 1.38 (app. d, $J = 13.2$ Hz, 2H), 1.28-1.10 (m, 3H), 1.16 (d, $J = 6.9$ Hz, 3H), 0.99 (app. d, $J = 10.2$ Hz, 1H), 0.95 (app. d, $J = 10.2$ Hz, 1H), 0.89 (s, 3H), 0.84 (s, 3H), 0.75 (s, 3H); ¹³C NMR (75 MHz, CDCl₃) (major imine geometric isomer (±)-**319A**): δ 165.6, 60.7, 48.3, 43.0, 42.3, 37.4, 36.3, 34.6, 34.1, 33.9, 24.0, 21.7, 19.6, 19.5, 18.6; IR (NaCl/CDCl₃) (major imine geometric isomer (±)-**319A**) : 3233 (broad), 2927, 1457, 1382, 1363, 994, 979, 962, 881 cm⁻¹; HRMS-EI⁺ (m/z): [M]⁺ calc'd for C₁₅H₂₇ON, 237.2093; found, 237.2087. X-Ray-quality crystals of the minor imine geometric isomer (±)-**319B** were obtained by taking the (±)-**319A**/(±)-**319B** mixture and dissolving it in heptane. The solution was allowed to undergo negative vapor diffusion within a sealed chamber containing heavy mineral oil.



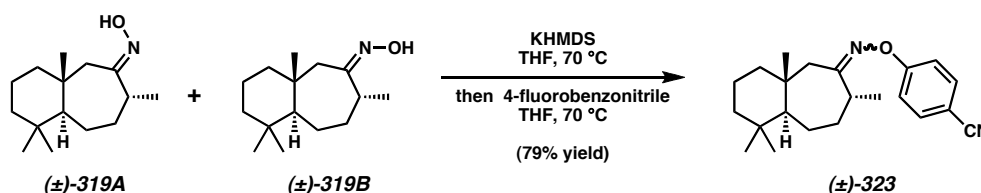
O-Aryloxime 321. In the glovebox, a flamedried round-bottom flask under argon was charged with KHMDS (484.1 mg, 2.43 mmol) and removed from the glovebox. A solution of cyclohexanoxime (**320**) (250 mg, 2.21 mmol) in THF (20 mL) was added. The reaction was fitted with a reflux condenser and heated to 70 °C for 1 h. Then, a solution of 4-fluorobenzonitrile (267.7 mg, 2.21 mmol) in THF (5 mL) was added.

Heating at 70 °C was continued for 4 h. The reaction was cooled to 23 °C and quenched with sat. aq NH₄Cl (8 mL). 5 min later, H₂O and hexanes were added. The reaction was extracted with EtOAc (3 x 20 mL). Organic layers were combined, dried (Na₂SO₄), filtered, and concentrated. The compound was purified by flash chromatography on silica gel (5:95 EtOAc:hexane eluent), affording **321** (yield not determined) as a white semisolid. *R_f* 0.59 (20:80 EtOAc/hexane), (*p*-Anisaldehyde, red spot); mp 66-68 °C (CDCl₃); ¹H NMR (300 MHz, CDCl₃): δ 7.57 (app. ddd, *J* = 9.1 Hz, 2.5 Hz, 2.1 Hz, 2H), 7.24 (app. ddd, *J* = 8.8 Hz, 2.5 Hz, 1.9 Hz, 2H), 2.65 (app. dd, *J* = 6.6 Hz, 6.0 Hz, 2H), 2.35 (app. dd, *J* = 6.6 Hz, 6.0 Hz, 2H), 1.80-1.60 (m, 6H); ¹³C NMR (75 MHz, CDCl₃): δ 165.9, 162.8, 133.9, 119.6, 115.1, 104.6, 32.2, 27.1, 26.4, 26.0, 25.7; IR (NaCl/CDCl₃): 2927, 2860, 2224, 1645, 1601, 1572, 1501, 1449, 1238, 1214, 1162, 892, 836 cm⁻¹; HRMS-EI⁺ (*m/z*): [M]⁺ calc'd for C₁₃H₁₄N₂O, 214.1106; found, 214.1104.



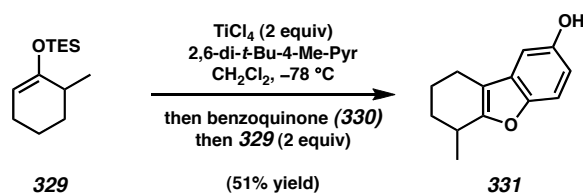
Cyanobenzofuran 322. A vial containing *O*-aryloxime **321** (20 mg, 93.3 μmol) was treated with a preformed solution of acetyl chloride (100 μL, 1.41 mmol) and absolute EtOH (1.0 mL). The vial was sealed and heated to 65 °C for 4.5 h. After cooling to 23 °C, the reaction was concentrated, and the residue immediately diluted with H₂O and CH₂Cl₂. The organic layer was collected and the aqueous layer extracted with CH₂Cl₂ (1 x). Organic layers were combined, dried (Na₂SO₄), filtered, and concentrated. The residue was purified on a preparative thin layer plate of silica gel (20:80 EtOAc:hexane

eluent), affording **322** (yield not determined) as a white powder. R_f 0.58 (20:80 EtOAc/hexane), (UV, 254 nm); mp 99-101 °C (CHCl_3); ^1H NMR (300 MHz, CDCl_3): δ 7.72 (app. s, 1H), 7.48 (dd, $J = 8.5$ Hz, 1.7 Hz, 1H), 7.44 (app. dd, $J = 8.5$ Hz, 0.8 Hz, 1H), 2.76 (app. tt, $J = 6.0$ Hz, 2.0 Hz, 2H), 2.62 (app. tt, $J = 6.0$ Hz, 2.0 Hz, 2H), 2.01-1.91 (m, 2H), 1.91-1.81 (m, 2H); ^{13}C NMR (75 MHz, CDCl_3): δ 157.0, 129.8, 127.1, 123.5, 120.0, 113.2, 112.0, 106.1, 23.5, 22.8, 22.5, 20.3; IR (NaCl/ CDCl_3): 2940, 2862, 2220, 1638, 1462, 1440, 1295, 1228, 1106, 876, 810 cm^{-1} ; HRMS-EI $^+$ (m/z): $[\text{M}]^+$ calc'd for $\text{C}_{13}\text{H}_{11}\text{NO}$, 197.0841; found, 197.0843.



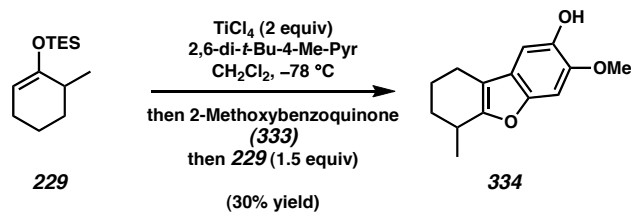
Aryloxime (±)-323. A solution of the two methylcyclohexanoximes (±)-319A and (±)-319B (59 mg total, 2.49 mmol) and THF (25 mL) was treated with KHMDS (52 mg, 2.61 mmol, weighed in glovebox). The reaction was heated to 70 °C for 1 h. 4-Fluorobenzonitrile (30.1 mg, 2.49 mmol) was introduced, and the heating at 70 °C was continued for 4 h. The reaction was quenched with sat. aq NH_4Cl (5 mL) and diluted with hexane (10 mL) and H_2O (5 mL). The suspension was extracted with Et_2O (3 x 15 mL). All organic layers were combined, washed (brine, 10 mL), dried (Na_2SO_4), filtered, and concentrated. The residue was purified by flash chromatography on silica gel (hexane \rightarrow 5:95 EtOAc:hexane eluent), affording (±)-323 as a 3 : 1 mixture of imine geometric isomers (66.2 mg, 79% yield) as a colorless oil. R_f 0.67 (20:80 EtOAc/hexane), (UV, 254 nm); ^1H NMR (300 MHz, CDCl_3): δ 7.58 (app. ddd, $J = 9.1$ Hz, 2.2 Hz, 1.7 Hz, 4H), 7.22

(app. ddd, $J = 8.8$ Hz, 1.9 Hz, 1.7 Hz, 4H), 3.18 (app. septet, $J_{\text{sept}} = 6.9$ Hz, 1.5H), 2.85 (AB spin system, d, $J_{\text{AB}} = 12.4$ Hz, 0.5H), 2.67 (app. d of septet, $J_{\text{d}} = 11.0$ Hz, $J_{\text{sept}} = 6.9$ Hz, 0.5H), 2.28 (AB spin system, d, $J_{\text{AB}} = 12.7$ Hz, 1.5H), 2.01 (AB spin system, d, $J_{\text{AB}} = 12.7$ Hz, 1.5H), 2.11-1.87 (m, 2H), 1.98 (AB spin system, d, $J_{\text{AB}} = 12.4$ Hz, 0.5H), 1.46-1.38 (m, 6H), 1.32-1.20 (m, 8H), 1.16 (d, $J = 6.9$ Hz, 1.5H), 1.11 (d, $J = 6.9$ Hz, 4.5H), 1.18-0.86 (m, 2H), 0.93 (s, 1.5H), 0.91 (s, 4.5H), 0.90 (s, 4.5H), 0.89 (s, 1.5H), 0.77 (s, 1.5H), 0.76 (s, 4.5H); ^{13}C NMR (75 MHz, CDCl_3): δ 171.2, 169.9, 162.9, 162.7, 133.9 (2C), 119.6, 115.3, 115.2, 104.6, 60.7, 60.3, 47.8, 43.0, 42.8, 42.3, 42.2, 42.0, 39.7, 38.0, 37.3, 36.2, 35.9, 35.3, 34.7, 34.6, 33.8, 33.7, 23.9, 23.8, 22.5, 21.7, 21.6, 19.8, 19.6, 19.50, 19.45, 19.1; IR (NaCl/ CDCl_3): 2928, 2868, 2224, 1601, 1576, 1501, 1458, 1311, 1242, 1161, 941, 911, 880, 836 cm^{-1} ; HRMS- EI^+ (m/z): $[\text{M}]^+$ calc'd for $\text{C}_{22}\text{H}_{30}\text{N}_2\text{O}$, 338.2358; found, 338.2363.



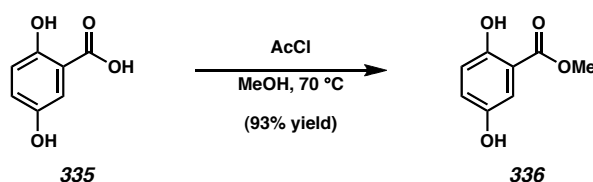
Hydroxybenzoquinone 331. A flamedried round-bottom flask under argon was charged with a solution of 2,6-di-*t*-butyl-4-methyl pyridine (307 mg, 1.49 mmol, 4 equiv) and CH_2Cl_2 (10 mL) and cooled to -78°C . Then, a solution of TiCl_4 (82 μL , 0.746 mmol) and CH_2Cl_2 (1.6 mL) was slowly introduced, followed by a solution of benzoquinone (**330**) (40.4 mg, 0.373 mmol, 1 equiv) in CH_2Cl_2 (10 mL). The reaction turned an orange-brown color. Then, a solution of silyl enol ether **229** (170 mg, 0.746 mmol, 2 equiv) in CH_2Cl_2 (5 mL) was added via syringe pump over a 3 h period, and the reaction became

maroon. Once the addition was complete, 6 M aq HCl (5 mL) was added at $-78\text{ }^{\circ}\text{C}$, and the reaction was warmed to $23\text{ }^{\circ}\text{C}$, becoming pale yellow. After 3 h, MeOH (25 mL) was added, and the reaction was refluxed overnight. The reaction was cooled to $23\text{ }^{\circ}\text{C}$, then diluted with H_2O and hexanes. The suspension was extracted with CH_2Cl_2 (2 x). All organic layers were combined and washed with brine. The combined aqueous layers were back-extracted with CH_2Cl_2 (3 x). All organic layers were combined, dried (Na_2SO_4), filtered, and concentrated. The residue was purified by flash chromatography on silica gel (hexane \rightarrow EtOAc:hexane 5:95 eluent), affording hydroxybenzofuran **331** (41.8 mg, 51% yield based on benzoquinone (**330**)) as a colorless oil. R_f 0.19 (20:80 EtOAc/hexane), (*p*-Anisaldehyde, purple spot, UV, 254 nm); ^1H NMR (300 MHz, CDCl_3): δ 7.25 (d, $J = 8.8$ Hz, 1H), 6.82 (d, $J = 2.5$ Hz, 1H), 6.71 (dd, $J = 8.8$ Hz, 2.5 Hz, 1H), 4.99 (s, 1H), 2.96 (app. d of sextuplet, $J_{\text{sext}} = 6.9$ Hz, $J_{\text{d}} = 1.4$ Hz, 1H), 2.55 (app. dd, $J = 5.2$ Hz, 1.9 Hz, 1H), 2.52 (app. dd, $J = 5.2$ Hz, 1.9 Hz, 1H), 2.00 (app. dddd, $J = 34.7$ Hz, 12.9 Hz, 5.8 Hz, 2.8 Hz, 1H), 1.99 (app. dddd, $J = 32.2$ Hz, 12.9 Hz, 5.5 Hz, 2.5 Hz, 1H), 1.69 (app. dddd, $J = 63.8$ Hz, 20.4 Hz, 10.2 Hz, 2.8 Hz, 1H), 1.68 (app. dddd, $J = 56.9$ Hz, 15.7 Hz, 7.7 Hz, 2.5 Hz, 1H), 1.31 (d, $J = 6.9$ Hz, 3H); ^{13}C NMR (75 MHz, CDCl_3): δ 159.3, 151.2, 149.5, 129.9, 112.4, 111.3, 104.2, 32.2, 29.5, 21.5, 20.9, 18.9; IR (NaCl/ CDCl_3): 3338 (br), 2962, 2932, 2854, 1619, 1596, 1456, 1395, 1377, 1336, 1283, 1191, 1152, 1125, 931, 800 cm^{-1} ; HRMS-FAB $^+$ (m/z): $[\text{M}+\text{H}]^+$ calc'd for $\text{C}_{13}\text{H}_{15}\text{O}_2$, 203.1072; found, 203.1079.

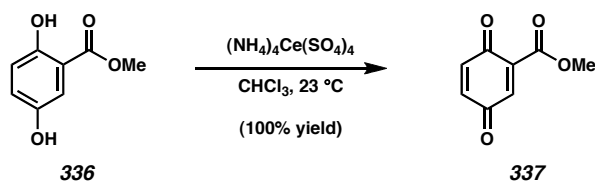


5-Hydroxy-6-Methoxybenzoquinone 334. A flamedried round-bottom flask under argon was charged with a solution of 2,6-di-*t*-butyl-4-methyl pyridine (309 mg, 1.50 mmol, 4 equiv) and CH₂Cl₂ (10 mL) and cooled to -78°C . Then, a solution of TiCl₄ (83 μL , 0.751 mmol) and CH₂Cl₂ (1.6 mL) was slowly introduced, followed by a solution of 2-methoxybenzoquinone (**333**) (51.9 mg, 0.373 mmol, 1 equiv) in CH₂Cl₂ (8.0 mL). The reaction turned a red-brown color. Then, a solution of silyl enol ether **229** (128 mg, 0.563 mmol, 1.5 equiv) in CH₂Cl₂ (5 mL) was added via syringe pump over a 2 h period, and the reaction became violet. Once the addition was complete, 6 M aq HCl (5 mL) was added at -78°C , and the reaction was warmed to 23°C , becoming orange-brown. THF (20 mL) was added, and the reaction was concentrated in vacuo to ~ 25 mL. More THF (20 mL) and 6 M aq HCl (3 mL) were added, and the pink reaction was heated to 65°C overnight. The reaction was cooled to 23°C and diluted with H₂O and hexanes. The suspension was extracted with Et₂O (3 x 20 mL). All organic layers were combined and washed with brine. The combined aqueous layers were back-extracted with CH₂Cl₂ (2 x). All organic layers were combined, dried (Na₂SO₄), filtered, and concentrated. The residue was purified by flash chromatography on silica gel (hexane \rightarrow EtOAc:hexane 5:95 eluent), affording 5-hydroxy-6-methoxybenzofuran **334** (28.3 mg, 30% yield based on 2-methoxybenzoquinone (**333**)) white powder. *R*_f 0.40 (20:80 EtOAc/hexane), (*p*-Anisaldehyde, blue spot, UV, 254 nm); mp $127\text{--}129^\circ\text{C}$ (CHCl₃); ¹H NMR (300 MHz, CDCl₃): δ 6.99 (s, 1H), 6.92 (s, 1H), 5.52 (s, 1H), 3.91 (s, 3H), 2.94 (app. d of sextuplet,

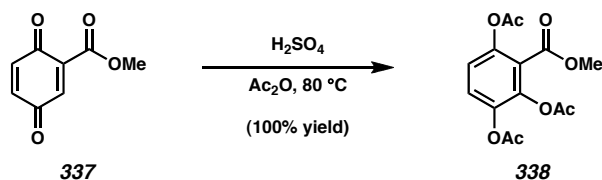
$J_{\text{sext}} = 6.9 \text{ Hz}$, $J_{\text{d}} = 1.9 \text{ Hz}$, 1H), 2.56 (app. dd, $J = 5.5 \text{ Hz}$, 1.9 Hz, 1H), 2.53 (app. dd, $J = 5.5 \text{ Hz}$, 1.9 Hz, 1H), 2.00 (app. dddd, $J = 34.7 \text{ Hz}$, 12.9 Hz, 5.8 Hz, 2.8 Hz, 1H), 1.99 (app. dddd, $J = 32.2 \text{ Hz}$, 12.9 Hz, 5.5 Hz, 2.5 Hz, 1H), 1.69 (app. dddd, $J = 63.8 \text{ Hz}$, 20.4 Hz, 10.2 Hz, 2.8 Hz, 1H), 1.68 (app. dddd, $J = 56.9 \text{ Hz}$, 15.7 Hz, 7.7 Hz, 2.5 Hz, 1H), 1.30 (d, $J = 6.9 \text{ Hz}$, 3H); ^{13}C NMR (75 MHz, CDCl_3): δ 157.2, 148.4, 144.2, 142.2, 121.7, 112.3, 103.0, 94.9, 56.6., 32.3, 29.5, 21.6, 21.0, 19.0; IR (NaCl/ CDCl_3): 3436 (br), 2959, 2928, 2854, 1623, 1595, 1491, 1445, 1374, 1343, 1318, 1189, 1136 cm^{-1} ; LRMS-EI $^{+}$ (m/z): $[\text{M}]^{+}$ calc'd for $\text{C}_{14}\text{H}_{16}\text{O}_3$, 232.1; found, 232.1106.



2,5 Dihydroxy Methylbenzoate (336). A round-bottom flask containing MeOH (40 mL) was treated slowly with AcCl (460 μL) at 23 $^{\circ}\text{C}$. Then, gentisic acid (**335**) (5.00 g, was added, and the reaction was heated to 70 $^{\circ}\text{C}$ for 21 h. Then, more AcCl (690 μL) was cautiously added to facilitate conversion. Heating to 70 $^{\circ}\text{C}$ was continued for 2 d. KHCO_3 and H_2O were added to quench the acid. The reaction was extracted with EtOAc (3 x 50 mL). Organic layers were combined, washed with brine, dried (Na_2SO_4), filtered, and concentrated. The residue was concentrated from PhH, taken up in EtOAc:PhH (1:1), then purified via flash column chromatography on silica gel (EtOAc:hexane 30:70 eluent), giving 2,5 dihydroxy methylbenzoate (**336**) (5.06 g, 93% yield). Characterization data for this compound was identical to previously reported data.⁵¹

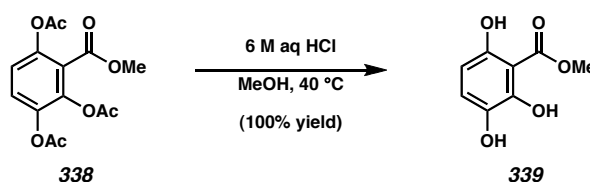


2-Methoxycarbonyl-1,4-benzoquinone (337). A round-bottom flask containing 2,5-dihydroxy methylbenzoate (**336**) (5.06 g, 30.1 mmol, 1.0 equiv) was charged with ceric ammonium sulfate (54.0 g, 90.3 mmol, 3.0 equiv) and CHCl_3 (stabilized with amylenes, 200 mL). The reaction was stirred vigorously for 20 h at 23 °C. It was then filtered over glass frits with the aid of CHCl_3 (stabilized with amylenes). The filtrate was concentrated in vacuo, giving 2-methoxycarbonyl-1,4-benzoquinone (**337**) (5.04 g, 100% yield). Characterization data for this compound was identical to previously reported data.⁵²



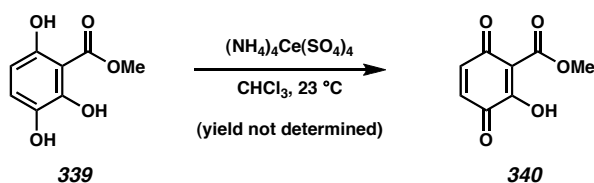
2,3,6-Triacetoxy-methylbenzoate (338). A round-bottom flask was charged with acetic anhydride (98%, 5 mL), and 10 drops of conc. aq H_2SO_4 were cautiously added (reaction tends to exotherm) from a glass pipet. Then, this solution was added slowly (exothermic reaction begins) to another round-bottom flask containing 2-Methoxycarbonyl-1,4-benzoquinone (**337**) (427 mg, 2.57 mmol). The flask was capped and warmed slowly to 60 °C and kept at this temperature for 3 h. The reaction was cooled to 23 °C and added slowly to a rapidly stirred suspension of H_2O (30 mL) and EtOAc (30 mL). The reaction was stirred vigorously for 15 min and the organic phase was collected. The aqueous layer

was extracted with EtOAc (2 x 20 mL). All organic layers were combined, dried (Na_2SO_4), filtered, and concentrated multiple times from toluene (to remove residual acetic acid), giving 2,3,6-triacetoxy-methylbenzoate (**338**) as a viscous orange-yellow oil, which solidified to a tan solid in vacuo (820 mg, 100% yield). R_f 0.55 (3:97 MeOH/DCM), (UV, 254 nm); mp 68-70 °C (CHCl_3); ^1H NMR (500 MHz, CDCl_3): δ 7.32 (d, $J = 9.0$ Hz, 1H), 7.05 (d, $J = 9.0$ Hz, 1H), 3.85 (s, 3H), 2.278 (s, 3H), 2.276 (s, 3H), 2.274 (s, 3H); ^{13}C NMR (125 MHz, CDCl_3): δ 168.9, 168.0, 167.7, 163.1, 147.0, 141.7, 141.0, 126.2, 121.4, 121.0, 52.8, 20.9, 20.8, 20.5; IR (NaCl/ CDCl_3): 2955, 1774, 1733, 1617, 1479, 1455, 1372, 1281, 1188, 1040, 1018, 902, 878 cm^{-1} ; HRMS-EI $^+$ (m/z): $[\text{M}]^+$ calc'd for $\text{C}_{14}\text{H}_{14}\text{O}_8$, 310.0688; found, 310.0683.

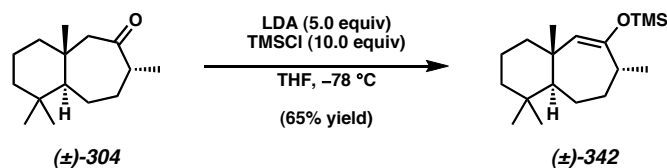


2,3,6-Trihydroxy-methylbenzoate (339). A round-bottom flask was charged with 2,3,6-triacetoxy-methylbenzoate (**338**) (1.00 g, 3.22 mmol), MeOH (40 mL), and 6 M aq HCl (8 mL). The reaction was warmed to 40 °C for 21 h. The reaction was then poured into H_2O (80 mL) and extracted with CH_2Cl_2 (3 x 40 mL). All organic layers were combined, dried (Na_2SO_4), filtered, and concentrated, giving 2,3,6-trihydroxy-methylbenzoate (**339**) (595 mg, 100% yield) as a pale yellow powder. R_f 0.49 (50:50 EtOAc/hexane), (UV, 254 nm); mp 132-134 °C (CHCl_3); ^1H NMR (500 MHz, CDCl_3): δ 9.89 (s, broad, 1H), 9.81 (s, broad, 1H), 7.05 (d, $J = 8.5$ Hz, 1H), 6.42 (d, $J = 8.5$ Hz, 1H), 5.22 (s, broad, 1H), 4.09 (s, 3H); ^{13}C NMR (125 MHz, CDCl_3): δ 170.0, 153.1, 146.7, 137.7, 122.4, 107.5, 100.1,

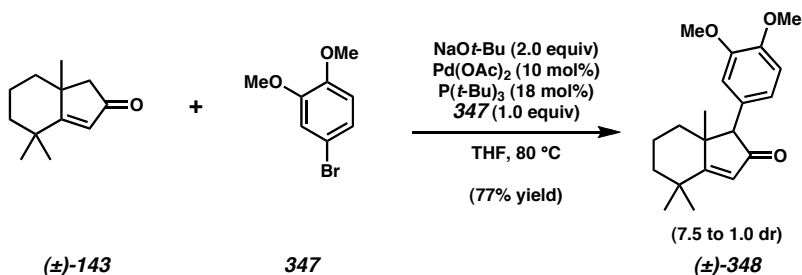
53.2; IR (NaCl/CDCl₃): 3434 (br), 1680, 1460, 1325, 1283, 1192, 1165, 1127, 1031, 996, 834, 811, 792 cm⁻¹; HRMS-EI⁺ (*m/z*): [M]⁺ calc'd for C₈H₈O₅, 184.0372; found, 184.0375.



2-Methoxycarbonyl-3-hydroxy-1,4-benzoquinone (340). A round-bottom flask was charged with 2,3,6-trihydroxy-methylbenzoate (**339**) (50 mg, 0.271 mmol) and ceric ammonium sulfate (487 mg, 0.814 mmol, 3 equiv), followed by CHCl₃ (10 mL, stabilized with amylenes). The reaction was stirred vigorously at 23 °C for 6 h, during which time the solvent became very orange-red. After the reaction was complete, it was filtered over glass frits, and the filtrate was concentrated, giving 2-methoxycarbonyl-3-hydroxy-1,4-benzoquinone (**340**) (yield not determined). *R_f* 0.30 (50:50 EtOAc/hexane), (visible red spot), (compound is unstable on silica gel); ¹H NMR (500 MHz, CDCl₃): δ 13.40 (s, broad, 1H), 6.79 (d, *J* = 10.2 Hz, 1H), 6.72 (d, *J* = 10.2 Hz, 1H), 3.98 (s, 3H); ¹³C NMR (125 MHz, CDCl₃): δ 181.7, 180.7, 171.1, 165.1, 139.2, 133.3, 132.5(?), 107.6(?), 53.8(?), 53.7(?) ; IR (NaCl/CDCl₃/CHCl₃): 3300 (br), 1734, 1682, 1662, 1575, 1449, 1393, 1356, 1325, 1249, 1210, 1117, 1030, 980, 850 cm⁻¹; HRMS-EI⁺ (*m/z*): [M]⁺ calc'd for C₈H₆O₅, 182.0215; found, 182.0223.

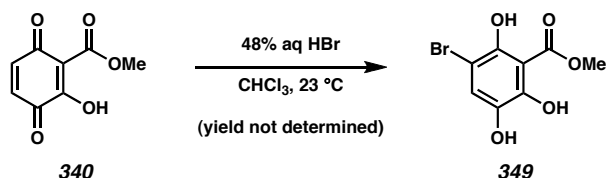


Silyl Enol Ether (±)-342. A flamedried round-bottom flask was charged with THF (6.0 mL) and *i*-Pr₂NH (240 μL, 1.71 mmol) and cooled to 0 °C. *n*-BuLi (2.5 M in hexanes, 624 μL, 1.56 mmol) was added dropwise. After 30 min, the reaction was cooled to −78 °C, and TMSCl (395 μL, 3.11 mmol, freshly distilled) was added. 5 min later, a solution of methylcycloheptanone (±)-304 (69.3 mg, 0.311 mmol), and THF (2.0 mL) was introduced dropwise over a 10 min period. 20 min later, the reaction was quenched at −78 °C via addition of Et₃N (500 μL), followed by sat. aq NaHCO₃ (1.0 mL). The reaction was allowed to thaw to 25 °C. The reaction was diluted with H₂O (10 mL) and hexanes (5 mL). The suspension was extracted with Et₂O (3 x 10 mL). The organic layers were collected and the aqueous layer was extracted with Et₂O (3 x 15 mL). All org layers were combined, washed with water (20 mL) followed by brine (10 mL), dried (K₂CO₃), filtered, and concentrated. The residue was evaporated 3x from PhH to remove residual water and TMSOH, giving (±)-342 (59.2 mg, 65% yield) as a colorless oil. *R*_f 0.53 (10:90 Et₃N/hexane), (*p*-Anisaldehyde, purple spot); ¹H NMR (300 MHz, C₆D₆): δ 4.75 (s, 1H), 2.45 (app. qdd, *J*_q = 7.2 Hz, *J*_{d1} = 7.2 Hz, *J*_{d2} = 2.5 Hz, 1H), 1.98-1.74 (m, 3H), 1.62-1.22 (m, 8H), 1.18 (d, *J* = 7.2 Hz, 3H), 1.11 (s, 3H), 0.89 (s, 3H), 0.86 (s, 3H), 0.22 (s, 3H); ¹³C NMR (75 MHz, C₆D₆): δ 155.1, 124.1, 51.9, 45.9, 43.6, 38.4, 37.1, 34.8, 33.9, 33.2, 24.5, 22.5, 21.5, 19.7, 18.0, 1.1(3C); IR (NaCl/neat film): 2929, 2868, 2846, 1685, 1655, 1645, 1460, 1384, 1375, 1251, 1168, 1150, 1131, 892, 841 cm^{−1}; HRMS-EI⁺ (*m/z*): [M]⁺ calc'd for C₁₈H₃₄OSi, 294.2379; found, 294.2365.

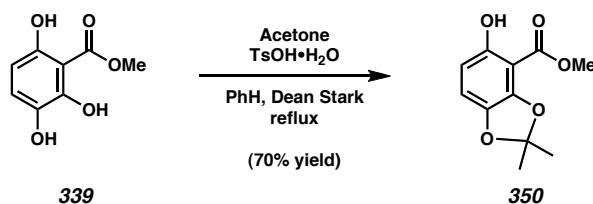


Aryl Enone (±)-348. In the glovebox, a vial was charged with NaOt-Bu (50.4 mg, 0.524 mmol), Pd(OAc)₂ (5.9 mg, 26.2 μmol), and a solution of P(*t*-Bu)₃ (9.5 mg, 47.2 μmol) in THF (1.0 mL). Then, a solution of the enone (±)-143 (47 mg, 0.262 mmol), 4-bromoveratrole (347) (56.9 mg, 0.262 mmol), and THF (1.0 mL) was introduced. The vial was cycled out of the glovebox, sealed, and heated to 80 °C for 24 h. Then, the reaction was cooled to 23 °C and quenched with sat. aq NH₄Cl (1.0 mL). After 5 min, the reaction was diluted with H₂O and hexane, then extracted with EtOAc (4 x 8 mL). All organic layers were combined, washed with brine, dried (Na₂SO₄), filtered, and concentrated. The residue was purified by flash column chromatography on silica gel (hexane → 7:93 EtOAc:hexane → 15:85 EtOAc:hexane → 30:70 EtOAc:hexane eluent), affording aryl enone (±)-348 (63.7 mg, 77% yield) as a yellow powder in 7.5:1.0 dr (major diastereomer not identified). *R_f* 0.57 (50:50 EtOAc/hexane), (UV, 254 nm); mp 132-136 °C (CHCl₃); ¹H NMR (500 MHz, CDCl₃)(Major Diastereomer Only): δ 6.83 (app. d, *J* = 8.1 Hz, 1H), 6.64 (app. d, *J* = 8.1 Hz, 1H), 6.59 (s, 1H), 6.00 (s, 1H), 3.86 (s, 3H), 3.84 (s, 3H), 3.49 (s, 1H), 1.98 (app. d, *J* = 12.7 Hz, 1H), 1.83 (app. dd, *J* = 27.6 Hz, 13.7 Hz, 1H), 1.71-1.50 (m, 3H), 1.46 (app. dd, *J* = 13.4 Hz, 11.9 Hz, 1H), 1.27 (s, 3H), 1.25 (s, 3H), 0.89 (s, 3H); ¹³C NMR (125 MHz, CDCl₃)(Major Diastereomer Only): δ 207.5, 192.1, 148.8, 148.3, 128.9, 125.9, 122.8, 113.6, 111.3, 68.6, 56.1, 56.0, 49.1, 41.1, 39.9, 36.3, 31.4, 27.4, 25.1, 18.9; IR (KBr): 3082, 2965, 2939, 2915, 2838, 1692, 1602,

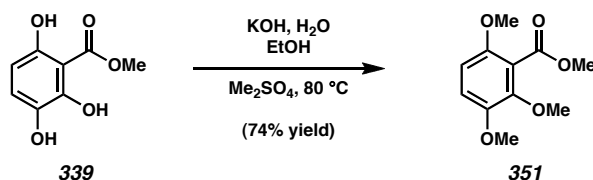
1520, 1470, 1255, 1235, 1165, 1143, 1028 cm^{-1} ; HRMS-EI⁺ (m/z): [M]⁺ calc'd for $\text{C}_{20}\text{H}_{26}\text{O}_3$, 314.1882; found, 314.1875.



5-Bromo-2,3,6-trihydroxy-methylbenzoate (349). A vial was charged with 2-methoxycarbonyl-3-hydroxy-1,4-benzoquinone (**340**) (9 mg, 49.3 μmol) as a solution in CHCl_3 (1.0 mL, stabilized with amylenes). 48% aq HBr (200 μL) was added, causing the reaction to turn from yellow to red. Once the reaction was complete, it was diluted with H_2O and extracted with CHCl_3 (3 x). All organic layers were combined, dried (Na_2SO_4), filtered, and concentrated. The residue was purified on a flash pipet column (2:98 EtOAc:hexane \rightarrow 5:95 EtOAc:hexane \rightarrow 10:90 EtOAc:hexane eluent), affording 5-bromo-2,3,6-trihydroxy-methylbenzoate (**349**) (yield was not determined) as a white powder. R_f 0.41 (50:50 EtOAc/hexane), (visible yellow spot); ^1H NMR (500 MHz, CDCl_3): δ 9.84 (s, 1H), 9.46 (s, 1H), 7.34 (s, 1H), 5.24 (s, 1H), 4.13 (s, 3H); ^{13}C NMR (125 MHz, CDCl_3): δ 169.5, 149.4, 146.4, 138.3, 125.4, 100.7, 99.5, 53.7; IR (NaCl/ CDCl_3): 3427 (br), 3116, 2960, 2917, 2849, 1680, 1630, 1474, 1438, 1398, 1367, 1308, 1278, 1181 cm^{-1} ; HRMS-EI⁺ (m/z): [M]⁺ calc'd for $\text{C}_8\text{H}_7\text{O}_5\text{Br}$, 261.9477; found, 261.9474.

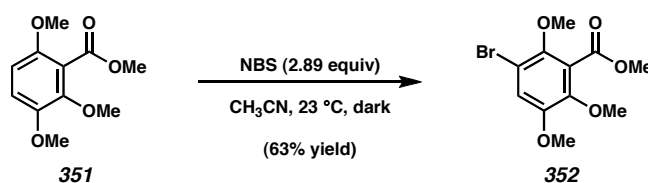


Acetonide 350. A round-bottom flask was charged with 2,3,6-trihydroxy-methylbenzoate (**339**) (100 mg, 0.543 mmol), PhH (10 mL), acetone (10 mL, Aldrich), and TsOH•H₂O (10.3 mg, 0.543 mmol, 1.0 equiv). The reactor was fitted with a Dean-Stark trap and heated to reflux (90 °C) for 20 h. Then, the reaction was cooled to 23 °C and concentrated in vacuo. The residue was purified by flash column chromatography on silica gel (hexane → 10:90 EtOAc:hexane eluent), giving acetonide **350** (85.6 mg, 70% yield) as a yellow-white powder. *R_f* 0.72 (50:50 EtOAc/hexane), (*p*-Anisaldehyde, pink spot); mp 78-80 °C (PhH); ¹H NMR (300 MHz, C₆D₆): δ 10.99 (s, 1H), 6.59 (d, *J* = 8.5 Hz, 1H), 6.45 (d, *J* = 8.5 Hz, 1H), 3.38 (s, 3H), 1.37 (s, 3H); ¹³C NMR (75 MHz, C₆D₆): δ 170.4, 156.6, 148.7, 141.1, 119.7, 114.9, 107.9, 99.8, 52.2, 26.0 (2C); IR (KBr): 3110, 2994, 2953, 1810, 1683, 1634, 1490, 1468, 1440, 1390, 1376, 1358, 1223, 1124, 1099, 1029, 1010, 802 cm⁻¹; HRMS-EI⁺ (*m/z*): [M]⁺ calc'd for C₁₁H₁₂O₅, 224.0685; found, 224.0690.



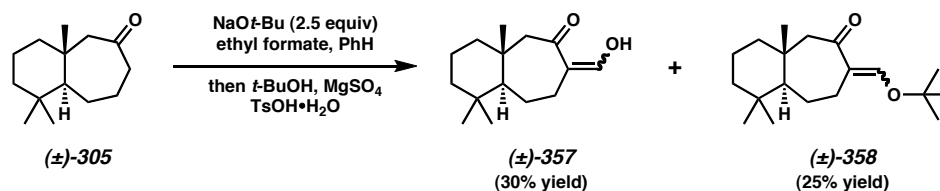
2,3,6-Trimethoxy-methylbenzoate (351). A vial containing 2,3,6-trihydroxy-methylbenzoate (**339**) (50 mg, 0.271 mmol) was charged with absolute EtOH (1.0 mL) and Me₂SO₄ (500 μL, fractionally distilled at ambient pressure). The reaction was

warmed until all solids had dissolved, then conc. aq KOH (500 μ L) was added dropwise (there was a mild exotherm, and each drop caused a slight reddening of the reaction which quickly faded). Once the addition was complete, the reaction was sealed and heated to 80 $^{\circ}$ C. A precipitate gradually formed. At 3 h, the reaction was diluted with H₂O and extracted with Et₂O (4 x). All organic layers were combined, dried (Na₂SO₄), filtered, and concentrated from CH₂Cl₂. The residue was purified by flash column chromatography on silica gel (hexane \rightarrow 10:90 EtOAc:hexane \rightarrow 30:70 EtOAc:hexane eluent), affording 2,3,6-trimethoxy-methylbenzoate (**351**) (45.4 mg, 74% yield) as a colorless liquid. *R_f* 0.55 (50:50 EtOAc/hexane), (*p*-Anisaldehyde, pink spot); ¹H NMR (500 MHz, CDCl₃): δ 6.87 (d, *J* = 9.0 Hz, 1H), 6.58 (d, *J* = 9.0 Hz, 1H), 3.91 (s, 3H), 3.86 (s, 3H), 3.80 (s, 3H), 3.76 (s, 3H); ¹³C NMR (125 MHz, CDCl₃): δ 166.6, 150.7, 147.2, 147.0, 119.4, 114.5, 106.4, 61.6, 56.7, 56.4, 52.6; IR (NaCl/CDCl₃): 3002, 2947, 2908, 2839, 1736, 1591, 1493, 1465, 1285, 1257, 1212, 1190, 1167, 1141, 1098, 1062, 1014 cm⁻¹; HRMS-EI⁺ (*m/z*): [*M*]⁺ calc'd for C₁₁H₁₄O₅, 226.0841; found, 226.0840.



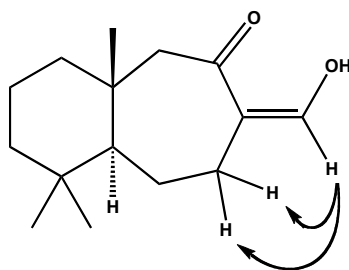
5-Bromo-2,3,6-trimethoxy-methylbenzoate (352). A vial was charged with a solution of 2,3,6-trimethoxy-methylbenzoate (**351**) (110 mg, 0.486 mmol) and CH₃CN (1.0 mL). *N*-bromosuccinimide (250 mg, 1.40 mmol) was added in one portion. The vial was sealed, and the reaction was stirred in the dark for 44 h. The reaction was then adsorbed directly onto silica gel, which was dried-loaded onto a silica gel column. The material was purified by flash column chromatography (10:90 EtOAc:hexane eluent), affording 5-

bromo-2,3,6-trimethoxy-methylbenzoate (**352**) (94.2 mg, 63% yield) as a colorless oil. R_f 0.39 (20:80 EtOAc/hexane), (UV, 254 nm); ^1H NMR (500 MHz, CDCl_3): δ 7.08 (s, 1H), 3.97 (s, 3H), 3.83 (s, 3H), 3.82 (s, 3H), 3.81 (s, 3H); ^{13}C NMR (125 MHz, CDCl_3): δ 165.6, 149.8, 147.6, 146.0, 125.3, 117.9, 110.9, 62.4, 61.7, 56.6, 52.7; IR (NaCl/ CHCl_3): 3090, 3002, 2946, 2841, 1737, 1594, 1571, 1481, 1423, 1281, 1224, 1080, 1059, 1000, 937 cm^{-1} ; HRMS-FAB $^+$ (m/z): $[\text{M}+\text{H}]^+$ calc'd for $\text{C}_{11}\text{H}_{14}\text{O}_5\text{Br}$, 305.0024; found, 305.0030.



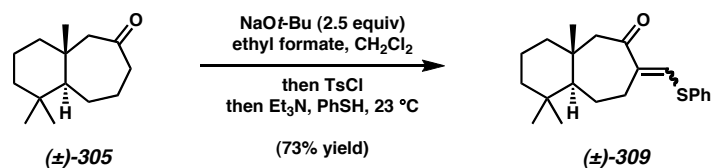
Vinylogous Acid (±)-357 and Vinylogous Ester (±)-358. A round-bottom flask was charged with a solution of cycloheptanone (**±**)-**305** (40 mg, 0.192 mmol, 1 equiv) in PhH (4.0 mL). Ethyl formate (78 μL , 0.960 mmol, 5 equiv) was introduced, followed by NaO*t*-Bu (46 mg, 0.480 mmol, 2.5 equiv). The reaction immediately turned yellow and was stirred vigorously at 23 °C for 30 min. The reaction was concentrated to a thick residue and *t*-BuOH (4.0 mL) was added along with MgSO₄ (231 mg, 1.92 mmol, 10 equiv), followed by TsOH·H₂O (128 mg, 0.672 mmol, 3.75 equiv). The vessel was closed and warmed to 65 °C for 48 h. Then, the reaction was cooled to 23 °C, diluted with PhH, and filtered through celite over glass frits with the aide of PhH. The filtrate was concentrated and evaporated from PhH several times to remove residual *t*-BuOH. The residue was then purified by flash chromatography on silica gel (hexane → 2:98 EtOAc:hexane → 8:92 EtOAc:hexane → 20:80 EtOAc:hexane eluent), giving vinylogous acid (**±**)-**357** (13.4 mg, 30% yield) as yellow oil. R_f 0.63 (20:80 EtOAc/hexane),

(KMnO₄, yellow spot, UV, 254 nm); ¹H NMR (300 MHz, C₆D₆): δ 7.38 (app. d, *J* = 8.6 Hz, 1H), 2.21 (AB spin system, d, *J*_{AB} = 13.0 Hz, 1H), 2.00 (AB spin system, d, *J*_{AB} = 13.0 Hz, 1H), 1.84-1.78 (m, 2H), 1.64-1.54 (m, 1H), 1.41 (app. qt, *J*_q = 13.2 Hz, *J*_t = 3.6 Hz, 1H), 1.26-1.18 (m, 2H), 1.15 (app. d, *J* = 14.6 Hz, 1H), 1.08-0.82 (m, 3H), 0.89-0.75 (m, 1H), 0.82 (s, 3H), 0.78 (s, 3H), 0.66 (s, 3H); ¹³C NMR (75 MHz, C₆D₆): δ 201.9, 171.5, 114.8, 59.7, 59.3, 43.8, 42.9, 36.4, 34.8, 33.9, 29.3, 26.4, 22.1, 19.5, 18.9; IR (NaCl/CH₂Cl₂): 2929, 2867, 2845, 1642, 1586, 1446, 1272, 1209, 1089, 978 cm⁻¹; HRMS-EI⁺ (*m/z*): [M]⁺ calc'd for C₁₅H₂₄O₂, 236.1776; found, 236.1780. ¹H-nOesy-1D spectra were obtained for (±)-**357** (300 MHz, CDCl₃); the results are shown below:

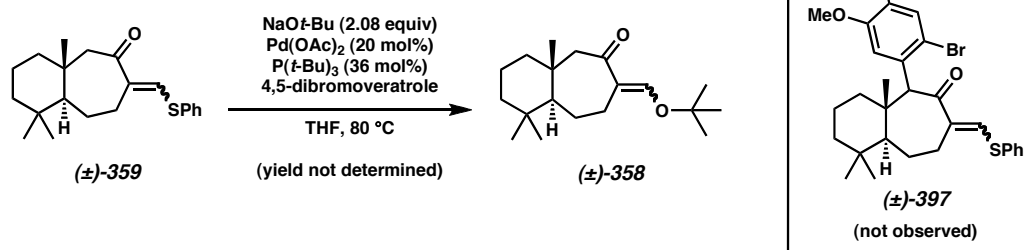


nOe's detected for (±)-**357**

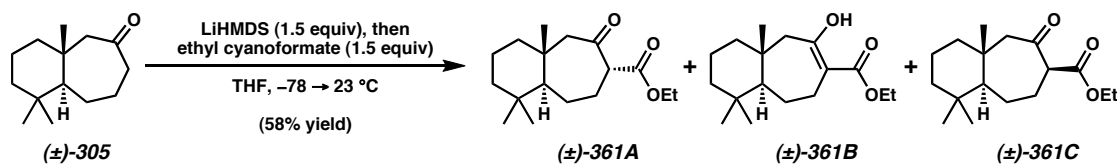
Additionally, vinylogous ester (±)-**358** (14.2 mg, 25% yield) was obtained as a yellow oil. *R*_f 0.43 (20:80 EtOAc/hexane), (KMnO₄, yellow spot); ¹H NMR (300 MHz, C₆D₆): δ 7.90 (s, 1H), 3.24 (app. dd, *J* = 14.8 Hz, 7.4 Hz, 1H), 2.56 (AB spin system, d, *J*_{AB} = 12.4 Hz, 1H), 2.31 (AB spin system, d, *J*_{AB} = 12.4 Hz, 1H), 1.96-1.80 (m, 2H), 1.57-1.37 (m, 1H), 1.32-1.20 (m, 4H), 1.16-0.88 (m, 3H), 1.02 (s, 3H), 1.00 (s, 9H), 0.82 (s, 3H), 0.69 (s, 3H); ¹³C NMR (75 MHz, C₆D₆): δ 201.1, 150.1, 120.1, 79.1, 62.2, 59.7, 44.2, 43.1, 36.7, 34.8, 34.1, 28.3 (3C), 26.9, 25.2, 22.1, 19.8, 19.2; IR (NaCl/CH₂Cl₂): 2968, 2936, 2868, 2845, 1678, 1594, 1464, 1370, 1265, 1210, 1165 cm⁻¹; HRMS-EI⁺ (*m/z*): [M]⁺ calc'd for C₁₉H₃₂O₂, 292.2402; found, 292.2410.



Vinylogous Thioester (±)-359. A round-bottom flask was charged with a solution of cycloheptanone (±)-305 (100 mg, 0.48 mmol, 1.0 equiv), ethyl formate (200 μL , 2.4 mmol, 5 equiv), and CH_2Cl_2 (10 mL). NaOt-Bu (92 mg, 0.960 mmol, 2.0 equiv, weighed in glovebox) was then added, and the yellow reaction was stirred for 3.5 h at 23 $^\circ\text{C}$. Then TsCl (recrystallized from Et_2O at -78 $^\circ\text{C}$) (183 mg, 0.960 mmol, 2.0 equiv) was introduced, and the reaction was stirred at 23 $^\circ\text{C}$ for 5 min. Finally, Et_3N (1.0 mL) was added, followed by thiophenol (100 μL , 0.960 mmol, 2.0 equiv). After 4 h at 23 $^\circ\text{C}$, the reaction was directly loaded onto a silica gel column and subjected to flash chromatography (5:95 EtOAc :hexane eluent). Semipure (±)-359 thus obtained was repurified via flash column chromatography on silica gel (2:98 EtOAc :hexane eluent), affording pure vinylogous thioester (±)-359 (114.7 mg, 73% yield) as a yellow oil. R_f 0.57 (20:80 EtOAc /hexane), (KMnO_4 , yellow spot); ^1H NMR (300 MHz, C_6D_6): δ 7.94 (s, 1H), 7.32-7.23 (m, 2H), 6.94-6.86 (m, 3H), 2.88 (app. dd, $J = 14.8$ Hz, 7.4 Hz, 1H), 2.41 (AB spin system, d, $J_{\text{AB}} = 12.6$ Hz, 1H), 2.25 (AB spin system, d, $J_{\text{AB}} = 12.6$ Hz, 1H), 2.19 (app. dd, $J = 13.4$ Hz, 13.2 Hz, 1H), 1.83 (app. dd, $J = 14.3$ Hz, 7.7 Hz, 1H), 1.46-1.36 (m, 1H), 1.28-1.16 (m, 4H), 1.10-0.80 (m, 3H), 0.88 (s, 3H), 0.80 (s, 3H), 0.65 (s, 3H); ^{13}C NMR (75 MHz, C_6D_6): δ 197.4, 137.8, 137.0, 134.7, 131.5, 130.9 (2C), 130.0 (2C), 61.0, 59.3, 44.0, 42.9, 37.0, 34.8, 34.0 30.7, 26.1, 22.0, 19.6, 19.2; IR ($\text{NaCl}/\text{CH}_2\text{Cl}_2$): 3058, 2930, 2866, 1671, 1561, 1480, 1441, 1321, 1209, 1195, 750 cm^{-1} ; HRMS-FAB $^+$ (m/z): $[\text{M}+\text{H}]^+$ calc'd for $\text{C}_{21}\text{H}_{29}\text{SO}$, 329.1939; found, 329.1933.

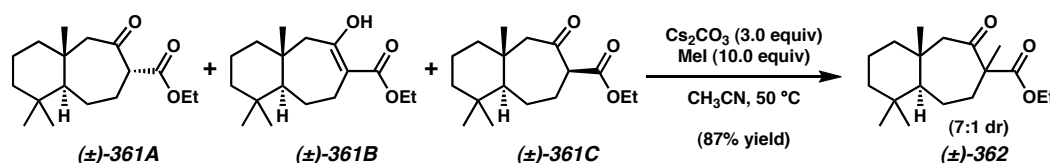


Attempted α -Arylation of (±)-359. In the glovebox, a vial was charged with $\text{P}(t\text{-Bu})_3$ (7.5 mg, 36 μmol , 36 mol%), Pd(OAc)_2 (4.5 mg, 20 μmol , 20 mol%), and NaOt-Bu (20.0 mg, 0.208 mmol, 2.08 equiv). The vial was removed from the glovebox and charged with a solution of vinylogous thioester **(±)-359** (32.8 mg, 0.100 mmol, 1.00 equiv), 4,5-dibromoveratrole (29.7 mg, 0.100 mmol, 1.00 equiv), and THF (1.0 mL). The vial was sealed and heated to 80°C for 22 h. The reaction was cooled to 23°C and quenched with sat. aq NH_4Cl (1 mL) and diluted with H_2O (5 mL) and hexane (3 mL). The biphasic mixture was extracted with EtOAc (3 x 8 mL). All organic layers were combined, dried (Na_2SO_4), filtered, and concentrated. The residue was purified by flash chromatography on silica gel (hexane \rightarrow 2:98 EtOAc:hexane \rightarrow 5:95 EtOAc:hexane \rightarrow 8:92 EtOAc:hexane \rightarrow 20:80 EtOAc:hexane eluent), giving vinylogous ester **(±)-358** (yield was not determined). No α -aryl vinylogous ester **(±)-397** was observed. Characterization data for **(±)-358** can be found on page 356 above.



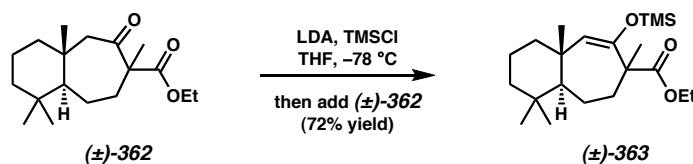
Ethyl β -Ketoester (as tautomers **(±)-361A**, **(±)-361B**, and **(±)-361C**). In the glovebox, a flamedried flask was charged with LiHMDS (77.1 mg, 0.461 mmol, 1.5 equiv) and removed from the glovebox. THF (10 mL) was introduced at $23\text{ }^{\circ}\text{C}$, followed by a solution of cycloheptanone (**(±)-305**) (64 mg, 0.307 mmol, 1.0 equiv) in THF (2.0 mL). After 30 min, the reaction was cooled to $-78\text{ }^{\circ}\text{C}$, and ethyl cyanoformate (45.5 μL , 0.461 mmol, 1.5 equiv) was introduced. The reaction was allowed to warm to $23\text{ }^{\circ}\text{C}$ and stirred for 16 h. Then, the reaction was quenched with sat. aq NH_4Cl (3.0 mL) and diluted with H_2O and hexanes. The biphasic mixture was extracted with EtOAc (3 x 20 mL). All organic layers were combined, dried (Na_2SO_4), filtered, and concentrated. The residue was purified by flash column chromatography on silica gel (3:97 EtOAc:hexane eluent), giving the ethyl β -Ketoester (50.1 mg, 58% yield) as a mixture of tautomers **(±)-361A**, **(±)-361B**, and **(±)-361C** in the form of a pale yellow oil. R_f (3 tautomers): 0.66 (20:80 EtOAc/hexane), (*p*-Anisaldehyde, sharp green spot), 0.64 (20:80 EtOAc/hexane), (*p*-Anisaldehyde, sharp red spot), 0.64 (20:80 EtOAc/hexane), (*p*-Anisaldehyde, broad yellow spot); ^1H NMR (300 MHz, CDCl_3) (**(±)-361B** only): δ 12.58 (s, 1H), 4.19 (q, $J = 7.0\text{ Hz}$, 1H), 4.18 (q, $J = 7.0\text{ Hz}$, 1H), 2.88 (app. dd, $J = 15.4\text{ Hz}$, 6.6 Hz, 1H), 2.44 (AB spin system, $J_{\text{AB}} = 13.5\text{ Hz}$, 1H), 1.90 (AB spin system, $J_{\text{AB}} = 13.5\text{ Hz}$, 1H), 1.77 (app. dd, $J = 13.5\text{ Hz}$, 7.7 Hz, 1H), 1.62 (app. qt, $J_q = 13.9\text{ Hz}$, $J_t = 3.3\text{ Hz}$, 1H), 1.46-1.34 (m, 3H), 1.30 (t, $J = 7.0\text{ Hz}$, 3H), 1.32-1.14 (m, 5H), 0.94 (s, 3H), 0.88 (s, 3H), 0.77 (s, 3H); ^{13}C NMR (75 MHz, CDCl_3) (**(±)-361B** only): δ 176.9, 172.8, 101.4, 60.4, 60.2, 52.8,

43.2, 42.7, 35.1, 34.6, 33.6, 25.3, 23.6, 21.8, 19.3, 18.2, 14.5; IR (NaCl/CDCl₃): 2931, 2867, 2845, 1742, 1703, 1644, 1614, 1463, 1401, 1379, 1306, 1276, 1247, 1216, 1178, 1047, 976, 861 cm⁻¹; HRMS-EI⁺ (*m/z*): [M]⁺ calc'd for C₁₇H₂₈O₃, 280.2038; found, 280.2031.



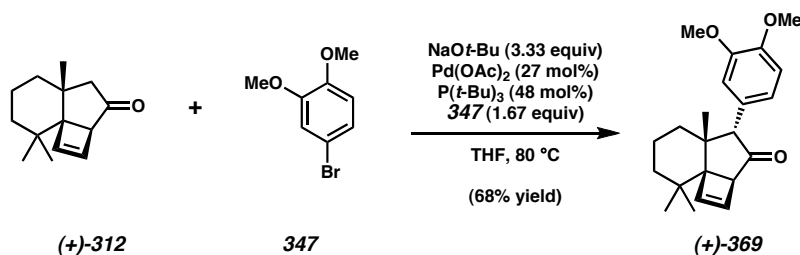
α-Methyl-β-Ketoester (±)-362. A vial was charged with anhydrous Cs₂CO₃ (174 mg, 0.535 mmol, 3.0 equiv), followed by a solution of β-Ketoester (50 mg, 0.178 mmol, 1.0 equiv) (as a tautomeric mixture of (±)-361A, (±)-361B, and (±)-361C), MeI (111 μL, 1.78 mmol, 10.0 equiv), and CH₃CN (2.0 mL). The vessel was sealed and heated to 50 °C for 16 h. The reaction was then cooled to 23 °C and filtered over glass frits. The filtrate was concentrated in vacuo, then taken up in CHCl₃ and filtered through silica gel with the aid of CHCl₃. The pink filtrate was washed with sat. aq Na₂SO₃. The washing was back-extracted with CHCl₃ (2 x). All organic layers were combined, dried (Na₂SO₄), filtered, and concentrated, giving α-methyl-β-ketoester (±)-362 as a mixture of diastereomers (>7:1 dr, major diastereomer unidentified) (45.5 mg, 87% yield) in the form of a colorless oil. R_f 0.57 (20:80 EtOAc/hexane), (*p*-Anisaldehyde, pink spot); ¹H NMR (300 MHz, CDCl₃): δ 4.15 (app. q, *J* = 7.1 Hz, 2H), 2.46 (AB spin system, d, *J*_{AB} = 11.5 Hz, 1H), 2.23 (app. ddd, *J* = 14.7 Hz, 8.1 Hz, 2.1 Hz, 1H), 2.19 (AB spin system, d, *J*_{AB} = 11.5 Hz, 1H), 1.84-1.66 (m, 2H), 1.66-1.48 (m, 2H), 1.45-1.31 (m, 3H), 1.26 (s, 3H), 1.30-1.08 (m, 2H), 1.23 (t, *J* = 7.1 Hz, 3H), 0.96 (s, 3H), 0.88 (s, 3H), 0.79 (s, 3H); ¹³C NMR (75

MHz, CDCl₃): δ 210.7, 173.6, 61.1, 28.9, 58.2, 57.9, 42.6, 37.23, 37.19, 34.7, 33.5, 23.3, 22.1, 21.6, 20.0, 19.2, 14.1; IR (NaCl/CDCl₃): 2930, 2869, 2847, 1738, 1703, 1460, 1389, 1311, 1261, 1180, 1102, 1057, 1035, 1018, 862 cm⁻¹; HRMS-EI⁺ (m/z): [M]⁺ calc'd for C₁₈H₃₀O₃, 294.2195; found, 294.2182.



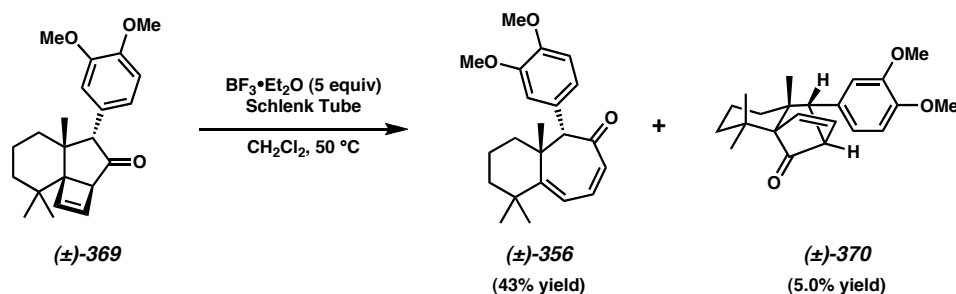
Silyl Enol Ether (±)-363. A flamedried round-bottom flask was charged with THF (8.0 mL) and *i*-Pr₂NH (137 μ L, 0.979 mmol, 6.0 equiv) and cooled to 0 $^{\circ}$ C. *n*-BuLi (2.5 M in hexanes, 326 μ L, 0.816 mmol, 5.0 equiv) was added dropwise. After 30 min, the reaction was cooled to -78 ° C, and TMSCl (186 μ L, 1.47 mmol, 9.0 equiv, freshly distilled) was added. After 5 min, a solution of α -Methyl- β -Ketoester (>7:1 dr, major diastereomer unidentified) (±)-362 (>7:1 dr, major diastereomer unidentified) (48 mg, 0.163 mmol, 1.0 equiv) in THF (2.0 mL) was added. After 1 h, Et₃N (1.0 mL) was added, followed by sat. aq NaHCO₃ (2.5 mL). The reaction was warmed to 23 $^{\circ}$ C, then diluted with H₂O and hexanes. The organic phase was collected, and the aqueous layer was extracted with Et₂O (2 x). All organic layers were combined, dried (K₂CO₃), filtered, and concentrated. The residue was concentrated several times from PhMe to remove residual H₂O and TMSOH, giving silyl enol ether (±)-363 (43.2 mg, 72% yield) as a diastereomeric mixture (> 7:1 dr, major diastereomer not identified) in the form of a pale yellow oil. *R*_f 0.74 (2:20:80 Et₃N/EtOAc/hexane), (I₂/Sand, white spot); ¹H NMR (300 MHz, C₆D₆): δ 4.71 (s, 1H), 4.04 (app. q, *J* = 7.1 Hz, 2H), 2.53 (app. ddd, *J* = 13.5 Hz, 10.7 Hz, 4.1 Hz, 1H), 1.83-

1.69 (m, 1H), 1.69-1.55 (m, 1H), 1.54 (s, 3H), 1.52-1.24 (m, 8H), 1.12 (s, 3H), 1.03 (t, J = 7.1 Hz, 3H), 0.83 (s, 3H), 0.81 (s, 3H), 0.22 (s, 9H); ^{13}C NMR (75 MHz, C_6D_6): δ 175.5, 151.9, 124.7, 60.7, 52.2, 52.0, 45.9, 43.3, 37.4, 35.7, 34.8, 33.6, 23.1, 22.2, 21.91, 21.88, 19.7, 14.7, 1.0 (3C); IR (NaCl/ CH_2Cl_2): 2933, 2905, 2868, 2847, 1738, 1655, 1461, 1384, 1251, 1172, 1141, 1093, 878, 842 cm^{-1} ; HRMS-FAB $^+$ (m/z): $[\text{M}+\text{H}]^+$ calc'd for $\text{C}_{21}\text{H}_{39}\text{O}_3\text{Si}$, 367.2669; found, 367.2676.



Aryl Cyclobutene (+)-369. In the glovebox, a round-bottom flask was charged with NaOt-Bu (913 mg, 9.50 mmol, 3.33 equiv), Pd(OAc)₂ (171 mg, 0.760 mmol, 27 mol%), and P(*t*-Bu)₃ (277 mg, 1.37 mmol, 48 mol%). The vessel was removed from the glovebox, and THF (27 mL) was added. The reaction was stirred at 23 °C for 15 min (solution was bright orange-red) and a solution of semipure cyclobutene (+)-312 (75% pure by mass, 776 mg total mass, (2.85 mmol pure cyclobutene, 582 mg pure cyclobutene)), 4-bromoveratrole (**347**) (1.031 g, 4.75 mmol, 1.67 equiv), and THF (10 mL) was added. The reaction was fitted with a condenser and heated to 80 °C for 30 h. Reaction went from bright red to chalky reddish-brown. Then the reaction was cooled to 23 °C and quenched with sat. aq NH_4Cl (12.0 mL) and diluted with H_2O (25 mL) and hexane (15 mL). The suspension was extracted with EtOAc (3 x 40 mL). All organic layers were combined, dried (Na_2SO_4), filtered, and concentrated. The residue was purified by flash column chromatography on silica gel (5:95 EtOAc:hexane \rightarrow 20:80

EtOAc:hexane eluent), affording aryl cyclobutene **(+)-369** (655 mg, 68% yield based on pure cyclobutene **(+)-312**) as a white powder. R_f 0.28 (20:80 EtOAc/hexane), (UV, 254 nm); mp 154-156 °C (EtOAc/hexane) (racemate), 145-147 °C (EtOAc/hexane) (95% ee); ^1H NMR (500 MHz, C_6D_6): δ 6.80 (d, $J = 2.2$ Hz, 1H), 6.74 (dd, $J = 8.3$ Hz, 2.2 Hz, 1H), 6.68 (d, $J = 8.3$ Hz, 1H), 6.15 (app. dd, $J = 2.9$ Hz, 0.9 Hz, 1H), 6.05 (app. dd, $J = 2.9$ Hz, 1.5 Hz, 1H), 4.35 (s, 1H), 3.54 (s, 3H), 3.46 (s, 3H), 3.12 (app. dd, $J = 1.5$ Hz, 0.9 Hz, 1H), 1.37-1.18 (m, 3H), 1.09 (app. ddd, $J = 13.7$ Hz, 3.7 Hz, 3.4 Hz, 1H), 1.08-1.02, (m, 1H), 1.07 (app. ddd, $J = 12.9$ Hz, 3.7 Hz, 3.2 Hz, 1H), 1.02 (s, 3H), 0.93 (s, 3H), 0.89 (s, 3H); ^{13}C NMR (125 MHz, C_6D_6): δ 212.8, 149.93, 149.92, 142.6, 140.4, 126.9, 125.1, 117.1, 112.3, 63.1, 60.7, 57.1, 56.3, 56.0, 40.5, 39.3, 34.0, 33.6, 28.7, 25.9, 20.7, 18.6; IR (NaCl/ CHCl_3): 2930, 2871, 2842, 1732, 1608, 1588, 1517, 1464, 1253, 1146, 1030, 739 cm^{-1} ; HRMS- EI^+ (m/z): $[\text{M}]^+$ calc'd for $\text{C}_{22}\text{H}_{28}\text{O}_3$, 340.2039; found, 340.2040. $[\alpha]_D^{25} +575.36^\circ$ (c 0.620, CHCl_3), 95% ee.

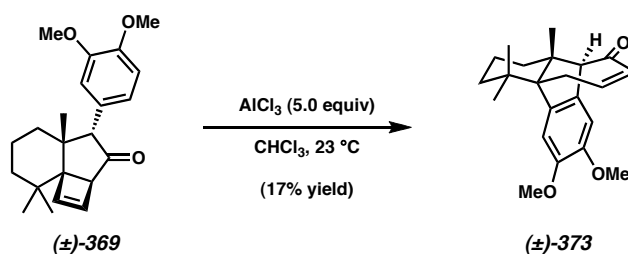


Aryl Cycloheptadienone (±)-356 and Cargill Rearrangement Adduct (±)-370. A Schlenk flask was charged with a solution of aryl cyclobutene **(±)-369** (563 mg, 1.65 mmol) and CH_2Cl_2 (52 mL). $\text{BF}_3 \cdot \text{Et}_2\text{O}$ (1.05 mL, 8.27 mmol) was then introduced. The vessel was sealed and heated with stirring to 50 °C behind a blast shield for 20 h. The

reaction was cooled to 23 °C and added slowly to a suspension of brine (25 mL), sat. aq NaHCO₃ (25 mL), and CH₂Cl₂ (25 mL). After addition was complete, the reaction was stirred vigorously for 5 min. The organic layer was collected, and the aqueous layer was extracted with CH₂Cl₂ (2 x 30 mL). All organic layers were combined, dried (Na₂SO₄), filtered, and concentrated. The residue was purified by flash column chromatography on silica gel (hexane → 20:80 EtOAc:hexane → 30:70 EtOAc:hexane → 40:60 EtOAc:hexane eluent), affording aryl cycloheptadienone (**±**)-**356** (242 mg, 43% yield) as a yellow oil. *R_f* 0.61 (50:50 EtOAc/hexane), (*p*-Anisaldehyde, green spot, UV, 254 nm); ¹H NMR (500 MHz, C₆D₆): δ 7.01 (app. d, *J* = 2.0 Hz, 1H), 6.95 (app. dd, *J* = 8.3 Hz, 2.0 Hz, 1H), 6.53 (d, *J* = 8.3 Hz, 1H), 6.17 (d, *J* = 6.8 Hz, 1H), 6.16 (d, *J* = 2.0 Hz, 1H), 5.91 (dd, *J* = 6.8 Hz, 2.0 Hz, 1H), 3.55 (s, 1H), 3.48 (s, 3H), 3.38 (s, 3H), 1.82 (app. td, *J_t* = 13.2 Hz, *J_d* = 5.1 Hz, 1H), 1.53-1.43 (m, 1H), 1.29-1.16 (m, 2H), 1.24 (s, 3H), 1.13-1.00 (m, 2H), 1.00 (s, 3H), 0.93 (s, 3H); ¹³C NMR (125 MHz, C₆D₆): δ 198.5, 166.8, 150.1, 150.0, 137.0, 129.8, 129.5, 123.1, 121.0, 114.8, 112.3, 70.6, 56.1, 55.9, 41.0, 38.6, 38.3, 36.8, 33.6, 31.7, 25.2, 17.9; IR (NaCl/CHCl₃): 2924, 1645, 1573, 1516, 1463, 1419, 1264, 1236, 1148, 1028 cm⁻¹; HRMS-EI⁺ (*m/z*): [M]⁺ calc'd for C₂₂H₂₈O₃, 340.2039; found, 340.2038.

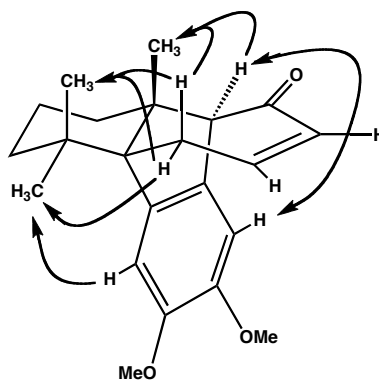
In addition to (**±**)-**356**, several fractions containing a second compound in semipure form were collected from the flash column above. These fractions were combined and concentrated. The residue was purified by flash column chromatography on silica gel (50:50 CH₂Cl₂:PhH → 10:50:50 EtOAc:CH₂Cl₂:PhH), affording pure Cargill rearrangement adduct (**±**)-**370** (28.1 mg, 5.0% yield) as colorless crystals. One of these crystals was suitable for X-Ray analysis, allowing for determination of the relative

stereochemistry of the compound. R_f 0.74 (50:50 EtOAc/hexane), (*p*-Anisaldehyde, brown spot, UV, 254 nm); mp 116-118 °C (C_6D_6); 1H NMR (500 MHz, C_6D_6): δ 6.79 (app. d, J = 8.3 Hz, 1H), 6.78 (app. s, 1H), 6.57 (app. d, J = 8.3 Hz, 1H), 6.32 (app. dd, J = 7.1 Hz, 3.9 Hz, 1H), 6.20 (app. dd, J = 7.1 Hz, 1.2 Hz, 1H), 3.54 (s, 3H), 3.44 (s, 3H), 2.83 (app. dd, J = 3.9 Hz, 0.7 Hz, 1H), 2.23 (s, 1H), 2.04 (app. td, J_t = 13.4 Hz, J_d = 3.9 Hz, 1H), 1.47 (app. qt, J_q = 13.7 Hz, J_t = 3.2 Hz, 1H), 1.35 (app. d, J = 14.2 Hz, 1H), 1.32-1.13 (m, 2H), 1.29 (s, 3H), 1.05 (s, 3H), 1.00 (s, 3H), 0.74 (app. d, J = 13.9 Hz, 1H); ^{13}C NMR (125 MHz, C_6D_6): δ 206.5, 150.2, 149.4, 134.6, 134.4, 134.1, 121.0, 113.2, 112.5, 64.0, 56.1, 56.0, 53.4, 40.2, 37.1, 34.3, 32.5, 32.4, 28.1, 26.9, 26.6, 19.6; IR (NaCl/ $CHCl_3$): 2995, 2934, 2867, 2834, 1772, 1518, 1464, 1267, 1254, 1241, 1147, 1030, 750 cm^{-1} ; HRMS-EI $^+$ (m/z): $[M]^+$ calc'd for $C_{22}H_{28}O_3$, 340.2039; found, 340.2034.

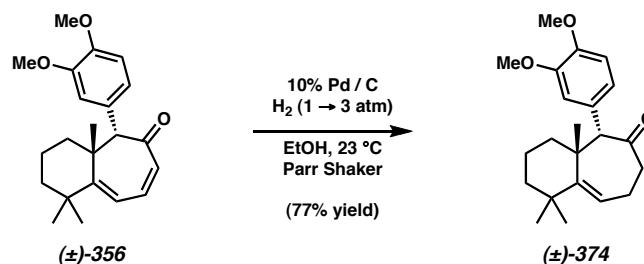


Friedel-Crafts Adduct (\pm) -373. A solution of aryl cyclobutene $(+)$ -369 (50 mg, 0.147 mmol, 1.0 equiv) in $CHCl_3$ (15.0 mL) was treated with $AlCl_3$ (98.0 mg, 0.735 mmol, 5.0 equiv, weighed in the glovebox). As the reaction stirred for 48 h, it went from peach-colored to maroon. After the reaction was complete, it was added dropwise to a solution of brine (20 mL) and sat. aq $NaHCO_3$ (20 mL) at 23 °C. The suspension was then extracted with $CHCl_3$ (2 x 20 mL). All organic layers were combined, dried (Na_2SO_4), filtered, and concentrated to ~500 μ L total volume. The brown oil was purified by

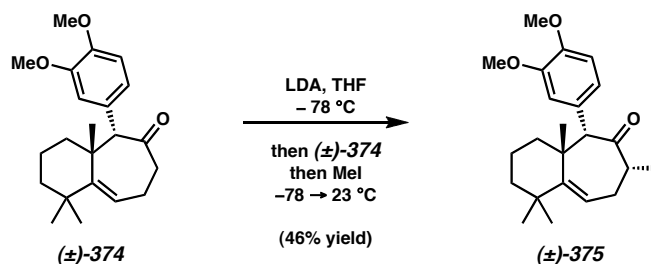
preparative TLC (20:80 EtOAc:hexane eluent), affording the Friedel-Crafts adduct (\pm)-**373** (8.3 mg, 17% yield) as a yellow powder. R_f 0.24 (20:80 EtOAc/hexane), (UV, 254 nm); mp 152-155 °C (CHCl_3); ^1H NMR (300 MHz, CDCl_3): δ 7.09 (s, 1H), 6.64 (s, 1H), 6.04 (app. ddd, $J = 12.6$ Hz, 5.5 Hz, 3.6 Hz, 1H), 5.66 (app. dd, broad, $J = 12.6$ Hz, 1.9 Hz, 1H), 3.84 (s, 3H), 3.81 (s, 3H), 3.33 (app. d, broad, $J = 1.6$ Hz, 1H), 2.84 (app. d, broad, $J = 1.9$ Hz, 1H), 2.84 (app. dd, $J = 9.0$ Hz, 1.6 Hz, 1H), 1.72-1.58 (m, 1H), 1.54-1.26 (m, 4H), 1.43 (s, 3H), 1.26 (s, 3H), 1.24-1.00 (m, 1H), 1.19 (s, 3H); ^{13}C NMR (75 MHz, CDCl_3): δ 148.8, 148.4, 142.9, 139.5, 135.5, 128.7, 110.2, 107.6, 73.1, 57.5, 56.3, 55.9, 46.4, 40.8, 39.9, 38.9, 37.5, 29.6, 26.9, 20.7, 18.4; IR (NaCl/ CDCl_3): 2932, 1659, 1605, 1504, 1464, 1402, 1295, 1206, 1096, 1036, 914, 857, 755 cm^{-1} ; HRMS-EI $^+$ (m/z): $[\text{M}]^+$ calc'd for $\text{C}_{22}\text{H}_{28}\text{O}_3$, 340.2039; found, 340.2039. ^1H -nOesy-1D spectra were obtained for (\pm)-**373** (300 MHz, CDCl_3); the results are shown below:



nOe's detected for (\pm)-**373**

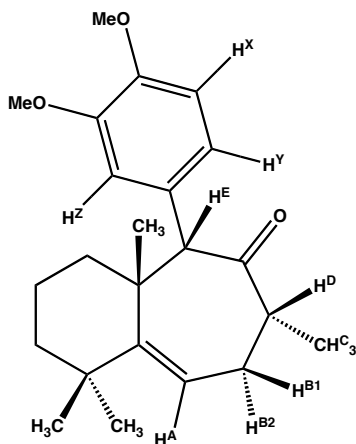


γ,δ -Unsaturated Aryl Cycloheptanone (\pm)-374. A Parr flask was charged with 10% w/w Pd/C (38 mg, 35.3 μmol , 5 mol%), followed by a solution of aryl cycloheptadienone (\pm)-356 (240 mg, 0.705 mmol) in absolute EtOH (40 mL). The reaction was placed under H_2 (1 atm) at 23 $^\circ\text{C}$ on a Parr shaker for 40 h. At this time, more 10% w/w Pd/C (114 mg, 0.106 mmol, 15 mol%) was carefully added. The reaction was continued under H_2 (now 3 atm) for 20 h. Once the reaction was complete, it was filtered through celite over glass frits with the aide of EtOAc. The filtrate was concentrated and purified by flash chromatography on silica gel (hexane \rightarrow 20:80 EtOAc:hexane eluent), giving γ,δ -unsaturated aryl cycloheptanone (\pm)-374 (188 mg, 77% yield) as a colorless oil. R_f 0.31 (20:80 EtOAc/hexane), (*p*-Anisaldehyde, blue spot); ^1H NMR (300 MHz, C_6D_6): δ 7.17 (app. d, $J = 2.1$ Hz, 1H), 7.09 (app. dd, $J = 8.2$ Hz, 2.1 Hz, 1H), 6.59 (app. d, $J = 8.2$ Hz, 1H), 5.77 (dd, $J = 8.2$ Hz, 5.2 Hz, 1H), 3.85 (s, 1H), 3.49 (s, 3H), 3.43 (s, 3H), 2.60 (app. td, $J_t = 13.8$ Hz, $J_d = 4.7$ Hz, 1H), 2.30-1.86 (m, 5H), 1.60-1.42 (m, 1H), 1.36-1.20 (m, 1H), 1.27 (s, 3H), 1.16 (s, 3H), 1.01 (s, 3H), 0.98-0.68 (m, 1H); ^{13}C NMR (75 MHz, C_6D_6): δ 210.0, 153.5, 150.1, 149.7, 130.5, 123.6, 123.5, 115.3, 112.3, 71.8, 56.2, 55.9, 42.0, 41.0, 40.2, 37.8 (2C), 33.8, 33.7, 28.4, 23.7, 18.6; IR (NaCl/ CHCl_3): 2933, 1695, 1603, 1588, 1515, 1464, 1379, 1252, 1146, 1029, 756 cm^{-1} ; HRMS-EI $^+$ (m/z): $[\text{M}]^+$ calc'd for $\text{C}_{22}\text{H}_{30}\text{O}_3$, 342.2195; found, 342.2183.



γ,δ -Unsaturated Methyl Aryl Cycloheptanone (\pm)-375. A round-bottom flask was charged with THF (4.2 mL) and *i*-Pr₂NH (29 μ L, 0.209 mmol, 1.2 equiv), then cooled to 0 $^{\circ}$ C. *n*-BuLi (2.5 M in hexanes, 77 μ L, 0.192 mmol, 1.1 equiv) was added dropwise. After 30 min, the reaction was cooled to -78 ° C, and a solution of γ,δ -unsaturated aryl cycloheptanone (\pm)-374 (60 mg, 0.174 mmol, 1 equiv) in THF (2.8 mL) was added dropwise via syringe pump over 1 h. Then, iodomethane (65 μ L, 1.04 mmol, 6.0 equiv) was added swiftly. The reaction was kept at -78 ° C for 6 h, then warmed to 23 $^{\circ}$ C and stirred for 16 h. Reaction gradually went from yellow to colorless. The reaction was quenched with sat. aq NH₄Cl (4 mL) and diluted with H₂O and hexanes. The suspension was extracted with EtOAc (3 x 20 mL). All organic layers were combined, dried (Na₂SO₄), filtered, and concentrated. The residue was purified by flash column chromatography on silica gel (hexane \rightarrow 5:95 EtOAc:hexane \rightarrow 12:88 EtOAc:hexane eluent), giving unreacted starting material ((\pm)-374) (22.6 mg, 38% yield) and γ,δ -unsaturated methyl aryl cycloheptanone (\pm)-375 (29.0 mg, 46% yield) as a colorless oil. *R*_f 0.48 (25:75 EtOAc/hexane), (*p*-Anisaldehyde, blue spot, UV, 254 nm); ¹H NMR (300 MHz, CDCl₃): δ 7.32 (d, *J* = 1.9 Hz, 1H), 6.99 (dd, *J* = 8.3 Hz, 1.9 Hz, 1H), 6.75 (d, *J* = 8.3 Hz, 1H), 5.84 (app. t, *J* = 7.3 Hz, 1H), 4.37 (s, 1H), 3.87 (s, 3H), 3.85 (s, 3H), 2.90-2.70 (m, 2H), 2.08-1.88 (m, 2H), 1.68-1.28 (m, 4H), 1.31 (s, 3H), 1.16 (s, 3H), 1.12 (s, 3H), 1.04 (d, *J* = 6.8 Hz, 3H), 1.00-0.88 (m, 1H); ¹³C NMR (75 MHz, CDCl₃): δ 212.6,

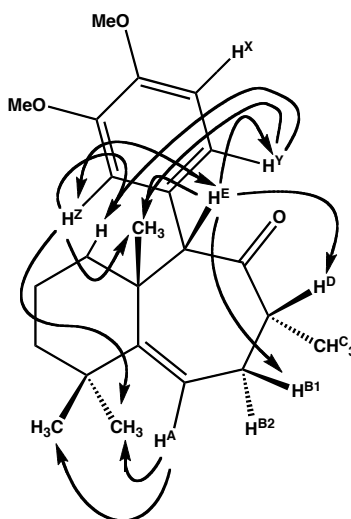
153.8, 148.1, 148.0, 128.2, 123.3, 21.1, 114.0, 110.2, 65.0, 56.0, 55.9, 49.0, 43.0, 40.2, 37.7, 35.4, 34.1, 32.2, 30.4, 28.1, 18.3, 15.5; IR (NaCl/CHCl₃): 2933, 1714, 1694, 1515, 1464, 1374, 1261, 1236, 1145, 1030, 757 cm⁻¹; HRMS-EI⁺ (*m/z*): [M]⁺ calc'd for C₂₃H₃₂O₃, 356.2352; found, 356.2352. ¹H-¹H gCOSY experiments (300 MHz, CDCl₃), were performed on (±)-**375**. The following spin systems were observed:



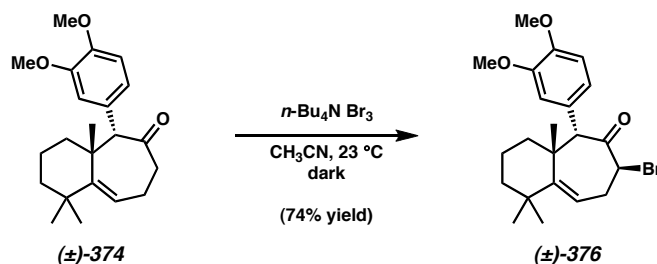
Resonance	Proton	Coupled Proton Spins
δ 5.84, t	H ^A	H ^{B1} , H ^{B2}
δ 2.85, m	H ^{B1}	H ^A , H ^{B2} , H ^D
δ 2.03, m	H ^{B2}	H ^A , H ^{B1} , H ^D
δ 1.04, d	3H ^C	H ^D
δ 2.75, m	H ^D	H ^{B1} , H ^{B2} , 3H ^C
δ 4.37, s	H ^E	NONE
δ 6.75, d	H ^X	H ^Y
δ 6.99, dd	H ^Y	H ^X , H ^Z
δ 7.32, d	H ^Z	H ^Y

spin systems found for (±)-**375**

Using the data from the gCOSY experiments along with proton assignments allowed for the assignments of some nOe's. ¹H-nOesy-1D spectra were obtained for (±)-**375** (300 MHz, CDCl₃); the results are shown below:

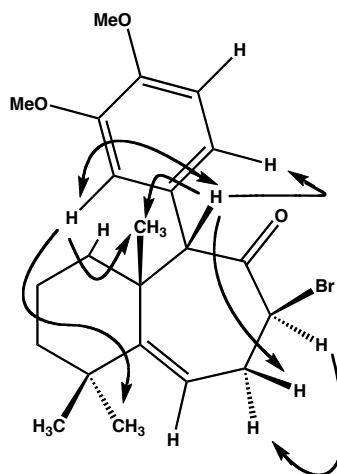


nOe's detected for (±)-**375**

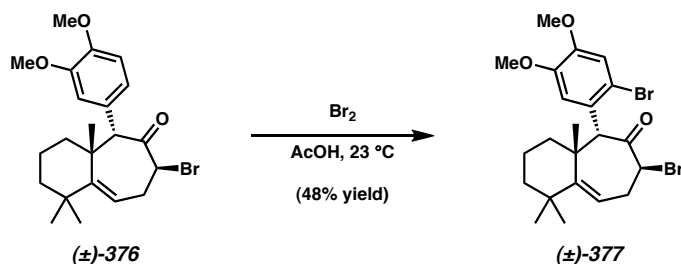


α -Bromo Aryl Ketone (\pm)-376. A round-bottom flask containing γ,δ -unsaturated aryl cycloheptanone (\pm)-374 (75.4 mg, 0.220 mmol) was charged with CH_3CN (12 mL) and treated with $n\text{-Bu}_4\text{N Br}_3$ (106.2 mg, 0.220 mmol) at 23 $^\circ\text{C}$ in the dark. After 16 h, the pale yellow reaction was diluted with CH_2Cl_2 (20 mL) and sat. aq NaHCO_3 (10 mL), and the reaction became colorless. The organic phase was collected, and the aqueous and the aqueous layer was extracted with CH_2Cl_2 (2 x). All organic layers were combined, dried (Na_2SO_4), filtered, and concentrated. The residue was purified by flash column chromatography on silica gel (hexane \rightarrow 8:92 EtOAc:hexane eluent), affording α -Bromo aryl ketone (\pm)-376 (68.5 mg, 74% yield) as a white powder. R_f 0.40 (20:80 EtOAc/hexane), (*p*-Anisaldehyde, blue spot, UV, 254 nm); mp 159-161 $^\circ\text{C}$ (MeOH); ^1H NMR (300 MHz, CDCl_3): δ 7.25 (d, $J = 1.5$ Hz, 1H), 7.03 (dd, $J = 8.2$ Hz, 1.5 Hz, 1H), 6.78 (d, $J = 8.2$ Hz, 1H), 5.79 (dd, $J = 9.3$ Hz, 5.8 Hz, 1H), 4.58 (s, broad, 1H), 4.22 (app. s, broad, 1H), 3.89 (s, 3H), 3.85 (s, 3H), 3.09-2.93 (m, 1H), 2.79 (app. ddd, $J = 15.1$ Hz, 9.3 Hz, 5.8 Hz, 1H), 1.80 (app. td, $J_t = 12.4$ Hz, $J_d = 5.8$ Hz, 1H), 1.58-1.22 (m, 4H), 1.31 (s, 3H), 1.14 (s, 3H), 1.18-1.06 (m, 1H), 1.10 (s, 3H); ^{13}C NMR (75 MHz, CDCl_3): δ 202.8, 148.4, 148.1, 128.2, 123.6, 119.2, 114.5, 110.3, 56.1, 55.9, 45.0 (broad), 39.5, 38.1, 34.8, 33.8, 33.0, 32.4, 26.6, 22.8, 18.0, 14.3; IR (NaCl/ CHCl_3): 2954, 2868, 2837, 1723, 1515, 1464, 1375, 1273, 1254, 1238, 1145, 1029, 756 cm^{-1} ; HRMS-FAB $^+$ (m/z): $[\text{M}]^+$ calc'd for $\text{C}_{22}\text{H}_{29}\text{BrO}_3$, 420.1308; found, 420.1300. ^1H - ^1H homodecoupling

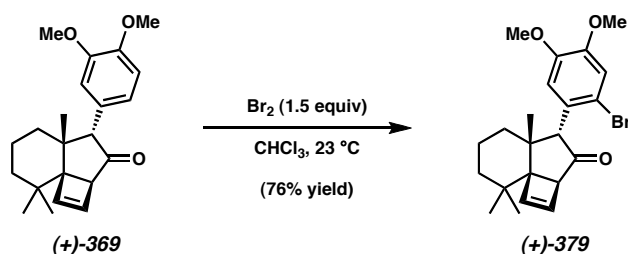
experiments (300 MHz, CDCl_3) were performed on (\pm)-**376**: The signal at δ 2.79 (app. ddd, $J = 15.1$ Hz, 9.3 Hz, 5.8 Hz, 1H) was suppressed with a decoupling current, resulting in a splitting change at δ 5.79 (dd, $J = 9.3$ Hz, 5.8 Hz, 1H \rightarrow app. d, $J \sim 9$ Hz, broad, 1H). The signal at δ 3.09-2.93 (m, 1H) was suppressed with a decoupling current, resulting in splitting changes at δ 5.79 (dd, $J = 9.3$ Hz, 5.8 Hz, 1H \rightarrow app. d, $J \sim 9$ Hz, broad, 1H) and δ 2.79 (app. ddd, $J = 15.1$ Hz, 9.3 Hz, 5.8 Hz, 1H \rightarrow app. dd, $J \sim 15$ Hz, ~ 6 Hz, broad, 1H). The signal at δ 4.22 (app. s, broad, 1H) was suppressed with a decoupling current, resulting in splitting changes at δ 3.09-2.93 (m, 1H \rightarrow m, 1H: lineshape change only) and δ 2.79 (app. ddd, $J = 15.1$ Hz, 9.3 Hz, 5.8 Hz, 1H \rightarrow app. dd, $J \sim 15$ Hz, ~ 9 Hz, broad, 1H). The signal at δ 4.57 (s, 1H) was suppressed with a decoupling current, resulting no noticeable splitting changes. This information allowed for key nOe's to be correctly assigned. ^1H -nOesy-1D spectra were obtained for (\pm)-**376** (300 MHz, CDCl_3); the results are shown below:



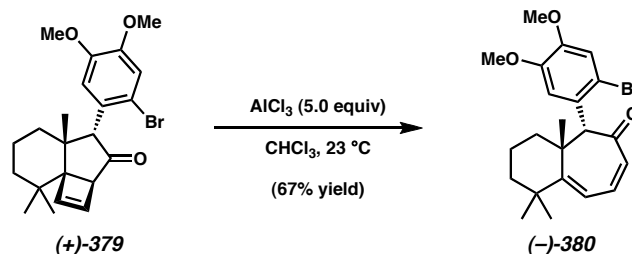
nOe's detected for (\pm)-**376**



Bromoarene (\pm)-377. α -Bromo aryl ketone (\pm)-376 (50 mg, 0.119 mmol) was dissolved in glacial AcOH (3.0 mL), and the solution was treated with a solution of Br_2 (19 mg, 0.119 mmol) in glacial AcOH (500 μL) at 23 $^\circ\text{C}$. After 6 h, the reaction was added dropwise to a suspension of H_2O (30 mL) and CHCl_3 (30 mL). The organic phase was carefully treated with sat. aq NaHCO_3 (20 mL). The organic layer was then collected, dried (Na_2SO_4), filtered, and concentrated. The residue was purified by flash column chromatography on silica gel (1:50:50 MeOH: CH_2Cl_2 :PhH eluent), giving bromoarene (\pm)-377 (28.6 mg, 48% yield) as a white semisolid. R_f 0.47 (20:80 EtOAc/hexane), (UV, 254 nm); mp 163-165 $^\circ\text{C}$ (dec.); ^1H NMR (300 MHz, CDCl_3): δ 7.69 (s, 1H), 7.04 (s, 1H), 5.83 (app. dd, $J = 9.6$ Hz, 5.8 Hz, 1H), 5.55 (s, 1H), 4.15 (app. dd, $J = 11.6$ Hz, 5.8 Hz, 1H), 3.91 (s, 3H), 3.86 (s, 3H), 3.21 (app. ddd, $J = 14.6$ Hz, 11.8 Hz, 5.8 Hz, 1H), 2.80 (app. ddd, $J = 15.4$ Hz, 9.6 Hz, 6.0 Hz, 1H), 1.88 (app. td, $J_t = 12.4$ Hz, $J_d = 5.2$ Hz, 1H), 1.63-1.39 (m, 3H), 1.34 (s, 3H), 1.27-1.21 (m, 2H), 1.15 (s, 3H), 1.09 (s, 3H); ^{13}C NMR (75 MHz, CDCl_3): δ 202.5, 158.3, 148.8, 147.3, 126.5, 119.2, 117.5, 116.0, 115.3, 56.3, 56.2, 55.1 (broad), 50.3, 47.3, 39.7, 38.3, 34.6, 34.1, 32.9, 32.0, 27.0, 18.0; IR (NaCl/ CDCl_3): 2953, 2936, 2869, 2846, 1723, 1661, 1508, 1463, 1440, 1368, 1316, 1255, 1213, 1166, 1031, 912, 732 cm^{-1} ; HRMS-FAB $^+$ (m/z): $[\text{M}]^+$ calc'd for $\text{C}_{22}\text{H}_{28}\text{Br}_2\text{O}_3$, 500.0385; found, 500.0382.

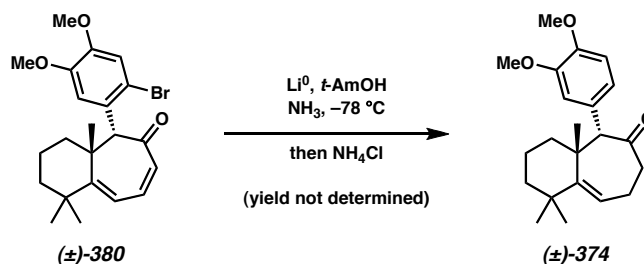


Bromoaryl Cyclobutene (+)-379. A round-bottom flask containing aryl cyclobutene (+)-**369** (652 mg, 1.92 mmol, 1.0 equiv) in CHCl_3 (35 mL) was treated with Br_2 (460 mg, 2.87 mmol, 1.5 equiv) in CHCl_3 at 23 °C over a 3 min period of slow addition. Once the addition was complete, the reaction was stirred for 1.5 h at 23 °C. Then, a mixture of sat. aq Na_2SO_3 (17.5 mL) and sat. aq NaHCO_3 (17.5 mL) was added. After 10 min, the organic phase was collected, and the aqueous layer was extracted with CHCl_3 (3 x 30 mL). All organic layers were combined, dried (Na_2SO_4), filtered, and concentrated. The residue was purified by flash column chromatography on silica gel (15:85 EtOAc:hexane eluent), affording bromoaryl cyclobutene (+)-**379** (610 mg, 76% yield) as a white solid. R_f 0.39 (20:80 EtOAc/hexane), (UV, 254 nm); mp 215-217 °C (EtOAc/hexane)(racemate), mp 240-242 °C (95% ee); ^1H NMR (300 MHz, CDCl_3): δ 7.02 (s, 1H), 6.65 (s, 1H), 6.57 (app. dd, J = 2.7 Hz, 0.8 Hz, 1H), 6.52 (app. dd, J = 2.7 Hz, 1.6 Hz, 1H), 5.21 (s, 1H), 3.84 (app. s, 6H), 3.13 (app. s, 1H), 1.60-1.40 (m, 3H), 1.34 (app. dd, J = 12.9 Hz, 3.8 Hz, 1H), 1.28-1.04 (m, 2H), 1.19 (s, 3H), 1.11 (s, 3H), 1.00 (s, 3H); ^{13}C NMR (75 MHz, CDCl_3): δ 214.8, 148.7, 147.5, 142.7, 140.2, 125.0, 118.2, 115.9, 115.4, 62.9, 58.6, 56.3, 56.21, 56.18, 42.0, 39.0, 33.8, 33.5, 28.4, 25.6, 20.7, 17.9; IR (NaCl/ CDCl_3): 2931, 2870, 2844, 1732, 1603, 1571, 1508, 1464, 1379, 1258, 1211, 1166, 1032, 914, 845, 735 cm^{-1} ; HRMS-FAB $^+$ (m/z): $[\text{M}+\text{H}]^+$ calc'd for $\text{C}_{22}\text{H}_{27}\text{O}_3^{\text{81}}\text{Br}$, 420.1123; found, 420.1119. $[\alpha]_{\text{D}}^{23} +527.47^\circ$ (c 1.82, CHCl_3), 95% ee.

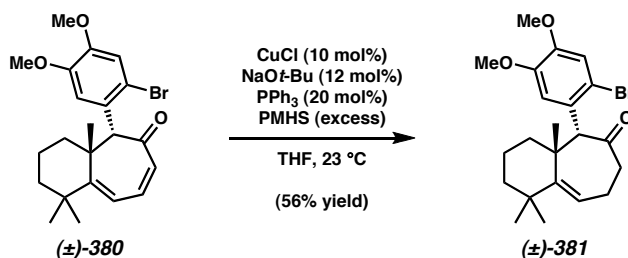


Bromoaryl Cycloheptadienone (–)-380. A round-bottom flask was charged with a solution of bromoaryl cyclobutene (+)-**379** (605 mg, 1.44 mmol, 1.0 equiv) and CHCl_3 (36 mL). The reaction was degassed with argon for 10 min. Then, AlCl_3 (959 mg, 7.20 mmol, 5.0 equiv, weighed in glovebox) was added at 23 °C, and the reaction went from pale yellow to deep maroon. After 24 h, the reaction was added at 0 °C to a rapidly stirred suspension of brine (35 mL), sat. aq NaHCO_3 (35 mL), and CHCl_3 (35 mL). The organic layer was collected, and the aqueous phase was extracted with CHCl_3 (3 x 35 mL). All organic layers were combined, dried (Na_2SO_4), filtered, and concentrated. The residue was purified by flash column chromatography on silica gel (10:90 EtOAc:hexane → 20:80 EtOAc:hexane eluent), affording bromoaryl cycloheptadienone (–)-**380** (404 mg, 67% yield) as a yellow solid. R_f 0.28 (20:80 EtOAc/hexane), (visible yellow spot, UV, 254 nm); mp 146–147 °C (EtOAc/hexane)(racemate), mp 144–147 °C (EtOAc/hexane)(95% ee); ^1H NMR (300 MHz, CDCl_3): δ 7.21 (s, 1H), 7.03 (s, 1H), 6.70 (dd, $J = 12.4$ Hz, 8.8 Hz, 1H), 6.30 (d, $J = 8.8$ Hz, 1H), 6.08 (d, $J = 12.4$ Hz, 1H), 4.16 (s, 1H), 3.82 (s, 3H), 3.72 (s, 3H), 1.75–1.33 (m, 5H), 1.37 (s, 3H), 1.21 (s, 3H), 1.22–1.04 (m, 1H), 1.05 (s, 3H); ^{13}C NMR (75 MHz, CDCl_3): δ 198.7, 168.4, 148.4, 148.0, 137.6, 129.5, 128.1, 120.4, 118.0, 115.8, 112.4, 66.3, 56.1, 55.8, 42.8, 38.4, 37.9, 35.4, 33.5, 31.5, 25.3, 17.0; IR (NaCl/ CDCl_3): 2934, 1644, 1572, 1509, 1463, 1440, 1377, 1267,

1248, 1230, 1205, 1159, 1030, 837 cm^{-1} ; HRMS-EI⁺ (m/z): $[\text{M}]^+$ calc'd for $\text{C}_{22}\text{H}_{27}\text{BrO}_3$, 418.1144; found, 418.1158. $[\alpha]_D^{24} -437.31^\circ$ (c 0.985, CHCl_3), 95% ee.



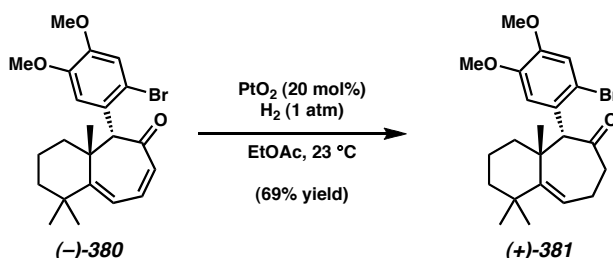
γ,δ -Unsaturated Aryl Cycloheptanone (\pm)-374. A 3-neck round-bottom flask fitted with a cold finger condenser, argon inlet, and mineral oil bubbler was cooled to -78°C . The cold finger was charged with dry ice and acetone, and the system placed under a continuous flow of argon. Ammonia gas was flushed through the system until the condensed volume of liquid NH_3 was ~ 10 mL. A solution of bromoaryl cycloheptadienone (\pm)-380 (10 mg, 23.8 μmol), *tert* amyl alcohol (10.5 mg, 0.118 mmol), and THF (2 mL) was added. Lithium wire (1.2 mm diameter x 5 mm length, ~ 50 mg) was introduced. A deep blue coloration developed, and the reaction was stirred for 15 min. While the system was still under a steady flow of argon, more THF (10 mL) was added, followed by dropwise addition of sat. aq NH_4Cl (3.0 mL). The reaction became colorless and was carefully warmed to 0°C . Once all of the ammonia had evaporated, the reaction was diluted with H_2O and hexanes and thawed to 23°C . The organic phase was collected. The aqueous layer was extracted with EtOAc (1 x). All organic layers were combined, dried (Na_2SO_4), filtered, and concentrated. The residue was purified by preparative TLC on silica gel (EtOAc:hexane 20:80 eluent), giving γ,δ -Unsaturated Aryl Cycloheptanone (\pm)-374 (yield was not determined). Characterization data for this compound can be found on page 367 above.



Bromoaryl- γ,δ -Unsaturated Cycloheptanone (\pm)-381**.** In the glovebox, a flamedried round-bottom flask was charged with CuCl (7.4 mg, 73.4 μ mol, 5 mol%) and NaOt-Bu (8.5 mg, 88.1 μ mol, 6 mol%). The reactor was cycled out of the glovebox and charged with PPh₃ (38.6 mg, 0.147 mmol, 10 mol%). THF (5.0 mL) was added, and the reaction was stirred for 20 min. PMHS (1.006 g/cm³, high viscosity, 447 mg, 4.00 hydride equivalents) was introduced, immediately followed by a solution of bromoaryl cycloheptadienone (\pm)-**380** (617 mg, 1.47 mmol) in THF (5.0 mL). After 2 h, more PMHS (1.006 g/cm³, high viscosity, ~1 g) was added to aide conversion. Additionally, a solution of CuCl (7.4 mg, 73.4 μ mol, 5 mol%), NaOt-Bu (8.5 mg, 88.1 μ mol, 6 mol%), PPh₃ (38.6 mg, 0.147 mmol, 10 mol%), and THF (1.0 mL) was added. Within 2 h, the reaction had become a thick, brown suspension. Sat. aq NH₄Cl (10 mL) was introduced, followed by 6 M aq HCl (5.0 mL). EtOAc (30 mL) was then added, and the polyphasic mixture was extracted with EtOAc (3 x 20 mL). The EtOAc-containing phases were combined, dried (Na₂SO₄), filtered, and concentrated. The residue was purified by flash chromatography on silica gel (5:95 EtOAc:hexane \rightarrow 30:70 EtOAc:hexane \rightarrow EtOAc eluent), giving semipure bromoaryl- γ,δ -unsaturated cycloheptanone (\pm)-**381**. The material was purified on a second silica gel flash column (5:95 EtOAc:hexane \rightarrow 10:90 EtOAc:hexane eluent), giving pure bromoaryl- γ,δ -unsaturated cycloheptanone (\pm)-**381**.

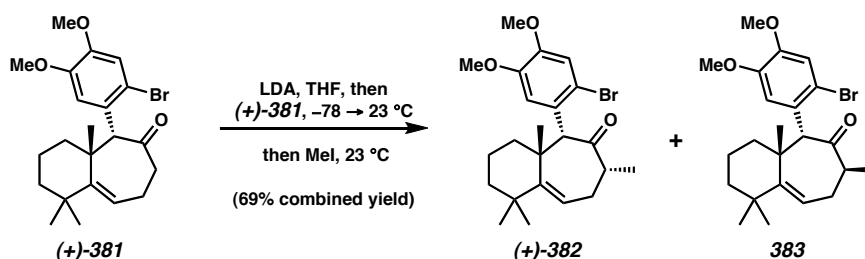
(365 mg, 56% yield) and unreacted starting material (\pm)-**380** (200 mg, 32% yield).

Characterization data for (+)-**381** can be found on pages 377 and 378 below.



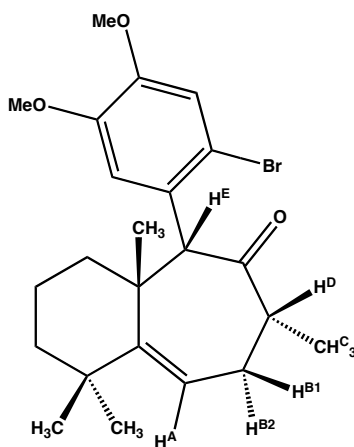
Bromoaryl- γ,δ -Unsaturated Cycloheptanone (+)-381. A round-bottom flask containing bromoaryl cycloheptadienone (\pm)-**380** (400 mg, 0.952 mmol) in EtOAc (ACS grade, 50 mL) was degassed with argon for 5 min. Then, PtO_2 (43.2 mg, 0.190 mmol, 20 mol%) was carefully added. The reaction was cooled to -78 °C, then evacuated/backfilled (vacuum/ H_2 (1 atm)) (3 x). With vigorous stirring, the reaction was warmed to 23 °C under H_2 (1 atm). After 30 min, the reaction was concentrated, and the residue was taken up in PhH. It was purified by flash chromatography on silica gel (10:90 EtOAc:hexane eluent), giving bromoaryl- γ,δ -unsaturated cycloheptanone (+)-**381** (277 mg, 69% yield) as a white solid. R_f 0.41 (20:80 EtOAc/hexane), (*p*-Anisaldehyde, blue spot, UV, 254 nm); mp 114-116 °C (EtOAc/hexane)(racemate), mp 121-123 °C (EtOAc/hexane)(95% ee) ; ^1H NMR (300 MHz, CDCl_3): δ 7.58 (s, 1H), 7.02 (s, 1H), 6.00 (dd, J = 9.9 Hz, 4.4 Hz, 1H), 4.68 (s, 1H), 3.87 (s, 3H), 3.85 (s, 3H), 2.71-2.49 (m, 2H), 2.43-2.32 (m, 2H), 1.79-1.57 (m, 2H), 1.51-1.39 (m, 2H), 1.36-1.24 (m, 2H), 1.28 (s, 3H), 1.19 (s, 3H), 1.17 (s, 3H); ^{13}C NMR (75 MHz, CDCl_3): δ 210.0, 153.8, 148.6, 147.8, 128.2, 122.7, 118.4, 115.6, 115.0, 66.0, 56.7, 56.2, 43.9, 41.5, 39.7, 37.8, 36.4, 33.7, 33.3, 27.5, 23.4, 17.9; IR (NaCl/ CDCl_3): 2936, 2845, 1716, 1699, 1600, 1567,

1506, 1463, 1440, 1374, 1254, 1212, 1159, 1030, 732 cm^{-1} ; HRMS-FAB⁺ (m/z): $[M]^+$ calc'd for $\text{C}_{22}\text{H}_{29}\text{BrO}_3$, 420.1300; found, 420.1303. $[\alpha]_D^{25} +162.47^\circ$ (c 1.250, CHCl_3), 95% ee.



Bromoaryl Methyl γ,δ -Unsaturated Cycloheptanones (+)-382 and 383. A flamedried round-bottom flask was charged with THF (8.0 mL) and $i\text{-Pr}_2\text{NH}$ (129 μL , 0.920 mmol, 1.2 equiv) and cooled to 0 $^\circ\text{C}$. $n\text{-BuLi}$ (2.5 M in hexanes, 338 μL , 0.844 mmol, 1.1 equiv) was added dropwise. After 30 min, the reaction was cooled to -78 $^\circ\text{C}$. A solution of bromoaryl- γ,δ -unsaturated cycloheptanone (+)-381 (324 mg, 0.767 mmol, 1.0 equiv) in THF (6.0 mL) was added, and the reaction gradually went from colorless to yellow. After 30 min, the reaction was warmed to 23 $^\circ\text{C}$ for 30 min. MeI (143 μL , 2.30 mmol, 3.0 equiv) was added. After 2 h had passed, the reaction was quenched with sat. aq NH_4Cl (5.0 mL). Then, H_2O (20 mL), hexanes (10 mL), and EtOAc (20 mL) were added. The organic layer was collected, and the aqueous layer was extracted with EtOAc (2 x 20 mL). All organic layers were combined, dried (Na_2SO_4), filtered, and concentrated. The residue was purified by flash chromatography on silica gel (5:95 EtOAc:hexane \rightarrow 20:80 EtOAc:hexane eluent), giving 4 main fractions. The first contained bromoaryl methyl γ,δ -unsaturated cycloheptanone (+)-382 (130 mg, 39% yield) in pure enough form for characterization. The compound was a white solid. R_f 0.49 (20:80 EtOAc/hexane), (p -

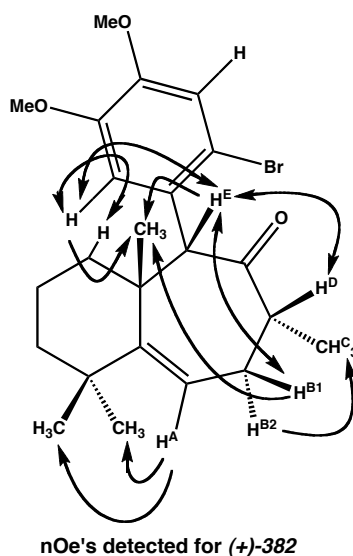
Anisaldehyde, blue spot); mp 53-57 °C (EtOAc)(racemate); ^1H NMR (300 MHz, CDCl_3): δ 7.73 (s, 1H), 6.97 (s, 1H), 5.87 (dd, $J = 9.3$ Hz, 6.0 Hz, 1H), 5.55 (s, 1H), 3.87 (s, 3H), 3.81 (s, 3H), 3.29 (app. dt, $J_d = 15.1$ Hz, $J_t = 6.0$ Hz, 1H), 2.77 (app. dq, $J_d = 8.2$ Hz, $J_q = 6.6$ Hz, 1H), 2.07 (app. ddd, $J = 15.1$ Hz, 9.3 Hz, 1.9 Hz, 1H), 1.91 (app. td, $J_t = 12.6$ Hz, $J_d = 4.9$ Hz, 1H), 1.61-1.19 (m, 5H), 1.27 (s, 3H), 1.11 (s, 3H), 1.05 (s, 3H), 1.03 (d, $J = 6.6$ Hz, 3H); ^{13}C NMR (75 MHz, CDCl_3): δ 211.6, 154.5, 148.4, 147.1, 126.9, 121.7, 117.8, 116.1, 114.8, 58.1, 56.02, 55.98, 50.4, 40.0, 37.8, 34.4, 34.2, 31.8, 29.9, 27.2, 18.1, 14.1; IR (NaCl/ CDCl_3): 2934, 2869, 2846, 1716, 1601, 1569, 1506, 1464, 1440, 1370, 1302, 1255, 1212, 1163, 1032, 915, 733 cm^{-1} ; HRMS-FAB $^+$ (m/z): $[\text{M}]^+$ calc'd for $\text{C}_{23}\text{H}_{31}\text{O}_3^{81}\text{Br}$, 436.1436; found, 436.1437. $[\alpha]_D^{25} +37.00^\circ$ (c 0.885, CHCl_3), 95% ee. ^1H gCOSY experiments (300 MHz, CDCl_3), were performed on (+)-**382**. The following spin systems were observed:



spin systems found for (+)-**382**

Resonance	Proton	Coupled Proton Spins
δ 5.87, dd	H^A	$\text{H}^{B1}, \text{H}^{B2}$
δ 3.29, dt	H^{B1}	$\text{H}^A, \text{H}^{B2}, \text{H}^D$
δ 2.07, ddd	H^{B2}	$\text{H}^A, \text{H}^{B1}$
δ 1.03, d	3H^C	H^D
δ 2.77, dq	H^D	$\text{H}^{B1}, 3\text{H}^C$
δ 5.55, s	H^E	NONE

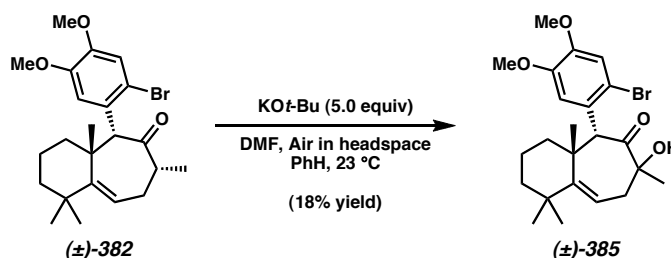
Using the data from the gCOSY experiments along with proton assignments allowed for the assignments of some nOe's. ^1H -nOesy-1D spectra were obtained for (+)-**382** (300 MHz, CDCl_3); the results are shown below:



The second fraction contained a mixture of (+)-**382** and **383** (52.4 mg, 16% yield). The third fraction contained bromoaryl methyl γ,δ -unsaturated cycloheptanone **383** (47.8 mg, 14% yield) in pure enough form for characterization. The compound was a white semisolid. R_f 0.44 (20:80 EtOAc/hexane), (*p*-Anisaldehyde, blue spot); ^1H NMR (300 MHz, CDCl_3): δ 7.61 (s, 1H), 7.02 (s, 1H), 5.93 (dd, $J = 9.6$ Hz, 5.2 Hz, 1H), 4.89 (s, broad, 1H), 3.89 (s, 3H), 3.85 (s, 3H), 2.70 (app. septet, $J = 5.2$ Hz, 1H), 2.42-2.20 (m, 1H), 2.24 (app. ddd, $J = 14.8$ Hz, 9.6 Hz, 5.2 Hz, 1H), 1.77 (app. ddd, $J = 25.5$ Hz, 12.9 Hz, 4.4 Hz, 1H), 1.64 (app. qt, $J_q = 12.1$ Hz, $J_t = 3.3$ Hz, 1H), 1.55-1.37 (m, 2H), 1.36-1.04 (m, 2H), 1.26 (s, 3H), 1.16 (app. s, 6H), 0.99 (d, $J = 6.9$ Hz, 3H); ^{13}C NMR (125 MHz, CDCl_3): δ 212.3 (broad), 153.8, 148.5, 147.5, 128.0 (broad), 122.0, 117.9, 115.6 (broad), 115.3, 56.6, 56.1, 44.5 (broad), 40.0, 37.8, 35.9 (broad), 33.9, 32.8, 31.9, 27.2, 18.1, 16.7; IR (NaCl/ CDCl_3): 2933, 2869, 1716, 1600, 1569, 1505, 1463, 1440, 1374,

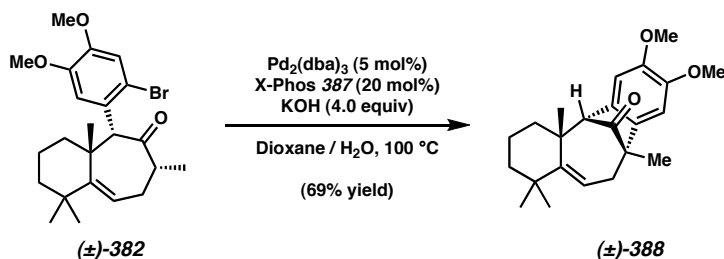
1254, 1213, 1160, 1031, 732; HRMS-FAB⁺ (*m/z*): [M]⁺ calc'd for C₂₃H₃₁O₃⁸¹Br, 436.1436; found, 436.1422.

The fourth fraction contained unreacted starting material (+)-**381** (40.0 mg, 12% yield).



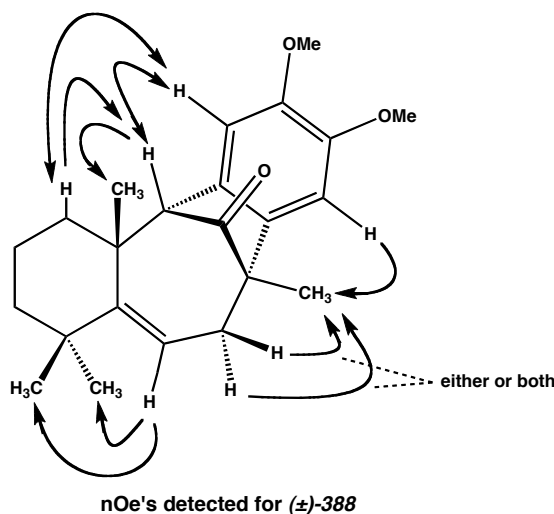
α-Hydroxyketone (±)-385. A vial (open to the air) was charged with KO*t*-Bu (28.0 mg, 0.229 mmol, 5.0 equiv) and dry, argon-degassed DMF (500 μL). The vial was then capped with air in the headspace, and a solution of bromoaryl methyl γ,δ-unsaturated cycloheptanone (+)-**382** (20.0 mg, 45.8 μmol, 1.0 equiv) in PhH (660 μL) was added at 23 °C. After 48 min, the reaction was quenched with sat. aq NH₄Cl (2.0 mL) and H₂O (1.0 mL). The reaction was diluted with more H₂O (4 mL), then extracted with CHCl₃ (3 x 8 mL). All organic layers were combined, dried (Na₂SO₄), filtered, and concentrated. The residue was purified on a 0.5 mm silica preparative TLC plate (20:80 EtOAc:hexane eluent), affording α-hydroxyketone (±)-**385** (3.8 mg, 18% yield) as a white semisolid. (The relative stereochemistry of the hydroxyl stereocenter was not determined, but it was entirely one epimer.) *R*_f 0.34 (20:80 EtOAc/hexane), (*p*-Anisaldehyde, purple spot, UV, 254 nm); ¹H NMR (300 MHz, CDCl₃): δ 7.42 (s, 1H), 6.97 (s, 1H), 5.65 (app. dd, *J* = 6.6 Hz, 1.9 Hz, 1H), 4.00 (s, 1H), 3.84 (s, 3H), 3.80 (s, 3H), 2.76 (AB spin system, app. dd, *J*_{AB} = 16.6 Hz, *J*_d = 1.9 Hz, 1H), 2.12 (s, 3H), 2.11 (app. td, *J*_t = 12.1 Hz, *J*_d = 3.8 Hz,

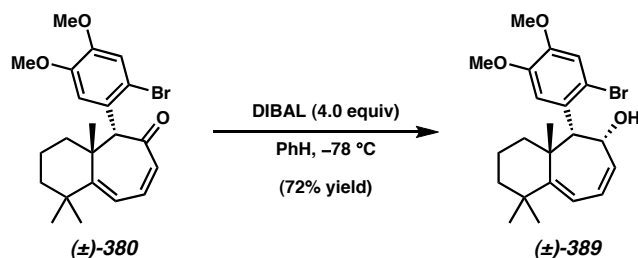
1H), 1.97 (AB spin system, app. dd, $J_{\text{dAB}} = 16.6$ Hz, $J_{\text{d}} = 6.6$ Hz, 1H), 1.73 (app. qt, $J_{\text{q}} = 13.2$ Hz, $J_{\text{t}} = 3.6$ Hz, 1H), 1.58-1.20 (m, 4H), 1.31 (s, 3H), 1.24 (s, 3H), 1.18 (s, 3H), 1.10-1.02 (m, 1H); ^{13}C NMR (125 MHz, CDCl_3): δ 211.8, 151.3, 148.5, 147.6, 129.3, 117.7, 115.4, 114.83, 114.80, 81.4, 56.1, 53.2, 43.1, 42.3, 37.8, 37.5, 35.7, 34.2, 28.9, 27.8, 24.4, 19.3; IR (NaCl/ CDCl_3): 3437 (broad), 2930, 1704, 1602, 1505, 1464, 1251, 1211, 1162, 1103, 1029, 913, 731 cm^{-1} ; HRMS-FAB $^+$ (m/z): $[\text{M}]^+$ calc'd for $\text{C}_{23}\text{H}_{31}\text{BrO}_4$, 450.1406; found, 450.1401.



Tetracyclic Ketone (\pm)-388. In the glovebox, a vial was charged with $\text{Pd}_2(\text{dba})_3$ (0.5 mg, 0.575 μmol , 5 mol%), X-Phos (**387**) (1.1 mg, 2.30 μmol , 20 mol%), and anhydrous, powdered KOH (2.6 mg, 46 μmol , 4.0 equiv). The vessel was cycled out, and a solution of bromoaryl methyl γ,δ -unsaturated cycloheptanones (\pm)-**382** (5.0 mg, 11.5 μmol , 1.0 equiv) in dioxane (250 μL) was added, followed by degassed H_2O (250 μL). The vial was sealed and heated to 100 °C. With time, the reaction went from colorless to yellow, but by 3.5 h, there was Pd black observed, and the reaction was once again colorless. At this time, the reaction was cooled to 23 °C and treated with 6 M aq HCl (50 μL) and diluted with H_2O (1 mL) and extracted with CHCl_3 (3 x 1 mL). All organic layers were combined, dried (Na_2SO_4), and concentrated to ~300 μL . The residue purified on a silica gel preparative TLC plate (20:80 EtOAc:hexane eluent), affording tetracyclic ketone (\pm)-

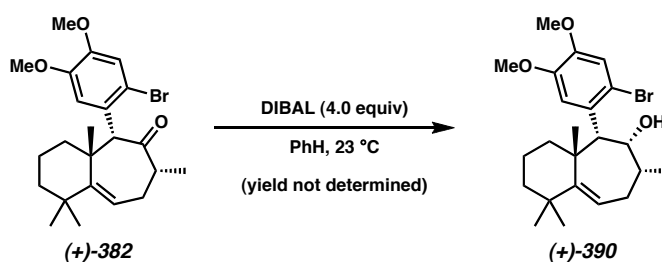
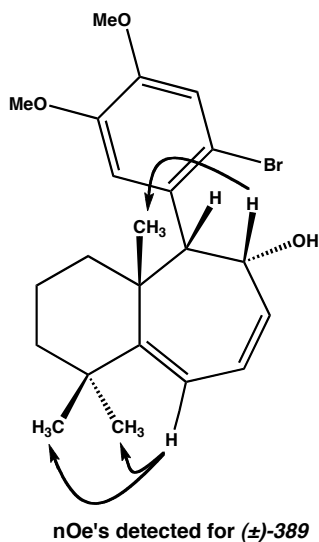
388 (2.8 mg, 69% yield) as a colorless oil. R_f 0.37 (20:80 EtOAc/hexane), (*p*-Anisaldehyde, blue spot); ^1H NMR (300 MHz, CDCl_3): δ 6.85 (s, 1H), 6.64 (s, 1H), 5.32 (app. t, $J = 6.0$ Hz, 1H), 3.90 (s, 3H), 3.88 (s, 3H), 2.80 (s, 1H), 2.23 (app. td, $J_t = 12.6$ Hz, $J_d = 6.0$ Hz, 1H), 2.18 (app. d, $J = 6.0$ Hz, 2H), 1.84-1.68 (m, 1H), 1.68-1.18 (m, 4H), 1.36 (s, 3H), 1.20 (s, 3H), 0.99 (s, 3H), 0.72 (s, 3H); ^{13}C NMR (125 MHz, CDCl_3): δ 216.9, 150.9, 149.3, 148.2, 137.3, 131.7, 119.1, 108.6, 105.2, 64.3, 56.6, 56.2, 52.0, 43.1, 40.5, 38.6, 37.3, 37.2, 32.9, 32.6, 25.5, 18.5, 17.7; IR (NaCl/ CDCl_3): 2928, 1747, 1608, 1500, 1464, 1310, 1244, 1058 cm^{-1} ; HRMS- EI^+ (m/z): $[\text{M}]^+$ calc'd for $\text{C}_{23}\text{H}_{30}\text{O}_3$, 354.2195; found, 354.2183. ^1H - ^1H homodecoupling experiments (300 MHz, CDCl_3) were performed on (\pm)-**388**: The signal at δ 5.32 (app. t, $J = 6.0$ Hz, 1H) was suppressed with a decoupling current, resulting in a splitting change at δ 2.18 (app. d, $J = 6.0$ Hz, 2H \rightarrow app. s, 2H). The signal at δ 2.18 (app. d, $J = 6.0$ Hz, 2H) was suppressed with a decoupling current, resulting in a splitting change at δ 5.32 (app. t, $J = 6.0$ Hz, 1H \rightarrow app. s, broad, 1H). This information allowed for key nOe's to be correctly assigned. ^1H -nOesy-1D spectra were obtained for (\pm)-**388** (300 MHz, CDCl_3); the results are shown below:





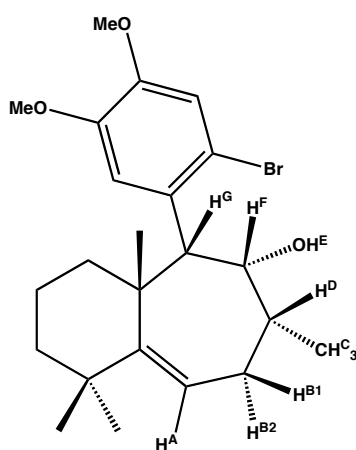
Bromoaryl Cycloheptadienol (\pm)-389. A flamedried round-bottom flask was charged with a solution of bromoaryl cycloheptadienone (\pm)-380 (50 mg, 0.119 mmol, 1.0 equiv) and PhMe (10 mL), then cooled to $-78\text{ }^{\circ}\text{C}$. DIBAL (0.67 M in PhMe, 721 μL , 0.476 mmol, 4.0 equiv) was added dropwise. After 15 min, the reaction was quenched at $-78\text{ }^{\circ}\text{C}$ with 1.0 M aq sodium, potassium tartrate (5.0 mL). Then, the reaction was warmed to $23\text{ }^{\circ}\text{C}$. The biphasic mixture was diluted with H_2O (25 mL) and extracted with PhH (3 x 30 mL). All organic layers were combined, dried (Na_2SO_4), filtered, and concentrated. The residue was purified by flash chromatography on silica gel (hexane \rightarrow 5:95 EtOAc:hexane eluent), affording bromoaryl cycloheptadienol (\pm)-389 (36.2 mg, 72% yield) as an off-white semisolid. R_f 0.24 (20:80 EtOAc/hexane), (*p*-Anisaldehyde, blue spot, UV, 254 nm); ^1H NMR (300 MHz, CDCl_3): δ 7.29 (s, 1H), 7.03 (s, 1H), 6.08 (d, J = 8.5 Hz, 1H), 5.93 (app. ddd, J = 12.1 Hz, 8.5 Hz, 2.7 Hz, 1H), 5.72 (app. d, broad, J = 12.1 Hz, 1H), 4.89 (app. ddt, J_{d1} = 9.3 Hz, J_{d2} = 6.9 Hz, J_t = 2.7 Hz, 1H), 3.84 (s, 3H), 3.73 (s, 3H), 3.62 (app. dd, J = 6.9 Hz, 1.4 Hz, 1H), 1.78-1.62 (m, 1H), 1.43-1.32 (m, 4H), 1.33 (s, 3H), 1.17 (s, 3H), 1.11-1.00 (m, 1H), 1.01 (s, 3H); ^{13}C NMR (75 MHz, CDCl_3): δ 159.0, 148.1, 147.8, 135.3, 130.8, 123.1, 120.0, 119.7, 115.0, 114.1, 71.4, 56.1, 55.7, 53.5, 44.0, 38.8, 37.6, 36.5, 33.7, 32.6, 29.9, 17.4; IR (NaCl/ CDCl_3): 3516 (broad), 2934, 2866, 1601, 1571, 1506, 1463, 1440, 1371, 1259, 1204, 1172, 1031, 912, 856, 793, 731 cm^{-1} ; HRMS-EI $^+$ (m/z): $[\text{M}]^+$ calc'd for $\text{C}_{22}\text{H}_{29}\text{O}_3$ ^{81}Br , 422.1280; found,

422.1283. ^1H -nOesy-1D spectra were obtained for (\pm)-**389** (300 MHz, CDCl_3); the results are shown below:



Bromoaryl Methyl Cycloheptanol (+)-390. A round-bottom flask containing bromoaryl methyl γ,δ -unsaturated cycloheptanone (+)-**382** (128.0 mg, 0.293 mmol, 1.0 equiv) in PhH (10.0 mL) was treated with DIBAL (0.67 M in PhMe, 1.78 mL, 1.17 mmol, 4.0 equiv) at 23 °C. After 15 min, the reaction was added slowly to a rapidly stirred suspension of 1.0 M aq sodium, potassium tartrate (20.0 mL) and PhH (20.0 mL). After 90 min, the organic phase was collected. The aqueous layer was extracted with PhH (3 x 30 mL). All organic layers were combined, dried (Na_2SO_4), filtered, and concentrated, giving bromoaryl methyl cycloheptanol (+)-**390** (135.8 mg, app. 106% yield) as a white

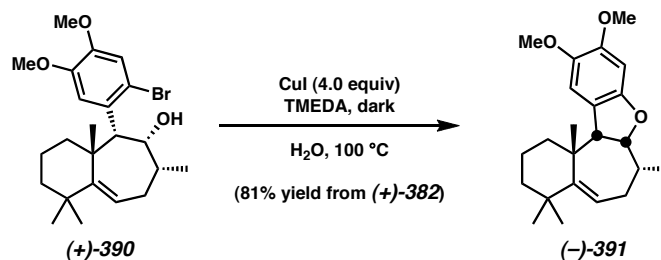
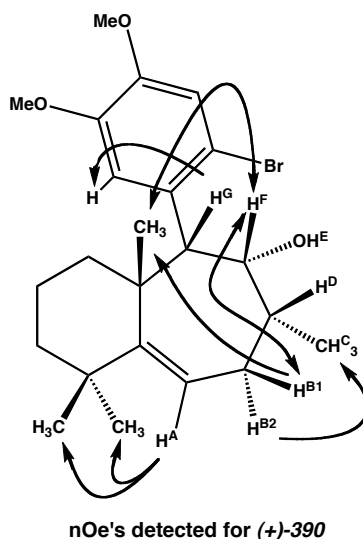
semisolid, which was immediately carried on to the next reaction. (The material was sufficiently pure for characterization.) R_f 0.45 (1:9 MeOH/DCM), (I₂/Sand); mp 203-205 °C (water); ¹H NMR (300 MHz, CDCl₃): δ 7.46 (s, 1H), 6.95 (s, 1H), 6.10 (dd, J = 8.8 Hz, 6.3 Hz, 1H), 4.01 (app. dd, J = 9.6 Hz, 8.5 Hz, 1H), 3.86 (s, 3H), 3.85 (s, 3H), 2.88 (app. dt, J_d = 14.3 Hz, J_t = 6.9 Hz, 1H), 2.43 (d, J = 12.1 Hz, 1H), 2.23 (app. td, J_t = 13.7 Hz, J_d = 6.9 Hz, 1H), 1.95 (app. td, J_t = 12.9 Hz, J_d = 4.4 Hz, 1H), 1.83 (app. dd, J = 14.3 Hz, 9.1 Hz, 1H), 1.65-1.55 (m, 1H), 1.44-1.28 (m, 4H), 1.41 (s, 3H), 1.21 (s, 3H), 1.17 (s, 3H), 1.05 (d, J = 7.4 Hz, 3H), 0.92 (d, broad, J = 12.9 Hz, 1H); ¹³C NMR (75 MHz, CDCl₃): δ 156.7, 148.0, 136.5, 124.3, 115.8, 115.2, 114.5, 80.4, 56.5, 56.2, 56.1, 43.5, 39.8, 39.7, 38.8, 37.8, 34.6, 33.4, 30.1, 28.5, 18.6, 16.8; IR (NaCl/CDCl₃): 3552 (broad), 2928, 1602, 1504, 1464, 1376, 1244, 1209, 1161, 1031 cm⁻¹; HRMS-ESI⁺ (m/z): [M+H]⁺ calc'd for C₂₃H₃₄O₃Br, 437.1691; found, 437.1678. [α]_D²⁵ +14.21° (c 2.00, CHCl₃), 95% ee. ¹H gCOSY experiments (300 MHz, CDCl₃) were performed on (+)-**390**. The following spin systems were observed:



spin systems found for (+)-**390**

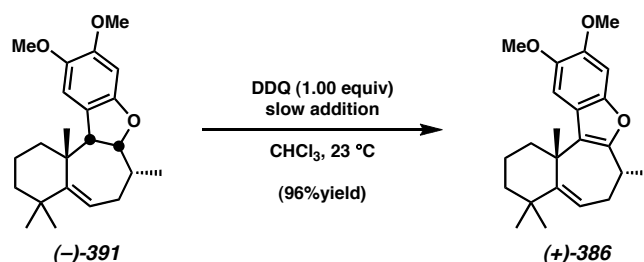
Resonance	Proton	Coupled Proton Spins
δ 6.10, dd	H ^A	H ^{B1} , H ^{B2}
δ 2.88, dt	H ^{B1}	H ^A , H ^{B2}
δ 1.83, dd	H ^{B2}	H ^A , H ^{B1}
δ 1.05, d	3H ^C	H ^D
δ 2.23, td	H ^D	3H ^C
uncertain	H ^E	uncertain
δ 4.01, dd	H ^F	H ^G
δ 2.34, d	H ^G	H ^F

Using the data from the gCOSY experiments along with proton assignments allowed for the assignments of some nOe's. ¹H-nOesy-1D spectra were obtained for (+)-**390** (300 MHz, CDCl₃); the results are shown below:



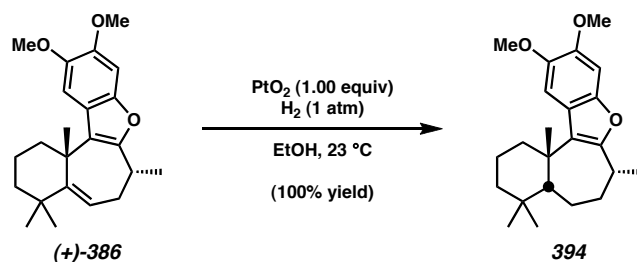
Dihydrobenzofuran (-)-391. A round-bottom flask containing bromoaryl methyl cycloheptanol **(+)-390** (~128 mg (from the previous reaction), 0.293 mmol (estimated), 1.0 equiv) was charged with freshly distilled TMEDA (5.0 mL) and H₂O (5.0 mL). The suspension was degassed with argon for 10 min and CuI (223 mg, 1.17 mmol, 4.0 equiv) was introduced. The reactor was fitted with a reflux condenser and heated to 100 °C in the dark under N₂ for 18 h. The reaction was cooled to 23 °C and diluted with H₂O (50 mL). The suspension was then extracted with CH₂Cl₂ (3 x 25 mL). All organic layers

were combined, dried (Na₂SO₄), filtered, and concentrated. The residue was purified by flash column chromatography on silica gel (5:95 EtOAc:hexane eluent), affording dihydrobenzofuran (–)-**391** (85.7 mg, 81% over 2 steps from (+)-**382**) as a yellow oil. *R*_f 0.48 (20:80 EtOAc/hexane), (UV, 254 nm); ¹H NMR (300 MHz, CDCl₃): δ 6.70 (s, 1H), 6.29 (s, 1H), 5.29 (dd, *J* = 5.2 Hz, 4.9 Hz, 1H), 4.71 (dd, *J* = 8.9 Hz, 3.6 Hz, 1H), 3.73 (s, 3H), 3.69 (s, 3H), 3.54 (d, *J* = 8.9 Hz, 1H), 2.30 (app. ddd, *J* = 14.3 Hz, 6.9 Hz, 3.6 Hz, 1H), 2.19 (app. td, *J*_t = 13.5 Hz, *J*_d = 4.4 Hz, 1H), 1.82 (app. qt, *J*_q = 12.2 Hz, *J*_t = 4.4 Hz, 1H), 1.60 (app. dd, *J* = 6.9 Hz, 5.8 Hz, 1H), 1.62–1.34 (m, 4H), 1.43 (s, 3H), 1.18–0.95 (m, 1H), 1.04 (s, 3H), 1.00 (s, 3H), 0.92 (d, *J* = 6.9 Hz, 3H); ¹³C NMR (75 MHz, CDCl₃): δ 156.3, 148.9, 141.7, 128.4, 123.7, 120.5, 110.8, 93.8, 88.4, 58.6, 57.1, 56.0, 41.7, 41.2, 39.8, 36.8, 35.7, 34.1, 32.9, 32.4, 30.5, 18.6, 18.3; IR (NaCl/CDCl₃): 2933, 2970, 2841, 1618, 1494, 1454, 1377, 1303, 1210, 1165, 1097, 996, 976, 908, 832 cm^{–1}; HRMS-ESI⁺ (*m/z*): [M+H]⁺ calc'd for C₂₃H₃₃O₃, 357.2430; found, 357.2419. [α]_D²⁷ –59.10° (*c* 1.385, CHCl₃), 95% ee.



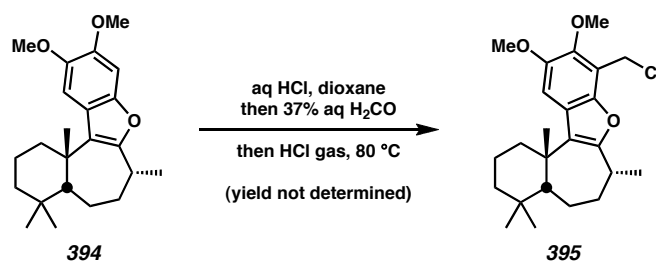
Benzofuran (+)-386. A round-bottom flask containing dihydrobenzofuran (–)-**391** (27.7 mg, 77.7 μmol) was charged with CHCl₃ (9.0 mL). A solution of DDQ (17.6 mg, 77.7 μmol) in CHCl₃ (5.0 mL) was added via syringe pump over a 5 h period at 23 °C. Then the reaction was filtered through a short plug of silica gel with the aid of CHCl₃, giving benzofuran (+)-**386** (26.6 mg, 96% yield) as a white semisolid. *R*_f 0.50 (20:80

EtOAc/hexane), (UV, 254 nm); ^1H NMR (300 MHz, CDCl_3): δ 7.14 (s, 1H), 6.94 (s, 1H), 5.95 (app. dd, $J = 9.6$ Hz, 5.8 Hz, 1H), 3.92 (s, 3H), 3.89 (s, 3H), 3.13 (app. qt, $J_q = 6.9$ Hz, $J_t = 3.4$ Hz, 1H), 2.70-2.60 (m, 2H), 2.20 (app. ddd, $J = 14.0$ Hz, 9.6 Hz, 4.4 Hz, 1H), 1.90-1.75 (m, 2H), 1.75-1.53 (m, 2H), 1.63 (s, 3H), 1.47-1.33 (m, 1H), 1.30 (d, $J = 6.9$ Hz, 3H), 1.24 (s, 3H), 1.22 (s, 3H); ^{13}C NMR (75 MHz, CDCl_3): δ 157.0, 154.2, 148.2, 146.9, 144.9, 121.9, 121.4, 120.5, 106.1, 95.1, 57.2, 56.3, 40.6, 38.6, 37.8, 37.6, 34.0, 33.8, 33.5, 31.7, 27.1, 18.7, 18.4; IR (NaCl/ CDCl_3): 3056, 2930, 2868, 2832, 1624, 1489, 1464, 1440, 1313, 1276, 1213, 1198, 1165, 1124, 1002, 733 cm^{-1} ; HRMS- EI^+ (m/z): $[\text{M}]^+$ calc'd for $\text{C}_{23}\text{H}_{30}\text{O}_3$, 354.2195; found, 354.2199.



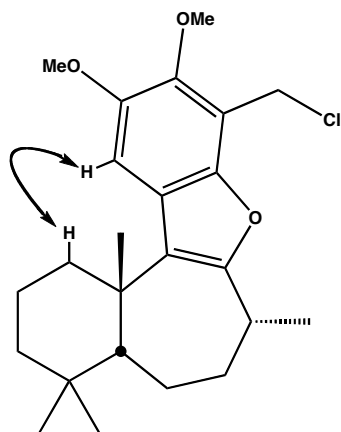
Benzofuran 394. A round-bottom flask containing benzofuran **(+)-386** (5.0 mg, 14.1 μmol , 1.0 equiv) was charged with absolute EtOH (2.0 mL). The solution was degassed with argon for 5 min. Then, PtO_2 (3.0 mg, 14.1 μmol , 1.0 equiv) was introduced. The reaction was cooled to -78 °C and purged/backfilled with vacuum and H_2 (1 atm) (3 x). Then, the reaction was warmed to 23 °C and stirred vigorously under H_2 (1 atm) for 20 h. The reaction was then concentrated and taken up in EtOAc. The mixture was filtered through silica gel with the aid of EtOAc. The filtrate was concentrated, affording benzofuran **394** (5.0 mg, 100% yield) as a white semisolid. R_f 0.48 (20:80 EtOAc/hexane), (UV, 254 nm); ^1H NMR (500 MHz, CDCl_3): δ 7.18 (s, 1H), 6.98 (s, 1H),

3.901 (s, 3H), 3.896 (s, 3H), 3.19-3.10 (m, 1H), 2.80-2.68 (m, 1H), 2.27-2.15 (m, 1H), 1.98 (app. q, $J = 12.7$ Hz, 1H), 1.80 (app. q, $J = 12.4$ Hz, 1H), 1.67-1.59 (m, 1H), 1.41 (d, $J = 6.8$ Hz, 3H), 1.50-0.80 (m, 6H), 1.31 (s, 3H), 0.97 (s, 3H), 0.65 (s, 3H); ^{13}C NMR (125 MHz, CDCl_3): δ 148.2, 146.5, 145.3, 120.4, 104.7, 95.0, 56.7, 56.2, 54.2 (broad), 45.7 (broad), 41.8 (broad), 38.8 (broad), 35.8, 35.1 (broad), 32.7, 32.5 (broad), 30.6, 29.8, 26.6, 21.5, 18.8; IR (NaCl/ CDCl_3): 2944, 2863, 1622, 1489, 1383, 1322, 1294, 1217, 1198, 1138, 1044 cm^{-1} ; HRMS- EI^+ (m/z): $[\text{M}]^+$ calc'd for $\text{C}_{23}\text{H}_{32}\text{O}_3$, 356.2352; found, 356.2351.

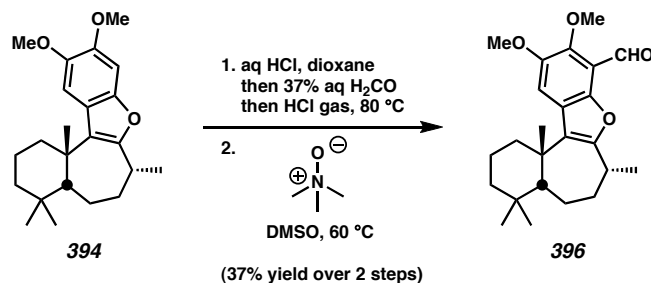


Benzyl Chloride 395. A vial containing benzofuran **394** (4.0 mg, 11.2 μmol) and dioxane (degassed with argon, 100 μL) was treated dropwise with conc. aq HCl (100 μL) at 23 $^\circ\text{C}$. The reaction turned yellow. 37% aq formaldehyde (100 μL) was introduced, followed by HCl gas (generated via slow addition of conc. aq H_2SO_4 to NaCl), which was bubbled in steadily for 3 min. The reaction became yellow-orange. The vessel was sealed and heated to 50 $^\circ\text{C}$ for 30 min followed by 80 $^\circ\text{C}$ for 30 min, during which time the reaction turned maroon. The vessel was cooled to 23 $^\circ\text{C}$ and 6 M aq HCl (1 mL) was added along with CHCl_3 (1 mL). The reaction was stirred vigorously for 10 min, then the organic phase was collected. The aqueous layer was extracted with CHCl_3 (2 x 1 mL). All organic layers were combined, carefully washed with sat. aq NaHCO_3 (2 x 1 mL),

dried (Na_2SO_4), filtered, and concentrated. The residue was purified on a pipet flash column containing silica gel (10:90 EtOAc:hexane eluent), giving semipure benzyl chloride **395** (yield not determined) as a yellow oil. R_f 0.60 (20:80 EtOAc/hexane), (UV, 254 nm); ^1H NMR (300 MHz, CDCl_3): δ 7.22 (s, 1H), 4.933 (app. s, 1H), 4.929 (app. s, 1H), 3.97 (s, 3H), 3.89 (s, 3H), 3.24-3.08 (m, 1H), 2.70 (app. d, broad, $J = 14.1$ Hz, 1H), 2.32-2.12 (m, 2H), 1.71-1.59 (m, 2H), 1.48-1.05 (m, 6H), 1.45 (d, $J = 7.1$ Hz, 3H), 1.26 (s, 3H), 0.98 (s, 3H), 0.67 (s, 3H); ^{13}C NMR (not performed); IR (not performed); LCMS-APCI $^+$ (m/z): $[\text{M}+\text{H}]^+$ calc'd for $\text{C}_{24}\text{H}_{34}\text{O}_3^{35,37}\text{Cl}$, 404, 406; found, 404, 406, and 369 ($\text{M}+\text{H}-^{35,37}\text{Cl})^+$. ^1H -nOesy-1D spectra were obtained for **395** (300 MHz, CDCl_3); the results are shown below:



nOe's detected for **395**

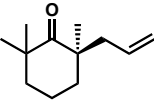
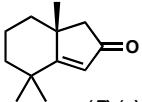
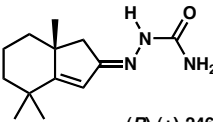


Benzaldehyde 396. A vial containing benzofuran **394** (4.0 mg, 11.2 μ mol) and dioxane (degassed with argon, 100 μ L) was treated dropwise with conc. aq HCl (100 μ L) at 23 °C. The reaction turned yellow. 37% aq formaldehyde (100 μ L) was introduced, followed by HCl gas (generated via slow addition of conc. aq H₂SO₄ to NaCl), which was bubbled in steadily for 3 min. The reaction became yellow-orange. The vessel was sealed and heated to 80 °C for 50 min, during which time the reaction turned maroon. The vessel was cooled to 23 °C and 6 M aq HCl (1 mL) was added along with CHCl₃ (1 mL). The reaction was stirred vigorously for 10 min, and the organic phase was collected. The aqueous layer was extracted with CHCl₃ (2 x 1 mL). All organic layers were combined, carefully washed with sat. aq NaHCO₃ (1 x 500 μ L), dried (Na₂SO₄), and filtered through a pipet of silica with the aide of CHCl₃. The filtrate, which contained benzyl chloride **395**, was concentrated and immediately used in the next reaction.

The benzyl chloride **395** was treated with DMSO (distilled from CaH₂, 200 μ L), followed by trimethylamine *N*-oxide (4.2 mg, 5.60 mmol, 5.0 equiv relative to **394**). The vessel was sealed and heated to 60 °C for 20 min. The reaction was purified on an preparative TLC plate (20:80 EtOAc:hexane eluent), giving benzaldehyde **396** (1.6 mg, 37% yield from **394**) as a yellow oil. *R*_f 0.46 (20:80 EtOAc/hexane), (UV, 356 nm, yellow spot, and UV, 254 nm); ¹H NMR (500 MHz, CDCl₃): δ 10.59 (s, 1H), 7.51 (s, 1H), 3.98 (s, 3H), 3.92 (s, 3H), 3.23-3.10 (m, 1H), 2.70 (app. d, broad, *J* = 11.0 Hz, 1H),

2.28-2.16 (m, 2H), 1.91 (app. q, $J = 11.1$ Hz, 1H), 1.89-1.75 (m, 1H), 1.69-1.62 (m, 2H), 1.50 (d, $J = 6.8$ Hz, 3H), 1.43-1.22 (m, 4H), 1.30 (s, 3H), 0.98 (s, 3H), 0.64 (s, 3H); ^{13}C NMR (75 MHz, CDCl_3): δ 188.7, 149.2, 148.5, 125.2, 115.0, 63.0, 57.0, 35.7, 29.9, 26.4, 21.5, 18.7; IR (NaCl/ CDCl_3): 2930, 2864, 1689, 1605, 1464, 1386, 1363, 1327, 1297, 1238, 1139, 1057, 979, 732 cm^{-1} ; HRMS-EI $^+$ (m/z): $[\text{M}]^+$ calc'd for $\text{C}_{24}\text{H}_{32}\text{O}_4$, 384.2301; found, 384.2306.

4.11.3 Methods for the Determination of Enantiomeric Excess

Entry	Substrate	Assay	Column	Method	Retention Time (min)
1.	 (R)-(+)-75	Enantiomeric Excess	Chiral GC	80 °C isotherm	Minor (S) 29.1
			Agilent GT-A Column	40 min	Major (R) 30.5
2.	 (R)-(+)-143	Enantiomeric Excess	Chiral HPLC	3%EtOH/Hex monitor@254nm	Major (R) 9.1
			Chiralcel AD Column	20 min	Minor (S) 10.2
3.	 (R)-(+)-246	Enantiomeric Excess	Chiral HPLC	10%EtOH/Hex monitor@254nm	Major (R) 9.3
			Chiralcel AD Column	20 min	Minor (S) 12.1

4.12 Notes and Citations

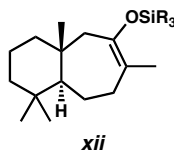
- (1) Marion, F.; Williams, D. E.; Patrick, B. O.; Hollander, I.; Mallon, R.; Kim, S. C.; Roll, D. M.; Feldberg, L.; van Soest, R.; Andersen, R. J. *Org. Lett.* **2006**, *8*, 321-324.
- (2) (a) Varticovski, L.; Druker, B.; Morrison, D.; Cantley, L.; Roberts, T. *Nature* **1989**, *342*, 699-702. (b) Fruman, D. A.; Cantley, L. C. *Signaling Networks and Cell Cycle Control* **2000**, 247-266. (c) Cantley, L. C. *Science* **2002**, *296*, 1655-1657. (d) Fruman, D. A.; Cantley, L. C. *Seminars in Immunology* **2002**, *14*, 7-18. (e) Isakoff, S. J.; Engelman, J. A.; Irie, H. Y.; Luo, J.; Brachmann, S. M.; Pearline, R. V.; Cantley, L. C.; Brugge, J. S. *Cancer Res.* **2005**, *65*, 10992-11000. (f) Brachmann, S. M.; Yballe, C. M.; Innocenti, M.; Deane, J. A.; Fruman, D. A.; Thomas, S. M.; Cantley, L. C. *Mol. Cell. Biol.* **2005**, *25*, 2593-2606. (g) Brachmann, S. M.; Ueki, K.; Engelman, J. A.; Kahn, R. C.; Cantley, L. C. *Mol. Cell. Biol.* **2005**, *25*, 1596-1607. (h) Luo, J.; Sobkiw, C. L.; Logsdon, N. M.; Watt, J. M.; Signoretti, S.; O'Connell, F.; Shin, E.; Shim, Y.; Pao, L.; Neel, B. G.; DePinho, R. A.; Loda, M.; Cantley, L. C. *Proc. Natl. Acad. Sci. U.S.A.* **2005**, *102*, 10238-10243.
- (3) (a) Ward, S. G.; Sotsios, Y.; Dowden, J.; Bruce, I.; Finan, P. *Chem. Biol.* **2003**, *10*, 207-213. (b) Ward, S. G.; Finan, P. *Curr. Opin. Pharmacol.* **2003**, *3*, 426-434. (c) Wymann, M. P.; Zvelebil, M.; Laffargue, M. *Trends Pharmacol. Sci.* **2003**, *24*, 366-376.
- (4) Yang, L.; Williams, D. E.; Mui, A.; Ong, C.; Krystal, G.; van Soest, R.; Andersen, R. *J. Org. Lett.* **2005**, *7*, 1073-1076.

-
- (5) Knight, Z. A.; Gonzalez, B.; Feldman, M. E.; Zunder, E. R.; Goldenberg, D. D.; Williams, O.; Loewith, R.; Stokoe, D.; Balla, A.; Toth, B.; Balla, T. Weiss, W. A.; Williams, R. L.; Shokat, K. M. *Cell*, **2006**, *125*, 733-737.
- (6) (a) Robertson, A. J.; Jackson, S.; Kenche, V.; Yaip, C.; Parbaharan, H.; Thompson, P. Int. Patent Appl. WO 0181346 A2, **2001**. (b) Hayakaa, M.; Kaizawa, H.; Kawaguchi, K. I.; Matsuda, K.; Ishikawa, N.; Koizumi, T.; Yamanao.; M.; Ohta, M. U.S. Patent US 6403588, **2002**. (c) Sadhu, C.; Masinovsky, B.; Dick, K.; Sowell, G. C.; Staunton, D. E. *J. Immunol.* **2003**, *170*, 2647-2654.
- (7) Andersen prepared liphagal (**271**) in 5.6% yield over a 12 step longest linear sequence from 2,4,5-trimethoxybenzaldehyde (**290**), which can be purchased from Aldrich for \$1.34/g (\$134/100 g).
- (8) McFadden, R. M.; Stoltz, B. M. *J. Am. Chem. Soc.* **2006**, *128*, 7738-7739.
- (9) Smith, A. B., III; Cho, Y. S.; Friestad, G. K. *Tetrahedron Lett.* **1998**, *39*, 8765-8768.
- (10) Thomas, A. F.; Ozainne, M.; Guntz-Dubini, R. *Can. J. Chem.* **1980**, *58*, 1810-1820.
- (11) Our synthesis of bicyclic enone (+)-**143** constitutes a formal total synthesis of *nat*-(-)-dichroanone ((-)-**150**); see chapter three and reference 8 for details.
- (12) For investigations of the stereochemistry of [2+2] cycloadditions of alkenes to enones, see: (a) Shih, C.; Fritzen, E. L.; Swenton, J. S. *J. Org. Chem.* **1980**, *45*, 4462-4471. (b) Shen, R.; Corey, E. *J. Org. Lett.* **2007**, *9*, 1057-1059.
- (13) For examples of ethylene photoadditions, see: (a) Eaton, P. E.; Nyi, K. *J. Am. Chem. Soc.* **1971**, *93*, 2786-2788. (b) Cargill, R. L.; Wright, B. W. *J. Org. Chem.* **1975**, *40*, 120-122. (c) Tsutsumi, K.; Nakano, H.; Furutani, A.; Endou, K.; Merpuge, A.; Shintani, T.; Morimoto, T.; Kakiuchi, K. *J. Org. Chem.* **2004**, *69*, 785-789.

-
- (14) For examples of cyclobutane rearrangements, see: (a) Kakiuchi, K.; Ue, M.; Tsukahara, H.; Shimizu, T.; Miyao, T.; Tobe, Y.; Odaira, Y.; Yasuda, M.; Shima, K. *J. Am. Chem. Soc.* **1989**, *111*, 3707-3712. (b) Kakiuchi, K.; Ohnishi, Y.; Kobiro, K.; Tobe, Y.; Odaira, Y. *J. Org. Chem.* **1991**, *56*, 463-466.
- (15) For studies of cyclobutadiene analogues prepared via alkyne photoadditions, see: (a) Breslow, R.; Grubbs, R. H.; Murahashi, S.-I. *J. Am. Chem. Soc.* **1970**, *92*, 4139-4140. (b) Breslow, R.; Murayama, D. R.; Murahashi, S.-I. *J. Am. Chem. Soc.* **1973**, *95*, 6688-6699.
- (16) For examples of acetylene photoadditions, see: (a) Sunder-Plassman, P.; Nelson, P. H.; Boyle, P. H.; Cruz, A.; Iriarte, J.; Crabbé, P.; Zderic, J. A.; Edwards, J. A.; Fried, J. H. *J. Org. Chem.* **1969**, *34*, 3779-3784. (a) White, J. D.; Avery, M. A.; Carter, J. P. *J. Am. Chem. Soc.* **1982**, *104*, 5486-5489.
- (17) A small sample of solid cyclobutene (\pm)-**312** evaporated during attempted solvent removal under high vacuum.
- (18) For the first synthesis of the parent compound—bicyclo[1.1.0]butane—reported in the peer-reviewed literature, see: Lemal, D. M.; Menger, F.; Clark, G. W. *J. Am. Chem. Soc.* **1963**, *85*, 2529-2530.
- (19) A dissertation surrounding bicyclo[1.1.0]butane has also been published: Ciula, R. P. Bicyclo[1.1.0]butane. Ph.D. Dissertation, Univ. of Washington, Seattle, WA, **1960**.
- (20) For an excellent review on oxa-di- π -methane rearrangements, see: Hixson, S. S.; Mariano, P. S.; Zimmerman, H. E. *Chem. Rev.* **1973**, *73*, 531-551.
- (21) For applications and studies of the oxa-di- π -methane rearrangement of cyclobutenes, see: (a) Sugihara, Y.; Yamato, A.; Murata, I. *Tetrahedron Lett.* **1981**, *22*, 3257-3260.

-
- (b) Hussain, S.; Schuster, D. I.; El-Bayoumy, K. *Tetrahedron Lett.* **1982**, 23, 153-156.
- (c) Cavazza, M.; Pietra, F. *J. Chem. Soc. Perkin Trans. 1* **1985**, 2283-2287. (d) Cavazza, M.; Guerriero, A.; Pietra, F. *J. Chem. Soc. Perkin Trans. 1* **1986**, 2005-2008. (e) Wakabayashi, S.; Saito, N.; Sugihara, Y.; Sugimura, T.; Murata, I. *Synth. Commun.* **1995**, 25, 2019-2027.
- (22) A related bicyclobutane rearrangement to a cyclobutene mediated by AlBr_3 has been reported: Razin, V. V.; Mostova, M. I.; D'yakonov, I. A. *Zh. Organich. Khim.* **1968**, 4, 535.
- (23) For studies of transition metal-catalyzed rearrangements of bicyclobutanes, see: (a) Gassman, P. G.; Atkins, T. J.; Williams, F. J. *J. Am. Chem. Soc.* **1971**, 93, 1812-1813. (b) Gassman, P. G.; Williams, F. J. *Tetrahedron Lett.* **1971**, 18, 1409-1412. (c) Gassman, P. G.; Meyer, R. G.; Williams, F. J. *J. Chem. Soc. Sect. D: Chem. Commun.* **1971**, 842-843. (d) Gassman, P. G.; Takeshi, N. *J. Am. Chem. Soc.* **1971**, 93, 5897-5899. (e) Gassman, P. G.; Williams, F. J. *J. Chem. Soc., Chem. Commun.* **1972**, 80-81. (f) Gassman, P. G.; Takeshi, N. *J. Am. Chem. Soc.* **1972**, 94, 2877-2879. (g) Gassman, P. G.; Nakai, T. *J. Am. Chem. Soc.* **1972**, 94, 5497-5499. (h) Gassman, P. G. *Angew. Chem., Int. Ed.* **1972**, 11, 323.
- (24) For studies regarding 4π -electrocyclic ring openings, see: (a) Ben-Nun, M.; Martínez, T. J. *J. Am. Chem. Soc.* **2000**, 122, 6299-6300. (b) Bajorek, T.; Werstiuk, N. H. *Chem. Commun.* **2003**, 648-649.
- (25) For excellent discussion on the Fischer indole synthesis, see: (a) Robinson, B. *Chem. Rev.* **1969**, 69, 227-250. (b) Robinson, B. In *The Fischer Indole Synthesis*. John

- Wiley and Sons: New York, **1982**. (c) Hughes, D. L. *Org. Prep. Proced. Int.* **1993**, 25, 609-632.
- (26) Miyata, O.; Takeda, N.; Morikami, Y.; Naito, T. *Org. Biomol. Chem.* **2003**, 1, 254-256.
- (27) For a synthesis of electron-rich *O*-aryl oximes, see: Alemagna, A.; Baldoli, C.; Del Buttero, P.; Licandro, E.; Maiorana, S. *Synthesis* **1987**, 2, 192-196.
- (28) Robertson, D. W.; Lacefield, W. B.; Bloomquist, W.; Pfiefer, W.; Simon, R. L.; Cohen, M. L. *J. Med. Chem.* **1992**, 35, 310-319.
- (29) Holmes, T. J.; John, V.; Vennerstrom, J.; Choi, K. E. *J. Org. Chem.* **1984**, 49, 4736-4738.
- (30) Wilgus, H. S.; Gates, J. W. *Can. J. Chem.* **1967**, 45, 1975-1980.
- (31) Stoltz, B. M.; Kano, T.; Corey, E. J. *J. Am. Chem. Soc.* **2000**, 122, 9044-9045.
- (32) Although the products from these reactions were not fully characterized, ^1H NMR data suggested they had the structure below:



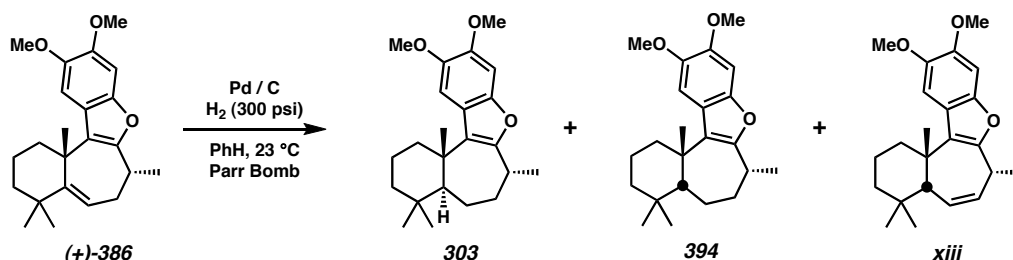
- (33) Carril, M.; SanMartin, R.; Tellitu, I.; Domínguez, E. *Org. Lett.* **2006**, 8, 1467-1470.
- (34) For an excellent theoretical discussion of “on-water” chemical phenomena, see: Jung, Y.; Marcus, R. A. *J. Am. Chem. Soc.* **2007**, 129, 5492-5502.
- (35) (a) Palucki, M.; Buchwald, S. L. *J. Am. Chem. Soc.* **1997**, 119, 11108-11109. (b) Kawatsura, M.; Hartwig, J. F. *J. Am. Chem. Soc.* **1999**, 121, 1473-1478. (c) Fox, J. M.; Huang, X.; Chieffi, A.; Buchwald, S. L. *J. Am. Chem. Soc.* **2000**, 122, 1360-

-
1370. (d) Culkin, D. A.; Hartwig, J. F. *Acc. Chem. Res.* **2003**, *36*, 234-245.
- (36) Su, W.; Raders, S.; Verkade, J. G.; Liao, X.; Hartwig, J. F. *Angew. Chem., Int. Ed.* **2006**, *45*, 5852-5855.
- (37) The relative stereochemistry of the major diastereomer was not assigned.
- (38) Cargill, R. L.; Jackson, T. E.; Peet, N. P.; Pond, D. M. *Acc. Chem. Res.* **1974**, *7*, 106-113.
- (39) A beautiful application of the Cargill rearrangement in the total synthesis of verrucarol has been detailed. The authors noted dramatic substituent effects when attempting the key cyclobutene opening. See: White, J. D.; Kim, N.-S.; Hill, D. E.; Thomas, J. A. *Synthesis* **1998**, 619-626.
- (40) Lipshutz, B. H.; Servesko, J. M.; Peterson, T. B.; Papa, P. P.; Lover, A. A. *Org. Lett.* **2004**, *6*, 1273-1275.
- (41) Anderson, K. W.; Ikawa, T.; Tundel, R.; Buchwald, S. L. *J. Am. Chem. Soc.* **2006**, *128*, 10694-10695.
- (42) (a) Sondheimer, F.; Elad, D. *J. Am. Chem. Soc.* **1958**, *80*, 1967-1971. (b) Mueller, R.; Ruedi, P. *Helv. Chim. Acta* **2003**, *86*, 439-456. (c) Takikawa, H.; Ueda, K.; Sasaki, M. *Tetrahedron Lett.* **2004**, *45*, 5569-5572. (d) Pollini, G. P.; Bianchi, A.; Casolari, A.; De Risi, C.; Zanirato, V.; Bertolasi, V. *Tetrahedron Asym.* **2004**, *15*, 3223-3232. (e) Foot, J. S.; Phillis, A. T.; Sharp, P. P.; Willis, A. C.; Banwell, M. G. *Tetrahedron Lett.* **2006**, *47*, 6817-6820.
- (43) (a) Enzell, C. *Acta Chem. Scand.* **1962**, *16*, 1553-1568. (b) Harayama, T.; Sakurai, K.; Tanaka, K.; Hashimoto, Y.; Fukushi, H.; Inubushi, Y. *Chem. Pharm. Bull.* **1987**, *35*, 1434-1442.

(44) See the experimental section for details.

(45) Paquette, W. D.; Taylor, R. E. *Org. Lett.* **2004**, 6, 103-106.

(46) A variety of hydrogenation conditions were tested on (+)-**386** in an attempt to produce **303**. One reaction produced an apparent 2:1:2 mixture of **303**, **394**, and **xiii**. See below:



(47) We have initiated a collaboration with Lewis Cantley, a pioneer in the field of PI3K biology² to investigate the structure activity relationship of liphaganes. Appendix nine gives a detailed list of compounds to be investigated.

(48) (a) Peer, M.; de Jong, J. C.; Kiefer, M.; Langer, T.; Riech, H.; Schell, H.; Sennhenn, P.; Sprinz, J.; Steinhagen, H.; Wiese, B.; Helmchen, G. *Tetrahedron* **1996**, 52, 7547-7583. (b) Behenna, D. C.; Stoltz, B. M. *J. Am. Chem. Soc.* **2004**, 126, 15044-15045. (c) Tani, K.; Behenna, D. C.; McFadden, R. M.; Stoltz, B. M. *Org. Lett.* **2007**, 9, 2529-2931.

(49) When a subscript is shown with the coupling constant, it indicates what type of splitting the constant is associated with. For example (td, $J_t = 5.0$ Hz, $J_d = 3.3$ Hz, 1H) indicates that the triplet splitting has a 5.0 Hz coupling constant and the doublet has a 3.3 Hz coupling constant.

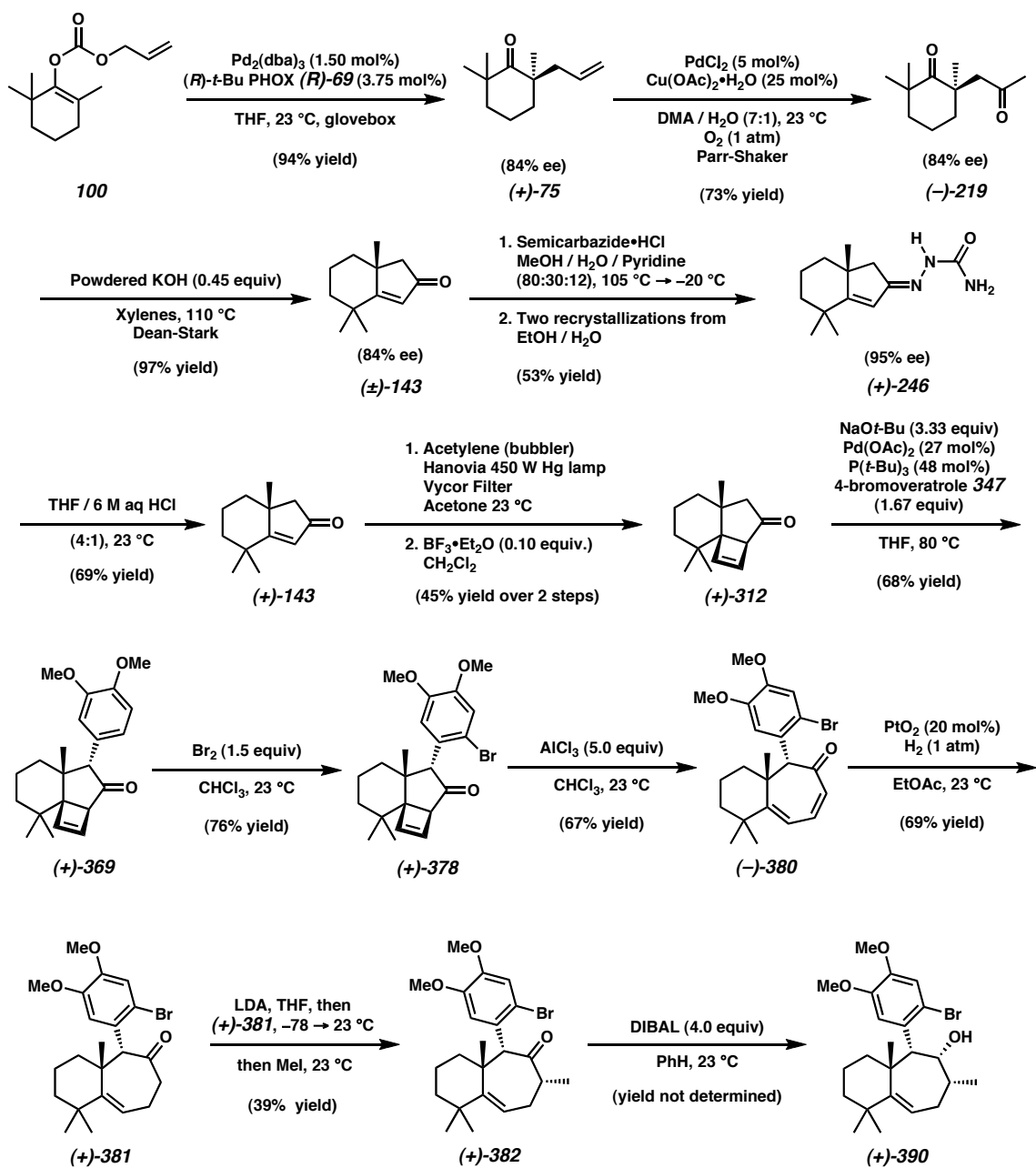
(50) Allowing the recrystallization to cool below 23 °C led to crystals having less enantioenrichment.

-
- (51) (a) Mamaghani, M.; Pourali, A. *Zh. Org. Khim.* **2002**, *38*, 369-371. (b) Legrand, S.; Nordlander, G.; Nordenhem, H.; Borg-Karlson, A.-K.; Unelius, C. R. *Z. Naturforsch* **2004**, *59*, 829-835.
- (52) (a) Ansell, M. F.; Clements, A. H. *J. Chem. Soc., Sect. C* **1971**, 269-275. (b) Brimble, M. A.; Burgess, C.; Halim, R.; Petersson, M.; Ray, J. *Tetrahedron* **2004**, *60*, 5751-5758.

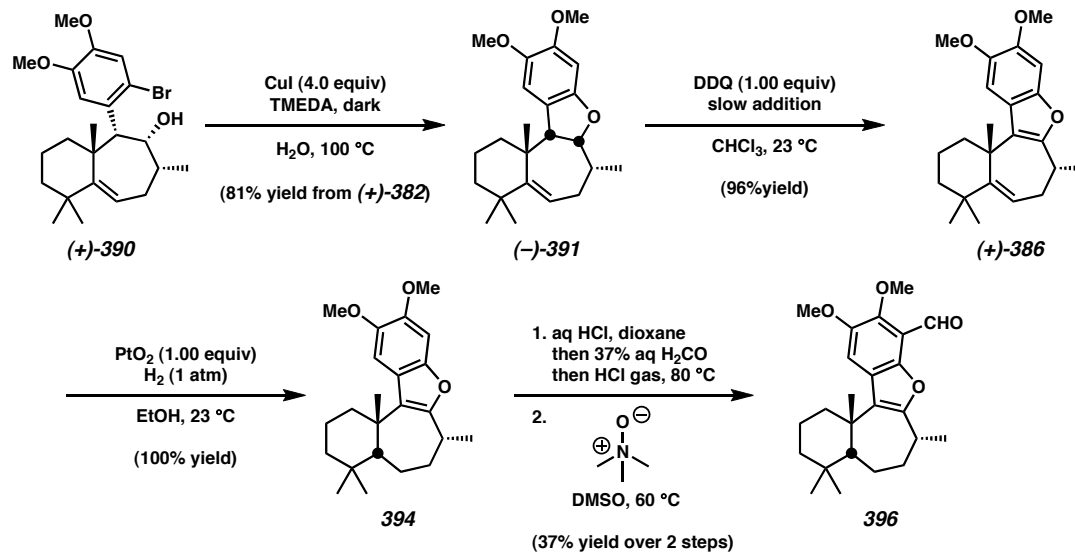
Appendix SIX

Synthetic Summary of Progress Toward the Enantioselective Total Syntheses of Liphagal

Scheme A6.1 Toward the Enantioselective Total Synthesis of Liphagal: Part 1



Scheme A6.2 Toward the Enantioselective Total Synthesis of Liphagal: Part 2



Appendix SEVEN

Spectra of Compounds Relevant to Chapter 4

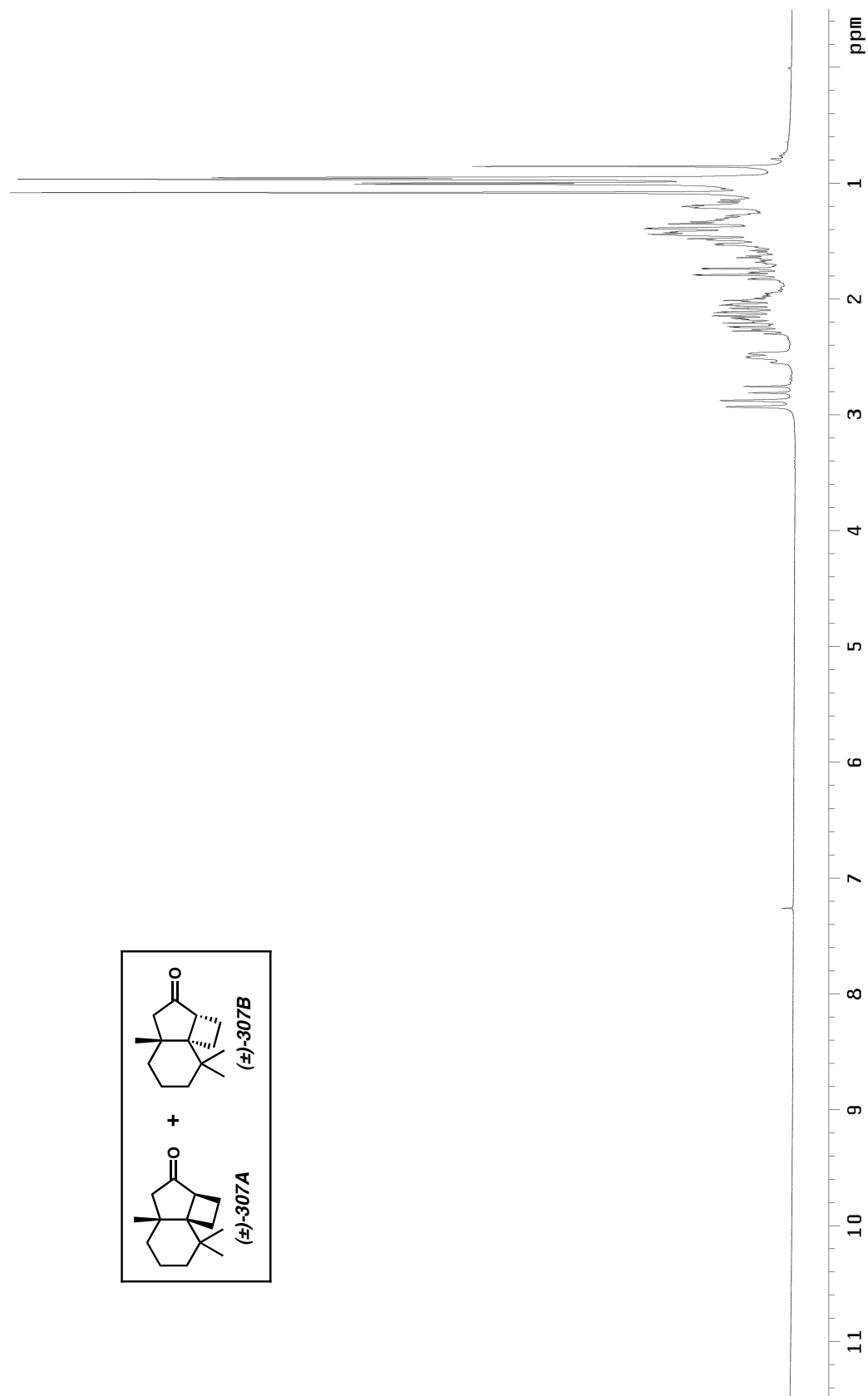


Figure A7.1 ^1H NMR (300 MHz, CDCl_3) of compounds **307A** and **307B**.

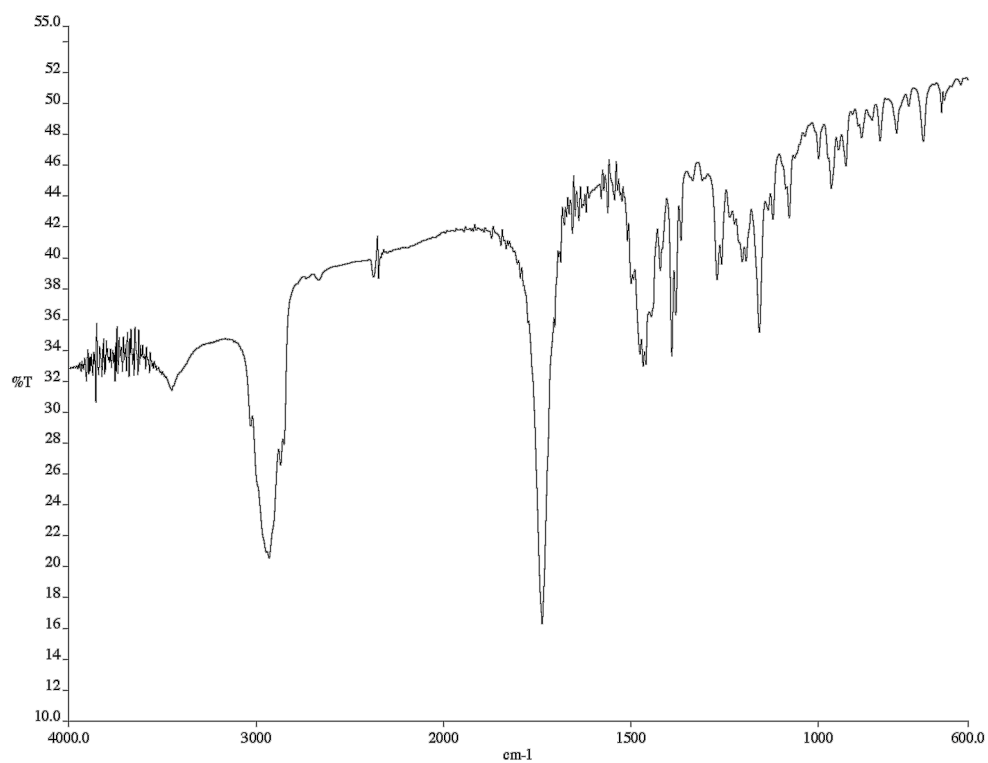


Figure A7.2 Infrared spectrum (KBr) of compounds **307A** and **307B**.

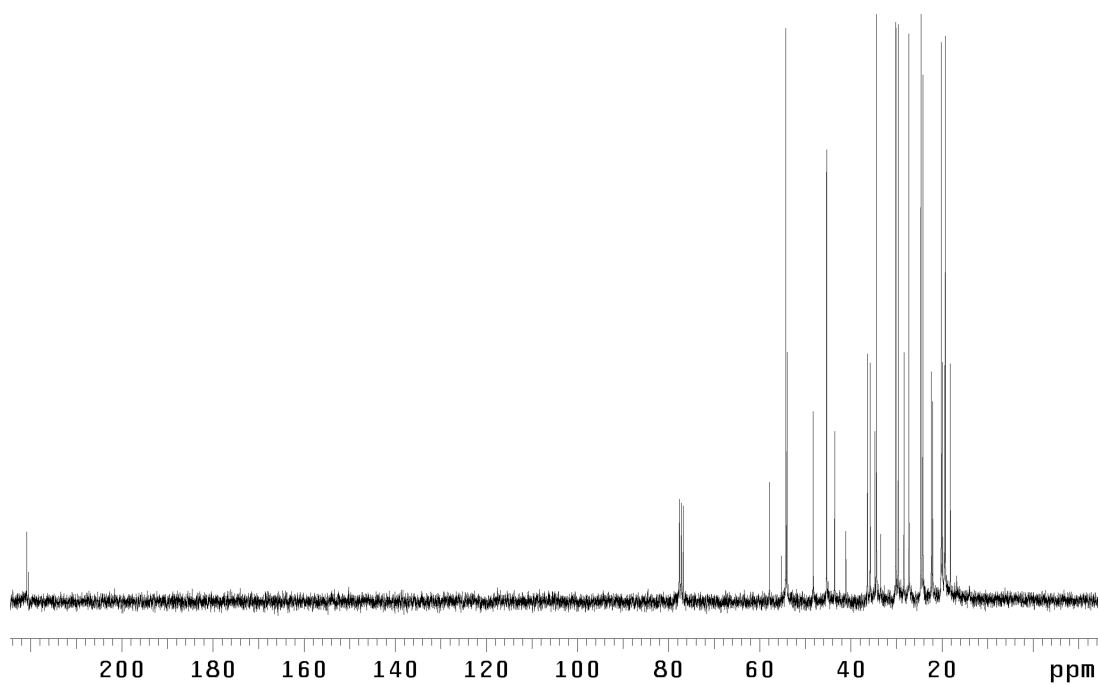


Figure A7.3 ¹³C NMR (75 MHz, CDCl₃) of compounds **307A** and **307B**.

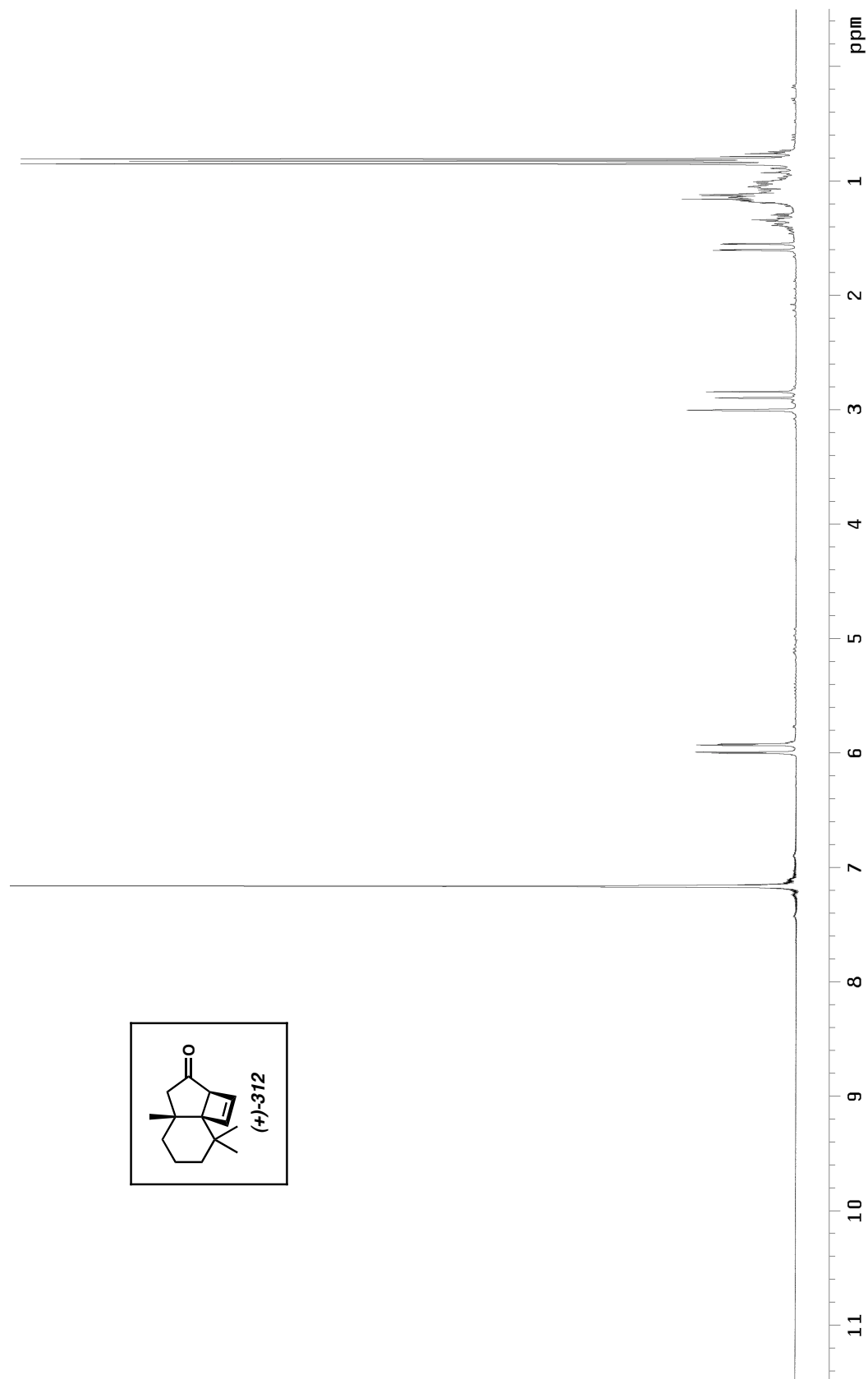


Figure A7.4 ^1H NMR (300 MHz, C_6D_6) of compound **312**.

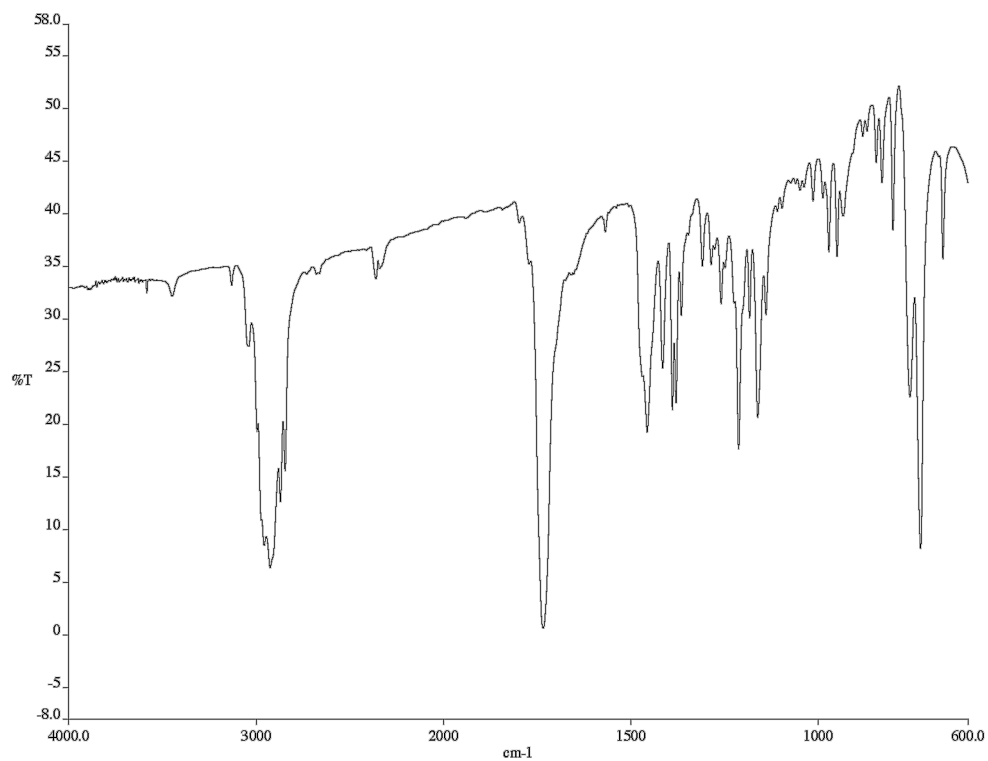


Figure A7.5 Infrared spectrum (NaCl/CHCl₃) of compound **312**.

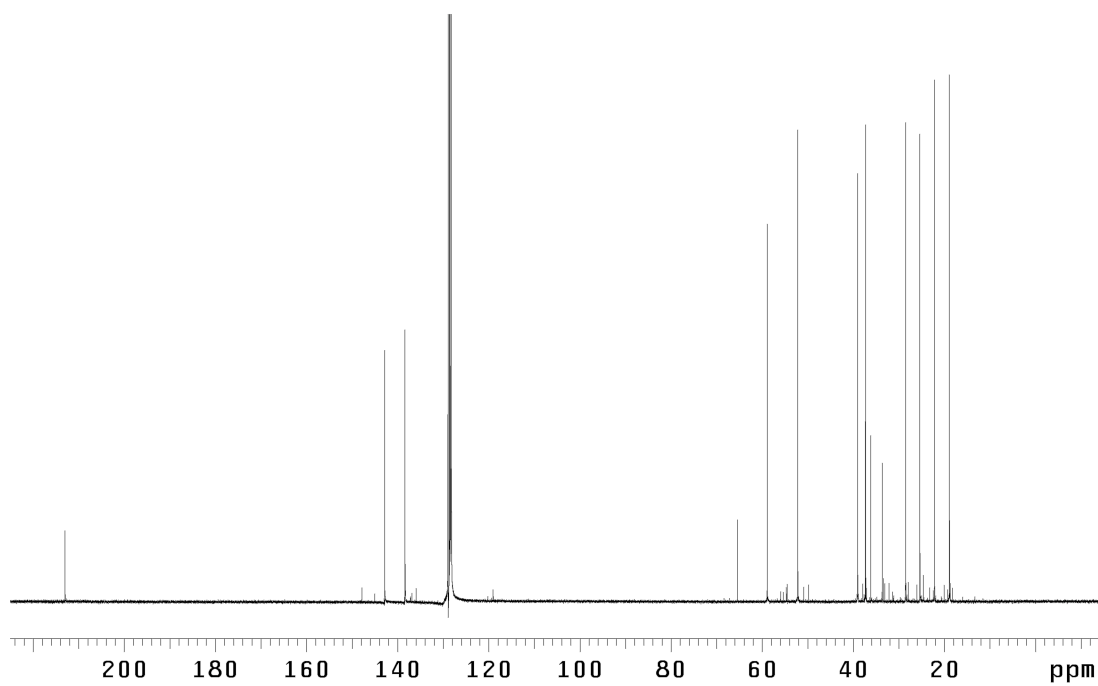


Figure A7.6 ¹³C NMR (125 MHz, C₆D₆) of compound **312**.

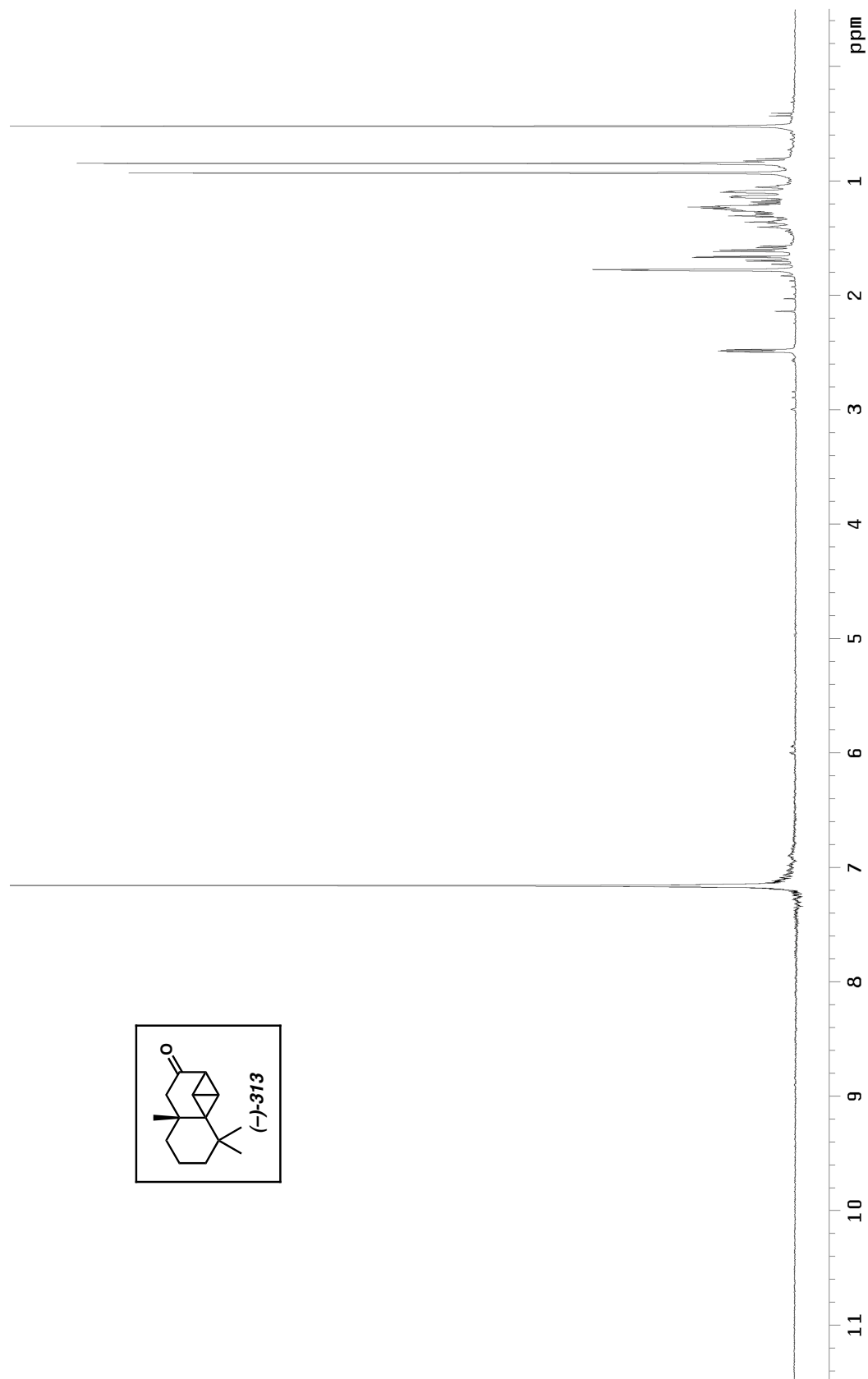


Figure A7.7 ^1H NMR (300 MHz, C_6D_6) of compound **313**.

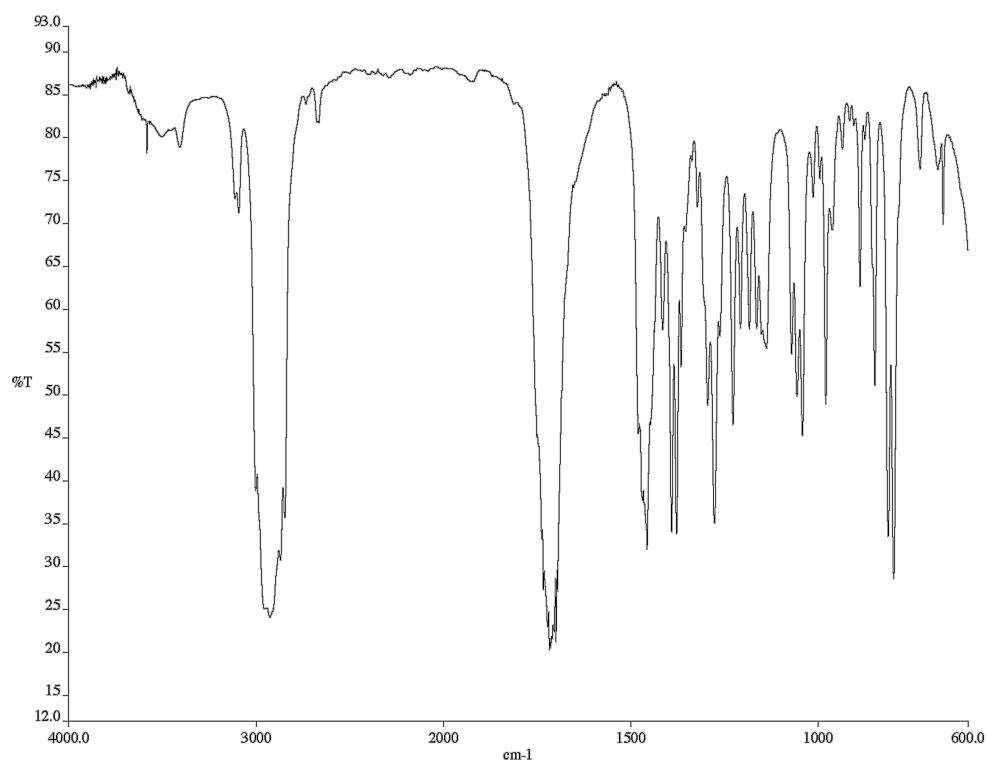


Figure A7.8 Infrared spectrum (NaCl/neat) of compound **313**.

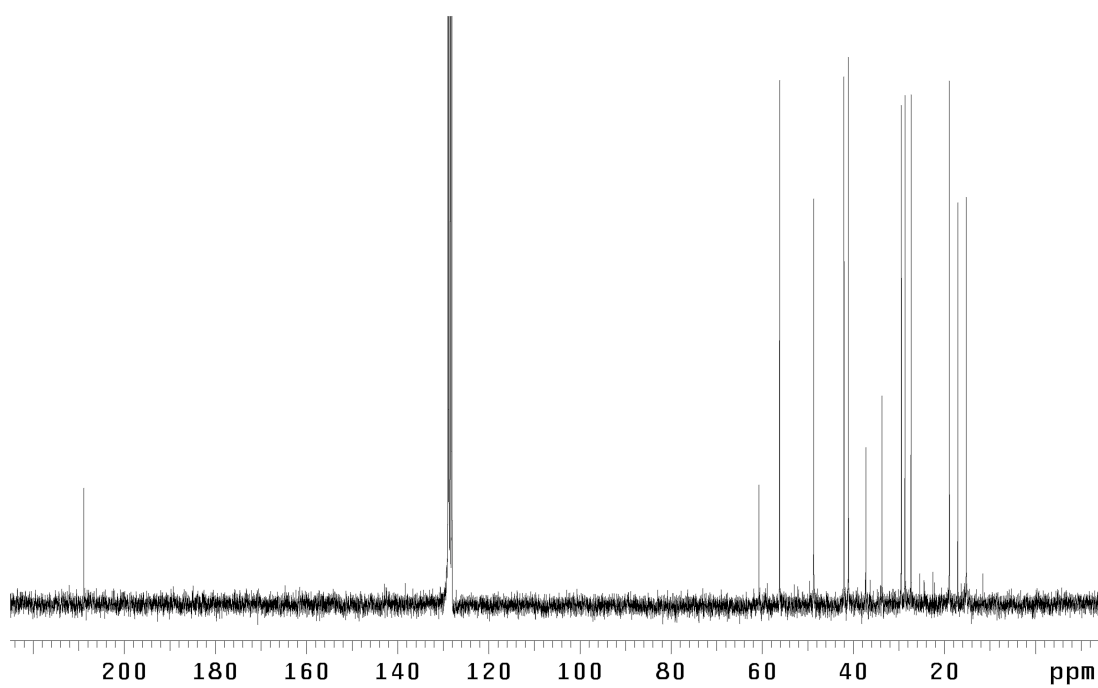


Figure A7.9 ¹³C NMR (75 MHz, C₆D₆) of compound **313**.



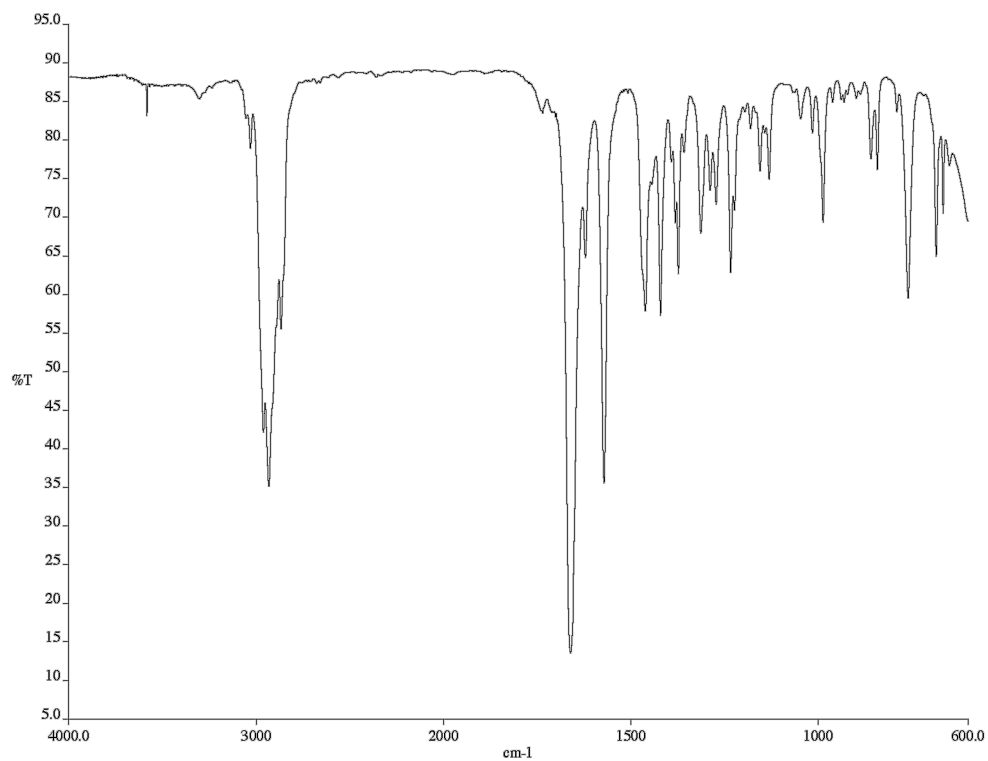


Figure A7.11 Infrared spectrum (NaCl/CDCl₃) of compound **318**.

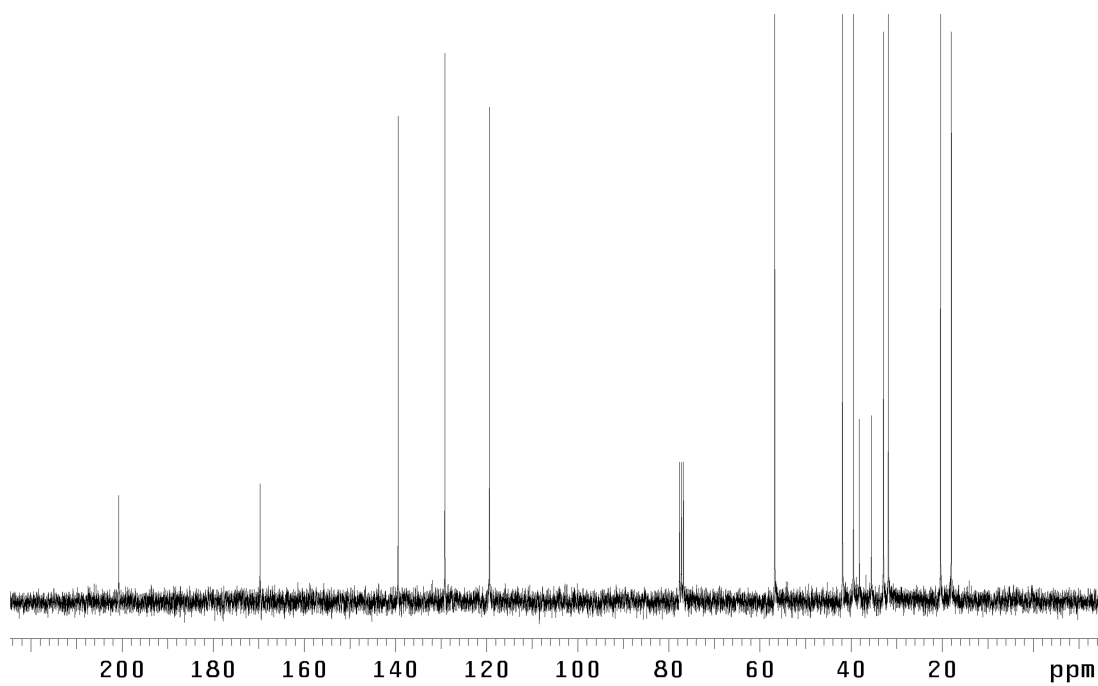


Figure A7.12 ¹³C NMR (75 MHz, CDCl₃) of compound **318**.

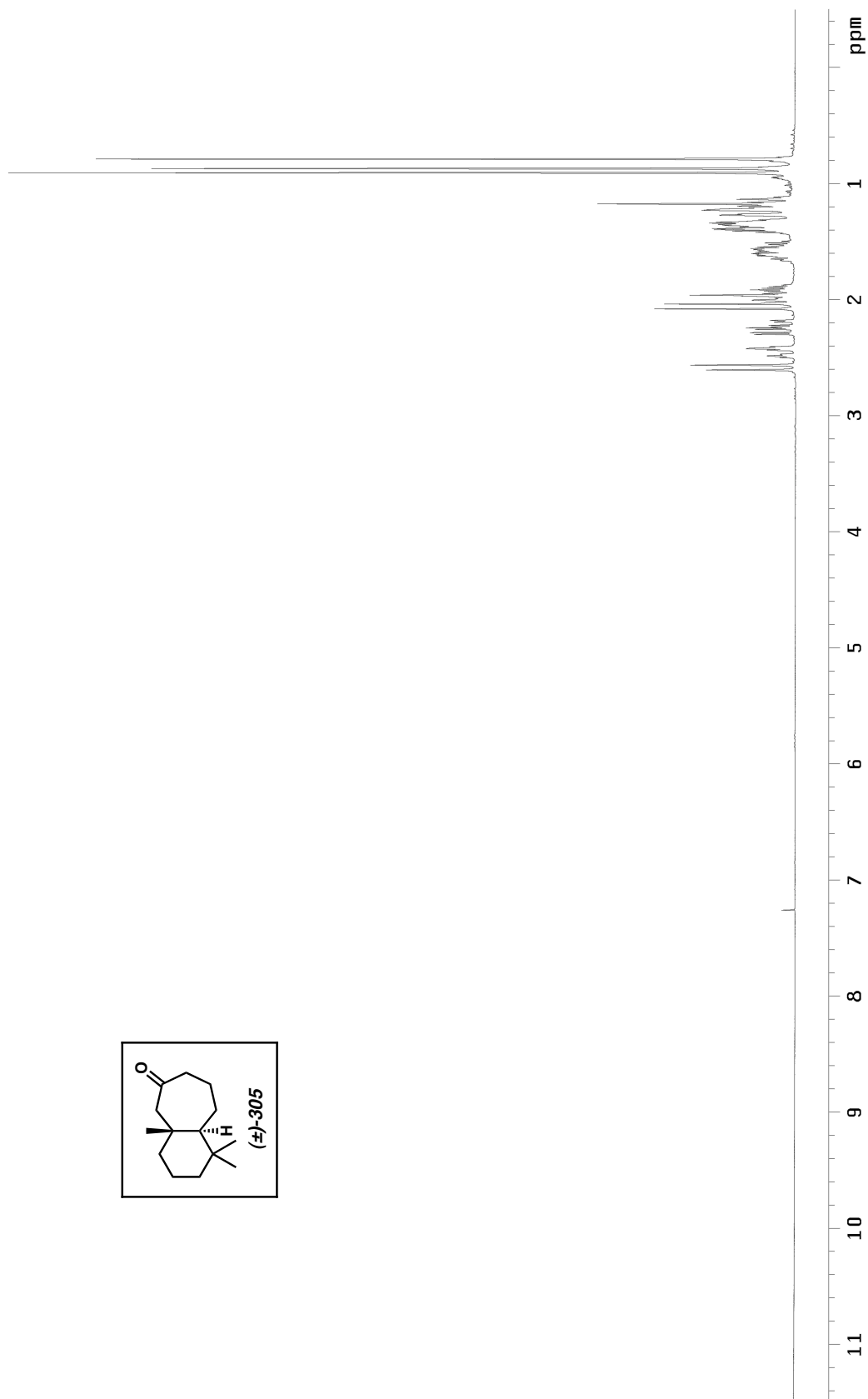
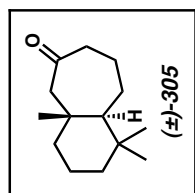


Figure A7.13 ¹H NMR (300 MHz, CDCl₃) of compound **305**.

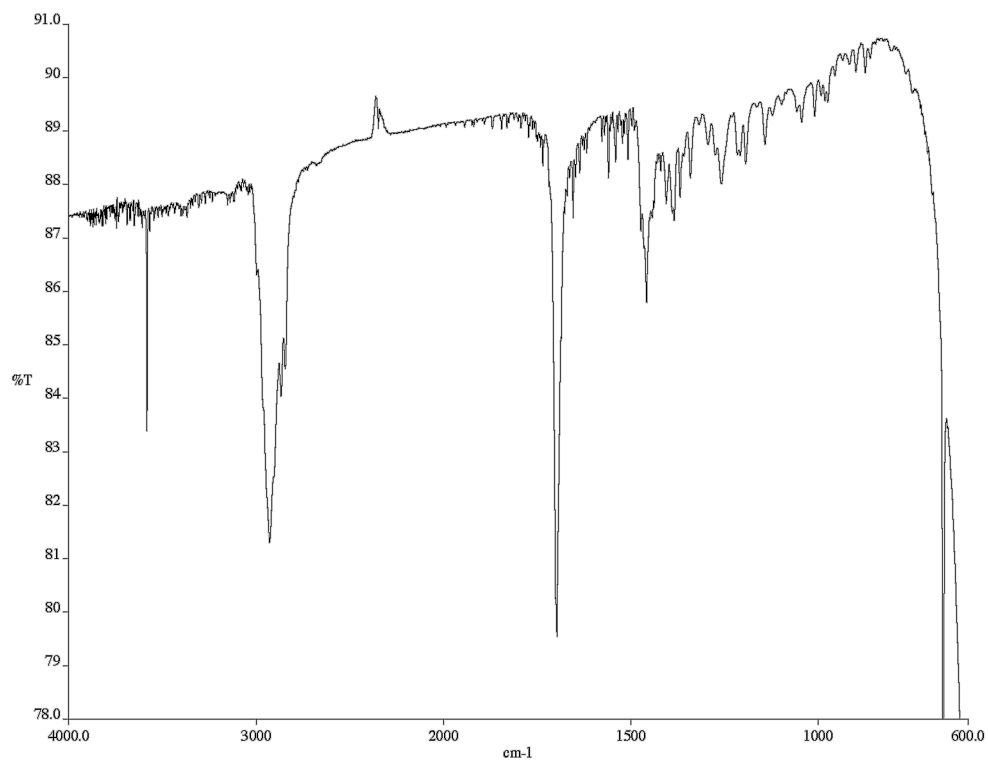


Figure A7.14 Infrared spectrum (NaCl/CDCl₃) of compound **305**.

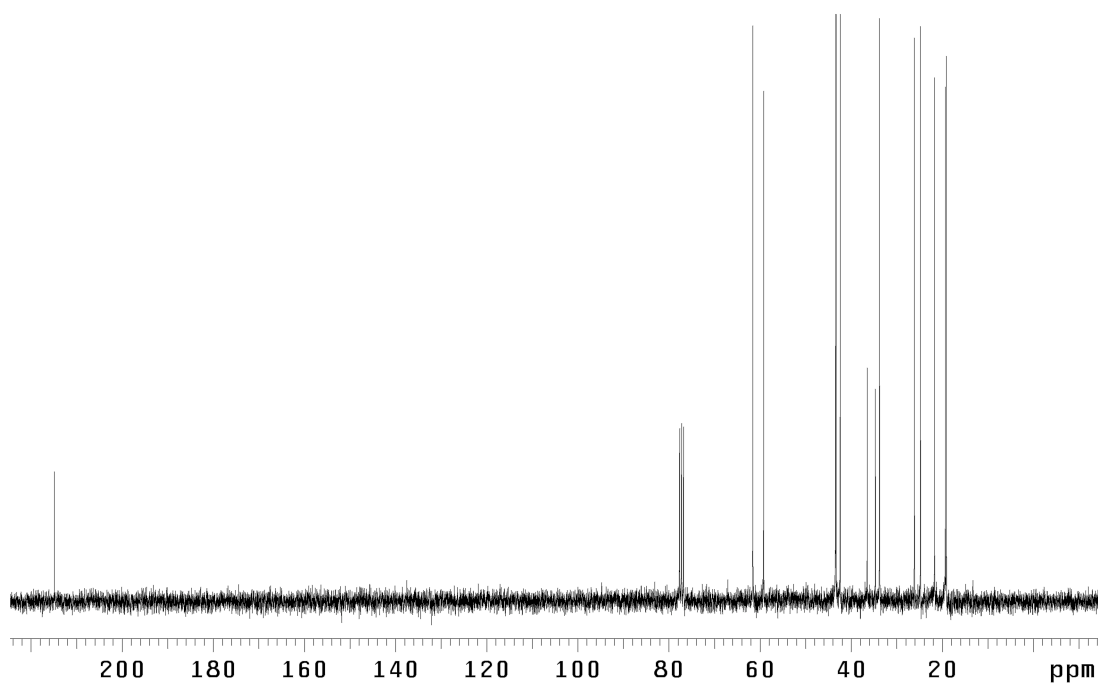


Figure A7.15 ¹³C NMR (75 MHz, CDCl₃) of compound **305**.

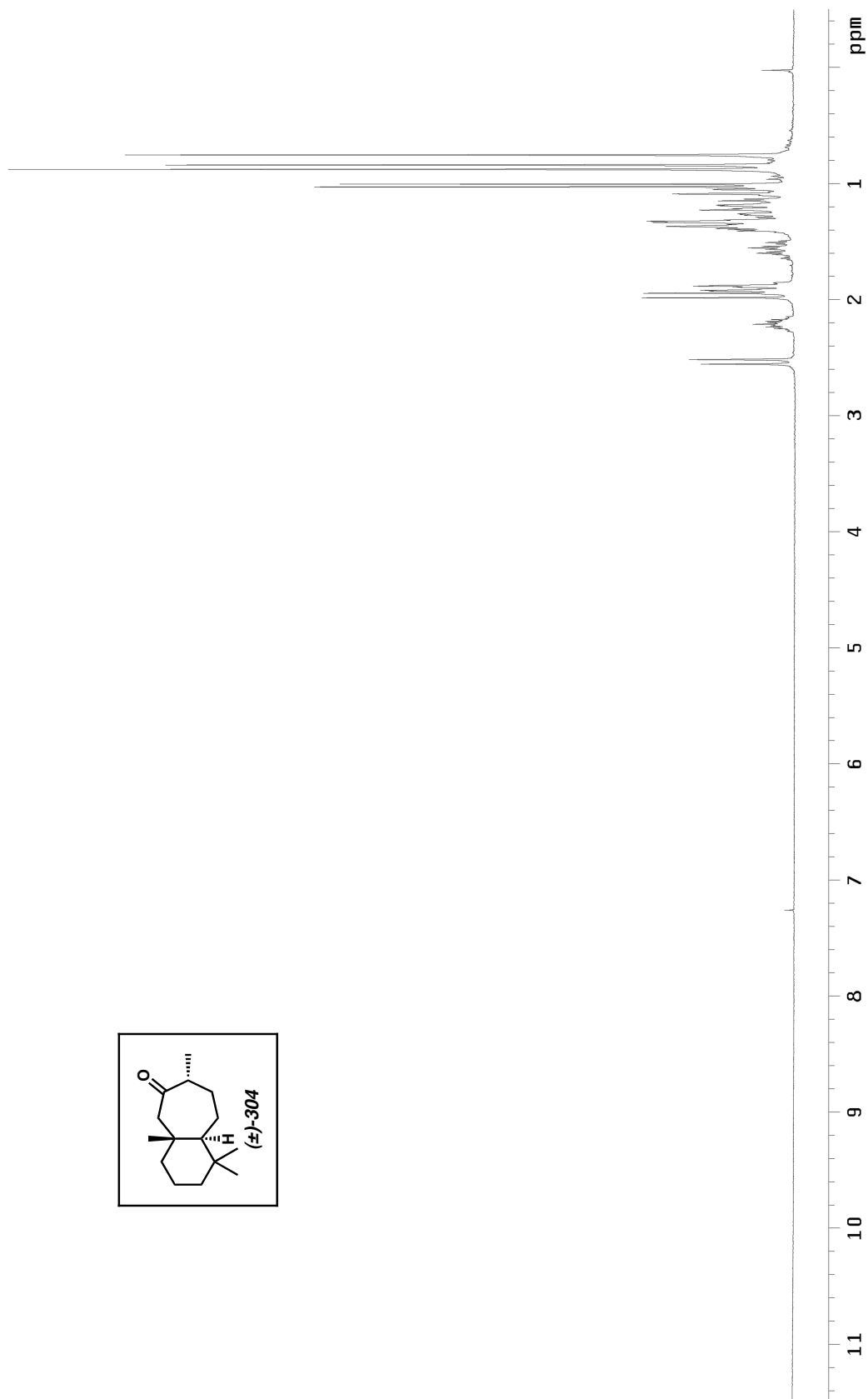
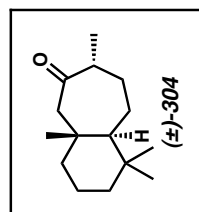


Figure A7.16 ¹H NMR (300 MHz, CDCl₃) of compound **304**.

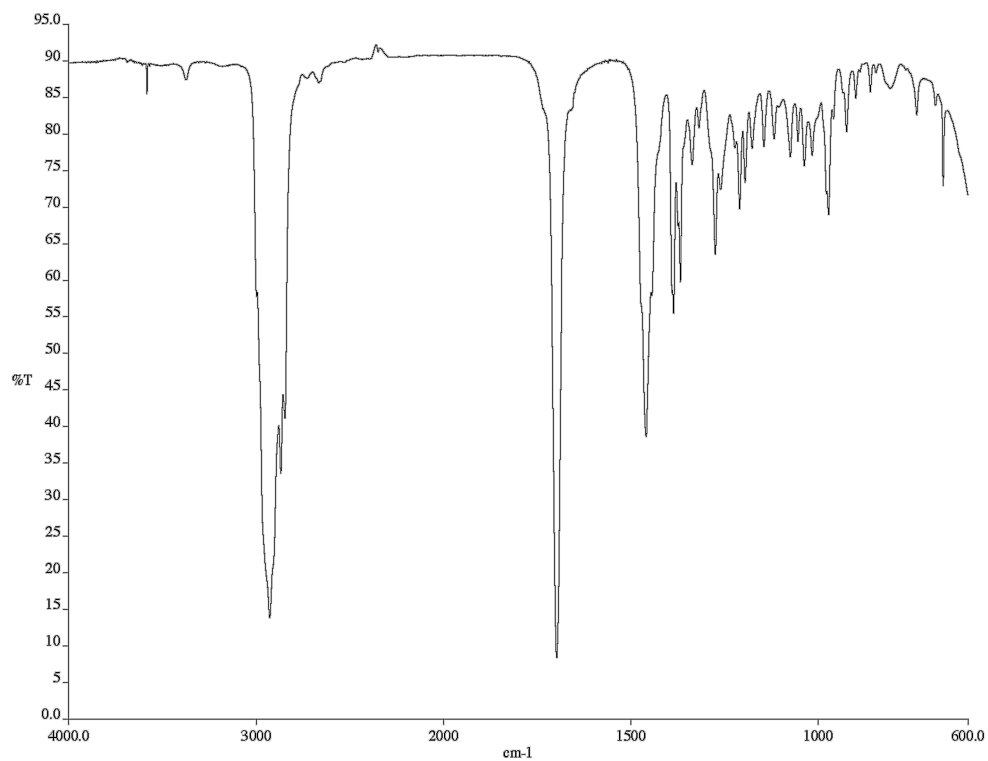


Figure A7.17 Infrared spectrum (NaCl/CDCl₃) of compound **304**.

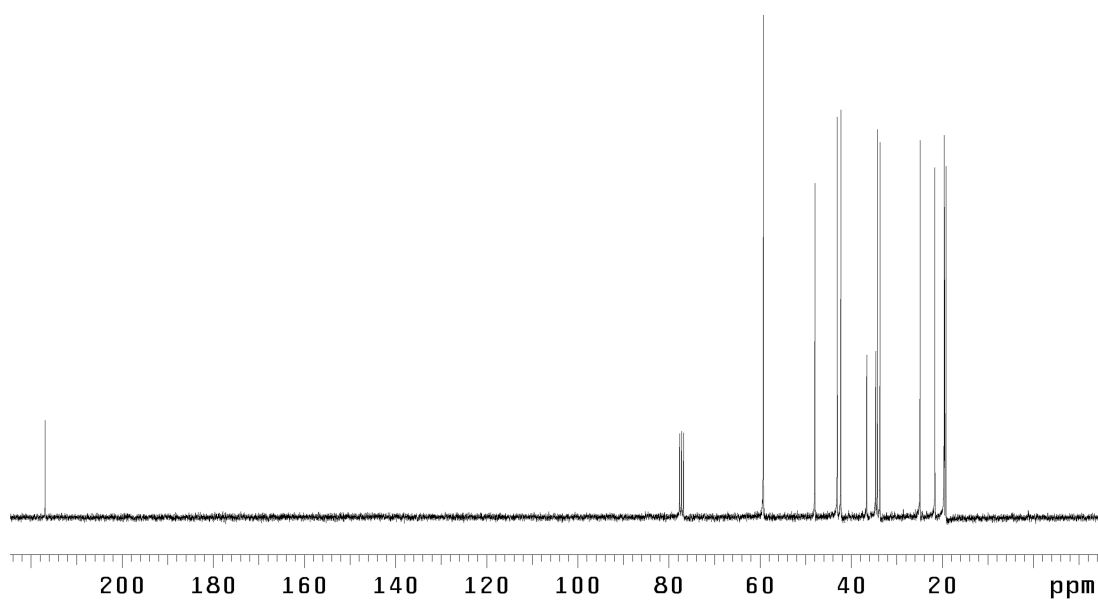


Figure A7.18 ¹³C NMR (75 MHz, CDCl₃) of compound **304**.

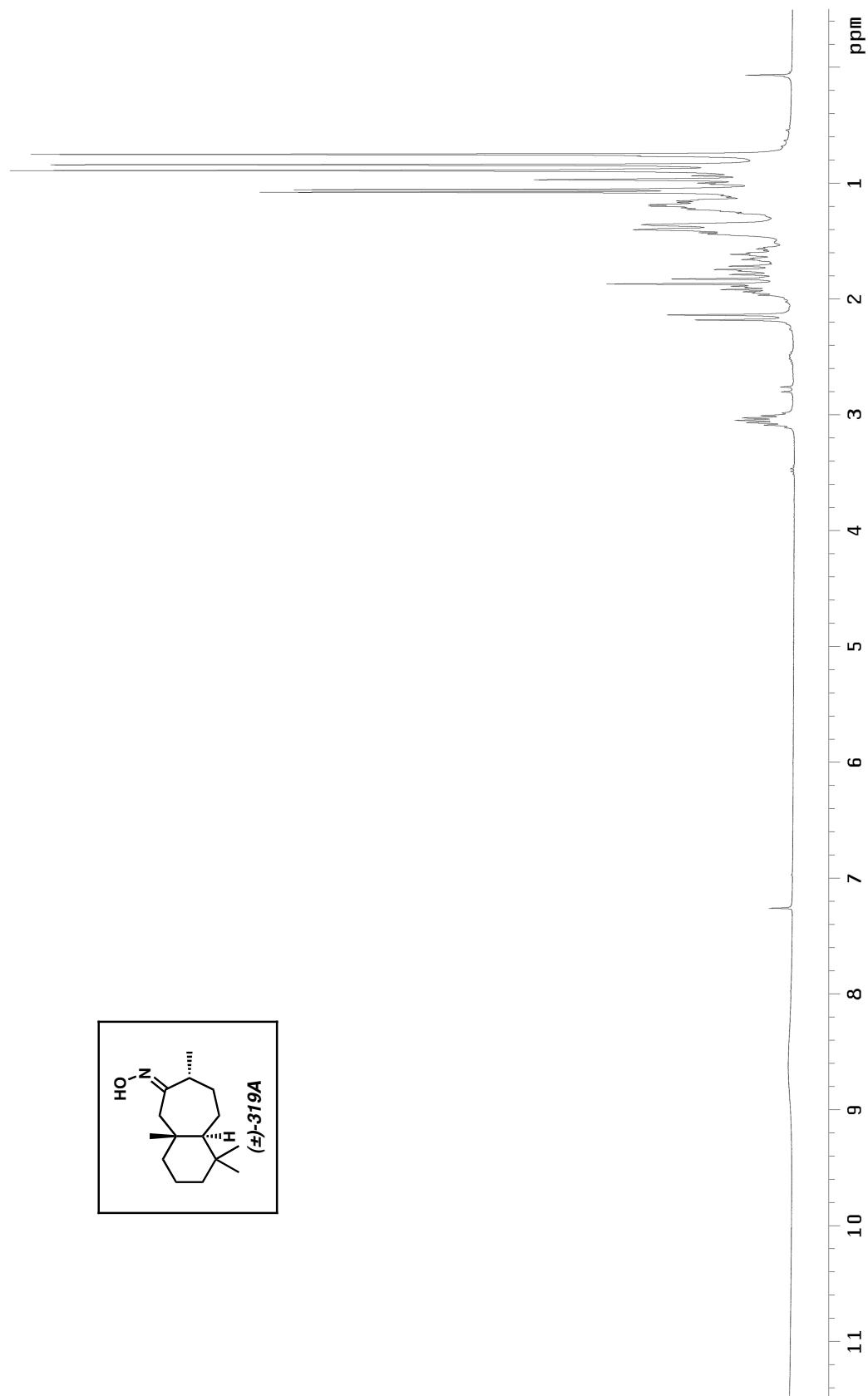


Figure A7.19 ^1H NMR (300 MHz, CDCl_3) of compounds **319A**.

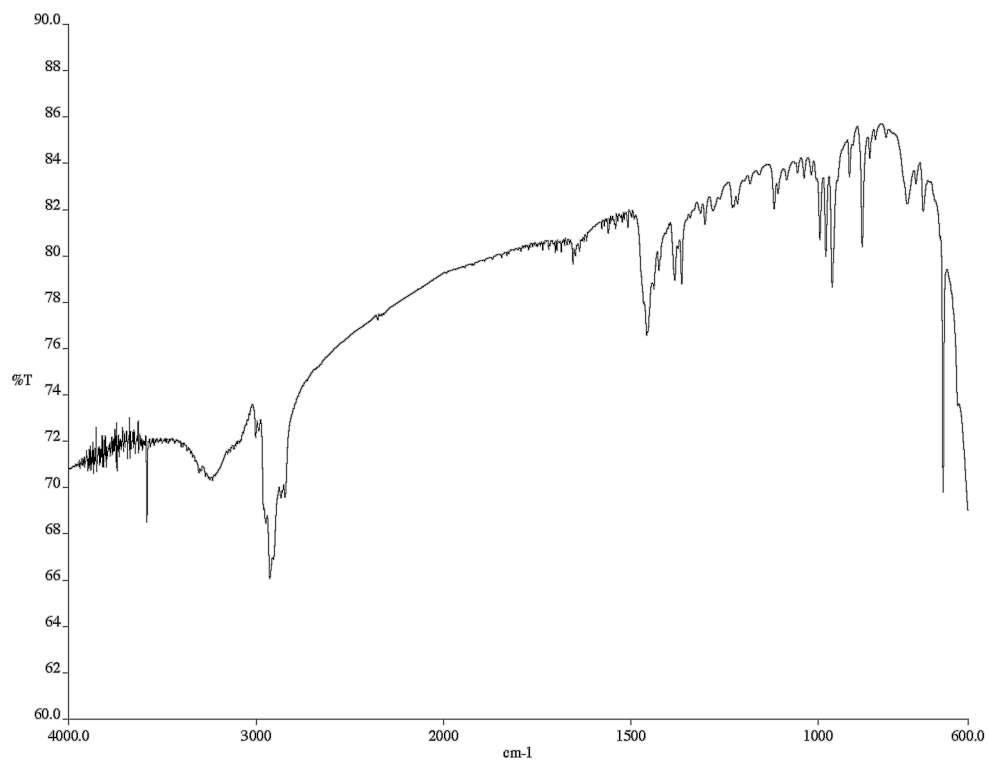


Figure A7.20 Infrared spectrum (NaCl/CDCl₃) of compounds **319A**.

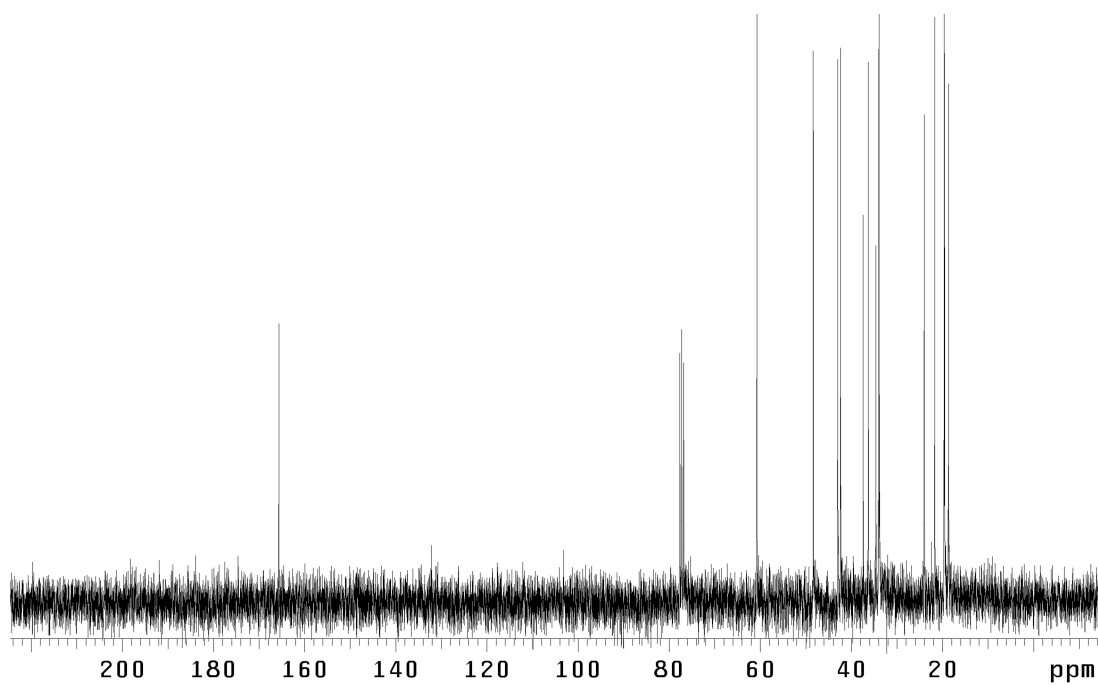


Figure A7.21 ¹³C NMR (75 MHz, CDCl₃) of compound **319A**.

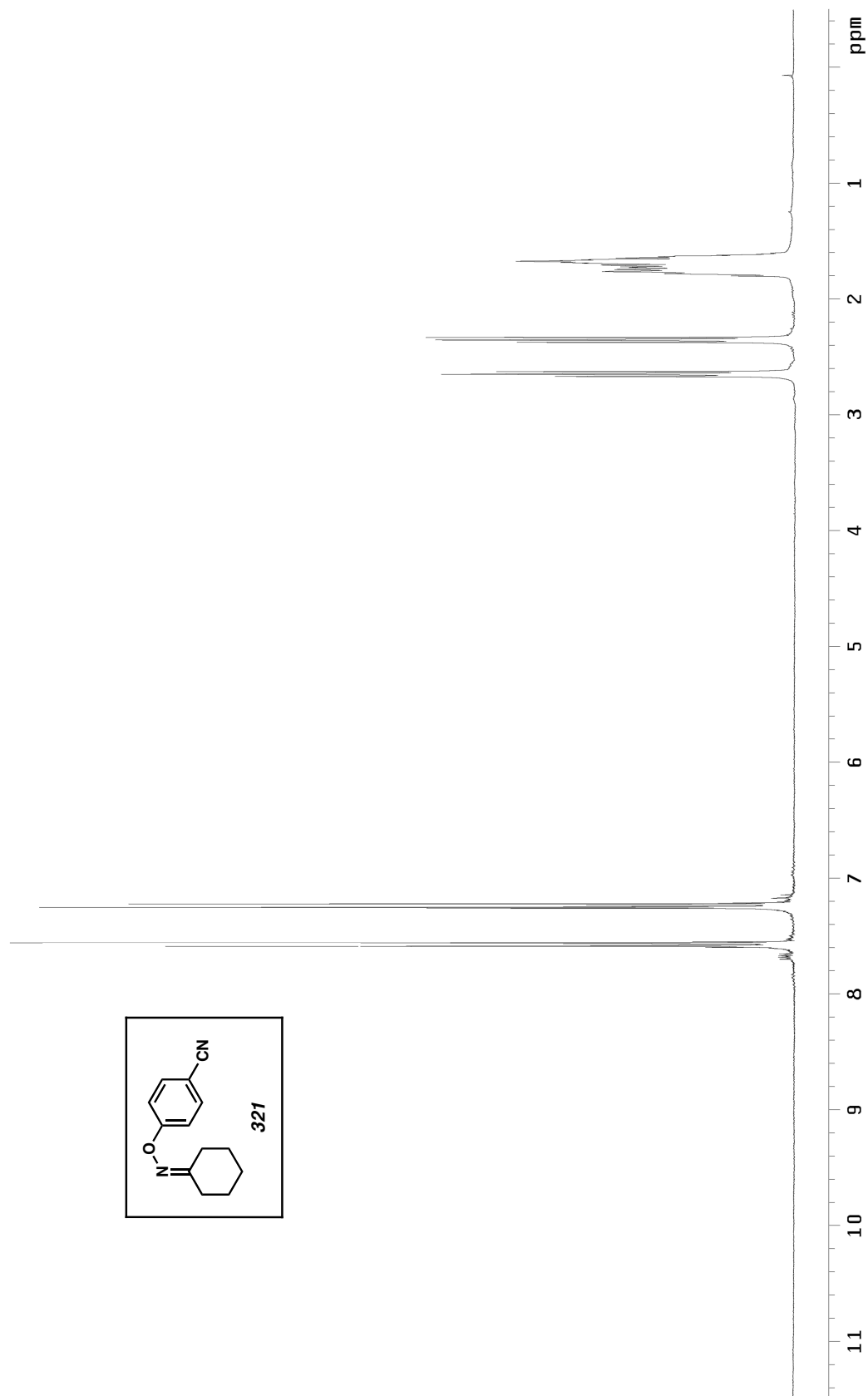


Figure A7.22 ^1H NMR (300 MHz, CDCl_3) of compound **321**.

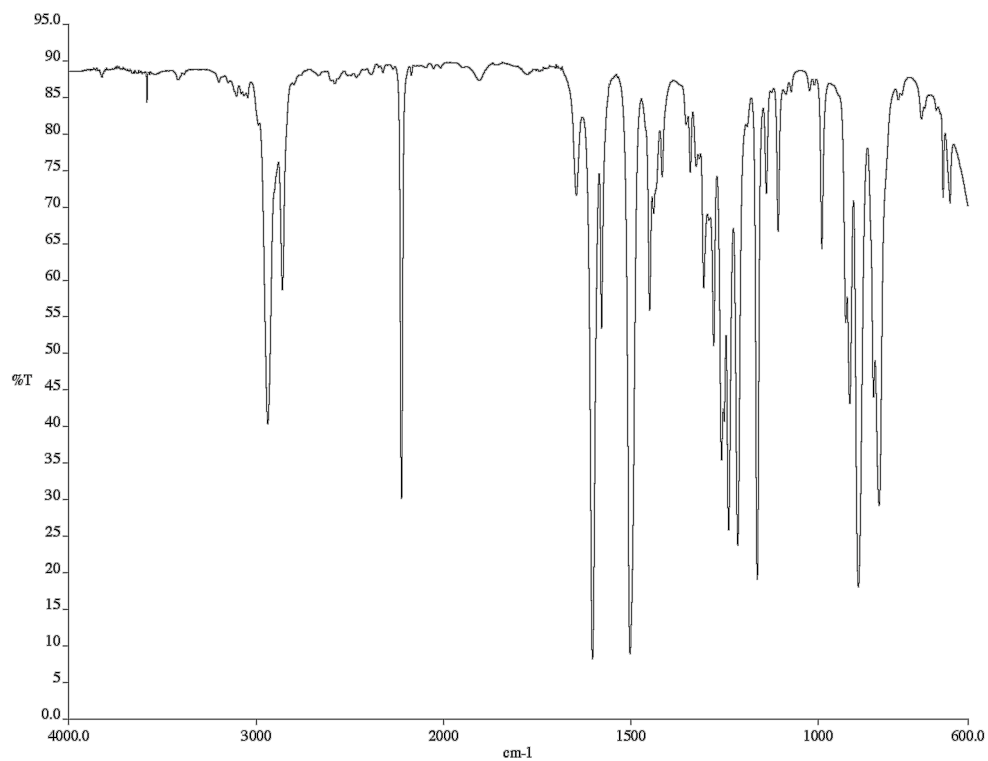


Figure A7.23 Infrared spectrum (NaCl/CDCl₃) of compound **321**.

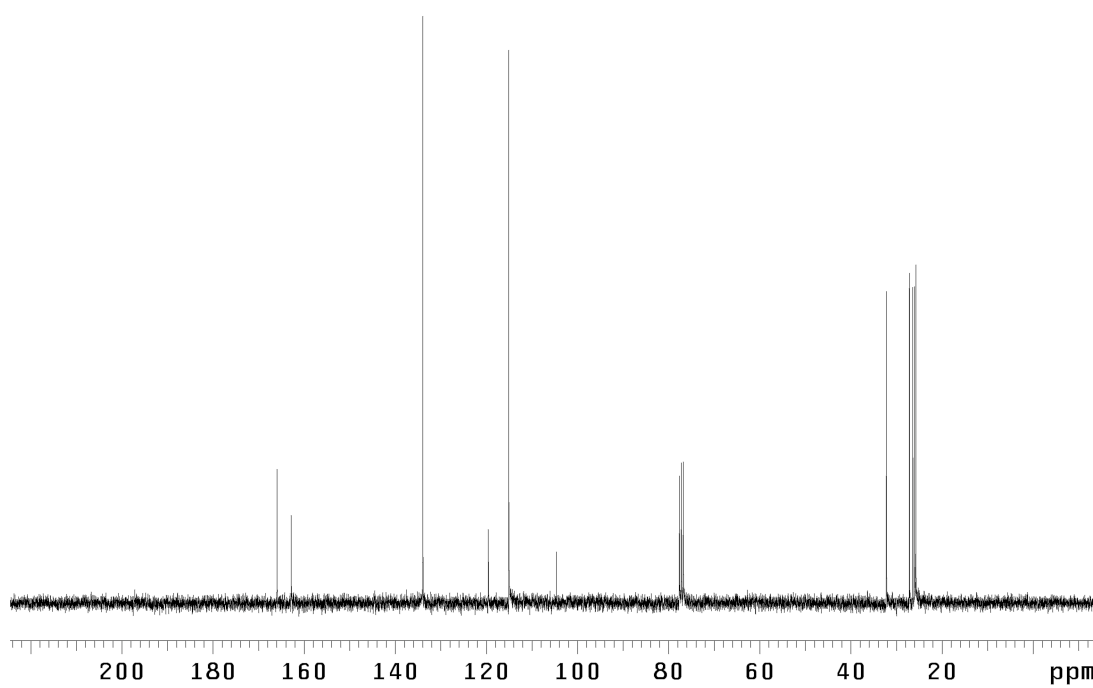


Figure A7.24 ¹³C NMR (75 MHz, CDCl₃) of compound **321**.

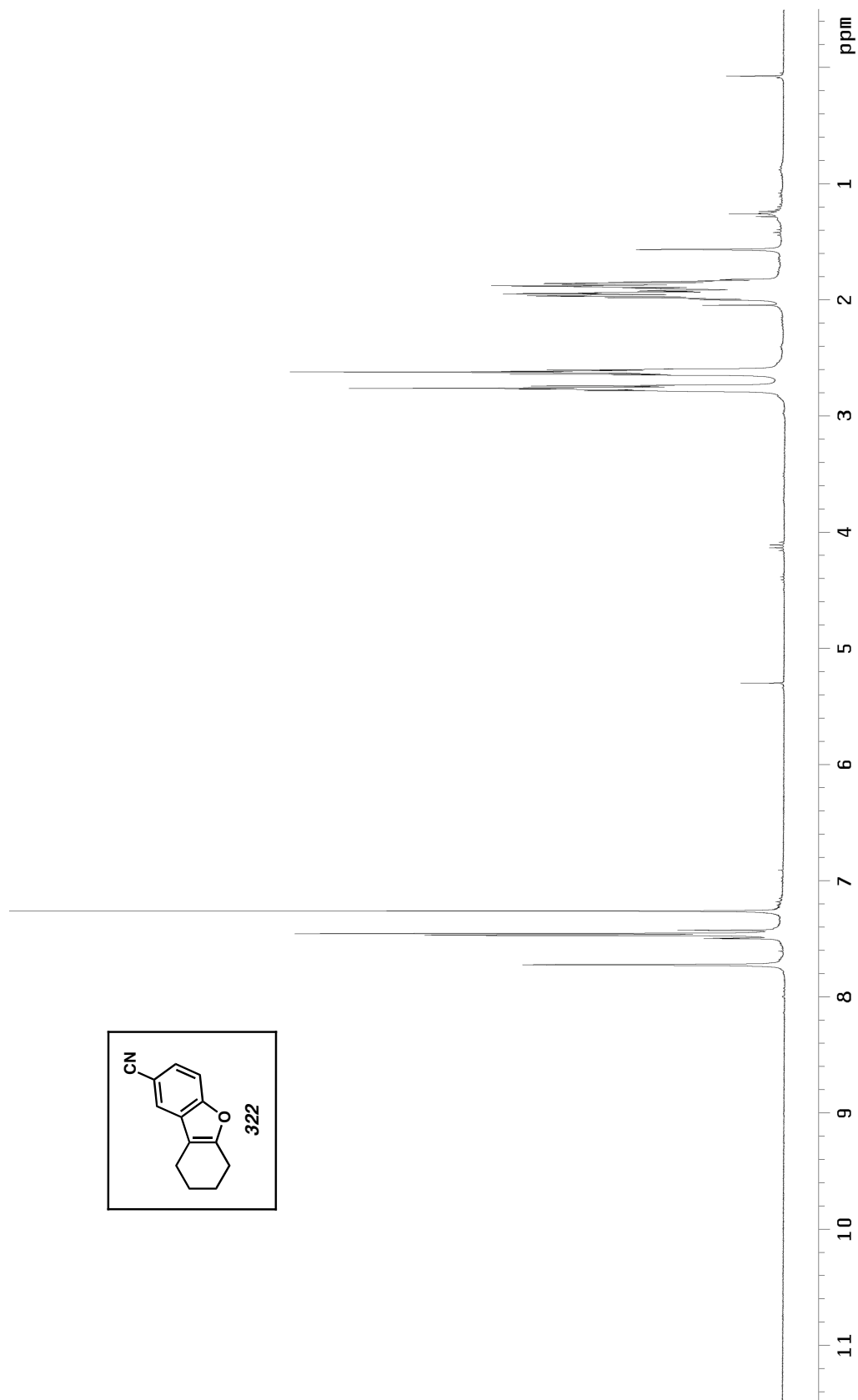


Figure A7.25 ^1H NMR (300 MHz, CDCl_3) of compound **322**.

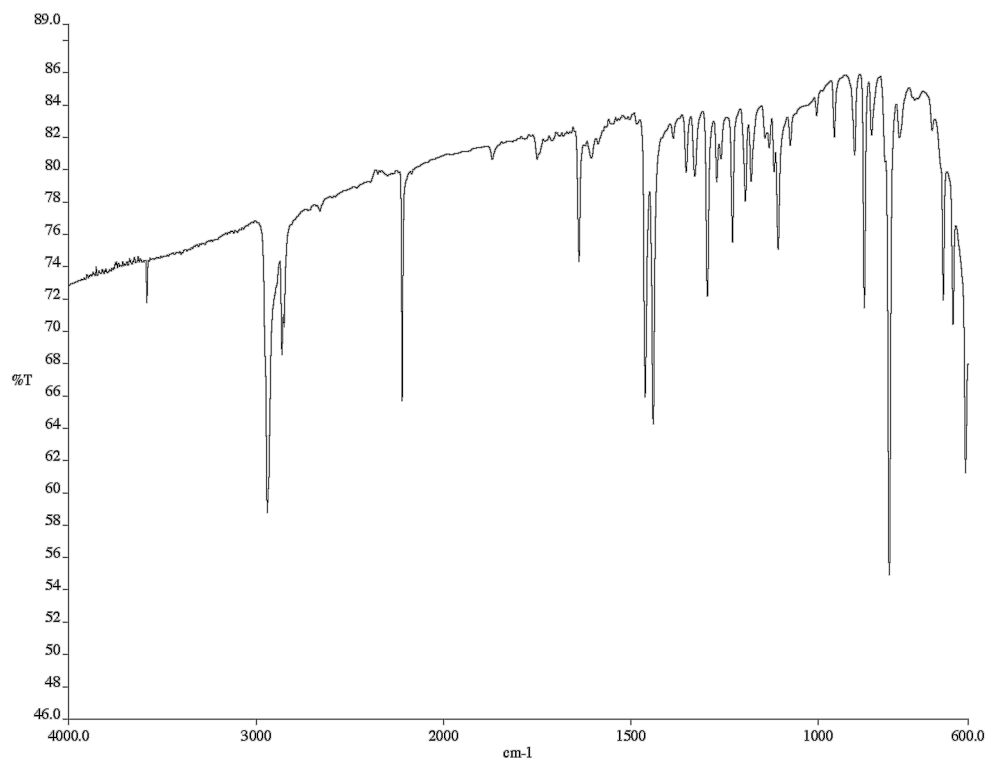


Figure A7.26 Infrared spectrum (NaCl/CDCl₃) of compound **322**.

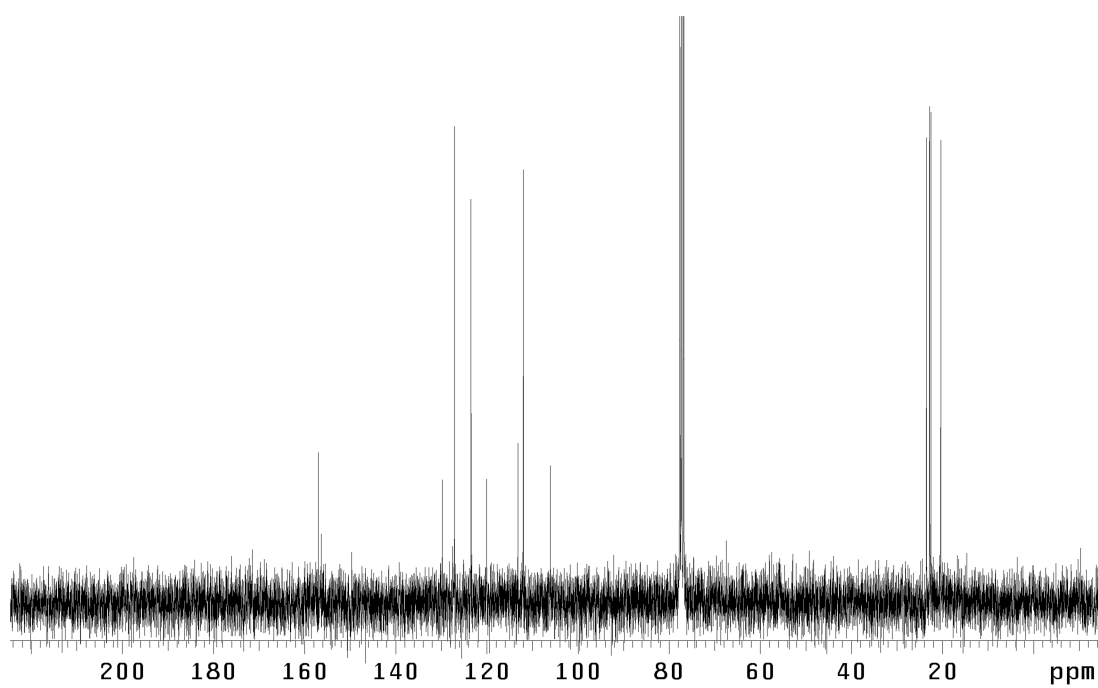


Figure A7.27 ¹³C NMR (75 MHz, CDCl₃) of compound **322**.

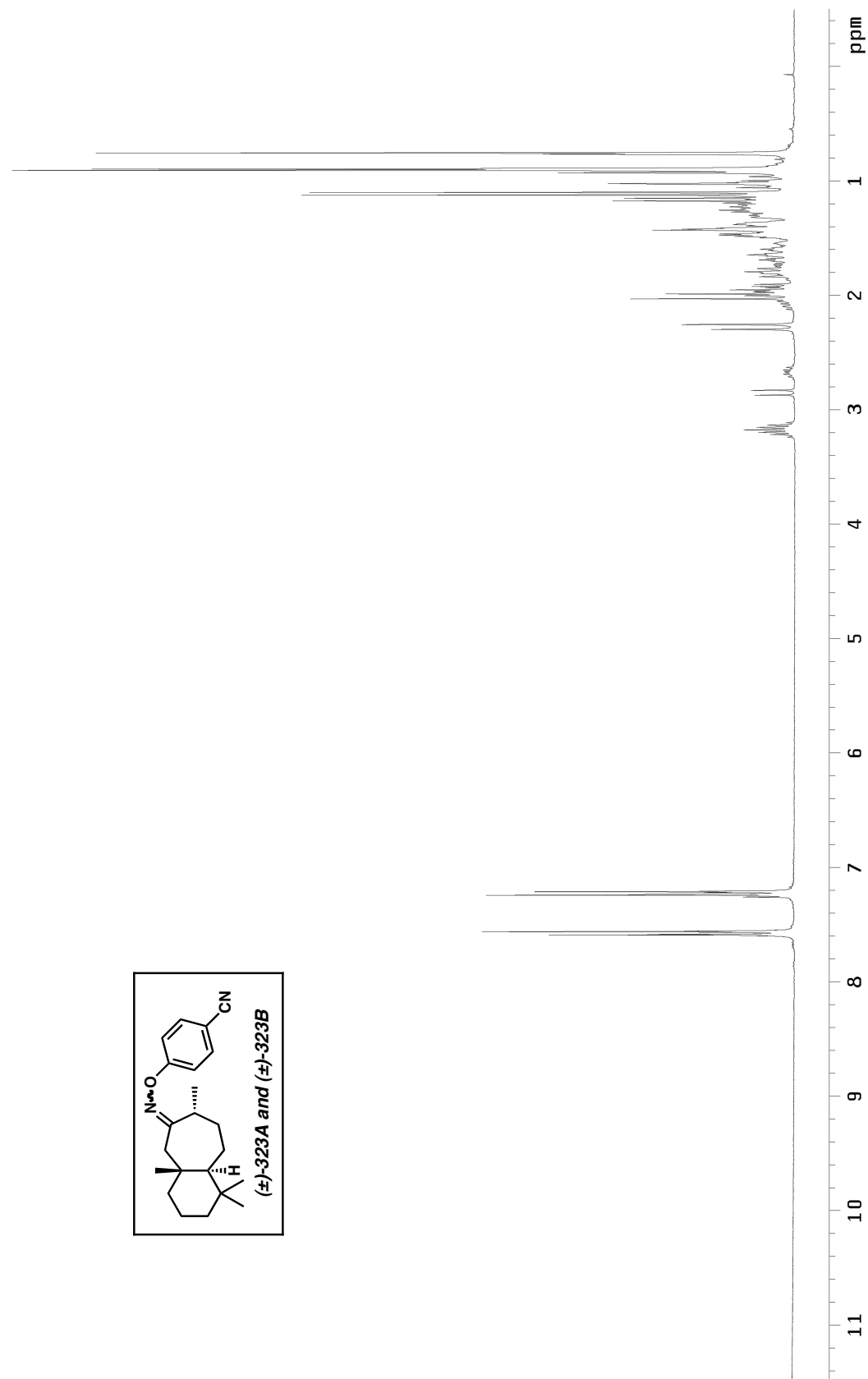


Figure A7.28 ^1H NMR (300 MHz, CDCl_3) of compound **323A** and **323B**.

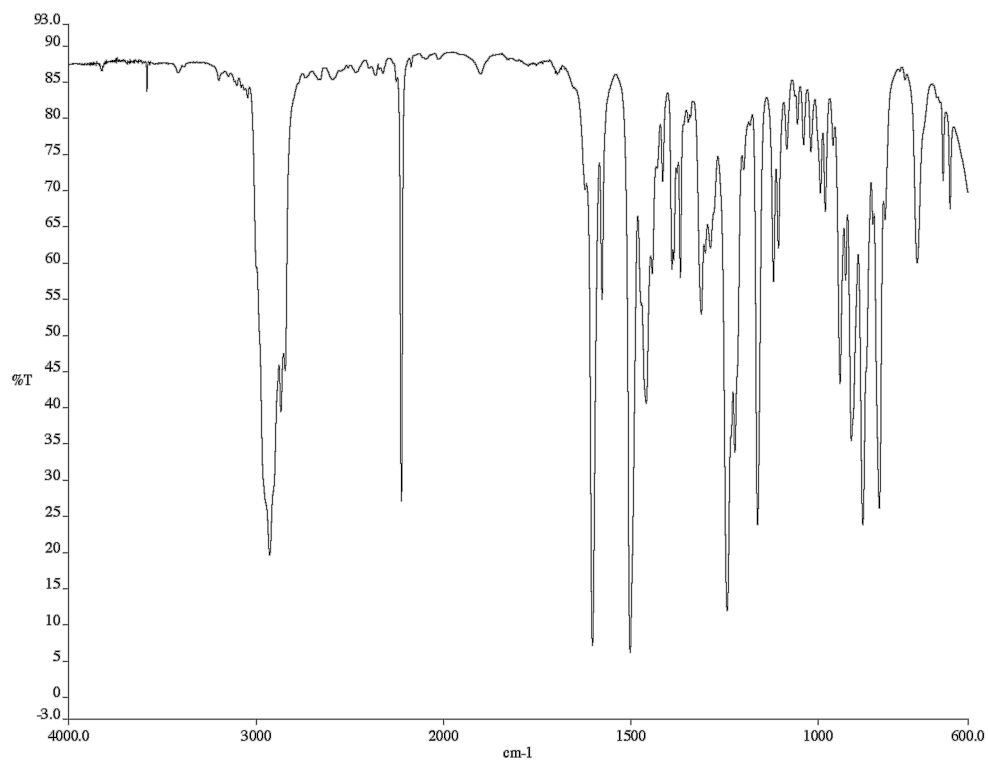


Figure A7.29 Infrared spectrum (NaCl/CDCl₃) of compound **323A** and **323B**.

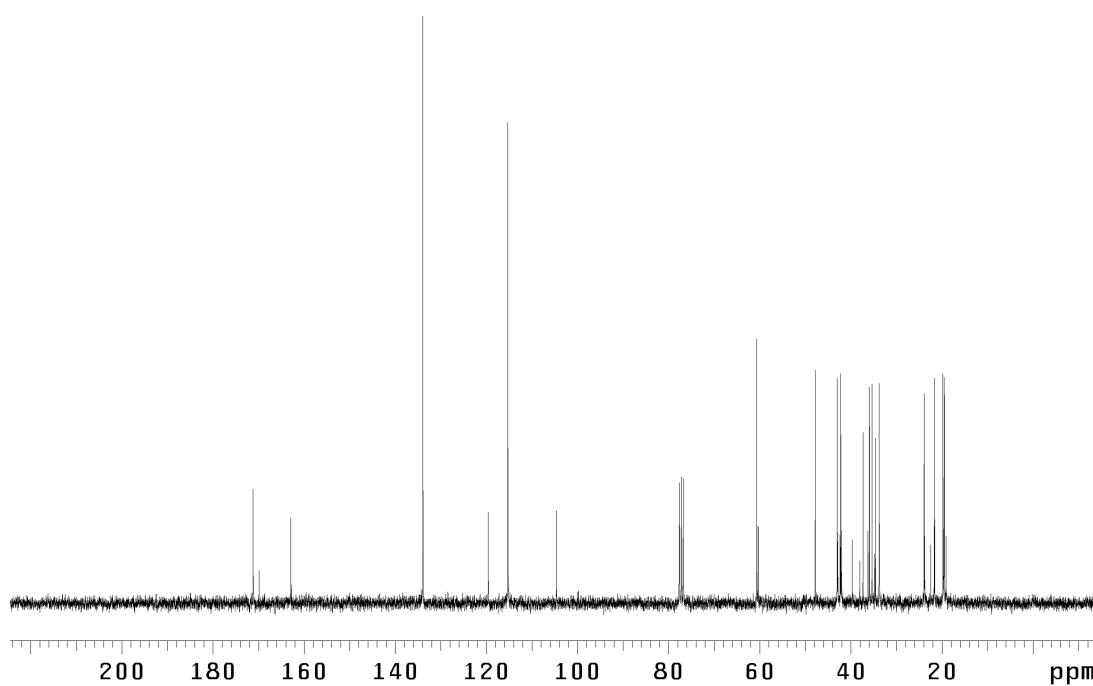


Figure A7.30 ¹³C NMR (75 MHz, CDCl₃) of compound **323A** and **323B**.

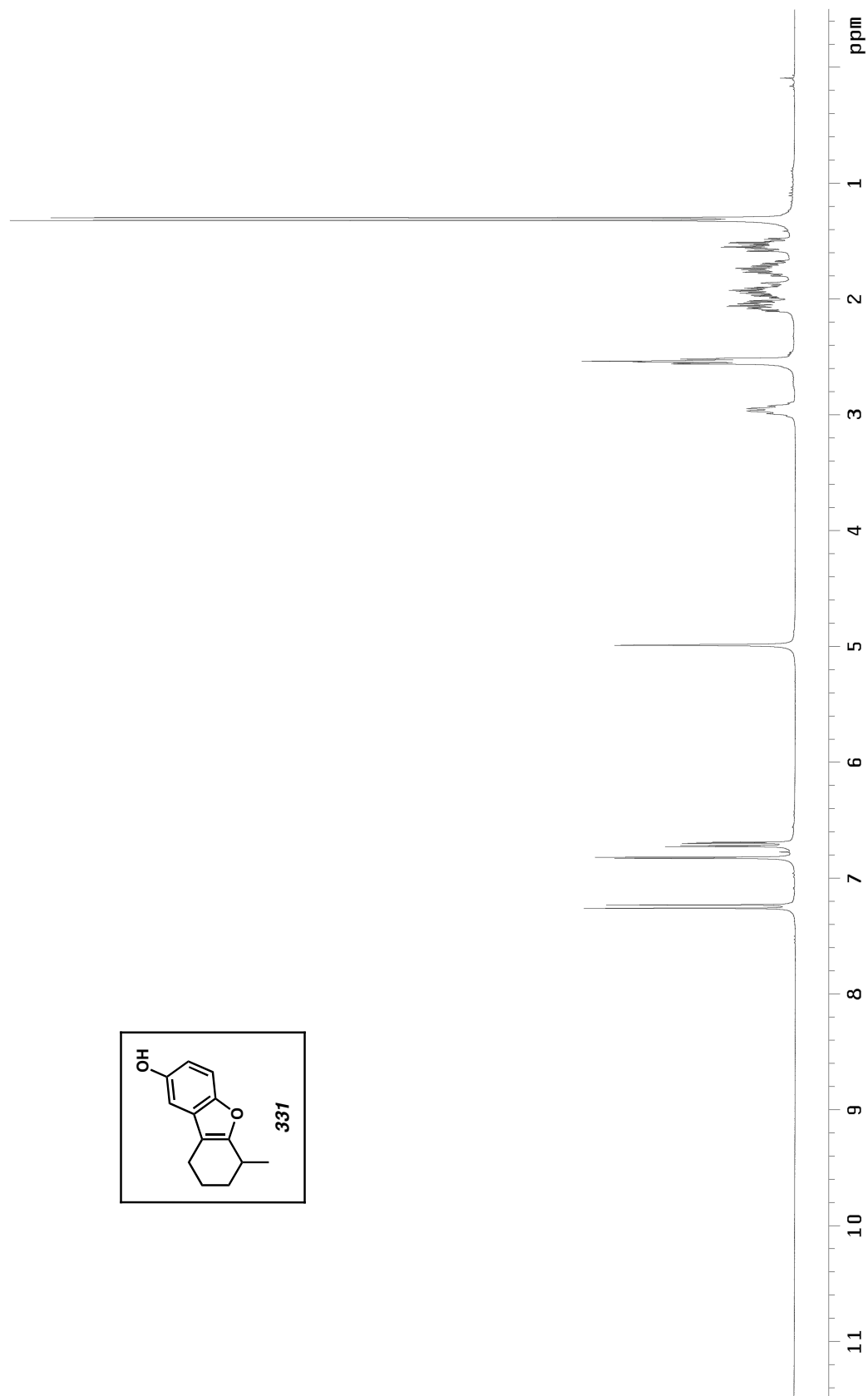


Figure A7.31 ^1H NMR (300 MHz, CDCl_3) of compound **331**.

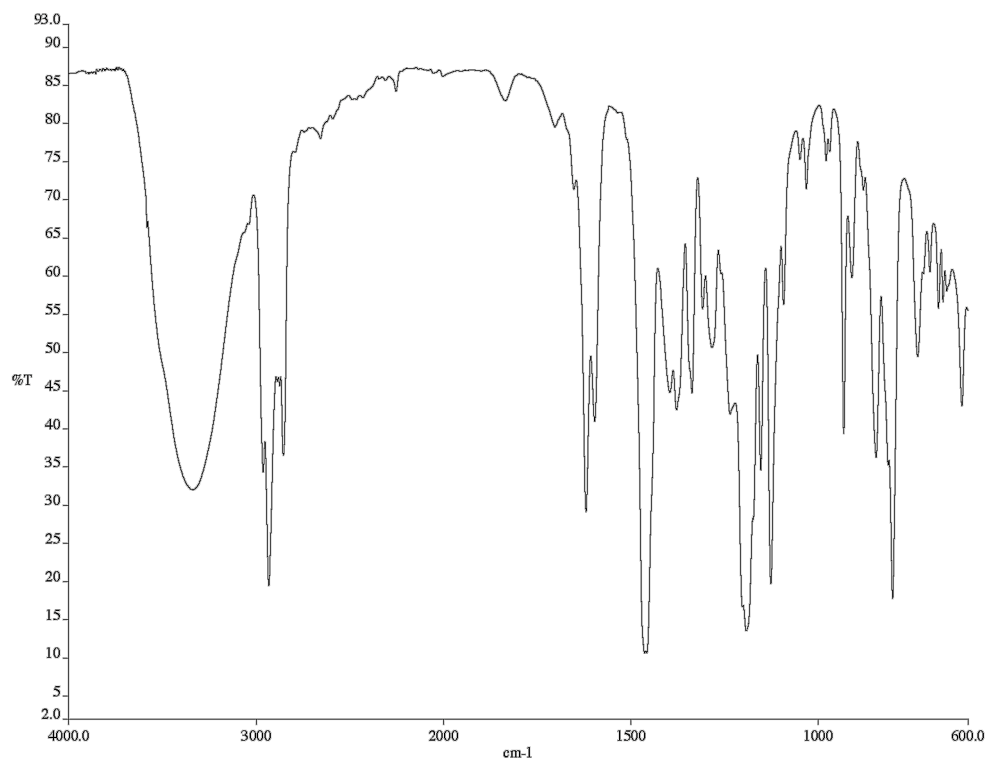


Figure A7.32 Infrared spectrum ($\text{NaCl}/\text{CDCl}_3$) of compound **331**.

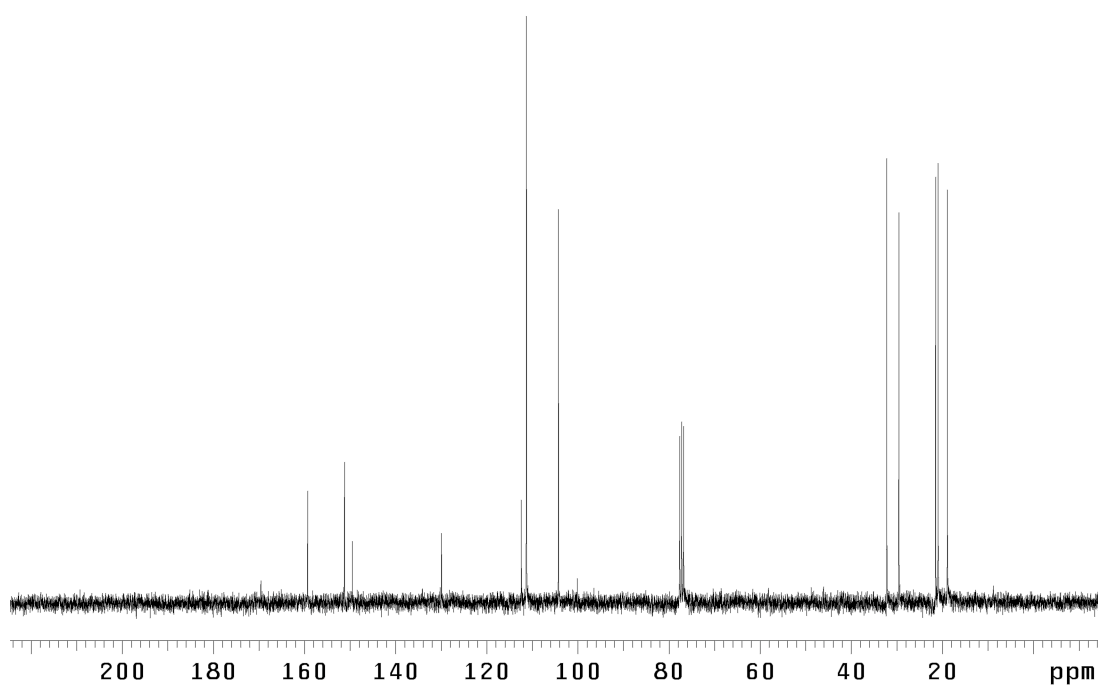


Figure A7.33 ^{13}C NMR (75 MHz, CDCl_3) of compound **331**.

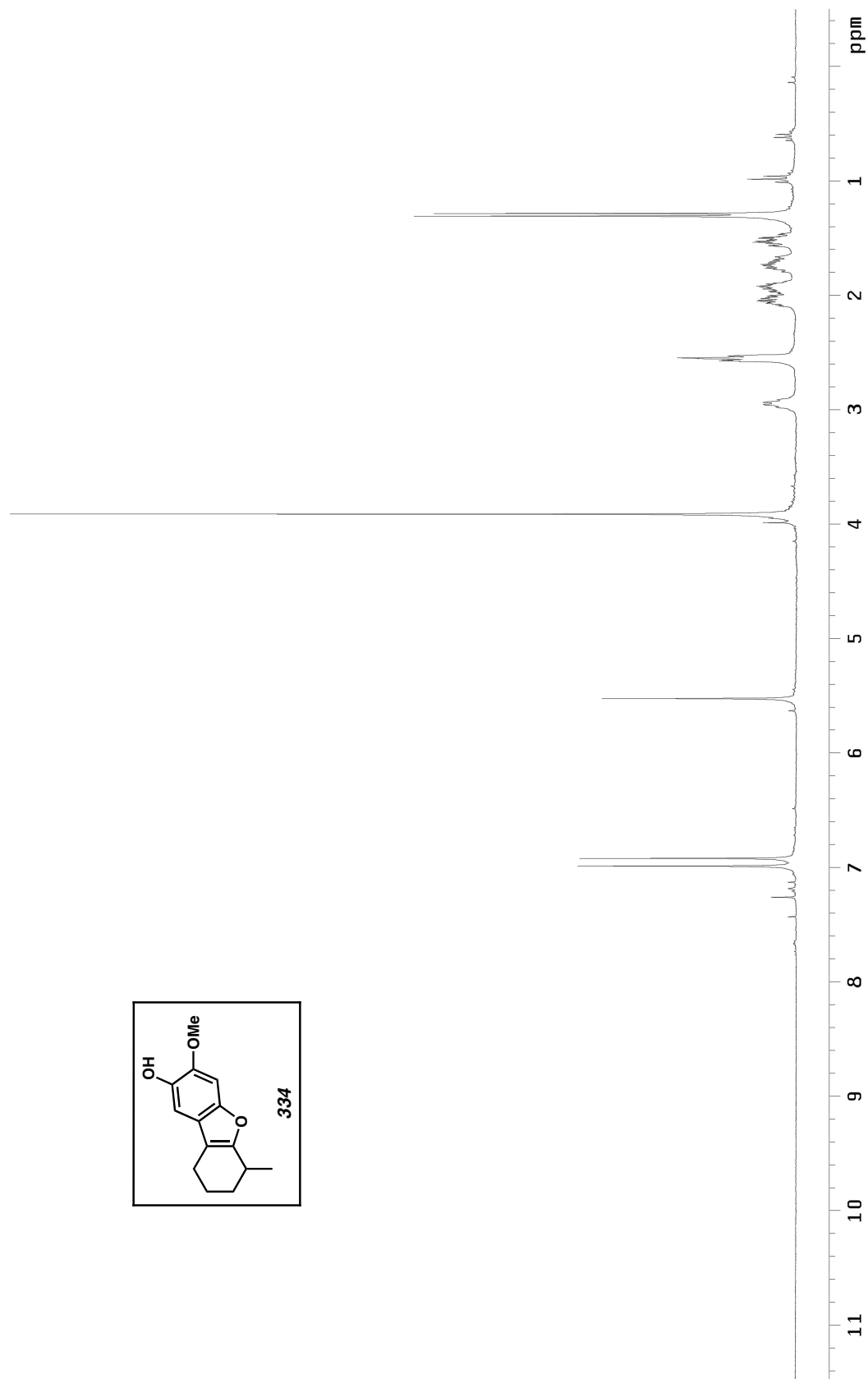


Figure A7.34 ^1H NMR (300 MHz, CDCl_3) of compound 334.

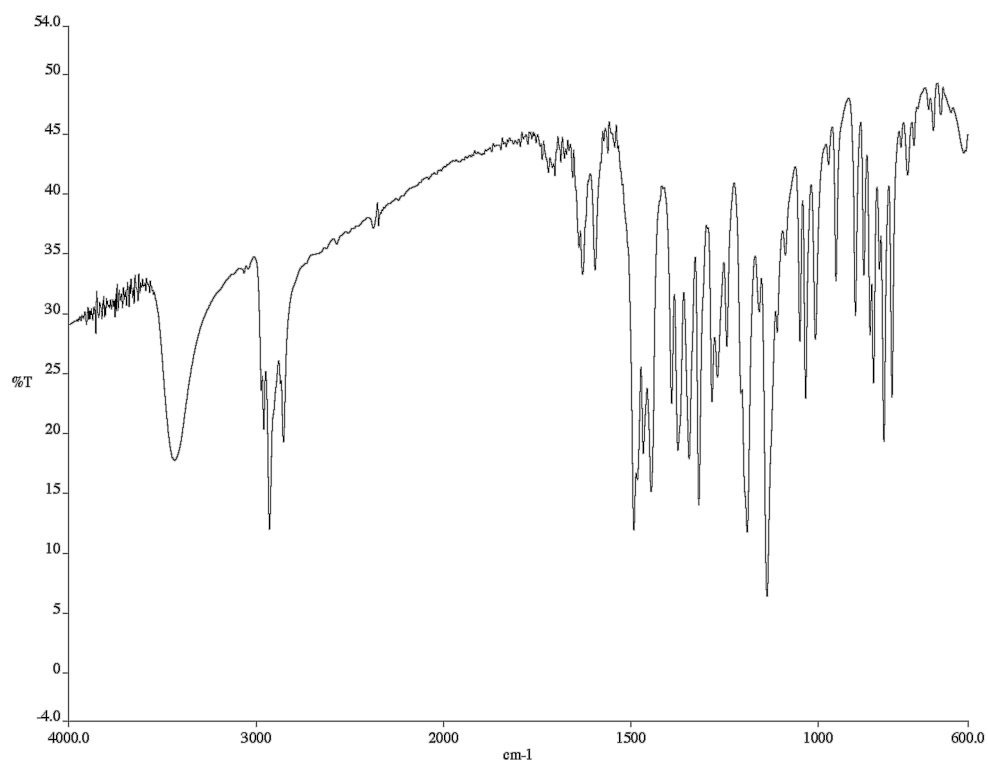


Figure A7.35 Infrared spectrum (KBr) of compound **334**.

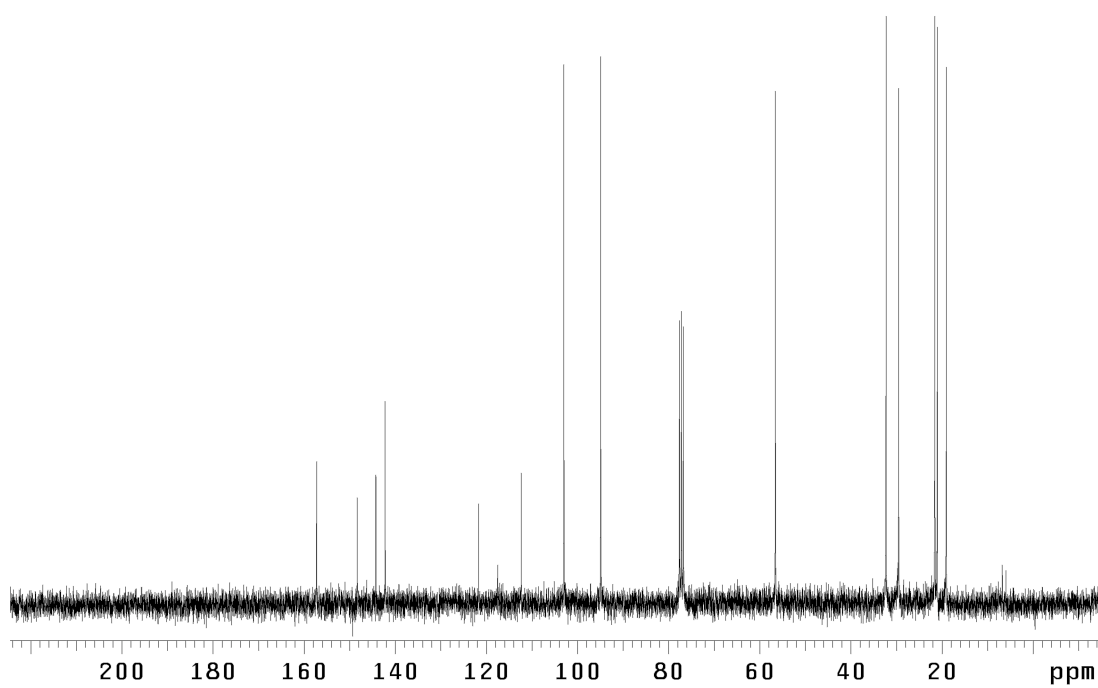


Figure A7.36 ¹³C NMR (75 MHz, CDCl₃) of compound **334**.

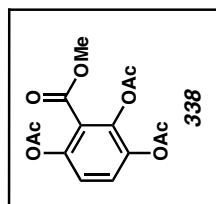
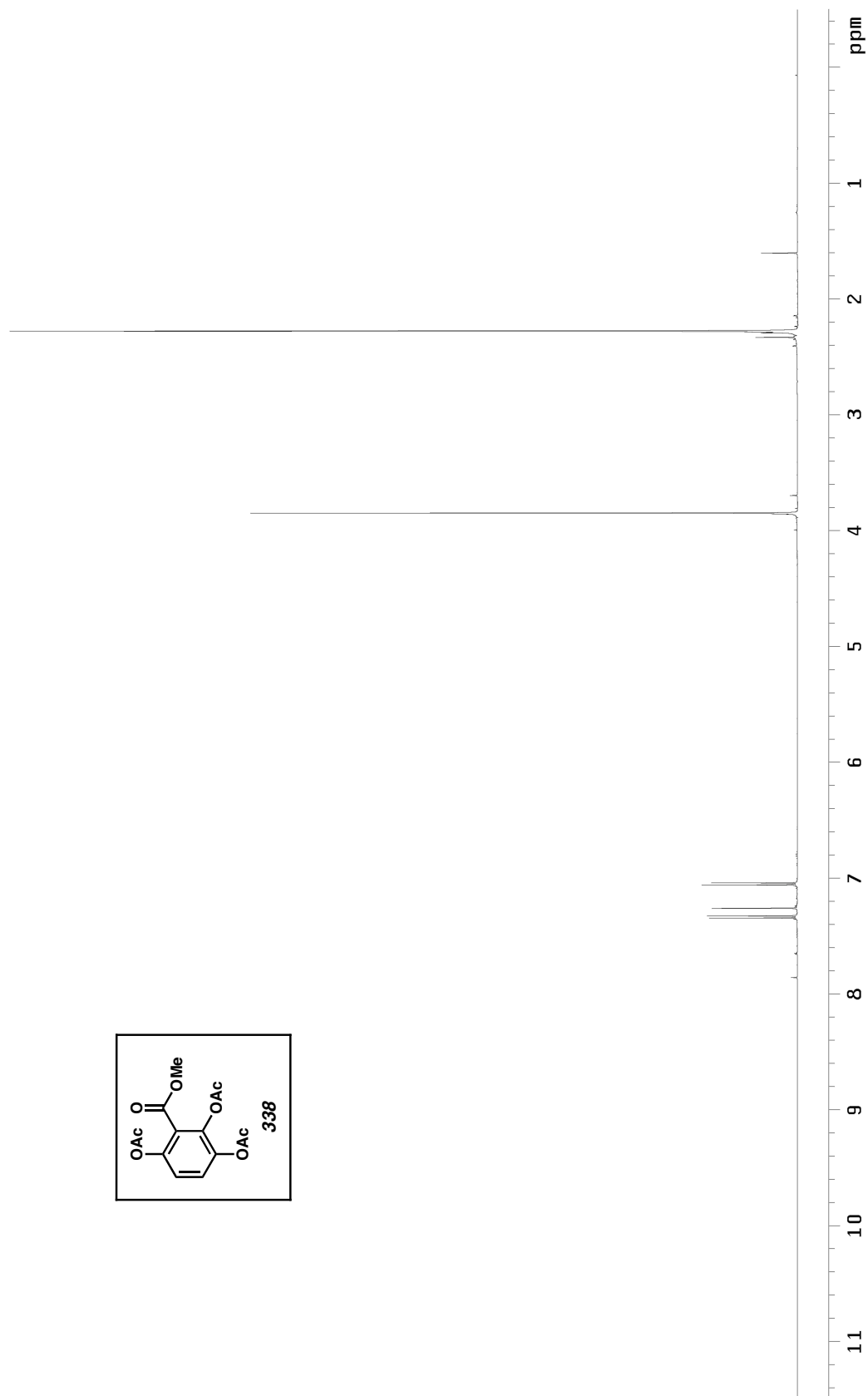


Figure A7.37 ^1H NMR (500 MHz, CDCl_3) of compound 338.

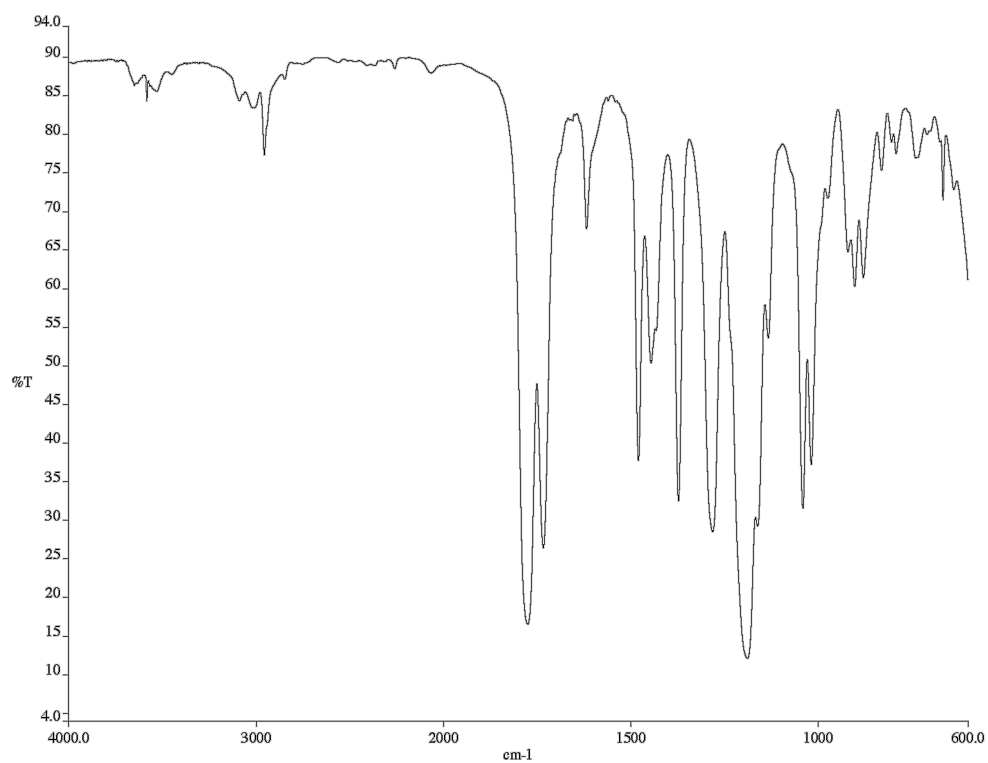


Figure A7.38 Infrared spectrum (NaCl/CDCl₃) of compound **338**.

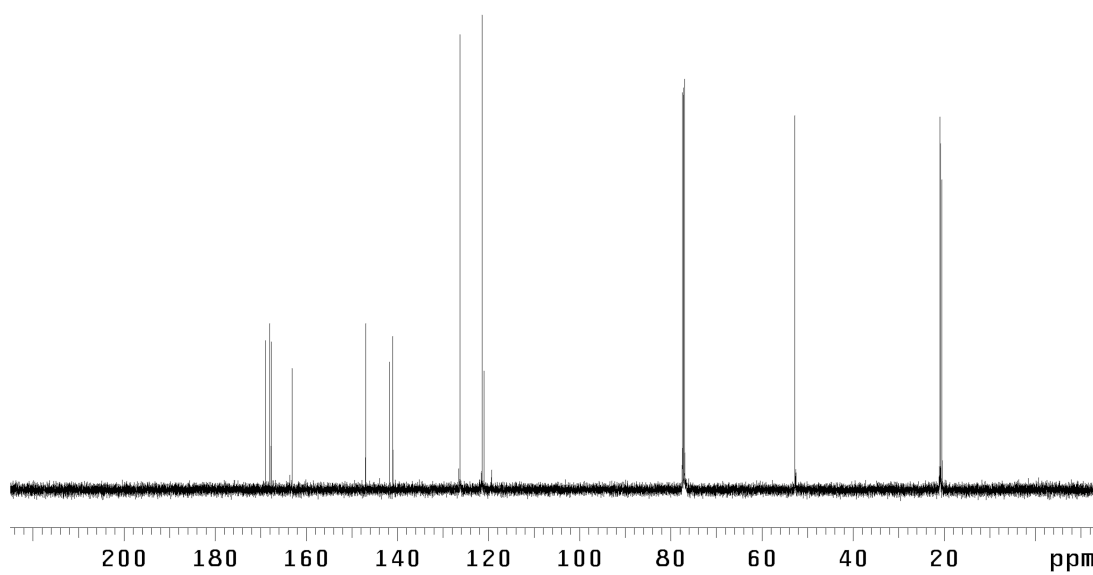


Figure A7.39 ¹³C NMR (125 MHz, CDCl₃) of compound **338**.

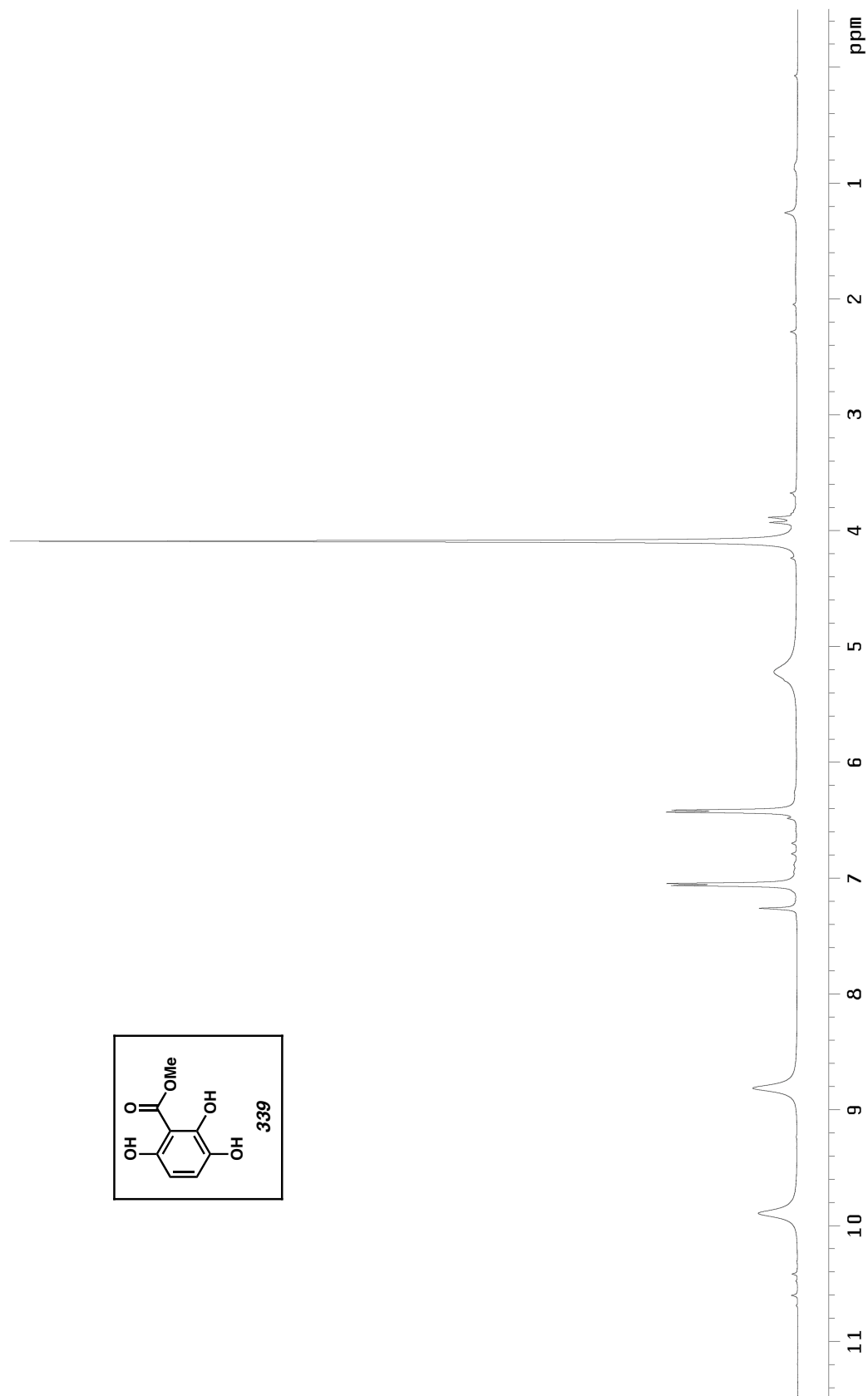


Figure A7.40 ^1H NMR (500 MHz, CDCl_3) of compound **339**.

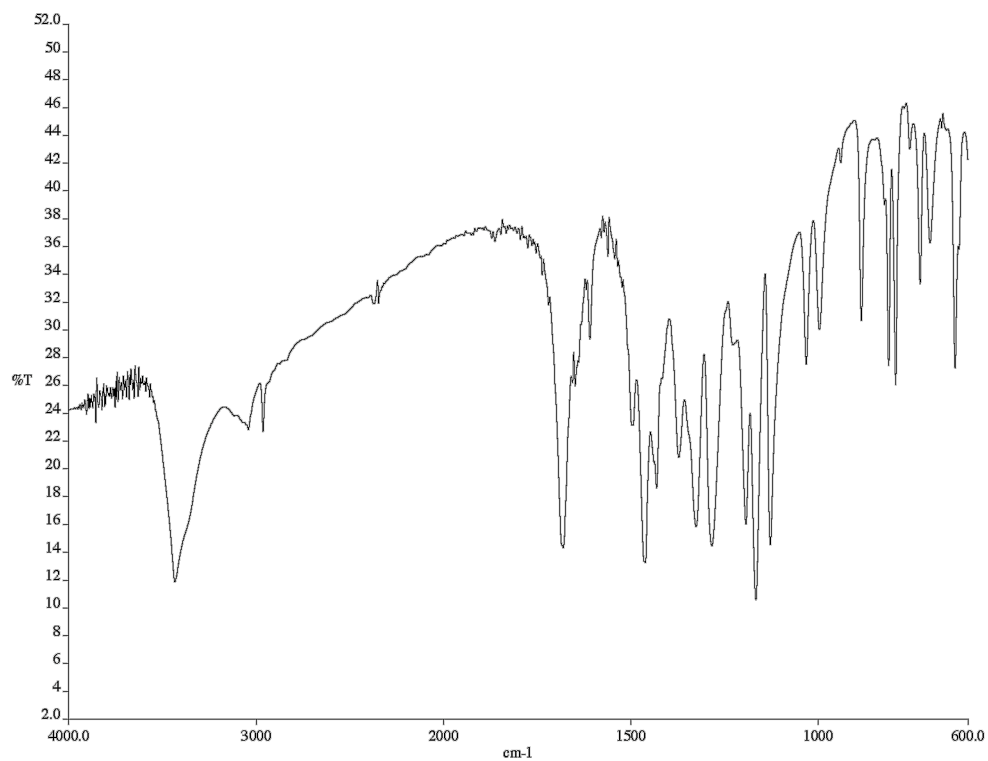


Figure A7.41 Infrared spectrum (KBr) of compound **339**.

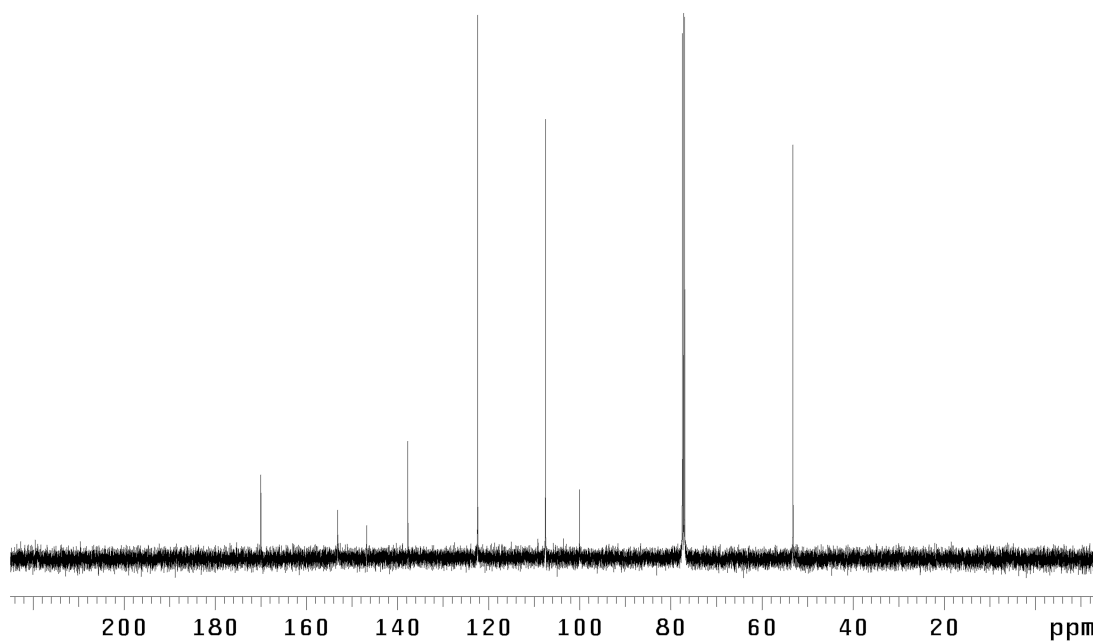


Figure A7.42 ^{13}C NMR (125 MHz, CDCl_3) of compound **339**.

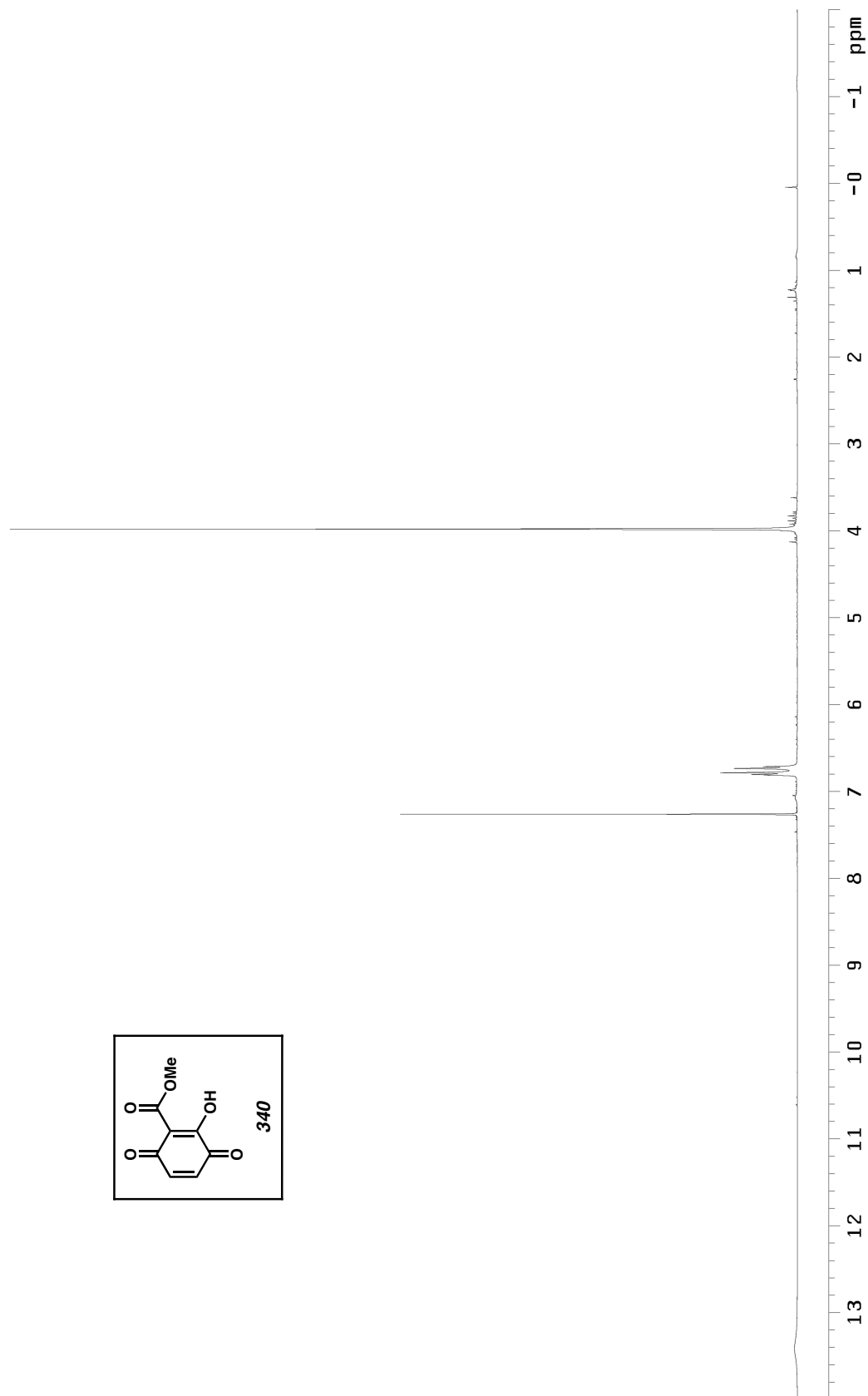


Figure A7.43 ^1H NMR (500 MHz, CDCl_3) of compound **340**.

Figure A7.45 ^{13}C NMR (125 MHz, CDCl_3) of compound **340**.

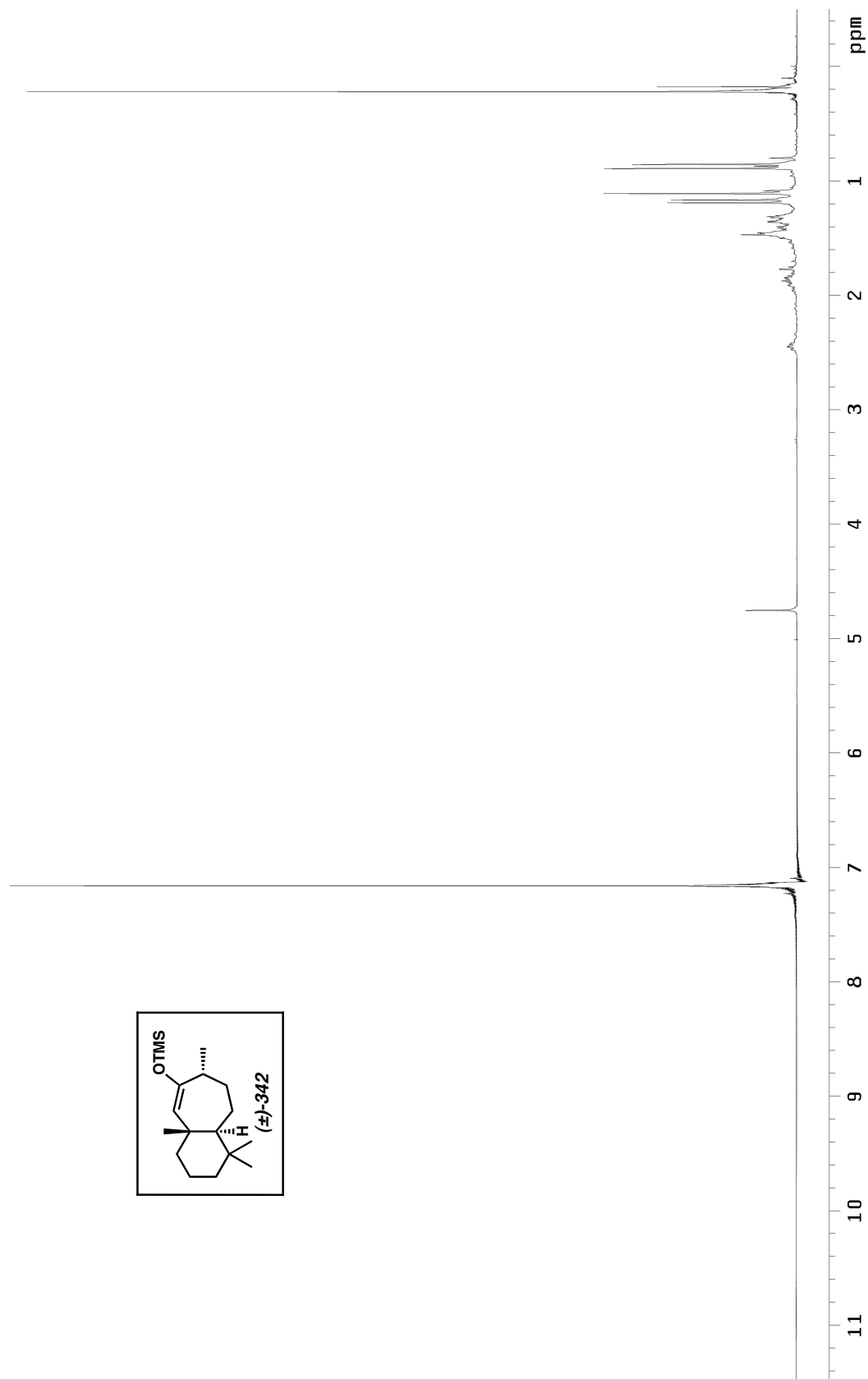


Figure A7.46 ¹H NMR (300 MHz, C₆D₆) of compound **342**.

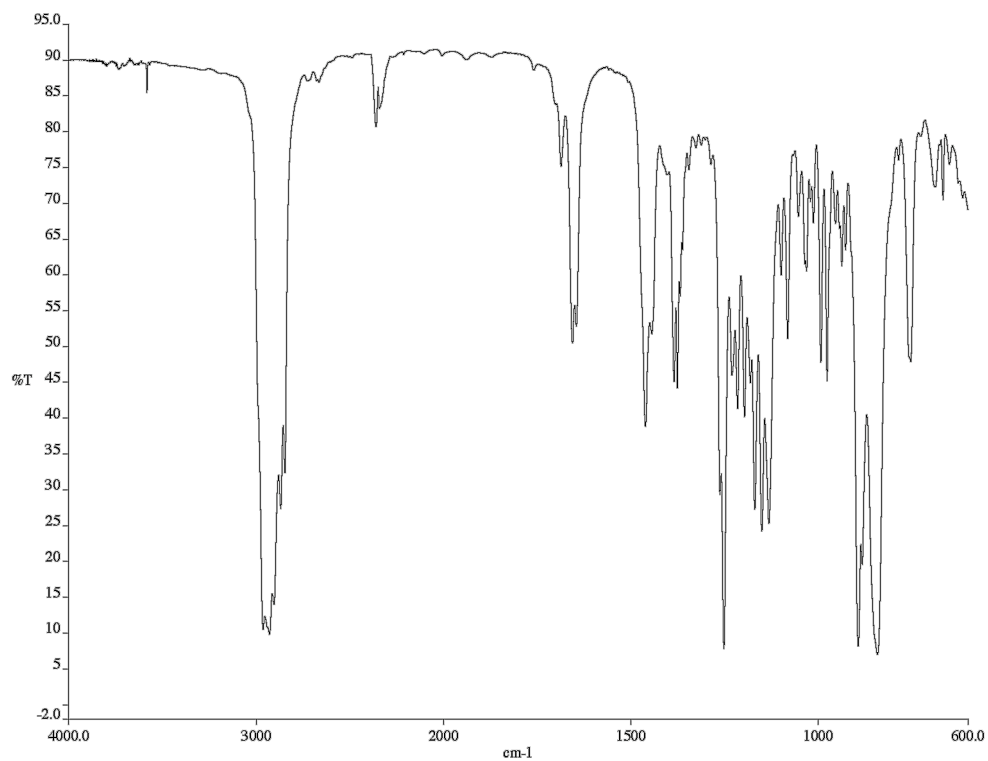


Figure A7.47 Infrared spectrum (NaCl/neat) of compound **342**.

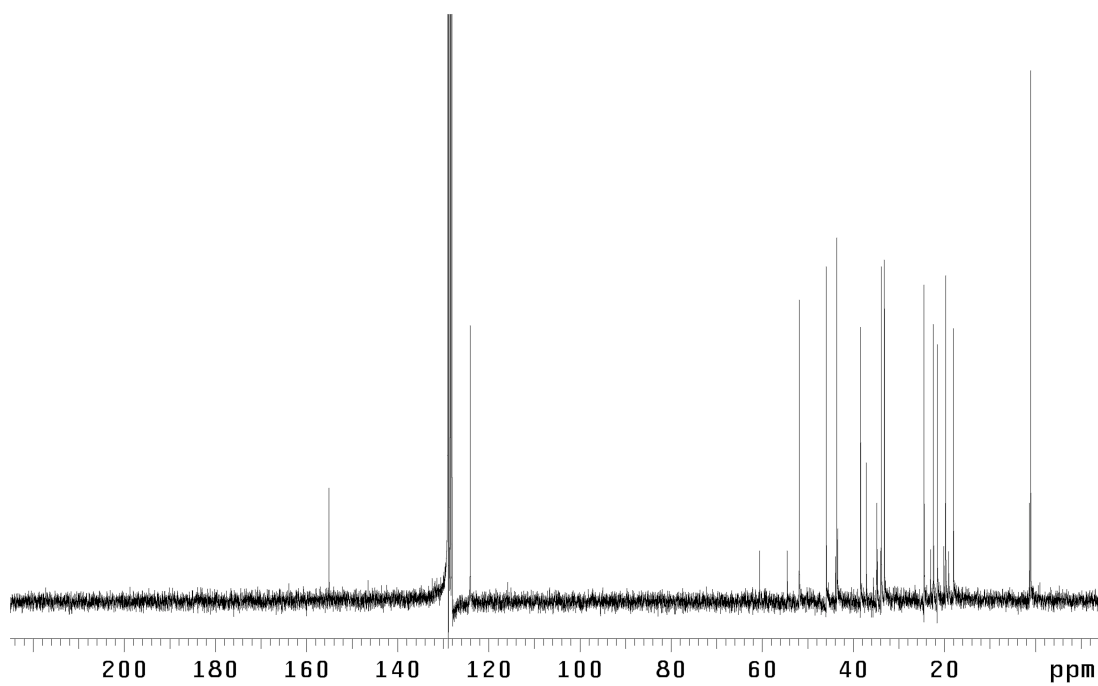


Figure A7.48 ¹³C NMR (75 MHz, C₆D₆) of compound **342**.

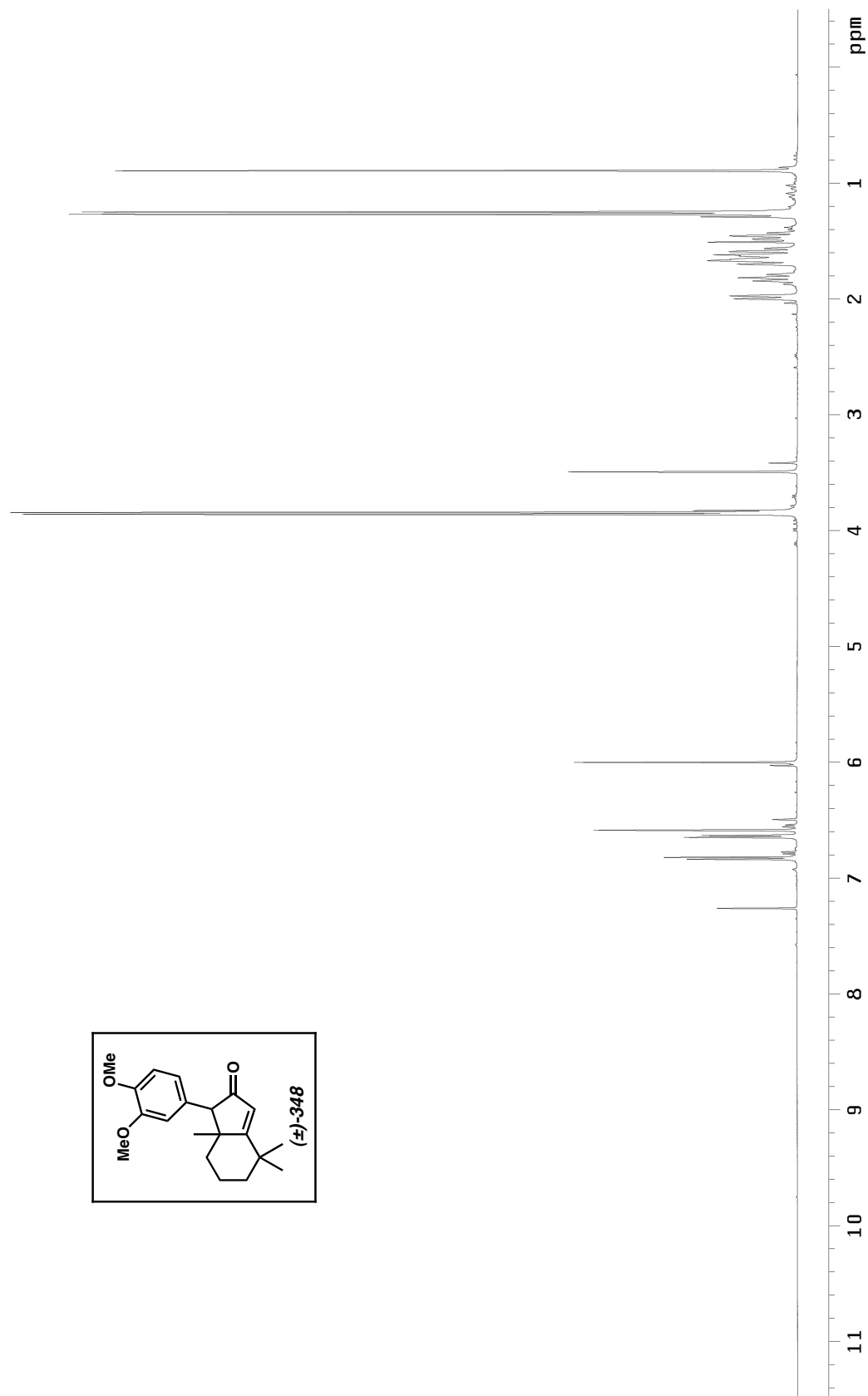


Figure A7.49 ¹H NMR (500 MHz, CDCl₃) of compound **348**.

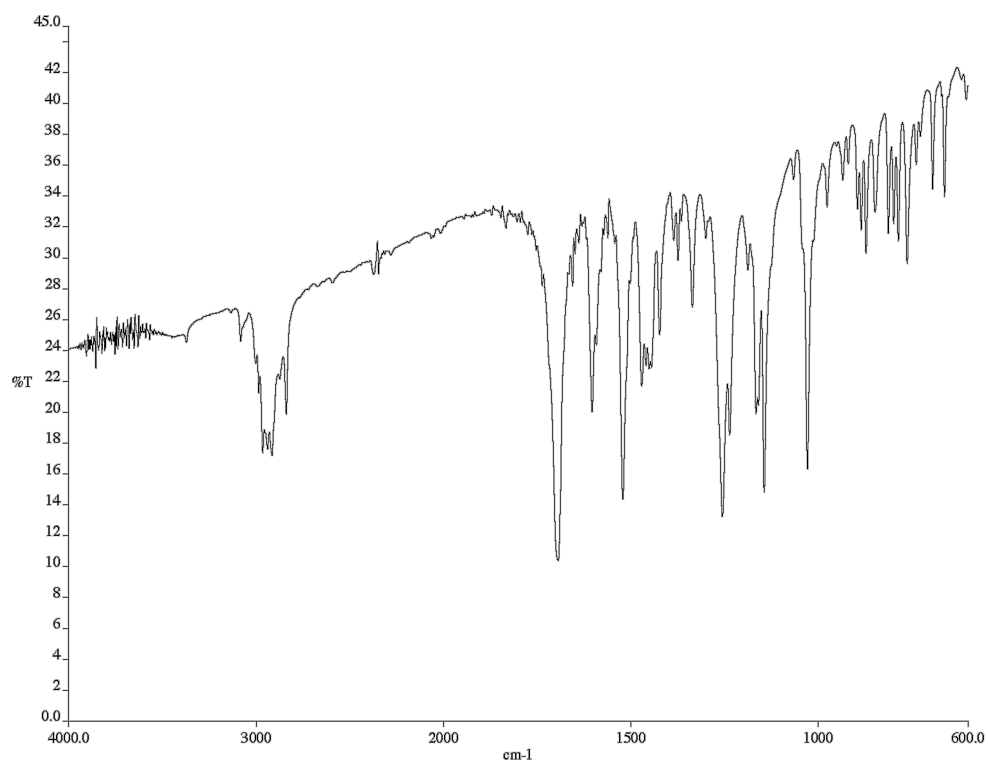


Figure A7.50 Infrared spectrum (KBr) of compound **348**.

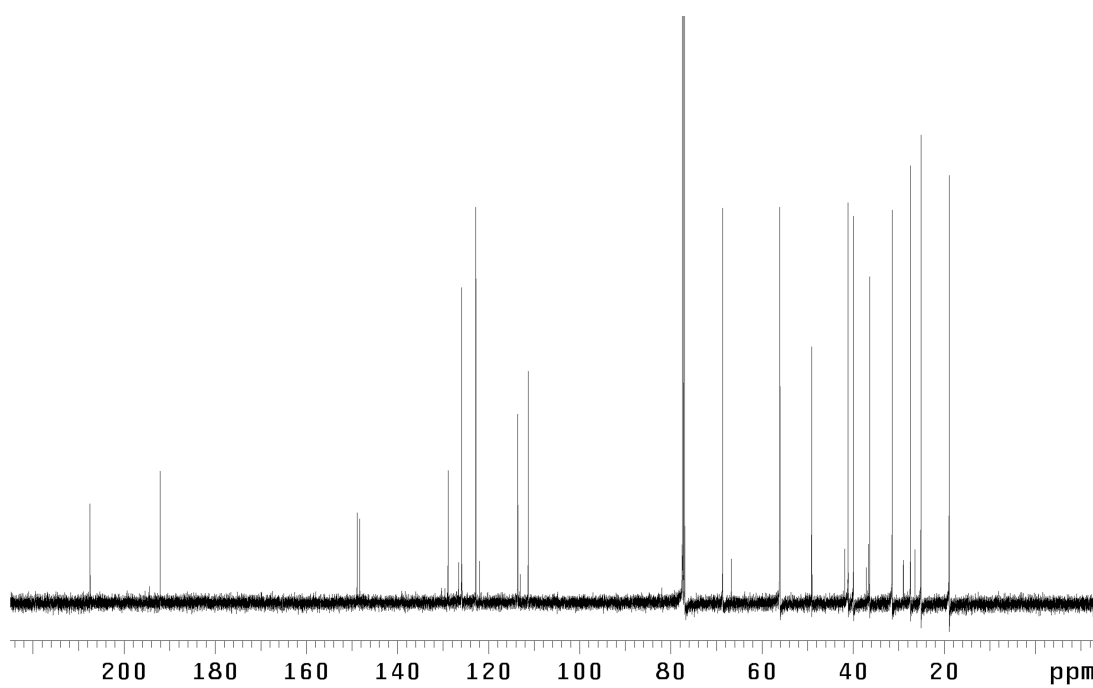


Figure A7.51 ¹³C NMR (125 MHz, CDCl₃) of compound **348**.



Figure A7.52 ^1H NMR (500 MHz, CDCl_3) of compound **349**.

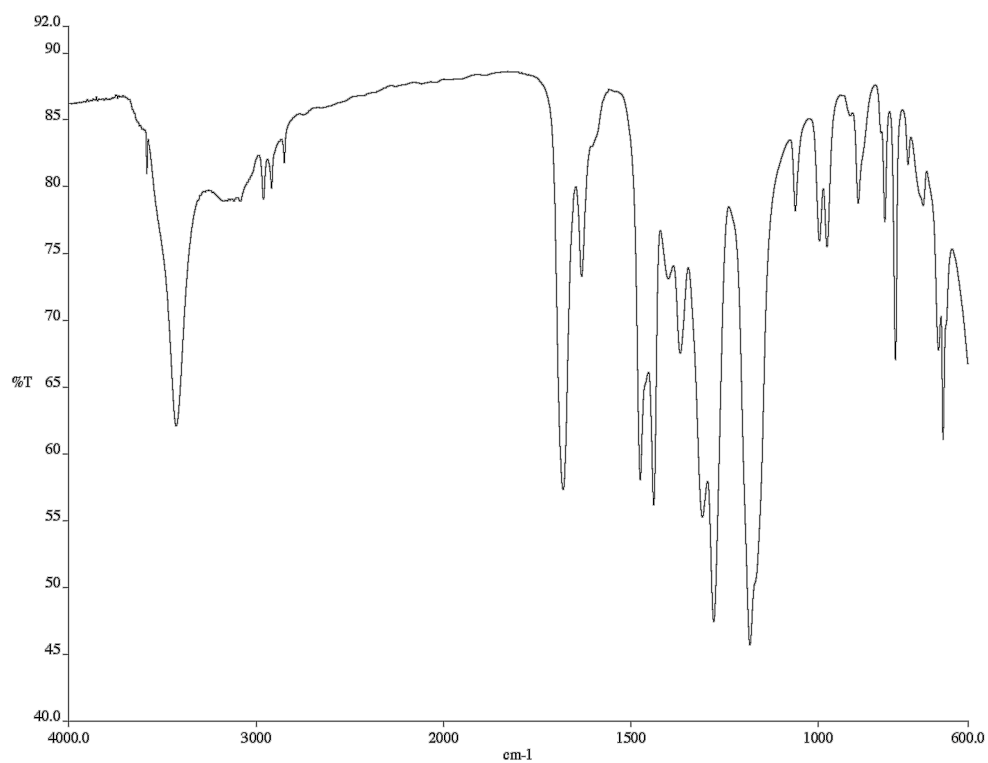


Figure A7.53 Infrared spectrum (NaCl/CDCl₃) of compound **349**.

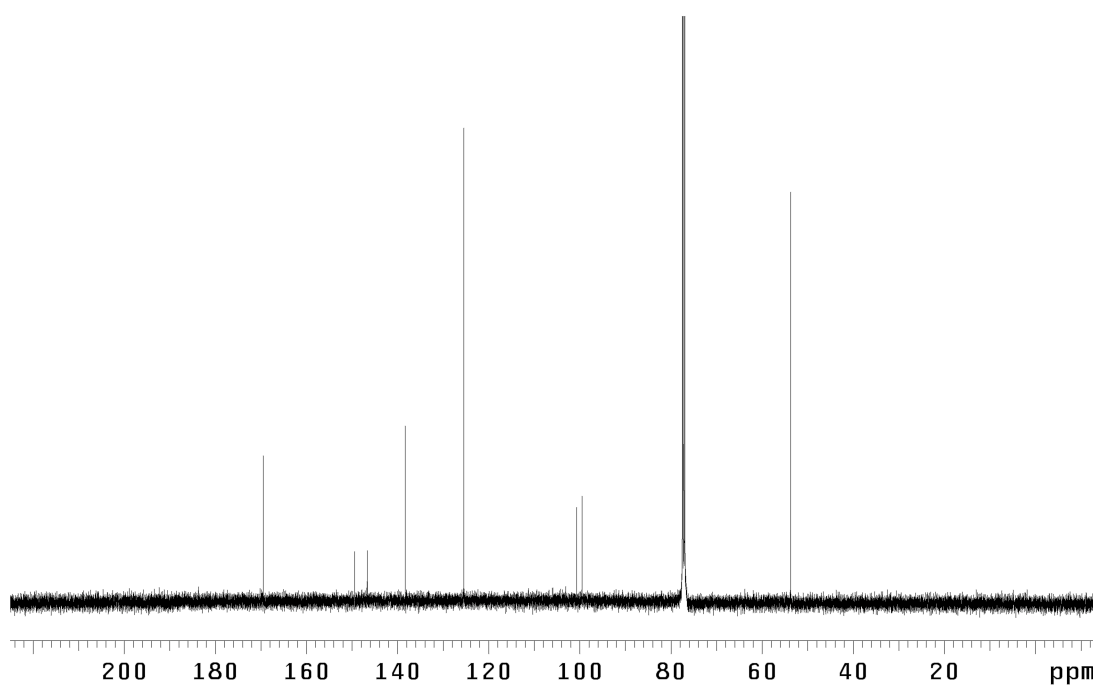


Figure A7.54 ¹³C NMR (125 MHz, CDCl₃) of compound **349**.

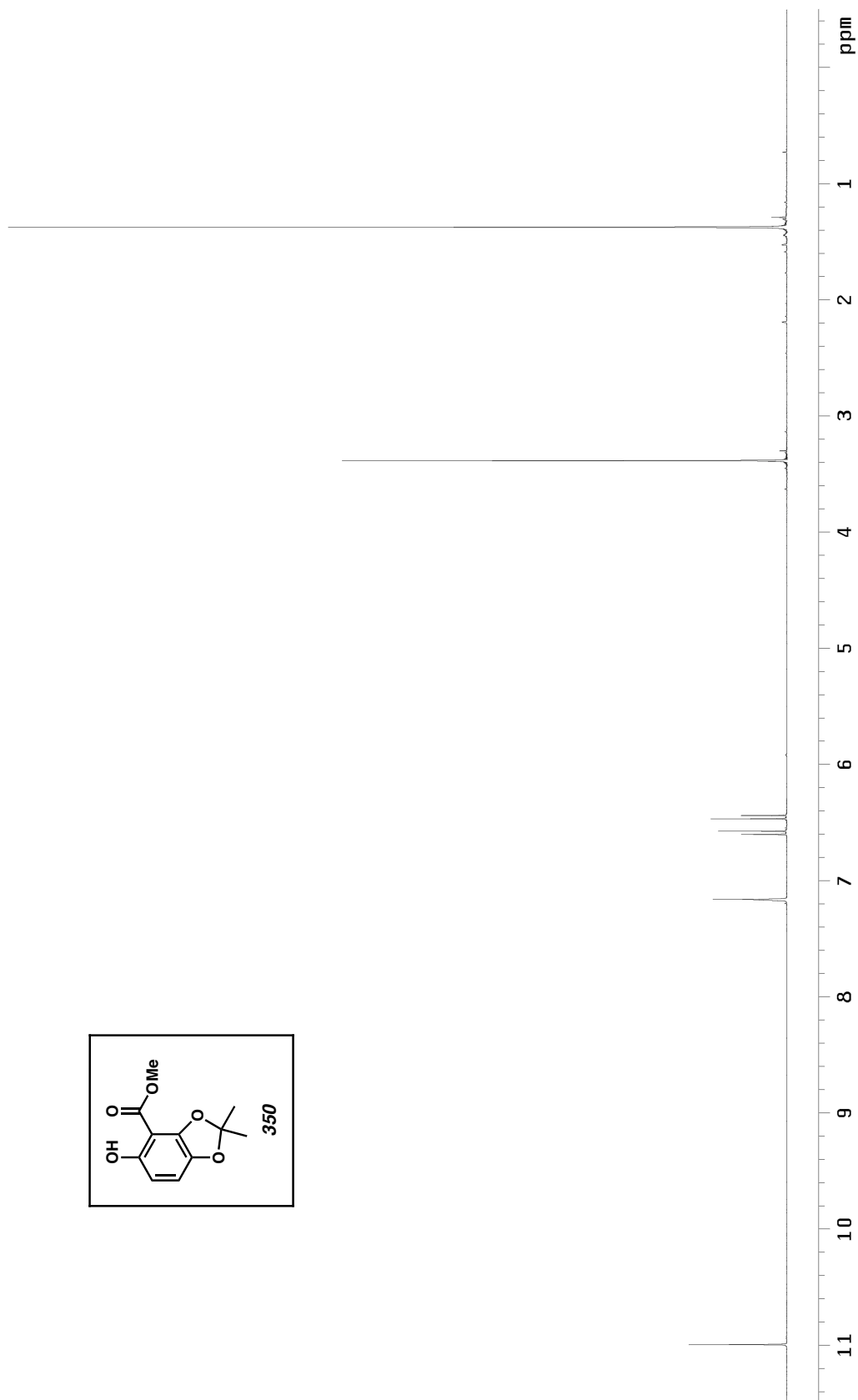


Figure A7.55 ^1H NMR (300 MHz, C_6D_6) of compound 350.

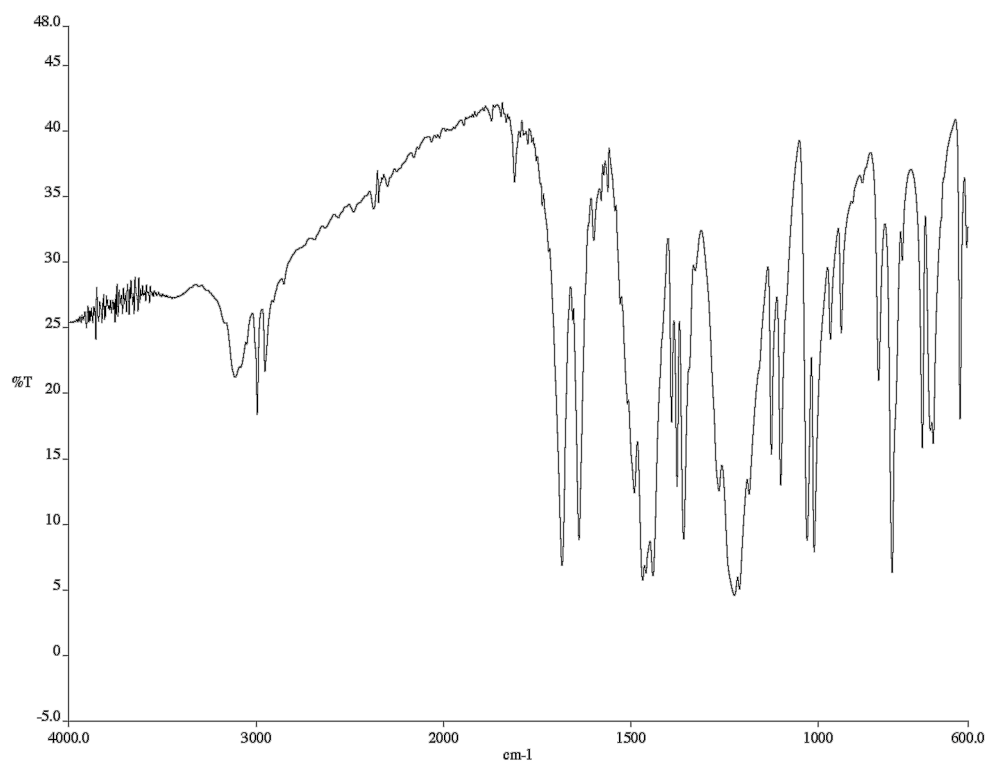


Figure A7.56 Infrared spectrum (KBr) of compound **350**.

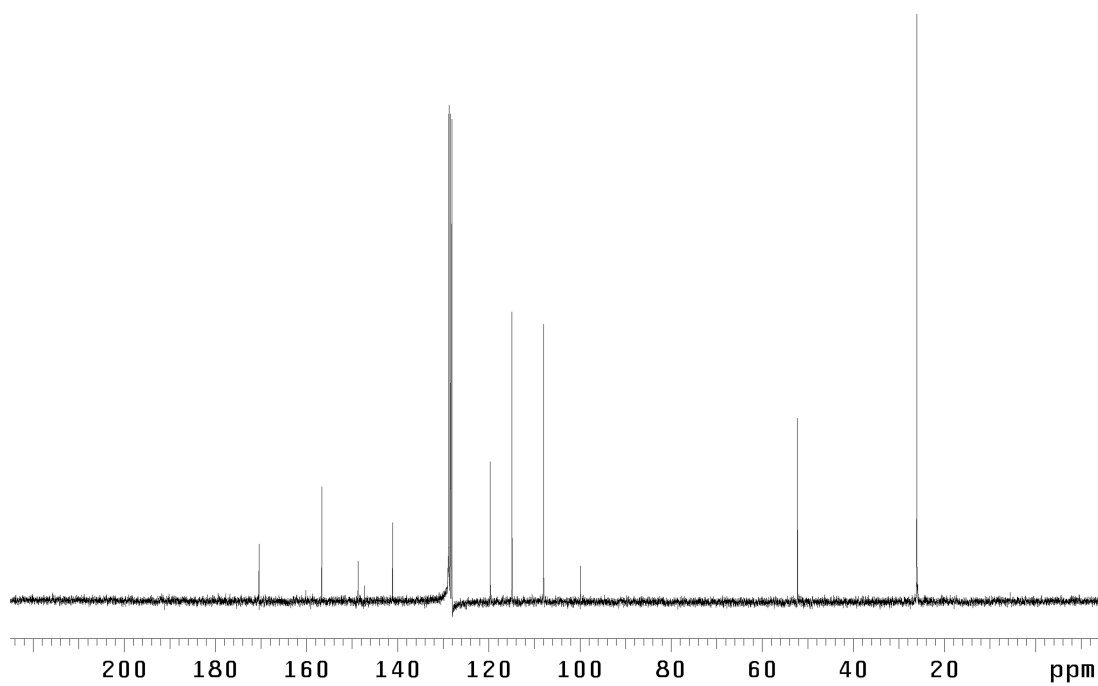


Figure A7.57 ¹³C NMR (75 MHz, C₆D₆) of compound **350**.

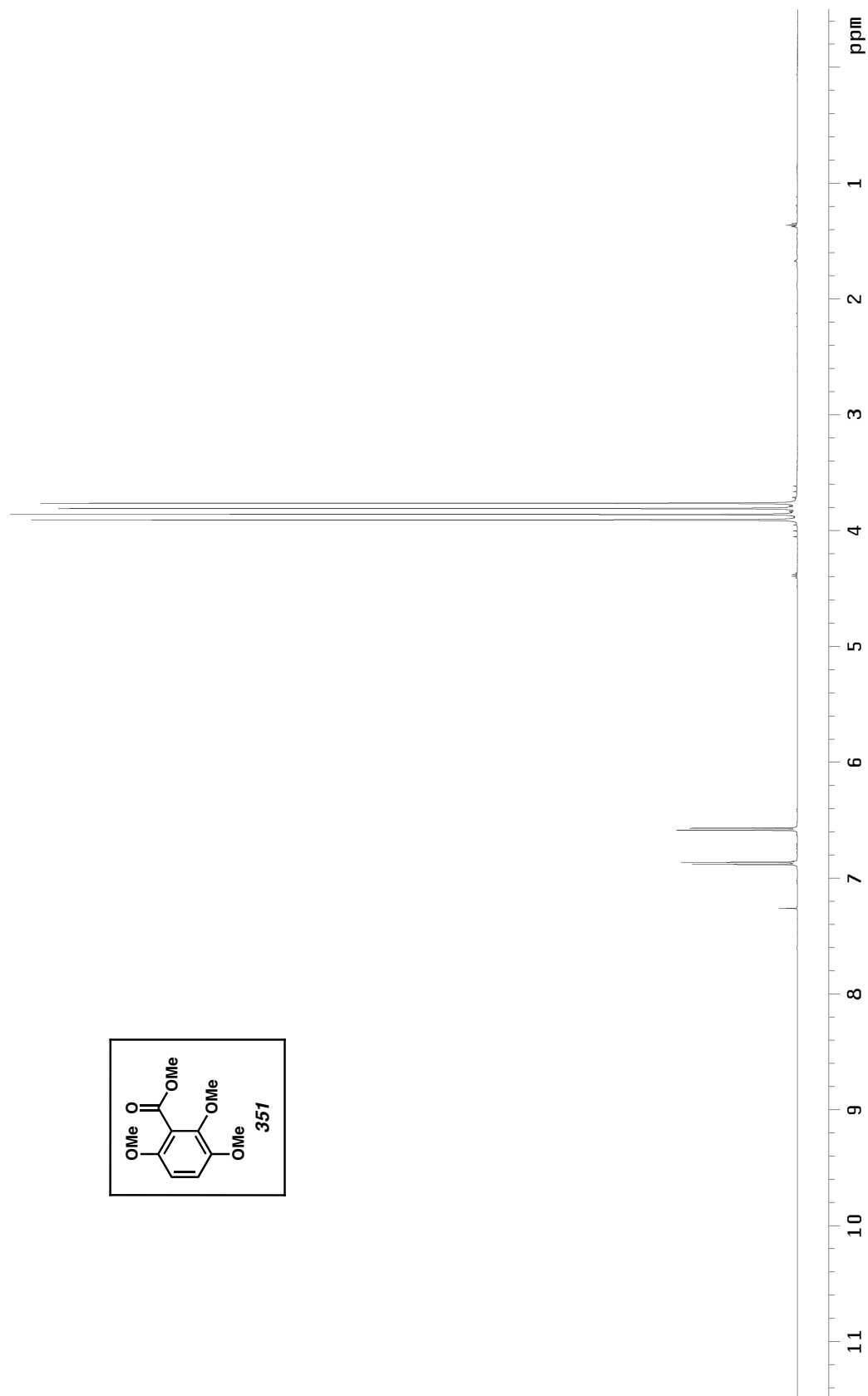
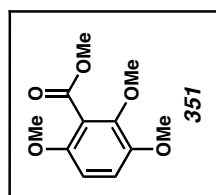


Figure A7.58 ^1H NMR (500 MHz, CDCl_3) of compound **351**.

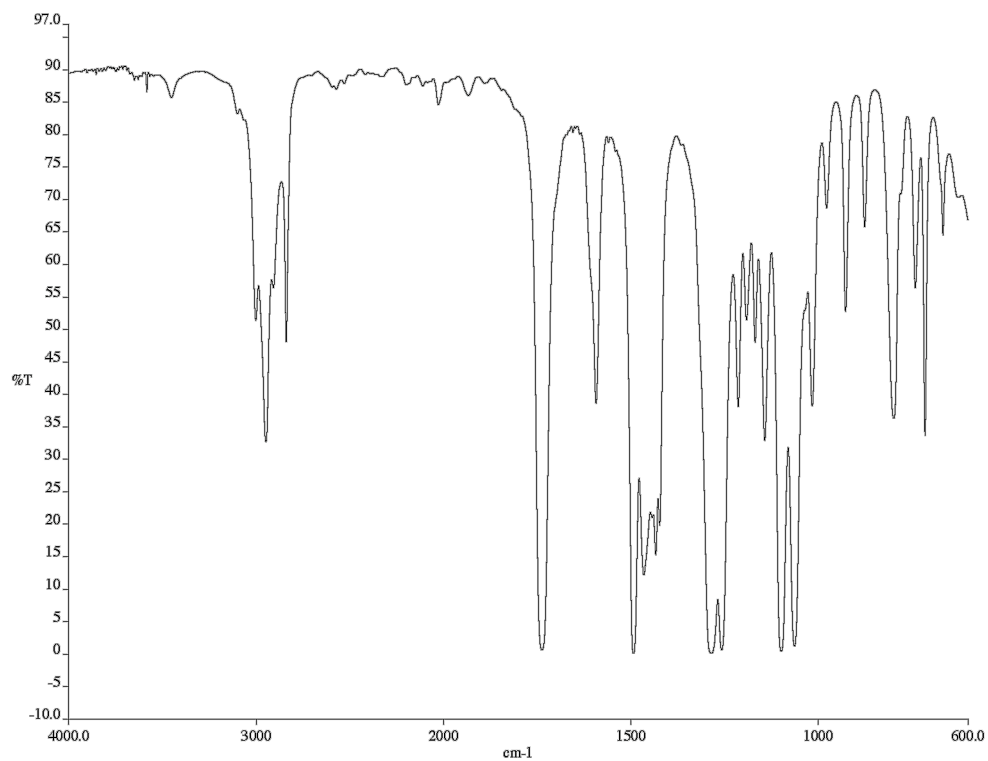


Figure A7.59 Infrared spectrum (NaCl/CDCl₃) of compound **351**.

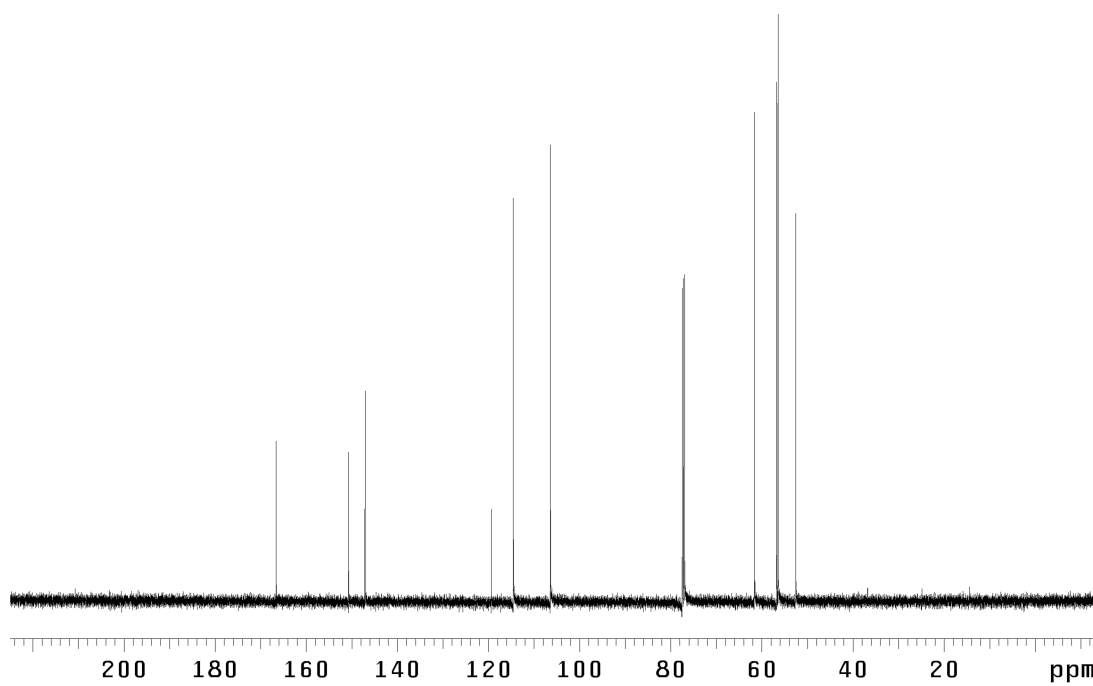


Figure A7.60 ¹³C NMR (125 MHz, CDCl₃) of compound **351**.

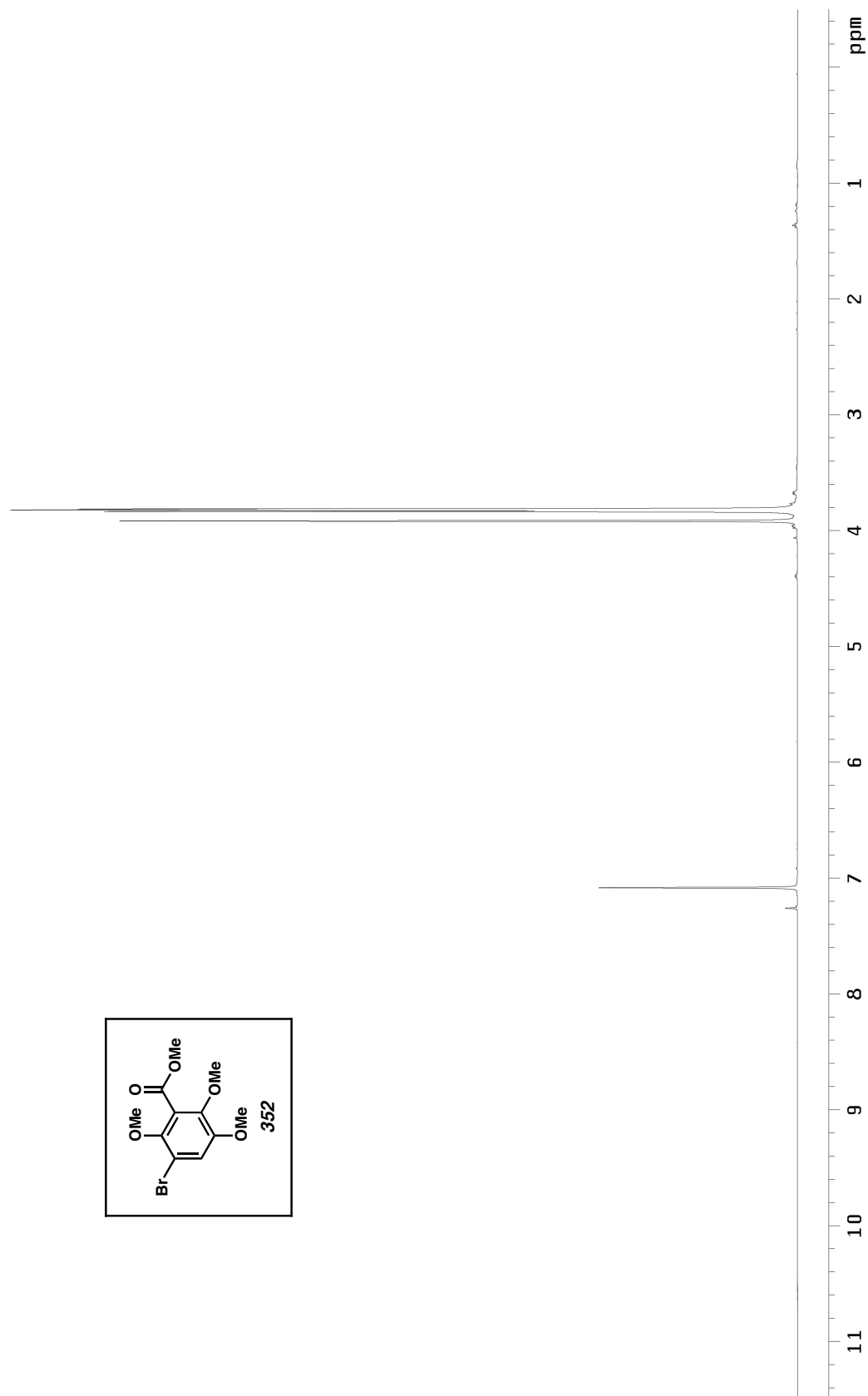


Figure A7.61 ^1H NMR (500 MHz, CDCl_3) of compound **352**.

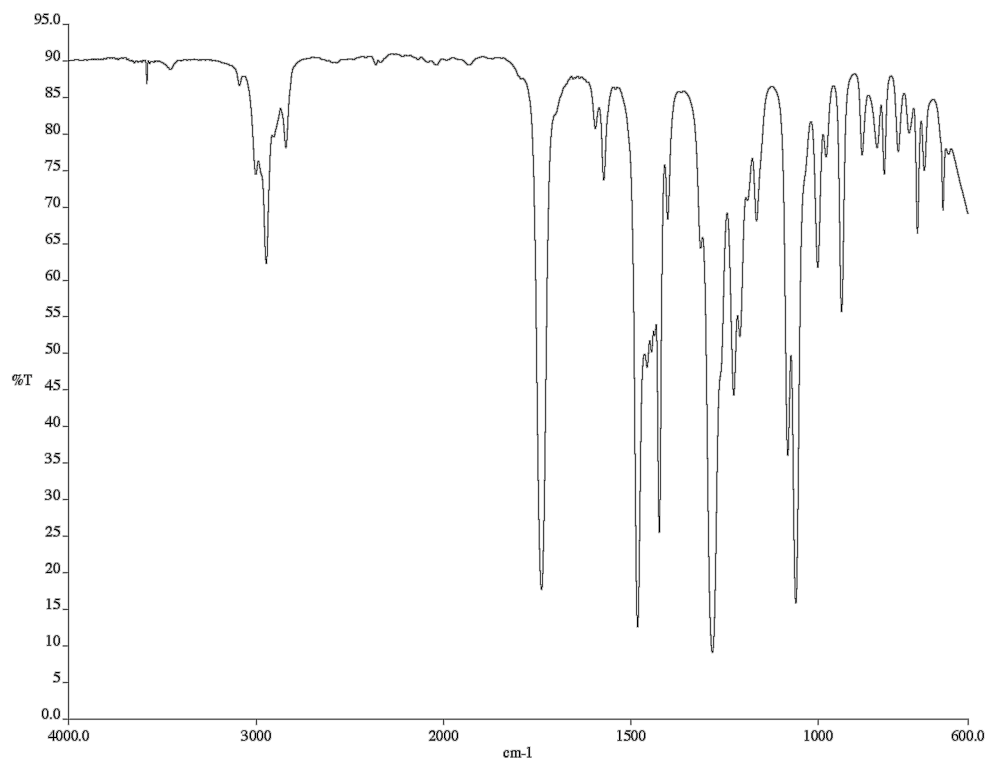


Figure A7.62 Infrared spectrum (NaCl/CHCl₃) of compound **352**.

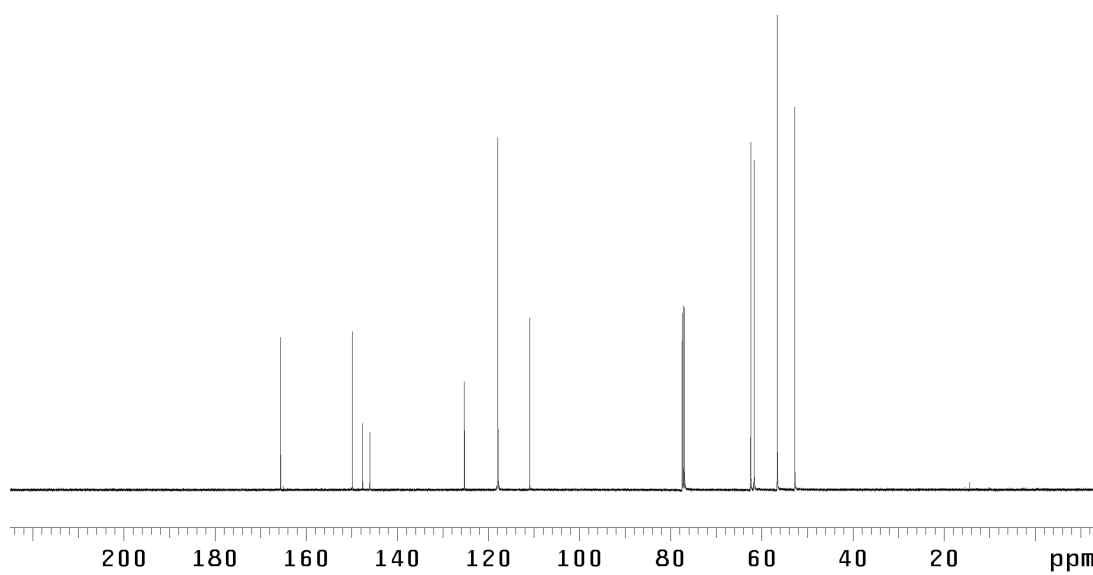


Figure A7.63 ¹³C NMR (125 MHz, CDCl₃) of compound **352**.

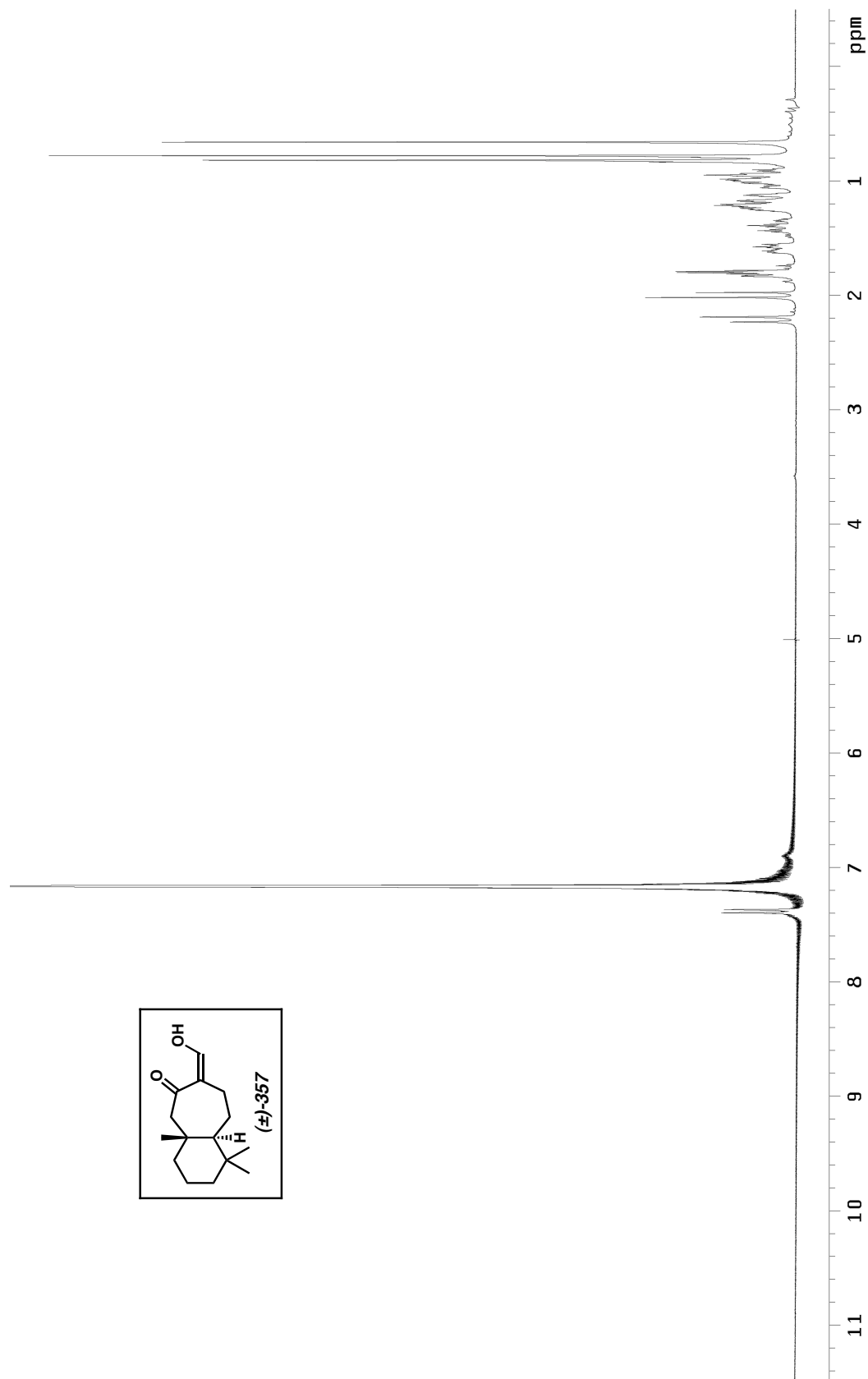


Figure A7.64 ^1H NMR (300 MHz, C_6D_6) of compound **357**.

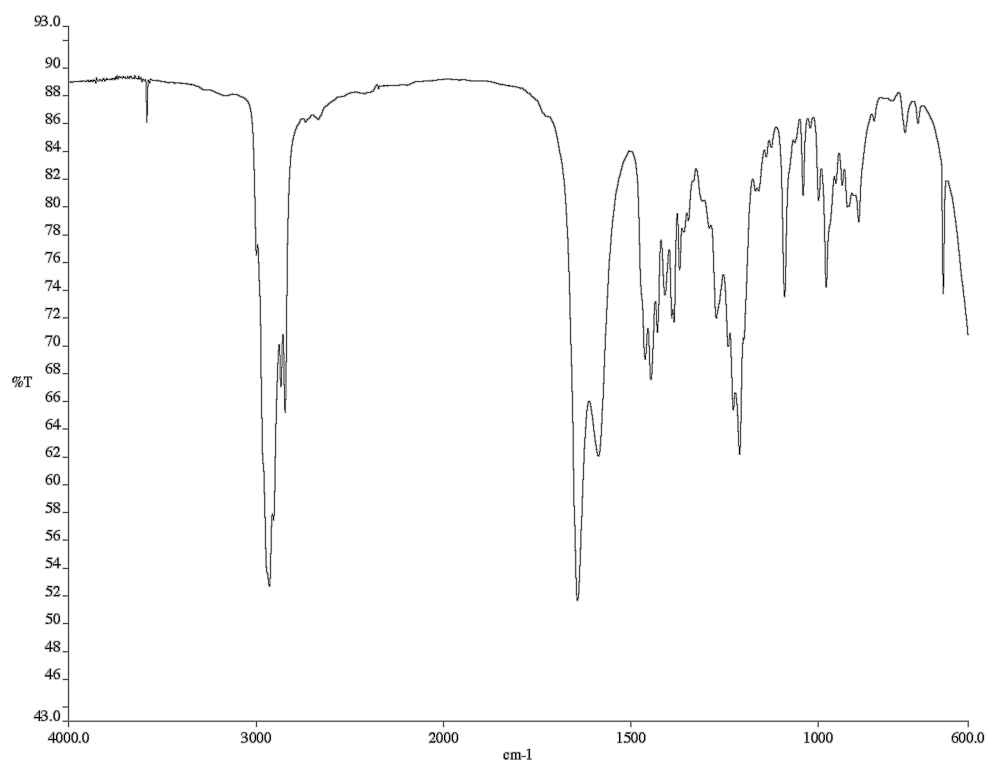


Figure A7.65 Infrared spectrum (NaCl/CH₂Cl₂) of compound **357**.

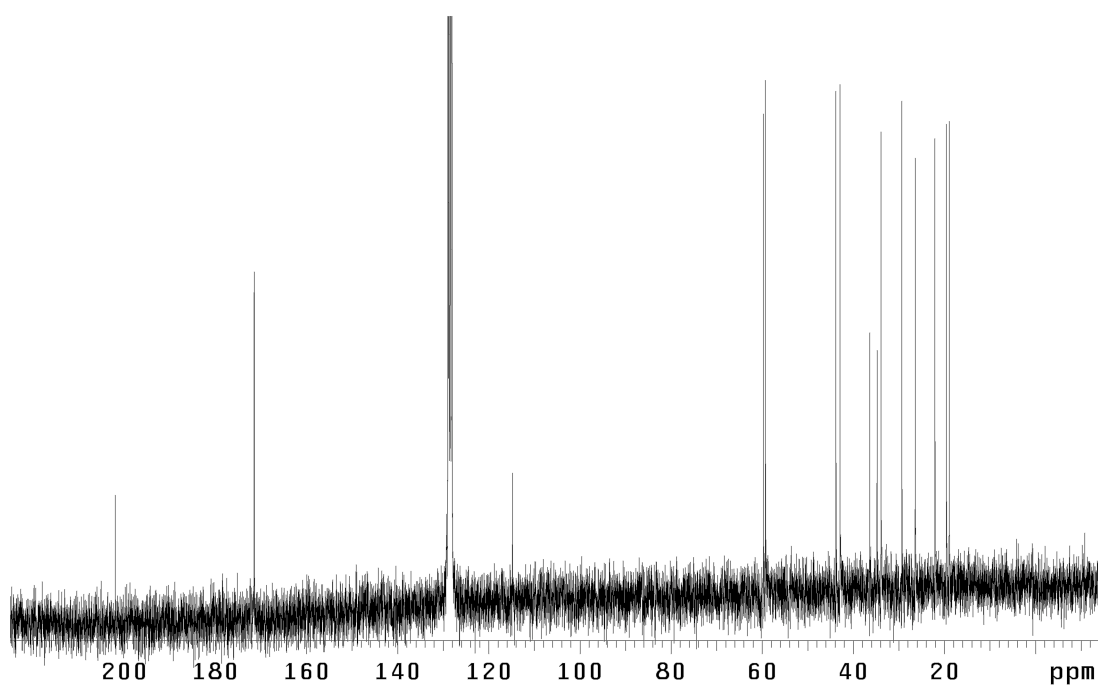


Figure A7.66 ¹³C NMR (75 MHz, C₆D₆) of compound **357**.

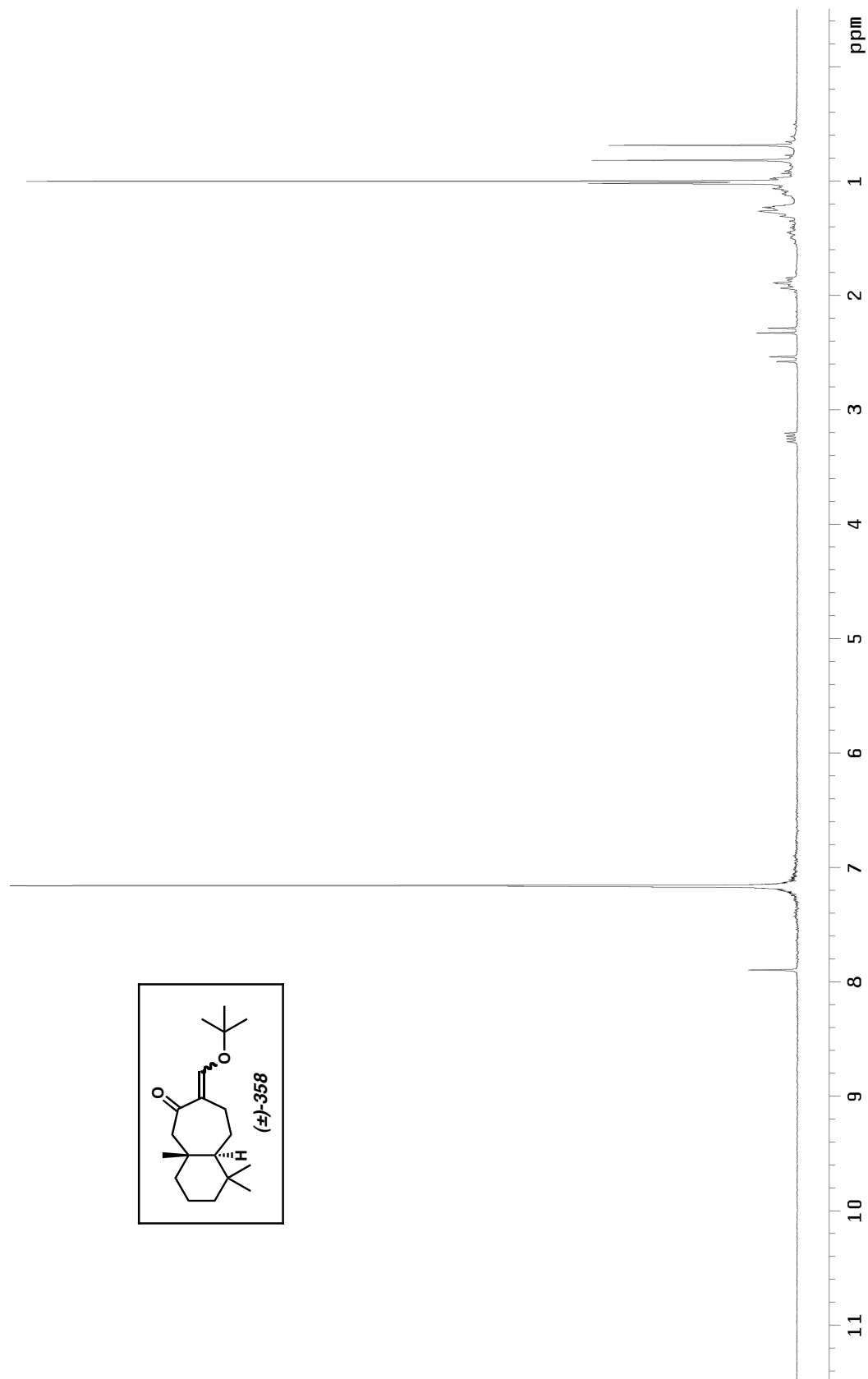


Figure A7.67 ^1H NMR (300 MHz, C_6D_6) of compound **358**.

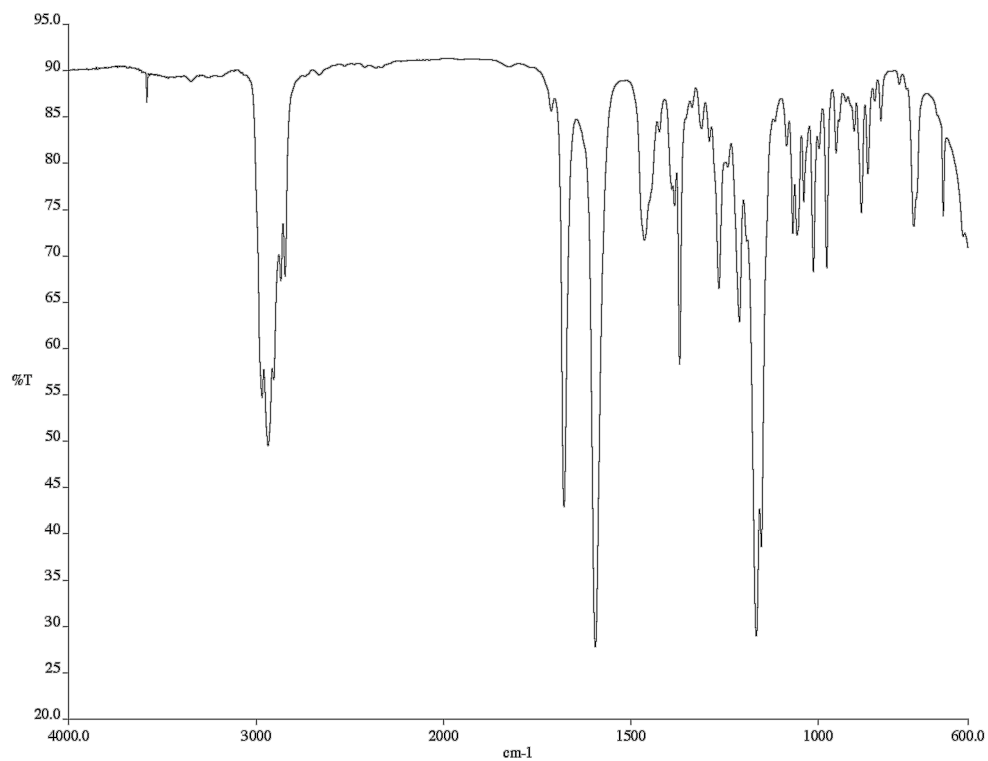


Figure A7.68 Infrared spectrum (NaCl/CH₂Cl₂) of compound **358**.

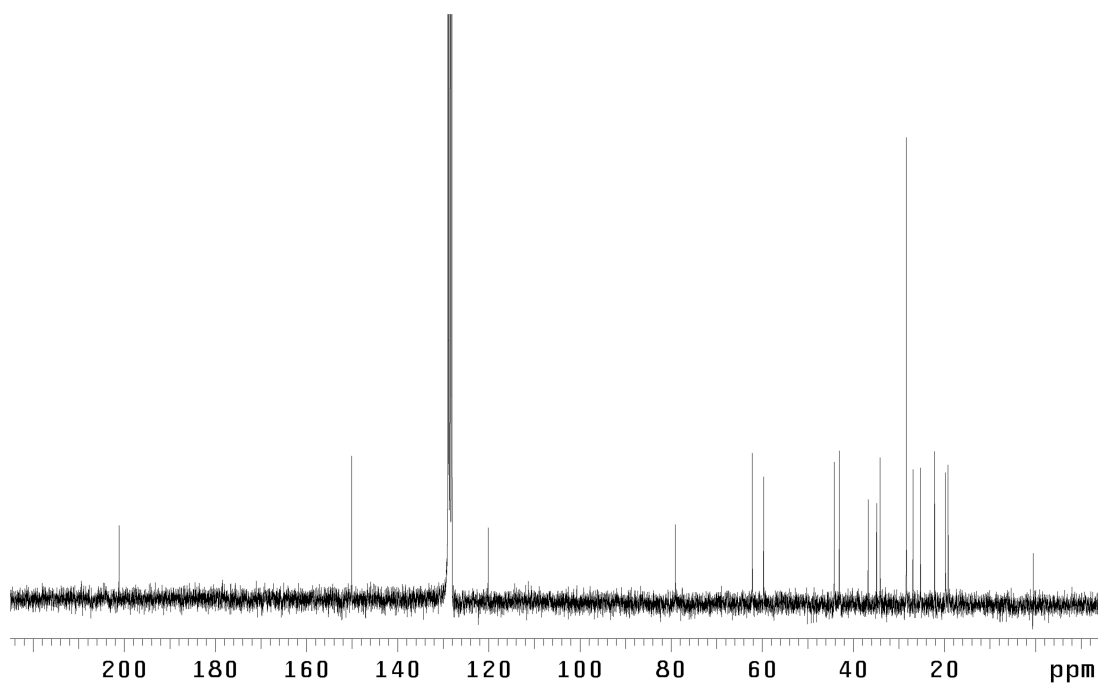


Figure A7.69 ¹³C NMR (75 MHz, C₆D₆) of compound **358**.

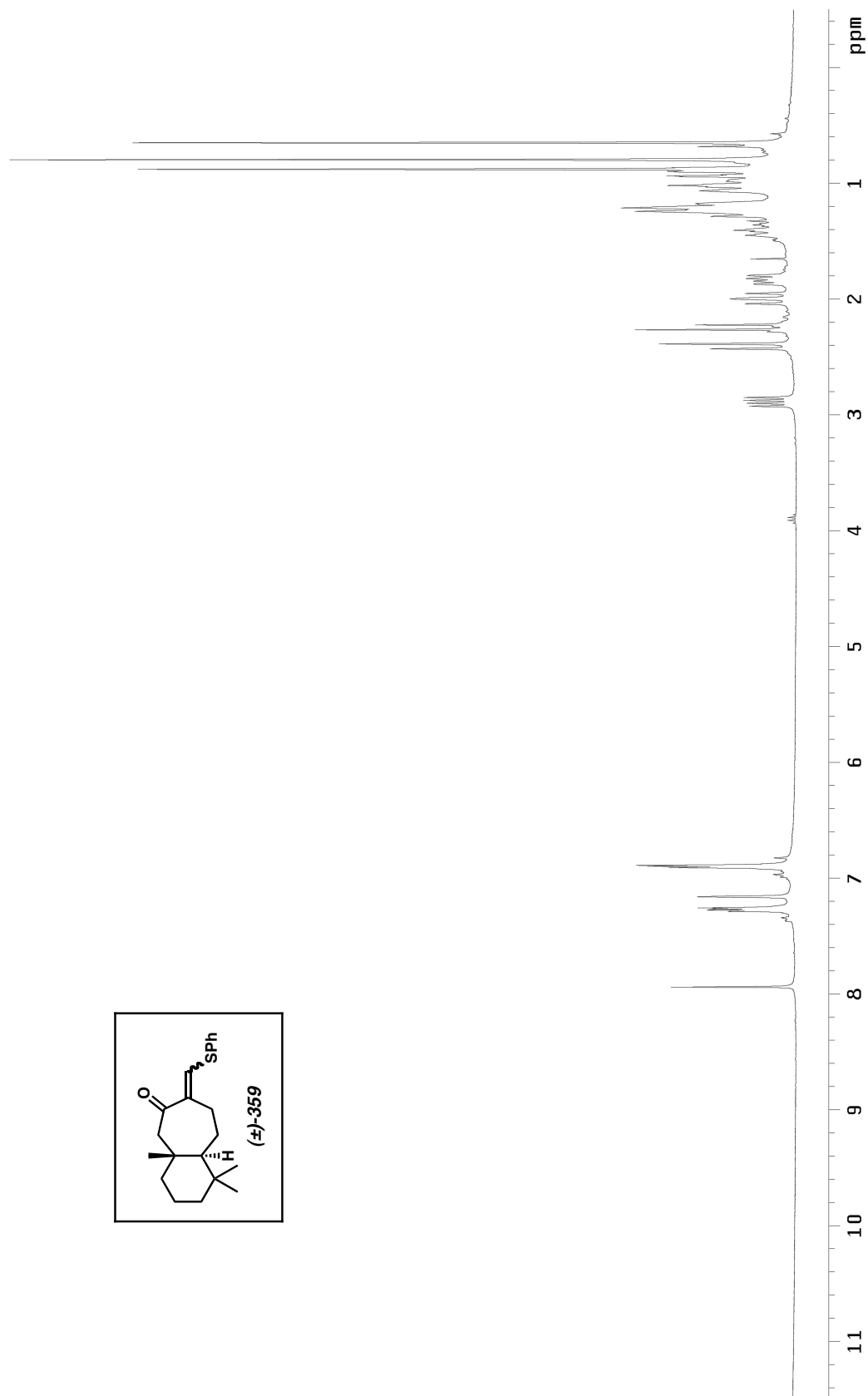


Figure A7.70 ^1H NMR (300 MHz, C_6D_6) of compound **359**.

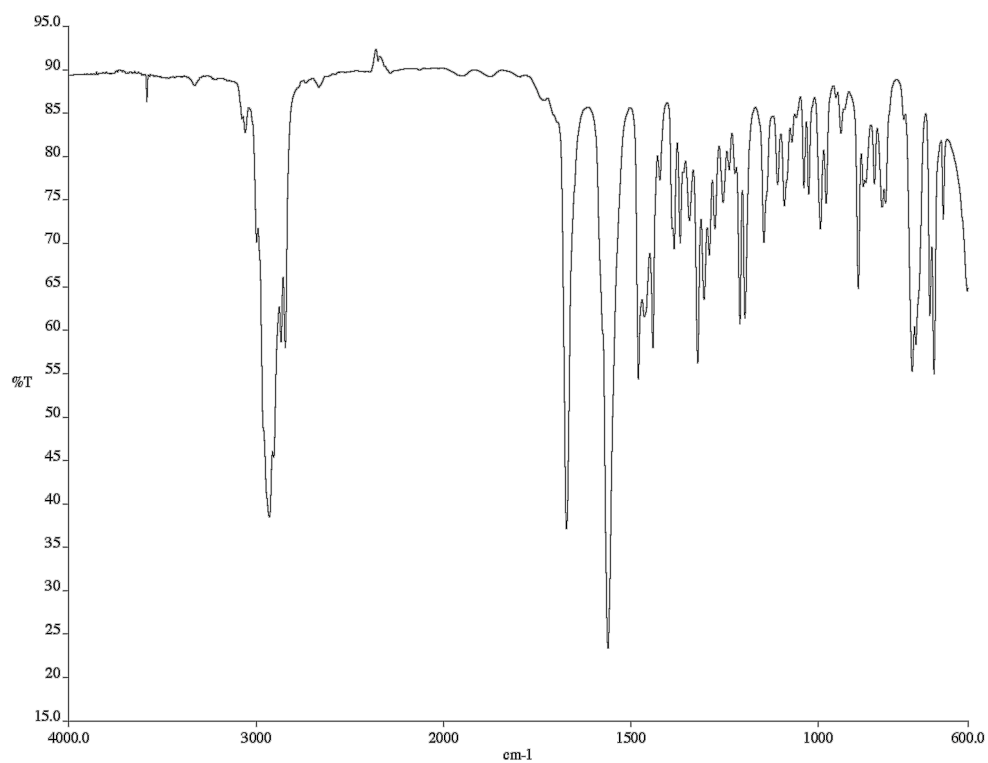


Figure A7.71 Infrared spectrum (NaCl/CH₂Cl₂) of compound **359**.

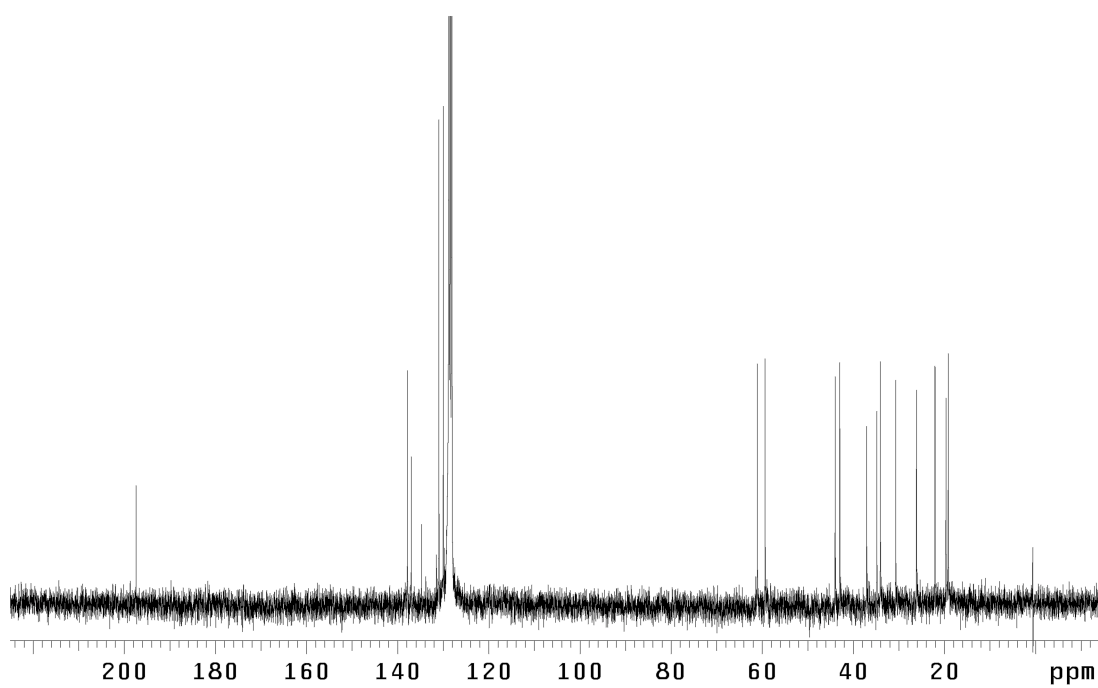


Figure A7.72 ¹³C NMR (75 MHz, C₆D₆) of compound **359**.

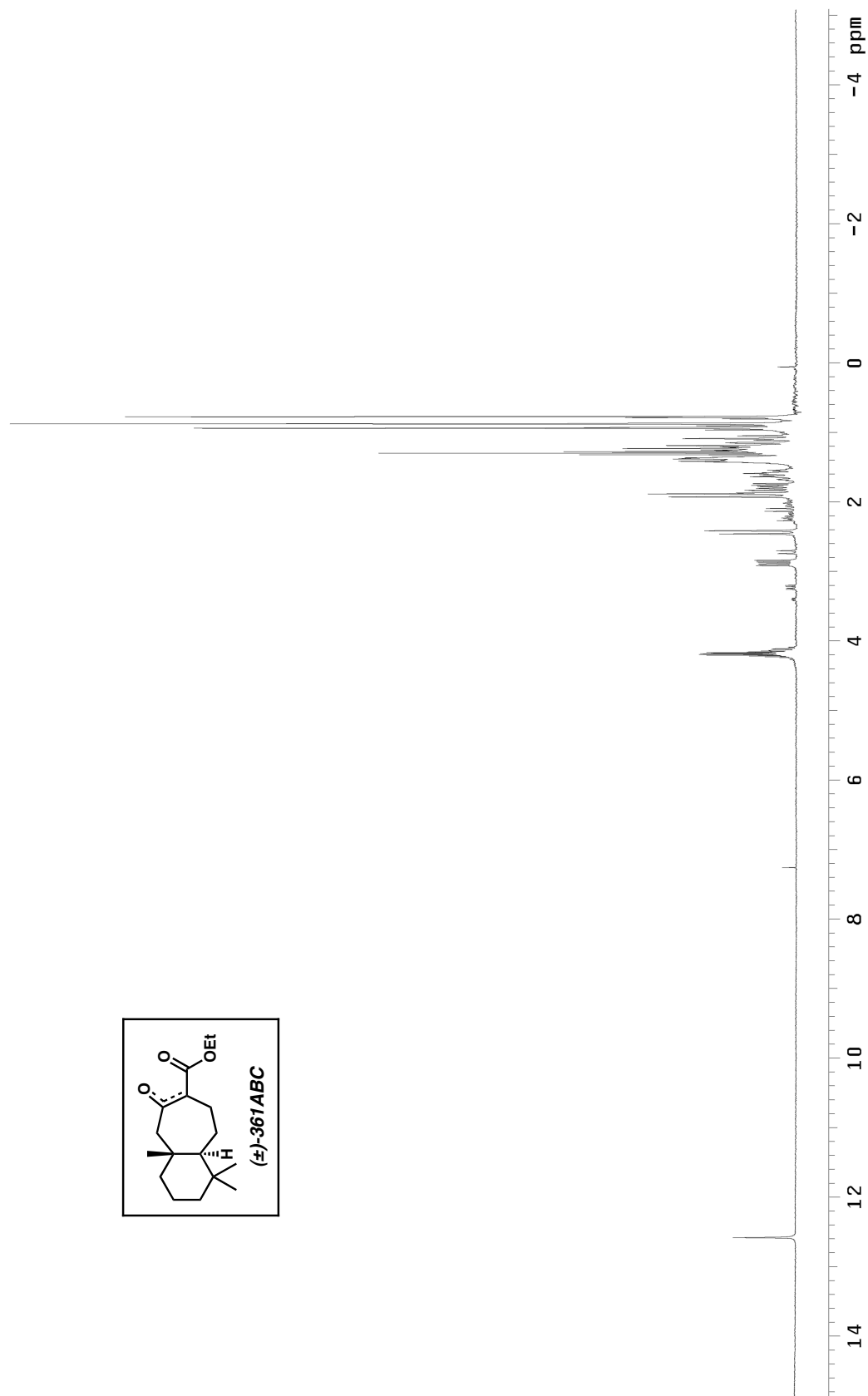


Figure A7.73 ^1H NMR (300 MHz, CDCl_3) of compounds 361A, 361B, and 361C.

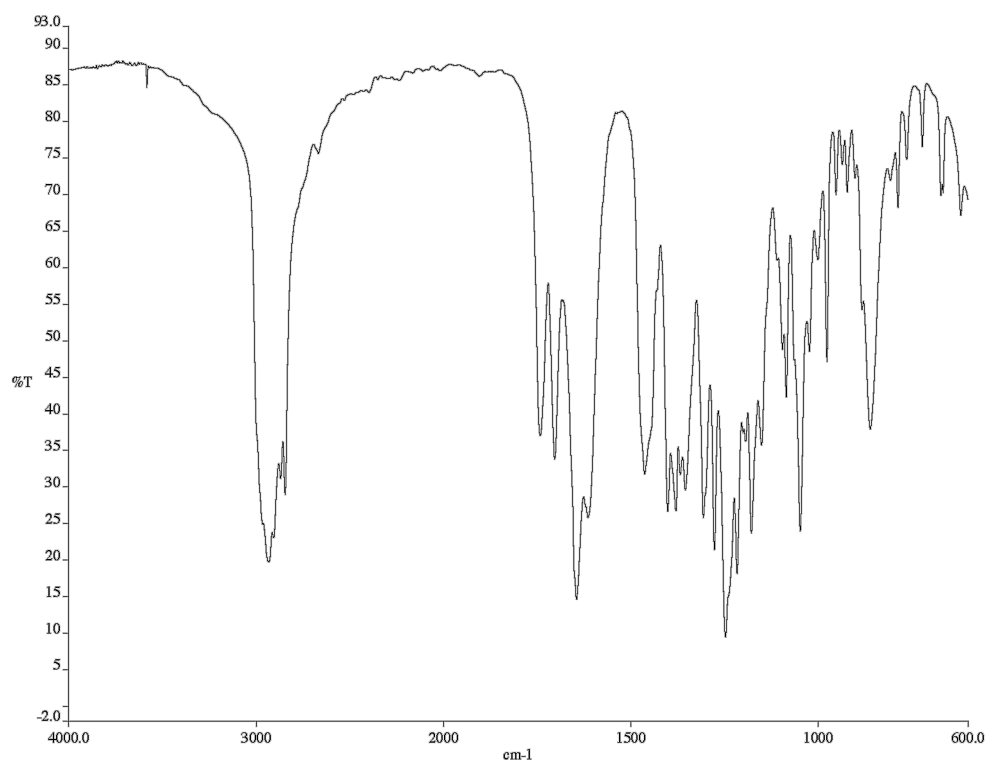


Figure A7.74 Infrared spectrum (NaCl/CDCl₃) of compounds **361A**, **361B**, and **361C**.

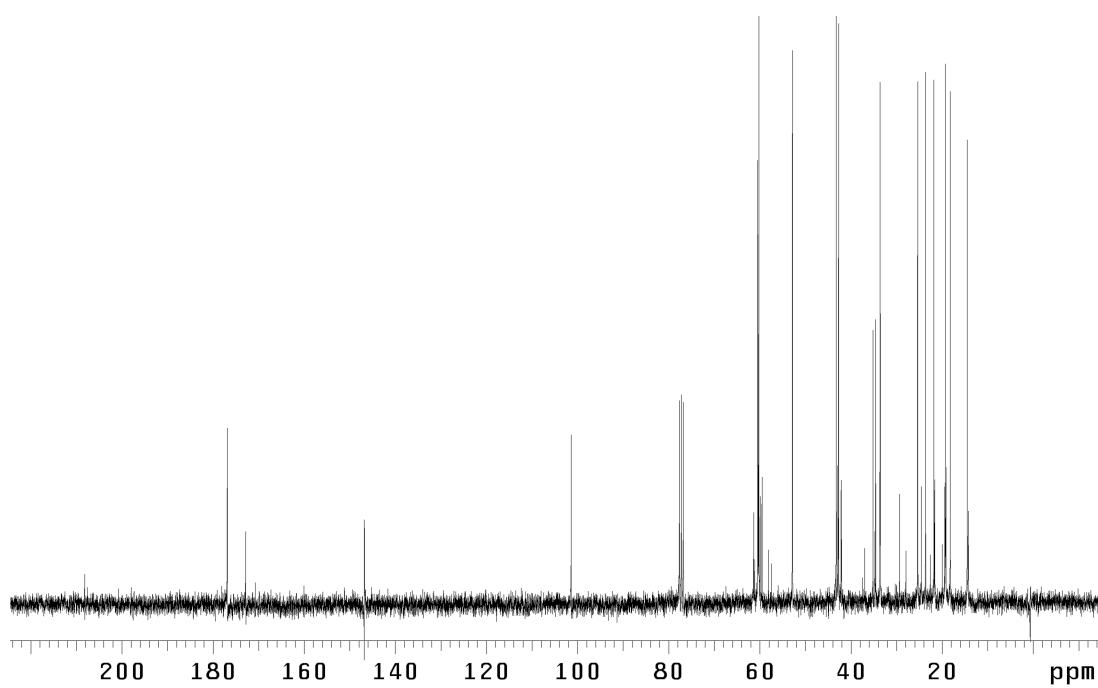


Figure A7.75 ¹³C NMR (75 MHz, CDCl₃) of compound **361A**, **361B**, and **361C**.

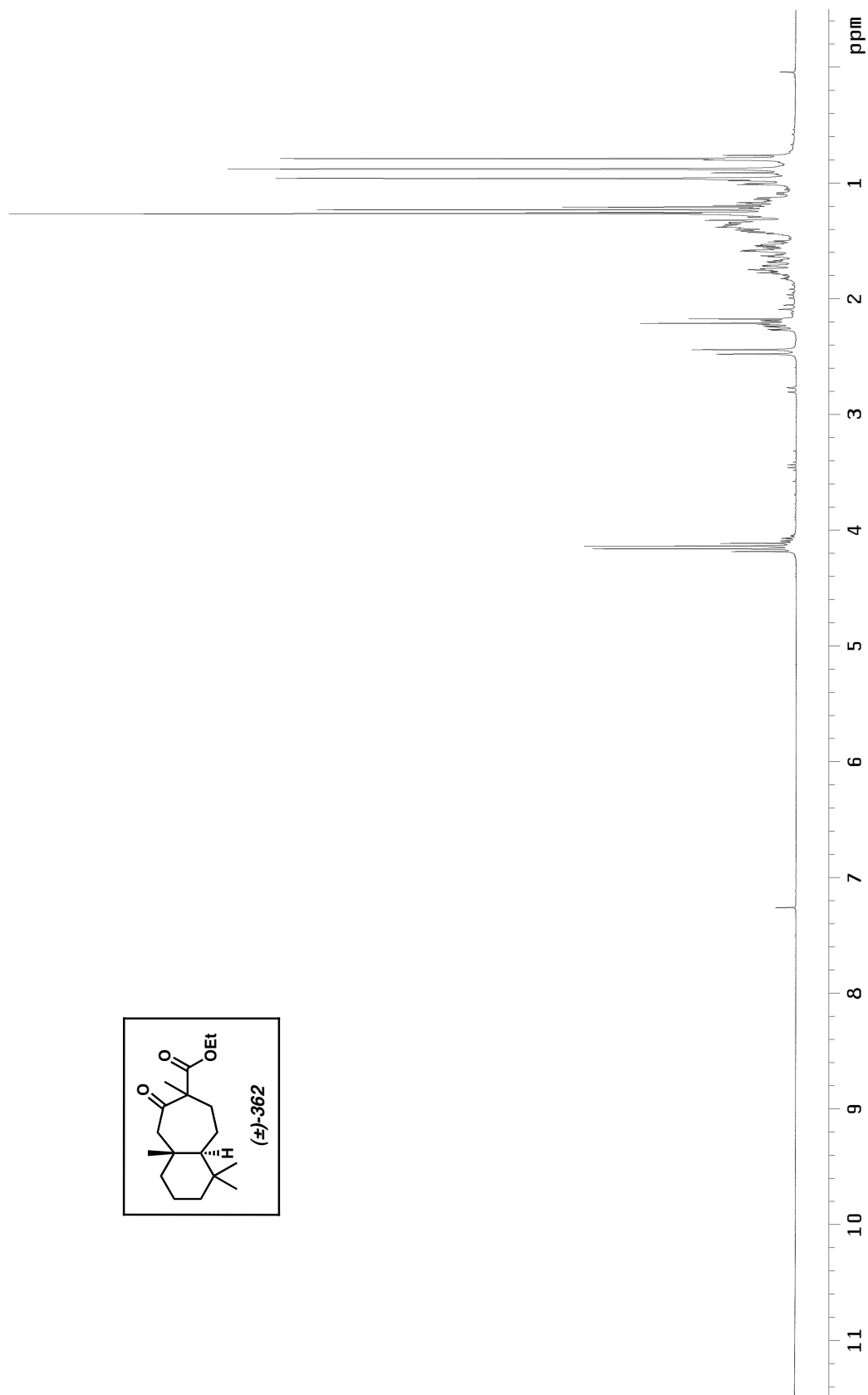


Figure A7.76 ^1H NMR (300 MHz, CDCl_3) of compound **362**.

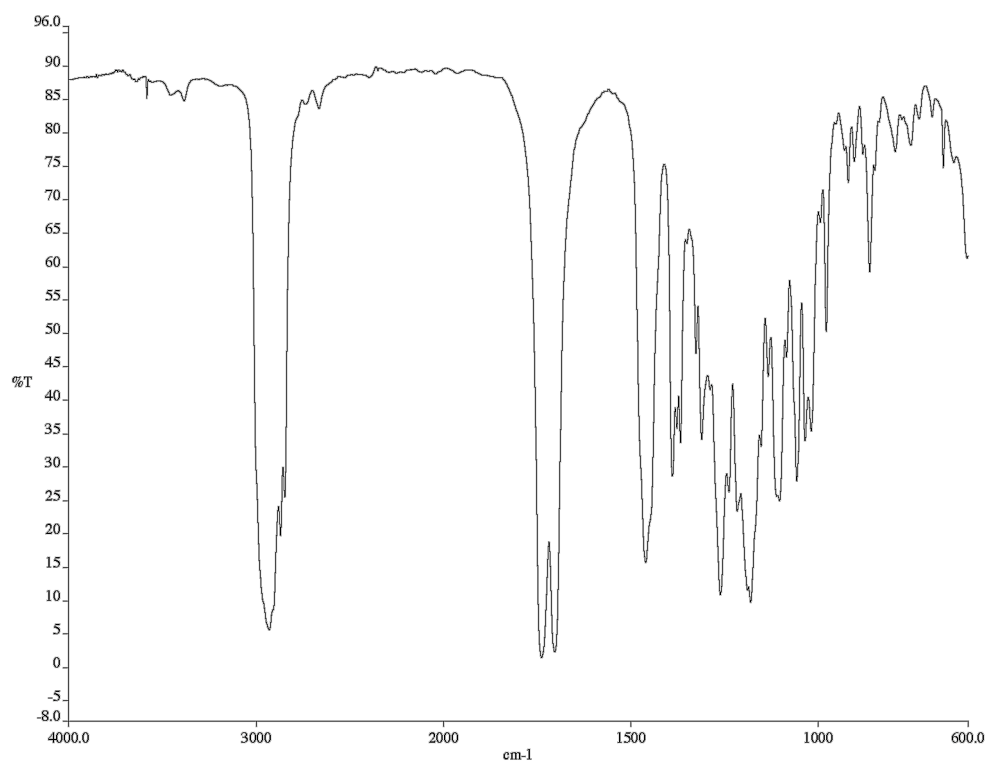


Figure A7.77 Infrared spectrum (NaCl/CDCl₃) of compound **362**.

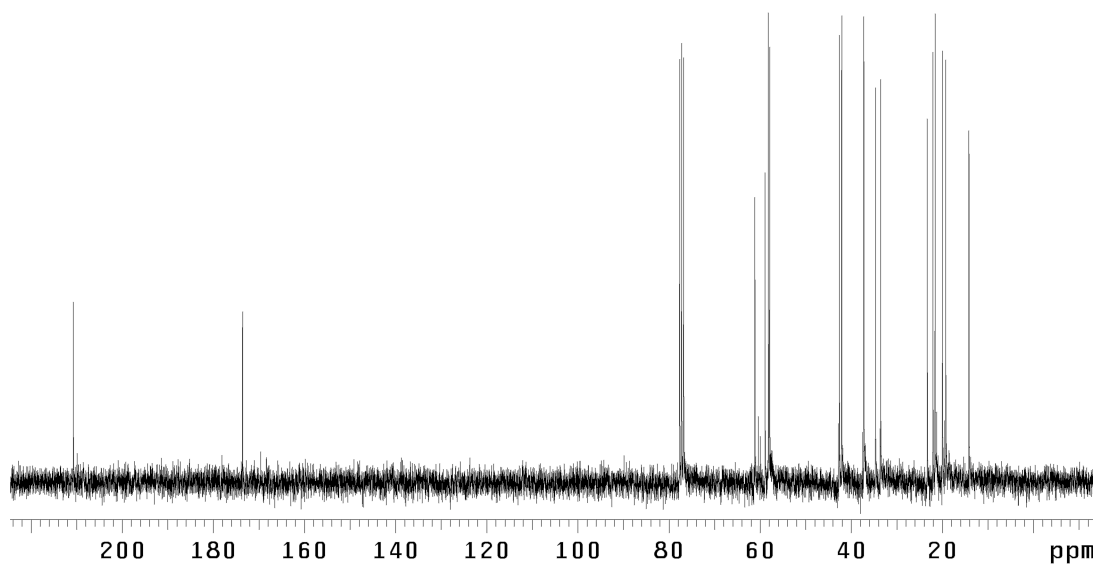


Figure A7.78 ¹³C NMR (75 MHz, CDCl₃) of compound **362**.

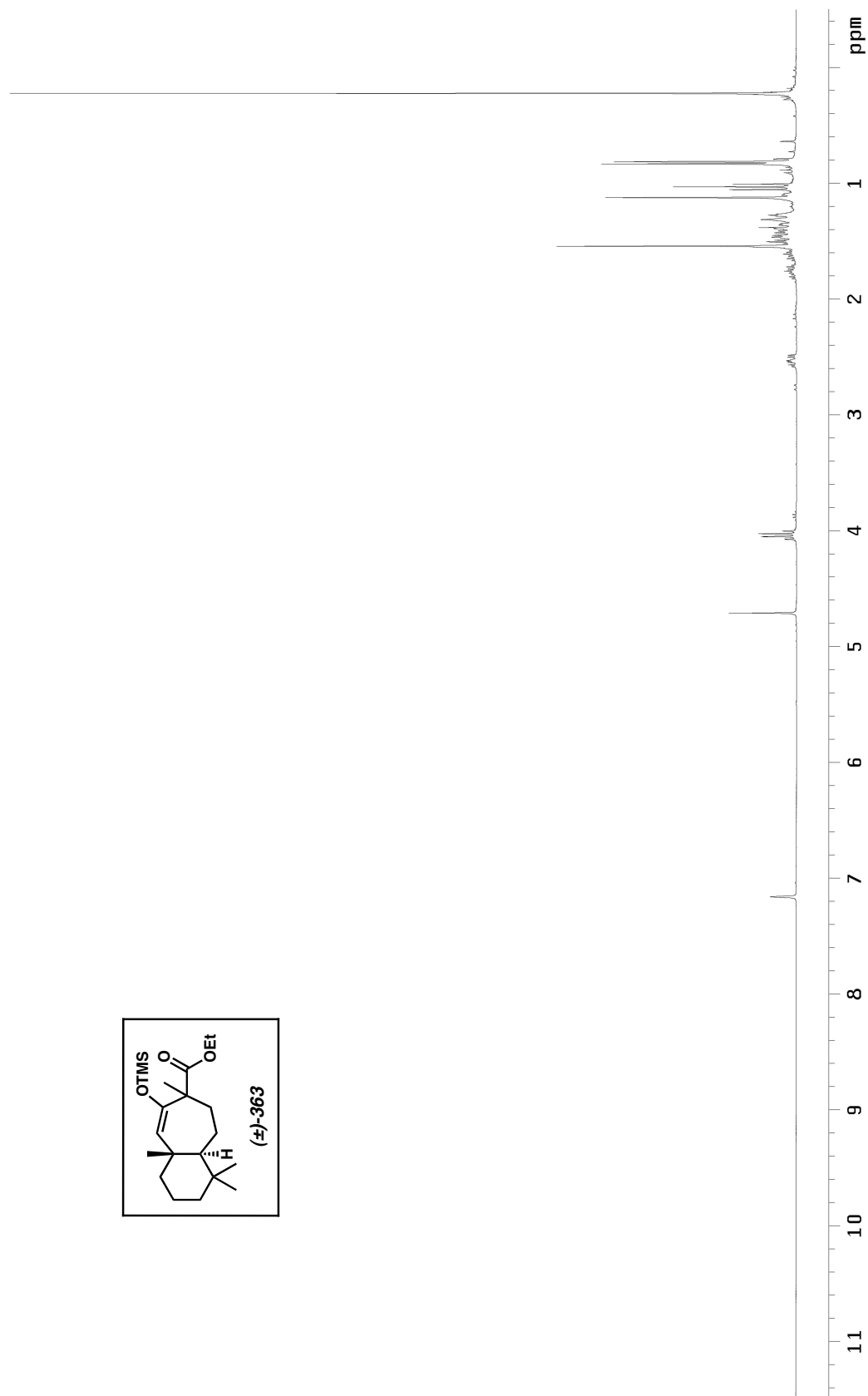


Figure A7.79 ^1H NMR (300 MHz, C_6D_6) of compound **363**.

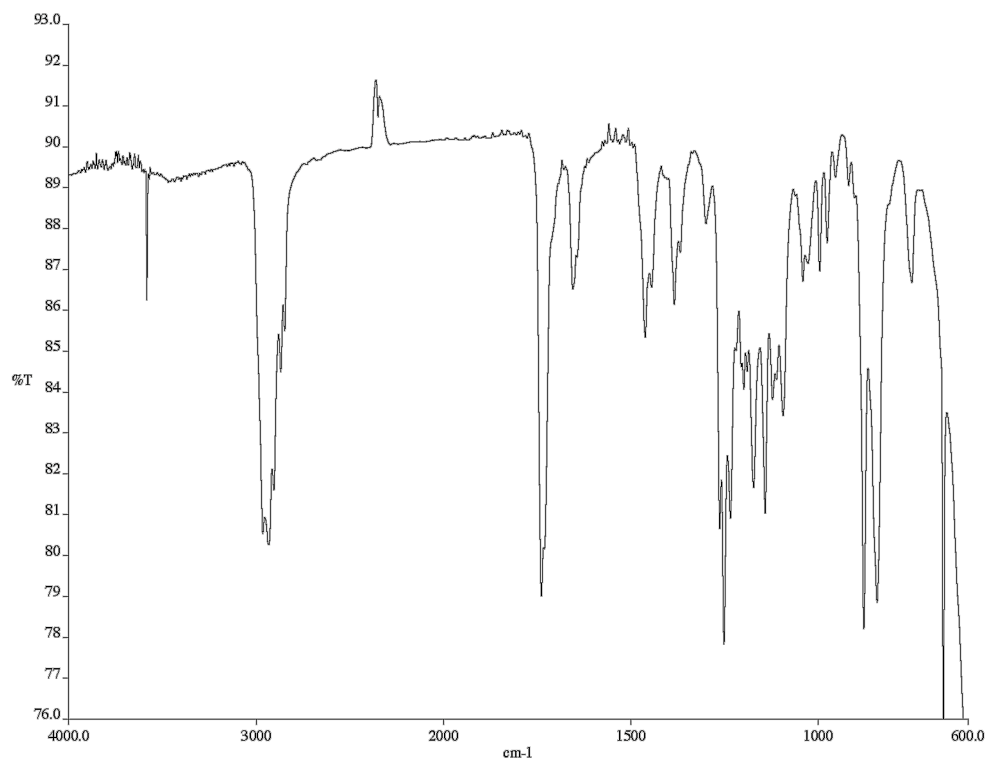


Figure A7.80 Infrared spectrum (NaCl/CH₂Cl₂) of compound **363**.

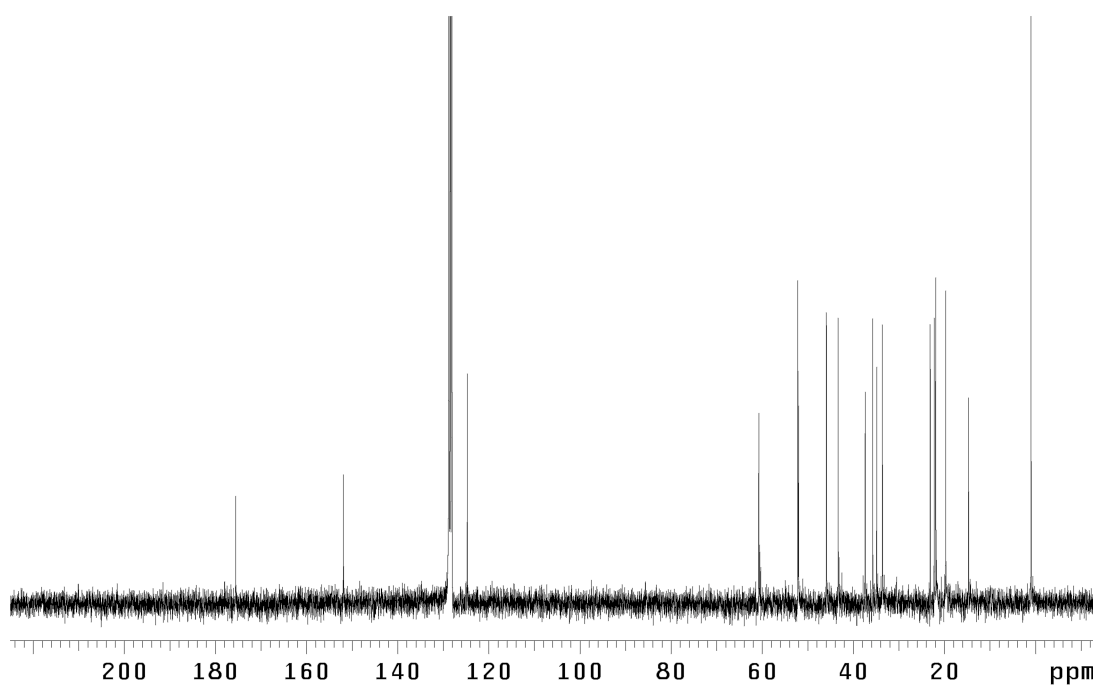
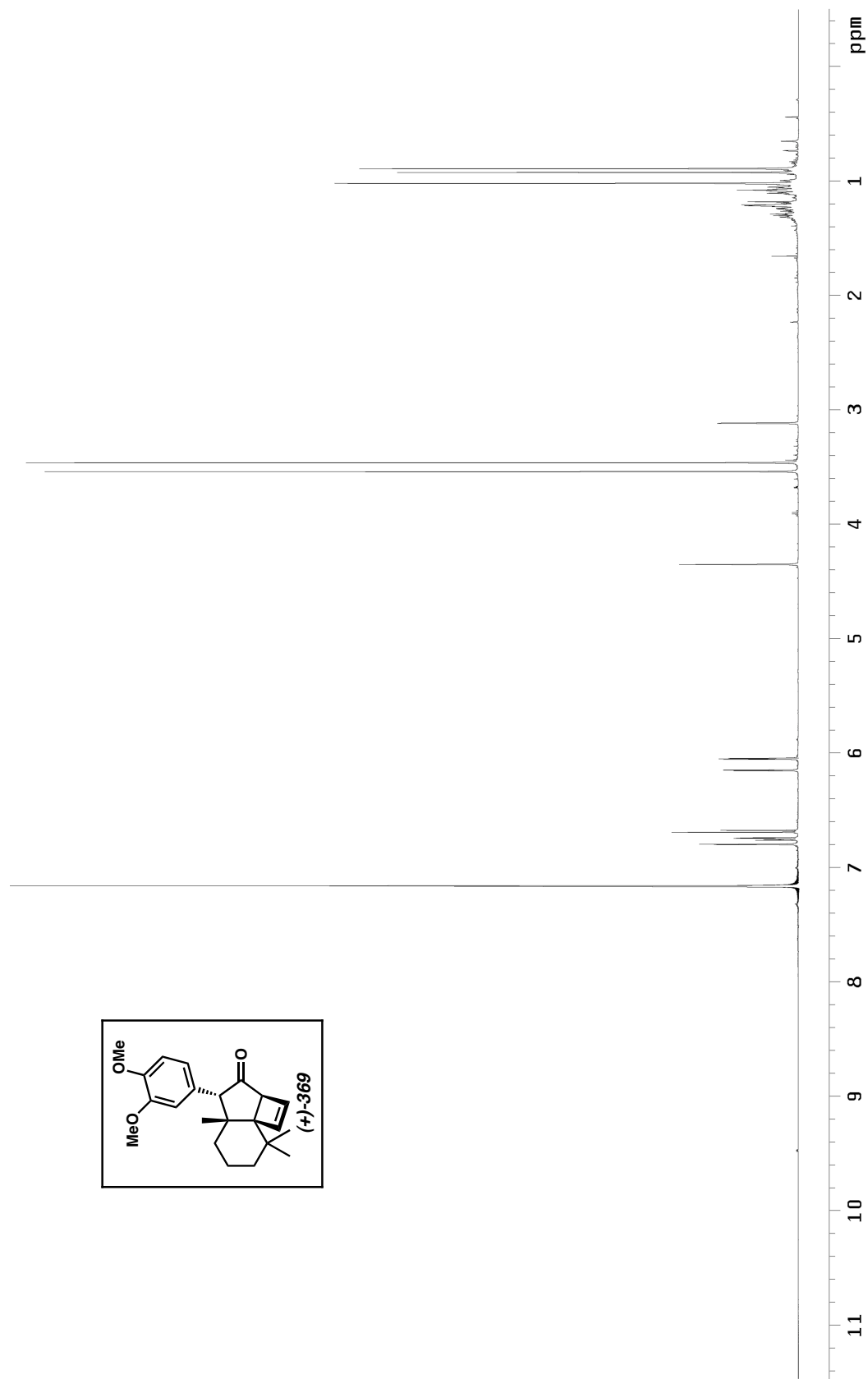


Figure A7.81 ¹³C NMR (75 MHz, C₆D₆) of compound **363**.

Figure A7.82 ^1H NMR (500 MHz, C_6D_6) of compound **369**.

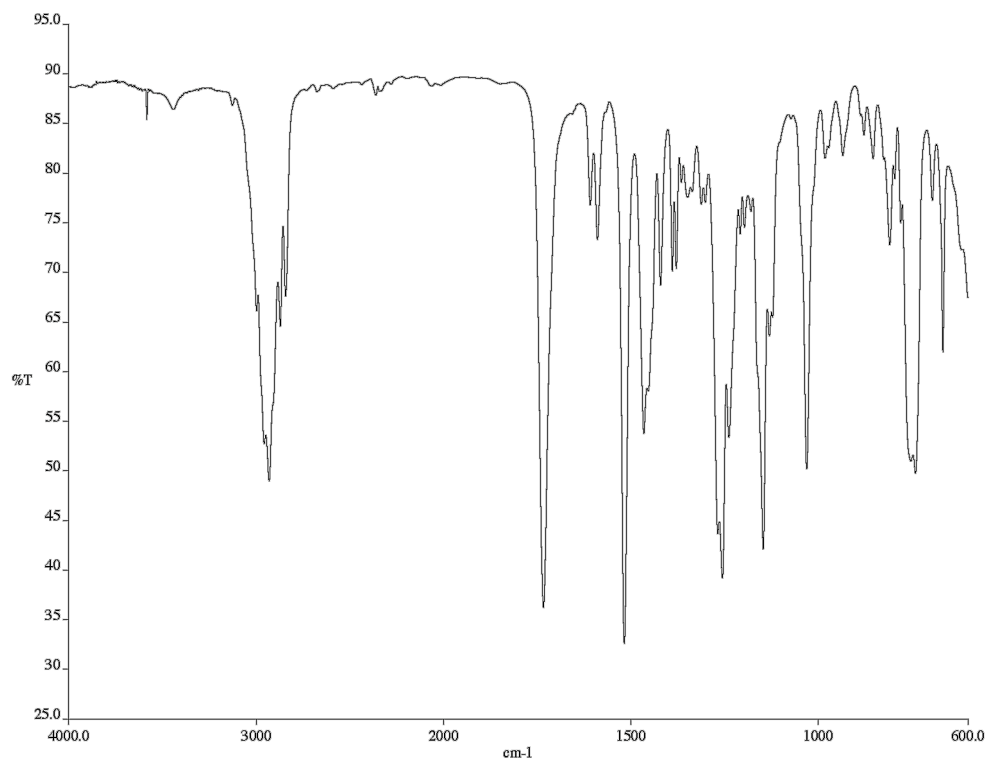


Figure A7.83 Infrared spectrum (NaCl/CHCl₃) of compound **369**.

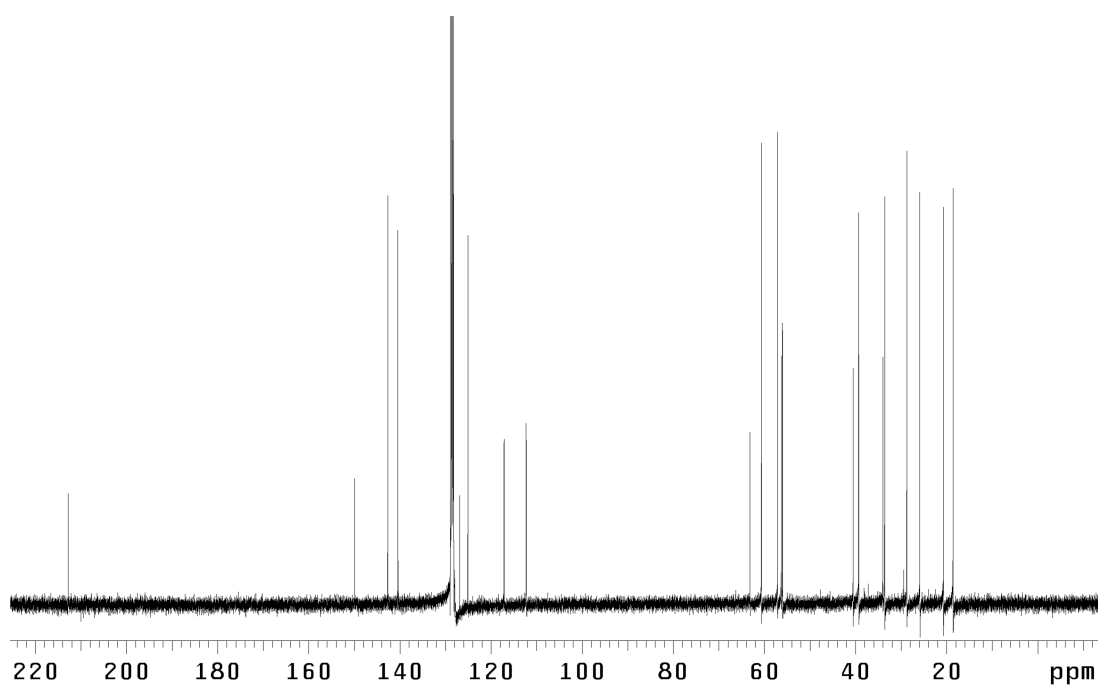
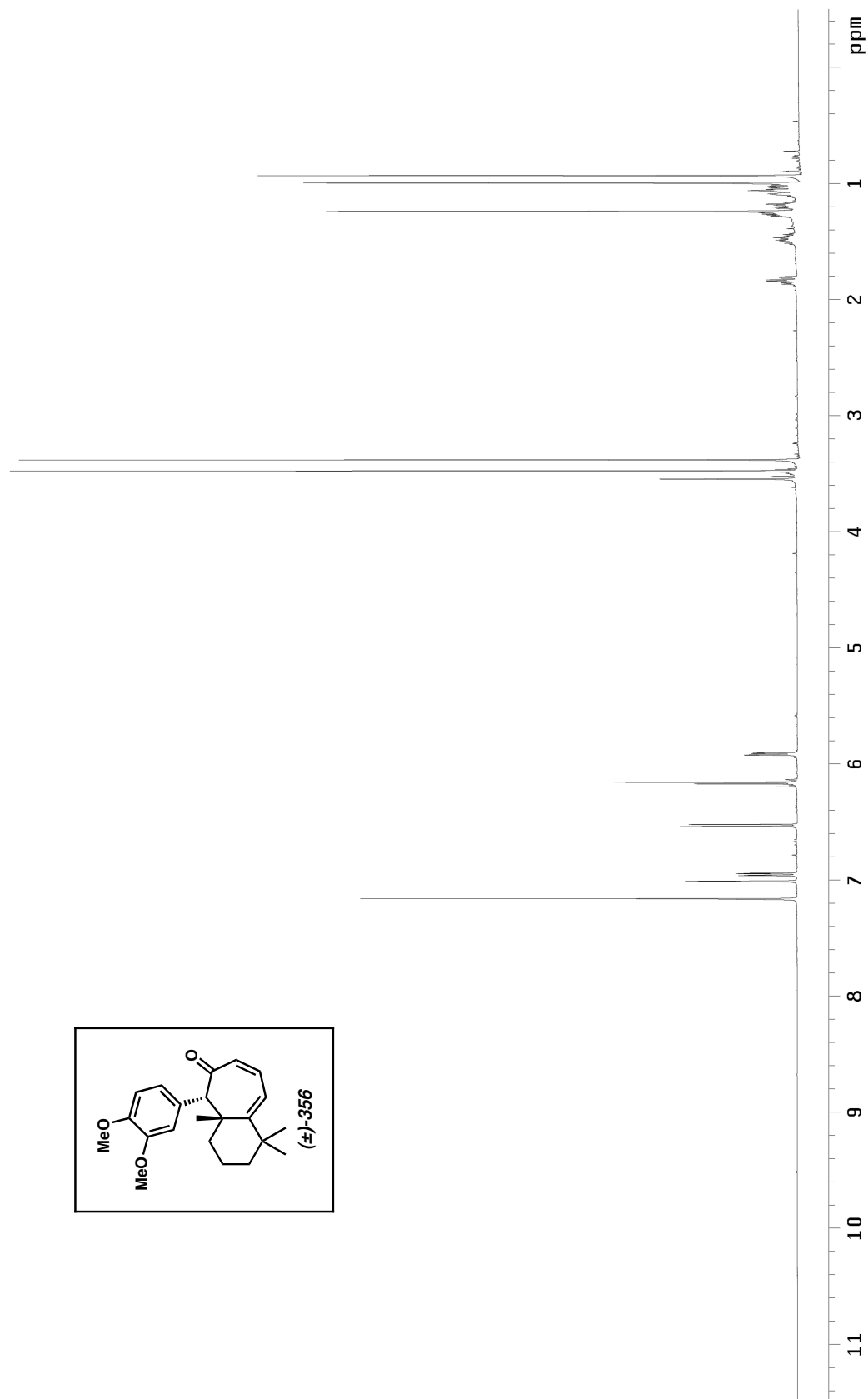


Figure A7.84 ¹³C NMR (125 MHz, C₆D₆) of compound **369**.

Figure A7.85 ^1H NMR (500 MHz, C_6D_6) of compound **356**.

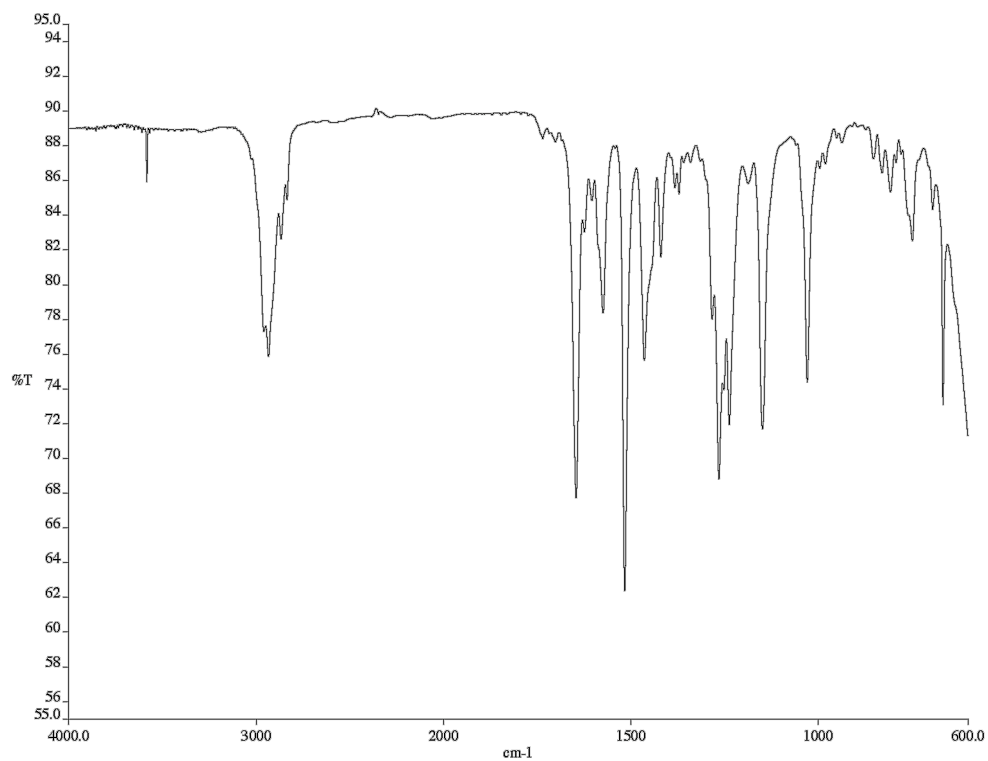


Figure A7.86 Infrared spectrum (NaCl/CHCl₃) of compound **356**.

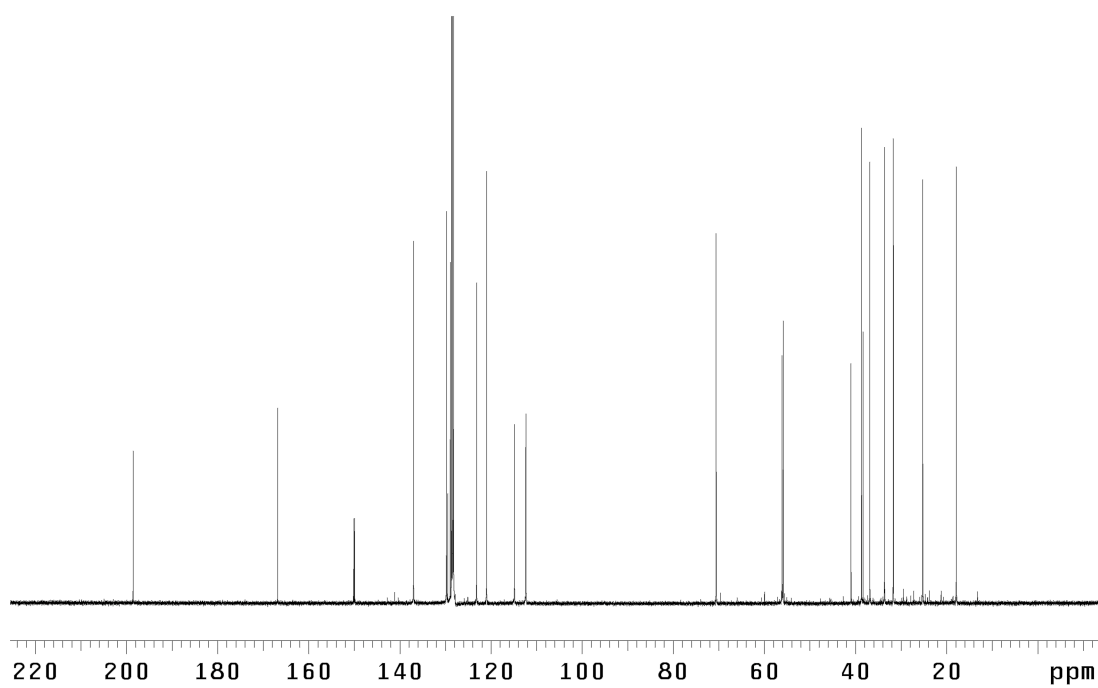
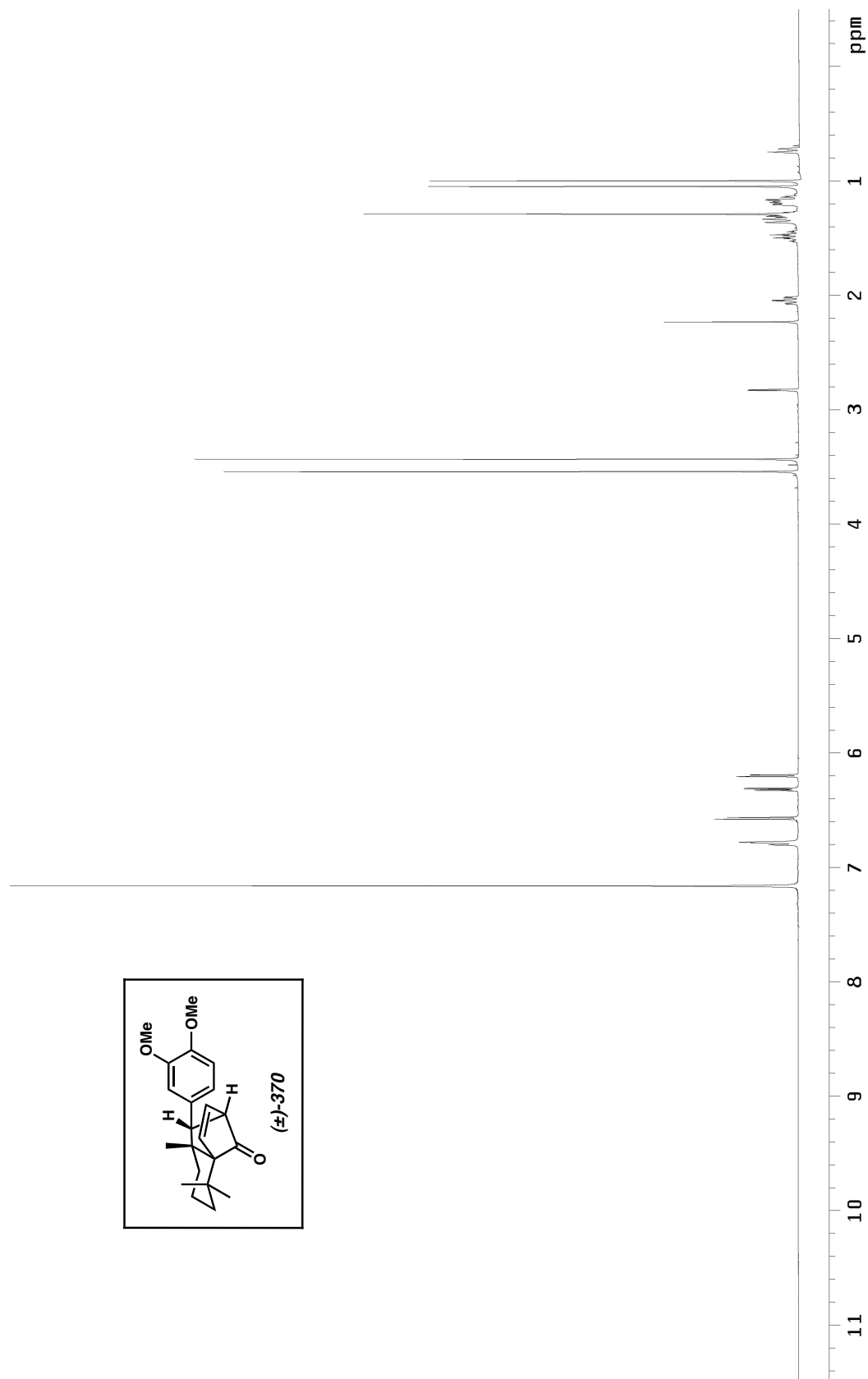


Figure A7.87 ¹³C NMR (125 MHz, C₆D₆) of compound **356**.

Figure A7.88 ¹H NMR (500 MHz, C₆D₆) of compound 370.

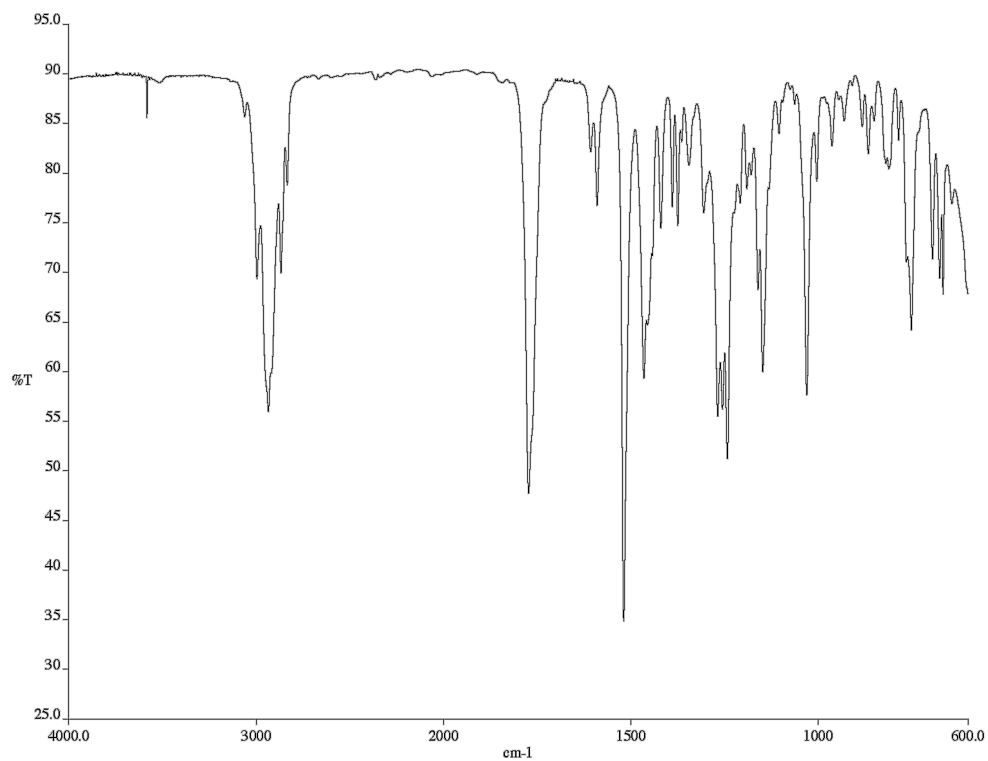


Figure A7.89 Infrared spectrum (NaCl/CHCl₃) of compound **370**.

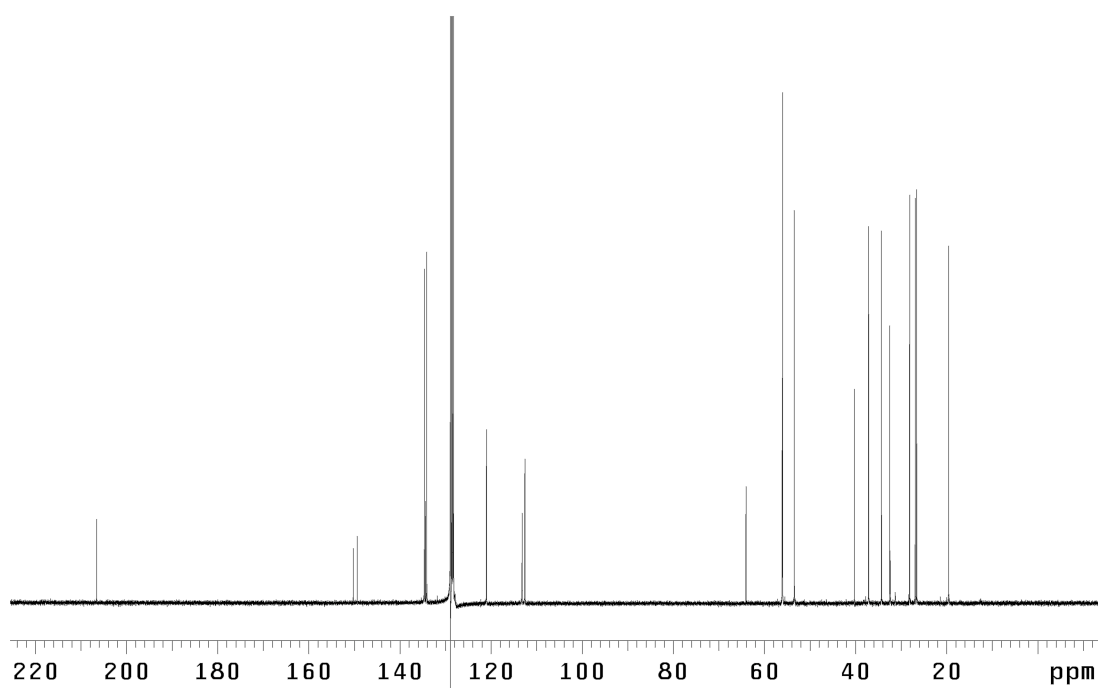
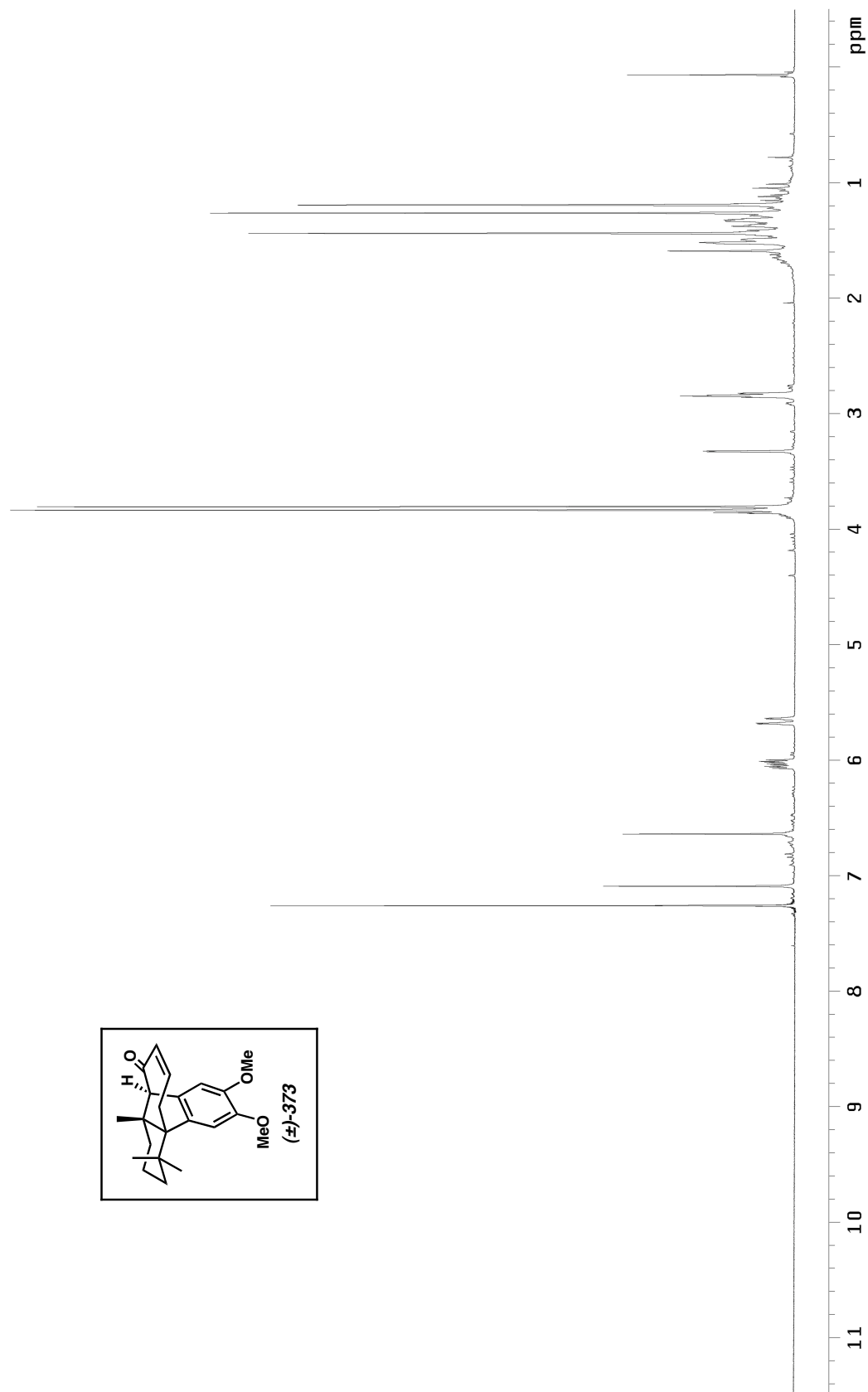


Figure A7.90 ¹³C NMR (125 MHz, C₆D₆) of compound **370**.



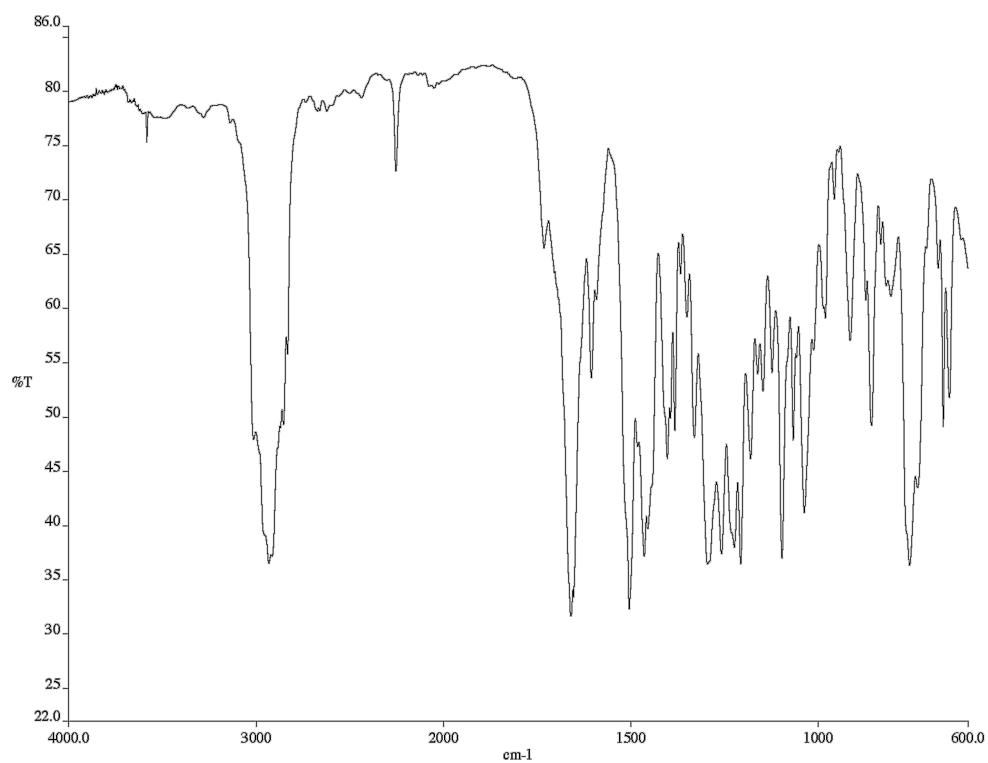


Figure A7.92 Infrared spectrum (NaCl/CDCl₃) of compound **373**.

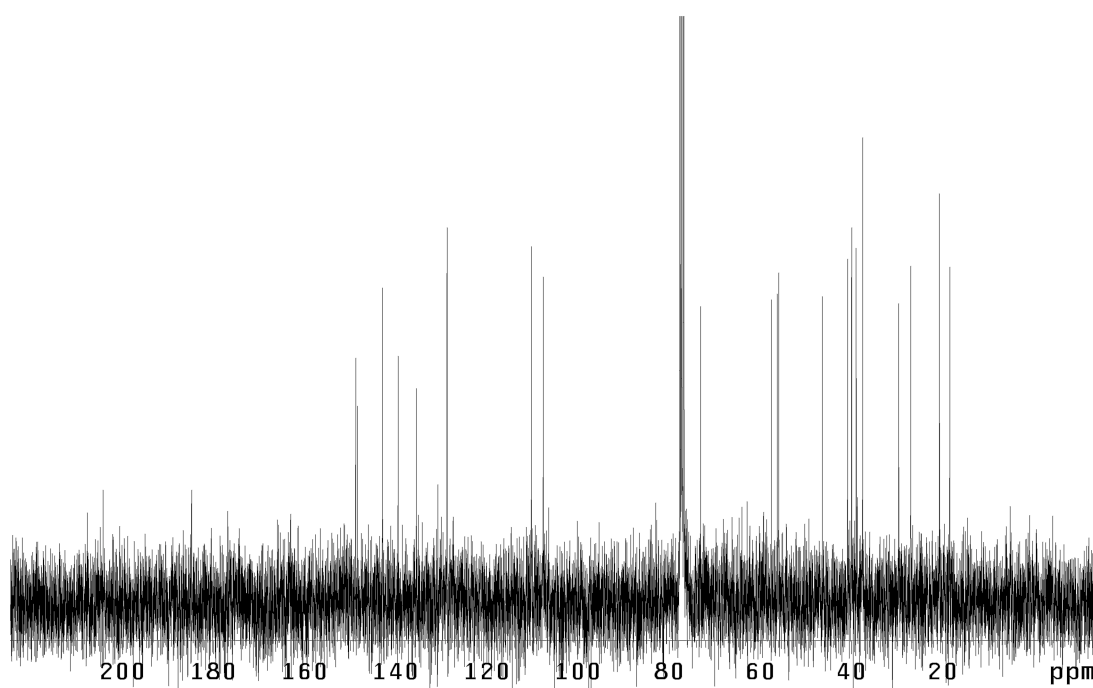
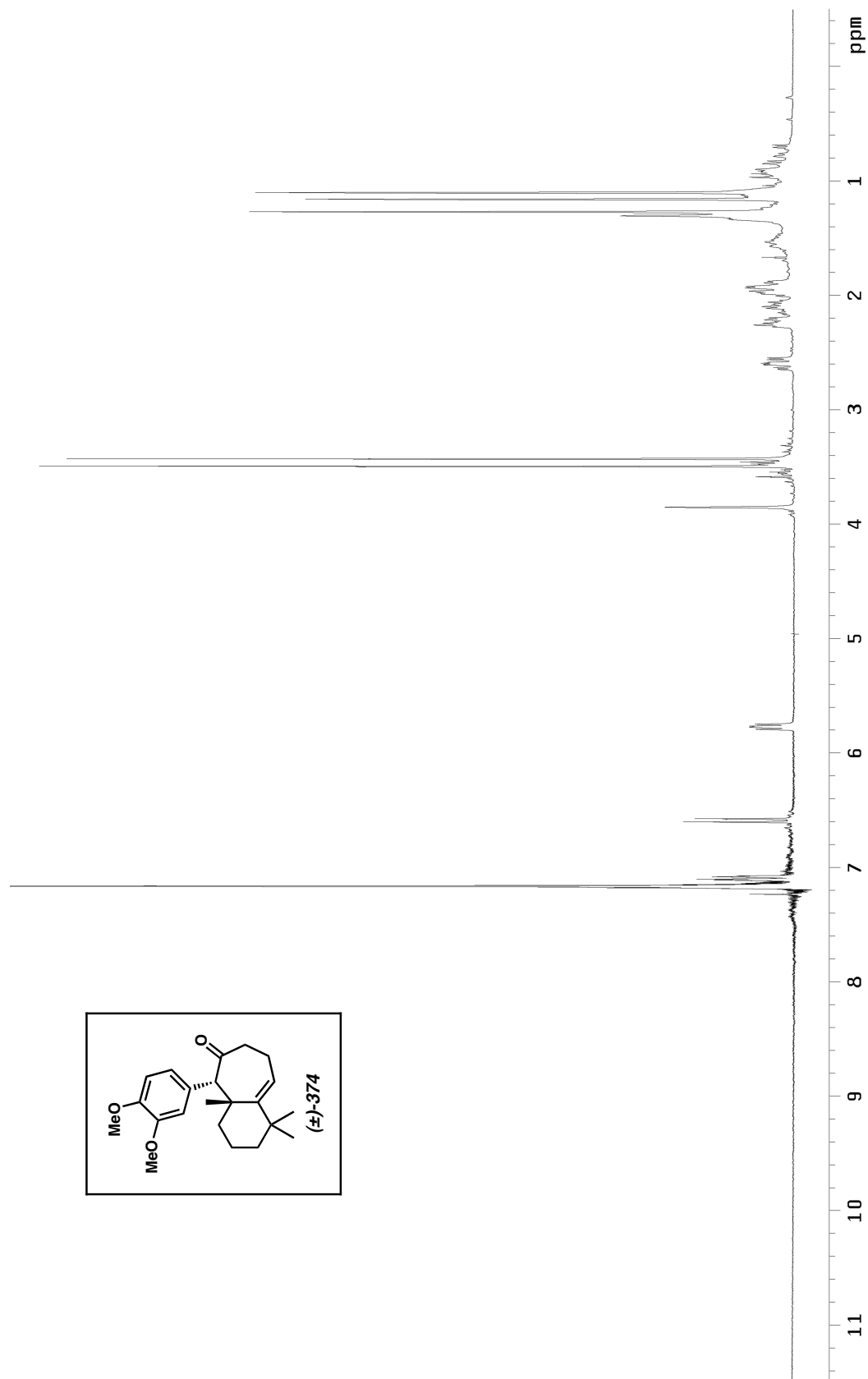


Figure A7.93 ¹³C NMR (75 MHz, CDCl₃) of compound **373**.

Figure A7.94 ^1H NMR (300 MHz, C_6D_6) of compound **374**.

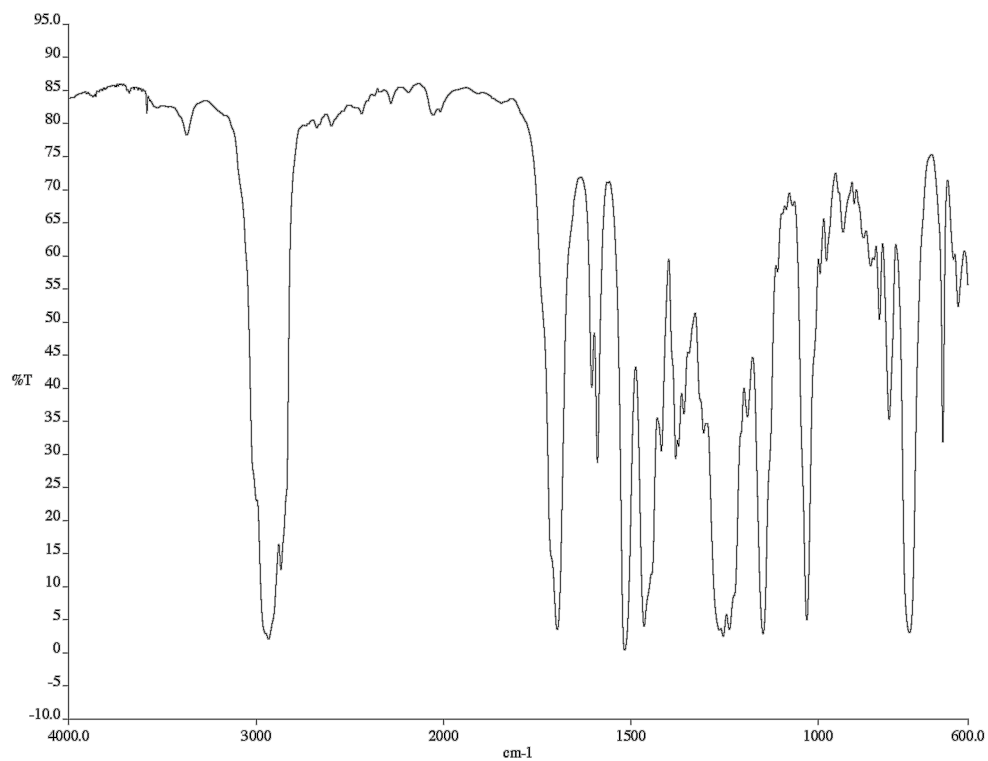


Figure A7.95 Infrared spectrum (NaCl/CHCl₃) of compound **374**.

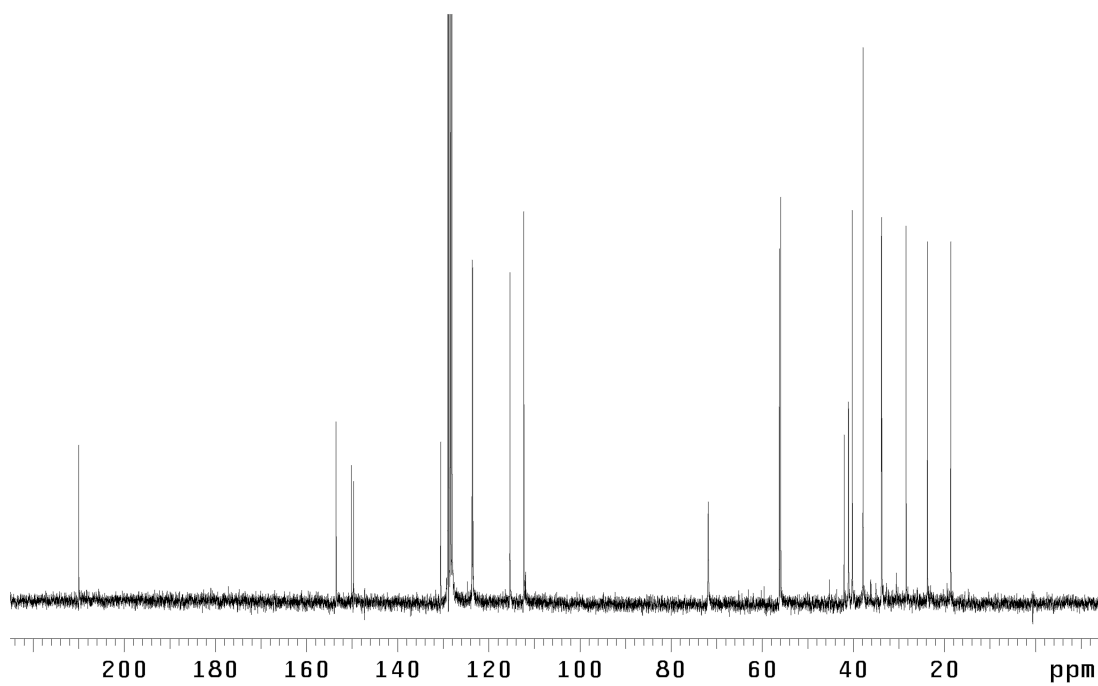


Figure A7.96 ¹³C NMR (75 MHz, C₆D₆) of compound **374**.

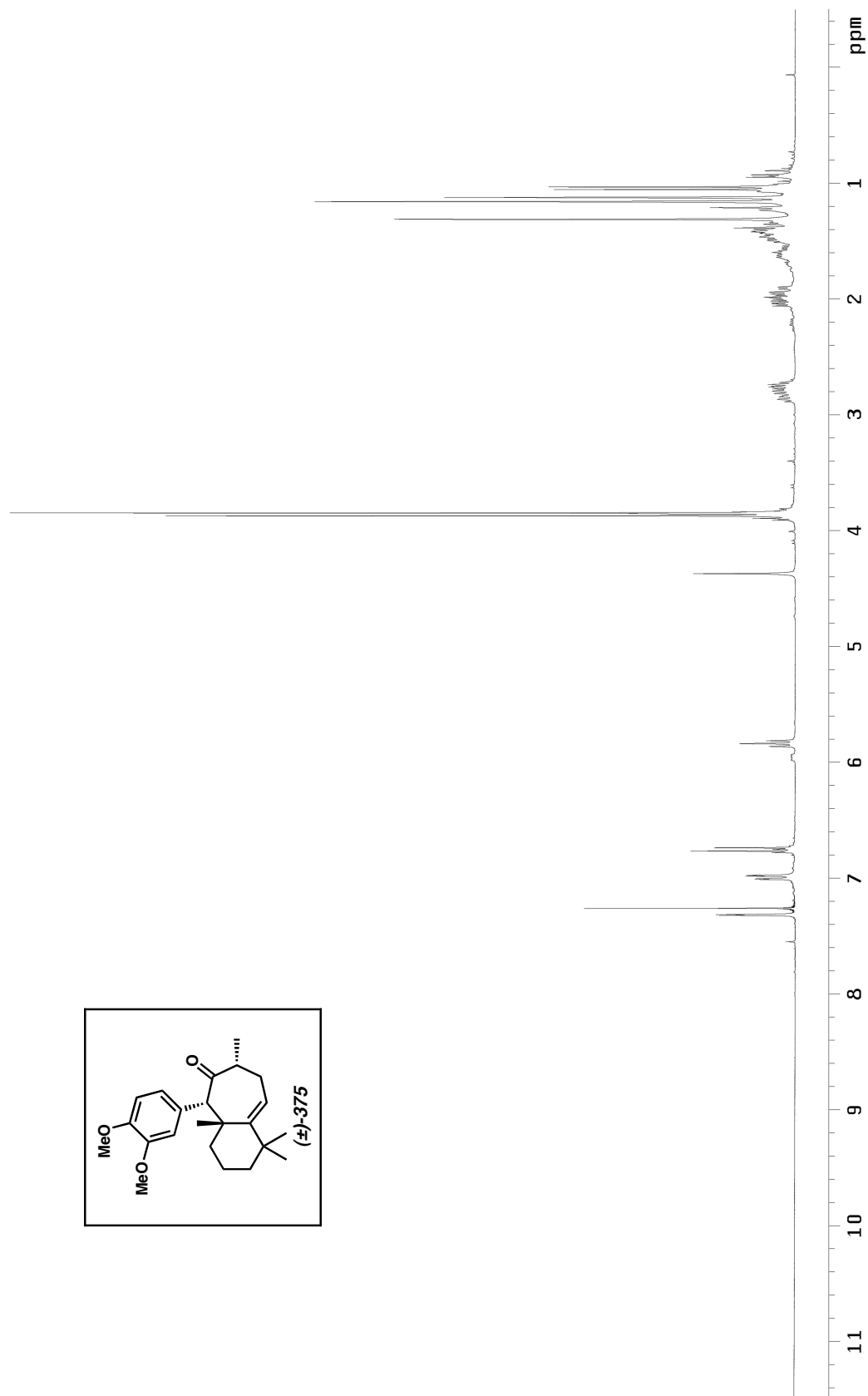


Figure A7.97 ^1H NMR (300 MHz, CDCl_3) of compound **375**.

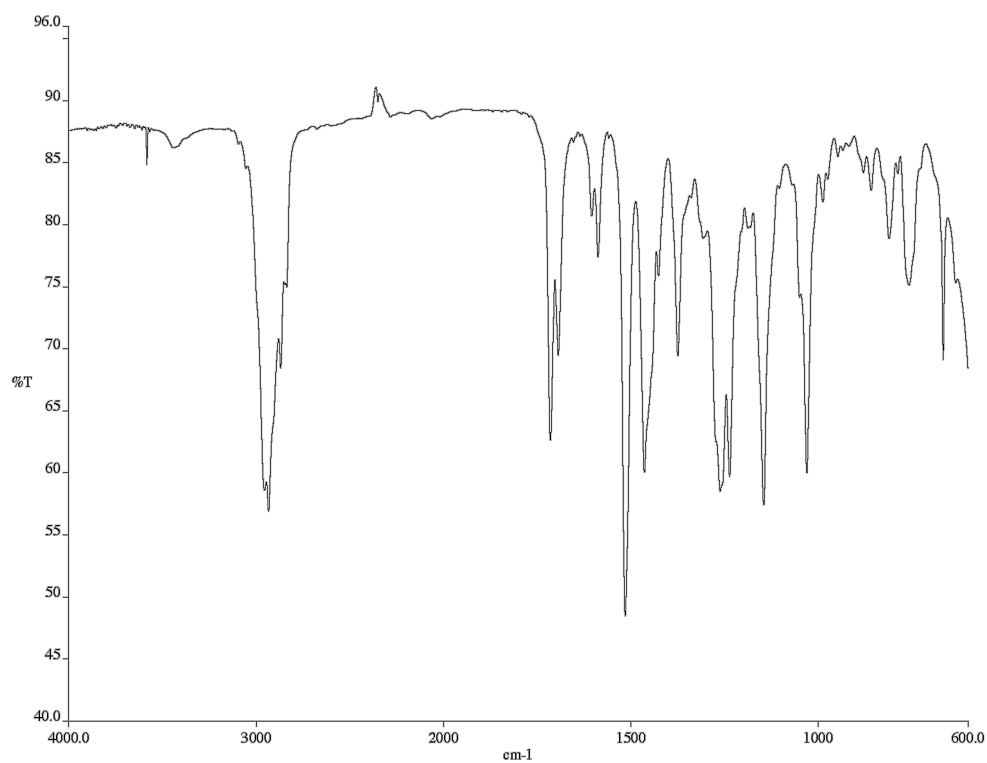


Figure A7.98 Infrared spectrum (NaCl/CHCl₃) of compound **375**.

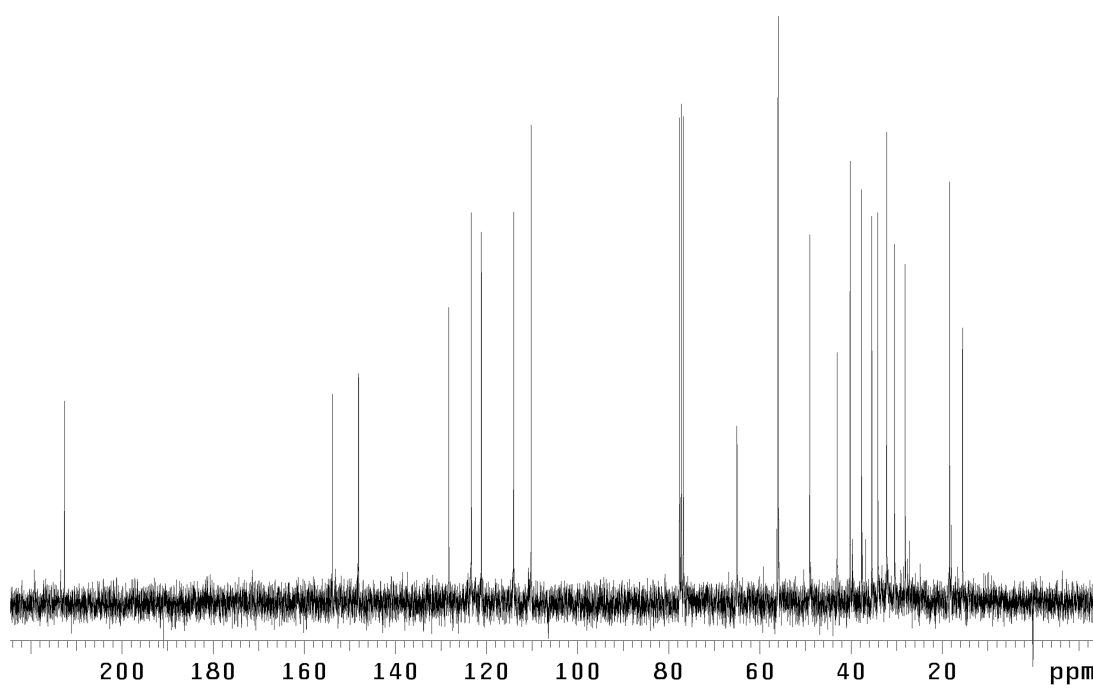


Figure A7.99 ¹³C NMR (75 MHz, CDCl₃) of compound **375**.

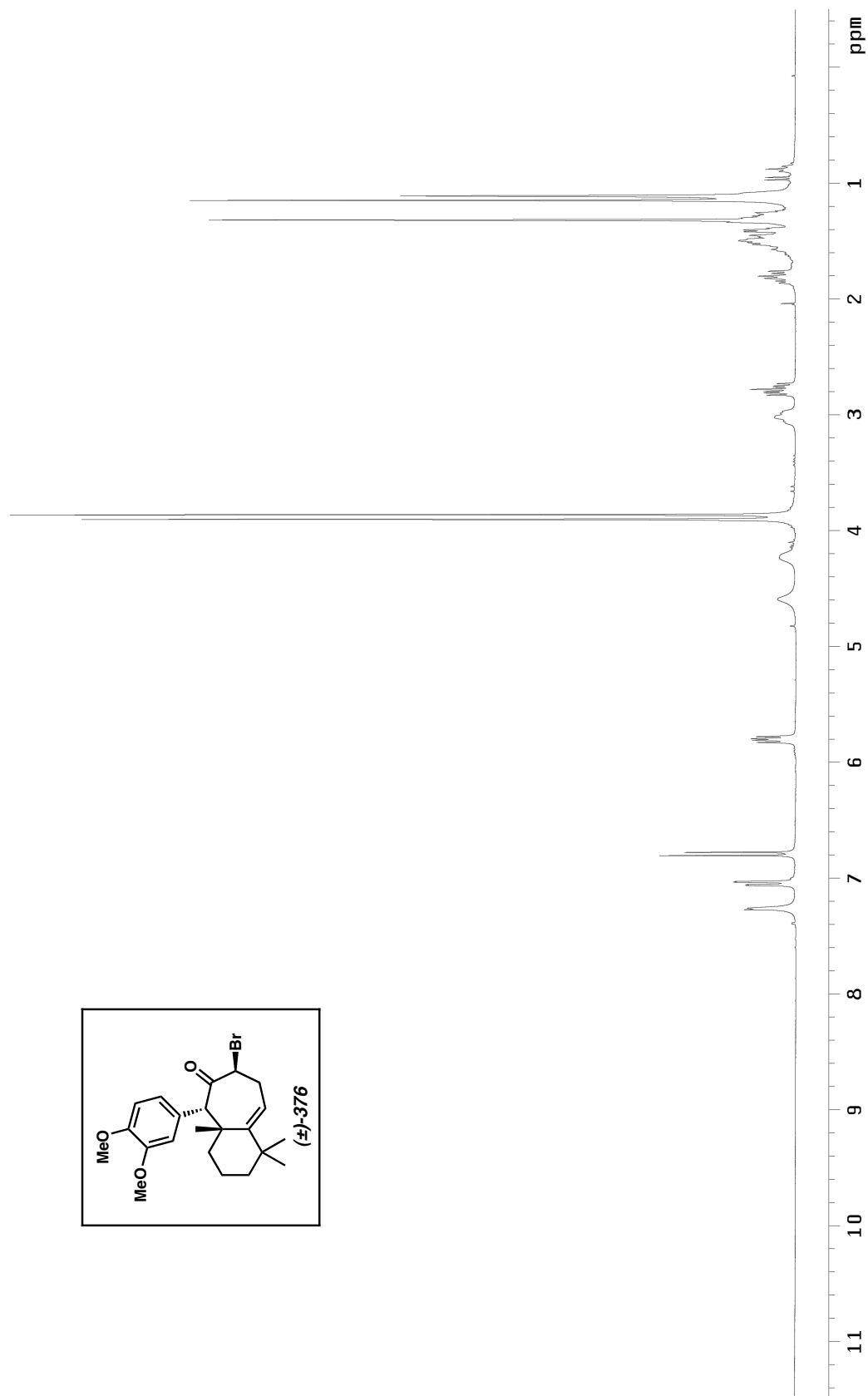


Figure A7.100 ^1H NMR (300 MHz, CDCl_3) of compound **376**.

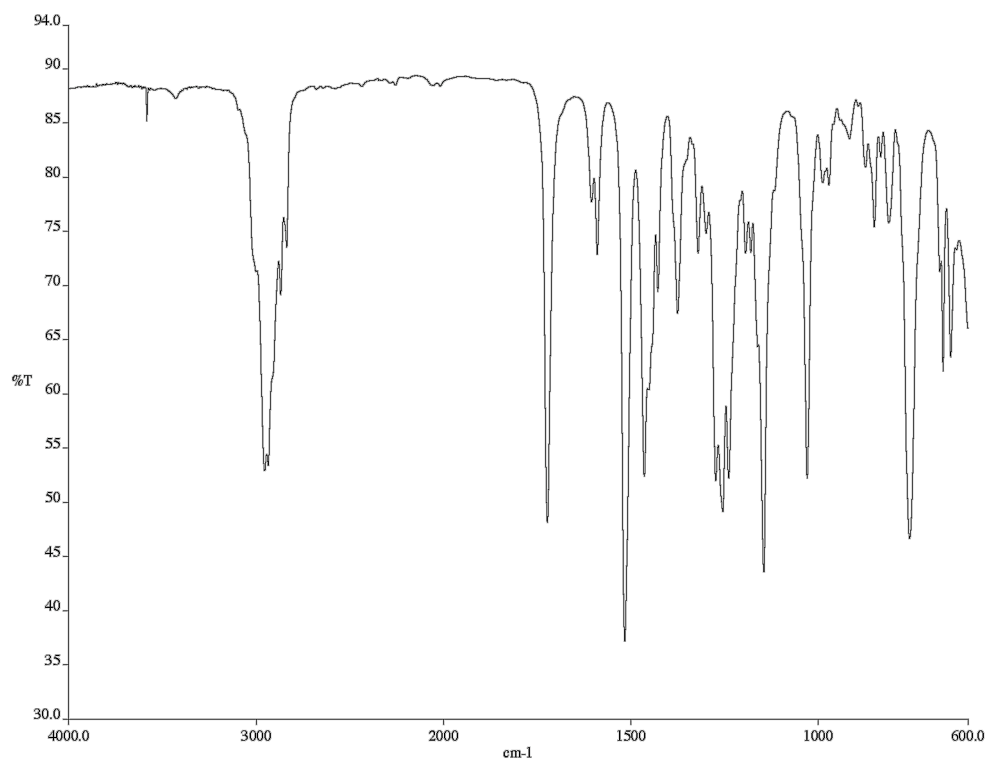


Figure A7.101 Infrared spectrum (NaCl/CHCl₃) of compound **376**.

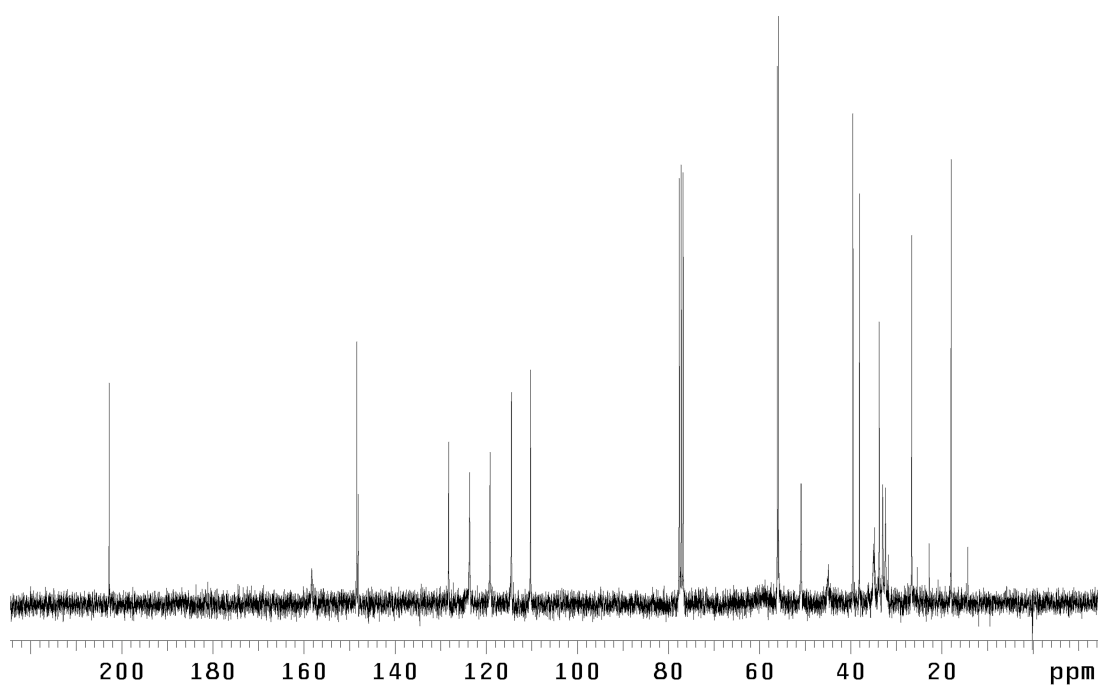


Figure A7.102 ¹³C NMR (75 MHz, CDCl₃) of compound **376**.

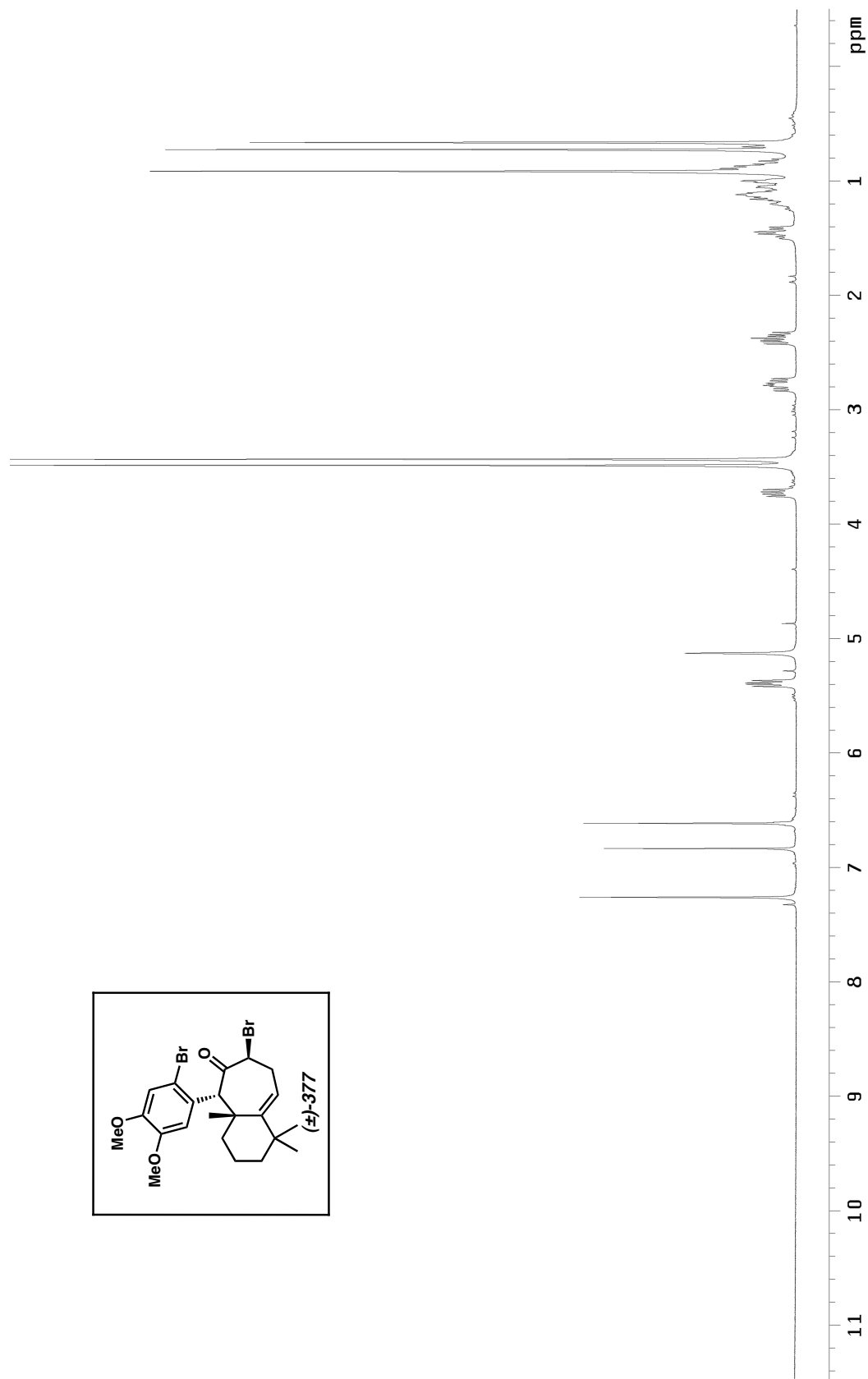


Figure A7.103 ^1H NMR (300 MHz, CDCl_3) of compound **377**.

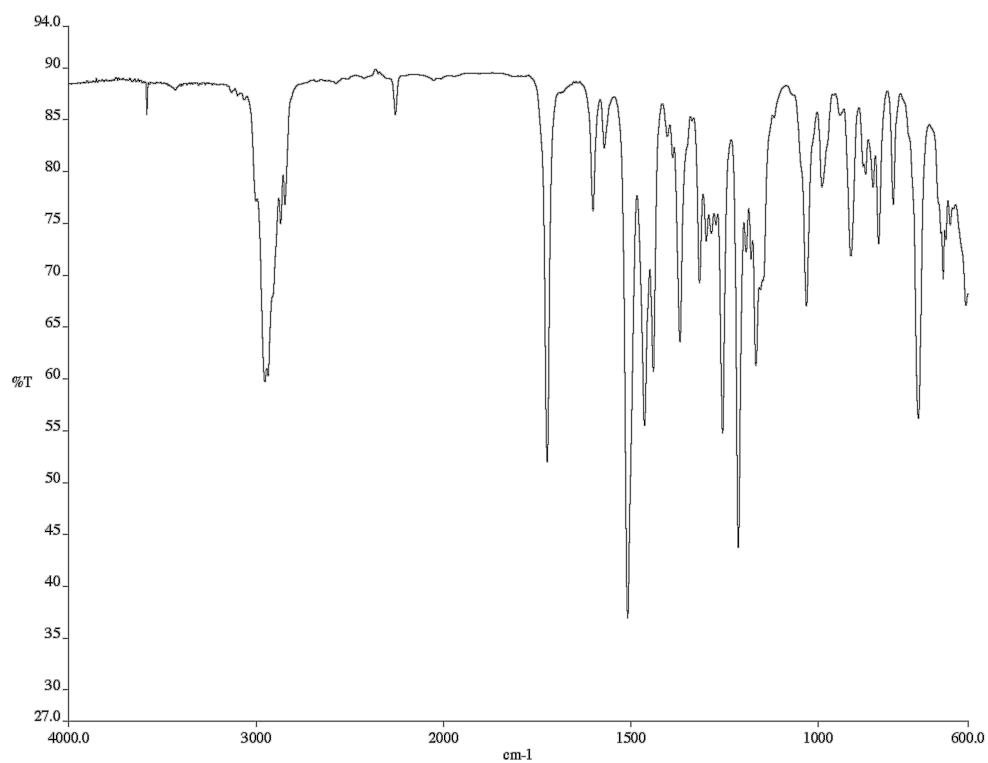


Figure A7.104 Infrared spectrum (NaCl/CDCl₃) of compound **377**.

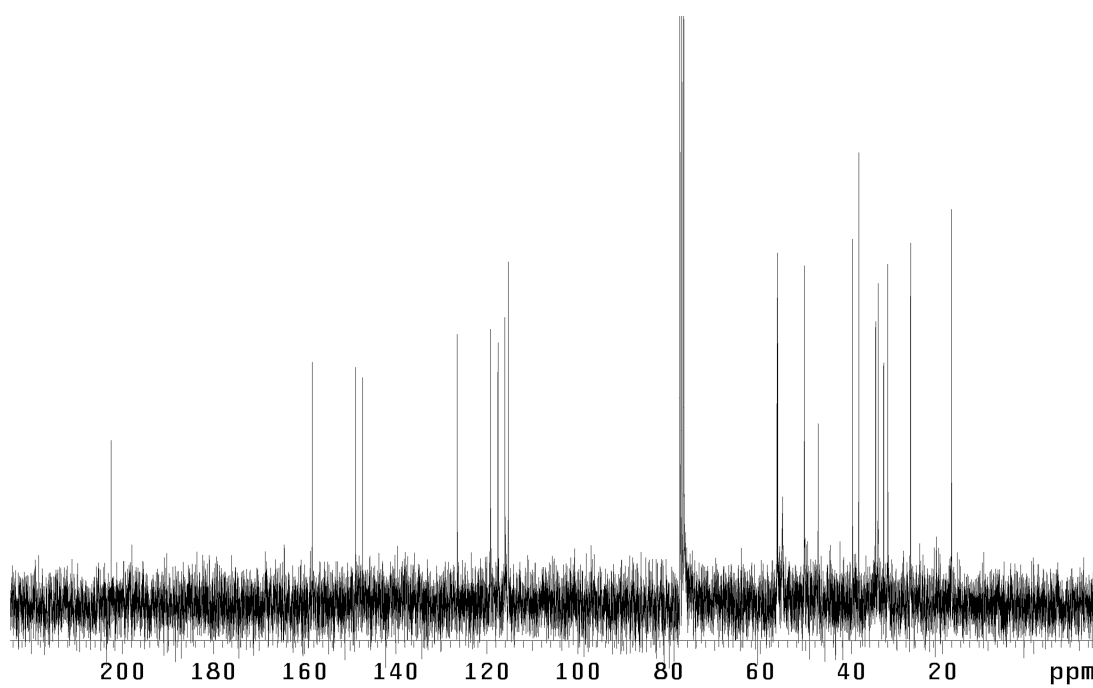


Figure A7.105 ¹³C NMR (75 MHz, CDCl₃) of compound **377**.



Figure A7.106 ^1H NMR (300 MHz, CDCl_3) of compound **379**.

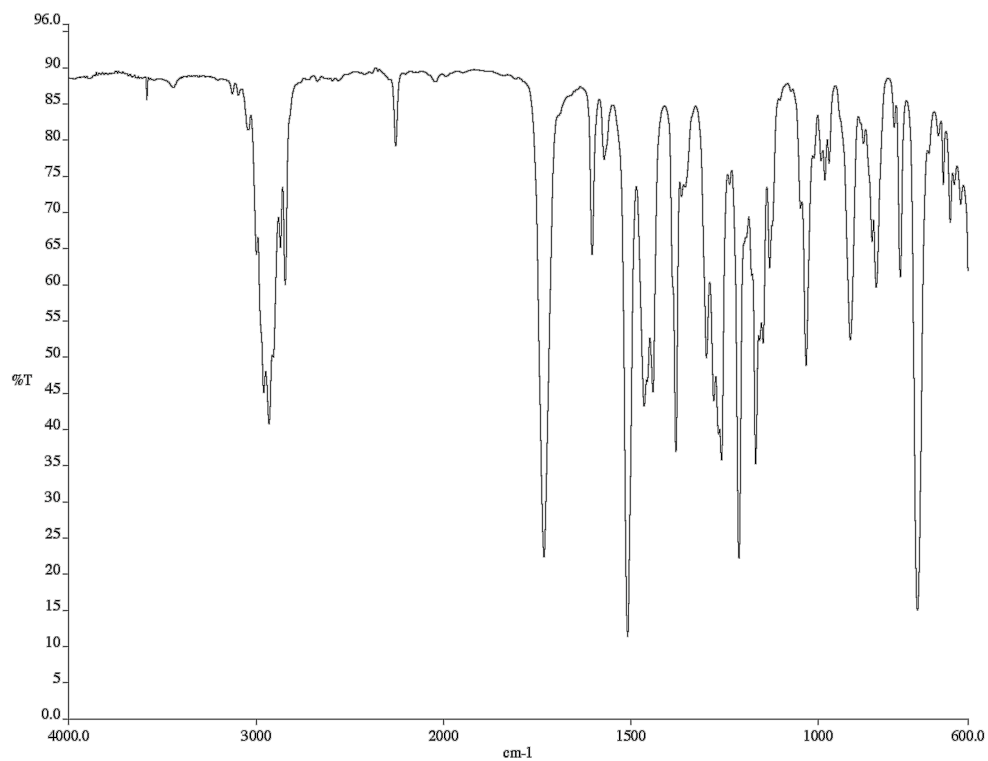


Figure A7.107 Infrared spectrum (NaCl/CDCl₃) of compound **379**.

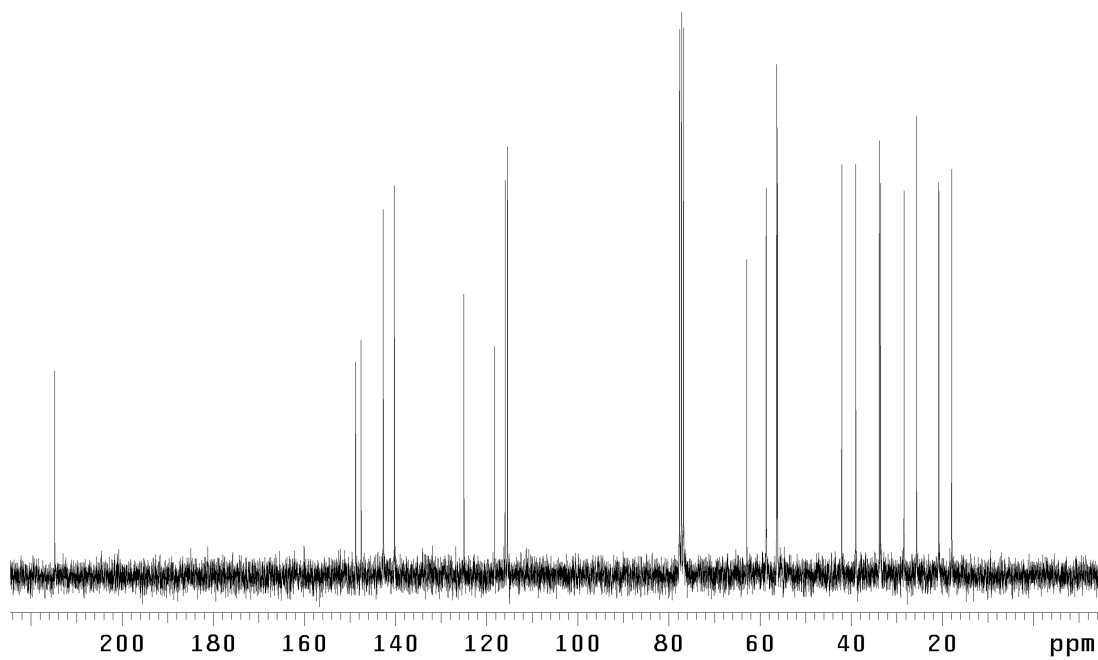


Figure A7.108 ¹³C NMR (75 MHz, CDCl₃) of compound **379**.

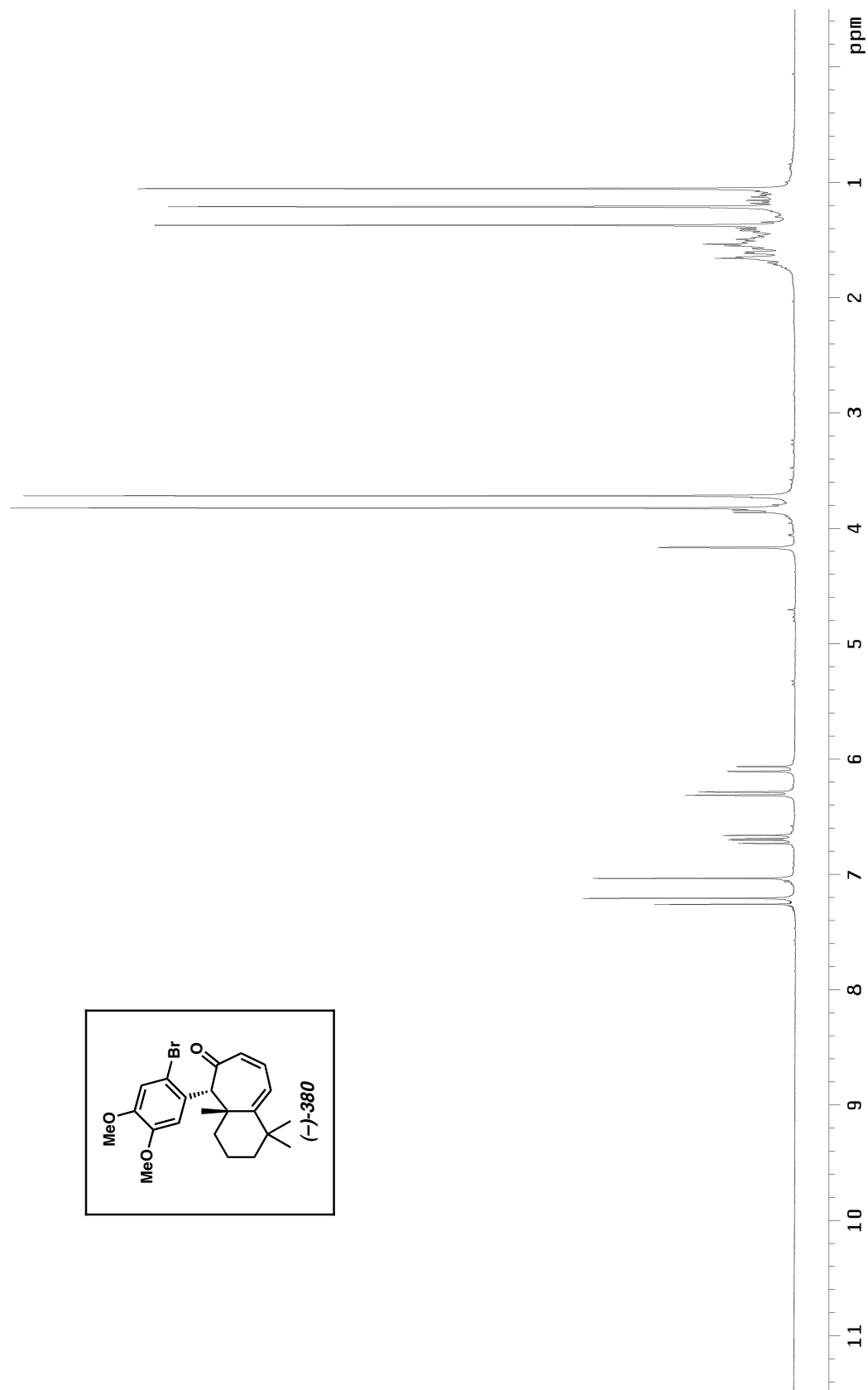


Figure A7.109 ^1H NMR (300 MHz, CDCl_3) of compound **380**.

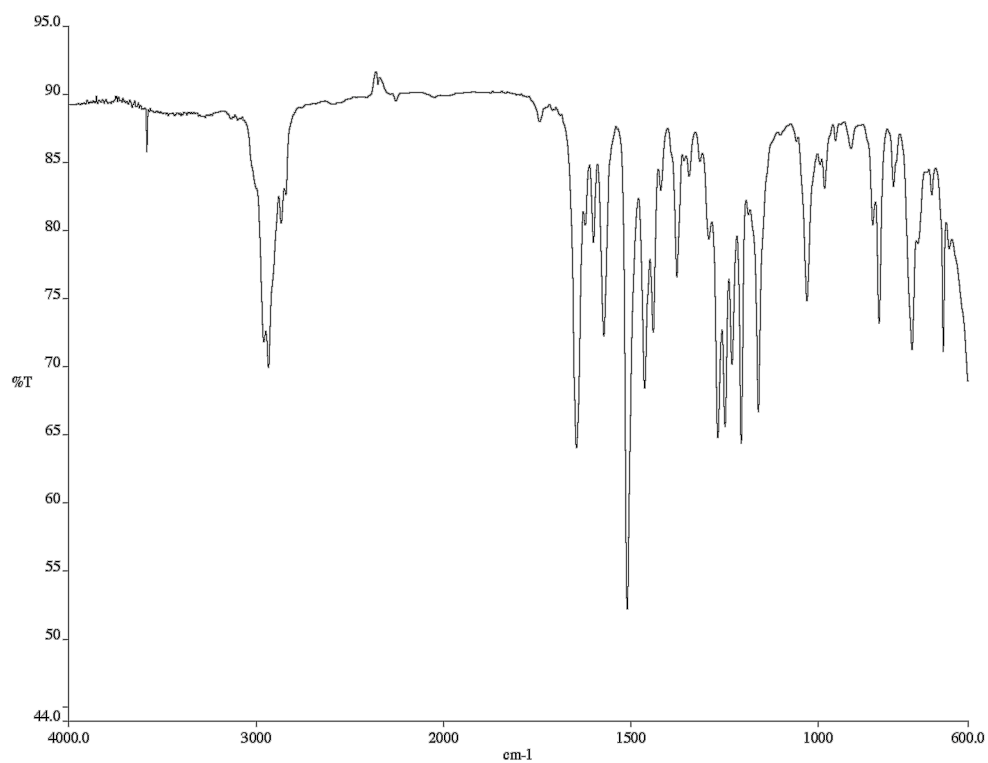


Figure A7.110 Infrared spectrum (NaCl/CDCl₃) of compound **380**.

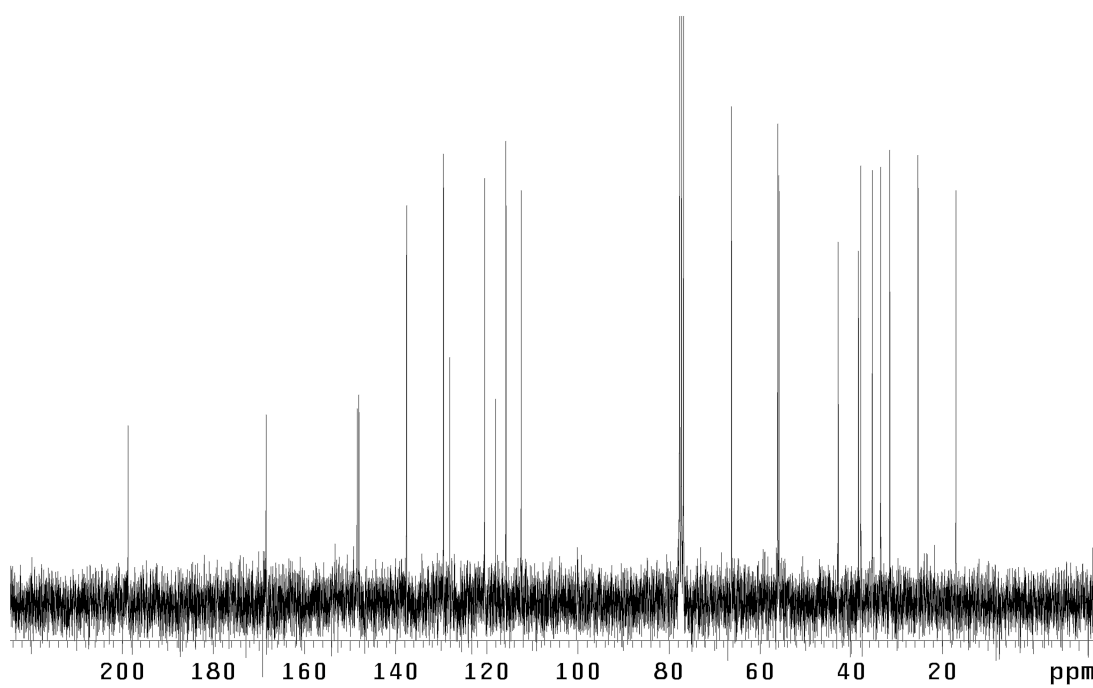


Figure A7.111 ¹³C NMR (75 MHz, CDCl₃) of compound **380**.

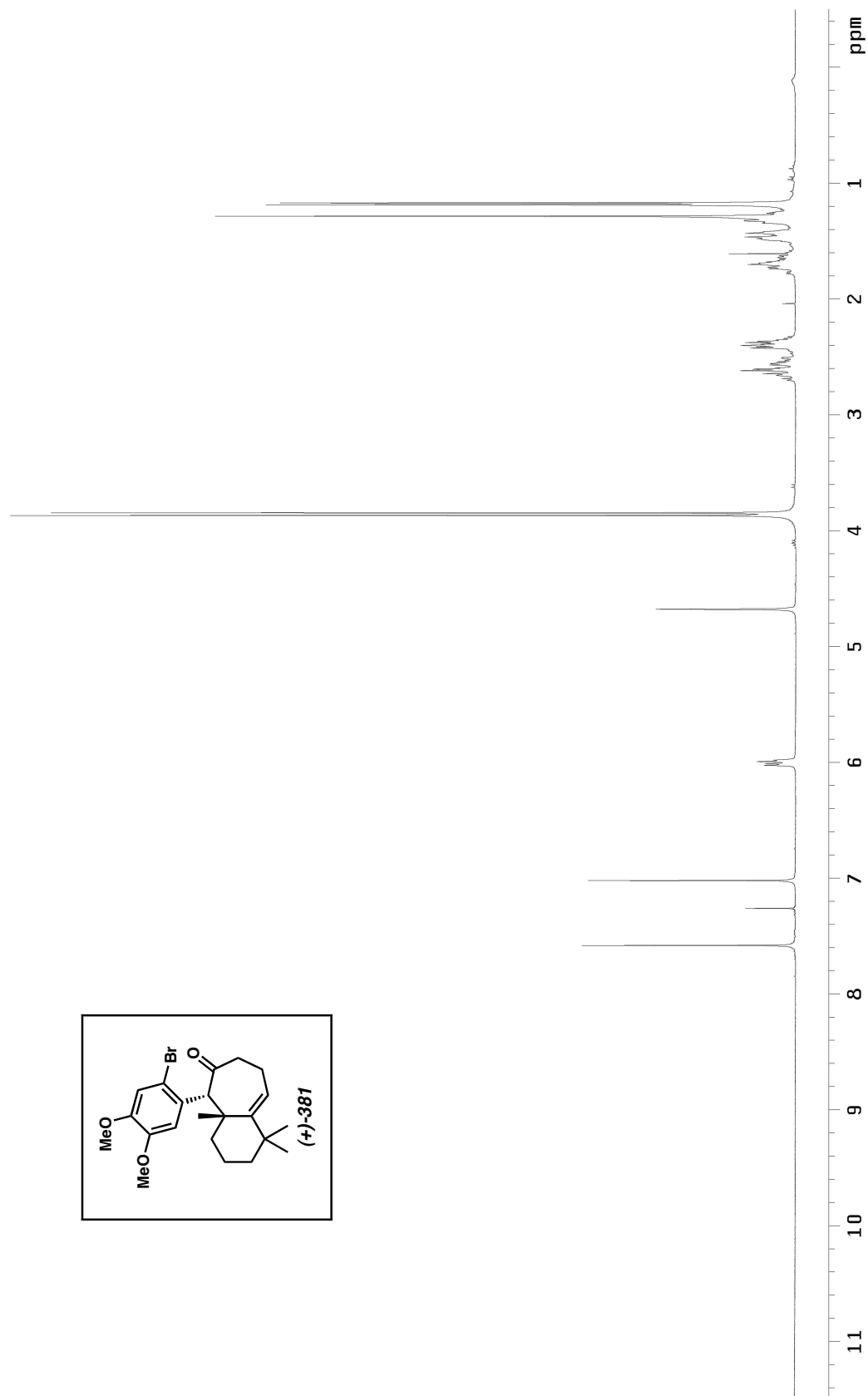


Figure A7.112 ^1H NMR (300 MHz, CDCl_3) of compound **381**.

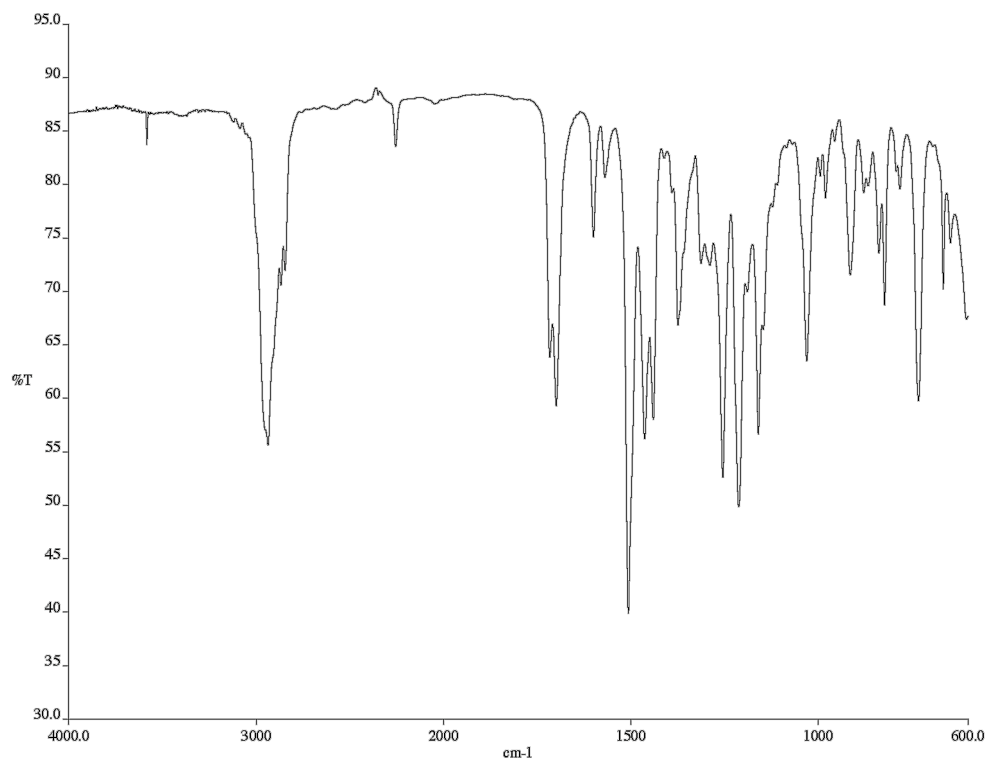


Figure A7.113 Infrared spectrum (NaCl/CDCl₃) of compound **381**.

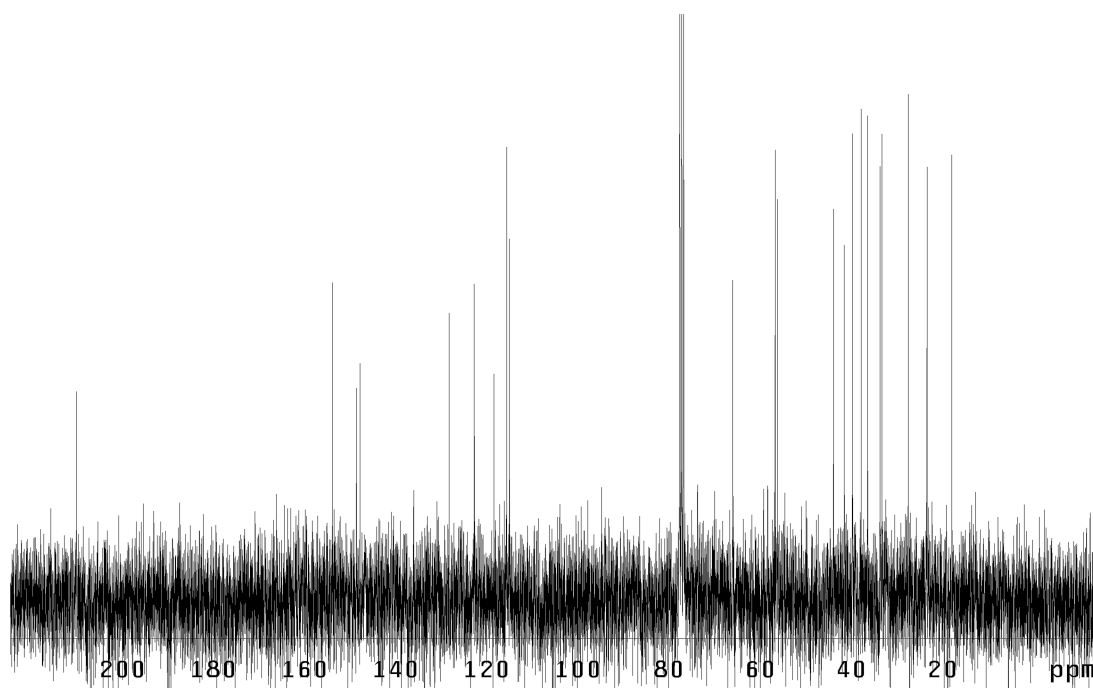


Figure A7.114 ¹³C NMR (75 MHz, CDCl₃) of compound **381**.

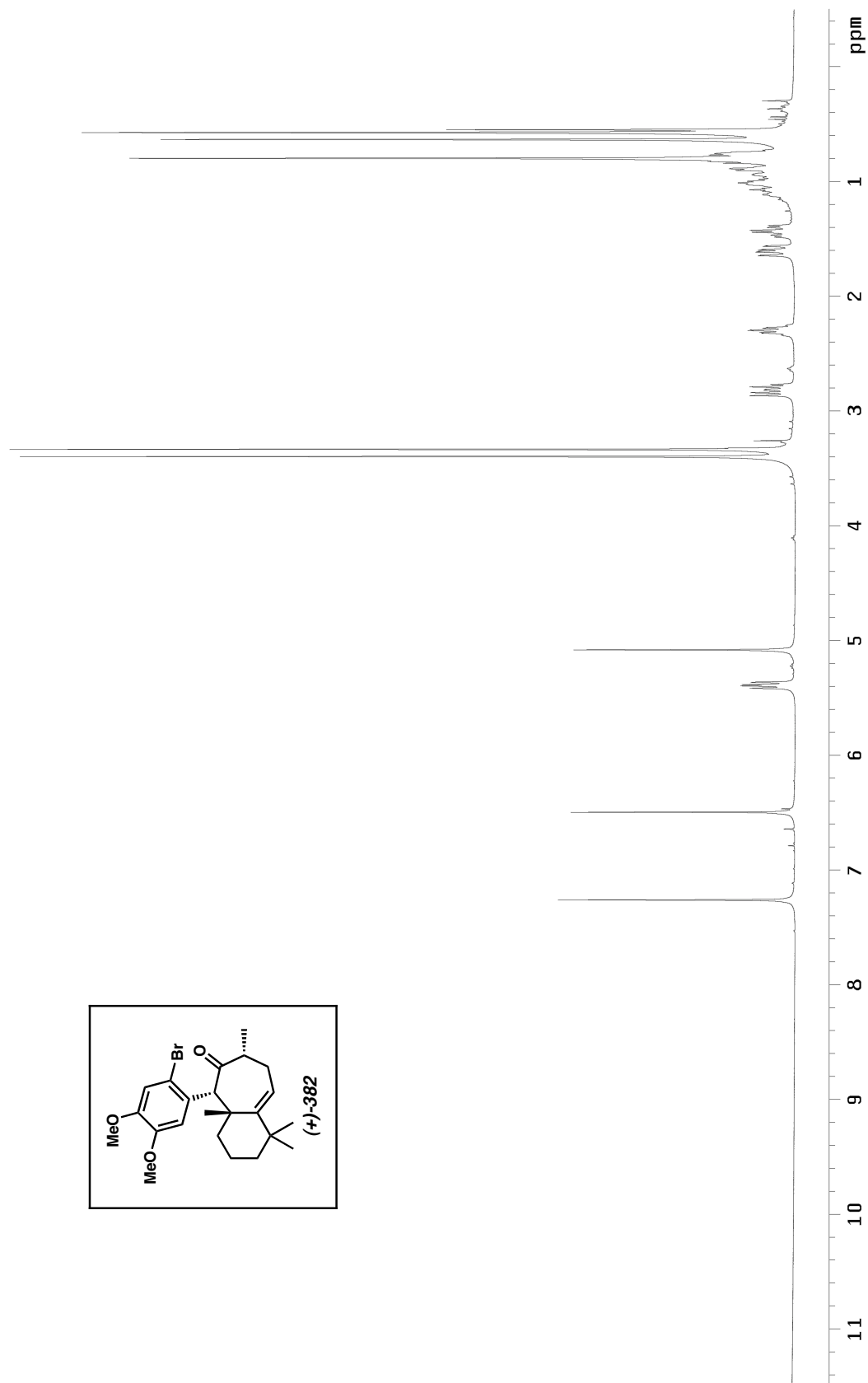


Figure A7.115 ^1H NMR (300 MHz, CDCl_3) of compound 382.

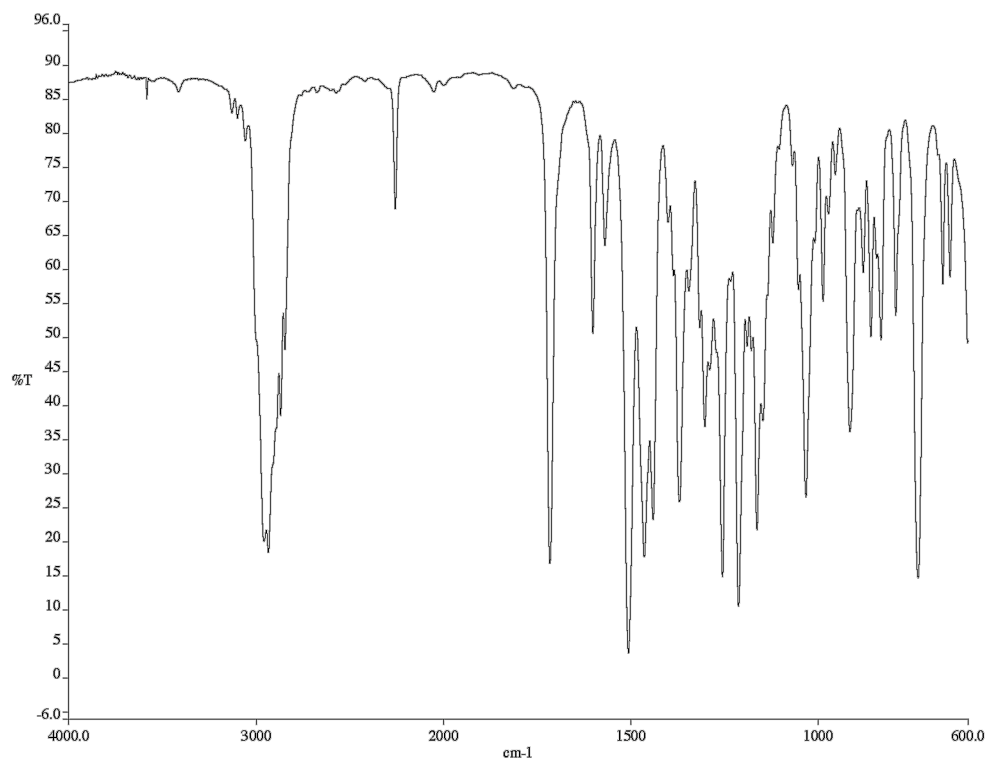


Figure A7.116 Infrared spectrum (NaCl/CDCl₃) of compound **382**.

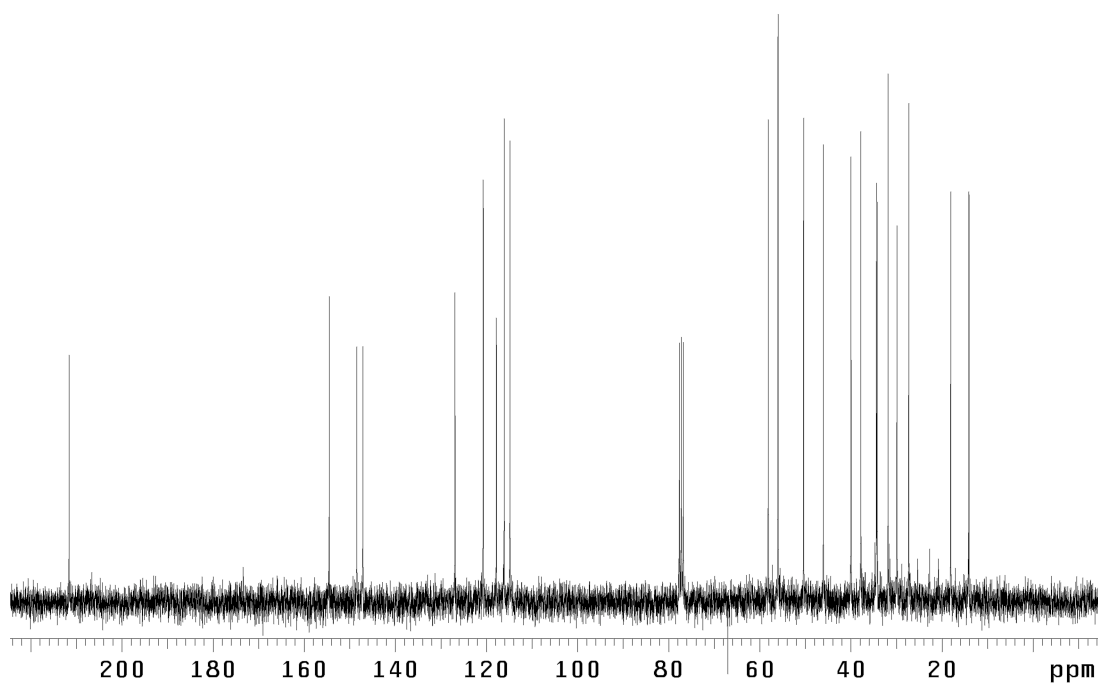


Figure A7.117 ¹³C NMR (75 MHz, CDCl₃) of compound **382**.

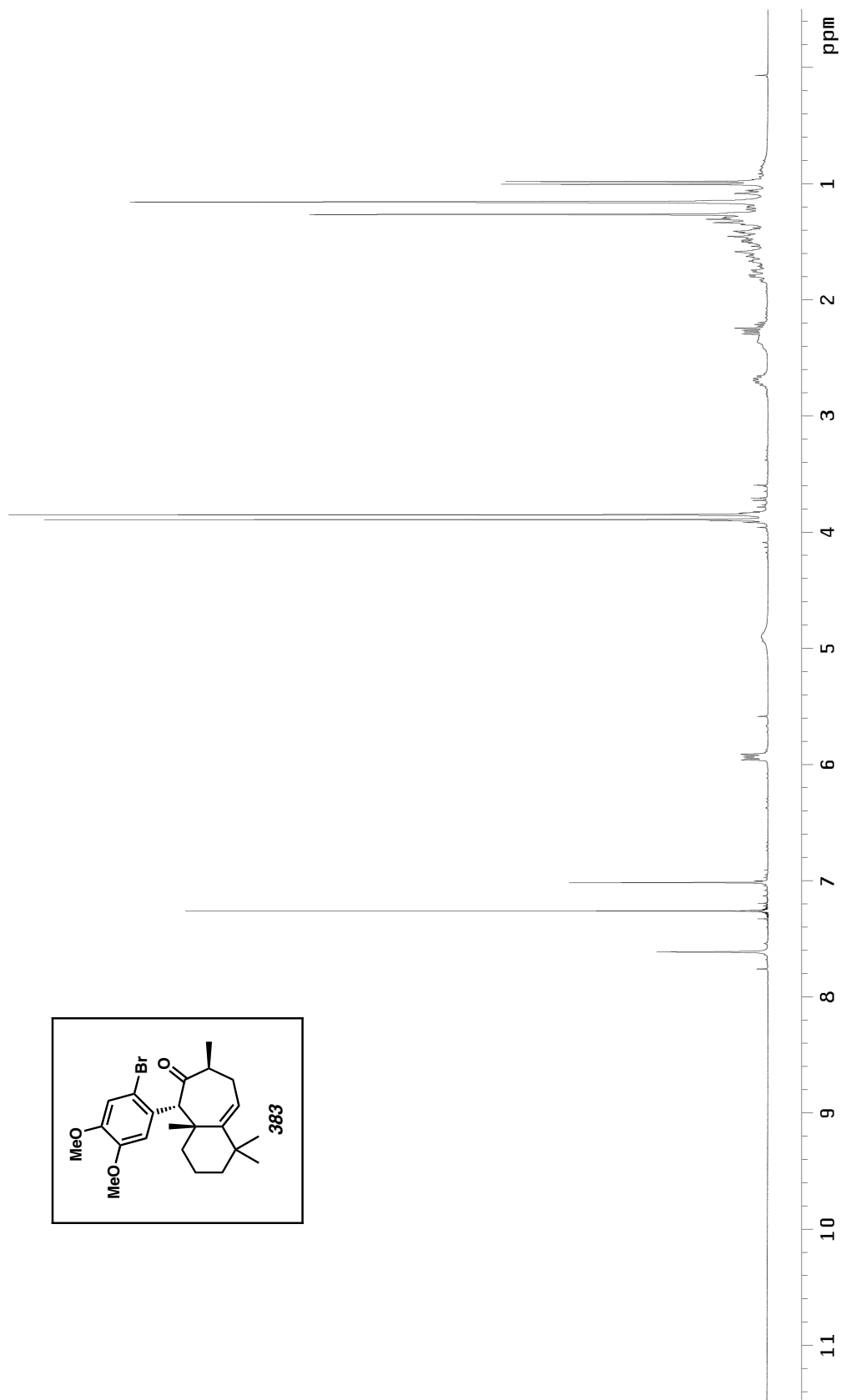


Figure A7.118 ^1H NMR (300 MHz, CDCl_3) of compound **383**.

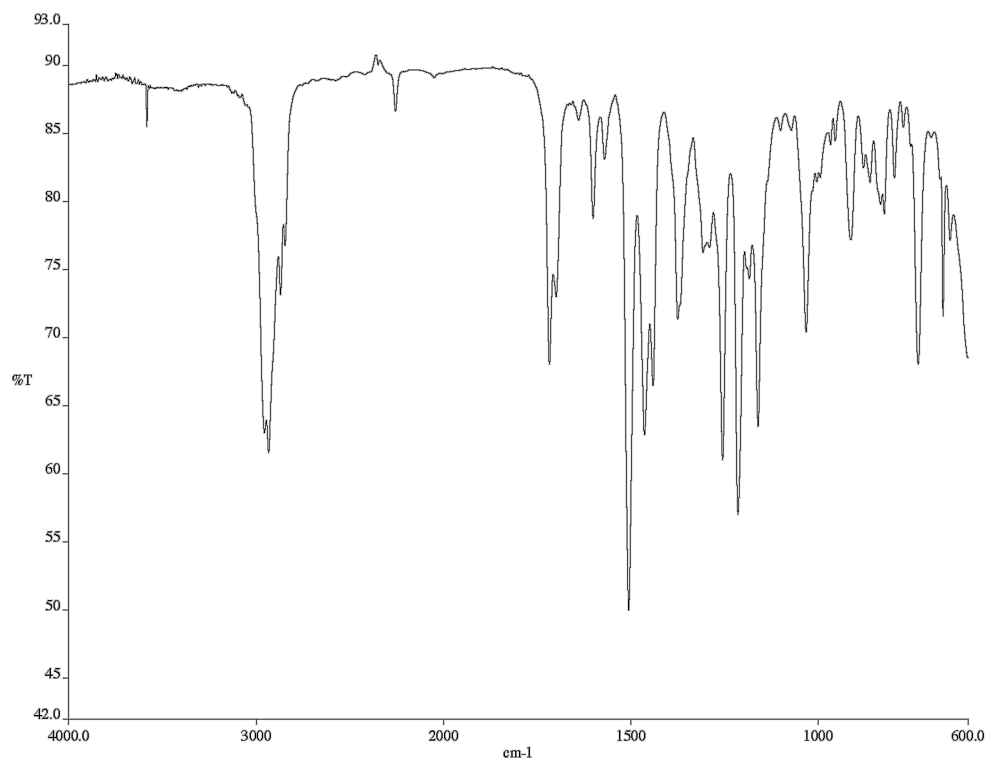


Figure A7.119 Infrared spectrum (NaCl/CDCl₃) of compound **383**.

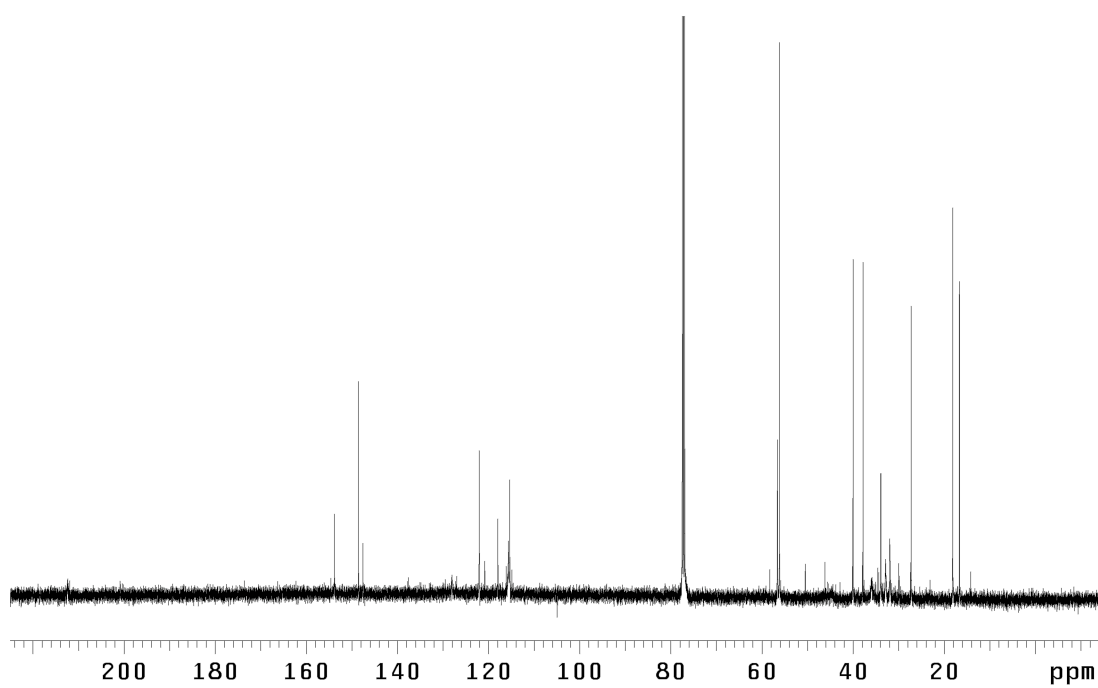


Figure A7.120 ¹³C NMR (125 MHz, CDCl₃) of compound **383**.

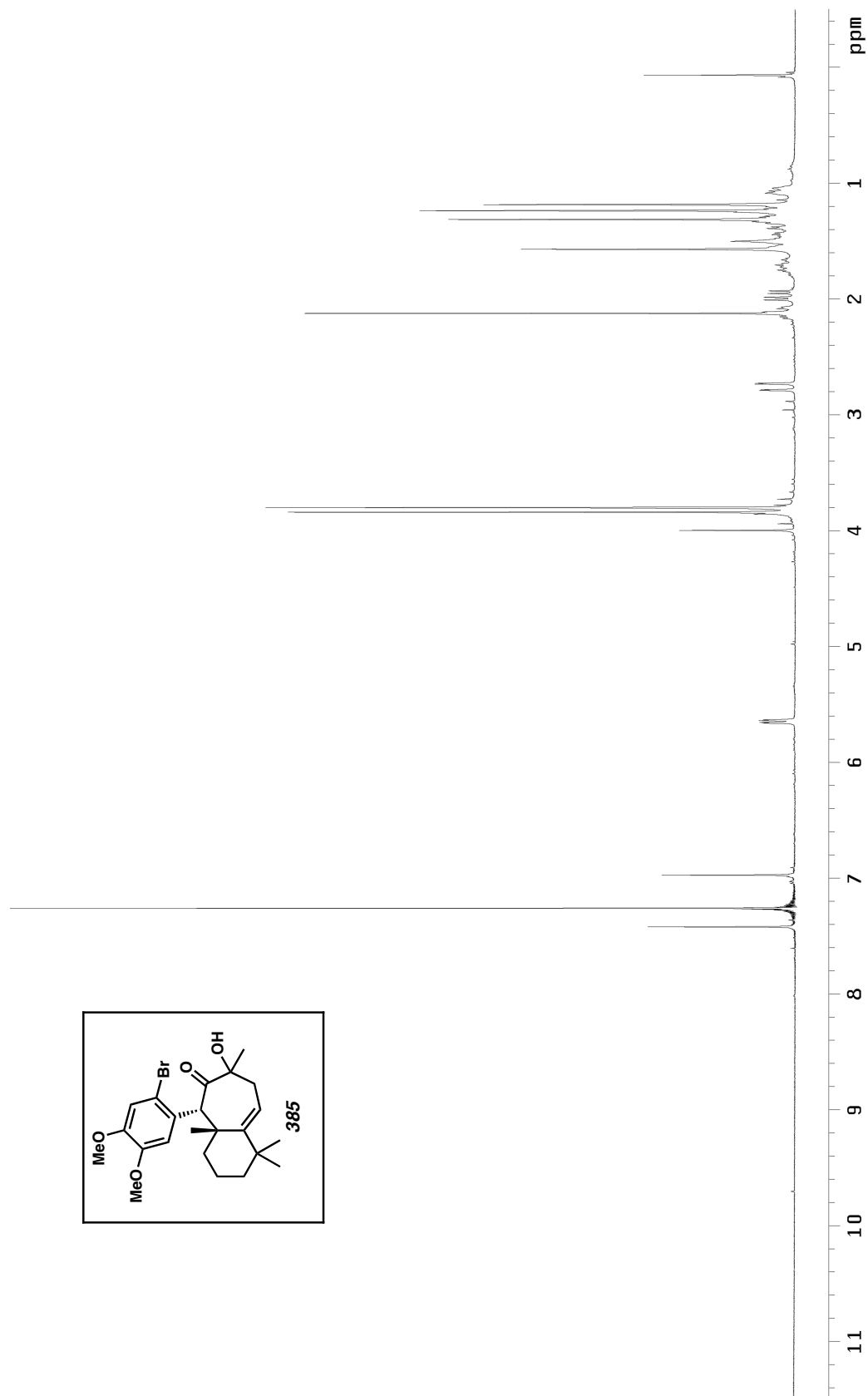


Figure A7.121 ^1H NMR (300 MHz, CDCl_3) of compound **385**.

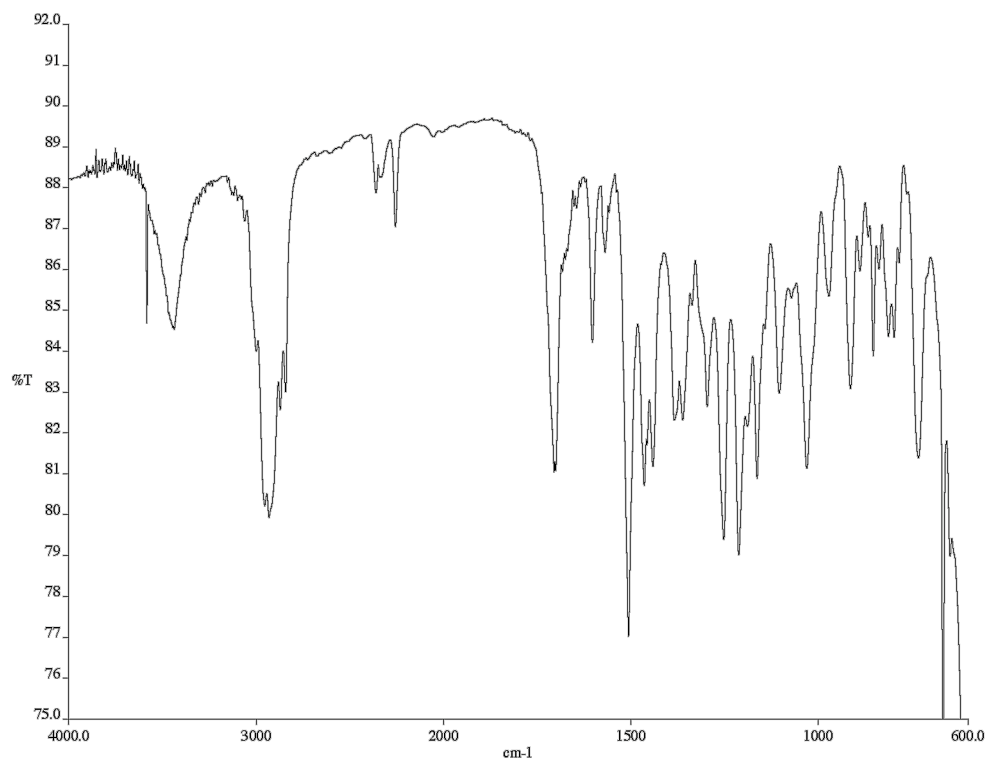


Figure A7.122 Infrared spectrum (NaCl/CDCl₃) of compound **385**.

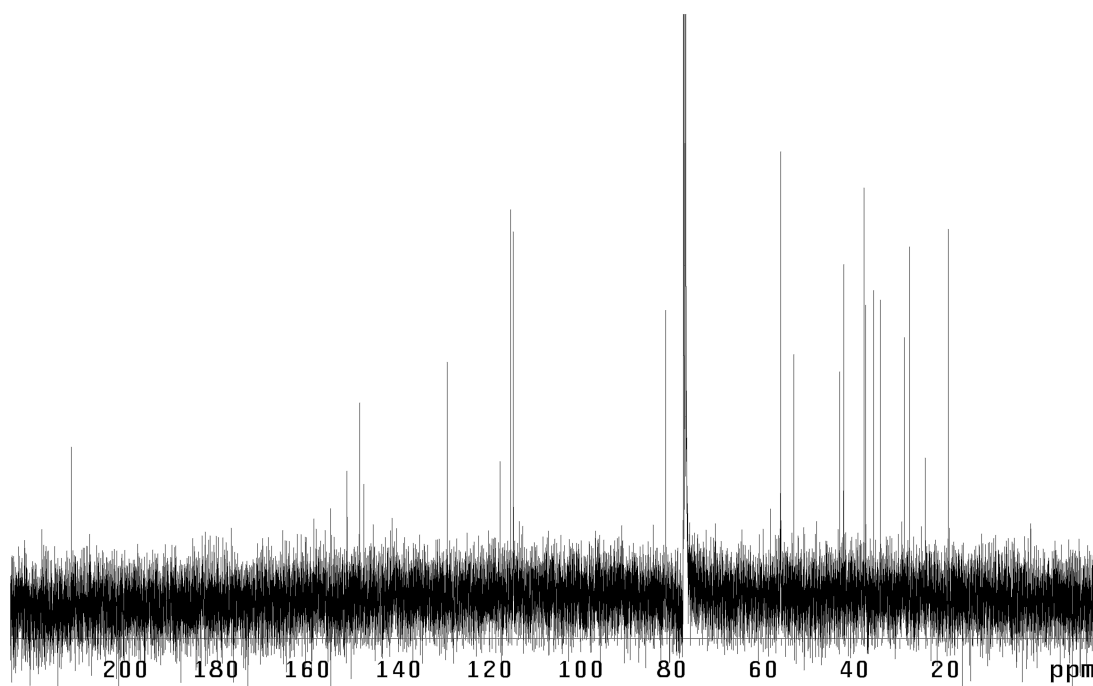


Figure A7.123 ¹³C NMR (125 MHz, CDCl₃) of compound **385**.

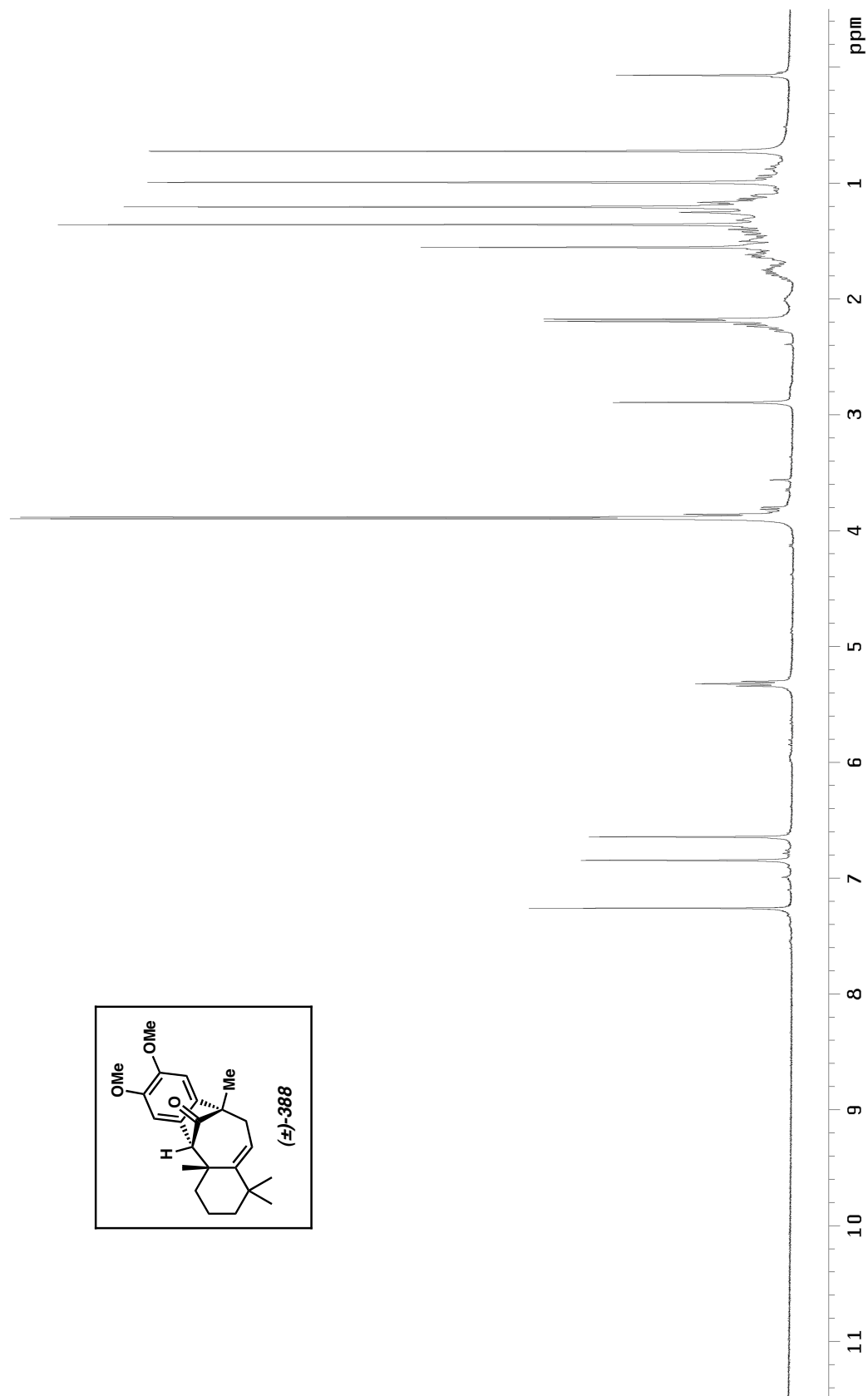
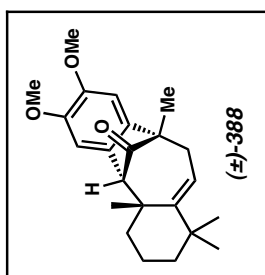


Figure A7.124 ^1H NMR (300 MHz, CDCl_3) of compound **388**.



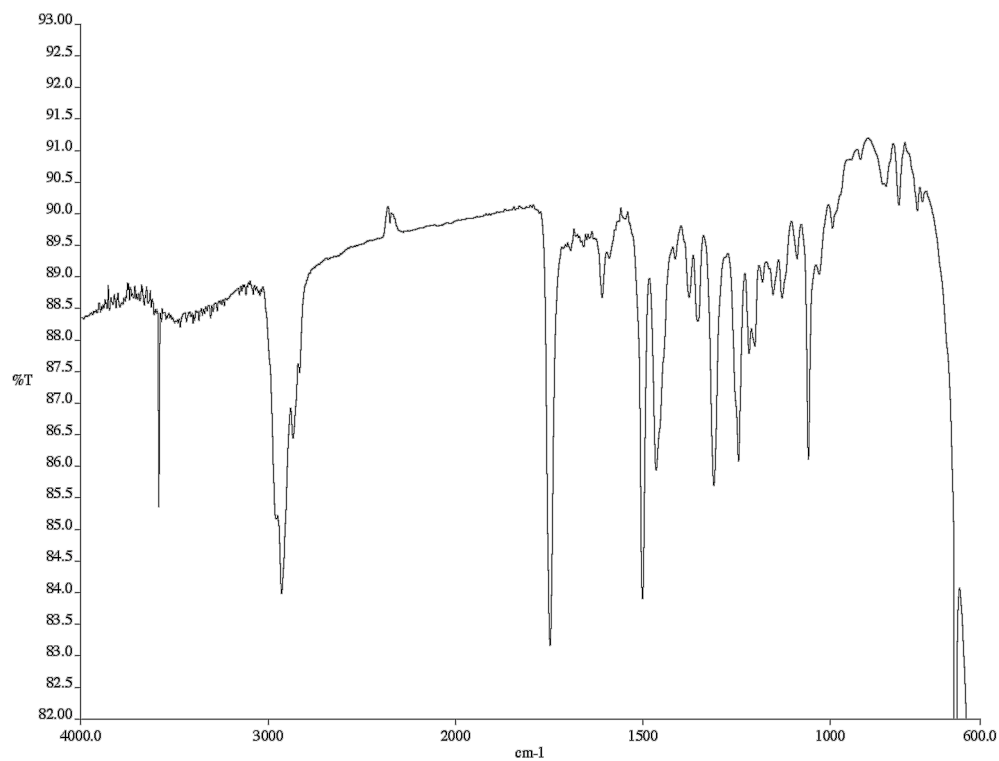


Figure A7.125 Infrared spectrum (NaCl/CDCl₃) of compound **388**.

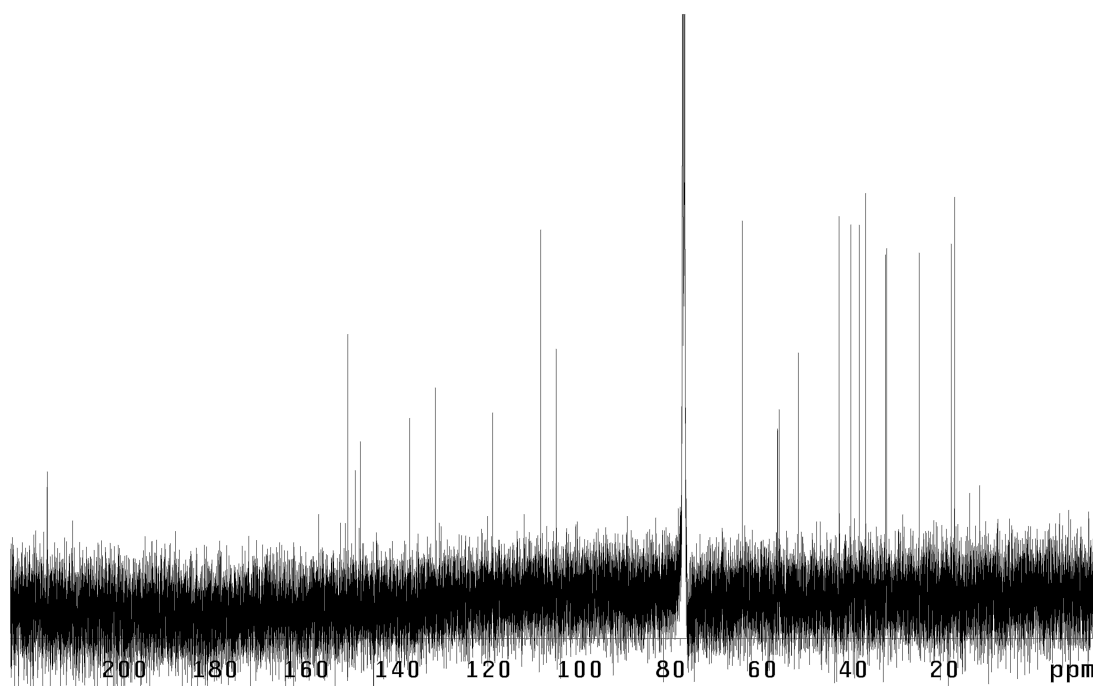
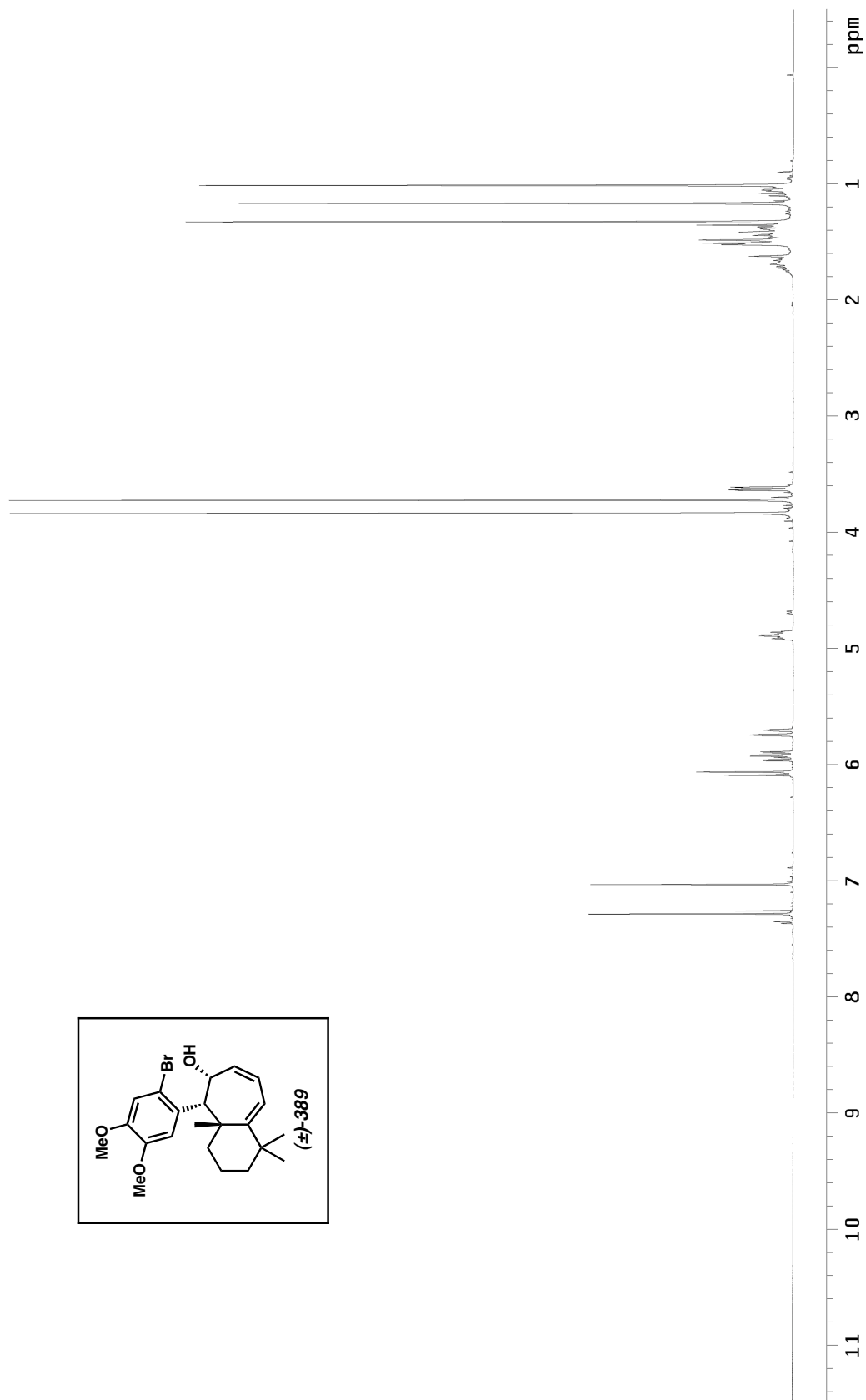


Figure A7.126 ¹³C NMR (125 MHz, CDCl₃) of compound **388**.

Figure A7.127 ^1H NMR (300 MHz, CDCl_3) of compound **389**.

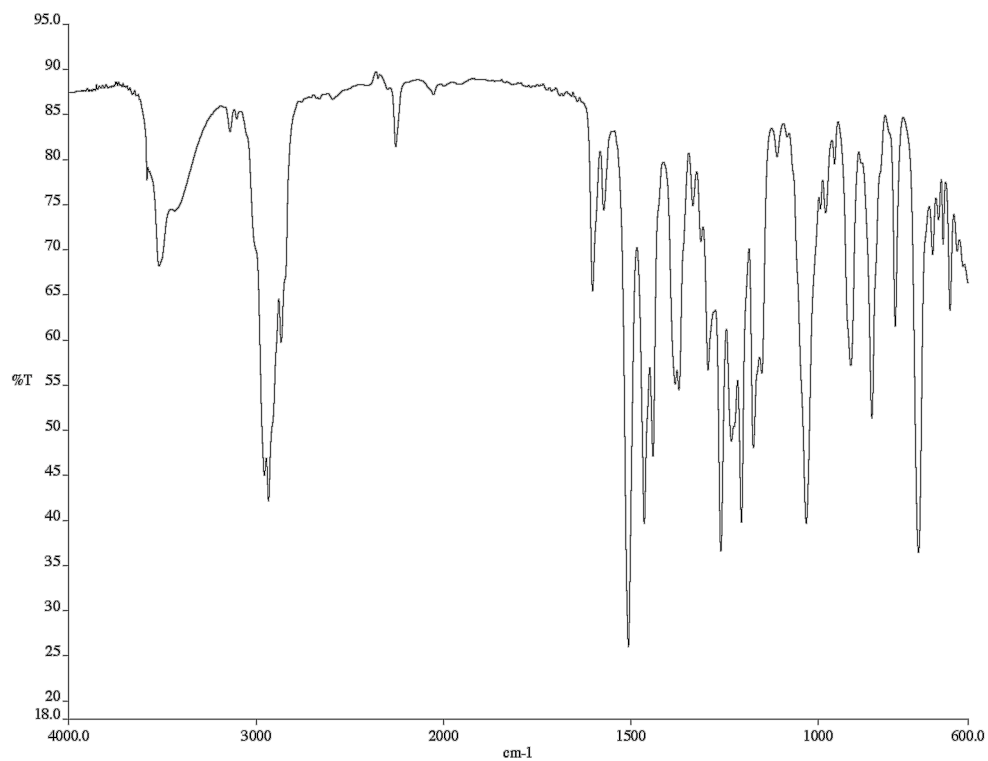


Figure A7.128 Infrared spectrum (NaCl/CDCl₃) of compound **389**.

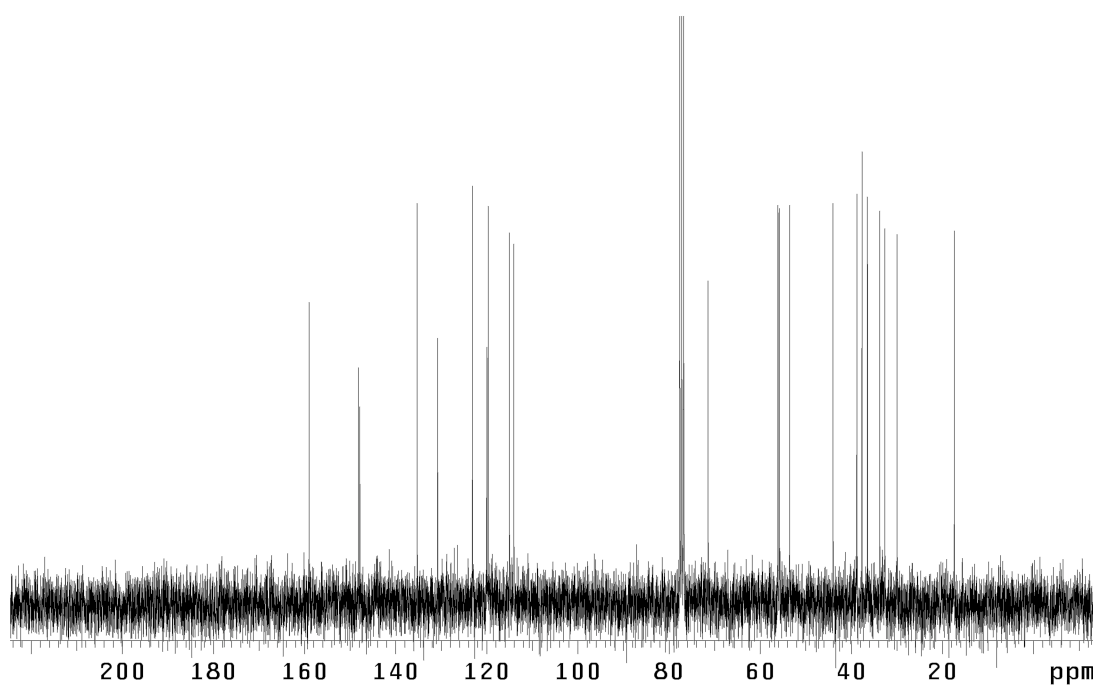


Figure A7.129 ¹³C NMR (75 MHz, CDCl₃) of compound **389**.

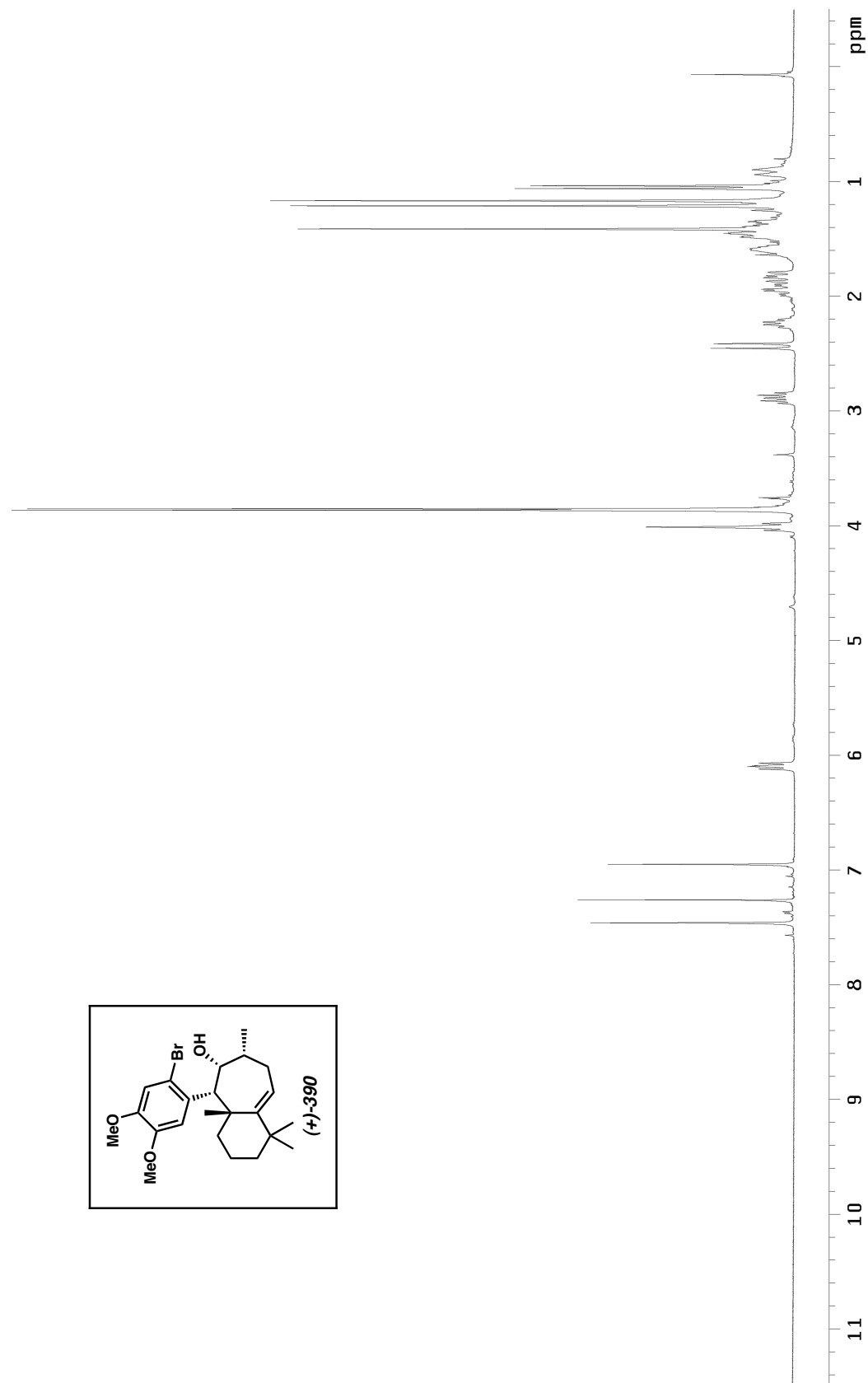


Figure A7.130 ^1H NMR (300 MHz, CDCl_3) of compound **390**.

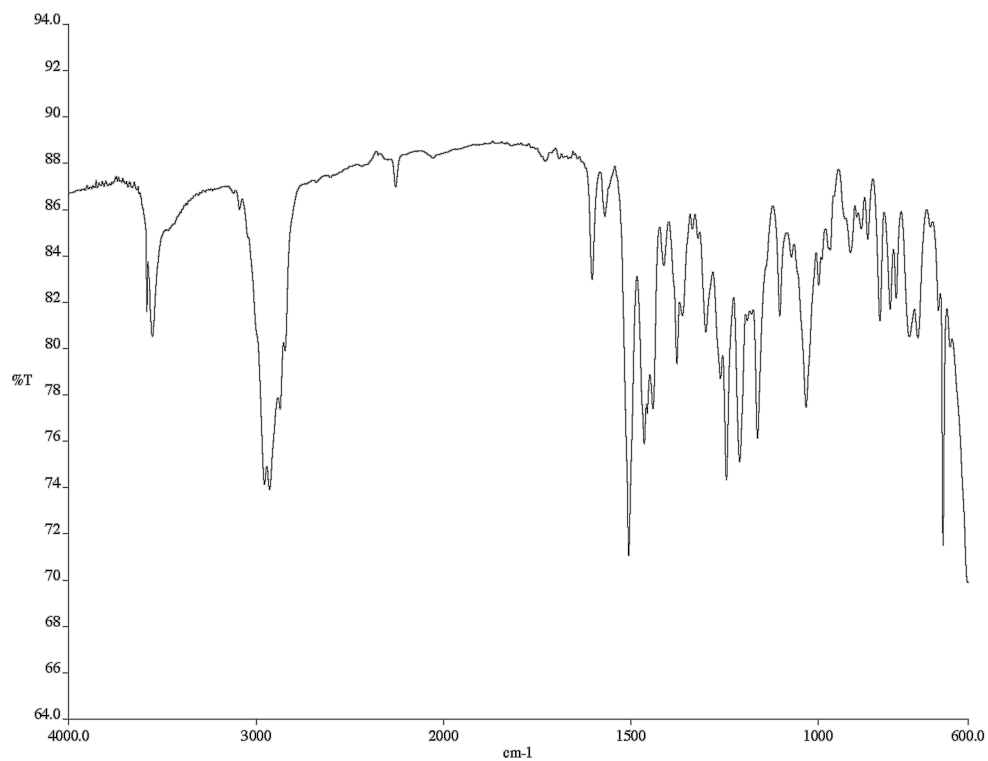


Figure A7.131 Infrared spectrum (NaCl/CDCl₃) of compound **390**.

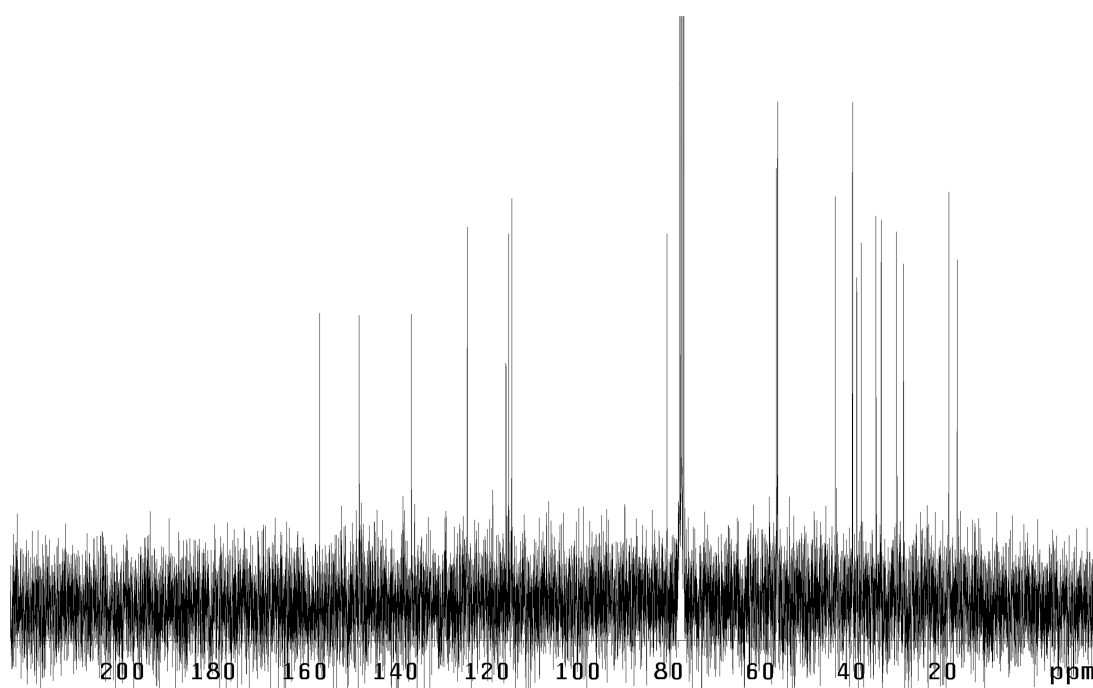


Figure A7.132 ¹³C NMR (75 MHz, CDCl₃) of compound **390**.

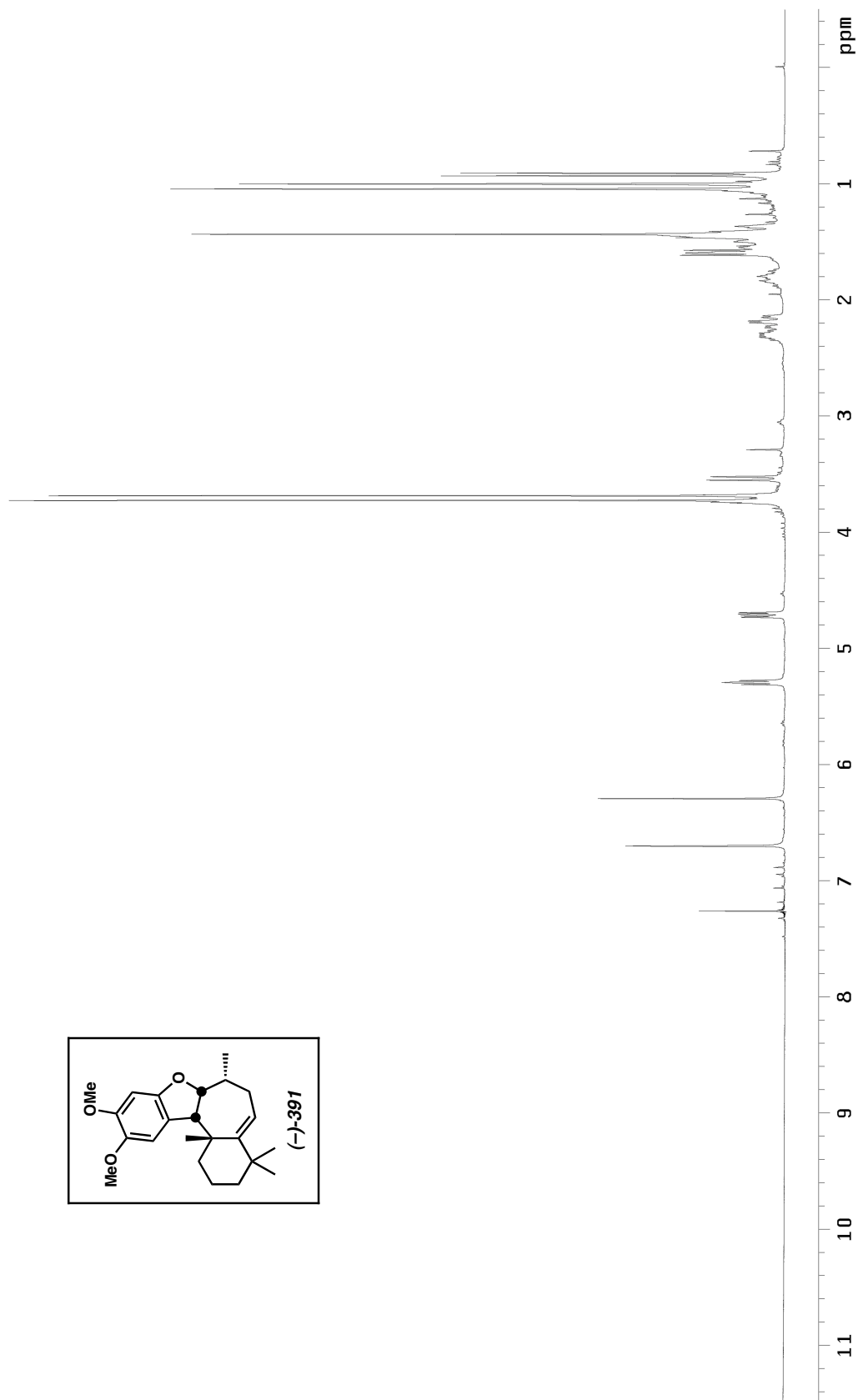


Figure A7.133 ^1H NMR (300 MHz, CDCl_3) of compound **391**.

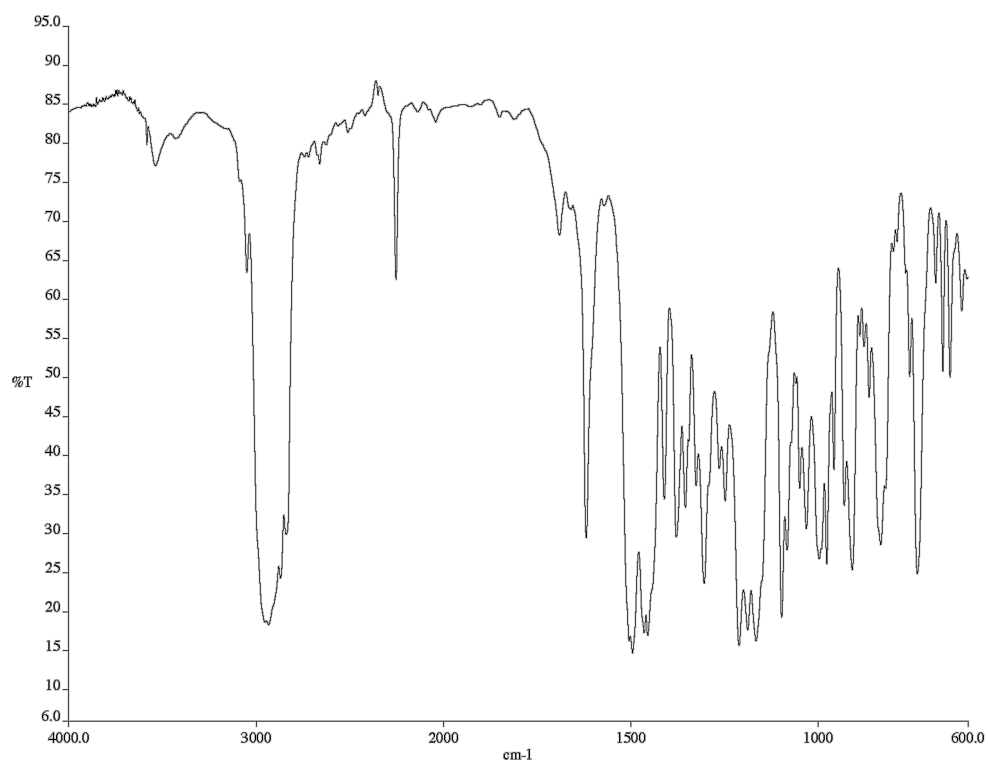


Figure A7.134 Infrared spectrum (NaCl/CDCl₃) of compound **391**.

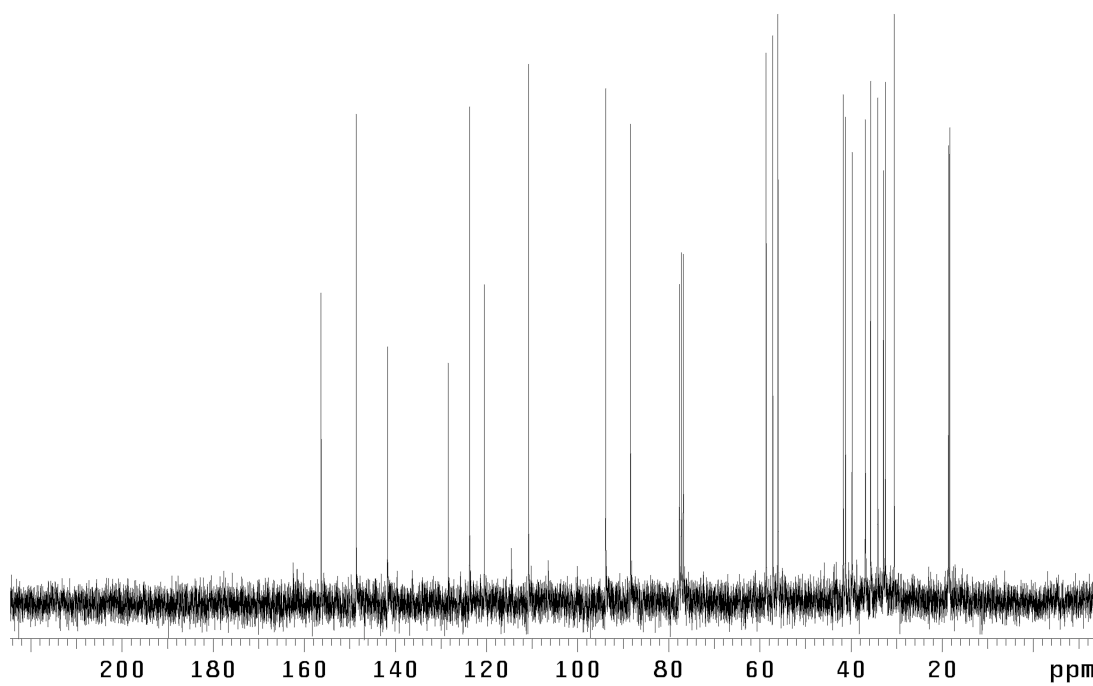


Figure A7.135 ¹³C NMR (75 MHz, CDCl₃) of compound **391**.

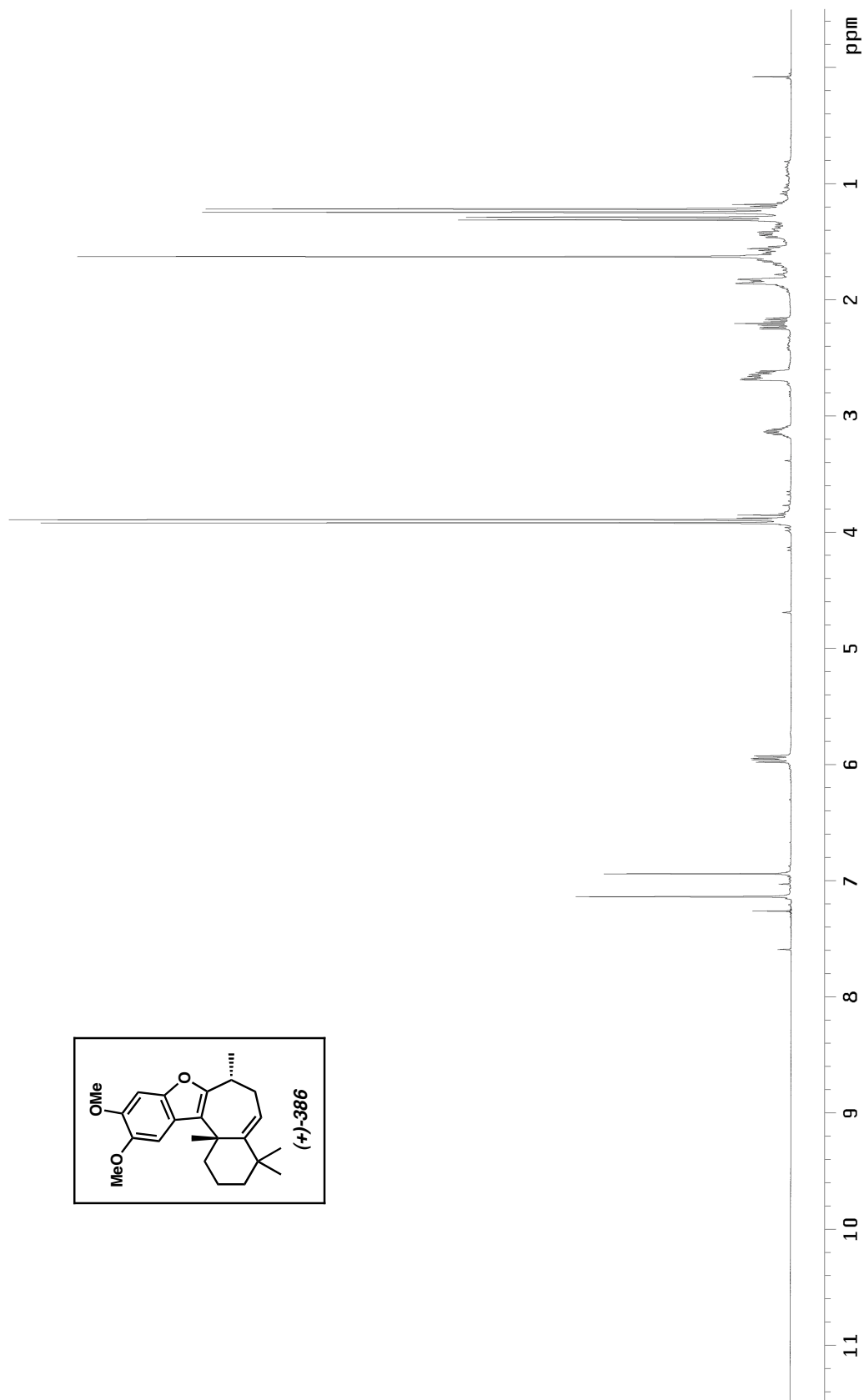


Figure A7.136 ^1H NMR (300 MHz, CDCl_3) of compound **386**.

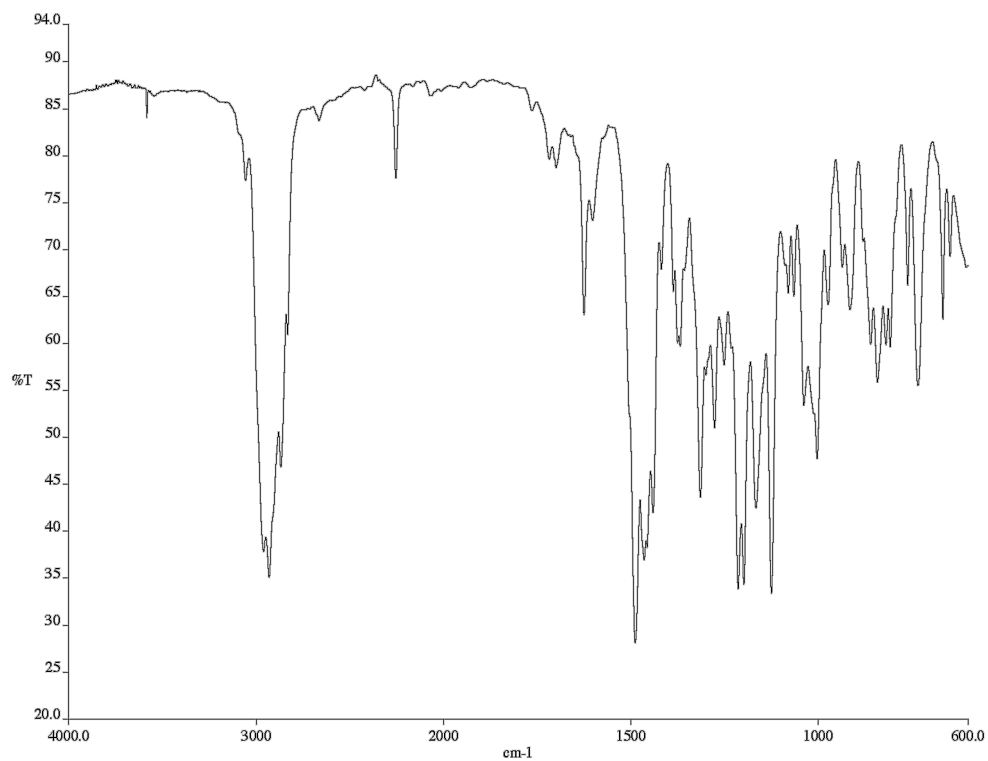


Figure A7.137 Infrared spectrum (NaCl/CDCl₃) of compound **386**.

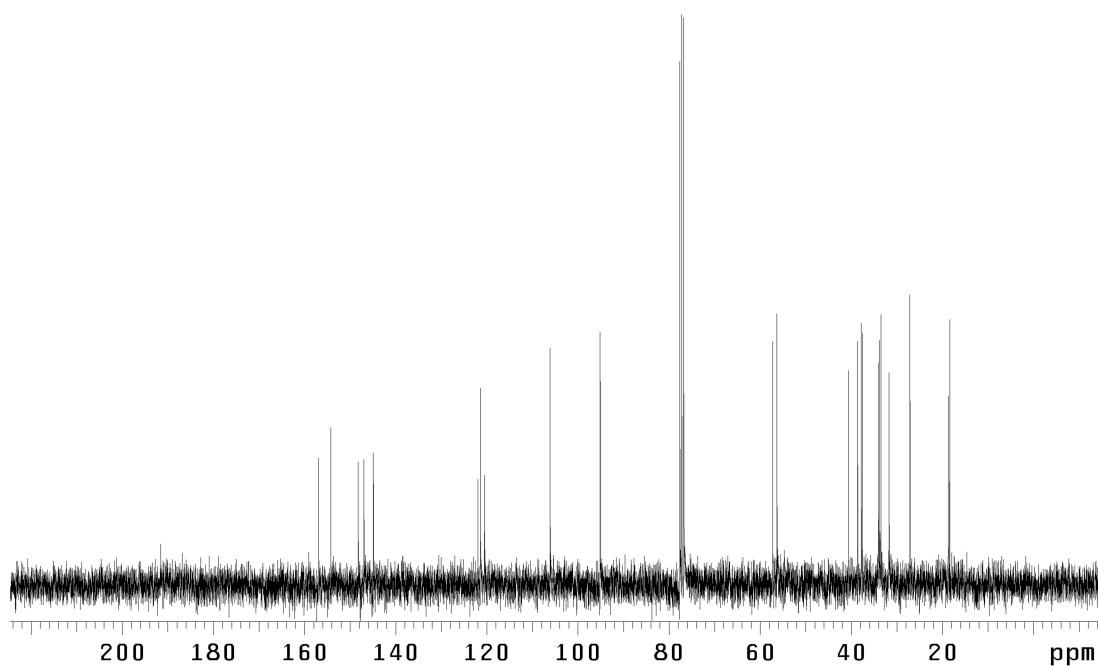


Figure A7.138 ¹³C NMR (75 MHz, CDCl₃) of compound **386**.

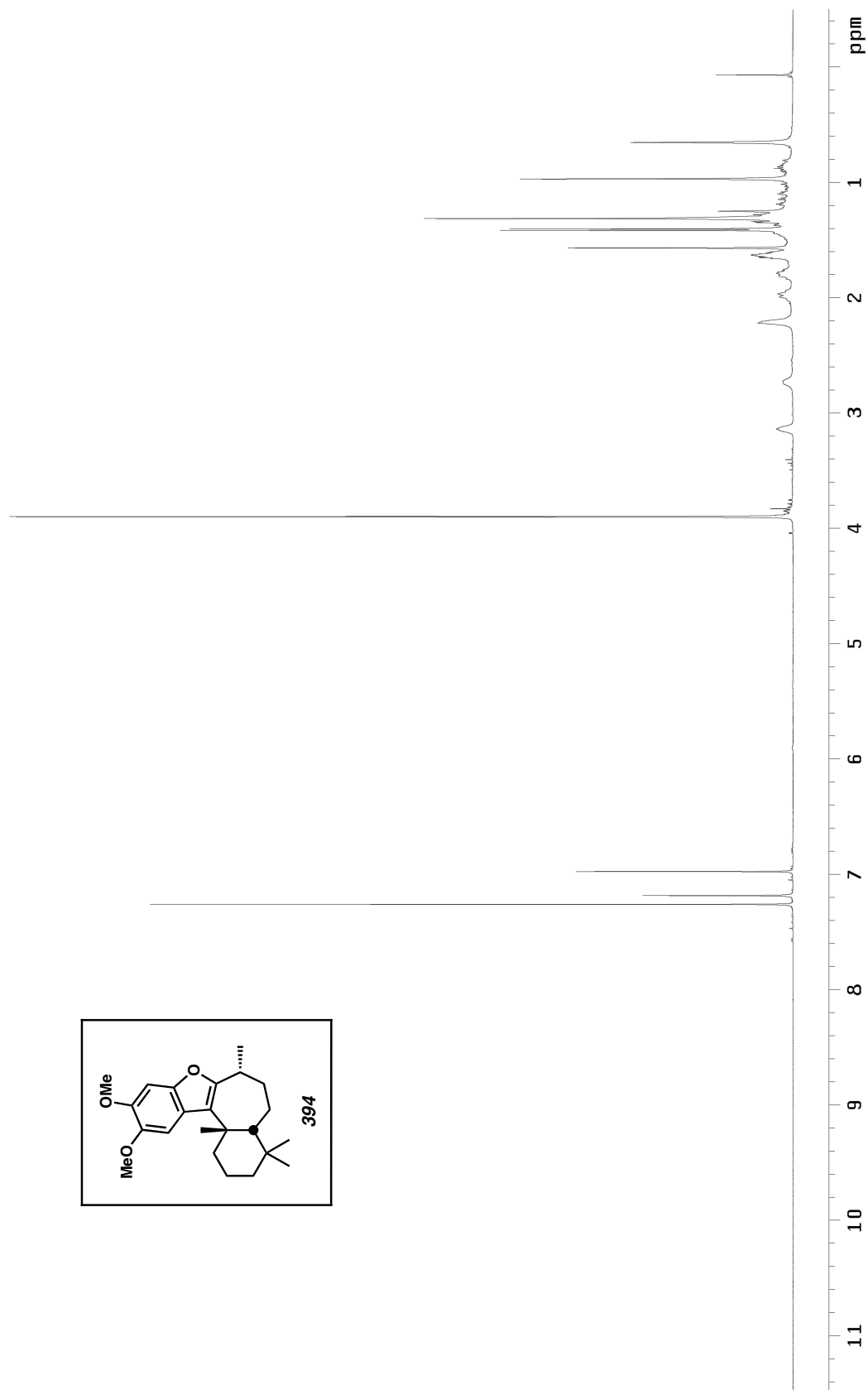


Figure A7.139 ^1H NMR (500 MHz, CDCl_3) of compound 394.

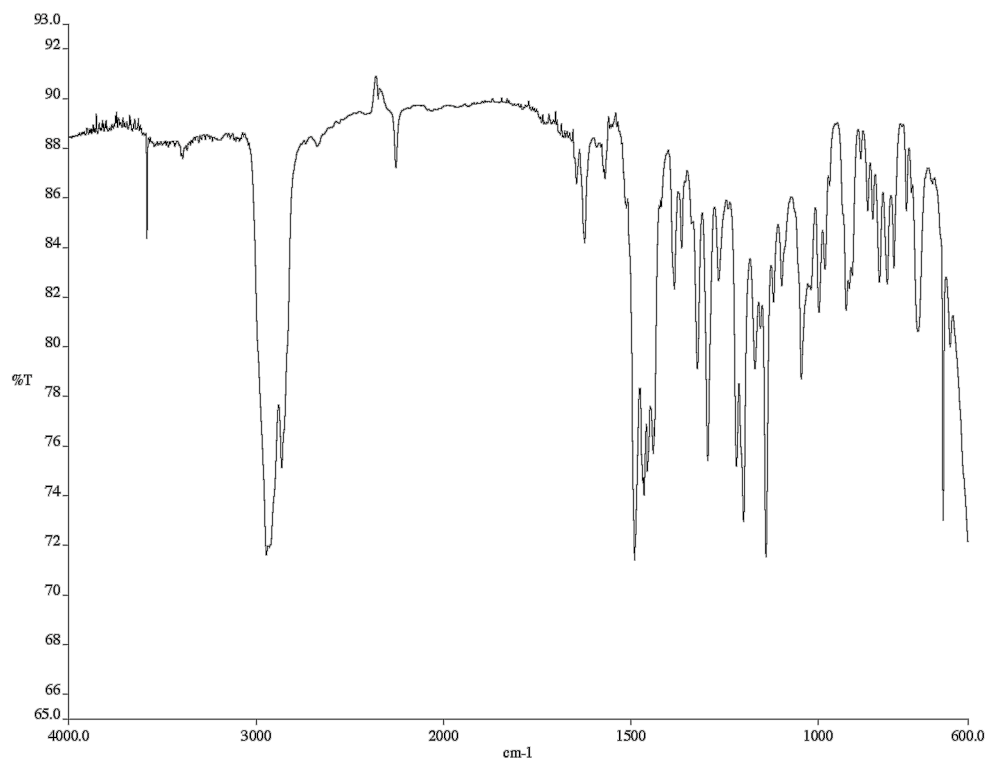


Figure A7.140 Infrared spectrum (NaCl/CDCl₃) of compound **394**.

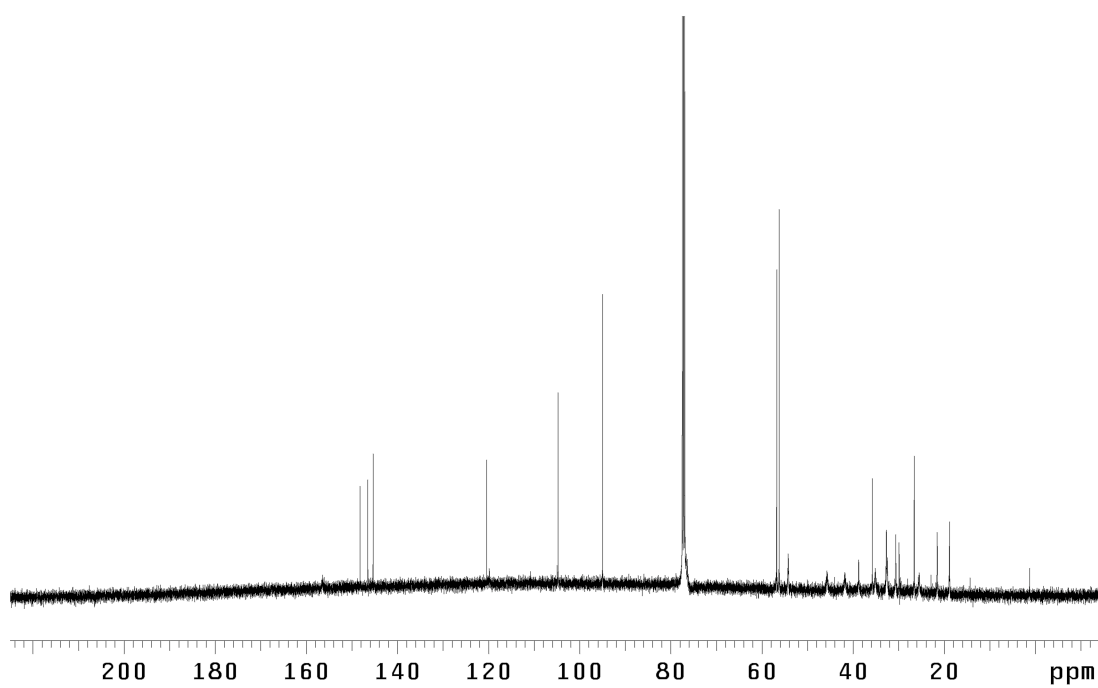


Figure A7.141 ¹³C NMR (125 MHz, CDCl₃) of compound **394**.

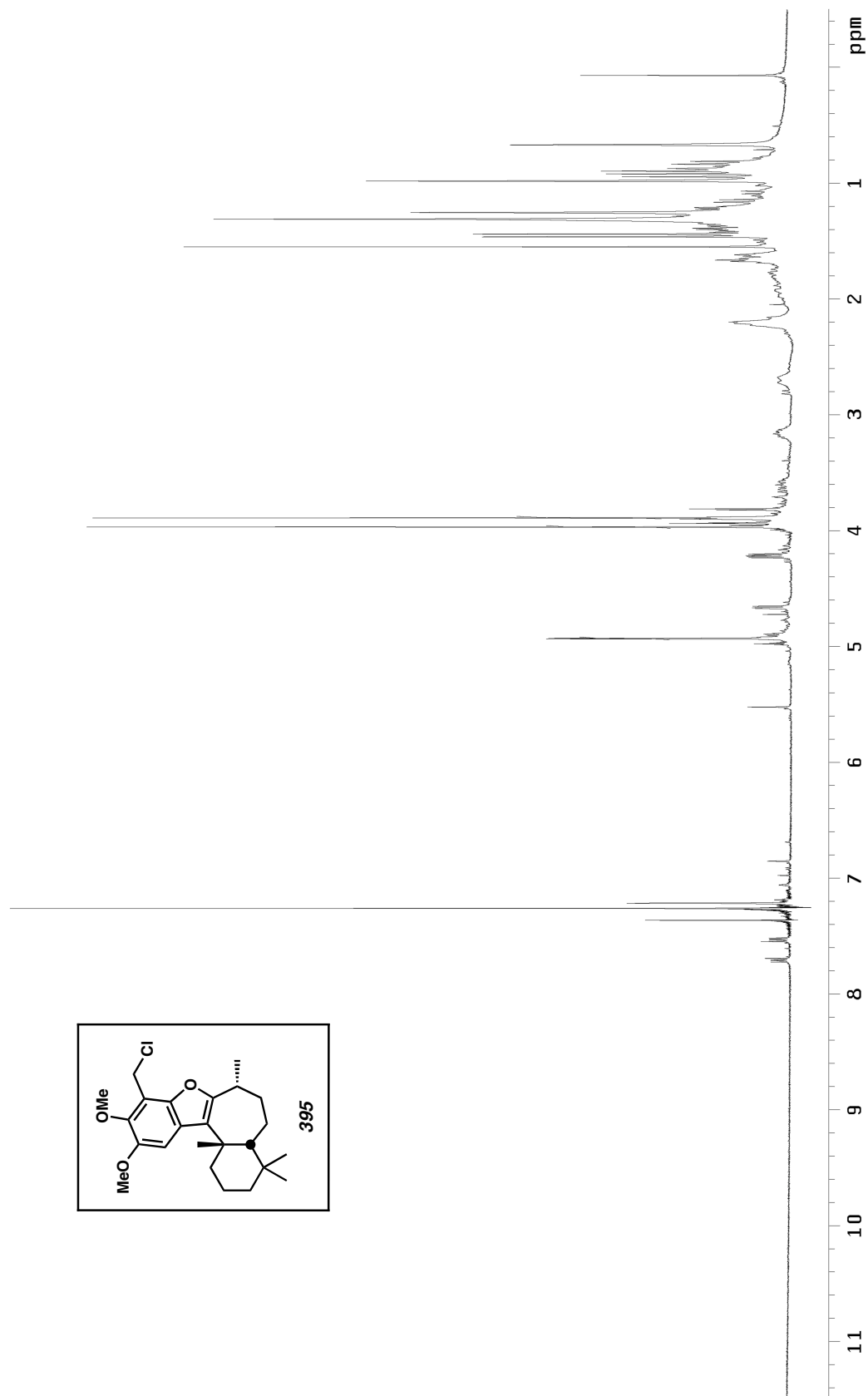
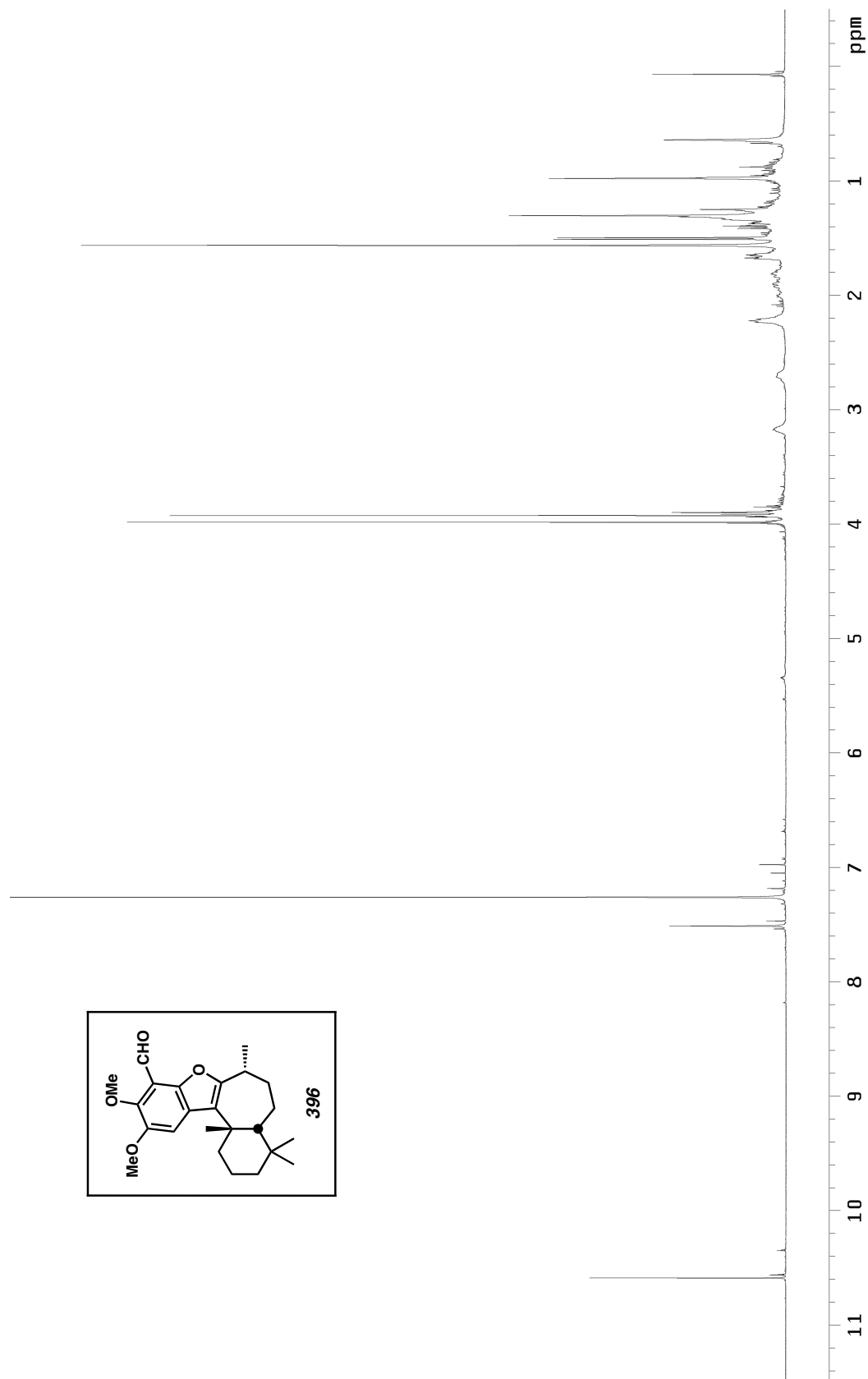


Figure A7.142 ^1H NMR (300 MHz, CDCl_3) of compound 395.

Figure A7.143 ^1H NMR (500 MHz, CDCl_3) of compound **396**.

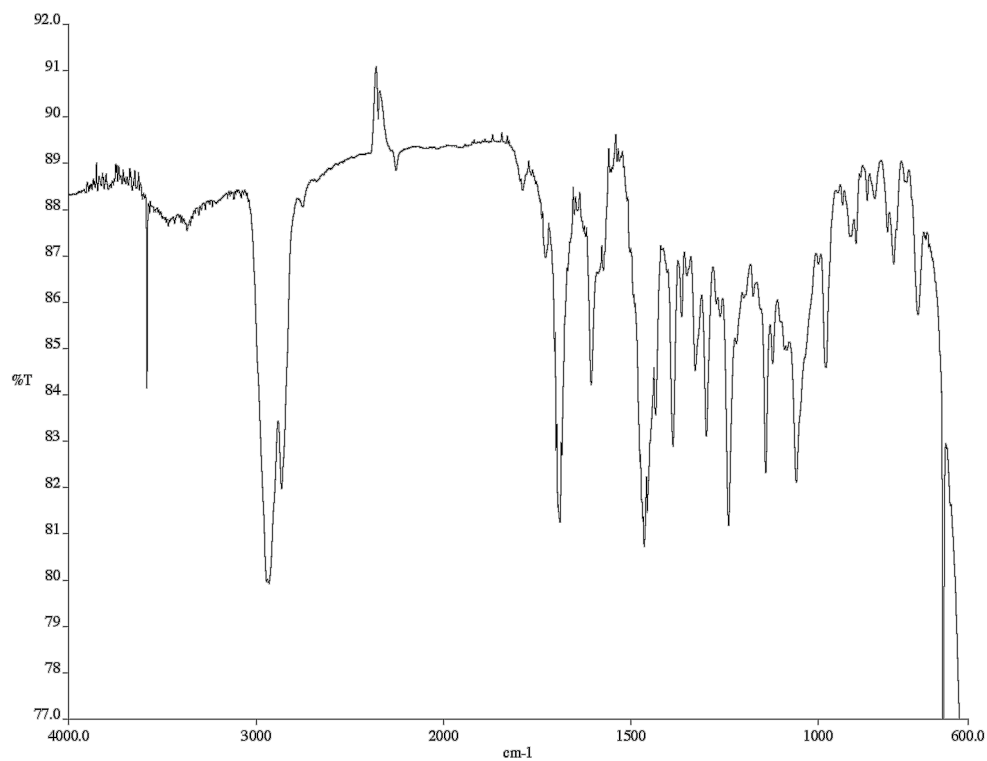


Figure A7.144 Infrared spectrum (NaCl/CDCl₃) of compound **396**.

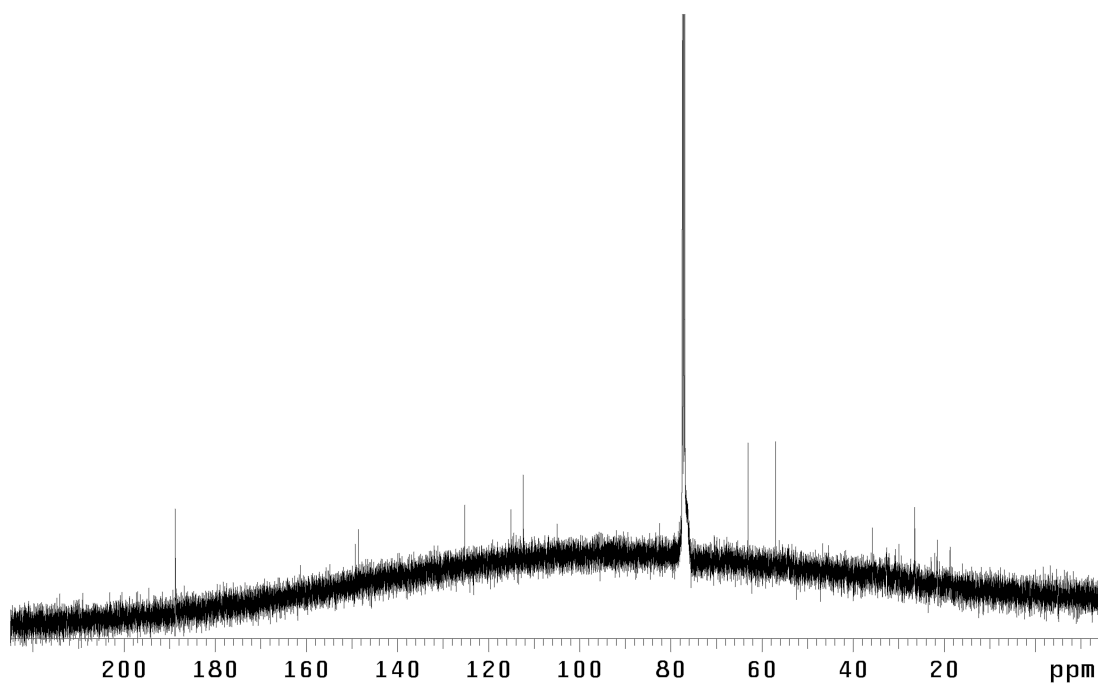


Figure A7.145 ¹³C NMR (125 MHz, CDCl₃) of compound **396**.

Appendix EIGHT

X-Ray Crystallographic Data Relevant to Chapter 4

CALIFORNIA INSTITUTE OF TECHNOLOGY
BECKMAN INSTITUTE
X-RAY CRYSTALLOGRAPHY LABORATORY

Date 1 May 2006

Crystal Structure Analysis of:

319B

(shown below)

For	Investigator: Ryan McFadden	ext. 6131
	Advisor: B. M. Stoltz	ext. 6064
	Account Number: BMS1.SQUIBB-2.22-GRANT.SQUIBB1	
By	Michael W. Day	116 Beckman ext. 2734 e-mail: mikeday@caltech.edu

Contents

Table 1. Crystal data

Figures Minimum overlap, unit cell contents, stereo view of unit cell contents

Table 2. Atomic Coordinates

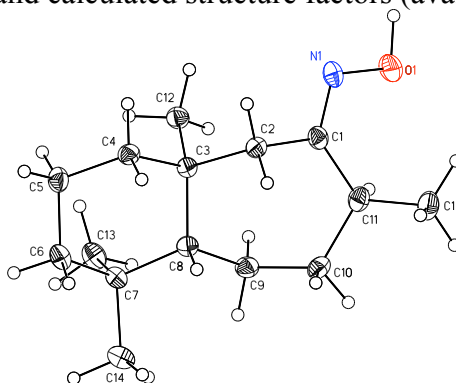
Table 3. Full bond distances and angles

Table 4. Anisotropic displacement parameters

Table 5. Hydrogen atomic coordinates

Table 6. Hydrogen bond distances and angles

Table 7. Observed and calculated structure factors (available upon request)



319B

Note: The crystallographic data have been deposited in the Cambridge Database (CCDC) and have been placed on hold pending further instructions from me. The deposition number is 606034. Ideally, the CCDC would like the publication to contain a footnote of the type: "Crystallographic data have been deposited at the CCDC, 12 Union Road, Cambridge CB2 1EZ, UK and copies can be obtained on request, free of charge, by quoting the publication citation and the deposition number 606034."

Table 1. Crystal data and structure refinement for 319B (CCDC 606034).

Empirical formula	C ₁₅ H ₂₇ NO		
Formula weight	237.38		
Crystallization Solvent	Heptane		
Crystal Habit	Column		
Crystal size	0.41 x 0.15 x 0.13 mm ³		
Crystal color	Colorless		
Data Collection			
Type of diffractometer	Bruker SMART 1000		
Wavelength	0.71073 Å MoKα		
Data Collection Temperature	100(2) K		
θ range for 6053 reflections used in lattice determination	2.39 to 30.07°		
Unit cell dimensions	a = 6.0159(7) Å b = 10.0422(12) Å c = 12.4023(14) Å	α= 74.349(2)° β= 81.140(2)° γ = 77.614(2)°	
Volume	700.99(14) Å ³		
Z	2		
Crystal system	Triclinic		
Space group	P-1		
Density (calculated)	1.125 Mg/m ³		
F(000)	264		
Data collection program	Bruker SMART v5.630		
θ range for data collection	1.71 to 30.48°		
Completeness to θ = 30.48°	88.4 %		
Index ranges	-8 ≤ h ≤ 8, -13 ≤ k ≤ 14, -17 ≤ l ≤ 17		
Data collection scan type	ω scans at 7 φ settings		
Data reduction program	Bruker SAINT v6.45A		
Reflections collected	15201		
Independent reflections	3787 [R _{int} = 0.0535]		
Absorption coefficient	0.069 mm ⁻¹		
Absorption correction	None		
Max. and min. transmission	0.9911 and 0.9723		

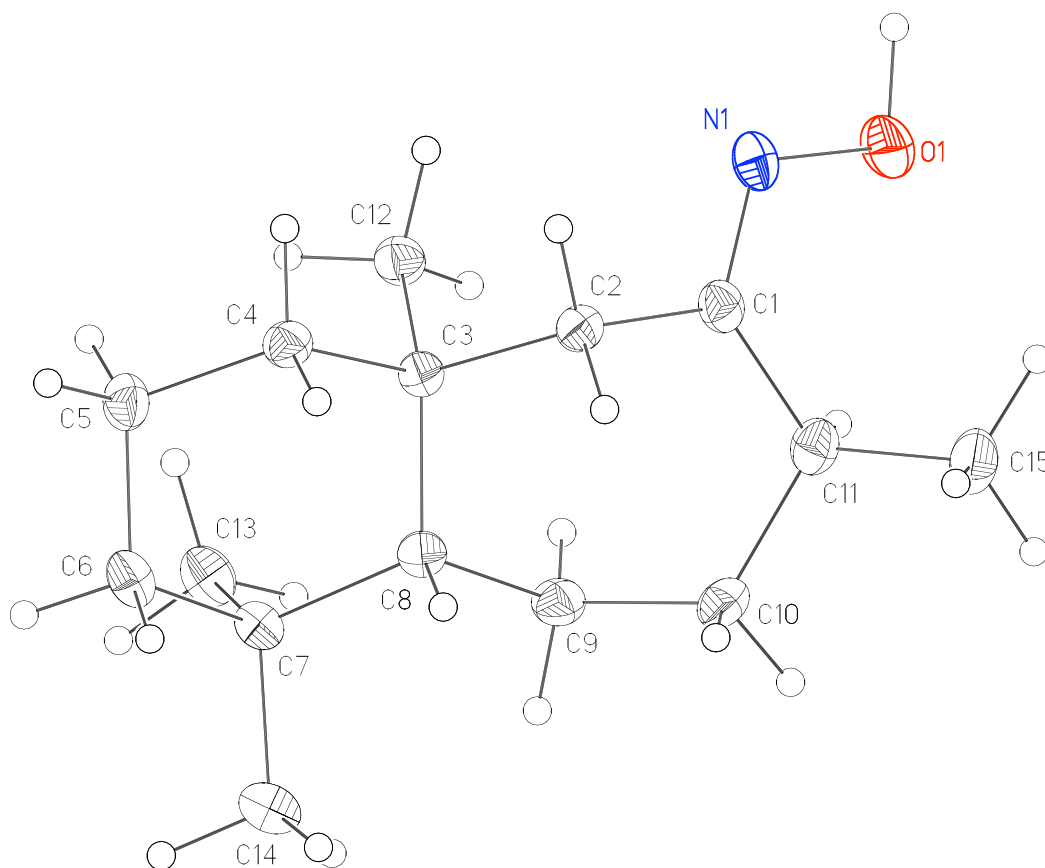
Table 1 (cont.)**Structure solution and Refinement**

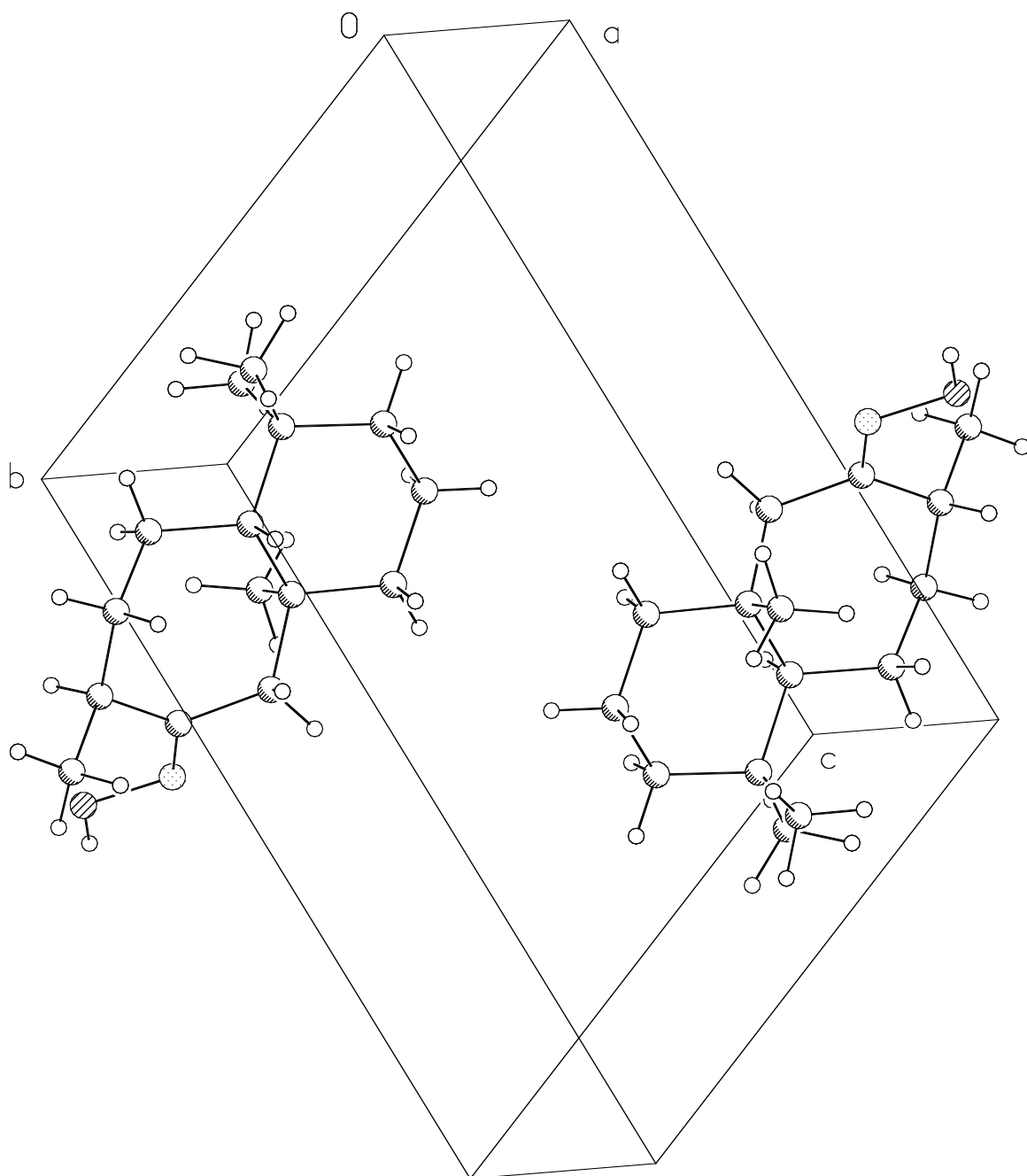
Structure solution program	Bruker XS v6.12
Primary solution method	Direct methods
Secondary solution method	Difference Fourier map
Hydrogen placement	Difference Fourier map
Structure refinement program	Bruker XL v6.12
Refinement method	Full matrix least-squares on F^2
Data / restraints / parameters	3787 / 0 / 262
Treatment of hydrogen atoms	Unrestrained
Goodness-of-fit on F^2	1.727
Final R indices [$I > 2\sigma(I)$, 2680 reflections]	$R1 = 0.0472$, $wR2 = 0.0748$
R indices (all data)	$R1 = 0.0689$, $wR2 = 0.0772$
Type of weighting scheme used	Sigma
Weighting scheme used	$w = 1/\sigma^2(F_o^2)$
Max shift/error	0.001
Average shift/error	0.000
Largest diff. peak and hole	0.339 and -0.260 e.Å ⁻³

Special Refinement Details

Refinement of F^2 against ALL reflections. The weighted R-factor (wR) and goodness of fit (S) are based on F^2 . Conventional R-factors (R) are based on F , with F set to zero for negative F^2 . The threshold expression of $F^2 > 2\sigma(F^2)$ is used only for calculating R-factors(gt), etc., and is not relevant to the choice of reflections for refinement. R-factors based on F^2 are statistically about twice as large as those based on F , and R-factors based on ALL data will be even larger.

All esds (except the esd in the dihedral angle between two l.s. planes) are estimated using the full covariance matrix. The cell esds are taken into account individually in the estimation of esds in distances, angles and torsion angles; correlations between esds in cell parameters are only used when they are defined by crystal symmetry. An approximate (isotropic) treatment of cell esds is used for estimating esds involving l.s. planes.





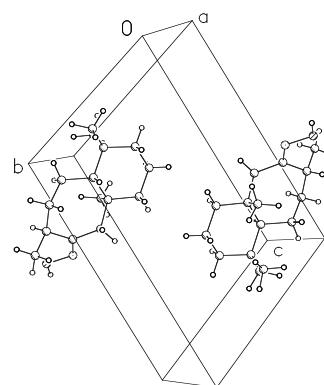
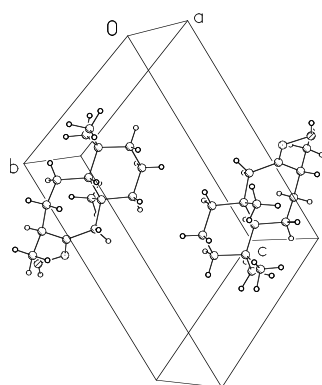


Table 2. Atomic coordinates ($\times 10^4$) and equivalent isotropic displacement parameters ($\text{\AA}^2 \times 10^3$) for 319B (CCDC 606034). $U(\text{eq})$ is defined as the trace of the orthogonalized U^{ij} tensor.

	x	y	z	U_{eq}
O(1)	-4505(1)	11144(1)	3840(1)	28(1)
N(1)	-2790(2)	9957(1)	4223(1)	21(1)
C(1)	-964(2)	9902(1)	3535(1)	18(1)
C(2)	877(2)	8645(1)	3887(1)	17(1)
C(3)	1046(2)	7415(1)	3314(1)	15(1)
C(4)	2524(2)	6123(1)	4021(1)	18(1)
C(5)	3103(2)	4868(1)	3493(1)	21(1)
C(6)	4334(2)	5257(1)	2315(1)	21(1)
C(7)	3040(2)	6534(1)	1514(1)	18(1)
C(8)	2286(2)	7777(1)	2102(1)	16(1)
C(9)	1074(2)	9121(1)	1332(1)	20(1)
C(10)	1234(2)	10493(1)	1604(1)	22(1)
C(11)	-655(2)	11007(1)	2448(1)	20(1)
C(12)	-1380(2)	7122(1)	3382(1)	19(1)
C(13)	1049(2)	6122(1)	1112(1)	24(1)
C(14)	4725(2)	6957(2)	471(1)	26(1)
C(15)	-230(3)	12347(1)	2687(1)	28(1)

Table 3. Bond lengths [Å] and angles [°] for 319B (CCDC 606034).

O(1)-N(1)	1.4241(11)	C(1)-C(2)-C(3)	115.86(9)
O(1)-H(1)	1.017(16)	C(1)-C(2)-H(2A)	109.5(6)
N(1)-C(1)	1.2844(14)	C(3)-C(2)-H(2A)	106.0(6)
C(1)-C(2)	1.5045(15)	C(1)-C(2)-H(2B)	109.3(6)
C(1)-C(11)	1.5119(15)	C(3)-C(2)-H(2B)	109.1(6)
C(2)-C(3)	1.5612(14)	H(2A)-C(2)-H(2B)	106.8(8)
C(2)-H(2A)	0.982(11)	C(12)-C(3)-C(4)	109.18(9)
C(2)-H(2B)	0.987(11)	C(12)-C(3)-C(8)	114.96(9)
C(3)-C(12)	1.5346(15)	C(4)-C(3)-C(8)	108.42(8)
C(3)-C(4)	1.5404(14)	C(12)-C(3)-C(2)	107.57(9)
C(3)-C(8)	1.5570(14)	C(4)-C(3)-C(2)	106.39(8)
C(4)-C(5)	1.5243(15)	C(8)-C(3)-C(2)	109.98(9)
C(4)-H(4A)	1.022(11)	C(5)-C(4)-C(3)	113.13(9)
C(4)-H(4B)	0.993(10)	C(5)-C(4)-H(4A)	109.2(6)
C(5)-C(6)	1.5226(16)	C(3)-C(4)-H(4A)	108.3(6)
C(5)-H(5A)	0.963(12)	C(5)-C(4)-H(4B)	110.5(6)
C(5)-H(5B)	1.017(11)	C(3)-C(4)-H(4B)	108.1(6)
C(6)-C(7)	1.5365(15)	H(4A)-C(4)-H(4B)	107.4(8)
C(6)-H(6A)	1.004(11)	C(6)-C(5)-C(4)	110.84(10)
C(6)-H(6B)	1.011(11)	C(6)-C(5)-H(5A)	109.6(7)
C(7)-C(13)	1.5369(15)	C(4)-C(5)-H(5A)	109.6(7)
C(7)-C(14)	1.5378(16)	C(6)-C(5)-H(5B)	110.0(6)
C(7)-C(8)	1.5626(15)	C(4)-C(5)-H(5B)	110.9(6)
C(8)-C(9)	1.5364(15)	H(5A)-C(5)-H(5B)	105.7(9)
C(8)-H(8)	0.985(10)	C(5)-C(6)-C(7)	114.42(10)
C(9)-C(10)	1.5297(16)	C(5)-C(6)-H(6A)	110.0(6)
C(9)-H(9A)	0.984(12)	C(7)-C(6)-H(6A)	109.6(6)
C(9)-H(9B)	1.021(10)	C(5)-C(6)-H(6B)	107.7(6)
C(10)-C(11)	1.5254(16)	C(7)-C(6)-H(6B)	109.0(6)
C(10)-H(10A)	0.980(11)	H(6A)-C(6)-H(6B)	105.8(8)
C(10)-H(10B)	0.985(11)	C(6)-C(7)-C(13)	110.26(10)
C(11)-C(15)	1.5327(16)	C(6)-C(7)-C(14)	106.92(9)
C(11)-H(11)	0.962(11)	C(13)-C(7)-C(14)	107.11(9)
C(12)-H(12A)	1.003(11)	C(6)-C(7)-C(8)	109.36(9)
C(12)-H(12B)	0.997(11)	C(13)-C(7)-C(8)	113.71(9)
C(12)-H(12C)	0.994(12)	C(14)-C(7)-C(8)	109.24(9)
C(13)-H(13A)	0.969(12)	C(9)-C(8)-C(3)	113.62(9)
C(13)-H(13B)	0.990(12)	C(9)-C(8)-C(7)	112.57(9)
C(13)-H(13C)	0.996(13)	C(3)-C(8)-C(7)	115.88(9)
C(14)-H(14A)	0.979(13)	C(9)-C(8)-H(8)	106.2(6)
C(14)-H(14B)	1.005(13)	C(3)-C(8)-H(8)	103.6(6)
C(14)-H(14C)	0.997(12)	C(7)-C(8)-H(8)	103.5(6)
C(15)-H(15A)	1.014(12)	C(10)-C(9)-C(8)	115.08(9)
C(15)-H(15B)	1.000(12)	C(10)-C(9)-H(9A)	107.3(6)
C(15)-H(15C)	0.989(13)	C(8)-C(9)-H(9A)	107.9(6)
		C(10)-C(9)-H(9B)	108.8(6)
N(1)-O(1)-H(1)	103.0(8)	C(8)-C(9)-H(9B)	111.7(6)
C(1)-N(1)-O(1)	112.92(9)	H(9A)-C(9)-H(9B)	105.6(9)
N(1)-C(1)-C(2)	114.97(10)	C(11)-C(10)-C(9)	115.95(10)
N(1)-C(1)-C(11)	123.26(10)	C(11)-C(10)-H(10A)	106.0(6)
C(2)-C(1)-C(11)	121.77(10)	C(9)-C(10)-H(10A)	109.8(6)

C(11)-C(10)-H(10B)	108.9(6)
C(9)-C(10)-H(10B)	110.2(6)
H(10A)-C(10)-H(10B)	105.5(9)
C(1)-C(11)-C(10)	113.20(9)
C(1)-C(11)-C(15)	110.49(9)
C(10)-C(11)-C(15)	110.64(10)
C(1)-C(11)-H(11)	106.7(7)
C(10)-C(11)-H(11)	107.9(7)
C(15)-C(11)-H(11)	107.6(7)
C(3)-C(12)-H(12A)	113.6(6)
C(3)-C(12)-H(12B)	114.1(7)
H(12A)-C(12)-H(12B)	106.8(9)
C(3)-C(12)-H(12C)	109.7(6)
H(12A)-C(12)-H(12C)	105.8(9)
H(12B)-C(12)-H(12C)	106.3(9)
C(7)-C(13)-H(13A)	109.4(7)
C(7)-C(13)-H(13B)	111.3(7)
H(13A)-C(13)-H(13B)	106.3(9)
C(7)-C(13)-H(13C)	112.7(7)
H(13A)-C(13)-H(13C)	107.4(9)
H(13B)-C(13)-H(13C)	109.5(9)
C(7)-C(14)-H(14A)	111.5(7)
C(7)-C(14)-H(14B)	113.5(7)
H(14A)-C(14)-H(14B)	107.7(10)
C(7)-C(14)-H(14C)	110.1(7)
H(14A)-C(14)-H(14C)	105.0(10)
H(14B)-C(14)-H(14C)	108.7(10)
C(11)-C(15)-H(15A)	111.2(7)
C(11)-C(15)-H(15B)	107.8(7)
H(15A)-C(15)-H(15B)	110.5(9)
C(11)-C(15)-H(15C)	110.3(7)
H(15A)-C(15)-H(15C)	107.5(10)
H(15B)-C(15)-H(15C)	109.6(10)

Table 4. Anisotropic displacement parameters ($\text{\AA}^2 \times 10^4$) for 319B (CCDC 606034). The anisotropic displacement factor exponent takes the form: $-2\pi^2 [h^2 a^{*2} U^{11} + \dots + 2 h k a^* b^* U^{12}]$

U^{11}	U^{22}	U^{33}	U^{23}	U^{13}	U^{12}
O(1)229(5)	225(5)	330(5)	-51(4)	-13(4)	65(4)
N(1)201(5)	170(5)	247(5)	-64(4)	-44(4)	23(4)
C(1)195(6)	172(6)	201(6)	-80(5)	-24(5)	-39(5)
C(2)175(6)	167(6)	161(6)	-36(5)	-17(5)	-42(5)
C(3)147(5)	158(6)	159(5)	-40(4)	-19(4)	-29(5)
C(4)185(6)	180(6)	162(6)	-23(5)	-13(5)	-25(5)
C(5)225(6)	159(6)	229(6)	-37(5)	-42(5)	2(5)
C(6)179(6)	205(6)	254(6)	-103(5)	-27(5)	4(5)
C(7)164(6)	193(6)	181(6)	-65(5)	-8(5)	-13(5)
C(8)147(6)	180(6)	165(6)	-40(5)	-21(5)	-36(5)
C(9)222(6)	212(6)	149(6)	-26(5)	-8(5)	-30(5)
C(10)250(7)	180(6)	195(6)	10(5)	-6(5)	-52(5)
C(11)205(6)	167(6)	227(6)	-22(5)	-51(5)	-17(5)
C(12)164(6)	202(7)	218(6)	-61(5)	-3(5)	-41(5)
C(13)228(7)	257(7)	247(7)	-112(6)	-42(6)	-10(6)
C(14)237(7)	306(8)	232(7)	-100(6)	35(5)	-33(6)
C(15)351(8)	171(7)	310(7)	-56(6)	-31(6)	-39(6)

Table 5. Hydrogen coordinates ($\times 10^4$) and isotropic displacement parameters ($\text{\AA}^2 \times 10^3$) for 319B (CCDC 606034).

	x	y	z	U_{iso}
H(1)	-5840(30)	11001(16)	4446(13)	67(5)
H(2A)	611(17)	8240(11)	4700(9)	18(3)
H(2B)	2372(19)	8949(11)	3752(8)	18(3)
H(4A)	4005(19)	6406(11)	4113(9)	22(3)
H(4B)	1692(17)	5871(11)	4782(9)	14(3)
H(5A)	4060(20)	4102(13)	3959(10)	29(3)
H(5B)	1668(19)	4503(11)	3465(9)	24(3)
H(6A)	4678(17)	4427(12)	1973(9)	21(3)
H(6B)	5870(19)	5459(11)	2391(9)	21(3)
H(8)	3746(18)	7985(10)	2218(8)	12(3)
H(9A)	1780(19)	9161(11)	556(10)	23(3)
H(9B)	-608(19)	9093(11)	1319(9)	19(3)
H(10A)	1180(18)	11255(12)	916(10)	21(3)
H(10B)	2728(19)	10415(11)	1870(9)	18(3)
H(11)	-2074(19)	11239(11)	2116(9)	22(3)
H(12A)	-1412(17)	6178(12)	3264(9)	20(3)
H(12B)	-2364(19)	7833(12)	2839(10)	27(3)
H(12C)	-2179(19)	7128(11)	4145(10)	23(3)
H(13A)	1653(19)	5487(13)	629(10)	31(3)
H(13B)	110(20)	6953(13)	651(10)	29(3)
H(13C)	50(20)	5634(13)	1746(10)	35(4)
H(14A)	5910(20)	7379(12)	643(10)	31(3)
H(14B)	3970(20)	7639(13)	-182(11)	37(4)
H(14C)	5570(20)	6104(13)	222(10)	32(3)
H(15A)	-1510(20)	12715(12)	3225(10)	26(3)
H(15B)	-120(20)	13063(13)	1952(11)	31(3)
H(15C)	1210(20)	12151(13)	3037(10)	41(4)

Table 6. Hydrogen bonds for 319B (CCDC 606034) [\AA and $^\circ$].

D-H...A	d(D-H)	d(H...A)	d(D...A)	$\angle(\text{DHA})$
O(1)-H(1)...N(1)#1	1.017(16)	1.843(16)	2.7884(13)	153.2(12)
O(1)-H(1)...O(1)#1	1.017(16)	2.584(15)	3.2256(17)	120.8(10)

Symmetry transformations used to generate equivalent atoms:

#1 $-x-1, -y+2, -z+1$

CALIFORNIA INSTITUTE OF TECHNOLOGY
BECKMAN INSTITUTE
X-RAY CRYSTALLOGRAPHY LABORATORY

Date 23 January 2007

Crystal Structure Analysis of:

370

(shown below)

For	Investigator: Ryan McFadden	ext. 6131
	Advisor: B. M. Stoltz	ext. 6064
	Account Number: BMS1.SQUIBB-2.22-GRANT.SQUIBB1	
By	Michael W. Day	116 Beckman ext. 2734
	e-mail: mikeday@caltech.edu	

Contents

Table 1. Crystal data

Figures Minimum overlap, unit cell contents, stereo view of unit cell contents

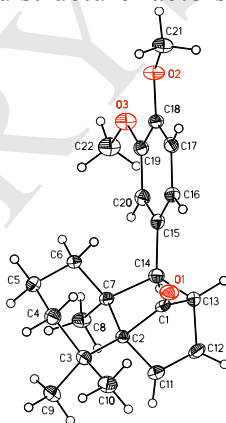
Table 2. Atomic Coordinates

Table 3. Full bond distances and angles

Table 4. Anisotropic displacement parameters

Table 5. Hydrogen atomic coordinates

Table 6. Observed and calculated structure factors (available upon request)



370

Note: The crystallographic data have been deposited in the Cambridge Database (CCDC) and has been placed on hold pending further instructions from me. The deposition number is 634511. Ideally the CCDC would like the publication to contain a footnote of the type: "Crystallographic data have been deposited at the CCDC, 12 Union Road, Cambridge CB2 1EZ, UK and copies can be obtained on request, free of charge, by quoting the publication citation and the deposition number 634511."

Table 1. Crystal data and structure refinement for 370 (CCDC 634511).

Empirical formula	C ₂₂ H ₂₈ O ₃
Formula weight	340.44
Crystallization Solvent	Hexanes/ethylacetate
Crystal Habit	Fragment
Crystal size	0.26 x 0.22 x 0.17 mm ³
Crystal color	Colorless

Data Collection

Type of diffractometer	Bruker SMART 1000
Wavelength	0.71073 Å MoK α
Data Collection Temperature	100(2) K
θ range for 8994 reflections used in lattice determination	2.29 to 34.45°
Unit cell dimensions	a = 23.2678(15) Å b = 13.8762(9) Å β = 108.548(2)° c = 11.8122(8) Å
Volume	3615.7(4) Å ³
Z	8
Crystal system	Monoclinic
Space group	C2/c
Density (calculated)	1.251 Mg/m ³
F(000)	1472
Data collection program	Bruker SMART v5.630
θ range for data collection	1.73 to 34.57°
Completeness to θ = 34.57°	89.7 %
Index ranges	-36 \leq h \leq 36, -21 \leq k \leq 21, -18 \leq l \leq 18
Data collection scan type	ω scans at 5 ϕ settings
Data reduction program	Bruker SAINT v6.45A
Reflections collected	37303
Independent reflections	37303 [R _{int} = 0.0000]
Absorption coefficient	0.081 mm ⁻¹
Absorption correction	TWINABS
Max. and min. transmission	1.0000 and 0.7508

Table 1 (cont.)**Structure solution and Refinement**

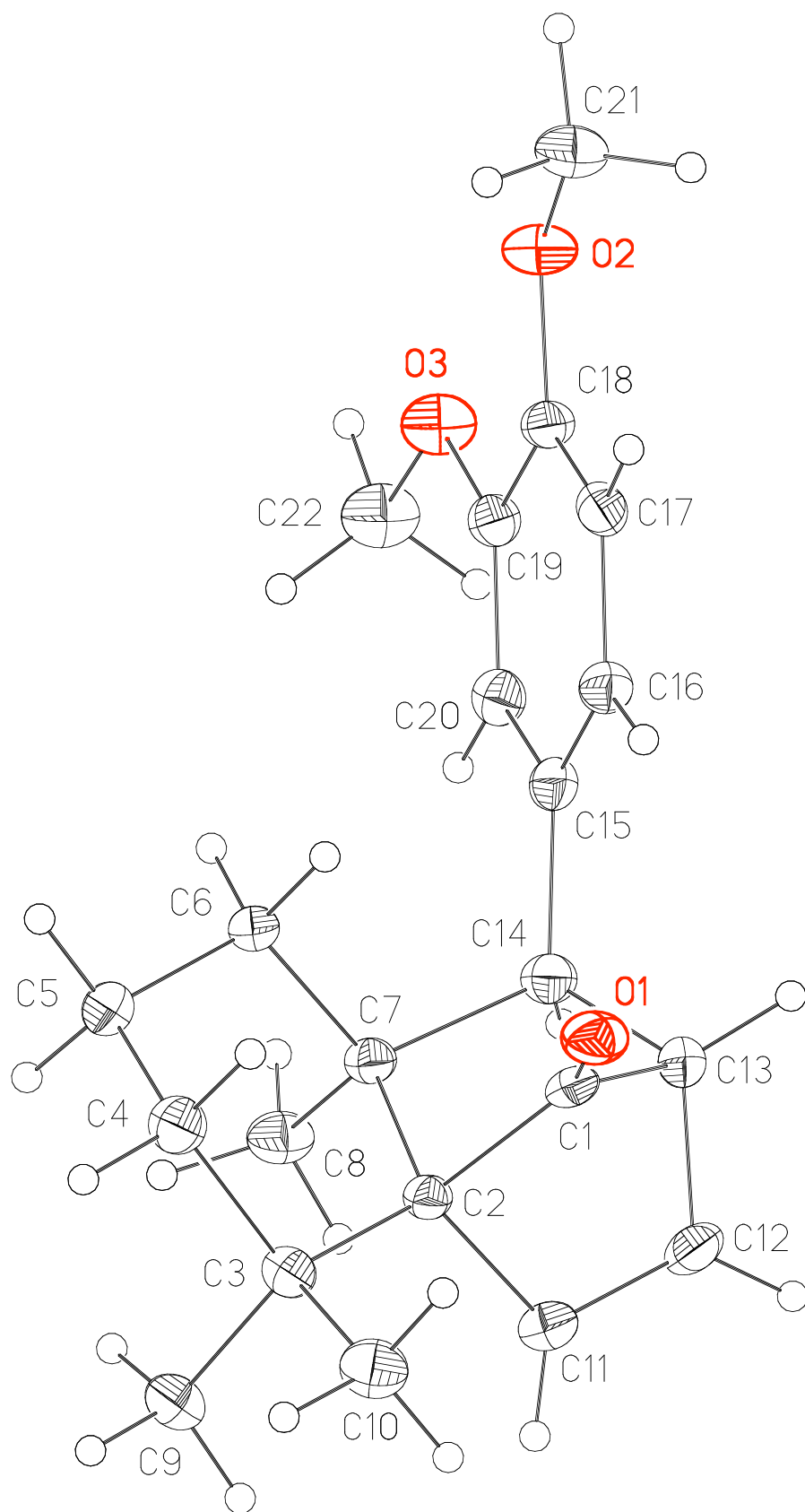
Structure solution program	Bruker XS v6.12
Primary solution method	Direct methods
Secondary solution method	Difference Fourier map
Hydrogen placement	Difference Fourier map
Structure refinement program	Bruker XL v6.12
Refinement method	Full matrix least-squares on F^2
Data / restraints / parameters	37303 / 0 / 339
Treatment of hydrogen atoms	Unrestrained
Goodness-of-fit on F^2	1.182
Final R indices [$I > 2\sigma(I)$, 21619 reflections]	$R1 = 0.0601$, $wR2 = 0.1106$
R indices (all data)	$R1 = 0.1018$, $wR2 = 0.1173$
Type of weighting scheme used	Sigma
Weighting scheme used	$w = 1/\sigma^2(F_o^2)$
Max shift/error	0.001
Average shift/error	0.000
Largest diff. peak and hole	0.570 and -0.427 e. \AA^{-3}

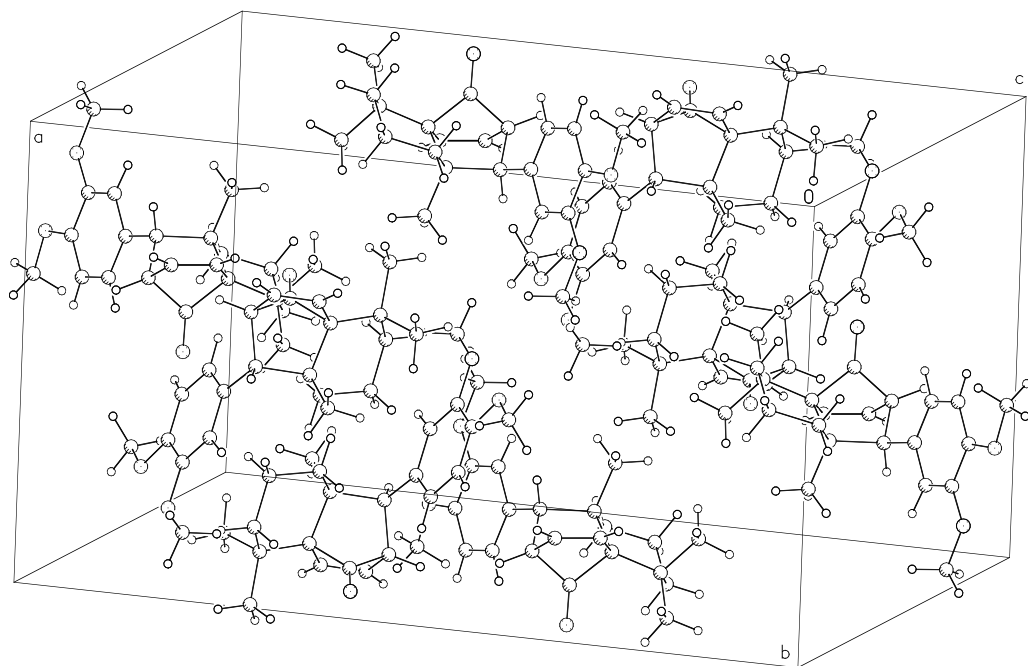
Special Refinement Details

This crystal is a non-merohedral twin and data were integrated and the structure refined as such.. The twin law (179.8° rotation around the c -axis) was determined using CELL_NOW on a group of orientation reflections, 690/781 reflections were assigned to domain 1 and 452/781 were assigned to domain 2, 89 of which were exclusive to this domain.

Refinement of F^2 against ALL reflections. The weighted R-factor (wR) and goodness of fit (S) are based on F^2 , conventional R-factors (R) are based on F , with F set to zero for negative F^2 . The threshold expression of $F^2 > 2\sigma(F^2)$ is used only for calculating R-factors(gt) etc. and is not relevant to the choice of reflections for refinement. R-factors based on F^2 are statistically about twice as large as those based on F , and R-factors based on ALL data will be even larger.

All esds (except the esd in the dihedral angle between two l.s. planes) are estimated using the full covariance matrix. The cell esds are taken into account individually in the estimation of esds in distances, angles and torsion angles; correlations between esds in cell parameters are only used when they are defined by crystal symmetry. An approximate (isotropic) treatment of cell esds is used for estimating esds involving l.s. planes.





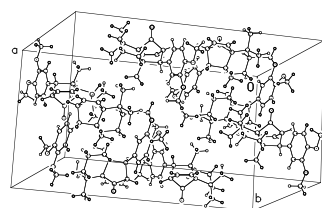
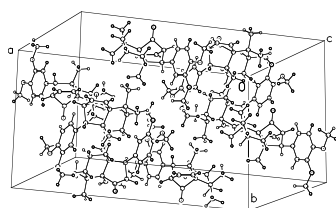


Table 2. Atomic coordinates ($\times 10^4$) and equivalent isotropic displacement parameters ($\text{\AA}^2 \times 10^3$) for 370 (CCDC 634511). $U(\text{eq})$ is defined as the trace of the orthogonalized U^{ij} tensor.

	x	y	z	U_{eq}
O(1)	1481(1)	5234(1)	2876(1)	28(1)
O(2)	684(1)	1843(1)	6684(1)	28(1)
O(3)	623(1)	556(1)	5078(1)	28(1)
C(1)	1332(1)	4548(1)	2231(1)	21(1)
C(2)	1679(1)	3923(1)	1575(1)	16(1)
C(3)	2328(1)	4235(1)	1655(1)	20(1)
C(4)	2752(1)	4090(1)	2946(1)	24(1)
C(5)	2709(1)	3082(1)	3421(1)	25(1)
C(6)	2065(1)	2867(1)	3409(1)	20(1)
C(7)	1593(1)	2918(1)	2152(1)	19(1)
C(8)	1643(1)	2037(1)	1419(1)	25(1)
C(9)	2569(1)	3662(1)	794(1)	26(1)
C(10)	2332(1)	5298(1)	1303(1)	27(1)
C(11)	1203(1)	4003(1)	347(1)	21(1)
C(12)	657(1)	4078(1)	469(1)	25(1)
C(13)	721(1)	4029(1)	1779(1)	23(1)
C(14)	912(1)	2985(1)	2204(1)	21(1)
C(15)	836(1)	2720(1)	3400(1)	20(1)
C(16)	873(1)	3401(1)	4275(1)	22(1)
C(17)	826(1)	3130(1)	5385(1)	22(1)
C(18)	736(1)	2184(1)	5622(1)	20(1)
C(19)	699(1)	1478(1)	4742(1)	21(1)
C(20)	746(1)	1757(1)	3647(1)	21(1)
C(21)	803(1)	2524(1)	7636(1)	29(1)
C(22)	592(1)	-189(1)	4224(1)	33(1)

Table 3. Bond lengths [Å] and angles [°] for 370 (CCDC 634511).

O(1)-C(1)	1.1998(9)	C(21)-H(21B)	1.028(9)
O(2)-C(18)	1.3818(9)	C(21)-H(21C)	0.987(8)
O(2)-C(21)	1.4275(10)	C(22)-H(22A)	1.018(10)
O(3)-C(19)	1.3677(9)	C(22)-H(22B)	1.033(8)
O(3)-C(22)	1.4304(10)	C(22)-H(22C)	1.036(10)
C(1)-C(13)	1.5297(12)		
C(1)-C(2)	1.5508(11)	C(18)-O(2)-C(21)	115.88(7)
C(2)-C(11)	1.5236(10)	C(19)-O(3)-C(22)	116.95(7)
C(2)-C(3)	1.5449(11)	O(1)-C(1)-C(13)	130.05(8)
C(2)-C(7)	1.5923(11)	O(1)-C(1)-C(2)	132.08(8)
C(3)-C(9)	1.5311(12)	C(13)-C(1)-C(2)	97.86(7)
C(3)-C(10)	1.5324(12)	C(11)-C(2)-C(3)	115.97(7)
C(3)-C(4)	1.5432(11)	C(11)-C(2)-C(1)	95.61(6)
C(4)-C(5)	1.5230(12)	C(3)-C(2)-C(1)	117.85(6)
C(4)-H(4A)	0.992(8)	C(11)-C(2)-C(7)	108.61(6)
C(4)-H(4B)	0.996(8)	C(3)-C(2)-C(7)	118.24(6)
C(5)-C(6)	1.5221(12)	C(1)-C(2)-C(7)	96.91(6)
C(5)-H(5A)	1.030(8)	C(9)-C(3)-C(10)	106.53(7)
C(5)-H(5B)	0.966(8)	C(9)-C(3)-C(4)	109.50(7)
C(6)-C(7)	1.5426(10)	C(10)-C(3)-C(4)	109.68(7)
C(6)-H(6A)	0.988(8)	C(9)-C(3)-C(2)	111.79(7)
C(6)-H(6B)	0.996(7)	C(10)-C(3)-C(2)	110.12(7)
C(7)-C(8)	1.5238(11)	C(4)-C(3)-C(2)	109.18(7)
C(7)-C(14)	1.6080(11)	C(5)-C(4)-C(3)	112.82(7)
C(8)-H(8A)	0.980(8)	C(5)-C(4)-H(4A)	112.3(4)
C(8)-H(8B)	0.967(8)	C(3)-C(4)-H(4A)	107.6(5)
C(8)-H(8C)	0.992(9)	C(5)-C(4)-H(4B)	107.9(5)
C(9)-H(9A)	1.001(9)	C(3)-C(4)-H(4B)	108.1(4)
C(9)-H(9B)	0.993(9)	H(4A)-C(4)-H(4B)	108.0(6)
C(9)-H(9C)	0.981(9)	C(6)-C(5)-C(4)	110.87(7)
C(10)-H(10A)	0.988(9)	C(6)-C(5)-H(5A)	109.0(4)
C(10)-H(10B)	0.997(8)	C(4)-C(5)-H(5A)	110.2(4)
C(10)-H(10C)	0.982(9)	C(6)-C(5)-H(5B)	109.2(5)
C(11)-C(12)	1.3280(12)	C(4)-C(5)-H(5B)	109.6(5)
C(11)-H(11)	0.901(7)	H(5A)-C(5)-H(5B)	107.9(6)
C(12)-C(13)	1.5082(12)	C(5)-C(6)-C(7)	113.39(7)
C(12)-H(12)	0.951(8)	C(5)-C(6)-H(6A)	108.5(4)
C(13)-C(14)	1.5519(11)	C(7)-C(6)-H(6A)	109.1(4)
C(13)-H(13)	0.950(8)	C(5)-C(6)-H(6B)	111.6(4)
C(14)-C(15)	1.5240(11)	C(7)-C(6)-H(6B)	108.4(4)
C(14)-H(14)	0.968(7)	H(6A)-C(6)-H(6B)	105.5(6)
C(15)-C(16)	1.3829(11)	C(8)-C(7)-C(6)	110.53(7)
C(15)-C(20)	1.3977(11)	C(8)-C(7)-C(2)	114.65(7)
C(16)-C(17)	1.4002(12)	C(6)-C(7)-C(2)	107.68(6)
C(16)-H(16)	1.004(8)	C(8)-C(7)-C(14)	108.84(7)
C(17)-C(18)	1.3713(11)	C(6)-C(7)-C(14)	112.01(7)
C(17)-H(17)	0.939(8)	C(2)-C(7)-C(14)	102.98(6)
C(18)-C(19)	1.4120(11)	C(7)-C(8)-H(8A)	112.0(5)
C(19)-C(20)	1.3868(11)	C(7)-C(8)-H(8B)	111.8(5)
C(20)-H(20)	1.015(7)	H(8A)-C(8)-H(8B)	107.1(7)
C(21)-H(21A)	0.990(9)	C(7)-C(8)-H(8C)	109.6(5)

H(8A)-C(8)-H(8C)	109.5(7)	H(21A)-C(21)-H(21C)	108.8(7)
H(8B)-C(8)-H(8C)	106.7(7)	H(21B)-C(21)-H(21C)	110.8(7)
C(3)-C(9)-H(9A)	112.5(5)	O(3)-C(22)-H(22A)	109.2(5)
C(3)-C(9)-H(9B)	109.4(5)	O(3)-C(22)-H(22B)	106.3(5)
H(9A)-C(9)-H(9B)	110.4(7)	H(22A)-C(22)-H(22B)	109.3(7)
C(3)-C(9)-H(9C)	110.5(5)	O(3)-C(22)-H(22C)	109.9(5)
H(9A)-C(9)-H(9C)	106.6(7)	H(22A)-C(22)-H(22C)	110.2(7)
H(9B)-C(9)-H(9C)	107.2(7)	H(22B)-C(22)-H(22C)	111.8(7)
C(3)-C(10)-H(10A)	110.1(5)		
C(3)-C(10)-H(10B)	107.9(5)		
H(10A)-C(10)-H(10B)	108.8(7)		
C(3)-C(10)-H(10C)	113.3(5)		
H(10A)-C(10)-H(10C)	108.1(7)		
H(10B)-C(10)-H(10C)	108.5(7)		
C(12)-C(11)-C(2)	109.50(8)		
C(12)-C(11)-H(11)	123.9(4)		
C(2)-C(11)-H(11)	126.6(5)		
C(11)-C(12)-C(13)	108.78(8)		
C(11)-C(12)-H(12)	130.1(5)		
C(13)-C(12)-H(12)	121.1(5)		
C(12)-C(13)-C(1)	96.58(7)		
C(12)-C(13)-C(14)	107.33(7)		
C(1)-C(13)-C(14)	100.80(6)		
C(12)-C(13)-H(13)	116.9(5)		
C(1)-C(13)-H(13)	116.6(5)		
C(14)-C(13)-H(13)	115.8(5)		
C(15)-C(14)-C(13)	114.77(7)		
C(15)-C(14)-C(7)	115.31(6)		
C(13)-C(14)-C(7)	103.12(6)		
C(15)-C(14)-H(14)	108.7(4)		
C(13)-C(14)-H(14)	109.7(4)		
C(7)-C(14)-H(14)	104.6(5)		
C(16)-C(15)-C(20)	118.28(8)		
C(16)-C(15)-C(14)	122.09(7)		
C(20)-C(15)-C(14)	119.60(7)		
C(15)-C(16)-C(17)	120.80(8)		
C(15)-C(16)-H(16)	120.5(4)		
C(17)-C(16)-H(16)	118.7(4)		
C(18)-C(17)-C(16)	120.70(8)		
C(18)-C(17)-H(17)	120.1(5)		
C(16)-C(17)-H(17)	119.2(5)		
C(17)-C(18)-O(2)	125.25(7)		
C(17)-C(18)-C(19)	119.42(7)		
O(2)-C(18)-C(19)	115.32(7)		
O(3)-C(19)-C(20)	126.04(7)		
O(3)-C(19)-C(18)	114.77(7)		
C(20)-C(19)-C(18)	119.19(7)		
C(19)-C(20)-C(15)	121.61(8)		
C(19)-C(20)-H(20)	120.7(4)		
C(15)-C(20)-H(20)	117.6(4)		
O(2)-C(21)-H(21A)	109.7(5)		
O(2)-C(21)-H(21B)	103.5(4)		
H(21A)-C(21)-H(21B)	111.6(7)		
O(2)-C(21)-H(21C)	112.4(5)		

Table 4. Anisotropic displacement parameters ($\text{\AA}^2 \times 10^4$) for 370 (CCDC 634511). The anisotropic displacement factor exponent takes the form: $-2\pi^2 [h^2 a^{*2} U^{11} + \dots + 2 h k a^* b^* U^{12}]$

	U^{11}	U^{22}	U^{33}	U^{23}	U^{13}	U^{12}
O(1)	395(4)	242(3)	222(3)	3(3)	138(3)	53(3)
O(2)	369(4)	292(3)	190(3)	-1(3)	115(3)	-64(3)
O(3)	365(4)	231(3)	251(3)	-21(3)	101(3)	-68(3)
C(1)	263(5)	231(5)	134(4)	83(4)	61(3)	32(4)
C(2)	179(4)	175(4)	143(4)	-1(3)	56(3)	3(3)
C(3)	204(4)	213(5)	192(4)	-6(3)	60(3)	-12(3)
C(4)	186(4)	314(5)	212(5)	-24(4)	56(4)	-23(4)
C(5)	197(5)	344(6)	191(4)	33(4)	47(4)	49(4)
C(6)	215(4)	237(5)	162(4)	19(4)	66(3)	43(4)
C(7)	190(4)	211(4)	154(4)	1(3)	54(3)	3(3)
C(8)	306(5)	232(5)	210(5)	-8(4)	94(4)	-18(4)
C(9)	260(5)	306(6)	255(5)	-1(4)	117(4)	3(4)
C(10)	265(5)	266(5)	290(5)	9(4)	98(4)	-44(4)
C(11)	259(5)	207(5)	166(4)	8(4)	55(4)	-14(4)
C(12)	222(5)	295(5)	197(4)	67(4)	10(4)	0(4)
C(13)	190(4)	293(5)	235(5)	58(4)	91(4)	56(4)
C(14)	212(4)	237(5)	177(4)	13(4)	50(3)	-12(4)
C(15)	140(4)	252(5)	207(4)	24(4)	39(3)	5(3)
C(16)	202(4)	227(5)	239(5)	35(4)	79(4)	9(4)
C(17)	192(4)	247(5)	207(4)	-27(4)	64(3)	16(4)
C(18)	170(4)	262(5)	183(4)	25(4)	57(3)	-14(4)
C(19)	152(4)	237(5)	222(4)	29(4)	38(3)	-25(4)
C(20)	171(4)	257(5)	202(4)	-18(4)	38(3)	-23(4)
C(21)	380(6)	307(6)	219(5)	-22(4)	128(4)	-24(5)
C(22)	453(7)	236(6)	314(6)	-27(4)	137(5)	-30(5)

Table 5. Hydrogen coordinates ($\times 10^4$) and isotropic displacement parameters ($\text{\AA}^2 \times 10^3$) for 370 (CCDC 634511).

	x	y	z	U_{iso}
H(4A)	3170(4)	4250(5)	2959(7)	23(2)
H(4B)	2632(3)	4559(6)	3468(7)	23(2)
H(5A)	2835(3)	2575(6)	2907(7)	20(2)
H(5B)	2981(4)	3027(6)	4229(8)	32(2)
H(6A)	1955(3)	3335(5)	3935(6)	14(2)
H(6B)	2036(3)	2221(6)	3755(6)	14(2)
H(8A)	2064(4)	1905(5)	1462(7)	22(2)
H(8B)	1413(4)	2116(6)	584(8)	29(2)
H(8C)	1473(4)	1466(6)	1705(7)	28(2)
H(9A)	2575(4)	2951(6)	943(7)	30(2)
H(9B)	2982(4)	3894(6)	856(8)	35(3)
H(9C)	2312(4)	3763(6)	-34(8)	32(2)
H(10A)	2060(4)	5396(6)	478(8)	33(3)
H(10B)	2753(4)	5468(6)	1337(7)	26(2)
H(10C)	2205(4)	5737(6)	1830(7)	28(2)
H(11)	1272(3)	4011(5)	-362(6)	7(2)
H(12)	269(4)	4139(6)	-120(7)	26(2)
H(13)	399(4)	4292(5)	2014(7)	20(2)
H(14)	684(3)	2531(5)	1606(6)	15(2)
H(16)	941(3)	4098(6)	4131(6)	18(2)
H(17)	868(3)	3601(6)	5976(7)	20(2)
H(20)	739(3)	1260(5)	3013(7)	16(2)
H(21A)	1225(4)	2762(6)	7834(7)	31(2)
H(21B)	741(4)	2132(6)	8327(7)	31(2)
H(21C)	524(4)	3080(6)	7436(7)	30(2)
H(22A)	230(4)	-69(7)	3483(9)	51(3)
H(22B)	529(4)	-826(6)	4621(7)	29(2)
H(22C)	989(4)	-199(7)	4001(8)	47(3)

Appendix NINE

Compounds Submitted for PI3K Biological Screening

Table A9.1 Compounds Submitted for PI3K Biological Screening: Part 1

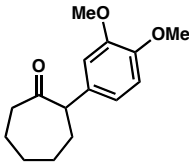
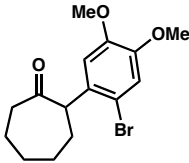
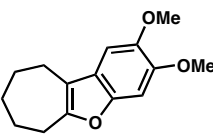
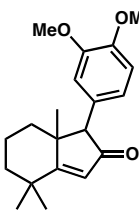
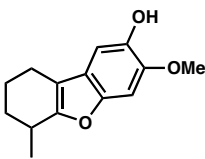
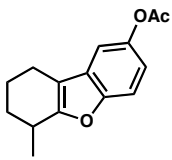
Compound Structure	Cantley#	Notebook#	%ee	Quantity (mg)	Storage Method
 (±)-398	1	16RMM2-1129135	0	12	Solution in Benzene
 (±)-399	2	16RMM1-1212203	0	6.8	Solution in Benzene
 (±)-400	3	16RMM1-1213207	NA	4.3	Solution in Benzene
 (7.5 to 1.0 dr) (±)-348	4	16RMM1-1107101	0	6.1	Solid
 (±)-334	5	15RMM1-0917163	0	4.0	Solution in Benzene
 (±)-401	6	14RMM1-0809259	0	1.5	Solution in Benzene

Table A9.2 Compounds Submitted for PI3K Biological Screening: Part 2

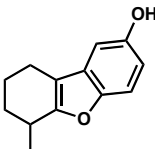
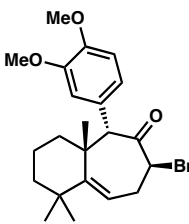
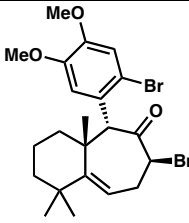
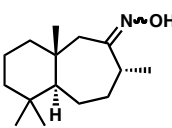
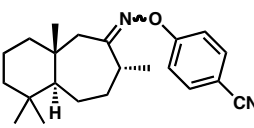
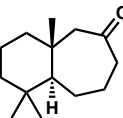
Compound Structure	Cantley#	Notebook#	%ee	Quantity (mg)	Storage Method
 (\pm) -331	7	14RMM1-0706161	0	5	Solution in Benzene
 (\pm) -376	8	16RMM2-0121289	0	30±5	Solution in Benzene
 (\pm) -377	9	16RMM1-0119289	0	2.0	Solid
 (\pm) -319A and (\pm) -319B	10	17RMM1-0227145	0	9.7	Solid
 (\pm) -323A and (\pm) -323B	11	14RMM1-0619109	0	3.0	Solution in Benzene
 (\pm) -305	12	16RMM2-0118287	0	3.1	Solution in Benzene

Table A9.3 Compounds Submitted for PI3K Biological Screening: Part 3

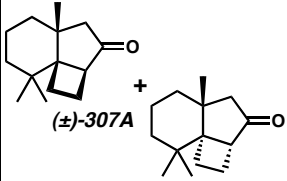
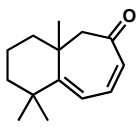
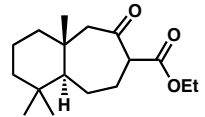
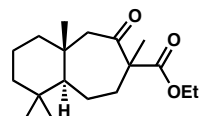
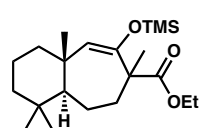
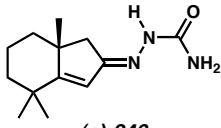
Compound Structure	Cantley#	Notebook#	%ee	Quantity (mg)	Storage Method
 <p>(±)-307A + (±)-307B (2 : 1 mixture; major diastereomer unassigned)</p>	13	13RMM1-0324231	0	8.7	Solid
 <p>(±)-318</p>	14	13RMM2-0907277	0	2.2	Solid
 <p>(±)-361ABC (tautomeric mixture)</p>	15	17RMM1-012437	0	2.1	Solid
 <p>(±)-362</p>	16	17RMMc-0209103	0	6.0	Solution in Benzene
 <p>(±)-363</p>	17	17RMMc-0211107	0	8.6	Solution in Benzene
 <p>(+)-246</p>	18	15RMM1-0906111	95	16	Solid

Table A9.4 Compounds Submitted for PI3K Biological Screening: Part 4

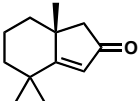
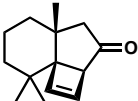
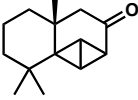
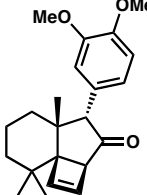
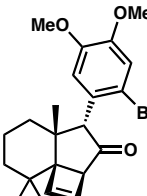
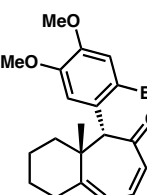
Compound Structure	Cantley#	Notebook#	%ee	Quantity (mg)	Storage Method
 (+)-143	19	19RMM6-090937	95	10	Neat Oil
 (+)-312	20	19RMM1-091151	95	8±3 Compound is Volatile!	Solution in Benzene
 (-)-313	21	19RMM4-090937	95	2.6±0.6	Solution in Benzene
 (±)-369	22	17RMM2-0211113	0	7.3	Solid
 (+)-379	23	19RMM1-091471	95	2.1	Solid
 (-)-380	24	19RMM1-091675	95	6.0	Solid

Table A9.5 Compounds Submitted for PI3K Biological Screening: Part 5

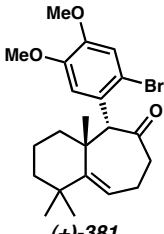
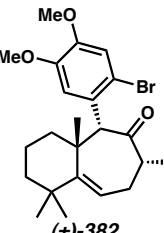
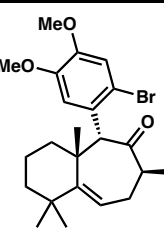
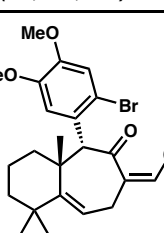
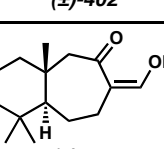
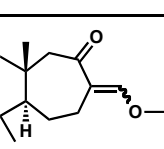
Compound Structure	Cantley#	Notebook#	%ee	Quantity (mg)	Storage Method
 (+)-381	25	19RMM1-091889	95	1.6	Solid
 (±)-382	26	17RMM1-0425227	0	3.3	Solution in Benzene
 (8R,10S,11R)-383	27	19RMMmethylepi	95	3.8	Solution in Benzene
 (±)-402	28	19RMM1-091155	0	3.2	Solution in Benzene
 (±)-357	29	16RMM1-0103235	0	3.3	Solution in Benzene
 (±)-358	30	16RMM2-0103235	0	3.5	Solution in Benzene

Table A9.6 Compounds Submitted for PI3K Biological Screening: Part 6

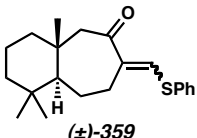
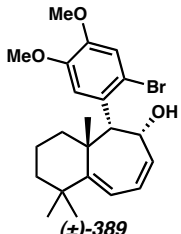
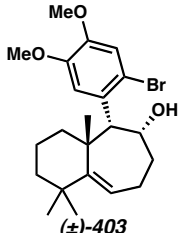
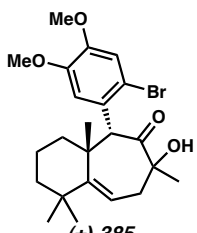
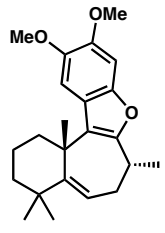
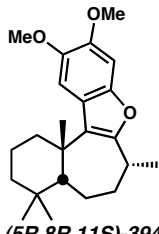
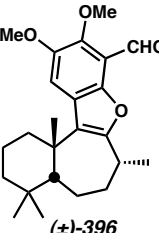
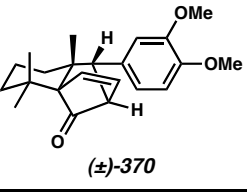
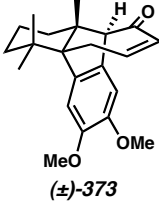
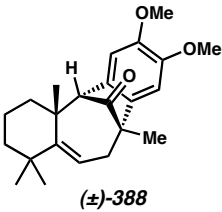
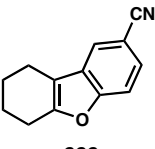
Compound Structure	Cantley#	Notebook#	%ee	Quantity (mg)	Storage Method
 <p>(±)-359</p>	31	16RMM3-0114261	0	6.8	Solution in Benzene
 <p>(±)-389</p>	32	18RMM2-071897	0	1.8	Solution in Benzene
 <p>(±)-403</p>	33	18RMMx-0718101	0	8±2	Solution in Benzene
 <p>(±)-385</p>	34	18RMM5-070851	0	4.2	Solution in Benzene
 <p>(±)-386</p>	35	18RMMc-0722119	0	1.5	Solution in Benzene

Table A9.7 Compounds Submitted for PI3K Biological Screening: Part 7

Compound Structure	Cantley#	Notebook#	%ee	Quantity (mg)	Storage Method
 (5R,8R,11S)-394	36	19RMM1-1026197	95	2.5	Solution in Benzene
 (±)-396	37	19RMM1-1024191	0	1.0	Solution in Benzene
 (±)-370	38	16RMM5-1130137	0	4.0	Solution in Benzene
 (±)-373	39	17RMM2-0318197	0	2.0±0.5	Solution in Benzene
 (±)-388	40	17RMM1-0504233	0	1.4	Solution in Benzene
 322	41	17RMM1-0312171	NA	1.0	Solid

Appendix Ten

Cross References to Characterization Binders and Notebooks

Table A10.1 Cross References for Compounds from Chapter 2: Thujopsene

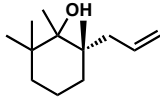
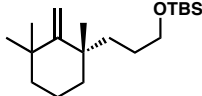
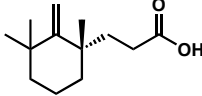
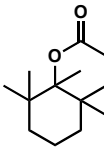
Characterization Binder #	Structure (Thesis #)	Spectral Data
TH01	 <p>99A and 99B</p>	¹ H NMR: 1-jm-062007-112H ¹³ C NMR : 1-jm-062007-112C13C IR: jm-1-061907-111NaCD
TH02	 <p>(-)-104</p>	¹ H NMR: 18RMM1-0820221H ¹³ C NMR : 18RMM1-0820221C13C IR: 18RMM1-0820221NaCD
TH03	 <p>(-)-94</p>	¹ H NMR: 18RMM1-0822229H ¹³ C NMR : 18RMM1-822229C13C IR: 1jm-072707157NaCD
TH04	 <p>103A and 103B</p>	¹ H NMR: 19RMMx-lactoneH ¹³ C NMR : 19RMMx-lactoneC IR: 19RMMx-lactoneNaCD

Table A10.2 Cross References for Compounds from Chapter 2: Dysidiolide

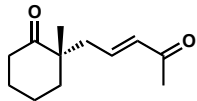
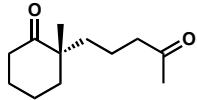
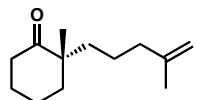
Characterization Binder #	Structure (Thesis #)	Spectral Data
DY01	 (-)-113	¹ H NMR: 7RMM1-0211109H ¹³ C NMR : 17RMM1-0211109C13C IR: 17RMM1-0211109NaCD
DY02	 (-)-112	¹ H NMR: 17RMMc-0212115H ¹³ C NMR : 17RMMc-0212115C13C IR: 17RMMc-0212115NaCD
DY03	 (-)-109	¹ H NMR: 17RMM1-0219139H ¹³ C NMR : 17RMM1-0219137C13C IR: 17RMM1-0218137NaCD

Table A10.3 Cross References for Compounds from Chapter 2: Aspidospermine

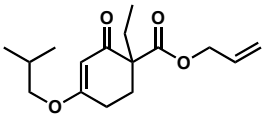
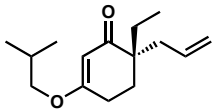
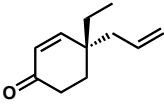
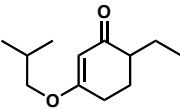
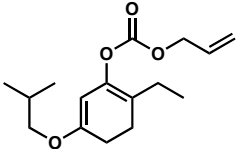
Characterization Binder #	Structure (Thesis #)	Spectral Data
AS01	 <p>121</p>	¹ H NMR: 17RMM2-0228151H ¹³ C NMR : 17RMM2-0228151C13C IR: 17RMM2-0228151NaCD
AS02	 <p>(+)-79</p>	¹ H NMR: 18RMM1-0726157H ¹³ C NMR : 17RMM1-0312169C13C IR: 17RMM1-0312169NaCD
AS03	 <p>(+)-120</p>	¹ H NMR: 18RMM1-0729161H ¹³ C NMR : 18RMM1-0729161C13C IR: 18RMM1-0729161NaCD
AS04	 <p>125</p>	¹ H NMR: 17RMM2-0401201H ¹³ C NMR : 17RMM2-0401201C13C IR: 17RMM2-0401201NaCD
AS05	 <p>124</p>	¹ H NMR: 17RMM1-0402209H ¹³ C NMR : 17RMM1-0402209C13C IR: 17RMM2-0402209NaCD

Table A10.4 Cross References for Compounds from Chapter 3: Dichroanone: Part 1

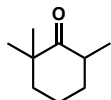
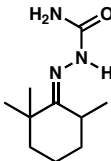
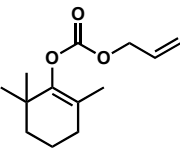
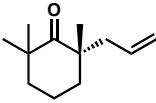
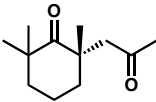
Characterization Binder #	Structure (Thesis #)	Spectral Data
DM01	 <p>101</p>	¹ H NMR: 11RMM1-0916107CH1H ¹³ C NMR : 11RMM1-0916107CC13C IR: 11RMM1-0916107CIRNaCD
DM02	 <p>222</p>	¹ H NMR: 11RMMC-918111CH1H ¹³ C NMR : 11RMMC-0918111CC13C IR: 11RMMC-0918111CIRKBr
DM03	 <p>100</p>	¹ H NMR: 13RMM3-0321215H ¹³ C NMR : 11RMM1-1003179CC13C IR: 11RMM1-1003179CIRNaCD
DM04	 <p>(-)-75</p>	¹ H NMR: 17RMM1-0617255CH1H ¹³ C NMR : 17RMM1-0617255C13C IR: 11RMM1-1006193CIRNaCD
DM05	 <p>(+)-219</p>	¹ H NMR: 11RMM1-1013203CH1H ¹³ C NMR : 11RMM1-1013203CC13C IR: 11RMM1-1013203CIRNaCD

Table A10.5 Cross References for Compounds from Chapter 3: Dichroanone: Part 2

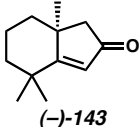
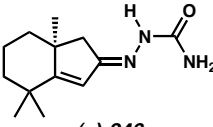
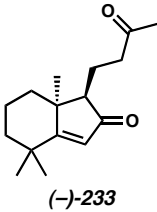
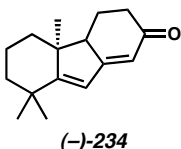
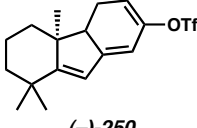
Characterization Binder #	Structure (Thesis #)	Spectral Data
DM06	 <chem>C[C@H]1CC[C@@H]2C(=O)C=C[C@H]1C2</chem> (-)-143	¹ H NMR: 12RMM3-0110665CH1H ¹³ C NMR : 11RMM1-1016215CC13C IR: 11RMM1-1016215CIRNaCD
DM07	 <chem>C[C@H]1CC[C@@H]2C(=O)C=C[C@H]1C2C(=O)N</chem> (-)-246	¹ H NMR: 12RMM2-110665CH1H ¹³ C NMR : 12RMM2-110665CC13C IR: 12RMM2-110665KBr
DM08	 <chem>CC(=O)CC[C@H]1C[C@@H]2C(=O)C=C[C@H]1C2</chem> (-)-233	¹ H NMR: 11RMM2-1018221CH1H ¹³ C NMR : 1RMM2-1018221CC13C IR: 11RMM2-1018221CIRKBr
DM09	 <chem>C[C@H]1CC[C@@H]2C(=O)C=C[C@H]1C2C(=O)C3=CC=CC=C3</chem> (-)-234	¹ H NMR: 12RMM2-111679CH1H ¹³ C NMR : 12RMM2-111679CC13C IR: 12RMM2-111679CIRNaCD
DM10	 <chem>C[C@H]1CC[C@@H]2C(=O)C=C[C@H]1C2C(=O)C3=CC=CC=C3OC(F)(F)F</chem> (-)-250	¹ H NMR: 12RMM1-112189CH1H ¹³ C NMR : 12RMM1-112189CC13C ¹⁹ F NMR: 12RMM1-112189CF19F IR: 12RMM1-112189CIRNaHex

Table A10.6 Cross References for Compounds from Chapter 3: Dichroanone: Part 3

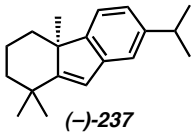
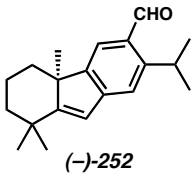
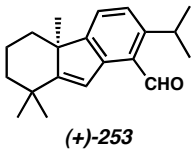
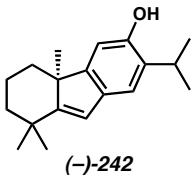
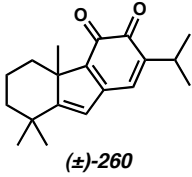
Characterization Binder #	Structure (Thesis #)	Spectral Data
DM11	 (-)-237	¹ H NMR: 12RMM1-112087CH1H ¹³ C NMR : 12RMM1-112087CC13C IR: 12RMM1-112087CIRNaCD
DM12	 (-)-252	¹ H NMR: 12RMM2-112293CH1H ¹³ C NMR : 12RMM2-112293CC13C IR: 12RMM2-112293CIRNaCD
DM13	 (+)-253	¹ H NMR: 12RMM1-112293CH1H ¹³ C NMR :12RMM1-112293CC13C IR: 12RMM1-112293CIRNaCD
DM14	 (-)-242	¹ H NMR: 12RMM1-1204105CC13C ¹³ C NMR : 12RMM1-112599CH1H IR: 12RMM1-112599CIRKBr
DM15	 (±)-260	¹ H NMR: 11RMM1-0920123-100H ¹³ C NMR : IR: RacoQuinoneNaNeat

Table A10.7 Cross References for Compounds from Chapter 3: Dichroanone: Part 4

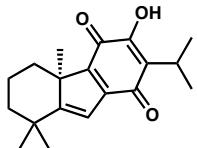
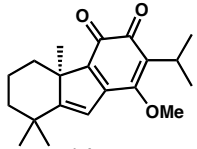
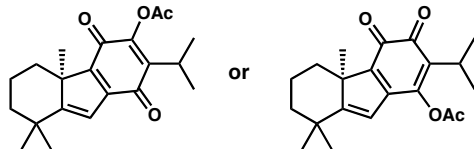
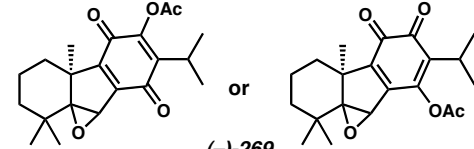
Characterization Binder #	Structure (Thesis #)	Spectral Data
DM16	 (+)-150	¹ H NMR: 12RMM1-1128101CH1H ¹³ C NMR : 12RMM1-1128101C13C IR: 12RMM1-1128101KBr DichroanoneNaCl
DM17	 (+)-267	¹ H NMR: 12RMM1-1213109CH1H ¹³ C NMR : 12RMM1-1213109CC13C IR: 12RMM1-1213109CIRNaCD
DM18	 (+)-268	¹ H NMR: 13RMM1-0209121CH1H ¹³ C NMR : 13RMM1-0209121CC13C IR: 13RMM1-0209121CIRNaCH
DM19	 (-)-269	¹ H NMR: 13RMM4-0212123CH1H ¹³ C NMR : 13RMM4-0212123CC13xC IR: 13RMM4-0212123CIRNaCH

Table A10.8 Cross References for Compounds from Chapter 3: Dichroanone: Part 5

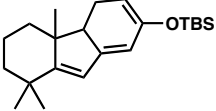
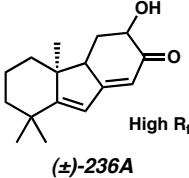
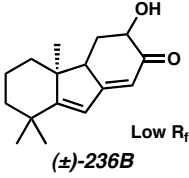
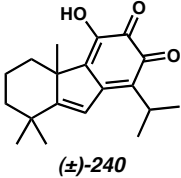
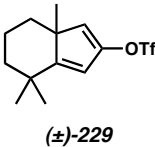
Characterization Binder #	Structure (Thesis #)	Spectral Data
DX01	 <p>(±)-235</p>	¹ H NMR: 8RMM1-020739CH1H ¹³ C NMR : 8RMM1-020739CC13C IR: 8RMM1-020739CIRNeat
DX02	 <p>(±)-236A</p>	¹ H NMR: 8RMM1-020947CH1H ¹³ C NMR : 8RMM1-020947CC13C IR: 8RMM1-020947CIRNaCD
DX03	 <p>(±)-236B</p>	¹ H NMR: 8RMM2-020947CH1H ¹³ C NMR : 8RMM2-020947CC13C IR: 8RMM2-020947CIRNaCD
DX04	 <p>(±)-240</p>	¹ H NMR: 7RMMx-0116235CH1H ¹³ C NMR : 7RMM1-0116235CC13-500C IR: 7RMMx-0116235CIR2NaCD
DX05	 <p>(±)-229</p>	¹ H NMR: 8RMM1-0327143CH1H ¹³ C NMR : 8RMM1-0327143CC13C ¹⁹ F NMR: 8RMM1-0327143CF19F

Table A10.9 Cross References for Compounds from Chapter 3: Dichroanone: Part 6

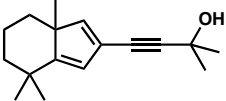
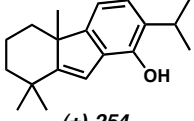
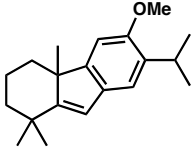
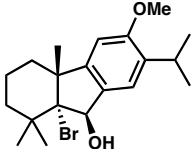
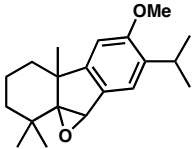
Characterization Binder #	Structure (Thesis #)	Spectral Data
DX06	 <p>(±)-231</p>	¹ H NMR: 8RMM1-0324141CH1H ¹³ C NMR : 8RMM1-0324141CC13C IR: 8RMM1-0324141NaCD
DX07	 <p>(±)-254</p>	¹ H NMR: 8RMM1-0408181CH1H ¹³ C NMR : 8RMM1-0408181CC13C IR: 8RMM1-0408181CIRNaCD
DX08	 <p>(±)-257</p>	¹ H NMR: 8RMM1-0408185CH1H ¹³ C NMR : 8RMM1-0408185CC13C IR: 8RMM1-0408185CIRNaCD
DX09	 <p>(±)-258</p>	¹ H NMR: 8RMM2-0410187H ¹³ C NMR : 8RMM2-0414187C13C IR: 8RMM2-0410187IRNaCD
DX10	 <p>(±)-259</p>	¹ H NMR: 8RMM1-0414205H ¹³ C NMR : 8RMM1-0414205C13C IR: 8RMM1-0414205NaCDD2O

Table A10.10 Cross References for Compounds from Chapter 3: Dichroanone: Part 7

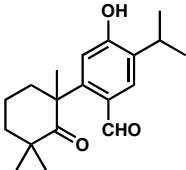
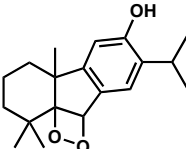
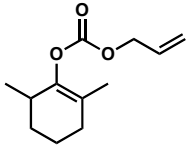
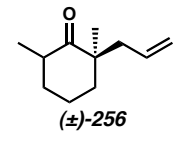
Characterization Binder #	Structure (Thesis #)	Spectral Data
DX11	 <p>245A and 245B</p>	¹ H NMR: 10RMMx-0901249H ¹³ C NMR : 10RMMx-0901249C13C IR: 11RMM4-1005191NaCD
DX12	 <p>244</p>	¹ H NMR: 11RMM3-1005191H ¹³ C NMR : None IR: None
<hr/>		
LI32	 <p>(±)-255</p>	¹ H NMR: 17RMM1-012961H ¹³ C NMR : 17RMM1-012961C13C IR: 17RMM1-012961NaCD
LI33	 <p>(±)-256</p>	¹ H NMR: 17RMM1-013163H ¹³ C NMR : 17RMM1-013163C13C IR: 17RMM1-013163NaCD

Table A10.11 Cross References for Compounds from Chapter 4: Liphagal: Part 1

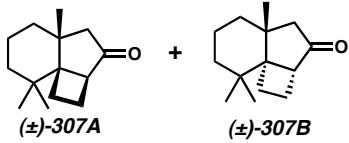
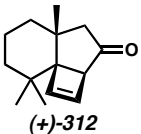
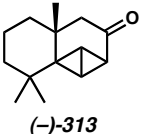
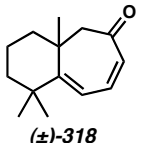
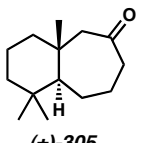
Characterization Binder #	Structure (Thesis #)	Spectral Data
LI01	 <p>(±)-307A + (±)-307B</p>	¹ H NMR: 13RMM1-0324231CH1H ¹³ C NMR : 13RMM1-0324231C13C IR: 13RMM1-0324231CIRKBr
LI02	 <p>(+)-312</p>	¹ H NMR: 15RMM1-cyclobuteneH ¹³ C NMR : 15RMM1-cyclobuteneCC13C IR: 15RMM1-cyclobuteneCIRNaCH
LI03	 <p>(-)-313</p>	¹ H NMR: 14RMM3-0814271CH1H ¹³ C NMR : 14RMM3-0814271CC13C IR: 14RMM3-0814271CIRNaNeat
LI04	 <p>(±)-318</p>	¹ H NMR: 13RMM2-0407275CH1H. ¹³ C NMR : 13RMM2-0407275CC13C IR: 13RMM2-0407275CIRNaCD
LI05	 <p>(±)-305</p>	¹ H NMR: 14RMM1-061599CH1H. ¹³ C NMR : 14RMM1-061599CC13C IR: 14RMM1-061599CIRNaCD

Table A10.12 Cross References for Compounds from Chapter 4: Liphagal: Part 2

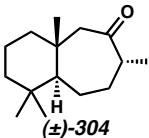
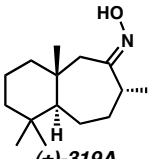
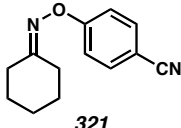
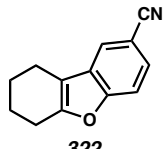
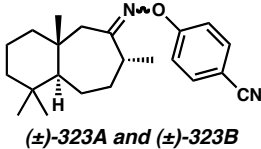
Characterization Binder #	Structure (Thesis #)	Spectral Data
LI06	 <p>(±)-304</p>	¹ H NMR: 13RMM1-0411287CH1H ¹³ C NMR : 13RMM1-0411287CC13C IR: 13RMM1-0411287CIRNaCD
LI07	 <p>(±)-319A</p>	¹ H NMR: 14RMM1-0618107CH1H ¹³ C NMR : 14RMM1-0618107CC13C IR: 14RMM1-0618107CIRNaNaCD
LI08	 <p>321</p>	¹ H NMR: 14RMM1-061397CH1H ¹³ C NMR : 14RMM1-061397CC13C IR: 14RMM1-061397CIRNaCD
LI09	 <p>322</p>	¹ H NMR: 17RMM1-0312171H ¹³ C NMR : 17RMM1-0312171C13C IR: 17RMM1-0312171NaCD
LI10	 <p>(±)-323A and (±)-323B</p>	¹ H NMR: 14RMM1-0619109CH1H ¹³ C NMR : 14RMM1-0619109CC13C IR: 14RMM1-0619109CIRNaCD

Table A10.13 Cross References for Compounds from Chapter 4: Liphagal: Part 3

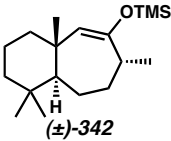
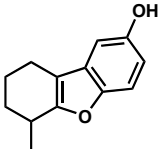
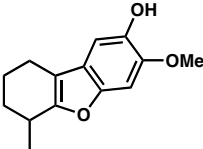
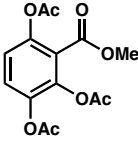
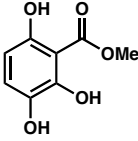
Characterization Binder #	Structure (Thesis #)	Spectral Data
LI11	 <p>(±)-342</p>	¹ H NMR: 14RMMc-0625125H ¹³ C NMR : 14RMMc-0625125C13C IR: 14RMM1-0625125NaNeat
LI12	 <p>331</p>	¹ H NMR: 14RMM1-0703151CH1H ¹³ C NMR : 14RMM1-0703151CC13C IR: 14RMM1-0703151CIRNaCD
LI13	 <p>334</p>	¹ H NMR: 15RMM1-0917163H ¹³ C NMR : 15RMM1-0917163CC13C IR: 15RMM1-0917163KBr
LI14	 <p>338</p>	¹ H NMR: 15RMM1-0921189CH1H ¹³ C NMR : 15RMM1-0921189CC13C IR: 15RMM1-0921189CIRNaCD
LI15	 <p>339</p>	¹ H NMR: 15RMM1-1001207CH1H ¹³ C NMR : 15RMM1-1001207CC13C IR: 15RMM1-1001207CIRxKBr

Table A10.14 Cross References for Compounds from Chapter 4: Liphagal: Part 4

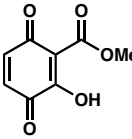
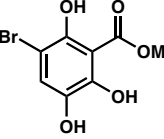
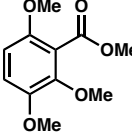
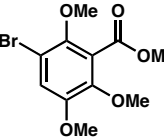
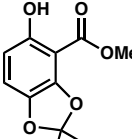
Characterization Binder #	Structure (Thesis #)	Spectral Data
LI16	 <p>340</p>	¹ H NMR: 15RMMc-1002215H ¹³ C NMR : 15RMMc-1002215C13C. IR: 15RMMc-1002215NaCDCH
LI17	 <p>349</p>	¹ H NMR: 15RMM1-1008263H ¹³ C NMR : 15RMM1-1008263C13C IR: 15RMM1-1008263NaCD
LI18	 <p>351</p>	¹ H NMR: 16RMM1-102651CH1H. ¹³ C NMR : 16RMM1-102651CC13C IR: 16RMM1-102651CIRNaCD
LI19	 <p>352</p>	¹ H NMR: 16RMM2-110389CH1H ¹³ C NMR : 16RMM2-110389CC13C IR: 16RMM2-110389CIRNaCH
LI20	 <p>350</p>	¹ H NMR: 16RMM1-102445CH1H ¹³ C NMR : 16RMM1-102445CC13C IR: 16RMM1-102445CIRKBr

Table A10.15 Cross References for Compounds from Chapter 4: Liphagal: Part 5

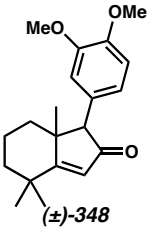
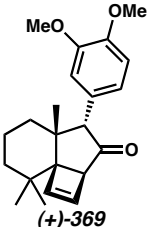
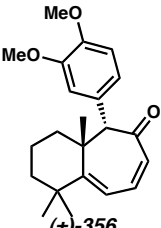
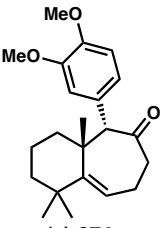
Characterization Binder #	Structure (Thesis #)	Spectral Data
LI21	 <p>(±)-348</p>	¹ H NMR: 16RMM1-1107101H ¹³ C NMR : 16RMM1-1107101C13C IR: 16RMM1-1107101KBr
LI22	 <p>(+)-369</p>	¹ H NMR: 16RMM1-1126123H ¹³ C NMR : 16RMM1-1126123C13C IR: 16RMM1-1126123NaCH
LI23	 <p>(±)-356</p>	¹ H NMR: 16RMM2-1130137H ¹³ C NMR : 16RMM2-1130137C13C IR: 16RMM2-1130137NaCH
LI24	 <p>(±)-374</p>	¹ H NMR: 16RMMc-1201145H ¹³ C NMR : 16RMMc-1201145C13C IR: 16RMMc-1201145NaCH

Table A10.16 Cross References for Compounds from Chapter 4: Liphagal: Part 6

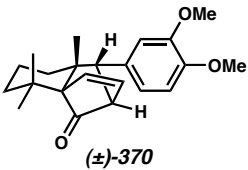
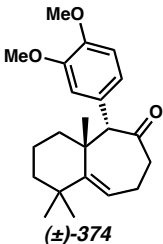
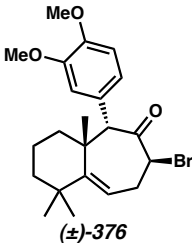
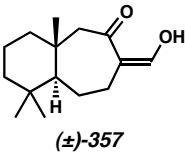
Characterization Binder #	Structure (Thesis #)	Spectral Data
LI25	 <p>(±)-370</p>	¹ H NMR: 16RMM4-1130137H ¹³ C NMR : 16RMM4-1130137C13C IR: 16RMM4-1130137NaCH
LI26	 <p>(±)-374</p>	¹ H NMR: 16RMMc-1201145H ¹³ C NMR : 16RMMc-1201145C13C IR: 16RMMc-1201145NaCH
LI27	 <p>(±)-376</p>	¹ H NMR: 16RMM1-0103237H ¹³ C NMR : 16RMM1-0103237C13C IR: 16RMM1-0103237NaCH
LI28	 <p>(±)-357</p>	¹ H NMR: 16RMM1-0103235H ¹³ C NMR : 16RMM1-0103235C13C IR: 16RMM1-0103235

Table A10.17 Cross References for Compounds from Chapter 4: Liphagal: Part 7

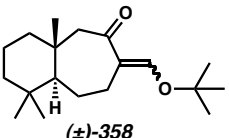
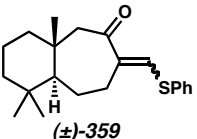
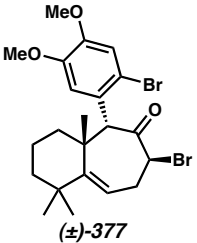
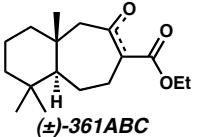
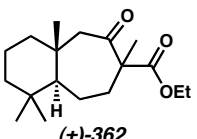
Characterization Binder #	Structure (Thesis #)	Spectral Data
LI29	 <p>(±)-358</p>	¹ H NMR: 16RMM2-0103235H ¹³ C NMR : 16RMM2-0103235C13C IR: 16RMM2-0103235NaDCM
LI30	 <p>(±)-359</p>	¹ H NMR: 16RMM3-0114261CH1H ¹³ C NMR : 16RMM3-0114261CC13C IR: 16RMM3-0114261NaDCM
LI31	 <p>(±)-377</p>	¹ H NMR: 16RMM1-0119289H ¹³ C NMR : 16RMM1-0119289C13xC IR: 16RMM1-0119289NaCD
LI34	 <p>(±)-361ABC</p>	¹ H NMR: 17RMM1-013169C ¹³ C NMR : 17RMM1-013169C13C IR: 17RMM1-013169NaCD
LI35	 <p>(±)-362</p>	¹ H NMR: 17RMM1-020175H ¹³ C NMR : 17RMM1-020175C13C IR: 17RMM1-020175

Table A10.18 Cross References for Compounds from Chapter 4: Liphagal: Part 8

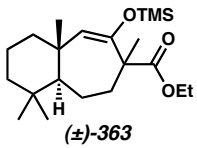
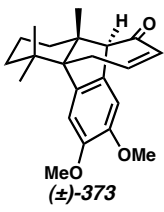
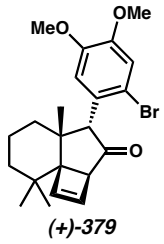
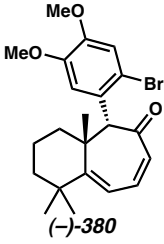
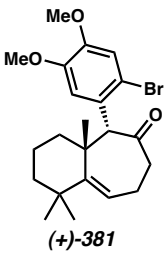
Characterization Binder #	Structure (Thesis #)	Spectral Data
LI36	 <p>(±)-363</p>	¹ H NMR: 17RMMc-0211107H ¹³ C NMR : 17RMMc-0211107C13C IR: 17RMMc-0211107NaDCM
LI37	 <p>(±)-373</p>	¹ H NMR: 17RMM2-0318197H ¹³ C NMR : 17RMM2-0318197C13C IR: 17RMM2-0318197NaCD
LI38	 <p>(+)-379</p>	¹ H NMR: 17RMM1-0406219H ¹³ C NMR : 17RMM1-0406219C13C IR: 17RMM1-0406219NaCD
LI39	 <p>(-)-380</p>	¹ H NMR: 17RMM2-0401205H ¹³ C NMR : 17RMM2-0401205C13C IR: 17RMM2-0401205NaCD
LI40	 <p>(+)-381</p>	¹ H NMR: 17RMMx-0422223H ¹³ C NMR : 17RMMx-0422223C13C IR: 17RMMx-0422223NaCD

Table A10.19 Cross References for Compounds from Chapter 4: Liphagal: Part 9

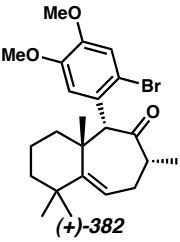
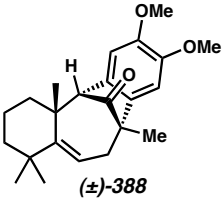
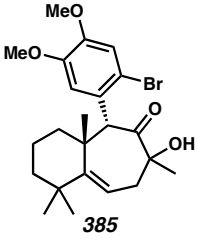
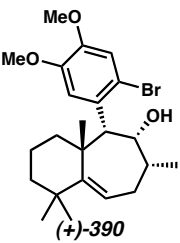
Characterization Binder #	Structure (Thesis #)	Spectral Data
LI41	 <p>(+)-382</p>	¹ H NMR: 17RMM1-0425227H ¹³ C NMR : 17RMM1-0425227C13C IR: 17RMM1-0425227NaCD
LI42	 <p>(±)-388</p>	¹ H NMR: 17RMM3-0503231H ¹³ C NMR : 17RMM1-0504233C IR: 17RMM1-0504233NaCD
LI43	 <p>385</p>	¹ H NMR: 18RMM5-070851H ¹³ C NMR : 18RMM5-070851C13C IR: 18RMM5-070851NaCD
LI44	 <p>(+)-390</p>	¹ H NMR: 18RMMc-071065H ¹³ C NMR : 18RMMc-071065C13C IR: 18RMMc-071065NaCD

Table A10.20 Cross References for Compounds from Chapter 4: Liphagal: Part 10

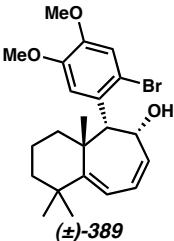
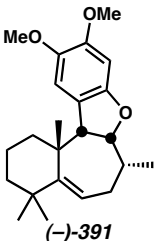
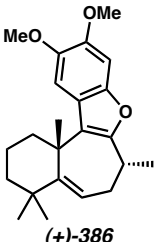
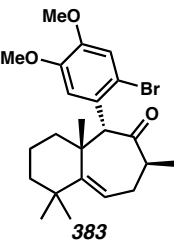
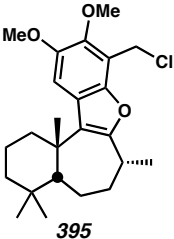
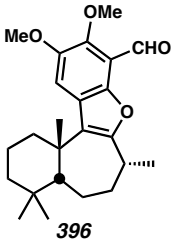
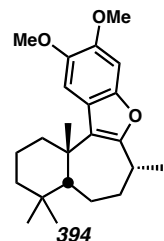
Characterization Binder #	Structure (Thesis #)	Spectral Data
LI45	 <p>(±)-389</p>	¹ H NMR: 18RMM2-071897H ¹³ C NMR : 18RMM2-071897C13C IR: 18RMM2-071897NaCD
LI46	 <p>(-)-391</p>	¹ H NMR: 18RMM1-0828251H ¹³ C NMR : 18RMM1-0828251C13C IR: 18RMM1-0828251
LI47	 <p>(+)-386</p>	¹ H NMR: 19RMM1-0926127H ¹³ C NMR : 19RMM1-0926127C13C IR: 19RMM1-0926127NaCD
LI48	 <p>383</p>	¹ H NMR: 19RMMx-MethylEpiH ¹³ C NMR : 19RMMx-MethylEpiC13C IR: 19RMMx-MethylEpiNaCD

Table A10.21 Cross References for Compounds from Chapter 4: Liphagal: Part 11

Characterization Binder #	Structure (Thesis #)	Spectral Data
LI49	 <p>395</p>	¹ H NMR: 19RMM1-0924121H ¹³ C NMR : None IR: None
LI50	 <p>396</p>	¹ H NMR: 19RMM1-1024191H ¹³ C NMR : 19RMM1-1024191C13C IR: 19RMM1-1024191NaCD
LI51	 <p>394</p>	¹ H NMR: 19RMM1-1026197H ¹³ C NMR : 19RMM1-1026197C13C IR: 19RMM1-1026197NaCD

Comprehensive Bibliography

- Aboulhoda, S. J.; Hénin, F.; Muzart, J.; Thorey, C. *Tetrahedron Lett.* **1995**, *36*, 4795-4796.
- Adam, W.; Chan, Y.-Y.; Cremer, D.; Gauss, J.; Scheutzow, D.; Schindler, M. *J. Org. Chem.* **1987**, *52*, 2800-2803.
- Alemagna, A.; Baldoli, C.; Del Buttero, P.; Licandro, E.; Maiorana, S. *Synthesis* **1987**, *2*, 192-196.
- Anderson, J. C.; Smith, S. C. *Synlett* **1990**, 107-108.
- Anderson, K. W.; Ikawa, T.; Tundel, R.; Buchwald, S. L. *J. Am. Chem. Soc.* **2006**, *128*, 10694-10695.
- Anderson, P. L. Use of Cyclopropyl Intermediates in Angular Methylation and a Total Synthesis of dl-Thujopsene. Ph. D. Dissertation, University of Michigan, Ann Arbor, MI, USA, **1967**.
- Ansell, M. F.; Clements, A. H. *J. Chem. Soc., Sect. C* **1971**, 269-275.
- Bajorek, T.; Werstiuk, N. H. *Chem. Commun.* **2003**, 648-649.
- Ban, Y.; Sato, Y.; Inoue, I.; Nagai, M.; Oishi, T.; Terashima, M.; Yonematsu, O.; Kanaoka, Y. *Tetrahedron Lett.* **1965**, *6*, 2261-2268.
- Banerjee, M.; Mukhopadhyay, R.; Achari, B.; Banerjee, A. Kr. *Org. Lett.* **2003**, *5*, 3931-3933.
- Banerjee, M.; Mukhopadhyay, R.; Achari, B.; Banerjee, A. Kr. *J. Org. Chem.* **2006**, *71*, 2787-2796.
- Barrate, B.; Meijer, L.; Galaktionov, K.; Beach, D. *Anticancer Res.* **1992**, *12*, 873-880.

- Behenna, D. C.; Stoltz, B. M. *J. Am. Chem. Soc.* **2004**, *126*, 15044-15045.
- Bell, M.; Poulsen, T. B.; Jørgensen, K. A. *J. Org. Chem.* **2007**, *72*, 3053-3056.
- Bella, M.; Kobbelgaard, S.; Jørgensen, K. A. *J. Am. Chem. Soc.* **2005**, *127*, 62-63.
- Ben-Nun, M.; Martínez, T. J. *J. Am. Chem. Soc.* **2000**, *122*, 6299-6300.
- Beuchi, G.; White, J. D. *J. Am. Chem. Soc.* **1964**, *86*, 2884-2887.
- Bhattacharya, A.; Dolling, U.-H.; Grabowski, E. J. J.; Karady, S.; Ryan, K. M.; Weinstock, L. *Angew. Chem., Int. Ed.* **1986**, *25*, 476-477.
- Blatt, A. H. *Org. React.* **1942**, *1*, 342-369.
- Boukouvalas, J.; Cheng, Y.-X.; Robichaud, J. *J. Org. Chem.* **1998**, *63*, 228-229.
- Brachmann, S. M.; Ueki, K.; Engelman, J. A.; Kahn, R. C.; Cantley, L. C. *Mol. Cell. Biol.* **2005**, *25*, 1596-1607.
- Brachmann, S. M.; Yballe, C. M.; Innocenti, M.; Deane, J. A.; Fruman, D. A.; Thomas, S. M.; Cantley, L. C. *Mol. Cell. Biol.* **2005**, *25*, 2593-2606.
- Branca, S. J.; Lock, R. L.; Smith, A. B., III *J. Org. Chem.* **1977**, *42*, 3165-3168.
- Breslow, R.; Grubbs, R. H.; Murahashi, S.-I. *J. Am. Chem. Soc.* **1970**, *92*, 4139-4140.
- Breslow, R.; Murayama, D. R.; Murahashi, S.-I. *J. Am. Chem. Soc.* **1973**, *95*, 6688-6699.
- Brimble, M. A.; Burgess, C.; Halim, R.; Petersson, M.; Ray, J. *Tetrahedron* **2004**, *60*, 5751-5758.
- Brunner, H.; Kraus, J.; Lautenschlager, H. J. *Monatsch. Chem.* **1988**, *119*, 1161-1167.
- Buono, G.; Chiodi, O.; Wills, M. *Synlett* **1999**, 377-388.
- Burger, A. P. N.; Brandt, E. V.; Roux, D. G. *Phytochemistry* **1983**, *22*, 2813-2817.

- Caille, S. Enantioselective Syntheses of the Sesterterpenoid (–)-Dysidiolide and Structurally Related Analogues. Ph. D. Dissertation, University of British Columbia, Vancouver, BC, Canada, **2002**.
- Cantley, L. C. *Science* **2002**, *296*, 1655-1657.
- Cargill, R. L.; Jackson, T. E.; Peet, N. P.; Pond, D. M. *Acc. Chem. Res.* **1974**, *7*, 106-113.
- Cargill, R. L.; Wright, B. W. *J. Org. Chem.* **1975**, *40*, 120-122.
- Carpenter, N. E.; Kucera, D. J.; Overman, L. E. *J. Org. Chem.* **1989**, *54*, 5845-5848.
- Carril, M.; SanMartin, R.; Tellitu, I.; Domínguez, E. *Org. Lett.* **2006**, *8*, 1467-1470.
- Cavassa, M.; Guerriero, A.; Pietra, F. *J. Chem. Soc. Perkin Trans. I* **1986**, 2005-2008.
- Cavazza, M.; Pietra, F. *J. Chem. Soc. Perkin Trans. I* **1985**, 2283-2287.
- Chang, C.-I.; Chang, J.-Y.; Kuo, C.-C.; Pan, Y.-H.; Kuo, W.-Y. *Planta Med.* **2005**, *71*, 72-76.
- Chang, C.-I.; Chien, S.-C.; Lee, S.-M.; Kuo, Y.-H. *Chem. Pharm. Bull.* **2003**, *51*, 1420-1422.
- Charette, A. B.; Lebel, H. In *Comprehensive Asymmetric Catalysis*; Jacobsen, E. N.; Pfaltz, A.; Yamamoto, H., Eds.; Springer: New York, **1999**; Vol. 2, pp 581-603.
- Chetty, G. L.; Dev, S. *Tetrahedron Lett.* **1965**, *6*, 3773-3776.
- Cho, Y. S.; Carcache, D. A.; Tian, Y.; Li, Y.-M.; Danishefsky, S. J. *J. Am. Chem. Soc.* **2004**, *126*, 14358-14359.
- Christoffers, J.; Mann, A. *Angew. Chem., Int. Ed.* **2001**, *40*, 4591-4597.
- Ciula, R. P. Bicyclo[1.1.0]butane. Ph.D. Dissertation, Univ. of Washington, Seattle, WA, **1960**.
- Corey, E. J. *Angew. Chem., Int. Ed.* **2002**, *41*, 1650-1667.

- Corey, E. J.; Guzman-Perez, A. *Angew. Chem., Int. Ed.* **1998**, *37*, 388-401.
- Corey, E. J.; Lazerwith, S. E. *J. Am. Chem. Soc.* **1998**, *120*, 12777-12782.
- Corey, E. J.; Roberts, B. E. *J. Am. Chem. Soc.* **1997**, *119*, 12425-12431.
- Crimmins, M. T. *Chem. Rev.* **1988**, *88*, 1453-1473.
- Culkin, D. A.; Hartwig, J. F. *Acc. Chem. Res.* **2003**, *36*, 234-245.
- Daniewski, A. R.; Wojciechowska, W. *Synth. Commun.* **1986**, *16*, 535-536.
- Dauben, W. G.; Ashcraft, A. C. *J. Am. Chem. Soc.* **1963**, *85*, 3673-3676.
- Davies, H. M. L.; Beckwith, R. E. *J. Chem. Rev.* **2003**, *103*, 2861-2903.
- Davis, F. A.; Chattopadhyay, S.; Towson, J. C.; Lal, S.; Reddy, T. *J. Org. Chem.* **1988**, *53*, 2087-2089.
- Davis, F. A.; Lamendola, J., Jr.; Nadir, U.; Kluger, E. W.; Sedergran, T. C.; Panunto, T. W.; Billmers, R.; Jenkins, R., Jr.; Turchi, I. J.; Watson, W. H.; Chen, J. S.; Kimura, M. *J. Am. Chem. Soc.* **1980**, *102*, 2000-2005.
- Davis, F. A.; Sheppard, A. C. *J. Org. Chem.* **1987**, *52*, 955-957.
- Demeke, D. Total Synthesis of Dysidiolide and Cacospongionolide F: A General Approach to the Synthesis of Labadane, Isolabadane, and Clerodane Polyterpenes. Ph. D. Dissertation, Univ. of Minnesota, Minneapolis, MN, USA, **2003**.
- Demeke, D.; Forsyth, C. *Org. Lett.* **2000**, *2*, 3967-3969.
- Demeke, D.; Forsyth, C. J. *Tetrahedron* **2002**, *58*, 6531-6544.
- Denmark, S. E.; O'Connor, S. P. *J. Org. Chem.* **1997**, *62*, 584-594.
- Dolling, U.-H.; Davis, P.; Grabowski, E. J. J. *J. Am. Chem. Soc.* **1984**, *106*, 446-447.
- Donde, A.; Overman, L. E. In *Catalytic Asymmetric Synthesis*, 2nd ed.; Ojima, I., Ed.; Wiley-VCH: New York, **2000**; pp 675-697.

- Douglas, C. J.; Overman, L. E. *Proc. Natl. Acad. Sci. U.S.A.* **2004**, *101*, 5363-5367.
- Dounay, A. B.; Overman, L. E. *Chem. Rev.* **2003**, *103*, 2945-2963.
- Doyle, A. G.; Jacobsen, E. N. *J. Am. Chem. Soc.* **2005**, *127*, 62-63.
- Doyle, M. P. In *Catalytic Asymmetric Synthesis*, 2nd ed.; Ojima, I., Ed.; Wiley-VCH: New York, **2000**; pp 191-228.
- Eaton, P. E.; Nyi, K. *J. Am. Chem. Soc.* **1971**, *93*, 2786-2788.
- Enders, D.; Bartsch, M.; Backhaus, D.; Runsink, J.; Raabe, G. *Liebigs Ann.* **1996**, 1095-1116.
- Enders, D.; Zamponi, A.; Raabe, G.; Runsink, J. *Synthesis* **1993**, 725-728.
- Enders, D.; Zamponi, A.; Schäfer, T.; Nübling, C.; Eichenauer, H.; Demir, A. S.; Raabe, G. *Chem. Ber.* **1994**, *127*, 1707-1721.
- Enzell, C. *Acta Chem. Scand.* **1962**, *16*, 1553-1568.
- Evans, D. A.; Johnson, J. S. In *Comprehensive Asymmetric Catalysis*; Jacobsen, E. N., Pfaltz, A., Yamamoto, H., Eds.; Springer: New York, **1999**; Vol. 3, pp 1177-1235.
- Evans, D. A.; Wu, J. *J. Am. Chem. Soc.* **2003**, *125*, 10162-10163.
- Fillion, E.; Fishlock, D. *J. Am. Chem. Soc.* **2005**, *127*, 13144-13145.
- Foot, J. S.; Phillis, A. T.; Sharp, P. P.; Willis, A. C.; Banwell, M. G. *Tetrahedron Lett.* **2006**, *47*, 6817-6820.
- Fox, J. M.; Huang, X.; Chieffi, A.; Buchwald, S. L. *J. Am. Chem. Soc.* **2000**, *122*, 1360-1370.
- France, S.; Guerin, D. J.; Miller, S. J.; Lectka, T. *Chem. Rev.* **2003**, *103*, 2985-3012.
- Frigerio, M.; Santagostino, M.; Sputore, S. *J. Org. Chem.* **1999**, *64*, 4537-4538.
- Fruman, D. A.; Cantley, L. C. *Signaling Networks and Cell Cycle Control* **2000**, 247-266.

- Fruman, D. A.; Cantley, L. C. *Seminars in Immunology* **2002**, *14*, 7-18.
- Gagnepain, J.; Castet, F.; Quideau, S. *Angew. Chem., Int. Ed.* **2007**, *46*, 1533-1535.
- Gammill, R. B. *Tetrahedron Lett.* **1985**, *26*, 1385-1388.
- Gao, X.; Matsuo, Y.; Snider, B. B. *Org. Lett.* **2006**, *8*, 2123-2126.
- Gassman, P. G. *Angew. Chem., Int. Ed.* **1972**, *11*, 323.
- Gassman, P. G.; Atkins, T. J.; Williams, F. J. *J. Am. Chem. Soc.* **1971**, *93*, 1812-1813.
- Gassman, P. G.; Meyer, R. G.; Williams, F. J. *J. Chem. Soc. Sect. D: Chem. Commun.* **1971**, 842-843.
- Gassman, P. G.; Nakai, T. *J. Am. Chem. Soc.* **1972**, *94*, 5497-5499.
- Gassman, P. G.; Takeshi, N. *J. Am. Chem. Soc.* **1971**, *93*, 5897-5899.
- Gassman, P. G.; Takeshi, N. *J. Am. Chem. Soc.* **1972**, *94*, 2877-2879.
- Gassman, P. G.; Williams, F. J. *Tetrahedron Lett.* **1971**, *18*, 1409-1412.
- Gassman, P. G.; Williams, F. J. *J. Chem. Soc., Chem. Commun.* **1972**, 80-81.
- Gunasekera, S. P.; McCarthy, P. J.; Kelly-Borges, M. *J. Am. Chem. Soc.* **1996**, *118*, 8759-8760.
- Hajos, Z. G.; Parrish, D. R. *J. Org. Chem.* **1974**, *39*, 1615-1621.
- Hamashima, Y.; Hotta, D.; Sodeoka, M. *J. Am. Chem. Soc.* **2002**, *124*, 11240-11241.
- Hamashima, Y.; Sakamoto, N.; Hotta, D.; Somei, H.; Umebayashi, N.; Sodeoka, M. *Angew. Chem., Int. Ed.* **2005**, *44*, 1525-1529.
- Harayama, T.; Sakurai, K.; Tanaka, K.; Hashimoto, Y.; Fukushi, H.; Inubushi, Y. *Chem. Pharm. Bull.* **1987**, *35*, 1434-1442.
- Hayakaa, M.; Kaizawa, H.; Kawaguchi, K. I.; Matsuda, K.; Ishikawa, N.; Koizumi, T.; Yamanao.; M.; Ohta, M. U.S. Patent US 6403588, **2002**.

- Hayashi, T.; Kanehira, K.; Hagihara, T.; Kumada, M. *J. Org. Chem.* **1988**, *53*, 113-120.
- Hayashi, U. In *Cycloaddition Reactions in Organic Synthesis*; Kobayashi, S.; Jorgensen, K. A., Eds.; Wiley-VCH: New York, **2002**; pp 5-56.
- Hills, I. D.; Fu, G. C. *Angew. Chem., Int. Ed.* **2003**, *42*, 3921-3924.
- Himkus, J. M.; Majetich, G. Total synthesis of (\pm)-dichroanone and studies toward related diterpenoids. Abstracts, 58th Southeast Regional Meeting of the American Chemical Society, Augusta, GA, United States, November 1-4 (**2006**), SRM06-633.
- Hiramatsu, Y.; Miyazaki, Y. *J. Wood. Sci.* **2001**, *47*, 13-17. (b) Yatagai, M. *Curr. Top. Phytochem.* **1997**, *1*, 85-97.
- Hixson, S. S.; Mariano, P. S.; Zimmerman, H. E. *Chem. Rev.* **1973**, *73*, 531-551.
- Holmes, T. J.; John, V.; Vennerstrom, J.; Choi, K. E. *J. Org. Chem.* **1984**, *49*, 4736-4738.
- Hughes, D. L. *Org. Prep. Proced. Int.* **1993**, *25*, 609-632.
- Hussain, S.; Schuster, D. I.; El-Bayoumy, K. *Tetrahedron Lett.* **1982**, *23*, 153-156.
- Isakoff, S. J.; Engelman, J. A.; Irie, H. Y.; Luo, J.; Brachmann, S. M.; Pearline, R. V.; Cantley, L. C.; Brugge, J. S. *Cancer Res.* **2005**, *65*, 10992-11000.
- Ito, S.; Endo, K.; Honma, H.; Ota, K. *Tetrahedron Lett.* **1965**, *6*, 3777-3781.
- Ito, Y.; Saegusa, T. *J. Org. Chem.* **1978**, *43*, 1011-1013.
- Iwamoto, M.; Ohtsu, H.; Tokuda, H.; Nishino, H.; Matsunaga, S.; Tanaka, R. *Bioorg. Med. Chem.* **2001**, *9*, 1911-1921.
- Johnson, C. R.; Barbachyn, M. R. *J. Am. Chem. Soc.* **1982**, *104*, 4290-4291.
- Jung, M. E.; Murakami, M. *Org. Lett.* **2007**, *9*, 461-463.
- Jung, M. E.; Nishimura, N. *Org. Lett.* **2001**, *3*, 2113-2115.
- Jung, Y.; Marcus, R. A. *J. Am. Chem. Soc.* **2007**, *129*, 5492-5502.

- Kaji, A.; Saito, R.; Hata, Y.; Kiriya, N. *Chem. Pharm. Bull.* **1999**, *47*, 77-82.
- Kakiuchi, K.; Ohnishi, Y.; Kobiro, K.; Tobe, Y.; Odaira, Y. *J. Org. Chem.* **1991**, *56*, 463-466.
- Kakiuchi, K.; Ue, M.; Tsukahara, H.; Shimizu, T.; Miyao, T.; Tobe, Y.; Odaira, Y.; Yasuda, M.; Shima, K. *J. Am. Chem. Soc.* **1989**, *111*, 3707-3712.
- Katsumura, S.; Ise, S. *Chem. Lett.* **1982**, 1689-1692.
- Kawatsura, M.; Hartwig, J. F. *J. Am. Chem. Soc.* **1999**, *121*, 1473-1478.
- Kawazoe, K.; Yamamoto, M.; Takaishi, Y.; Honda, G.; Fujita, T.; Sezik, E.; Yesilada, E. *Phytochemistry* **1999**, *50*, 493-497.
- Kim, Y.-S.; Matsunaga, S.; Das, J.; Sekine, A.; Ohshima, T.; Shibasaki, M. *J. Am. Chem. Soc.* **2000**, *122*, 6506-6507.
- Knight, Z. A.; Gonzalez, B.; Feldman, M. E.; Zunder, E. R.; Goldenberg, D. D.; Williams, O.; Loewith, R.; Stokoe, D.; Balla, A.; Toth, B.; Balla, T. Weiss, W. A.; Williams, R. L.; Shokat, K. M. *Cell*, **2006**, *125*, 733-737.
- Kogen, H.; Tomioka, K.; Hashimoto, S.-i.; Koga, K. *Tetrahedron Lett.* **1980**, *21*, 4005-4008.
- Kurti, L.; Hurczech, P.; Visy, J.; Simonyi, M.; Antus, S.; Pelter, A. *J. Chem. Soc., Perkin Trans. 1: Organic and Bio-Organic Chemistry* **1999**, *4*, 379-380.
- Kuwano, R.; Uchida, K.-i.; Ito, Y. *Org. Lett.* **2003**, *5*, 2177-2179.
- Lawton, G.; Saxton, J. E.; Smith, A. J. *Tetrahedron* **1977**, *33*, 1641-1653.
- Lee, E.; Shin, I.-J.; Kim, T.-S. *J. Am. Chem. Soc.* **1990**, *112*, 260-264.
- Legrand, S.; Nordlander, G.; Nordenhem, H.; Borg-Karlson, A.-K.; Unelius, C. R. Z. *Naturforsch* **2004**, *59*, 829-835.

- Lemal, D. M.; Menger, F.; Clark, G. W. *J. Am. Chem. Soc.* **1963**, *85*, 2529-2530.
- Liang, G.; Xu, Y.; Seiple, I. B.; Trauner, D. *J. Am. Chem. Soc.* **2006**, *128*, 11022-11023.
- Lin, W.-H.; Fang, J.-M.; Cheng, Y.-S. *Phytochemistry* **1995**, *40*, 871-873.
- Lin, W.-H.; Fang, J.-M.; Cheng, Y.-S. *Phytochemistry* **1996**, *42*, 1657-1663.
- Liu, T.-Y.; Long, J.; Li, B.-J.; Jiang, L.; Li, R.; Wu, Y.; Ding, L.-S.; Chen, Y.-C. *Org. Biomol. Chem.* **2006**, *4*, 2097-2099.
- Lipshutz, B. H.; Servesko, J. M.; Peterson, T. B.; Papa, P. P.; Lover, A. A. *Org. Lett.* **2004**, *6*, 1273-1275.
- Luis, J. G.; Grillo, T. A. *Tetrahedron*, **1993**, *49*, 6277-6284.
- Luo, J.; Sobkiw, C. L.; Logsdon, N. M.; Watt, J. M.; Signoretti, S.; O'Connell, F.; Shin, E.; Shim, Y.; Pao, L.; Neel, B. G.; DePinho, R. A.; Loda, M.; Cantley, L. C. *Proc. Natl. Acad. Sci. U.S.A.* **2005**, *102*, 10238-10243.
- Lydon, K. M.; McKerverey, M. A. In *Comprehensive Asymmetric Catalysis*; Jacobsen, E. N.; Pfaltz, A.; Yamamoto, H., Eds.; Springer: New York, **1999**; Vol. 2, pp 539-580.
- Magdziak, D.; Rodriguez, A. A.; Van De Water, R. W.; Pettus, T. R. R. *Org. Lett.* **2002**, *4*, 285-288.
- Magnuson, S. R.; Sepp-Lorenzino, L.; Rosen, N.; Danishefsky, S. J. *J. Am. Chem. Soc.* **1998**, *120*, 1615-1616.
- Mamaghani, M.; Pourali, A. *Zh. Org. Khim.* **2002**, *38*, 369-371.
- Marion, F.; Williams, D. E.; Patrick, B. O.; Hollander, I.; Mallon, R.; Kim, S. C.; Roll, D. M.; Feldberg, L.; van Soest, R.; Andersen, R. J. *Org. Lett.* **2006**, *8*, 321-324.
- Maruoka, K. In *Catalytic Asymmetric Synthesis*, 2nd ed.; Ojima, I., Ed.; Wiley-VCH: New York, **2000**; pp 467-491.

- Mase, N.; Tanaka, F.; Barbas, C. F., III *Angew. Chem., Int. Ed.* **2004**, *43*, 2420-2423.
- McFadden, R. M.; Stoltz, B. M. *J. Am. Chem. Soc.* **2006**, *128*, 7738-7739.
- McMurry, J. E.; Blaszcak, L. C. *J. Org. Chem.* **1974**, *39*, 2217-2222.
- Mermerian, A. H.; Fu, G. C. *J. Am. Chem. Soc.* **2003**, *125*, 4050-4051.
- Meyers, A. I.; Berney, D. *J. Org. Chem.* **1989**, *54*, 4673-4676.
- Meyers, A. I.; Fleming, S. A. *J. Am. Chem. Soc.* **1986**, *108*, 306-307.
- Meyers, A. I.; Hanreich, R.; Wanner, K. T. *J. Am. Chem. Soc.* **1985**, *107*, 7776-7778.
- Meyers, A. I.; Harre, M.; Garland, R. *J. Am. Chem. Soc.* **1984**, *106*, 1146-1148.
- Meyers, A. I.; Lefker, B. A. *J. Org. Chem.* **1986**, *51*, 1541-1544.
- Millar, J. B. A.; Russel, P. *Cell* **1992**, *68*, 407-410.
- Minami, T.; Iwamoto, M.; Ohtsu, H.; Ohishi, H.; Tanaka, R.; Yoshitake, A. *Planta Med.* **2002**, *68*, 742-745.
- Miyaoka, H.; Kajiwar, Y.; Hara, Y.; Yamada, Y. *J. Org. Chem.* **2001**, *66*, 1429-1435.
- Miyaoka, H.; Kajiwar, Y.; Yamada, Y. *Tetrahedron Lett.* **2000**, *41*, 911-914.
- Miyaoka, H.; Yamada, Y. *Bull. Chem. Soc. Jpn.* **2002**, *75*, 203-222.
- Miyata, O.; Takeda, N.; Morikami, Y.; Naito, T. *Org. Biomol. Chem.* **2003**, *1*, 254-256.
- Miyazaki, Y. *Mokuzai Gakkaishi* **1996**, *42*, 624-626.
- Mohr, J. T.; Behenna, D. C.; Harned, A. M.; Stoltz, B. M. *Angew. Chem., Int. Ed.* **2005**, *44*, 6924-6927.
- Mohr, J. T.; Ebner, D. C.; Stoltz, B. M. *Org. Biomol. Chem.* **2007**, *5*, 3571-3576.
- Mohr, J. T.; Stoltz, B. M. *Chem. Asian J.* **2007**, (In Press: DOI: 10.1002/asia.200700183).
- Mori, K.; Ohki, M.; Kobayashi, A.; Matsui, M. *Tetrahedron*, **1970**, *26*, 2815-2819.
- Mueller, R.; Ruedi, P. *Helv. Chim. Acta* **2003**, *86*, 439-456.

- Nakamura, N.; Nojima, M.; Kusabayashi, S. *J. Am. Chem. Soc.* **1987**, *109*, 4969-4973.
- Nemoto, T.; Fukuda, T.; Matsumoto, T.; Hitomi, T.; Hamada, Y. *Adv. Synth. Catal.* **2005**, *347*, 1504-1506.
- Nishimura, N. I. Total Synthesis of Dysidiolide. II. [2+2] to [4+2] Rearrangements. Ph. D. Dissertation, University of California, Los Angeles, CA, USA, **2001**.
- Norin, T. *Acta Chem. Scand.* **1961**, *15*, 1676-1694.
- Norin, T. *Acta Chem. Scand.* **1963**, *17*, 738-748.
- Nozoe, T.; Takeshita, H.; Ito, S.; Ozeki, T.; Seto, S. *Chem. Pharm. Bull.* **1960**, *8*, 936-938.
- Ohtsu, H.; Iwamoto, M.; Ohishi, H.; Matsunaga, S.; Tanaka, R.; *Tetrahedron Lett.* **1999**, *40*, 6419-6422.
- Palucki, M.; Buchwald, S. L. *J. Am. Chem. Soc.* **1997**, *119*, 11108-11109.
- Paquette, W. D.; Taylor, R. E. *Org. Lett.* **2004**, *6*, 103-106.
- Peer, M.; de Jong, J. C.; Kiefer, M.; Langer, T.; Riech, H.; Schell, H.; Sennhenn, P.; Sprinz, J.; Steinhagen, H.; Wiese, B.; Helmchen, G. *Tetrahedron* **1996**, *52*, 7547-7583.
- Pfaltz, A. In *Comprehensive Asymmetric Catalysis*; Jacobsen, E. N., Pfaltz, A., Yamamoto, H., Eds.; Springer: New York, **1999**; Vol. 2, pp 513-538.
- Planas, L.; Mogi, M.; Takita, H.; Kajimoto, T.; Node, M. *J. Org. Chem.* **2006**, *71*, 2896-2898.
- Pollini, G. P.; Bianchi, A.; Casolari, A.; De Risi, C.; Zanirato, V.; Bertolasi, V. *Tetrahedron Asym.* **2004**, *15*, 3223-3232.
- Razin, V. V.; Mostova, M. I.; D'yakonov, I. A. *Zh. Organish. Khim.* **1968**, *4*, 535.

- Roberts, B. E. The Enantioselective Total Synthesis of the Marine Terpenes Fuscol and Dysidiolide. Ph. D. Dissertation, Harvard University, Cambridge, MA, USA, **1997**.
- Robertson, A. J.; Jackson, S.; Kenche, V.; Yaip, C.; Parbaharan, H.; Thompson, P. Int. Patent Appl. WO 0181346 A2, **2001**.
- Robertson, D. W.; Lacefield, W. B.; Bloomquist, W.; Pfiefer, W.; Simon, R. L.; Cohen, M. L. *J. Med. Chem.* **1992**, *35*, 310-319.
- Robinson, B. *Chem. Rev.* **1969**, *69*, 227-250.
- Robinson, B. In *The Fischer Indole Synthesis*. John Wiley and Sons: New York, **1982**.
- Roldán, E. A.-M.; Santiago, J. L. R.; Chahboun, R. *J. Nat. Prod.* **2006**, *69*, 563-566.
- Rubottom, G. M.; Juve, H. D., Jr. *J. Org. Chem.* **1983**, *48*, 422-425.
- Ryu, D. U.; Corey, E. J. *J. Am. Chem. Soc.* **2003**, *125*, 6388-6390.
- Sadhu, C.; Masinovsky, B.; Dick, K.; Sowell, G. C.; Staunton, D. E. *J. Immunol.* **2003**, *170*, 2647-2654.
- Sasai, H.; Emori, E.; Arai, T.; Shibasaki, M. *Tetrahedron Lett.* **1996**, *37*, 5561-5564.
- Sato, Y.; Sodeoka, M.; Shibasaki, M. *J. Org. Chem.* **1989**, *54*, 4738-4739.
- Sawamura, M.; Nagata, H.; Sakamoto, H.; Ito, Y. *J. Am. Chem. Soc.* **1992**, *114*, 2586-2592.
- Saxton, J. E. In *The Alkaloids*; Cordell, G. A., Ed.; Academic Press: New York, **1998**; Vol. 51, Chapter 1.
- Schulz, S. R.; Blechert, S. *Angew. Chem., Int. Ed.* **2007**, *46*, 3966-3970.
- Shaw, S. A.; Aleman, P.; Vedejs, E. *J. Am. Chem. Soc.* **2003**, *125*, 13368-13369.
- Shen, R.; Corey, E. J. *Org. Lett.* **2007**, *9*, 1057-1059.
- Shibasaki, M.; Yoshikawa, N. *Chem. Rev.* **2002**, *102*, 2187-2209.

- Shih, C.; Fritzen, E. L.; Swenton, J. S. *J. Org. Chem.* **1980**, *45*, 4462-4471.
- Shimizu, I.; Yamada, T.; Tsuji, J. *Tetrahedron Lett.* **1980**, *21*, 3199-3202.
- Sisido, K.; Nozaki, H.; Imagawa, T. *J. Org. Chem.* **1961**, *26*, 1964-1967.
- Smith, A. B., III; Cho, Y. S.; Friestad, G. K. *Tetrahedron Lett.* **1998**, *39*, 8765-8768.
- Sondheimer, F.; Elad, D. *J. Am. Chem. Soc.* **1958**, *80*, 1967-1971.
- Spielvogel, D. J.; Buchwald, S. L. *J. Am. Chem. Soc.* **2002**, *124*, 3500-3501.
- Srikrishna, A.; Anebouselvy, K. *J. Org. Chem.* **2001**, *66*, 7102-7106.
- Stoltz, B. M.; Kano, T.; Corey, E. J. *J. Am. Chem. Soc.* **2000**, *122*, 9044-9045.
- Stork, G.; Danheiser, R. L. *J. Org. Chem.* **1973**, *38*, 1775-1776.
- Stork, G.; Dolfini, J. E. *J. Am. Chem. Soc.* **1963**, *85*, 2872-2873.
- Su, W.; Raders, S.; Verkade, J. G.; Liao, X.; Hartwig, J. F. *Angew. Chem., Int. Ed.* **2006**, *45*, 5852-5855.
- Sugihara, Y.; Yamato, A.; Murata, I. *Tetrahedron Lett.* **1981**, *22*, 3257-3260.
- Sunder-Plassman, P.; Nelson, P. H.; Boyle, P. H.; Cruz, A.; Iriarte, J.; Crabbé, P.; Zderic, J. A.; Edwards, J. A.; Fried, J. H. *J. Org. Chem.* **1969**, *34*, 3779-3784.
- Syper, L.; Mlochowski, J.; Kloc, K. *Tetrahedron* **1983**, *39*, 781-792.
- Takahashi, M.; Dodo, K.; Hashimoto, Y.; Shirai, R. *Tetrahedron Lett.* **2000**, *41*, 2111-2114.
- Takano, S.; Sato, T.; Inomata, K.; Ogasawara, K. *J. Chem. Soc., Chem. Commun.* **1991**, *7*, 462-464.
- Takikawa, H.; Ueda, K.; Sasaki, M. *Tetrahedron Lett.* **2004**, *45*, 5569-5572.
- Tani, K.; Behenna, D. C.; McFadden, R. M.; Stoltz, B. M. *Org. Lett.* **2007**, *9*, 2529-2931.
- Taylor, M. S.; Jacobsen, E. N. *J. Am. Chem. Soc.* **2003**, *125*, 11204-11205.

- Tessier, P. E.; Nguyen, N.; Clay, M. D.; Fallis, A. G. *Org. Lett.* **2005**, *7*, 767-770.
- Thomas, A. F.; Ozainne, M.; Guntz-Dubini, R. *Can. J. Chem.* **1980**, *58*, 1810-1820.
- Trost, B. M.; Radinov, R.; Grenzer, E. M. *J. Am. Chem. Soc.* **1997**, *119*, 7879-7880.
- Trost, B. M.; Schroeder, G. M. *J. Am. Chem. Soc.* **1999**, *121*, 6759-6760.
- Trost, B. M.; Schroeder, G. M.; Kristensen, J. *Angew. Chem., Int. Ed.* **2002**, *41*, 3492-3495.
- Trost, B. M.; Xu, J. *J. Am. Chem. Soc.* **2005**, *127*, 2846-2847. (b) Trost, B. M.; Xu, J. *J. Am. Chem. Soc.* **2005**, *127*, 12180-17181.
- Trost, B. M.; Xu, J.; Reichle, M. *J. Am. Chem. Soc.* **2007**, *129*, 282-283.
- Tsuda, T.; Chujo, Y.; Nishi, S.; Tawara, K.; Saegusa, T. *J. Am. Chem. Soc.* **1980**, *102*, 6381-6384.
- Tsuji, J.; Minami, I.; Shimizu, I. *Chem. Lett.* **1983**, 1325-1326.
- Tsuji, J.; Minami, I.; Shimizu, I. *Tetrahedron Lett.* **1983**, *24*, 1793-1796.
- Tsutsumi, K.; Nakano, H.; Furutani, A.; Endou, K.; Merpuge, A.; Shintani, T.; Morimoto, T.; Kakiuchi, K. *J. Org. Chem.* **2004**, *69*, 785-789.
- Varticovski, L.; Druker, B.; Morrison, D.; Cantley, L.; Roberts, T. *Nature* **1989**, *342*, 699-702.
- Vedejs, E.; Engler, D. A.; Teclschow, J. E. *J. Org. Chem.* **1978**, *43*, 188-196.
- Wakabayashi, S.; Saito, N.; Sugihara, Y.; Sugimura, T.; Murata, I. *Synth. Commun.* **1995**, *25*, 2019-2027.
- Ward, S. G.; Finan, P. *Curr. Opin. Pharmacol.* **2003**, *3*, 426-434.
- Ward, S. G.; Sotsios, Y.; Dowden, J.; Bruce, I.; Finan, P. *Chem. Biol.* **2003**, *10*, 207-213.
- Watanabe, N.; Ogawa, T.; Ohtake, Y.; Ikegami, S.; Hashimoto, S. *Synlett* **1996**, 85-86.

- White, J. D.; Avery, M. A.; Carter, J. P. *J. Am. Chem. Soc.* **1982**, *104*, 5486-5489.
- White, J. D.; Kim, N.-S.; Hill, D. E.; Thomas, J. A. *Synthesis* **1998**, 619-626.
- Wilgus, H. S.; Gates, J. W. *Can. J. Chem.* **1967**, *45*, 1975-1980.
- Wu, M. H.; Hansen, K. B.; Jacobsen, E. N. *Angew. Chem., Int. Ed.* **1999**, *38*, 2012-2014.
- Wymann, M. P.; Zvelebil, M.; Laffargue, M. *Trends Pharmacol. Sci.* **2003**, *24*, 366-376.
- Yang, L.; Williams, D. E.; Mui, A.; Ong, C.; Krystal, G.; van Soest, R.; Andersen, R. J. *Org. Lett.* **2005**, *7*, 1073-1076.
- Yano, M. *J. Soc. Chem. Ind. Jpn.* **1913**, *16*, 443. (b) Uchida, S. *J. Soc. Chem. Ind. Jpn.* **1928**, *31*, 501.
- Yatagai, M. *Aroma Res.* **2007**, *8*, 88-93.
- Yoon, T. P.; Dong, V. M.; MacMillan, D. W. C. *J. Am. Chem. Soc.* **1999**, *121*, 9726-9727.
- Yoon, T. P.; MacMillan, D. W. C. *J. Am. Chem. Soc.* **2001**, *123*, 2911-2912.
- Yoshihiko, I.; Yasuhiro, M.; Yoshikazu, S.; Toshihoro, O.; Nakao, I. *Biocontrol science* **2006**, *11*, 49-54.
- You, S.-L.; Dai, L.-X. *Angew. Chem., Int. Ed.* **2006**, *45*, 5246-5248.
- You, S.-L.; Hou, X.-L.; Dai, L.-X.; Zhu, X.-Z. *Org. Lett.* **2001**, *3*, 149-151.
-

About the Author

Ryan Michael McFadden was born in Evansville, IN on October 15th, 1979. He is the son of Michael L. and Sharon A. McFadden and the brother of Erin and Kevin McFadden. He spent his younger years playing basketball and tennis, cub scouting, and building legos. His interest in chemistry began when he joined the science club at Plaza Park Middle School, led by James Kimsey. He took on a science project investigating the stoichiometry of the reaction between vinegar and baking soda, winning the science fair in eighth grade. Later, he attended William Henry Harrison high school, where he pursued the clarinet, marched four years in the band, and participated in community outreach.

In the fall of 1998, Ryan began his undergraduate studies in chemistry at Purdue University in West Lafayette, IN. He served as concertmaster of the Purdue Symphonic Band and treasurer of Shreve Residence Hall Club, while actively participating in Campus Crusade for Christ. It was at Purdue where he undertook undergraduate research with Dr. Timothy Zwier, studying the chemistry of hydrogen-bonded clusters. He later began undergraduate research in the labs of Dr. Hicham Fenniri, where he found his true love for organic chemistry. He graduated from Purdue with honors, earning an ACS accredited Bachelors in chemistry and a BS in Chemistry and Biochemistry in May of 2002.

In the Fall of 2002, he moved to Pasadena, CA to begin graduate studies at the California Institute of Technology. He joined the labs of Dr. Brian M. Stoltz, where he investigated the applications of palladium-catalyzed enantioselective decarboxylative alkylation in total synthesis. On July 30th, 2005 he married Marcia Jean Liem, the daughter of Bian Bie and Linny Liem. He is eagerly looking forward to starting a new life with Marcia in the San Francisco area, where he will be working as a medicinal chemist at Gilead Pharmaceuticals.